Synthesis and Development of Light-Activated Molecular Probes



Michelle L. Savage

Prof. T. Brown & Prof. S. J. Conway

Pembroke College

University of Oxford

A thesis submitted in partial fulfilment of the requirement for the degree of

Doctor of Philosophy (D. Phil.)

Trinity 2017

清者自清

Acknowledgements

My heartfelt gratitude goes out to Prof. Tom Brown for taking a chance on me, his kindness, generosity and the graciousness with which he accepted me into his group and for his advice, encouragement and support, without which I would never have had this opportunity.

I thank Prof. Stuart Conway for giving me the opportunity to work on this challenging, yet fulfilling project that pushed me out of my comfort zone, taught me many a life lesson along the way and helped me grow as an individual.

Many thanks to Afaf for her guidance and encouragement on an almost daily basis and for imparting so many anecdotes and words of wisdom to me. I will always remember to "Try my best and leave the rest!"

To the Brown and Conway groups, it has been an absolute pleasure to work alongside all of you.
I am especially grateful to Sara who so promptly and meticulously proof-read my work.

To all the CRL Support Staff, NMR Team, MS Team, Stores and Workshop Staff, thank you for working tirelessly behind the scenes, and for designing and assembling my LEDs and light box. Special mention must go to Dr James Wickens who saved the day by painstakingly running hundreds of LCMS samples for me.
I will be forever grateful to Prof. John Foord for always lending me a helping hand and pointing me in the right direction every time I faced a road-block from the very first day I became his student.
To Dr Green and Prof. Schofield, I thank you both for the part you played in making this possible.

To all the people at Peptide Protein Research Ltd., particularly Bob, Michele, John and Jack, many thanks for imparting so much knowledge to me and for extending your hospitality and allowing me to work alongside you.

Simply too many people have contributed to bringing this project to fruition in one way or another and I extend my thanks to all of you.

To my beloved PoPo, Mommie and Daddy, I am where I am today because of your love and sacrifices, and because you believed in me, even when no one else would. You stood by me every step of the way and saw me through it all. I hope I made you proud.
Stephen and Sophia, my siblings and best friends, you have kept me smiling all the way through and made each and every day just that little bit brighter.

To Martin, thank you for your constant encouragement and for helping in whatever way you knew how.

To all my family and friends, none of this would have been possible without each and every single one of you.

Declaration

I, Michelle L. Savage, hereby declare, that this dissertation has been written by me, that it is the record of work carried out by me and that it has not been submitted in any previous application for a higher degree at this or any other university or institute of learning.

I was admitted as a probationary research student in October 2011 and as a candidate for the degree of Doctor of Philosophy in October 2012; the higher study for which this is a record was carried out in the University of Oxford between 2011 and 2017.

Michelle L. Savage

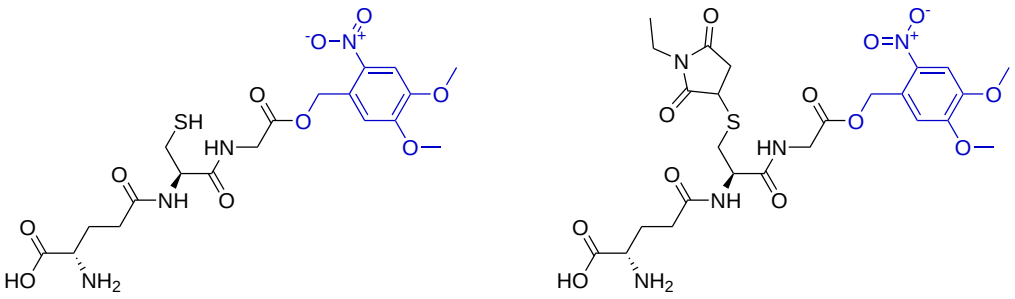
In submitting this thesis to the University of Oxford, I understand that I am giving permission for it to be made available for use in accordance with the regulations of the University Library for the time being in force, subject to any copyright vested in the work not being affected thereby. I also understand that the title and the abstract will be published, and that a copy of the work may be made available and supplied to any *bona fide* library or research worker, that this thesis will be electronically accessible for personal or research use, and that the library has the right to migrate this thesis into new electric forms as required to ensure continued access to the thesis. I have obtained any third-party copyright permissions that may be required in order to allow such access and migration.

Abstract

Synthesis & Development of Light-Activated Molecular Probes
Michelle L. Savage
Supervisor: Prof. Tom Brown & Prof. Stuart J. Conway
Pembroke College, University of Oxford
Submitted for the degree of D. Phil.: Trinity 2017

Judicious addition of photolabile caging groups (PCGs) to protect biologically important molecules, has enabled the development of many powerful chemical tools for the study of biological processes. These tools have the potential to be activated in a cellular setting by irradiation with light of appropriate wavelengths, restoring functionality, with excellent spatial and temporal control.

This D. Phil. dissertation highlights two biologically relevant examples where PCGs can be applied: (i) 4,5-dimethoxynitrobenzyl (DMNB) caged derivatives of GSH (**1**) and ESG (**2**), were synthesised and uncaging of the DMNB group at 350 nm to reveal the free α-carboxylic acid of the glycine residue was demonstrated. These molecules (**Figure 1**) have the potential to probe the binding mode within the KefC KTN binding domain, a ligand-gated K^+ efflux system, critical for bacterial response to electrophilic assault. The molecules are currently with collaborators awaiting further evaluation.



1 **2**

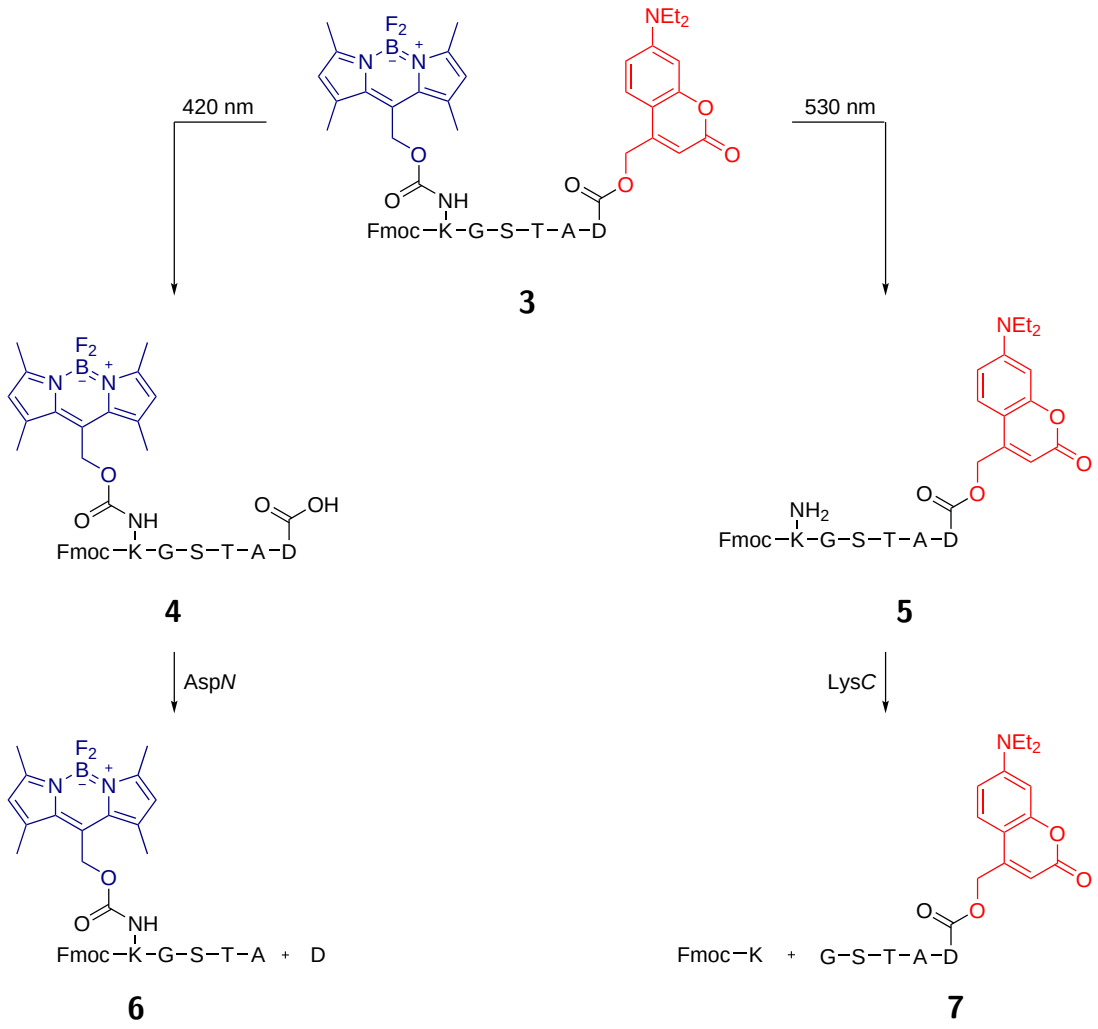
Figure 1: DMNB-caged GSH and ESG to probe the binding mode within the KefC KTN binding domain.

(ii) The wavelength-dependent application of PCGs toward the study of protein post-translational modifications (PTMs) was developed. PTMs modulate protein function and have a ubiquitous role in a diverse range of cellular functions.

A wavelength selective sequential pair of PCGs was developed and demonstrated in a tripeptide (**225**), using the diethylamino coumarin (DEACM), which was cleaved at 420 nm, and the DMNB caging group, which was subsequently cleaved at 350 nm.

A chromatically orthogonal pair of PCGs, with possible applications in both organic synthesis and biological systems, incorporating the BODIPY-based and DEACM caging groups, which could be cleaved at 530 nm and 420 nm, respectively, was also developed.
Photolysis was conducted on a tripeptide (**266**) and hexapeptide (**3**) and an *in vitro* application was demonstrated where when caged, the peptide (**3**) was not susceptible to peptidolysis when incubated with enzymes. Following irradiation at 420 nm, the DEACM group was uncaged and the peptide underwent peptidolysis in the presence of Endoproteinase Asp*N*, whereas following irradiation at 530 nm to uncage the BODIPY group, the peptide underwent peptidolysis in the presence of Endoproteinase Lys*C* (**Scheme 1**). These results not only provide conclusive evidence of the ability of this pair of caging groups to act in a wavelength orthogonal sense but also demonstrates the potential applicability of the pair to biochemical studies.

This pair of PCGs represents the first example of an orthogonal pair of caging groups where both PCGs could be cleaved, at wavelengths longer than 400 nm, in a sequence independent manner.



Scheme 1: Peptidolysis of hexapeptide following irradiation at 420 and 530 nm.

Abbreviations

AA	Amino acid
Ac	Acetyl
Alloc	Allyloxycarbonyl
4AP	4-Aminopyridine
aq.	Aqueous
Asp	Aspartic acid
ATP	Adenosine triphosphate
Bn	Benzoyl
Boc	*tert*-Butyloxycarbonyl
BODIPY	Boron-dipyrromethene
Bpy	2,2'-Bipyridine
$BTMABr_3$	Benzyltrimethylammonium tribromide
Bu	Butyl
CASPT2	Complete active space with second-order perturbation theory
Cbz	Carboxybenzyl
CDNI	4-Carboxymethoxy-5,7-dinitroindoline
Conc.	Concentrated
CS	Charge separation
CTD	C-terminal domain
Cy	Cyclohexyl
Cys	Cysteine
DBU	1,8-Diazabicyclo[5.4.0]undec-7-ene
DCAC	7-(Dicarboxymethyl)-aminocoumarin
Ddz	α,α-Dimethyl-3,5-dimethoxybenzyloxycarbonyl
DEACM	7-Diethylaminocoumarin-4-yl
DEATC	7-Diethylamino-1-thiocoumarin
DFT	Density functional theory
DIPEA	*N*,*N*-Diisopropylethylamine
DMAP	4-(Dimethylamino)pyridine
DMB	3',5'-Dimethoxybenzoin
DMBF	2-Phenyl-5,7-dimethoxybenzofuran
DMF	*N*,*N*-Dimethylformamide
DMFDMA	*N*,*N*-Dimethylformamide dimethyl acetal
DMNB	4,5-Dimethoxy nitrobenzyl
DMP	2, 5-Dimethylphenacyl
DMSO	Dimethyl sulfoxide
EDC	*N*-(3-Dimethylaminopropyl)-*N*'-ethylcarbodiimide hydrochloride

eq.	Equivalents
ESG	*N*-Ethylsuccinimido-*S*-glutathione
Et	Ethyl
FCC	Flash column chromatography
Fmoc	9-Fluorenylmethoxycarbonyl
GABA	γ-aminobutyric acid
Glu	Glutamic acid
Gly	Glycine
GSH	Glutathione
GSX	Glutathione-*S*-conjugates
HATs	Histone acetylases
HBTU	*N*,*N*,*N*',*N*'-tetramethyl-*O*-(1*H*-benzotriazol-1-yl)uronium hexafluorophosphate
HDACs	Histone deacetylases
HKMTs	Histone lysine methyltransferases
HMTs	Histone methyltransferases
HOBt	1-Hydroxybenzotriazole
HOMO	Highest occupied molecular orbital
HPLC	High performance light
HRMS	High resolution mass spectrometry
5-HT	5'-Hydroxytryptophan
Im	Imidazole
IR	Infrared
ISC	Intersystem crossing
Kch	K^+ channels
Kef	K^+ efflux systems
KTN	K^+ transport and nucleotide
Ktr	K^+ uptake systems
KTRT	Kerr-gated resonance Raman spectroscopy
LFP	Laser flash photolysis
LRMS	Low resolution mass spectrometry
LUMO	Lowest unoccupied molecular orbital
Lys	Lysine
MCM	7-Methoxycoumarin-4-ylmethyl
Me	Methyl
MEM	2-Methoxyethoxymethyl
MPH	4-Methoxyphenacyl
Mtt	4-Methyltrityl
MudPIT	Multidimensional protein identification technology
NAD	Nicotinamide adenine dinucleotide
NBS	*N*-Bromosuccinimide
NDBF	1-(3-Nitrobenzofuran-1-yl)ethyl
NIR	Near infrared
NMM	*N*-Methylmorpholine
NPE	1-(2-Nitrophenyl)ethyl

NP-EGTA	Nitrophenyl ethylene glycol-bis(2-aminoethylether)-*N*,*N*,*N*',*N*'-tetraacetic acid
NPEOC	2-(4-Nitrophenyl)ethoxycarbonyl
NPP	2-(*o*-nitrophenyl)propyl
NPPOC	2-(2-Nitrophenyl)propoxycarbonyl
*o*NB	*o*-Nitrobenzyl
*o*NT	*o*-Nitrotoluene
PCG	Photolabile caging group
2PE	Two photon excitation
PeT	Photoinduced electron transfer
Ph	Phenyl
pHA	4-Hydroxyacetophenone
Phe	Phenylalanine
pHP	4-Hydroxyphenacyl
PKs	Protein kinases
PKU	Phenylketonuria
PPG	Photolabile protecting group
PPIs	Protein-protein interactions
PPs	Phosphatases
Pr	Propyl
ps-TR-RR	Picosecond time-resolved resonance Raman
PTM	Post-translational modification
PyBop	(Benzotriazol-1-yloxy)tripyrrolidinophosphonium hexafluorophosphate
RDS	Rate-determining step
RGS	Regulators of G-protein signalling
RP	Reverse phase
RT	Room temperature
Ser	Serine
SOMO	Singly occupied molecular orbital
SPPS	Solid phase peptide synthesis
TBDPS	*tert*-Butyldiphenylsilyl
^{t}Bu	*tert*-Butyl
TFA	Trifluoroacetic acid
TFE	2,2,2-Trifluoroethanol
THF	Tetrahydrofuran
TIPS	Triisopropylsilyl
TLC	Thin layer chromatography
TMS	Trimethylsilyl
TMSOTf	Trimethylsilyl trifluoromethanesulfonate
Trk	K^+ uptake systems
Trt	Triphenylmethyl
TR-TA	Time-resolved transient absorption
Tyr	Tyrosine
Ub	Ubiquitin

UV	Ultraviolet
Vis	Visible

Contents

1 Introduction **1**

1.1 Importance of Photolabile Caging Groups 3
1.2 An "Ideal" Photolabile Caging Group 4
1.3 General Mechanism of Photorelease 6
1.4 Common Photolabile Caging Groups 7
1.4.1 Arylcarbonylmethyl Groups 8
1.4.1.1 Phenacyl and Other Related Arylcarbonylmethyl Groups 9
1.4.1.2 Alkylphenacyl Groups 9
1.4.2 *p*-Hydroxyphenacyl Groups 10
1.4.3 Benzoin Groups 13
1.4.4 Nitroaryl Groups 15
1.4.5 *o*-Nitroanilide Groups 17
1.4.6 Coumarin Groups 18
1.5 Improvements and Recent Advances 20
1.5.1 Substituent Modification 20
1.5.2 Sensitised Release 21
1.5.3 Longer Wavelength PCGs 22
1.5.4 Two Photon Excitation 26
1.6 Biological Applications 27
1.6.1 Caged Small Molecules 27
1.6.1.1 Caged Neurotransmitters 28
1.6.2 Caged Nucleic Acids 29
1.6.3 Caged Peptides and Proteins 30
1.7 Chromatic Orthogonality 32
1.7.1 Design of Chromatically Orthogonal Systems 33
1.7.2 Applications of Chromatic Orthogonality 35
1.8 General Aims & Hypothesis 40

2 Caged Kef Ligands for the Study of Kef Ion Channels 42
2.1 Introduction . . . 42
2.2 Project Aims . . . 47
2.3 Synthesis of DMNB-Caged GSH and ESG . . . 47
2.4 Photolysis Studies . . . 51
2.5 Summary and Future Work . . . 59

3 Caged Amino Acids Towards the Development of Photoactive Tools for the Analysis of Protein Post-Translational Modification 60
3.1 Introduction . . . 60
3.1.1 Acetylation . . . 61
3.1.2 Carbonylation . . . 62
3.1.3 Glycosylation & Glycation . . . 62
3.1.4 Hydroxylation . . . 63
3.1.5 Methylation . . . 63
3.1.6 Nitration . . . 64
3.1.7 Palmitoylation . . . 64
3.1.8 Phosphorylation . . . 65
3.1.9 Sulfation . . . 65
3.1.10 Ubiquitination . . . 66
3.2 Current Methods of Studying PTMs . . . 66
3.3 Y-Box Binding Protein 1 . . . 67
3.4 Project Aims . . . 68
3.4.1 Prospective Caging Groups . . . 69
3.5 Synthesis of Photolabile Caged Amino Acids . . . 71
3.5.1 The Phenacyl-Based Caging Group . . . 71
3.5.2 The DMNB Caging Group . . . 73
3.5.3 The DEACM Caging Group . . . 74
3.6 Synthesis of Protected Amino Acids - Boc & *tert*-Butyl Strategy . . . 75
3.7 Synthesis of Caged Amino Acids - Boc & *tert*-Butyl Strategy . . . 75
3.7.1 Phenacyl-Based Caged Amino Acids - Boc & *tert*-Butyl Strategy 76
3.7.2 DMNB-Caged Amino Acids – Boc & *tert*-Butyl Strategy . . . 81
3.7.3 DEACM-Caged Amino Acids – Boc & *tert*-Butyl Strategy . . 81
3.8 Summary & Conclusions – Boc & *tert*-Butyl Strategy . . . 83
3.9 Synthesis of Protected Amino Acid – Fmoc and tert-Butyl Strategy . 84
3.10 Synthesis of Caged Amino Acids – Fmoc and *tert*-Butyl Strategy . . . 86

3.10.1 Phenacyl-Based Caged Amino Acids – Fmoc & *tert*-Butyl Strategy 86
3.10.2 DMNB-Caged Amino Acids – Fmoc & *tert*-Butyl Strategy . . 92
3.10.3 DEACM Caged Amino Acids – Fmoc & *tert*-Butyl Strategy . 94
3.11 Photolysis of Photolabile-Caged Amino Acids 98
3.11.1 Irradiation Control Reactions 100
3.11.2 Irradiation of MPH-Caged Amino Acids 103
3.11.3 Irradiation of DMNB-Caged Amino Acids 106
3.11.4 Irradiation of DEACM-Caged Amino Acids 108
3.11.5 Development of a Sequential System 111
3.12 Sequential Light-Activated Caged Tripeptide 114
3.12.1 Synthesis of DEACM- and DMNB-Caged Tripeptide 114
3.13 Photolysis of the Sequentially-Caged Tripeptide 116
3.14 Summary & Conclusions 121

4 Red Shifted Caging Groups Towards the Development of Photoactive Tools for the Analysis of Protein Post-Translational Modification 122
4.1 Inorganic Ruthenium Polypyridyl Caging Group 123
4.1.1 Towards the Synthesis of Ru(bpy) Caged Amino Acids 123
4.2 Diethylamino-Thiocoumarin (DEATC) Caging Group 125
4.2.1 Synthesis, Photolysis and Evaluation of DEATC-Caged Amino Acids 125
4.3 BODIPY Dyes as Caging Groups 130
4.3.1 Synthesis, Photolysis and Evaluation of BODIPY Dyes as Caging groups for Amino Acids 130
4.4 Chromatically Orthogonal Light-Activated Tripeptide 151
4.4.1 Synthesis of Tripeptide 151
4.4.2 Photolysis of the Wavelength-Orthogonally Caged Tripeptide . 153
4.5 Summary and Future Work 157

5 Optimisation of Photolysis Studies & Application to Peptides 158
5.1 Introduction and Aims 158
5.2 Photolysis of Caged Amino Acids 159
5.3 Synthesis of Caged Peptides 163
5.4 Photolysis of Caged Peptides 166
5.4.1 Photolysis of Caged Tripeptide 166
5.4.2 Photolysis of Caged Hexapeptides 172

5.5 Biochemical Studies on Caged Peptides . . . 178
5.6 Summary and Future Work . . . 180

6 Conclusions & Future Work **181**
6.1 Caged Kef Ligands as Tools to Probe Binding within the KefC KTN Domain . . . 181
6.2 Caged Amino Acids & Peptides Towards the Development of Photoactive Tools to Probe Protein PTMs . . . 183

7 Experimental **189**
7.1 General Experimental . . . 189
7.2 Photolysis Experiments . . . 193
7.2.1 Experimental Setup . . . 193
7.2.2 Analysis of Photolysis Results . . . 197
7.2.3 Determination of Calibration Curves by HPLC . . . 198
7.2.4 Photolysis Data as Measured by HPLC . . . 199
7.2.5 Determination of Calibration Curves by LCMS . . . 200
7.2.6 Photolysis Data as Measured by LCMS . . . 201
7.3 Quantum Yield of Uncaging . . . 202
7.3.0.1 Ferrioxalate Actinometry Protocol . . . 202
7.3.0.2 Photon Flux Measurements . . . 204
7.3.0.3 Quantum Yield Measurements . . . 205
7.4 Enzyme Catalysed Proteolysis . . . 206
7.4.1 Preparation of Buffer Solutions . . . 206
7.4.1.1 250 mM Sodium Phosphate Buffer, pH 8.0 . . . 206
7.4.1.2 500 mM Ammonium Bicarbonate Buffer, pH 8.0 . . . 206
7.4.2 Enzyme Catalysed Digestion Protocol . . . 206
7.4.2.1 Asp-*N* . . . 206
7.4.2.2 Lys-*C* . . . 207
7.5 DMNB Caged GSH and ESG . . . 208
7.6 Amino Acids Residues . . . 225
7.7 DEACM Caged Amino Acids . . . 252
7.8 DMNB Caged Amino Acids . . . 275
7.9 Phenacyl Caged Amino Acids . . . 285
7.10 Red-Shifted Caging Groups . . . 314
7.10.1 Ruthenium Bipyridyl Caging Group . . . 314
7.10.2 DEATC Caged Amino Acids . . . 318

7.10.3 BODIPY Caged Amino Acids 326
7.11 Caged Peptides - Solution Phase Synthesis 355
7.12 Caged Peptides - Solid Phase Peptide Synthesis 369
7.12.1 Linking Amino Acid to Resin 369
7.12.2 Addition of Amino Acid to Peptide Chain 369
7.12.3 Cleavage of Peptide from CTR Resin 369
7.12.4 Experimental Data 370
7.12.4.1 Tripeptides 370
7.12.4.2 Hexapeptides 370

A NMR Spectra **372**
A.1 DMNB Caged GSH and ESG 373
A.2 Amino Acid Residues 383
A.3 DEACM Caged Amino Acids 398
A.4 DMNB Caged Amino Acids 410
A.5 Phenacyl Caged Amino Acids 415
A.6 Red-Shifted Caging Groups 435
A.6.1 Ruthenenium Bipyridyl Caging Group 435
A.6.2 DEATC Caged Amino Acids 438
A.6.3 BODIPY Caged Amino Acids 442
A.7 Caged Peptides 469

B Photolysis Experiments **476**
B.1 Determination of Calibration Curves by HPLC 477
B.1.1 Calibration of Fmoc-Asp-O^{t}Bu (**221**) 477
B.1.2 Calibration of Fmoc-Ser-O^{t}Bu (**185**) 478
B.1.3 Calibration of Fmoc-Asp(DEACM)-O^{t}Bu (**215**) 479
B.1.4 Calibration of Fmoc-Ser(DEACM)-O^{t}Bu (**217**) 480
B.1.5 Calibration of Fmoc-Asp(DMNB)-O^{t}Bu (**212**) 481
B.1.6 Calibration of Fmoc-Ser(DMNB)-O^{t}Bu (**213**) 482
B.1.7 Calibration of Fmoc-Asp(MPH)-O^{t}Bu (**209**) 483
B.1.8 Calibration of Fmoc-Asp(DEATC)-O^{t}Bu (**232**) 484
B.1.9 Calibration of Fmoc-Asp(BODIPY-2)-O^{t}Bu (**251**) 485
B.2 Photolysis Data as Measured by HPLC 486
B.2.1 Irradiation at $\lambda = 310$ nm 486
B.2.2 Irradiation at $\lambda = 350$ nm 491
B.2.3 Irradiation at $\lambda = 365$ nm 497

B.2.4 Irradiation at $\lambda = 420$ nm . . . 501
B.2.5 Irradiation at $\lambda = 520$ nm . . . 508
B.2.6 Irradiation of a Sequential System . . . 510
B.2.7 Irradiation of an Orthogonal System . . . 515
B.3 Determination of Calibration Curves by LCMS . . . 520
B.3.1 Calibration of Fmoc-Asp-O^{t}Bu (**221**) . . . 520
B.3.2 Calibration of Fmoc-Asp(DEACM)-O^{t}Bu (**215**) . . . 521
B.3.3 Calibration of Fmoc-Asp(BODIPY-2)-O^{t}Bu (**251**) . . . 522
B.3.4 Calibration of KLD (**269**) . . . 523
B.3.5 Calibration of KLD-DEACM (**267**) . . . 524
B.3.6 Calibration of BODIPY-KLD (**268**) . . . 525
B.3.7 Calibration of BODIPY-KLD-DEACM (**266**) . . . 526
B.3.8 Calibration of KGSTAD (**270**) . . . 527
B.3.9 Calibration of KGSTAD-DEACM (**5**) . . . 528
B.3.10 Calibration of BODIPY-KGSTAD (**4**) . . . 529
B.3.11 Calibration of BODIPY-KGSTAD-DEACM (**3**) . . . 530
B.4 Photolysis Data as Measured by LCMS . . . 531
B.4.1 Irradiation at $\lambda = 420$ nm . . . 531
B.4.2 Irradiation at $\lambda = 530$ nm . . . 540

C Photolysis LCMS-UV Curves **548**
C.1 Monomers . . . 549
C.1.1 420 nm Irradiation of Fmoc-Asp(DEACM)-O^{t}Bu (**215**) . . . 549
C.1.2 420 nm Irradiation of Fmoc-Asp(BODIPY)-O^{t}Bu (**251**) . . . 550
C.1.3 530 nm Irradiation of Fmoc-Asp(DEACM)-O^{t}Bu (**215**) . . . 551
C.1.4 530 nm Irradiation of Fmoc-Asp(BODIPY)-O^{t}Bu (**251**) . . . 552
C.2 Trimers . . . 553
C.2.1 420 nm Irradiation of KLD-DEACM (**267**) . . . 553
C.2.2 420 nm Irradiation of BODIPY-KLD (**268**) . . . 554
C.2.3 420 nm Irradiation of BODIPY-KLD-DEACM (**266**) . . . 555
C.2.4 530 nm Irradiation of KLD-DEACM (**267**) . . . 556
C.2.5 530 nm Irradiation of BODIPY-KLD (**268**) . . . 557
C.2.6 530 nm Irradiation of BODIPY-KLD-DEACM (**266**) . . . 558
C.3 Hexamers . . . 559
C.3.1 420 nm Irradiation of KGSTAD-DEACM (**5**) . . . 559
C.3.2 420 nm Irradiation of BODIPY-KGSTAD (**4**) . . . 560

C.3.3 420 nm Irradiation of BODIPY-KGSTAD-DEACM (**3**) 561
C.3.4 530 nm Irradiation of KGSTAD-DEACM (**5**) 562
C.3.5 530 nm Irradiation of BODIPY-KGSTAD (**4**) 563
C.3.6 530 nm Irradiation of BODIPY-KGSTAD-DEACM (**3**) 564

D Enzyme Proteolysis Mass Spectrometry Data **565**
D.1 Fmoc-KGSTAD (**270**) 566
D.2 Fmoc-KGSTAD-DEACM (**5**) 566
D.3 BODIPY-K(Fmoc)GSTAD (**4**) 567
D.4 BODIPY-K(Fmoc)GSTAD-DEACM (**3**) 567
D.5 BODIPY-K(Fmoc)GSTAD-DEACM (**3**) following irradiation at 420 nm 568
D.6 BODIPY-K(Fmoc)GSTAD-DEACM (**3**) following irradiation at 530 nm 568

References **569**

Chapter 1

Introduction

The development and advancement of novel therapeutics presents one of the biggest scientific challenges of our present day.[1] Much progress in this field has been attributed to a deeper molecular-level understanding.[2] In 2015, approximately USD 58.8 billion was spent by PhRMA members on R&D toward this end,[2] and eight of ten Chemistry Nobel Prizes in the last decade were awarded for the advancement of the study of complex and highly dynamic biological processes.[3] Despite these recent advances, there still exists great difficulty in achieving the spatial and temporal control required to study these multifarious systems and control the many convoluted, simultaneously occurring processes, while only perturbing the system in the desired manner.

Light offers a unique opportunity to overcome a number of these challenges through its ability to act as an external trigger that can be manipulated precisely. The accompanying spatio-temporal control imparted through the use of light over area, time, and dosage[4] has led to development of four main classes of photoresponsive molecules:
(i) Photosensitised reactions involve the photocontrolled excitation of a sensitiser that provides the energy to trigger downstream processes, such as inducing targeted cell death in photodynamic therapy.[6] Upon irradiation, the photosensitiser is excited to a short lived singlet excited state ($^1PS_1*$) which can proceed, *via* intersystem crossing (ISC), to the longer lived triplet state ($^3PS_1*$). The triplet state species can undergo electronic decay to return to the ground state or transfer charge (Type I) or energy (Type II) to a substrate or molecular oxygen to generate reactive oxygen species (**Figure 1.1**).[5]

(ii) Photoswitches make use of photoisomerisation for reversible regulation. This type of photoinduced control was demonstrated by the inclusion of an azobenzene moiety

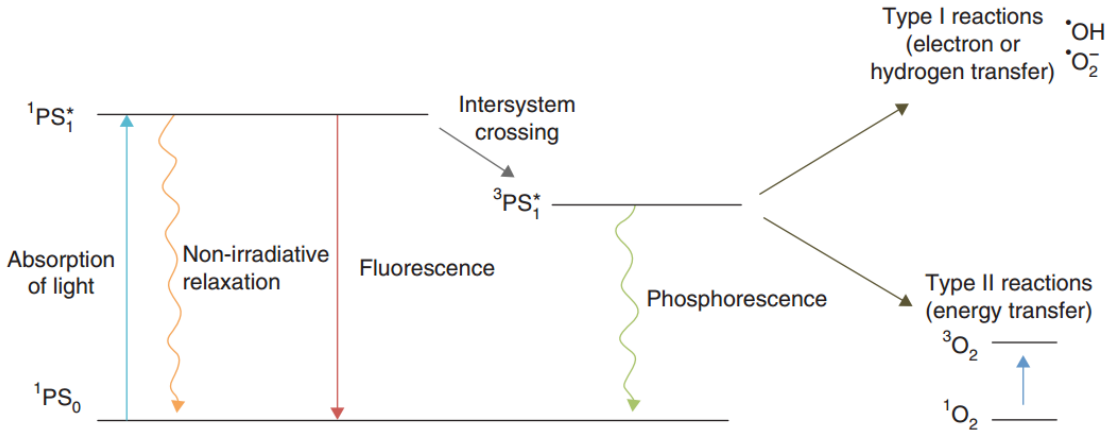
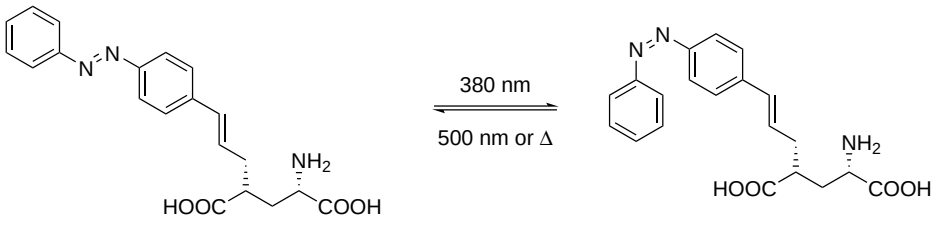


Figure 1.1: Jablonski diagram detailing photosensitisation pathways.[5]

in the development of a photochromic agonist of ionotropic glutamate receptors.[7] Whole cell voltage clamp recordings showed that the *cis*-form (**9**) of the compound was able to trigger a depolarising action potential, whilst in the *trans*-form (**8**), the action potential was extinguished (**Scheme 1.1**).[7]



8 **9**

Scheme 1.1: Photoinduced *cis-trans* isomerisation of azobenzene photochromic moiety.[7]

(iii) Photolabile caging groups (PCGs), synonymous with photolabile protecting groups (PPGs), are phototriggers which render a molecule temporarily inactive when covalently bonded to the functionally active part of the molecule (**Figure 1.2**). Photochemically induced bond cleavage restores the functionality and has enabled widespread application of PCGs in biomedical fields.[8]

(iv) Optogenetics combines the use of light and genetically encoded photosensitive actuator proteins used to render targets, particularly neurons, responsive to light.[9]

All four classes have found important biological and chemical applications. However, previous experience with PCGs and their potential for a wide array of applications, led to a focus of this study on their development and possible biological uses.

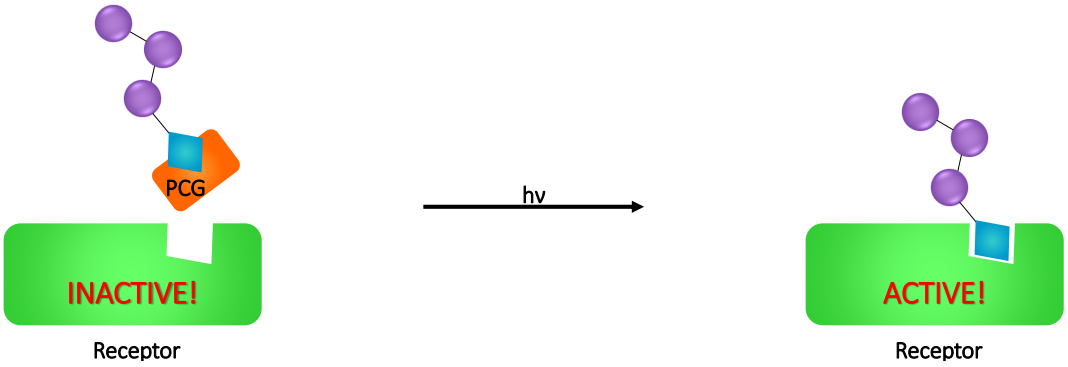


Figure 1.2: Photolysis of PCG to reveal active biomolecule.

1.1 Importance of Photolabile Caging Groups

Synthesis of caged species are usually straightforward, and diverse strategies have been developed for the effective caging of different functional groups. Photolysis of the temporarily inactive caged species, to reveal the active molecule, requires no reagents, only light, and is often rapid, allowing uncaging to be conducted with respect to activity.[8]

In 1962, Barltrop and Schofield published the first known report of PCGs when the pair observed that upon exposure to UV irradiation, benzyloxycarbonylglycine appeared to liberate free glycine.[10] Several months later, Barton and co-workers discussed the photolysis of 2,4-dinitrophenylthio-derivatives of carboxylic acids and a variety of β-naphthyl esters as photosensitive protecting groups for phenols.[11, 12] Engels and Schlaeger first demonstrated the biological applicability of PCGs when they employed the *o*-nitrobenzyl ester as a photosensitive protecting group for adenosine cyclic 3',5'-phosphate (cAMP). An increase in stimulation of protein kinase, to nearly the same level as with endogenous cAMP, was observed due to the release of cAMP following irradiation at 366 nm.[13]

In 1978, Hoffman *et. al.* adopted the term "caging" somewhat misleadingly to describe this phenomenon when the group published their work on "caged" ATP.[14] "Caging" is a problematic misnomer for several reasons; it brings to mind molecules caged in the topological sense e.g. inside a C60 molecule, or the "cage effect" observed in the recombination of radicals. As such, some authors have opted to use the term "light-activated" or alternatives along those lines.

Since their advent, PCGs have found their way into an array of applications in biochemistry, bio-technology and cell biology, including and not limited to, bioimaging, photoregulation of gene expression, photomodulation of protein splicing, photorelease of drugs, analysis of neurological processes and cellular signalling processes.[6]

1.2 An "Ideal" Photolabile Caging Group

The design specifications for effective PCGs are heavily dependent upon the intended applications. In general, good PCGs will fulfil most or all of the following criteria:
(i) Light must be absorbed by the caged molecules to trigger photochemical cleavage. It thus follows that the greater the proportion of molecules absorbing the light, the more substrate will be released.
Two laws relate extinction coefficient(ε) to measurements of absorption (A):[15]

(a) The Lambert law states that the proportion of light absorbed (I_{A}) is independent of initial intensity (I_0)

(b) The Beer law states that transmitted light intensity (I_{T}) is proportional to the concentration (c) of absorbing molecules
Hence the absorbance (A) of a solution is given by (**Equation 1.1**):

$$A = log\frac{I_0}{I_{\mathrm{T}}} \tag{1.1}$$

and ε is given by (**Equation 1.2**):

$$log\frac{I_0}{I_{\mathrm{T}}} = \varepsilon cl \tag{1.2}$$

where (l) is the optical pathlength:
This reduces to the Beer-Lambert law (**Equation 1.3**) which determines absorbance (A) of a caged molecule in solution by:

$$A = \varepsilon cl \tag{1.3}$$

The larger the ε, the more likely a photon will be absorbed. Thus for efficient photolysis, ε should be high at wavelengths triggering the photochemical reactions.
However, it should be noted that the magnitude of ε can also become limiting; a high ε can lead to poor and uneven photolysis in thick preparations because the molecules at the front surface may absorb much of the light before it reaches the centre.[15]

(ii) Quantum yield can be defined as the ratio of the amount of substrate released to

the amount of photons absorbed by the caged compound at the irradiation wavelength (**Equation 1.4**). The greater the propensity for photocleavage to release the substrate upon absorption of a photon, the greater the quantum yield and hence the greater the efficacy. This is particularly important where time-resolved work is being undertaking or the system under investigation displays rapid kinetics.[8]

$$\phi = \frac{\eta_{rel}}{\eta_p} \tag{1.4}$$

(iii) Clean photoreaction with high efficacy. The product of quantum yield (ϕ) and molar decadic absorption coefficient (ε) for a given wavelength (λ) of irradiation is a means of determining the efficacy of a PCG, as it is proportional to the amount of release at the given excitation wavelength (**Equation 1.5**).[8] This is an important parameter of caged compounds and may constrain feasible applications. High efficacy can thus result from high ϕ or large ε at the excitation wavelength.[15]

$$Efficacy = \phi\varepsilon \tag{1.5}$$

(iv) Where biological samples are concerned, a high ε at $\lambda > 300$ nm is ideal. The use of longer wavelengths reduces the likelihood that irradiation will be absorbed by and hence damage the biological environment; penetration in biological tissues increases at longer wavelengths making it more likely that light reaches the sample.[8]

(v) The by-products of the photolysis reaction should be transparent at the wavelength of irradiation to avoid competitive absorption with the caged compound. Practical considerations usually call for optical densities of caged compounds in cells to be less than 20%, to minimise the effects of inhomogeneous uncaging resulting from inner filtering effects during rapid photolysis.[15] Biocompatibility is essential as the by-products must not interfere with the system under investigation.

(vi) Where time-resolved work is being conducted and where the study of the kinetics of rapid responses is being undertaken, the rate (k_{app}) of uncaging to release the desired active biomolecule must exceed that of the response under investigation.

(vii) Caged compounds may be required to pass through biological barriers, commonly cell membranes. They are thus required to be soluble in the targeted media, often water.

(viii) Successful detection, particularly in systems requiring a great degree of sensitivity,

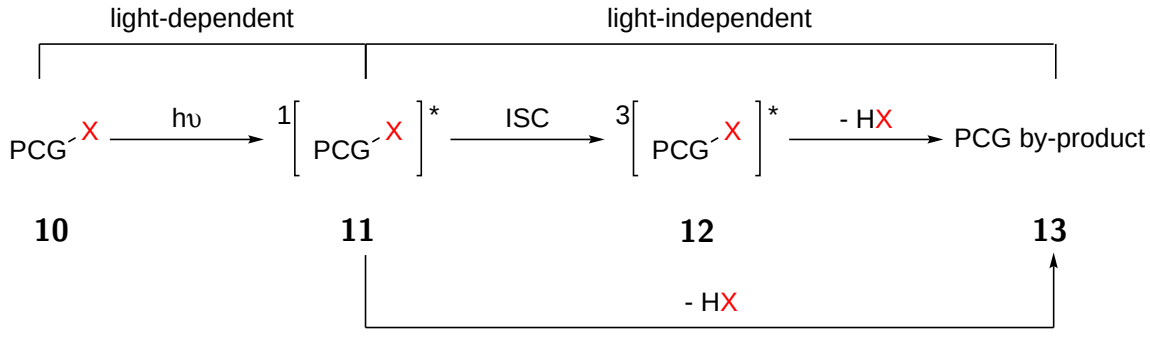
of the response under investigation, requires a large $\phi\varepsilon$ and minimal background activity prior to irradiation. Background activity might arise from contamination of the sample e.g. by deprotected material. Therefore, it is imperative that the PCGs and their caged analogues are analytically pure, have low intrinsic activity and are stable in the media prior to and during irradiation.[16]

1.3 General Mechanism of Photorelease

A comprehensive understanding of photorelease reaction mechanisms and their associated rate-determining steps (RDSs) is important for analysis when using PCGs, for example to study biological response times. This detailed knowledge may also serve the purpose of enabling designed improvements of PCGs by structural variation.

Most photoreactions proceed *via* a cascade of reaction steps, involving ground state (GS) and excited state (ES) intermediates. Following initial excitation by light to form the ES intermediates, release of the substrate often occurs by heterolytic elimination, or requires proton transfer. These light independent reactions may occur with considerable delay following initial irradiation becoming rate-limiting. This could present limitations with applications of PCGs as time taken for photorelease could exceed the biological process under investigation. Consequently, rates and efficiencies of substrate release may be heavily dependent upon solvent, pH, and buffer concentration.[8]

Following irradiation, several means of photorelease can be identified:[16]
(i) Direct elimination of the substrate from a reactive singlet (**11**) or triplet excited state (**12**) (**Scheme 1.2**).

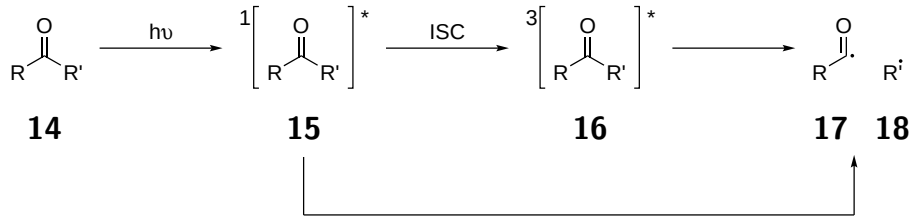


Scheme 1.2: Photorelease by direct elimination from reactive singlet or triplet excited states.

(ii) Release of the substrate following light-induced formation of reactive ground-state intermediates with a strong driving force and low energy barrier to elimination.

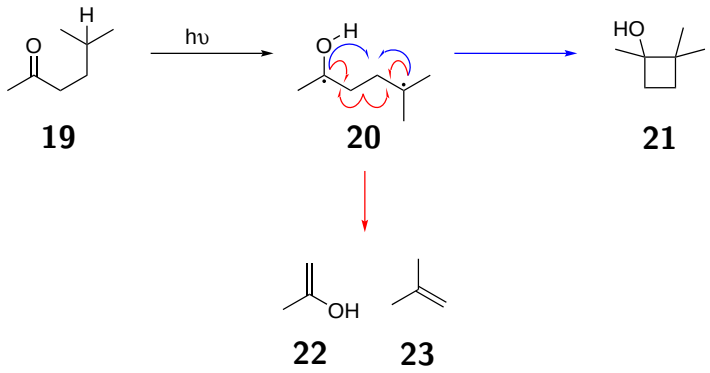
(iii) Use of carbonic or carbamic acids, which undergo decarboxylation, to increase the thermodynamic driving force for poor leaving groups, such as alcohols and amines. It is, however, possible for decarboxylation to become the rate limiting step.[16]

For carbonyl compounds, Norrish *et al.* observed two processes:[17]
(i) Norrish type I reaction (**Scheme 1.3**) - following excitation of the carbonyl compound (**14**) by absorption of a photon, homolysis of the (C=O)-R' bond may result, frequently followed by decarbonylation of the carbonyl radical (**17**).



Scheme 1.3: Norrish type I reaction.

(ii) Norrish type II reaction (**Scheme 1.4**) - hydrogen abstraction from the γ-position, following excitation, to form a highly reactive diradical species (**20**).



Scheme 1.4: Norrish type II reaction.

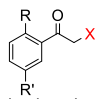
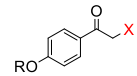
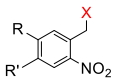
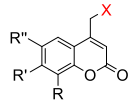
It is worthwhile to note that often a combination of these processes can occur, following excitation of the PCG chromophore, leading to release of the desired substrate.

1.4 Common Photolabile Caging Groups

Extensive research into the development of novel PCGs has been undertaken by numerous groups. The common classes of PCGs are shown below (**Table 1.1**).

Consequently this introduction focusses on those classes of PCGs that are most relevant to this work.

Table 1.1: Common classes of photolabile caging groups.

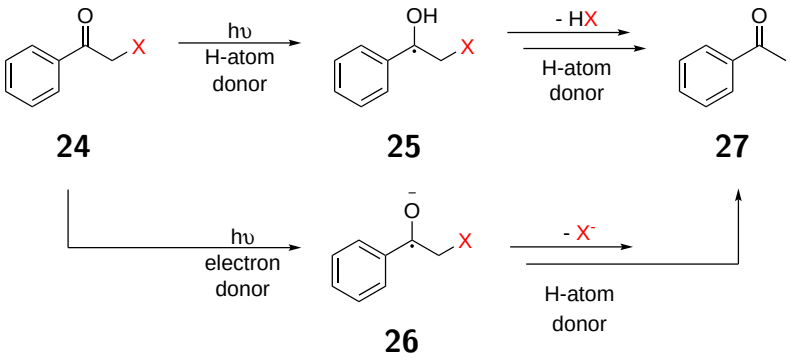
Entry	Reference	PCG Class	λ_{max} (nm)	Notable Examples
1	1.4.1	 Arylcarbonylmethyl	267	**Phenacyl**: R, R' = H **2-Methylphenacyl**: R = H, R' = Me **2,5-Dimethylphenacyl**: R, R' = Me
2	1.4.2	 *p*-Substitutedphenacyl	268	**4-Hydroxyphenacyl**: R = H **4-Methoxyphenacyl**: R = Me
3	1.4.3	 Benzoin	247	**Benzoin**: R, R' = H **Dimethoxybenzoin**: R, R' = OMe
4	1.4.4	 Nitroaryl	346	***o*-Nitrobenzyl**: R, R' = H **4,5-Dimethoxynitrobenzyl**: R, R' = OMe
5	1.4.5	 *o*-Nitroanilides	363	**5-Bromo-7-Nitroindoline**: R = Br **5-Nitro-7-Nitroindoline**: R = NO_2
6	1.4.6	 Coumarin	385	**(Coumarin-4-yl)methyl**: R, R', R'' = H **(7-Hydroxycoumarin-4-yl)methyl**: R, R'' = H; R' = OH **(7-Methoxycoumarin-4-yl)methyl**: R, R'' = H; R' = OMe **[7-(Diethylamino)coumarin-4-yl]methyl**: R, R'' = H; R' = NMe_2 **(6-methoxycoumarin-4-yl)methyl**: R, R' = H; R'' = Me **[6,7-dimethoxy(coumarin-4-yl)]methyl**: R = H; R', R'' = OMe

1.4.1 Arylcarbonylmethyl Groups

The carbonyl group of aromatic ketones lies at the centre of the photochemical reactivity; ketones bearing n-π^* lowest triplets, with a half vacant n-orbital localised on the carbonyl oxygen are more reactive than ketones with π-π^* lowest triplets, in which spins delocalise onto the aromatic ring.[18] They are thermally stable and synthetically readily available. Sensitivity to solvent polarity and substitutions on the phenyl ring are characteristic of the electronic transitions of aromatic ketones. Protic solvents stabilise the oxygen non-bonding orbital, through hydrogen bonding to the carbonyl oxygen, giving rise to a hypsochromic shift of the n-π^* absorption band to shorter wavelengths while both electron-donating groups and polar solvents tend to stabilise the π-π^* states.[19]

1.4.1.1 Phenacyl and Other Related Arylcarbonylmethyl Groups

α-Substituted esters of the phenyl chromophore are typical of the PCG framework for release of carboxylic acids.[20] The mechanism of photorelease, involving hydrogen abstraction from a hydrogen-atom donor by the singlet or triplet n-π^* states of the excited carbonyl group of the phenacyl ester, *via* a ketyl ester intermediate (**25**), was established using laser flash photolysis (LFP) (**Scheme 1.5**).[21] The presence of an electron donor allows for a mechanism involving electron transfer to the carbonyl group, resulting in reduction in energy of both n-π^* and π-π^* states, prior to release of the leaving group.



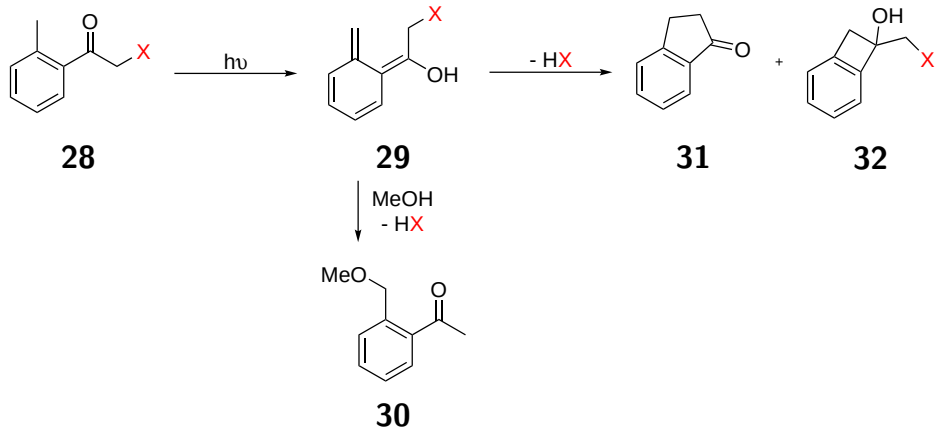
Scheme 1.5: General photorelease mechanism of phenacyl-type PCGs.

1.4.1.2 Alkylphenacyl Groups

Klán and co-workers demonstrated the ability of the 2-methylphenacyl moiety[22] (**28**) and later the 2,5-dimethylphenacyl (DMP) (**33**), to act as PCGs for carboxylic acids,[23] phosphate, sulfonates,[24] alcohols[25] and amines[26] as carbonates and carbamates respectively. One drawback is the requirement for a good leaving group for effective release within the photoenol lifetime.

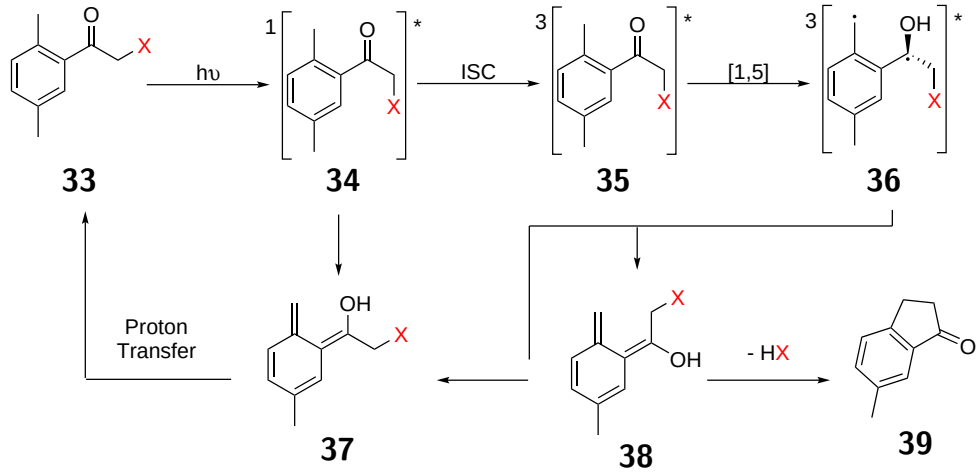
Leaving groups on the α-carbon of 2-alkylphenacyl derivatives (**28**) are released from the photoenol intermediates (**29**). In general, indanone (**31**) and benzocyclobutenol (**32**) side products are formed in non-nucleophilic solvents, whereas acetophenone derivatives, substituted on the 2-methyl group (**30**), are produced in the presence of a nucleophile such as methanol (**Scheme 1.6**).[24]

The mechanism of photorelease by DMP esters (**33**) was elucidated by LFP in degassed methanol. A short-lived intermediate, and two longer-lived ones, attributed to the triplet 1,4-biradical (**36**) and the Z- (**37**) and E-photoenols (**38**) respectively, were



Scheme 1.6: General photorelease mechanism of alkylphenacyl-type PCGs.

formed. However, only the longer-lived E-photoenol (**38**) resulted in release of benzoic acid *via* a triplet pathway (**Scheme 1.7**).

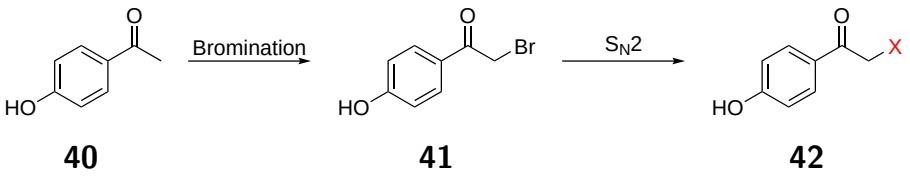


Scheme 1.7: General photorelease mechanism of dialkylphenacyl-type PCGs.

1.4.2 *p*-Hydroxyphenacyl Groups

The 4-hydroxyphenacyl (pHP) group (**42**) pioneered by Park and Givens,[27],[28] has found widespread applications in neurobiology, enzyme catalysis and synthetic organic chemistry.[8] This PCG has emerged as a promising candidate owing to its relative hydrophilicity, the high photolysis quantum yield and the unusually clean photoreaction.

Most leaving groups have been introduced by means of bromination of pHA (**40**) and subsequent S_N2 displacement with the conjugate base of the leaving group under



Scheme 1.8: General synthesis towards pHP-caged compounds.[8]

basic conditions (**Scheme 1.8**). Occasionally, for more complex reactions, protection of the phenol group is required, which is commonly achieved through benzylation, silylation or acetylation.[8] Of the rapidly growing number of leaving groups that can be accommodated, sulfonates, phosphates and carboxylates proved to be most easily uncaged, and thus most commonly encountered.

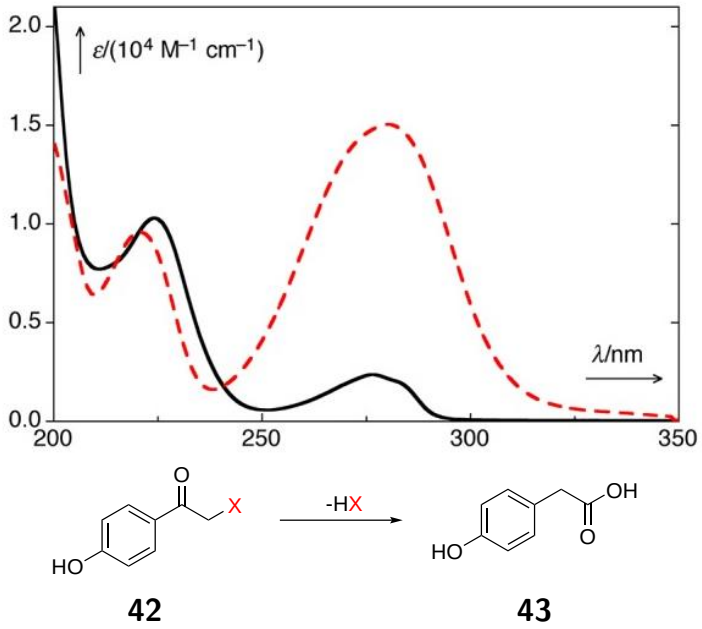
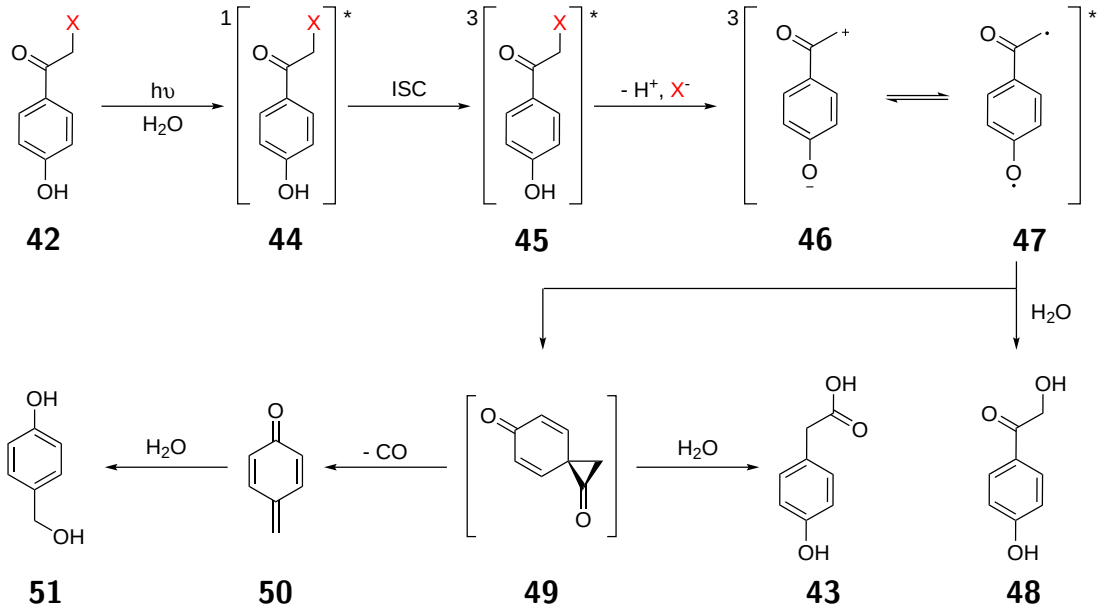


Figure 1.3: UV/Vis absorption spectra of (**42**), where X = $OPO(OEt)_2$ (red) and (**43**) (black).[29]

A dramatic change is observed in the absorption spectrum over the course of the photolysis reaction as it progresses from a conjugated phenyl ketone (**42**) to the non-conjugated 4-hydroxyphenyl acetate (**43**). The transformation is thought to proceed *via* a photo-Favorskii rearrangement (**Figure 1.3**).[29]

Philips *et al.* used a combination of techniques including time-resolved transient absorption and Kerr-gated resonance Raman spectroscopy (KTRF) to assign electronic configurations to the key excited states and confirmed the reactive species to be the

triplet state (**45**).[30] Picosecond time-resolved resonance Raman spectroscopy (ps-TR-RR) scans taken in the first few ps showed only diffuse, weak absorption signals belonging to the excited singlet (**44**) and triplet states (**45**) of the pHP-caged compound (**42**). Four new bands emerged at 300 ps, becoming prominent at 0.7 - 1.0 ns and by 6 ns, were the only bands remaining; the four peaks corresponded precisely to those obtained with an authentic sample of 4-hydroxyphenylacetic acid (**43**).[30]



Scheme 1.9: General mechanism of pHP PCG photolysis, based on time-resolved transient absorption analysis.[31]

Time-resolved transient absorption (TR-TA) studies revealed two additional reactive intermediates. An early, extremely short-lived transient species, appearing on the tail of the triplet decay, was attributed to the triplet biradical (**47**), assumed to form adiabatically by extrusion from the excited triplet-state pHP-caged analogue (**45**), with concerted departure of the leaving group and a proton in the ground state, conforming to the Wigner spin rule. Following ISC, the triplet biradical (**47**) was converted to the spirodienedione (**49**), which very rapidly hydrolysed to 4-hydroxyphenylacetic acid (**43**). The latter longer-lived species was identified as the *p*-quinone methide (**50**) which was hydrolysed to form 4-hydroxybenzyl alcohol (**51**) (**Scheme 1.9**).[31] Validation for the existence of the spirodienedione intermediate (**49**) was based on the requirement for the carbon skeleton organisation and a very facile CO extrusion owing to the strained nature of the bicyclic structure and complemented by DFT calculations.

Corrie *et al.* provided further supporting evidence for the photorelease mechanism by examining the photolysis products from a series of pHP-substituted acetate esters; the acetates had been specifically chosen for their increasing propensity towards decarboxylation *via* photoinduced homolysis of the corresponding arylmethyl esters to form carboxy radicals. However, they were only able to detect carboxylic acids in excess of 90% yields, providing further proof of a heterolytic pathway.[32]

The quantum yields of photolysis were found to monotonically decrease with increasing pK_a of the leaving group, suggesting a Brønsted leaving group relationship. The best leaving groups were conjugate bases of moderate to strong acids, including sulfates, phosphates, thiophosphates, carboxylates, phenolates and thiolates.[8]

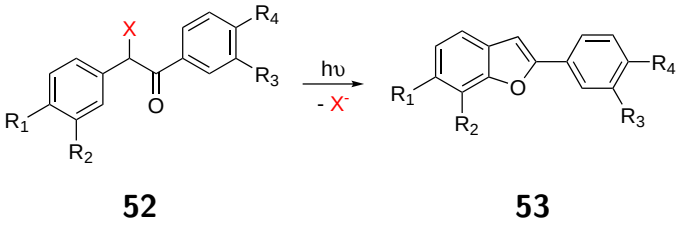
To build upon the versatility of the pHP family of PCGs (**42**), substituent modifications were employed at the 2- and 3-positions to shift the absorption to longer wavelengths and alter the solubility properties. 3-Electron donors were generally found to display lowered quantum yields relative to the parent PCG (**42**), whereas electron withdrawing groups gave rise to slight increases in quantum yields.

Introduction of the 4-OH modification to the parent phenacyl chromophore (**24**), resulted in a profound alteration to the photochemical behaviour from a photoreduction mechanism of unsubstituted phenacyl to the photo-Favorskii rearrangement of the pHP group (**42**). Modifications involving electron donors such as 4-methoxy and 2-methoxyphenacyl have been attempted, however, here the photoreduction and photo-Favorskii rearrangement pathways are in competition, resulting in mixtures of the corresponding methoxyacetophenones and phenyl acetates.[33] Yet other groups such as the 3-nitro, 3-OH and 3-acetyl resulted in complete quenching of the photo-Favorskii rearrangement reaction when present as substituents on the parent chromophore.[34]

1.4.3 Benzoin Groups

In 1964, Sheehan *et. al.* demonstrated that upon irradiation, benzoin-caged compounds (**52**) cyclised to give 2-substituted benzofuran (**53**) (**Scheme 1.10**).[35]

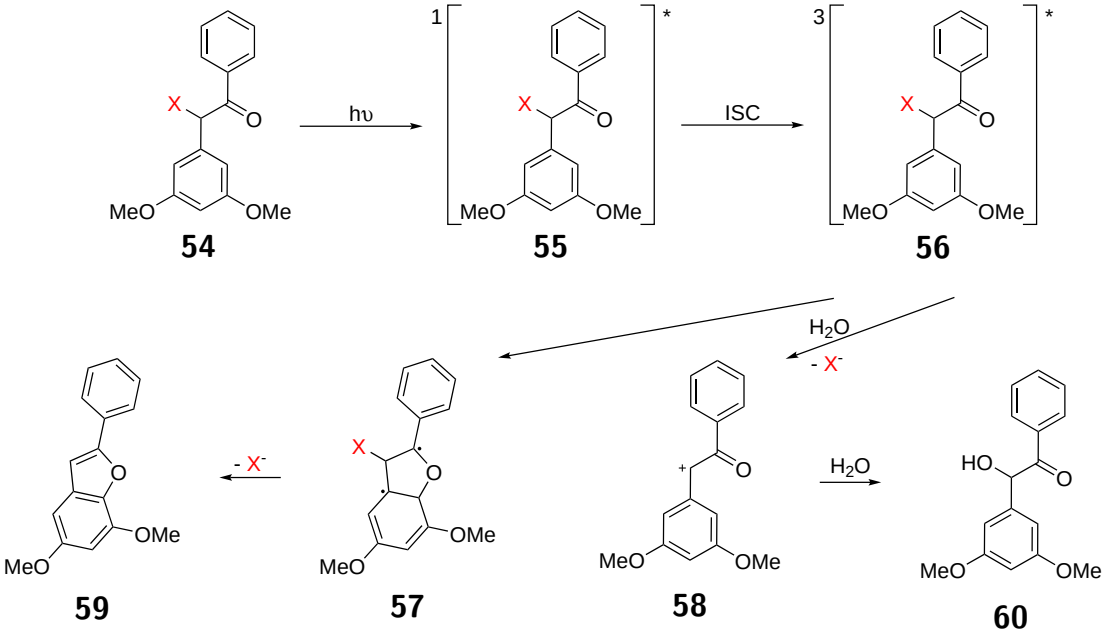
The benzofuran by-product (**53**) competed with the original caged compound for absorption of light, acting as an internal filter, reducing overall photolysis efficiency.[36] The yield was found to be dependent on both the solvent and the nature of the leaving group however, high quantum yields and rates of release make this an attractive PCG.



52 **53**

Scheme 1.10: Photolysis of benzoin-caged analogues.

The most common PCG in this class is the 3,5-dimethoxybenzoin (DMB) group (**54**), which was found to undergo smooth and rapid cyclisation, following irradiation, to release the leaving group in high yields (>65%). The DMB group (**54**) has been extensively employed in a range of settings, varying from drug delivery to biochip fabrication.[37]



54 **55** **56** **59** **57** **58** **60**

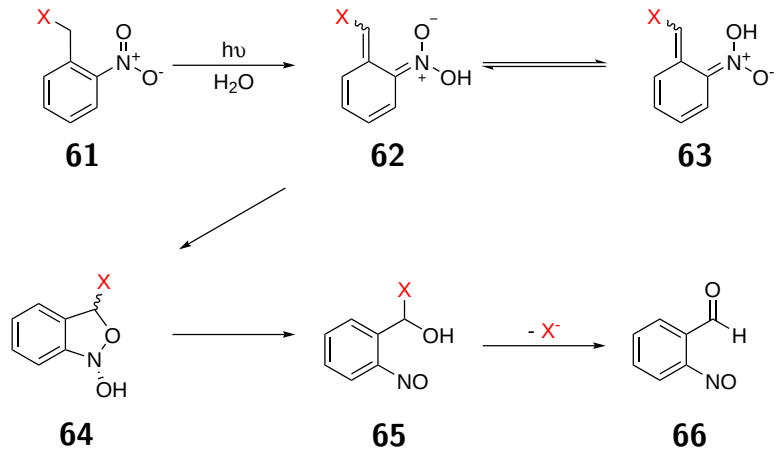
Scheme 1.11: Photocyclisation mechanism of DMB-caged analogues.

Phillips and co-workers used a variety of techniques to investigate the primary photophysical processes involved in the photolysis of the DMB group (**54**). They provided evidence for the formation of an intramolecular charge transfer singlet state (**55**) and found that the final cyclised product (DMBF) (**59**) was formed by concerted leaving group elimination directly from the biradical, largely independent of the solvent (**Scheme 1.11**).[38]

1.4.4 Nitroaryl Groups

2-Nitrobenzylic groups were first proposed as PCGs in the 1970s,[39] and have since found widespread application.[8]

The parent *ortho*-nitrobenzyl (*o*-NB) structure (**61**), although not the most widely used, represents the generic form of this PCG family. Direct attachment of the leaving group to the benzylic position is typical for carboxylic acids, thiols, histidines and phosphates. Although it is possible to directly attach alcohols and amines in a similar manner, they are more commonly linked as carbonic acid derivatives, a strategy which is not feasible when rapid release is required, as the post photolytic fragmentation becomes rate determining.



Scheme 1.12: Photolysis mechanism of *o*-NB caging groups.[40]

LFP and time-resolved IR studies, with methanol as the leaving group, were used to elucidate the mechanisms of photorelease from these PCGs.[225]
The primary photoreaction is often thought to be hydrogen transfer from the *o*-alkyl substituent to the nitro group, proceeding *via* *aci*-nitro intermediates (**62**), (**63**), which follow a biexponential rate law for decay, the rate constants of which are of the order 10^2 - 10^4 s^{-1} and show strong variations with substitution, solvent, and pH in aqueous solution (**Scheme 1.12**).
Formation of the reactive *aci*-nitro intermediates (**62**), (**63**) may proceed from either the excited singlet or triplet states. Irreversible cyclisation from the neutral *aci*-compound (**62**) occurs to afford the 1,3-dihydrobenz-[*c*]isoxazol-1-ol intermediate (**64**). At pH < 8, elimination of the leaving group from the hemiacetal intermediate (**65**), formed by ring opening of the cyclised product (**64**), was found to be the RDS for the

release of methanol and possibly with other poor leaving groups. The rate was many orders of magnitude slower than decay of the *aci*-intermediates (**62**), (**63**), at near neutral pH vales.[40]

There are, however, major drawbacks associated with the use of this class of PCGs. This includes the condensation of amines with the nitrosoaldehyde by-product (**66**), resulting in the formation of stable imines. Whilst this reaction can be minimised through the use of carbonyl scavengers, the formation of nitrosobenzaldehyde (**66**) itself, is a major limitation, as it yields brown-coloured degradation products, which absorb incident light and hence act as internal filters.[37]

Despite these limitations, *o*-NB PCGs have found application in various synthetic and biological examples, ranging from caged biomolecules to protecting groups in natural product synthesis and over the years, numerous modifications have been developed to improve the properties of this class of PCGs.[16] These derivatives have mostly been geared towards increasing the quantum yield, release rates and absorbance wavelengths. In general, substitutions at the benzylic site have mainly affected quantum yield, whilst those on the aromatic moiety have mostly affected absorbance wavelengths.[8]

Various substituents at the benzylic position of *o*-NB were found to enhance their performance as PCGs. This was attributed to both electronic effects and the addition of a second unit capable of performing hydrogen-abstractions. The reactivity of the photolysis by-product is also affected through generation of the less electrophilic ketone. However, substitutions at this position generate a stereogenic centre which can become problematic if the leaving group is a chiral molecule, due to the formation of diastereoisomers.[37]
A carboxylate at this position was found to increase release rates,[41] while the presence of a hydroxyl group opened a new pathway for decay of the *aci*-nitro intermediate *via* a nitroso hydrate.[42] Simpler substituents such as a methyl group were also found to have a beneficial impact on the quantum yield. Specht *et. al.*[43] and Jullien *et. al.*[44], both proposed the use of strongly electron-withdrawing groups but despite having a positive effect on quantum efficiency, these derivatives were not widely adopted due to the required use of a Mitsunobu reaction for their assembly.

Modifications on the aromatic ring allowed for tuning of three features:[8]
(i) the absorbance with concomitant effects on quantum yield,

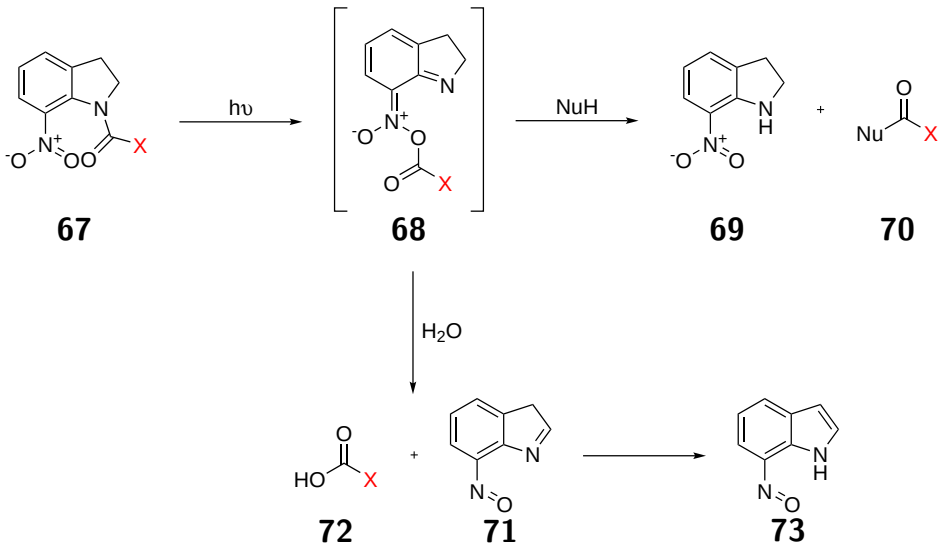
(ii) the possibility of anchoring the group on a solid support or linker,

(iii) modulation of solubility of the group.

Electron withdrawing groups, such as a second nitro group have been introduced to increase the hydrogen abstraction capacity and increase the efficiency of uncaging.[45] Groups have also been included to increase hydrophilicity to overcome water-solubility issues.[46] The addition of methoxy groups had the effect of lowering the HOMO-LUMO energy gap and reducing the energy of excitation, hence increasing the absorbance wavelength; a very prominent example is the 4,5-dimethoxy 2-nitrobenzyl (DMNB) caging group, which is undoubtedly one of the most frequently employed PCGs both in solid and solution phase.[8]

1.4.5 *o*-Nitroanilide Groups

Nitroanilide derivatives have been shown to act as PCGs releasing carboxylic acids and various by-products, depending on the conditions and substitution pattern.[47] Cyclic anilides were also shown to act as PCGs but their cyclic nature prevented a direct hydrogen abstraction on the amide alkyl substituent.[48] Variations in the substitution pattern on the indoline aromatic ring were shown to influence the nature of the side products obtained.[49] The size of the fused heterocyclic ring was critical for reactivity, with the 5-membered ring of the 7-nitroindoline (**69**) being most efficient.



Scheme 1.13: Photolysis mechanism of 7-nitroindoline PCGs.[49]

Corrie *et. al.* proposed a comprehensive photolysis mechanism for these PCGs. Photoinduced acyl migration from the indoline nitrogen atom (**69**) to one of the nitro-group oxygens results in formation of a highly electrophilic N-O acyl intermediate (**68**), which could lead to one of two distinct pathways (**Scheme 1.13**):
(i) In H_2O, the product is released following deprotonation with concomitant formation of a nitrosoindole (**73**).

(ii) In wet organic solvents, the acyl moiety undergoes nucleophilic attack, either by the solvent, or an external nucleophile.

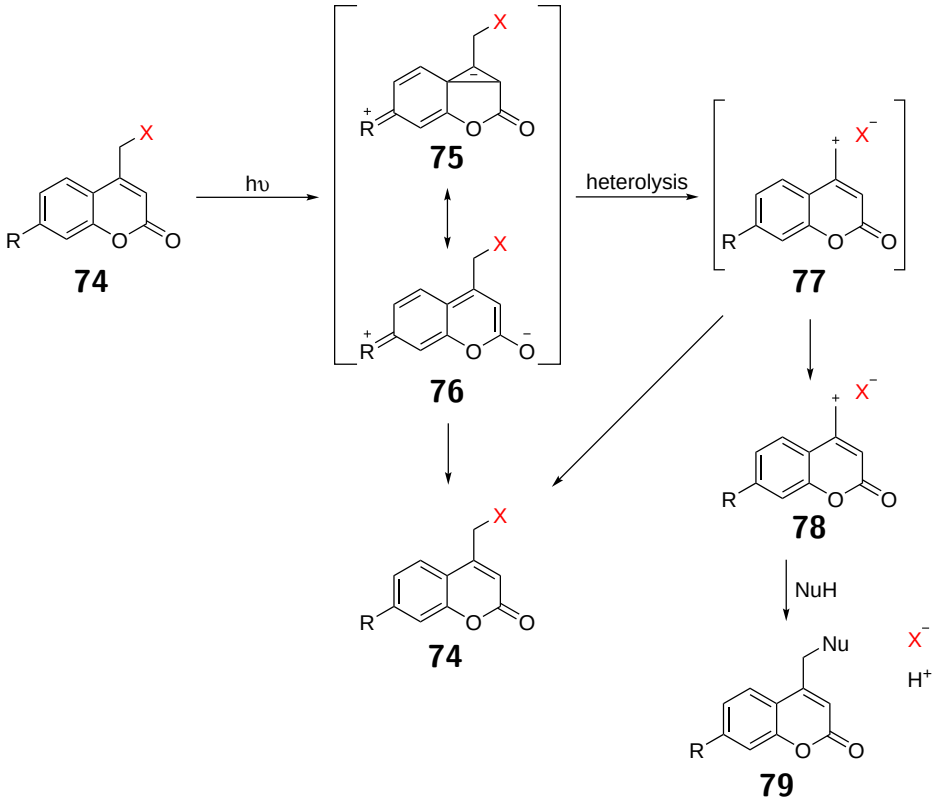
7-Nitroindolines release their leaving groups efficiently and tuning of the aromatic substituents at C-4 and C-5 have the greatest impact on their reactivity.[49] These properties have enabled these PCGs to find application in neuronal studies, particularly for the study of activation of ion channels, and other physiological sciences.[8]

1.4.6 Coumarin Groups

The use of coumarin derivatives as PCGs is relatively recent,[37] although an initial report on the photoactivity of 7-methoxycoumarin-4-ylmethyl esters (MCM) (**83**) first appeared in 1984.[50] The spectral range of irradiation for this class of PCGs extends to the visible region and can be shifted further by addition of suitable substituents. Modifications of the substituents at C-6 and C-7 have addressed issues of poor water solubility, in addition to improving quantum yield.[16]

A general mechanism was proposed for the photolysis of coumarin-caged compounds (**Scheme 1.14**).[51] After initial excitation to the lowest singlet π^*-state, relaxation to the lowest singlet π-state occurs. This can then undergo radiationless decay, fluorescence or heterolytic C-X bond cleavage, resulting in formation of the key intermediate tight ion pair (**77**). The coumarinylmethylene cation (**78**) can either react directly with adventitious nucleophiles or the solvent to generate a new stable coumarylmethyl product (**79**) or alternatively, the tight ion pair (**77**) may escape the solvent cage and react with available nucleophiles or undergo recombination to regenerate the ground state (**74**). Although, evidence of ISC has been observed, there has been no indication of triplet reactivity.[52]
Though time-resolved absorption studies have shown that the heterolytic bond cleavage is extremely rapid,[53] the subsequent reactions are dominated by ion pair recombination

that is approximately ten times faster than nucleophile trapping of the cationic intermediate by the solvent.[51]



Scheme 1.14: General mechanism for photorelease from coumarin-caged compounds.[51]

Coumarin-caged species bearing poor leaving groups, such as alcohols, phenols and thiols, are resistant to heterolysis. Uncaging is more efficient when these species are caged through carbonates and thiocarbonates. However, decarboxylation of the liberated carbonic or thiocarbonic acid becomes the rate limiting step, which may restrict applications requiring very rapid substrate release.[54]

Coumarin derivatives are suitable as PCGs for a number of applications, ranging from photorelease of carboxylic acids and phosphates to cyclic nucleotides and amino acids. This applicability is largely due to the potential for tuning the photophysical properties of these PCGs, through the use of substituents, the high absorption coefficient, and fast rate of photorelease.

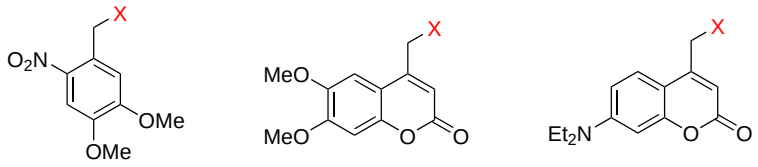
1.5 Improvements and Recent Advances

One of the primary advantages associated with the use of PCGs in biological systems is the spatio-temporal control conferred. However, cleavage often requires the use of UV irradiation; whilst this may limit *in vitro* applications, it may not be compatible with many *in vivo* or biomedical applications.[55]

This is the result of two factors, which in concert, define the phototherapeutic window, the region of relative tissue transparency that lies between 650 - 950 nm; the major absorbing species in vertebral tissue is oxyheamoglobin which filters all light of wavelengths shorter than 640 nm, while water becomes increasingly absorbent at wavelengths longer than 950 nm. Lower scattering and reduced phototoxic effects accompany the increased depth of tissue penetration in this region.[56] Continued growth in the field thus requires the development of new PCGs, susceptible to cleavage within the phototherapeutic window. However, red and NIR photons possess relatively low energy which limits the range of processes they are capable of initiating. In addition, the majority of chromophores with useful single-photon absorbance which fall in the phototherapeutic window are also sensitive to visible light, hence complicating the handling of their caged substrates. To date, several strategies have been developed to achieve longer wavelength excitation which will be discussed in turn.

1.5.1 Substituent Modification

The introduction of various substituents or extending the degree of conjugation of the chromophore are the most common methods for increasing the absorption of PCGs at longer wavelengths. Notable examples include the addition of two methoxy groups to the *meta*- and *para*-positions of *o*-NB (**80**) to extend the absorbance to $\lambda_{max} = 350$ nm.[57]



80 **81** **82**

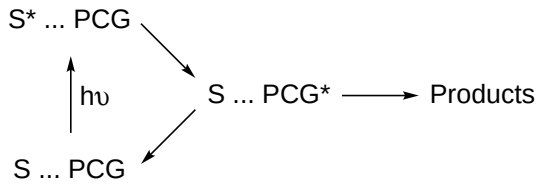
Figure 1.4: Structures of PCGs bearing substituent modifications.[57]

Incorporation of two methoxy groups at the C-6 and C-7 positions of the coumaryl moiety (**81**) red shifted the absorbance by 40 nm whilst preserving the photochemical

properties. Substitution with a dialkylamino group at the C-7 position (**82**) remarkably improved the spectroscopic and photochemical properties of this PCG relative to the parent compound and red shifted the absorption maximum, resulting in the highest quantum yields recorded among the coumaryl analogues.[6]

1.5.2 Sensitised Release

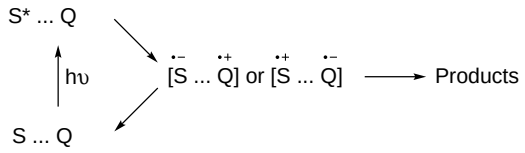
A photosensitised cleavage system provides a means to decouple the light absorption step from the photoresponsive release, such that each step can be optimised independently. It is usually composed of two molecular components comprising the photosensitiser and the trigger for cleavage. Photorelease occurs in two steps; initial excitation of the photosensitiser enables activation of the neighbouring molecule through energy or electron transfer, which is then followed by photocleavage of the trigger. The donor molecule is required to have a high absorption coefficient at the irradiation wavelength to be capable of undergoing efficient ISC and have a sufficiently long triplet lifetime to allow for quantitative energy transfer.[58] When the acceptor molecule is a PCG, this process leads to release of the leaving group (**Scheme 1.15**).



Scheme 1.15: Photoinduced energy transfer.[58]

The release of leaving groups can also be driven by photoinduced electron transfer (PET). In general, electron transfer to a quencher (Q) results in quenching of the excited state sensitiser (S). These species can be separate or linked *via* a tether. If both S and Q are neutral prior to the commencement of the reaction, a radical ion pair will be formed which can then undergo further chemical reaction to afford the desired product.[59] Alternatively, the reverse reaction may occur to regenerate S and Q (**Scheme 1.16**). This is an important bifurcation in the reaction sequence that determines the overall release quantum yields.

Theoretically, two major mechanistic strategies can be designed; either S or Q can represent a PCG bearing a leaving group. Thus, the PCG can either be oxidised by loss of an electron or reduced by accepting an electron in a direct or sensitised manner. PET-based PCGs and their applications have been comprehensively reviewed elsewhere and have not been included in this introduction.[60]



Scheme 1.16: Photoinduced electron transfer.[59]

1.5.3 Longer Wavelength PCGs

The use of red-shifted caging groups presents advantages for applications in biological systems, through increased penetration and reduced photo-damage.

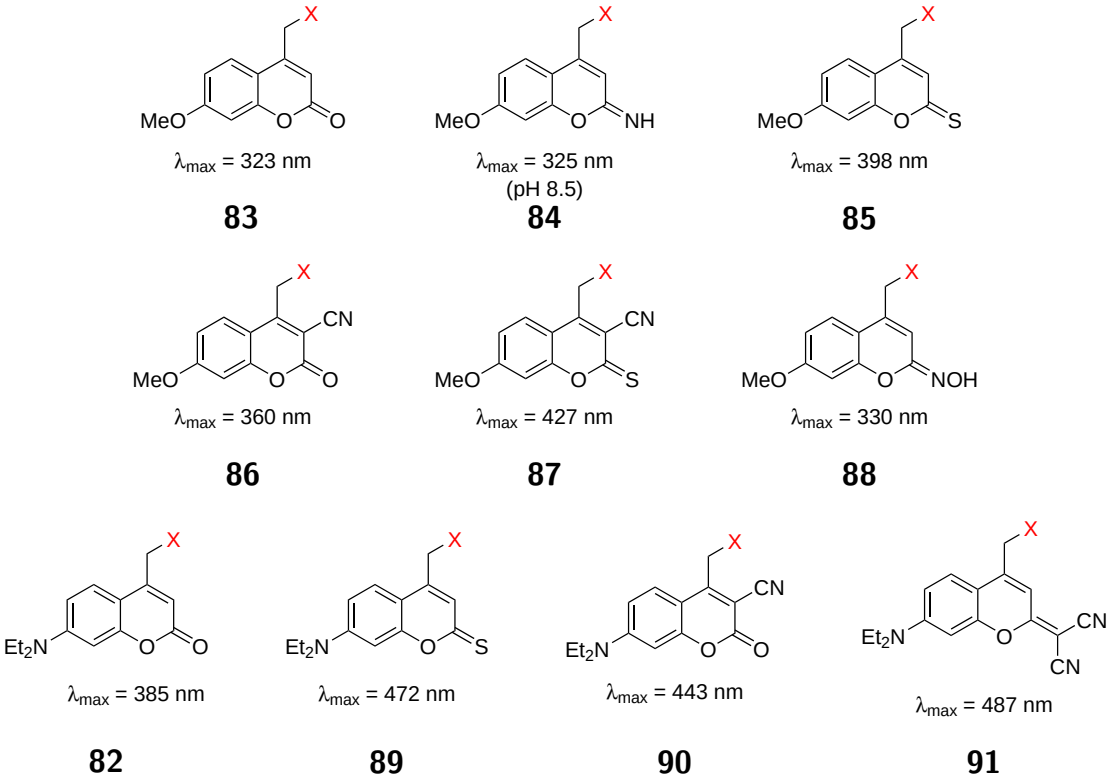


Figure 1.5: Red-shifted family of coumarin-based caging groups by Jullien *et. al.*; X = LG.[61]

Absorption peak wavelengths have a tendency to shift to longer wavelengths with increased conjugation of the system, resulting from the greater ease of excitation of the π-electrons.

This strategy was used to develop red-shifted PCGs by extending the conjugation of the absorbing moiety of established PCGs. Jullien *et. al.* demonstrated the red-shifted absorption of a family of modified coumarins (**Figure 1.5**) by introducing electron-donating groups in the 7-position and electron withdrawing groups in the 2-

or 2- and 3-positions (**Figure 1.5**).[61]

The development of ruthenium polypyridyl phototriggers (**92**) presents a prominent example of a strategy around designing new caging groups based on existing chromophores, known to absorb in the visible range.
The photoreactivity of these compounds was first reported in 1963,[62] but it was not until two decades later that a systematic study provided evidence for their potential utility as phototriggers.[63] The photochemistry of $[Ru(bpy)_2XY]^{n+}$ complexes (**92**) bearing two bipyridines and two monodentate ligands, is distinguished by the well-defined photodissociation of one or both monodentate ligands.

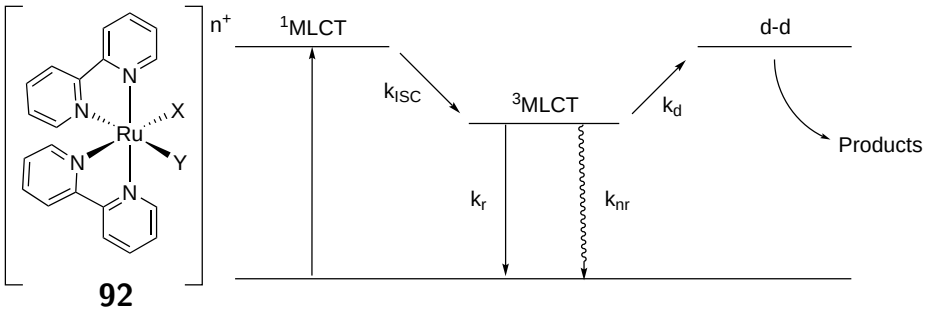


Figure 1.6: Structure and electronic states of $[Ru(bpy)_2XY]^{n+}$ complexes.[64]

The photodissociation observed with these complexes can be modelled by a state diagram (**Figure 1.6**). An electron is excited to the singlet metal to ligand charge transfer band (^{1}MLCT), the maximum of which lies at 400 - 500 nm, allowing visible light to be used. The excited singlet species undergoes efficient ISC to populate the triplet (^{3}MLCT) band. The ground state can then be reaccessed *via* emission or non-radiative pathways. Alternatively, population of the non-bonding *d-d* state could lead to dissociation of the ligand. The ligands coordinated to the Ru centre are released as whole molecules, with no further dark reactions that could potentially introduce unwanted side-products.

Only one of six available ligand sites around the octahedral Ru centre needs to be occupied by the leaving group. The other five sites are available to various ligands for fine-tuning to alter the physical and chemical properties of the phototrigger.[64] Members of the phosphine family of the form PPh_nMe_{3-n} are typically chosen for this role. The weaker σ-donor and stronger π-acceptor properties of the phosphine groups result in the ruthenium (II) centre becoming electronically depleted and shifting the position of the ^{1}MLCT band from 489 nm to 424 nm. In the case of $Ru(bpy)_2$-caged

GABA, the increase in energy of the MLCT band led to a dramatic increase in the quantum yield of photodissociation.[65]

The inert character of the phosphine ligand can also be exploited to force bidentate ligands to coordinate through only one position (**94**) (**Figure 1.7**). This approach had the effect of vastly increasing the quantum yield of the photodissociation reaction by preventing the very rapid recoordination often observed with bidentate coordinated ligands.[66]

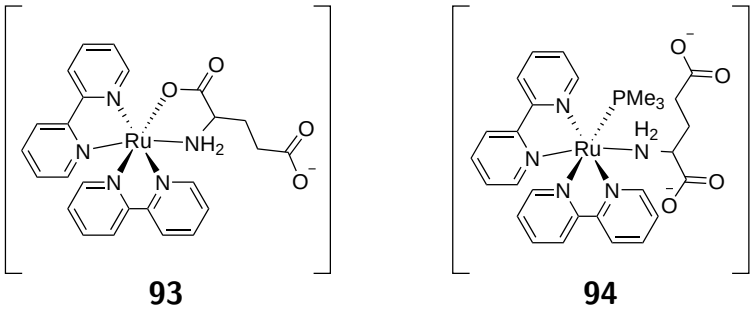


Figure 1.7: $Ru(bpy)_2$ caged through bidentate and monodentate coordination as forced by PMe_3.[66]

This strategy was similarly adopted by Wirz and Klán for their development of xanthene- (**95**),[67] and pyronin-based (**96**) caging groups (**Figure 1.8**).[68]

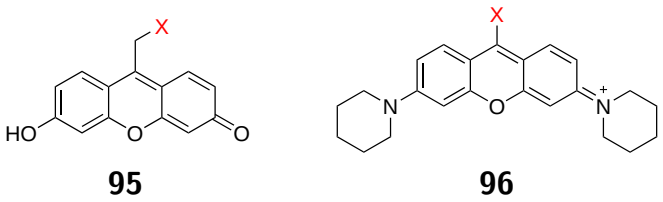


Figure 1.8: Xanthene and pyronin caging groups designed by Wirz and Klán.[67], [68]

The authors were able to effect photorelease of diethyl phosphate, acetate, and bromide upon irradiation of the fluorescein analogues (**95**) at wavelengths longer than 500 nm in aqueous solutions.[67]

A potential application in bioimaging was highlighted for the pyronin-caged analogues (**96**); these compounds exhibited strong fluorescence in the near IR region when irradiated with light in the visible range, allowing *in vivo* visualisation of mitochondria in myeloma cells in the tissue-transparent window.[68]

A third strategy was recently developed by Winter *et. al.*, who hypothesised that photoheterolysis reactions were under the control of conical intersections.[69] They

postulated that photoheterolysis of C-X bonds (X = leaving group), to generate ion pairs, would be favoured if the ion pair had access to a nearby productive conical intersection that provided an efficient channel for decay of the excited state to the ground-state ion pair. They simplified their computation of conical intersections by suggesting the use of the vertical energy gap of the carbocation to its first excited state, as a simple predictor of a nearby conical intersection. A low lying S_0 - S_1 energy gap of the cation would be indicative of a potential nearby conical intersection between the two surfaces and hence, the potential for a productive mechanistic channel for the photolysis to proceed from excited state to ion pair.[69]

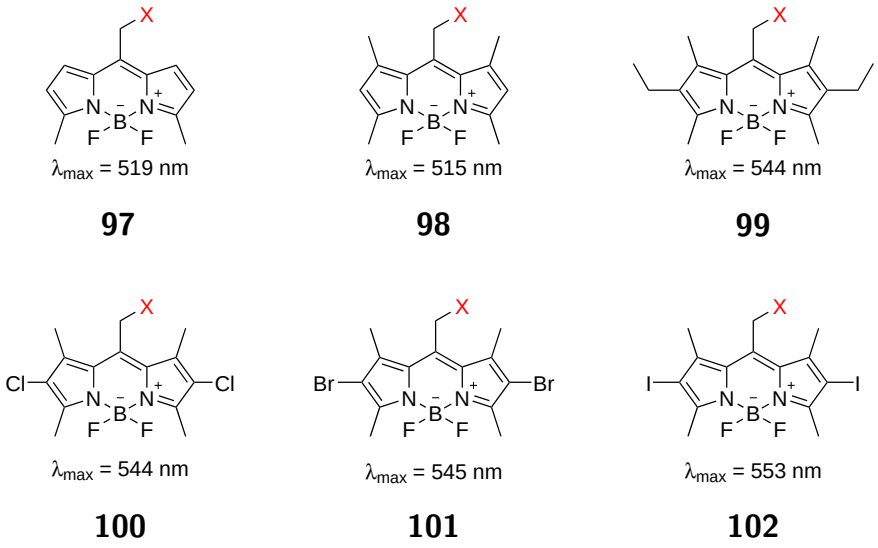
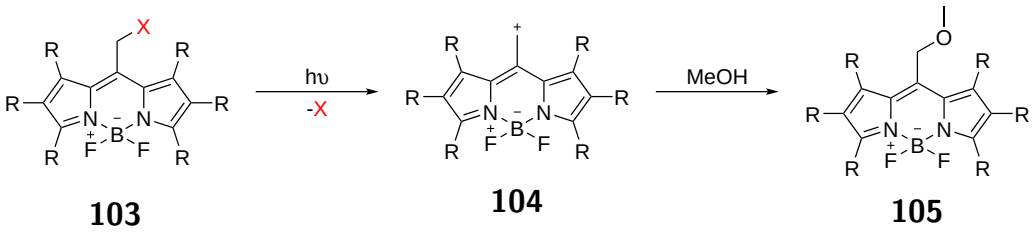


Figure 1.9: BODIPY-based caging groups developed by Winter *et. al.*.[70]

Previous computational work[69] led Winter *et. al.* to synthesise a family of caging groups based on the BODIPY-scaffold (**Figure 1.9**) which demonstrated photolysis of the C-X bond in the visible range ($\lambda > 500$ nm).[70]

They found the quantum yields of the BODIPY dyes (**Figure 1.9**) to be lower than those of the better known phototriggers based on coumaryl or *o*-NB scaffolds but argued that the higher extinction coefficients resulted in them possessing practically useful quantum efficiencies. A potential mechanism for the process was postulated (**Scheme 1.17**), which involved the generation of carbocations with low-lying diradical states.[70]

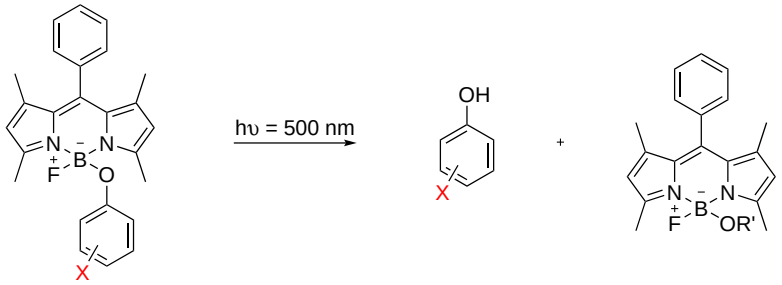
Umeda *et. al.* reported their independent findings on the photoelimination reaction of some 4-aryloxy BODIPY derivatives (**106**) when exposed to irradiation of blue-green visible light of approximately 500 nm.[71]



103 **104** **105**

Scheme 1.17: Hypothesised mechanism of photolysis by Winter *et. al.* where X = acetic acid.[70]

The group postulated that the photolysis proceeded *via* a photoinduced electron transfer (PeT) mechanism, that resulted in formation of a charge-separation intermediate (CS state) involving the cation radical of the aryl group and the anion radical of the fluorophore. This was followed by solvolysis of the B-O bond of the positively charged aryl group (**Scheme 1.18**).[71]



106 **107** **108**

Scheme 1.18: Umeda *et. al.*'s photoelimination of 4-aryloxy BODIPY derivatives; X = 3-NME_2PhOH, 3,4-$(OMe)_2PhOH$, 4-OMePhOH, 7-hydroxycoumarin, 4-COOMePhOH, 4-CNPhOH, 4-NO_2PhOH; R‘ = H, Me.[71]

Despite the growing interest in designing and developing novel red-shifted caging groups, that can be activated by one-photon excitation, the area is still in its infancy, owing to the difficulty in predicting *a priori* which structures will undergo efficient photoheterolysis. Much of the work in this area still relies on serendipity for its growth.[8]

1.5.4 Two Photon Excitation

The use of nonresonant two-photon excitation (2PE) replaces UV irradiation by simultaneous absorption of two IR photons, of equivalent total energy, to generate higher-energy excited states, the same as or similar to those accessible by direct excitation with UV photons.[72] This enables excitation to be achieved with longer

wavelengths of light, thus increasing biological compatibility.

The photosensitivity of a molecule to 2PE is expressed by its two-photon action cross section (δ_u). The application of this technique has thus far been limited by currently available PCGs possessing too low δ_u. It has been estimated that for practical application at safe laser power, the δ_u needed to be higher than that for any known PCG, 3 - 30 GM.[73]

Although IR photons are known to be less likely to cause damage to biological molecules, 2PE requires very high light intensities, which can only be achieved using ultrafast pulsed lasers. However, some recent studies have shown that toxicity of irradiation is related to laser power and in the system investigated, an upper limit of 5 - 10 mW was established, above which damage due to multiphoton absorption was observed.[73]

1.6 Biological Applications

PCGs have found widespread application in biological study owing to the spatial and temporal control conferred on release of the substrate, following irradiation at a specific site at the time point when a concentrate jump of the active biomolecule is required. This added control is in stark contrast to simple addition of the active biomolecule, as often, all control over the biomolecule is lost following its introduction. This specificity has allowed PCGs to become an excellent tool to study dynamic biological processes. Many biological application incorporating PCGs have been successfully demonstrated and extensively reviewed;[8], [37], [16], [74], [15] only a select few examples will be highlighted to give a general overview of the interdisciplinary research PCGs have facilitated.

1.6.1 Caged Small Molecules

A significant number of small molecules have been successfully caged and applied to the investigation of the pathways of numerous cellular processes.
Adenosine triphosphate (ATP) (**109**) plays a fundamental role in biological systems and was the first caged biomolecule to be applied in cell biology.[14] A variety of caged ATP derivatives, e.g. DMNB-caged ATP, were found to be useful in biological study, such as in the investigation of charge translocation in a number of ion translocating membrane proteins.[75]

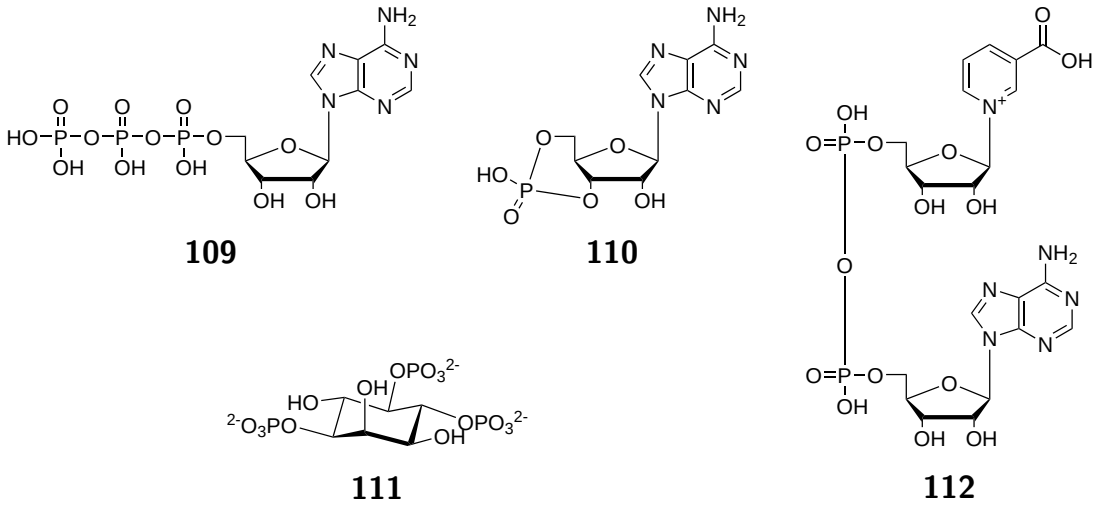


Figure 1.10: Notable small molecules caged for the study of cellular signal-transduction pathways.

Cyclic adenosine 3',5'-monophosphate (cAMP) (**110**) has been caged with a variety of PCGs, including DEACM[76] and MCM[77], [78] and shown to release free cAMP upon irradiation, leading to stimulation of the systems under investigation.

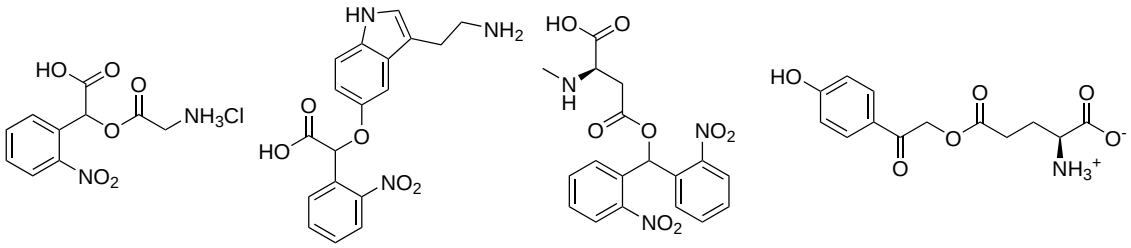
Photoactivatable inositol 1,4,5-triphosphate ($InsP_3$) (**111**), e.g. DMNB-caged $InsP_3$ analogues are widely-used in cell biology and can be used to induce a Ca^{2+} concentration jump in cells.[79] Upon binding to its receptors, $InsP_3$ initiates the release of Ca^{2+} from intracellular stores and triggers complex waves and oscillations in levels of cytosolic free Ca^{2+}. Delivery of exogenous $InsP_3$ into populations of unpermeabilised cells with high spatio-temporal control is extremely useful in determining long-term responses, controlled by oscillations in $InsP_3$ and cytosolic free Ca^{2+}.[79]

Nanomolar concentrations of nicotinic acid adenine dinucleotide phosphate (NAADP) (**112**), a potent Ca^{2+} mobilising agent, is able to trigger Ca^{2+} release from intracellular stores by stimulating its receptors. NAADP was caged with 1-(2-nitrophenyl)-diazoethane and shown to induce Ca^{2+} oscillation. This provided unequivocal evidence that Ca^{2+} release occurred from intracellular stores.[80]

1.6.1.1 Caged Neurotransmitters

Neuroscience is one of the areas in which PCGs have proved most useful.
Binding of neurotransmitters to receptors causes the opening of ion channels, either directly or indirectly. Caged derivatives have been crucial in advancing investigations

on the mechanism of chemical synaptic transmission and monitoring the kinetics of these processes has been made possible in combination with patch-clamp techniques.



113 **114** **115** **116**

Figure 1.11: Representative structures of caged neurotransmitters.[81], [41], [82], [83]

The α-carboxy-2-nitrobenzyl PCG was used to cage both glycine (**113**) and serotonin (**114**) and shown, upon irradiation, to induce cell currents in HEK-293 cells,[81] and activate receptors in NIE-115 mouse neuroblastoma cells[41] respectively.

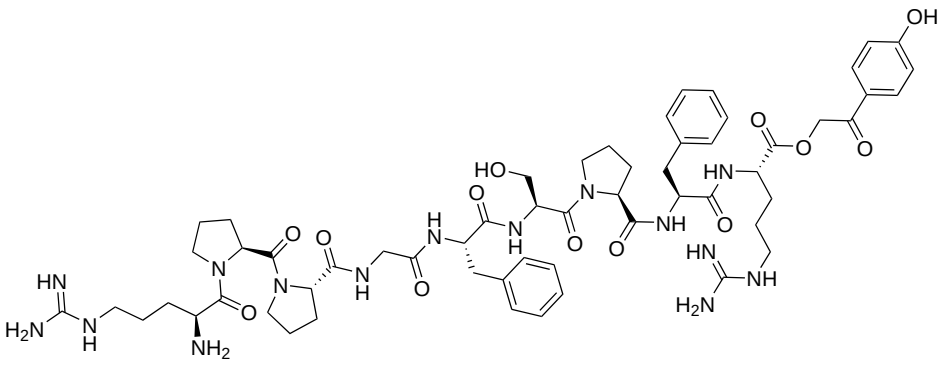
2,2'-Dinitrobenzyl (DNB) was used to cage *N*-methyl-*D*-aspartic acid (NMDA) (**115**) and applied to rat hippocampal neurons, where irradiation led to release of free NMDA, which elicited a current that rose with a rate constant of 100 s^{-1}.[82]

DMNB-caged nonivamide (**116**) was shown, following irradiation at 355 nm, to display fast responses, consistent with activation of TRPV1-receptors in cultured trigeminal neurons.[83]

pHP-caged Bradykinin (**117**) was applied to rat dorsal root ganglions, photolysed and the intracellular Ca^{2+} concentrations measured on single neurons, using a Ca^{2+}-sensitive fluorescent dye. A single laser pulse was sufficient to produce a detectable transient signal.[84]

1.6.2 Caged Nucleic Acids

The fundamental biological processes of gene transcription and protein translation are regulated by nucleic acids. The use of PCGs is an efficient method for the control of gene expression and serves as a good alternative to more traditional techniques of "knock-down" and ectopic gene expression technology. The use of NPE and Bhc as PCGs to modify nucleobases, internucleotide phosphates or hydroxyl groups on ribose rings has been well-established.[85] Caged DNA and RNA have been prepared by coupling of the selected PCG either randomly to backbone phosphates or to specific



117

Figure 1.12: Structure of pHP-caged Bradykinin.[84]

nucleobases in the nucleotide.[86]

Relative to conventional methods, many of which involve various genetic manipulations to regulate gene expression, the use of PCG protected-RNA is a rapid and economic means of realising conditional gene expression *in vivo*.[87] Bhc-caged green fluorescent protein (GFP) mRNA showed much reduced translational activity *in vitro* which could be partially recovered following photolysis of the caged species.[87]

1-(4,5-Dimethoxy-2-nitrophenyl) diazoethane (DMNPE) caged plasmids, that coded for luciferase, were transfected into a specific skin site of rats and no expression of luciferase was observed. Subsequent exposure to irradiation at 355 nm, induced luciferase expression proportional to the amount of light applied. This strategy provided an alternative means to target the expression of genetic material with spatio-temporal specificity.[88]

1.6.3 Caged Peptides and Proteins

Peptides and proteins are vital for the regulation of complex biological systems; the vast majority of biological processes are influenced by proteins through changes to its three-dimensional structure. Internal or external stimuli which can induce this 3D change often trigger cascade responses in cellular signal transduction through the ligand-receptor interaction with proteins. Chemical molecules have been used as probes to target specific proteins and to elucidate relative signalling pathways. However, the use of PCGs to cage peptides and proteins may offer a superior way to regulate the activity of proteins and the complex signal transduction pathways with enhanced spatial and temporal control.

Incorporation of a NPE-caged phosphoserine residue within a phosphopeptide was shown to be a useful tool for elucidating the role of a specific protein family in real-time studies of cell cycle regulation.[89] The caged phosphopeptide induced disruption to ligand binding and allowed for exploration of kinase-dependent signalling pathways in cells with temporal control. Other applications of caged peptides have included photocontrollable cell adhesion based on caged RGD 7-30 and caged peptide-based enzyme inhibitors.[74], [90]

Examples of caged proteins in the literature are limited, largely owing to synthetic complications as caged proteins are difficult to access by uniform chemistry. Great difficulty exists getting high contrast on the activity of caged proteins prior to and after photolysis as site-specific conjugation of PCGs with a specified amino acid residue in the protein is hard to realise and thus a variety of PCGs must be tested for a given protein. There exists a high probability of multi-site caging using conventional conjugation strategies making efficient uncaging to restore protein activity challenging to realise.

Chemical biologists have developed approaches to incorporate unnatural amino acids, including mutagenesis and protein ligation.[8]
Native chemical ligation enables the generation of long chain peptides and proteins through a convergent approach. Fragments can be synthesised using solid phase peptide synthesis (SPPS) technology, enabling the incorporation of unnatural caged amino acids into the sequence. Chemoselective reaction occurs between the free thiol group of an unprotected *N*-terminal Cys-polypeptide and a second unprotected peptide containing an α-thioester group. Trans-thioesterification reaction gives rise to a thioester-linked intermediate that spontaneously rearranges to form a normal peptide bond at the ligation site.[91]
Protein engineering methods involving the use of recombinant DNA have also enabled large quantities of recombinant protein to be produced, enabling biochemical characterisation. The use of site specific mutagenesis and nonsense codon suppression can complement this technique enabling the incorporation of unnatural amino acids into the protein sequence.[92]

Photocaged Tyr,[93] Cys,[94] Ser,[95] and Lys,[96] have all been genetically encoded and used in biological studies. Photocaged Ser was used to examine the contribution of two phosphorylation sites to its export from the nucleus, in the yeast transcription factor Pho4.[95] Photocaged Lys was genetically encoded in place of a key lysine residue, in

mammalian cells, within a nuclear localisation sequence fused to green fluorescent protein (GFP) in p53, that has been reported to be important for nuclear localisation.[96] This mislocalised both proteins to the cytosol, allowing the kinetics of their nuclear import to be measured reproducibly in single cells, following a millisecond-to-second pulse of light.[96]

Owing to the advantages conferred through the use of PCGs, including their non-contact mode of action and greatly enhanced spatio-temporal control, PCGs have established themselves as valuable molecular tools to both chemists and biological scientists for numerous photoregulation applications such as in proteins, genes, cells and even living organisms.

1.7 Chromatic Orthogonality

Biological systems, with their astonishing levels of complexity, are an excellent platform where the use of PCGs has particularly excelled. The dynamic interplay of single components and networks in combination with highly non-linear response curves for internal and external stimuli is what makes biological systems so intricate. Thus, it is not only important where and when something is activated or deactivated, but also the extent of the perturbation. However, many of the existing methods to probe biological functions and effects are either too invasive or lack the necessary levels of spatio-temporal control; once the biomolecule is injected, all control is often lost.

To separately address concurrent processes in an orthogonal manner requires the use of two or more PCGs with different spectral properties. These can include differences in absorption maximum (λ_{max}), molar absorptivity (ε), and quantum yield (ϕ). The ability to fine-tune the properties of PCGs, for example through the use of substituents, further enhances the potential of this method for achieving high levels of selectivity in the control of complex biological processes.[97]

The use of chromatic orthogonality was first described by Bochet *et. al.*, who demonstrated that the reactivity of PCGs with monochromatic light could be tuned by changing the substitution pattern around the aromatic ring to achieve orthogonal protection.[98] Selectivity was modest but since this seminal work, several systems have been reported where the use of wavelength-selective cleavage of PCGs has been employed to externally control multiple processes in parallel.

The terms wavelength orthogonality and wavelength selectivity are often used interchangeably but an important distinction exists:
Wavelength selectivity describes the situation where one PCG can be cleaved with a certain degree of selectivity over a second PCG; this includes sequential systems where the selective preference for uncaging only occurs in one direction.
Orthogonality refers to "a set of completely independent classes of PCGs where each class can be cleaved in any order and in the presence of all other classes".[99]
However, as orthogonality is much more challenging to achieve, few reports of true orthogonality exist in the literature with much of the work reported being more aptly classed as wavelength selective.

Despite the plethora of PCGs, not all are suitable for use in chromatically orthogonal systems. Multiple requirements need to be fulfilled, including distinct and narrow absorption maxima, high quantum yields, and suppressed intra- and intermolecular energy transfer.

1.7.1 Design of Chromatically Orthogonal Systems

Several property differences between PCGs can be exploited in the design of an orthogonal system.[100]
(i) Differences in absorbance: a combination of PCGs from different classes or from the same class can be used by employing substituents to shift λ_{max}. In an ideal situation, the PCGs would possess UV/vis absorption spectra that do not overlap, such that it would be possible to select a wavelength of irradiation at which the extinction coefficient of the other PCG is near zero, enabling perfect orthogonality to be attained. Such a system is incredibly rare and it is far more common that the spectra of different PCGs partially overlap. Most visible light sensitive PCGs also possess substantial absorbance in the UV region; photodeprotection of UV sensitive PCGs is likely to result in partial or complete cleavage of the visible light sensitive PCG resulting in only a sequentially wavelength selective system. The use of red-shifted PCGs can present an advantage, by means of reduced spectral overlap, when coupled with PCGs absorbing in the 200 - 300 nm range. It should, however, be noted that the use of short irradiation wavelengths will limit the application in biological systems.

(ii) Differences in the kinetics of photolysis: although spectral overlap means it is extremely difficult to achieve full, sequence independent orthogonality, the difference in kinetics of uncaging may be exploited should they prove large enough for the intended

purposes, especially if full uncaging is not necessary.[101] The first order reaction rate constant (k) of a PCG deprotection, under irradiation with light of a given wavelength, is proportional to the molar extinction coefficient (ε) at the wavelength and the quantum yield (ϕ) of the process (**Equation 1.6**).

$$k \propto \varepsilon\phi \tag{1.6}$$

where:

k - first order photolysis rate constant
ε - molar extinction coefficient at a given wavelength
ϕ - quantum yield of photolysis at given wavelength

(iii) Use of $\lambda_{irradiation}$ other than λ_{max}: since irradiation at λ_{max} does not guarantee optimal selectivity, the use of different wavelengths that provide a more favourable ratio of uncaging can be used as a means to improve selectivity of a system. Careful selection of the irradiation wavelength enabled Bochet *et. al.* to define sets of PCGs that could address selectivity in one system using sequential uncaging. They were also able to define several pairs of PCGs that could be uncaged in a near orthogonal manner.[101]

(iv) Differences in quantum yield (ϕ): most strategies for achieving wavelength orthogonality have been underpinned by the exploitation of differences in absorbance. However, even if strong absorbance overlap were present, a sufficiently large difference in ϕ would still allow for photo-orthogonal systems to be achieved.[102]

(v) Alterations in starting concentrations: one of the major applications for chromatically orthogonal PCGs, is to induce downstream effects in biological systems following photolysis. In many cases, dose-response curves are typically non-linear resulting in differing potencies and selectivities within the system. This can be advantageous for the translation of imperfect selectivity in photodeprotection into perfect orthogonality within the biological system under investigation.

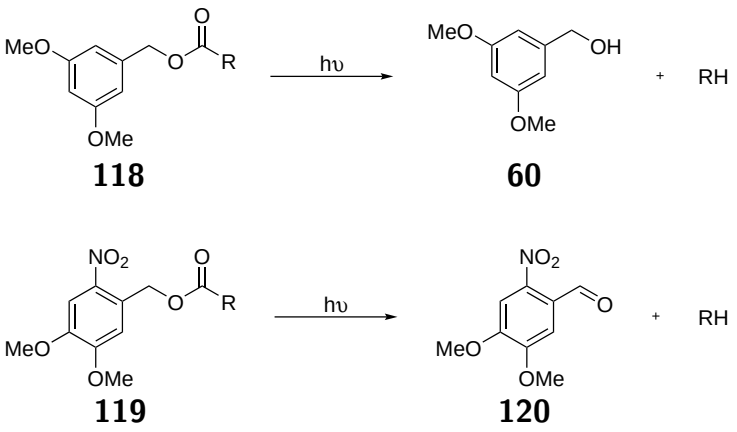
(vi) Use of two-photon excitation PCGs: the use of 2PE has also been proposed as a means of increasing selectivity, in spite of the requirement for the use of stronger light sources. The nitroindolinyl and nitrobenzyl groups have typically dominated this approach with wavelengths of irradiation generally occurring in the range of 710 - 740 nm.[100]

To date, most reported systems have focussed heavily on gaining leverage through differences in absorbance and hence the extinction coefficient (ε) of PCGs at a given wavelength, which is usually more pronounced than differences in quantum yield (ϕ).[103]

Chromatic orthogonality has huge potential for use and application in the elucidation of many complex chemical and biological processes. However, its design and hence implementation is limited by several prerequisites that must be fulfilled. Namely, light exposure must be adjusted so as not to cause any disturbance to biological samples, both positive and negative such as phototoxicity. The by-products of photolysis must be non-toxic to biological samples. This is of particular importance when highly reactive aldehydes are generated. The solubility of the caged and uncaged species can vary remarkable and thus must be taken into account when designing the system, as well as the solvent effects on the kinetics and behaviour of the photo-induced uncaging process.

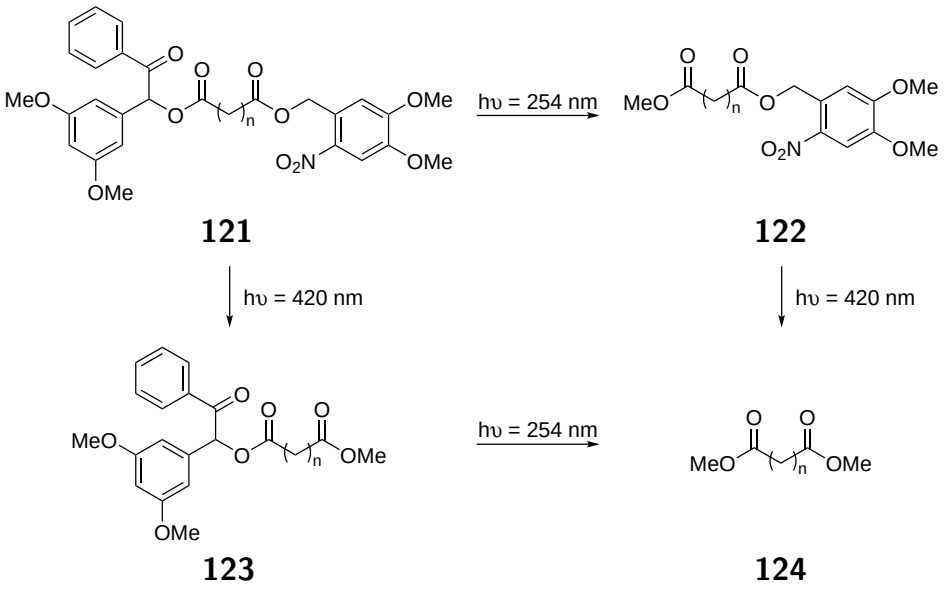
1.7.2 Applications of Chromatic Orthogonality

The potential of wavelength selectivity addressing multiple levels in one system has been showcased in a diverse set of disciplines, ranging from organic synthesis and materials sciences to molecular biology and neurophysiology. However, only a handful of examples have demonstrated true orthogonality. As such, examples discussed will focus on work carried out towards chromatic orthogonality, which include the use of sequentially uncaged PCGs on multiple functional levels and cases in which true chromatic orthogonality have been achieved. Bochet first highlighted the potential for



Scheme 1.19: Photolysis of DMB alcohol and DMNB caged carboxylic acids and amines at 254 nm and 350 nm; R = $HNC_{12}H_{25}$ or $C_{11}H_{23}$.[98]

chromatic orthogonality in seminal proof of concept studies using 3,5-dimethoxybenzyl (DMB) alcohol and 3,5-dimethoxynitrobenzyl (DMNB) groups to protect carboxylic acids or amines. Irradiation of the DMB alcohol caged species (**118**) at 254 nm released the substrates with rate constants of the order $10^{-3}s^{-1}$ whilst at 350 nm, the rate was close to zero. The DMNB-caged species (**119**) was found to have one of the slowest rates of cleavage at 254 nm, with a rate constant of the order $10^{-6}s^{-1}$. Following irradiation at 350 nm, the substrate was released with a rate constant of the order $10^{-4}s^{-1}$. However, despite these encouraging results, the selectivity was not transferable to mixtures of the two caged species and it appeared that following irradiation at 254 nm, the more reactive DMB alcohol (**118**) acted as a sensitizer for the DMNB group, resulting in intermolecular energy transfer interfering with wavelength selectivity.[98]



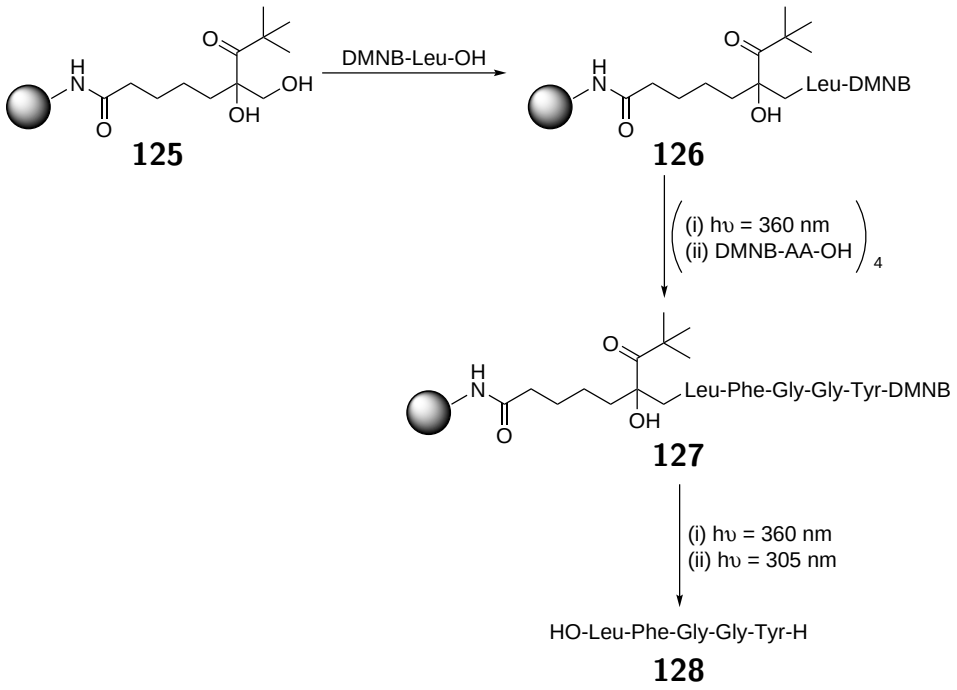
Scheme 1.20: Chromatic orthogonality employing benzoin PCG cleaved at 254 nm and DMNB PCG cleaved at 420 nm.[104]

Through rational design, this issue was circumvented by modification of the DMB alcohol (**118**) to incorporate a benzoyl moiety (**121**). The result was a shortened excited state lifetime, suppressing the energy transfer. This structural modification led to the first instance of both inter- and intramolecular chromatic orthogonality (**Scheme 1.20**).[104]

The chemical synthesis of biopolymers, e.g. nucleic acids, peptides and proteins, requires the use of a multitude of orthogonal protecting groups which need to be

removable under mild conditions to prevent interference with other functionalities. The use of PCGs confers a great advantage owing to its orthogonality to most other functional groups.

Bochet *et. al.* employed a *tert*-butyl ketone linker, sensitive to irradiation at 305 nm, attached to a TentaGel-resin (**125**) and the DMNB PCG, cleaved at 360 nm, to protect the α-amine terminus of the amino acid residues. This strategy enabled the synthesis of 5-mer peptide Leu-Enkephalin (**128**) in an overall 55% yield (**Scheme 1.21**).[105]



125 **126** **127** **128**

Scheme 1.21: Synthesis of Ley-Enkephalin *via* PCG mediated solid-phase peptide synthesis.[105]

Conway *et. al.* demonstrated the applicability of wavelength orthogonality *in vitro* on Glu and GABA receptors in hippocampal neurons, by caging glutamic acid (Glu) and γ-amino butyric acid (GABA) with the MPH and DMNB groups respectively. Wavelength orthogonality was demonstrated by irradiation at 405 nm to effect uncaging of the DMNB group and at 260 nm to release the MPH protected glutamate. The MPH PCG does not absorb at wavelengths longer than 330 nm and was not affected by the irradiation at longer wavelengths. Although, the UV-vis absorption spectrum of the DMNB species did reflect absorption at the shorter wavelength chosen for irradiation, the interplay of ϕ, ε, and cleavage kinetics enabled selectivity to be achieved. An inhibitory response was observed, from released GABA, following

irradiation at 405 nm and an excitatory response from irradiation at 260 nm to release free Glu (**Figure 1.13**).[106]

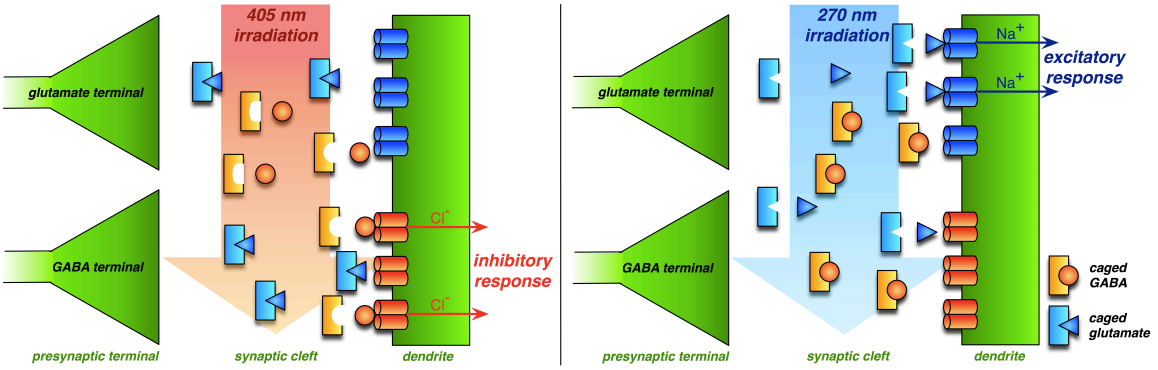


Figure 1.13: One-photon chromatic orthogonality to selectively uncage Glu-GABA pair. Adapted from [106] with permission of The Royal Society of Chemistry.[106]

Ellis-Davis *et. al.* were able to demonstrate selective uncaging of the Glu-GABA pair with two colour, 2PE, using the 4-carboxymethoxy-5,7-dinitroindolin (CDNI) and 7-(dicarboxymethyl)-aminocoumarin (DCAC) caging groups. Selective uncaging of caged CDNI-glutamate with 2PE at 720 nm or caged *N*-DCAC-GABA at 830 nm, allowed the control of neuronal firing rates in rat brain slices with single-synapse precision. However, as the absorption spectra of CDNI and DCAC overlap at 720 nm, orthogonality could only be achieved by taking advantage of differences in cleavage kinetics by optimising concentrations and laser power.[107]

Wavelength selectivity is not limited to the use of simple pairs of PCGs. The number of functional levels that can be selectively addressed is dependent on the number of distinct wavelength selective deprotections that can be achieved for a given system and poses a limiting factor for the complexity of possible applications. To date, a total of four functional wavelength-selective levels have been achieved and although orthogonality in these instances has not yet been possible, they represent a step forward in the ability to address a larger number of functionalities in a single system.

Bochet *et. al.* were able to demonstrate up to four independent functional levels on a single surface that could be selectively addressed with irradiation wavelengths ranging from 255 - 435 nm. The group generated photoactivatable surfaces by protecting surface-attached silanes with seven different PCGs through amine-, thiol- or carboxylic acid groups and screened the photorelease reaction of the protected surface silanes at

different wavelengths and irradiation powers.[101]

Heckel *et. al.* extended this work to demonstrate four levels of wavelength-selective uncaging in oligonucleotides. Caging of oligonucleotides presents an interesting approach to achieve light-control of biological function at the genomic level. The group employed the (7-diethylaminocoumarin-4-yl)methyl (DEACM), 1-(3-nitrobenzofuran-1-yl)ethyl (NDBF), 2-(o-nitrophenyl)propyl (NPP) and 4-hydroxyphenacyl (pHP) caging groups to cage phosphoramidites which were used as building blocks for the solid-phase synthesis of the caged oligonucleotides. By HPLC analysis, the authors were able to determine that sequential photolysis at 505 nm (DEACM), 440 nm (NDBF), 365 nm (NPP) and lastly 313 nm (pHP), enabled them to afford four levels of wavelength-selective uncaging of the oligonucleotides. They noted however, that the pHP caging groups necessitated irradiation at 313 nm for its cleavage and as other biomolecules were also susceptible to undergoing photoreactions at this short wavelength, it was likely to be less suitable for intracellular applications.[102]

Heckel *et. al.* further successfully achieved four levels of uncaging, through a combination of exploiting the differences in absorbance and quantum yield. Nucleosides were caged with the DEACM or pHP groups, through an oxygen or nitrogen atom, the nature of which demonstrated a strong influence on the ϕ of uncaging. Irradiation at 420 nm initially resulted in selective uncaging of the DEACM-caged oligonucleotide, attached through the oxygen atom. Prolonged exposure to irradiation at 420 nm then led to selective uncaging of the DEACM-caged oligonucleotide, attached through the nitrogen atom, leaving the pHP-caged analogues undisturbed. When irradiation was subsequently performed with 313 nm, the pHP-caged analogues displayed the same trend with the caged oligonucleotide attached *via* the oxygen atom undergoing photolysis much more readily than the derivative caged through the nitrogen atom. Thus, four levels of selective uncaging were achieved using only two PCGs and irradiation with only two wavelengths of light, through manipulation of a combination of time and wavelength selectivity of the PCGs.[108]

Despite considerable progress in the field of PCGs, more than a decade on from the first report of wavelength selective application of a pair of PCGs, only a few examples of true chromatic orthogonality have been reported. Though efforts have been made to increase selectivity and applications in more complex systems through the use of multiple functional levels, the lack of progress exemplifies the difficulty in obtaining and developing these systems.

1.8 General Aims & Hypothesis

The work in this dissertation has been aimed at adding to the relevance of PCGs and expanding its scope through development of the first pair of chromatically orthogonal caging groups capable of undergoing photolysis above 300 nm, in addition to extending the applications of PCGs to biologically relevant problems.
Two distinct biological systems form the basis from which to develop the proficiency of PCGs as tools to offer greater insights and understanding of biological problems.

The first system is the bacterial K^+ efflux system, Kef, which protects bacteria against the detrimental effects of electrophilic compounds *via* acidification of the cytoplasm. It was hypothesised that the use of a PCG attached to the endogenous agonist and antagonist of the receptor would provide conclusive evidence for the binding mode in the pocket. More specifically, it was the intention to synthesise both DMNB-caged glutathione (GSH) and the *N*-ethylmaleimide glutathione adduct (ESG). The uncaging of the DMNB group could then be tested and if successful, the compounds would be sent to collaborators for further biological evaluation.

The second biological system is that of protein post-translational modification (PTM); extremely convoluted and highly dynamic biological processes that serve to impart complexity to the proteome through a series of covalent modifications, usually at the side chain functional group termini of amino acid residues. PTMs are vital for the regulation of the cellular environment and have been linked to neurodegenerative and cardiovascular diseases. Despite much work carried out to better identify PTMs, current techniques lack the spatial and temporal control necessary to gain deeper levels of understanding of the processes involved. Examples where single caging groups were used have previously been reported and it was hypothesised that extending this to the use of a pair of chromatically orthogonal caging groups would be an invaluable tool that could be used to gain additional insights into the complex workings of PTMs. The benefit of this would be the ability to probe two amino acids, using light, simultaneously and independently of one another.
The aim was to synthesise a series of amino acids, caged through the side chain functional groups. The amino acids chosen would be those commonly known to undergo protein PTMs possessing differing functionalities at the side chain, namely aspartic acid, glutamic acid, serine, tyrosine, and lysine. The caged amino acids would then be evaluated based on their propensity to undergo photolysis at wavelengths longer than 300 nm. This cut-off was chosen to minimise phototoxic damage to

biological systems and increase penetration in tissues. The caged amino acids would be photolysed at various wavelengths, including 530 nm, 520 nm, 420 nm, 365 nm, 350 nm, and 310 nm. Once an orthogonal system was established, the caged amino acids would then be incorporated into peptides and the photolysis of the caging groups demonstrated in these systems. The relationship between the two caging groups (e.g. propensity towards energy transfer) would also be investigated by synthesis and photolysis of caged peptides with increasing distance between the pair of PCGs. Lastly, the biological relevance of these caged peptides would be demonstrated in an *in vitro* setting.

Chapter 2

Caged Kef Ligands for the Study of Kef Ion Channels

2.1 Introduction

Cellular homeostasis is imperative to cell survival. In bacterial pathogens, this is achieved through the regulation of cytoplasmic membrane permeability to ions and solutes.[109]
The K^+ transport and nucleotide-binding (KTN) domain is central to the regulation of intracellular K^+, important in maintaining cytoplasmic pH and cell turgor, as it links K^+ uptake systems (Trk, Ktr), channels (Kch), and efflux systems (Kef).[110] The Kef system, which comprises both KefC and KefB in *Escherichia coli* (*E. coli*), is a ligand-gated K^+ efflux system, critical for the bacterial response to electrophilic assault and presents a novel target for antimicrobial agent development.[111]

KefC, a system with homologues in the majority of Gram negative pathogens, is a K^+/H^+ antiporter. Formation of a complex of KefC with a small flavoprotein, KefF, which binds directly to the KTN domain, results in maximum activity.[112] Cytoplasmic glutathione (GSH), a thiol-containing tripeptide, acts as a scavenger for electrophiles. The electrophiles react either by direct and spontaneous reaction with GSH, or conjugation to the nucleophile by glutathione *S*-transferase to form adducts (GSX). Exposure to GSX gives rise to activation of the Kef system, resulting in rapid K^+ efflux and a concomitant H^+ influx, leading to cytoplasmic acidification which protects the cells. This observation can be rationalised by a decrease in nucleophile reactivity caused by protonation (or partial protonation) of nucleophiles at lower pH values; despite the process of active detoxification, potentially lethal direct reaction of electrophiles with DNA and other important macromolecules might occur, resulting

in ancillary damage.[113]

Large hydrophobic adducts, such as *N*-ethylsuccinimido-*S*-glutathione (ESG), activate all Kef systems, whilst glutathione-*S*-conjugates with smaller adducts formed in the presence of electrophiles, activate only a subset. GSH and structurally-related γ-linked peptides, such as ophthalmic acid, maintain Kef systems inactive. For *E. coli* KefC, strongest activation is observed with hydrophobic conjugates such as *N*-ethylsuccinimido-S-glutathione (ESG).[113] Kef activity is thus a reflection of electrophilic stress (**Figure 2.1**).[114] Perturbation of Kef activity stands out as a potentially novel target for antibiotic drug development. However, development of Kef-targeting compounds requires thorough understanding of Kef activation at a molecular level.

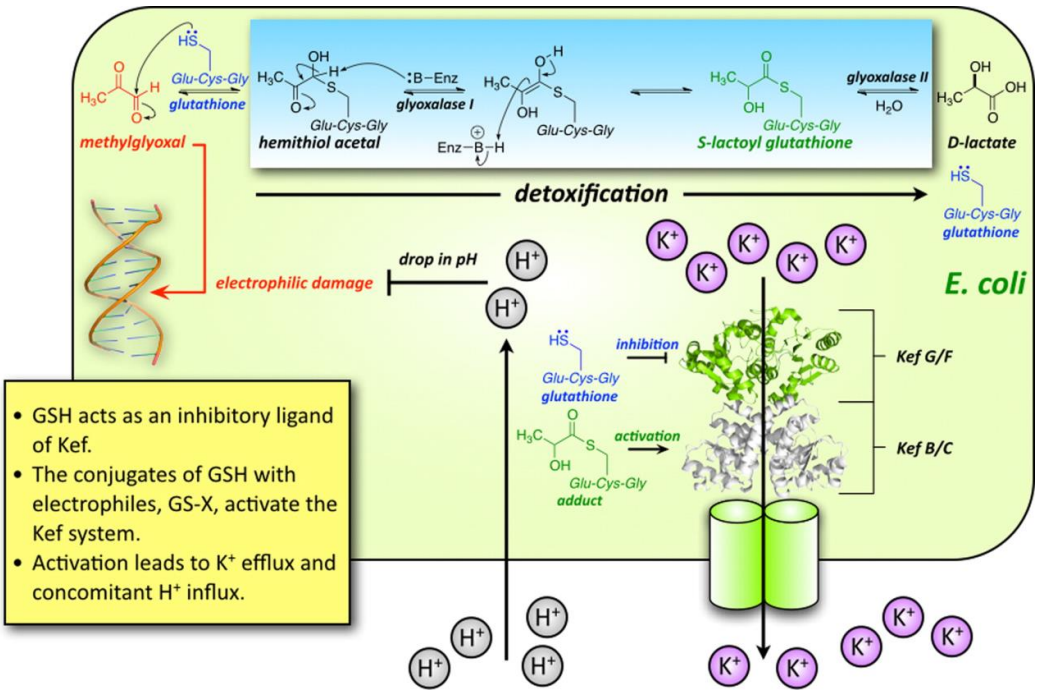


Figure 2.1: Synergistic action of Kef system in *E. coli*; Exposure to toxic electrophiles results in rapid K^+ efflux and concomitant H^+ influx, protecting cells from electrophilic assault. Adapted with permission from ref [114]. Copyright 2014 American Chemical Society.[114]

A combination of crystallographic studies and classical bacterial mutational analysis provided a mechanistic model for the binding of GSH and GSX to Kef, and their modulation of activity. Kef proteins are homodimeric and possess a carboxy-terminal K^+ KTN domain, which contains a Rossmann fold that binds a nucleotide. This

domain is critical to sensing cytoplasmic cues, and gating the associated transmembrane pore-forming domain. KTN domains are small, consisting of approximately 140 amino acids, and are invariably positioned near the base of pore-forming helices.
The GSH/GSX binding site, resides at the interface of two KTN domains. A number of key residues were implicated in the binding of the peptide components to the *E. coli* KefC protein. Classical bacterial genetics identified three critical residues, R416, R516 and N551, as defining the GSH binding site; mutations at these points resulted in a phenotype equivalent to that of loss of GSH from the cell.[115] Crystallographic studies, further reinforced the importance of these three residues for binding to a structured water molecule that binds to the GSH glycine carboxylate residue. However, despite numerous studies, the conformational changes associated with ligand-mediated control of their associated channel or transporter remain elusive.

Cocrystals of KefC C-terminal domain (KefC-CTD) with Kef ligands, produced by recombinant bacterial protein expression using *E. coli* colonies,[116] showed GSH to be bound within a crevice formed at the junction of the two KTN folds. Residues from both KTN subunits contributed to the coordination of the molecule, including R416, R516, and N551, which coordinated the carboxylate of glycine in GSH. These structures also predicted other residues to be critical for ligand affinity, including Q412, R498, D499, and the backbone carbonyl of V500 (**Figure 2.2**).[116]

Comparison of the structure of KefC-CTD with bound ESG, relative to the GSH structure, was used to propose a model for the ligand gating mechanism. ESG and GSH were found to occupy overlapping binding sites and make contacts with the same residues in the KTN domain. However, in the GSH-bound structure, residue F441 protruded into a well-defined, hydrophobic pocket on the opposing KTN subunit. The free thiol group of GSH was believed to stabilise both the protein-ligand association, and resulting protein conformation by displacing water from the cavity adjacent to the phenyl ring of F441. Superposition of the GSH and ESG structures showed that the *N*-ethylsuccinimide substituent overlapped with the phenyl ring of F441. The protein oscillates between the inactive and active forms, and upon binding of ESG, the active form where the F441 phenylalanine residue is displaced from its original position in the pocket is stabilised. This repositioning to an alternative conformation, in which it pulled away from the adjoining KTN fold and now associated solely with other amino acids from its own chain (**Figure 2.3**),[116] is believed to result in activation of the Kef system.

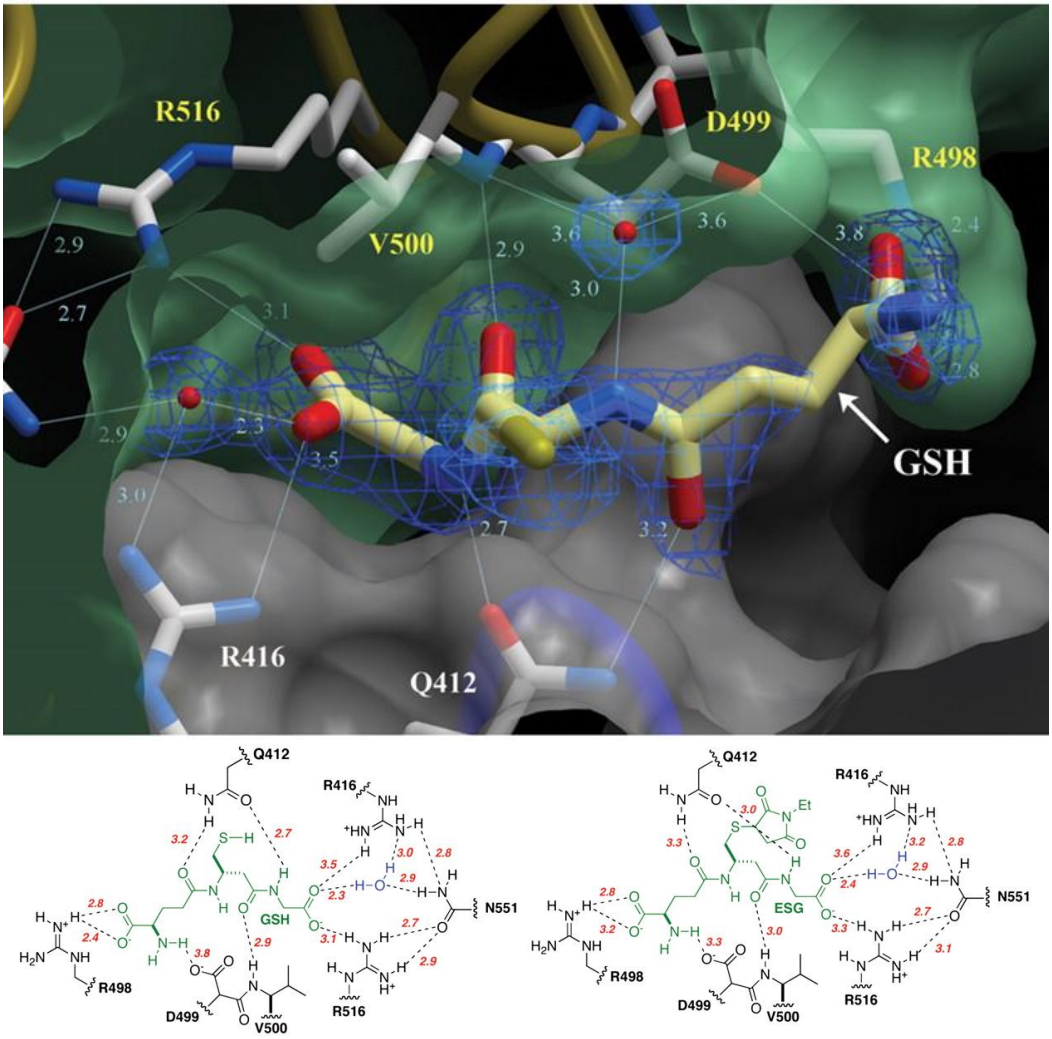


Figure 2.2: GSH and ESG binding to KefC-CTD:KefF fusion protein produced by recombinant bacterial protein expression using *E. coli* colonies, showing the residues important for coordination of the tripeptides.[116]

GSH is abundant in cells, therefore, activating ligands must show preferential affinity for binding over GSH. Competition assays using fluorescent reporter ligand analogues of GSH (DNGSH), complemented by direct binding assays and thermal shift measurements, revealed a 10 - 20 fold higher affinity of ESG for KefC over GSH.[114] A strategy employing PCGs was previously used to provide conclusive evidence for

binding of GSH to glutathione *S*-transferase (GST). Based on X-ray crystallographic data of GSH bound GST, GSH was caged at the glutamyl carboxy residue with nitrophenylpropyl (NPP) to strongly impact the recognition of GSH by GST. A FRET

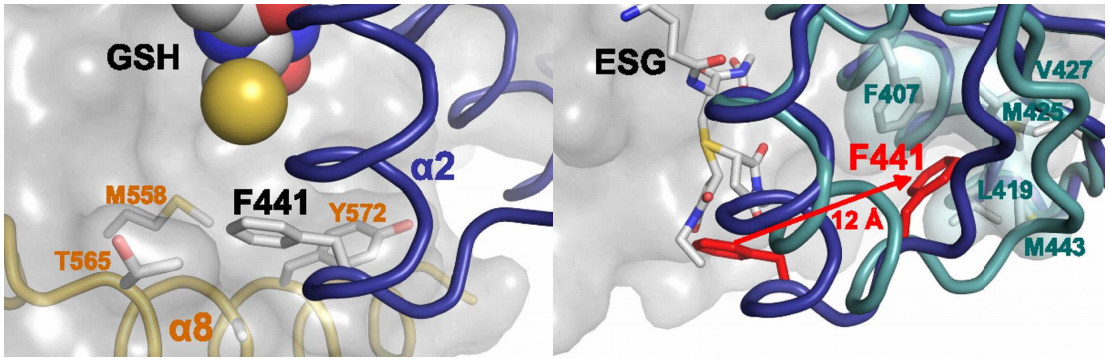


Figure 2.3: Mechanism of GSX modulation of KTN conformation; F441 displaced to alternative conformation.[116]

assay was then used to follow the GSH-protein interaction in real time under the control of light.[117] Prior to irradiation, titration with NPP-caged ATTO565-labelled GSH showed no significant FRET. Illumination of caged GSH, led to uncaging of NPP to reveal the active GSH molecule. This molecule was able to bind to GST which had been C-terminal fused to enhanced green fluorescent protein (eGFP). This result was observed as an increase and decrease of acceptor and donor fluorescence respectively. This provided support for use of the developed strategy to provide conclusive evidence for the binding mode of GSH and ESG within the KefC KTN binding domain.

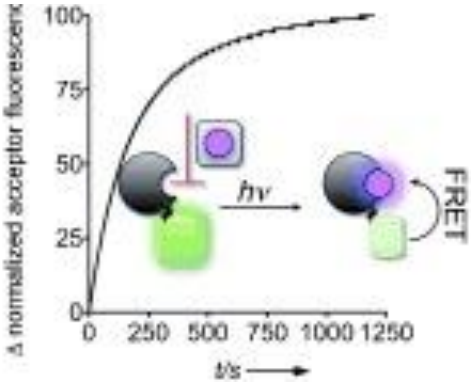


Figure 2.4: Acceptor fluorescence at 592nm was recorded by simultaneous excitation of the donor and uncaging of NPP at 366nm.[117]

2.2 Project Aims

Despite the wealth of research conducted in the field, including strong interactions observed between the α-carboxy terminus of the glycine residue of GSH and ESG to the binding pocket, no definitive evidence has been provided for the importance of the glycine residue α-carboxy terminus of the tripeptides for binding within the KefC pocket. As such, it was hypothesised that covalently caging GSH (**1**) and ESG (**2**) with the DMNB group, at this site (**Figure 2.6**), would prevent the ligand from fitting into the pocket, hence disrupting its ability to bind. Irradiation with light of an appropriate wavelength would cleave the caging group, with spatial and temporal control, revealing the free biomolecule and restoring the appropriate interactions for binding (**Figure 2.5**). The added spatial and temporal control would, in addition to binding, shed light on the effects of concentration, time delays and recovery of action in binding to Kef, following exposure to toxic electrophiles.

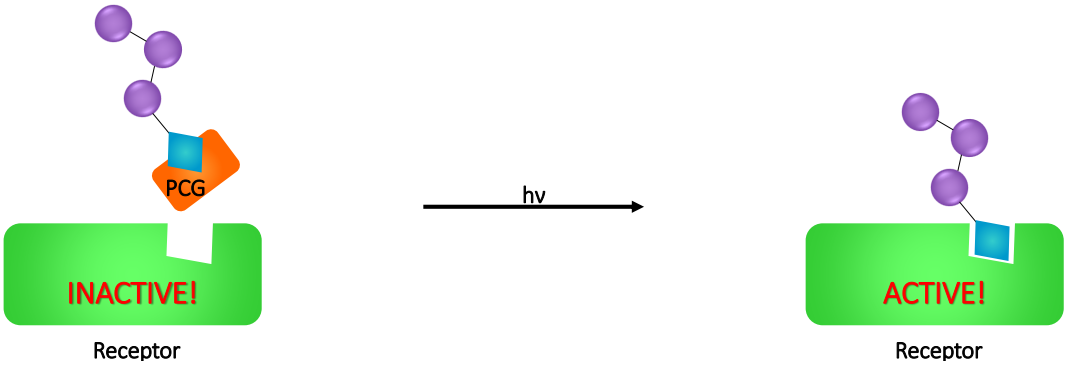


Figure 2.5: Photolysis of caged tripeptide to reveal active biomolecule capable of binding to KefC.

The commonly used DMNB caging group was selected due to its well-characterised nature and its ability to be uncaged at wavelengths longer than 300 nm. Moreover, the precursor compound is readily commercially available.

2.3 Synthesis of DMNB-Caged GSH and ESG

The synthesis of DMNB-caged GSH (**1**) and ESG (**2**) commenced with *N*-Boc protection of glycine (**129**) using 1.1 eq of Boc anhydride which allowed the reaction to proceed in 63% yield. Although this was not representative of typical amine Boc protections which usually proceed in $>$ 90% yield,[118] the reaction was readily performed

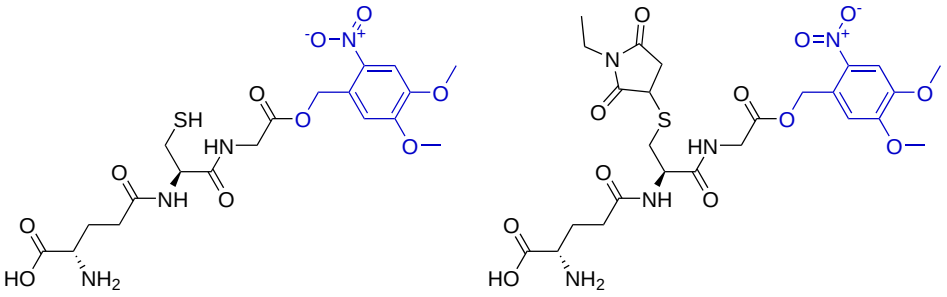


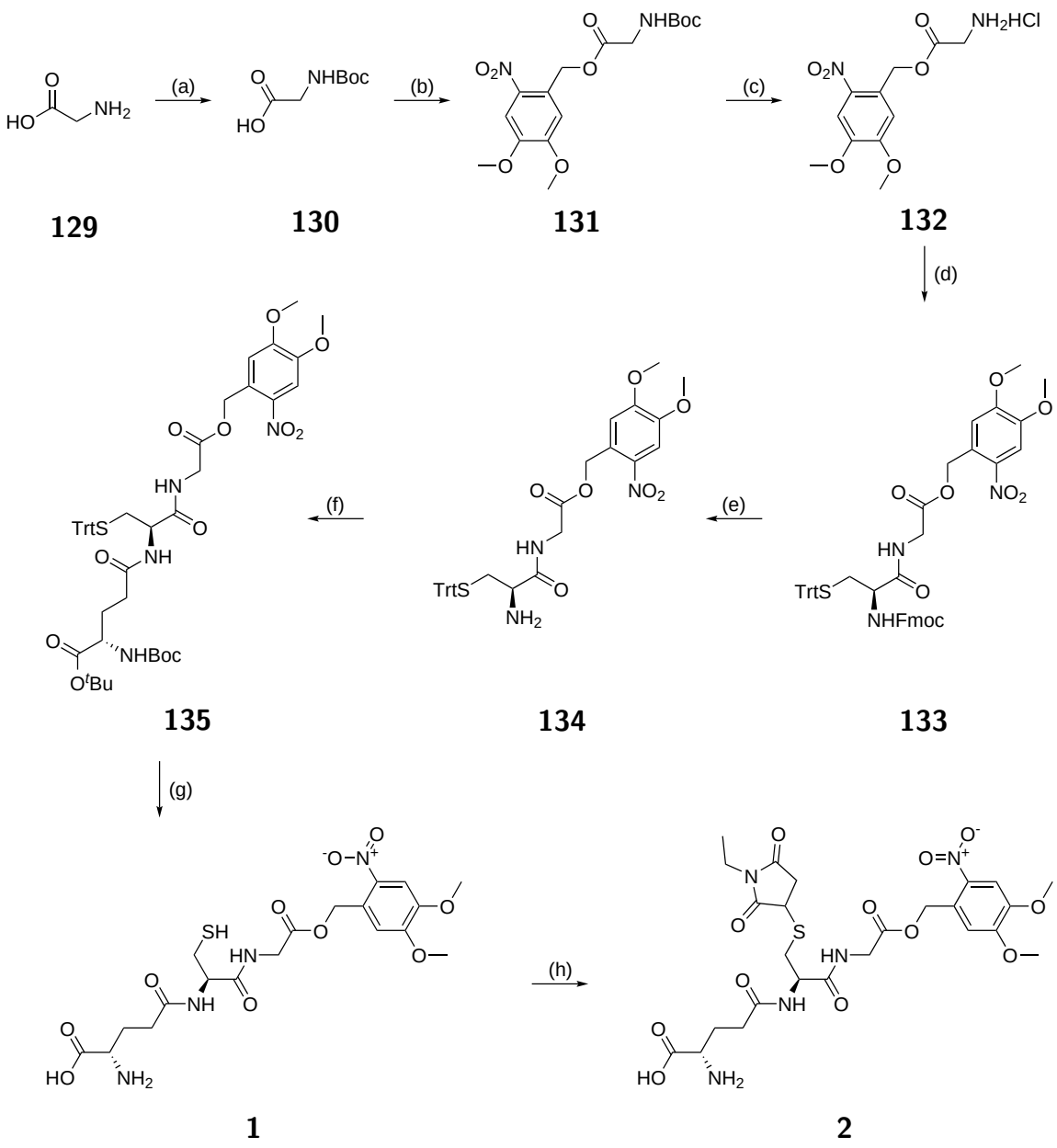
Figure 2.6: DMNB-caged GSH and ESG to probe the binding mode within the KefC KTN binding domain.

on a 10 g scale and thus further optimisation was not performed (**Scheme 2.1**).

The purified *N*-Boc glycine residue (**130**) was protected at the carboxylic acid terminal with the DMNB-photolabile caging group. Optimised conditions employing HBTU as the activating agent enabled the desired caged compound (**131**) to be isolated in 90% yield. This procedure was scalable to 5 g with consistent yields (**Scheme 2.1**).
It was opted to use HBTU due to the *in situ* release of OBt, following initial activation of the carboxylic acid group. The presence of OBt reduces the negative effects on yield of base-mediated epimerisation (for amino acids where R $\neq$ H) and the competing intramolecular side reaction, leading to the formation of the unreactive *N*-acylurea by-product, which often occurs when employing carbodiimide reagents. This occurs through displacement of the carbodiimide as the urea by-product, through formation of the less reactive activated ester.

Deprotection of the *N*-Boc group revealed the free amine hydrochloride salt (**132**), under acidic conditions using HCl. Using 1 M HCl in 1,4-dioxane, the reaction did not proceed to completion after 24 h at RT, and the product was afforded in only 51% yield. Increasing both the number of equivalents and the concentration of HCl used allowed the reaction to proceed to completion after 3 h, giving the desired DMNB-caged primary amine (**132**) in 97% yield (**Scheme 2.1**).
Following optimisation toward DMNB-caged glycine (**132**), the synthesis of the DMNB-caged dipeptide (**133**) by reaction with Fmoc-Cys(Trt)-OH was attempted. Optimised conditions employing HBTU as the activating agent allowed the desired caged dipeptide (**133**) to be isolated in 98% yield.

Fmoc deprotection was subsequently conducted to reveal the free α-amine of the



Scheme 2.1: Synthesis of DMNB-caged GSH (**1**) and ESG (**2**); Reagents & Conditions: (a) Boc_2O, NaOH, THF/H_2O, RT, 24 h, 63%; (b) DMNB-OH, HBTU, DIPEA, DMF, RT, N_2, 3 h, 90%; (c) 4 M HCl in 1,4-dioxane, RT, N_2, 3 h, 97%; (d) Fmoc-Cys(Trt)-OH, HBTU, DIPEA, DMF, RT, N_2, 18 h, 98%; (e) 20% piperidine in DMF, 0 °C, N_2, 1 h, 56%.; (f) Boc-Glu-O^{t}Bu, HBTU, DIPEA, DMF, RT, N_2, 24 h, 99%; (g) 50% TFA in CH_2Cl_2, Et_3SiH, RT, N_2, 24 h, 66%; (h) *N*-ethylmaleimide, NaOH, H_2O, RT, N_2, 3 h, 51%.

cysteine residue (**134**). However, this well-characterised reaction posed a considerable challenge to afford the free amine product in practical yields (**Table 2.1**).
Initially, this reaction was attempted under standard Fmoc deprotection conditions, employing 20% piperidine in DMF, however, no product could be isolated. This was due to degradation of the starting material and deprotection of the DMNB-photolabile caging group through hydrolysis of the ester bond.
It was postulated that the rate of Fmoc deprotection exceeded that of ester hydrolysis and thus a reduced reaction time was trialled. However, this conferred no additional advantage and no product was isolated but significant amounts of degradation products were observed.
The reaction was carried out at 0 °C to reduce the reaction rates. Fewer equivalents of base were also used in an attempt to reduce the amount of degradation and ester hydrolysis and instead allow the more favourable Fmoc deprotection to occur. The highest yielding conditions, 56%, were found to be 15 eq 20% piperidine in DMF, stirring at 0 °C for 1 h (**Table 2.1**).

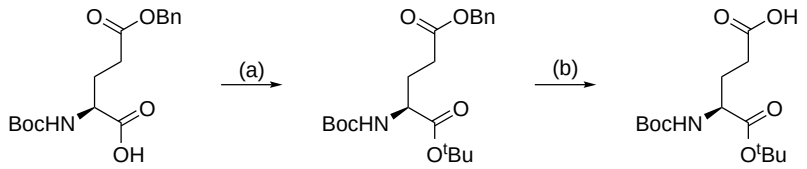
Table 2.1: Optimisation of Fmoc deprotection to afford DMNB-caged dipeptide bearing free amine on cysteine residue (**134**). [a]Hexanethiol was employed as a scavenger for the reaction.

Entry	Base	Equivalents	Solvent	T (° C)	Time	Yield (%)
1	20 % Piperidine	25.0	DMF	RT	24 h	-
2	20 % Piperidine	25.0	DMF	RT	5 min	-
3	20 % Piperidine	10.0	DMF	0	5 min	9
4	20 % Piperidine	10 + 10	DMF	0	1 h	46
5	20 % Piperidine	15	DMF	0	1 h	56
6	20 % DBU[a]	0.03	DMF	RT	24 h	30
7	50 % DIPEA	25.0	DMF	RT	24 h	-

Other bases, such as DIPEA and DBU, were also explored for the Fmoc deprotection reaction. The use of 20% DBU in DMF resulted in isolation of the desired Fmoc deprotected species (**134**) in 30% yield. However, this set of conditions required the use of the extremely pungent hexanethiol as an additive and the yield was only modest. 50% DIPEA on the other hand afforded no product and only degraded ester hydrolysis products were observed (**Table 2.1**).

In order to effect the synthesis of DMNB-caged GSH (**1**) and ESG (**2**), the glutamic acid amino acid residue (**138**) had to be synthesised with the *tert*-butyl and Boc-protected α-carboxylic acid and amine respectively, for coupling to the previously

synthesised DMNB-caged dipeptide (**134**) to afford the fully protected DMNB-caged GSH compound (**135**).



136 **137** **138**

Scheme 2.2: Synthesis of Boc-Glu-O^{t}Bu (**138**); Reagents & Conditions: (a) Boc_2O, DMAP, ^{t}BuOH, RT, N_2, 2 h, 79%; (b) 10% Pd/C, MeOH, RT, H_2, 3 h, 80%.

The *tert*-butyl ester protection of the free α-carboxylic acid was attempted with *tert*-butanol, using DCC as the activating agent in an ester coupling. Although the product (**137**) could be isolated in 38% yield, this reaction was often poor yielding and not reproducible. Moreover, the possibility of epimerisation and yield erosion due to formation of the *N*-acylurea by-product also presented a concern. Alternative conditions were sought to effect this transformation; employing Boc anhydride and DMAP, stirring in *tert*-butanol led to isolation of the *tert*-butyl ester protected glutamate residue (**137**) in 79% yield (**Scheme 2.2**).
Palladium catalysed hydrogenolysis of the benzyl ester under an atmosphere of H_2, subsequently afforded the desired carboxylic acid (**138**) in 80% yield (**Scheme 2.2**).

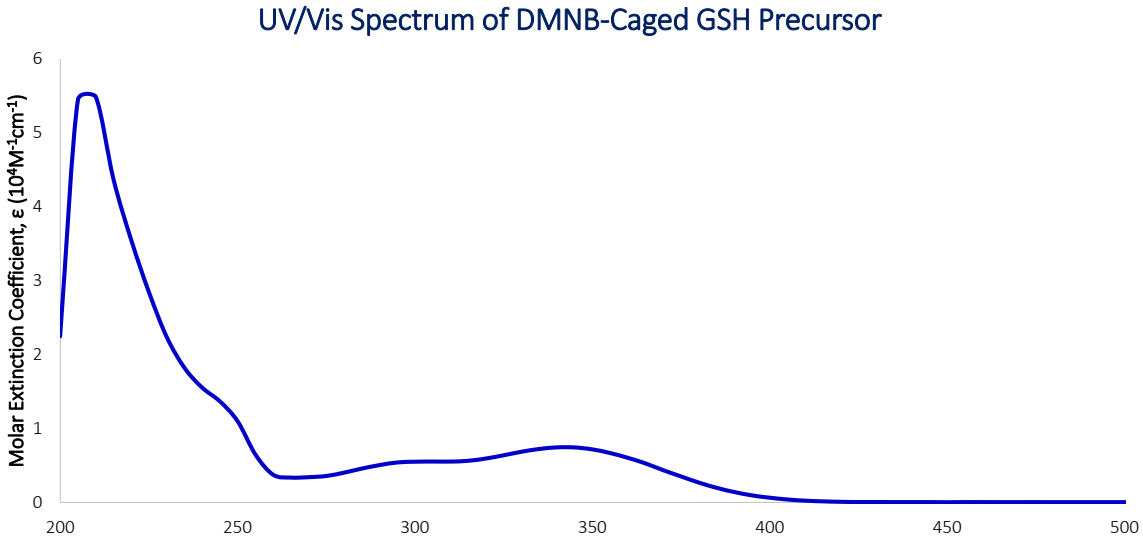
With both fragments (**134**) and (**138**) in hand, synthesis of the tripeptide could be attempted. Initial activation of the free carboxylic acid of the glutamic acid residue (**138**) with HBTU and subsequent trapping using the DMNB-caged dipeptide moiety (**134**), allowed isolation of the desired fully protected tripeptide (**135**) in near quantitative ($> 99\%$) yields (**Scheme 2.1**).

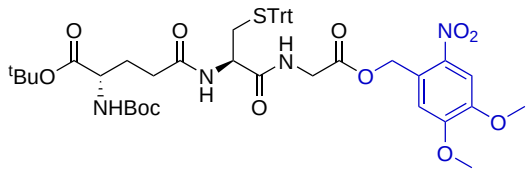
Removal of the acid labile protecting groups was achieved by treatment with 50% TFA in CH_2Cl_2, enabling the desired DMNB-caged GSH (**1**) to be isolated in 66% yield (**Scheme 2.1**), whilst synthesis of DMNB-caged ESG (**2**) was accomplished by conjugate addition of the mercaptan to *N*-ethylmaleimide under basic conditions of aqueous NaOH, yielding the product (**2**) in 51% (**Scheme 2.1**).

2.4 Photolysis Studies

Following successful synthesis of DMNB-caged GSH (**1**) (111 mg) and ESG (**2**) (37.9 mg), photolysis and uncaging of the DMNB photolabile caging group to reveal the

free carboxylic acid of the glycine residue was demonstrated, which would then be available for binding to the KefC KTN domain.





135

Entry	Conc (mM)	λ_{max} (nm)	Transition	A	ε ($M^{-1}cm^{-1}$)
1	0.04	340	n – π*	0.298	7447

Figure 2.7: UV/vis absorption spectrum of DMNB-caged protected GSH precursor (**135**) [λ_{max} = 340 nm (n - π^*); Concentration = 0.04 mM [MeOH].

As only limited amounts of the final compounds had been synthesised and were required for biological testing, it was opted to conduct the photolysis experiments on the fully protected DMNB-caged precursor species (**135**). Moreover, as it was intended to monitor the photolysis reaction by HPLC, both the caged and uncaged compounds were required to bear a chromophore, which the trityl group was suitable for.

The UV/vis absorption spectra (**Figure 2.7**) was measured to identify the appropriate wavelength with which to irradiate the DMNB-caged GSH analogue (**135**) and effect

photorelease of the tripeptide. To minimise UV damage to biological material and to increase penetration, only wavelengths longer than 300 nm were considered suitable. The maximum absorbance was determined to lie at λ_{max} = 340 nm (**Figure 2.7**) for the n - π^* transition, which is important for the photolysis of the DMNB-photolabile caging group. Consequently, the photolysis experiments were performed with light of 350 nm wavelength with an optical output power of 8 W and radiant intensity of 25,620 mW/sm.
Unfortunately, the DMNB-caged molecule (**135**) was found to be unstable under the reverse phase HPLC conditions used to monitor the photolysis reaction. This instability was attributed to deprotection of the acid-labile *S*-trityl moiety due to the presence of TFA in the eluent. The photolysis experiments, for proof of principle, were thus monitored by **^{1}H NMR** analysis, concentrating on the changes in the shifts of characteristic peaks to determine the photolysis and hence cleavage of the DMNB-photolabile caging group. The other protecting groups present in the caged tripeptide, including the *tert*-butyl ester, *N*-Boc protected amine and *S*-trityl moiety were thought to have no effect on the photolysis characteristics of the DMNB photolabile caging group and hence the results obtained from the photolysis of the DMNB-caged GSH analogue (**135**) could be extended to DMNB-caged GSH (**1**) and ESG (**2**).

Examining the aromatic region from 7.50 - 7.00 ppm of the DMNB-caged compound (**135**), it could be seen that over time, the doublet peak belonging to the aromatic trityl proton at 7.34 ppm diminished, whilst a new doublet peak appeared at 7.40 ppm. The same was observed for the triplet aromatic peak of the trityl moiety at 7.26 ppm, which shifted to a new triplet at 7.29 ppm. In addition, the peak belonging to the aromatic proton on the DMNB ring at 7.06 was also observed to diminish (**Figure 2.8**).

For the region between 4.30 - 3.80 ppm, a shift of the doublet of doublet peak belonging to the α-proton of the glutamic acid residue from 4.25 to 4.22 ppm was observed. A similar change was also observed for the CH_2 protons of the glycine residue, shifting from 4.01 to a multiplet between 4.00 - 3.85 ppm. This region of the **^{1}H NMR** spectra also showcased the decrease in intensity of the two methoxy peaks of the DMNB-ring and the growth of new singlets at 3.86 and 3.84 ppm (**Figure 2.9**).

The last region of the **^{1}H NMR** spectra with characteristic peaks, fell between 2.70 - 1.80 ppm. Here, marginal shifts could be observed for the CH_2 peaks of glutamic acid, one pair lying at 2.62 and 2.53 which shifted slightly to 2.64 and 2.56, the other at

2.05 and 1.83 ppm which shifted to 2.07 and 1.85 ppm, respectively. In addition, a shift was also observed in the CH_2 triplet of the cysteine residue from 2.28 ppm to 2.31 ppm (**Figure 2.10**).

The identity of the uncaged tripeptide was confirmed to be that of the desired product following cleavage of the DMNB-photolabile caging group, after 8 h of irradiation at 350 nm, by mass spectrometry.

The **^{1}H NMR** spectra integrals were used to calculate the change in composition of the caged and uncaged species over the course of the reaction (**Figure 2.11**). Following 8 h of irradiation, the amount of caged material had dropped to 18%, with a first order rate constant $k_{irrad} = 0.156$ s^{-1}, accompanied by 80% released of the uncaged tripeptide with a rate constant $k_{release} = 0.147$ s^{-1}.
Owing to the light sources available for the photolysis studies, long irradiation times were required to effect uncaging of the tripeptide. This issue was addressed in later photolysis studies where the use of higher powered LED light sources substantially reduced irradiation times.

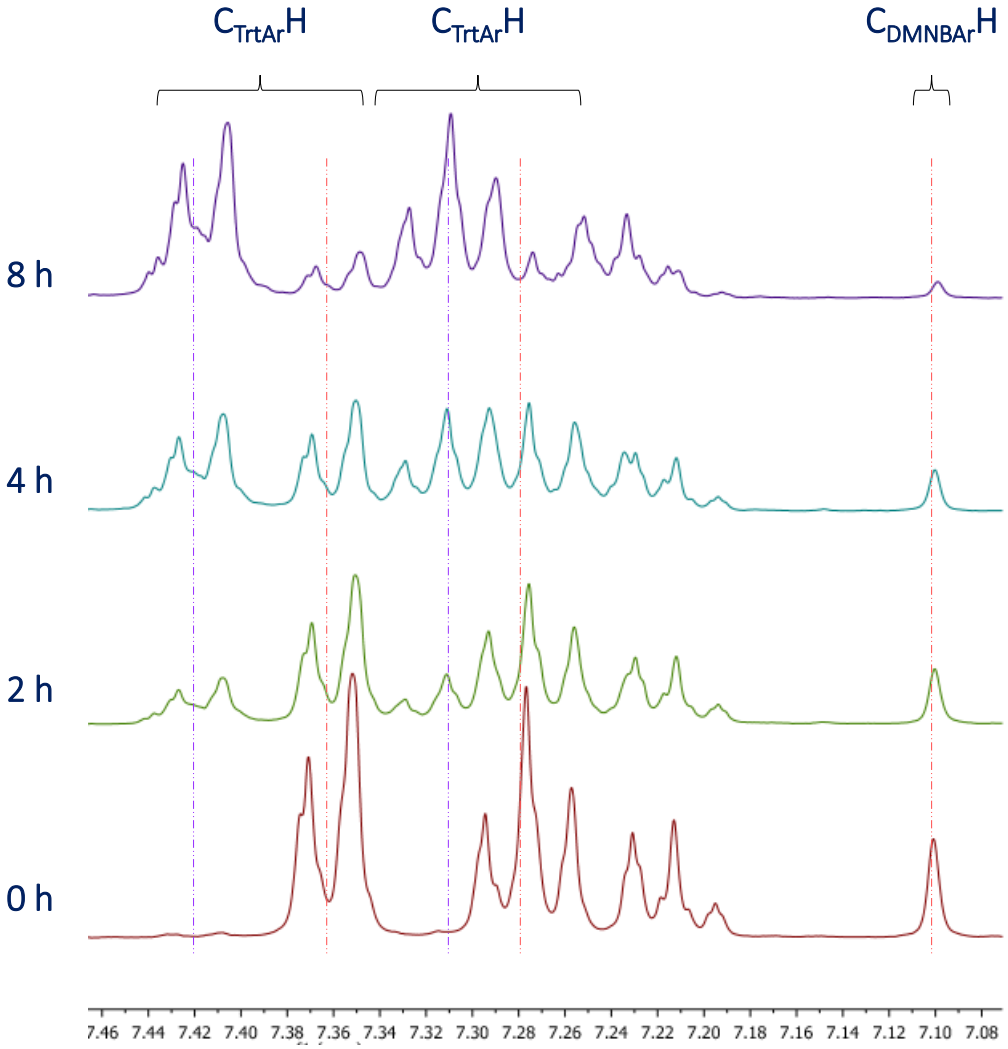


Figure 2.8: Partial **^{1}H NMR** spectra 7.50 - 7.00 ppm; Spectra recorded at 0 h, 2 h, 4 h and 8 h after irradiation at 350 nm with an optical output power of 8 W and radiant intensity of 25,620 mW/sm; Concentration = 11.1 mM [MeOD]; (Pink lines highlight disappearance of peaks of starting material; Purple lines highlight appearance of peaks of product).

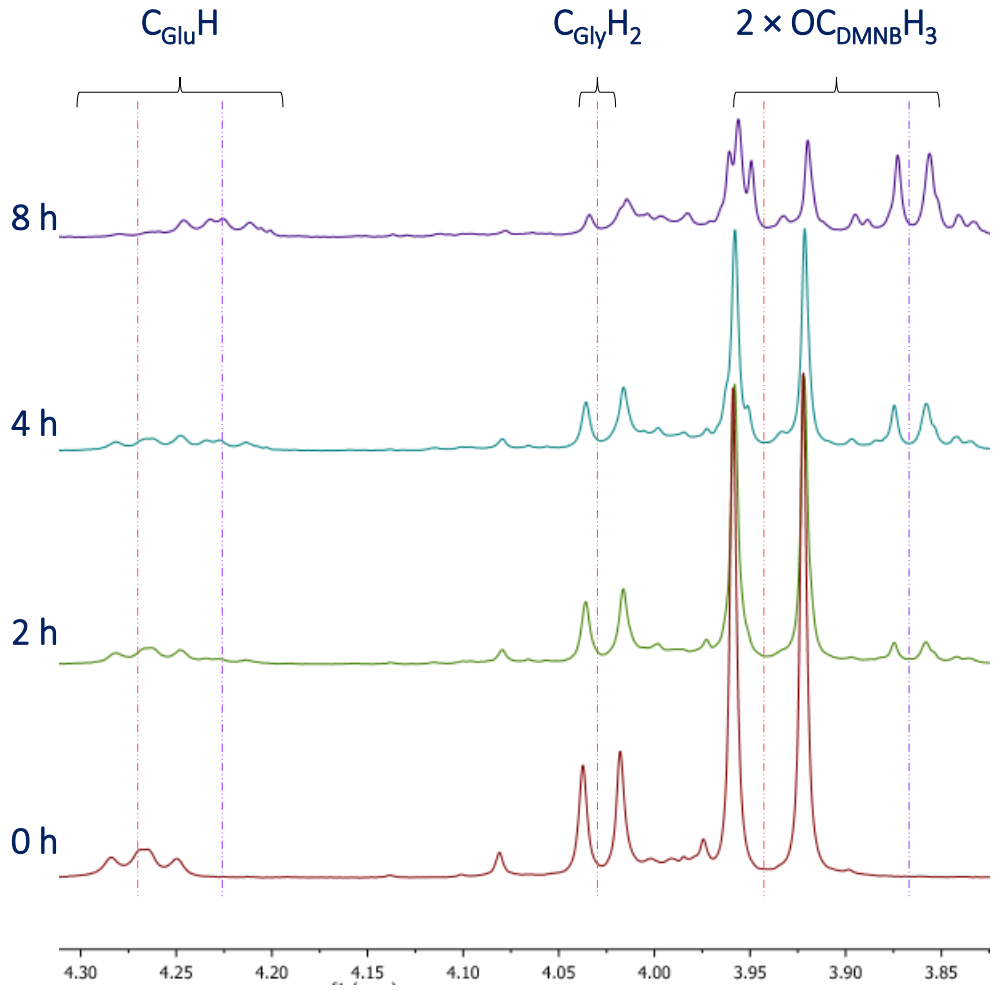


Figure 2.9: Partial **^{1}H NMR** spectra 4.30 - 3.80 ppm; Spectra recorded at 0 h, 2 h, 4 h and 8 h after irradiation at 350 nm with an optical output power of 8 W and radiant intensity of 25,620 mW/sm; Concentration = 11.1 mM [MeOD]; (Pink lines highlight disappearance of peaks of starting material; Purple lines highlight appearance of peaks of product).

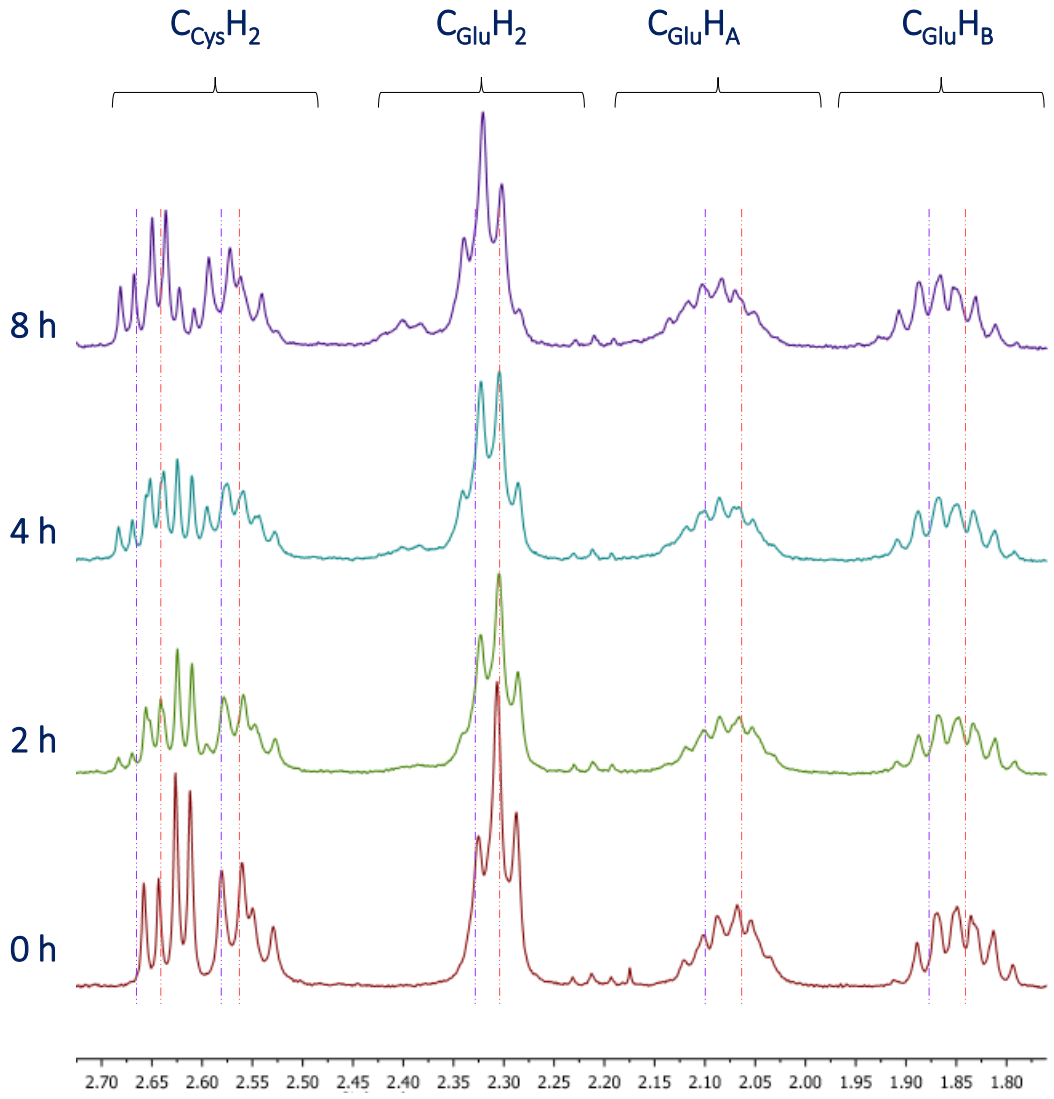
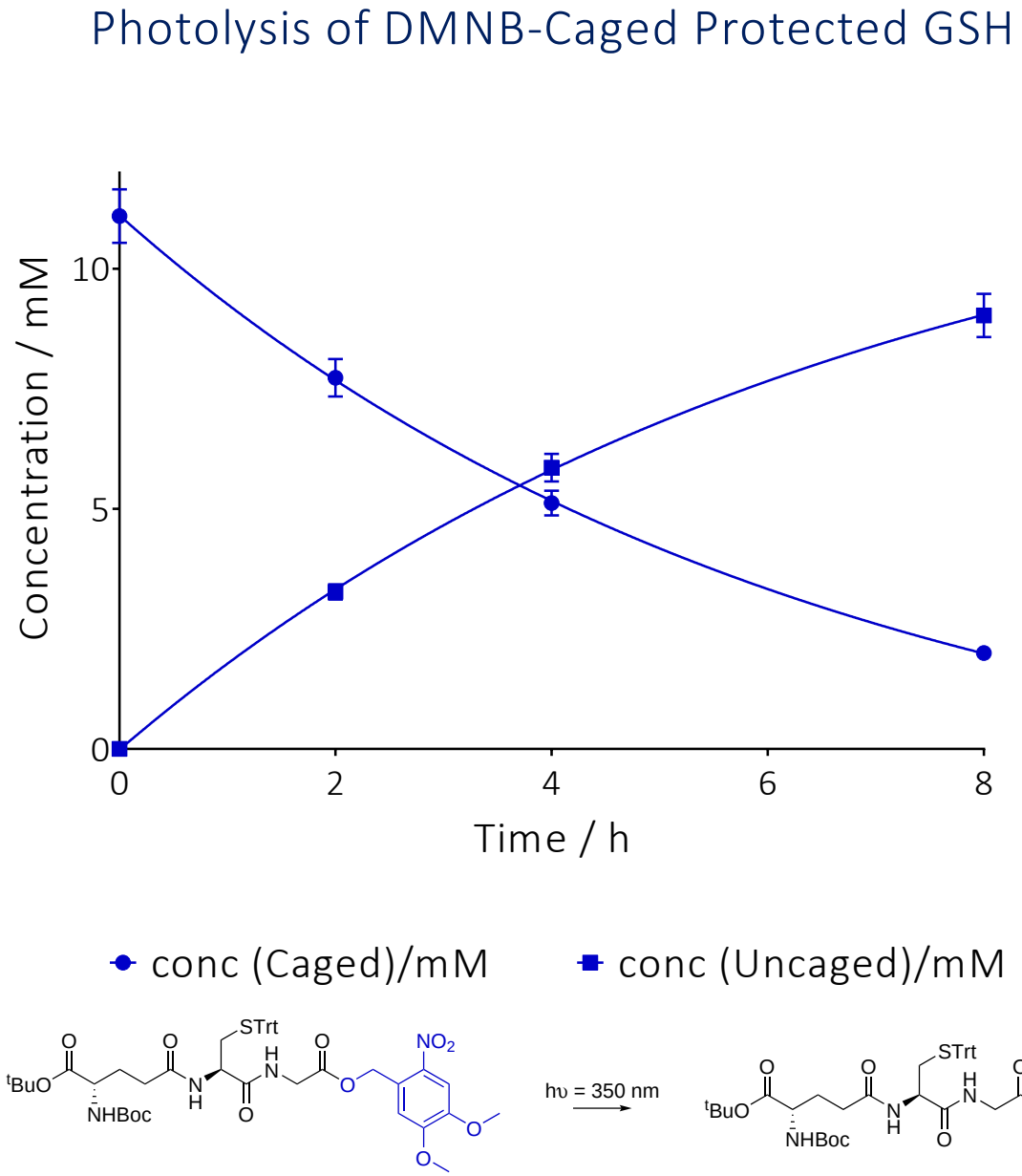


Figure 2.10: Partial **^{1}H NMR** spectra 2.70 - 1.80 ppm; Spectra recorded at 0 h, 2 h, 4 h and 8 h after irradiation at 350 nm with an optical output power of 8 W and radiant intensity of 25,620 mW/sm Concentration = 11.1 mM [MeOD]; (Pink lines highlight disappearance of peaks of starting material; Purple lines highlight appearance of peaks of product).



Entry	λ_{irrad} (nm)	k_{caged} (s^{-1})	N_{caged}	R^2_{caged}	$k_{uncaged}$ (s^{-1})	$N_{uncaged}$	$R^2_{uncaged}$
1	350	0.155	4	1.00	0.149	4	1.00

Figure 2.11: Composition of caged and uncaged protected GSH following irradiation at 350 nm with an optical output power of 8 W and radiant intensity of 25,620 mW/sm, as calculated using **^{1}H NMR** integrals.

2.5 Summary and Future Work

The carboxylic acid moiety of the terminal glycine residue of GSH and ESG was thought to be imperative to the binding of these molecules in the KefC KTN-domain. To investigate this hypothesis, both DMNB-caged GSH (**1**) and ESG (**2**) with the photolabile caging group attached *via* an ester linkage at the carboxylic acid of the glycine residue were successfully synthesised. The presence of the DMNB caging group at this position was hypothesised to result in inhibition of binding. Further to this, the DMNB-caged GSH analogue (**135**) was demonstrated to be successfully photolysed to reveal the free carboxylic acid residue following irradiation at 350 nm. The experiments were monitored by **^{1}H NMR** analysis and the final product confirmed to be that of the uncaged tripeptide by mass spectrometry.

To supplement this work, further photolytic studies could be performed, analysing the samples using LCMS-UV, for a greater number of time points. In addition, different aqueous buffer and solvent conditions could be trialled as well as investigating the concentration and temperature dependence of the photolysis reaction.

Biological testing of the DMNB-caged GSH (**1**) and ESG (**2**) are currently underway with collaborators and it is hoped that these caged compounds will help provide conclusive evidence of the binding mode in the KefC KTN-domain.

Chapter 3

Caged Amino Acids Towards the Development of Photoactive Tools for the Analysis of Protein Post-Translational Modification

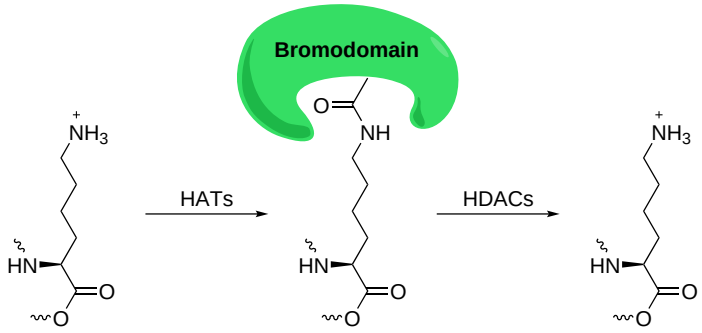
3.1 Introduction

Biological systems are often extremely complex and despite the added spatial and temporal control offered, use of a single PCG is insufficient. In such instances, the use of more than one caging group, particularly in a wavelength orthogonal manner, can provide more in depth information about the system. This is particularly true of the relationship between concurrently occurring phenomena in biological systems, such as that of protein post-translational modifications (PTMs).

PTMs modulate protein function in most eukaryotes and play a key role in a diverse range of cellular functions. Through this biochemical mechanism, in which amino-acid residues in a protein are covalently modified, complexity of several orders of magnitude greater than the coding capacity of the genome can be imparted to the eukaryotic proteomes. Understanding the functional significance of PTMs in a biological context relies on the identification, characterisation, and mapping of these modifications to specific amino acid residues on proteins. PTMs have been linked to many life-threatening diseases, including cancer,[119] cardiovascular,[120] and neurodegenerative disorders.[121] An in-depth understanding of protein PTMs is thus important, not only for gaining knowledge of a wide array of cellular functions but also towards developing drug therapies for many diseases.[122]

Regulation of most protein PTMs is usually controlled by enzymes that directly alter the chemical makeup of the protein. These enzymes can be proteases, transferases, or enzymes that remove groups. PTMs are known to act both alone and in combination to regulate nearly all aspects of protein function. Deciphering how PTMs are coordinately regulated is of fundamental importance to our understanding of chemical biology. In all, more than 400 discrete types of modifications can occur, and to date, more than 90000 individual PTMs have been identified through biochemical and biophysical analysis.[123] A select few major modifications, which have received significant attention by the research community in the past few decades, will be discussed below.

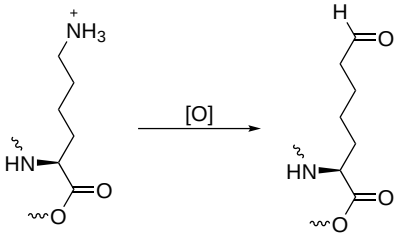
3.1.1 Acetylation



Scheme 3.1: Histone acetylation and deacetylation of lysine mediated by HATs and HDACs; Bromodomain reader of acetylated histones.

The acetylation of lysine residues is one of the most common PTMs; in excess of 3500 sites for lysine acetylation on both histone and non-histone proteins have been identified.[124] Histone acetylation and deacetylation on the *N*-terminal tail of the lysine residue of histone proteins, facilitated by histone acetylase (HAT) and histone deacetylase (HDAC) enzymes, are of particular interest due to their role in gene regulation (**Scheme 3.1**). The acetylation status of histones mediate protein-protein interactions (PPIs) *via* bromodomains resulting in the regulation of various transcription factors, molecular chaperones and cellular metabolism,[125] with significant impact on cellular homeostasis.[126] Acetylation of glutamic acid and aspartic acid in prokaryotes has also been observed and the conversion of glutamic acid to *N*-acetylglutamic acid is an important intermediate step of ornithine synthesis in bacteria.[127]

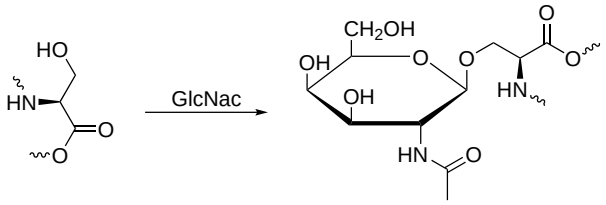
3.1.2 Carbonylation



Scheme 3.2: Carbonylation of lysine residue, resulting in formation of non-functional proteins.

Protein carbonylation has received significant attention as an indicator of oxidative or genotoxic stress.[128] Carbonylation of amino acids including proline, arginine, lysine, threonine, glutamate and aspartate is irreversible and may result in the formation of non-functional proteins (**Scheme 3.2**), which in turn leads to many diseases, especially those that are influenced by the state of oxidative stress in a cell.[129] Protein carbonylation may also play a role in protein quality control. Carbonylated proteins are more susceptible to proteolytic degradation than non-oxidised proteins and thus the rapid carbonylation of mistranslated or aberrant proteins may act as a signal ensuring damaged proteins enter degradation pathways.[128]

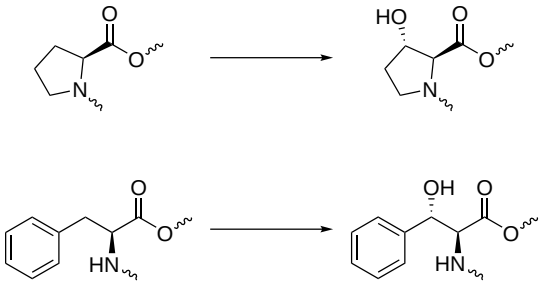
3.1.3 Glycosylation & Glycation



Scheme 3.3: *N*-acetylgalactosamine *O*-glycosylation of serine residue on protein.

Glycosylation and glycation involve the addition of sugar moieties to proteins (**Scheme 3.3**). Glycosylation is enzyme-directed, while glycation refers to random events that mostly result in the formation of defective or non-functional biomolecules. Glycosylation plays a central role in protein localisation, protein-protein interactions (PPIs), structural stability of the cell, immune responses, and modulating of cell signalling.[130] Therefore, dysfunctional glycans formed in the cell could lead to diseases including cancer,[131] liver cirrhosis,[132] diabetes,[133] and exacerbated HIV infection.[134]

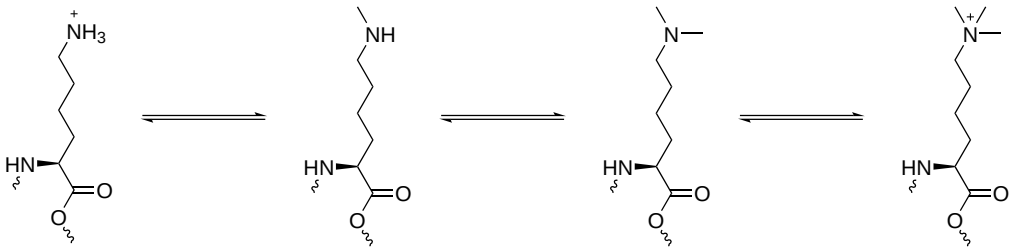
3.1.4 Hydroxylation



Scheme 3.4: Hydroxylation of proline and phenylalanine residues.

Hydroxylation, an important detoxification reaction in the cell with prominent relevance to cellular physiology, is mostly facilitated by the group of enzymes called hydroxylases (**Scheme 3.4**). Some cancers or metabolic disorders, such as scurvy, are linked to a lack of proline hydroxylation due to ascorbate deficiencies.[135] Amino acids possessing aromatic side-chains such as phenylalanine [136], tyrosine [137] and tryptophan [138] are also known to undergo hydroxylation (**Scheme 3.4**).[139] Hydroxylation of amino acids occurs in the liver, central nervous system, adrenal glands and brain. Several genetic diseases, such as phenylketonuria (PKU) and hyperphenylalaninemia, are linked to a lack of hydroxylation on aromatic amino acids.[140] Tyrosine hydroxylase is used as a molecular target to treat hypertension,[141] whilst tryptophan hydroxylation, catalysed by tryptophan hydroxylase, is a critical regulatory step in the production of the important neurotransmitter, 5'-hydroxytryptophan (5-HT, serotonin).[142]

3.1.5 Methylation

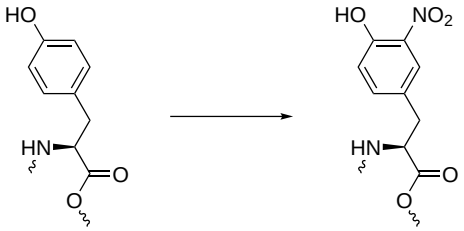


Scheme 3.5: Lysine mono-, di-, and tri-methylation.

The impacts of protein methylation are wide spread, from embryonic to postnatal developmental stages, and in numerous physiological conditions including cancer.[143]

Lysine and arginine are the most commonly methylated amino acid residues with lysine methylation being of particular prominence owing to its role in epigenetics and chromatin remodelling (**Scheme 3.5**).[144] Histone methyltransferases (HMTs) or histone lysine methyltransferases (HKMTs) specifically target lysine residues in histones, leading to transcriptional activation or inhibition, thus playing a regulatory role in gene expression.[145] The role of methyltransferases in various diseases, such as colorectal,[146] ovarian,[147] and lung cancer,[148] has also been widely noted.[149]

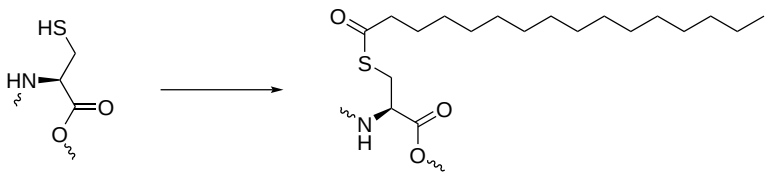
3.1.6 Nitration



Scheme 3.6: Tyrosine nitration in response to nitrating agent or oxidative stress.

Protein nitration occurs in response to protein oxidation reactions (**Scheme 3.6**). Reversible and stable nitration is initiated when amino acids are exposed to nitrating agents, such as peroxynitrite formed by combination of nitric oxide and superoxide,[150] or oxidative stress.[140] Formation of protein nitroderivatives is another classic hallmark of exposure to genotoxic stress.[151] Nitroproteins, of which nitrotyrosines are the primary product, are thought to be involved in a plethora of diseases ranging from neurodegenerative diseases to lung diseases,[152] inflammation,[153] coronary artery disease,[154] and cancer.[155]

3.1.7 Palmitoylation

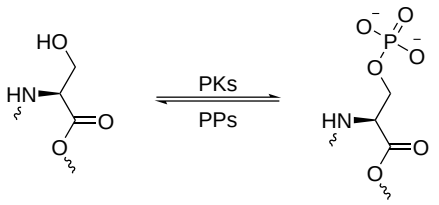


Scheme 3.7: *S*Palmitoylation of cysteine residue on protein.

Palmitoylation compromises the covalent attachment of fatty acids, mainly palmitic acid, to the protein molecule, making it more hydrophobic and most commonly

occurs as a cysteine thioacylation modification (**Scheme 3.7**). This class of PTMs is reversible in nature and is involved in cell trafficking, membrane stimuli, and PPIs.[156] Palmitoylation is also closely involved in the neural inflammatory response including demyelinating diseases, as well as T-cell autoimmune responses.[157] Numerous diseases and disorders, such as diabetic vascular diseases, have also been linked to reduced or dysfunctional palmitoylation.[158]

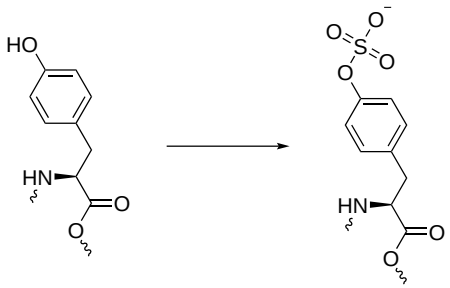
3.1.8 Phosphorylation



Scheme 3.8: Phosphorylation catalysed by PKs and dephosphorylation catalysed by PPs of serine residue of protein.

Phosphorylation is the addition of a phosphate group to an amino acid residue (**Scheme 3.8**). It is mediated by protein kinases (PKs) and is one of the primary reversible PTMs involved in the regulation of cellular metabolism, PPIs, enzyme reactions, and protein degradation for a myriad of proteins. These processes are important for intracellular signalling cascades. Dephosphorylation, the removal of phosphate groups, is catalysed by various phosphatases (PPs).[159] The maintenance of cellular homeostasis is dependent on the proper balance of action between the PKs and PPs. Phosphorylation has been implicated in the progression of cancers and neurological diseases, with serine, threonine and tyrosine being the most commonly observed phosphorylated amino acid residues.[160]

3.1.9 Sulfation



Scheme 3.9: *O*-Sulfation of tyrosine residue of protein.

N- and *O*-sulfation, the addition of a sulfate group (**Scheme 3.9**), is a protein PTM commonly observed on membrane and secreted proteins.[161] Sulfated proteins have been implicated in PPIs, G-protein-coupled receptor signalling, chemokine signalling, and immune responses,[162] however, their precise role in cellular regulation still remains elusive.[163]

3.1.10 Ubiquitination

Ubiquitination, a highly dynamic, coordinated, and multi-step enzymatically-catalysed PTM that targets proteins for degradation and recycling occurs by covalent attachment of a small regulatory protein tag, ubiquitin (Ub).[164] Depending on the substrate type and localisation, proteins targeted for degradation can be mono-Ub or poly-Ub. This PTM plays a critical role in virtually all cellular process. Ubiquitination's involvement in modulating diverse cellular functions including cell proliferation and differentiation, autophagy, apoptosis, immune response, DNA repair, neural degeneration, myogenesis, and stress response, gives it a vital role in almost any disease or disorder.[165] It affects the outcome of many life-threatening diseases like cancer, neurodegenerative disorders, HIV infection, Herpes, and liver diseases.[166]

3.2 Current Methods of Studying PTMs

Given the pivotal role of PTMs in the maintenance of cellular homeostasis, a constant effort exists to develop novel, highly sensitive, and sophisticated tools and techniques for the identification of PTMs. Some of these are targeted towards identifying specific PTMs, such as the modification of histone tails, whilst others are more comprehensive, like surface-enhanced Raman spectroscopy and mass spectrometry.[167] A novel technology known as "multidimensional protein identification technology" (MudPIT), a combinatorial method of chromatography in conjunction with mass spectrometry, has been efficient in discovering global PTMs, i.e. PTMs that can occur on all modifiable residues in proteins. Traditional biochemical methods like Western blotting and SDS-PAGE are widely used to confirm the high-throughput results obtained from the spectroscopic methods and for investigating the *in vivo* biological significance of PTMs. In addition, successful attempts in developing *in silico* algorithms that can reliably predict various PTMs in a given protein sample have been achieved. Other PTMs like biotinylation, which attach a prosthetic group to a protein, are frequently used to understand PPIs that result from the changes in three-dimensional structures of protein.

3.3 Y-Box Binding Protein 1

The multifunctional vertebrate Y-box binding protein 1 (YBX1) belongs to a large family of proteins with an evolutionally ancient cold shock domain (CSD) and is involved in a number of cellular processes, ranging from proliferation to differentiation, and stress response. A DNA- and RNA-binding protein possessing properties of a nucleic acid chaperone, it interacts with a great variety of other proteins and is involved in almost all DNA- and mRNA-dependent processes including DNA replication and repair, transcription, pre-mRNA splicing, and mRNA translation.[168]
Human YBX1 is a 35.9 kDa protein with an extremely high isoelectric point of approximately 9.5, consisting of 324 amino acid residues; the predominating ones being arginine (11.7%), glycine (12%), proline (11%), and glutamic acid (8.3%).[169]

YBX1 is considered to be one of the most indicative markers of malignant tumours and a possible therapeutic target for cancer due to its upregulation in tumour cells.[168]
For example, YBX1 has been observed to be overexpressed in about 40 % of breast cancers but absent in normal breast tissue.[170]
In addition, YBX1 nuclear localisation is thought to be an early marker of multidrug resistance of malignant cells. By passing from the cytoplasm to cell nucleus, YBX1 activates transcription of genes of several protective proteins, including proteins that provide multidrug resistance of cells. When involved in DNA repair in the nucleus, YBX1 also enhances resistance of cells to xenobiotics and ionizing radiation.[171]
An increase of YBX1 level in the cytoplasm prevents oncogenic cell transformation and simultaneously promotes transformation of differentiated epithelial cells into mesenchymal ones with higher migration activity. This is favourable for cell spreading in the organism and metastasis, leading YBX1 to be considered a marker of metastasis in remote organs.[172]

YBX1 has emerged as a protein undergoing substantial PTMs with many PTMs having been identified. Several of these PTMs have been linked with oncogenic activity. This is the case for phosphorylation at S102.[173] Ubiquitylation of YBX1 is thought to lead to proteasomal degradation where dysregulation may contribute to oncogenic capability.[174] Acetylation of K81 may affect interaction of YBX1 with p53 (gene) and hence regulation of YBX1 nuclear localisation may be affected leading to disruptions to cell function,[175] whilst methylation of YBX1 may play an important role in regulation of interaction with NF-kB (transcription factor), contributing to dysfunction in cancer cells.[176]

YBX1 presents an exciting research area for further exploration where the use of PCGs would provide the necessary level of spatial and temporal control for the elucidation and characterisation of PTMs. The unique PTMs of YBX1 could represent a disease-specific signature which may help with oncogenic diagnosis and treatment. With the identification of numerous potential PTMs sites on the protein, the biological role of each confirmed site could be further examined in cancer or other YBX1 related diseases.

Discovery and analysis of the enzymes that may catalyse the specific modifications also presents an additional avenue of inquiry; enzymes are often better targets in the development of drugs to treat cancer. The study of PTMs of YBX1 will not only lead to a better understanding of the mechanisms underlying biological processes regulated by YBX1, but may also help to develop effective pathway-specific therapeutic strategies against YBX1 in different types of cancer and YBX1-related diseases.

3.4 Project Aims

Whilst there exists a continuum in the development of novel tools to study PTMs, they lack the spatial and temporal control that the use of PCGs can offer. Whilst the use of a single PCG has previously been used to investigate PTMs,[96], [95], [93], elucidation of the complex processes of protein PTMs would greatly benefit from the use of two PCGs in a wavelength orthogonal fashion. This approach would have the added advantage of both spatial and temporal control over conventional methods, as well as to obtain information regarding PTMs of amino acid residues at more than one site of the same protein or on different protein chains.

PTMs are most prevalent as covalent modifications at the side chain termini of amino acids. Thus, it was sought to demonstrate the use of wavelength orthogonal PCGs as tools for studying PTMs by attaching the PCGs at the side chains of amino acids bearing different functional groups. Aspartic acid (**140**) and glutamic acid (**141**), bearing carboxylic acids, serine (**142**), bearing a hydroxyl group, tyrosine (**143**), bearing a phenol ring and lysine (**144**), bearing a primary amine, were chosen as the amino acids to be caged (**Figure 3.1**).

The premise of this work is that when caged, the amino acid residues would no longer be available to PTM. Upon irradiation, the free side chain functional group would be released, enabling protein PTM to occur at this site. The use of two wavelength orthogonal PCGs would give rise to an increase in spatio-temporal control as two amino acid residues, on the same or different protein chains could be concurrently

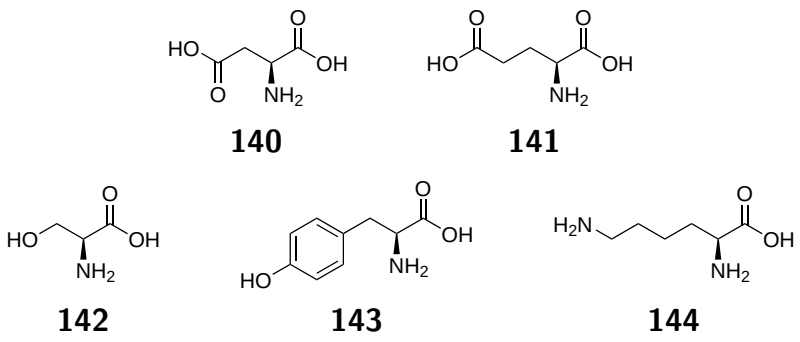


Figure 3.1: Selected amino acids to be caged bearing differing side chain functionalities.

caged. Irradiation with specified wavelengths of light would allow selective uncaging, in any order, to reveal the free side chain functional group of the amino acid residue on which PTMs and their effects could be observed. This would enable more in depth analysis of the position and time-dependence of these PTMs, as well as their interrelation to one another, providing a more comprehensive understanding of PTMs, which have been linked to numerous disease states (**Figure 3.2**).

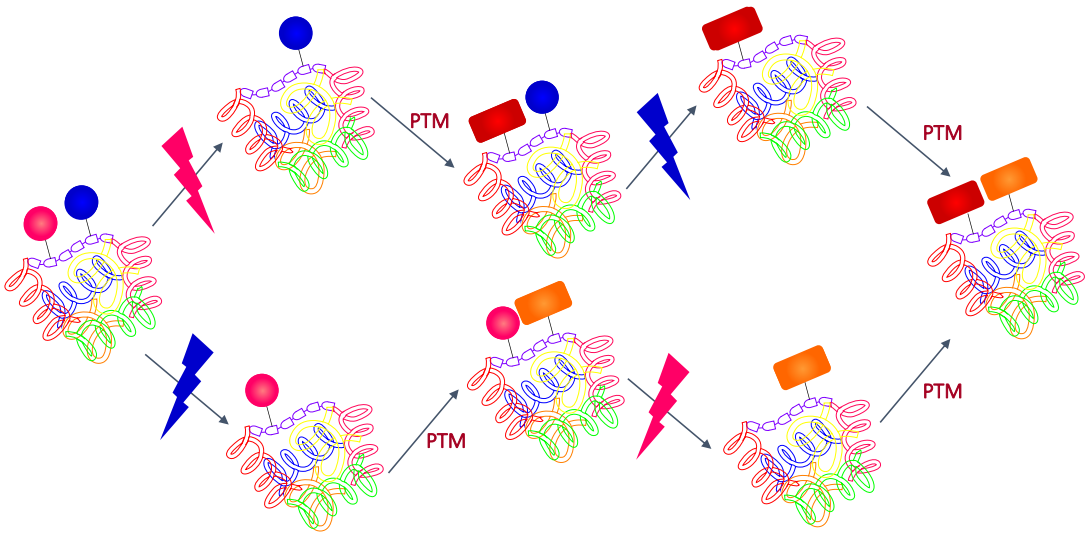


Figure 3.2: Application of wavelength orthogonal PCGs to the study of protein PTMs.

3.4.1 Prospective Caging Groups

A plethora of PCGs exist and thus to obtain a starting point of potential PCGs for the development of an orthogonal pair of caging groups, capable of cleavage above 300 nm, the work of Bochet *et. al.*, who had characterised the photophysical properties

of several well established PCGs as caged silanes on surfaces,[101] was referred to. In order to limit damage to biological specimen and increase penetration through cellular media and tissue, an additional constraint was imposed that the wavelength of irradiation for uncaging had to be longer than 300 nm.

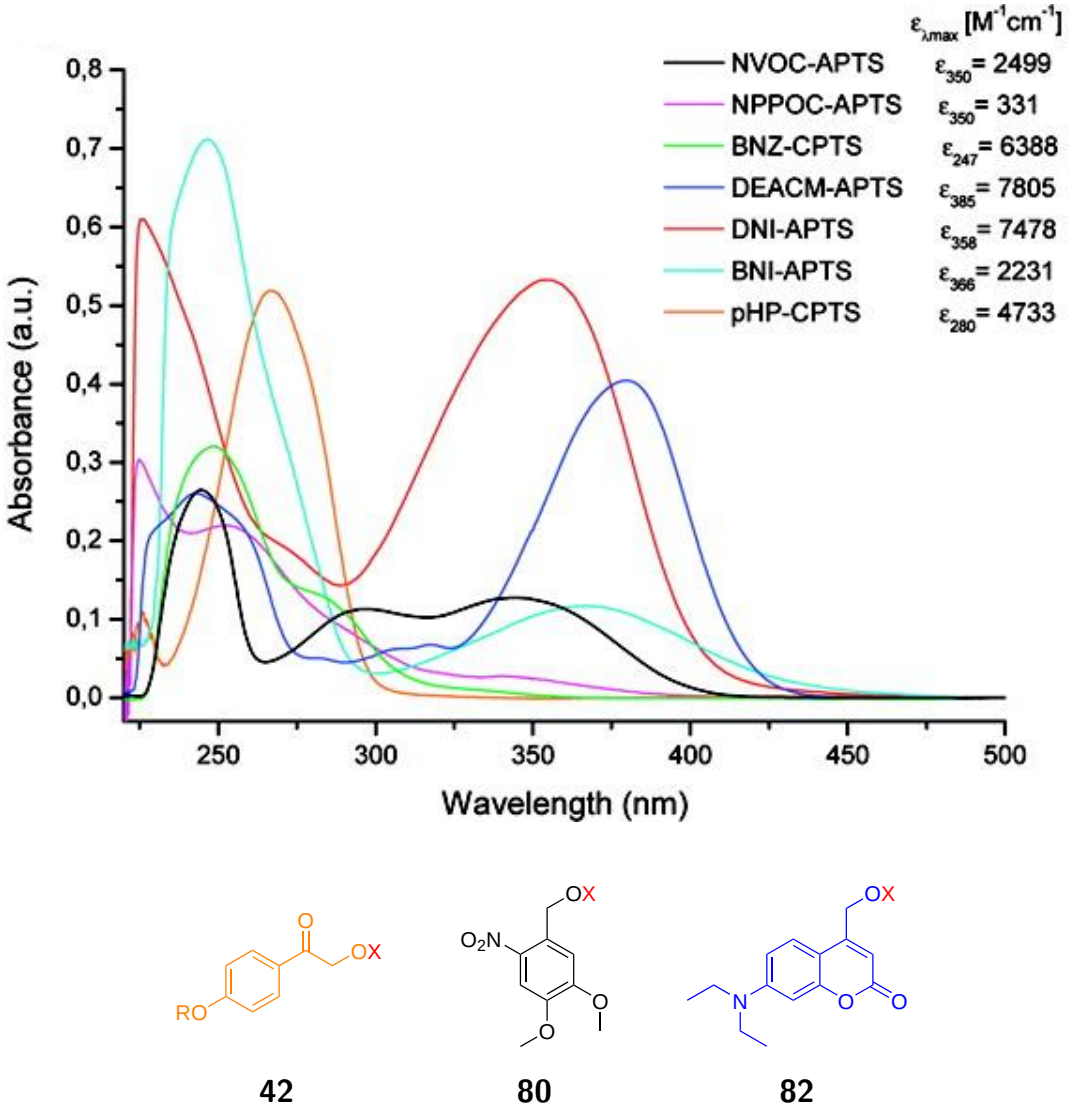


Figure 3.3: UV/vis absorption spectra measured by Bochet *et. al.*[101]; selected PCGs for wavelength orthogonal protection of R-groups of amino acid residues; R = H or Me; X = leaving groups. Adapted with permission from ref [101]. Copyright 2011 American Chemical Society.

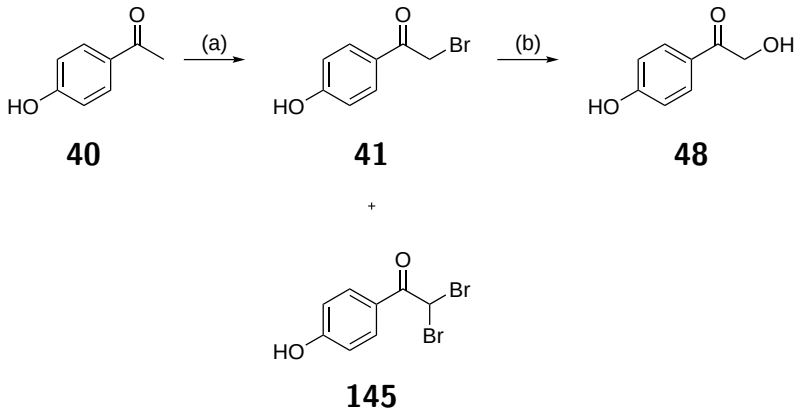
A simplified approach for predicting the potential of PCGs toward wavelength orthogonality is to compare their UV/vis absorption spectra. PCGs that display minimal

overlap in their UV/vis absorption spectra at defined wavelengths (i.e. DEACM, pHP and DMNB) are more likely to be wavelength orthogonal when irradiated at those wavelengths as opposed to PCGs that possess overlapping spectra (i.e. DEACM and DNI). Bochet *et. al.* measured the UV/vis spectra of the PCGs used in their study (**Figure 3.3**)[101] and by comparing the overlap of the UV/vis absorption spectra, the phenacyl- (**42**) (orange; λ_{max} = 268 nm), DMNB- (**80**) (black; λ_{max} = 346 nm) and DEACM caging groups (**82**) (blue; λ_{max} = 385 nm) were selected as starting points for the development of an orthogonally caged amino acid system for application in the study of protein PTM (**Figure 3.3**), owing to the minimised overlap in their UV/vis spectra.

3.5 Synthesis of Photolabile Caged Amino Acids

3.5.1 The Phenacyl-Based Caging Group

The strategy to obtain 4-hydroxyphenacyl (pHP) caged amino acids involved the coupling of amino acid side chains to the caging group bearing an α-hydroxyl (**48**). Synthesis of this parent caging group (**48**) proceeded *via* bromination of the commercially available 4-hydroxyacetophenone (**40**) to afford the α-bromo ketone (**41**), followed by substitution with a hydroxyl group (**Scheme 3.10**).



Scheme 3.10: Bromination of 4'-hydroxyacetophenone (**40**); Reagents & Conditions: (a) Br_2, $CHCl_3$, RT, N_2, 18 h or Br_2, acetic acid, RT, N_2, 4 h or $CuBr_2$ - see (**Table 3.1**); (b) Formic acid, DBU, toluene, 0 °C - RT, N_2, 24 h, 97%.

Two brominating reagents, Br_2 and $CuBr_2$, were trialled to effect the halogenation reaction, however, the reaction proved to be challenging due to an inseparable mixture of starting material (**40**), and mono- (**41**), and di-brominated (**145**) products being obtained (**Scheme 3.10**). Various conditions were trialled with Br_2,[177], [178] including

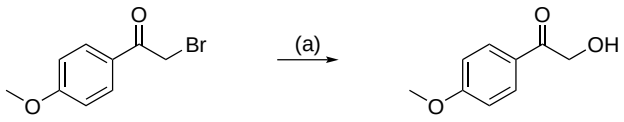
changing the number of equivalents, solvent, and time, however, no improvements in selectivity for the mono-brominated product (**41**) were observed. Further optimisation experiments focussed on the use of $CuBr_2$, which had previously been shown to demonstrate excellent selectivity for the mono-brominated product when tested on hydroxyacetophenones.[179]

Varying the number of equivalents of $CuBr_2$, solvent, temperature, and reaction time was required in order to determine conditions favouring mono-bromination (**Table 3.1**). There was little difference in polarity between the mono- (**41**) and di-brominated (**145**) products, making it difficult to separate out the unwanted side-product (**145**) by column chromatography. It was thus imperative to find conditions which disfavoured formation of the di-brominated compound (**145**).
The reaction is thought to require two equivalents of $CuBr_2$; the first equivalent is involved in coordination of Cu to the carbonyl oxygen, whilst the second equivalent delivers Br at the α-position, resulting in the formation of HBr and Cu(I)Br as side products. Polar solvents were required for the reaction as it was previously reported that no conversion was observed when the reaction was conducted in carbon tetrachloride.[179] A mixture of $CHCl_3$ and EtOAc was originally used, as this had been shown to produce cleaner product than either solvent on its own.[179]. However, studies conducted revealed the best selectivity for the mono-brominated product (**41**) was observed when 2.1 eq $CuBr_2$ in EtOAc were used, allowing the desired product (**41**) to be isolated in 46% yield (**Table 3.1**).

Table 3.1: Optimisation of conditions for the bromination of 4'-hydroxyacetophenone (**40**) with $CuBr_2$; [(a)]conversion determined by comparing integrals in **^{1}H NMR** spectra; [(b)]isolated yield.

Entry	Eq. of $CuBr_2$	Solvent	T (° C)	Time (h)	SM (%)[a]	Mono (%)[a]	Di (%)[a]
1	2.0	EtOAc/$CHCl_3$	100	24	8	72	20
2	5.0	EtOAc/$CHCl_3$	100	18	-	-	100
3	2.1	EtOAc/$CHCl_3$	100	2	-	-	100
4	1.7	EtOAc/$CHCl_3$	100	24	10	71	19
5	2.0	EtOAc/$CHCl_3$	40	24	3	71	26
6	1.7	EtOAc/$CHCl_3$	40	24	19	68	13
7	2.0	$CHCl_3$	40	24	11	75	14
8	2.0	EtOAc	RT	2	100	-	-
9	2.1	EtOAc	100	24	48	52 (46)[b]	-

Substitution of the bromine for a hydroxyl group to obtain the desired 4-hydroxyphenacyl parent caging group (pHP-OH) (**48**) proceeded smoothly in the presence of formic acid and 1,8-diazabicyclo[5.4.0]undec-7-ene (DBU) to give the product in 97% yield (**Scheme 3.10**).
It was also found that the crude mixture of products obtained from the bromination reaction could be directly subjected to the S_N2 reaction without purification. pHP-OH (**48**) could then be isolated after purification by silica gel flash column chromatography in 73% yield over two steps.



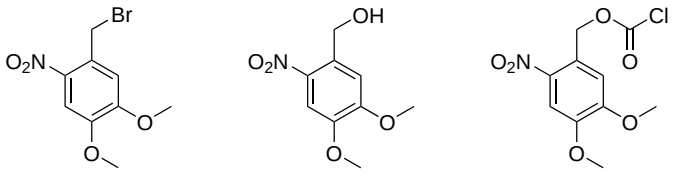
146 **147**

Scheme 3.11: Synthesis of MPH-OH; Reagents & Conditions: (a) HCOONa, EtOH, reflux, 4 h, 73%.

The methoxy-protected phenacyl caging group (MPH-OH) (**147**), an analogue of pHP-OH (**48**), was also synthesised in 73% yield, by employing a similar procedure to that above, refluxing commercially available 2‘-bromo-4‘-methoxyacetophenone (**146**) with sodium formate (**Scheme 3.11**). It was thought that the methoxy-protection on the phenol ring would circumvent possible selectivity issues in later reactions pertaining to the caging of the amino acid side chains.

3.5.2 The DMNB Caging Group

All precursors required for the synthesis of DMNB-caged amino acids are commercially available and do not require any additional synthetic manipulation. These include the 4,5-dimethoxy-2-nitrobenzyl bromide (DMNB-Br) (**148**), 4,5-dimethoxy-2-nitrobenzyl alcohol (DMNB-OH) (**149**), and 4,5-dimethoxy-2-nitrobenzyl chloroformate (DMNB-OCOCl) (**150**).

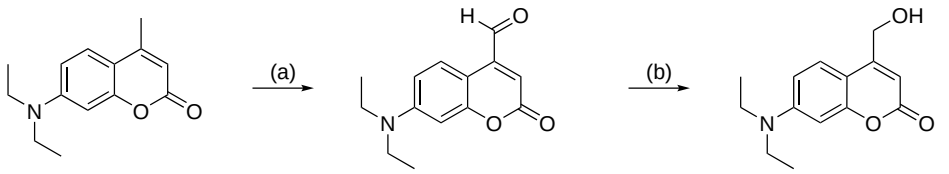


148 **149** **150**

Figure 3.4: Commercially available DMNB precursors.

3.5.3 The DEACM Caging Group

Two primary routes exist for synthesising the desired coumarin caging group bearing a primary hydroxyl group (**153**).
The more commonly reported route involves SeO_2-mediated oxidation of commercially available 4-methyl-7-diethyl aminocoumarin (**151**) in a Riley-type reaction, followed by reduction to the alcohol using $NaBH_4$ (**Scheme 3.12**).[8]

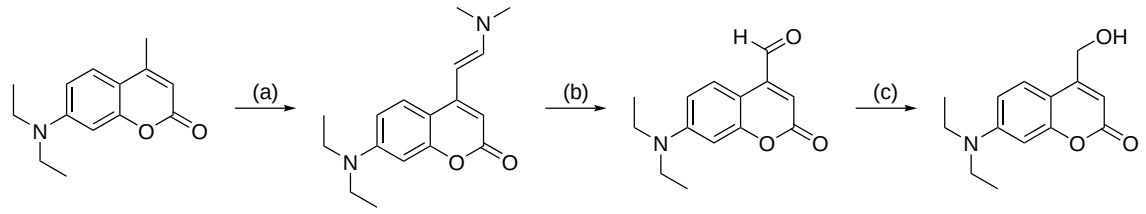


151 **152** **153**

Scheme 3.12: Synthesis of DEACM-OH (**153**) *via* SeO_2 mediated oxidation; Reagents & Conditions: (a) SeO_2, toluene, reflux, N_2, 24 h; (b) $NaBH_4$, MeOH, RT, N_2, 3 h, 29% over 2 steps.

Despite isolating the desired caging group (**153**), this method presented a problem with scaling up of the procedure, and yields were consistently low (< 20%) when performing the reaction on multigram scale (> 2.00 g). In addition, it was hoped to identify a method that circumvented use of toxic SeO_2. A report by Barone and co workers[180] detailed functionalisation of the methyl group by condensation with *N,N*-dimethylformamide dimethyl acetal (DMF·DMA), a procedure first reported by Thummel *et. al.*. [136]

The γ-proton of the α,β-unsaturated ester moiety ($pK_a \approx 4.25$) could be deprotonated, allowing the enol to react with DMF·DMA to afford the enamine (**154**) in near quantitative yields. This could then be oxidised to the aldehyde (**152**) using $NaIO_4$ in 83% yield. Finally, $NaBH_4$ reduction allowed the desired parent caging group (**153**) to be isolated in 52% yield (**Scheme 3.13**).
Although this route involved an additional step, the overall yield was greater (42% vs 20%) and circumvented the use of toxic SeO_2. In addition, purification was simplified as the workup for the SeO_2 reaction was troublesome, and required the disposal of large quantities of toxic waste. The procedure could easily be scaled up (> 5.00 g) with little to no erosion in yields (38 - 42% over three steps).

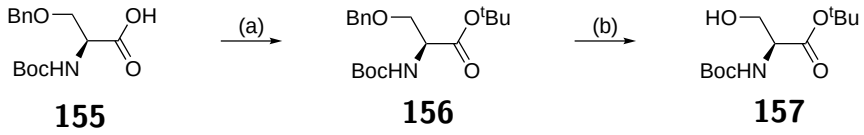


Scheme 3.13: Synthesis of DEACM-OH (**153**) *via* condensation with DMFDMA; Reagents & Conditions: (a) DMFDMA, DMF, 140 °C, Ar, 18 h, 98%; (b) $NaIO_4$, THF:H_2O = 1:1, RT, 18 h, 83%; (c) $NaBH_4$, MeOH, RT, Ar, 4 h, 52%.

3.6 Synthesis of Protected Amino Acids - Boc & *tert*-Butyl Strategy

PTMs most commonly occur on the side chain functional groups of amino acid residues, the points at which to attach PCGs. To minimise interference during attachment of PCGs, it was decided to protect the α-amine and carboxyl groups. The acid labile Boc and *tert*-butyl protecting groups were initially selected as both would undergo simultaneous facile deprotection in TFA.

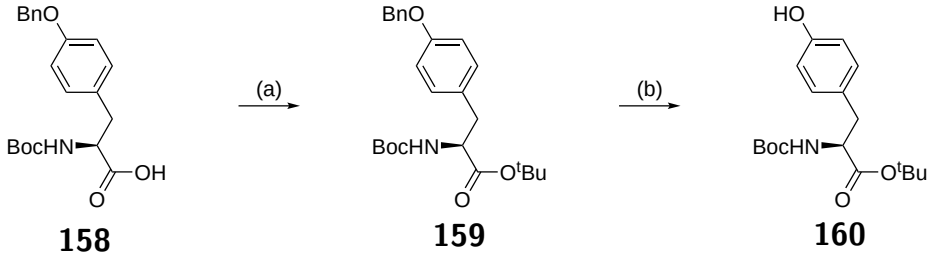
Glutamic acid was commercially available in the required protected form, while serine, tyrosine, and lysine could be purchased as the *N*-Boc and Bzl or CBz protected form. The synthesis for all three compounds followed a similar strategy, involving initial *tert*-butyl ester protection of the α-carboxylic acid[181] and subsequent Pd-catalysed hydrogenolysis reaction[182] to afford the desired amino acids, serine (**157**) [62%], tyrosine (**160**) [73%], and lysine (**163**) [88%], over 2 steps.



Scheme 3.14: Synthesis of Boc-Ser-O^{t}Bu; Reagents & Conditions: (a) Boc_2O, DMAP, ^{t}BuOH, RT, N_2, 3 h, 69%; (b) 10% Pd/C, MeOH, RT, H_2, 48 h, 90%.

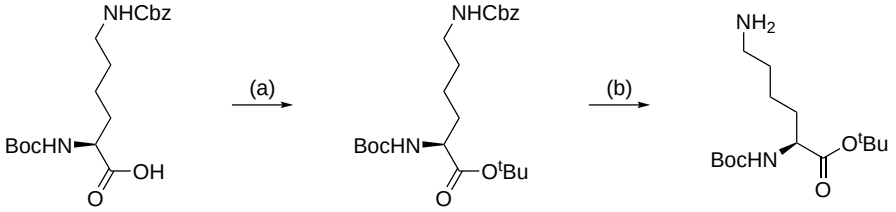
3.7 Synthesis of Caged Amino Acids - Boc & *tert*-Butyl Strategy

Following synthesis of the appropriately protected amino acids and PCGs, these could be coupled to afford the caged amino acids. These compounds could then be evaluated



158 **159** **160**

Scheme 3.15: Synthesis of Boc-Tyr-O^{t}Bu; Reagents & Conditions: (a) Boc_2O, DMAP, ^{t}BuOH, RT, N_2, 3 h, 76%; (b) 10% Pd/C, MeOH, RT, H_2, 3 h, 96%.



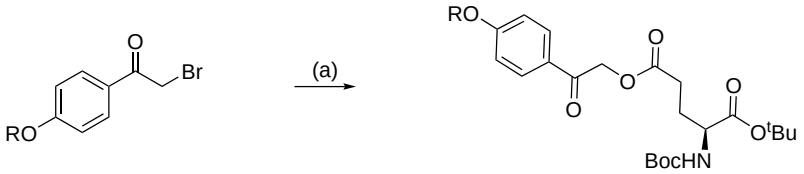
161 **162** **163**

Scheme 3.16: Synthesis of Boc-Lys-O^{t}Bu; Reagents & Conditions: (a) Boc_2O, DMAP, ^{t}BuOH, RT, N_2, 3 h, 90%; (b) 10% Pd/C, MeOH, RT, H_2, 3 h, 98%.

for their propensity to act as a wavelength orthogonal pair.

3.7.1 Phenacyl-Based Caged Amino Acids - Boc & *tert*-Butyl Strategy

Caging of the amino acid side chain functional groups with the 4‘-hydroxyphenacyl caging (pHP) group commenced with coupling of the carboxylic acid side chain of glutamic acid (**138**) by reaction of pHP-Br (**41**) with commercially available Boc-Glu-O^{t}Bu (**138**) in the presence of DBU to afford the desired pHP-caged glutamate (**199**) in 84% yield (**Scheme 3.17**).



R = H **41** **164**

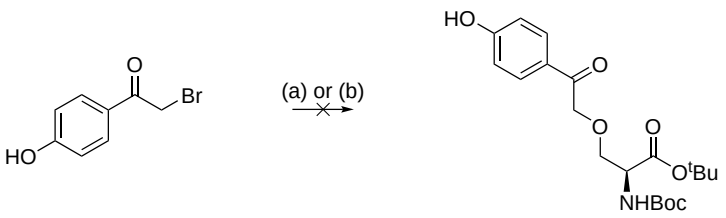
R = Me **146** **165**

Scheme 3.17: Synthesis of phenacyl-caged Boc-Glu-O^{t}Bu; Reagents & Conditions: (a) Boc-Glu-O$_t$Bu (**138**), DBU, THF, 0 °C - RT, Ar, 24 h, 84% (R = H) or 74% (R = Me).

The same reaction with 2-bromo-4'-methoxyacetophenone (MPH-Br) (**146**) yielded the MPH-caged product (**165**) in 74% yield (**Scheme 3.17**).

Having successfully demonstrated that a carboxylic acid side chain functional group could be caged, coupling the phenacyl-based caging groups with the hydroxyl side chain of serine and tyrosine *via* an ether linker was attempted.

pHP-Br (**41**) was reacted with Boc-Ser-O^{t}Bu (**157**) in the presence of DBU [conjugate acid pK_a ≈ 12] or KO^{t}Bu [conjugate acid pK_a ≈ 17] (**Scheme 3.18**) however, in both instances, no product could be isolated. This was attributed to the greater ease with which the phenolic proton could be deprotonated relative to the hydroxyl side chain [pKa ≈ 16], hence hindering progress of the desired reaction and leading to the formation of numerous potential side-products.



41 **166**

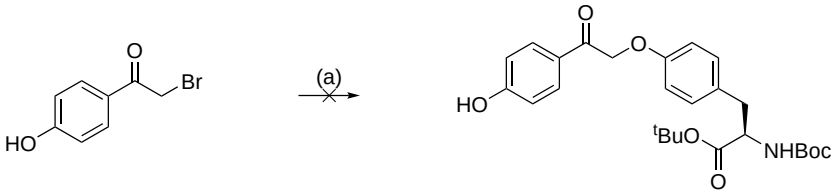
Scheme 3.18: Attempted synthesis of Boc-Ser(pHP)-O^{t}Bu *via* an ether linkage; Reagents & Conditions: (a) Boc-Ser-O^{t}Bu, DBU, 1,4-dioxane, 0 °C- RT, N_2, 18 h; (b) Boc-Ser-O^{t}Bu, KO^{t}Bu, THF, RT, N_2, 5 h.

In the case of tyrosine, the reaction proceeded with KO^{t}Bu, as the more acidic phenolic proton [pka ≈ 10] could be deprotected to facilitate the S_N2 reaction. However, these conditions gave rise to complex mixtures which could have been the result of the starting material reacting with itself or other addition-eliminated based side reactions (**Scheme 3.19**).

To reduce the likelihood of side reactions occurring, the analogous MPH PCG was employed, where the phenolic group was protected as the methoxy ether.

KO^{t}Bu was used to effect the S_N2 transformation between MPH-Br (**146**) and Boc-Tyr-O^{t}Bu (**160**) but again, a complex mixture was obtained, likely due to addition-elimination side reactions occurring (**Scheme 3.19**). In addition to this, the possibility of racemisation at the α-stereogenic centre under basic conditions, led to trialling of alternative possible linking strategies.

The use of a carbonate linker between the pHP-based caging group and the amino acid side chain was postulated, as this would additionally give rise to a favourable



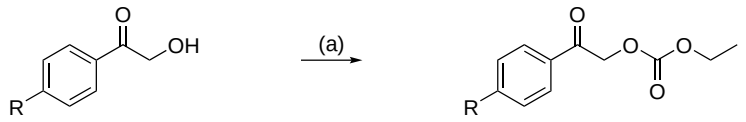
R = H **41** **167**

R = Me **146** **168**

Scheme 3.19: Attempted synthesis of phenacyl-caged Boc-Tyr-O^{t}Bu *via* an ether linkage; Reagents & Conditions: (a) Boc-Tyr-O^{t}Bu, KO^{t}Bu, THF, RT, N_2, 24 h.

entropic driving force, associated with the release of CO_2, during photorelease, possibly enhancing the rate of photolysis.
The commercially available 2-hydroxyacetophenone (**169**) was chosen as a model system from which to optimise the initial activation of the alcohol, due to its structural similarity to the phenacyl-based PCGs.

The base, solvent, and temperature were varied for the reaction with ethyl carbonate and conversion to product (**170**) was observed with either pyridine or NMM in CH_2Cl_2 (**Scheme 3.20**).



R = H **169** **170**

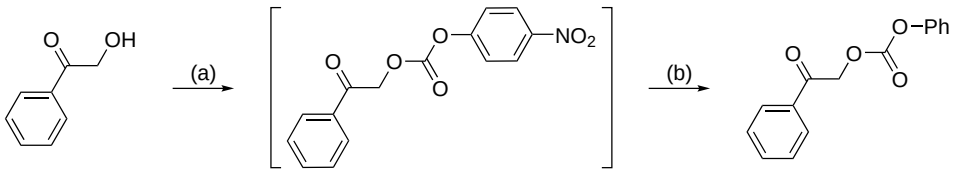
R = OTBDPS **171** **172**

Scheme 3.20: Synthesis of ethyl carbonate analogues; Reagents & Conditions: (a) Ethyl chloroformate, pyridine, 80 °C, N_2, 18 h, R = H 78%, R = OTBDPS 98%.

However, subsequent displacement of the ethoxy group with protected Boc-Ser-O^{t}Bu (**157**) could not be effected. This lack of reactivity was attributed to the ethoxy group not being a sufficiently good leaving group [pKa EtOH $\approx$ 16].

Applying the optimised conditions to the use of 4-nitrophenyl chloroformate as the activating reagent and phenol for the subsequent displacement reaction, it was believed that the greater leaving group ability of the 4-nitrophenyl moiety [conjugate acid pKa $\approx$ 7.1] would enable the displacement reaction to occur (**Scheme 3.21**).

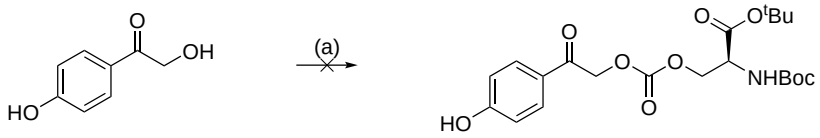
Test reactions were conducted on a 10 mg of 2-hydroxyacetophenone (**169**) scale, with several organic bases trialled. Conversions were judged by TLC and formation of the product was confirmed by mass spectrometry. NMM was found to be the most effective base for formation of the nitrophenyl carbonate intermediate, producing the cleanest reaction with the highest rate of conversion, whilst the nucleophilic base, DMAP, was observed to be superior at promoting the addition elimination reaction.



169 **173** **174**

Scheme 3.21: Synthesis of model phenyl carbonate; Reagents & Conditions: (a) 4-Nitrophenyl chloroformate, base, RT, N_2, 2 h; (b) Phenol, base, RT, N_2, 2 h.

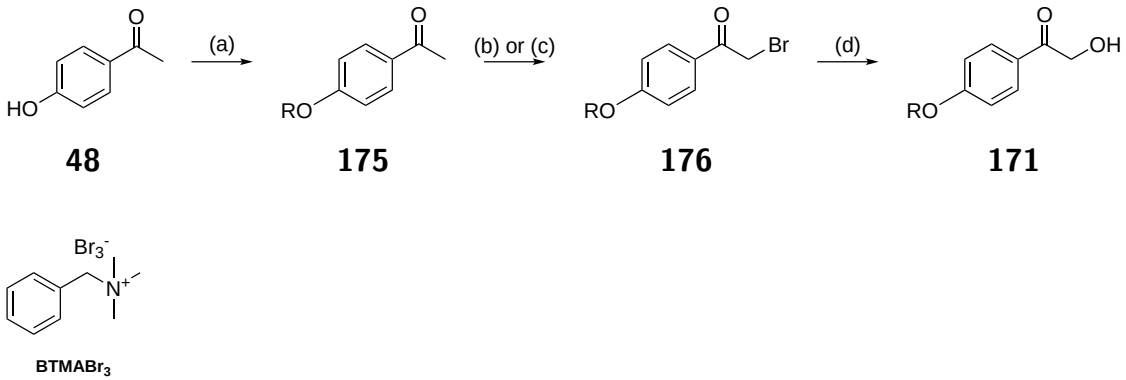
The optimised conditions from the model system were applied to formation of the pHP-nitrophenyl carbonate intermediate *in situ* by reaction of pHP-OH (**48**) with 4-nitrophenyl chloroformate. Boc-Ser-O^{t}Bu (**157**) was then added to the reaction mixture to displace the 4-nitrohydroxyphenyl leaving group (**Scheme 3.22**). However, it was observed by TLC that the reaction produced a complex mixture of numerous side-products, including those from self-coupling of both the pHP caging group and the amino acid, as determined by mass spectrometry.



48 **166**

Scheme 3.22: Attempted synthesis of Boc-Ser(pHP)-O^{t}Bu *via* a carbonate linker; Reagents & Conditions: (a) 4-Nitrophenyl chloroformate, DMAP, CH_2Cl_2, RT, N_2, 18 h then Boc-Ser-O^{t}Bu, DMAP, NEt_3, RT, N_2, 18 h.

The 4-hydroxyl group appeared to be interfering with the reaction by competing with the primary hydroxyl group in the initial formation of the nitrophenyl carbonate intermediate. The phenolic group was thus protected as the *tert*-butyldiphenylsilyl ether (**171**) to circumvent this issue, due to its ease of synthesis and removal, and its relative stability in both acidic and basic conditions (**Scheme 3.23**). The reactions



Scheme 3.23: Synthesis of TBDPS-protected pHP-OH [R = TBDPS]; Reagents & Conditions: (a) TBDPS-Cl, imidazole, DMF, RT, N_2, 18 h, > 99%; (b) TMSOTf, DIPEA, 0 °C, N_2, 0.5 h then NBS, 0 °C - RT, N_2, 0.5 h, 41%; (c) $BTMABr_3$, CH_2Cl_2/MeOH = 5/2, RT, 4 h, 92%; (d) HCOONa, EtOH, reflux, 10 h, 32%.

proceeded smoothly to afford the TBDPS-protected caging group (**171**) in 30% yield over 3 steps.

The previously optimised conditions were then applied to TBDPS-pHP-OH (**171**) enabling the ethyl carbonate (**172**) to be isolated in 98% yield (**Scheme 3.20**).

The coupling reactions were next attempted using 4-nitrophenyl chloroformate as the activating agent but in all cases, with serine (**157**), tyrosine (**160**), and lysine (**163**), complex mixtures were afforded, as determined by TLC and crude **^{1}H NMR**. These were partly attributed to the instability of the TBDPS protecting group to the reaction conditions, resulting in numerous side-products, including self-coupling variants amongst others.

The obstacles encountered with the chloroformate activating compounds, led to exploration of other potential activating groups, including the carbonyl diimidazole (CDI) group and triphosgene.

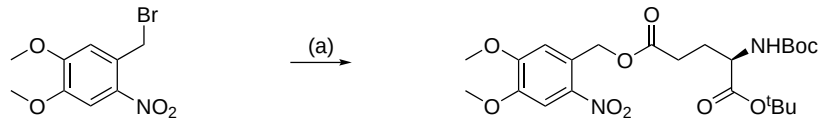
Where CDI was used, the imidazole carbamate intermediate (**276**) was isolated in 25% yield. However, any further attempts to displace the imidazole leaving group [pKa $\approx$ 18.6] provided limited developments. It is possible that the addition elimination reaction could not be effected as the carbamate was more stable in relation to the carbonates to be formed.

When using triphosgene to form the chloroformate intermediate, several procedures were trialled, however, in all cases, only the pyridinium or triethylammonium adduct was formed and no chloroformate could be detected (TLC, mass spectrometry or crude **^{1}H NMR**) or isolated.

Ultimately, despite trialling numerous conditions, progress in attempts to cage serine, tyrosine, or lysine with the pHP or MPH caging groups proved to be challenging.

3.7.2 DMNB-Caged Amino Acids – Boc & *tert*-Butyl Strategy

DMNB-caged glutamic acid (**177**) was synthesised by reaction of 4,5-dimethoxy-2-nitrobenzyl bromide (**148**) with Boc-Glu-O^{t}Bu (**138**) under basic conditions in 62% yield (**Scheme 3.24**).



148 **177**

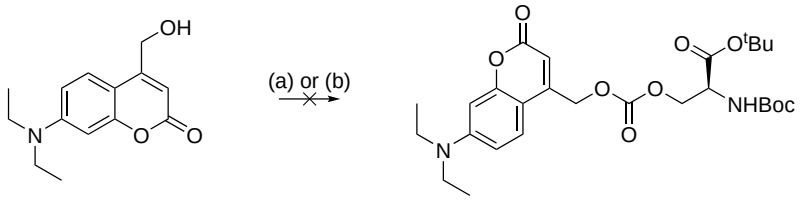
Scheme 3.24: Synthesis of Boc-Glu(DMNB)-O^{t}Bu; Reagents & Conditions: (a) Boc-Glu-O^{t}Bu, DBU, THF, 0 °C - RT, Ar, 24 h, 62%.

3.7.3 DEACM-Caged Amino Acids – Boc & *tert*-Butyl Strategy

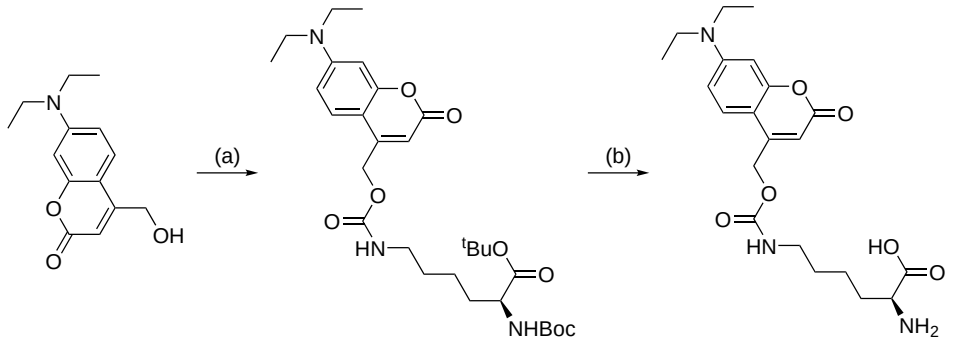
The carbonate and carbamate linking strategies were opted for linking the hydroxyl group of serine and tyrosine and the amine group of lysine to the DEACM caging group, respectively. DEACM-OH (**153**) was activated with 4-nitrophenyl chloroformate and when complete consumption of the starting material (**153**) was observed by TLC, Boc-Ser-O^{t}Bu (**157**) was added (**Scheme 3.25**). Although conversion to the desired product (**178**) was observed by TLC, mass spectrometry and crude **^{1}H NMR**, these reaction conditions produced a complex mixture from which the desired product could not be isolated, even after successive purifications by silica gel flash chromatography. This was attributed to the high reactivity of the intermediate (**273**) formed, as well as difficulties in separating out reaction by-products and side-products.

To minimise this, the less reactive 4-nitrophenyl imidazole carboxylate (**180**) was synthesised and used to activate the DEACM caging group (**153**) to the subsequent addition-elimination reaction by the amino acid.

However, despite observing the formation of what appeared to be the intermediate by TLC, decomposition was observed upon addition of the amino acid, and no product could be isolated (**Scheme 3.26**). This was also the case when the reaction was attempted with Boc-Tyr-O^{t}Bu (**160**).


OH
(a) or (b)
O
O
O

For both tyrosine and lysine, the use of 4-nitrophenyl chloroformate led to isolation of the protected carbonate and carbamate in 29% and 28%, respectively. It is likely the carbonate formation reaction for tyrosine was favoured over that of serine due to the more acidic phenolic proton, whilst that of lysine was favoured due to the formation of the more stable carbamate.



153 **182** **183**

Scheme 3.28: Synthesis of Boc-Lys(DEACM)-O^{t}Bu; Reagents & Conditions: (a) 4-Nitrophenyl chloroformate, DMAP, CH_2Cl_2, RT, N_2, 18 h, then Boc-Lys-O^{t}Bu, DMAP, RT, N_2, 18 h, 28%; (b) TFA, Et_3SiH, CH_2Cl_2, RT, N_2, 4 h, 80%.

In the case of DEACM-caged lysine (**182**), an analytically pure sample of the global deprotection DEACM-caged lysine product (**183**), bearing a free α-amine and carboxylic acid group, was also obtained in 80% yield by treatment with 50% TFA in CH_2Cl_2 (v/v) (**Scheme 3.28**).

3.8 Summary & Conclusions – Boc & *tert*-Butyl Strategy

The Boc and *tert*-butyl protecting strategy was originally chosen for the ease of preparation of the amino acid precursors and that the protecting groups would not interfere with reactions to attach the chosen photolabile caging groups. As both protecting groups were acid-labile, deprotection to afford the free amino acid could occur in 1 step using either TFA or 4 M HCl.

With this protecting group strategy, pHP- (**199**), MPH- (**165**), and DMNB-protected glutamic acid (**177**), attached at the γ-carboxylic acid were synthesised. However, despite numerous attempts, caging of serine, tyrosine or lysine with the phenacyl class of caging group was not achieved.

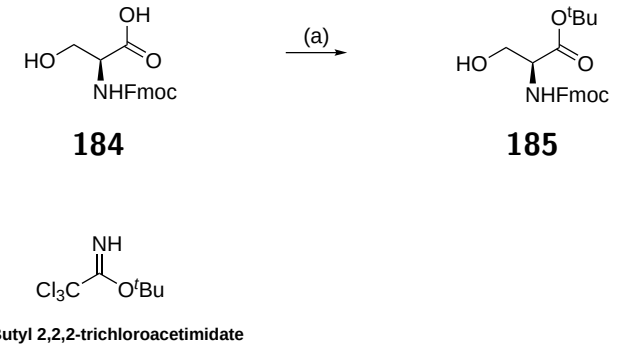
With the DEACM group, more success was achieved and both tyrosine (**181**) and lysine (**182**) were successfully caged. However, yields remained low despite attempts at optimising the reaction. In addition, the amount of material afforded was insufficient to perform photolysis reactions, which had to be monitored by **^{1}H NMR** as the photoreleased products lacked a chromophore, and hence their evolution could not be monitored by HPLC.
It was reasoned that the presence of a chromophore on the amino acid and hence the photoreleased product, would enable progression of the photolysis experiments and evolution of photoreleased product to be monitored by HPLC, a technique that would demand far less material per run. To this end, the Fmoc-group was selected as it could function with the dual purpose of acting as a protecting group to prevent side reactions at the α-amine, as well as serving as a chromophore to allow the released amino acid, following uncaging, to be detected by HPLC. In addition, this protecting groups strategy would render the caged amino acids amenable to solid phase peptide synthesis (SPPS).

3.9 Synthesis of Protected Amino Acid – Fmoc and tert-Butyl Strategy

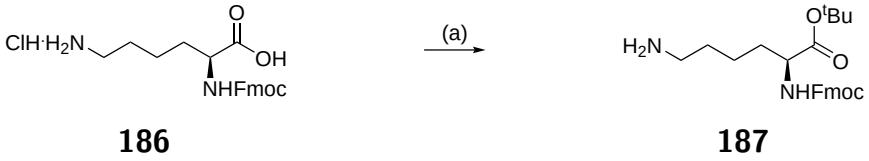
This strategy required the synthesis of protected amino acids bearing the Fmoc protecting group on the α-amine and the *tert*-butyl ester on the α-carboxylic acid. Fmoc-Asp-O^{t}Bu was commercially available and thus, chosen as the model system to evaluate the photolytic properties of the various caging groups.

Fmoc-Ser-O^{t}Bu (**185**) was obtained by treatment of the commercially available *N*-Fmoc-Ser-OH (**184**) with *tert*-butyl 2,2,2-trichloroacetimidate to afford the *tert*-butyl ester (**185**) in 51% yield (**Scheme 3.29**).
When the same conditions were applied to the lysine analogue, no conversion to product was observed and only starting material (**186**) could be isolated. It was postulated that the HCl salt of the lysine precursor (**186**) was interfering with the reaction, and when a base wash with sat. aq. $NaHCO_3$ was carried out prior to reaction with *tert*-butyl 2,2,2-trichloroacetimidate, the desired product (**187**) was isolated in 10% yield (**Scheme 3.30**).

Owing to the low yield, alternative routes to the product (**187**) were sought. These involved the *tert*-butyl esterification of α and ε-protected lysine, followed by deprotection



Scheme 3.29: Synthesis of Fmoc-Ser-O^{t}Bu; Reagents & Conditions: (a) *tert*-Butyl 2,2,2-trichloroacetimidate, EtOAc:cyclohexane (2:1), RT, 18 h, 51%.



Scheme 3.30: Synthesis of Fmoc-Lys-O^{t}Bu; Reagents & Conditions: (a) sat. aq. $NaHCO_3$ then *tert*-butyl 2,2,2-trichloroacetimidate, EtOAc:cyclohexane (2:1), RT, 4 h, 10%.

at the ε-amine.

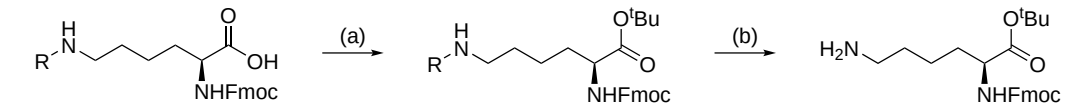
Where R = Cbz, Boc, Trt and Mtt, the *tert*-butyl ester formation reaction proceeded in moderate to good yields following treatment with Boc_2O in ^{t}BuOH. The substrate where R = Alloc presented an exception and the fully protected lysine product could only be isolated in 29% yield. The *tert*-butyl ester protection of the Alloc-protected lysine variant proceeded far more smoothly, and in good yield, when the reaction was conducted using $POCl_3$ to afford the desired product in 71% yield (**Scheme 3.31**).

With the fully protected lysine analogues successfully synthesised, deprotection conditions were investigated (**Scheme 3.31**). Some optimisation was required to obtain the product and it was found that when R = Mtt, the best yield of the desired Fmoc-Lys-O^{t}Bu (**187**) could be obtained.

Cbz and Fmoc were found not to be orthogonal as the hydrogenolysis conditions used also resulted in removal of the Fmoc group.

Where the Boc group was used to protect the ε-amine, it was possible to effect selective cleavage through the use of 2.0 M HCl in Et_2O to obtain the product (**187**) in 38% yield. The selectivity was attributed to reduced solubility of the HCl salt which limited deprotection of the also acid labile *tert*-butyl ester.[183]

Selective deprotection of the Alloc group proved to be extremely challenging. On attempting numerous conditions, varying the catalyst, additives and solvent used,



R = CBz	**188**	**189**	(84%)	**187**
R = Boc	**190**	**191**	(95%)	
R = Alloc	**192**	**193**	(29% or 71%)	
R = Trt	**194**	**195**	(55%)	
R = Mtt	**196**	**197**	(71%)	

Scheme 3.31: Synthesis of Fmoc-Lys(R)-O^{t}Bu; Reagents & Conditions: (a) Boc_2O, DMAP, ^{t}BuOH, RT, N_2, 3 h, 29 - 95% or $POCl_3$, pyridine, ^{t}BuOH, 5 °C, 5 h, 71%; (b) See (**Table 3.2**) for conditions.

only $Pd(PPh_3)_4$ as the catalyst with $Me_2NH.BH_3$ as additive allowed the product (**187**) to be afforded in 14% yield.

The use of the acid labile Trt and Mtt protecting groups allowed isolation of the product (**187**) in excellent yields with the Mtt group offering a slightly superior yield of 92% as well as simpler purification procedures. This was thus adopted as the synthesis of choice (**Table 3.2**).

3.10 Synthesis of Caged Amino Acids – Fmoc and *tert*-Butyl Strategy

Following successful synthesis of the amino acid precursors, the previously synthesised PCGs could be used for caging at the side chain functional groups of the amino acid residues.

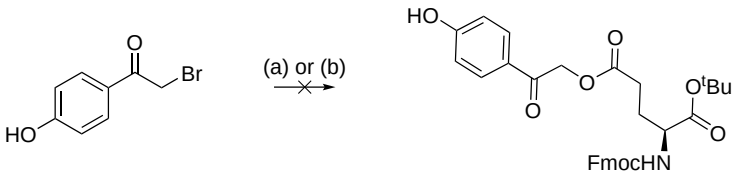
3.10.1 Phenacyl-Based Caged Amino Acids – Fmoc & *tert*-Butyl Strategy

To synthesise pHP-caged glutamate (**198**) bearing the Fmoc and *tert*-butyl ester, previously used conditions were replicated but DBU was found to result in cleavage of the Fmoc group, whilst in the presence of DIPEA, the reaction did not proceed (**Scheme 3.32**).

The conditions used for the S_N2-type displacement of Br had the potential for many side reactions, including self-coupling, addition to the carbonyl and interference from the free phenolic OH. To circumvent these, the TBDPS-protected variant (**171**) was

Table 3.2: Optimisation for selective deprotection of ε-amine of lysine.

Entry	R	Conditions	Yield (%)
1	Cbz	10 % Pd/C (20 mol %), Et_2O, RT, H_2, 24 h	-
2	Boc	2.0 M HCl in Et_2O, 0 ° C - RT, N_2, 6 h	38
3	Boc	4.0 M HCl in Dioxane, 0 ° C - RT, Ar, 0.5 h	-
4	Alloc	$Pd(PPh_3)_4$, $Me_2NH.BH_3$, CH_2Cl_2, RT, Ar, 18 h	14
5	Alloc	$Pd(PPh_3)_4$, DABCO, CH_2Cl_2, RT, Ar, 18 h	-
6	Alloc	$Pd(PPh_3)_4$, K_2CO_3, MeOH, RT, Ar, 18 h	-
7	Alloc	$Pd(dba)_2$, dppe, pyrrolidine, THF, RT, Ar, 18 h	-
8	Alloc	$Pd(dba)_2$, dppe, NEt_3, THF, RT, Ar, 18 h	-
9	Alloc	$Pd(dba)_2$, dppe, pyrrolidine, MeCN, RT, Ar, 18 h	-
10	Alloc	$Pd(dba)_2$, dppe, NEt_3, MeCN, RT, Ar, 18 h	-
11	Trt	5 % TFA in CH_2Cl_2, $HSiEt_3$, RT, Ar, 2 h	83
12	Mtt	1 % TFA in CH_2Cl_2, $HSiEt_3$, RT, Ar, 40 min	92



41 **198**

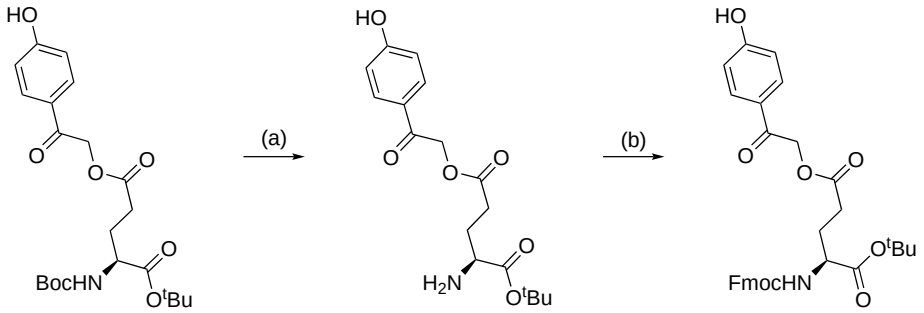
Scheme 3.32: Attempted synthesis of Fmoc-Glu(pHP)-O^{t}Bu; Reagents & Conditions: (a) Fmoc-Glu-O^{t}Bu, DBU, THF, 0 °C - RT, Ar, 24 h; (b) Fmoc-Glu-O^{t}Bu, DIPEA, CH_2Cl_2, RT, Ar, 18 h.

used to access the product by means of an esterification reaction with HBTU. This would be followed by deprotection of the silyl group in the presence of TBAF to afford the final product (**198**). However, the silyl group appeared to be unstable to the reaction conditions and would be cleaved resulting in side-product formation of the esterified product with the phenolic OH, amongst others.

As the caged product could not be synthesised through conventional means, an alternative route was hypothesised involving selective deprotection of the Boc group from Boc-Glu(pHP)-O^{t}Bu (**199**) to reveal the free amine, which could subsequently be protected with the Fmoc group at the α-amine (**Scheme 3.33**).

Both the Boc and *tert*-butyl ester protecting groups are acid labile and few distinctions in their selectivity have been made with regards to conditions for their deprotection.

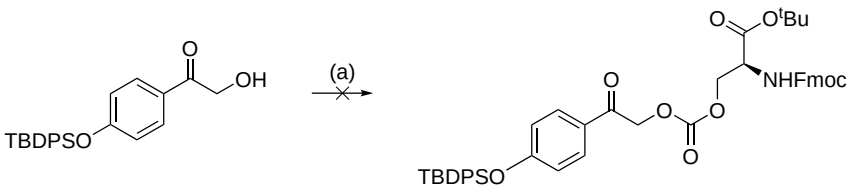
It was possible to selectively cleave the Boc group over the *tert*-butyl ester through the use of 2.0 M HCl in Et_2O, playing on the insolubility of the HCl salt to minimise further deprotection of the ^{t}Bu ester.



Scheme 3.33: Synthesis of Fmoc-Glu(pHP)-O^{t}Bu *via* Boc deprotection followed by Fmoc protection of Boc-Glu(pHP)-O^{t}Bu; Reagents & Conditions: (a) 2.0 M HCl in Et_2O, RT, Ar, 24 h, 98%; (b) $NaHCO_3$, H_2O, RT, 0.5 h then Fmoc-OSu, 1,4-dioxane, RT, 18 h, 25%.

Following a simple filtration, the product was obtained in 98% yield and subsequent protection of the free α-amine using Fmoc-OSu gave Fmoc-Glu(pHP)-O^{t}Bu (**198**) in 25% yield (**Scheme 3.33**). Whilst this is not representative of typical Fmoc protections,[184] no further optimisations were performed as the reaction had yielded sufficient material for testing purposes.

Based on previous optimisation studies, the hydroxyl group was found to interfere with the carbonate and carbamate forming reactions and thus TBDPS-pHP-OH (**171**) was adopted for the coupling reaction to serine (**185**). However, in all cases trialled with 4-nitrophenyl chloroformate, the TBDPS protecting group appeared not to be compatible with the reaction conditions, resulting in its deprotection to reveal the free phenolic group which interfered with the reaction leading to the generation of multiple side products (**Scheme 3.34**).
CDI was trialled as base was not required for the initial activation and thus the TBDPS group would be less susceptible to cleavage. However, in the absence of base, Fmoc-Ser-O^{t}Bu could not be activated to displace the imidazole leaving group and the addition of base resulted in cleavage of Fmoc leading to the formation of numerous side-products.
The use of triphosgene for the synthesis of chloroformates was also attempted[185] but only formation of the carbamate adduct formed with the base used was observed, from which no further reaction took place.



171 **201**

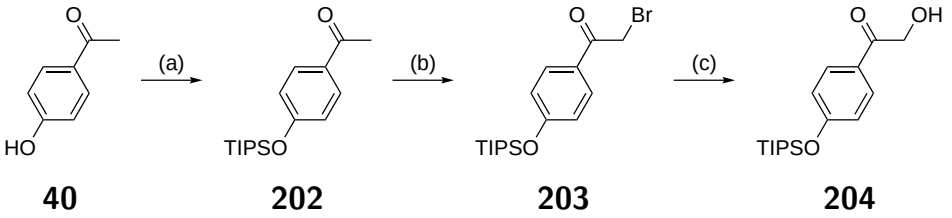
Scheme 3.34: Attempted synthesis of TBDPS-pHP-caged serine; Reagents & Conditions: (a) See (**Table 3.3**) for conditions.

Table 3.3: Trials towards the synthesis of TBDPS-protected Fmoc-Ser(pHP)O^{t}Bu; [a]Base used for activation of PCG; [b]Base used in addition of Fmoc-Ser-O^{t}Bu.

Entry	Activating Agent	Base[a]	Solvent	T (° C)	Base[b]
1	4-Nitrophenyl chloroformate	NMM	CH_2Cl_2	RT	DMAP
2	4-Nitrophenyl chloroformate	DMAP	CH_2Cl_2	RT	DMAP
3	4-Nitrophenyl chloroformate	NEt_3, DMAP	CH_2Cl_2	RT	DMAP
4	Carbonyl-diimidazole	-	THF	RT	LiH
5	Carbonyl-diimidazole	-	THF	RT	-
6	Carbonyl-diimidazole	-	THF then CH_2Cl_2	RT	DMAP, NMM
7	Triphosgene	Pyridine	THF then CH_2Cl_2	0 - RT	DMAP
8	Triphosgene	Pyridine, NEt_3	CH_2Cl_2	0 - RT	DMAP
9	Triphosgene	Na_2CO_3, NEt_3	Toluene	0 - RT	NMM

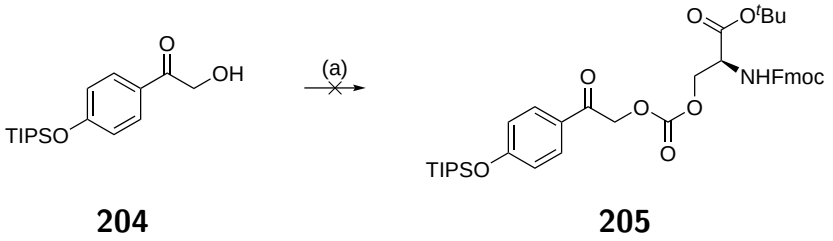
Attempts were also made to first activate the amino acid using the methods described above, prior to addition of the protected caging group. Unfortunately, this also yielded no caged product (**201**).

The TIPS group is known to be more stable in basic media and was thought to be less likely to undergo cleavage under the reaction conditions. The TIPS-protected pHP analogue (**204**) was synthesised by treatment of 4'-hydroxyacetophenone (**40**) with triisopropylsilane to afford the product (**202**) in $>$ 99% yield. Bromination at the α-position using $AlCl_3$ and Br_2 afforded the α-bromo compound (**203**) in 87% yield and heating under reflux with sodium formate in EtOH afforded the desired product in 21% yield (**Scheme 3.35**).
Employing the optimised conditions to activate the caging group using 4-nitrophenyl chloroformate by stirring with NMM and subsequently reacting this intermediate *in*



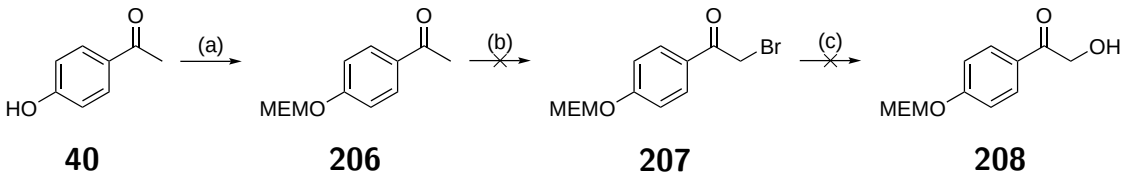
Scheme 3.35: Synthesis of TIPS-pHP-OH; Reagents & Conditions: (a) TIPS-Cl, Imidazole, DMF, RT, N_2, 4 h, > 99%; (b) $AlCl_3$, Br_2, Et_2O, 0 °C - RT, Ar, 18 h, 87%; (c) HCOONa, EtOH, reflux, 4 h, 21%.

situ with Fmoc-Ser-O^{t}Bu (**185**) in the presence of DMAP, resulted in conversion to the desired product (**205**) as observed by mass spectrometry and crude **^{1}H NMR** but despite numerous attempts and successive purifications by silica gel flash chromatography, the product (**205**) could not be afforded in sufficient purity (**Scheme 3.36**). In addition, decomposition of the starting materials or formation of other undesired by-products were also observed.



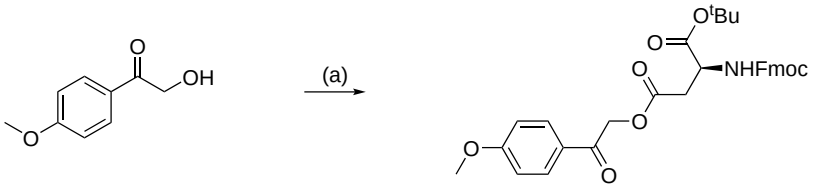
Scheme 3.36: Attempted synthesis of TIPS-protected Fmoc-Ser(pHP)-O^{t}Bu; Reagents & Conditions: (a) 4-Nitrophenyl chloroformate, NMM, CH_2Cl_2, RT, Ar, 18 h then Fmoc-Ser-O^{t}Bu, DMAP, RT, Ar, 18 h.

The MEM-protecting group was also trialled as this group was known to be stable to basic conditions. However, the MEM group was unstable to silica gel purification and it was believed that continued use of this group would cause even more purification issues at subsequent stages.



Scheme 3.37: Synthesis of MEM-pHP-OH; Reagents & Conditions: (a) MEM-Cl, DIPEA, CH_2Cl_2, RT, Ar, 18 h, 51%; (b) Br_2, $AlCl_3$, Et_2O, 0 °C- RT, Ar, 18 h; (c) HCOONa, EtOH, reflux, 4 h.

Focus was shifted to the methoxy protected pHP analogue (mPH) (**147**). The two PCGs have very similar photolytic properties and it was thought that the methoxy protection would ease some of the synthetic challenges previously encountered.
The synthesis of MPH-caged aspartic acid (**209**) was achieved by activation with HBTU, to afford the product (**209**) in 81% yield (**Scheme 3.38**).

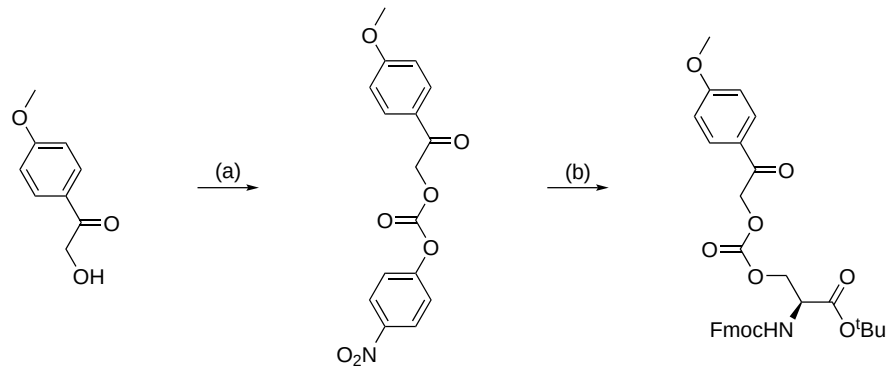


147 **209**

Scheme 3.38: Synthesis of MPH-protected Fmoc-Asp-O^{t}Bu; Reagents & Conditions: (a) Fmoc-Asp-O^{t}Bu, HBTU, DIPEA, DMF, RT, Ar, 18 h, 81%.

In an attempt to obtain MPH-caged glutamic acid, selective deprotection of the *N*-Boc group on the previously synthesised Boc-Glu-O^{t}Bu (**165**) was undertaken in 49% yield. However, attempts to install the Fmoc protecting group on the α-amine were unsuccessful.
However, as caged aspartic acid (**209**) bearing the MPH protection at the β-carboxylic acid had been successfully synthesised, this route was not pursued any further.

The synthesis of MPH-caged serine (**211**) bearing the carbonate linker required optimisation.
The reaction was trialled with 4-nitrophenyl chloroformate, *N*,*N*-carbonyldiimidazole (CDI), and triphosgene as activating agents. The highest yield was obtained when using 4-nitrophenyl chloroformate as the activating agents in the presence of pyridine and sub-stoichiometric amounts of DMAP to obtain the activated intermediate (**210**). The addition-elimination reaction conducted with $NaHCO_3$ allowed the desired product (**211**) to be furnished in 40% yield (**Scheme 3.39**).
The activated species was obtained with the use of CDI, however, no further reaction took place, likely due to the carbamate intermediate possessing greater stability over the carbonate product.
The use of triphosgene allowed isolation of the desired product (**211**) in 4% yield. This could have been the result of the basicity of the reaction, resulting in cleavage of the Fmoc-group, leading to the formation of numerous side reactions with the highly reactive chloroformate intermediate.



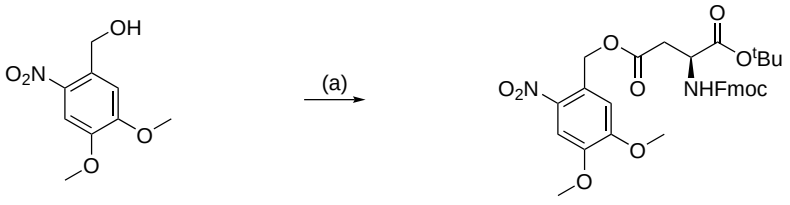
147 **210** **211**

Scheme 3.39: Synthesis of Fmoc-Ser(MPH)-O^{t}Bu; Reagents & Conditions: (a) 4-Nitrophenyl chloroformate, pyridine, DMAP, CH_2Cl_2, RT, Ar, 18 h; (b) Fmoc-Ser-O^{t}Bu, $NaHCO_3$, RT, 18 h, 40%.

The synthesis of MPH-caged lysine through the carbamate linker was also attempted. However, despite observing conversion to the product by mass spectrometry and crude **^{1}H NMR**, the desired product could not be isolated in sufficient analytical purity following successive purifications by silica gel flash chromatography.
As both pHP- and MPH-caged amino acids had been obtained, the syntheses of other caged amino acids were attempted in search of an orthogonal pair.

3.10.2 DMNB-Caged Amino Acids – Fmoc & *tert*-Butyl Strategy

The DMNB caging group is commercially available as both the alcohol (**149**) and chloroformate (**150**) and is therefore amenable to the devised synthetic strategy. DMNB-caged aspartic acid (**212**) was readily synthesised from the DMNB alcohol (**149**) in 79% yield (**Scheme 3.40**).



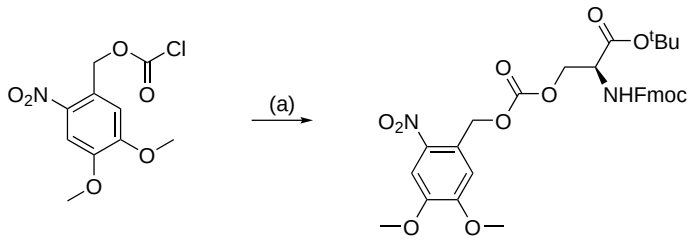
149 **212**

Scheme 3.40: Synthesis of DMNB-caged aspartic acid; Reagents & Conditions: (a) Fmoc-Asp-O^{t}Bu, HBTU, DIPEA, DMF, RT, Ar, 18 h, 79%.

However, when this reaction was conducted with the commercially available Fmoc-Glu-O^{t}Bu, only starting material could be isolated.
An alternative route was thus sought to access the product, through selective deprotection of the Boc group of previously synthesised DMNB-caged glutamate (**177**) to reveal the free α-amine (**275**) in 42%, using 2.0 M HCl in Et_2O. However, subsequent protection of the α-amine with the Fmoc group proved to be unsuccessful and no desired product was obtained.

The synthesis of DMNB-caged serine (**213**) (**Scheme 3.41**) required optimisation to obtain sufficient quantities of the product (**213**). (**Table 3.4**).
Bases trialled included NEt_3, NMM, pyridine, DIPEA, and DMAP, with addition of the bases conducted at 0 °C or RT. Addition at 0 °C was attempted to hinder the rate of formation of side products but the desired product (**213**) was not isolated under these conditions.
To ease the purification procedures, a base wash with sat. aq. $NaHCO_3$ or an acid wash with 1 M HCl were trialled. The base wash was found to be detrimental to the yield, resulting in breakdown of the product as observed by the formation of several additional spots by TLC. The product was stable to 1 M HCl acid wash, which hydrolysed the unreacted chloroformate, simplifying subsequent silica gel flash chromatography purification.
Two successive purifications by fractional column chromatography were required to obtain the pure sample (**213**) and it must be noted that the order of eluents used was crucial.

The best yield was obtained through the use of DMAP, incorporating a 1 M HCl acid wash, followed by two successive silica gel chromatography purifications.



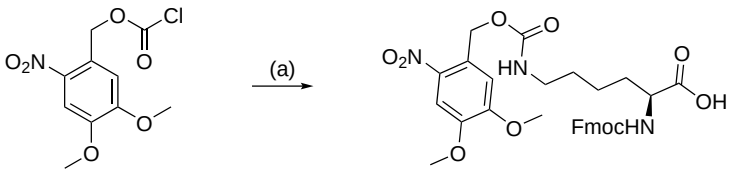
150 **213**

Scheme 3.41: Synthesis of Fmoc-Ser(DMNB)-O^{t}Bu; Reagents & Conditions: (a) See (**Table 3.4**) for conditions.

Table 3.4: Optimisation table for synthesis of Fmoc-Ser(DMNB)-O^{t}Bu; [a]eluents for siliga gel flash column chromatography.

Entry	Base	T (° C)	Work Up	Purification[a]	Yield (%)
1	NEt_3	0 - RT	Concentrate	$CHCl_3$	-
2	DMAP	0 - RT	Concentrate	$CHCl_3$	-
3	NMM	RT	Concentrate	1. $CHCl_3$; 2. Petrol:Acetone = 9:1/ - 1:1	-
4	NMM	RT	Concentrate	1. Petrol:$CHCl_3$ = 1:1; 2. Petrol:Et_2O = 7:3 - 1:1	7
5	NMM	RT	sat. aq. $NaHCO_3$ wash	1. $CHCl_3$; 2. Petrol:Et_2O = 1:1 - 3:7; 3. Petrol:$CHCl_3$ = 1:1	9
6	Pyridine	RT	sat. aq. $NaHCO_3$ wash	1. Petrol:Acetone = 8:2; 2. Petrol:$CHCl_3$ = 2:8	8
7	DMAP, $NaHCO_3$	RT	Concentrate	1. Petrol:Acetone = 8:2; 2. $CHCl_3$	13
8	DIPEA	RT	1 M HCl wash	1. Petrol:Acetone = 8:2; 2. Petrol:$CHCl_3$ = 2:8	19
9	DMAP	RT	1 M HCl wash	1. Petrol:Acetone = 8:2; 2. Petrol:$CHCl_3$ = 2:8	37

This methodology was extended to synthesis of the carbamate-linked DMNB-protected lysine analogue (**214**). Following the procedure reported by Rusiecki and Warne,[186] the reaction proceeded smoothly with commercially available Fmoc-Lys-OH·HCl, in the presence of $NaHCO_3$, to afford the desired product (**214**) in 57%. The free carboxylic acid group present on the molecule would make this caged amino acid suitable for the Sheppard peptide synthesis approach.[187]



150 **214**

Scheme 3.42: Synthesis of Fmoc-Lys(DMNB)-OH; Reagents & Conditions: (a) Fmoc-Lys-OH.HCl, $NaHCO_3$, H_2O:1,4-dioxane:MeCN (1:1:1), RT, 18 h, 57%.

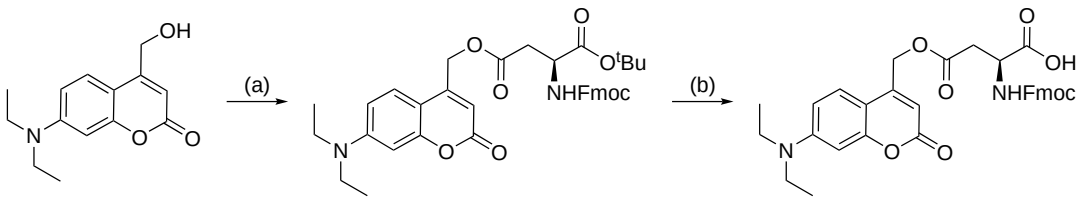
Having demonstrated the ability of the DMNB photolabile caging group to be coupled to a variety of amino acid side chain functional groups, ranging from aspartic acid to serine and lysine *via* ester, carbonate and carbamate linkers respectively, these transformations were attempted with the DEACM caging group to enable comparison of their photolytic properties to establish the potential for orthogonality.

3.10.3 DEACM Caged Amino Acids – Fmoc & *tert*-Butyl Strategy

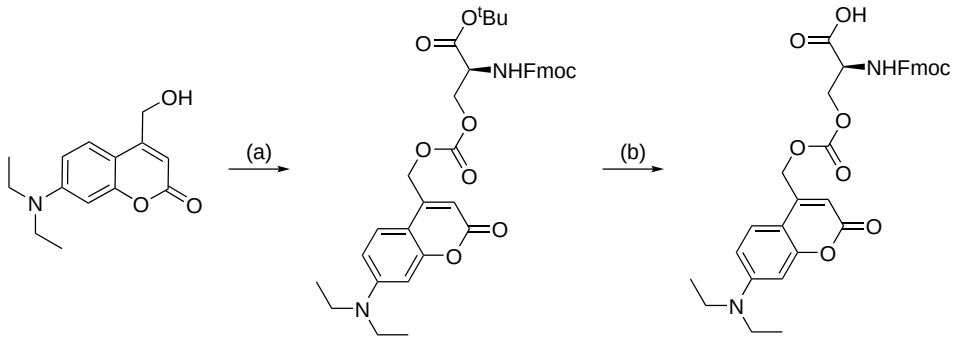
The last caging group selected, based on the report by Bochet *et. al.*,[**275**] was the diethylaminocoumarin (DEACM) caging group. The authors showed this caging group

to have a λ_{max} of 385 nm and that it could be uncaged at longer wavelengths of 412 nm.

Synthesis of DEACM-caged aspartic acid (**215**) was achieved by reaction of the previously synthesised DEACM-OH (**153**) with commercially available Fmoc-Asp-O^{t}Bu to yield the product (**215**) in 75% yield (**Scheme 3.43**).


OH
(a)
O
O
O

and the second with $CHCl_3$ (**Scheme 3.44**). These conditions were reproducible and scalable up to 400 mg.

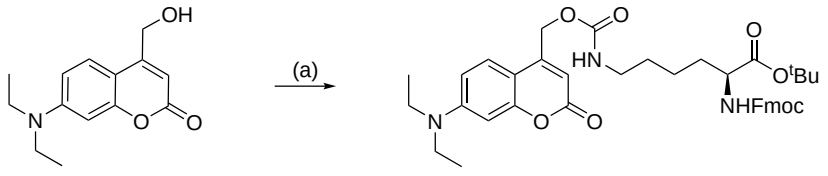


153 **217** **218**

Scheme 3.44: Synthesis of DEACM-caged serine; Reagents & Conditions: (a) 4-Nitrophenyl chloroformate, NMM, CH_2Cl_2, RT, Ar, 8 h then Fmoc-Ser-O^{t}Bu, DMAP, RT, 18 h, 24%; (b) 50% TFA in CH_2Cl_2, $HSiEt_3$, RT, 12 h, 92%.

Deprotection of the *tert*-butyl ester to reveal the free carboxylic acid (**218**) was also achieved in 29% yield, the product of which could then be used for later peptide synthesis (**Scheme 3.44**).

DEACM-caged lysine (**219**) was synthesised by employing a procedure reported by Palomo *et. al.*.[188] The activated DEACM-nitrophenyl intermediate was synthesised by treatment of DEACM-OH (**153**) with 4-nitrophenyl chloroformate and pyridine. Following an acid work-up with 1 M HCl, the residue was then subjected to further reaction with Fmoc-Lys-O^{t}Bu (**187**) to afford the product (**219**) in 22% yield (**Scheme 3.45**).

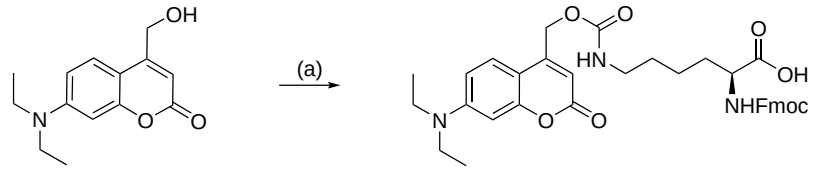


153 **219**

Scheme 3.45: Synthesis of DEACM-caged Fmoc-Lys-O^{t}Bu; Reagents & Conditions: (a) 4-Nitrophenyl chloroformate, pyridine, CH_2Cl_2, 0 °C - RT, Ar, 18 h then Fmoc-Lys-O^{t}Bu, 10% Na_2CO_3, DMF, 0 °C - RT, 22%.

In addition, DEACM-caged lysine bearing a free carboxylic acid (**220**), which could later be employed in peptide synthesis, was also successfully synthesised. DEACM-OH (**153**) was activated with 4-nitrophenyl chloroformate, prior to treatment with

Fmoc-Lys-OH·HCl to afford the desired DEACM-caged lysine (**220**) in 44% yield (**Scheme 3.46**).

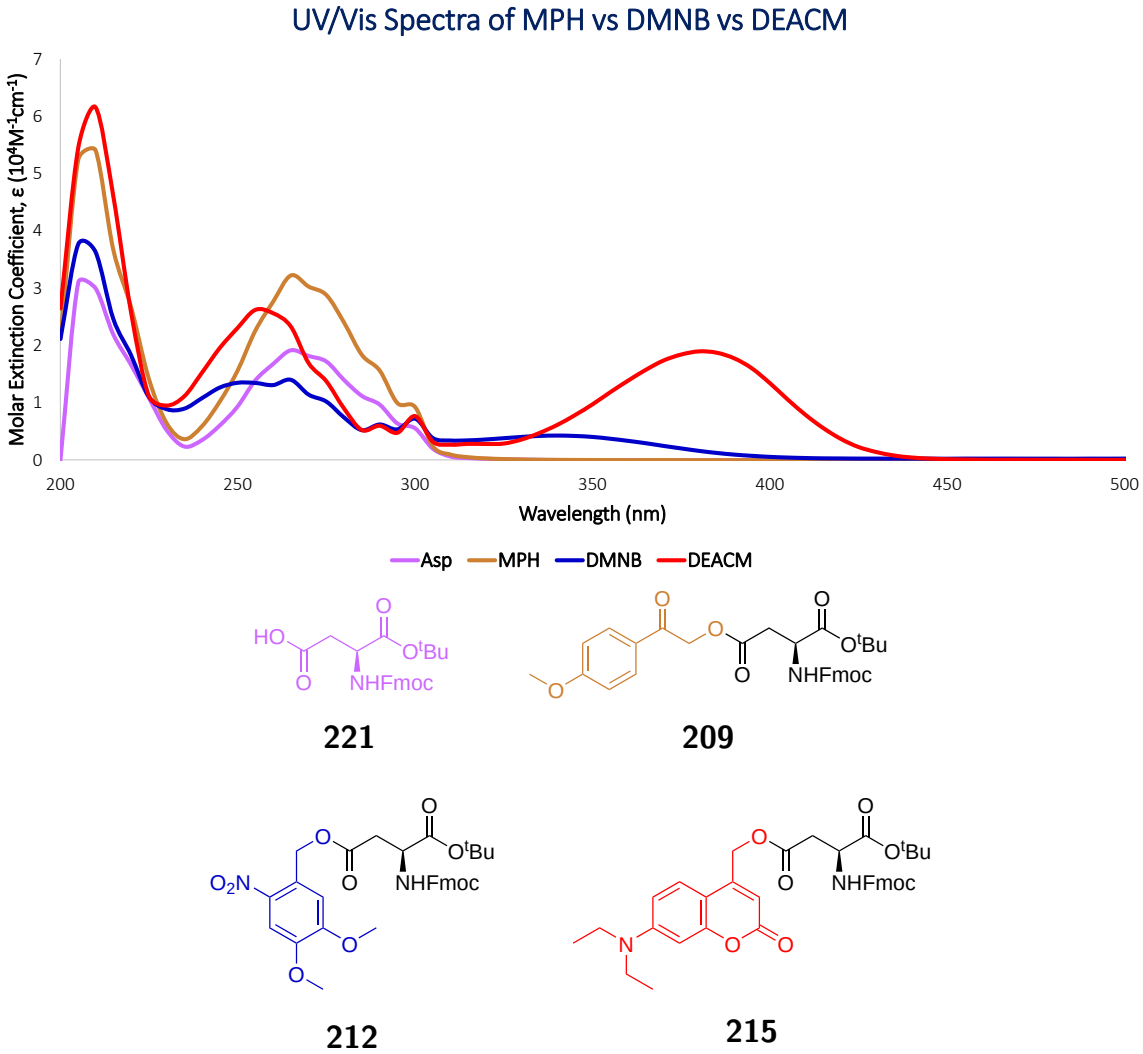


153 **220**

Scheme 3.46: Synthesis of Fmoc-Lys(DEACM)-OH; (a) 4-Nitrophenyl chloroformate, NMM, CH_2Cl_2, RT, Ar, 2 h then Fmoc-Lys-OH·HCl, $NaHCO_3$, CH_2Cl_2:MeCN:H_2O (1:4:1), RT, 18 h, 44%.

Following the synthesis of this series of caged amino acids, measurements and comparison of the UV/vis spectra were undertaken as a simplistic means of predicting the ability of the caged amino acids to undergo photolysis as well as the potential for orthogonality at various wavelengths. Photolysis experiments would then be conducted to test the photolabile caging groups for wavelength orthogonality.

3.11 Photolysis of Photolabile-Caged Amino Acids



Entry	Conc (mM)	λ_{max} (nm)	Transition	A	ε ($M^{-1}cm^{-1}$)
1	0.04	205	n – π*	1.24	30950
2	0.04	265	n – π*	1.29	32204
3	0.04	340	n – π*	0.170	4250
4	0.04	380	π – π*	0.758	18961

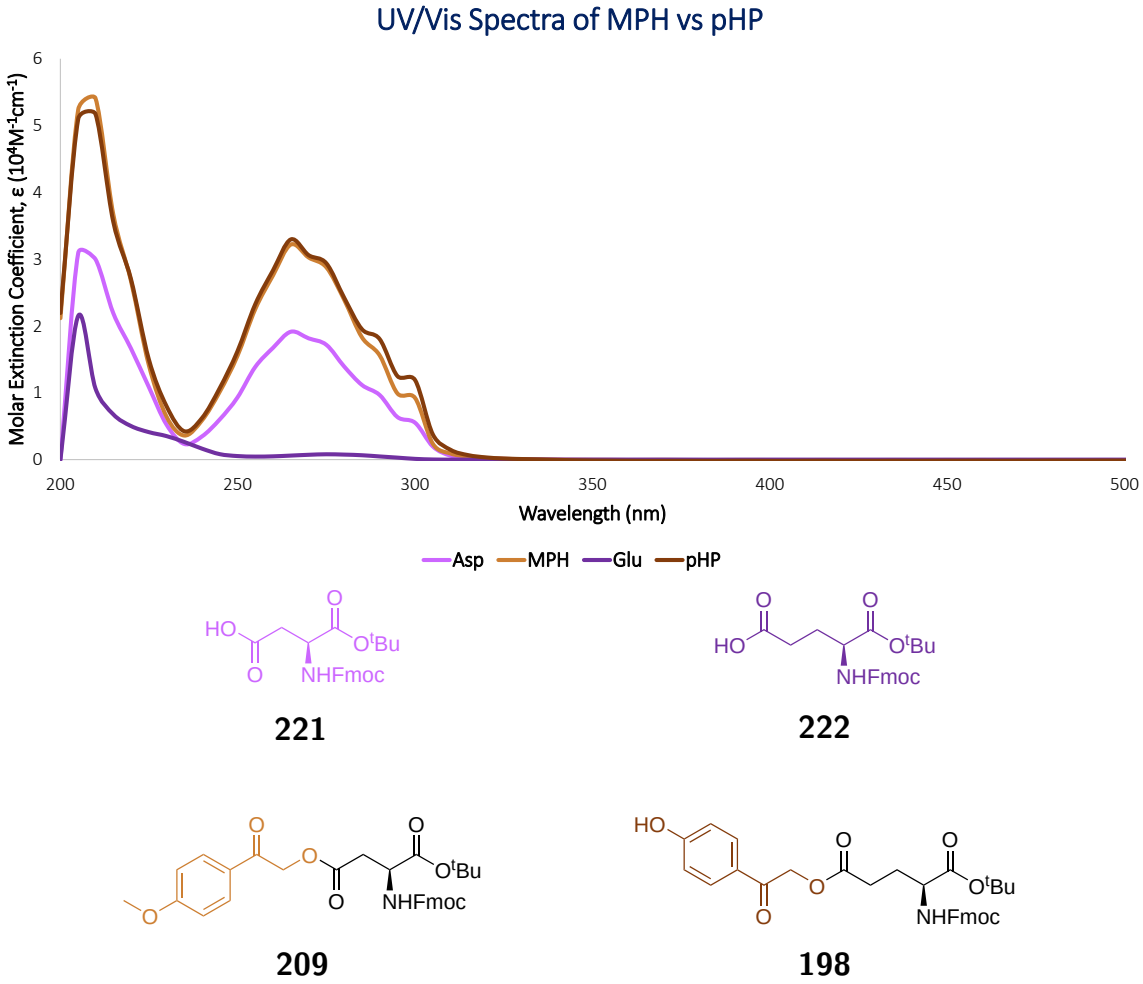
Figure 3.5: UV/vis spectra comparing Fmoc-Asp-O^{t}Bu [purple], MPH- [bronze; λ_{max} = 265 nm (n - π*)], DMNB- [blue; λ_{max} = 340 nm (n - π*)] and DEACM- [red; λ_{max} = 380 nm (π - π*)] caged Fmoc-Asp-O^{t}Bu; Concentration = 0.04 mM [MeOH].

Comparisons of the UV/vis absorption spectra of the photocaged amino acids was used as an indicator of which wavelengths would be most suitable for irradiation and photolysis.
With exception of the pHP caging group, which was measured as the glutamic acid caged compound (**198**), all other PCGs were measured as the aspartic acid caged variant.
Based on previously elucidated mechanisms of photolysis,[8] the photochemical transitions of greatest interest were those of the n - π^* [pHP, MPH, DMNB] or π to π^* [DEACM], which are responsible for the photochemical cleavage required to release the caged biomolecule.

Measurements were consistent with those reported by Bochet *et. al.*[101] and showed that the amino acid fragment had minimal effect on the absorption spectra in the region of the n - π^* or π to π^* transition.
DEACM (**215**) was shown to exhibit its transition at λ_{max} = 380 nm, whilst for DMNB (**212**), the transition occurred at λ_{max} = 340 nm and at λ_{max} = 265 nm for the MPH caging group (**209**) (**Figure 3.5**).

The pHP caging group and the MPH caging group showed little variation in their absorption properties as witnessed by their UV/vis spectra; indeed, both compounds exhibited their n - π^* transition at λ_{max} = 265 nm (**Figure 3.6**).

Based on comparisons of the measured UV/vis spectra, photolysis experiments were performed to determine which wavelengths the various caging groups were labile at. As the aim was to develop a chromatically orthogonal set of caging groups that could be cleaved at wavelengths of irradiation longer than 300 nm, the region above 300 nm of the UV/vis spectra was set as the focus for comparison. In addition, limitations in the light sources available led to the decision to irradiate the caged compounds at wavelengths of 420 nm, 365 nm, 350 nm and 310 nm. Inclusion of the Fmoc protecting group and its ability to act as a chromophore enabled formation of the photoreleased amino acid products to be monitored and quantified by HPLC analysis at hourly intervals.



Entry	Conc (mM)	λ_{max} (nm)	Transition	A	ε ($M^{-1}cm^{-1}$)
1	0.04	205	n – π*	1.24	30950
2	0.04	265	n – π*	1.29	32204
3	0.04	205	n – π*	0.861	21516
4	0.04	265	n – π*	1.32	32962

Figure 3.6: UV/vis spectra comparing Fmoc-Asp-O^{t}Bu [purple], Fmoc-Glu-O^{t}Bu [dark purple], MPH-caged [bronze; λ_{max} = 265 nm (n - π*)] Fmoc-Asp-O^{t}Bu and pHP-caged [brown; λ_{max} = 265 nm (n - π*)] Fmoc-Glu-O^{t}Bu; Concentration = 0.04 mM [MeOH].

3.11.1 Irradiation Control Reactions

Control experiments were conducted by exposing Fmoc-Asp-O^{t}Bu (**221**) to the various irradiation wavelengths. This was to demonstrate that over the course of the reaction, any photolysis observed was solely the result of uncaging of the photolabile caging

group and not any change in the expected photoreleased product.

No significant change was observed over the course of irradiation, indicating that photolysis resulted in formation of the product (**221**) at 420 nm, 365 nm, and 350 nm. However, when irradiated at 310 nm, a significant decrease of approximately 40% was observed in the composition of (**221**) after irradiating for 4 h, with a rate constant of 0.278 s^{-1} (**Figure 3.8**). This was observed as a decrease in the peak at 13.3 min and accompanied by the appearance of a new peak in the HPLC spectrum at 13.5 min (**Figure 3.7**).

Mass spectrometry revealed the new peak to have a mass corresponding to that of the original amino acid (**221**). This led to the hypothesis that the new peak corresponded to a product (**223**) derived from the photoisomerisation of the *tert*-butyl ester from the α-carboxylic acid to that of the β-carboxylic acid position (**Figure 3.8**). Further evidence for this was provided by doping studies which confirmed that Fmoc-Asp(O^{t}Bu)-OH (**223**) has the same retention time as that of the new peak under identical HPLC conditions.

It was postulated that the new isomer (**223**) was favoured owing to the decrease in steric clash of the two bulky protecting groups when in the α-positions; this line of inquiry was not pursued any further.

Thus, whilst irradiation at 310 nm resulted in photolysis of all three caging groups, the short wavelength in addition to the photoinduced isomerisation observed for the photoreleased aspartic acid product prohibited the use of this wavelength in further photolysis experiments.

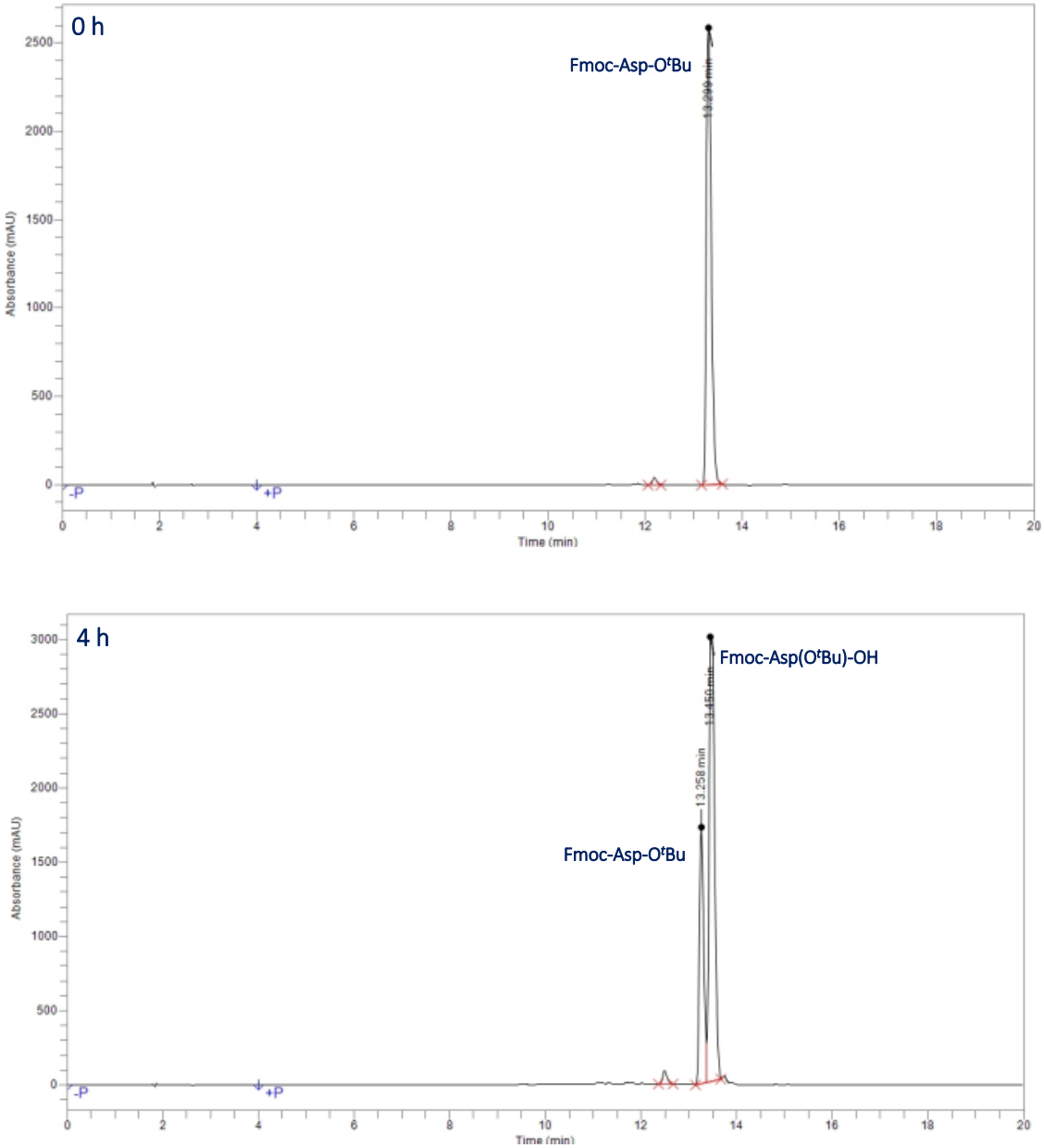
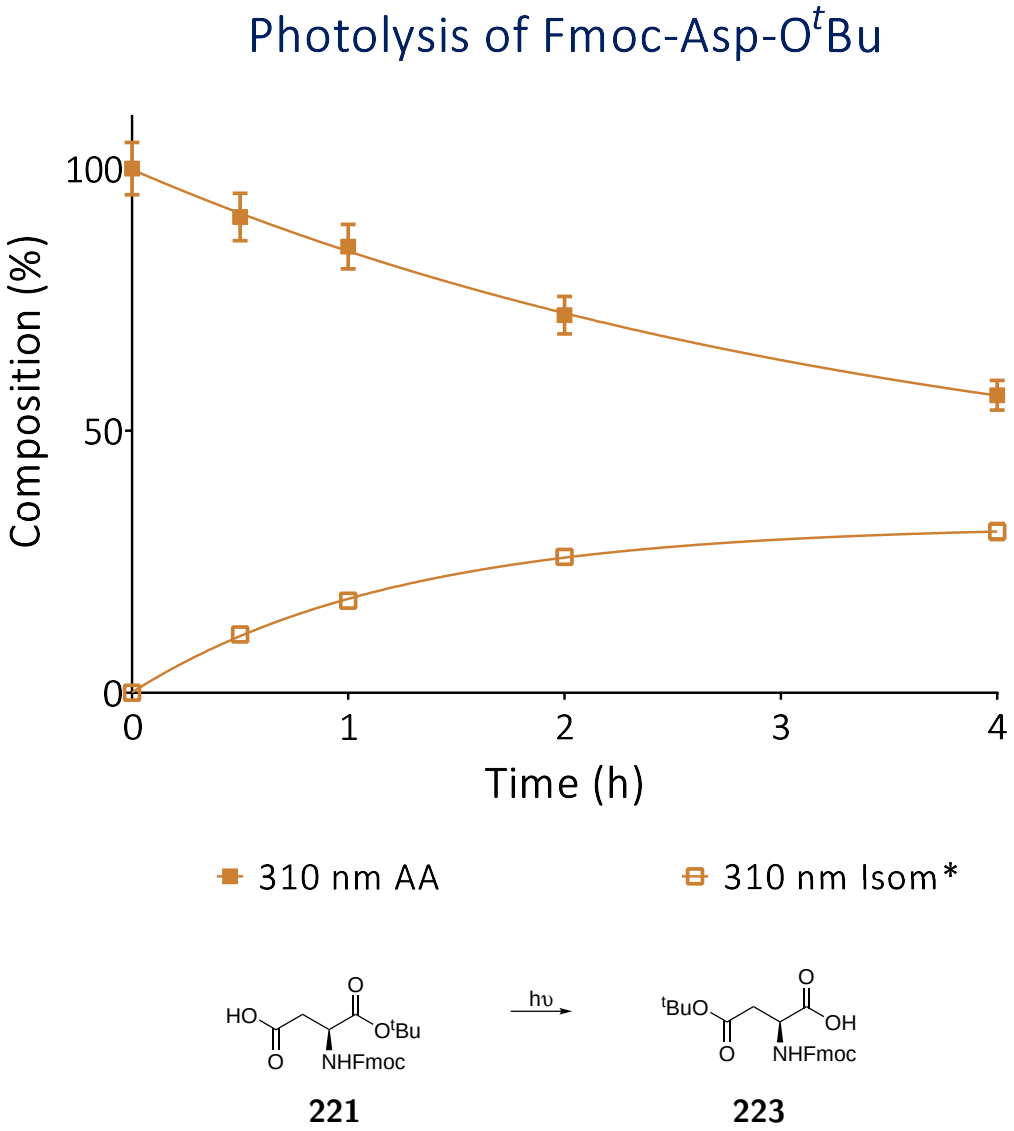


Figure 3.7: RP-HPLC spectra of control experiment following irradiation, at 310 nm, of Fmoc-Asp-O^{t}Bu at 0 h and 4 h.



Entry	λ_{irrad} (nm)	k_{AA} (s^{-1})	N_{AA}	R^2_{AA}	k_{isom} (s^{-1})	N_{isom}	R^2_{isom}
1	310	0.278	5	1.00	0.8205	5	1.00

Figure 3.8: Photoisomerisation of Fmoc-Asp-O^{t}Bu following irradiation at 310 nm in MeOH.

3.11.2 Irradiation of MPH-Caged Amino Acids

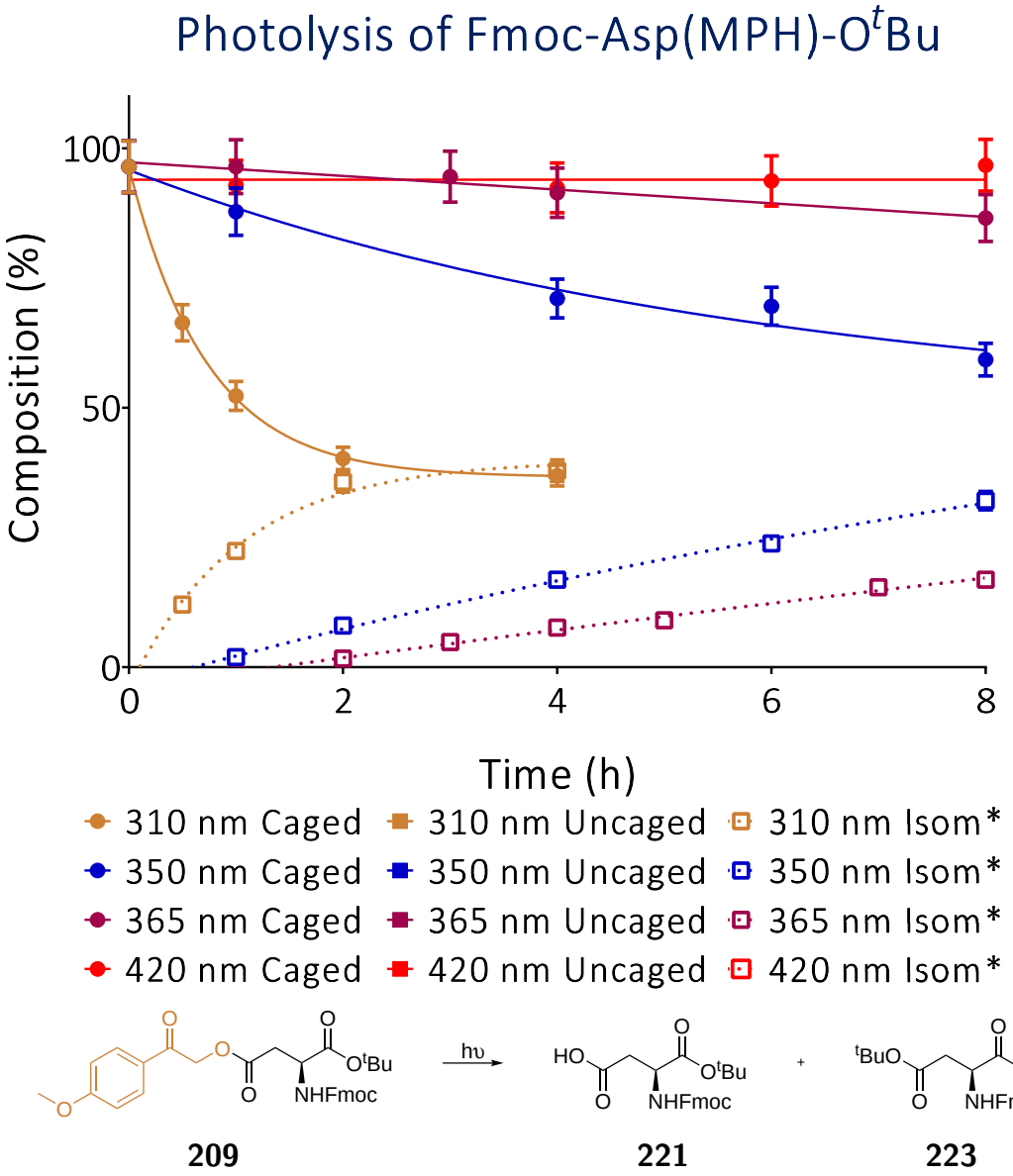
The n - π^* transition for the MPH caging group was shown to lie at $\lambda_{max} = 265$ nm. The MPH-caged amino acids were thus expected to undergo photolysis at 310 nm and remain stable at longer wavelengths of irradiation.

Despite observing a significant decrease in the percentage composition of the starting caged compound of approximately 60% over the course of 4 h with a rate constant of 1.37 s^{-1}, no photoreleased amino acid product could be detected following irradiation at 310 nm (**Figure 3.9**). This was attributed to the rate of photoinduced *tert*-butyl isomerisation exceeding that of photolysis; any photoreleased product was converted into the photoisomerised product upon release with a rate constant of 0.967 s^{-1} (see section 3.11.1).

Irradiation of Fmoc-Asp(MPH)-O^{t}Bu (**209**) at 350 nm over the course of 8 h resulted in an approximate 40% decrease of the caged amino acid with a rate constant of 0.170 s^{-1} (**Figure 3.9**). However, no photoreleased product was observed and thus the decrease was attributed to loss of starting material by photodegradation with a rate constant of 0.0733 s^{-1}.

Approximately 10% decrease was observed in the percentage composition of starting material, with a rate constant of 8.72×10^{-5} s^{-1}, over the course of irradiation of MPH-caged aspartic acid (**209**) at 365 nm. However, no formation of Fmoc-Asp-O^{t}Bu (**221**) was detected (**Figure 3.9**). The decline in starting material was attributed to photodegradation of the caged starting material, though it remains possible that the amount of product formed was too small to be detected. The light source used for irradiation at 365 nm possessed a broad spectrum, which may also have resulted in anomalous effects during photolysis.

No significant change was observed in either the composition of caged material or of any photoreleased product when MPH-caged aspartic acid (**209**) was irradiated at 420 nm; the MPH caging group was inert at this wavelength (**Figure 3.9**).



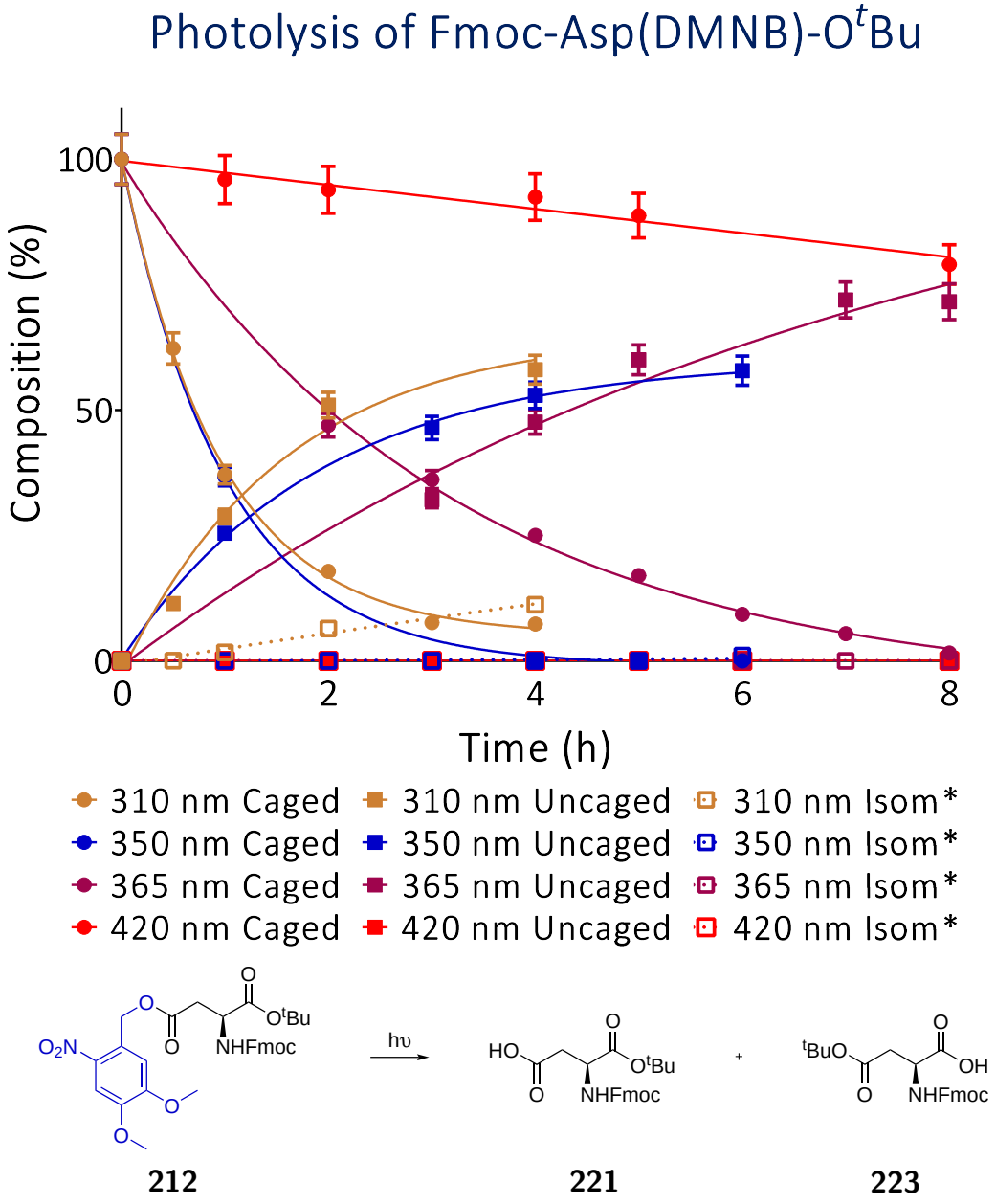
Entry	λ_{irrad} (nm)	k_{caged} (s^{-1})	N_{caged}	R^2_{caged}	$k_{uncaged}$ (s^{-1})	$N_{uncaged}$	$R^2_{uncaged}$	k_{isom} (s^{-1})	N_{isom}	R^2_{isom}
1	310	1.37	5	1.00	-	-	-	0.967	5	0.99
2	350	0.170	6	0.98	-	-	-	0.0733	6	1.00
3	365	8.72×10^{-5}	5	0.96	-	-	-	0.0236	5	1.00
4	420	-	-	-	-	-	-	-	-	-

Figure 3.9: Photolysis of MPH-caged and uncaged aspartic acid [MeOH].

3.11.3 Irradiation of DMNB-Caged Amino Acids

The n - π^* transition for the DMNB caging group was found to lie at $\lambda_{max} = 340$ nm. Uncaging was thus expected at 350 nm and 365 nm. A trough was observed around $\lambda = 310$ nm, which indicated the caging group could be stable at this wavelength. Absorbance was not observed at wavelengths longer than 400 nm; the DMNB caging group was thus expected to be stable at wavelengths longer than this.

However, complete photolysis of DMNB-caged aspartic acid (**212**) with a rate constant of 1.05 s^{-1} was observed after 3 h, with a maximum percentage composition of 67% of Fmoc-Asp-O^{t}Bu (**221**) released, as observed by HPLC, following irradiation at 310 nm (**Figure 3.10**).
Irradiation at 350 nm also resulted in complete consumption of the starting material after 4 h for DMNB-caged aspartic acid (**212**) (**Figure 3.10**) with a rate constant of 0.990 s^{-1}. The maximum percentage composition of Fmoc-Asp-O^{t}Bu (**221**) observed for the photorelease was 73% after 5 h with a rate constant of 0.522 s^{-1}. Longer irradiation times resulted in a decline of photoreleased product. This was attributed to a photoinduced isomerisation of the *tert*-butyl ester group of the Fmoc-Asp-O^{t}Bu (**221**) photoreleased product (see section 3.11.1).
DMNB-caged Asp (**212**) also displayed complete consumption of starting material, as observed by the disappearance of the peak belonging to this by HPLC, after irradiation at 365 for 7 h with a rate constant of 0.316 s^{-1}. Approximately 78% Fmoc-Asp-O^{t}Bu (**221**) was released in the 7 h timeframe measured (**Figure 3.10**) with a rate constant of 0.134 s^{-1}.
Following irradiation at 420 nm, no photoreleased Fmoc-Asp-O^{t}Bu (**221**) was detected by HPLC. However, some photodegradation of DMNB-caged aspartic acid (**212**) was observed, with the percentage composition of the caged-starting material dropping to 80% following 8 h of irradiation (**Figure 3.10**) with a rate constant of 6.75 $\times$ 10^{-5} s^{-1}. This result suggested that while some degree of photodegradation of the DMNB-caged aspartic acid starting material (**212**) was occurring, the compound was stable to photolysis with no release of uncaged aspartic acid (**221**) at 420 nm.

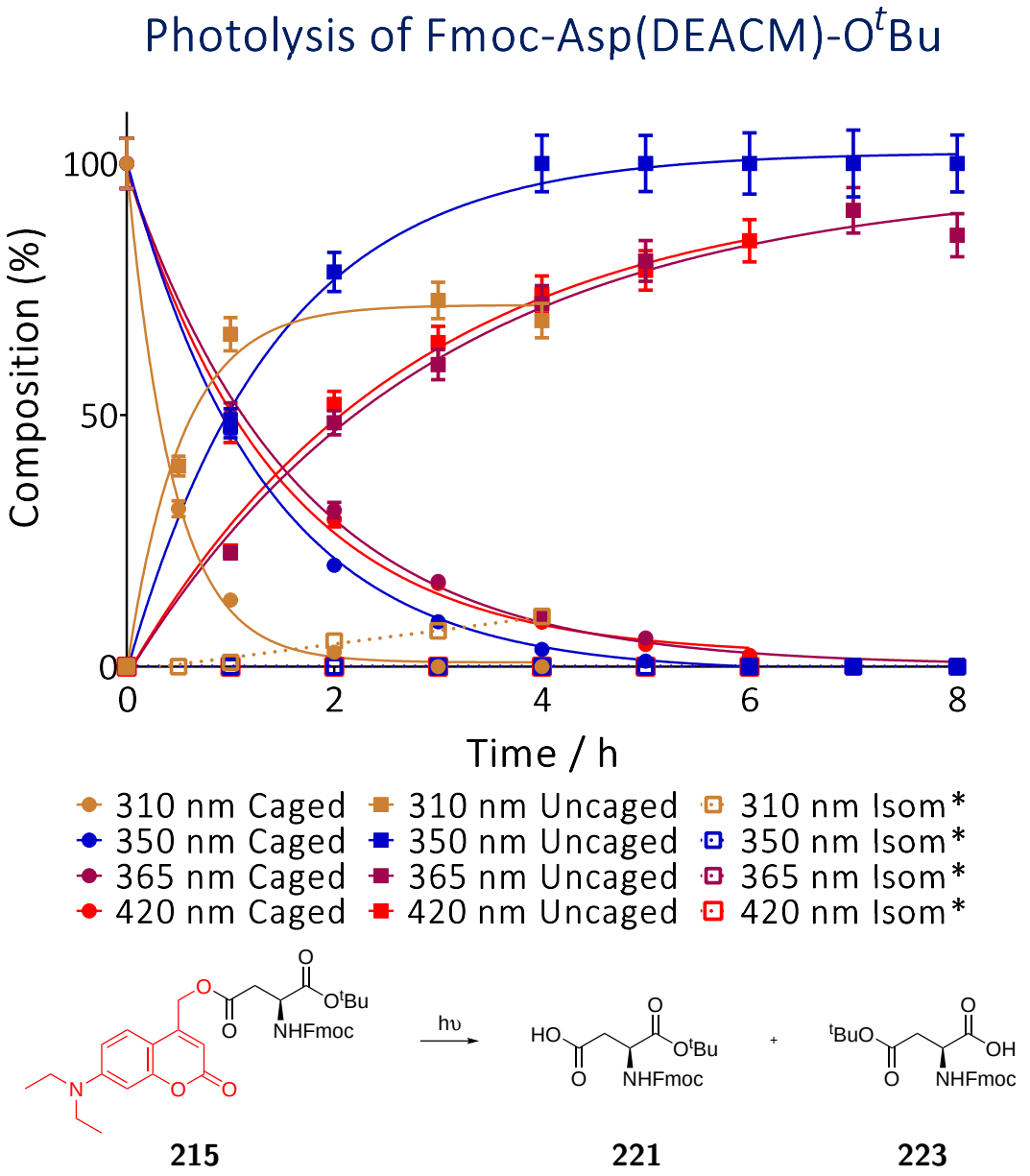

Photolysis of Fmoc-Asp(DMNB)-O^{t}Bu
Composition (%)
100
50
0
0
2
4
6
8
Time (h)
310 nm Caged
310 nm Uncaged
310 nm Isom*
350 nm Caged
350 nm Uncaged
350 nm Isom*
365 nm Caged
365 nm Uncaged
365 nm Isom*
420 nm Caged
420 nm Uncaged
420 nm Isom*
O2N
O
O
O

3.11.4 Irradiation of DEACM-Caged Amino Acids

The π - π^* transition for the DEACM caging group occurred at $\lambda_{max} = 380$ nm. It was expected that photolysis would occur following irradiation at 420 nm. Absorbance was found to be much lower in the region of 300 - 350 nm; it was postulated that kinetics could be exploited to achieve orthogonality when irradiating at shorter wavelengths.

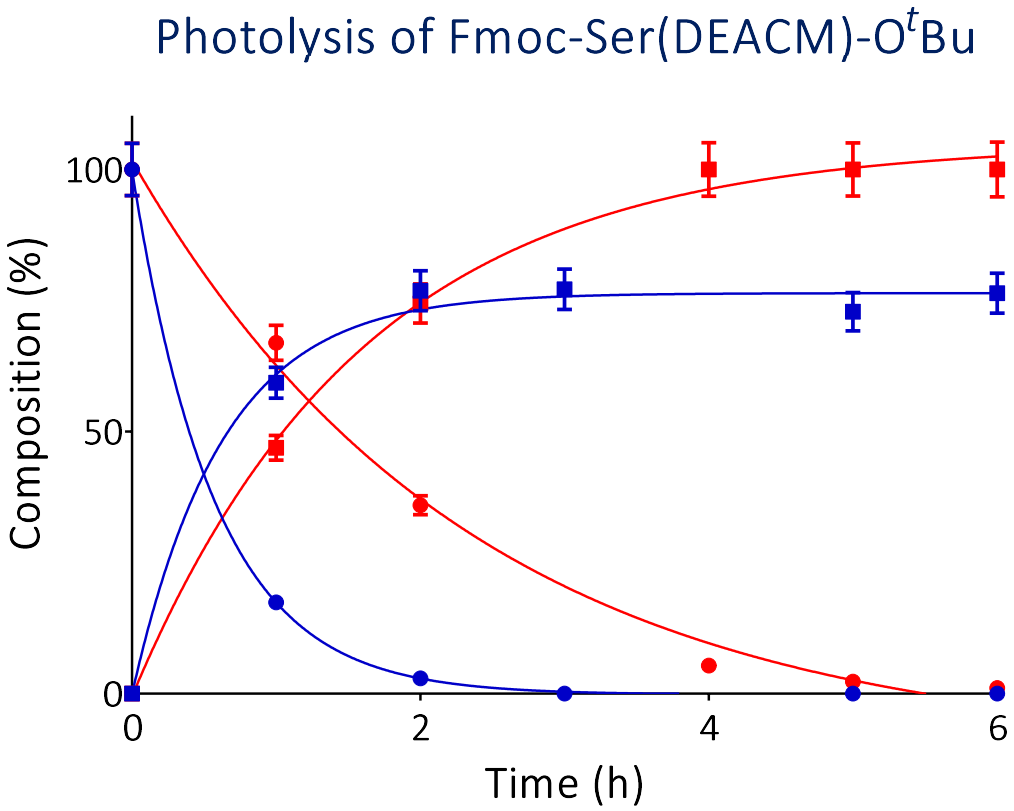
However, following irradiation at 310 nm for DEACM-caged aspartic acid (**215**), the photolysis reaction was complete after 2 h with a rate constant of 2.26 s^{-1}. This occured with a maximum of 91% photoreleased product (**221**) observed, which later decreased over time (**Figure 3.11**).
Complete consumption of the starting material (**215**) also occurred after 6 h of irradiation at 350 nm (**Figure 3.11**) with a rate constant of 0.751 s^{-1}. The maximum percentage composition of Fmoc-Asp-O^{t}Bu (**221**) observed for the photorelease from the DEACM caging group was 100% after 6 h with a rate constant of 0.703 s^{-1}.
DEACM-Asp (**215**) displayed complete consumption of starting material, as observed by the disappearance of the peak belonging to the starting material by HPLC after 7 h with a rate constant of 0.611 s^{-1}, following irradiation at 365 nm. Approximately 94% Fmoc-Asp-O^{t}Bu (**221**) was released (**Figure 3.11**) with a rate constant of 0.341 s^{-1}.
When irradiation was conducted with a light source at 420 nm, DEACM-caged aspartic acid (**215**) was observed to undergo photolysis with a rate constant of 0.689 s^{-1}. After 6 hours, the peak belonging to the starting material could no longer be observed and conversion to photoreleased aspartic acid (**221**) plateaued at a maximum of 90% (**Figure 3.11**) with a rate constant of 0.367 s^{-1}.

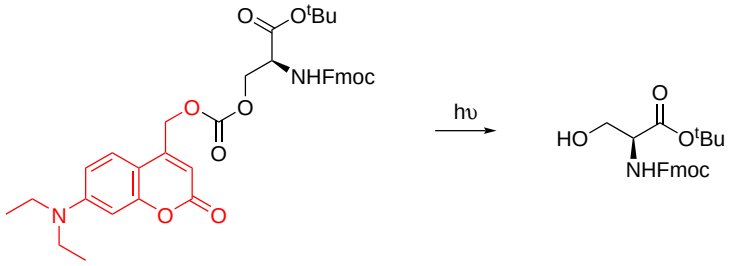
The photolysis reactions were also conducted for DEACM-caged serine (**217**) and found to mimic that of the aspartic acid caged species (**215**).
Full conversion to uncaged amino acid (**185**) for DEACM-caged serine was observed after 3 h irradiation at 350 nm (**Figure 3.12**) with a rate constant of 1.74 s^{-1}. The increased rate was attributed to the entropic effect from the decarboxylation of the carbonate following irradiation.
The photolysis reaction at 420 nm was also conducted and after 6 h, the starting material peak had completely disappeared with a rate constant of 0.427 s^{-1} and full conversion to the released amino acid (**185**) was observed (**Figure 3.12**) with a rate constant of 0.622 s^{-1}.



Entry	λ_{irrad} (nm)	k_{caged} (s^{-1})	N_{caged}	R^2_{caged}	$k_{uncaged}$ (s^{-1})	$N_{uncaged}$	$R^2_{uncaged}$	k_{isom} (s^{-1})	N_{isom}	R^2_{isom}
1	310	2.26	6	1.00	1.90	5	0.99	9.64×10^{-5}	6	0.97
2	350	0.751	9	1.00	0.703	8	1.00	-	-	-
3	365	0.611	8	1.00	0.341	8	0.99	-	-	-
4	420	0.689	7	1.00	0.367	7	0.99	-	-	-

Figure 3.11: Photolysis of DEACM-caged and uncaged aspartic acid [MeOH].





217 **221**

Entry	λ_{irrad} (nm)	k_{caged} (s^{-1})	N_{caged}	R^2_{caged}	$k_{uncaged}$ (s^{-1})	$N_{uncaged}$	$R^2_{uncaged}$	k_{isom} (s^{-1})	N_{isom}	R^2_{isom}
1	350	1.74	6	1.00	1.60	6	0.99	-	-	-
2	420	0.427	6	0.99	0.622	6	0.99	-	-	-

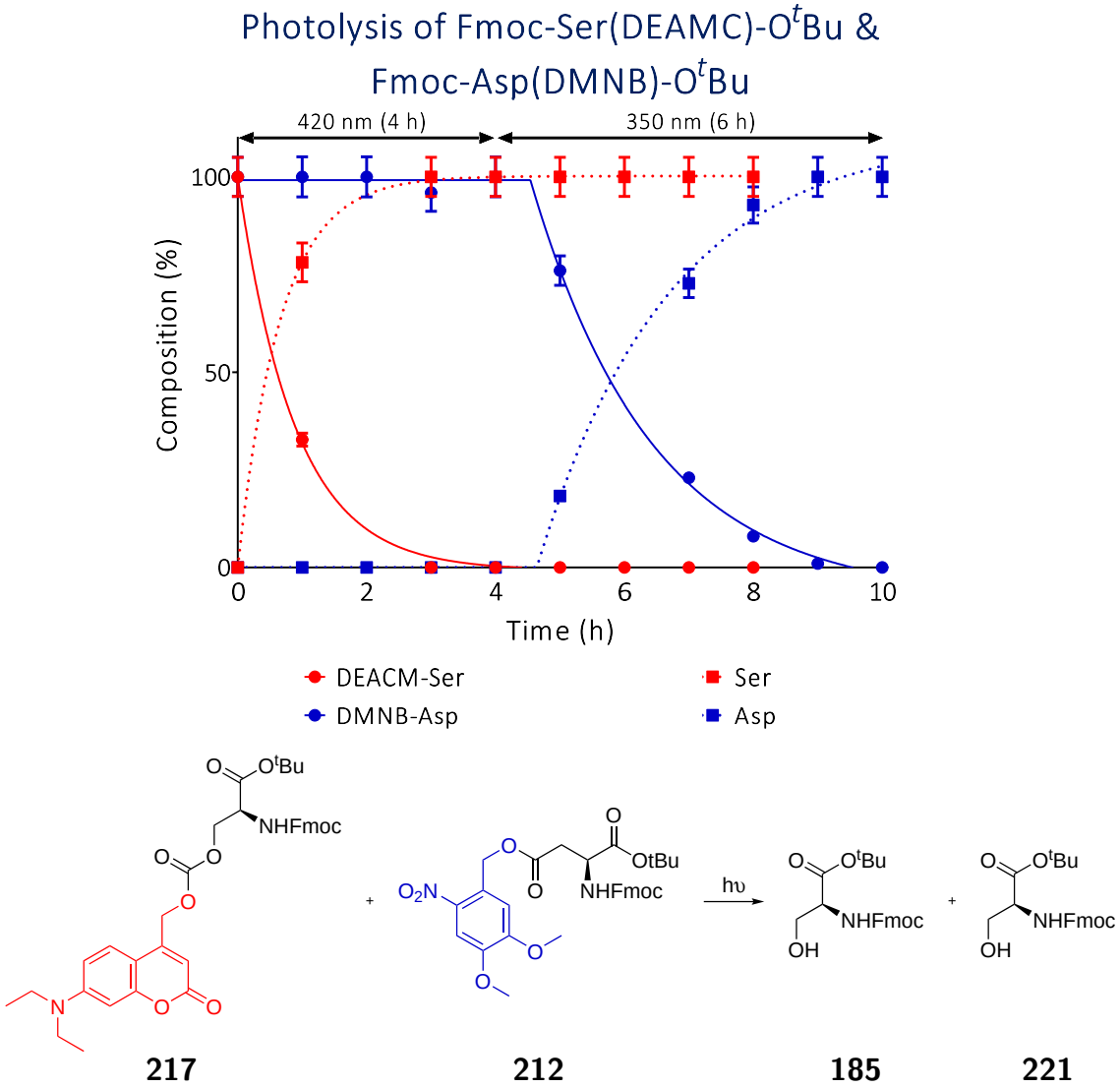
Figure 3.12: Photolysis of DEACM-caged and uncaged serine [MeOH].

3.11.5 Development of a Sequential System

It was hypothesised that a sequential system could be developed using the DEACM and DMNB caging groups.
To confirm this, a mixture of DEACM-caged serine (**217**) and DMNB-caged aspartic acid (**212**) was irradiated, first at 420 nm for 4 h, followed by 350 nm for 6 h (**Figure 3.13**).
After 4 h exposure to irradiation at 420 nm, DEACM-caged serine (**217**) had undergone complete and exclusive photolysis with a rate constant of 1.13 s^{-1}, releasing uncaged serine (**185**). At this wavelength, the DMNB-group demonstrated no significant change in its percentage composition over the course of the irradiation. Upon switching the wavelength of irradiation to 350 nm, DMNB-caged aspartic acid (**212**) underwent photolysis with a rate constant of 0.530 s^{-1} to reveal the released aspartic acid (**221**) (**Figure 3.13**).

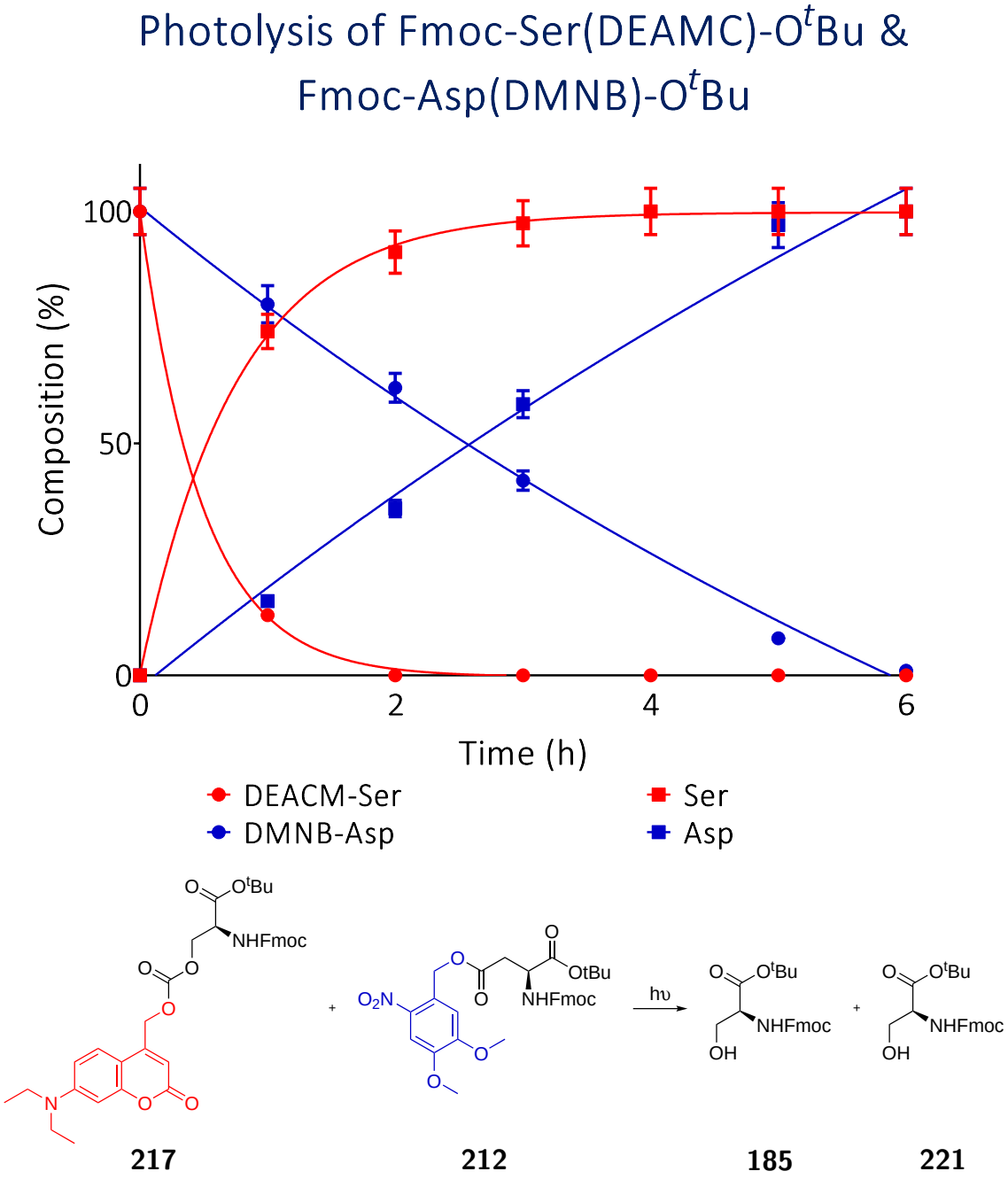
When irradiated at 350 nm (**Figure 3.14**), both compounds underwent photolysis with little distinction between the two PCGs (**Figure 3.14**) .
DEACM-caged serine (**217**) had undergone complete photolysis with a rate constant of 2.05 s^{-1} after 2 h of irradiation to release serine (**185**). The photolysis of DMNB-caged aspartic acid (**212**), with a rate constant of 0.0961 s^{-1}, was complete after 6 h to afford uncaged aspartic acid (**221**) (**Figure 3.14**).

These results were indicative of the development of a sequential system of caged amino acids bearing the DEACM and DMNB caging groups, which could undergo unidirectional photolysis i.e. only in one specific order. First, irradiation at 420 nm would reveal the uncaged biomolecule released from the photolysis of the caged DEACM species. Irradiation at 350 nm could then reveal the uncaged biomolecule from photolysis of the DMNB-species. However, if irradiation was first conducted at 350 nm, both DEACM and DMNB caging groups would undergo photolysis with little selectivity.



Entry	λ_{irrad} (nm)	k_{caged} (s^{-1})	N_{caged}	R^2_{caged}	$k_{uncaged}$ (s^{-1})	$N_{uncaged}$	$R^2_{uncaged}$
1	420	1.13	8	1.00	1.52	8	1.00
2		-	-	-	-	-	-
3	350	-	-	-	-	-	-
4		0.530	10	1.00	0.490	10	1.00

Figure 3.13: Percentage composition of DEACM-caged (red) & DMNB-caged (blue) and uncaged serine and aspartic acid following irradiation at 420 nm then 350 nm for 4 h and 6 h; [MeOH].



Entry	λ_{irrad} (nm)	k_{caged} (s^{-1})	N_{caged}	R^2_{caged}	$k_{uncaged}$ (s^{-1})	$N_{uncaged}$	$R^2_{uncaged}$
1	350	2.05	7	1.00	1.32	7	1.00
2		0.0961	6	1.00	0.078	6	1.00

Figure 3.14: Percentage composition of DEACM-caged (yellow) & DMNB-caged (blue) and uncaged serine and aspartic acid following irradiation at 350 nm for 8 h; [MeOH].

3.12 Sequential Light-Activated Caged Tripeptide

Use of the DEACM and DMNB caging groups allowed demonstration of a sequential pair of caging groups following irradiation, first at 420 nm to effect uncaging of the DEACM caging group, then at 350 nm to afford photorelease from the DMNB caging group as shown with a 1:1 mixture of DEACM-caged serine (**217**) and DMNB-caged aspartic acid (**212**) (**Figure 3.13**). As this was a tool being developed for use in peptides and proteins to study protein PTMs, the application was extended to a tripeptide bearing the two caging groups. This would be more representative of the developed system's ability to be applicable to its eventual goal.

3.12.1 Synthesis of DEACM- and DMNB-Caged Tripeptide

For the synthesis of a tripeptide bearing both the DEACM and DMNB groups, DEACM-caged aspartic acid (**215**) and DMNB-caged lysine (**214**) were chosen. Glycine was adopted as the amino acid residue linking the two caged amino acids, owing to the simplicity of its structure.

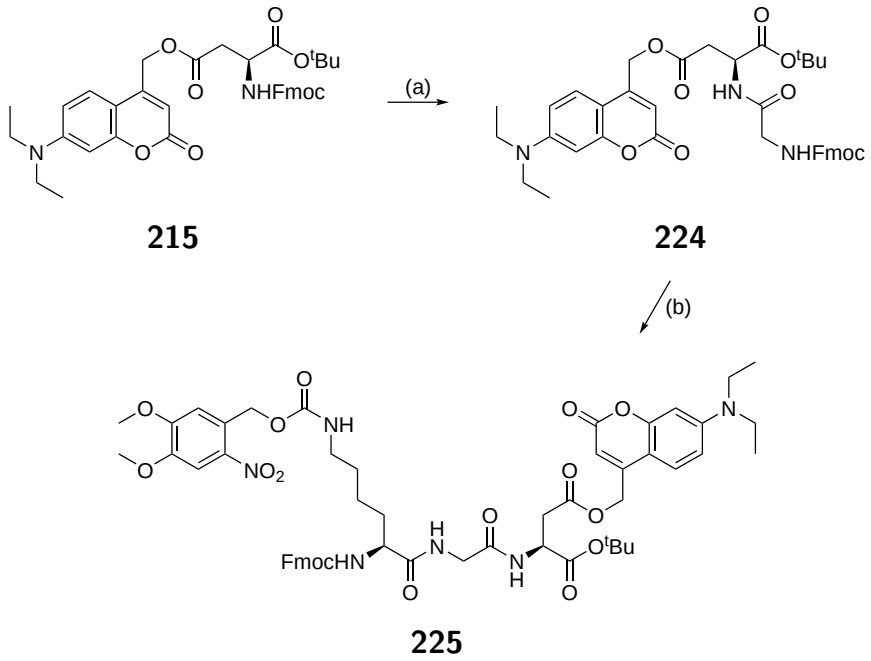
It had been the intention to use a phenylalanine residue to link the two caged amino acids, as it would be able to act as a chromophore and allow the uncaged tripeptide to be detected by HPLC. However, over the course of synthesis of the peptide, it was found that the desired tripeptide could not be isolated. This was attributed to the steric bulk of the two caging groups and the phenyl ring side chain of phenylalanine. The Fmoc protecting group was thus retained such that following photolysis, the released tripeptide could still be observed by HPLC, with the Fmoc group acting as a chromophore.

Fmoc deprotection was first performed on DEACM-caged aspartic acid (**215**), followed by reaction with commercially available Fmoc-Gly-OH to afford the desired dipeptide (**224**) in 53% yield over 2 steps (**Scheme 3.47**).

The second Fmoc deprotection and peptide coupling to afford the tripeptide presented more of a challenge. Conducting the reaction as before, no product could be isolated; this was thought to be the result of excess piperidine in the reaction mixture from the Fmoc deprotection step eroding the yield by facilitating the ester hydrolysis of the DEACM caging group on the side chain carboxylic acid of the aspartic acid residue. Decreasing the amount of piperidine conferred no additional advantage but instead prolonged the reaction time for Fmoc deprotection. Attempting to include an acid wash to remove the excess piperidine also proved to be futile as the dipeptide bearing

the free amine was simultaneously drawn into the aqueous layer. Basifying this and extracting with Et_2O once again simply resulted in both compounds being drawn back into the organic layer.
The best solution found, in order to separate the excess piperidine from the dipeptide, was to employ a silica gel plug; loading the crude reaction mixture directly onto silica gel and eluting with a mixture of petroleum ether and acetone. Following removal of the volatiles, the crude residue was then further reacted with Fmoc-Lys(DMNB)-OH (**214**), affording the desired tripeptide (**225**) bearing the DEACM and DMNB caging groups in 21% yield over 2 steps (**Scheme 3.47**).

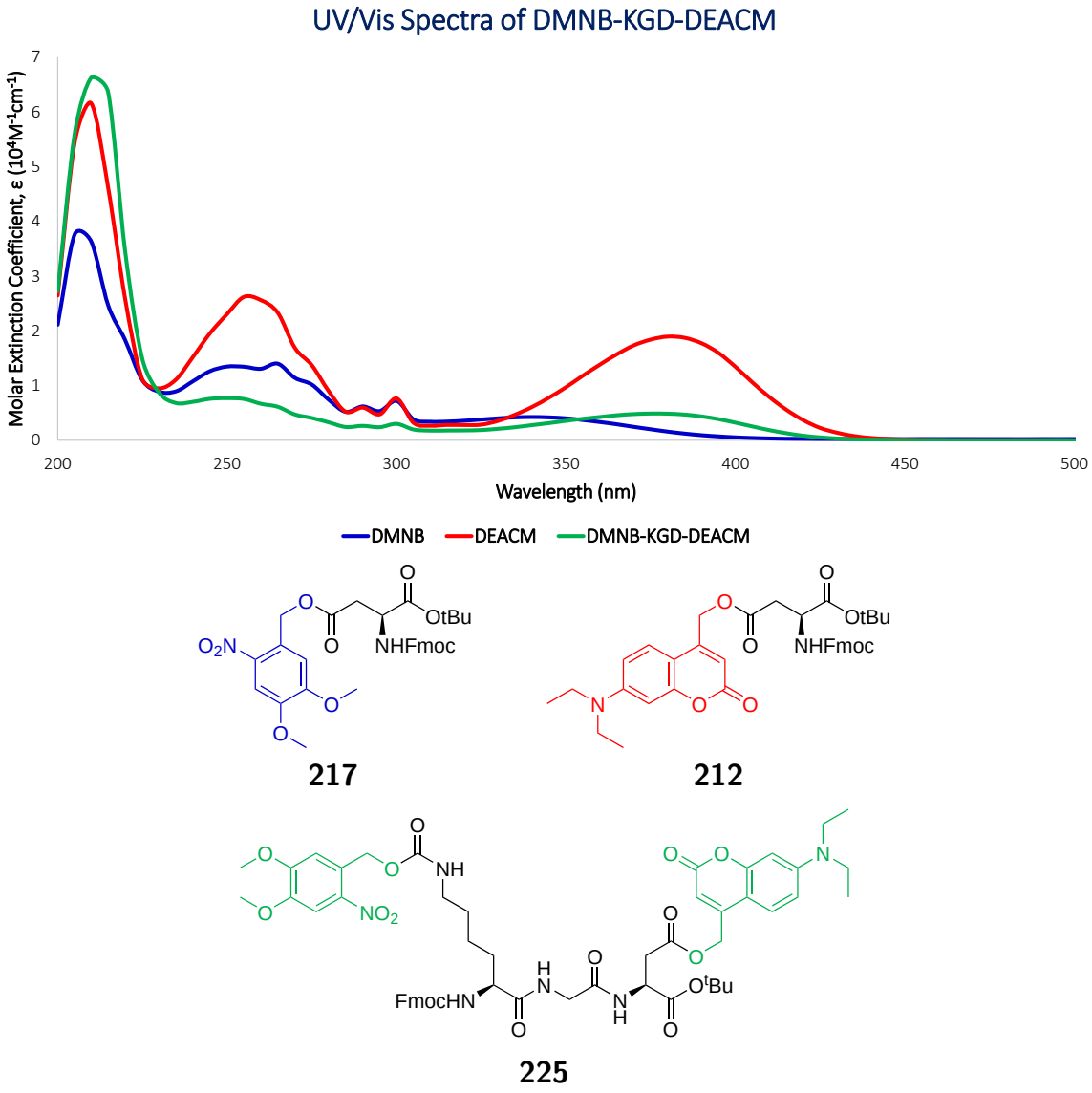
With the synthesis of the dual caged tripeptide (**225**) bearing the DMNB and DEACM caging groups complete, it was possible to commence investigation of its photophysical and photolytic properties.



215 **224** **225**

Scheme 3.47: Synthesis of tripeptide incorporating DEACM-caged aspartic acid, DMNB-caged lysine and a glycine linker; Reagents & Conditions: (a) 10% Piperidine in DMF, 0 °C, Ar, 0.5 h then Fmoc-Gly-OH, HBTU, DIPEA, DMF, RT, Ar, 18 h, 53% over 2 steps; (b) 10% Piperidine in DMF, 0 °C, Ar, 1 h then Fmoc-Lys(DMNB)-OH, HBTU, DIPEA, DMF, RT, Ar, 24 h, 21% over 2 steps.

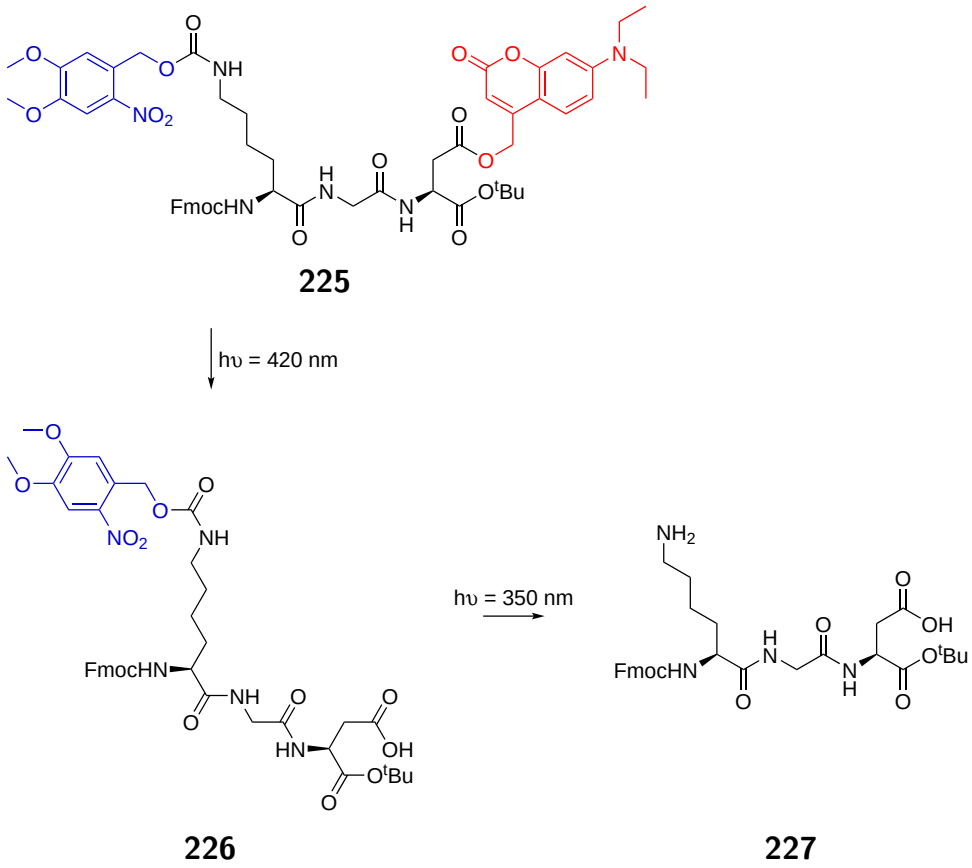
3.13 Photolysis of the Sequentially-Caged Tripeptide



Entry	Conc (mM)	λ_{max} (nm)	Transition	A	ε ($M^{-1}cm^{-1}$)
1	0.04	340	n – π*	0.170	4250
2	0.04	380	π – π*	0.758	18961
3	0.04	375	n – π*	0.196	4891
			π – π*		

Figure 3.15: UV/vis Spectra of DEACM- & DMNB-caged tripeptide [green; λ_{max} = 378 nm (n - π*)] overlaid on DEACM-caged aspartic acid [yellow; λ_{max} = 380 nm (π - π*)] and DMNB-caged aspartic acid [blue; λ_{max} = 340 nm (n - π*)]; [0.04 mM in MeOH].

The UV/vis spectrum of the DEACM- and DMNB-caged tripeptide (**225**) was measured and λ_{max} was determined to lie at 378 nm (**Figure 3.15**).
The UV/vis spectra of the tripeptide (**225**) suggested that the molecule would display similar photolytic properties to the mixture of the two individual caged amino acids. Based on these results, the photolysis experiments were conducted at 420 nm and 350 nm and monitored by HPLC. The peaks were manually collected and the identities of the species confirmed by mass spectrometry.



Scheme 3.48: Photolysis of DEACM- & DMNB-caged tripeptide by irradiation at 420 nm (4 h) followed by 350 nm (4 h); [MeOH].

The dual caged tripeptide (**225**) was first irradiated at 420 nm then 350 nm.
After 4 h of irradiation at 420 nm, the DEACM caging group had undergone complete and exclusive photolysis, evident from the decline of the peak at 14.8 min, with **LRMS *m/z* (ESI$^+$)**: 1065 [(M + H)$^+$]. The tripeptide product (**226**) bore the free carboxylic acid side chain of aspartic acid, with the DMNB caging group still intact at the ε-amine side chain of the lysine residue. This was observed as a peak at 12.9 min in the HPLC spectrum (**Figure 3.16**), with **LRMS *m/z* (ESI$^+$)**: 836 [(M + H)$^+$, 858 [(M + Na)$^+$].

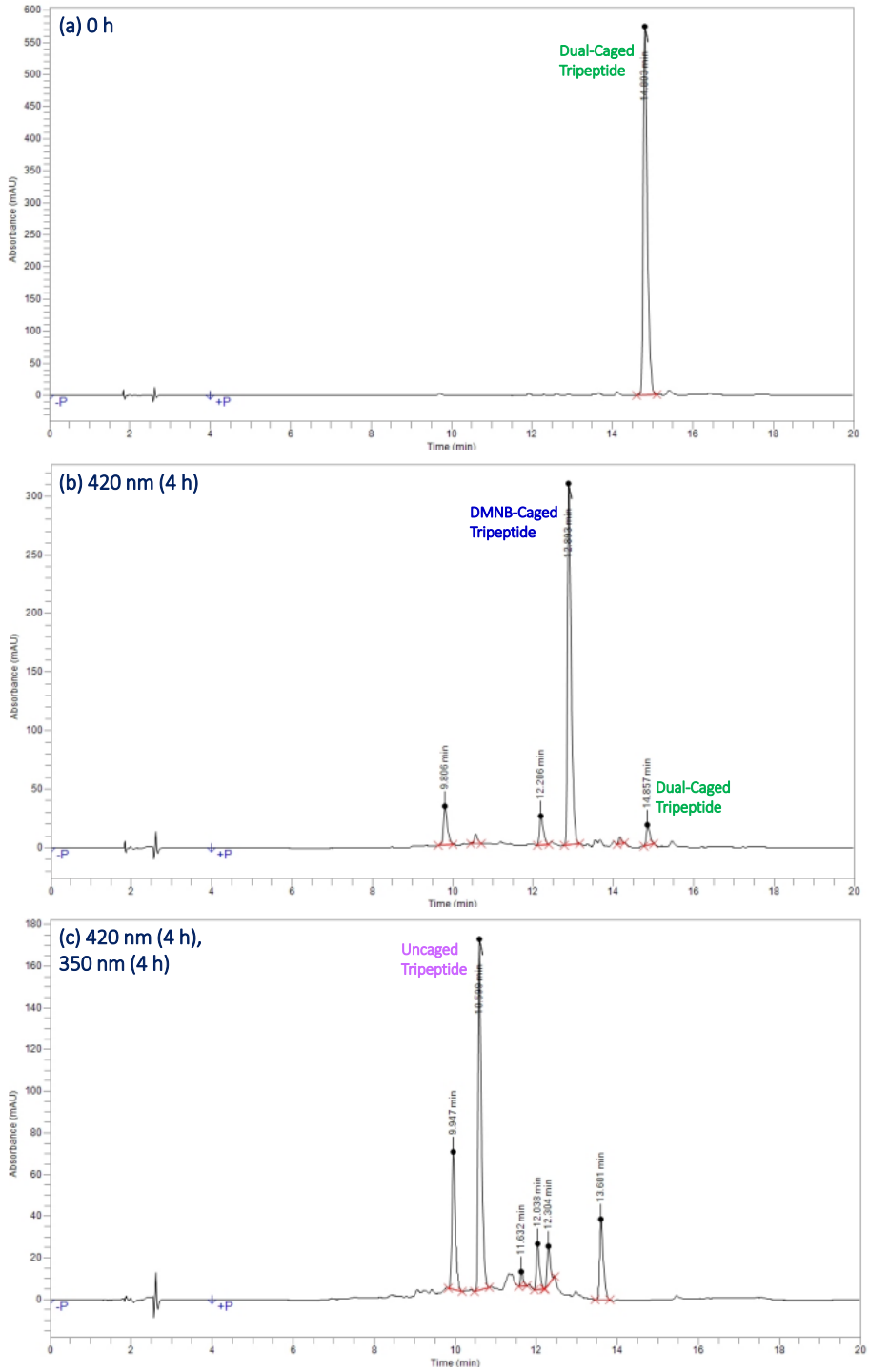
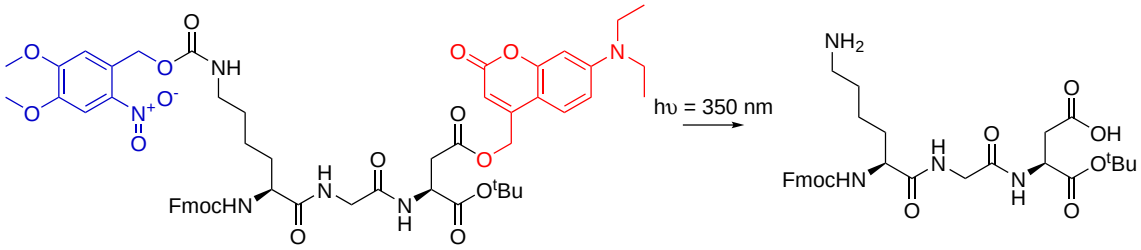


Figure 3.16: RP-HPLC traces following irradiation of DEACM- and DMNB-caged tripeptide at 420 nm (4 h) then 350 nm (4 h); (a) 0 h: caged tripeptide = 14.8 min; (b) 4 h at 420 nm: caged tripeptide = 14.8 min, DMNB-caged tripeptide = 12.9 min, DEACM photolysis by-product = 12.2 min, DEACM photolysis by-product = 9.8 min; (c) 4 h at 420 nm then 4 h at 350 nm: DEACM photolysis by-product = 12.3 min, DMNB photolysis by-product = 11.6 min, uncaged tripeptide = 10.6 min, DEACM photolysis by-product = 9.9 min.

Following this, the compound was exposed to irradiation at 350 nm for 4 h and this resulted in the cleavage of the DMNB group at the side chain ε-amine of the lysine residue to reveal the fully uncaged tripeptide (**227**), as a peak at 10.6 min in the HPLC spectrum (**Figure 3.16**), with **LRMS *m/z* (ESI$^+$)**: 597 [(M + H)$^+$].

When the dual caged tripeptide (**225**) was exposed to irradiation at 350 nm for 6 h (**Scheme 3.49**), as had been observed for the mixture of the individual caged amino acids, little to no selectivity was afforded in terms of the photolysis observed for the two caging groups.
Both DEACM and DMNB were photolysed simultaneously to afford the fully uncaged tripeptide (**227**), evident as a peak at 10.6 min in the HPLC spectrum (**Figure 3.17**), with **LRMS *m/z* (ESI$^+$)**: 597 [(M + H)$^+$], bearing the free carboxylic acid side chain of aspartic acid and the free ε-amine side chain of the lysine residue.

These results supported initial findings that a sequential pair of photolabile caging groups had been developed, through use of the DEACM and DMNB caging groups. These could be selectively cleaved, first by irradiation at 420 nm to cleave the DEACM group followed by irradiation at 350 nm to photolyse the DMNB group. Irradiation at 350 nm afforded little to no selectively in terms of the order of photolysis of the two caging groups.



Scheme 3.49: Photolysis of DEACM- & DMNB-caged tripeptide by irradiation at 350 nm (6 h); [MeOH].

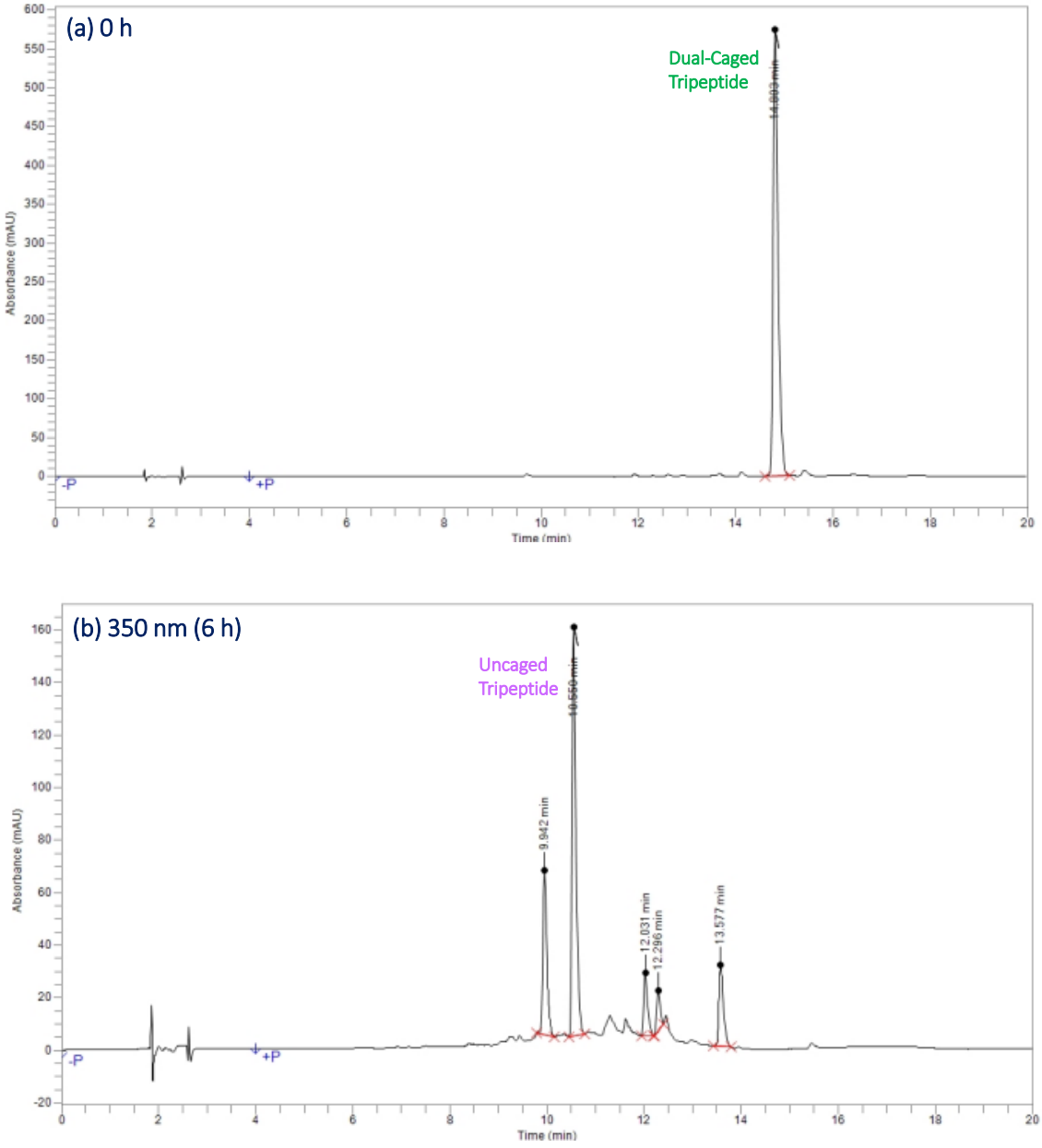


Figure 3.17: RP-HPLC traces following irradiation of DEACM- and DMNB-caged tripeptide at 350 nm (6 h); (a) 0 h: caged tripeptide = 14.8 min; (b) 6 h at 350 nm: DEACM photolysis by-product = 12.3 min, DMNB photolysis by-product = 11.3 min, uncaged tripeptide = 10.6 min, DEACM photolysis by-product = 9.8 min.

3.14 Summary & Conclusions

In this chapter, three of the more commonly used and better characterised caging groups, the MPH, DMNB, and DEACM groups, were explored for their potential to act as orthogonal sets of caging groups. As it was intended to apply this to the study of protein PTMs, amino acid biomolecules with side chains bearing differing functional groups commonly known to undergo PTM were selected to be caged. This included aspartic acid and glutamic acid bearing carboxylic acid side chains, serine with a primary hydroxyl side chain, tyrosine which possesses a phenolic side chain moiety, and lysine, bearing a primary amine at its side chain. At the onset, the amino acids were synthesised bearing Boc and *tert*-butyl ester protecting groups at the α-amine and carboxylic acid moieties. However, difficulties with the synthesis and purification of their caged variants led to adoption of the Fmoc and *tert*-butyl ester protection strategy, which would make this approach compatible for analysis by HPLC, owing to the Fmoc group's ability to act as a chromophore.

Aspartic acid caged species were selected as the model system, and following the successful synthesis of these and other caged amino acid analogues, their UV/vis spectra were measured and compared. Content that the results matched those of Bochet *et. al.*[101] and others,[8] initial photolysis studies were conducted by irradiating at 420 nm, 365 nm, 350 nm, and 310 nm. These results provided evidence that the current selection of photolabile caging groups afforded a sequential pair. As such, a mixture of DEACM-caged serine (**217**) and DMNB-caged aspartic (**212**) acid was irradiated at 420 nm and 350 nm.
It was found that at these wavelengths, the pair of PCGs was sequential, first by cleaving the DEACM group at 420 nm, followed by the DMNB at 350 nm. Irradiation at 350 nm offered little to no selectivity with respect to the photolysis of the two caging groups.

In culmination, a tripeptide (**225**), bearing both the DEACM and DMNB photolabile caging groups, was synthesised and subjected to irradiation at 420 nm and 350 nm. The results clearly reflected what had previously been observed for the mixture of the individual caged amino acids and provided conclusive evidence that a sequential pair of caging groups had been successfully developed, with great potential for use in peptides and proteins for the study of protein post-translational modifications.

Chapter 4

Red Shifted Caging Groups Towards the Development of Photoactive Tools for the Analysis of Protein Post-Translational Modification

The more commonly used caging groups often require irradiation in the UV region for one-photon photoactivation. Consequently, it was necessary to explore alternative caging groups capable of absorbing in the visible region, despite obvious difficulties in predicting which structures will undergo useful photolysis reactions. Photolysis employing wavelengths in the visible region would have the advantage of enhanced optical penetration into tissues and reduced photodamage to cells. Use of longer wavelengths would increase the applicability and compatibility of this methodology for use in biological systems and confer economical benefits as cheaper light sources and ordinary pyrex glass could be used.

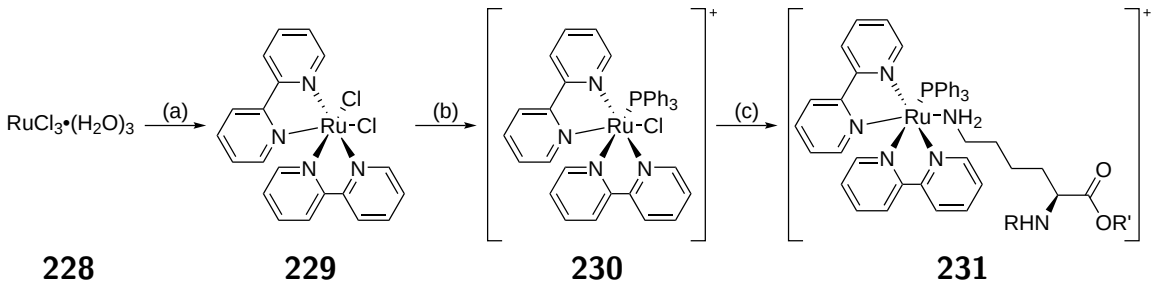
Caging groups trialled included the inorganic ruthenium bipyridyl group, to which the amino acid side chain functional groups could be coordinated, a thiocoumarin group, and two BODIPY variants. These caging groups were shown to possess red shifted λ_{max} and could be photolysed at longer wavelengths. The aim was to synthesise caged amino acids protected by these caging groups, employing aspartic acid as the model system for comparison purposes. The UV/vis spectra could then be measured and compared and preliminary photolysis experiments conducted to assess the potential for orthogonality with other caging groups.

4.1 Inorganic Ruthenium Polypyridyl Caging Group

The inorganic ruthenium polypyridyl caging group had been shown to uncage at $\lambda_{irradiation} = 450$ nm and had the potential to demonstrate orthogonality with the DMNB caging group [$\lambda_{irradiation} = 350$ nm].
Coordination of lysine to the ruthenium centre through the ε-amine of the side chain would inhibit PTM at this site. This mode of coordination most closely resembled prior literature examples published for this type of caged compounds.[64] Photolysis and hence release of the lysine residue to protein PTM would occur at longer wavelengths.

4.1.1 Towards the Synthesis of Ru(bpy) Caged Amino Acids

The $Ru(bpy)_2$ core bearing two bipyridyl groups and a triphenyl phosphine ligand, to act as the tuning ligand, were chosen due to their commercial availability and ease of synthesis of the photocaging building block.
Two Bpy groups were initially coordinated to the Ru centre by reaction of hydrated $RuCl_3$ (**228**) with Bpy as reported by Viala and Coudret.[189] Black microcrystals of the desired compound (**229**) were afforded in 35% yield upon crystallising from acetone (**Scheme 4.1**).
The PPh_3 group coordination to the Ru-centre was then achieved by heating with PPh_3 under reflux to afford the desired $Ru(bpy)_2(PPh_3)Cl$ caging group (**230**) in 94% yield (**Scheme 4.1**).[65]



Scheme 4.1: Synthesis of $Ru(bpy)_2$-caged lysine; Reagents & Conditions: (a) Bpy, LiCl, anhydrous DMF, reflux, Ar atm, 8 h, 35%;[189] (b) PPh_3, $MeOH/H_2O$, reflux, 2 h, 94%;[65] (c) For conditions, see (**Table 4.1**).

Various conditions were explored to coordinate the primary ε-amine of the lysine side chain to the Ru centre (**Scheme 4.1**).[190], [65], [191]

Table 4.1: Conditions attempted for the coordination of R-group amine of lysine to Ru-centre.

Entry	Amino Acid	Additive	Solvent	T (° C)
1	H-Lys-OH·HCl	aq. NaOH (1.0 M)	H_2O	80
2	H-Lys-OH·HCl	aq. NaOH (2.0 M)	H_2O	80
3	Fmoc-Lys-OtBu	aq. NaOH (1.0 M)	H_2O	80
4	Fmoc-Lys-OtBu	-	H_2O /EtOH	90
5	Fmoc-Lys-OtBu	-	EtOH	120
6	Fmoc-Lys-OtBu	-	H_2O /MeOH	110
7	Boc-Lys-OH	-	H_2O	80
8	Boc-Lys-OH	-	H_2O	85
9	Boc-Lys-OH	-	MeOH	80
10	Fmoc-Lys-OH·HCl	$KHCO_3$	H_2O	80
11	H-Lys-OH·HCl	K_2CO_3	EtOH	80
12	Fmoc-Lys-OH·HCl	K_2CO_3	EtOH	100
13	H-Lys-OH·HCl	K_2CO_3	EtOH	100
14	Fmoc-Lys-OtBu	LiCl	DMF	170
15	Boc-Lys-OH	$AgSO_3CF_3$	MeOH	80
16	Fmoc-Lys-OH	$AgSO_3CF_3$	MeOH	80
17	Boc-Lys-OH	$AgSO_3CF_3$	EtOH	100
18	Boc-Lys-OH	$AgSO_3CF_3$	EtOH	100

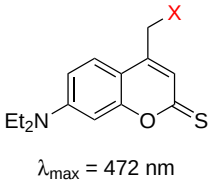
The reaction was screened with several different lysine analogues and additives in a variety of solvents at different temperatures.
Unprotected lysine was trialled to mitigate concerns that protecting groups on the α-amine or α-carboxylic acid could potentially interfere with the coordination reactions. Coordination to the Ru centre was postulated to preferentially occur through the ε-amine instead of the α-amine, because the ϵ-amine is more accessible. Unfortunately, the desired product could not be isolated nor was it possible to obtain any evidence for its formation.
Some milder conditions, to effect the coordination in the absence of base, were trialled, where Fmoc-Lys-O^{t}Bu or Boc-Lys-OH were investigated as potential ligands to prevent deprotection of the protecting groups under basic conditions. However, once again no formation of the product (**231**) was observed with any of these conditions.
Some mild bases, such as K_2CO_3, were also screened but no conversion to product was observed, as adjudged by **^{1}H NMR** and mass spectrometry.

As a final attempt, $AgSO_3CF_3$ was used as an additive to promote the exchange of the Cl^- ligand for H_2O at the Ru centre prior to the substitution by the ε-amine

of lysine.[192] It was thought that the precipitation of the AgCl salt would shift the equilibrium to favour the formation of the hydrate. Precipitation of AgCl as a colourless solid, which turned grey on exposure to air, indicated the ligand exchange had been effected. Product formation could also be observed by mass spectrometry, however attempts to precipitate out the desired product as the PF_6 salt were unsuccessful. Despite numerous attempts, formation of the desired complex (**231**) could not be achieved.

4.2 Diethylamino-Thiocoumarin (DEATC) Caging Group

Based on the work of Jullien *et. al.*,[193] the DEATC caging group (λ_{max} = 467 nm) stood out as a strong contender for the possibility of affording a chromatically orthogonal pair of PCGs, in combination with other PCGs, including the DMNB group, which has previously shown to undergo photolysis at 350 nm but not at 420 nm.

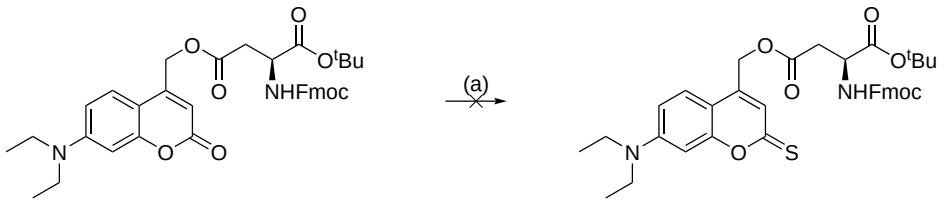


89

Figure 4.1: The DEATC caging group.

4.2.1 Synthesis, Photolysis and Evaluation of DEATC-Caged Amino Acids

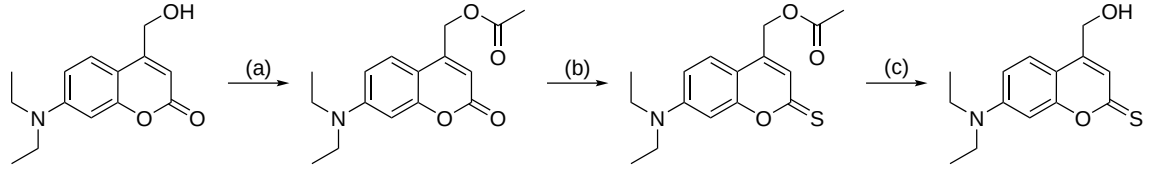
The synthesis of DEATC-caged aspartic acid (**232**) was initially attempted by treating DEACM-caged aspartic acid (**215**) with Lawesson's reagent (**Scheme 4.2**), as it was believed that the carbonyl group of the lactone would be more susceptible to the reaction, to afford the thiolactone. Unfortunately, it was not possible to isolate the desired product and instead a complex mixture was obtained as observed by TLC, arising from sulphur-oxygen substitution at various carbonyl groups within the molecule.



215 **232**

Scheme 4.2: Attempted synthesis of DEATC-caged aspartic acid; Reagents & Conditions: (a) Lawesson's reagent, toluene, reflux, Ar, 12 h.

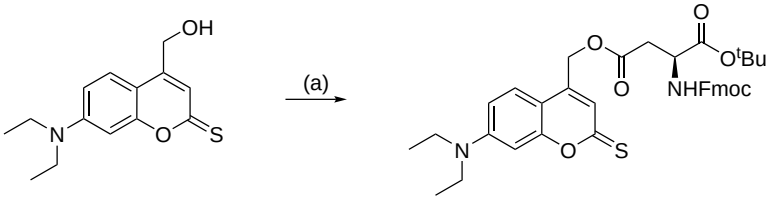
Thus, the DEATC caging group (**235**) was synthesised prior to coupling with the desired amino acid side chain functional group. This was achieved by acetate protection of the primary alcohol of the previously synthesised DEACM caging group (**153**), through the use of glacial acetic acid and DCC in 87% yield. The key step in this sequence was achieved by reacting the ester (**233**) with Lawesson's reagent under reflux in toluene, to afford the acetate protected DEATC caging group (**234**) in 68% yield. The final desired caging group (**235**) was then obtained by ester cleavage under acidic conditions, affording DEATC-OH (**235**) in 50% yield (**Scheme 4.3**).



153 **233** **234** **235**

Scheme 4.3: Synthesis of DEATC caging group; Reagents & Conditions: (a) DCC, DMAP, glacial acetic acid, anhydrous CH_2Cl_2, 0 °C - RT, Ar, 16 h, 87%; (b) Lawesson's reagent, toluene, reflux, Ar, 12 h, 68%; (c) Ethanolic HCl (1.25 M), reflux, Ar, 18 h, 50%.

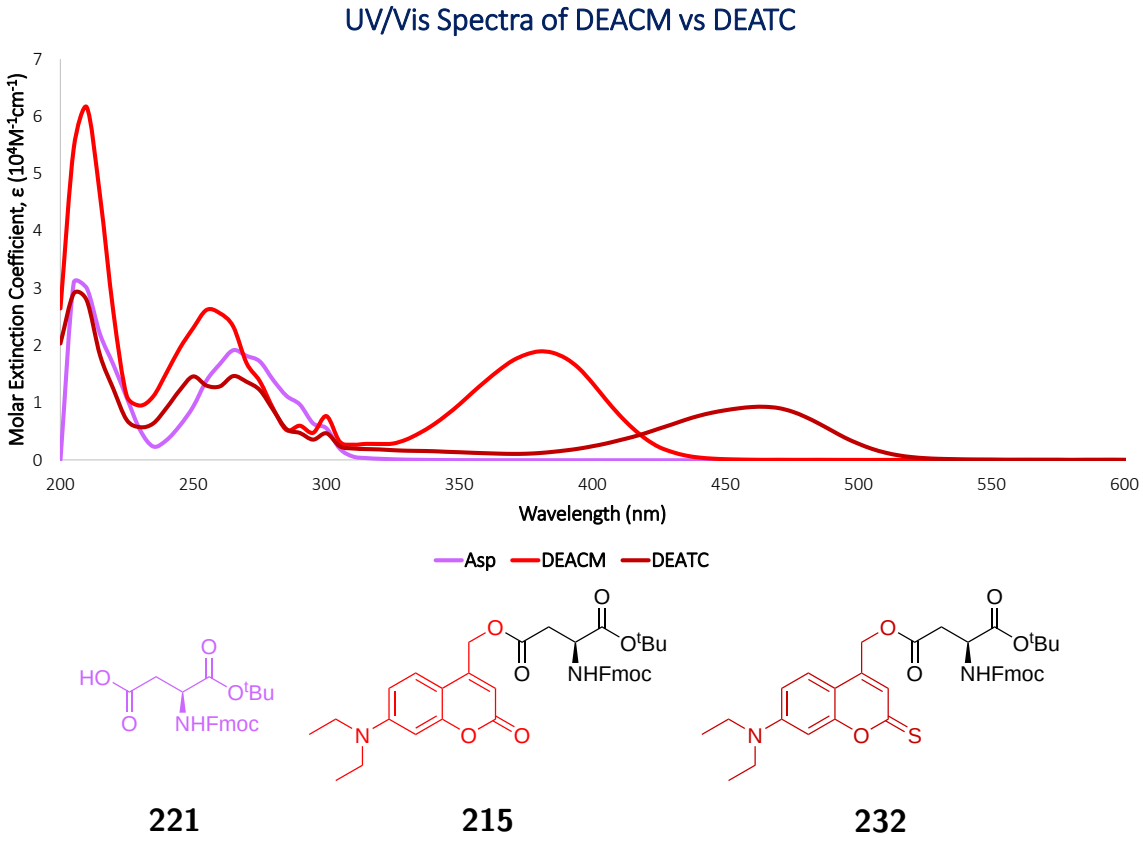
Through the use of HBTU, aspartic acid (**221**) was caged at the side chain carboxylic acid to furnish the caged amino acid (**232**) in near quantitative yield (**Scheme 4.4**).



235 **232**

Scheme 4.4: Synthesis of DEATC-caged aspartic acid; Reagents & Conditions: (a) Fmoc-Asp-O^{t}Bu, HBTU, DIPEA, anhydrous DMF, RT, Ar, 24 h, 97%.

In concordance with previous literature results,[193] the DEATC group possessed its maxima at longer wavelengths relative to the DEACM parent compound, with λ_{max} increasing from 382 nm to 463 nm (**Figure 4.2**). This can be rationalised on the basis of the reduced energy gap difference between the C=S HOMO-LUMO (principle quantum number, $n = 3$) relative to the C=O HOMO-LUMO energy gap (principle quantum number, $n = 2$) responsible for the π - π^* transition.[194]



Entry	Conc (mM)	λ_{max} (nm)	Transition	A	ε ($M^{-1}cm^{-1}$)
1	0.04	205	n – π*	1.24	30950
2	0.04	380	π – π*	0.758	18961
3	0.04	465	π – π*	0.371	9283

Figure 4.2: UV/vis absorption spectrum of DEATC-caged aspartic acid [dark red; λ_{max} = 465 nm (π - π^*)]; DEACM-caged aspartic acid [red; λ_{max} = 380 nm (π - π^*)] and aspartic acid [purple] are included for comparison; Concentration = 0.04 mM [MeOH].

Based on these results, photolysis studies were conducted to evaluate the use of the DEATC caging group as a viable wavelength orthogonal partner to the DEACM or

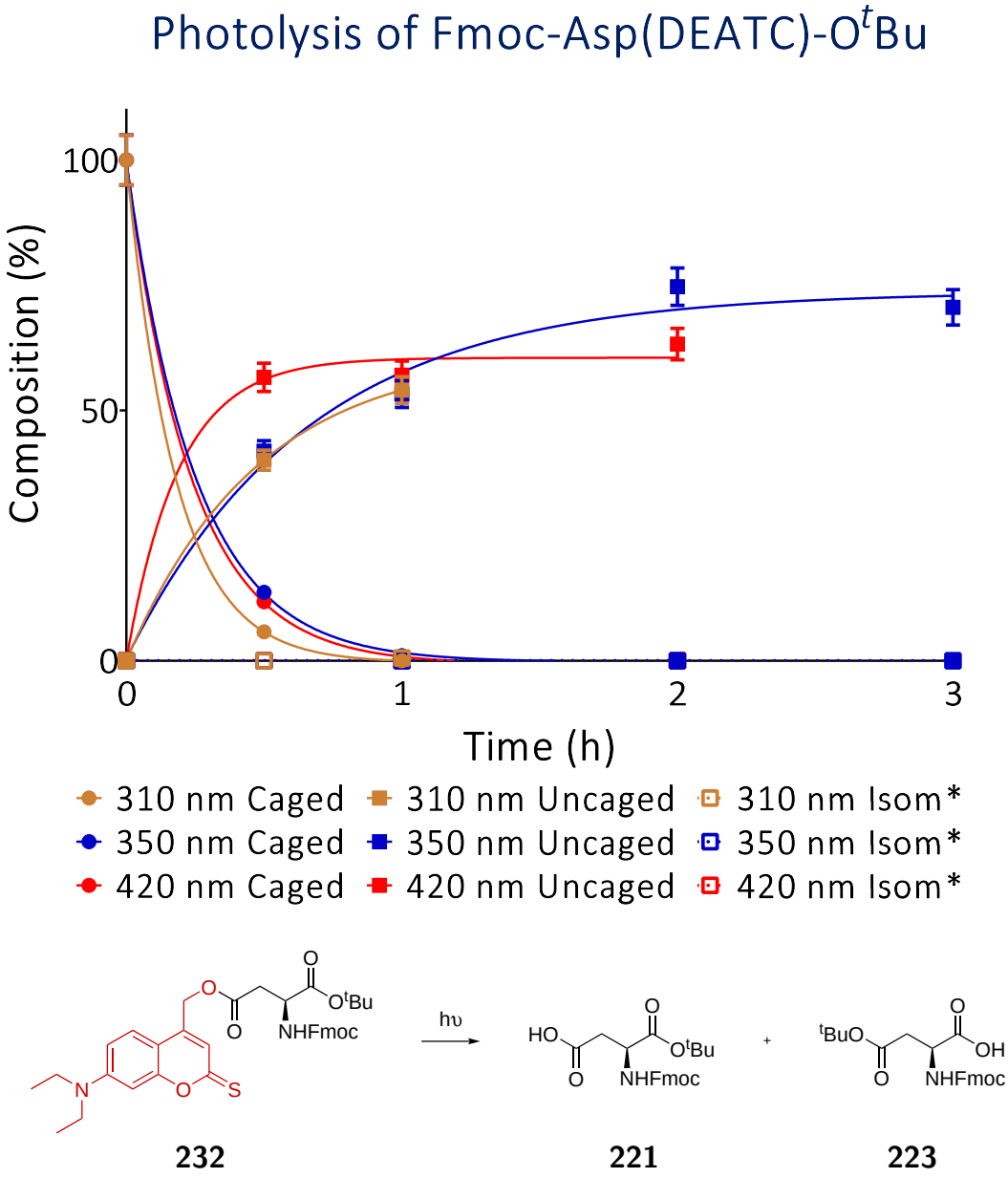
DMNB caging groups.

Irradiation was conducted at λ = 420 nm, 350 nm and 310 nm; the DEATC-caged molecule (**232**) was found to undergo complete photolysis at all three wavelengths measured, with rate constants of 4.21 s^{-1}, 3.97 s^{-1} and 5.58 s^{-1} respectively, to release aspartic acid (**221**) (**Figure 4.3**).

The resulting uncaged amino acid (**221**) was obtained in 60 - 75% yields upon complete photolysis of the starting caged amino acid (**232**). As was previously observed, conversion to the uncaged amino acid product started to decline upon prolonged exposure to UV irradiation at wavelengths of λ = 350 nm and 310 nm, which was attributed to the photoisomerisation of the *tert*-butyl protecting group.

To confirm that uncaging was the result of photolysis and not hydrolysis of the caged compound in MeOH, control experiment were performed, stirring DEATC-caged aspartic acid (**232**) in MeOH for the duration of the photolysis reaction. Importantly, in the absence of irradiation, no uncaging was observed; the formation of aspartic acid (**221**) was the result of photorelease and solvent dependent degradation could not account for conversion to the product.

These photolysis experiments demonstrated that the DEATC caging group would not be a suitable orthogonal partner to the previously used DEACM, DMNB, or MPH caging groups, as the DEATC caging group rapidly underwent photolysis at all wavelengths used for irradiation.



Entry	λ_{irrad} (nm)	k_{caged} (s^{-1})	N_{caged}	R^2_{caged}	$k_{uncaged}$ (s^{-1})	$N_{uncaged}$	$R^2_{uncaged}$
1	310	5.58	3	1.00	2.11	3	1.00
2	350	3.97	5	1.00	1.52	5	0.99
3	420	4.21	4	1.00	5.25	4	0.99

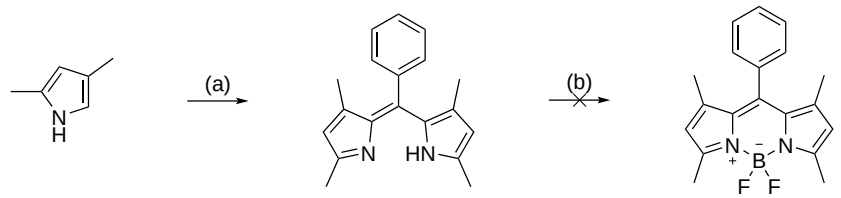
Figure 4.3: Photolysis of DEATC-caged and uncaged aspartic acid [MeOH].

4.3 BODIPY Dyes as Caging Groups

A series of BODIPY dyes was shown to have red-shifted λ_{max} of absorption beyond 500 nm; [71], [70] it was hypothesised that these BODIPY-based phototriggers would be suitable partners to the DEACM or DMNB caging groups to form a chromatically orthogonal pair, irradiating at wavelengths around 500 nm for photolysis of the BODIPY phototriggers, to release the free amino acid, while leaving the DEACM or DMNB caging groups intact. Irradiation at 420 nm or 350 nm would cleave the DEACM or DMNB groups respectively, while leaving the BODIPY PCG untouched. Two BODIPY structures were synthesised and used to cage the side chains of amino acids, aspartic acid and tyrosine to evaluate their photolytic properties.

4.3.1 Synthesis, Photolysis and Evaluation of BODIPY Dyes as Caging groups for Amino Acids

The BODIPY derivative (BODIPY-1) (**238**), employed by Umeda *et. al.*,[71] was synthesised, through reaction of 2,4-dimethylpyrrole (**236**) and benzaldehyde, followed by complexation with boron trifluoride etherate (**Scheme 4.5**).[71]

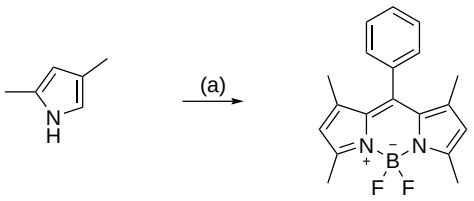


236 **237** **238**

Scheme 4.5: Synthesis of BODIPY-1 precursor *via* dipyrromethane; Reagents & Conditions: (a) Benzaldehyde, CH_2Cl_2, RT, Ar, 18 h then DDQ, RT, Ar, 0.5 h; (b) $BF_3.OEt_2$, DIPEA, toluene, RT, Ar, 2 h.[71]

Despite observing the formation of the dipyrromethane intermediate (**237**) by mass spectrometry, the complexation with boron could not be effected and no product (**238**) was isolated.

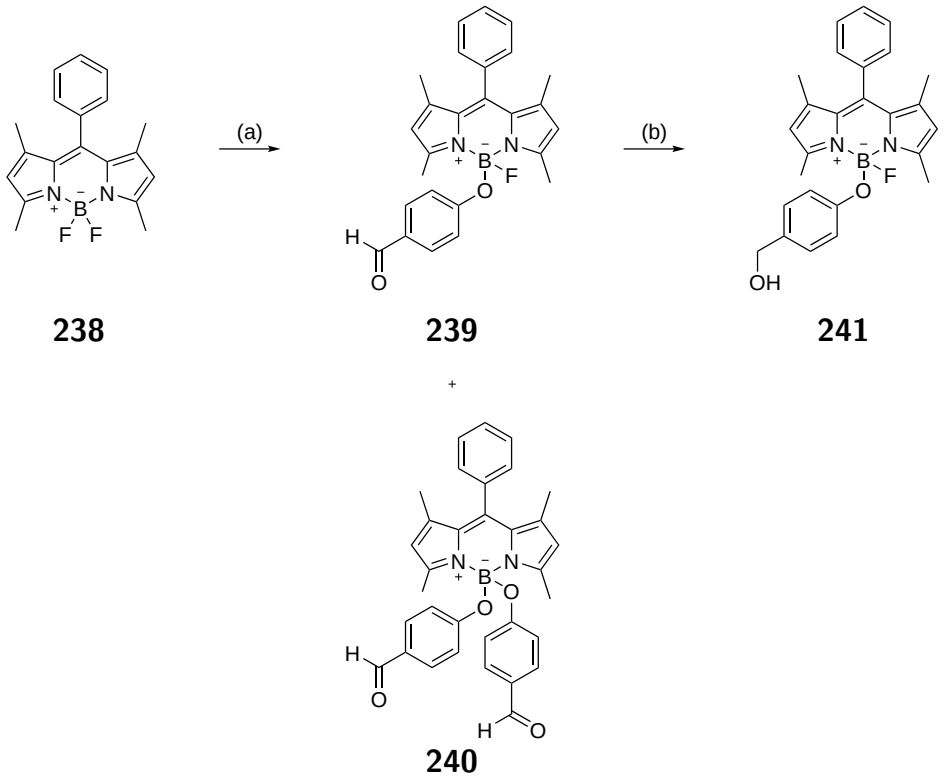
Product formation was effected by reacting 2,4-dimethylpyrrole (**236**) with a slight excess of benzoyl chloride. *In situ* complexation with boron trifluoride etherate was then performed in the presence of triethylamine to afford the desired BODIPY-1 precursor (**238**) as a bright orange solid in 25% yield (**Scheme 4.6**).
Activation of the boron centre by heating with $AlCl_3$ under reflux, followed by addition of 4-hydroxybenzaldehyde and subsequent stirring under reflux, allowed the desired



236 **238**

Scheme 4.6: Synthesis of BODIPY-1 precursor; Reagents & Conditions: (a) Benzoyl chloride, CH_2Cl_2, RT, Ar, 18 h, $BF_3.OEt_2$, NEt_3, 0 °C - RT, Ar, 6 h, 25%.[195]

product (**239**) to be isolated in 35% yield. In addition to the mono-substituted product (**239**), the di-substituted product (**240**) was also obtained in 19% yield (**Scheme 4.7**).



238 **239** **241**

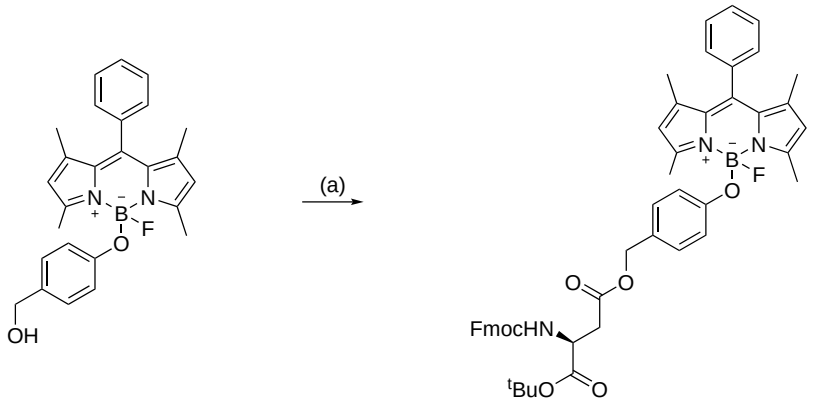
240

Scheme 4.7: Synthesis of BODIPY-1 phototrigger bearing 4-hydroxyaryl linker; Reagents & Conditions: (a) $AlCl_3$, CH_2Cl_2, reflux, Ar, 10 min then 4-hydroxybenzaldehyde, reflux, Ar, 0.5 h, 35%; (b) $NaBH_4$, MeOH, RT, 2.5 h, 77%.[71]

Reduction of the aldehyde with $NaBH_4$ afforded the desired product (**241**) in 77% yield (**Scheme 4.7**).

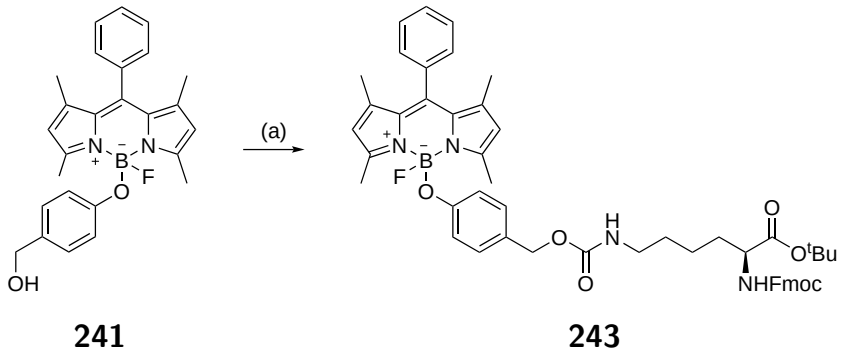
PyBOP was employed as the activating agent to afford the desired BODIPY-1-caged

aspartic acid (**242**) in 84% yield (**Scheme 4.8**).



Scheme 4.8: Synthesis of BODIPY-1-caged aspartic acid; Reagents & Conditions: (a) Fmoc-Asp-O^{t}Bu, PyBOP, DIPEA, RT, Ar, 18 h, 84%.

It was possible to synthesise BODIPY-1-caged lysine (**243**), through the ε-amine. This was achieved through activation of the primary alcohol of the BODIPY caging group (**241**) with 4-nitrophenyl chloroformate. The nitrophenyl alcohol leaving group was subsequently displaced *via* an addition-elimination reaction with the ε-amine of Fmoc-Lys-O^{t}Bu (**187**) to form the carbamate linker and afford the desired product (**243**) in 14% yield (**Scheme 4.9**).



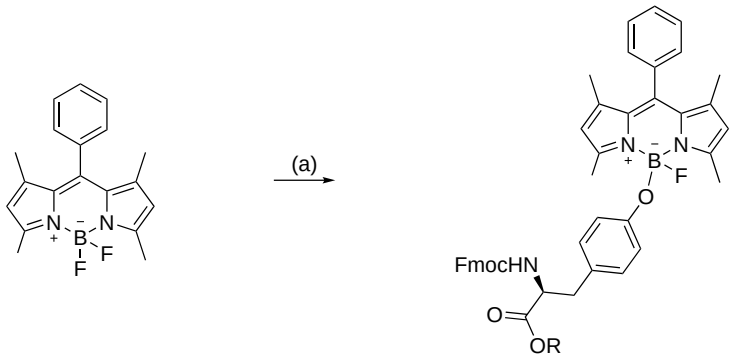
Scheme 4.9: Synthesis of BODIPY-1-caged lysine; Reagents & Conditions: (a) 4-Nitrophenyl chloroformate, NMM, CH_2Cl_2, 0 °C - RT, Ar, 3 h then Fmoc-Lys-O^{t}Bu, DMAP, RT, Ar, 18 h, 14%.

N,*N*-carbonyldiimidazole (CDI) was trialled as an activating agent, in an attempt to improve the yield, however, no product could be isolated despite observing formation of the intermediate as adjudged by TLC and mass spectrometry. This was due to the formation of a number of side products which made purification very challenging. In

addition, the lower reactivity of CDI relative to 4-nitrophenyl chloroformate resulted in lower conversion to the product.

Caging of the side chain hydroxyl group of Fmoc-Ser-O^{t}Bu (**185**) with the BODIPY-1 caging group (**241**) was also attempted but no product formation was observed as adjudged by TLC, **^{1}H NMR** and mass spectrometry. *N*,*N*-Carbonyldiimidazole and 4-nitrophenyl chloroformate were trialled as activating agents. However, with the former, it was postulated that the greater stability of the imidazole carbamate relative to the carbonate product accounted for the lack of reactivity, whilst in the latter, the inability to isolate any product was attributed to the reaction conditions being insufficiently basic to deprotonate the serine hydroxyl group to effect the addition-elimination reaction.

Noting the parallels between the aryloxy linker and the phenolic side chain functional group of tyrosine, the reaction to install the aryloxy linker (**Scheme 4.7**) was envisaged to enable formation of BODIPY-1-caged tyrosine (**244**), (**245**), directly through the boron centre and the phenol group (**Scheme 4.10**). Both the Fmoc-protected tyrosine residue bearing a free α-carboxylic acid (**244**) and the dual protected tyrosine residue bearing both the Fmoc and methyl ester protection on the α-amine and α-carboxylic acid groups (**245**) were synthesised under these conditions in 8% and 28%, respectively (**Scheme 4.10**).



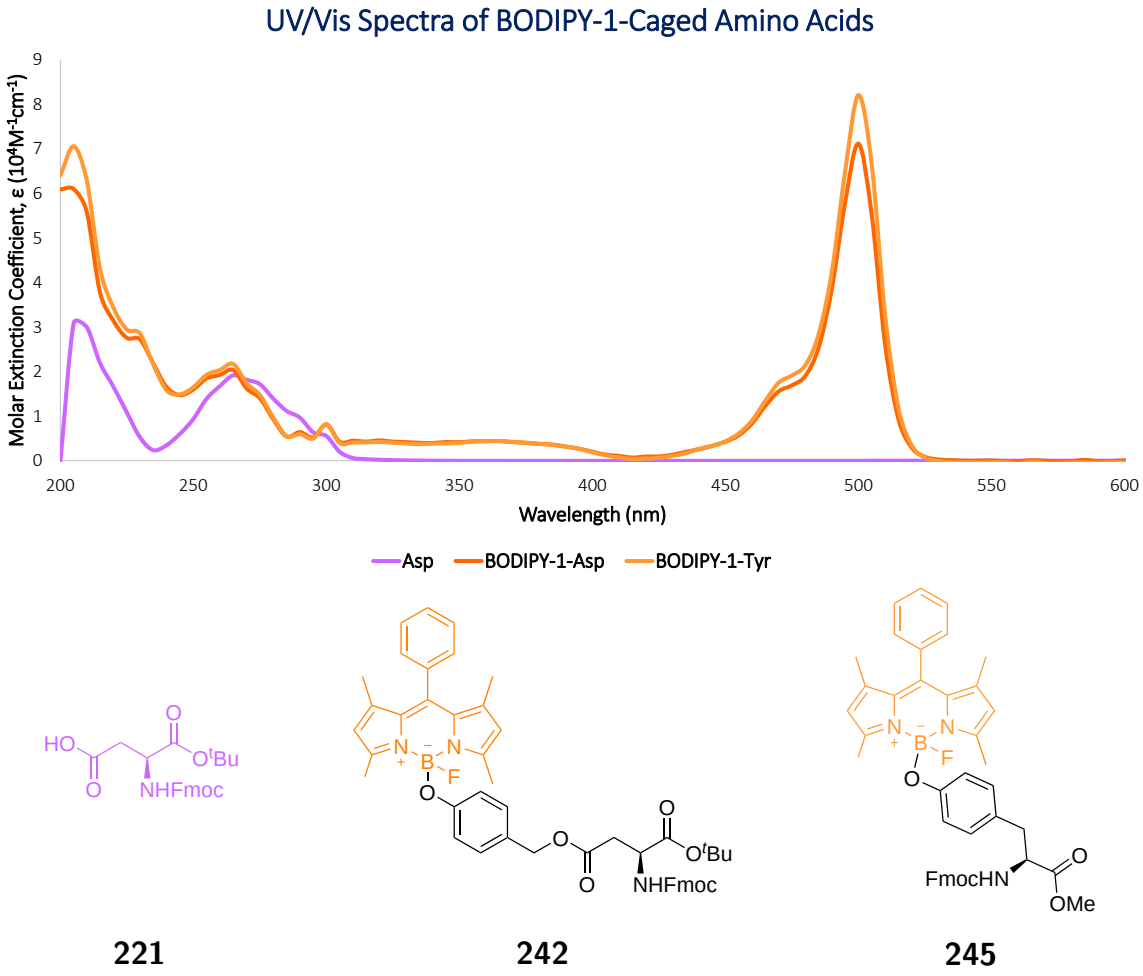
238 **244** **245**

Scheme 4.10: Synthesis of BODIPY-1-caged tyrosine; Reagents & Conditions: (a) R = H: $AlCl_3$, CH_2Cl_2, reflux, Ar, 10 min then Fmoc-Tyr-OH, reflux, Ar, 0.5 h, 8 % or R = Me: $AlCl_3$, CH_2Cl_2, reflux, Ar, 15 min then Fmoc-Tyr-OMe, reflux, Ar, 0.5 h, 28 %.

Although both reactions gave rise to the desired products, the reaction with the free α-carboxylic acid (**244**) proceeded in much lower yield. This was attributed to

interference of the carboxylic acid with the reaction, hindering the formation of the product; the free carboxylic acid could also coordinate to the boron atom.

Successful synthesis of the BODIPY-1-caged amino acids made it possible to measure the UV/vis absorption spectra and assess the photolytic properties of the compounds.



Entry	Conc (mM)	λ_{max} (nm)	Transition	A	ε ($M^{-1}cm^{-1}$)
1	0.04	205	n – π*	1.24	30950
2	0.004	500	π – π*	0.285	71191
3	0.004	500	π – π*	0.328	82094

Figure 4.4: UV/vis absorption spectrum of BODIPY-1-caged aspartic acid [orange; λ_{max} = 500 nm (π - π*)], BODIPY-1-caged tyrosine [light orange; λ_{max} = 500 nm (π - π*); Concentration = 0.004 mM [MeOH]; and aspartic acid [purple]; Concentration = 0.04 mM [MeOH].

The maximum of BODIPY-1-caged aspartic acid (**242**) and that of the caged tyrosine analogue (**245**) lie at 500 nm (**Figure 4.4**). The UV/vis spectra alongside Umeda's reported results,[71] provided a good indication that irradiation at 520 nm would facilitate uncaging with photorelease of the free amino acid. In addition, the trough in the UV/vis spectra in the region of 410 - 430 nm, and the comparatively low absorption in the region centred around 350 nm was also noted. It was thus hypothesised that this caging group would demonstrate wavelength orthogonality alongside either the previously discussed DEACM or DMNB caging groups.

Initial photolysis experiments showed BODIPY-1-caged aspartic acid (**242**) to be incompatible for analysis by HPLC. It appeared that the compound was partially decomposing under the reverse phase conditions of H_2O/MeOH/TFA eluents. **^{1}H NMR** was thus used to monitor the uncaging of these compounds.

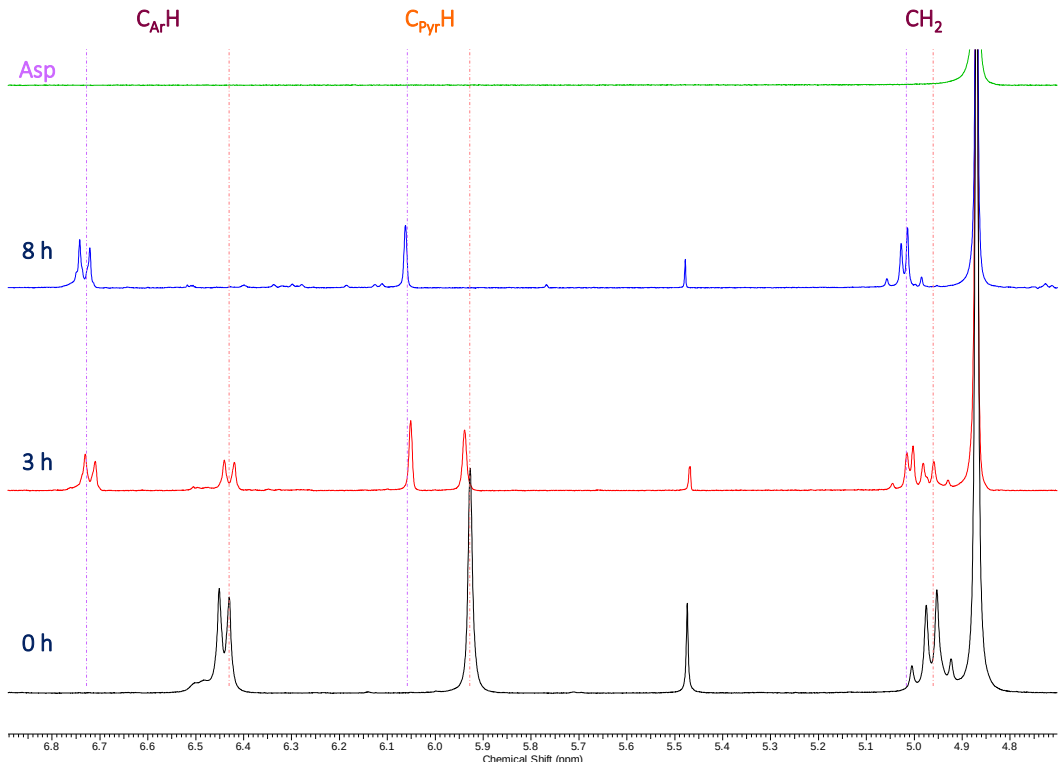


Figure 4.5: Partial **^{1}H NMR** spectra 6.80 - 4.80 ppm; Spectra recorded at 0 h, 3 h and 8 h after irradiation at 520 nm (MeOD); spectrum of Fmoc-Asp-O^{t}Bu (Asp) included for comparison [Pink lines highlight disappearance of peaks of starting material; Purple lines highlight appearance of peaks of product].

Commencing with irradiation of BODIPY-1-caged aspartic acid (**242**), changes in the characteristic peaks in the **^{1}H NMR** spectra over the course of an 8 h period were

observed. The regions of the NMR spectra experiencing the most significant changes lay between 6.80 - 4.80 ppm (**Figure 4.5**), and 4.60 - 4.00 ppm (**Figure 4.6**). The diagnostic peaks highlighted in the former region belong to the aromatic protons and the alkoxy protons of the linker, and the pyrrole protons of the BODIPY-1 scaffold. In the latter region the defining peaks belonged to the alkyl proton and the alkoxy protons of the Fmoc protecting group and the α-proton of the amino acid.

The first region, between 6.80 - 4.80 ppm, clearly showed a decline in the peaks belonging to the original caged compound (**242**) and the formation of a new set of peaks after 3 h. Exposure to irradiation at 520 nm for 8 h resulted in the complete disappearance of the peaks belonging to the caged aspartic acid species (**242**) and full conversion to the new set of peaks. All the original peaks had shifted to their corresponding peaks at higher ppms in the formed products (**Figure 4.5**). The peaks corresponding to the photolysed product did not match the data for the quinone methide by-product or the 4-hydroxybenzyl alcohol hydrolysed form as obtained by Umeda and co-workers[71] for decomposition of the linker to release the free amino acid.
In the latter region, between 4.60 - 4.40 ppm, comparing the peaks of aspartic acid in the caged form (**242**) to the expected photoreleased product of free Fmoc-Asp-O^{t}Bu (**221**), a change was observed between the peaks prior to, and following, photolysis. However, the product peaks did not appear to correspond to that of the expected uncaged aspartic acid (**221**) when the spectra were compared (**Figure 4.6**). Both mass spectrometry and TLC data supported the findings observed by **^{1}H NMR** and distinctly showed the disappearance of the starting caged material. Irradiation was thought to have resulted in photolysis of the boron-oxygen bond but decomposition of the released species (**246**) had not occurred. This was possibly due to the strength of the ester bond in addition to the lack of entropic driving force from release of CO_2 accompanied by the photodecomposition of carbonate or carbamate bonds. Thus, the linker and the amino acid were still attached *via* the ester bond (**Scheme 4.11**) and free aspartic acid (**221**) had not been formed. Mass spectrometry data corroborated this hypothesis, revealing a peak corresponding to the released compound comprising of the linker and aspartic acid. This line of investigation was discontinued.
Successful cleavage in previous photolysis studies and similarities of the side chain of tyrosine and the aryloxy linker led to the hypothesis that uncaging to release tyrosine would be feasible. Irradiation experiments of the BODIPY-1-caged tyrosine (**245**) at 520 nm, 420 nm and 350 nm were thus carried out.

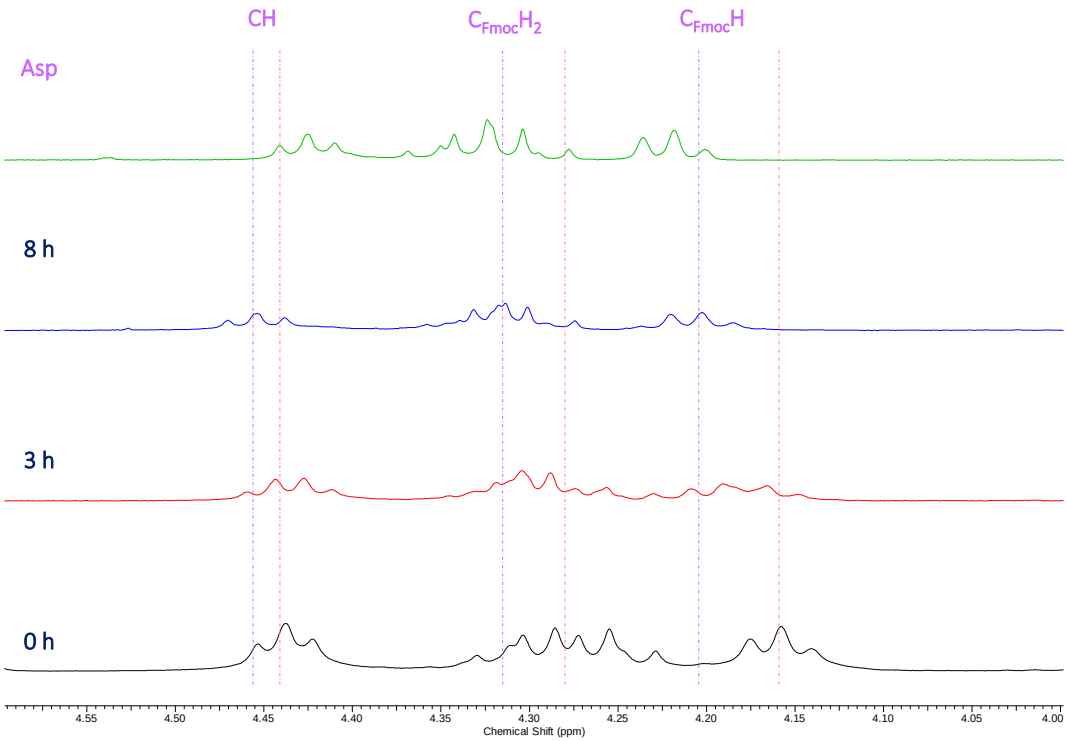
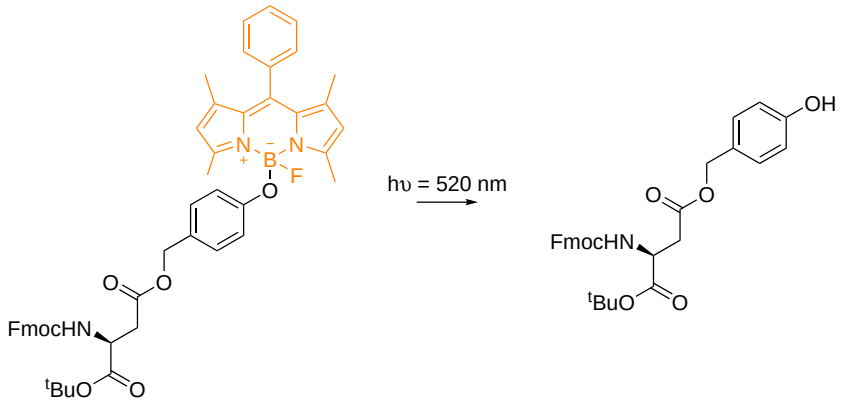
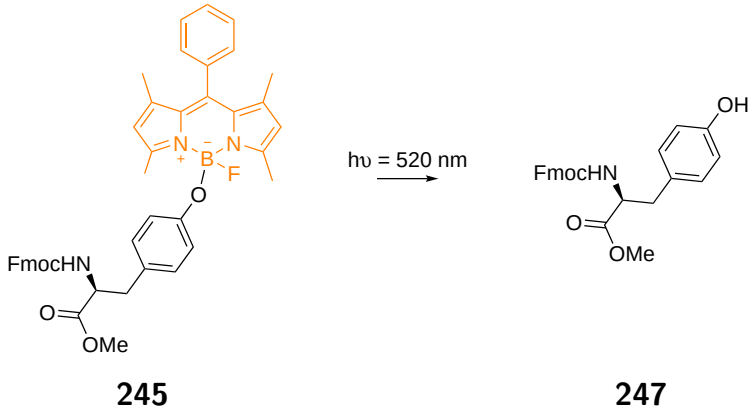


Figure 4.6: Partial **^{1}H NMR** spectra 4.60 - 4.00 ppm; Spectra recorded at 0 h, 3 h and 8 h after irradiation at 520 nm (MeOD); spectrum of Fmoc-Asp-O^{t}Bu (Asp) included for comparison [Pink lines highlight disappearance of peaks of starting material; Purple lines highlight appearance of peaks of product].

Irradiation experiments were conducted at 520 nm and the **^{1}H NMR** spectra were compared after 4 h and 8 h. The regions in the spectra displaying the most characteristic peaks were analysed. These included the region between 7.10 - 5.70 ppm (**Figure 4.7**), which showed the aromatic peaks of the tyrosine side chain phenolic group and the pyrrole proton of the BODIPY-1 scaffold and the region between 4.40 - 3.55 ppm, which included the methyl ester protecting group and the less characteristic α-proton of tyrosine and the Fmoc-protecting group alkoxy protons (**Figure 4.8**).
After 8 h, a diminishing of the peaks in these regions belonging to the original BODIPY-1-caged species (**245**) and the formation of new peaks belonging to the BODIPY-1 photolysed by-product and the released species (**247**) were observed. Comparing the spectra with that of Fmoc-Tyr-OMe, revealed that the peaks in the aromatic region and those of the methyl ester protecting group matched those of the desired product. In addition, mass spectrometry and TLC evidence corroborated this result.
It was concluded that photolysis of BODIPY-1-caged Fmoc-Tyr-OMe (**245**) led to the formation of the desired uncaged amino acid (**247**) (**Scheme 4.12**).



Scheme 4.11: Hypothesised product formed from the photolysis of BODIPY-1-caged aspartic acid; no further decomposition following irradiation to release free amino acid.



Scheme 4.12: Photolysis of BODIPY-1-caged tyrosine at 520 nm in MeOD to reveal uncaged Fmoc-Tyr-OMe.

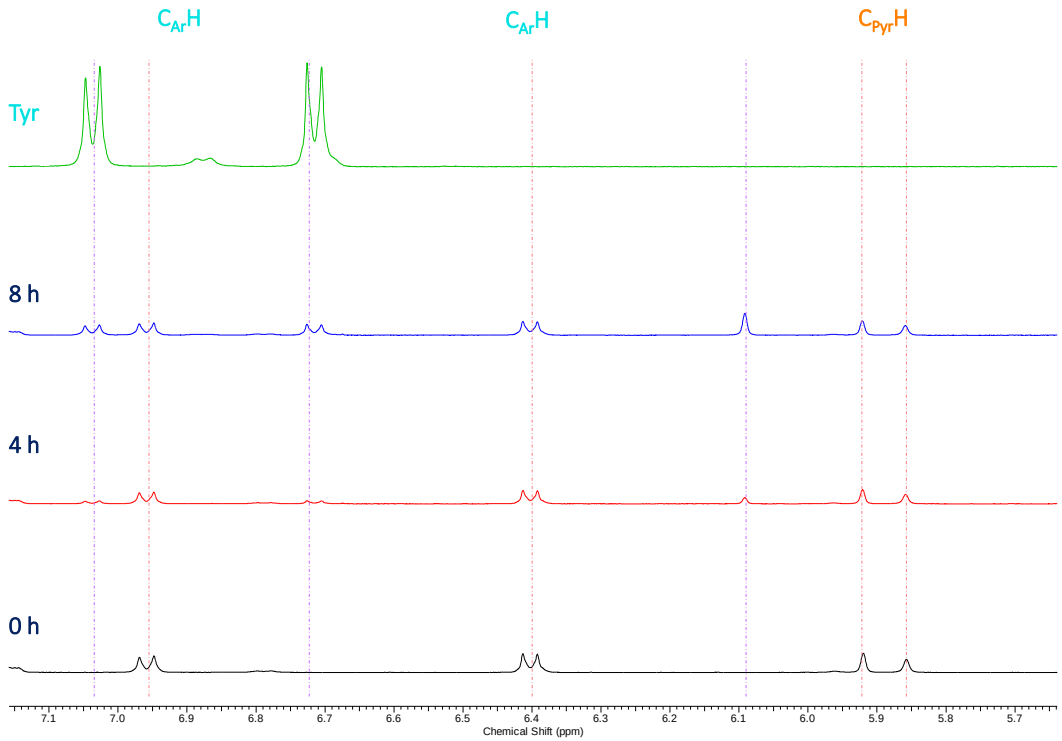


Figure 4.7: Partial **^{1}H NMR** spectra 7.10 - 5.70 ppm; Spectra recorded at 0 h, 4 h and 8 h after irradiation at 520 nm (MeOD); spectrum of Fmoc-Tyr-OMe included for comparison [Pink lines highlight disappearance of peaks of starting material; Purple lines highlight appearance of peaks of product].

The inclusion of hexamethyldisiloxane as an internal standard allowed for quantification of the degree of photolysis that had occurred at the various wavelengths over a specific period of time. Following 8 h of irradiation at 520 nm, 45% of the caged species (**245**) had undergone photolysis to reveal the tyrosine product (**247**). At 420 nm, 46% had undergone photolysis to release tyrosine (**247**) and at 350 nm, a total of 87% of the initial caged species (**245**) had been converted to uncaged product (**247**). The photolysis reaction appeared to be clean with little to no photodegradation or the formation of unwanted by-products observed. However, despite the clean photoreaction, BODIPY-1 was no longer investigated any further as it did not appear to possess the potential for chromatic orthogonality with any of the previously investigated caging groups.

Interest was, however, piqued by the long-wavelength absorbing BODIPY scaffold and it was opted to pursue the BODIPY variant, BODIPY-2 (**250**) investigated by Winter *et. al.*,[70] in the search for an orthogonal pair.

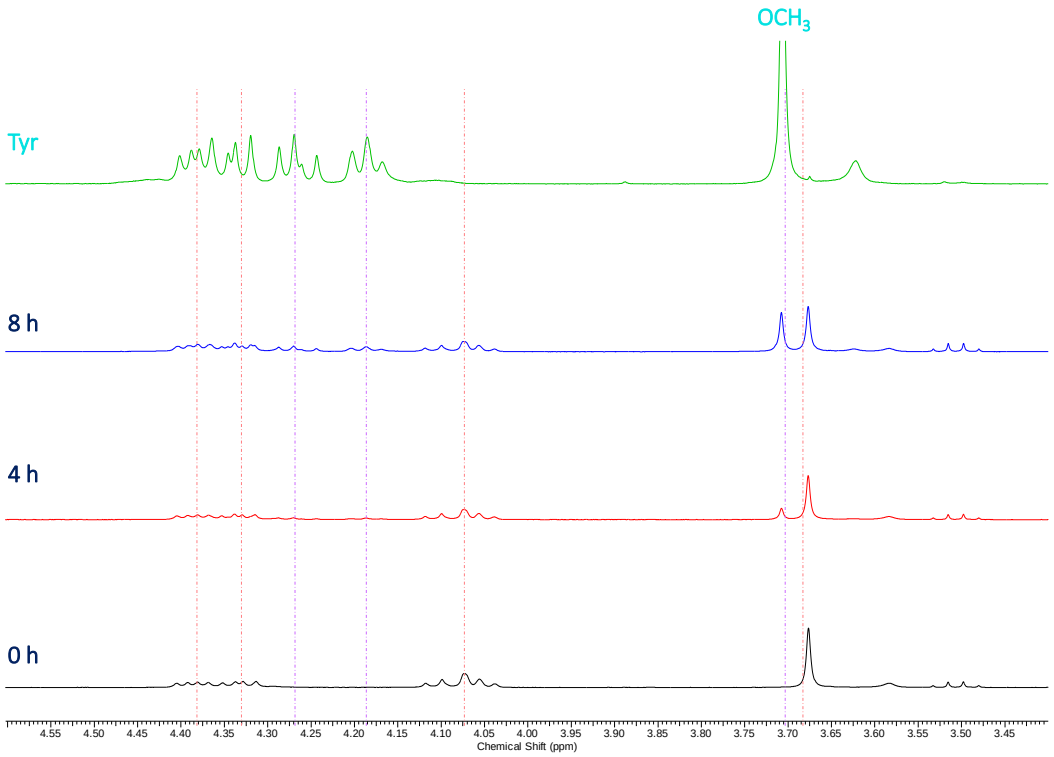
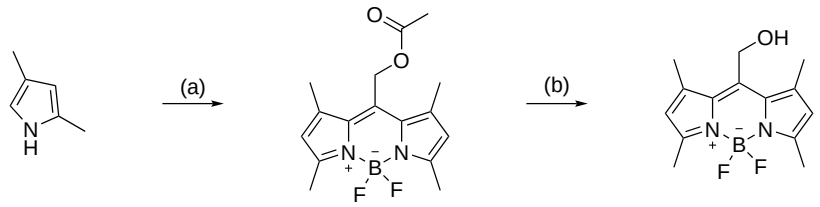


Figure 4.8: Partial **^{1}H NMR** spectra 4.40 - 3.55 ppm; Spectra recorded at 0 h, 4 h and 8 h after irradiation at 520 nm (MeOD); spectrum of Fmoc-Tyr-OMe included for comparison [Pink lines highlight disappearance of peaks of starting material; Purple lines highlight appearance of peaks of product].

The synthesis of this BODIPY analogue (**250**) was effected through the use of a one-pot method, owing to the greater simplicity of this reaction.
Commercially available 2,4-dimethyl pyrrole (**236**) was stirred with a slight excess of acetoxyacetyl chloride, before dropwise addition of NEt_3 and boron trifluoride etherate, leading to isolation of the acyl protected species (**249**) in 60% yield (**Scheme 4.13**).
The acyl deprotection of the BODIPY-2 species (**249**) was attempted in basic conditions (**Scheme 4.13**). Several conditions were investigated to find a set that would afford the product in practical yields.

It was found that the BODIPY core was very sensitive to decomposition, following exposure to basic conditions. It was necessary to optimise the reaction and find conditions favouring acyl deprotection over BODIPY decomposition.
Several bases were tested at 0 °C and RT.
With LiOH, only decomposition was observed. The use of 2.0 M NaOH afforded the product in 11% yield, whilst the weaker NaOMe base gave the product in 43%, when



Scheme 4.13: Synthesis of BODIPY-2 caging group; Reagents & Conditions: (a) Acetoxyacetyl chloride, CH_2Cl_2, RT, Ar, 18 h then NEt_3, $BF_3.OEt_2$, 0 °C - RT, Ar, 18 h, 60%;[195] (b) See (**Table 4.2**).

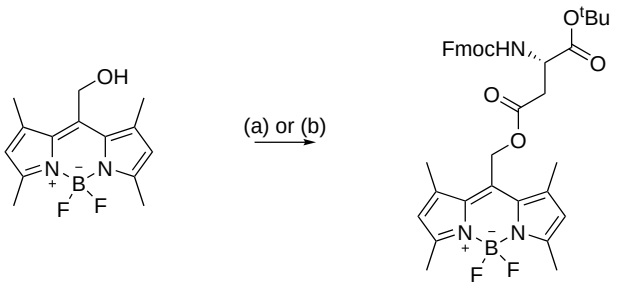
Table 4.2: Optimisation of acyl deprotection conditions to afford BODIPY-2 caging precursor.

Entry	Base	Equivalents	Solvent	T (° C)	Time (h)	Yield (%)
1	$LiOH.H_2O$	5.0	THF/H_2O = 1/1	RT	24	-
2	2.0 M NaOH (aq.)	300	CH_2Cl_2/MeOH = 1/2	RT	2.5	11
3	0.2 M NaOMe in MeOH	1.5	CH_2Cl_2	0	4	43
4	K_2CO_3	2.0	MeOH	RT	1.5	39
5	K_2CO_3	1.2	MeOH	0	1	50

the reaction was conducted at 0 °C.
The best yields, 50%, were obtained when K_2CO_3 was employed, stirring at 0 °C for 1 h. It was found that to avoid erosion of yields, it was imperative to neutralise any excess base prior to workup. This could be readily achieved through the use of H^+ form Dowex resin, which could be filtered off prior to concentration.

Having synthesised the BODIPY-2 caging precursor (**250**) bearing the primary hydroxyl group, it was possible to synthesise the caged amino acids, commencing with caged aspartic acid as the model system.
The synthesis of the BODIPY-2-caged aspartic acid species (**251**) was conducted with PyBOP or DCC as the activating agent, resulting in isolation of the product in 24% and 21% yields respectively. PyBOP was the preferred reagent as in addition to problems associated with epimerisation at the α-stereocentre, DCC-mediated couplings are also open to the possibility of low yields through the formation of *N*-acylureas.

The synthesis of BODIPY-2-caged Fmoc-Lys-O^{t}Bu (**253**) *via* a carbamate linker was next attempted. This presented a challenge, with initial attempts proving unsuccessful. A commonly used method of carbamate formation is the reaction between an oxygen-

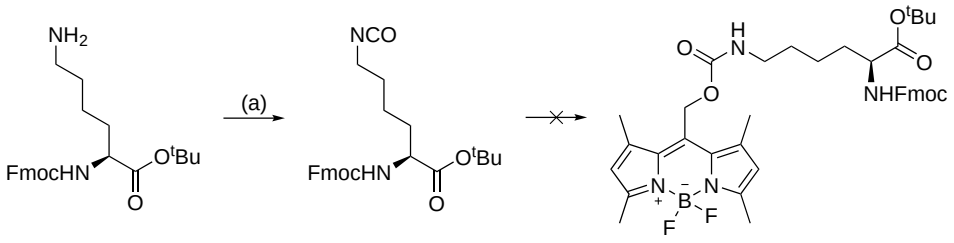


250 **251**

Scheme 4.14: Synthesis of BODIPY-2-caged aspartic acid; Reagents & Conditions: (a) Fmoc-Asp-O^{t}Bu, PyBOP, DIPEA, CH_2Cl_2, RT, Ar, 24 h, 24%; (b) Fmoc-Asp-O^{t}Bu, DCC, DMAP, CH_2Cl_2, 0 °C - RT, Ar, 18 h, 21%.

nucleophile and an isocyanate. These species are relatively reactive, affording the desired carbamate product in good yields.

Though it was possible to form the isocyanate on the ε-amine of lysine (**252**), as evidenced by TLC and a peak by mass spectrometry corresponding to the desired isocyanate, subsequent reaction with the BODIPY caging group (**250**) would not proceed under the basic conditions trialled with NMM or DMAP (**Scheme 4.15**).



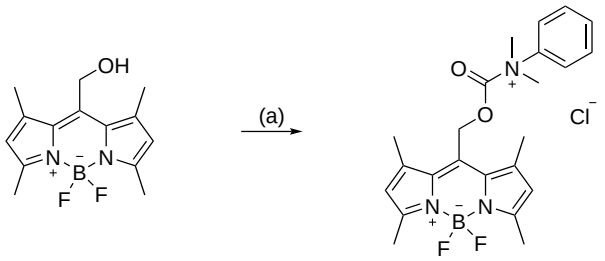
187 **252** **253**

Scheme 4.15: Synthesis of lysine isocyanate intermediate for coupling with BODIPY-2 precursor to form BODIPY-2-caged lysine; Reagents & Conditions: (a) triphosgene, sat. aq. $NaHCO_3$, CH_2Cl_2, 0 °C, 2 h.[196]

Formation of the chloroformate *via* reaction of the BODIPY caging group (**250**) with triphosgene (**Scheme 4.16**), prior to addition of lysine (**187**) was attempted. However, the reaction with triphosgene afforded the *N*,*N*-dimethylaniline adduct (**254**) from which no further reaction with this species took place.

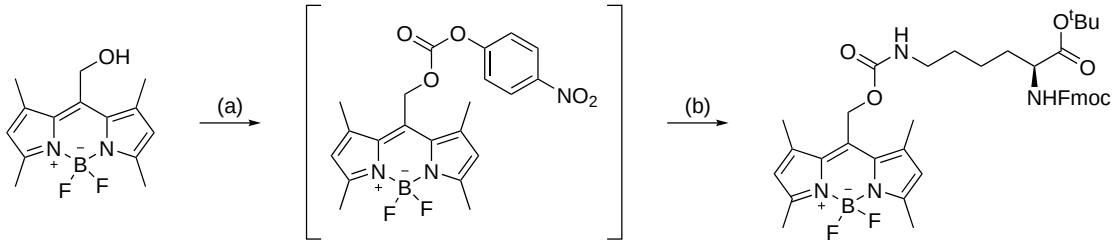
CDI was also trialled as the activating agent and although the formation of what appeared to be the imidazole carbonate intermediate was evidenced by TLC, no further reaction between the lysine side chain ε-amine (**187**) and the activated BODIPY-2-species (**250**) occurred. This was attributed to the imidazole group being too poor a

leaving group to be displaced by the BODIPY-2-hydroxyl.



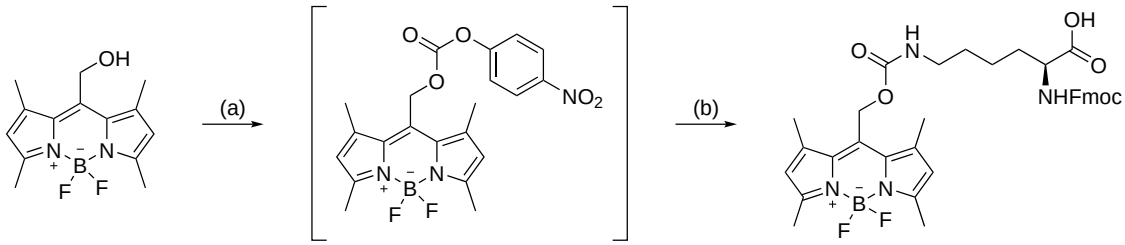
250 **254**

Scheme 4.16: Attempted synthesis of BODIPY-2-chloroformate; Reagents & Conditions: (a) trisphosgene, *N*,*N*-dimethylaniline, toluene, 0 °C - RT, 4 h.



250 **255** **253**

Scheme 4.17: Synthesis of BODIPY-2-caged lysine; Reagents & Conditions: (a) 4-Nitrophenyl chloroformate, NMM, CH_2Cl_2, 0 °C - RT, Ar, 18 h then Fmoc-Lys-O^{t}Bu, DMAP, RT, Ar, 18 h, 15%.

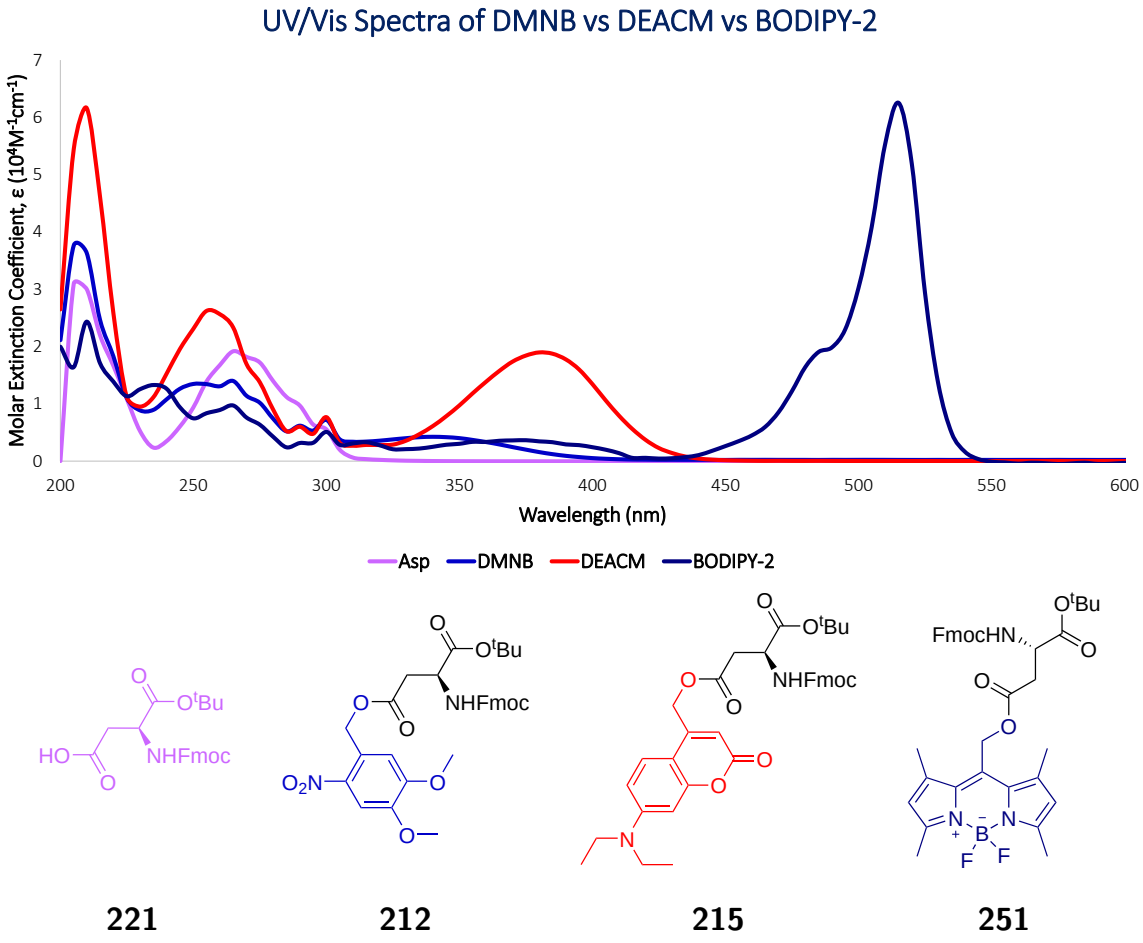


250 **255** **256**

Scheme 4.18: Synthesis of BODIPY-2-caged Fmoc-Lys-OH; Reagents & Conditions: (a) 4-Nitrophenyl chloroformate, NMM, CH_2Cl_2, 0 °C - RT, Ar, 3 h then Fmoc-Lys-OH, $NaHCO_3$, DMAP, H_2O:MeCN:CH_2Cl_2 (1:1:2), RT, Ar, 18 h, 33%.

Using 4-nitrophenyl chloroformate and adding the BODIPY-2 precursor (**250**) dropwise, as a solution in CH_2Cl_2, to minimise formation of the self-coupled product, allowed the desired product (**253**) to be afforded in 15% yield (**Scheme 4.17**).

The synthesis of the BODIPY-2-caged lysine (**256**) bearing a free α-carboxylic acid was effected by reaction of the BODIPY-2 precursor (**250**) and 4-nitrophenyl chloroformate, followed by addition of commercially available Fmoc-Lys-OH, which led to isolation of the product (**256**) in 33% yield (**Scheme 4.18**).



Entry	Conc (mM)	λ_{max} (nm)	Transition	A	ε ($M^{-1}cm^{-1}$)
1	0.04	205	n – π*	1.24	30950
2	0.04	340	n – π*	0.170	4250
3	0.04	380	π – π*	0.758	18961
4	0.004	515	π – π*	0.250	62533

Figure 4.9: UV/vis absorption spectrum comparing BODIPY-2 [pink; λ_{max} = 515 nm (π - π^*)]; Concentration = 0.004 mM [MeOH]; DEACM- [yellow; λ_{max} = 380 nm (π - π^*)] and DMNB-caged [blue; λ_{max} = 340 nm (n - π^*)] aspartic acid, Fmoc-Asp-OtBu [purple] is included; Concentration = 0.04 mM [MeOH].

Having synthesised a series of BODIPY-2-caged amino acids, their UV/vis spectra

were measured to determine the optimum wavelengths for irradiation as well as the potential for orthogonality with previously discussed phototriggers.
The BODIPY-2 caging group was found to be the most red-shifted caging group of those synthesised, possessing an absorption $\lambda_{max} = 513$ nm (**Figure 4.9**). In addition, a decrease in absorption around 420 nm was observed. The absorption at 350 nm was also shown to be lower. It appeared that this caging group presented one of the best opportunities for establishing a chromatically orthogonal pair with the previously discussed DEACM phototrigger.

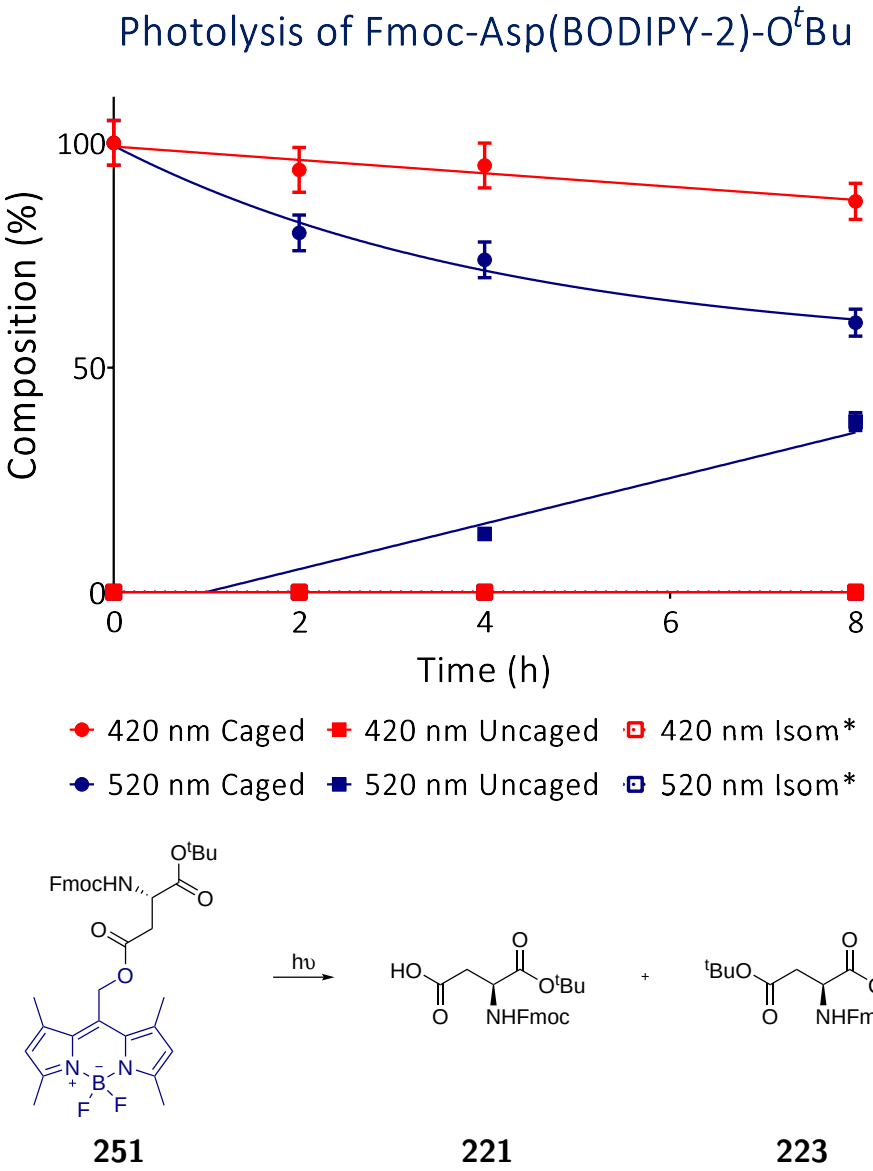
Photolysis studies were conducted, concentrating on irradiating with light-sources at 520 nm and 420 nm. It was hypothesised that the BODIPY-2-caged species (**251**) would be photolysed at 520 nm to release the free uncaged amino acid (**221**) but would be photostable at 420 nm, i.e. no uncaging to release free uncaged amino acid should be observed. The DEACM caging group was previously shown to undergo photolysis to release the free amino acid at 420 nm. As the DEACM photolabile caging group displayed no absorption at 520 nm according to its UV/vis spectrum, the group was expected to be photostable at this wavelength. If so, these two groups would indeed demonstrate chromatic orthogonality.

Irradiation of BODIPY-2-caged aspartic acid (**251**) at 520 nm resulted in a decline of the percentage composition of the caged material with a rate constant of 0.234 s^{-1} and appearance of uncaged aspartic acid (**221**) was observed with a rate constant of 4.60×10^{-5} s^{-1}. After 8 h, the percentage composition of the BODIPY-2-caged aspartic acid (**251**) had dropped to approximately 60% accompanied by 40% release of uncaged aspartic acid (**221**) (**Figure 4.10**).

When irradiation was conducted with a light source at 420 nm, 13% released aspartic acid (**221**) was observed with a rate constant of 0.00129 s^{-1}, after 8 h of irradiation (**Figure 4.10**). However, as the rate of photolysis of the DEACM caging group at 420 nm ($k = 0.427$ s^{-1}) greatly exceeded that of the BODIPY-2 caging group, it would be possible to take advantage of the differences in kinetics to achieve chromatic orthogonality.

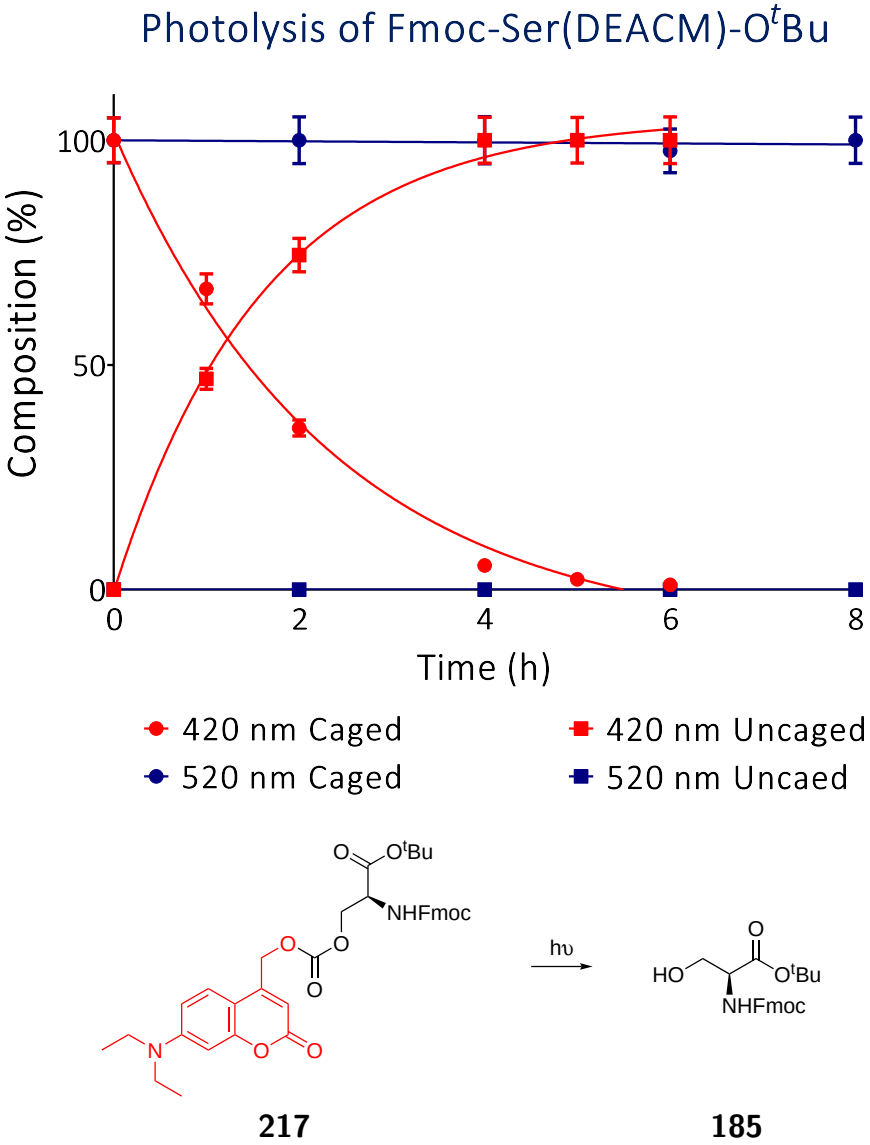
Although the UV/vis spectrum of the DEACM caging group displayed no absorption in the region above 450 nm and was thus expected to be photostable at 520 nm, it was still imperative to test this hypothesis. DEACM-caged Fmoc-Ser-O^{t}Bu (**217**) was

irradiated at 520 nm and 5% release of serine (**185**) was observed following 8 h of irradiation (**Figure 4.11**).



Entry	λ_{irrad} (nm)	k_{caged} (s^{-1})	N_{caged}	R^2_{caged}	$k_{uncaged}$ (s^{-1})	$N_{uncaged}$	$R^2_{uncaged}$
1	420	0.00129	4	0.90	-	-	-
2	520	0.234	4	0.99	4.60×10^{-5}	4	0.94

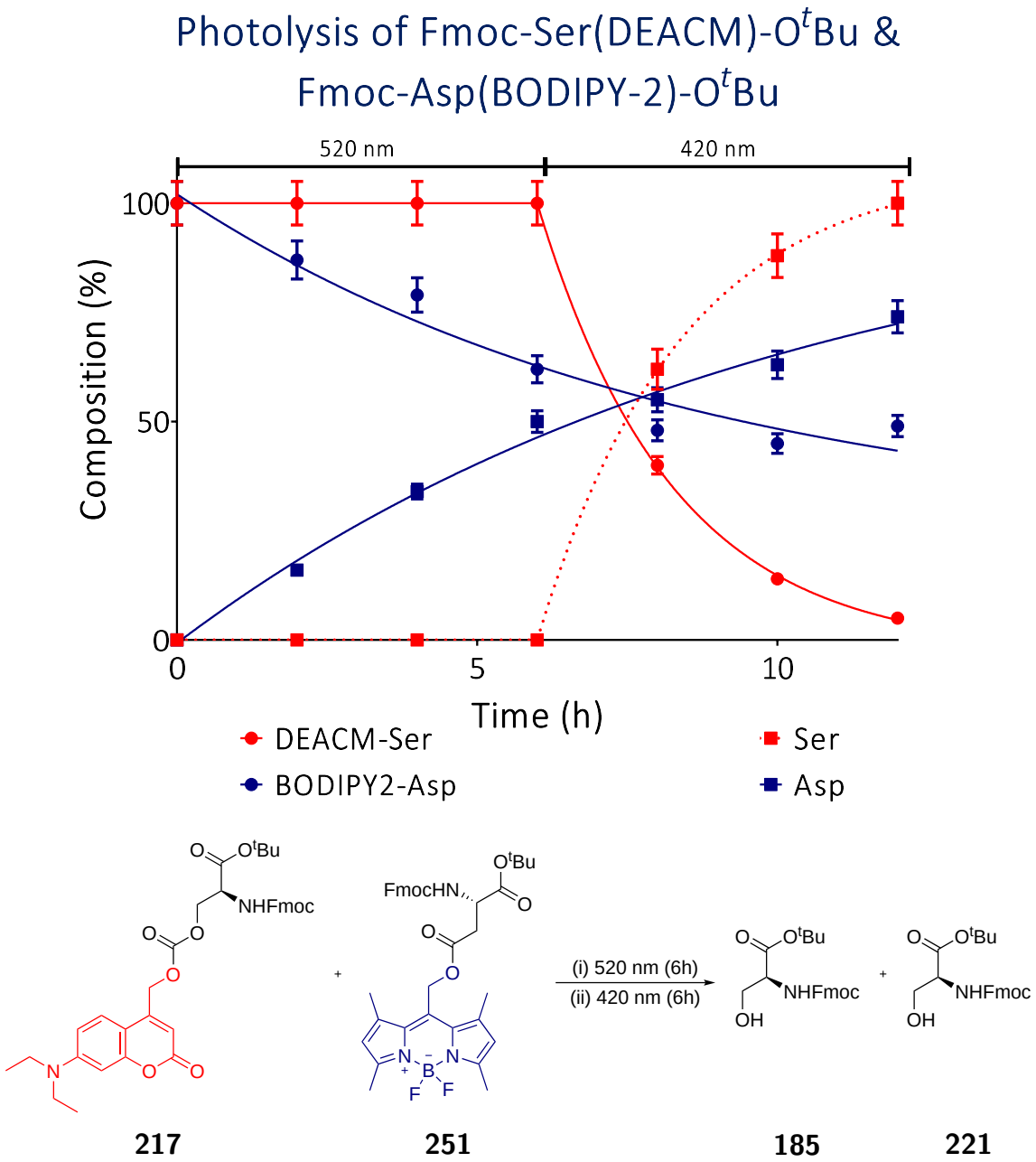
Figure 4.10: Percentage composition of BODIPY-2-caged and uncaged aspartic acid following irradiation (MeOH).



Entry	λ_{irrad} (nm)	k_{caged} (s^{-1})	N_{caged}	R^2_{caged}	$k_{uncaged}$ (s^{-1})	$N_{uncaged}$	$R^2_{uncaged}$
1	420	0.427	6	0.99	0.622	6	1.00
2	520	-	-	-	-	-	-

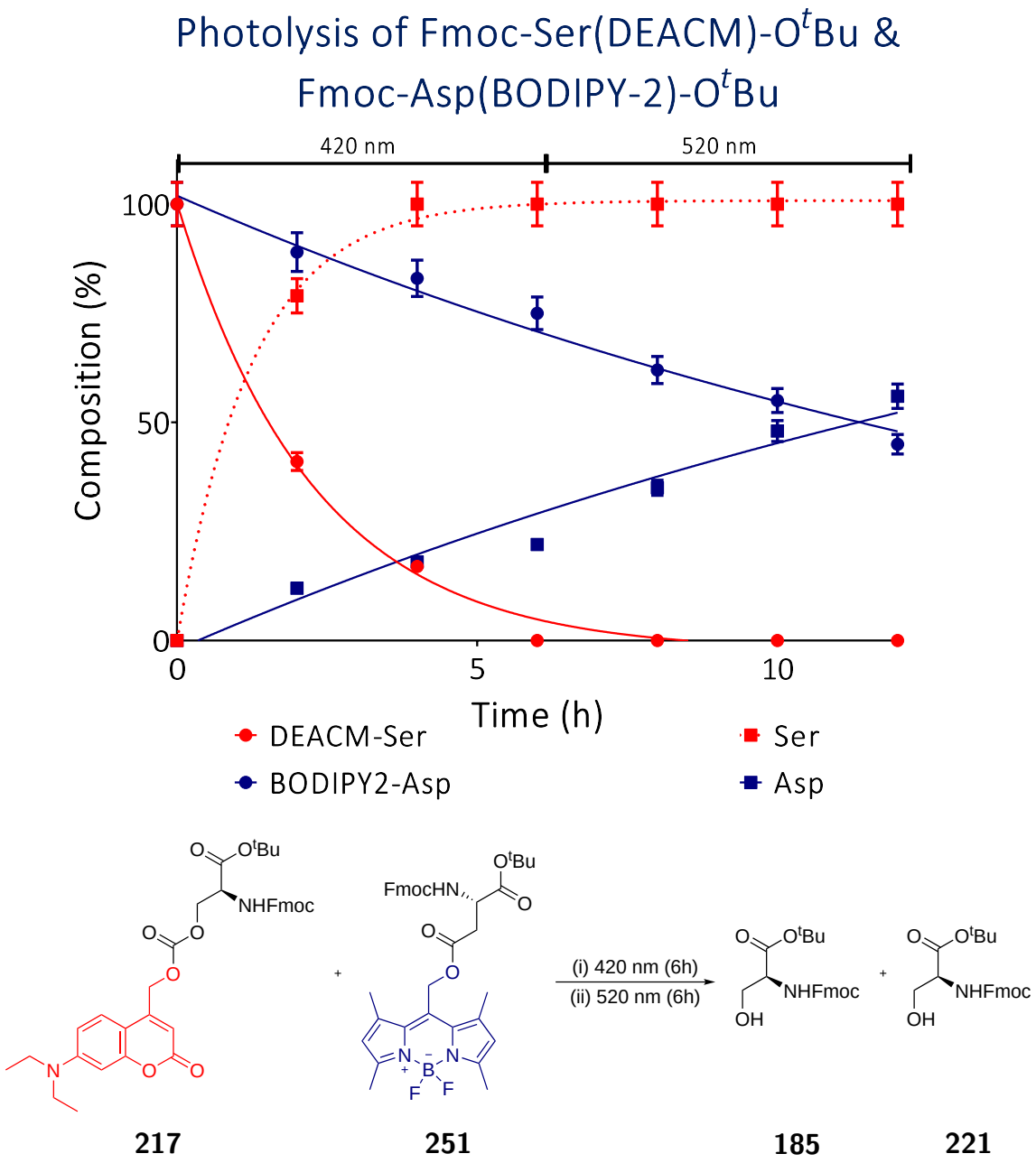
Figure 4.11: Percentage composition of DEACM-caged and uncaged serine following irradiation at 520 nm (MeOH).

Despite the small amount of photolysis observed at the corresponding wavelengths, the differences in rates of photolysis could lead to the potential for a wavelength orthogonal system to exist.



Entry	λ_{irrad} (nm)	k_{caged} (s^{-1})	N_{caged}	R^2_{caged}	$k_{uncaged}$ (s^{-1})	$N_{uncaged}$	$R^2_{uncaged}$
1	520	-	-	-	-	-	-
2		0.118	7	0.95	0.0990	7	0.99
3	420	0.445	7	1.00	0.422	7	1.00
4		-	-	-	-	-	-

Figure 4.12: Percentage composition of DEACM-caged (yellow) & BODIPY-2-caged (pink) and uncaged serine & aspartic acid following irradiation at 520 nm then 420 nm both for 6 h [MeOH].



Entry	λ_{irrad} (nm)	k_{caged} (s^{-1})	N_{caged}	R^2_{caged}	$k_{uncaged}$ (s^{-1})	$N_{uncaged}$	$R^2_{uncaged}$
1	420	0.441	7	1.00	0.798	7	1.00
2		-	-	-	-	-	-
3	520	-	-	-	-	-	-
4		0.0513	7	0.98	0.0500	7	0.961

Figure 4.13: Percentage composition of DEACM-caged (yellow) & BODIPY-2-caged (pink) and uncaged serine & aspartic acid following irradiation at 420 nm then 520 nm both for 6 h [MeOH].

To test this hypothesis further, a solution containing a mixture of DEACM-caged serine (**217**) and BODIPY-2-caged aspartic acid (**251**) was irradiated at both 520 nm and 420 nm. If only the BODIPY-2 caging group was photolysed at 520 nm and only the DEACM caging group was photolysed at 420 nm, it would provide further evidence of chromatic orthogonality for this pair of phototriggers (**Figure 4.12**).

When the mixture of DEACM-caged serine (**217**) and BODIPY-2-caged aspartic acid (**251**) was irradiated at 520 nm for 6 h, no significant change was observed in the percentage composition of DEACM-caged serine (**217**) and no uncaged photoreleased serine (**185**) was detected. The percentage composition of the BODIPY-2-caged species (**251**) had dropped to approximately 60% with a rate constant of 0.118 s^{-1}, releasing aspartic acid (**221**) with a rate constant of 0.0990 s^{-1}. After 6 h, the wavelength of irradiation was changed to 420 nm. Over the first 2 h of irradiation at 420 nm, extremely rapid photolysis of the DEACM-caged species (**217**) was observed with a rate constant of 0.445 s^{-1}, and the percentage composition dropping to 60%, accompanied by the photorelease of Fmoc-Ser-O^{t}Bu (**185**) with a rate constant of 0.422 s^{-1}. Over the course of 6 h, a small drop in the percentage composition of the BODIPY-2 species (**251**) was observed alongside a minor increase in the percentage composition of free aspartic acid (**221**) (**Figure 4.12**). The decline in the caged species was attributed to photodegradation and the small increase in uncaged amino acid was attributed to a delayed release of the amino acid, following irradiation at 520 nm, as had been observed with the single species irradiation experiments (**Figure 4.10**).

The photolysis experiments were also carried out, irradiating the mixture of DEACM-caged serine (**217**) and BODIPY-2-caged aspartic acid (**251**), first at 420 nm for 6 h followed by 520 nm for another 6 h (**Figure 4.13**).
For the first 6 h, irradiation with a light source of 420 nm was used and very rapid decline of the DEACM-caged serine (**217**) was observed with a rate constant of 0.441 s^{-1}, and the accompanied release of serine (**185**). An approximate drop of 25% was observed for the BODIPY-2-caged aspartic acid (**251**) which was accompanied by release of free Fmoc-Asp-O^{t}Bu (**221**). Relative to the rate of photolysis of the DEACM photolabile caging group, the rate of photolysis of the BODIPY-2 phototrigger at this wavelength (k = 0.0513 s^{-1}) was deemed to be sufficiently slow. When the wavelength of irradiation was switched to 520 nm, photolysis continued to be observed for the BODIPY-2-caged species (**251**) with a rate constant of 0.0513 s^{-1}, and the percentage composition dropping to approximately 45% accompanied by an excess of

50% formation of free uncaged aspartic acid (**221**) with a rate constant of 0.0500 s^{-1}.

This experiment demonstrated that the DEACM- and BODIPY-2 caging groups have the potential to act as a pair of chromatically orthogonal photolabile caging groups when irradiation at wavelengths of 420 nm to selectively cleave the DEACM photolabile caging group and 520 nm to photolyse the BODIPY-2 photolabile caging group were used.

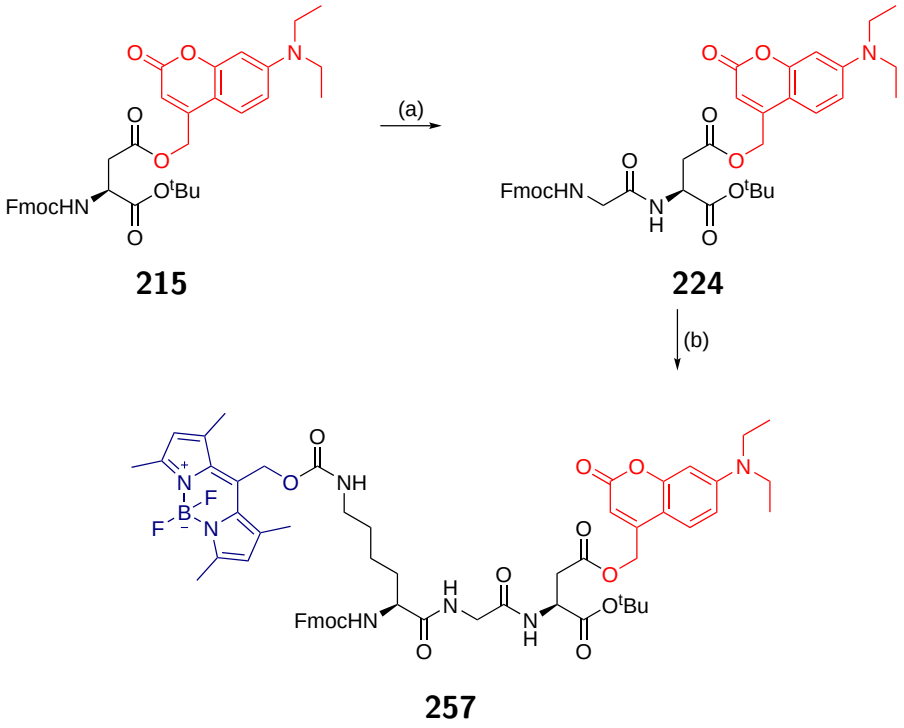
4.4 Chromatically Orthogonal Light-Activated Tripeptide

As the aim was to develop a pair of wavelength orthogonal photolabile caging groups that could be applied as a tool to enhance the study of protein PTM, the investigation was extended to incorporate this pair of PCGs into a model peptide. This would enable demonstration of wavelength orthogonal photolysis in a peptide system bearing the DEACM and BODIPY-2 caging groups.

4.4.1 Synthesis of Tripeptide

Synthesis of the tripeptide incorporating DEACM-caged aspartic acid (**215**) and BODIPY-2-caged lysine (**256**), subtended by a glycine residue, commenced with the Fmoc deprotection of DEACM-caged Fmoc-Asp-O^{t}Bu (**215**) by stirring in 10% piperidine. This was followed by reaction with commercially available Fmoc-Gly-OH, employing HBTU as the activating agent, affording the desired dipeptide product (**224**) in 53% yield over two steps (**Scheme 4.19**).

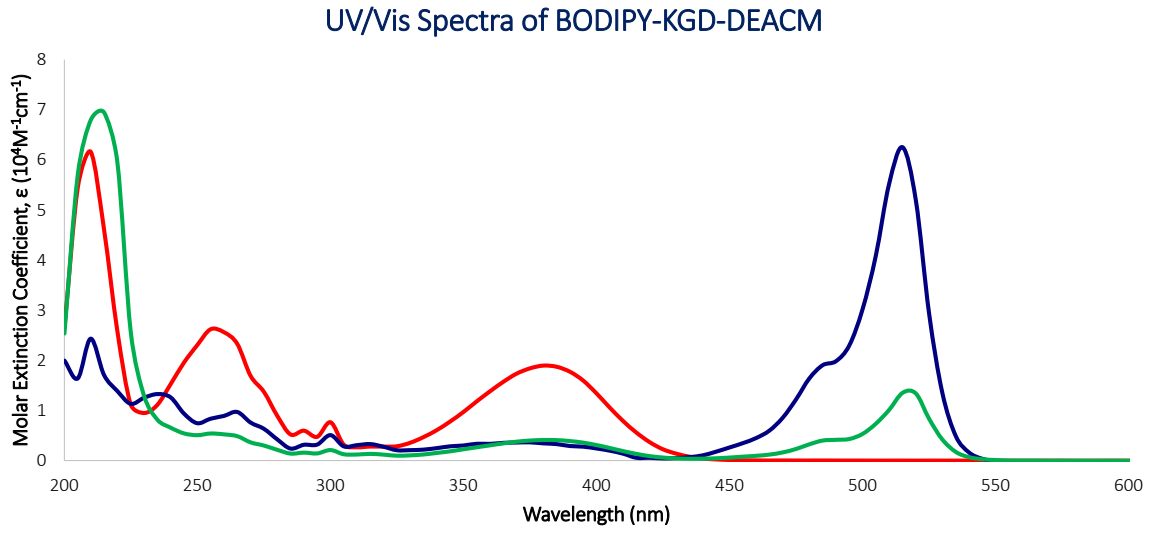
The next stage of the tripeptide synthesis involved another Fmoc-deprotection prior to peptide coupling with the previously synthesised BODIPY-2-caged Fmoc-protected lysine (**256**) bearing the free α-carboxylic acid. Fmoc-deprotection was conducted with 5% piperidine at 0 °C. The low temperature was chosen to minimise decomposition due to any excess piperidine. The crude residue was then reacted with BODIPY-2-caged lysine, bearing the free α-carboxylic acid (**256**), in the presence of PyBOP to give the desired dual caged tripeptide (**257**) in 21% yield over 2 steps (**Scheme 4.19**).

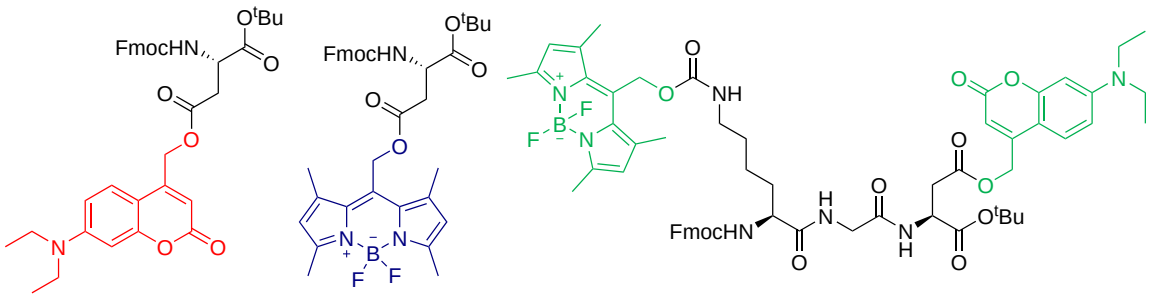


Scheme 4.19: Synthesis of tripeptide incorporating DEACM-caged aspartic acid, BODIPY-2-caged lysine and a glycine linker; Reagents & Conditions: (a) 10% Piperidine in DMF, 0 °C, Ar, 0.5 h then Fmoc-Gly-OH, HBTU, DIPEA, DMF, RT, Ar, 18 h, 53% over 2 steps; (b) 5% Piperidine in DMF, 0 °C, Ar, 10 min then Fmoc-Lys(BODIPY-2)-OH, PyBOP, DIPEA, DMF/CH_2Cl_2, RT, Ar, 18 h, 21% over 2 steps.

4.4.2 Photolysis of the Wavelength-Orthogonally Caged Tripeptide

Following synthesis of the dual-caged tripeptide (**257**) bearing the DEACM and BODIPY-2 photolabile caging groups, the UV/vis absorption spectrum of the compound was measured.



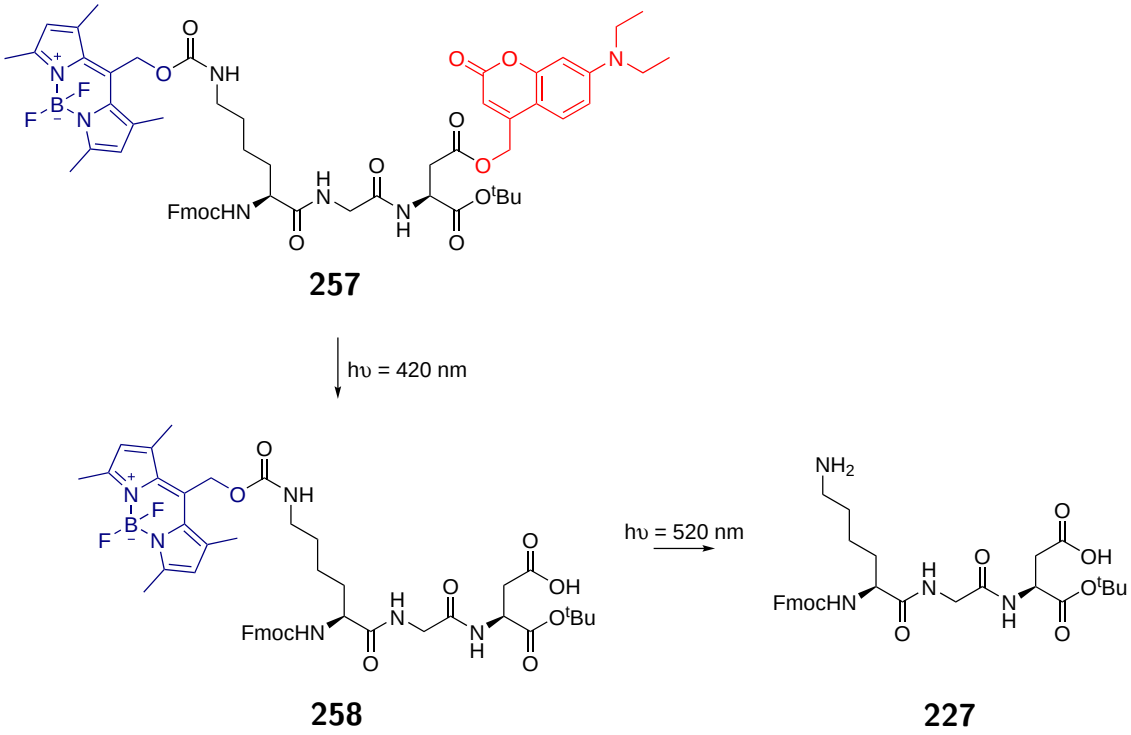


215 **251** **257**

Entry	Conc (mM)	λ_{max} (nm)	Transition	A	ε ($M^{-1}cm^{-1}$)
1	0.04	380	π – π*	0.758	18961
2	0.004	515	π – π*	0.250	62533
3	0.04	380	π – π*	0.164	4112
		515	π – π*	0.542	13539

Figure 4.14: UV/vis Spectra of DEACM- & BODIPY-2-caged tripeptide [green; λ_{max} = 517 nm (π - π*)] overlaid on DEACM-caged aspartic acid [yellow; λ_{max} = 382 nm (π - π*)] and BODIPY-2-caged aspartic acid [pink; λ_{max} = 519 nm (π - π*)]; [c0.2 mM in MeOH].

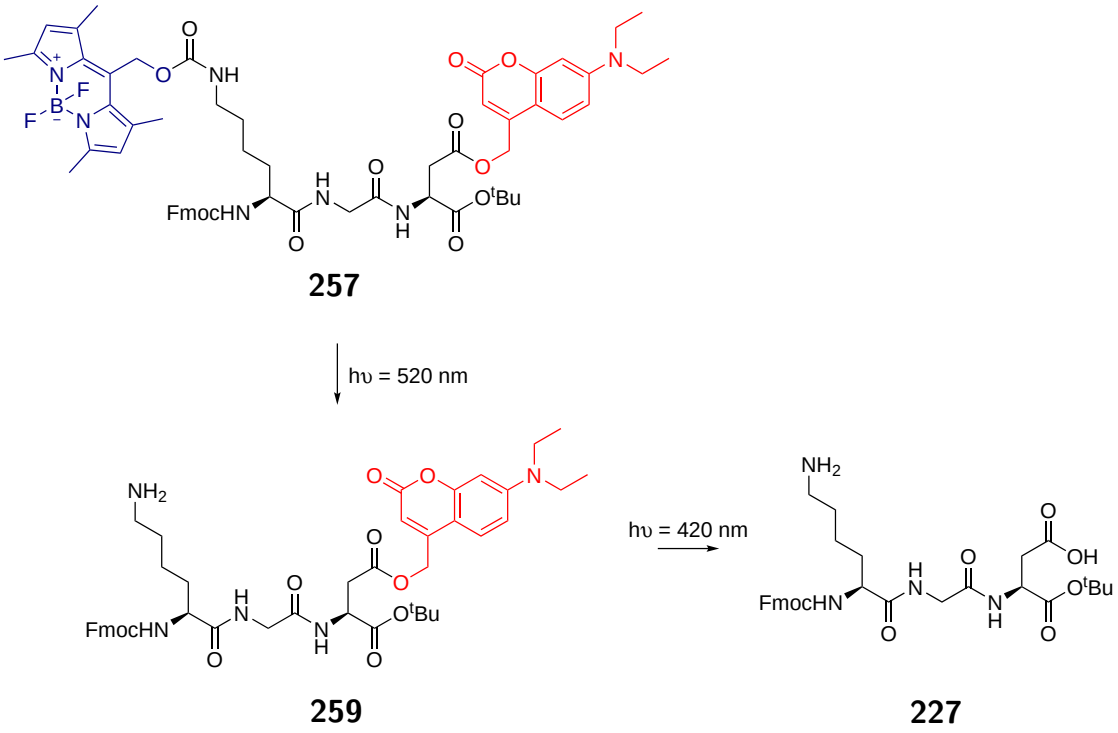
The tripeptide was found to possess two absorption maxima centred at 517 nm and 379 nm. These were found to correspond almost directly to the absorption maxima of the individual phototriggers. The individual contributions to the absorbance of the dual-caged tripeptide from the component photolabile caging groups were particularly evident when the UV/vis absorption spectra were overlaid (**Figure 4.14**). This gave confidence that the results from the previously conducted photolysis experiments could be extrapolated to the dual-caged tripeptide system.



Scheme 4.20: Photolysis of DEACM- & BODIPY-2-caged tripeptide by irradiation at 420 nm (10 h) followed by 520 nm (3 h) [MeOH].

The dual-caged tripeptide (**257**) was subjected to irradiation at 520 nm and 420 nm. Irradiating at 420 nm uncaged the DEACM photolabile caging group and afforded the tripeptide (**258**) bearing the free side chain carboxylic acid of the aspartic acid residue, resulting in formation of a new peak in the HPLC spectrum centred at 14.0 min; the identity of the product was confirmed by mass spectrometry. Swapping the wavelength of irradiation to 520 nm resulted in uncaging of the BODIPY-2 phototrigger, evident as a decrease of the peak at 14.0 min and the growth of a new peak at 10.1 min, the mass of which corresponded to the fully uncaged tripeptide (**227**) bearing the free side chain carboxylic acid of aspartic acid and ε-amine of the lysine residue (**Scheme 4.20**). After irradiation at 420 nm for 10 h, dual-caged tripeptide (**257**)

remained, evident by the peak in the HPLC spectrum at 15.6 min. Thus, when the wavelength of irradiation was changed to 520 nm, the formation of a peak at 12.3 min, attributed to the DEACM-caged tripeptide (**259**) was simultaneously observed alongside formation of the peak of the fully uncaged tripeptide (**227**) at 10.1 min (**Figure 4.15**).



Scheme 4.21: Photolysis of DEACM- & BODIPY-2-caged tripeptide by irradiation at 520 nm (10 h) followed by 420 nm (2 h) [MeOH].

When the order of irradiation was reversed (**Scheme 4.21**), and photolysis was first performed with the light source of 520 nm, cleavage of the BODIPY-2 photolabile group to reveal the free side chain ε-amine of the lysine residue commenced, resulting in formation of a new peak at 12.3 min in the HPLC, the mass of which was confirmed to be that of the now mono-caged tripeptide (**259**). Prolonged exposure to irradiation at 520 nm ($>$ 2 h), gave rise to some deprotection of the DEACM caging group, resulting in formation of the mono BODIPY-2-caged tripeptide (**258**), evident from the formation of a peak in the HPLC spectrum at 13.2 min. The dominant product, even after prolonged irradiation at 520 nm (10 h) was still the DEACM-caged tripeptide (**259**), derived from cleavage of the BODIPY-2 caging group (**Figure 4.15**). Irradiation of the DEACM-caged tripeptide (**259**) compound with a light source of 420 nm resulted in subsequent photocleavage of the DEACM caging group to reveal the fully uncaged

tripeptide (**227**) as witnessed by the growth of the peak at 10.1 min in the HPLC, the mass of which was confirmed to be that of the desired fully uncaged tripeptide (**227**) (**Figure 4.15**).

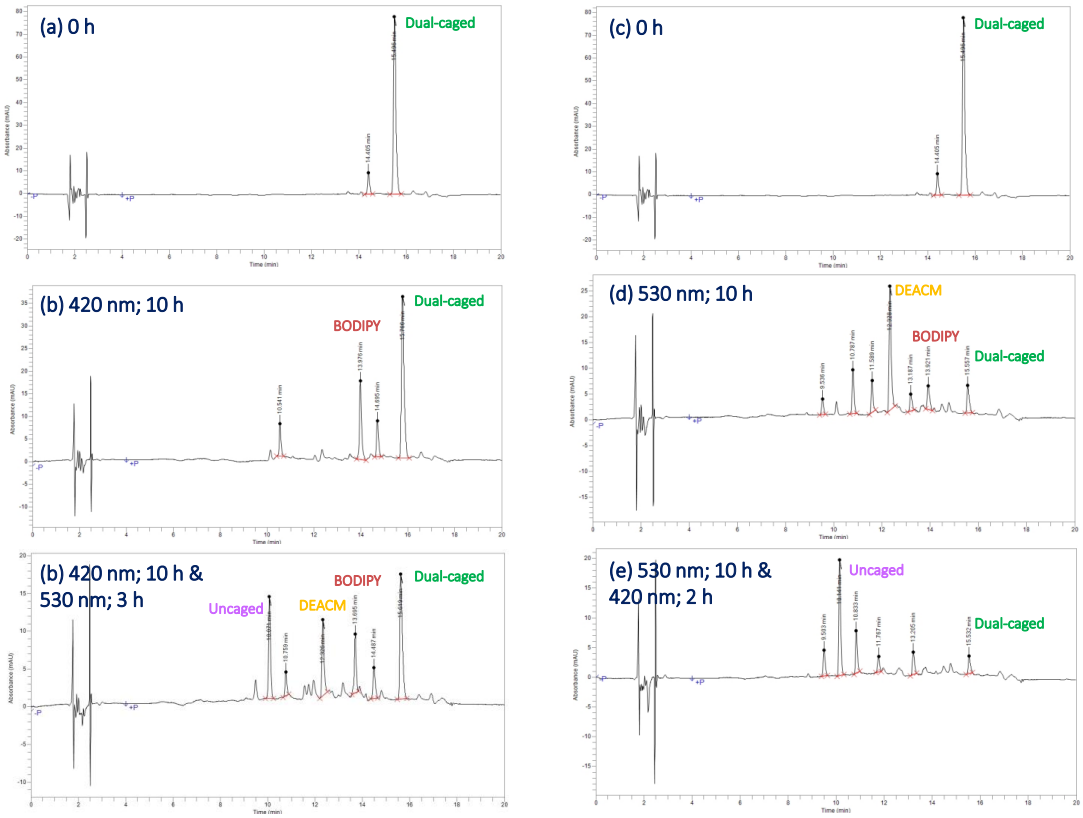


Figure 4.15: HPLC traces following irradiation of BODIPY-2- and DEACM-caged tripeptide at 420 nm and 520 nm; (a) 0 h: caged tripeptide = 15.6 min (92 %), impurity = 14.5 min (8 %); (b) 10 h at 420 nm: caged tripeptide = 15.8 min, impurity = 14.7 min, BODIPY-2-caged tripeptide = 14.0 min, DEACM photolysis by-product = 10.5 min; (c) 10 h at 420 nm then 3 h at 520 nm: caged tripeptide = 15.6 min, impurity = 14.5 min, BODIPY-2-caged tripeptide = 13.7 min, DEACM-caged tripeptide = 12.3 min, DEACM photolysis by-product = 10.8 min, uncaged tripeptide = 10.1 min; (d) 0 h: caged tripeptide = 15.6 min (92 %), impurity = 14.5 min (8 %); (e) 10 h at 520 nm: caged tripeptide = 15.6 min, BODIPY-2-caged tripeptide = 13.9 min, BODIPY-2 photolysis by-product = 13.2 min, DEACM-caged tripeptide = 12.3 min, BODIPY-2 photolysis by-product = 11.6 min, DEACM photolysis by-product = 10.8 min, BODIPY-2 photolysis by-product = 9.5 min; (f) 10 h at 520 nm then 2 h at 420 nm: caged tripeptide = 15.5 min, BODIPY-2 photolysis by-product = 13.2 min, BODIPY-2 photolysis by-product = 11.7 min, DEACM photolysis by-product = 10.8 min, uncaged tripeptide = 10.1 min, BODIPY-2 photolysis by-product = 9.5 min.

These results supported the development of a chromatically orthogonal pair of photolabile caging groups, employing the DEACM phototrigger that could be selectively

cleaved at 420 nm and the BODIPY-2 phototrigger that could be selectively cleaved at 520 nm, and showed great potential for application as a tool to aid the investigation of protein PTMs. Most importantly, the use of these two caging groups minimised restrictions in terms of the sequence in which the irradiation and hence photolysis had to occur and is the first known example of wavelength orthogonality where both wavelengths of irradiation used are longer than 300 nm.

4.5 Summary and Future Work

Through the use of red-shifted photolabile caging groups, a chromatically orthogonal pair of photolabile caging groups was developed, the orthogonal photolysis of which was demonstrated in a tripeptide system. Various red-shifted caging groups were investigated, which included the RuBpy group, the DEATC caging group and two BODIPY dye derived variants. Wavelength orthogonality could only be achieved with the second BODIPY variant and the DEACM phototrigger. By irradiating at 420 nm, selective uncaging of the DEACM photolabile caging group was achieved, while at 520 nm, selective photolysis of the BODIPY-2 caging group was observed. To date, this is the first example of the development of chromatically orthogonal PCGs as a tool to study protein PTMs with enhanced spatial and temporal control, where both wavelengths of irradiation exceed 400 nm.

To further build upon this work, two lines of inquiry can be pursued. The first would involve investigation into novel red-shifted caging groups which could potentially be applied for the purpose of developing new chromatically orthogonal pairs of photolabile caging groups. The second line of inquiry would revolve around further developing the chromatically orthogonal pair of caging groups as tools for the investigation of protein PTMs. This would involve incorporating the pair of caging groups into longer peptides and eventually proteins, through the use of solid phase peptide synthesis (SPPS) or mutagenesis, to demonstrate their utility as tools to aid the study of protein PTMs.

Chapter 5

Optimisation of Photolysis Studies & Application to Peptides

5.1 Introduction and Aims

Previous experimental work detailed in this dissertation laid the foundations for the development of a chromatically orthogonal pair of photolabile caging groups that had the potential to be applied to the study of protein post-translational modifications. Long irradiation times required to effect photolysis would however, limit applications, especially for time sensitive studies and thus it was imperative to increase the rate of photolysis. In addition, it was likely that a reduction in irradiation times would lead to an improvement in selectivity.

To achieve this, higher power LED light sources would be employed. In addition, to improve on previous studies, solutions of a lower concentration would be subjected to irradiation; this was to better mimic biological settings and reduce irradiation times. The concentration of 4.0 μM in MeOH was chosen such that UV/vis absorbance was less than one absorbance unit (A.U.). It was thought that this would minimise the effects of inhomogeneous uncaging due to inner filtering effects, as the light would not be fully absorbed at the surface and be able to pass through the sample.

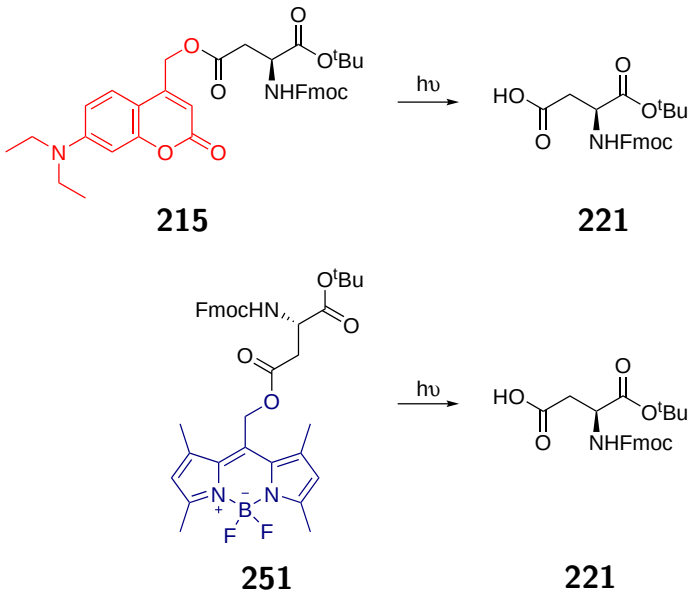
In order to further demonstrate the applicability of the developed photolabile caging group system to the study of PTMs, caged tripeptides, and hexapeptides would be synthesised by solid phase peptide synthesis and be subsequently exposed to irradiation at 420 nm and 530 nm. The effects of irradiation would be observed to determine the compatibility of the caging groups with the model peptide systems as well as to further assess the pair of caging groups for orthogonality.

Finally, the caged hexapeptides would be subjected to incubation with proteolysis enzymes *in vitro*, prior to and following photolysis, as a means of demonstrating the ability of the pair of caging groups to be used for the study of protein PTMs. It was envisaged that prior to photolysis, whilst caged, the peptides would not undergo peptidolysis following incubation with the respective enzymes, whereas following irradiation and hence uncaging of the photolabile group, incubation with the enzymes would result in peptidolysis at their respective sites.

5.2 Photolysis of Caged Amino Acids

As a result of the lower concentrations, LCMS was adopted as the method of analysis owing to its greater sensitivity relative to traditional methods such as **^{1}H NMR** and HPLC-UV. For quantitative measurements to be performed, a series of calibration experiments were undertaken, for the caged and uncaged amino acid analogues [See Experimental Chapter (**7**) for further details].

To enhance the rate of photolysis, stronger light sources were also employed. For irradiation at 420 nm, the previously used 15 mW LED was replaced by a 750 mW LED whilst for irradiation conducted at 530 nm, the LED strip was replaced by a 350 mW LED. Irradiation experiments were conducted in triplicates for varying time frames before analysis of the samples by LCMS.

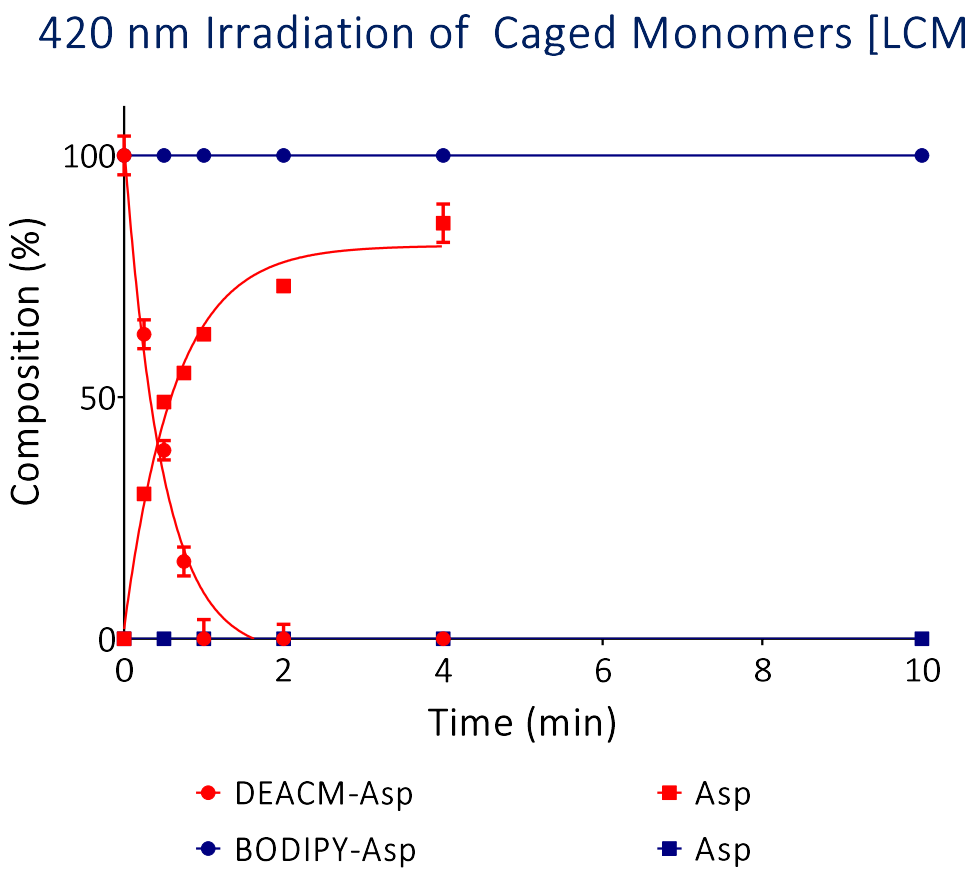

O
O
O

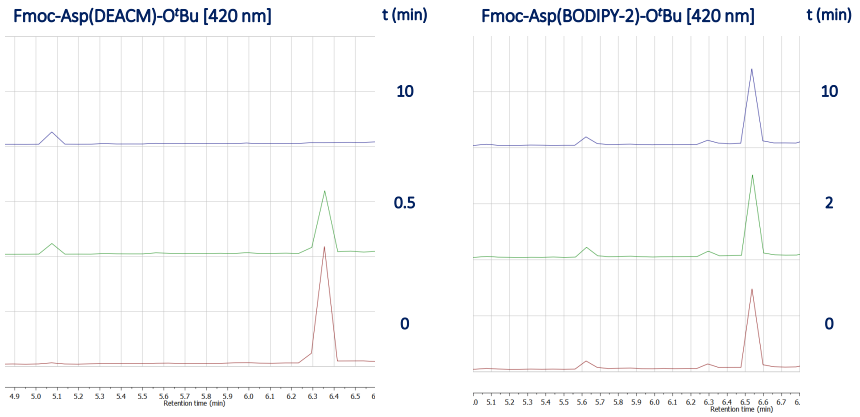
When subjecting the DEACM-caged aspartic acid (**215**) to irradiation at 420 nm, the rate of photolysis was greatly enhanced, from 0.689 s^{-1} to 2.10 s^{-1}, as a result of the stronger light source and reduced concentration used. The percentage composition of the caged species had dropped to 0% in 1 minute, relatively to the 7 h previously required, accompanied by 63% conversion to uncaged aspartic acid (**221**), rising to 86% after 4 minutes of irradiation, with a rate constant of 1.57 s^{-1} and a quantum yield of 2.28×10^{-4}. This delayed product release indicated the possibility of the reaction rate limiting step following initial light-mediated excitation (**Figure 5.1**). The increased power of the light source and the reduced concentration used, had no effect on the photostability of the BODIPY-2 caging group at 420 nm and after 10 minutes of irradiation at this wavelength, there was no decline in the percentage composition of BODIPY-2 caged aspartic acid (**251**) and no formation of uncaged aspartic acid (**221**) was observed (**Figure 5.1**).

Irradiation at 530 nm resulted in the caged BODIPY-2 compound (**251**) undergoing complete photolysis with a rate constant of 0.0190 s^{-1} by 120 min, and a quantum yield of 0.398×10^{-4}, to release uncaged aspartic acid (**221**) in 63% yield with a rate constant of 0.0251 s^{-1} (**Figure 5.2**).

When DEACM-caged aspartic acid (**215**) was irradiated at 530 nm, no change in percentage composition of the caged species was observed. In addition, no formation of the uncaged aspartic acid (**221**) could be detected by LCMS, suggesting the caging group was stable at this wavelength (**Figure 5.2**).

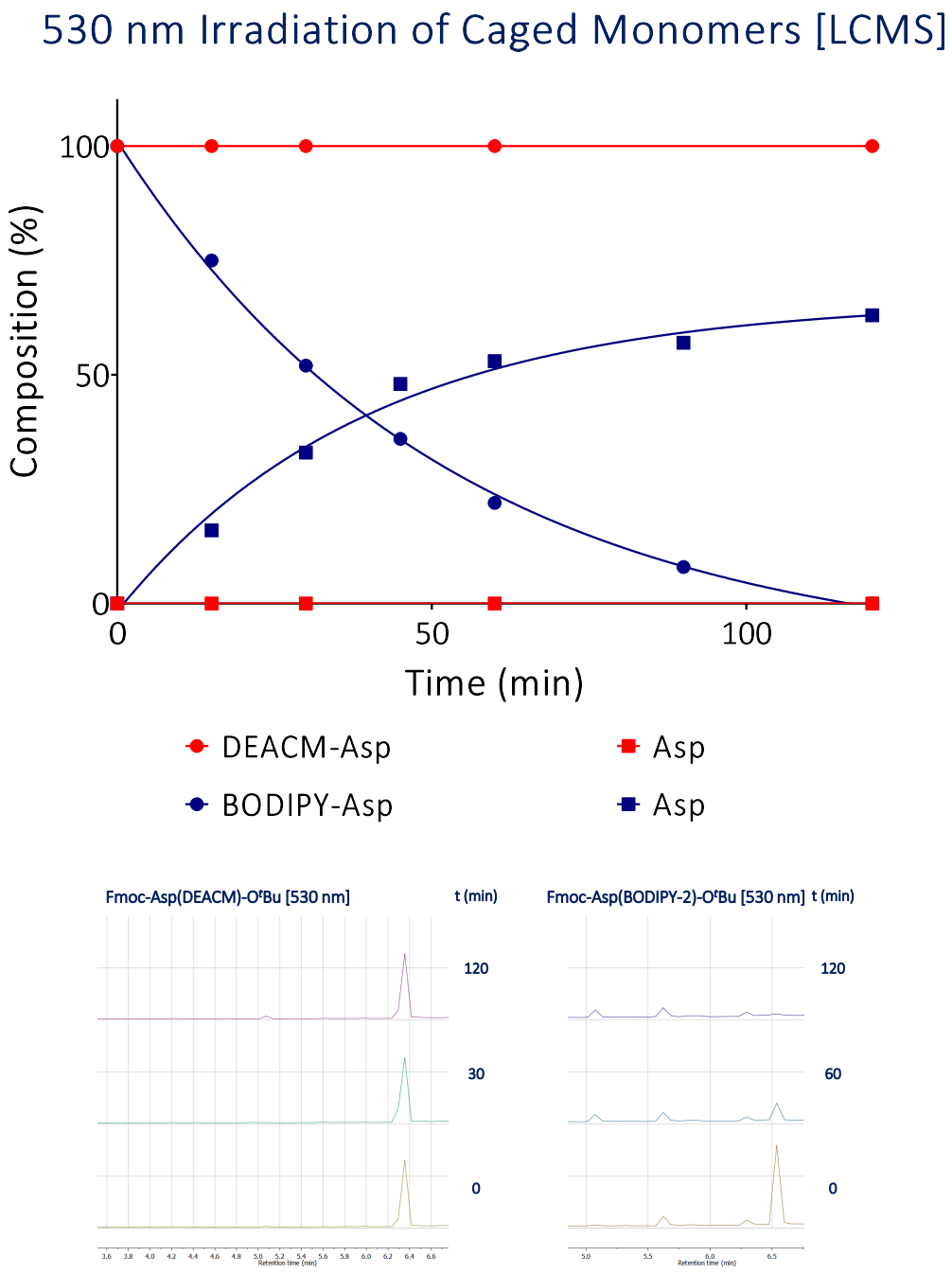
The use of a lower concentration and stronger light sources for the irradiation experiments led to a dramatic decline in the photolysis time frames required for complete disappearance of the caged species. Moreover, selectivity was enhanced, providing further support for the development of an orthogonal system using the DEACM and BODIPY-2 caging groups.





Entry	λ_{irrad} (nm)	k_{caged} (s^{-1})	N_{caged}	R^2_{caged}	$k_{uncaged}$ (s^{-1})	$N_{uncaged}$	$R^2_{uncaged}$
1	420	2.10	7	0.98	1.57	7	0.98
2	420	-	-	-	-	-	-

Figure 5.1: Percentage composition of caged and uncaged aspartic acid following irradiation at 420 nm as monitored by LCMS; Concentration = 4.0 μM [MeOH].



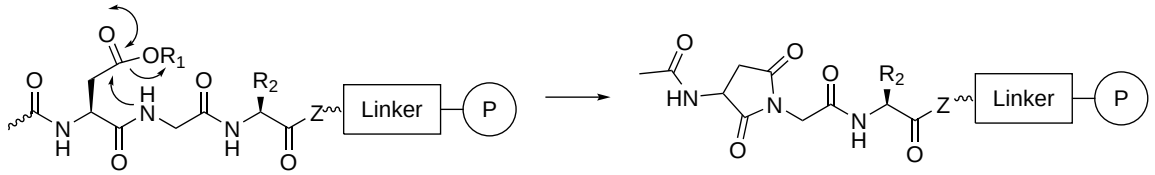
Entry	λ_{irrad} (nm)	k_{caged} (s^{-1})	N_{caged}	R^2_{caged}	$k_{uncaged}$ (s^{-1})	$N_{uncaged}$	$R^2_{uncaged}$
1	530	-	-	-	-	-	-
2	530	0.0190	7	1.00	**0.0251**	7	0.99

Figure 5.2: Percentage composition of caged and uncaged aspartic acid following irradiation at 530 nm as monitored by LCMS; Concentration = 4.0 μM [MeOH].

5.3 Synthesis of Caged Peptides

To further demonstrate the applicability of the orthogonal pair of caging groups that had been developed, the solid phase peptide synthesis (SPPS) strategy was employed to synthesise a series of peptides bearing the DEACM and BODIPY-2 caging groups; this included a series of tripeptides and hexapeptides. The increasing distance between the two caging groups as the length of the peptides increased could also offer insight into any interactions occurring between the two caging groups.

For the initial tripeptide, the sequence K-G-D (Lys-Gly-Asp) was selected. However, it was found that the G-D (Gly-Asp) sequence suffered from issues of aspartimide formation in the presence of base, which eroded the yield (**Scheme 5.2**).



260 **261**

Scheme 5.2: Aspartimide formation between G (Gly) and D (Asp).

Therefore, in order to avoid the issues of aspartimide formation, the sequence D-L-K (Asp-Leu-Lys) was chosen for the tripeptide. The DEACM caging group was shown to be stable to peptide synthesis conditions, however, the propensity of the BODIPY-2 group to undergo decomposition under strongly acidic and basic conditions led to three strategies being trialled for the synthesis of the caged peptides:

(i) Strategy 1: The first strategy involved addition of the BODIPY-2 group to the free side-chain ϵ-amine of the lysine residue following assembly of the peptide *via* SPPS and cleavage from the Wang resin.

(ii) Strategy 2: The second strategy required coupling of the BODIPY-caging group to the free side-chain ϵ-amine of the assembled peptide whilst still attached to the CTR resin, prior to cleavage.

Both these routes however, proved to be ineffective and the desired peptide could not be isolated. One possible explanation for this could be steric hindrance which disfavoured the reaction. The coupling reactions were attempted with 4-nitrophenyl

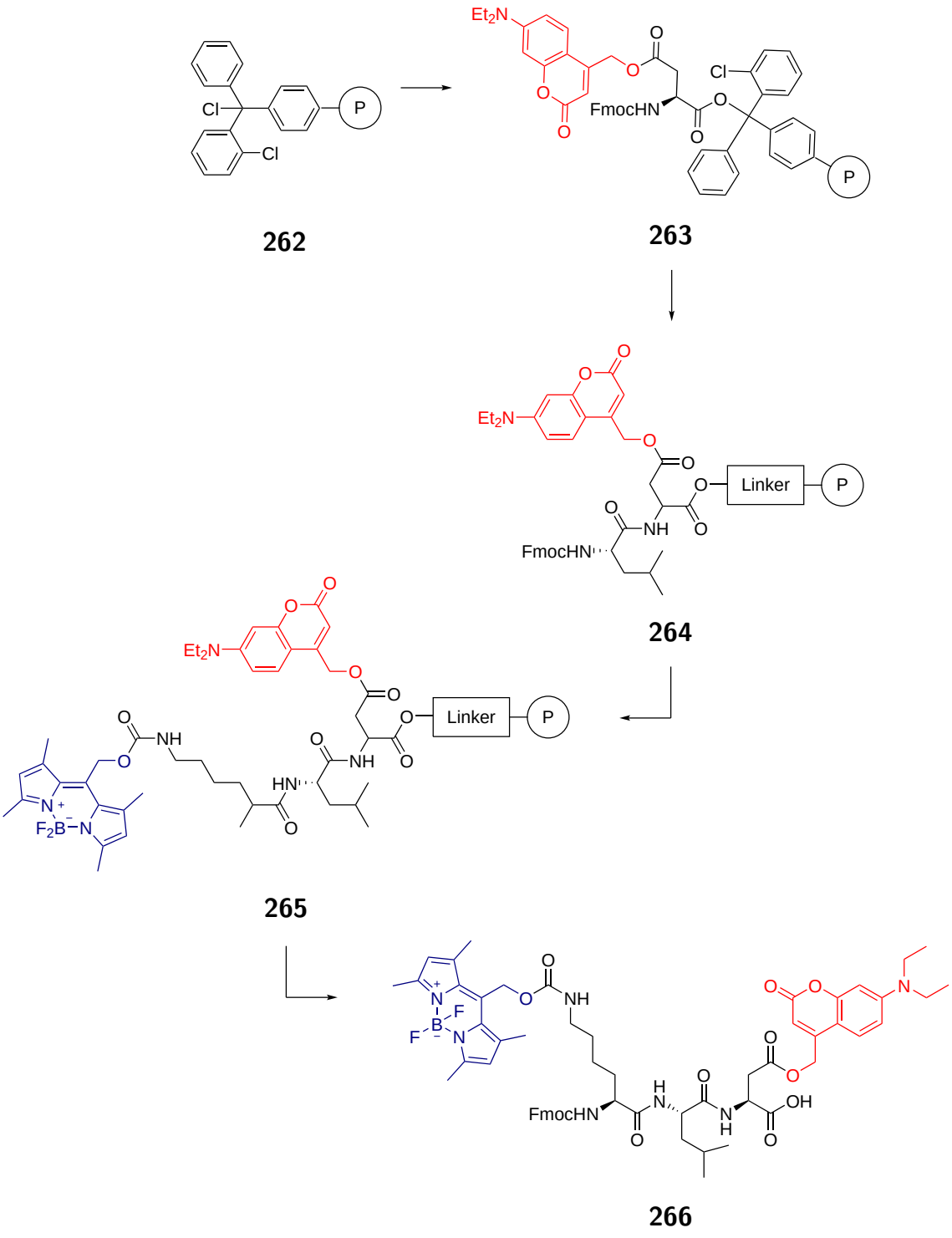
chloroformate or CDI, either as a biphasic mixture in CH_2Cl_2 or THF and H_2O or in DMSO, with a variety of bases ranging from NMM to 4-DMAP and sodium bicarbonate. The reactions were also carried out *in-situ* or following isolation of the active intermediate. However, in all cases, the desired caged peptide could not be isolated.

(iii) Strategy 3: The third strategy involved the SPPS assembly of the peptide using modified amino acids as residues. For this, the CTR resin was employed as the high acid lability would allow cleavage of the peptide from the resin using HFIP, to which the BODIPY-2 group had been shown to be stable. In addition, both the BODIPY-2 and DEACM caging groups were shown to be stable to Fmoc deprotection conditions of piperidine in DMF as well as standard peptide coupling conditions with a variety of activating agents in NMP or DMF. Amino acids residues are also commercially available as trityl and methyl trityl protected variants thus allowing ready synthesis of caged peptides up to the limit of SPPS.

Synthesis of the tripeptide commenced with coupling of DEACM-caged aspartic acid (**216**) to the CTR resin in the presence of DIPEA. Any unreacted resin was capped with MeOH to prevent it interfering with downstream reactions. The addition of the standard non-modified amino acid, leucine, was then conducted using a peptide synthesiser, following standard protocols. Lastly, BODIPY-caged lysine was coupled to the growing amino acid chain following standard peptide coupling protocol prior to cleavage from the resin in the presence of HFIP. The use of amino acids protected with highly acid labile Trt and Mtt groups would allow for global deprotection in the final stage (**Scheme 5.3**).

Syntheses of caged hexapeptides followed a similar strategy. The base sequence chosen was K-G-S-T-A-D (Lys-Gly-Ser-Thr-Ala-Asp).

This strategy allowed the synthesis of the caged amino acid containing peptides on scales of between 25 - 100 mg.



Scheme 5.3: Synthesis of caged tripeptide *via* SPPS.

5.4 Photolysis of Caged Peptides

Successful syntheses of the caged peptides enabled the UV/vis spectra to be measured and photolysis reactions to be undertaken by subjecting the modified peptides to irradiation at 420 nm and 530 nm. Comparison of the mono-caged and dual-caged peptides would enable interactions, if any, between the two caging groups to be investigated; interactions if present would be expected to decrease with increasing distance between the caging groups. Analysis of the irradiated samples by LCMS-UV would then allow for quantification of the photolysis reactions.

5.4.1 Photolysis of Caged Tripeptide

Prior to conducting the photolysis reactions, the UV/vis spectra of the caged tripeptides was measured and compared (**Figure 5.3**). The absorbance of BODIPY-KLD-DEACM (**266**) reflected a combination of the absorbance of the individual caging groups, with λ_{max} at 380 and 520 nm (**Figure 5.3**).

Photolysis reactions commenced with irradiation of the caged peptides at 420 nm.
As observed with the caged amino acids (**Figure 5.1**), uncaging at 420 nm proceeded very rapidly for the DEACM mono-caged tripeptide (**267**), with complete photolysis of KLD-DEACM (**267**) occurring after 4 min, with a rate constant of 1.49 s^{-1} and a quantum yield of 15.8×10^{-4}, accompanied by 93% release of uncaged KLD (**269**) (**Figure 5.4**).
No change in percentage composition was observed for BODIPY-KLD (**268**) following irradiation at 420 nm and no uncaged tripeptide (**269**) was detected (**Figure 5.4**).

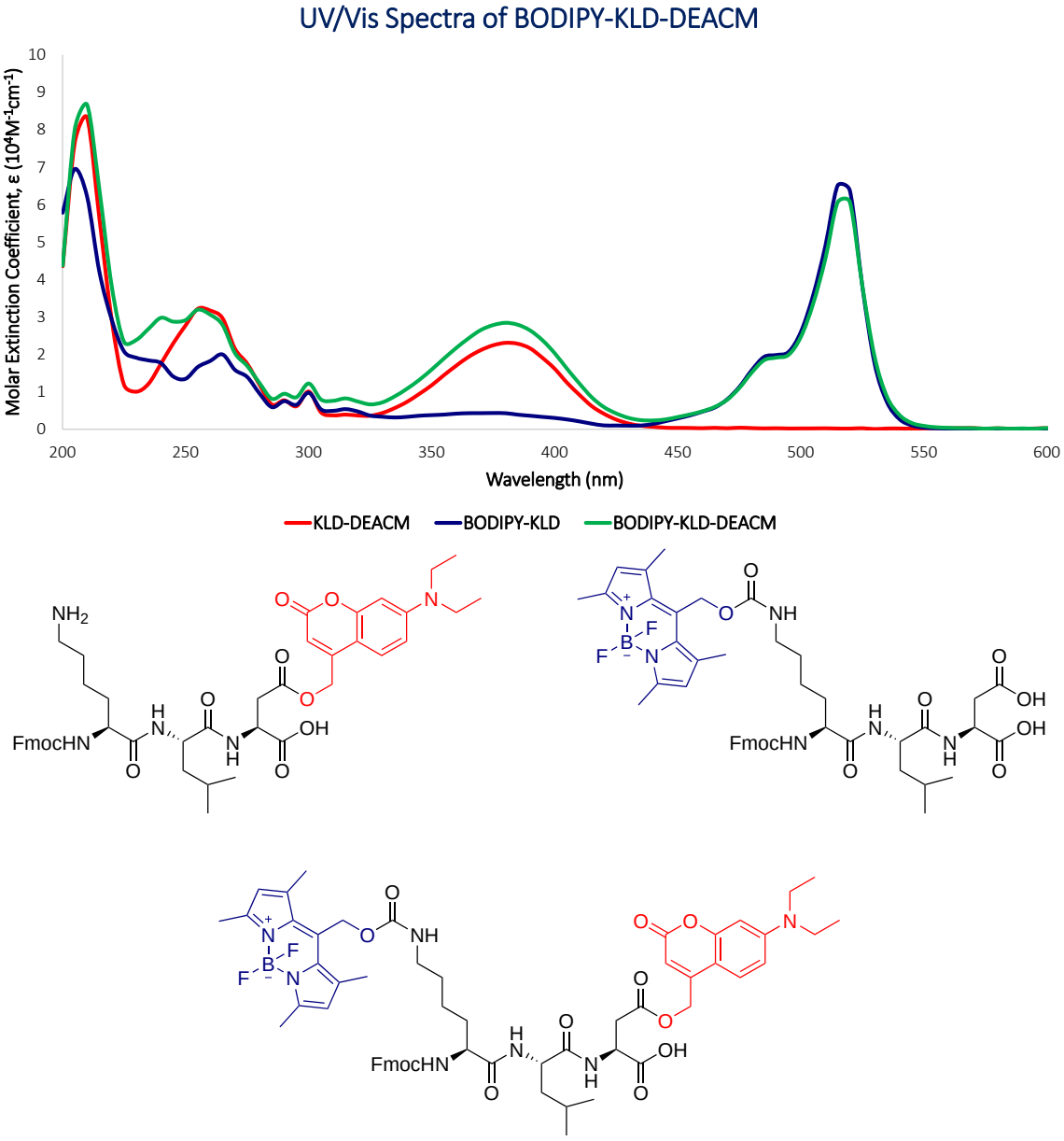
When the dual caged tripeptide (**266**), bearing both the BODIPY- and DEACM-caging groups was subjected to irradiation at 420 nm, in excess of 90% consumption of BODIPY-KLD-DEACM (**266**) was observed with a rate constant of 0.0222 s^{-1} following 2 h of irradiation. This was accompanied by 65% formation of BODIPY-KLD (**268**) with a rate constant of 0.0147 s^{-1}, resulting from photorelease of the DEACM-caging group with a quantum yield of photolysis of 0.0991×10^{-4}. The lower than expected product yield could be due to dark-reactions resulting in delayed on-set of product release. Importantly, no uncaging was observed from photorelease of the BODIPY-group which had been demonstrated to be photostable at this wavelength (**Figure 5.4**).

The increased duration required for photolysis and reduced quantum yield of the dual-caged tripeptide (**266**) relative to the mono-DEACM-caged tripeptide (**267**) was likely due to internal filtering effects arising from competitive absorbance of light at 420 nm by the BODIPY-group.

When irradiated at 530 nm, KLD-DEACM (**267**) showed no change in percentage composition over a 2 h period and no released KLD (**269**) was detected (**Figure 5.5**). In comparison, when BODIPY-caged KLD (**268**) was subjected to irradiation at 530 nm, the percentage composition dropped to 5% following 2 h of irradiation with a rate constant of 0.0248 s^{-1} a quantum yield of 0.315×10^{-4}. This was accompanied by 79% released uncaged tripeptide (**269**) with a rate constant of 0.0259 s^{-1} (**Figure 5.5**). These results are in line with photolysis studies conducted on the caged amino acids (**Figure 5.2**).

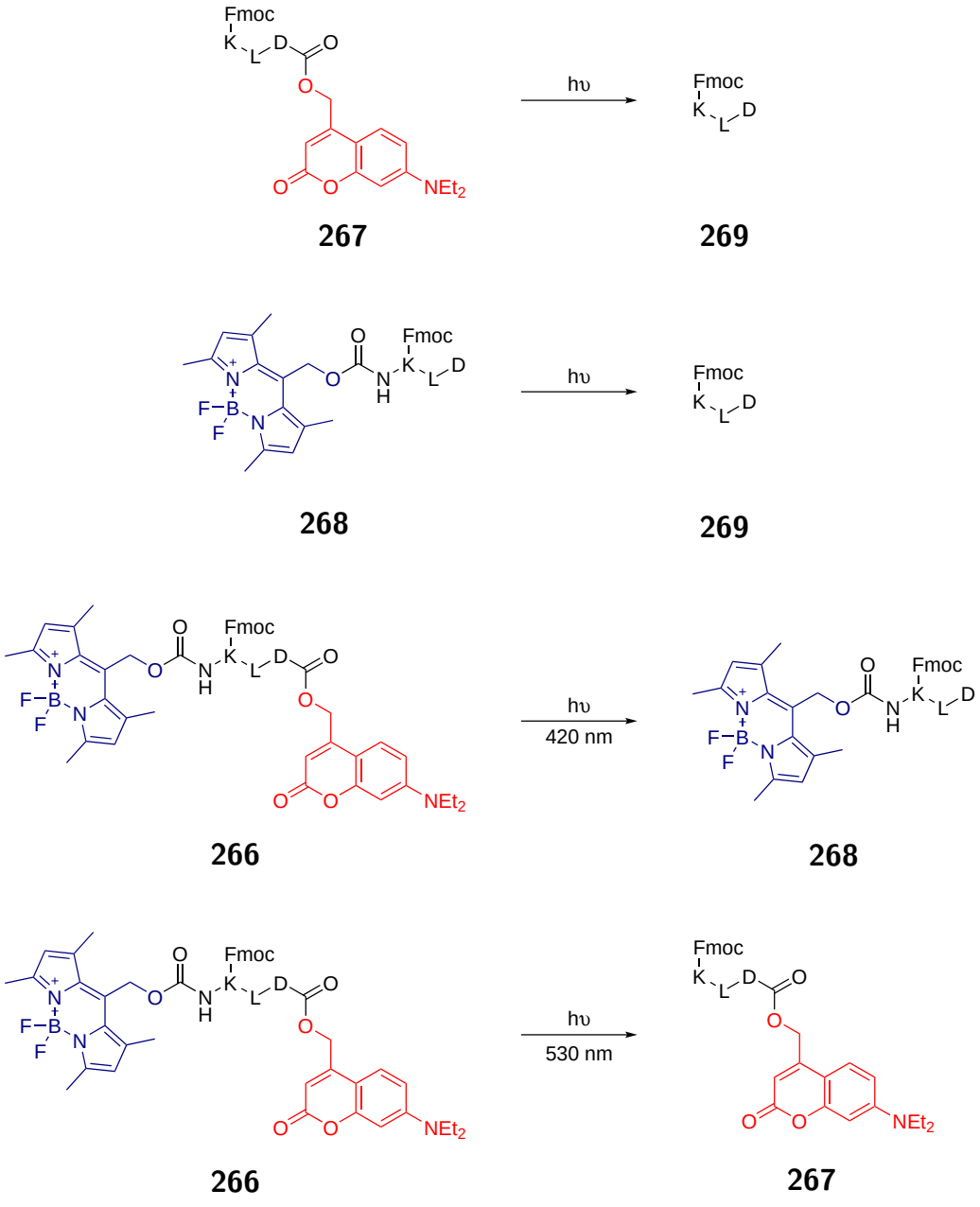
Subjecting the dual-caged tripeptide (**266**) to irradiation at 530 nm led to complete consumption of BODIPY-KLD-DEACM (**266**) after 2 h with a rate constant of 0.0267 s^{-1}, alongside the formation of 78% KLD-DEACM (**267**), resulting from photorelease of the BODIPY-caging group with a quantum yield of 0.388×10^{-4}. No product from photorelease of the DEACM-group was observed.

These results provided further support and evidence for the ability of the DEACM and BODIPY-2 groups to act as a pair of orthogonal caging groups when irradiated at 420 nm and 530 nm to cleave the DEACM and BODIPY-2 groups respectively.

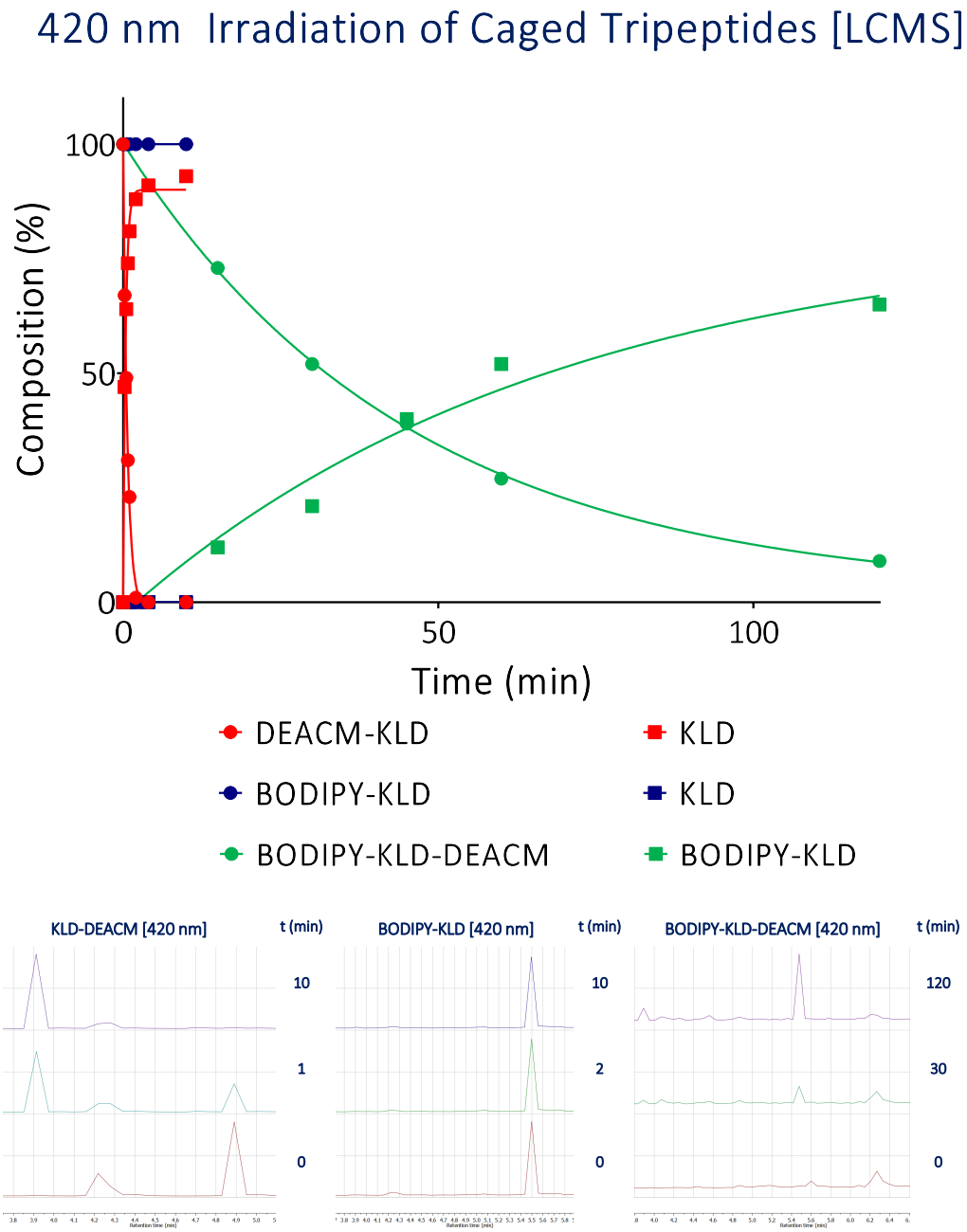


Entry	Conc (mM)	λ_{max} (nm)	Transition	A	ε ($M^{-1}cm^{-1}$)
1	0.004	380	$\pi - \pi^*$	0.0924	23091
2	0.004	515	$\pi - \pi^*$	0.260	65098
3	0.004	380	$\pi - \pi^*$	0.114	28422
		515	$\pi - \pi^*$	0.243	60659

Figure 5.3: UV/Vis absorption spectra of caged tripeptides; Concentration = 4.0 μM [MeOH].

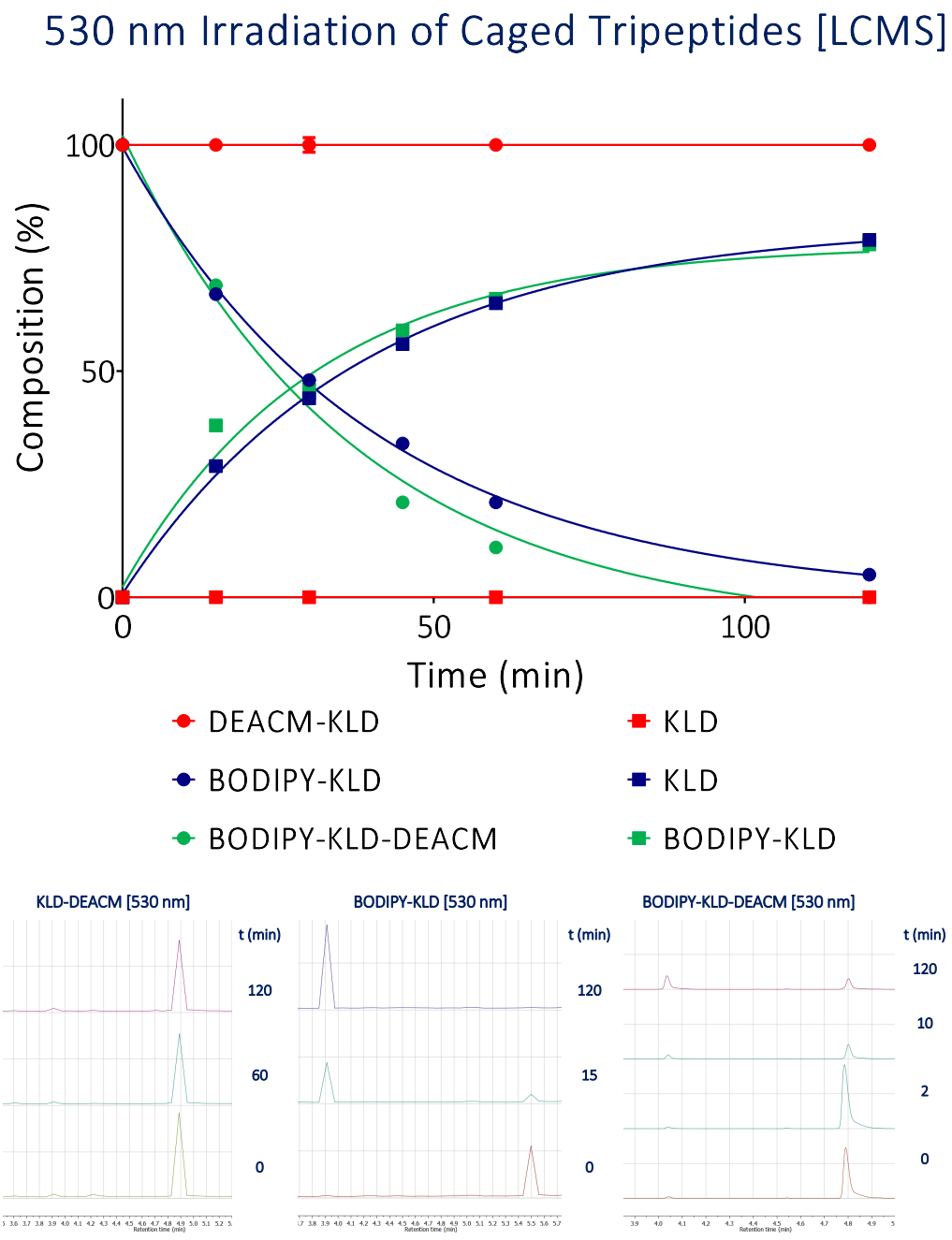


Scheme 5.4: Photolysis of DEACM- and/or BODIPY-caged tripeptides.



Entry	λ_{irrad} (nm)	k_{caged} (s^{-1})	N_{caged}	R^2_{caged}	$k_{uncaged}$ (s^{-1})	$N_{uncaged}$	$R^2_{uncaged}$
1	420	1.49	8	1.00	2.51	8	0.99
2	420	-	-	-	-	-	-
3	420	0.0222	6	1.00	**0.0147**	6	0.97

Figure 5.4: Percentage composition of caged and uncaged tripeptides following irradiation at 420 nm as monitored by LCMS; Concentration = 4.0 μM [MeOH].



Entry	λ_{irrad} (nm)	k_{caged} (s^{-1})	N_{caged}	R^2_{caged}	$k_{uncaged}$ (s^{-1})	$N_{uncaged}$	$R^2_{uncaged}$
1	530	-	-	-	-	-	-
2	530	0.0248	6	1.00	**0.0259**	6	1.0
3	530	0.0267	6	0.99	**0.0321**	6	0.98

Figure 5.5: Percentage composition of caged tripeptides and uncaged tripeptides following irradiation at 530 nm as monitored by LCMS; Concentration = 4.0 μM [MeOH].

5.4.2 Photolysis of Caged Hexapeptides

The UV/vis spectra of the caged hexapeptides were also measured and compared (**Figure 5.6**). The absorbance of BODIPY-KGSTAD-DEACM (**3**) reflected a combination of the absorbance of the individual caging groups, with λ_{max} at 380 nm and 525 nm (**Figure 5.6**).

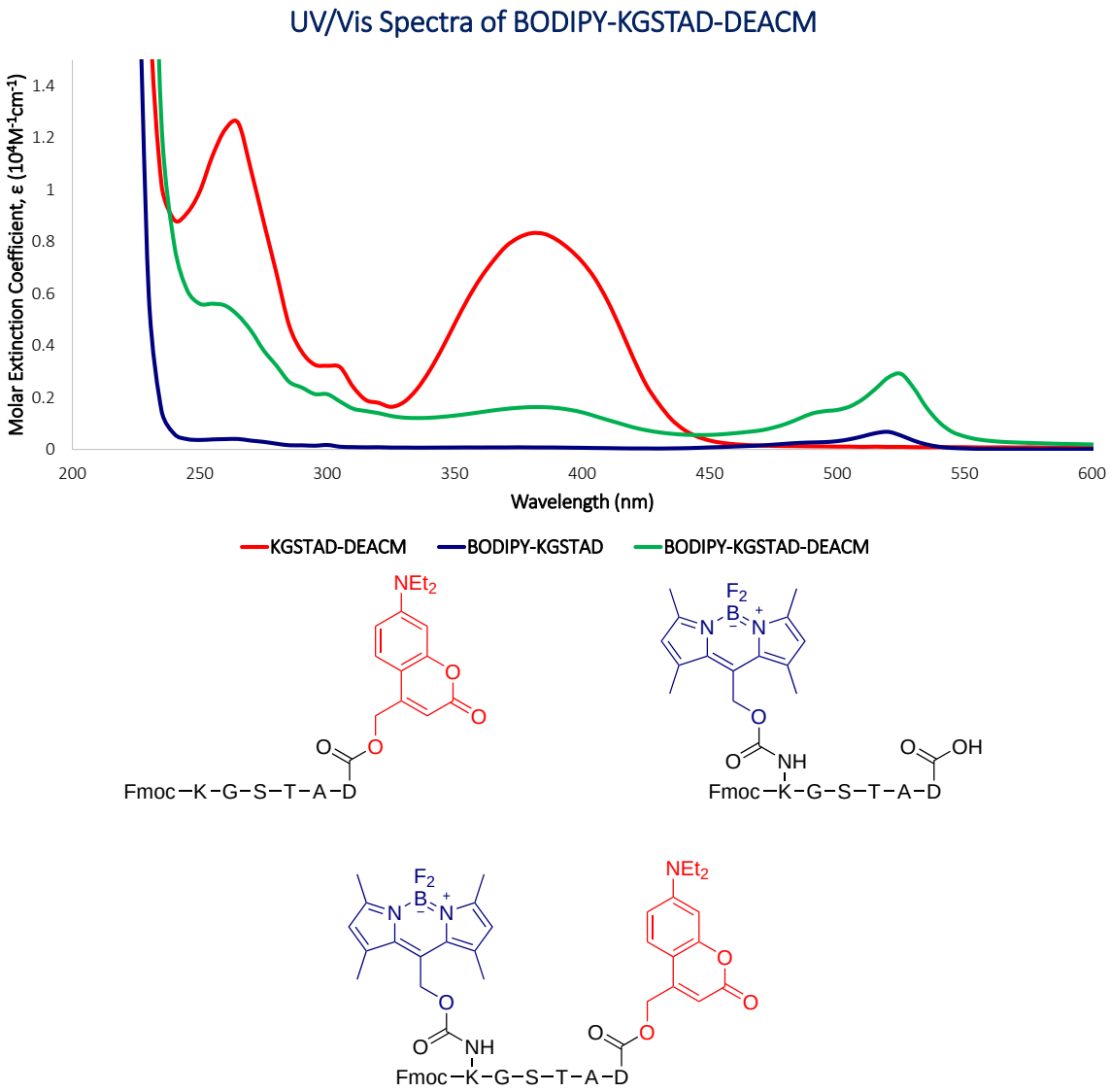
Photolysis reactions were monitored by LCMS-UV, however, issues were encountered with instrument sensitivity and ion-suppression. The data obtained revealed that photolytic trends for uncaging of the hexapeptides matched those observed for the caged amino acids and tripeptides thus, quantitative conversion could be modelled using data trends based on assumptions from prior results obtained.

Photolysis studies for the caged hexapeptide series commenced with irradiation of the caged peptides at 420 nm in an aqueous environment.
As observed with the caged amino acids (**Figure 5.1**) and tripeptides (**Figure 5.4**), uncaging at 420 nm proceeded very rapidly for the DEACM mono-caged hexapeptide (**5**) with a rate constant of 0.819 s^{-1}. Complete photolysis of KGSTAD-DEACM (**5**) occurred within 5 min, with a quantum yield of 8.02×10^{-4}, accompanied by 86% release of uncaged KGSTAD (**270**) (**Figure 5.7**).
No change in percentage composition was observed for BODIPY-KGSTAD (**4**) following irradation at 420 nm and no uncaged hexapeptide (**270**) was detected after 5 min (**Figure 5.7**). However, prolonged irradiation at 420 nm resulted in uncaging of BODIPY-caged KGSTAD, with its composition dropping to 21% after 2 h with a much reduced rate constant of 0.0482 s^{-1} (**Figure 5.7**).
When the dual caged hexapeptide (**3**), bearing both the BODIPY- and DEACM-caging groups was subjected to irradiation at 420 nm, complete consumption of BODIPY-KGSTAD-DEACM (**3**) was observed following 20 min of irradiation with a rate constant of 0.845 s^{-1}. This was the result of uncaging of the DEACM-caging group with the rate constant being in line with that of the mono-caged hexapeptide and with a quantum yield of photolysis of 406×10^{-4}. Importantly, no uncaging was observed from photorelease of the BODIPY-group (**Figure 5.7**). The photolysis was accompanied by a maximum of 74% formation of BODIPY-KGSTAD (**4**); this decreased following prolonged irradiation at 420 nm and was accompanied by release of fully uncaged KGSTAD (**270**).
The increased duration of photolysis required for the dual-caged hexapeptide (**3**) to go to completion relative to the mono-DEACM-caged hexapeptide (**5**) was likely due

to internal filtering effects arising from competitive absorbance of light at 420 nm by the BODIPY-group.

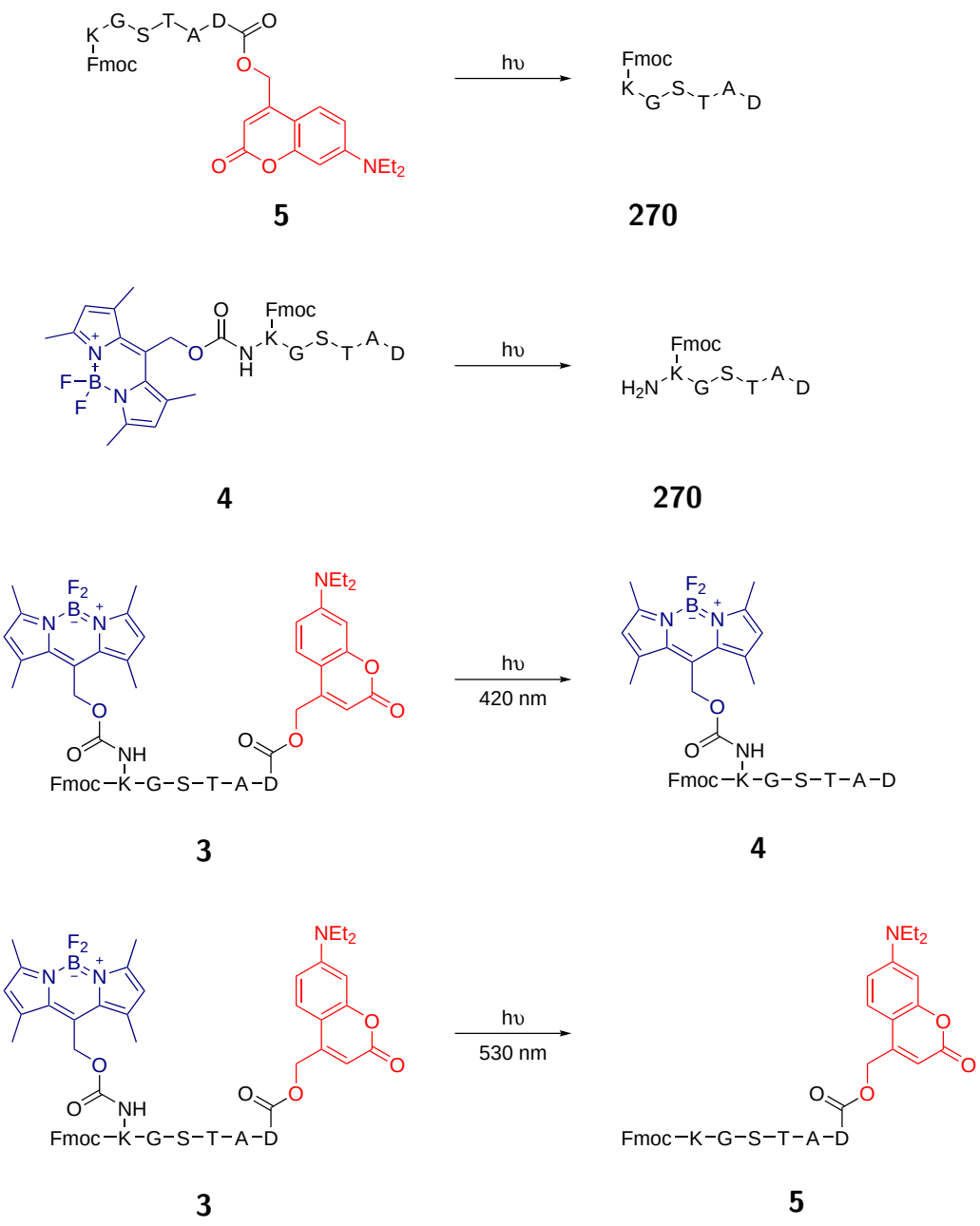
When irradiated at 530 nm, KGSTAD-DEACM (**5**) showed no initial change in percentage composition over the first 5 min with no release of uncaged KGSTAD (**270**). However, prolonged irradiation at 530 nm resulted in cleavage of the DEACM group with a rate constant of 0.00590 s^{-1}, accompanied by release of the uncaged hexapeptide (**270**) (**Figure 5.8**).
On the contrary, when BODIPY-caged KGSTAD (**4**) was subjected to irradiation at 530 nm, the percentage composition dropped to 0% following 30 min of irradiation with a rate constant of 0.518 s^{-1} and a quantum yield of 187×10^{-4}. This was accompanied by in excess of 60% released uncaged hexapeptide (**270**) with a rate constant of 0.558 s^{-1} (**Figure 5.8**). These results are in line with photolysis studies conducted on caged amino acids (**Figure 5.2**) and tripeptides (**Figure 5.5**).
Subjecting the dual-caged hexapeptide (**3**) to irradiation at 530 nm led to complete consumption of BODIPY-KGSTAD-DEACM (**3**) after 20 min with a rate constant of 0.629 s^{-1}, alongside the formation of nearly 60% KGSTAD-DEACM (**5**), resulting from photorelease of the BODIPY-caging group with a quantum yield of 82.2×10^{-4}. No product from photorelease of the DEACM-group was observed (**Figure 5.8**). However, continued irradiation at 530 nm resulted in photolysis of the DEACM-KGSTAD product leading to formation of the fully uncaged hexapeptide (**270**).

These results further support the ability of the DEACM and BODIPY-2 groups to act as a pair of orthogonal caging groups when irradiated at 420 and 530 nm to cleave the DEACM and BODIPY-2 groups respectively. In addition, the similarities in photolytic data trends indicate little to no interactions between the two caging groups and that they act independently of one another. However, the possibility of peptide sequence dependency may exist and should not be ignored when selecting caging groups to be employed.



Entry	Conc (mM)	λ_{max} (nm)	Transition	A	ε ($M^{-1}cm^{-1}$)
1	0.1	380	π – π*	0.834	8326
2	0.1	520	π – π*	0.0681	681
3	0.1	380	π – π*	0.163	1629
		525	π – π*	0.291	2911

Figure 5.6: UV/Vis absorption spectra of caged hexapeptides; Concentration = 0.1 mM [H_2O].



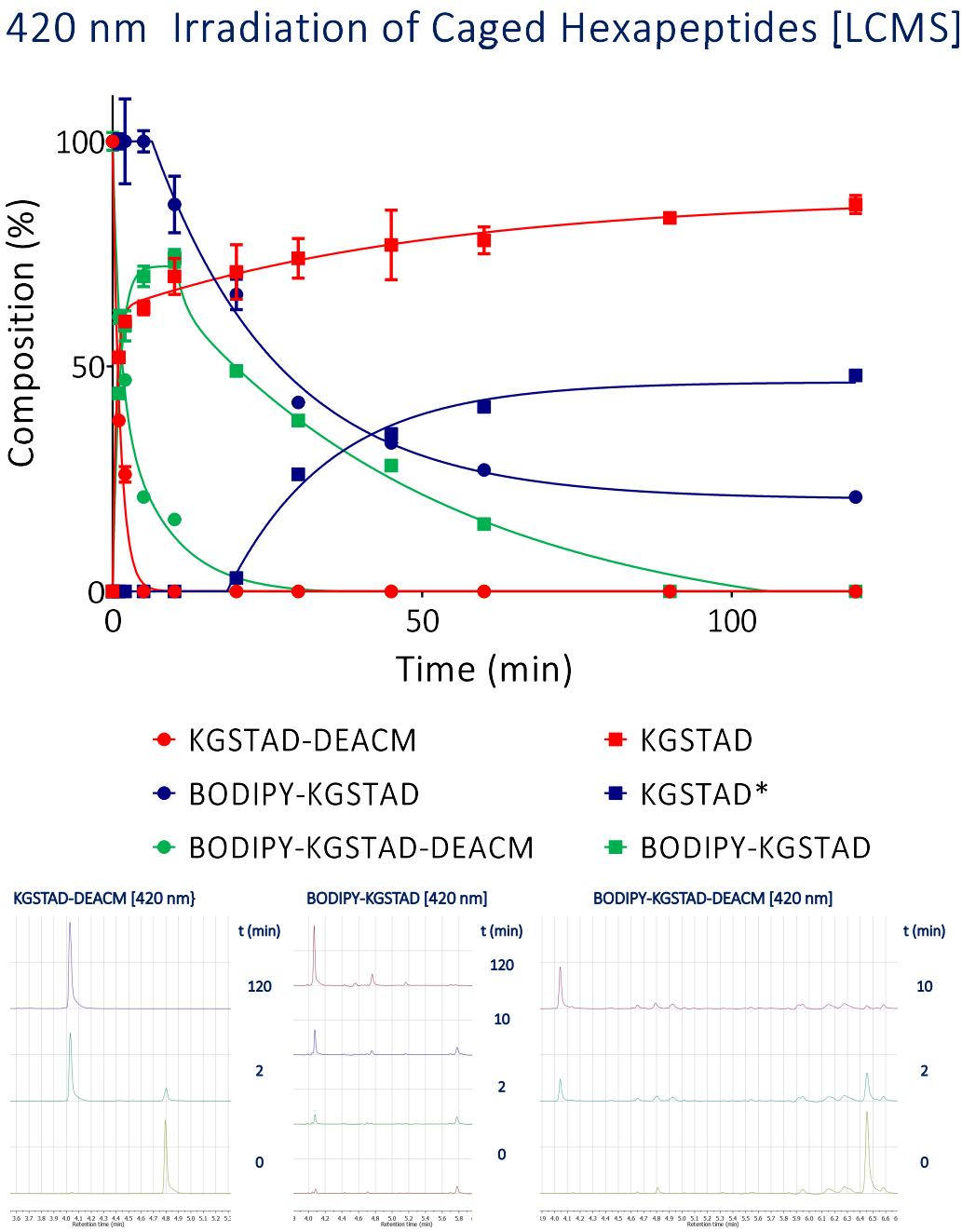
5 **270**

4 **270**

3 **4**

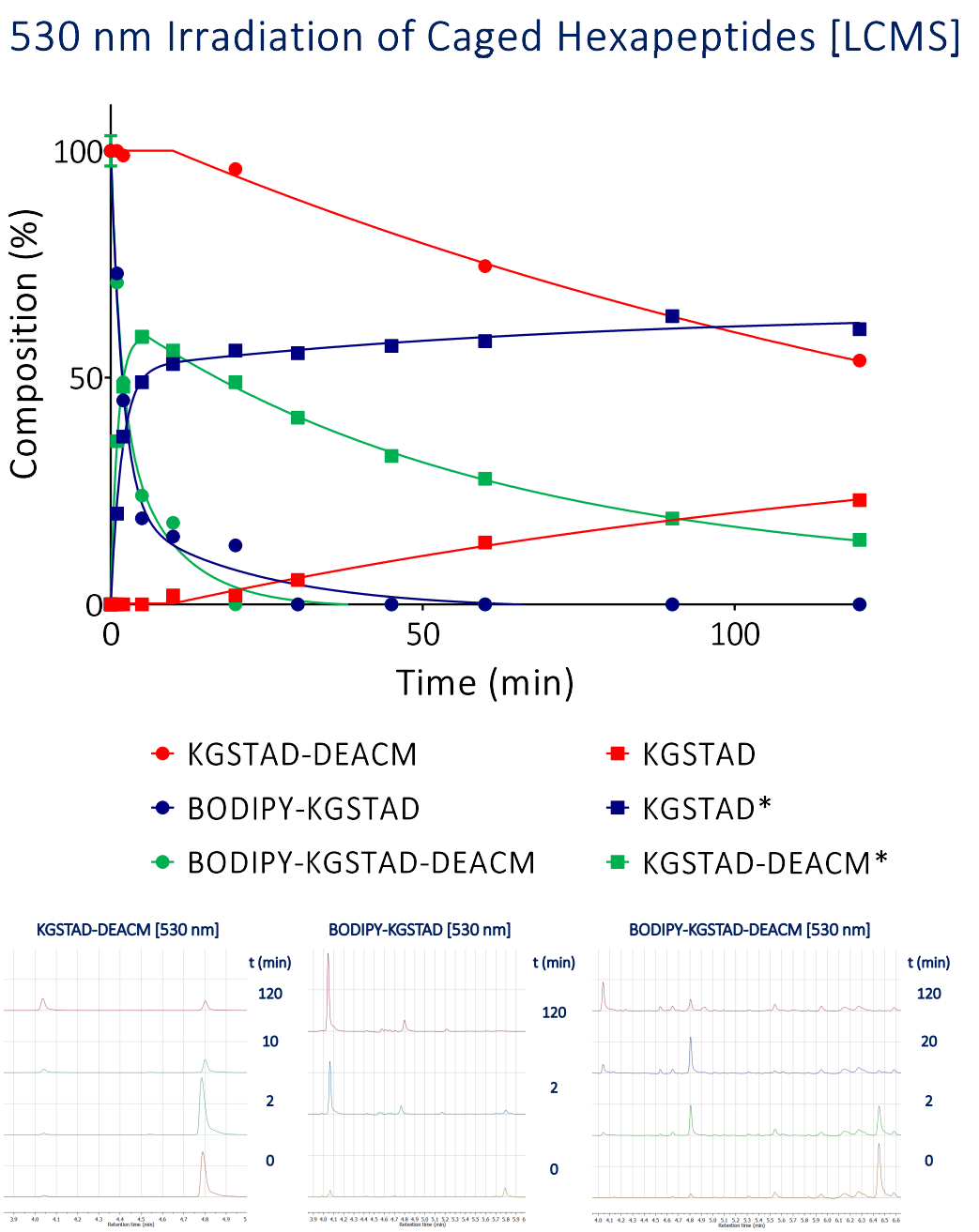
3 **5**

Scheme 5.5: Photolysis of DEACM- and/or BODIPY-caged hexapeptides.



Entry	λ_{irrad} (nm)	k_{caged} (s^{-1})	N_{caged}	R^2_{caged}	$k_{uncaged}$ (s^{-1})	$N_{uncaged}$	$R^2_{uncaged}$	$K_{uncaged'}$ (s^{-1})	$N_{uncaged'}$	$R^2_{uncaged'}$
1	420	0.819	11	0.99	1.21	11	1.00	-	-	-
2	420	0.0482	10	1.00	0.0594	10	0.99	-	-	-
3	420	0.845	11	1.00	0.894	11	1.00	0.0103	11	0.99

Figure 5.7: Percentage composition of caged and uncaged hexapeptides following irradiation at 420 nm as monitored by LCMS [c 0.1 mM in H_2O] [* denotes quantification by modelling].



Entry	λ_{irrad} (nm)	k_{caged} (s^{-1})	N_{caged}	R^2_{caged}	$k_{uncaged}$ (s^{-1})	$N_{uncaged}$	$R^2_{uncaged}$	$K_{uncaged'}$ (s^{-1})	$N_{uncaged'}$	$R^2_{uncaged'}$
1	530	0.00590	11	1.00	0.00718	11	0.99	-	-	-
2	530	0.518	11	0.99	0.558	11	0.99	-	-	-
3	530	0.620	11	1.00	0.893	11	1.00	0.0170	11	1.00

Figure 5.8: Percentage composition of caged and uncaged hexapeptides following irradiation at 530 nm as monitored by LCMS [c 0.1 mM in H_2O] [* denotes quantification by modelling].

5.5 Biochemical Studies on Caged Peptides

Proteolysis involves the breakdown of proteins into smaller polypeptides or amino acids. This process, catalysed by proteases through hydrolysis of peptide bonds, represents an irreversible and ubiquitous post-translational modification that can result in activation, inactivation or completely altered protein function.[197] Proteolysis is thus involved in the regulation of a vast array of biological processes, ranging from DNA replication and cell cycle progression to pathological processes such as inflammation, cancer and cardiovascular diseases.[197]

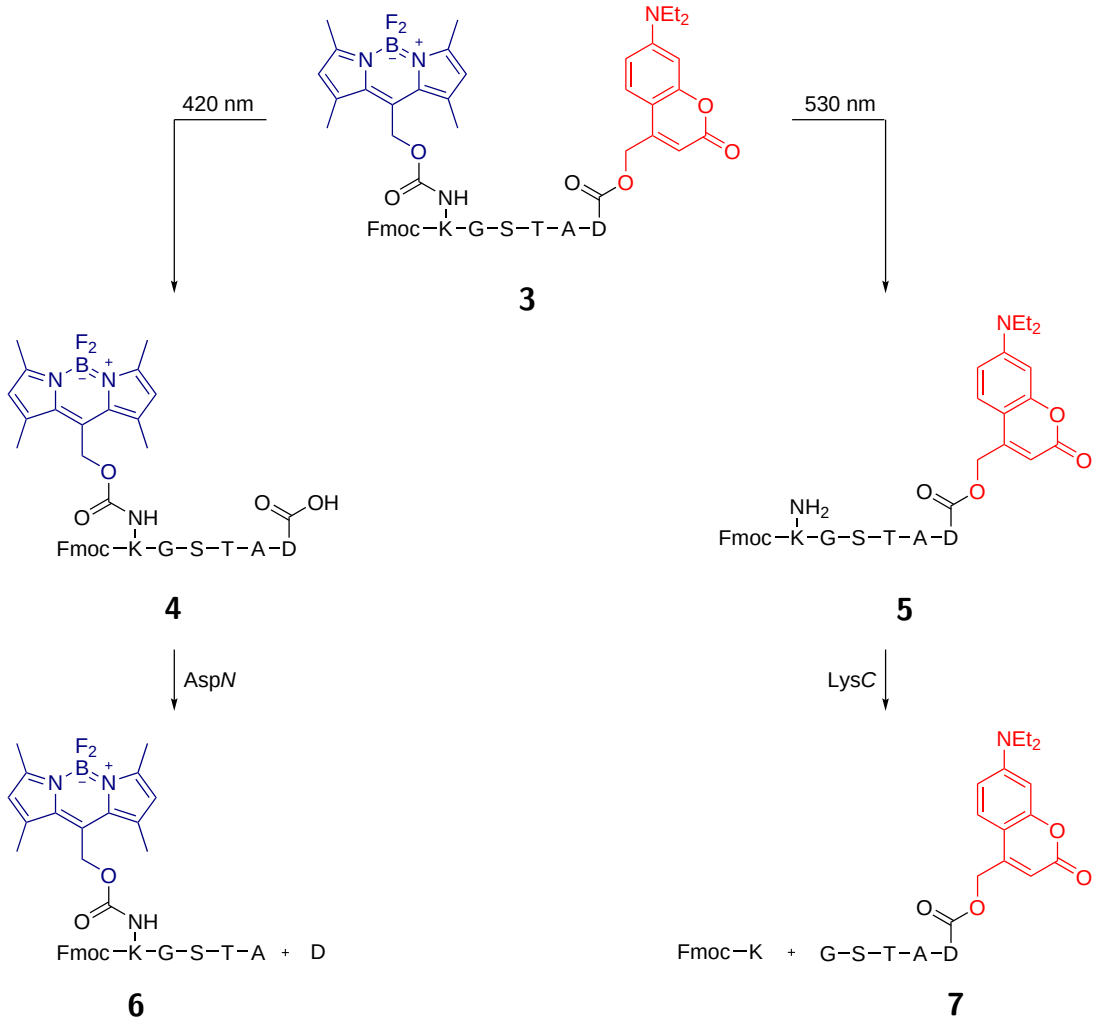
Proteases constitute one of the largest families of enzymes in humans where more than half have no known substrates.[198] Owing to the extensive part it plays in biological processes, proteolysis forms an important sub-field for the study of protein PTMs. Full comprehension of the cellular functions of proteases requires not only knowledge of the proteins processes but also the function of the substrates and the specific processing events.[199]

Current methods for the study of proteases involves degradomics, the application of high-throughput approaches on a system-wide scale. However, this method is inherently restricted to single peptide identifications and has largely focussed on large-scale identification of cleavage sites and PTMs;[197] targeted analyses remain challenging. This presents an opportunity for the use of caging groups as this would enable study of proteolytic events with enhanced spatial and temporal control. Moreover, the application of an orthogonal pair of caging groups would allow for more than one peptide or cleavage site to be simultaneously probed.

As a proof of principle, two proteases, Asp-*N* and Lys-*C* were employed and incubated with the caged hexapeptides prior to and following irradiation at 420 nm and 530 nm. Asp-*N* is a metalloprotease which preferentially cleaves peptides and proteins at the *N*-terminus of aspartic and cysteic acid residues with high specificity,[200] whilst Lys-*C* is a serine protease with high specificity for cleavage at the *C*-terminus of lysine residues.[201]
Both enzymes are commercially available and were incubated with the peptide samples at 37 °C.

When caged, the hexapeptides were shown not to undergo peptidolysis at their site specific residues following incubation with the enzymes, i.e. when the aspartic acid

residue was caged with DEACM (**3**), (**5**), incubation with Asp-*N* did not result in peptidolysis at the *N*-terminus of aspartic acid. Similarly, when the lysyl residue was caged with BODIPY-2 (**3**), (**4**), incubation with Lys-*C* did not lead to cleavage at the *C*-terminus of the lysyl residues. However, when these residues were not caged, the peptides were free to undergo peptidolysis with their corresponding proteases.



Scheme 5.6: Peptidolysis of hexapeptides following irradiation at 420 and 530 nm.

Prior to and following photolysis in aqueous conditions at 420 nm and 530 nm for 5 min, BODIPY-KGSTAD-DEACM (**3**) was incubated with Asp-*N* and Lys-*C* and the samples analysed for peptidolysis by mass spectrometry. It was revealed by mass spectrometry that prior to photolysis, the fully caged hexapeptide (**3**) did not undergo proteolysis with either protease. Following irradiation at 420 nm, the DEACM group was uncaged to reveal the free aspartic acid residue, whist the lysyl residue remained caged by the BODIPY-2 group. Incubation with Asp-*N*, led to peptidolysis at the

N-terminus of the aspartic acid residue whilst incubation with Lys-*C* led to no peptide cleavage. Irradiation at 530 nm resulted in photolysis of the BODIPY-2 group to reveal the free lysine residue whilst the aspartic acid residue remained protected by the DEACM caging group. Incubation with Asp-*N* led to no cleavage at the aspartic acid residue whilst incubation with Lys-*C* resulted in peptidolysis at the *C*-terminus of the lysyl residue (**Scheme 5.6**).

This *in vitro* biological application demonstrates the ability to control and hence study biological processes with enhanced spatial and temporal control through the use of photolabile caging groups and provides further evidence for the development and applicability of this pair of photolabile caging groups for the study of protein PTMs.

5.6 Summary and Future Work

A pair of orthogonal photolabile caging groups, employing the DEACM and BODIPY-2 group, was developed. The ability to incorporate these caging groups into peptides was demonstrated through the use of solid phase peptide synthesis and uncaging of these peptides was undertaken and quantified in a tripeptide and hexapeptide series. These studies provided conclusive evidence for the orthogonal nature of this pair of caging groups. It is valuable to note though, that a sequence dependent nature may exist when applying caging groups to more complex peptides and proteins.

Lastly, an *in vitro* biological application was demonstrated involving the use of two proteases, Asp-*N* and Lys-*C*. These peptides were shown to be stable to peptidolysis when caged at the aspartic acid and lysine residues, respectively. However, following photolysis at 420 nm or 530 nm to reveal the free uncaged aspartic acid and lysine residues, respectively, peptidolysis was able to proceed with the corresponding proteases. This study highlighted the applicability of this orthogonal pair of caging groups for potential use in the study of protein PTMs.

Chapter 6

Conclusions & Future Work

The work in this dissertation has been aimed at contributing to the relevance of PCGs and expanding its scope through development of the first pair of chromatically orthogonal caging groups capable of undergoing photolysis above 300 nm, in addition to extending the applications of PCGs to biologically relevant problems.
Two distinct biological systems formed the basis from which to develop the proficiency of PCGs as tools to offer greater insights into and enhance our understanding of biological systems - (i) KefC KTN-domain; (ii) protein post-translational modifications (PTMs).

6.1 Caged Kef Ligands as Tools to Probe Binding within the KefC KTN Domain

The first system targeted was the bacterial K^+ efflux system, Kef, which protects bacteria against the detrimental effects of electrophilic stress *via* acidification of the cytoplasm. It was hypothesised that use of the DMNB caging group attached to the endogenous agonist, GSH, and antagonist, ESG, of the receptor would provide conclusive evidence for the binding mode in the pocket. The carboxylic acid moiety of the terminal glycine residue of the tripeptide was thought to be imperative to binding of these molecules in the KefC KTN-domain. Validation for the hypothesis would come in the form of inhibition of binding to the KefC KTN-domain due to the presence of the DMNB caging group at this position. Following irradiation to photolyse the DMNB group and liberate the free uncaged GSH and ESG molecules, activity would be restored.

To this end, DMNB-caged GSH (**1**) and ESG (**2**) were synthesised (**Figure 6.1**)

with the DMNB group was attached, through an ester linkage, to the α-carboxy acid terminus of the glycine residue of GSH and ESG.

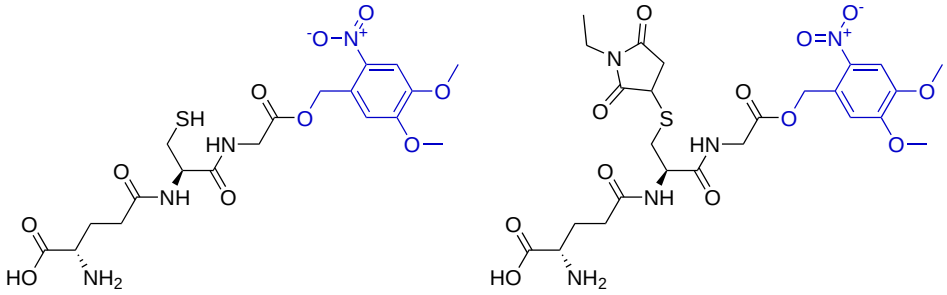
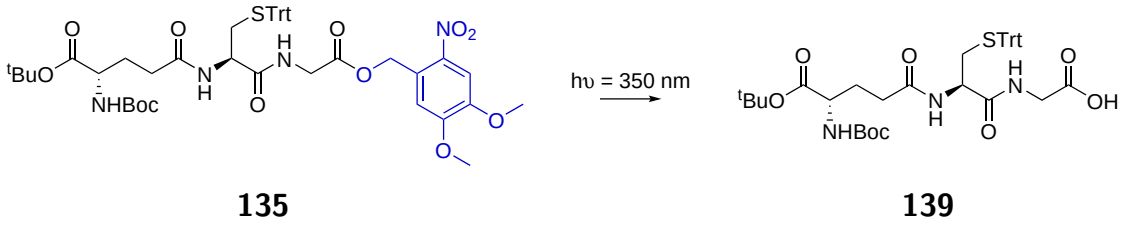


Figure 6.1: DMNB-caged GSH and ESG to probe the binding mode within the KefC KTN binding domain.

Photolysis studies were performed on the fully protected DMNB-caged GSH precursor (**135**) and monitored by **^{1}H NMR** and mass spectrometry. The DMNB-caging group was cleaved upon irradiation at 350 nm to reveal the uncaged GSH protected compound (**139**) (**Scheme 6.1**); 8 h of exposure to irradiation at 350 nm led to 82% decrease in the percentage composition of the DMNB-caged GSH precursor (**135**), accompanied by 80% release of the uncaged tripeptide (**139**).



Scheme 6.1: Photolysis of DMNB-caged protected GSH (**135**) following irradiation at 350 nm.

DMNB-caged GSH (**1**) and ESG (**2**) are currently with collaborators awaiting biological testing.

The caged compounds need to be tested *in vitro* for binding to the protein in order to access background activity whilst photolysis studies have to be performed and the uncaged species shown to bind to the protein. To improve cell permeability, the DMNB-caged derivatives of GSH (**1**) and ESG (**2**) will have to be esterified. The photolysis reactions will then be conducted in E. *coli*. It must be ensured that the photolysis by-products do not interfere with the Kef system or show toxicity in E. *coli*. By monitoring the photolysis reactions and observing binding of the released GSH

and ESG compounds, conclusive proof for the binding mode through the α-carboxylic acid of the glycine residue can be ascertained.

6.2 Caged Amino Acids & Peptides Towards the Development of Photoactive Tools to Probe Protein PTMs

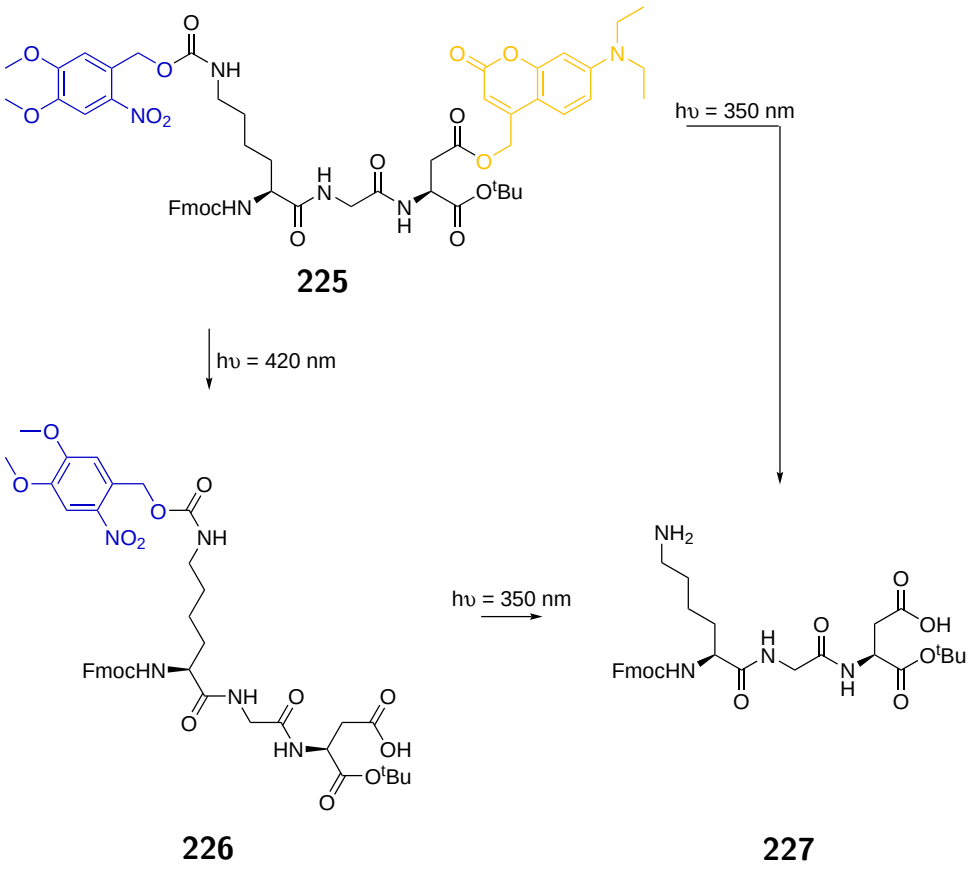
The second biological system explored was that of protein post-translational modification (PTM); biological processes that impart complexity to the genome through a series of covalent modifications, usually at the side chain functional group termini of amino acid residues. PTMs are vital for the regulation of the cellular environment and have been linked to cancer, neurodegenerative, and cardiovascular diseases. Despite much work carried out to better identify PTMs, current techniques lack the spatial and temporal control necessary to gain deeper level understanding of the processes involved.
It was hypothesised that use of a pair of chromatically orthogonal caging groups would provide an invaluable tool that could be used to gain additional insights into the complex workings of PTMs. The benefit of this would be the ability to probe two amino acids, using light, simultaneously and independently of one another.

Commencing this study, a series of amino acids, including aspartic acid, glutamic acid, serine, lysine, and tyrosine, were caged with pHP, MPH, DMNB, DEACM, DEATC, BODIPY-1 and BODIPY-2 caging groups.

Photolysis studies were performed on the caged amino acids, irradiating with light at wavelengths of 530 nm, 520 nm, 420 nm, 365 nm, 350 nm, and 310 nm and monitored by HPLC, LCMS-UV, **^{1}H NMR** and mass spectrometry analysis.

The DMNB and DEACM caging groups were shown to be a wavelength selective pair capable of undergoing unidirectional sequential uncaging when irradiating at 420 nm to cleave the DEACM group, followed by 350 nm to cleave the DMNB group.
Irradiation at 350 nm resulted in non-selective simultaneous cleavage of both groups. This approach was further demonstrated in a tripeptide bearing both caging groups. The results of irradiation at 420 nm and 350 nm reflected those observed for the caged amino acids. Subjecting the dual-caged tripeptide to irradiation at 420 nm led to

uncaging of the DEACM group whilst leaving the DMNB group in tact. Irradiation at 350 nm then led to uncaging of the DMNB group. When the dual caged tripeptide was subjected to irradiation at 350 nm, both caging groups underwent simultaneous photolysis with little to no selectivity.

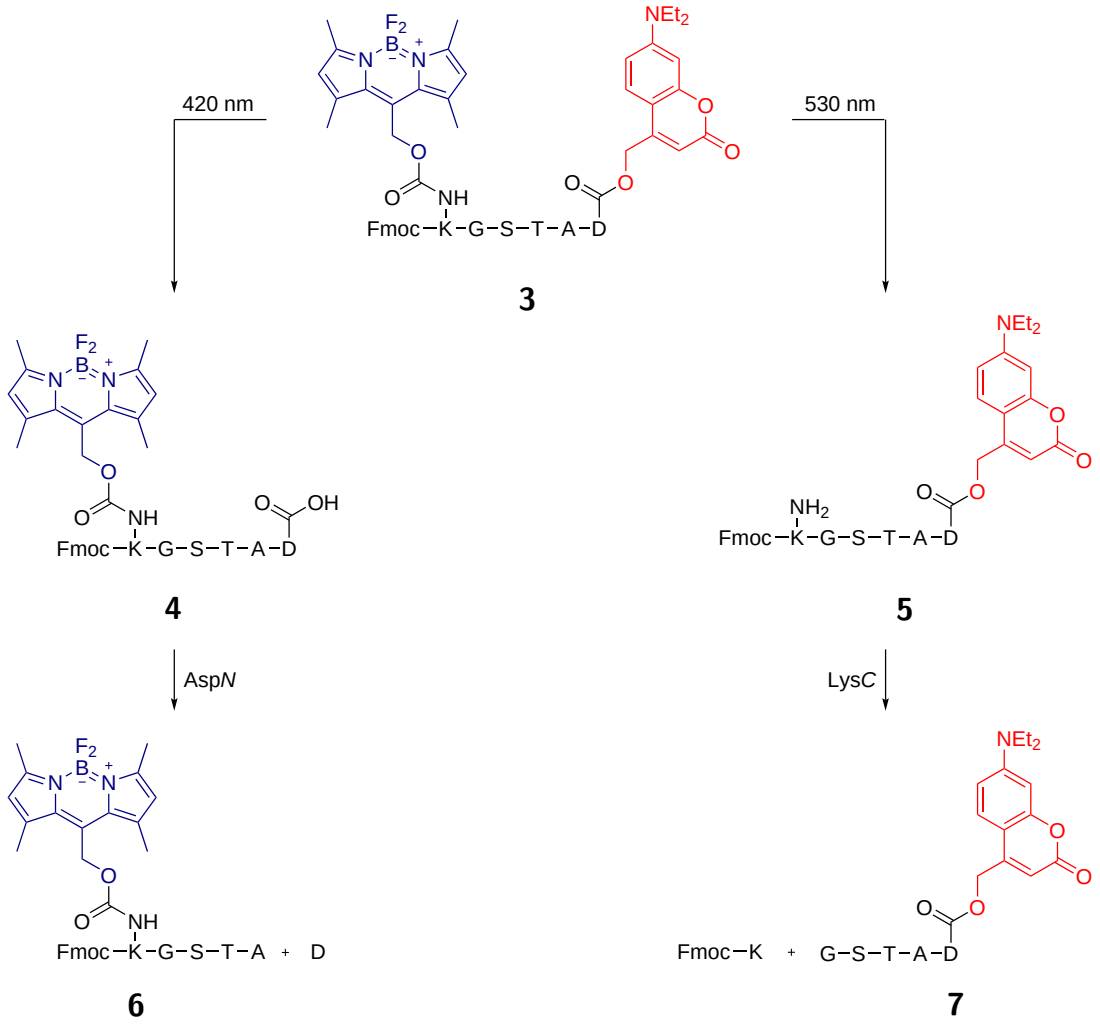


Scheme 6.2: Irradiation of wavelength selectively caged tripeptide bearing the DEACM and DMNB caging groups.

This provided further evidence that the DEACM and DMNB caging groups were capable of acting as a sequential wavelength selective pair of caging groups with the potential to be applied to peptides and proteins for the study of protein PTMs where only unidirectional control is required.

The combination of the DEACM and BODIPY-2 caging groups allowed an orthogonal pair to be established when irradiating at 530 nm to selectively cleave the BODIPY-2 caging group and at 420 nm to selectively cleave the DEACM caging group. The use of these two caging groups circumvented the limitation of the order in which the wavelengths of light had to be applied i.e. either caging group could be selectively removed in the presence of the other. This approach was demonstrated using caged

amino acids and further extended to a tripeptide and hexapeptide series. The photolysis reactions were monitored by LCMS-UV and calibration experiments were performed to allow for quantification of the degree of photolysis and to establish the yields of photoreleased products.



Scheme 6.3: Peptidolysis of hexapeptide following irradiation at 420 and 530 nm.

Having demonstrated the ability of the two caging groups to act as an orthogonal pair, the caged hexapeptide were subjected to incubation with two proteases, Asp-*N* and Lys-*C*, prior to and following irradiation at 530 nm and 420 nm in an aqueous environment (**Scheme 6.3**), and the samples analysed by mass spectrometry, to demonstrate their applicability to the study of protein PTMs.
Asp-*N* shows high specificity for cleavage at the *N*-terminus of aspartic acid residues whilst Lys-*C* shows high specificity for cleavage at the *C*-terminus of lysine residues.

Prior to irradiation, the caged peptides were shown to be stable to proteolysis. Following irradiation at 420 nm to reveal the free aspartic acid residue (**4**), incubation with Asp-*N* led to peptidolysis at the *N*-terminus of the aspartic acid residue but incubation with Lys-*C* resulted in no peptidolysis. Irradiation at 530 nm resulted in photolysis of the BODIPY-2 group to reveal the free lysine residue (**5**). Incubation with Asp-*N* resulted in no peptidolysis whilst incubation with Lys-*C* resulted in cleavage at the *C*-terminus of the lysine residue (**Scheme 6.3**).

This pair of caging groups, consisting of DEACM and BODIPY-2, presents the first example where orthogonality has been achieved using a pair of caging groups where both could be cleaved at wavelengths longer than 400 nm in both organic and aqueous media, thus allowing its applicability to extend to both classical organic synthesis and the study of biological systems.

To further build upon this project, several avenues could be explored.
Additional photolysis studies with the current wavelength orthogonal pair of the DEACM and BODIPY-2 caging groups could be conducted to investigate the effects of different aqueous solvents and buffers on photolysis rates as well as potential concentration and temperature dependence. Additionally, peptides with thiol groups e.g. cysteine could be caged and photolysis studies undertaken with these as cysteine residues commonly undergo PTMs e.g. disulfide bridge formation.

Another area could involve synthesis of other variants of the BODIPY-2 caging groups to improve photolytic properties as well as enhance the stability of this group to acidic and basic conditions to ease peptide synthesis by SPPS and its incorporation into peptides and proteins. This could be achieved through substituent modifications to increase the stability of the boron centre and inhibit deboronation reactions in the presence of acidic or basic conditions. It would have to be ensured that modifications to the BODIPY-2 structure did not adversely affect the photolytic properties of the compound but instead added to it e.g. by increasing quantum efficiency or red-shifting the absorption maximum.

Alternatively, other novel and red-shifted caging groups, such as the RuBpy, fluorescein, pyronin or rhodamine based PCGs could be explored to design new wavelength orthogonal pairs to improve selectivity of uncaging and red-shift the absorption maxima to allow uncaging to be conducted with light of longer wavelengths. A possible route to designing new PCGs could also be through rational computational based design,

exploiting currently available data and relating structure and activity of PCGs to their energetics, absorbance, and mechanism of uncaging. This could then be used to model novel PCGs which could lead to new hits.

Another area could involve incorporation of the caging groups into longer functional peptides, such as histone tails, and/or proteins, such as enzymes and antibodies. The use of PCGs would enable defined functions of specific peptides and proteins to be rapidly and specifically activated inside living cells and organisms thereby facilitating the study of resulting adaptive changes. Several key peptides and proteins could be targeted, including and not limited to:

(i) Proteases, enzymes which play a pivotal role in the bioregulation of healthy and disease states due to their propensity to extensively catalyse post-translational modifications and the presence of endogenous inhibitors. Spatio-temporal activity-based measurements could provide valuable insights into the diverse and important roles proteases play in physiology and disease, including influencing critical processes in development, immune responses, and malignancies. Both the abundance and activity of these enzymes are tightly regulated and highly contextual; the use of PCGs would give rise to precise control of both the location and time of activity-based sensing, enabling elucidation of specific impacts on disease progression, through precise monitoring of *in situ* protease activity.

(ii) Cyclic or conformationally constrained peptides represent an important class of bioactive molecules with the ability to act as peptidic lead compounds or research tools. Due to their rigidity, these privileged structures for inhibitor design are able to compensate for the energetic loss of the entropic contribution when binding to a protein target. Their large size and protein-like structure make them particularly promising candidates for the inhibition of protein–protein interactions. The incorporation of PCGs would enable activity of these peptides to be probed in living cells in order to gain insight into the mode of action and lead to identification of new bioactive molecules.

(iii) Photocaged antibodies and/or photoactivatable protein antigens for biophysical and cellular studies could shed light on fundamental aspects of B-cell responses, including antibody discrimination, antibody memory immunity and even B-cell tumourigenesis. Use of PCGs would evoke induction of activity with spatial and temporal control, enabling the study and light controlled manipulation of antigen-antibody

interactions to probe targets and the mode of action. Orthogonal caging groups emerge as promising molecular tools to unravel the complex and dynamic events of B-cell activation by giving rise to simultaneous control of both the photocaged antibody and target.

Photocaged peptides and proteins are typically derived by masking the critical functionality for enzyme activity, protein–protein interaction or peptide backbones.
One method by which this could be achieved is through the use of four base codons or the more commonly used amber stop codon method.[202] Possible issues of biocompatibility may have to be addressed; these could include assessing the protein to ensure that the caging groups do not interfere with the folding of the protein, solubility of the resulting protein and that the photolysis by-products do not interfere with the PTM processes being analysed, damage the protein or are toxic to the systems being analysed.

In closing, photolabile caging groups possess the potential to be applied in a wide array of settings, ranging from total synthesis to photoresists and tools to probe biological mechanisms. The development of a pair of orthogonal photolabile caging groups, employing the DEACM and BODIPY-2 groups, serves to add to the utility of this umbrella of compounds through increasing the spatial and temporal control imparted to the experimenter and enabling the study of more complex systems with simultaneously occurring convoluted processes. Furthermore, the ability to use wavelengths longer than 300 nm to selectively cleave the DEACM and BODIPY-2 caging groups, in addition to their ability to act as dyes, increases their applicability in biological settings by reducing the likelihood of imparting photodamage and allowing convenient visualisation of the compounds when caged.

This pair of caging groups presents the first example of a pair of wavelength orthogonal caging groups with possible applications in both organic synthesis and biological systems that can be cleaved using light of wavelengths greater than 400 nm in a sequence independent manner.

Chapter 7

Experimental

Experimental methods have been included in this chapter in the sections below. Experimental results have been included in Appendices. See:
Appendix A - NMR Spectra
Appendix B - Photolysis Experimental Data
Appendix C - Photolysis LCMS-UV Curves
Appendix D - Enzyme Proteolysis Mass Spectrometry Data.

7.1 General Experimental

^{1}H NMR Spectra: Proton (**^{1}H NMR**) spectra were recorded at 298 K on a Bruker DQX-400 (400 MHz) or Bruker DPX-400 (400 MHz) spectrometer. Proton (δH) chemical shifts are quoted in ppm and referenced to tetramethylsilane ($\delta = 0$ ppm) with residual protonated solvent as a reference for internal deuterium lock. The number of protons (η) for a given resonance signal is indicated by ηH. Assignments were made on the basis of chemical shift, coupling constants, COSY and HSQC data and comparison with spectra of related compounds. Resonances are described as s (singlet), d (doublet), t (triplet), q (quartet), qn (quintet), sx (sextet), sp (septet), m (multiplet), dd (doublet of doublets) and so on. Coupling constants (J) are given in Hz and are rounded to the nearest 0.1 Hz. Values for identical coupling constants are averaged and were determined by analysis using Advanced Chemical Developments Spectrus software.

^{13}C NMR Spectra: Carbon (**^{13}C NMR**) spectra were recorded at 298 K on a Bruker DQX-400 (100 MHz) or Bruker DPX-400 (100 MHz) spectrometer. Carbon

(δC) chemical shifts are quoted in ppm and referenced to tetramethylsilane ($\delta = 0$ ppm) with residual protonated solvent as a reference for internal deuterium lock. Assignments were made on the basis of chemical shift, coupling constants, COSY and HSQC data and comparison with spectra of related compounds.

^{19}F NMR Spectra: Fluorine (**^{19}F NMR**) spectra were recorded at 298 K on a Bruker DQX-400 (376 MHz) or a Bruker AVII 500 (470 MHz) using a broadband proton decoupling pulse sequence and deuterium internal lock. The chemical shift data for each signal are given as δFin units of parts per million (ppm).

Mass Spectra: Low resolution mass spectra were recorded on a Fisons Platform spectrometer (ESI). *m/z* values are reported in Daltons, followed by their percentage abundance in parentheses and where known, the relevant fragment ion in parentheses. High resolution mass spectra were recorded by the Mass Spectrometry Service at the University of Oxford Chemical Research Laboratory, using a Bruker Daltronics microTOF spectrometer (ESI), operating in positive or negative mode as indicated, from solutions of methanol, water or acetonitrile or a Micromass (GCT) (FI). High resolution values are calculated to four decimal places from the molecular formula, all found values being within a tolerance of 5 ppm.

Infrared Spectra: Infrared spectra were recorded on a Bruker Tensor 27 Fourier Transform spectrophotometer using thin films on NaCl plates (for all non solid compounds) or solid samples using a diamond ART module as stated. Absorption maxima (ν_{max}) are classified as strong (s), medium (m), weak (w) and broad (br) and are quoted in wavenumbers (cm^{-1}).

Chromatography: Analytical TLC was performed on Merck DC-Alufolien 60 F254 0.23mm pre-coated plates and visualised using a UV lamp ($\lambda_{max} = 254$ or 365 nm), or thermal development following immersion in basic potassium permanganate, vanillin or ninhydrin dips. Retention factors (R_f) are reported with the solvent system used in parentheses.

Flash Column Chromatography: Flash column chromatography was performed on Merck 60 silica (particle size 40-63 μm, pore diameter 60 Å) and the solvent system is recorded in parentheses.

Melting points: Crystallised samples were employed, using a Kofler hot stage micro-

scope and are uncorrected. The solvent of crystallisation is recorded in parentheses.

Specific optical rotations: A Perkin Elmer 341 polarimeter was used, in cells with a path length of 1 dm. The light source was maintained at 589 nm. The concentration (c) is expressed in g/100 mL (equivalent to g/0.1 dm^3). Specific rotations are denoted $[\alpha]_D^T$ and are given in implied units of $10^{-1} deg cm^2 g^{-1}$ (where T = ambient temperature in °C).

Microanalyses: Obtained at the Elemental Analysis Service, London Metropolitan University, London. Elemental analysis was carried out in duplicate; average values are reported.

Analytical HPLC: Carried out on a PerkinElmer Flexar system with a Binary Lc Pump and UV/VIS LC Detector. For determination of compound purity, a Dionex Acclaim® 120 column (C18, 5 μm, 120 Å, 4.6 × 150 mm) was employed, with a 10 minute gradient of 95% H_2O/ 5% MeCN + 0.1% TFA (Solvent A) to 95% MeCN/ 5% H_2O + 0.1% TFA (Solvent B), flow rate 1 mL/min and detection at 254 nm (unless stated otherwise). Samples were injected in DMSO, MeOH, or DMSO/acetone or DMSO/chloroform mixtures. The method was as described below (**Table 7.1**):

Table 7.1: Analytical HPLC method.

Entry	Step Length (min)	Elapsed Time (min)	A (%)	B (%)
1	1	1	100	0
2	10	11	0	100
3	3	14	0	100
4	1	15	100	0
5	5	20	100	0

Anhydrous solvents: Obtained under the following conditions: anhydrous DMF, anhydrous MeOH and anhydrous EtOH were purchased from Sigma-Aldrich UK in SureSeal™bottles and used without further purification; anhydrous THF and Et_2O were dried over activated 3 Å molecular sieves under an Ar or N_2 atmosphere, where stated, THF was distilled from sodium and benzophenone.

Chemicals: Purchased from Acros UK, Sigma-Aldrich UK, Alfa Aesar UK or Fisher UK. Where appropriate and if not stated otherwise, all non-aqueous reactions were

performed in a flame-dried flask under an inert atmosphere of N_2 or Ar. Where necessary, K_2CO_3 and $NaHCO_3$ were dried in an oven prior to use. "Under reduced pressure" refers to the use of a rotary evaporator attached to a diaphragm pump. Brine refers to a saturated aqueous solution of sodium chloride. Petroleum ether refers to the fraction boiling between 40 - 60 °C, unless otherwise stated.

UV/Vis Spectra: Carried out on a Perkin Elmer Lambda 25, with a range of 190 nM - 1100 nm, and fixed bandwidth of 1 nm. Samples were made up as stock solutions in MeOH (c 1.0 mM) and subsequently diluted with MeOH to obtain 2.0 mL samples of appropriate concentrations for which $\lambda_{max} < 1$. All measurements were obtained in quartz cuvettes, with a pathlength (l) of 1.0 cm. UVWinlab software was used for analysis of the obtained data.

Photolysis Experiments: Carried out with the light sources outlined below. For general procedures used in photolysis experiments refer to section 8.9.
$\lambda = 310$ nm: LZC-UVB (8 W) lamps in Luzchem UV/Vis Photoreactor LZC-5 (refer to manufacturer's guide for further details).
$\lambda = 350$ nm: LZC-UVA (8 W) lamps in Luzchem UV/Vis Photoreactor LZC-5 (refer to manufacturer's guide for further details).
$\lambda = 365$ nm: Philips Cleo Compact (15 W) fluorescent tubes in Philips HB175/01 Facial Tanner (refer to manufacturer's guide for further details).
$\lambda = 420$ nm: Roithner LaserTechnik GmbH InGaN LED (15 mW) (refer to manufacturer's guide for further details).
$\lambda = 520$ nm: Ec Technology SMD 5050 RGB LED strip (60 W) (refer to manufacturer's guide for further details).

7.2 Photolysis Experiments

7.2.1 Experimental Setup

Photolysis experiments were conducted following the general procedures outlined below, for each of the different wavelengths at λ = 310 nm, 350 nm, 420 nm and 520 nm.

λ = 310 nm: Luzchem UV/vis Photoreactor LZC-5 was used, with 8 × 12 inch (4 on each side) LZC-UVB lamps [λ_{max} = 313 nm; Bandwidth (FWHM) = 37.5 nm / 115 THz; Radiant Intensity = 39,390 mW/sm], each with an optical output power of 8 W (refer to manufacturer's guide for further details). Lamps were switched on and allowed to warm up for 0.5 h, prior to commencement of the experiment. The samples (*c* 1.0 mg/mL in MeOH, 2.00 mL) were irradiated in quartz cuvettes, placed 1.0 cm away from the light source. An elevated platform was used to support the samples such that irradiation was focussed on the centre of the sample (**Figure 7.1**). The ventilation system in the Luzchem photoreactor was used to maintain the temperature of the samples below 30 °C.

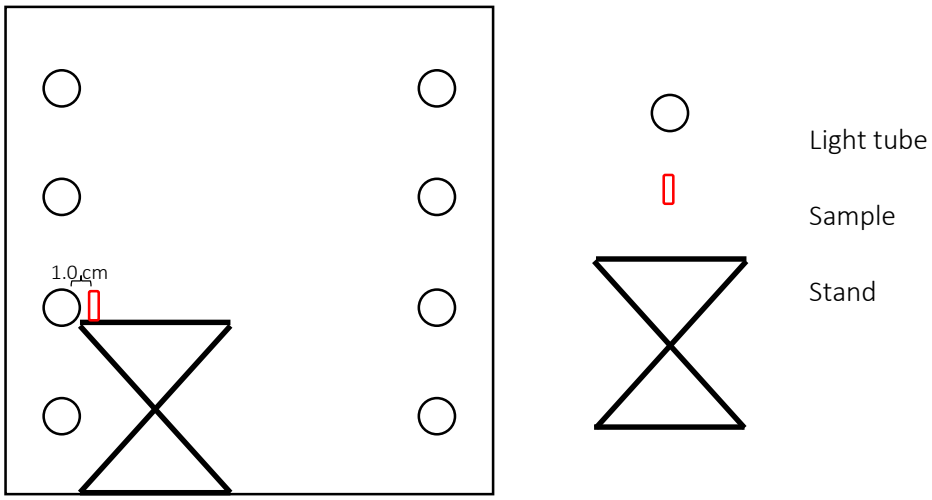


Figure 7.1: Saggital cross-section of photolysis setup for irradiation of samples with Luzchem phororeactor at λ = 310 nm and λ = 350 nm.

λ = 350 nm: Luzchem UV/Vis Photoreactor LZC-5 was used, with 8 × 12 inch (4 on

each side) LZC-UVA lamps [λ_{max} = 351 nm; Bandwidth (FWHM) = 35 nm / 85.2 THz; Radiant Intensity = 25,620 mW/sm], each with an optical output power of 8 W (refer to manufacturer's guide for further details). Lamps were switched on and allowed to warm up for 0.5 h, prior to commencement of the experiment. The samples (*c* 1.0 mg/mL in MeOH, 2.00 mL) were irradiated in glass vials, placed 1.0 cm away from the light source. An elevated platform was used to support the samples such that irradiation was focussed on the centre of the sample (**Figure 7.1**). The ventilation system in the Luzchem photoreactor was used to maintain the temperature of the samples below 30 °C.

λ = 365 nm: A Philips HB175/01 Facial Tanner was used with 4 × 29 cm Philips Cleo Compact vertical fluorescent tubes (emission spectrum: 300 - 400 nm; maximum ≈ 365 nm; Incident light flux = 2.45 × 10^{-8} photons mol $cm^{-2}s^{-1}$), each with an optical output power of 15 W (refer to manufacturer's guide for further details). Philips HB175/01 Facial Tanner was switched on and allowed to warm up for 0.5 h, prior to commencement of the experiment. The samples (*c* 1.0 mg/mL in MeOH, 2.00 mL) were irradiated in glass vials, placed 5.0 cm away from the light source. An elevated platform was used and samples were placed directly in front of a Philips Cleo Compact vertical fluorescent tube (**Figure 7.2**). As a safety precaution, the experiments were conducted in a fumehood with aluminium sheets covering the sash. The temperature of the samples was kept below 30 °C by exposure to a stream of N_2 gas, clamped in place above the sample.

λ = 420 nm: A InGaN LED light source [λ_{max} = 420 nm; Bandwidth (FWHM) = 15 nm / 25.5 THz; Radiant Intensity = 60 mW/sr], mounted on a lead frame and encapsulated in a clear epoxy silicone lens, purchased from Roithner LaserTechnik GmbH, with an optical output power of 15 mW, and a viewing half angle of ± 8 °, was used (refer to manufacturer's guide for further details). The LED was switched on and allowed to warm up for 0.5 h, prior to commencement of the experiment. The samples (*c* 1.0 mg/mL in MeOH, 2.00 mL) were irradiated in glass vials and placed 1.0 cm away from the light source. An elevated platform was used to support the samples such that irradiation was focussed on the centre of the sample. As a safety precaution, the photolysis experiments were conducted in a square black box, fashioned out of aluminium sheets (**Figure 7.3**). As no appreciable increase in temperature (remained at RT) of the samples was observed, no cooling was required.

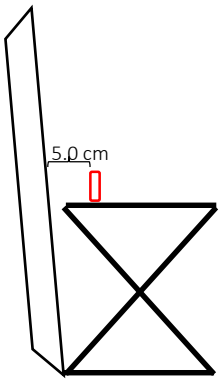


Figure 7.2: Saggital cross-section of photolysis setup for irradiation of samples using Philips HB175/01 at $\lambda = 365$ nm.

$\lambda = 420$ nm: A LED light source [$\lambda_{max} = 420$ nm; Bandwidth (FWHM) = 15 nm / 25.5 THz; Irradiance = 13.1 µW mm^{-2}], with integrated EEPROM for automated LED settings, mounted on a ϕ30.5mm heat sink, purchased from Thorlabs, Inc., with an optical output power of 750 mW, and a viewing half angle of ± 125 °, was used (refer to manufacturer's guide for further details). The LED was switched on and allowed to warm up for 0.5 h, prior to commencement of the experiment. The samples (c 0.004 mM in MeOH or 0.10 mM in H_2O, 1.80 mL) were irradiated in glass vials and placed 1.0 cm away from the light source. An elevated platform was used to support the samples such that irradiation was focussed on the centre of the sample. As a safety precaution, the photolysis experiments were conducted in a square black box, fashioned out of aluminium sheets (**Figure 7.3**). As no appreciable increase in temperature (remained at RT) of the samples was observed, no cooling was required.

$\lambda = 530$ nm: A LED light source [$\lambda_{max} = 530$ nm; Bandwidth (FWHM) = 33 nm / 35.2 THz; Irradiance = 9.5 μW mm^{-2}], with integrated EEPROM for automated LED settings, mounted on a ϕ30.5mm heat sink, purchased from Thorlabs, Inc., with an optical output power of 350 mW, and a viewing half angle of ± 80 °, was used (refer

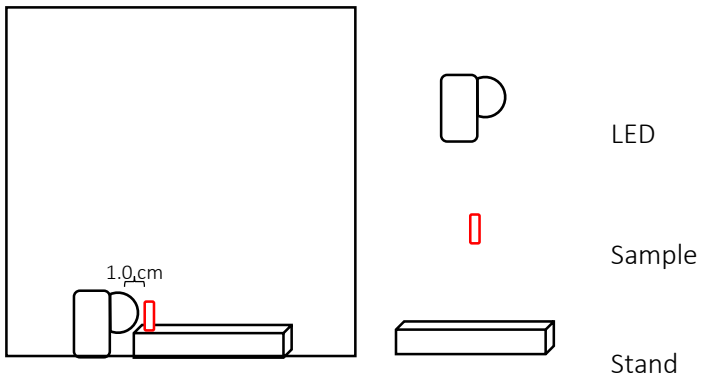


Figure 7.3: Saggital cross-section of photolysis setup for irradiation of samples using LED at $\lambda = 420$ nm.

to manufacturer's guide for further details). The LED was switched on and allowed to warm up for 0.5 h, prior to commencement of the experiment. The samples (c 0.004 mmol in MeOH or 0.10 mmol in H_2O, 1.80 mL) were irradiated in glass vials and placed 1.0 cm away from the light source. An elevated platform was used to support the samples such that irradiation was focussed on the centre of the sample. As a safety precaution, the photolysis experiments were conducted in a square black box, fashioned out of aluminium sheets (**Figure 7.3**). As no appreciable increase in temperature (remained at RT) of the samples was observed, no cooling was required.

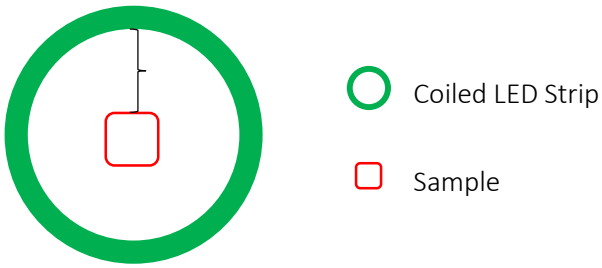


Figure 7.4: Transverse cross-section of photolysis setup for irradiation of samples using LED strip at $\lambda = 520$ nm.

λ = 520 nm: A LED strip containing 300 SMD 5050 RGB LEDs [λ_{max} = 525 nm; Bandwidth (FWHM) = 36 nm / 39.2 THz], purchased from EC Technology, with an optical output power of 60 W, was used (refer to manufacturer's guide for further details). The LED strip was switched on and allowed to warm up for 0.5 h, prior to commencement of the experiment. The LED strip was fashioned into a coil and the samples (*c* 1.0 mg/mL in MeOH, 2.00 mL) were irradiated in glass vials, placed at the centre of the coil, 2.0 cm radius away from the light source (**Figure 7.4**). As a safety precaution, the experiments were conducted in a fumehood with aluminium sheets covering the sash. Samples were kept below 30 °C by exposure to a stream of N_2 gas, through a rubber tube, held in place with a clamp, above the photolysis set up.

7.2.2 Analysis of Photolysis Results

i) Analysis by HPLC: Samples (*c* 1.0 mg/mL in MeOH, 2.00 mL) were irradiated at a given wavelength (λ), in quartz cuvettes (λ = 310 nm) or glass vials (λ = 350 nm, 420 nm, 520 nm) and 25 μL aliquots were taken at hourly intervals. Samples were diluted two fold (*c* 0.5 mg/mL in MeOH) prior to injection (20 μL) for analysis by HPLC. Percentage conversions were determined based on changes in absorbance (calibration curves were obtained determining linear relationship between concentration and absorbance).

ii) Analysis by 1H NMR: Samples (*c* 10.0 mg/mL in CD_3OD) were irradiated at a given wavelength (λ), in quartz NMR tubes (λ = 310 nm, 0.50 mL) or glass vials (λ = 350 nm, 420 nm, 520 nm, 0.70 mL). Hexamethyldisiloxane (*c* 0.035 mM in CD_3OD, 0.20 mL) was employed as an internal standard for quantification of percentage conversions, following irradiation of samples. For samples irradiated in quartz NMR tubes, the internal standard was added directly prior to NMR analysis. For samples in glass vials, the sample (0.50 mL) was transferred to an NMR tube, followed by addition of the internal standard prior to the NMR. Effects of photolysis and uncaging were monitored by comparison of characteristic peaks in the **^{1}H NMR** spectra obtained for samples after irradiation to those of of the caged compound prior to irradiation and the expected product.

iii) Analysis by LCMS-UV: Samples (*c* 0.004 mmol in MeOH or 0.10 mmol in H_2O, 1.80 mL) were irradiated at a given wavelength (λ), in mass spectrometry vials (λ =

420 nm, 5e0 nm) and analysed by LCMS. Percentage conversions were determined based on changes in intensity (calibration curves were obtained determining linear relationship between concentration and intensity).

Standard deviations were calculated using the error propagation formula (**Equation 7.1**).

$$\sigma_f = \sqrt{(\frac{\delta_f}{\delta_x})\sigma_x^2 + (\frac{\delta_f}{\delta_y})\sigma_y^2 + ...} \tag{7.1}$$

This enabled the standard errors to be calculated (**Equation 7.2**).

$$\sigma_m = \frac{\sigma_f}{\sqrt{N}} \tag{7.2}$$

7.2.3 Determination of Calibration Curves by HPLC

To allow for quantitative conversion measurements, calibration studies were performed for both the caged and uncaged amino acid variants by measuring the change in absorbance with concentration. Stock solutions were prepared in MeOH and diluted to the desired concentrations. Absorbance data were collected at different concentrations by HPLC analysis and plotted to obtain the linear relationship between the two variables. The linear relationship between the absorbance and concentration can be modelled by the Beer-Lambert law equation (**Equation 7.3**):

$$A = \varepsilon cl \tag{7.3}$$

By establishing the extinction coefficient, ε for the compound, where pathlength, $l = 1$, given the absorbance, A, it is possible to determine the concentration, c, of the species present in the sample.
Where HPLC was being used for analysis, the area under the curve represented the absorbance of the compounds and was used for the calculations to obtain the relationship between absorbance and concentration.
These figures were determined by analysis using Microsoft Office Excel 2016. Values shown are the average of a minimum of three concordant sets of repetitions.

The linear relationship between the absorbance and concentration can be modelled by the equation (**7.4**):

$$A = mc + j \tag{7.4}$$

where:

A - absorbance

m - gradient

c - concentration

j - coefficient

By establishing the gradient, m, and the coefficient ,j, which was shown for Fmoc-Asp-O^{t}Bu (**221**) to be m = 12500461.46 with a standard error of 797634.27638 and c = 1436167.13 with a standard error of 242044.00167 with an R^2 value of 1.00, it would be possible to determine the quantity of Fmoc-Asp-O^{t}Bu (**221**) present in the sample.

For example, if the absorbance was measured to be 9227657, this and the values of m and j could be substituted into the above equation to obtain the concentration:

$$9227657 = 12500401(c) + 1436167.13 \tag{7.5}$$

Rearrangement of the equation to make the concentration, c, the subject, yields:

$$c = \frac{9227657 - 1436167.13}{12500461.46} = 0.623(3s.f.) \tag{7.6}$$

This allows the concentration of Fmoc-Asp-O^{t}Bu (**221**) in the sample to be determined as 0.623 mM. For a reaction with an initial caged-aspartic acid concentration of 1.00 mM, the percentage conversion to product can be determined using the following equation:

$$conversion = \frac{0.623}{1.00} \times 100\% = 62.3\%(3s.f.) \tag{7.7}$$

This gives the overall percentage conversion to product as 62.3%.

By obtaining the linear relationship for the caged amino acids as well as the expected photoreleased products, the rate of photolysis of both photolytic uncaging as well as product formation can be determined by the percentage conversion per unit time. This could then be plotted as graphs to display the results.

7.2.4 Photolysis Data as Measured by HPLC

By employing the linear relationship between the absorbance and concentration, the Beer-Lambert law, as established in the calibration studies, given the absorbance, as

measured by the area under the curve by HPLC analysis, it is possible to determine the concentration, c of the species. The change in concentration, c, then enables the percentage composition of the caged and uncaged species present in the sample to be determined (**Equation 7.8**).

$$PercentageComposition = \frac{c'}{c} \times 100\% \tag{7.8}$$

where:

c - initial concentration of caged amino acid at start of experiment
c' - concentration of caged or uncaged amino acid present in sample

Calculations were performed using Microsoft Office Excel 2016. Values shown are the average of a minimum of three concordant sets of repetitions. Values for percentage composition were rounded to the nearest whole number. The initial percentage composition of caged amino acid at the start of the photolysis experiment (0 h) was taken to be 100%. Where no absorbance peak was detected by HPLC analysis, absorbance, concentration and hence percentage composition were taken to be 0. Where such a small absorbance was observed so as to result in a negative concentration, both concentration and percentage composition were taken to be 0. Where absorbance resulted in a concentration greater than the initial concentration and hence a conversion greater than 100%, the conversion was taken to be 100%. Percentage conversions were found to be accurate within ± 5%. Graphs obtained from these results are shown in the 'Results & Discussion' chapters. For a worked example, refer to 'Results & Discussion.

7.2.5 Determination of Calibration Curves by LCMS

To allow for quantitative conversion, calibration studies were performed for both the caged and uncaged amino acid variants by measuring the change in intensities with concentration. Stock solutions were prepared and diluted to the desired concentrations. Intensity data was collected at different concentrations by LCMS analysis and plotted to obtain the linear relationship between the two variables.

Where LCMS was being used for analysis, the area under the curve represented the mass spectrometry intensity of the compounds and was used for the calculations to obtain the relationship between intensities and concentration.

These figures were determined by analysis using Microsoft Office Excel 2016. Values shown are the average of a minimum of three concordant sets of repetitions.

7.2.6 Photolysis Data as Measured by LCMS

By employing the linear relationship between the intensity and concentration, as measured by the area under the curve by LCMS analysis, it is possible to determine the concentration, c of the species. The change in concentration, c, then enables the percentage composition of the caged and uncaged species present in the sample to be determined (**Equation 7.8**).

Calculations were performed using Microsoft Office Excel 2016. Values shown are the average of a minimum of three concordant sets of repetitions. Values for percentage composition were rounded to the nearest whole number. The initial percentage composition of caged amino acid at the start of the photolysis experiment (0 h) was taken to be 100%. Where no peak was detected by LCMS analysis, intensity, concentration and hence percentage composition were taken to be 0. Where such a small intensity peak was observed so as to result in a negative concentration, both concentration and percentage composition were taken to be 0. Where the intensity peak resulted in a concentration greater than the initial concentration and hence a conversion greater than 100%, the conversion was taken to be 100%. Percentage conversions were found to be accurate within ± 5%. Graphs obtained from these results are shown in the 'Results & Discussion' chapters. For a worked example, refer to 'Results & Discussion.

7.3 Quantum Yield of Uncaging

The quantum yield of photolysis, ϕ_p, is a measure of the number of excited state molecules leading to uncaging, relative to the number of photons absorbed by irradiation (**Equation 7.9**).[15]

$$\phi_p = \frac{kcVN_{\mathrm{A}}}{f(1-10^{-\mathrm{A}})} \tag{7.9}$$

where:

ϕ_p - quantum yield of photolysis
k - photolysis rate constant
c - concentration of irradiated solution (M)
V - volume of irradiated solution (dm^3)
N_A - Avogadro's number
f - photon flux i.e. number of photons administered
$(1-10^{-A})$ - factor for correction of % light transmission
A - absorbance of sample at irradiation wavelength

Following the reaction progress by LCMS enabled the number of molecules released per second to be determined. The photolysis reactions followed first-order reaction kinetics (**Equation 7.10**).

$$Rate = -\frac{d[A]}{dt} Rate = k[A] \frac{d[A]}{[A]} = -kdt \tag{7.10}$$

This enabled the rate constant, k, to be calculated by means of the integrated first-order rate equation (**Equation 7.11**).

$$ln[A] = -kt + I \tag{7.11}$$

Plotting ln [A] vs t gave a straight line, the gradient of which was equal to the rate constant, k.

The number of photons absorbed was equated to the photon flux administered and included a factor for correction of the percentage light transmission. The photon flux of the light source was measured using ferrioxalate actinometry.[232]

7.3.0.1 Ferrioxalate Actinometry Protocol

Colorimetric ferrioxalate actinometry experiments were used to determine the photon flux produced by the light sources used for the irradiation experiments. All actinometry

experiments were performed in the dark to eliminate external light contributing to the decomposition of the ferrioxalate. Autopipettes were used to ensure accuracy of the measured solutions.



Scheme 7.1: Photodecomposition of ferrioxalate.

Potassium ferrioxalate undergoes photodecomposition to form Fe^{2+} ions upon irradiation (**Scheme 7.1**). Complexation with 1,10-phenanthroline forms $[Fe(phen)_3]^{2+}$, which has a strong absorption at 510 nm, and enables the concentration of Fe^{2+} produced to be determined spectrophotometrically. The intensity of the red solution can be measured as a function of irradiation time to gauge the conversion rate of potassium ferrioxalate to Fe^{2+}, thereby enabling light intensity to be determined, as the quantum yield for this reaction is well-established.[232]

Preparation of Solutions:
(i) Ferric oxalate solution (6 mM) was prepared by dissolving 300 mg of potassium ferric oxalate trihydrate ($K_3[Fe(C_2O_4)_3]3H_2O$) in 100 mL of 0.05 M H_2SO_4.
(ii) Phenanthroline solution (0.1% w/v) was prepared by dissolving 22.5 g of $CH_3CO_2Na3H_2O$ and 0.100 g of phenanthroline in 100 mL of 0.5 M H_2SO_4).

Irradiation of Samples:
Ferric oxalate solution (1.80 mL) was irradiated in a glass vial, using the light sources according to the set-ups listed above (**7.2.1**), while an identical control sample (1.80 mL) was kept in the dark. Following irradiation for pre-determined time periods, aliquots of the irradiated and non-irradiated ferric oxalate solution (0.2 mL) were transferred to vials containing a mixture of the above prepared phenanthroline solution (0.9 mL) and H_2O (0.9 mL). The mixtures were kept in the dark for 1 h to allow for complexation to occur, after which their absorbance, at 510 nm, was measured.
Irradiation times were chosen to ensure that the photoconversion of ferric oxalate did not exceed 5%, as the production of the photoproduct results in a diminished absorbance at the wavelengths of photolysis, as well as an accumulation of $Fe(C_2O_4)$, which precipitates out of solution, and that the absorption of the $Fe(phen)_3{}^{2+}$ complex was within 0.5 – 1.

Calculation of Photon Flux:

Determination of the photon flux (**Equation 7.12**) required knowledge of the amount of Fe^{2+} formed, the quantum yield of the ferrioxalate conversion and the absorbance of the ferrioxalate solution at the irradiation wavelength.

$$f = \frac{\eta(Fe^{2+})}{\phi_{Fe} t(1 - 10^{A})} \tag{7.12}$$

where:

f - photon flux
$\eta(Fe^{2+})$ - number of moles of Fe^{2+}
ϕ_{Fe} - quantum yield of ferrioaxalate conversion at irradiation wavelength
t - photolysis time (s)
$(1 - 10^{-A})$ - factor for correction of% light transmission
A - absorbance of ferrioxalate solution at irradiation wavelength

Complexation with 1,10-phenanthroline solution to generate the red coloured $Fe(phen)_3{}^{2+}$ complex (ε = 11,100 M–1 cm–1) allowed quantification of the number of moles of Fe^{2+} formed following the photodecomposition of the ferrioxalate solution, by measuring the difference in absorbance between the irradiated and non-irradiated ferrioxalate solutions (**Equation 7.13**).

$$\eta(Fe^{2+}) = \frac{V_1 V_3 \Delta A_{510nm}}{V_2 l \varepsilon} \tag{7.13}$$

where:

$\eta(Fe^{2+})$ - number of moles of Fe^{2+}
V_1 - volume of irradiated solution (dm^3)
V_2 - aliquot of irradiated solution tranferred for complexation (dm^3)
V_3 - final volume of complexation solution (dm^3)
ΔA_{510nm} - difference in absorbance between irradiated and non-irradiated ferrioxalate solution
ε - extinction coefficient of the ferrioxalate solution
l - path length (cm)

The photon flux was converted from the calculated Es^{-1} to moles of $photonss^{-1}$ by multiplying by Avogadro's number.

7.3.0.2 Photon Flux Measurements

The use of ferrioxalate actinometry allowed to photon flux of the light sources used for the irradiation experiments to be determined (**Table 7.2**).

Table 7.2: Photon Flux of light sources used for irradiation.

Entry	Light Source (nm)	Manufacturer	Photon Flux ($E \cdot s^{-1}$)	Photon Flux (moles of photons$\cdot s^{-1}$)
1	420	Thorlabs	1.16×10^{18}	6.99×10^{42}
2	530	Thorlabs	1.84×10^{17}	1.11×10^{42}

7.3.0.3 Quantum Yield Measurements

By following the progression of the photolysis reactions to determine the rate of photolysis and through the use of ferrioxalate chemistry, it was possible to determine the quantum yields of uncaging for the following caged specied (**Table 7.3**).

Table 7.3: Quantum Yield of Photolysis.

Photolysis Quantum Yield						
Entry	Compound	$\lambda_{irradiation}$ (nm)	k ($10^{-4}s^{-1}$)	ε ($10^{4}M^{-1}cm^{-1}$)	ϕ (10^{-4}) [SE]	ε ϕ [SE]
1	Fmoc-Asp(DEACM)-O^{t}Bu	420	174	3.65	2.28 ± 0.0147	8.31 ± 0.0538
2	Fmoc-Asp(BODIPY)-O^{t}Bu	530	2.01	1.38	0.398 ± 0.00231	0.548 ± 0.00319
3	KLD-DEACM	420	154	0.40	15.8 ± 0.0930	6.37 ± 0.0376
4	BODIPY-KLD	530	1.99	1.75	0.315 ± 0.00183	0.552 ± 0.00321
5	BODIPY-KLD-DEACM	420	1.45	0.61	0.0991 ± 0.000641	0.06051 ± 0.000391
6	BODIPY-KLD-DEACM	530	2.67	1.93	0.388 ± 0.00225	0.747 ± 0.00434
7	KGSTAD-DEACM	420	49.0	0.37	8.02 ± 0.0519	2.95 ± 0.0191
8	BODIPY-KGSTAD	530	24.0	0.034	187 ± 1.08	6.39 ± 0.0372
9	BODIPY-KGSTAD-DEACM	420	1301	0.15	406 ± 2.63	1.01 ± 0.00655
10	BODIPY-KGSTAD-DEACM	530	21.0	0.071	82.2 ± 0.478	5.83 ± 0.0339

7.4 Enzyme Catalysed Proteolysis

7.4.1 Preparation of Buffer Solutions

7.4.1.1 250 mM Sodium Phosphate Buffer, pH 8.0

Stock solutions of 1 M monobasic NaH_2PO_4 (13.8 g NaH_2PO_4 in 100 mL double-distilled millipore H_2O) and 1 M dibasic Na_2HPO_4 (14.2 g Na_2HPO_4 in 100 mL double-distilled millipore H_2O) were prepared.

For preparation of 250 mM sodium phosphate buffer, pH 8.0, aliquots of 1 M NaH_2PO_4 (1.70 mL) and 1 M $Na_2HPO_4$23.3 mL stock solutions were pipetted and brought to a total volume of 100 mL with double-distilled millipore H_2O. If necessary, the pH of the solution was adjusted through the addition of additional 1 M NaH_2PO_4 or 1 M Na_2HPO_4 stock solutions as necessary.

7.4.1.2 500 mM Ammonium Bicarbonate Buffer, pH 8.0

Concentrated NH_3 solution (33%, 6.00 mL) was added to make up a 100 mL solution in double-distilled millipore H_2O. Through this solution was bubbled CO_2 until a pH of 8.0 for the buffer solution was obtained. If necessary, the solution was adjusted with additional NH_3 or CO_2 to obtain the desired pH.

7.4.2 Enzyme Catalysed Digestion Protocol

7.4.2.1 Asp-*N*

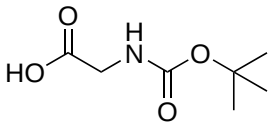
250 mM sodium phosphate buffer, pH 8.0 (10 µL) was added to an eppendorf containing the peptide (0.1 mM in double-distilled millipore H_2O, 40 µL) to be digested, to give a final concentration of 50 mM sodium phosphate buffer. To this solution was added Asp-*N* (2 µg in 20 µL double-distilled millipore H_2O) to give a final 1:200 to 1:20 enzyme to protein by weight ratio. The samples were incubated at 37 °C for 8 h before being analysed by mass spectrometry.
Note: All volumes were measured using micro-pipettes; New vials of enzyme were used when repeating digestions to minimize risks of contamination or autolysis; Incubation temperature was not allowed to exceed 37 °C to avoid autolysis.

7.4.2.2 Lys-*C*

500 mM ammonium bicarbonate buffer, pH 8.0 (10 µL) was added to an eppendorf containing the peptide (0.1 mM in double-distilled millipore H_2O, 40 µL) to be digested, to give a final concentration of 100 mM ammonium bicarbonate buffer. To this solution was added Lys-*C* (20 µg in 200 µL double-distilled millipore H_2O) to give a final 1:20 enzyme to protein by weight ratio. The samples were incubated at 37 °C for 20 h before being analysed by mass spectrometry.
Note: All volumes were measured using micro-pipettes; Remaining reconstituted enzyme was aliquoted into single-use volumes and stored at -80 °C; New vials of enzyme were used when repeating digestions to minimize risks of contamination or autolysis; Incubation temperature was not allowed to exceed 37 °C to avoid autolysis.

7.5 DMNB Caged GSH and ESG

2-((*tert*-Butoxycarbonyl)amino)acetic acid



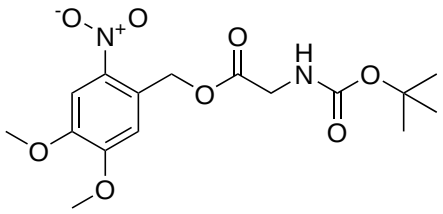
130

Glycine (**129**) (10.00 g, 133 mmol, 1.00 eq) was dissolved in a solution of NaOH (8.00 g, 200 mmol, 1.50 eq) in H_2O/THF (1/1, 600 mL). A solution of di-*tert*-butyl dicarbonate (32.0 g, 147 mmol, 1.0 eq) in THF (200 mL) was added dropwise over 1 h. The resulting solution was stirred at RT for 24 h, after which time the reaction was adjudged to be complete by TLC analysis. The solvent was concentrated under reduced pressure and the resulting residue was redissolved in H_2O (200 mL). The resulting aqueous solution was washed with EtOAc (2 × 250 mL), and acidified with solid citric acid to pH = 4, before being extracted with EtOAc (3 × 100 mL). The organic layers were combined, washed with brine (250 mL), dried over $MgSO_4$, and filtered. The solvent was removed under reduced pressure to afford 2-((*tert*-butoxycarbonyl)amino)acetic acid (**130**) as a colourless solid (14.64 g, 63%).

R_f: 0.24 (Petroleum ether:EtOAc = 8:2);
m.p.: 88 - 90 °C (Petroleum ether/EtOAc) [Literature value: 88 - 90 °C][203];
^{1}H NMR (400 MHz, $CDCl_3$) δH: 11.55 (1H, br s, COO**H**), 5.29 - 5.11 (1H, m, N**H**), 3.99 - 3.85 (2H, m, C$\mathbf{H}_2$), 1.47 (9H, s, (C$\mathbf{H}_3$)$_3$);
^{13}C NMR (100 MHz, $CDCl_3$) δC [Rotamers]: 174.8 (**C**OOH), 174.0 (**C**OOH), 157.3 (NH**C**O), 156.0 (NH**C**O), 81.8 (O**C**(CH$_3$)$_3$), 80.4 (O**C**(CH$_3$)$_3$), 43.4 (**C**H$_2$NH), 42.2 (**C**H$_2$NH), 28.3 (C(**C**H$_3$)^3);
LRMS *m/z* (ESI$^+$): 131 (100%), 176 (78% [M + H]$^+$);
IR (ν_{max} cm^{-1}): 2978 (w, br), 1738 (m, C=O), 1666 (m), 1530 (m), 1196 (s, C-N), 1158 (s, C-O), 857 (m).

Data are concordant with literature values.[204]

4,5-Dimethoxy-2-nitrobenzyl 2-((*tert*-butoxycarbonyl)amino)acetate



131

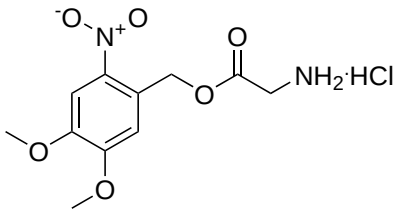
2-((*tert*-Butoxycarbonyl)amino)acetic acid (**130**) (2.00 g, 11.4 mmol, 1.00 eq), 4,5-dimethoxy-2-nitrobenzyl alcohol (**149**) (2.56 g, 12.0 mmol, 1.05 eq) and *N*,*N*,*N'*,*N'*-tetramethyl-*O*-(1*H*-benzotriazol-1-yl)uronium hexafluorophosphate (4.55 g, 12.0 mmol, 1.05 eq) were dissolved in anhydrous DMF (20.0 mL) and the resulting solution was stirred at RT for 10 mins. *N*,*N*-Diisopropylethylamine (2.95 g, 3.97 mL, 22.8 mmol, 2.00 eq) was added dropwise and the resulting solution was stirred at RT under a N_2 atmosphere for 3 h, after which time the reaction was adjudged to be complete by TLC analysis. The reaction was quenched with EtOAc (150 mL) and washed sequentially with aqueous 1 M HCl (150 mL), sat. aqueous $NaHCO_3$ (150 mL), H_2O (150 mL) and brine (150 mL), dried over $MgSO_4$ and filtered. The solvent was removed under reduced pressure and the resulting crude product was purified by silica gel flash column chromatography, eluting with petroleum ether:EtOAc = 6:4, to afford 4,5-dimethoxy-2-nitrobenzyl 2-((*tert*-butoxycarbonyl)amino)acetate (**131**) as a yellow foam (3.81 g, 90%).

R_f: 0.37 (Petroleum ether:EtOAc = 6:4);
m.p.: 153 - 155 °C (Petroleum ether/EtOAc) [Literature value: 152 - 154 °C][205];
UV λ_{max}/nm (ϵ/$M^{-1}cm^{-1}$): 340 (7920) [MeOH];
^{1}H NMR (400 MHz, $CDCl_3$) δH: 7.73 (1H, s, C_{Ar}**H**), 7.03 (1H, s, C_{Ar}**H**), 5.60 (2H, s, $C_{Ar}C$**H**$_2$O), 5.13 - 5.04 (1H, m, CH_2N**H**), 4.04 - 3.95 (5H, m, C**H**$_2$NH, OC**H**$_3$), 3.96 (3H, s, OC**H**$_3$), 1.44 (9H, s, C(C**H**$_3$)$_3$);
^{13}C NMR (100 MHz, $CDCl_3$) δC: 170.0 (**C**O), 155.8 (**C**O), 153.7 (**C**$_{Ar}$), 148.3 (**C**$_{Ar}$) 139.7 (**C**$_{Ar}$), 126.7 (**C**$_{Ar}$), 110.1 (**C**$_{Ar}$H), 108.2 (**C**$_{Ar}$H), 80.2 (O**C**(CH$_3$)$_3$), 63.9 (C_{Ar}**C**H$_2$O), 56.6 (O**C**H$_3$), 56.4 (O**C**H$_3$), 42.5 (**C**H$_2$NH), 28.3 (OC(**C**H$_3$)$_3$);
LRMS *m/z* (ESI$^+$): 371 (18% $[M + H]^+$), 804 (100%);
HRMS *m/z* (ESI$^+$): Found 393.1271 $[M + Na]^+$ ($C_{16}H_{22}N_2NaO_8^+$ requires 393.1268 $[M + Na]^+$);

IR (ν_{max} cm^{-1}): 3352 (w, N-H), 1737 (m, C=O), 1677 (m, C=O), 1580 (w), 1521 (s, N-O), 1451 (w), 1275 (m), 1226 (m), 1161 (s, C-O), 1065 (m), 986 (w), 870 (w), 794 (w).

Data are concordant with literature values.[205]

4,5-Dimethoxy-2-nitrobenzyl glycinate hydrochloride



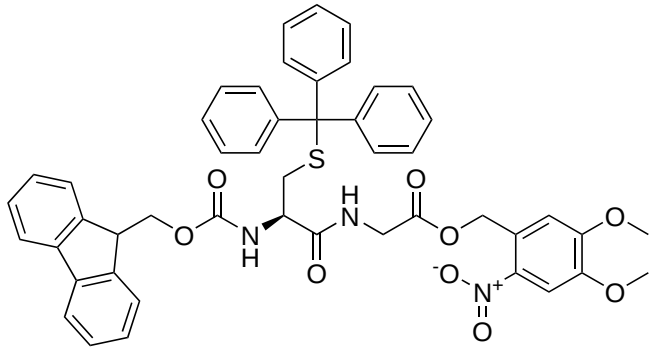
132

4,5-Dimethoxy-2-nitrobenzyl 2-((*tert*-butoxycarbonyl)amino)acetate (**131**) (7.80 g, 21.1 mmol, 1.00 eq) was dissolved in a solution of 4 M HCl in anhydrous 1,4-dioxane (79.0 mL, 316 mmol, 15.0 eq). The reaction solution was stirred under a N_2 atmosphere at RT for 3 h, after which time the reaction was adjudged to complete by TLC analysis. The solvent was removed under reduced pressure and the crude mixture was purified by trituration with Et_2O to afford 4,5-dimethoxy-2-nitrobenzyl glycinate hydrochloride (**132**) as a yellow solid (6.26 g, 97%).

R_f: 0.37 (Reverse phase; MeOH:H_2O = 1:1);
m.p.: 169 - 171 °C (Et_2O) [Literature value: 168 - 170 °C][106];
UV λ_{max}/nm (ϵ/$M^{-1}cm^{-1}$): 340 (6390) [MeOH];
^{1}H NMR (500 MHz, D_2O) δH: 7.69 (1H, s, C_{Ar}**H**), 7.10 (1H, s, C_{Ar}**H**), 5.51 (2H, s, C$\mathbf{H}_2$O), 4.00 (2H, s, C$\mathbf{H}_2$N), 3.93 (3H, s, OC$\mathbf{H}_3$), 3.87 (3H, s, OC$\mathbf{H}_3$);
^{13}C NMR (125 MHz, D_2O) δC: 167.8 (**C**O), 153.1 ($\mathbf{C}_{Ar}$), 148.0 ($\mathbf{C}_{Ar}$), 139.8 ($\mathbf{C}_{Ar}$), 125.1 ($\mathbf{C}_{Ar}$), 112.0 ($\mathbf{C}_{Ar}$H), 108.5 ($\mathbf{C}_{Ar}$H), 65.2 (**C**H_2O), 56.3 (O**C**H_3), 56.1 (O**C**H_3), 40.0 (**C**H_2N);
LRMS *m/z* (ESI$^+$): 271 (100% $[M + H]^+$), 293 (85% $[M + Na]^+$);
HRMS *m/z* (ESI$^+$)(FI$^+$): Found 270.0756 [M] ($C_{11}H_{14}N_2O_6$ requires 270.0852 [M]);
IR (ν_{max} cm^{-1}): 2951 (w, br), 1742 (w, C=O), 1523 (m, N-O), 1449 (w), 1326 (w), 1278 (s, C-O), 1214 (s, C-N), 1123 (w), 1059 (m), 940 (w), 903 (w), 864 (w), 800 (w).

Data are concordant with literature values.[106]

(*R*)-4,5-Dimethoxy-2-nitrobenzyl 2-(2-((((9*H*-fluoren-9-yl)methoxy)carbonyl)amino)-3-(tritylthio)propanamido)acetate



133

4,5-Dimethoxy-2-nitrobenzyl glycinate hydrochloride (**132**) (2.10 g, 7.80 mmol, 1.00 eq), Fmoc-Cys(Trt)-OH (4.80 g, 8.20 mmol, 1.05 eq), and *N*,*N*,*N*',*N*'-tetramethyl-*O*-(1*H*-benzotriazol-1-yl)uronium hexafluorophosphate (3.11 g, 8.20 mmol, 1.05 eq) were dissolved in anhydrous DMF (45.0 mL), and the solution was stirred at RT for 10 min. After this time, *N*,*N*-diisopropylethylamine (2.02 g, 2.72 mL, 15.6 mmol, 2.00 eq) was added dropwise and the resulting solution was stirred at RT under an atmosphere of N_2 for 18 h, after which time the reaction was adjudged to be complete by TLC analysis. The reaction was quenched with EtOAc (200 mL), washed with H_2O (2 × 200 mL) and brine (200 mL), dried over $MgSO_4$, and filtered. The solvent was removed under reduced pressure and the crude residue was purified by silica gel flash column chromatography, eluting with petroleum ether:EtOAc = 7:3, to afford (*R*)-4,5-dimethoxy-2-nitrobenzyl 2-(2-(((9*H*-fluoren-9-yl)methoxy)carbonyl)amino)-3-(tritylthio)propanamido)acetate (**133**) as a yellow foam (6.37 g, 98%).

R_f: 0.55 (Petroleum ether:EtOAc = 6:4);
m.p.: 97 - 98 °C (Petroleum ether/EtOAc);
$[\alpha]_D^{26}$: -0.78 (***c*** 0.9 in $CHCl_3$);
UV λ_{max}/nm (ϵ/$M^{-1}cm^{-1}$): 345 (6790) [MeOH];
^{1}H NMR (500 MHz, $CDCl_3$) **δ**H: 7.77 - 7.73 (2H, m, C_{FmocAr}**H**), 7.71 (1H, s, C_{Ar}**H**), 7.57 (2H, d, J = 7.0 Hz, C_{FmocAr}**H**), 7.45 - 7.36 (8H, m, C_{Ph}**H**, C_{FmocAr}**H**), 7.32 - 7.18 (8H, m, C_{Ph}**H**, C_{FmocAr}**H**), 6.96 (1H, s, C_{Ar}**H**), 6.50 - 6.39 (1H, m, N**H**CH_2), 5.56 (2H, s, OC**H**$_2C_{Ar}$), 4.96 (1H, d, J = 7.6 Hz, N**H**$CHCH_2$), 4.41 (2H, d, J = 6.5 Hz, C_{Fmoc}**H**$_2$), 4.19 (1H, t, J = 6.5 Hz, C_{Fmoc}**H**), 4.11 - 4.01 (2H, m, NHC**H**$_2$), 3.98

(3H, s, OC$\mathbf{H}_3$), 3.95 (3H, s, OC$\mathbf{H}_3$), 3.88 - 3.83 (1H, m, NHC$\mathbf{H}$C$\mathrm{H_2}$S), 2.76 - 2.56 (2H, m, CHC$\mathbf{H}_2$S);

^{13}C NMR (125 MHz, $\mathrm{CDCl_3}$) $\boldsymbol{\delta}$C: 170.6 (**C**O), 168.7 (**C**O), 156.0 (**C**O), 153.7 ($\mathbf{C}_{\mathrm{Ar}}$), 148.2 ($\mathbf{C}_{\mathrm{Ar}}$), 144.2 ($\mathbf{C}_{\mathrm{Ph}}$), 143.6 ($\mathbf{C}_{\mathrm{FmocAr}}$), 141.3 ($\mathbf{C}_{\mathrm{FmocAr}}$), 139.5 ($\mathbf{C}_{\mathrm{Ar}}$), 129.4 ($\mathbf{C}_{\mathrm{Ph}}$H), 128.1 ($\mathbf{C}_{\mathrm{Ph}}$H), 127.7 ($\mathbf{C}_{\mathrm{FmocAr}}$H), 127.9 ($\mathbf{C}_{\mathrm{FmocAr}}$H), 126.5 ($\mathbf{C}_{\mathrm{Ar}}$), 124.9 ($\mathbf{C}_{\mathrm{FmocAr}}$H), 120.0 ($\mathbf{C}_{\mathrm{FmocAr}}$H), 110.0 ($\mathbf{C}_{\mathrm{Ar}}$H), 108.0 ($\mathbf{C}_{\mathrm{Ar}}$H), 67.3 ($\mathbf{C}_{\mathrm{Fmoc}}\mathrm{H_2}$), 66.9 (S$\mathbf{C}_{\mathrm{Ph3}}$), 64.0 (O$\mathbf{C}\mathrm{H_2C_{Ar}}$), 56.6 (O$\mathbf{C}\mathrm{H_3}$), 56.3 (O$\mathbf{C}\mathrm{H_3}$), 53.7 (NH$\mathbf{C}HC\mathrm{H_2}$S), 47.0 ($\mathbf{C}_{\mathrm{Fmoc}}$H), 41.4 (NH$\mathbf{C}\mathrm{H_2CO}$), 33.4 (NHCH$\mathbf{C}\mathrm{H_2}$S);

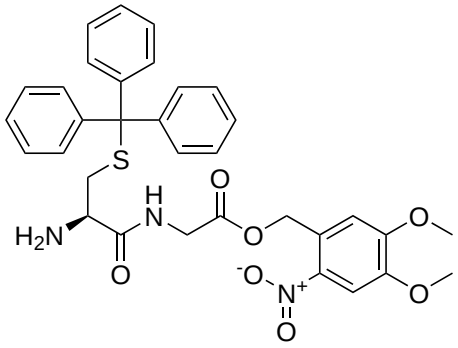
LRMS *m/z* (ESI$^+$): 860 (100% $[\mathrm{M + Na}]^+$);

HRMS *m/z* (ESI$^+$): Found 860.2618 $[\mathrm{M + Na}]^+$ ($\mathrm{C_{48}H_{43}N_3NaO_9S^+}$ requires 860.2618 $[\mathrm{M + Na}]^+$);

IR ($\boldsymbol{\nu}_{\mathbf{max}}$ cm^{-1}): 3370 (w, br), 1720 (w, C=O), 1676 (w, C=O), 1516 (m, N-O), 1446 (w), 1327 (w), 1274 (m), 1177 (w), 1066 (w), 870 (w), 745 (m), 700 (m);

Elemental Analysis: Found C = 68.7%, H = 5.2%, N = 4.9% ($\mathrm{C_{48}H_{43}N_3O_9S}$ requires c = 68.8%, H = 5.2%, N = 5.0%).

(*R*)-4,5-Dimethoxy-2-nitrobenzyl 2-(2-amino-3-(tritylthio)propanamido)acetate



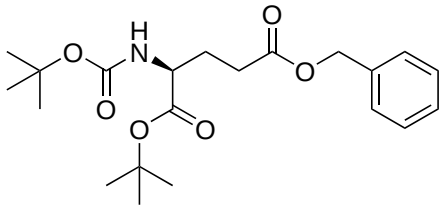
134

20% v/v Piperidine (9.20 g, 10.7 mL, 108 mmol, 15.0 eq) in DMF (42.8 mL) was added to (*R*)-4,5-dimethoxy-2 nitrobenzyl 2-(2-((((9*H*-fluoren-9-yl)methoxy)carbonyl)amino)-3-(tritylthio)propanamido)acetate (**133**) (6.00 g, 7.20 mmol, 1.00 eq) at 0 °C. The resulting solution was stirred at 0 °C under a N_2 atmosphere for 1 h, after which time the reaction was adjudged to be complete by TLC analysis. The reaction was quenched with EtOAc (200 mL), washed with H_2O (3 × 300 mL) and brine (200 mL), dried over $MgSO_4$, and filtered. The solvent was removed under reduced pressure, and the crude mixture further purified by silica gel flash column chromatography, eluting with petroleum ether:EtOAc:NEt_3 = 50:49:1 to EtOAc:NEt_3 = 99:1, to afford (*R*)-4,5-dimethoxy-2-nitrobenzyl 2-(2-amino-3-(tritylthio)propanamino)acetate (**134**) as a yellow foam (2.48 g, 56%).

R_f: 0.52 (Petroleum ether:EtOAc = 1:1);
m.p.: 135 - 137 °C (Petroleum ether/EtOAc);
$[\alpha]_D^{26}$: +14.2 (***c*** 0.95 in $CHCl_3$);
UV λ_{max}/nm (ϵ/$M^{-1}cm^{-1}$): 345 (7160) [MeOH];
^{1}H NMR (500 MHz, $CDCl_3$) **δ**H: 7.72 (1H, s, C_{Ar}**H**), 7.43 (6H, d, J = 7.3 Hz, C_{Ph}**H**), 7.31 (6H, t, J = 7.3 Hz, C_{Ph}**H**), 7.24 (3H, t, J = 7.3 Hz, C_{Ph}**H**), 7.19 (1H, s, C_{Ar}**H**), 6.23 - 6.17 (1H, m, N**H**CH_2CO) 4.97 (2H, s, OC**H**$_2C_{Ar}$), 4.01 (3H, s, OC**H**$_3$), 3.97 (3H, s, OC**H**$_3$), 3.87 (2H, d, J = 5.9 Hz, NHC**H**$_2$CO), 3.34 (1H, ddt, J = 8.3, 3.6, 1.2 Hz, NH_2C**H**CH_2S), 2.86 (1H, dd, J = 13.4, 3.6 Hz, NHCHC**H**$_A$H$_B$S), 2.75 (1H, dd, J = 13.4, 8.3 Hz, $CHCH_A$**H**$_B$S);
^{13}C NMR (125 MHz, $CDCl_3$) **δ**C: 166.6 (**C**O), 164.8 (**C**O), 153.9 (**C**$_{Ar}$), 148.0 (**C**$_{Ar}$), 144.1 (**C**$_{Ph}$), 139.8 (**C**$_{Ar}$), 132.3 (**C**$_{Ar}$), 129.5 (**C**$_{Ph}$H), 128.2 (**C**$_{Ph}$H), 127.1

($\mathbf{C}_{\mathrm{Ph}}$H), 111.0 ($\mathbf{C}_{\mathrm{Ar}}$H), 108.1 ($\mathbf{C}_{\mathrm{Ar}}$H), 67.5 (S$\mathbf{C}_{\mathrm{Ph3}}$), 62.8 (O$\mathbf{C}H_2C_{\mathrm{Ar}}$), 56.5 (O$\mathbf{C}H_3$), 56.4 (O$\mathbf{C}H_3$), 53.1 (NH$_2\mathbf{C}HCH_2$S), 44.9 (NH$\mathbf{C}H_2$CO), 36.0 (NH$_2CH\mathbf{C}H_2$S);
LRMS *m/z* (ESI$^+$): 425 (100%), 616 (30% [M + H]$^+$), 638 (25% [M + Na]$^+$);
HRMS *m/z* (ESI$^+$): Found 638.1932 [M + Na]$^+$ ($C_{33}H_{33}N_3NaO_7S^+$ requires 638.1937 [M + Na]$^+$);
IR ($\boldsymbol{\nu}_{\mathbf{max}}$ cm^{-1}): 3496 (w), 2917 (w), 1681 (s, C=O), 1580 (w, N-H), 1513 (m, N-O), 1456 (w), 1324 (m, N-O), 1270 (s, C-N), 1211 (m, C-O), 1154 (w), 1068 (s, C-N), 978 (w), 869 (m), 794 (w), 746 (m), 697 (s);
Elemental Analysis: Found C = 64.4%, H = 5.6%, N = 6.8% ($C_{33}H_{33}N_3O_7S$ requires c = 64.4%, H = 5.4%, 6.8%).

(*S*)-5-Benzyl 1-*tert*-butyl 2-((*tert*-butoxycarbonyl)amino)pentanedioate



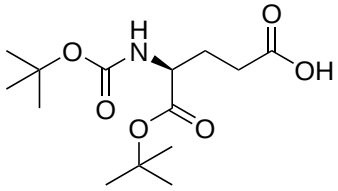
137

A solution of Boc-Glu(OBzl)-OH (**136**) (2.00 g, 5.90 mmol, 1.00 eq), di-*tert*-butyl dicarbonate (2.60 g, 2.72 mL, 11.9 mmol, 2.00 eq), and 4-(dimethylamino)pyridine (220 mg, 1.80 mmol, 0.30 eq) in anhydrous *tert*-butanol (40.0 mL) was stirred at RT under a N_2 atmosphere for 2 h, after which time the reaction was adjudged to be complete by TLC analysis. The solvent was removed under reduced pressure and the residue was dissolved in EtOAc, washed with 10% citric acid (100 mL), and brine (100 mL), dried over $MgSO_4$, and filtered. The solvent was removed under reduced pressure and the resulting oil was purified by silica gel flash column chromatography, eluting with petroleum ether:EtOAc = 9:1, to afford (*S*)-5-benzyl 1-*tert*-butyl 2-((*tert*-butoxycarbonyl)amino)pentanedioate (**137**) as a colourless oil (1.84 g, 79%).

R_f: 0.37 (Petroleum ether:EtOAc = 85:15);
$[\alpha]_D^{26}$: -11.0 (***c*** 0.7 in MeOH) [Literature value: -12.0 (***c*** 1.7 in MeOH][206];
^{1}H NMR (400 MHz, $CDCl_3$) ***δ***H: 7.42 - 7.29 (5H, m, C_{Bzl}**H**), 5.13 (2H, s, OC**H**$_2$$C_{Bzl}$), 5.11 - 5.05 (1H, m, N**H**CHCH$_2$), 4.22 (1H, ddd, J = 7.0, 6.5, 6.5 Hz, NHC**H**CH$_2$), 2.55 - 2.34 (2H, m, NHCHCH$_2$C**H**$_2$), 2.19 (1H, ddt, J = 13.6, 7.0, 6.5 Hz, NHCHC**H**$_A$H$_B$), 2.00 - 1.87 (1H, m, NHCHCH$_A$**H**$_B$), 1.46 (9H, s, OC(C**H**$_3$)$_3$), 1.44 (9H, s, OC(C**H**$_3$)$_3$);
^{13}C NMR (100 MHz, $CDCl_3$) ***δ***H: 172.7 (**C**O), 171.3 (**C**O), 155.4 (**C**O), 135.81 (**C**$_{Bzl}$), 128.6 (**C**$_{Bzl}$H), 128.2 (**C**$_{Bzl}$H), 128.2 (**C**$_{Bzl}$H), 82.2 (O**C**(CH$_3$)$_3$), 79.8 (O**C**(CH$_3$)$_3$), 66.4 (O**C**H$_2$C$_{Bzl}$), 53.4 (NH**C**HCH$_2$), 30.3 (NHCHCH$_2$**C**H$_2$), 28.3 (OC(**C**H$_3$)$_3$), 28.1 (NHCH**C**H$_2$CH$_2$), 28.0 (OC(**C**H$_3$)$_3$);
LRMS *m/z* (ESI$^+$): 326 (100% [M + Na]$^+$);
IR (ν_{max} cm^{-1}): 3422 (w, br), 2978 (m), 1717 (s, C=O), 1582 (w, Ar C-C), 1512 (w), 1448 (w), 1368 (m), 1253 (m), 1161 (s), 1103 (w), 1053 (w), 936 (w), 853 (w), 736 (w);
HPLC (AS-H, IPA: Heptane = 1:19): 9.24 min (0.68 mAU*min, (+)), 9.83 min (44.78 mAU*min, (-)), data are in accordance with the racemate.

Data are concordant with literature values.[206]

(*S*)-5-(*tert*-butoxy)-4-((*tert*-butoxycarbonyl)amino)-5-oxopentanoic acid



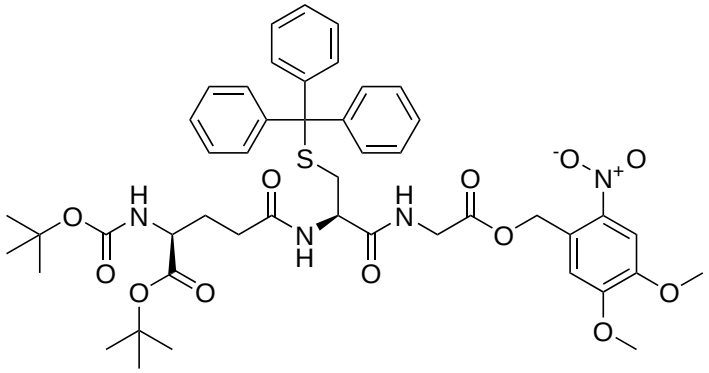
138

(*S*)-5-Benzyl 1-*tert*-butyl 2-((*tert*-butoxycarbonyl)amino)pentanedioate (**137**) (1.00 g, 2.50 mmol, 1.00 eq) and 10% Pd/C (138 mg, 0.10 mmol, 0.05 eq) were stirred in anhydrous MeOH (20.0 mL) at RT under an atmosphere of H_2 for 3 h, after which time the reaction was adjudged to be complete by TLC analysis. The reaction mixture was filtered through a pad of Celite eluting with MeOH. The solvent was removed under reduced pressure to afford (*S*)-5-(*tert*-butoxy)-4-((*tert*-butoxycarbonyl)amino)-5-oxopentanoic acid (**138**) as a colourless oil (616 mg, 81%).

R_f: 0.47 (Petroleum ether:EtOAc = 6:4);
$[\alpha]_D^{26}$: -29.0 (***c*** 0.6 in MeOH) [Literature value: -27.5 (***c*** 0.6 in MeOH)][206];
^{1}H NMR (400 MHz, $CDCl_3$) **δ**H: 5.19 (1H, d, J = 7.6 Hz, N**H**CHCH$_2$CH$_2$), 4.33 - 4.15 (1H, m, NHC**H**CH$_2$CH$_2$), 2.53 - 2.35 (2H, m, NHCHCH$_2$C**H**$_2$), 2.23 - 2.09 (1H, m, NHCHC**H**$_A$H$_B$CH$_2$), 2.00 - 1.83 (1H, m, NHCHCH$_A$**H**$_B$CH$_2$), 1.47 (9H, s, OC(C**H**$_3$)$_3$), 1.45 (9H, s, OC(C**H**$_3$)$_3$);
LRMS *m/z* (ESI$^+$): 326 (100% [M + Na]$^+$);
IR (ν_{max} cm^{-1}): 3422 (w, br, O-H), 2978 (m), 1717 (s, C=O), 1582 (w), 1512 (w), 1448 (w), 1368 (m), 1253 (m, C-N), 1161 (s, C-O), 1103 (w), 1053 (w), 936 (w), 853 (w), 736 (w).

Data are concordant with literature values.[206]

(6*S*, 11*R*)-4,5-Dimethoxy-2-nitrobenzyl-(*tert*-butoxycarbonyl)-2,2-dimethyl-4,9,12-trioxo-11-((tritylthio)methyl)-3-oxa-5,10,13-triazapentadecan-15-oate



135

(*R*)-4,5-Dimethoxy-2-nitrobenzyl 2-(2-amino-3-(tritylthio)propanamido)acetate (**134**) (2.00 g, 3.30 mmol, 1.0 eq), (*S*)-5-(*tert*-butoxy)-4-((*tert*-butoxycarbonyl)amino)-5-oxopentanoic acid (**138**) (1.03 g, 3.40 mmol, 1.05 eq) and *N*,*N*,*N*',*N*'-tetramethyl-*O*-(1*H*-benzotriazol-1-yl)uronium hexafluorophosphate (1.29 g, 3.40 mmol, 1.05 eq) were dissolved in anhydrous DMF (6.00 mL) and the resulting solution was stirred at RT for 10 min under an atmosphere of N_2. After this time, *N*,*N*-diisopropylethylamine (840 mg, 1.53 mL, 6.50 mmol, 2.00 eq) was added dropwise and the resulting solution was stirred at RT under a N_2 atmosphere for 24 h, after which time the reaction was adjudged to be complete by TLC analysis. The reaction was quenched with EtOAc (200 mL), washed with H_2O (3 × 200 mL), and brine (200 mL), dried over $MgSO_4$, and filtered. The solvent was removed under reduced pressure and the crude mixture was purified by silica gel flash column chromatography, eluting with petroleum ether:EtOAc:NEt_3 = 50:49:1 to EtOAc:NEt_3 = 9.9:0.1, to afford (6*S*, 11*R*)-4,5-dimethoxy-2-nitrobenzyl 6-(*tert*-butoxycarbonyl)-2,2-dimethyl-4,9,12-trioxo-11-((tritylthio)methyl)-3-oxa-5,10,13-triazapentadecan-15-oate (**135**) as a yellow foam (1.68 g, 99%).

R_f: 0.15 (Petroleum ether:EtOAc = 1:1);
m.p.: 81 - 84 °C (Petroleum ether/EtOAc);
$[\alpha]_D^{26}$: -4.3 (***c*** 0.9 in $CHCl_3$);
UV λ_{max}/nm (ϵ/$M^{-1}cm^{-1}$): 340 (7260) [MeOH];

^{1}H NMR (500 MHz, $CDCl_3$) δH: 7.72 (1H, s, C_{Ar}**H**), 7.43 (6H, d, J = 7.4 Hz, C_{Ph}**H**), 7.29 (6H, t, J = 7.4 Hz, C_{Ph}**H**), 7.22 (3H, t, J = 7.4 Hz, C_{Ph}**H**), 7.00 (1H, s, C_{Ar}**H**), 6.91 - 6.83 (1H, m, N**H**CH_2CO), 6.29 (1H, d, J = 6.3 Hz, N**H**$CHCH_2S$), 5.57 (2H, d, J = 3.2 Hz, OC**H**$_2C_{Ar}$), 5.23 (1H, d, J = 8.2 Hz, NHC**H**CH_2CH_2), 4.24 - 4.16 (1H, m, NHC**H**CH_2CH_2), 4.12 - 4.02 (2H, m, NHC**H**$_2$CO), 4.03 - 3.99 (4H, m, NHC**H**CH_2S, OC**H**$_3$), 3.96 (3H, s, OC**H**$_3$), 2.85 - 2.81 (1H, m, NHCHC**H**$_A$H$_B$S) 2.62 (1H, dd, J = 13.2, 5.0 Hz, NHCHC**H**$_A$**H**$_B$S) 2.29 - 2.14 (2H, m, NHCHC**H**$_2$C**H**$_2$), 2.14 - 2.05 (1H, m, NHCHC**H**$_A$H$_B$$CH_2$), 1.88 - 1.75 (1H, m, NHCHC**H**$_A$**H**$_B$$CH_2$), 1.43 (9H, s, OC(C**H**$_3$)$_3$), 1.43 (9H, s, OC(C**H**$_3$)$_3$);

^{13}C NMR (125 MHz, $CDCl_3$) δC: 172.4 (**C**O) 171.4 (**C**O), 170.7 (**C**O), 168.9 (**C**O), 155.8 (**C**O), 153.8 (**C**$_{Ar}$), 148.2 (**C**$_{Ar}$), 144.4 (**C**$_{Ph}$), 139.6 (**C**$_{Ar}$), 129.5 (**C**$_{Ph}$H), 128.1 (**C**$_{Ph}$H), 126.9 (**C**$_{Ph}$H), 126.8 (**C**$_{Ar}$), 110.1 (**C**$_{Ar}$H), 108.1 (**C**$_{Ar}$H), 82.4 (O**C**$(CH_3)_3$), 80.1 (OC$(CH_3)_3$), 67.2 (S**C**$_{Ph}$3), 63.9 (O**C**H_2C_{Ar}), 56.7 (O**C**H_3), 56.5 (NH**C**H_2CO), 56.4 (O**C**H_3), 53.2 (NH**C**HCH_2CH_2), 52.2 (NH**C**HCH_2S), 32.5 (NHCH**C**H_2S), 32.3 (NHCHCH_2**C**H_2), 28.3 (OC(**C**$H_3)_3$), 28.2 (NHCH**C**H_2CH_2), 27.9 (OC(**C**$H_3)_3$);

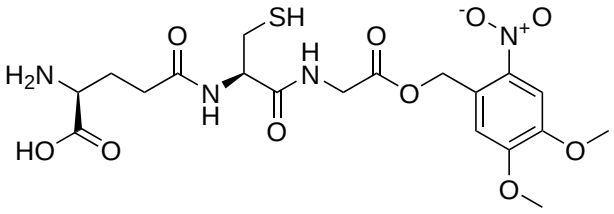
LRMS *m/z* (ESI$^+$): 901 ([M + H]$^+$, 25%), 923 ([M + Na]$^+$, 100%);

HRMS *m/z* (ESI$^+$): Found 923.3516 [M + Na]$^+$ ($C_{47}H_{56}N_4NaO_{12}S^+$ requires 923.3513 [M + Na]$^+$);

IR (ν_{max} cm^{-1}): 3084 (w), 1740 (m, C=O), 1657 (w), 1518 (s, N-O), 1445 (w, Ar C-C), 1370 (m, N-O), 1327 (w), 1276 (s, C-O), 1221 (m, C-N), 1158 (s, C-O), 1066 (m, C-N), 979 (w), 863 (w), 797 (w), 748 (m), 702 (m);

Elemental Analysis: Found C = 62.3%, H = 6.2%, N = 6.2% ($C_{47}H_{56}N_4O_{12}S$ requires c = 62.7%, H = 6.3%, N = 6.2%).

(*S*)-2-Amino-5-(((*R*)-1-((2-((4,5-dimethoxy-2-nitrobenzyl)oxy)-2-oxoethyl)amino)-3-mercapto-1-oxopropan-2-yl)amino)-5-oxopentanoic acid



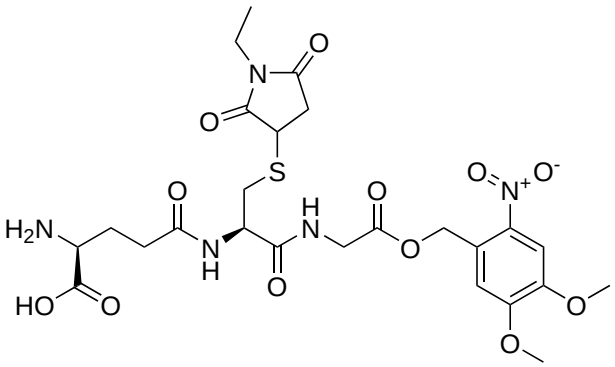
1

To a solution of (6*S*, 11*R*)-4,5-dimethoxy-2-nitrobenzyl 6-(*tert*-butoxycarbonyl)-2,2-dimethyl-4,9,12-trioxo-11-((tritylthio)methyl)-3-oxa-5,10,13-triazapentadecam-15-oate (**135**) (300 mg, 0.30 mmol, 1.00 eq) and triethylsilane (314 mg, 0.42 mL, 2.70 mmol, 8.00 eq) in CH_2Cl_2 (2.55 mL) was added trifluoroacetic acid (3.79 g, 2.55 mL, 33.3 mmol, 100 eq). The reaction vessel was wrapped in foil and the reaction solution was stirred at RT under a N_2 atmosphere for 24 h, after which time the reaction was adjudged to be complete by TLC analysis. The crude reaction solution was concentrated under reduced pressure by azeotropic distillation with cyclohexane, purified by reverse phase silica gel flash column chromatography, eluting with H_2O to H_2O:MeOH = 1:1, and lyophilised to afford (*S*)-2-Amino-5-(((*R*)-1-((2-((4,5-dimethoxy-2-nitrobenzyl)oxy)-2-oxoethyl)a-mino)-3-mercapto-1-oxopropan-2-yl)amino)-5-oxopentanoic acid (**1**) as a hygroscopic pale yellow powder (111 mg, 66%).

R_f: 0.45 (Reverse Phase; H_2O:MeOH = 3:7);
m.p.: 168 - 170 °C (H_2O/MeOH);
UV λ_{max}/nm (ϵ/$M^{-1}cm^{-1}$): 340 (4530) [MeOH];
^{1}H NMR (500 MHz, DMSO) **δ**H: 9.19 (1H, t, J = 5.7 Hz, N**H**CH_2CO), 8.45 (1H, d, J = 8.3 Hz, N**H**$CHCH_2S$), 7.71 (1H, s, C_{Ar}**H**), 7.17 (1H, s, C_{Ar}**H**), 5.46 (1H, d, J = 14.4 Hz, $OCH_AH_BC_{Ar}$), 5.42 (1H, d, J = 14.4 Hz, $OCH_AH_BC_{Ar}$), 4.36 (1H, td, J = 8.3, 4.4 Hz, $NHCHCH_2S$), 3.96 (3H, s, OCH_3), 3.95 - 3.91 (2H, m, $NHCH_2CO$), 3.87 (3H, s, OCH_3), 3.34 (3H, br. s, $NH_2CHCH_2CH_2$, $NHCHCH_2SH$), 3.25 (1H, t, J = 7.0 Hz, $NH_2CHCH_2CH_2$), 2.84 - 2.79 (1H, m, $NHCHCH_AH_BS$), 2.72 - 2.66 (1H, m, $NHCHCH_AH_BS$), 2.41 - 2.26 (2H, m, $NH_2CHCH_2CH_2$), 1.98 - 1.88 (1H, m, $NH_2CHCH_AH_BCH_2$), 1.85 - 1.75 (1H, m, $NH_2CHCH_AH_BCH_2$);
^{13}C NMR (125 MHz, DMSO) **δ**C: 172.0 (**C**OOH), 171.1 (**C**O), 170.0 (**C**O), 169.4 (**C**O), 153.5 (C_{Ar}), 147.9 (C_{Ar}), 139.3 (C_{Ar}), 126.5 (C_{Ar}), 110.8 (C_{Ar}H), 108.2 (C_{Ar}H), 62.9 (OCH_2C_{Ar}), 56.4 (OCH_3), 56.1 (OCH_3), 55.4 ($NHCHCH_2S$), 53.1

($NH_2\mathbf{C}HCH_2CH_2$), 41.0 ($NH\mathbf{C}H_2CO$), 31.5 ($NH_2CHCH_2\mathbf{C}H_2$), 26.8 ($NH_2CH\mathbf{C}H_2CH_2$), 26.0 ($NHCH\mathbf{C}H_2S$);
LRMS *m/z* ($\mathbf{ESI^+}$): 503 ($[M + H]^+$, 20%), 525 ($[M + Na]^+$, 45%), 545 (100%);
HRMS *m/z* ($\mathbf{ESI^+}$): Found 525.1257 $[M + Na]^+$ ($C_{19}H_{26}N_4NaO_{10}S^+$ requires 525.1262 $[M + Na]^+$);
IR ($\boldsymbol{\nu_{max}}$ $\mathbf{cm^{-1}}$): 3598 (w, br, O-H), 3299 (w), 1735 (m, C=O), 1638 (m), 1522 (s, N-O), 1456 (w), 1332 (m, N-O), 1280 (s, C-O), 1223 (m, C-O), 1182 (m, C-N), 1117 (w), 1067 (m, C-N), 978 (w), 872 (w), 800 (w), 754 (w), 717 (w), 662 (w).

(2*S*)-2-Amino-5-(((2*R*)-1-((2-((4,5-dimethoxy-2-nitrobenzyl)oxy)-2-oxoethyl)amino)-3-((1-ethyl-2,5-dioxopyrrolidin-3-yl)thio)-1-oxopropan-2-yl)amino)-5-oxopentanoic acid



2

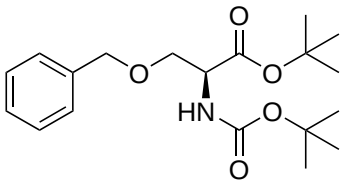
(6*S*,11*R*)-4,5-Dimethoxy-2-nitrobenzyl 6-(*tert*-butoxycarbonyl)-2,2-dimethyl-4,9,12-trioxo-11-((tritylthio)methyl)-3-oxa-5,10,13-triazapentadencan-15-oate (**1**) (60.0 mg, 0.12 mmol, 1.00 eq) and *N*-ethylmaleimide (15.0 mg, 0.12 mmol, 1.00 eq) were dissolved in H_2O (0.30 mL). NaOH (4.80 mg, 0.12 mmol, 1.00 eq) was added and the reaction vessel was wrapped in foil and the reaction solution was stirred at RT under a N_2 atmosphere for 3 h, after which time the reaction was adjudged to be complete by TLC analysis. The crude mixture was directly loaded onto a column and purified by reverse phase silica gel flash column chromatography, eluting with H_2O to H_2O:MeOH = 1:1, and lyophilised to afford (2*S*)-2-amino-5-(((2*R*)-1-((2-((4,5-dimethoxy-2-nitrobenzyl)oxy)-2-oxoethyl)amino-3-((1-ethyl-2,5-dioxopyrrolidin-3-yl)thio)-1-oxopropan-2-yl)amino)-5-oxopentanoic acid (**2**) as a hygroscopic pale yellow powder (37.9 mg, 51%).

R_f: 0.39 (Reverse Phase; H_2O:MeOH = 3:7);
m.p.: 125 - 127 °C (H_2O/MeOH);
$[\alpha]_D^{26}$: +58.2 (***c*** 0.2 in $CHCl_3$)
UV λ_{max}/nm (ϵ/$M^{-1}cm^{-1}$): 340 (5540) [MeOH];
^{1}H NMR (500 MHz, D_2O) δH: 7.61 (1H, s, C_{Ar}**H**), 6.97 (1H, s, C_{Ar}**H**), 5.35 (2H, s, OC**H**$_2C_{Ar}$), 4.62 - 4.56 (1H, m, NHC**H**CH_2S), 4.15 - 4.09 (1H, m, NHC**H**$_A$H$_B$CO), 4.08 - 4.01 (1H, m, NHCH$_A$**H**$_B$CO), 3.90 (3H, s, OC**H**$_3$), 3.84 (3H, s, OC**H**$_3$), 3.72 (1H, t, J = 5.4 Hz, NH_2C**H**CH_2CH_2), 3.44 (2H, qd, J = 7.3, 2.5 Hz, NC**H**$_2CH_3$), 3.31 (1H, br s, SC**H**CH_2) 3.20 - 3.08 (2H, m, NHCHC**H**$_A$H$_B$S, SCHC**H**$_A$H$_B$), 3.05 (1H, dd, J = 14.2, 5.7 Hz, SCHCH$_A$**H**$_B$), 2.88 (1H, dd, J = 14.2, 8.2 Hz, NHCHCH$_A$**H**$_B$S),

2.54 - 2.42 (2H, m, $NH_2CHCH_2C\mathbf{H}_2$), 2.14 - 2.06 (2H, m, $NH_2CHC\mathbf{H}_2CH_2$), 1.04 (3H, t, J = 7.3 Hz, $NCH_2C\mathbf{H}_3$);
^{13}C NMR (125 MHz, D_2O) $\boldsymbol{\delta}$C: 179.3 ($\mathbf{C}$OOH), 179.1 ($\mathbf{C}$OOH), 178.0 ($\mathbf{C}$O), 177.9 ($\mathbf{C}$O), 174.7 ($\mathbf{C}$O), 174.7 ($\mathbf{C}$O), 173.9 ($\mathbf{C}$O), 172.4 ($\mathbf{C}$O), 170.7 ($\mathbf{C}$O), 170.6 ($\mathbf{C}$O), 153.1 ($\mathbf{C}_{Ar}$), 153.1 ($\mathbf{C}_{Ar}$), 147.7 ($\mathbf{C}_{Ar}$), 147.7 ($\mathbf{C}_{Ar}$), 139.6 ($\mathbf{C}_{Ar}$), 138.9 ($\mathbf{C}_{Ar}$), 126.0 ($\mathbf{C}_{Ar}$), 126.0 ($\mathbf{C}_{Ar}$), 111.5 ($\mathbf{C}_{Ar}$H), 111.4 ($\mathbf{C}_{Ar}$H), 108.3 ($\mathbf{C}_{Ar}$H), 108.3 ($\mathbf{C}_{Ar}$H), 64.4 ($O\mathbf{C}H_2C_{Ar}$), 56.4 ($O\mathbf{C}H_3$), 56.1 ($O\mathbf{C}H_3$), 56.1 ($O\mathbf{C}H_3$), 56.0 ($O\mathbf{C}H_3$), 54.0 ($NH_2\mathbf{C}HCH_2CH_2$), 53.2 ($NH\mathbf{C}HCH_2S$), 52.7 ($NH\mathbf{C}HCH_2S$), 48.8 ($S\mathbf{C}HCH_2$), 41.4 ($NH\mathbf{C}H_2CO$), 35.9 ($SCH\mathbf{C}H_2$), 35.5 ($SCH\mathbf{C}H_2$), 34.2 ($N\mathbf{C}H_2CH_3$), 34.2 ($N\mathbf{C}H_2CH_3$), 32.8 ($NHCH\mathbf{C}H_2S$), 32.5 ($NHCH\mathbf{C}H_2S$), 31.2 ($NH_2CHCH_2\mathbf{C}H_2$), 31.1 ($NH_2CHCH_2\mathbf{C}H_2$), 26.1 ($NHCH\mathbf{C}H_2CH_2$), 26.1 ($NHCH\mathbf{C}H_2CH_2$), 11.7 ($NCH_2\mathbf{C}H_3$);
LRMS *m/z* (ESI$^+$): 628 ($[M + H]^+$, 25%), 650 ($[M + Na]^+$, 100%);
HRMS *m/z* (ESI$^+$): Found 650.1733 $[M + Na]^+$ ($C_{25}H_{33}N_5NaO_{12}S^+$ requires 650.1739 $[M + Na]^+$);
IR ($\boldsymbol{\nu}_{\mathbf{max}}$ cm^{-1}): 3590 (w, br, O-H), 3366 (w), 2474 (w), 2179 (w), 2047 (w), 1766 (w), 1698 (m, C=O), 1649 (w), 1579 (w), 1520 (s, N-O), 1402 (m), 1331 (m, N-O), 1276 (s, C-O), 1228 (w), 1181 (m, C-O), 1124 (w), 1069 (m, C-N), 982 (w), 874 (w), 796 (w), 760 (w), 687 (w).

7.6 Amino Acids Residues

(*S*)-*tert*-Butyl 3-(benzyloxy)-2-((*tert*-butoxycarbonyl)amino)propanoate



156

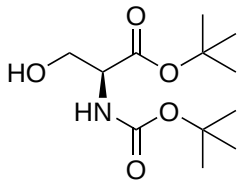
Boc-Ser(Bzl)-OH (**155**) (1.00 g, 3.40 mmol, 1.0 eq), di-*tert*-butyl dicarbonate (1.49 g, 6.80 mmol, 2.0 eq) and 4-(dimethylamino)pyridine (122 mg, 1.00 mmol, 0.30 eq) were dissolved in a solution of anhydrous *tert*-butanol (20.0 mL). The resulting solution was stirred at RT under a N_2 atmosphere for 3 h, after which time the reaction was adjudged to be complete by TLC analysis. The solvent was removed under reduced pressure and the resulting residue was redissolved in EtOAc (100 mL), washed with 10% citric acid (100 mL), and brine (100 mL), dried over $MgSO_4$, and filtered. The solvent was removed under reduced pressure and the resulting oil was purified by silica gel flash column chromatography, eluting with petroleum ether:EtOAc = 7:3, to afford (*S*)-*tert*-butyl 3-(benzyloxy)-2-((*tert*-butoxycarbonyl)amino)propanoate (**156**) as a colourless oil (824 mg, 69%).

$\mathbf{R_f}$: 0.68 (Petroleum ether:EtOAc = 1:1);
$[\boldsymbol{\alpha}]_{\boldsymbol{D}}^{\mathbf{26}}$: -5.5 (***c*** 1.2 in $CHCl_3$) [Literature value: -15.0 (***c*** 1.0 in $CHCl_3$)][207];
^{1}H NMR (400 MHz, $CDCl_3$) $\boldsymbol{\delta}$H: 7.35 - 7.28 (5H, m, $C_{Ar}\mathbf{H}$), 5.38 (1H, d, J = 8.5 Hz, N**H**$CHCH_2$), 4.53 (2H, s, $C_{Ar}\mathbf{H}_2O$), 4.32 (1H, ddd, J = 8.5, 3.0, 3.0 Hz, $NHC\mathbf{H}CH_2$), 3.86 (1H, dd, J = 9.2, 3.0 Hz, $OC\mathbf{H}_AH_BCH$), 3.66 (1H, dd, J = 9.2, 3.0 Hz, $OCH_A\mathbf{H}_BCH$), 1.48 (9H, s, $OC(C\mathbf{H}_3)_3$), 1.48 (9H, s, $OC(C\mathbf{H}_3)_3$;
^{13}C NMR (100 MHz, $CDCl_3$) $\boldsymbol{\delta}$C: 169.7 (**C**O), 155.5 (**C**O), 137.7 ($\mathbf{C}_{Ar}$), 128.4 ($\mathbf{C}_{Ar}$H), 127.7 ($\mathbf{C}_{Ar}$H), 127.6 ($\mathbf{C}_{Ar}$H), 82.0 ($O\mathbf{C}(CH_3)_3$), 79.7 ($O\mathbf{C}(CH_3)_3$), 73.3 ($\mathbf{C}_{Ar}H_2O$), 70.5 ($O\mathbf{C}H_2CH$), 54.5 (**C**H), 28.3 ($OC(\mathbf{C}H_3)_3$), 28.0 ($OC(\mathbf{C}H_3)_3$;
LRMS *m/z* (ESI$^+$): 352 ($[M + H]^+$, 100%), 374 ($[M + Na]^+$, 35%);
HRMS *m/z* (ESI$^+$): Found 374.1938 $[M + Na]^+$ ($C_{19}H_{29}NNaO_5{}^+$ requires 374.1938 $[M + Na]^+$);
IR ($\boldsymbol{\nu}_{\mathbf{max}}$ cm^{-1}): 3446 (w), 2977 (w), 1716 (s, C=O), 1497 (m, Ar C-C), 1363 (m), 1251 (w), 1158 (s, C-O), 1110 (w), 1061 (w), 1021 (w), 851 (w), 740 (m), 699 (w);

Elemental Analysis: Found C = 64.7%, H = 8.3%, N = 4.1% ($C_{19}H_{29}NO_5$ requires c = 64.9%, H = 8.3%, N = 4.0%).

Data are concordant with literature values.[207]

(*S*)-*tert*-Butyl 2-((*tert*-butoxycarbonyl)amino)-3-hydroxypropanoate



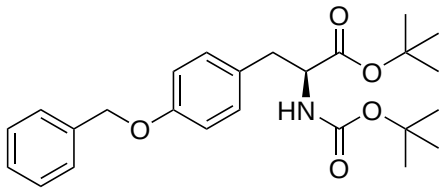
157

10% Pd/C (3.79 g, 3,56 mmol, 0.50 eq) was added to a solution of (*S*)-*tert*-butyl 3-(benzyloxy)-2-((*tert*-butoxycarbonyl)amino)propanoate (**156**) (2.50 g, 7.12 mmol, 1.00 eq) in anhydrous Et_2O (40.0 mL) under a N_2 atmosphere. The suspension was flushed with N_2, followed by H_2. The reaction mixture was stirred at RT under a H_2 atmosphere for 24 h, after which time the reaction was adjudged to be complete by TLC analysis. The suspension was filtered through a pad of Celite and eluted with MeOH. The solvent was removed under reduced pressure to afford (*S*)-*tert*-butyl 2-((*tert*-butoxycarbonyl)amino)-3-hydroxypropanoate (**157**) as a colourless oil (1.76 g, 95%).

R_f: 0.28 (Petrol 40 - 60:EtOAc = 7:3);
$[\alpha]_D^{26}$: -5.4 (***c*** 1.0 in $CHCl_3$) [Literature value: -25.0 (***c*** 2.0 in EtOH)][207];
^{1}H NMR (400 MHz, $CDCl_3$) **δ**H: 5.43 (1H, br s, N**H**), 4.27 (1H, br s, C**H**), 3.95 - 3.89 (2H, m, C$\mathbf{H}_2$), 2.32 (1H, br s, O**H**), 1.49 (9H, s, C(C$\mathbf{H}_3$)$_3$), 1.46 (9H, s, C(C$\mathbf{H}_3$)$_3$);
^{13}C NMR (100 MHz, $CDCl_3$) **δ**C: 170.3 (**C**O), 155.8 (**C**O), 82.6 (O**C**(CH$_3$)$_3$), 79.8 (O**C**(CH$_3$)$_3$), 63.1 (**C**H$_2$), 56.2 (**C**H), 28.1 (C(**C**H$_3$)$_3$), 27.8 (C(**C**H$_3$)$_3$;
LRMS *m/z* (ESI$^+$): 262 ([M + H]$^+$, 100%), 284 ([M + Na]$^+$, 78%);
HRMS *m/z* (ESI$^+$): Found 284.1465 [M + Na]$^+$ ($C^{12}H^{23}NNaO_5^+$ requires 284.1468 [M + Na]$^+$);
IR (ν_{max} cm^{-1}): 3436 (w, br, O-H), 2978 (w), 1709 (s, C=O), 1509 (m), 1452 (w), 1366 (m), 1248 (w), 1160 (s, C-O), 1062 (m, C-N), 850 (w), 746 (w);
Elemental Analysis: Found C = 55.0%, H = 8.8%, N = 5.5% ($C_{12}H_{23}NO_5$ requires c = 55.2%, H = 8.9%, N = 5.4%).

Data are concordant with literature values.[207]

(*S*)-*tert*-Butyl 3-(4-(Benzyloxy)phenyl)-2-((*tert*-butoxycarbonyl)amino)propanoate



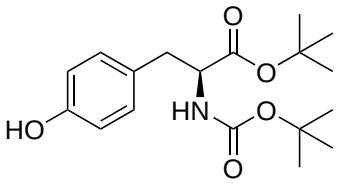
159

Boc-Tyr(Bzl)-OH (**158**) (2.00 g, 5.40 mmol, 1.00 eq), di-*tert*-butyl dicarbonate (2.36 g, 10.8 mmol, 2.00 eq) and 4-(dimethylamino)pyridine (195 mg, 1.60 mmol, 0.30 eq) were dissolved in a solution of anhydrous *tert*-butanol (40.0 mL). The resulting solution was stirred at RT under a N_2 atmosphere for 3 h, after which time the reaction was adjuged to be complete by TLC analysis. The solvent was removed under reduced pressure and the resulting residue was redissolved in EtOAc (100 mL), washed with 10% citric acid (100 mL), and brine (100 mL), dried over $MgSO_4$, and filtered. The solvent was removed under reduced pressure and the resulting oil was purified by silica gel flash column chromatography, eluting with petroleum ether:EtOAc = 9:1, to afford (*S*)-*tert*-butyl 3-(4-(benzyloxy)phenyl)-2-((*tert*-butoxycarbonyl)amino)propanoate (**159**) as a colourless oil (1.75 g, 76%).

R_f: 0.60 (Petroleum ether:EtOAc = 7:3);
$[\alpha]_D^{26}$: +28.0 (***c*** 1.0 in $CHCl_3$);
^{1}H NMR (400 MHz, $CDCl_3$) ***δ***H: 7.46 - 7.30 (5H, m, C_{Bzl}**H**), 7.11 (2H, d, J = 8.7 Hz, C_{Ar}**H**), 6.92 (2H, d, J = 8.7 Hz, C_{Ar}**H**), 5.08 (1H, d, J = 8.1 Hz, N**H**CHCH$_2$), 5.04 (2H, s, C_{Ar}**H**$_2$O), 4.48 - 4.41 (1H, m, NHC**H**CH$_2$), 3.05 - 3.00 (2H, m, NHCHC**H**$_2$), 1.46 (9H, s, OC(C**H**$_3$)$_3$), 1.43 (9H, s, OC(C**H**$_3$)$_3$);
^{13}C NMR (100 MHz, $CDCl_3$) ***δ***C: 170.1 (**C**O), 157.6 (**C**O), 154.9 (**C**$_{Ar}$), 136.9 (**C**$_{Ar}$), 130.4 (**C**$_{Bzl}$H), 130.3 (**C**$_{Ar}$), 128.4 (**C**$_{Ar}$H), 127.7 (**C**$_{Bzl}$H), 127.2 (**C**$_{Bzl}$H), 114.5 (**C**$_{Ar}$H), 81.7 (O**C**(CH$_3$)$_3$), 79.3 (O**C**(CH$_3$)$_3$), 69.7 (Ph**C**H$_2$O), 54.8 (NH**C**HCH$_2$), 37.4 (NHCH**C**H$_2$), 28.1 (OC(**C**H$_3$)$_3$), 27.8 (O**C**(CH$_3$)$_3$;
LRMS *m/z* (ESI$^+$): 428 ([M + H]$^+$, 22%), 450 ([M + Na]$^+$, 80%) 877 (100%);
HRMS *m/z* (ESI$^+$): Found 450.2235 [M + Na]$^+$ ($C_{25}H_{33}NNaO_5^+$ requires 450.2251 [M + Na]$^+$);
IR (ν_{max} cm^{-1}): 3376 (w), 2977 (w), 1710 (s, C=O), 1612 (w), 1503 (m, Ar C-C), 1449 (w), 1365 (m), 1236 (m), 1154 (s, C-O), 1013 (w), 850 (w), 735 (m);

Elemental Analysis: Found C = 70.2%, H = 7.7%, N = 3.4% ($C_{25}H_{33}NO_5$ requires C = 70.2%, H = 7.8%, N = 3.3%).

(*S*)-*tert*-Butyl 2-((*tert*-butoxycarbonyl)amino)-3-(4-hydroxyphenyl)propanoate



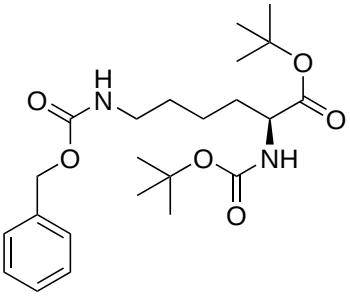
160

10% Pd/C (255 mg, 0.24 mmol, 0.20 eq) was added to a solution of (*S*)-*tert*-butyl 3-(4-(benzyloxy)phenyl-2-((*tert*-butoxycarbonyl)amino)propanoate (**159**) (500 mg, 1.20 mmol, 1.00 eq) in anhydrous MeOH (10.0 mL) under a N_2 atmosphere. The reaction mixture was flushed with N_2, then with H_2. The reaction mixture was stirred at RT under a H_2 atmosphere for 3 h, after which time the reaction was adjudged to be complete by TLC analysis. The suspension was filtered through a pad of Celite and eluted with MeOH. The solvent was removed under reduced pressure to afford (*S*)-*tert*-butyl 2-((*tert*-butoxycarbonyl)amino)-3-(4-hydroxyphenyl)propanoate (**160**) as a colourless foam (399 mg, 96%).

R_f: 0.33 (Petroleum ether:EtOAc = 7:3);
$[\alpha]_D^{26}$: +32.8 (***c*** 1.1 in $CHCl_3$) [Literature value: +36.2 (***c*** 1.0 $CHCl_3$)][208];
^{1}H NMR (400 MHz, $CDCl_3$) **δ**H: 7.02 (2H, d, J = 8.4 Hz, C_{Ar}**H**), 6.74 (2H, d, J = 8.4 Hz, C_{Ar}**H**), 5.05 – 4.96 (2H, m, O**H**, N**H**), 4.45 - 3.37 (1H, m, C**H**), 3.04 - 2.93 (2H, m, C$\mathbf{H}_2$), 1.43 (9H, s, OC(C$\mathbf{H}_3$)$_3$), 1.42 (9H, s, OC(C$\mathbf{H}_3$)$_3$);
^{13}C NMR (100 MHz, $CDCl_3$) **δ**C: 171.3 (**C**O), 155.3 (**C**$_{Ar}$), 155.1 (**C**O), 130.6 (**C**$_{Ar}$H), 130.5 (**C**$_{Ar}$H), 127.8 (**C**$_{Ar}$), 115.4 (**C**$_{Ar}$H), 115.3 (**C**$_{Ar}$H), 82.2 (O**C**(CH$_3$)$_3$, 80.0 (O**C**(CH$_3$)$_3$, 55.1 (**C**H), 37.7 (C$\mathbf{H}_2$), 28.3 (OC(**C**H$_3$)$_3$), 28.0 (OC(**C**H$_3$)$_3$;
LRMS *m/z* (ESI$^+$): 360 ([M + Na]$^+$, 100%);
HRMS *m/z* (ESI$^+$): Found 360.1783 [M + Na]$^+$ ($C_{18}H_{27}NNaO_5^+$ requires 360.1783 [M + Na]$^+$);
IR (ν_{max} cm^{-1}): 3368 (w, br, O-H), 2978 (w), 1692 (s, C=O), 1610 (w), 1511 (m), 1448 (w), 1367 (m), 1254 (m), 1158 (s, C-O), 1058 (w), 840 (w), 739 (w);
Elemental Analysis: Found C = 64.0%, H = 8.0%, N = 4.3% ($C_{18}H_{27}NO_5$ requires c = 64.1%, H = 8.1%, N = 4.2%).

Data are concordant with literature values.[208]

(*S*)-*tert*-Butyl 6-(((benzyloxy)carbonyl)amino-2-((*tert*-butoxycarbonyl)amino) hexanoate



162

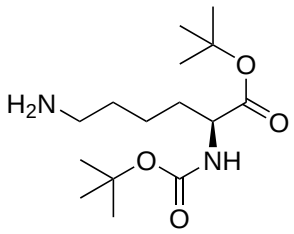
Boc-Lys(Cbz)-OH (**161**) (2.00 g, 5.40 mmol, 1.00 eq), di-*tert*-butyl dicarbonate (2.35 g, 10.8 mmol, 2.00 eq) and 4-(dimethylamino)pyridine (195 mg, 1.60 mmol, 0.30 eq) were dissolved in anhydrous *tert*-butanol (40.0 mL). The resulting solution was stirred at RT under a N_2 atmosphere for 3 h, after which time the reaction was adjudged to be complete by TLC analysis. The solvent was removed under reduced pressure and the resulting residue was redissolved in EtOAc (100 mL), washed with 10% citric acid (100 mL), and brine (100 mL), dried over $MgSO_4$, and filtered. The solvent was removed under reduced pressure and the resulting oil was purified by silica gel flash column chromatography, eluting with petroleum ether:EtOAc = 8:2, to afford (*S*)-*tert*-butyl 6-(((benzyloxy)carbonyl)amino)-2-(*tert*-butoxycarbonyl)amino)hexanoate (**162**) as a colourless oil (2.11 g, 90%).

$\mathbf{R_f}$: 0.38 (Petroleum ether:EtOAc = 7:3);
$[\boldsymbol{\alpha}]_{\boldsymbol{D}}^{\mathbf{26}}$: +4.5 (***c*** 1.3 in $CHCl_3$) [Literature value: +5.5 (***c*** 1.0 $CHCl_3$)][209];
^{1}H NMR (400 MHz, $CDCl_3$) $\boldsymbol{\delta}$H: 7.38 - 7.29 (5H, m, $C_{Ar}\mathbf{H}$), 5.09 (2H, s, $C\mathbf{H}_2O$), 4.25 - 4.14 (1H, m, $NHC\mathbf{H}CH_2$), 3.20 (2H, q, J = 6.6 Hz, $NHC\mathbf{H}_2CH_2$), 1.86 - 1.50 (4H, m, $NHCH_2C\mathbf{H}_2$, $NHCHC\mathbf{H}_2$), 1.46 (9H, s, $OC(C\mathbf{H}_3)_3$), 1.44 (9H, s, $OC(C\mathbf{H}_3)_3$), 1.39 - 1.30 (2H, m, $NHCHCH_2C\mathbf{H}_2$);
^{13}C NMR (100 MHz, $CDCl_3$) $\boldsymbol{\delta}$C: 172.0 ($\mathbf{C}O$), 156.5 ($NH\mathbf{C}OO$), 155.5 ($NH\mathbf{C}OO$), 136.7 ($\mathbf{C}_{Ar}$), 128.4 ($\mathbf{C}_{Ar}H$), 128.0 ($\mathbf{C}_{Ar}H$), 128.0 ($\mathbf{C}_{Ar}H$), 81.6 ($O\mathbf{C}(CH_3)_3$), 79.4 ($O\mathbf{C}(CH_3)_3$), 66.4 ($\mathbf{C}H_2O$), 53.7 ($\mathbf{C}H$), 40.6 ($\mathbf{C}H_2$), 32.4 ($\mathbf{C}H_2$), 29.3 ($\mathbf{C}H_2$), 28.3 ($OC(\mathbf{C}H_3)_3$), 28.0 ($OC(\mathbf{C}H_3)_3$), 22.3 ($\mathbf{C}H_2$);
LRMS *m/z* (ESI$^+$): 437 ($[M + H]^+$, 100%);
HRMS *m/z* (ESI$^+$): Found 459.2466 $[M + Na]^+$ ($C_{23}H_{36}N_2NaO_6^+$ requires 459.2457 $[M + Na]^+$);

IR (ν_{max} cm^{-1}): 3342 (w), 2974 (w), 2934 (w), 1703 (s, C=O), 1523 (m, Ar C-C), 1452 (w), 1365 (m), 1247 (m), 1155 (s, C-O), 1020 (w), 852 (w), 744 (w), 699 (w).

Data are concordant with literature values.[210]

***tert*-Butyl (*tert*-butoxycarbonyl)-*L*-lysinate**



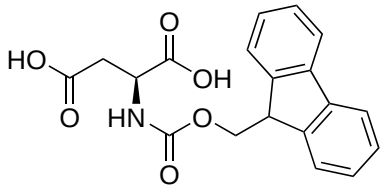
163

10% Pd/C (490 mg, 0.46 mmol, 0.20 eq) was added to a solution of (*S*)-*tert*-butyl 6-(((benzyloxy)carbonyl)amino)-2-(*tert*-butoxycarbonyl)amino)hexanoate (**162**) (1.00 g, 2.29 mmol, 1.00 eq) in anhydrous MeOH (20.0 mL) under a N_2 atmosphere. The suspension was flushed with N_2, then with H_2. The reaction mixture was stirred at RT under a H_2 atmosphere for 3 h, after which time the reaction was adjudged to be complete by TLC analysis. The suspension was filtered through a pad of Celite and eluted with MeOH. The solvent was removed under reduced pressure to afford *tert*-butyl (*tert*-butoxycarbonyl)-*L*-lysinate (**163**) as a colourless oil (678 mg, 98%).

R_f: 0.01 (Petroleum ether:EtOAc = 1:1);
$[\alpha]_D^{26}$: –24.2 (***c*** 1.0 in MeOH) [Literature value: –22.6 (***c*** 1.0 MeOH)][209];
^{1}H NMR (400 MHz, $CDCl_3$) **δ**H: 5.07 (1H, d, J = 7.3 Hz, N**H**CHCH$_2$), 4.20 - 4.11 (1H, m, NHC**H**CH$_2$), 2.68 (2H, t, J = 6.7 Hz, NH$_2$C**H**$_2$CH$_2$), 1.81 - 1.73 (1H, m, NHCHC**H**$_A$H$_B$CH$_2$), 1.67 - 1.56 (3H, m, NHCHCH$_A$**H**$_B$, NH$_2$CH$_2$C**H**$_2$), 1.45 (9H, s, OC(C**H**$_3$)$_3$), 1.43 (9H, s, OC(C**H**$_3$)$_3$), 1.40 - 1.29 (2H, m, NHCHCH$_2$C**H**$_2$) ;
^{13}C NMR (100 MHz, $CDCl_3$) **δ**C: 172.0 (**C**O), 155.4 (NH**C**OO), 81.7 (O**C**(CH$_3$)$_3$), 79.6 (O**C**(CH$_3$)$_3$), 53.9 (**C**H), 41.9 (**C**H$_2$), 33.2 (**C**H$_2$), 32.8 (**C**H$_2$), 28.3 (OC(**C**H$_3$)$_3$), 28.0 (OC(**C**H$_3$)$_3$), 22.5 (**C**H$_2$);
LRMS *m/z* (ESI$^+$): 303 ([M + H]$^+$, 100%);
HRMS *m/z* (ESI$^+$): Found 301.2126 [M - H]$^-$ ($C_{15}H_{29}N_2O_4^-$ requires 301.2128 [M - H]$^-$);
IR (ν_{max} cm^{-1}): 3374 (w, br, O-H), 2975 (w), 2933 (w), 1709 (s, C=O), 1501 (w), 1365 (m), 1248 (m), 1158 (s, C-O), 1053 (w), 853 (w), 737 (m).

Data are concordant with literature values.[209]

(((9*H*-Fluoren-9-yl)methoxy)carbonyl)-*L*-aspartic acid



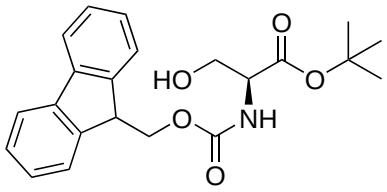
271

Fmoc-Asp-O^{t}Bu (**221**) (500 mg, 1.22 mmol, 1.00 eq) was dissolved in CH_2Cl_2 (2.34 mL). To this solution was added trifluoroacetic acid (3.49 g, 2.34 mL, 30.5 mmol, 25.0 eq) dropwise, followed immediately by triethylsilane (2.13 g, 2.92 mL, 18.3 mmol, 15.0 eq) and the reaction solution was stirred at RT for 7 h, after which time the reaction was adjudged to be complete by TLC analysis. The reaction solution was azeotroped with cyclohexane to afford (((9*H*-fluoren-9-yl)methoxy)carbonyl)-*L*-aspartic acid (**271**) as a colourless oil (535 mg, 97%) and used without further purification.

R_f: 0.69 ($CHCl_3$:MeOH = 9:1);
$[\alpha]_D^{26}$: -5.7 (***c*** 1.0 in MeOH) [Literature value: -4.0 (***c*** 1.0 in MeOH)][211];
^{1}H NMR (400 MHz, MeOD) **δ**H: 7.77 (2H, d, J = 7.5 Hz, C_{FmocAr}**H**), 7.64 (2H, d, J = 7.3 Hz, C_{FmocAr}**H**), 7.37 (2H, t, J = 7.5 Hz, C_{FmocAr}**H**), 7.29 (2H, t, J = 7.3 Hz, C_{FmocAr}**H**), 4.57 (1H, dd, J = 7.0, 5.2 Hz, NHC**H**CH_2) 4.34 - 4.29 (2H, m, C_{Fmoc}**H**$_2$) 4.21 (1H, t, J = 7.2 Hz, C_{Fmoc}**H**), 2.94 - 2.75 (2H, m, NHCHC**H**$_A$H$_B$, NHCHCH$_A$**H**$_B$);
^{13}C NMR (100 MHz, $CDCl_3$) **δ**C: 174.5 (**C**OOH), 174.2 (**C**OOH), 158.5 (NH**C**O), 145.3 ($\mathbf{C}_{FmocAr}$), 142.7 ($\mathbf{C}_{FmocAr}$), 128.9 ($\mathbf{C}_{FmocAr}$H), 128.3 ($\mathbf{C}_{FmocAr}$H), 126.4 ($\mathbf{C}_{FmocAr}$H), 121.0 ($\mathbf{C}_{FmocAr}$H), 68.3 ($\mathbf{C}_{Fmoc}H_2$), 52.0 (NH**C**HCH$_2$), 48.4 ($\mathbf{C}_{Fmoc}$H), 37.3 (NHCH**C**H$_2$);
LRMS *m/z* (ESI$^+$): 378 (49% [M + Na]$^+$), 658 (100%);
HRMS *m/z* (ESI$^+$): Found 354.0977 [M - H]$^-$($C_{19}H_{16}NO_6$-requires 354.0972 [M - H]$^-$);
IR (ν_{max} cm^{-1}): 3341 (w, br, O-H), 2945 (w), 2832 (w), 2387 (w), 1709 (s, C=O), 1523 (w, Ar C-C), 1448 (w), 1416 (w), 1335 (m), 1105 (m), 1055 (m), 1026 (s, C-O), 760 (w), 741 (m), 620 (w).

Data are concordant with literature values.[211]

***tert*-Butyl (((9*H*-fluoren-9-yl)methoxy)carbonyl)-*L*-serinate**



185

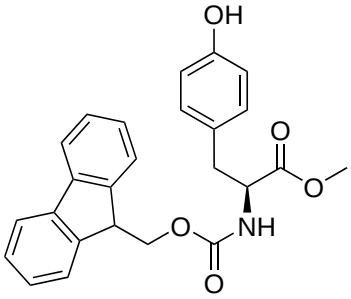
To a solution of *N*-Fmoc-Ser-OH (**184**) (2.00 g, 6.11 mmol, 1.00 eq) in a mixture of EtOAc:cyclohexane (2:1, 45.0 mL) was added *tert*-butyl 2,2,2-trichloroacetimidate (2.67 g, 2.18 mL, 12.2 mmol, 2.00 eq) dropwise and left to stir at RT for 18 h, after which time the reaction was adjudged to be complete by TLC analysis. The resulting solution was washed with sat. aq. $NaHCO_3$(200 mL), H_2O (200 mL), and brine (200 mL), dried over $MgSO_4$, and filtered. The solvent was removed under reduced pressure and the residual oil was purified by silica gel flash column chromatography, eluting with petroleum ether:EtOAc = 8:2, to afford *tert*-butyl (((9*H*-fluoren-9-yl)methoxy)carbonyl)-*L*-serinate (**185**) as a colourless solid (1.20 g, 51%).

R_f: 0.57 (Petroleum ether:EtOAc = 1:1);
m.p.: 129 - 130 °C (Petroleum ether/Et_2O) [Literature value: 130 °C][212];
$[\alpha]_D^{26}$: -3.8 (***c*** 1.0 in MeOH) [Literature value: +6.7 (***c*** 1.0 in $CHCl_3$)][213];
^{1}H NMR (400 MHz, $CDCl_3$) ***δ***H: 7.77 (2H, d, J = 7.6 Hz, C_{FmocAr}**H**), 7.61 (2H, d, J = 7.1 Hz, C_{FmocAr}**H**), 7.41 (2H, t, J = 7.6 Hz, C_{FmocAr}**H**), 7.32 (2H, t, J = 7.1 Hz, C_{FmocAr}**H**), 5.79 (1H, d, J = 7.1 Hz, N**H**CHCH$_2$), 4.42 (2H, d, J = 7.1 Hz, C_{Fmoc}**H**$_2$), 4.37 - 4.31 (1H, m, OCH$_2$C**H**NH), 4.23 (1H, t, J = 7.1 Hz, C_{Fmoc}**H**), 3.97 - 3.91 (2H, m, OC**H**$_2$CHNH), 1.50 (9H, s, OC(C**H**$_3$)$_3$);
^{13}C NMR (100 MHz, $CDCl_3$) ***δ***C: 169.6 (**C**O), 163.8 (**C**O), 143.8 ($\mathbf{C}_{FmocAr}$), 141.3 ($\mathbf{C}_{FmocAr}$), 127.8 ($\mathbf{C}_{FmocAr}$H), 127.1 ($\mathbf{C}_{FmocAr}$H), 125.1 ($\mathbf{C}_{FmocAr}$H), 120.0 ($\mathbf{C}_{FmocAr}$H), 83.0 (O**C**(CH$_3$)$_3$), 67.2 ($\mathbf{C}_{Fmoc}H_2$), 63.7 (O**C**H$_2$CHNH), 56.6 (OCH$_2$**C**HNH), 47.2 ($\mathbf{C}_{Fmoc}$H), 28.0 (OC(**C**H$_3$)$_3$);
LRMS *m/z* (ESI$^+$): 406 (100% [M + Na]$^+$);
HRMS *m/z* (ESI$^+$): Found 406.1625 [M + Na]$^+$ ($C_{22}H_{25}NNaO_5^+$ requires 406.1625 [M + Na]$^+$);
IR (ν_{max} cm^{-1}): 3361 (w, br, O-H), 3067 (w), 2979 (w), 1707 (s, C=O), 1608 (w), 1520 (w), 1478 (w), 1451 (w), 1370 (w), 1343 (w), 1232 (w), 1156 (m, C-O), 1106 (w), 1059 (m, C-O), 912 (w), 829 (m), 759 (m), 740 (m), 648 (w), 621 (w);

HPLC: 13.58 min (100%).

Data are concordant with literature values.[212]

Methyl (((9*H*-fluoren-9-yl)methoxy)carbonyl)-*L*-tyrosinate



247

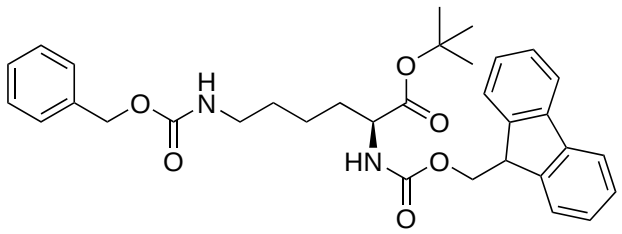
L-Tyrosine methyl ester (500 mg, 2.56 mmol, 1.00 eq) was added to an aqueous solution of $NaHCO_3$ (656 mg, 7.80 mmol, 3.00 eq) in H_2O (10.0 mL). The reaction mixture was stirred at RT until a clear solution was obtained. A solution of *N*-(9-fluorenylmethoxycarbonyloxy)succinimide (950 mg, 2.82 mmol, 1.10 eq) in dioxane (10.0 mL) was added dropwise to the above aqueous solution and the reaction mixture was stirred at RT for 18 h, after which time the reaction was adjudged to be complete by TLC analysis. The reaction mixture was adjusted to pH = 2 with aq. 1 M HCl and extracted with Et_2O (3 × 200 mL). The combined organic extracts were washed with brine (200 mL), dried over $MgSO_4$, and filtered. The solvent was removed under reduced pressure and the obtained residue was further purified by silica gel flash column chromatography, eluting with CH_2Cl_2 to CH_2Cl_2:Et_2O = 9:1, to afford methyl (((9*H*-fluoren-9-yl)methoxy)carbonyl)-*L*-tyrosinate (**247**) as a colourless solid (1.06 g, 99%).

$\mathbf{R_f}$: 0.70 (CH_2Cl_2:Et_2O = 9:1);
m.p.: 122 - 123 °C (Petroleum ether/Et_2O) [Literature value: 122 - 123 °C][214];
$[\boldsymbol{\alpha}]_{\boldsymbol{D}}^{\mathbf{26}}$: +42.3 (***c*** 1.0 in $CHCl_3$) [Literature value: +34.7 (***c*** 0.5 in $CHCl_3$)][214];
^{1}H NMR (400 MHz, $CDCl_3$) $\boldsymbol{\delta}$H: 7.77 (2H, d, J = 7.5 Hz, $C_{FmocAr}\mathbf{H}$), 7.57 (2H, d, J = 7.3 Hz, $C_{FmocAr}\mathbf{H}$), 7.41 (2H, t, J = 7.5 Hz, $C_{FmocAr}\mathbf{H}$), 7.32 (2H, t, J = 7.3 Hz, $C_{FmocAr}\mathbf{H}$), 6.95 (2H, d, J = 8.2 Hz, $C_{TyrAr}\mathbf{H}$), 6.74 (2H, d, J = 8.2 Hz, $C_{TyrAr}\mathbf{H}$), 6.01 (1H, s, $C_{TyrAr}O\mathbf{H}$), 5.37 (1H, d, J = 8.2 Hz, $CH_2CHN\mathbf{H}$), 4.70 - 4.61 (1H, m, $CH_2C\mathbf{H}NH$), 4.49 - 4.33 (2H, m, $C_{Fmoc}\mathbf{H}_2$), 4.21 (1H, t, J = 6.9 Hz, $C_{Fmoc}\mathbf{H}$), 3.74 (3H, s, $COOC\mathbf{H}_3$), 3.08 (1H, dd, J = 14.0, 5.8 Hz, $C\mathbf{H}_AH_BCHNH$), 3.01 (1H, dd, J = 14.0, 5.8 Hz, $CH_A\mathbf{H}_BCHNH$);

^{13}C NMR (100 MHz, $CDCl_3$) δC: 172.2 (**C**O), 155.8 ($\mathbf{C}_{\mathrm{TyrAr}}$OH), 155.1 (**C**O), 143.7 ($\mathbf{C}_{\mathrm{FmocAr}}$), 141.3 ($\mathbf{C}_{\mathrm{FmocAr}}$), 130.4 ($\mathbf{C}_{\mathrm{TyrAr}}$H), 127.7 ($\mathbf{C}_{\mathrm{FmocAr}}$H), 127.2 ($\mathbf{C}_{\mathrm{TyrAr}}$), 127.0 ($\mathbf{C}_{\mathrm{FmocAr}}$H), 125.0 ($\mathbf{C}_{\mathrm{FmocAr}}$H), 120.0 ($\mathbf{C}_{\mathrm{FmocAr}}$H), 115.5 ($\mathbf{C}_{\mathrm{TyrAr}}$H), 67.0 ($\mathbf{C}_{\mathrm{Fmoc}}H_2$), 54.9 ($CH_2$**C**HNH), 52.4 (COO**C**H_3), 47.1 ($\mathbf{C}_{\mathrm{Fmoc}}$H), 37.4 (**C**$H_2$CHNH);
LRMS *m/z* (ESI$^+$): 418 (30% $[M + H]^+$), 440 (100% $[M + Na]^+$);
HRMS *m/z* (ESI$^+$): Found 418.1647 $[M + H]^+$ ($C_{25}H_{24}NO_5{}^+$ requires 418.1649 $[M + H]^+$);
IR (ν_{max} cm^{-1}): 3423 (w), 3320 (w), 3030 (w), 2951 (w), 1722 (m), 1693 (s, C=O), 1614 (w), 1539 (m), 1516 (m), 1442 (m), 1353 (m), 1299 (w), 1262 (m), 1217 (m, C-O), 1147 (w), 1106 (w), 1082 (w), 1046 (w), 1002 (w), 939 (w), 828 (w), 800 (w), 736 (s), 676 (w).

Data are concordant with literature values.[214]

***tert*-Butyl N^2-(((9*H*-fluoren-9-yl)methoxy)carbonyl)-N^6-((benzyloxy)carbonyl)-*L*-lysinate**



189

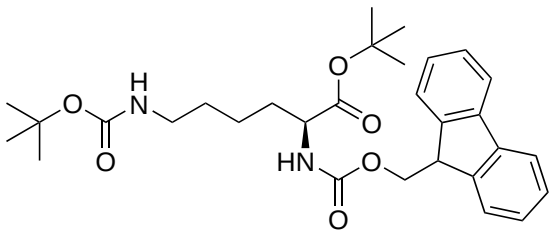
Fmoc-Lys(Z)-OH (**188**) (2.00 g, 3.98 mmol, 1.00 eq), di-*tert*-butyl dicarbonate (1.74 g, 7.96 mmol, 2.00 eq) and 4-(dimethylamino)pyridine (145 mg, 1.19 mmol, 0.30 eq) were dissolved in anhydrous *tert*-butanol (40.0 mL). The reaction solution was stirred at RT under a N_2 atmosphere for 3 h, after which time the reaction was adjudged to be complete by TLC analysis. The solvent was removed under reduced pressure and the resulting residue was redissolved in EtOAc (200 mL), washed with 10% citric acid (200 mL), and brine (200 mL), dried over $MgSO_4$, and filtered. The solvent was removed under reduced pressure prior to further purification by silica gel flash column chromatography, eluting with petroleum ether:EtOAc = 7:3, to afford *tert*-butyl N^2-(((9*H*-fluoren-9-yl)methoxy)carbonyl)-N^6-((benzyloxy)carbonyl)-*L*-lysinate (**189**) as a colourless oil (1.86 g, 84%).

$\mathbf{R_f}$: 0.31 (Petroleum ether:EtOAc = 7:3);
$[\boldsymbol{\alpha}]_{\boldsymbol{D}}^{\mathbf{26}}$: +4.2 (***c*** 1.0 in $CHCl_3$);
^{1}H NMR (400 MHz, $CDCl_3$) $\boldsymbol{\delta}$H: 7.77 (2H, d, J = 7.4 Hz, $C_{FmocAr}\mathbf{H}$), 7.62 (2H, d, J = 7.6 Hz, $C_{FmocAr}\mathbf{H}$), 7.41 (2H, t, J = 7.4 Hz, $C_{FmocAr}\mathbf{H}$), 7.37 – 7.29 (7H, m, $C_{Cbz}\mathbf{H}$, $C_{Cbz}\mathbf{H}$, $C_{FmocAr}\mathbf{H}$), 5.45 (1H, d, J = 8.2 Hz, N$\mathbf{H}$CHCH$_2$), 5.09 (2H, s, $C_{Cbz}C\mathbf{H}_2O$), 4.93 - 4.85 (1H, m, NHC$\mathbf{H}$CH$_2$), 4.40 (2H, d, J = 7.3 Hz, $C_{Fmoc}\mathbf{H}_2$), 4.31 - 4.25 (1H, m, $C_{Fmoc}\mathbf{H}$), 3.26 - 3.11 (2H, m, NHC$\mathbf{H}_2$CH$_2$), 1.91 - 1.81 (1H, m, NHCHC$\mathbf{H}_A$H$_B$CH$_2$), 1.75 - 1.63 (1H, m, NHCHCHCH$_A\mathbf{H}_B$CH$_2$), 1.62 - 1.50 (2H, m, NHCH$_2$C$\mathbf{H}_2$), 1.48 (9H, s, OC(C$\mathbf{H}_3$)$_3$), 1.44 - 1.31 (2H, m, NHCHCH$_2$C$\mathbf{H}_2$);
^{13}C NMR (100 MHz, $CDCl_3$) $\boldsymbol{\delta}$C: 171.5 (**C**O), 156.4 (**C**O), 155.9 (**C**O), 143.8 ($\mathbf{C}_{FmocAr}$), 143.7 ($\mathbf{C}_{FmocAr}$), 141.2 ($\mathbf{C}_{Cbz}$H), 136.5 ($\mathbf{C}_{Cbz}$), 128.4 ($\mathbf{C}_{Cbz}$H), 128.0 ($\mathbf{C}_{FmocAr}$H), 127.6 ($\mathbf{C}_{FmocAr}$H), 126.9 ($\mathbf{C}_{Cbz}$H), 125.0 ($\mathbf{C}_{FmocAr}$H), 119.9 ($\mathbf{C}_{FmocAr}$H), 82.0 (O**C**(CH$_3$)$_3$), 66.8 ($\mathbf{C}_{Fmoc}$H$_2$), 66.5 ($C_{Cbz}\mathbf{C}$H$_2$O), 54.0 (NH**C**HCH$_2$), 47.1 ($\mathbf{C}_{Fmoc}$H), 40.5 (NH**C**H$_2$CH$_2$), 32.3 (NHCH**C**H$_2$), 29.3 (NHCH$_2\mathbf{C}$H$_2$), 27.9 (OC(**C**H$_3$)$_3$), 22.1 (NHCHCH$_2\mathbf{C}$H$_2$);

LRMS *m/z* (ESI$^+$): 559 (100% $[M + H]^+$);
HRMS *m/z* (ESI$^+$): Found 581.2622 $[M + Na]^+$ ($C_{33}H_{38}N_2NaO_6^+$ requires 581.2622 $[M + Na]^+$);
IR (ν_{max} cm^{-1}): 3330 (w), 2945 (w), 2361 (s), 2338 (s), 1718 (s, C=O), 1525 (m, Ar C-C), 1452 (w), 1368 (w), 1234 (m), 1155 (m, C-O), 1033 (w), 740 (w), 672 (w), 618 (m).

Data are concordant with literature values.[215]

***tert*-Butyl N^2-(((9*H*-fluoren-9-yl)methoxy)carbonyl)-N^6-(*tert*- butoxycarbonyl)-*L*-lysinate**



191

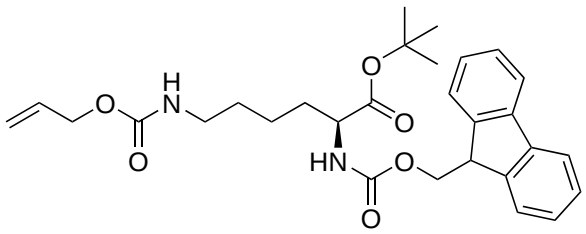
Fmoc-Lys(Boc)-OH (**190**) (1.00 g, 2.13 mmol, 1.00 eq), di-*tert*-butyl dicarbonate (930 mg, 4.26 mmol, 2.00 eq) and 4-(dimethylamino)pyridine (78.1 mg, 0.64 mmol, 0.30 eq) were dissolved in anhydrous *tert*-butanol (20.0 mL). The reaction solution was stirred at RT under a N_2 atmosphere for 3 h, after which time the reaction was adjudged to be complete by TLC analysis. The solvent was removed under reduced pressure and the resulting residue was redissolved in Et_2O (100 mL), washed with 10% citric acid (100 mL), sat. aq. $NaHCO_3$ (100 mL), and brine (100 mL), dried over $MgSO_4$, and filtered. The solvent was removed under reduced pressure and the crude residue was further purified by silica gel flash column chromatography, eluting with petroleum ether:Et_2O = 1:1 to Et_2O, to afford *tert*-butyl N^2-(((9*H*-fluoren-9-yl)methoxy)carbonyl)-N^6-(*tert*-butoxycarbonyl)-*L*-lysinate (**191**) as a colourless solid (2.13 g, 95%).

R_f: 0.54 (Petroleum ether:Et_2O = 1:1);
m.p.: 140 - 143 °C (Petroleum ether/Et_2O);
$[\alpha]_D^{26}$: +4.5 (***c*** 1.1 in $CHCl_3$);
^{1}H NMR (400 MHz, $CDCl_3$) δH: 7.77 (2H, d, J = 7.6 Hz, C_{FmocAr}**H**), 7.62 (2H, d, J = 7.3 Hz, C_{FmocAr}**H**), 7.41 (2H, t, J = 7.6 Hz, C_{FmocAr}**H**), 7.32 (2H, t, J = 7.3 Hz, C_{FmocAr}**H**), 5.41 (1H, d, J = 8.0 Hz, N**H**CHCH$_2$), 4.59 (1H, br s, N**H**CH$_2$CH$_2$), 4.44 - 4.36 (2H, m, C_{Fmoc}**H**$_2$), 4.29 - 4.19 (2H, m, C_{Fmoc}**H**, NHC**H**CH$_2$), 3.12 (2H, q, J = 5.8 Hz, NHC**H**$_2$CH$_2$), 1.91 - 1.78 (1H, m, NHCHC**H**$_A$H$_B$CH$_2$), 1.73 - 1.62 (1H, m, NHCHCH$_A$**H**$_B$CH$_2$), 1.58 - 1.50 (2H, m, NHCH$_2$C**H**$_2$), 1.48 (9H, s, OC(C**H**$_3$)$_3$), 1.44 (9H, s, OC(C**H**$_3$)$_3$), 1.42 - 1.31 (2H, m, NHCHCH$_2$C**H**$_2$);
^{13}C NMR (100 MHz, $CDCl_3$) δC: 171.7 (**C**O), 156.1 (**C**O), 151.9 (**C**O), 144.0 ($\mathbf{C}_{FmocAr}$), 141.3 ($\mathbf{C}_{FmocAr}$), 127.7 ($\mathbf{C}_{FmocAr}$H), 127.1 ($\mathbf{C}_{FmocAr}$H), 125.2 ($\mathbf{C}_{FmocAr}$H), 120.0 ($\mathbf{C}_{FmocAr}$H), 82.2 (O**C**(CH$_3$)$_3$), 79.5 (O**C**(CH$_3$)$_3$), 67.0 ($\mathbf{C}_{Fmoc}$H$_2$),

54.2 (NH**C**HCH$_2$), 47.2 (**C**$_{\text{Fmoc}}$H), 40.2 (NH**C**H$_2$CH$_2$), 32.5 (NHCH**C**H$_2$), 29.6 (NHCH$_2$**C**H$_2$), 28.5 (OC(**C**H$_3$)$_3$), 28.1 (OC(**C**H$_3$)$_3$), 22.3 (NHCHCH$_2$**C**H$_2$);
LRMS *m/z* (ESI$^+$): 369 (100%), 525 (90% [M + H]$^+$), 547 (80% [M + Na]$^+$);
HRMS *m/z* (ESI$^+$): Found 547.2781 [M + Na]$^+$ ($C_{30}H_{40}N_2NaO_6^+$ requires 547.2779 [M + Na]$^+$);
IR (ν_{max} cm^{-1}): 3345 (w), 2978 (w), 2933 (w), 2863 (w), 2362 (w), 1705 (s, C=O), 1518 (m, Ar C-C), 1450 (w), 1392 (w), 1367 (w), 1249 (m), 1161 (s, C-O), 1107 (w), 1043 (w), 849 (w), 757 (s), 742 (s), 666 (w), 620 (w).

Data are concordant with literature values.[216]

***tert*-Butyl N^2-(((9*H*-fluoren-9-yl)methoxy)carbonyl-N^6-((allyloxy)carbonyl)-*L*-lysinate**



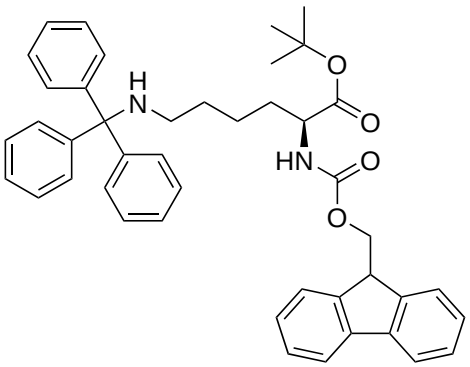
193

Method A:
Fmoc-Lys(Alloc)-OH (**192**) (1.00 g, 2.21 mmol, 1.00 eq), di-*tert*-butyl dicarbonate (964 mg, 4.42 mmol, 2.00 eq) and 4-(dimethylamino)pyridine (80.6 mg, 0.66 mmol, 0.30 eq) were dissolved in anhydrous *tert*-butanol (20.0 mL). The reaction solution was stirred at RT under an Ar atmosphere for 3 h, after which time the reaction was adjudged to be complete by TLC analysis. The solvent was removed under reduced pressure and the crude residue was redissolved in Et_2O (100 mL), washed with 10% citric acid (100 mL), sat. aq. $NaHCO_3$ (100 mL), and brine (100 mL), dried over $MgSO_4$, and filtered. The solvent was removed under reduced pressure and further purified by silica gel flash column chromatography, eluting with hexane:EtOAc = 2:1 to afford *tert*-butyl N^2-(((9*H*-fluoren-9-yl)methoxy)carbonyl)-N^6-((allyloxy)carbonyl)-*L*-lysinate (**193**) as a colourless solid (326 mg, 29%).

Method B:
Fmoc-Lys(Alloc)-OH (**192**) (1.00 g, 2.21 mmol, 1.00 eq) was dissolved in anhydrous *tert*-butanol (5.28 mL, 55.3 mmol, 25.0 eq). To this solution was added pyridine (2.18 g, 2.23 mL, 27.6 mmol, 1.10 eq). The solution was cooled to – 5 °C and $POCl_3$ (0.23 mL, 2.43 mmol, 1.10 eq) was added dropwise. The reaction solution was stirred at – 5 °C for 5 h, after which time the reaction was adjudged to be complete by TLC analysis. The reaction was quenched with H_2O (100 mL) and extracted with Et_2O (100 mL). The organic layer was washed with aq. 1 M HCl (100 mL), sat. aq. $NaHCO_3$ (100 mL), H_2O (100 mL), and brine (100 mL), dried over $MgSO_4$, and filtered. The solvent was removed under reduced pressure and the crude residue was further purified by silica gel flash column chromatography, eluting with hexane:EtOAc = 2:1, to afford *tert*-butyl N^2-(((9*H*-fluoren-9-yl)methoxy)carbonyl)-N^6-((allyloxy)carbonyl)-*L*-lysinate (**193**) as a colourless solid (797 mg, 71%).

R_f: 0.21 (Hexane:EtOAc = 2:1);
m.p.: 77 - 79 °C (Petroleum ether/Et_2O);
$[\alpha]_D^{26}$: -9.4 (***c*** 1.1 in MeOH);
^{1}H NMR (400 MHz, $CDCl_3$) **δ**H: 7.77 (2H, d, J = 7.6 Hz, $C_{FmocAr}\mathbf{H}$), 7.62 (2H, d, J = 7.3 Hz, $C_{FmocAr}\mathbf{H}$), 7.40 (2H, t, J = 7.6 Hz, $C_{FmocAr}\mathbf{H}$), 7.32 (2H, t, J = 7.3 Hz, $C_{FmocAr}\mathbf{H}$), 5.89 (1H, ddt, J = 16.7, 10.7, 5.2 Hz, $C_{Alloc}H$), 5.51 (1H, d, J = 7.9 Hz, N**H**CHCH_2), 5.27 (1H, d, J = 16.9 Hz, $C_{Alloc}\mathbf{H}_AH_B$), 5.18 (1H, d, J = 10.7 Hz, $C_{Alloc}H_A\mathbf{H}_B$), 4.98 - 4.88 (1H, m, N**H**CH_2CH_2), 4.54 (2H, d, J = 5.2 Hz, C_{Alloc}HC$\mathbf{H}_2$O), 4.39 (2H, d, J = 7.2 Hz, $C_{Fmoc}\mathbf{H}_2$), 4.31 - 4.24 (1H, m, NHC**H**CH_2), 4.23 (1H, t, J = 7.2 Hz, $C_{Fmoc}\mathbf{H}$), 3.19 (2H, q, J = 6.2 Hz, NHC$\mathbf{H}_2$CH_2), 1.90 - 1.78 (1H, m, NHCHC$\mathbf{H}_A$H$_B$CH_2), 1.74 - 1.62 (1H, m, NHCHC$H_A\mathbf{H}_B$CH_2), 1.61 - 1.51 (2H, m, NHCH_2C$\mathbf{H}_2$), 1.48 (9H, s, OC(C$\mathbf{H}_3$)$_3$), 1.43 - 1.31 (2H, m, NHCHCH_2C$\mathbf{H}_2$);
^{13}C NMR (100 MHz, $CDCl_3$) **δ**C: 171.5 (**C**O), 156.3 (**C**O), 155.9 (**C**O), 143.8 ($\mathbf{C}_{FmocAr}$), 141.2 ($\mathbf{C}_{FmocAr}$), 132.9 ($\mathbf{C}_{Alloc}$H), 127.6 ($\mathbf{C}_{FmocAr}$H), 127.0 ($\mathbf{C}_{FmocAr}$H), 125.0 ($\mathbf{C}_{FmocAr}$H), 119.9 ($\mathbf{C}_{FmocAr}$H), 117.5 ($\mathbf{C}_{Alloc}H_2$), 82.1 (O**C**(CH_3)$_3$), 66.8 ($\mathbf{C}_{Fmoc}H_2$), 65.3 (C_{Alloc}H**C**H_2O), 54.0 (NH**C**HCH_2), 47.1 ($\mathbf{C}_{Fmoc}$H), 40.5 (NH**C**H_2CH_2), 32.3 (NHCH**C**H_2), 29.3 (NHCH_2**C**H_2), 27.9 (OC(**C**H_3)$_3$), 22.1 (NHCHCH_2**C**H_2);
LRMS *m/z* (ESI$^+$): 509 (23% [M + H]$^+$), 531 (48% [M + Na]$^+$), 811 (100%);
HRMS *m/z* (ESI$^+$): Found 509.2644 [M + H]$^+$ ($C_{29}H_{37}N_2O_6^+$ requires 509.2646 [M + H]$^+$);
IR (ν_{max} cm^{-1}): 3332 (w), 3067 (w), 2940 (w), 2865 (w), 2383 (w), 2348 (w), 2304 (w), 1705 (s, C=O), 1531 (m, Ar C-C), 1450 (w), 1367 (w), 1324 (w), 1249 (m), 1156 (m, C-O), 1107 (m, C-O), 1083 (w), 992 (w), 930 (w), 847 (w), 760 (w), 741 (m), 644 (w), 624 (w).

***tert*-Butyl N^2-(((9*H*-fluoren-9-yl)methoxy)carbonyl)-N^6-trityl-*L*-lysinate**



195

Fmoc-Lys(Trt)-OH (**194**) (2.50 g, 4.09 mmol, 1.00 eq), di-*tert*-butyl dicarbonate (1.88 mL, 8.19 mmol, 2.00 eq) and 4-(dimethylamino)pyridine (150 mg, 1.23 mmol, 0.30 eq) were dissolved in anhydrous *tert*-butanol (50.0 mL). The reaction solution was stirred at RT under an Ar atmosphere for 2 h, after which time the reaction was adjudged to be complete by TLC analysis. The solvent was removed under reduced pressure and the crude residue was redissolved in EtOAc (250 mL), washed with 10% citric acid (250 mL), sat. aq. $NaHCO_3$ (250 mL), and brine (250 mL), dried over $MgSO_4$, and filtered. The solvent was removed under reduced pressure and the crude residue was further purified by silica gel flash column chromatography, eluting with $CHCl_3$, to afford *tert*-butyl N^2-(((9*H*-fluoren-9-yl)methoxy)carbonyl)-N^6-trityl-*L*-lysinate (**195**) as a colourless foam (1.50 g, 55%).

$\mathbf{R_f}$: 0.72 ($CHCl_3$:Acetone = 9:1);
m.p.: 62 - 65 °C (Petroleum ether/Acetone);
$[\boldsymbol{\alpha}]_{\boldsymbol{D}}^{\mathbf{26}}$: -11.6 (***c*** 1.0 in MeOH);
^{1}H NMR (400 MHz, $CDCl_3$) $\boldsymbol{\delta}$H: 7.77 (2H, d, J = 7.3 Hz, $C_{\text{FmocAr}}\mathbf{H}$), 7.61 (2H, d, J = 7.3 Hz, $C_{\text{FmocAr}}\mathbf{H}$), 7.49 (6H, d, J = 7.4 Hz, $C_{\text{Trt}}\mathbf{H}$), 7.40 (2H, t, J = 7.3 Hz, $C_{\text{FmocAr}}\mathbf{H}$), 7.34 - 7.25 (8H, m, $C_{\text{FmocAr}}\mathbf{H}$, $C_{\text{Trt}}\mathbf{H}$), 7.19 (3H, t, J = 7.4 Hz, $C_{\text{Trt}}\mathbf{H}$), 5.37 - 5.27(1H, m, N**H**CHCH$_2$), 5.12 - 5.01 (1H, m, N**H**CH$_2$CH$_2$), 4.40 (2H, d, J = 7.0 Hz, $C_{\text{Fmoc}}\mathbf{H}_2$), 4.36 - 4.26 (1H, m, NHC**H**CH$_2$), 4.23 (1H, t, J = 7.0 Hz, $C_{\text{Fmoc}}\mathbf{H}$), 2.21 - 2.06 (2H, m, NHC$\mathbf{H}_2$CH$_2$), 1.89 - 1.74 (1H, m, NHCHC$\mathbf{H}_\text{A}$H$_\text{B}$CH$_2$), 1.71 - 1.58 (1H, m, NHCHCH$_\text{A}\mathbf{H}_\text{B}CH_2$), 1.58 - 1.53 (2H, m, NHCH$_2$C$\mathbf{H}_2$), 1.48 (9H, s, OC(C$\mathbf{H}_3$)$_3$), 1.31 - 1.22 (2H, m, NHCHCH$_2$C$\mathbf{H}_2$);

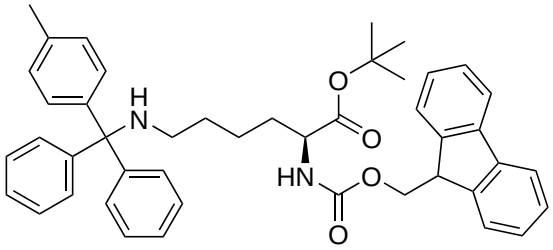
^{13}C NMR (100 MHz, $CDCl_3$) δC: 171.7 (**C**O), 155.8 (**C**O), 146.2 ($\mathbf{C}_{\mathrm{TrtAr}}$), 143.8 ($\mathbf{C}_{\mathrm{FmocAr}}$), 141.3 ($\mathbf{C}_{\mathrm{FmocAr}}$), 128.6 ($\mathbf{C}_{\mathrm{TrtAr}}$H), 127.7 ($\mathbf{C}_{\mathrm{TrtAr}}$H), 127.6 ($\mathbf{C}_{\mathrm{FmocAr}}$H), 127.0 ($\mathbf{C}_{\mathrm{FmocAr}}$H), 126.1 ($\mathbf{C}_{\mathrm{TrtAr}}$H), 125.1 ($\mathbf{C}_{\mathrm{FmocAr}}$H), 119.3 ($\mathbf{C}_{\mathrm{FmocAr}}$H), 82.0 (O**C**$(CH_3)_3$), 70.8 ($\mathbf{C}_{\mathrm{Trt}}$NH), 66.8 ($\mathbf{C}_{\mathrm{Fmoc}}H_2$), 54.2 (NH**C**HCH$_2$), 47.2 ($\mathbf{C}_{\mathrm{Fmoc}}$H), 43.3 (NH**C**H$_2CH_2$), 32.9 (NHCH**C**H$_2$), 30.5 (NHCH$_2$**C**H$_2$), 28.0 (OC(**C**H$_3$)$_3$), 22.9 (NHCHCH$_2$**C**H$_2$);

LRMS *m/z* (ESI$^+$): 243 (100%), 667 (56% $[M + H]^+$);

HRMS *m/z* (ESI$^+$): Found 667.3518 $[M + H]^+$ ($C_{44}H_{47}N_2O_4^+$ requires 667.3530 $[M + H]^+$);

IR (ν_{max} cm^{-1}): 3337 (w), 3059 (w), 2976 (w), 2934 (w), 2858 (w), 2381 (w), 2349 (w), 2303 (w), 1722 (s, C=O), 1597 (w), 1510 (m, Ar C-C), 1449 (m), 1368 (w), 1343 (w), 1248 (w), 1218 (w), 1154 (m), 1107 (m, C-O), 1035 (m), 901 (w), 847 (w), 762 (m), 741 (m), 706 (s), 645 (w), 622 (w).

***tert*-Butyl N^2-(((9*H*-fluoren-9-yl)methoxy)carbonyl)-N^6-(diphenyl(*p*-tolyl)methyl)-*L*-lysinate**



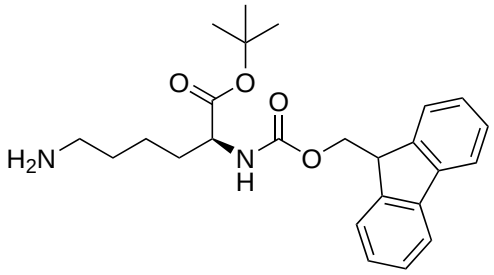
197

Fmoc-Lys(Mtt)-OH (**196**) (1.00 g, 1.60 mmol, 1.00 eq), di-*tert*-butyl dicarbonate (698 mg, 3.20 mmol, 2.00 eq) and 4-(dimethylamino)pyridine (58.6 mg, 0.48 mmol, 0.30 eq) were dissolved in anhydrous *tert*-butanol (20.0 mL). The reaction solution was stirred at RT under an Ar atmosphere for 2 h, after which time the reaction was adjudged to be complete by TLC analysis. The reaction was quenched with Et_2O (50.0 mL) and the solvent was removed under reduced pressure. The resulting residue was dissolved in Et_2O (100 mL), washed with 10% citric acid (100 mL), sat. aq. $NaHCO_3$ (100 mL), and brine (100 mL), dried over $MgSO_4$, and filtered. The solvent was removed under reduced pressure and the crude residue was further purified by silica gel flash column chromatography, eluting with CH_2Cl_2 to CH_2Cl_2:Et_2O = 9:1, to afford *tert*-butyl N^2-(((9*H*-fluoren-9-yl)methoxy)carbonyl-N^6-(diphenyl(*p*-tolyl)methyl)-*L*-lysinate (**197**) as a colourless foam (772 mg, 71%).

R_f: 0.63 (CH_2Cl_2:Et_2O = 9:1);
m.p.: 58 - 60 °C (Petroleum ether/Et_2O);
$[\alpha]_D^{26}$: +7.1 (***c*** 1.2 in $CHCl_3$);
^{1}H NMR (400 MHz, $CDCl_3$) ***δ***H: 7.78 (2H, d, J = 7.3 Hz, C_{FmocAr}**H**), 7.62 (2H, d, J = 7.3 Hz, C_{FmocAr}**H**), 7.50 (4H, d, J = 7.8 Hz, C_{MttPh}**H**), 7.44 - 7.36 (4H, m, C_{FmocAr}**H**, C_{MttPh}**H**), 7.35 - 7.28 (6H, m, C_{FmocAr}**H**, C_{MttPh}**H**), 7.23 - 7.16 (2H, m, C_{MttPh}**H**), 7.10 (2H, d, J = 7.8 Hz, C_{MttPh}**H**) 5.33 (1H, d, J = 8.1 Hz, N**H**$CHCH_2$), 4.41 (2H, d, J = 7.0 Hz, C_{Fmoc}**H**$_2$), 4.33 - 4.20 (2H, m, C_{Fmoc}**H**, NHC**H**CH_2), 2.33 (3H, s, $C_{MttPh}C$**H**$_3$), 2.21 - 2.09 (2H, m, NHC**H**$_2CH_2$), 1.90 - 1.75 (1H, m, NHCHC**H**$_A$H$_B$$CH_2$), 1.71 - 1.61 (1H, m, NHCHCH_A**H**$_B$$CH_2$), 1.57 - 1.52 (2H, m, $NHCH_2$C**H**$_2$), 1.49 (9H, s, OC(C**H**$_3$)$_3$), 1.37 (2H, qn, J = 7.0 Hz, $NHCHCH_2$C**H**$_2$);
^{13}C NMR (100 MHz, $CDCl_3$) ***δ***C: 171.7 (**C**O), 155.8 (**C**O), 146.3 ($\mathbf{C}_{MttPh}$), 143.9 ($\mathbf{C}_{MttPh}$), 143.2 ($\mathbf{C}_{FmocAr}$), 141.2 ($\mathbf{C}_{FmocAr}$), 135.6 ($\mathbf{C}_{MttPh}$), 128.6 ($\mathbf{C}_{MttPh}$H), 128.5

($\mathbf{C}_{\mathrm{MttPh}}$H), 128.4 ($\mathbf{C}_{\mathrm{MttPh}}$H), 127.7 ($\mathbf{C}_{\mathrm{MttPh}}$H), 127.6 ($\mathbf{C}_{\mathrm{FmocAr}}$H), 127.0 ($\mathbf{C}_{\mathrm{FmocAr}}$H), 126.1 ($\mathbf{C}_{\mathrm{MttPh}}$H), 125.1 ($\mathbf{C}_{\mathrm{FmocAr}}$H), 119.9 ($\mathbf{C}_{\mathrm{FmocAr}}$H) 82.0 (O$\mathbf{C}$($CH_3$)$_3$), 70.5 (NH$\mathbf{C}(Ph)_2$(Ph$CH_3$)), 66.8 ($\mathbf{C}_{\mathrm{Fmoc}}$H), 54.2 (NH$\mathbf{C}HCH_2$), 47.2 ($\mathbf{C}_{\mathrm{Fmoc}}$H), 43.3 (NH$\mathbf{C}H_2CH_2$), 32.9 (NHCH$\mathbf{C}H_2$), 30.5 (NHC$H_2\mathbf{C}H_2$), 28.0 (OC($\mathbf{C}H_3$)$_3$), 22.9 (NHCHC$H_2\mathbf{C}H_2$), 20.9 (Ph$\mathbf{C}H_3$);
LRMS m/z (ESI$^-$): 715 (100% [M + Cl]$^-$);
HRMS *m/z* (ESI$^+$): Found 681.3683 [M + H]$^+$ ($C_{45}H_{49}N_2O_4^+$ requires 681.3687 [M + H]$^+$);
IR ($\boldsymbol{\nu}_{\mathbf{max}}$ cm^{-1}): 3059 (w), 2928 (w), 2857 (w), 1719 (s, C=O), 1509 (m, Ar C-C), 1449 (m), 1367 (w), 1346 (w), 1218 (w), 1153 (s, C-O), 1108 (w), 1037 (w), 904 (w), 847 (w), 816 (m), 759 (s), 741 (s), 704 (s), 642 (w), 617 (w).

***tert*-Butyl (((9*H*-fluoren-9-yl)methoxy)carbonyl)-*L*-lysinate**



187

Method A:
Fmoc-Lys-OH·HCl (100 mg, 0.25 mmol, 1.00 eq) was washed with sat. aq. $NaHCO_3$ (20.0 mL) and extracted with EtOAc (3 × 20.0 mL). The solvent was removed under reduced pressure and the obtained residue was redissolved in EtOAc (2.00 mL). To this solution was added, dropwise, a solution of *tert*-butyl-2,2,2-trichloroacetimidate (0.90 mL, 0.50 mmol, 2.00 eq) in cyclohexane (1.00 mL). The reaction solution was stirred at RT for 4 h, after which time the reaction was adjudged to be complete by TLC analysis. The reaction was quenched with EtOAc (50.0 mL), washed with sat. aq. $NaHCO_3$ (50.0 mL), H_2O (50.0 mL), and brine (50.0 mL), dried over $MgSO_4$, and filtered. The solvent was removed under reduced pressure and the crude oil was purified by silica gel flash column chromatography, eluting with $CHCl_3$:MeOH = 99:1 - 9:1, to afford *tert*-butyl (((9*H*-fluoren-9-yl)methoxy)carbonyl)-*L*-lysinate (**187**) as a yellow oil (10.6 mg, 10%).

Method B:
tert-Butyl N^2-(((9*H*-fluoren-9-yl)methoxy)carbonyl)-N^6-((allyloxy)carbonyl)-*L*-lysinate (**193**) (500 mg, 0.98 mmol, 1.00 eq), $Pd(PPh_3)_4$ (231 mg, 0.20 mmol, 0.20 eq) and $Me_2NH{\cdot}BH_3$ (116 mg, 1.97 mmol, 2.00 eq) were dissolved in anhydrous CH_2Cl_2 (25.0 mL). The reaction solution was stirred at RT under an Ar atmosphere for 18 h, after which time the reaction was adjudged to be complete by TLC analysis. The reaction was quenched with CH_2Cl_2 (100 mL) and washed with sat. aq. $NaHCO_3$ (100 mL). The solvent was removed under reduced pressure and the crude oil was further purified by silica gel flash column chromatography, eluting with CH_2Cl_2:NEt_3 = 99:1 to CH_2Cl_2:MeOH:NEt_3 = 90:9:1, to afford *tert*-butyl (((9*H*-fluoren-9-yl)methoxy)carbonyl)-*L*-lysinate (**187**) as a dark yellow oil (58.3 mg, 14%).

Method C:

tert-Butyl N^2-(((9*H*-fluoren-9-yl)methoxy)carbonyl)-N^6-(*tert*-butoxycarbonyl)-*L*-lysinate (**191**) (4.30 g, 8.20 mmol, 1.00 eq) was dissolved in 2.0 M HCl in Et_2O (50.0 mL, 100 mmol, 12.5 eq) and the reaction solution was stirred at RT under an Ar atmosphere for 6 h. Additional 2.0 M HCl in Et_2O (50.0 mL, 100 mmol, 12.5 eq) was added and the reaction mixture was stirred at RT under an Ar atmosphere for a further 6 h, after which time the reaction was adjudged to be complete by TLC analysis. The resulting suspension was filtered and the white precipitate was washed with cold Et_2O and dried under suction. The precipitate was further purified by silica gel flash column chromatography, eluting with $CHCl_3$:MeOH = 99:1 - 9:1, to afford the HCl salt of *tert*-butyl (((9*H*-fluoren-9-yl)methoxy)carbonyl)-*L*-lysinate (**187**) as a hygroscopic colourless solid (1.32 g, 38%).

Method D:
Trifluoroacetic acid (1.71 g, 1.15 mL, 15.0 mmol, 10.0 eq) was added dropwise to a solution of *tert*-butyl N^2-(((9*H*-fluoren-9-yl)methoxy)carbonyl)-N^6-trityl-*L*-lysinate (**195**) (1.00 g, 1.50 mmol, 1.00 eq) in CH_2Cl_2 (23.0 mL). This was immediately followed with the addition of triethylsilane (872 mg, 1.20 mL, 7.50 mmol, 5.00 eq). The resulting reaction solution was stirred at RT for 2 h, after which time the reaction was adjudged to be complete by TLC analysis. The solvent was removed under reduced pressure by azeotroping with cyclohexane and the crude residue was purified by silica gel flash column chromatography, eluting with $CHCl_3$:MeOH = 99:1 - 9:1, to afford *tert*-butyl (((9*H*-fluoren-9-yl)methoxy)carbonyl)-*L*-lysinate (**187**) as a hygroscopic colourless solid (649 mg, 83%).

Method E:
tert-Butyl N^2-(((9*H*-fluoren-9-yl)methoxy)carbonyl-N^6-(diphenyl(*p*-tolyl)methyl)-*L*-lysinate (**197**) (600 mg, 0.90 mmol, 1.00 eq) was dissolved in a 1% v/v trifluoroacetic acid solution in CH_2Cl_2 (60.0 mL, c 100 mg in 10.0 mL). Triethylsilane (3.00 mL, 18.9 mmol, 20.9 eq) was immediately added thereafter and the reaction solution was stirred at RT for 40 min, after which time the reaction was adjudged to be complete by TLC analysis. The reaction mixture was azeotroped with cyclohexane and the crude residue was further purified by silica gel flash column chromatography, eluting with CH_2Cl_2 to CH_2Cl_2:MeOH = 95:5 - 9:1 - 8:2, to afford *tert*-butyl (((9*H*-fluoren-9-yl)methoxy)carbonyl)-*L*-lysinate (**187**) as a hygroscopic colourless solid (431 mg, 92%).

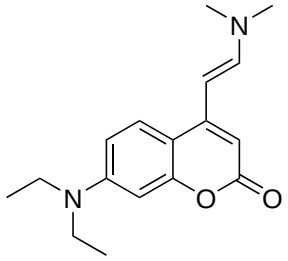
$\mathbf{R_f}$: 0.37 ($CHCl_3$:MeOH = 8:2);

m.p.: 79 - 82 °C (Hexane/MeOH);
$[\boldsymbol{\alpha}]_{\boldsymbol{D}}^{\mathbf{26}}$: -2.2 (***c*** 1.1 in $CHCl_3$);
^{1}H NMR (400 MHz, CD_3OD) $\boldsymbol{\delta}$H: 7.76 (2H, d, J = 7.5 Hz, $C_{FmocAr}\mathbf{H}$), 7.64 (2H, t, J = 7.5 Hz, $C_{FmocAr}\mathbf{H}$), 7.36 (2H, t, J = 7.5 Hz, $C_{FmocAr}\mathbf{H}$), 7.28 (2H, t, J = 7.5 Hz, $C_{FmocAr}\mathbf{H}$), 4.42 - 4.26 (2H, m, $C_{Fmoc}\mathbf{H}_2$), 4.18 (1H, t, J = 6.4 Hz, $C_{Fmoc}\mathbf{H}$), 4.14 - 4.00 (1H, m, NHC$\mathbf{H}$CH_2), 2.90 (2H, t, J = 7.3 Hz, NHC$\mathbf{H}_2$CH_2), 1.88 - 1.76 (1H, m, NHCHC$\mathbf{H}_A$H$_B$CH_2), 1.72 - 160 (3H, m, NHCHCH$_A\mathbf{H}_B$CH_2, $NH_2CH_2C\mathbf{H}_2$), 1.52 - 1.36 (2H, m, NHCHCH_2C$\mathbf{H}_2$), 1.44 (9H, s, OC(C$\mathbf{H}_3$)$_3$);
^{13}C NMR (100 MHz, CD_3OD) $\boldsymbol{\delta}$C: 173.3 (**C**O), 158.8 (**C**O), 145.4 ($\mathbf{C}_{FmocAr}$), 142.7 ($\mathbf{C}_{FmocAr}$), 128.9 ($\mathbf{C}_{FmocAr}$H), 128.3 ($\mathbf{C}_{FmocAr}$H), 126.3 ($\mathbf{C}_{FmocAr}$H), 121.1 ($\mathbf{C}_{FmocAr}$H), 82.9 (O**C**(CH$_3$)$_3$), 68.0 ($\mathbf{C}_{Fmoc}H_2$), 55.9 (NH**C**HCH_2), 48.5 ($\mathbf{C}_{Fmoc}$H), 40.6 ($NH_2\mathbf{C}H_2CH_2$), 32.1 (NHCH**C**H_2), 28.4 (OC(**C**H$_3$)$_3$), 28.1 ($NH_2CH_2\mathbf{C}H_2$), 24.0 (NHCHCH_2**C**H_2);
LRMS *m/z* (ESI$^+$): 426 (100% [M + H]$^+$);
HRMS *m/z* (ESI$^+$): Found 425.2430 [M + H]$^+$ ($C_{25}H_{33}N_2O_4^+$ requires 425.2446 [M + H]$^+$);
IR ($\boldsymbol{\nu}_{\mathbf{max}}$ cm^{-1}): 2981 (w), 2361 (w), 2110 (w), 1681 (s, C=O), 1527 (w, N-H), 1449 (w, Ar C-C), 1341 (w), 1205 (m, C-O), 1140 (m, C-N), 842 (w), 801 (w), 744 (w), 666 (w), 624 (w).

Data are concordant with literature values.[217]

7.7 DEACM Caged Amino Acids

(*E*)-7-(Diethylamino)-4-(2-(dimethylamino)vinyl)-2*H*-chromen-2-one



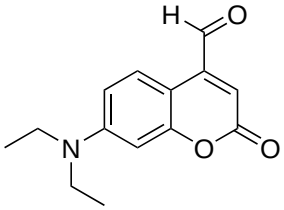
154

N,*N*-Dimethylformamide dimethylacetal (3.86 g, 4.30 mL, 32.4 mmol, 1.50 eq) was added to a solution of 4-methyl 7-diethylaminocoumarin (**151**) (5.00 g, 21.6 mmol, 1.00 eq) in anhydrous DMF (40.0 mL). The reaction mixture was heated to 140 °C and stirred under an Ar atmosphere for 18 h, after which time the reaction was adjudged to complete by TLC analysis. The resulting solution was allowed to cool to RT and the solvent was removed under reduced pressure. The residue was washed with hexane to afford (*E*)-7-(diethylamino)-4-(2-(dimethylamino)vinyl)-2*H*-chromen-2-one (**154**) as a brown solid (6.06 g, 98%).

R_f: 0.14 (Petroleum ether:Et_2O = 2:8);
m.p.: 180 - 182 °C (Hexane/MeOH);
UV λ_{max}/nm (ϵ/$M^{-1}cm^{-1}$): 385 (26700) [MeOH];
^{1}H NMR (400 MHz, $CDCl_3$) δH: 7.52 (1H, d, J = 9.0 Hz, C_{Ar}**H**), 7.21 (1H, d, J = 13.1 Hz, C**H**CHN$(CH_3)_2$), 6.54 (1H, dd, J = 9.0, 2.4 Hz, C_{Ar}**H**), 6,48 (1H, d, J = 2.4 Hz, C_{Ar}**H**), 5.84 (1H, s, $C_{Ring\text{-}Alkene}$**H**), 5.21 (1H, d, J = 13.1 Hz, CHC**H**N$(CH_3)_2$), 3.39 (4H, q, J = 7.1 Hz, N(C**H**$_2$$CH_3)_2$), 2.98 (6H, s, N(C**H**$_3)_2$), 1.19 (6H, t, J = 7.1 Hz, N(CH_2C**H**$_3)_2$);
^{13}C NMR (100 MHz, $CDCl_3$) δC: 163.4 (**C**O), 156.3 ($\mathbf{C}_{Ar}$), 152.3 ($\mathbf{C}_{Ar}$), 150.1 ($\mathbf{C}_{Ar}$), 146.5 ($\mathbf{C}_{Alkene}$H), 124.8 ($\mathbf{C}_{Ar}$H), 108.0 ($\mathbf{C}_{Ar}$), 107.8 ($\mathbf{C}_{Ring\text{-}Alkene}$H), 98.0 ($\mathbf{C}_{Ar}$H), 93.2 ($\mathbf{C}_{Ar}$H), 87.3 ($\mathbf{C}_{Alkene}$H), 44.6 (N(**C**$H_2CH_3)_2$), 39.6 (N(**C**$H_3)_2$), 12.4 (N($CH_2$**C**$H_3)_2$) ;
LRMS *m/z* (ESI$^+$): 288 (100% $[M + H]^+$);
HRMS *m/z* (ESI$^+$): Found 287.1754 $[M + H]^+$ ($C_{17}H_{23}N_2O_2^+$ requires 287.1754 $[M + H]^+$);

IR (ν_{max} cm^{-1}): 3655 (w), 2978 (w, Alkene C-H), 2887 (w), 2186 (w), 2022 (w), 1466 (w), 1385 (m), 1252 (m), 1154 (m, C-O), 1074 (m, C-N), 955 (m, Alkene C-H), 818 (w), 645 (w), 620 (w).

7-(Diethylamino)-2-oxo-2*H*-chromen-2-one



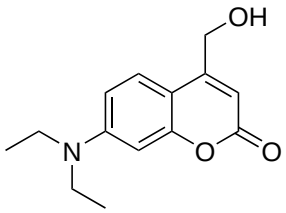
152

(*E*)-7-(Diethylamino)-4-(2-(dimethylamino)vinyl)-2*H*-chromen-2-one (**154**) (2.00 g, 6.99 mmol, 1.00 eq) and $NaIO_4$ (4.49 g, 21.0 mmol, 3.00 eq) were dissolved in a mixture of THF:H_2O (1:1, 80.0 mL). The reaction solution was stirred at RT for 18 h under an Ar atmosphere, after which time the reaction was adjudged to be complete by TLC analysis. The reaction mixture was filtered to remove any insolubles, diluted with EtOAc (100 mL), washed with sat. aq. $NaHCO_3$ (200 mL), and brine (200 mL), dried over $MgSO_4$, and filtered. The solvent was removed under reduced pressure and the crude oil was purified by silica gel flash column chromatography, eluting with petroleum ether:acetone = 9:1, to afford 7-(diethylamino)-2-oxo-2*H*-chromen-4-carbaldehyde (**152**) as a red oil (1.43 g, 83%).

R_f: 0.19 (Petroleum ether:Acetone = 9:1);
UV λ_{max}/nm (ϵ/M^{-1}cm^{-1}): 380 (15780) [MeOH];
^{1}H NMR (400 MHz, $CDCl_3$) δH: 10.03 (1H, s, $C_{Aldehyde}$**H**), 8.31 (1H, d, J = 9.3 Hz, C_{Ar}**H**), 6.63 (1H, dd, J = 9.3, 2.6 Hz, C_{Ar}**H**), 6.52 (1H, d, J = 2.6 Hz, C_{Alkene}**H**), 6.46 (1H, s, C_{Ar}**H**), 3.43 (4H, q, J = 7.1 Hz, N(C**H**$_2$CH$_3$)$_2$), 1.22 (6H, t, J = 7.1 Hz, N(CH$_2$C**H**$_3$)$_2$);
^{13}C NMR (100 MHz, $CDCl_3$) δC: 192.5 (**C**O), 161.9 (**C**O), 157.3 (**C**$_{Ar}$), 151.0 (**C**$_{Ar}$), 143.8 (**C**$_{Ar}$), 127.0 (**C**$_{Ar}$H), 117.3 (**C**$_{Ring\text{-}Alkene}$H), 109.5 (**C**$_{Ar}$H), 103.6 (**C**$_{Ring\text{-}Alkene}$), 97.6 (**C**$_{Ar}$H), 44.8 (N(**C**H$_2$CH$_3$)$_2$), 12.4 (N(CH$_2$**C**H$_3$)$_2$);
LRMS *m/z* (ESI$^+$): Ion observed in MS of product hydrolysed by MeOH, 279 (100% [M + H]$^+$);
HRMS *m/z* (ESI$^+$): Found 246.1126 [M + H]$^+$ ($C_{14}H_{16}NO_3^+$ requires 246.1125 [M + H]$^+$);
IR (ν_{max} cm^{-1}): 2975 (w, br), 1715 (s, C=O), 1607 (s, C=O), 1521 (m, Ar C-C), 1430 (m), 1356 (m), 1275 (w), 1199 (w), 1143 (w), 1058 (m, C-O), 826 (w).

Data are concordant with literature values.[61]

7-(Diethylamino)-4-(hydroxymethyl)-2*H*-chromen-2-one



153

Method A:
4-Methyl-7-diethyl aminocoumarin (**151**) (2.00 g, 8.65 mmol, 1.00 eq) was dissolved in anhydrous toluene (40.0 mL). To this was added SeO_2 (1.44 g, 13.0 mmol, 1.50 eq) and the resulting mixture was heated under reflux and stirred for 24 h, after which time the reaction was adjudged to be complete by TLC analysis. The crude reaction mixture was filtered and the solvent was removed under reduced pressure. The resulting solid was redissolved in MeOH (40.0 mL) and $NaBH_4$ (163 mg, 4.32 mmol, 0.50 eq) was added. The reaction mixture was stirred at RT under N_2 atmosphere for 3 h, after which time the reaction was adjudged to be complete by TLC analysis. The reaction was quenched by dropwise addition of aq. 1 M HCl (10.0 mL), diluted with H_2O (200 mL) and extracted with CH_2Cl_2 (3 $\times$ 200 mL). The organics were combined, washed with H_2O (500 mL), and brine (500 mL), dried over $MgSO_4$, and filtered. The solvent was removed under reduced pressure and the crude residue was purified by silica gel flash column chromatography, eluting with petroleum ether:acetone = 8:2, to afford 7-(diethylamino)-4-(hydroxymethyl)-2*H*-chromen-2-one (**153**) as a yellow solid (620 mg, 29% over 2 steps).

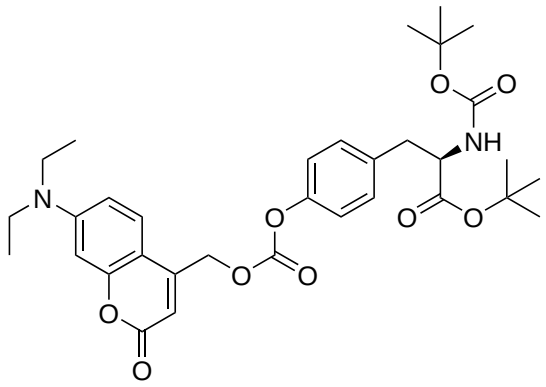
Method B:
To a solution of 7-(diethylamino)-2-oxo-2*H*-chromen-4-carbaldehyde (**152**) (1.43 g, 5.83 mmol, 1.00 eq) in MeOH (30.0 mL) was added $NaBH_4$ (441 mg, 11.7 mmol, 2.00 eq). After stirring at RT under an atmosphere of Ar for 1 h, additional $NaBH_4$ (441 mg, 11.7 mmol, 2.00 eq) was added. The reaction mixture was stirred at RT under an Ar atmosphere for 4 h, after which the reaction was adjudged to be complete by TLC analysis. The reaction was quenched with Et_2O (200 mL), washed with H_2O (200 mL), and brine (200 mL), dried over $MgSO_4$, and filtered. The solvent was removed under reduced pressure and the crude residue was purified by silica gel flash column chromatography, eluting with petroleum ether:acetone = 8:2, to afford 7-(diethylamino)-4-(hydroxymethyl)-2*H*-chromen-2-one (**153**) as a yellow solid (749

mg, 52%).

R_f: 0.23 (Petroleum ether:Acetone = 7:3);
m.p.: 141 - 143 °C (Petroleum ether/Et_2O) [Literature value: 146 - 147 °C][218];
UV λ_{max}/nm (ϵ/$M^{-1}cm^{-1}$): 375 (23860) [MeOH];
^{1}H NMR (400 MHz, $CDCl_3$) δH: 7.30 (1H, d, J = 9.0 Hz, C_{Ar}**H**), 6.54 (1H, dd, J = 9.0, 2.5 Hz, C_{Ar}**H**), 6.44 (1H, d, J = 2.5 Hz, C_{Ar}**H**), 6.28 (1H, s, $C_{Ring\text{-}Alkene}$**H**), 4.82 (2H, d, J = 5.5 Hz, C**H**$_2$OH), 3.38 (4H, q, J = 7.2 Hz, N(C**H**$_2$CH$_3$)$_2$), 3.31 (1H, t, J = 5.5 Hz, CH$_2$O**H**), 1.18 (6H, t, J = 7.2 Hz, N(CH$_2$C**H**$_3$)$_2$);
^{13}C NMR (100 MHz, $CDCl_3$) δC: 163.0 (**C**O), 156.0 ($\mathbf{C}_{Ar}$), 155.4 ($\mathbf{C}_{Ar}$), 150.4 ($\mathbf{C}_{Ar}$), 124.3 ($\mathbf{C}_{Ar}$H), 108.6 ($\mathbf{C}_{Ar}$H), 106.3 ($\mathbf{C}_{Ring\text{-}Alkene}$), 105.1 ($\mathbf{C}_{Ring\text{-}Alkene}$H), 97.5 ($\mathbf{C}_{Ar}$H), 60.7 (**C**H$_2$OH), 44.6 (N(**C**H$_2CH_3$)$_2$), 12.4 (N(CH$_2$**C**H$_3$)$_2$);
LRMS *m/z* (ESI^+): 248 (62% $[M + H]^+$), 270 (100% $[M + Na]^+$);
HRMS *m/z* (ESI^+): Found 270.1101 $[M + Na]^+$ ($C_{14}H_{17}NNaO_3^+$ requires 270.1101 $[M + Na]^+$);
IR (ν_{max} cm^{-1}): 3396 (w, br, O-H), 2973 (w), 2915 (w), 1691 (m, C=O), 1598 (s, Ar C-C), 1526 (m, Ar C-C), 1418 (m), 1345 (m), 1279 (m, C-O), 1198 (w), 1144 (w), 1084 (m, C-N), 998 (w), 910 (w), 836 (w, br), 732 (w), 654 (w).

Data are concordant with literature values.[219]

***tert*-Butyl (*R*)-2-((*tert*-butoxycarbonyl)amino)-3-(4-((((7-(diethylamino)-2-oxo-2*H*-chromen-4-yl)methoxy)carbonyl)oxy)phenyl)propanoate**



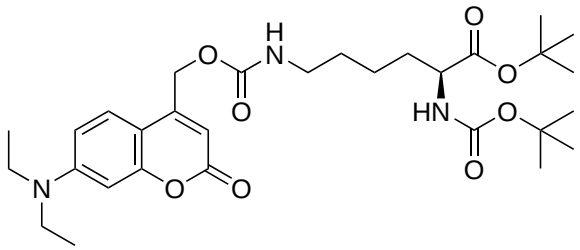
181

7-(Diethylamino)-4-(hydroxymethyl)-2*H*-chromen-2-one (**153**) (50.0 mg, 0.20 mmol, 1.00 eq), 4-nitrophenyl chloroformate (48.4 mg, 0.24 mmol, 1.20 eq) and 4-(dimethylamino)pyridine (29.3 mg, 0.24 mmol, 1.20 eq) were dissolved in anhydrous CH_2Cl_2 (2.00 mL). The resulting solution was stirred at RT under a N_2 atmosphere for 18 h, after which time the formation of the intermediate was adjudged to be complete by TLC analysis. To this solution was added (*S*)-*tert*-butyl 2-((*tert*-butoxycarbonyl)amino)-3-(4-hydroxyphenyl)propanoate (**160**) (67.4 mg, 0.20 mmol, 1.00 eq) and 4-(dimethylamino) pyridine (36.7 mg, 0.30 mmol, 1.50 eq). The reaction solution was stirred at RT under a N_2 atmosphere for 18 h, after which time the reaction was adjudged to be complete by TLC analysis. The reaction was quenched with CH_2Cl_2 (100 mL) and washed with sat. aq. $NaHCO_3$ (100 mL). The solvent was removed under reduced pressure and the crude oil was further purified by silica gel flash column chromatography, eluting with petroleum ether:EtOAc = 7:3, to afford *tert*-butyl (*R*)-((*tert*-butoxycarbonyl)amino)-3-(4-((((7-(diethylamino)-2-oxo-2*H*-chromen-4-yl)methoxy)carbonyl)oxy)phenyl)propanoate (**181**) as a dark yellow oil (35.3 mg, 29%).

$\mathbf{R_f}$: 0.26 (Petroleum ether:EtOAc = 7:3);
$\mathbf{[\alpha]_D^{26}}$: +8.6 (***c*** 0.5 in $CHCl_3$);
UV $\boldsymbol{\lambda_{max}}$/nm ($\boldsymbol{\epsilon}$/$\mathbf{M^{-1}cm^{-1}}$): 380 (740) [MeOH];
^{1}H NMR (400 MHz, $CDCl_3$) $\boldsymbol{\delta}$H: 7.37 (1H, d, J = 8.8 Hz, $C_{Ar}\mathbf{H}$), 7.22 (2H, d, J = 8.8 Hz, $C_{TyrAr}\mathbf{H}$), 7.14 (2 H, d, J = 8.8 Hz, $C_{TyrAr}\mathbf{H}$), 6.81 - 6.74 (1H, m, $C_{Ar}\mathbf{H}$), 6.68 - 6.63 (1H, m, $C_{Ar}\mathbf{H}$), 6.29 (1H, s, $C_{Ring\text{-}Alkene}\mathbf{H}$), 5.38 (2H, d, J = 1.3 Hz,

C$\mathbf{H}_2$O), 5.04 (1H, d, J = 8.2 Hz, N$\mathbf{H}$CHCH_2), 4.49 - 4.42 (1H, m, NHC$\mathbf{H}$CH_2), 3.44 (4H, q, J = 7.2 Hz, N(C$\mathbf{H}_2$CH_3)$_2$), 3.07 (2H, d, J = 5.7 Hz, NHCHC$\mathbf{H}_2$), 1.43 (9H, s, OC(C$\mathbf{H}_3$)$_3$), 1.40 (9H, s, OC(C$\mathbf{H}_3$)$_3$), 1.23 (6H, t, J = 7.2 Hz, N(CH_2C$\mathbf{H}_3$)$_2$);
^{13}C NMR (100 MHz, CDCl_3) $\boldsymbol{\delta}$C: 170.7 (**C**O), 161.4 (**C**O), 156.1 (**C**O), 155.1 (**C**O), 153.2 ($\mathbf{C}_{\mathrm{TyrAr}}$), 151.7 ($\mathbf{C}_{\mathrm{Ar}}$), 149.8 ($\mathbf{C}_{\mathrm{Ar}}$), 148.2 ($\mathbf{C}_{\mathrm{Ar}}$H), 147.7 ($\mathbf{C}_{\mathrm{Ar}}$), 137.2 ($\mathbf{C}_{\mathrm{Ring\text{-}Alkene}}$), 134.7 ($\mathbf{C}_{\mathrm{TyrAr}}$), 130.7 ($\mathbf{C}_{\mathrm{TyrAr}}$H), 126.2 ($\mathbf{C}_{\mathrm{Ar}}$H), 124.5 ($\mathbf{C}_{\mathrm{Ring\text{-}Alkene}}$H), 120.7 ($\mathbf{C}_{\mathrm{TyrAr}}$H), 115.7 ($\mathbf{C}_{\mathrm{Ar}}$H), 82.3 (O**C**(C$\mathrm{H}_3$)$_3$), 79.8 (O**C**(C$\mathrm{H}_3$)$_3$), 65.1 (**C**$\mathrm{H}_2$O), 54.8 (NH**C**HC$\mathrm{H}_2$), 45.7 (N(**C**$\mathrm{H}_2C\mathrm{H}_3$)$_2$), 37.9 (NHCH**C**$\mathrm{H}_2$), 28.3 (OC(**C**$\mathrm{H}_3$)$_3$), 27.9 (OC(**C**$\mathrm{H}_3$)$_3$), 12.2 (N(C$\mathrm{H}_2$**C**$\mathrm{H}_3$)$_2$);
LRMS *m/z* (ESI$^+$): 611 (100% [M + H]$^+$);
HRMS *m/z* (ESI$^+$): Found 633.2780 [M + Na]$^+$ ($\mathrm{C_{33}H_{42}N_2NaO_9}^+$ requires 633.2783 [M + Na]$^+$);
IR ($\boldsymbol{\nu}_{\mathbf{max}}$ cm^{-1}): 3351 (w), 2976 (w), 1715 (s, C=O), 1607 (s, C=O), 1516 (m, Ar C-C), 1432 (w), 1357 (m), 1241 (s, C-O), 1155 (m, C-O), 1087 (w), 845 (w), 735 (w).

***tert*-Butyl N^2-(*tert*-butoxycarbonyl)-N^6-(((7-(diethylamino)-2-oxo-2*H*-chromen-4-yl)methoxy)carbonyl)-*L*-lysinate**



182

7-(Diethylamino)-4-(hydroxymethyl)-2*H*-chromen-2-one (**153**) (250 mg, 1.01 mmol, 1.00 eq), 4-nitrophenyl chloroformate (244 mg, 1.21 mmol, 1.20 eq) and 4-(dimethylamino) pyridine (148 mg, 1.21 mmol, 1.20 eq) were dissolved in anhydrous CH_2Cl_2 (10.0 mL). The reaction solution was stirred at RT under a N_2 atmosphere for 18 h, after which time formation of the intermediate was adjudged to be complete by TLC analysis. *tert*-Butyl (*tert*-butoxycarbonyl)-*L*-lysinate (**163**) (275 mg, 0.91 mmol, 1.00 eq) and 4-(dimethylamino)pyridine (148 mg, 1.21 mmol, 1.20 eq) were added and the reaction solution was stirred at RT under a N_2 atmosphere for 18 h, after which time the reaction was adjudged to be complete by TLC analysis. The reaction was quenched with CH_2Cl_2 (50.0 mL) and washed with sat. aq. $NaHCO_3$ (50.0 mL). The solvent was removed under reduced pressure and the crude oil was further purified by silica gel flash column chromatography, eluting with petroleum ether:EtOAc = 7:3, to afford *tert*-butyl N^2-(*tert*-butoxycarbonyl)-N^6-(((7-(diethylamino)-2-oxo-2*H*-chromen-4-yl)methoxy)carbonyl)-*L*-lysinate (**182**) as a dark yellow oil (163 mg, 28%).

R_f: 0.44 (Petroleum ether:EtOAc = 7:3);
$[\alpha]_D^{26}$: +7.3 (***c*** 1.2 in $CHCl_3$);
UV λ_{max}/nm (ϵ/$M^{-1}cm^{-1}$): 380 (23420) [MeOH];
^{1}H NMR (400 MHz, $CDCl_3$) **δ**H: 7.31 (1H, d, J = 8.6 Hz, C_{Ar}**H**), 6.61 (1H, dd, J = 8.6, 1.3 Hz, C_{Ar}**H**), 6.54 (1H, d, J = 1.3 Hz, C_{Ar}**H**), 6.13 (1H, s, $C_{Ring\text{-}Alkene}$**H**), 5.22 (2H, s, C**H**$_2$O), 5.12 - 5.04 (2H, m, N**H**CH_2CH_2, N**H**$CHCH_2$), 4.21 - 4.14 (1H, m, NHC**H**CH_2), 3.42 (4H, q, J = 7.1 Hz, N(C**H**$_2CH_3)_2$), 3.27 - 3.20 (2H, m, NHC**H**$_2CH_2$), 1.85 - 1.75 (1H, m, NHCHC**H**$_A$H$_B$$CH_2$), 1.68 - 1.54 (3H, m, $NHCHCH_AH_BCH_2$, $NHCH_2CH_2$), 1.47 (9H, s, OC(C**H**$_3)_3$), 1.43 (9H, s, OC(C**H**$_3)_3$), 1.49 - 1.39 (2H, m, $NHCHCH_2CH_2$), 1.21 (6H, t, J = 7.1 Hz, N(CH_2C**H**$_3)_2$);

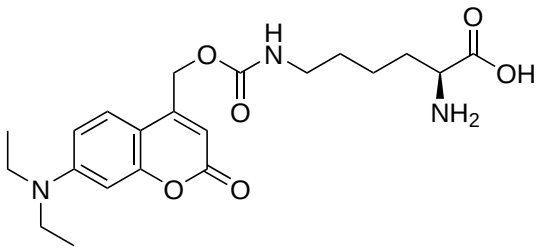
^{13}C NMR (100 MHz, $CDCl_3$) δC: 171.9 (**C**O), 162.0 (**C**O), 156.2 (**C**O), 155.6 (**C**O), 155.5 ($\mathbf{C}_{Ar}$), 150.4 ($\mathbf{C}_{Ar}$), 124.5 ($\mathbf{C}_{Ar}$H), 112.3 ($\mathbf{C}_{Ar}$), 108.9 ($C_{Ring\text{-}Alkene}$), 108.8 ($\mathbf{C}_{Ar}$H), 106.3 ($\mathbf{C}_{Ring\text{-}Alkene}$H), 98.1 ($C_{Ar}$H), 81.9 (O**C**($CH_3$)$_3$), 79.7 (O**C**($CH_3$)$_3$), 61.7 (**C**$H_2$O), 53.6 (NH**C**H$CH_2$), 45.0 (N(**C**$H_2CH_3$)$_2$), 40.9 (NH**C**$H_2CH_2$), 32.7 (NH**C**H$CH_2$), 29.2 (NH$CH_2$**C**$H_2$), 28.3 (OC(**C**$H_3$)$_3$), 28.0 (OC(**C**$H_3$)$_3$), 22.3 (NHCH$CH_2$**C**$H_2$), 12.4 (N($CH_2$**C**$H_3$)$_2$);

LRMS *m/z* (ESI$^+$): 576 (100% $[M + H]^+$);

HRMS *m/z* (ESI$^+$): Found 576.3279 $[M + H]^+$ ($C_{30}H_{46}N_3O_8^+$ requires 576.3279 $[M + H]^+$);

IR (ν_{max} cm^{-1}): 3429 (w), 3326 (w), 2974 (w), 2934 (w), 1716 (s, C=O), 1609 (s, C=O), 1522 (m, Ar C-C), 1423 (w), 1361 (m), 1245 (m), 1151 (m, C-O), 1071 (m, C-N), 1015 (w), 853 (w), 735 (w).

N^6-(((7-(Diethylamino)-2-oxo-2*H*-chromen-4-yl)methoxy)carbonyl)-*L*-lysine



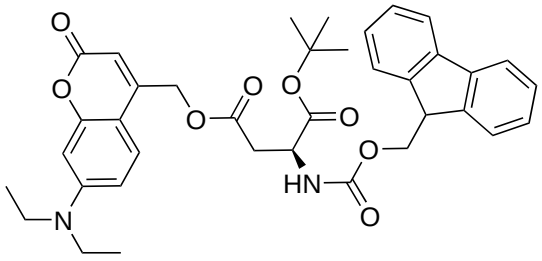
272

tert-Butyl N^2-(*tert*-butoxycarbonyl)-N^6-(((7-(diethylamino)-2-oxo-2*H*-chromen-4-yl) methoxy)carbonyl)-*L*-lysinate (**182**) (30.0 mg, 0.05 mmol, 1.00 eq) was dissolved in CH_2Cl_2 (0.40 mL). Trifluoroacetic acid (594 mg, 0.40 mL, 5.21 mmol, 100 eq) was added dropwise followed immediately by the addition of triethylsilane (60.4 mg, 0.08 mL, 0.52 mmol, 10.0 eq). The reaction solution was stirred at RT under a N_2 atmosphere for 4 h, after which time the reaction was adjudged to be complete by TLC analysis. The solvent was removed by azeotropic distillation with cyclohexane (3 × 2.00 mL) to afford N^6-(((7-(diethylamino)-2-oxo-2*H*-chromen-4-yl)methoxy)carbonyl)-*L*-lysine (**183**) as a yellow oil (16.8 mg, 80%).

R_f: 0.26 (MeOH:H_2O = 1:1);
$[\alpha]_D^{26}$: +59.5 (***c*** 0.5 in $CHCl_3$);
^{1}H NMR (400 MHz, CD_3OD) ***δ***H: 7.47 (1H, d, J = 9.1 Hz, C_{Ar}**H**), 6.74 (1H, dd, J = 9.1, 2.5 Hz, C_{Ar}**H**), 6.55 (1H, d, J = 2.5 Hz, C_{Ar}**H**), 6.05 (1H, s, $C_{Ring\text{-}Alkene}$**H**), 5.27 (2H, s, C**H**$_2$O), 3.54 (1H, dd, J = 6.6, 5.4 Hz, NHC**H**CH_2), 3.48 (4H, q, J = 7.0 Hz, N(C**H**$_2$$CH_3$)$_2$), 3.18 (2H, t, J = 6.8 Hz, NHC**H**$_2$$CH_2$), 1.96 - 1.87 (1H, m, NHCHC**H**$_A$$H_B$$CH_2$), 1.87 - 1.78 (1H, m, NHCHCH_A**H**$_B$$CH_2$), 1.62 - 1.54 (2H, m, NHCH_2C**H**$_2$), 1.52 - 1.42 (2H, m, NHCHCH_2C**H**$_2$), 1.21 (6H, t, J = 7.0 Hz, N(CH_2C**H**$_3$)$_2$);
^{13}C NMR (100 MHz, $CDCl_3$) ***δ***C: 174.6 (**C**O), 164.7 (**C**O), 158.2 (**C**O), 157.6 (**C**$_{Ar}$), 154.3 (**C**$_{Ar}$), 152.6 (**C**$_{Ar}$), 126.2 (**C**$_{Ar}$H), 110.6 (**C**$_{Ar}$H), 107.2 (**C**$_{Ring\text{-}Alkene}$), 105.5 (**C**$_{Ring\text{-}Alkene}$H), 98.4 (**C**$_{Ar}$H), 62.8 (**C**H_2O), 57.3 (NH**C**HCH_2), 45.8 (N(**C**$H_2$$CH_3$)$_2$), 41.7 (NH**C**$H_2$$CH_2$), 32.2 (NHCH**C**$H_2$), 30.7 (NHC$H_2$**C**$H_2$), 23.7 (NHCHC$H_2$**C**$H_2$), 12.9 (N($CH_2$**C**$H_3$)$_2$);
LRMS *m/z* (ESI$^+$): 420 (92% [M + H]$^+$), 434 (100%);

HRMS *m/z* (ESI$^+$): Found 420.2127 $[M + H]^+$ ($C_{21}H_{30}N_3O_6^+$ requires 420.2129 $[M + H]^+$);
IR (ν_{max} cm^{-1}): 3346 (w, br, O-H), 2939 (w), 1704 (s, C=O), 1608 (s, C=O), 1526 (m, Ar C-C), 1423 (m), 1347 (w), 1270 (w), 1137 (w), 1074 (w), 1023 (m, C-O), 832 (w).

1-(*tert*-Butyl) 4-((7-(diethylamino)-2-oxo-2*H*-chromen-4-yl)methyl) (((9*H*-fluoren-9-yl)methoxy)carbonyl-*L*-aspartate



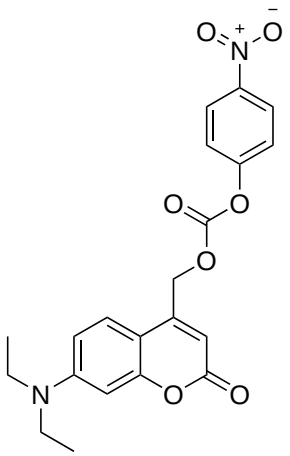
215

A solution of 7-(diethylamino)-4-(hydroxymethyl)-2*H*-chromen-2-one (**153**) (200 mg, 0.81 mmol, 1.00 eq), Fmoc-Asp-O^{t}Bu (**221**) (333 mg, 0.81 mmol, 1.00 eq) and *N*,*N*,*N*',*N*'-tetramethyl-*O*-(1*H*-benzotriazol-1-yl)uronium hexafluorophosphate (322 mg, 0.85 mmol, 1.05 eq) in anhydrous DMF (5.00 mL) was stirred at RT under an Ar atmosphere for 0.5 h. *N*,*N*-Diisopropylethylamine (209 mg, 0.28 mL, 1.62 mmol, 2.00 eq) was added dropwise and the reaction solution was stirred at RT under an Ar atmosphere for 18 h, after which time the reaction was adjudged to be complete by TLC analysis. The reaction was quenched with Et_2O (100 mL), washed with H_2O (100 mL), and brine (100 mL), dried over $MgSO_4$, and filtered. The solvent was removed under reduced pressure and the crude residue was purified by silica gel flash column chromatography, eluting with $CHCl_3$, to afford 1-(*tert*-butyl) 4-((7-(diethylamino)-2-oxo-2*H*-chromen-4-yl)methyl) (((9*H*-fluoren-9-yl)methoxy)carbonyl)-*L*-aspartate (**215**) as a yellow solid (418 mg, 75%).

R_f: 0.73 ($CHCl_3$:Acetone = 9:1);
m.p.: 78 - 81 °C (Petroleum ether/Acetone);
$[\alpha]_D^{26}$: +22.7 (***c*** 0.75 in $CHCl_3$);
UV λ_{max}/nm (ϵ/M^{-1}cm^{-1}): 380 (18930) [MeOH];
^{1}H NMR (400 MHz, $CDCl_3$) **δ**H: 7.77 (2H, d, J = 7.5 Hz, C_{FmocAr}**H**), 7.61 (2H, d, J = 7.5 Hz, C_{FmocAr}**H**), 7.40 (2H, t, J = 7.5 Hz, C_{FmocAr}**H**), 7.35 - 7.28 (3H, m, C_{FmocAr}**H**, C_{Ar}**H**), 6.56 (1H, dd, J = 9.0, 2.4 Hz, C_{Ar}**H**), 6.51 (1H, d, J = 2.4 Hz, C_{Ar}**H**), 6.13 (1H, s, $C_{Ring\text{-}Alkene}$**H**), 5.78 (1H, d, J = 7.8 Hz, N**H**CHCH$_2$), 5.31 - 5.19 (2H, m, C**H**$_2$O), 4.63 - 4.55 (1H, m, NHC**H**CH$_2$), 4.39 (2H, d, J = 7.0 Hz, C_{Fmoc}**H**$_2$), 4.23 (1H, t, J = 7.0 Hz, C_{Fmoc}**H**), 3.40 (4H, q, J = 7.2 Hz, N(C**H**$_2$CH$_3$)$_2$), 3.11 (1H, dd, J = 17.0, 4.7 Hz, NHCHC**H**$_A$H$_B$), 3.01 (1H, dd, J = 17.0, 4.7 Hz,NHCHCH$_A$**H**$_B$), 1.47 (9H, s, OC(C**H**$_3$)$_3$), 1.19 (6H, t, J = 7.2 Hz, N(CH$_2$C**H**$_3$);

^{13}C NMR (100 MHz, $CDCl_3$) δC: 170.4 (**C**O), 169.4 (**C**O), 161.7 (**C**O), 156.3 ($\mathbf{C}_{Ar}$), 155.9 (**C**O), 150.7 ($\mathbf{C}_{Ar}$), 148.8 ($\mathbf{C}_{Ar}$), 143.6 ($\mathbf{C}_{FmocAr}$), 141.3 ($\mathbf{C}_{FmocAr}$), 127.8 ($\mathbf{C}_{FmocAr}$H), 127.1 ($\mathbf{C}_{FmocAr}$H), 125.2 ($\mathbf{C}_{FmocAr}$H), 124.4 ($\mathbf{C}_{Ar}$H), 120.0 ($\mathbf{C}_{FmocAr}$H), 108.7 ($\mathbf{C}_{Ar}$H), 106.8 ($\mathbf{C}_{Ring\text{-}Alkene}$H), 105.9 ($\mathbf{C}_{Ring\text{-}Alkene}$), 97.9 ($\mathbf{C}_{Ar}$H), 83.1 (O**C**$(CH_3)_3$), 67.3 ($\mathbf{C}_{Fmoc}H_2$), 61.9 (**C**$H_2$O), 50.9 (NH**C**H$CH_2$), 47.1 ($\mathbf{C}_{Fmoc}$H), 44.8 (N(**C**$H_2CH_3)_2$), 36.8 (NHCH**C**$H_2$), 27.9 (OC(C**H**$_3)_3$), 12.4 (N($CH_2$C**H**$_3)_2$);
LRMS *m/z* (ESI$^+$): 641 (100% $[M + H]^+$);
HRMS *m/z* (ESI$^+$): Found 641.2855 $[M + H]^+$ ($C_{37}H_{41}N_2O_8^+$ requires 641.2857 $[M + H]^+$);
IR (ν_{max} cm^{-1}): 3360 (w, br), 2976 (w), 1719 (s, C=O), 1605 (s, C=O), 1528 (m, Ar C-C), 1448 (w), 1423 (m), 1340 (w), 1274 (w), 1227 (w), 1147 (m, C-O), 1076 (w), 845 (w), 758 (m); HPLC: 15.78 min (97.4%).

(7-(Diethylamino)-2-oxo-2*H*-chromen-4-yl)methyl (4-nitrophenyl) carbonate



273

Method A:
4-Nitrophenyl chloroformate (66.5 mg, 0.33 mmol, 1.10 eq) was dissolved in anhydrous CH_2Cl_2 (1.00 mL). To this solution was added pyridine (26.1 mg, 0.03 mL, 0.33 mmol, 1.10 eq) to afford a white slurry. The reaction mixture was cooled to 0 °C and 7-(diethylamino)-4-(hydroxymethyl)-2*H*-chromen-2-one (**153**) (50.0 mg, 0.30 mmol, 1.00 eq) was added. The reaction mixture was allowed to warm to RT and stirred under an Ar atmosphere for 12 h, after which time the reaction was adjudged to be complete by TLC analysis. The reaction was quenched with CH_2Cl_2 (50.0 mL), washed with aq. 1 M HCl (50.0 mL), H_2O (50.0 mL), and brine (50.0 mL), dried over $MgSO_4$, and filtered. The solvent was removed under reduced pressure to afford (7-(diethylamino)-2-oxo-2*H*-chromen-4-yl)methyl (4-nitrophenyl) carbonate (**273**) as a bright yellow solid (71.7 mg, 58%), that was used without further purification.

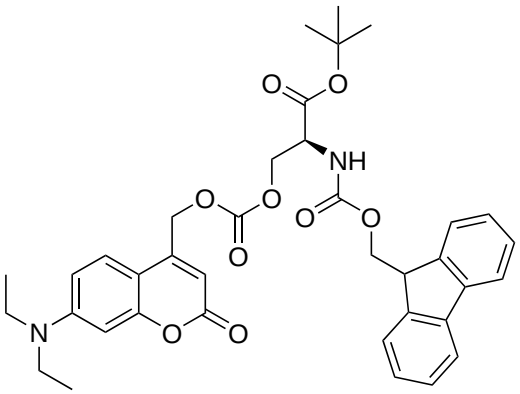
Method B:
7-(Diethylamino)-4-(hydroxymethyl)-2*H*-chromen-2-one (**153**) (200 mg, 0.81 mmol, 1.00 eq), 4-nitrophenyl chloroformate (244 mg, 1.21 mmol, 1.50 eq) and 4-(dimethylamino) pyridine (198 mg, 1.62 mmol, 2.00 eq) were dissolved in anhydrous CH_2Cl_2 (5.00 mL). The reaction solution was stirred at RT under an Ar atmosphere for 8 h, after which time the reaction was adjudged to be complete by TLC analysis. The reaction was quenched with CH_2Cl_2 (100 mL) and washed with aq. 1 M HCl (100 mL). The solvent was removed under reduced pressure and the crude residue was further purified by silica gel flash column chromatography, eluting with $CHCl_3$:petroleum ether = 6:4 - 7:3

to $CHCl_3$, to afford (7-(diethylamino)-2-oxo-2*H*-chromen-4-yl)methyl (4-nitrophenyl) carbonate (**273**) as a bright yellow solid (254 mg, 76%).

R_f: 0.64 (Petroleum ether:Acetone = 7:3);
m.p.: 168 - 170 °C (Petroleum ether/CH_2Cl_2);
^{1}H NMR (400 MHz, $CDCl_3$) **δ**H: 8.32 (2H, d, J = 9.3 Hz, C_{Ph}**H**), 7.43 (2H, d, J = 9.3 Hz, C_{Ph}**H**), 7.33 (1H, d, J = 9.1 Hz, C_{Ar}**H**), 6.65 (1H, dd, J = 9.1, 2.3 Hz, C_{Ar}**H**), 6.57 (1H, d, J = 2.3 Hz, C_{Ar}**H**), 6.25 (1H, s, $C_{Ring\text{-}Alkene}$**H**), 5.42 (2H, s, C**H**$_2$O), 3.44 (4H, q, J = 7.1 Hz, N(C**H**$_2$$CH_3$)$_2$), 1.23 (6H, t, J = 7.1 Hz, N(CH_2C**H**$_3$)$_2$);
^{13}C NMR (100 MHz, $CDCl_3$) **δ**C: 161.9 (**C**O), 156.3 (**C**O), 155.2 ($\mathbf{C}_{Ph}$), 152.1 ($\mathbf{C}_{Ph}$), 150.9 ($\mathbf{C}_{Ar}$), 148.0 ($\mathbf{C}_{Ar}$), 145.6 ($\mathbf{C}_{Ar}$), 125.4 ($\mathbf{C}_{Ph}$H), 124.3 ($\mathbf{C}_{Ar}$H), 121.7 ($\mathbf{C}_{Ph}$H), 108.9 ($\mathbf{C}_{Ar}$H), 106.6 ($\mathbf{C}_{Ring\text{-}Alkene}$H), 105.5 ($\mathbf{C}_{Ring\text{-}Alkene}$), 97.8 ($\mathbf{C}_{Ar}$H), 65.7 (**C**H$_2$O), 44.8 (N(**C**H$_2$$CH_3$)$_2$), 12.4 (N($CH_2$**C**H$_3$)$_2$);
LRMS *m/z* (ESI$^+$): 384 (100% $[M + H]^+$), 406 (33% $[M + Na]^+$;
HRMS *m/z* (ESI$^+$): Found 413.1344 $[M + H]^+$ ($C_{21}H_{21}N_2O_7^+$ requires 413.1343 $[M + H]^+$);
IR (ν_{max} cm^{-1}): 2969 (w), 2929 (w), 1773 (m), 1709 (s, C=O), 1610 (s, C=O), 1525 (m, N-O), 1489 (w), 1425 (w), 1359 (m), 1337 (w), 1272 (m), 1226 (w), 1198 (s, C-O), 1165 (s, C-O), 1143 (m), 1091 (m), 1072 (m),1041 (w), 1010 (w), 986 (w), 962 (w), 859 (m), 838 (s), 818 (w), 792 (w), 748 (m), 705 (w), 679 (w), 636 (w).

Data are concordant with literature values.[101]

***tert*-Butyl N-(((9*H*-fluoren-9-yl)methoxy)carbonyl)-*O*-(((7-(diethylamino)-2-oxo-2*H*-chromen-4-yl)methoxy)carbonyl)-*L*-serinate**



217

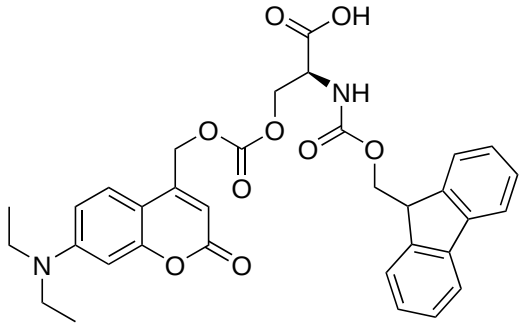
Method A:
N-Methylmorpholine (246 mg, 0.27 mL, 2.43 mmol, 1.50 eq) was added to an anhydrous solution of 4-nitrophenyl chloroformate (490 mg, 2.43 mmol, 1.50 eq) in CH_2Cl_2 (40.0 mL). The solution was cooled to 0 °C and a solution of 7-(diethylamino)-4-(hydroxymethyl)-2*H*-chromen-2-one (**153**) (400 mg, 1.62 mmol, 1.00 eq) in anhydrous CH_2Cl_2 (8.00 mL) was added dropwise. The reaction solution was warmed to RT and stirred under an Ar atmosphere for 8 h, after which time the formation of the intermediate was adjudged to be complete by TLC analysis. *tert*-Butyl (((9*H*-fluoren-9-yl)methoxy)carbonyl)-*L*-serinate (**185**) (621 mg, 1.62 mmol, 1.00 eq) and 4-(dimethylamino)pyridine (200 mg, 1.62 mmol, 1.00 eq) were added and the reaction solution was stirred at RT under an Ar atmosphere for 18 h, after which time the reaction was adjudged to be complete by TLC analysis. The reaction was quenched with CH_2Cl_2 (20.0 mL) and washed with aq. 1 M HCl (100 mL). The solvent was removed under reduced pressure and the crude residue was subjected to two successive purifications by silica gel flash column chromatography, eluting with petroleum ether:acetone = 8:2 then $CHCl_3$, to afford *tert*-butyl N-(((9*H*-fluoren-9-yl)methoxy)carbonyl)-*O*-(((7-(diethylamino)-2-oxo-2*H*-chromen-4-yl)methoxy)carbonyl)-*L*-serinate (**217**) as a yellow solid (258 mg, 24%).

Method B:
(7-(Diethylamino)-2-oxo-2*H*-chromen-4-yl)methyl (4-nitrophenyl) carbonate (**273**) (230 mg, 0.56 mmol, 1.00 eq), *tert*-butyl (((9*H*-fluoren-9-yl)methoxy)carbonyl)-*L*-serinate (**185**) (215 mg, 0.56 mmol, 1.00 eq) and 4-(dimethylamino)pyridine (137 mg,

1.12 mmol, 2.00 eq) were dissolved in anhydrous CH_2Cl_2 (10.0 mL). The reaction solution was stirred under an Ar atmosphere for 18 h, after which time the reaction was adjudged to be complete by TLC analysis. The reaction was quenched with CH_2Cl_2 (10.0 mL) and washed with aq. 1 M HCl (50.0 mL). The solvent was removed under reduced pressure and the crude residue was further subjected to two successive purifications by silica gel flash column chromatography, eluting with petroleum ether:acetone = 8:2 then $CHCl_3$, to afford *tert*-butyl *N*-(((9*H*-fluoren-9-yl)methoxy)carbonyl)-*O*-(((7-(diethylamino)-2-oxo-2*H*-chromen-4-yl)methoxy)carbonyl)-*L*-serinate (**217**) as a yellow solid (118 mg, 32%).

R_f: 0.34 (Petroleum ether:Acetone = 7:3);
m.p.: 79 - 82 °C (Petroleum ether/Acetone);
$[\alpha]_D^{26}$: +25.0 (***c*** 0.5 in $CHCl_3$);
UV λ_{max}/nm (ϵ/M^{-1}cm^{-1}): 380 (16570) [MeOH];
^{1}H NMR (400 MHz, $CDCl_3$) **δ**H: 7.76 (2H, d, J = 7.5 Hz, C_{Fmoc}**H**), 7.62 (2H, d, J = 7.5 Hz, C_{Fmoc}**H**), 7.40 (2H, t, J = 7.5 Hz, C_{Fmoc}**H**), 7.32 (2H, t, J = 7.5 Hz, C_{Fmoc}**H**), 7.26 (1H, d, J = 9.1 Hz, $C_{DEACMAr}$**H**), 6.56 (1H, dd, J = 9.1, 2.5 Hz, $C_{DEACMAr}$**H**), 6.50 (1H, d, J = 2.5 Hz, $C_{DEACMAr}$**H**), 6.15 (1H, s, $C_{DEACMAlkene}$**H**), 5.72 (1H, d, J = 7.3 Hz, N**H**), 5.26 (2H, d, J = 3.2 Hz, C**H**$_2$O), 4.63 - 4.55 (2H, m, NHC**H**CH$_2$, NHCHC**H**$_A$H$_B$), 4.55 - 4.50 (1H, m, NHCHCH$_A$**H**$_B$), 4.42 (1H, dd, J = 10.8, 7.1 Hz, C_{Fmoc}**H**$_A$H$_B$), 4.38 (1H, dd, J = 10.8, 7.1 Hz, C_{Fmoc}H$_A$**H**$_B$), 4.24 (1H, t, J = 7.1 Hz, C_{Fmoc}**H**), 3.40 (4H, q, J =7.1 Hz, N(C**H**$_2$CH$_3$)$_2$), 1.49 (9 H, s, OC(C**H**$_3$)$_3$), 1.20 (6H, t, J = 7.1 Hz, N(CH$_2$C**H**$_3$)$_2$);
^{13}C NMR (100 MHz, $CDCl_3$) **δ**C: 167.8 (**C**O), 161.7 (**C**O), 156.2 ($\mathbf{C}_{DEACMAr}$), 155.8 (**C**O), 154.3 (**C**O), 150.7($\mathbf{C}_{DEACMAr}$), 148.4 ($\mathbf{C}_{DEACMAr}$), 143.7 ($\mathbf{C}_{FmocAr}$), 141.2 ($\mathbf{C}_{FmocAr}$), 127.7 ($\mathbf{C}_{FmocAr}$H), 127.0 ($\mathbf{C}_{FmocAr}$H), 125.1 ($\mathbf{C}_{FmocAr}$H), 124.3 ($\mathbf{C}_{DEACMAr}$H), 119.9 ($\mathbf{C}_{FmocAr}$H), 108.7 ($\mathbf{C}_{DEACMAr}$H), 106.6 ($\mathbf{C}_{DEACMAlkene}$H), 105.6 ($\mathbf{C}_{DEACMAlkene}$), 97.7 ($\mathbf{C}_{DEACMAr}$H), 83.5 (O**C**(CH$_3$)$_3$), 68.2 (NH**C**HCH$_2$), 67.3 ($\mathbf{C}_{Fmoc}$H$_2$), 65.0 (**C**H$_2$O), 53.8 (NHCH**C**H$_2$), 47.00 ($\mathbf{C}_{Fmoc}$H), 44.7 (N(**C**H$_2$CH$_3$)$_2$), 27.9 (OC(**C**H$_3$)$_3$), 12.4 (N(CH$_2$**C**H$_3$)$_2$);
LRMS *m/z* (ESI$^+$): 657 (100% [M + H]$^+$);
HRMS *m/z* (ESI$^+$): Found 657.2802 [M + H]$^+$ ($C_{37}H_{41}N_2O_9^+$ requires 657.2807 [M + H]$^+$);
IR (ν_{max} cm^{-1}) 3336 (w, br), 2976 (w), 1719 (s, C=O), 1605 (s, C=O), 1528 (m, Ar C-C), 1450 (w), 1423 (w), 1355 (w), 1236 (m), 1154 (m, C-O), 1077 (w), 973 (w), 844 (w), 759 (m), 743 (m), 666 (w); HPLC: 15.70 min (99.4%).

***N*-(((9*H*-Fluoren-9-yl)methoxy)carbonyl)-*O*-(((7-(diethylamino)-2-oxo-2*H*-chromen-4-yl)methoxy)carbonyl)-*L*-serine**



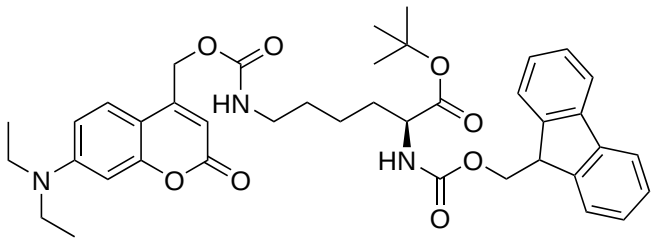
218

tert-Butyl *N*-(((9*H*-fluoren-9-yl)methoxy)carbonyl)-*O*-(((7-(diethylamino)-2-oxo-2*H*-chromen-4-yl)methoxy)carbonyl)-*L*-serinate (**217**) (100 mg, 0.15 mmol, 1.00 eq) was dissolved in CH_2Cl_2 (1.75 mL). To this solution was added trifluoroacetic acid (869 mg, 0.58 mL, 7.62 mmol, 50.0 eq) and immediately thereafter was added triethylsilane (142 mg, 0.19 mL, 1.22 mmol, 8.00 eq). The reaction solution was stirred at RT for 12 h, after which time the reaction was adjudged to be complete by TLC analysis. The solvent was removed by azeotropic distillation with cyclohexane (3 × 5.00 mL). The resulting residue was further purified by silica gel flash column chromatography, eluting with $CHCl_3$:AcOH = 100:1 to $CHCl_3$:MeOH:AcOH = 98:2:1, to afford *N*-(((9*H*-fluoren-9-yl)methoxy)carbonyl)-*O*-(((7-(diethylamino)-2-oxo-2*H*-chromen-4-yl)methoxy)carbonyl)-*L*-serine (**218**) as a yellow solid (96.2 mg, 92%).

R_f: 0.19 ($CHCl_3$:MeOH = 8:2);
m.p.: 132 - 133 °C (Hexane/MeOH);
$[\alpha]_D^{26}$: +52.9 (***c*** 1.0 in $CHCl_3$);
UV λ_{max}/nm (ϵ/$M^{-1}cm^{-1}$): 380 (21730) [MeOH];
^{1}H NMR (400 MHz, $CDCl_3$) **δ**H: 7.73 (2H, d, J = 7.2 Hz, $C_{FmocAr}\mathbf{H}$), 7.63 - 7.56 (2H, m, $C_{FmocAr}\mathbf{H}$), 7.41 - 7.33 (2H, m, $C_{FmocAr}\mathbf{H}$), 7.32 - 7.27 (2H, m, $C_{FmocAr}\mathbf{H}$), 7.23 (1H, d, J = 9.0 Hz, $C_{Ar}\mathbf{H}$), 6.57 (1H, d, J = 9.0 Hz, $C_{Ar}\mathbf{H}$), 6.50 (1H, s, $C_{Ar}\mathbf{H}$), 6.31 (1H, d, J = 7.4 Hz, $N\mathbf{H}CHCH_2$), 6.30 (1H, s, $C_{Alkene}\mathbf{H}$), 5.34 (1H, d, J = 15.4 Hz, $C\mathbf{H}_AH_BO$), 5.26 (1H, d, J = 15.4 Hz, $CH_A\mathbf{H}_BO$), 4.80 - 4.73 (1H, m, $NHC\mathbf{H}CH_2$), 4.72 - 4.66 (1H, m, $NHCHC\mathbf{H}_AH_B$), 4.66 - 4.60 (1H, m, $NHCHCH_A\mathbf{H}_B$), 4.47 - 4.33 (2H, m, $C_{Fmoc}\mathbf{H}_2$), 4.21 (1H, t, J = 7.0 Hz, $C_{Fmoc}\mathbf{H}$), 3.40 (4H, q, J = 6.9 Hz, $N(C\mathbf{H}_2CH_3)_2$), 1.20 (6H, t, J = 6.9 Hz, $N(CH_2C\mathbf{H}_3)_2$);

^{13}C NMR (100 MHz, $CDCl_3$) δC: 176.1 (**C**O), 171.8 (**C**O), 163.2 (**C**O), 156.0 ($\mathbf{C}_{Ar}$O), 154.3 (**C**O), 150.9 ($\mathbf{C}_{Ar}$N), 149.7 ($\mathbf{C}_{Ar}$), 143.8 ($\mathbf{C}_{FmocAr}$), 141.3 ($\mathbf{C}_{FmocAr}$), 127.7 ($\mathbf{C}_{FmocAr}$H), 127.1 ($\mathbf{C}_{FmocAr}$H), 125.2 ($\mathbf{C}_{FmocAr}$H), 124.2 ($\mathbf{C}_{Ar}$H), 119.9 ($\mathbf{C}_{FmocAr}$H), 109.1 ($\mathbf{C}_{Ar}$H), 105.7 ($\mathbf{C}_{Alkene}$), 105.4 ($\mathbf{C}_{Alkene}$H), 97.8 ($\mathbf{C}_{Ar}$H), 68.2 (NH**C**HCH$_2$), 67.4 ($\mathbf{C}_{Fmoc}$H$_2$), 64.6 (**C**H$_2$O), 53.2 (NHCH**C**H$_2$), 47.1 ($\mathbf{C}_{Fmoc}$H), 44.8 (N(**C**H$_2$CH$_3$)$_2$), 12.4 (N(CH$_2$**C**H$_3$)$_2$);
LRMS *m/z* (ESI$^+$): 601 (100% $[M + H]^+$);
HRMS *m/z* (ESI$^+$): Found 601.2180 $[M + H]^+$ ($C_{33}H_{33}N_2O_9^+$ requires 601.2181 $[M + H]^+$);
IR (ν_{max} cm^{-1}): 2973 (w), 1712 (s, C=O), 1598 (s, C=O), 1526 (m, Ar C-C), 1425 (m), 1351 (w), 1237 (s, C-O), 1142 (w), 1054 (m), 970 (w), 831 (w), 740 (s).

***tert*-Butyl N^2-(((9*H*-fluoren-9-yl)methoxy)carbonyl)-N^6-(((7-(diethylamino)-2-oxo-2*H*-chromen-4-yl)methoxy)carbonyl)-*L*-lysinate**



219

tert-Butyl (((9*H*-fluoren-9-yl)methoxy)carbonyl)-*L*-lysinate (**187**) (72.0 mg, 0.17 mmol, 1.00 eq) was dissolved in anhydrous DMF (0.17 mL). To this solution was added 10% aq. $NaHCO_3$ (0.45 mL). The solution was cooled to 0 °C and a solution of (7-(diethylamino)-2-oxo-2*H*-chromen-4-yl)methyl (4-nitrophenyl) carbonate (**273**) (70.0 mg, 0.17 mmol, 1.00 eq) in anhydrous DMF (0.51 mL) was added. The resulting solution was stirred at 0 °C for 1 h before being warmed to RT and stirred for a further 18 h under an Ar atmosphere, after which time the reaction was adjudged to be complete by TLC analysis. The reaction was quenched with H_2O (20.0 mL) and extracted with Et_2O (3 × 20.0 mL). The combined organics were washed with brine (50.0 mL), dried over $MgSO_4$ and filtered. The solvent was removed under reduced pressure and the crude oil was subjected to two successive purifications by silica gel flash column chromatography, eluting with petroleum ether:acetone = 8:2 then $CHCl_3$, to afford *tert*-butyl N^2-(((9*H*-fluoren-9-yl)methoxy)carbonyl)-N^6-(((7-(diethylamino)-2-oxo-2*H*-chromen-4-yl)methoxy)carbonyl)-*L*-lysinate (**219**) as a yellow oil (26.2 mg, 22%).

$\mathbf{R_f}$: 0.34 (Petroleum ether:Acetone = 7:3);
$\mathbf{[\alpha]_D^{26}}$: +4.7 (***c*** 5.1 in $CHCl_3$);
UV $\boldsymbol{\lambda_{max}}$/nm ($\boldsymbol{\epsilon}$/$\mathbf{M^{-1}cm^{-1}}$): 380 (32550) [MeOH];
^{1}H NMR (400 MHz, MeOD) $\boldsymbol{\delta}$H: 7.75 (2H, d, J = 7.5 Hz, $C_{FmocAr}\mathbf{H}$), 7.64 (2H, d, J = 7.1, Hz, $C_{FmocAr}\mathbf{H}$), 7.36 (2H, t, J = 7.5 Hz, $C_{FmocAr}\mathbf{H}$), 7.32 - 7.25 (3H, m, $C_{FmocAr}\mathbf{H}$, $C_{Ar}\mathbf{H}$), 6.59 (1H, dd, J = 8.9, 2.1 Hz, $C_{Ar}\mathbf{H}$), 6.46 (1H, d, J = 2.1 Hz, $C_{Ar}\mathbf{H}$), 6.02 (1H, s, $C_{Ring\text{-}Alkene}\mathbf{H}$), 5.24 (1H, d, J = 16.3 Hz, $C\mathbf{H}_AH_BO$), 5.19 (1H, d, J = 16.3 Hz, $CH_A\mathbf{H}_BO$), 4.35 - 4.23 (2H, m, $C_{Fmoc}\mathbf{H}_2$), 4.15 (1H, t, J = 7.0 Hz, $C_{Fmoc}\mathbf{H}$), 4.13 - 4.00 (1H, m, NHC**H**CH_2), 3.40 (4H, q, J = 7.0 Hz, $N(C\mathbf{H}_2CH_3)_2$), 3.18 (2H, t, J = 6.4 Hz, $NHC\mathbf{H}_2CH_2$), 1.88 - 1.76 (1H, m, $NHCHC\mathbf{H}_AH_BCH_2$),

1.76 - 1.65 (1H, m, $NHCHCH_A\mathbf{H}_BCH_2$), 1.63 - 1.51 (2H, m, $NHCH_2C\mathbf{H}_2$), 1.45 (9H, s, $OC(C\mathbf{H}_3)_3$), 1.50 - 1.37 (2H, m, $NHCHCH_2C\mathbf{H}_2$), 1.16 (6H, t, J = 7.0 Hz, $N(CH_2C\mathbf{H}_3)_2$);

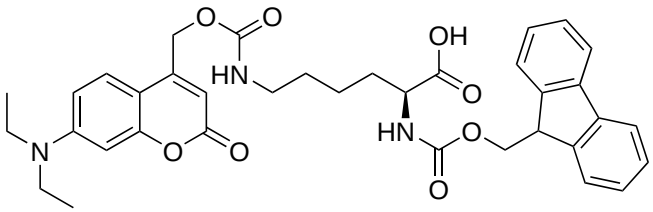
^{13}C NMR (100 MHz, $CDCl_3$) $\boldsymbol{\delta}$C: 171.3 ($\mathbf{C}O$), 164.7 ($\mathbf{C}O$), 158.8 ($\mathbf{C}O$), 157.5 ($\mathbf{C}O$), 154.1 ($\mathbf{C}_{Ar}$), 151.0 ($\mathbf{C}_{Ar}$), 148.5 ($\mathbf{C}_{Ar}$), 145.4 ($\mathbf{C}_{FmocAr}$), 142.7 ($\mathbf{C}_{FmocAr}$), 128.9 ($\mathbf{C}_{FmocAr}H$), 128.3 ($\mathbf{C}_{FmocAr}H$), 126.4 ($\mathbf{C}_{Ar}H$), 126.0 ($\mathbf{C}_{FmocAr}H$), 121.1 ($\mathbf{C}_{FmocAr}H$), 110.5 ($\mathbf{C}_{Ar}H$), 107.2 ($\mathbf{C}_{Ring\text{-}Alkene}$), 105.3 ($\mathbf{C}_{Ring\text{-}Alkene}H$), 98.3 ($\mathbf{C}_{Ar}H$), 82.8 ($O\mathbf{C}(CH_3)_3$), 68.1 ($\mathbf{C}_{Fmoc}H_2$), 62.8 ($\mathbf{C}H_2O$), 56.2 ($NH\mathbf{C}HCH_2$), 55.0 ($\mathbf{C}_{Fmoc}H$), 45.7 ($N(\mathbf{C}H_2CH_3)_2$), 41.4 ($NH\mathbf{C}H_2CH_2$), 32.1 ($NHCH\mathbf{C}H_2CH_2$), 30.5 ($NHCH_2\mathbf{C}H_2$), 28.4 ($OC(\mathbf{C}H_3)_3$), 24.0 ($NHCHCH_2\mathbf{C}H_2$), 12.9 ($N(CH_2\mathbf{C}H_3)_2$);

LRMS *m/z* (ESI$^+$): 698 (100% $[M + H]^+$);

HRMS *m/z* (ESI$^+$): Found 698.3425 $[M + H]^+$ ($C_{40}H_{49}N_3O_8{}^+$ requires 698.3436 $[M + H]^+$);

IR ($\boldsymbol{\nu}_{\mathbf{max}}$ cm^{-1}): 3432 (w, br), 2970 (w), 2483 (w), 1710 (s, C=O), 1606 (s, C=O), 1528 (w), 1432 (m, Ar C-C), 1342 (w), 1275 (w), 1153 (w), 1076 (w), 841 (w), 748 (w).

N^2-(((9*H*-Fluoren-9-yl)methoxy)carbonyl)-N^6-(((7-(diethylamino)-2-oxo-2*H*-chromen-4-yl)methoxy)carbonyl)-*L*-lysine



274

4-Nitrophenyl chloroformate (120 mg, 0.60 mmol, 1.50 eq) was dissolved in anhydrous CH_2Cl_2 (10.0 mL). To this solution was added *N*-methyl morpholine (81.9 mg, 0.09 mL, 0.81 mmol, 2.00 eq) and the resulting solution was stirred at RT for 5 min. A solution of 7-(diethylamino)-4-(hydroxymethyl)-2*H*-chromen-2-one (**153**) (100 mg, 0.40 mmol, 1.00 eq) in CH_2Cl_2 (5.00 mL) was added dropwise and the reaction solution was stirred at RT under an Ar atmosphere for 2 h, after which time the reaction was adjudged to be complete by TLC analysis. The reaction was quenched with CH_2Cl_2 (5.00 mL) and washed with aq. 1 M HCl (10.0 mL). The solvent was removed under reduced pressure and used without further purification. The above residue was resuspended in MeCN (10.0 mL) and CH_2Cl_2 (5.00 mL). Fmoc-Lys-OH·HCl (150 mg, 0.40 mmol, 1.00 eq) was dissolved in H_2O:MeCN (2:1, 15.0 mL) and $NaHCO_3$ (68.0 mg, 0.81 mmol, 2.00 eq) was added. To this solution was added dropwise a solution of the above-mentioned 4-nitrophenyl carbamate intermediate (**273**) in CH_2Cl_2 (2.00 mL). The resulting reaction mixture was stirred at RT for 18 h, after which time the reaction was adjudged to be complete by TLC analysis. The reaction was quenched with CH_2Cl_2 (5.00 mL) and the solvent was removed under reduced pressure. The crude residue was further purified by silica gel flash column chromatography, eluting with $CHCl_3$:AcOH = 100:1, to afford N^2-(((9*H*-fluoren-9-yl)methoxy)carbonyl)-N^6-(((7-(diethylamino)-2-oxo-2*H*-chromen-4-yl)methoxy)carbonyl)-*L*-lysine (**220**) as a yellow powder (113 mg, 44%).

R_f: 0.38 ($CHCl_3$:MeOH = 8:2);
m.p.: 181 - 183 °C (Hexane/MeOH);
$[\alpha]_D^{26}$: +13.7 (***c*** 1.1 in $CHCl_3$);
UV λ_{max}/nm (ϵ/M^{-1}cm^{-1}): 380 (23240) [MeOH];
^{1}H NMR (400 MHz, $(CD_3)_2SO$) **δ**H: 12.55 (1H, br s, COO**H**), 7.88 (2H, d, J = 7.5 Hz, C_{FmocAr}**H**), 7.72 (2H, d, J = 7.5 Hz, C_{FmocAr}**H**), 7.60 (1H, d, J = 8.0 Hz,

N**H**CHCH$_2$), 7.51 (1H, t, J = 5.6 Hz, N**H**CH$_2$CH$_2$), 7.45 - 7.37 (3H, m, C$_{\text{FmocAr}}$**H**, C$_{\text{Ar}}$**H**), 7.32 (2H, t, J = 7.5 Hz, C$_{\text{FmocAr}}$**H**), 6.67 (1H, dd, J = 8.9, 2.0 Hz, C$_{\text{Ar}}$**H**), 6.53 (1H, d, J = 2.0 Hz, C$_{\text{Ar}}$**H**), 5.96 (1H, s, C$_{\text{Alkene}}$**H**), 5.19 (2H, s, C**H**$_2$O), 4.28 (2H, d, J = 7.0 Hz, C$_{\text{Fmoc}}$**H**$_2$), 4.21 (1H, t, J = 7.0 Hz, C$_{\text{Fmoc}}$**H**), 3.92 (1H, ddd, J = 8.0, 8.0, 4.8 Hz, NHC**H**CH$_2$), 3.41 (4H, q, J = 6.9 Hz, N(C**H**$_2$CH$_3$)$_2$), 3.03 (2H, q, J = 5.6 Hz, NHC**H**$_2$CH$_2$), 1.77 - 1.66 (1H, m, NHCHC**H**$_{\text{A}}$H$_{\text{B}}$CH$_2$), 1.66 - 1.57 (1H, m, NHCHCH$_{\text{A}}$**H**$_{\text{B}}$CH$_2$), 1.50 - 1.39 (2H, m, NHCH$_2$C**H**$_2$), 1.39 - 1.26 (2H, m, NHCHCH$_2$C**H**$_2$), 1.11 (6H, t, J = 6.9 Hz, N(CH$_2$C**H**$_3$)$_2$);

^{13}C NMR (100 MHz, (CD$_3$)$_2$SO) δC: 173.9 (**C**OOH), 160.7 (**C**O), 156.1 (**C**$_{\text{Ar}}$O), 155.7 (**C**O), 155.4 (**C**O), 151.9 (**C**$_{\text{Ar}}$N), 150.4 (**C**$_{\text{Ar}}$), 143.8 (**C**$_{\text{FmocAr}}$), 140.7 (**C**$_{\text{FmocAr}}$), 127.6 (**C**$_{\text{FmocAr}}$H), 127.0 (**C**$_{\text{FmocAr}}$H), 125.3 (**C**$_{\text{FmocAr}}$H), 125.3 (**C**$_{\text{Ar}}$H), 120.1 (**C**$_{\text{FmocAr}}$H), 108.7 (**C**$_{\text{Ar}}$H), 105.3 (**C**$_{\text{Alkene}}$H), 104.5 (**C**$_{\text{Alkene}}$), 96.8 (**C**$_{\text{Ar}}$H), 65.6 (**C**$_{\text{Fmoc}}$H$_2$), 60.8 (**C**H$_2$O), 53.8 (**C**$_{\text{Fmoc}}$H), 46.7 (NH**C**HCH$_2$), 44.0 (N(**C**H$_2$CH$_3$)$_2$), 40.1 (NH**C**H$_2$CH$_2$), 30.4 (NHCH**C**H$_2$CH$_2$), 28.9 (NHCH$_2$**C**H$_2$), 22.9 (NHCHCH$_2$**C**H$_2$), 12.3 (N(CH$_2$**C**H$_3$)$_2$);

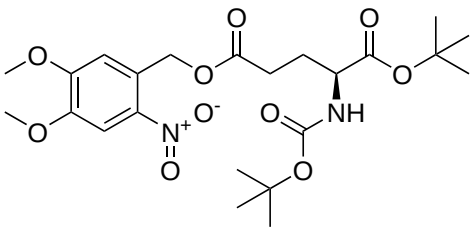
LRMS *m/z* (ESI$^+$): 642 (100% [M + H]$^+$);

HRMS *m/z* (ESI$^+$): Found 642.2811 [M + H]$^+$ (C$_{36}$H$_{40}$N$_3$O$_8$$^+$ requires 642.2810 [M + H]$^+$);

IR (ν_{max} cm^{-1}): 3332 (w), 2980 (w), 2941 (w), 2873 (w), 1734 (w), 1693 (s, C=O), 1665 (m), 1608 (s, C=O), 1526 (m, Ar C-C), 1441 (m), 1416 (m), 1346 (m), 1287 (w), 1262 (w), 1219 (w), 1196 (w), 1142 (w), 1110 (w), 1081 (m), 1014 (w), 988 (w), 933 (w), 867 (w), 823 (w), 800 (w), 776 (w), 734 (m), 696 (W), 669 (w).

7.8 DMNB Caged Amino Acids

1-(*tert*-Butyl) 5-(4,5-dimethoxy-2-nitrobenzyl) (*tert*-butoxycarbonyl)-*L*-glutamate



177

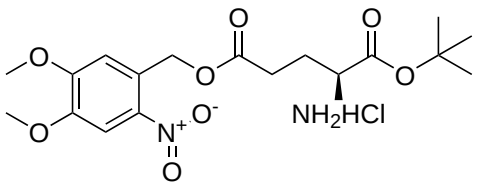
4,5-Dimethoxy-2-nitrobenzyl bromide (**148**) (200 mg, 0.72 mmol, 1.00 eq) and Boc-Glu-O^{t}Bu (**138**) (220 mg, 0.72 mmol, 1.00 eq) were dissolved in anhydrous THF (10.0 mL). The solution was cooled to 0 °C and 1,8-diazabicyclo[5.4.0]undec-7-ene (135 mg, 0.13 mL, 0.89 mmol, 1.10 eq) was added dropwise. The resulting mixture was stirred at RT under an Ar atmosphere for 24 h, after which time the reaction was adjudged to be complete by TLC analysis. The mixture was filtered and the solvent was removed under reduced pressure. The residue was redissolved in CH_2Cl_2 (200 mL), washed with H_2O (200 mL), dried over $MgSO_4$, and filtered. The solvent was removed under reduced pressure and the crude residue was purified by silica gel flash column chromatography, eluting with petroleum ether:Et_2O = 1:1, to afford 1-(*tert*-butyl) 5-(4,5-dimethoxy-2-nitrobenzyl) (*tert*-butoxycarbonyl)-*L*-glutamate (**177**) as a yellow solid (222 mg, 62%).

$\mathbf{R_f}$: 0.28 (Petroleum ether:Et_2O = 1:1);
m.p.: 105 - 107 °C (Petroleum ether/Et_2O) [Literature value: 106 - 107 °C (Petroleum ether/EtOAc)][205];
$[\boldsymbol{\alpha}]_{\boldsymbol{D}}^{\mathbf{26}}$: -5.2 (***c*** 0.9 in $CHCl_3$) [Literature value: -5.4 (***c*** 1.0 in $CHCl_3$)][205];
^{1}H NMR (400 MHz, $CDCl_3$) $\boldsymbol{\delta}$H: 7.72 (1H, s, $C_{Ar}\mathbf{H}$), 7.02 (1H, s, $C_{Ar}\mathbf{H}$), 5.55 (1H, d, J = 15.0 Hz, $C\mathbf{H}_AH_BO$), 5.50 (1H, d, J = 15.0 Hz, $CH_A\mathbf{H}_BO$), 5.11 (1H, d, J = 7.9 Hz, $N\mathbf{H}CHCH_2$), 4.27 - 4.18 (1H, m, $NHC\mathbf{H}CH_2$), 4.00 (3H, s, $OC\mathbf{H}_3$), 3.96 (3H, s, $OC\mathbf{H}_3$), 2.61 - 2.42 (2H, m, $NHCHCH_2C\mathbf{H}_2$), 2.29 - 2.16 (1H, m, $NHCHC\mathbf{H}_AH_BCH_2$), 2.02 - 1.90 (1H, m, $NHCHCH_A\mathbf{H}_BCH_2$), 1.47 (9H, s, $OC(C\mathbf{H}_3)_3$), 1.43 (9H, s, $OC(C\mathbf{H}_3)_3$);
^{13}C NMR (100 MHz, $CDCl_3$) $\boldsymbol{\delta}$C: 179.4 (**C**O), 175.0 (**C**O), 156.7 (**C**O), 153.5 ($\mathbf{C}_{Ar}$), 152.6 ($\mathbf{C}_{Ar}$), 131.6 ($\mathbf{C}_{Ar}$), 126.7 ($\mathbf{C}_{Ar}$), 110.3 ($\mathbf{C}_{Ar}$H), 108.2 ($\mathbf{C}_{Ar}$H), 82.3 (O**C**$(CH_3)_3$),

75.7 (O**C**$(CH_3)_3$), 63.4 (**C**H_2O), 56.5 (O**C**H_3), 56.4 (O**C**H_3), 55.4 (NH**C**HCH_2), 43.3 (NHCHCH_2**C**H_2), 31.3 (NHCH**C**H_2CH_2), 28.3 (OC(**C**$H_3)_3$), 28.0 (OC(**C**$H_3)_3$);
LRMS *m/z* (ESI$^+$): 499 (100% $[M + H]^+$);
IR (ν_{max} cm^{-1}): 3369 (w), 2968 (w), 2166 (w), 1970 (w), 1732 (s, C=O), 1716 (s, C=O), 1582 (w, Ar C-C), 1525 (s, N-O), 1332 (m), 1276 (s, C-O), 1224 (w), 1160 (m), 1066 (s, C-O), 982 (w), 878 (w), 840 (w), 749 (w), 680 (w).

Data are concordant with literature values.[205]

1-(*tert*-Butyl) 5-(4,5-dimethoxy-2-nitrobenzyl) *L*-glutamate hydrochloride



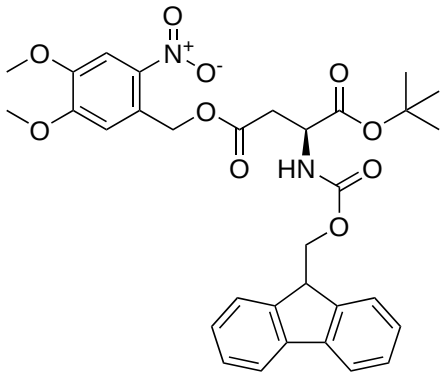
275

1-(*tert*-Butyl) 5-(4,5-dimethoxy-2-nitrobenzyl) (*tert*-butoxycarbonyl)-*L*-glutamate (**177**) (200 mg, 0.40 mmol, 1.00 eq) was dissolved in a solution of 2.0 M HCl in Et_2O (10.0 mL, 20.1 mmol, 50.0 eq). The reaction solution was stirred at RT under an Ar atmosphere for 24 h, after which time the reaction was adjudged to be complete by TLC analysis. The solid was filtered, washed with Et_2O, and dried under suction to afford 1-(*tert*-butyl) 5-(4,5-dimethyoxy-2-nitrobenzyl)-*L*-glutamate hydrochloride (**275**) as a colourless solid (72.8 mg, 42%).

R_f: 0.01 (Petroleum ether:Et_2O = 1:1);
m.p.: 155 - 157 °C (Petroleum ether/Et_2O);
$[\alpha]_D^{26}$: +19.5 (***c*** 0.3 in $CHCl_3$);
UV λ_{max}/nm (ϵ/$M^{-1}cm^{-1}$): 340 (6070) [MeOH];
^{1}H NMR (400 MHz, CD_3OD) **δ**H: 7.73 (1H, s, C_{Ar}**H**), 7.16 (1H, s, C_{Ar}**H**), 5.50 (1H, d, J = 13.8 Hz, $C_{Ar}C\mathbf{H}_AH_BO$), 5.46 (1H, d, J = 13.8 Hz, $C_{Ar}H_A\mathbf{H}_BO$), 4.01 (1H, dd, J = 7.0, 7.0 Hz, $NH_2C\mathbf{H}CH_2$), 3.96 (3H, s, $C_{Ar}OC\mathbf{H}_3$), 3.91 (3H, s, $C_{Ar}OC\mathbf{H}_3$), 2.76 - 2.58 (2H, m, $NHCHCH_2C\mathbf{H}_2$), 2.22 (1H, dtd, J= 14.1, 7.2, 7.0 Hz, $NH_2CHC\mathbf{H}_AH_BCH_2$), 2.17 (1H, dtd, J = 14.1, 7.2, 7.0 Hz, $NH_2CHCH_A\mathbf{H}_BCH_2$), 1.52 (9H, s, $OC(C\mathbf{H}_3)_3$);
^{13}C NMR (100 MHz, CD_3OD) **δ**C: 173.2 (**C**O) 169.4 (**C**O), 155.1 ($\mathbf{C}_{Ar}O$), 150.3 ($\mathbf{C}_{Ar}O$), 142.0 ($\mathbf{C}_{Ar}N$), 127.3 ($\mathbf{C}_{Ar}CH_2O$), 113.3 ($\mathbf{C}_{Ar}H$), 109.7 ($C_{Ar}H$), 85.8 ($O\mathbf{C}(CH_3)_3$), 65.1 ($C_{Ar}\mathbf{C}H_2O$), 57.2 ($C_{Ar}O\mathbf{C}H_3$), 57.0 ($C_{Ar}O\mathbf{C}H_3$), 53.7 ($NH_2\mathbf{C}HCH_2$), 30.6 ($NHCHCH_2\mathbf{C}H_2$), 28.3 ($OC(\mathbf{C}H_3)_3$), 26.9 ($NH_2CH\mathbf{C}H_2CH_2$);
LRMS *m/z* (ESI$^+$): 399 (100% $[M + H]^+$);
HRMS *m/z* (ESI$^+$): Found 399.1758 $[M + H]^+$ ($C_{18}H_{27}N_2O_8^+$ requires 399.1762 $[M + H]^+$);
IR (ν_{max} cm^{-1}): 2926 (w), 2853 (w), 2362 (m), 2164 (w), 2025 (w), 1974 (w), 1733 (s, C=O), 1694 (w), 1579 (m, Ar C-C), 1519 (s, N-O), 1440 (w), 1397 (w), 1370 (w),

1328 (m), 1275 (s), 1252 (s), 1224 (s, C-N), 1176 (s, C-O), 1153 (s, C-O), 1069 (s), 987 (w), 881 (w), 837 (w), 796 (w), 755 (w), 674 (w).

1-(*tert*-Butyl) 4-(4,5-dimethoxy-2-nitrobenzyl) (((9*H*-fluoren-9-yl)meth-oxy)carbonyl)-*L*-aspartate



212

Fmoc-Asp-O^{t}Bu (**221**) (387 mg, 0.94 mmol, 1.00 eq) and *N*,*N*,*N*',*N*'-tetramethyl-*O*-(1*H*-benzotriazol-1-yl)uronium hexafluorophosphate (374 mg, 0.99 mmol, 1.05 eq) were dissolved in anhydrous DMF (10.0 mL). *N*,*N*-Diisopropylethylamine (243 mg, 0.33 mL, 1.88 mmol, 2.00 eq) was added dropwise and the reaction solution was stirred under an Ar atmosphere for 1 h. 4,5-Dimethoxy-2-nitrobenzyl alcohol (**149**) (200 mg, 0.94 mmol, 1.00 eq) was added and the resulting solution was stirred at RT under an Ar atmosphere for 18 h, after which time the reaction was adjudged to be complete by TLC analysis. The reaction was quenched with Et_2O (200 mL), washed with H_2O (3 × 200 mL), and brine (200 mL), dried over $MgSO_4$, and filtered. The solvent was removed under reduced pressure and the crude residue was further purified by silica gel flash column chromatography, eluting with $CHCl_3$:petroleum ether 40 - 60 = 7:3, to afford 1-(*tert*-butyl) 4-(4,5-dimethoxy-2-nitrobenzyl) (((9*H*-fluoren-9-yl)methoxy)carbonyl)-*L*-aspartate (**212**) as a yellow solid (452 mg, 79%).

R_f: 0.67 ($CHCl_3$:Acetone = 9:1);
m.p.: 64 - 66 °C (Petroleum ether/Et_2O);
$[\alpha]_D^{26}$: +18.3 (***c*** 0.8 in $CHCl_3$);
UV λ_{max}/nm (ϵ/M^{-1}cm^{-1}): 340 (4070) [MeOH]:
^{1}H NMR (400 MHz, $CDCl_3$) **δ**H: 7.76 (2H, d, J = 7.6 Hz, C_{FmocAr}**H**), 7.73 (1H, s, C_{Ar}**H**), 7.60 (2H, d, J = 7.5 Hz, C_{FmocAr}**H**), 7.40 (2H, t, J = 7.6 Hz, C_{FmocAr}**H**), 7.31 (2H, t, J = 7.5 Hz, C_{FmocAr}**H**), 7.02 (1H, s, C_{Ar}**H**), 5.82 (1H, d, J = 8.1 Hz, N**H**CHCH$_2$), 5.60 (1H, d, J = 14.7 Hz, C**H**$_A$H$_B$O), 5.51 (1H, d, J = 14.7 Hz, CH$_A$**H**$_B$O), 4.58 (1H, ddd, J = 8.1, 4.8, 4.6 Hz, NHCHC**H**$_2$), 4.41 (1H, dd, J = 10.5,

7.2 Hz, $C_{Fmoc}\mathbf{H}_AH_B$), 4.34 (1H, dd, J = 10.5, 7.2 Hz, $C_{Fmoc}H_A\mathbf{H}_B$), 4.22 (1H, dd, J = 7.2, 7.2 Hz, $C_{Fmoc}\mathbf{H}$), 3.98 (3H, s, OC$\mathbf{H}_3$), 3.95 (3H, s, OC$\mathbf{H}_3$), 3.12 (1H, dd, J = 17.0, 4.8 Hz, NHCHC$\mathbf{H}_A$H$_B$), 2.98 (1H, dd, J = 17.0, 4.6 Hz, NHCHCH$_A\mathbf{H}_B$), 1.45 (9H, s, OC(C$\mathbf{H}_3$)$_3$);

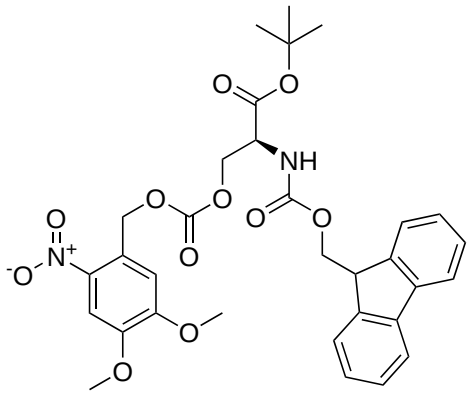
^{13}C NMR (100 MHz, $CDCl_3$) $\boldsymbol{\delta}$C: 170.3 (**C**O), 169.4 (**C**O), 155.9 (**C**O), 153.5 ($\mathbf{C}_{Ar}$), 148.3 ($\mathbf{C}_{Ar}$), 143.7 ($\mathbf{C}_{FmocAr}$), 141.2 ($\mathbf{C}_{FmocAr}$), 139.9 ($\mathbf{C}_{Ar}$), 127.7 ($\mathbf{C}_{FmocAr}$H), 127.0 ($\mathbf{C}_{FmocAr}$H), 126.4 ($\mathbf{C}_{Ar}$), 125.1 ($\mathbf{C}_{FmocAr}$H), 120.0 ($\mathbf{C}_{FmocAr}$H), 110.5 ($\mathbf{C}_{Ar}$H), 108.2 ($\mathbf{C}_{Ar}$H), 82.9 (O**C**(CH$_3$)$_3$), 67.2 ($\mathbf{C}_{Fmoc}H_2$), 63.8 (**C**H$_2$O), 56.5 (O**C**H$_3$), 56.4 (O**C**H$_3$), 50.9 (NH**C**HCH$_2$), 47.0 ($\mathbf{C}_{Fmoc}$H), 36.9 (NHCH**C**H$_2$), 27.8 (OC(**C**H$_3$)$_3$;

LRMS *m/z* (ESI$^+$): 629 (62% [M + Na]$^+$);

HRMS *m/z* (ESI$^+$): Found 607.2286 [M + H]$^+$ ($C_{32}H_{35}N_2O_{10}{}^+$ requires 607.2206 [M + H]$^+$);

IR ($\boldsymbol{\nu}_{\mathbf{max}}$ cm^{-1}): 3370 (w), 2977 (w), 1732 (s, C=O), 1580 (w, Ar C-C), 1521 (s, N-O), 1454 (w), 1333 (m), 1277 (s), 1223 (m), 1159 (m, C-N), 1067 (m, C-O), 869 (w), 749 (w); HPLC: 15.03 min (98.7%).

***tert*-Butyl *N*-(((9*H*-fluoren-9-yl)methoxy)carbonyl)-*O*-(((4,5-dimethoxy-2-nitrobenzyl)oxy)carbonyl)-*L*-serinate**



213

tert-Butyl (((9*H*-fluoren-9-yl)methoxy)carbonyl)-*L*-serinate (**185**) (69.0 mg, 0.18 mmol, 1.00 eq) and 4-(dimethylamino)pyridine (44.0 mg, 0.36 mmol, 2.00 eq) were dissolved in anhydrous CH_2Cl_2 (2.00 mL) and allowed to stir for 0.5 h at RT under an Ar atmosphere. 4,5-Dimethoxy-2-nitrobenzyl chloroformate (**150**) (49.6 mg, 0.18 mmol, 1.00 eq) was added and the reaction solution was again stirred at RT under an Ar atmosphere for 18 h, after which time the reaction was adjudged to be complete by TLC analysis. The reaction was quenched with CH_2Cl_2 (100 mL) and washed with aq. 1 M HCl (1 x 100 mL). The solvent was removed under reduced pressure and the crude residue was subjected to two successive purifications by silica gel flash column chromatography, eluting with petroleum ether:acetone = 8:2 then $CHCl_3$:petroleum ether = 9:1, to afford *tert*-butyl N-(((9*H*-fluoren-9-yl)methoxy)carbonyl)-*O*-(((4,5-dimethoxy-2-nitrobenzyl)oxy)carbonyl)-*L*-serinate (**213**) as a yellow foam (41.9 mg, 37%).

$\mathbf{R_f}$: 0.20 (Petroleum ether:Acetone = 7:3);
m.p.: 60 - 62 °C (Petroleum ether/Acetone);
$[\boldsymbol{\alpha}]_{\boldsymbol{D}}^{\mathbf{26}}$: +21.3 (***c*** 0.4 in $CHCl_3$);
UV $\boldsymbol{\lambda_{max}}$/nm ($\boldsymbol{\epsilon}$/$\mathbf{M^{-1}cm^{-1}}$): 340 (7020) [MeOH];
^{1}H NMR (400 MHz, $CDCl_3$) $\boldsymbol{\delta}$H: 7.76 (2H, d, J = 7.5 Hz, $C_{FmocAr}\mathbf{H}$), 7.72 (1H, s, $C_{Ar}\mathbf{H}$), 7.60 (2H, d, J = 7.3 Hz, $C_{FmocAr}\mathbf{H}$), 7.40 (2H, t, J = 7.5 Hz, $C_{FmocAr}\mathbf{H}$), 7.31 (2H, t, J = 7.3 Hz, $C_{FmocAr}\mathbf{H}$), 7.03 (1H, s, $C_{Ar}\mathbf{H}$), 5.66 (1H, d, J = 7.5 Hz, N**H**CHCH_2), 5.62, (1H, d, J = 15.2 Hz, C$\mathbf{H}_A$H$_B$O), 5.57 (1H, d, J = 15.2 Hz, CH$_A$$\mathbf{H}_B$O), 4.62 (1H, dd, J = 10.4, 4.0 Hz, NHCHC$\mathbf{H}_A$H$_B$), 4.59 – 4.55 (1H, m,

NHC**H**CH_2), 4.51 (1H, dd, J = 10.4, 4.0 Hz, NHCHCH_A**H**$_B$), 4.39 (2H, d, J = 7.0 Hz, C_{Fmoc}**H**$_2$), 4.22 (1H, t, J = 7.0 Hz, C_{Fmoc}**H**), 3.97 (3H, s, OC**H**$_3$), 3.95 (3H, s, OC**H**$_3$), 1.48 (9H, s, OC(C**H**$_3$)$_3$);

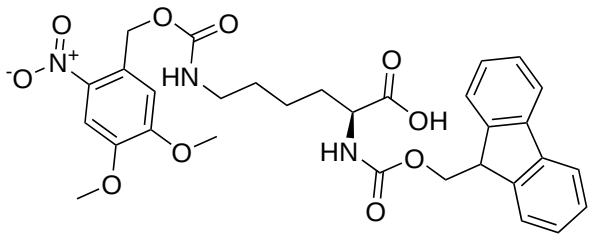
^{13}C NMR (100 MHz, $CDCl_3$) δC: 167.9 (**C**O), 155.8 (**C**O), 154. 4 (**C**O), 153.7 (**C**$_{Ar}$), 148.4 (**C**$_{Ar}$), 143.7 (**C**$_{FmocAr}$), 141.3 (**C**$_{FmocAr}$), 139.6 (**C**$_{Ar}$), 127.8 (**C**$_{FmocAr}$H), 127.1 (**C**$_{FmocAr}$H), 125.1 (**C**$_{FmocAr}$H), 120.0 (**C**$_{FmocAr}$H), 109.8 (**C**$_{Ar}$H), 108.2 (**C**$_{Ar}$H) 83.5 (O**C**$(CH_3)_3$), 68.0 (NH**C**HCH_2), 67.3 (**C**$_{Fmoc}H_2$), 66.7 (**C**H_2O), 56.5 (O**C**H_3), 56.4 (OCH_3), 54.0 (NHCH**C**H_2), 47.1 (**C**$_{Fmoc}$H), 27.9 (OC(**C**$H_3)_3$);

LRMS *m/z* (ESI$^+$): 183 (100%), 623 (21% $[M + H]^+$);

HRMS *m/z* (ESI$^+$): Found 623.2242 $[M + H]^+$ ($C_{32}H_{35}N_2O_{11}{}^+$ requires 623.2235 $[M + H]^+$);

IR (ν_{max} cm^{-1}): 3362 (w, br), 2977 (w), 2361 (w), 1751 (m, C=O), 1725 (m, C=O), 1582 (w, Ar C-C), 1524 (s, N-O), 1451 (w), 1394 (w), 1370 (w), 1332 (m), 1279 (s, C-N), 1221 (s, C-O), 1155 (m), 1066 (m), 974 (w), 873 (w), 796 (w) 758 (m), 667 (w); HPLC: 15.03 min (92.6%).

N^2-(((9*H*-Fluoren-9-yl)methoxy)carbonyl)-N^6-(((4,5-dimethoxy-2-nitrobenzyl)oxy)carbonyl)-*L*-lysine



214

Fmoc-Lys-OH·HCl (500 mg, 1.23 mol, 1.0 eq) was dissolved in a mixture of H_2O:1,4-dioxane:MeCN (1:1:1, 15.0 mL) and $NaHCO_3$ (207 mg, 2.46 mmol, 2.00 eq) was added. Additional H_2O (2.00 mL) and MeCN (2.00 mL) were added to ensure all solids were dissolved. 4,5-Dimethoxy-2-nitrobenzylchloroformate (**150**) (339 mg, 1.23 mmol, 1.00 eq) was dissolved in 1,4-dioxane (2.00 mL) and added dropwise to the aforementioned solution. The resulting bright yellow solution was stirred at RT for 18 h, after which time the reaction was adjudged to be complete by TLC analysis. The solvent was removed under reduced pressure and the obtained residue was partitioned between CH_2Cl_2 (200 mL) and aq. 1 N $NaHSO_4$ (200 mL). The organic layer was collected, the solvent was removed under reduced pressure, and the crude residue was further purified by silica gel flash column chromatography, eluting with $CHCl_3$:AcOH = 99:1 to $CHCl_3$:MeOH:AcOH = 94:5:1, to afford N^2-(((9*H*-fluoren-9-yl)methoxy)carbonyl)-N^6-(((4,5-dimethoxy-2-nitrobenzyl)oxy)carbonyl)-*L*-lysine (**214**) as a yellow foam (428 mg, 57%).

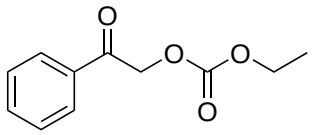
R_f: 0.43 ($CHCl_3$:MeOH:AcOH = 89:10:1);
m.p.: 68 - 70 °C (Hexane/MeOH);
$[\alpha]_D^{26}$: +3.4 (***c*** 8.8 in $CHCl_3$);
UV λ_{max}/nm (ϵ/$M^{-1}cm^{-1}$): 340 (4620) [MeOH];
^{1}H NMR (400 MHz, $(CD_3)_2SO$) **δ**H: 12.24 (1H, br s, COO**H**), 7.88 (2H, d, J = 7.3 Hz, C_{FmocAr}**H**), 7.72 (2H, d, J = 7.4 Hz, C_{FmocAr}**H**), 7.68 (1H, s, C_{Ar}**H**), 7.63 (1H, d, J = 7.9 Hz, N**H**CHCH$_2$), 7.47 (1H, t, J = 5.7 Hz, N**H**CH$_2$CH$_2$), 7.40 (2H, t, J = 7.3 Hz, C_{FmocAr}**H**), 7.32 (2H, t, J = 7.4 Hz, C_{FmocAr}**H**), 7.17 (1H, s, C_{Ar}**H**), 5.32 (2H, s, C**H**$_2$O), 4.31 - 4.24 (2H, m, C_{Fmoc}**H**$_2$), 4.24 - 4.19 (1H, m, C_{Fmoc}**H**), 3.95 - 3.89 (1H, m, NHC**H**CH$_2$), 3.88 (3H, s, OC**H**$_3$), 3.85 (3H, s, OC**H**$_3$), 3.07 - 2.96

(2H, m, NHC$\mathbf{H}_2$CH$_2$), 1.74 - 1.65 (1H, m, NHCHC$\mathbf{H}_A$H$_B$CH$_2$), 1.65 - 1.55 (1H, m, NHCHCH$_A$$\mathbf{H}_BCH_2$), 1.48 - 1.26 (4H, m, NHCH$_2$C$\mathbf{H}_2$, NHCHCH$_2$C$\mathbf{H}_2$);
^{13}C NMR (100 MHz, (CD$_3$)$_2$SO) $\boldsymbol{\delta}$C: 172.1 (**C**O), 156.2 (**C**O), 155.7 (**C**O), 153.3 (**C**$_{Ar}$), 147.7 (**C**$_{Ar}$), 143.8 (**C**$_{FmocAr}$), 140.7 (**C**$_{FmocAr}$), 139.3 (**C**$_{Ar}$), 128.0 (**C**$_{FmocAr}$H), 127.7 (**C**$_{Ar}$), 127.2 (**C**$_{FmocAr}$H), 125.3 (**C**$_{FmocAr}$H), 120.1 (**C**$_{FmocAr}$H), 110.5 (**C**$_{Ar}$H), 108.1 (**C**$_{Ar}$H), 65.6 (**C**$_{Fmoc}$H$_2$), 62.3 (**C**H$_2$O), 56.2 (O**C**H$_3$), 56.1 (O**C**H$_3$), 53.8 (NH**C**HCH$_2$), 46.7 (**C**$_{Fmoc}$H), 40.1 (NH**C**H$_2$CH$_2$), 30.4 (NHCH**C**H$_2$), 29.0 (NHCH$_2$**C**H$_2$), 23.0 (NHCHCH$_2$**C**H$_2$);
LRMS *m/z* (ESI$^+$): 564 (100%), 608 (60% [M + H]$^+$), 630 (100% [M + Na]$^+$); LRMS m/z (ESI$^-$): 606 (100% [M - H]$^-$);
HRMS *m/z* (ESI$^+$): Found 608.2237 [M + H]$^+$ ($C_{31}H_{34}N_3O_{10}^+$ requires 608.2239 [M + H]$^+$);
IR ($\boldsymbol{\nu}_{\mathbf{max}}$ cm^{-1}): 3339 (w), 2942 (w), 2024 (w), 1884 (w), 1705 (s, C=O), 1581 (w, Ar C-C), 1519 (s, N-O), 1447 (m), 1328 (m), 1273 (s, C-O), 1219 (m, C-N), 1168 (w), 1134 (w), 1066 (m), 1033 (m), 984 (w), 942 (w), 871 (m), 795 (m), 759 (s, N-H), 739 (s), 641 (w).

Data are concordant with literature values.[220]

7.9 Phenacyl Caged Amino Acids

Ethyl (2-oxo-2-phenylethyl) carbonate



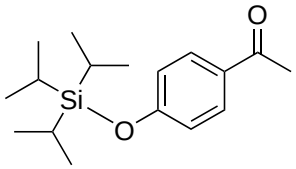
170

2-Hydroxyacetophenone (**169**) (250 mg, 1.84 mmol, 1.00 eq) was dissolved in anhydrous pyridine (10.0 mL). Ethyl chloroformate (0.35 mL, 3.67 mmol, 2.00 eq) was added dropwise and the resulting solution was stirred at 80 °C under a N_2 atmosphere for 18 h, after which time the reaction was adjudged to be complete by TLC analysis. The solution was cooled to RT and the reaction was quenched with Et_2O (100 mL), washed with aq. 1 M H_2SO_4 (100 mL), sat. aq. $NaHCO_3$ (100 mL), H_2O (100 mL) and brine (100 mL), dried over $MgSO_4$, and filtered. The solvent was removed under reduced pressure and the crude residue was further purified by silica gel flash column chromatography, eluting with petroleum ether:Et_2O = 7:3, to afford ethyl (2-oxo-2-phenylethyl) carbonate (**170**) as a yellow oil (299 mg, 78%).

$\mathbf{R_f}$: 0.28 (Petroleum ether:Et_2O = 7:3);
^{1}H NMR (400 MHz, $CDCl_3$) $\boldsymbol{\delta}$H: 7.92 (2H, d, J = 7.6 Hz, $C_{Ar}\mathbf{H}$), 7.63 (1H, t, J = 7.6 Hz, $C_{Ar}\mathbf{H}$), 7.50 (2H, t, J = 7.6 Hz, $C_{Ar}\mathbf{H}$), 5.36 (2H, s, $COC\mathbf{H}_2O$), 4.29 (2H, q, J = 7.2 Hz, $OC\mathbf{H}_2CH_3$), 1.37 (3H, t, J = 7.2 Hz, $OCH_2C\mathbf{H}_3$);
^{13}C NMR (100 MHz, $CDCl_3$) $\boldsymbol{\delta}$C: 191.8 ($\mathbf{C}O$), 154.9 ($\mathbf{C}O$), 134.0 ($\mathbf{C}_{Ar}H$), 128.9 ($\mathbf{C}_{Ar}H$), 127.7 ($\mathbf{C}_{Ar}$), 127.7 $\mathbf{C}_{Ar}H$), 68.5 ($CO\mathbf{C}H_2O$), 64.7 ($O\mathbf{C}H_2CH_3$), 14.2 ($OCH_2\mathbf{C}H_3$);
LRMS *m/z* (ESI$^+$): 209 (30% $[M + H]^+$), 231 (70% $[M + Na]^+$), 391 (100%).

Data are concordant with literature values.[221]

1-(4-((Triisopropylsilyl)oxy)phenyl)ethan-1-one



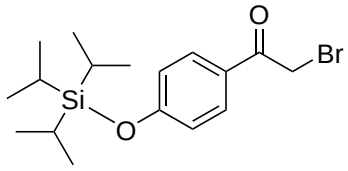
202

4'-Hydroxyacetophenone (**40**) (500 mg, 3.70 mmol, 1.00 eq) and imidazole (776 mg, 11.4 mmol, 3.10 eq) were dissolved in anhydrous DMF (5.00 mL). Triisopropylchlorosilane (925 mg, 1.02 mL, 4.80 mmol, 1.30 eq) was added dropwise and the reaction solution was stirred at RT under a N_2 atmosphere for 4 h, after which time the reaction was adjudged to be complete by TLC analysis. The reaction was quenched with EtOAc (200 mL), washed with H_2O (200 mL), and brine (200 mL), dried over $MgSO_4$, and filtered. The solvent was removed under reduced pressure and the crude residue was further purified by silica gel flash column chromatography, eluting with petroleum ether:EtOAc = 9:1, to afford 1-(4-((triisopropylsilyl)oxy)phenyl)ethan-1-one as a colourless oil (**202**) (1.07 g, > 99%).

R_f: 0.54 (Petroleum ether:EtOAc = 7:3);
UV λ_{max}/nm (ϵ/M^{-1}cm^{-1}): 270 (12140) [MeOH];
^{1}H NMR (400 MHz, $CDCl_3$) **δ**H: 7.88 (2H, d, J = 8.8 Hz, C_{Ar}**H**), 6.91 (2H, d, J = 8.8 Hz, C_{Ar}**H**), 2.55 (3H, s, COC**H**$_3$), 1.35 - 1.22 (3H, m, Si(CH(CH$_3$)$_2$)$_3$) 1.11 (18H, d, J = 7.3 Hz, Si(CH(C**H**$_3$)$_2$)$_3$);
^{13}C NMR (100 MHz, $CDCl_3$) **δ**C: 196.8 (**C**O), 160.7 (O**C**$_{Ar}$), 130.6 (**C**$_{Ar}$), 130.5 (**C**$_{Ar}$H), 119.7 (**C**$_{Ar}$H), 26.3 (CO**C**H$_3$), 17.8 (Si(**C**H(CH$_3$)$_2$)$_3$), 12.6 (Si(CH(**C**H$_3$)$_2$)$_3$);
LRMS m/z (ESI$^+$): 294 (88% [M + H]$^+$), 307 (100%);
IR (ν_{max} cm^{-1}): 3499 (w, br), 2947 (w), 2865 (w), 1677 (m, C=O), 1595 (m), 1507 (w), 1464 (w, Ar C-C), 1417 (w), 1358 (w), 1263 (s, C-O), 1166 (m), 1108 (w), 1069 (w), 1002 (w), 955 (m), 911 (w), 879 (m), 795 (w), 682 (m).

Data are concordant with literature values.[102]

2-Bromo-1-(4-((triisopropylsilyl)oxy)phenyl)ethan-1-one



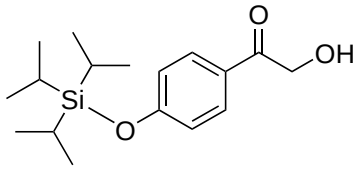
203

To a solution of 1-(4-((Triisopropylsilyl)oxy)phenyl)ethan-1-one (**202**) (10.7 g, 36.6 mmol, 1.00 eq) in anhydrous Et_2O (125 mL) was added $AlCl_3$ (2.44 g, 18.3 mmol, 0.50 eq). The resulting suspension was cooled to 0 °C and Br_2 (6.44 g, 2.06 mL, 40.3 mmol, 1.10 eq) was added dropwise. The resulting reaction mixture was allowed to warm to RT and stirred under an Ar atmosphere for 18 h, after which time the reaction was adjudged to be complete by TLC analysis. The reaction was quenched with sat. aq. $Na_2S_2O_3$ (200 mL) and filtered through a pad of Celite. The filtrate was partitioned between H_2O (100 mL) and Et_2O (250 mL), washed with brine (250 mL), dried over $MgSO_4$, and filtered. The solvent was removed under reduced pressure and the crude residue was further purified by silica gel flash column chromatography, eluting with CH_2Cl_2:Petroleum ether = 1:1, to afford 2-bromo-1-(4-((triisopropylsilyl)oxy)phenyl)ethan-1-one (**203**) as a colourless oil (11.8 g, 87%).

R_f: 0.54 (CH_2Cl_2);
UV λ_{max}/nm (ϵ/M^{-1}cm^{-1}): 285 (15050) [MeOH];
^{1}H NMR (400 MHz, $CDCl_3$) **δ**H: 7.92 (2H, d, J = 8.8 Hz, C_{Ar}**H**), 6.93 (2H, d, J = 8.8 Hz, C_{Ar}**H**), 4.41 (2H, s, COC**H**$_2$Br), 1.36 - 1.23 (3H, m, Si(C**H**$(CH_3)_2)_3$), 1.11 (18H, d, J = 7.6 Hz, Si(CH(C**H**$_3)_2)_3$);
^{13}C NMR (100 MHz, $CDCl_3$) **δ**C: 189.9 (**C**O), 161.4 (O**C**$_{Ar}$), 131.2 (**C**$_{Ar}$H), 127.2 (**C**$_{Ar}$), 120.0 (**C**$_{Ar}$H), 30.8 (**C**H$_2$Br), 17.8 (Si(**C**H$(CH_3)_2)_3$), 12.7 (Si(CH(**C**H$_3)_2)_3$);
LRMS *m/z* (ESI$^+$): 371 (100% $[M + H]^+$);
IR (ν_{max} cm^{-1}): 2946 (w), 2866 (w), 1676 (m, C=O), 1594 (s, Ar C-C), 1508 (m), 1464 (m), 1424 (w), 1389 (w), 1274 (s), 1197 (m), 1168 (m, C-O), 1112 (w), 1069 (w), 994 (w), 907 (s), 843 (m), 760 (w), 664 (s, C-Br).

Data are concordant with literature values.[102]

2-Hydroxy-1-(4-((triisopropylsilyl)oxy)phenyl)ethan-1-one

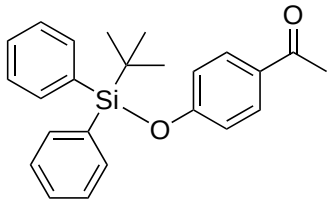


204

Sodium formate (21.2 g, 311 mmol, 10.0 eq) was stirred in EtOH (150 mL) for 15 min. To this was added 2-bromo-1-(4-((triisopropylsilyl)oxy)phenyl)ethan-1-one (**203**) (11.5 g, 31.1 mmol, 1.00 eq) and the reaction was stirred under reflux (88 °C) for 4 h. The hot solution was filtered and the solvent was removed under reduced pressure. The obtained crude oil was further purified by silica gel flash column chromatography, eluting with petroleum ether:Et_2O = 7:3, to afford 2-hydroxy-1-(4-((triisopropylsilyl)oxy)phenyl)ethan-1-one (**204**) as a yellow oil (1.99 g, 21%).

R_f: 0.41 (Petroleum ether:Et_2O = 1:1);
UV λ_{max}/nm (ϵ/$M^{-1}cm^{-1}$): 250 (9630) [MeOH];
^{1}H NMR (400 MHz, $CDCl_3$) **δ**H: 7.85 (2H, d, J = 8.7 Hz, C_{Ar}**H**), 6.95 (2H, d, J = 8.7 Hz, C_{Ar}**H**), 4.83 (2H, d, J = 4.6 Hz, C**H**$_2$OH), 3.58 (1H, t, J = 4.6 Hz, CH_2O**H**), 1.30 (3H, sp, J = 7.3 Hz, Si(C**H**$(CH_3)_2)_3$), 1.11 (18H, d, J = 7.3 Hz, Si(CH(C**H**$_3)_2)_3$);
^{13}C NMR (100 MHz, $CDCl_3$) **δ**C: 196.7 (**C**O), 161.7 (O**C**$_{Ar}$), 130.0 (**C**$_{Ar}$H), 126.5 (**C**$_{Ar}$), 120.1 (**C**$_{Ar}$H), 64.9 (**C**H_2OH), 17.8 (Si(**C**H$(CH_3)_2)_3$), 12.6 (Si(CH(**C**$H_3)_2)_3$);
LRMS *m/z* (ESI$^+$): 309 (50% $[M + H]^+$), 331 (100% $[M + Na]^+$);
HRMS *m/z* (ESI$^+$): Found 331.1708 $[M + Na]^+$ ($C_{17}H_{28}NaO_3Si^+$ requires 331.1700 $[M + Na]^+$);
IR (ν_{max} cm^{-1}): 3739 (w, br, O-H), 2968 (m), 2362 (s, C=O), 1385 (w, Ar C-C), 1260 (m, C-O), 1022 (m), 800 (m), 669 (m).

1-(4-((*tert*-Butyldiphenylsilyl)oxy)phenyl)ethan-1-one



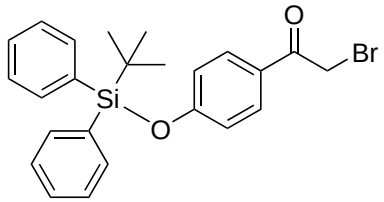
175

4'-Hydroxyacetophenone (**40**) (1.00 g, 7.34 mmol, 1.00 eq) and imidazole (600 mg, 8.81 mmol, 1.20 eq) were dissolved in anhydrous DMF (15.0 mL). *tert*-Butyl(chloro)diphenylsilane (3.03 g, 2.87 mL, 11.0 mmol, 1.50 eq) was added and the reaction solution was stirred at RT under a N_2 atmosphere for 18 h, after which time the reaction was adjudged to be complete by TLC analysis. The reaction was quenched with EtOAc (200 mL), washed with H_2O (200 mL), and brine (200 mL), dried over $MgSO_4$, and filtered. The solvent was removed under reduced pressure to afford 1-(4-((*tert*-butyldiphenylsilyl)oxy)phenyl)ethan-1-one (**175**) as a colourless solid (2.84 g, > 99%) that was used without further purification.

R_f: 0.74 (Petroleum ether:EtOAc = 1:1);
m.p.: 33 - 35 °C (Petroleum ether/Et_2O);
UV λ_{max}/nm (ϵ/$M^{-1}cm^{-1}$): 265 (24830) [MeOH];
^{1}H NMR (400 MHz, $CDCl_3$) δH: 7.77 - 7.73 (2H, m, C_{Ar}**H**), 7.71 (4H, m, C_{Ph}**H**), 7.40 (6H, m, C_{Ph}**H**), 6.80 (2H, d, J = 8.6 Hz, C_{Ar}**H**), 2.49 (3H, s, COC**H**$_3$), 1.12 (9H, s, $SiC_{Ph2}(CH_3)_3$);
^{13}C NMR (100 MHz, $CDCl_3$) δC: 196.9 (**C**O), 160.0 (**C**$_{Ar}$), 135.4 (**C**$_{Ph}$H), 132.1 (**C**$_{Ph}$), 130.3 (**C**$_{Ph}$H), 130.1 (**C**$_{Ar}$H), 129.6 (**C**$_{Ar}$), 127.9 (**C**$_{Ph}$H), 119.6 (**C**$_{Ar}$H), 26.5 (CO**C**H$_3$), 26.3 (SiC_{Ph2}(**C**H$_3$)$_3$), 19.4 (Si**C**$_{Ph2}$(CH$_3$)$_3$);
LRMS *m/z* (ESI$^+$): 338 (100%), 398 (12% $[M + Na]^+$);
IR (ν_{max} cm^{-1}): 2932 (w), 2892 (w), 2857 (w), 1674 (m, C=O), 1594 (m, Ar C-C), 1505 (m, Ar C-C), 1468 (w), 1413 (w), 1356 (w), 1255 (s, C-O), 1171 (m), 1107 (w), 1076 (w), 1006 (w), 962 (w), 910 (s), 837 (s), 780 (s), 679 (m).

Data are concordant with literature values.[222]

2-Bromo-1-(4-((*tert*-butyldiphenylsilyl)oxy)phenyl)ethan-1-one



176

Method A:
1-(4-((*tert*-Butyldiphenylsilyl)oxy)phenyl)ethan-1-one (**176**) (1.00 g, 2.67 mmol, 1.00 eq) was dissolved in anhydrous CH_2Cl_2 (10.0 mL). The solution was cooled to 0 °C and *N*,*N*-diisopropylethylamine (438 mg, 0.59 mL, 3.39 mmol, 1.27 eq) and trimethylsilyl trifluoromethanesulfonate (713 mg, 0.58 mL, 3.21 mmol, 1.20 eq) were added. The reaction was stirred at 0 °C for 0.5 h under a N_2 atmosphere. *N*-Bromosuccinimide (571 g, 3.21 mmol, 1.20 eq) was added and the reaction mixture was allowed to warm to RT and stirred for 0.5 h under a N_2 atmosphere. The reaction was quenched with CH_2Cl_2 (100 mL) and the solvent was removed under reduced pressure. The crude product was further purified by silica gel flash column chromatography, eluting with petroleum ether:EtOAc = 7:3, to afford 2-bromo-1-(4-((*tert*-butyldiphenylsilyl)oxy)phenyl)ethan-1-one (**176**) as a yellow oil (497 mg, 41%).

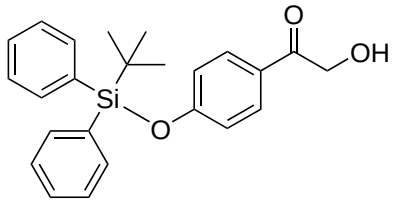
Method B:
1-(4-((*tert*-Butyldiphenylsilyl)oxy)phenyl)ethan-1-one (**175**) (10.0 g, 26.7 mmol, 1.00 eq) was dissolved in a mixture of CH_2Cl_2:MeOH (5:2, 70.0 mL). Benzyltrimethylammonium tribromide (10.4 g, 26.7 mmol, 1.00 eq) was added and the resulting mixture was stirred at RT for 4 h. The solvents were removed under reduced pressure and H_2O (500 mL) was added to the crude residue. The organic was extracted with Et_2O (3 × 500 mL) and the combined organic extracts were washed with brine (500 mL), dried over $MgSO_4$, and filtered. The solvent was removed under reduced pressure and the crude oil was further purified by silica gel flash column chromatography, eluting with petroleum ether:EtOAc = 7:3, to afford 2-bromo-1-(4-((*tert*-butyldiphenylsilyl)oxy)phenyl)ethan-1-one (**176**) as a colourless oil (11.1 g, 92%).

R_f: 0.59 (Petroleum ether:EtOAc = 1:1);
UV λ_{max}/nm (ϵ/$M^{-1}cm^{-1}$): 280 (11250) [MeOH];

^{1}H NMR (400 MHz, $CDCl_3$) $\boldsymbol{\delta}$H: 7.78 (2H, d, J = 9.0 Hz, $C_{Ar}\mathbf{H}$), 7.70 (4H, dd, J = 8.2, 1.4 Hz, $C_{Ph}\mathbf{H}$), 7.49 - 7.44 (2H, m, $C_{Ph}\mathbf{H}$), 7.42 - 7.37 (4H, m, $C_{Ph}\mathbf{H}$), 6.82 (2H, d, J = 9.0 Hz, $C_{Ar}\mathbf{H}$), 4.35 (2H, s, $C\mathbf{H}_2Br$), 1.12 (9H, s, $SiC_{Ph2}(C\mathbf{H}_3)_3$);
^{13}C NMR (100 MHz, $CDCl_3$) $\boldsymbol{\delta}$C: 189.9 ($\mathbf{C}O$), 160.7 ($\mathbf{C}_{Ar}$), 135.4 ($\mathbf{C}_{Ph}H$), 131.9 ($\mathbf{C}_{Ph}$), 131.0 ($\mathbf{C}_{Ar}H$), 130.2 ($\mathbf{C}_{Ph}H$), 128.0 ($\mathbf{C}_{Ph}H$), 127.3 ($\mathbf{C}_{Ar}$), 120.0 ($\mathbf{C}_{Ar}H$), 30.8 ($\mathbf{C}H_2Br$), 26.3 ($SiC_{Ph2}(\mathbf{C}H_3)_3$, 19.4 ($Si\mathbf{C}_{Ph2}(CH_3)_3$);
LRMS *m/z* (ESI$^+$): 455 (100% $[M + H]^+$);
IR ($\boldsymbol{\nu}_{\mathbf{max}}$ cm^{-1}): 3070 (w), 2957 (w), 2858 (w), 1676 (m, C=O), 1595 (s, Ar C-C), 1508 (m, Ar C-C), 1469 (w), 1426 (m), 1271 (s), 1195 (m), 1170 (m), 1110 (s, C-O), 1079 (m), 1000 (w), 911 (s), 842 (s, Ar C-H), 742 (m), 700 (s, C-Br), 665 (w).

Data are concordant with literature values.[222]

1-(4-((*tert*-Butyldiphenylsilyl)oxy)phenyl)-2-hydroxyethan-1-one



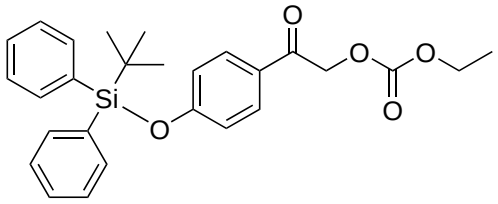
171

Sodium formate (979 mg, 14.4 mmol, 6.50 eq) was stirred in EtOH (5.00 mL) for 15 min. 2-Bromo-1-(4-((*tert*-butyldiphenylsilyl)oxy)phenyl)ethan-1-one (**176**) (1.00 g, 2.20 mmol, 1.00 eq) was added and the reaction mixture was gently heated under reflux (88 °C) for 10 h, after which time the reaction was adjudged to be complete by TLC analysis. The hot reaction mixture was filtered and the solvent was removed under reduced pressure. The crude residue was purified by silica gel flash column chromatography, eluting with petroleum ether:EtOAc = 8:2, to afford 1-(4-((*tert*-butyldiphenylsilyl)oxy)phenyl)-2-hydroxyethan-1-one (**171**) as a colourless solid (272 mg, 32%).

R_f: 0.26 (Petroleum ether:EtOAc = 8:2);
m.p.: 69 - 71 °C (Petroleum ether/Et_2O);
UV λ_{max}/nm (ϵ/$M^{-1}cm^{-1}$): 265 (18250) [MeOH];
^{1}H NMR (400 MHz, $CDCl_3$) δH: 7.75 - 7.68 (6H, m, C_{Ar}**H**, C_{Ph}**H**), 7.49 - 7.43 (2H, m, C_{Ph}**H**), 7.42 - 7.36 (4H, m, C_{Ph}**H**), 6.83 (2H, d, J = 8.8 Hz, C_{Ar}**H**), 4.75 (2H, d, J = 4.5 Hz, C**H_2**OH), 3.55 (1H, t, J = 4.5 Hz, CH_2O**H**), 1.12 (9H, s, $SiC_{Ph2}(CH_3)_3$);
^{13}C NMR (100 MHz, $CDCl_3$) δC: 196.7 (**C**O), 160.1 (**C_{Ar}**), 135.3 (**C_{Ph}**H), 131.8 (**C_{Ph}**), 130.3 (**C_{Ar}**H), 129.7 (**C_{Ph}**H), 128.0 (**C_{Ph}**H), 126.6 (**C_{Ar}**), 120.1 (**C_{Ar}**H), 64.9 (**C**H_2OH), 26.3 (SiC_{Ph2}(**C**H_3)$_3$), 19.4 (Si**C**$_{Ph2}$(CH_3)$_3$);
LRMS *m/z* (ESI$^+$): 391 (88% $[M + H]^+$), 414 (100% $[M + Na]^+$);
IR (ν_{max} cm^{-1}): 3424 (w, br, O-H), 2932 (w), 2858 (w), 1679 (m, C=O), 1597 (m, Ar C-C), 1509 (m, Ar C-C), 1468 (w), 1426 (m), 1360 (w), 1267 (s, C-O), 1236 (s, C-O), 1172 (m), 1110 (s), 980 (m), 913 (s), 842 (m), 821 (m), 735 (m), 699 (s), 636 (w).

Data are concordant with literature values.[222]

2-(4-((*tert*-Butyldiphenylsilyl)oxy)phenyl)-2-oxoethyl ethyl carbonate

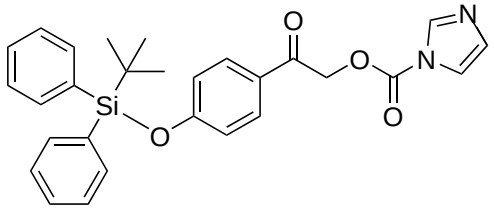


172

1-(4-((*tert*-Butyldiphenylsilyl)oxy)phenyl)-2-hydroxyethan-1-one (**171**) (50.0 mg, 0.13 mmol, 1.00 eq) was dissolved in anhydrous pyridine (1.00 mL). To this solution was added ethyl chloroformate (28.2 mg, 0.02 mL, 0.26 mmol, 2.00 eq) dropwise. The solution was stirred at 80 °C under an Ar atmosphere for 18 h, after which time the reaction was adjudged to be complete by TLC analysis. The reaction mixture was allowed to cool to RT and the reaction was quenched with Et_2O (20.0 mL). The organic layer was washed with aq. 2 M HCl (20.0 mL), sat. aq. $NaHCO_3$ (20.0 mL), H_2O (20.0 mL), and brine (20.0 mL), dried over $MgSO_4$, and filtered. The solvent was removed under reduced pressure and the crude oil was purified by silica gel flash column chromatography, eluting with petroleum ether:Et_2O = 6:4, to afford 2-(4-((*tert*-butyldiphenylsilyl)oxy)phenyl)-2-oxoethyl ethyl carbonate (**172**) as a pale yellow oil (58.9 mg, 98%).

$\mathbf{R_f}$: 0.38 (Petroleum ether:Et_2O = 1:1);
^{1}H NMR (400 MHz, $CDCl_3$) $\boldsymbol{\delta}$H: 7.72 - 7.68 (6H, m, $C_{Ph}\mathbf{H}$), 7.42 - 7.38 (6H, m, $C_{Ar}\mathbf{H}$, $C_{Ph}\mathbf{H}$), 6.82 (2H, d, J = 8.8 Hz, $C_{Ar}\mathbf{H}$), 5.23 (2H, s, $C\mathbf{H}_2O$), 4.26 (2H, q, J = 7.1 Hz, $OC\mathbf{H}_2CH_3$), 1.35 (3H, t, J = 7.1 Hz, $OCH_2C\mathbf{H}_3$), 1.13 - 1.11 (9H, s, $SiC_{Ph2}(C\mathbf{H}_3)_3$);
^{13}C NMR (100 MHz, $CDCl_3$) $\boldsymbol{\delta}$C: 190.8 ($\mathbf{C}O$), 161.2 ($\mathbf{C}_{Ar}$), 155.3 ($\mathbf{C}O$), 135.8 ($\mathbf{C}_{Ph}H$), 135.2 ($\mathbf{C}_{Ph}H$), 132.4 ($\mathbf{C}_{Ph}$), 128.4 ($\mathbf{C}_{Ph}H$), 128.2 ($\mathbf{C}_{Ar}H$), 127.8 ($\mathbf{C}_{Ar}$), 120.5 ($\mathbf{C}_{Ar}H$), 68.7 ($\mathbf{C}H_2O$), 65.1 ($O\mathbf{C}H_2CH_3$), 26.8 ($SiC_{Ph2}(\mathbf{C}H_3)_3$), 19.9 ($Si\mathbf{C}_{Ph2}(CH_3)_3$), 14.6 ($OCH_2\mathbf{C}H_3$);
LRMS *m/z* (ESI$^+$): 157 (100%), 463 (18% $[M + H]^+$).

2-(4-((*tert*-Butyldiphenylsilyl)oxy)phenyl)-2-oxoethyl 4-methyl-1*H*-imidazole-1-carboxylate

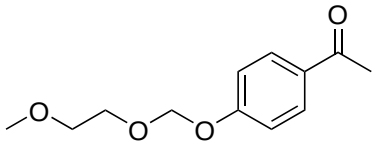


276

1-(4-((*tert*-Butyldiphenylsilyl)oxy)phenyl)-2-hydroxyethan-1-one (**171**) (78.0 mg, 0.20 mmol, 1.00 eq) was dissolved in anhydrous THF (2.50 mL). To this solution was added *N*,*N*,-carbonyldiimidazole (35.7 mg, 0.03 mL, 0.22 mmol, 1.10 eq) dropwise. The reaction mixture was stirred at RT under an Ar atmosphere for 18 h, after which time the reaction was adjudged to be complete by TLC analysis. The solvent was removed under reduced pressure and the crude oil was purified by silica gel flash column chromatography, eluting with petroleum ether:acetone = 7:3, to afford 2-(4-((*tert*-butyldiphenylsilyl)oxy)phenyl)-2-oxoethyl 4-methyl-1*H*-imidazole-1-carboxylate (**276**) as a colourless oil (25.2 mg, 25%).

$\mathbf{R_f}$: 0.18 (Petroleum ether:EtOAc = 7:3);
^{1}H NMR (400 MHz, $CDCl_3$) $\boldsymbol{\delta}$H: 8.22 (1H, s, $NC_{Im}H\mathbf{N}$), 7.75 - 7.67 (6H, m, $C_{Ph}\mathbf{H}$, $C_{Ph}\mathbf{H}$), 7.49 (1H, br s, $NC_{Im}\mathbf{H}C_{Im}HN$), 7.46 (2H, d, J = 8.1 Hz, $C_{Ar}\mathbf{H}$), 7.43 - 7.37 (4H, m, $C_{Ph}\mathbf{H}$), 7.11 (1H, br s, $NC_{Im}HC_{Im}\mathbf{H}N$), 6.85 (2H, d, J = 8.1 Hz, $C_{Ar}\mathbf{H}$), 5.51 (2H, s, $COC\mathbf{H}_2O$), 1.12 (9H, s, $SiC_{Ph2}(C\mathbf{H}_3)_3$).

1-(4-((2-Methoxyethoxy)methoxy)phenyl)ethan-1-one



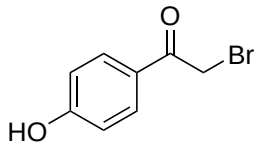
206

4'-Hydroxyacetophenone (**40**) (5.00 g, 36.7 mmol, 1.00 eq) was dissolved in anhydrous CH_2Cl_2 (50.0 mL). To this was added *N*,*N*-diisopropylethylamine (7.12 g, 9.60 mL, 55.1 mmol, 1.50 eq) to afford a pale orange solution. 2-Methoxyethoxymethyl chloride (6.86g, 6.29 mL, 55.1 mmol, 1.50 eq) was added dropwise and the reaction solution was stirred at RT under an Ar atmosphere for 18 h, after which time the reaction was adjudged to be complete by TLC analysis. The reaction was quenched with H_2O (50.0 mL), washed with aq. 1 M NaOH (100 mL) and H_2O (100 mL), dried over $MgSO_4$, and filtered. The solvent was removed under reduced pressure and the resulting crude oil was purified by silica gel flash column chromatography, eluting with CH_2Cl_2:Et_2O = 8:2, to afford 1-(4-((2-methoxyethoxy)methoxy)phenyl)ethan-1-one (**206**) as a pale pink oil (4.23 g, 51%).

R_f: 0.40 (CH_2Cl_2:Et_2O = 1:1);
UV λ_{max}/nm (ϵ/$M^{-1}cm^{-1}$): 265 (12460) [MeOH];
^{1}H NMR (400 MHz, $CDCl_3$) **δ**H: 7.92 (2H, d, J = 8.7 Hz, C_{Ar}**H**), 7.08 (2H, d, J = 8.7 Hz, C_{Ar}**H**), 4.76 (2H, s, OC_{MEM}**H_2**O), 3.74 – 3.68 (4H, m, OC_{MEM}**H_2**, C_{MEM}**H_2**O), 3.36 (3H, s, OC_{MEM}**H_3**), 2.55 (3H, s, CO**CH_3**);
^{13}C NMR (100 MHz, $CDCl_3$) **δ**C: 196.9 (**C**O), 161.0 (**C_{Ar}**), 130.4 (**C_{Ar}**H), 115.7 (**C_{Ar}**H), 95.6 (**$C_{MEM}H_2$**), 93.0 (**C_{Ar}**), 71.7 (**$C_{MEM}H_2$**), 66.7 (**$C_{MEM}H_2$**), 58.9 (**$C_{MEM}H_3$**), 26.3 (CO**C**H_3);
LRMS *m/z* (ESI$^+$): 187 (100%), 247 (25% $[M + Na]^+$);
IR (ν_{max} cm^{-1}): 2884 (w), 1676 (m, C=O), 1600 (m, Ar C-C), 1509 (w, Ar C-C), 1419 (w), 1360 (w), 1311 (w), 1269 (m, C-O), 1232 (m, C-O), 1170 (w), 1102 (m, C-O), 980 (s), 839 (s), 656 (w).

Data are concordant with literature values.[223]

2-Bromo-1-(4-hydroxyphenyl)ethan-1-one



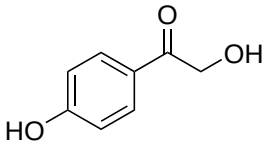
41

$CuBr_2$ (2.35 g, 10.5 mmol, 2.10 eq) was suspended in EtOAc (15.0 mL). A solution of 4'-hydroxyacetophenone (**40**) (681 mg, 5.00 mmol, 1.00 eq) in EtOAc (15.0 mL) was added at RT and the resulting mixture was stirred under reflux for 24 h under a N_2 atmosphere, after which time the reaction was adjudged to be complete by TLC analysis. The reaction mixture was allowed to cool to RT and filtered. The solvent was removed under reduced pressure and the obtained crude residue was redissolved in EtOAc (20.0 mL) and subjected to discolouration by stirring over activated charcoal for 1 h. The suspension was filtered and the solvent was removed under reduced pressure. The crude residue was further purified by silica gel flash column chromatography, eluting with $CHCl_3$:MeOH = 20:1, to afford 2-bromo-1-(4-hydroxyphenyl)ethan-1-one (**41**) as a colourless solid (490 mg, 46%).

R_f: 0.67 (Petroleum ether:EtOAc = 1:1);
m.p.: 121 - 122 °C (Hexane/MeOH) [Literature value: 124 - 126 °C (Benzene)][179];
UV λ_{max}/nm (ϵ/$M^{-1}cm^{-1}$): 290 (13960) [MeOH]
^{1}H NMR (400 MHz, CD_3OD) δH: 7.91 (2H, d, J = 9.0 Hz, C_{Ar}**H**), 6.86 (2H, d, J = 9.0 Hz, C_{Ar}**H**), 4.54 (2H, s, C**H**$_2$Br);
^{13}C NMR (100 MHz, CD_3OD) δC: 192.7 (**C**O), 164.8 (**C**$_{Ar}$), 133.1 (**C**$_{Ar}$H), 127.4 (**C**$_{Ar}$), 116.8 (**C**$_{Ar}$H), 32.3 (**C**H$_2$Br);
LRMS *m/z* (ESI$^+$): 214 (27% $[M + H]^+$), 217 (100%);
IR (ν_{max} cm^{-1}): 3325 (w, br, O-H), 1659 (m, C=O), 1601 (m), 1572 (s, Ar C-C), 1512 (w, Ar C-C), 1447 (w), 1382 (w), 1318 (w), 1281 (m), 1223 (m), 1197 (m), 1171 (s, C-O), 1115 (s), 989 (m), 837 (s), 811 (m), 759 (w), 684 (m, C-Br), 634 (w).

Data are concordant with literature values.[178]

2-Hydroxy-1-(4-hydroxyphenyl)ethan-1-one



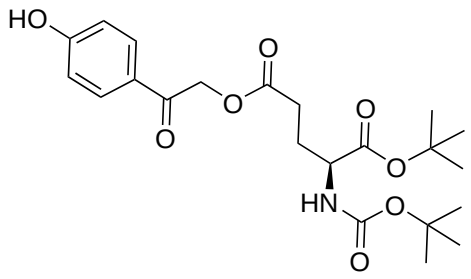
48

2-Bromo-1-(4-hydroxyphenyl)ethan-1-one (**41**) (590 mg, 2.70 mmol, 1.00 eq) and formic acid (157 mg, 0.13 mL, 3.40 mmol, 1.25 eq) were dissolved in toluene (30.0 mL). The solution was cooled to 0 °C and 1,8-diazabicyclo[5.4.0]undec-7-ene (518 mg, 0.52 mL, 3.40 mmol, 1.25 eq) was added dropwise. The reaction solution was allowed to warm to RT and stirred under a N_2 atmosphere for 24 h, after which time the reaction was adjudged to be complete by TLC analysis. The solvent was removed under reduced pressure and the crude residue was purified by silica gel flash column chromatography, eluting with, petroleum ether:EtOAc = 6:4, to afford 2-hydroxy-1-(4-hydroxyphenyl)ethan-1-one (**48**) as a pale pink solid (398 mg, 97%).

R_f: 0.34 (Petroleum ether:EtOAc = 1:1);
m.p.: 170 - 171 °C (Petroleum ether/Et_2O) [Literature value: 170 - 171 °C][224];
UV λ_{max}/nm (ϵ/$M^{-1}cm^{-1}$): 280 (14360) [MeOH];
^{1}H NMR (400 MHz, $(CD_3)_2SO$) δH: 10.53 (1H, s, O**H**), 8.40 (1H, s, O**H**), 7.85 (2H, d, J = 8.9 Hz, C_{Ar}**H**), 6.88 (2H, d, J = 8.9 Hz, C_{Ar}**H**), 5.49 (2H, s, C$\mathbf{H_2}$);
LRMS m/z (ESI^-): 151 (32% $[M - H]^-$);
IR (ν_{max} cm^{-1}): 3338 (m, O-H), 2923 (w), 1724 (m), 1673 (s, C=O), 1603 (m), 1575 (s, Ar C-C), 1514 (w, Ar C-C), 1433 (w), 1352 (w), 1312 (w), 1286 (m), 1247 (m), 1215 (m), 1191 (s, C-O), 1164 (s, C-O), 1110 (w), 1033 (w), 977 (w), 949 (m), 831 (s), 696 (w).

Data are concordant with literature values.[28]

1-(*tert*-Butyl) 5-(2-(4-hydroxyphenyl)-2-oxoethyl) (*tert*-butoxycarbonyl)-*L*-glutamate



199

2-Bromo-1-(4-hydroxyphenyl)ethan-1-one (**41**) (100 mg, 0.47 mmol, 1.00 eq) and Boc-Glu-O^{t}Bu (**138**) (143 mg, 0.47 mmol, 1.00 eq) were dissolved in anhydrous THF (5.00 mL). The solution was cooled to 0 °C and 1,8-diazabicyclo[5.4.0]undec-7-ene (77.6 mg, 0.08 mL, 0.51 mmol, 1.10 eq) was added dropwise. The resulting yellow solution was stirred RT under an Ar atmosphere for 24 h, after which time the reaction was adjudged to be complete by TLC analysis. The reaction mixture was filtered to remove the DBU salt and the solvent was removed under reduced pressure. The obtained crude residue was dissolved in CH_2Cl_2 (100 mL), washed with H_2O (100 mL), dried over $MgSO_4$, and filtered. The solvent was removed under reduced pressure and the crude residue was further purified by silica gel flash column chromatography, eluting with petroleum ether:Et_2O = 1:1 to Et_2O, to afford 1-(*tert*-butyl) 5-(2-(4-hydroxyphenyl)-2-oxoethyl) (*tert*-butoxycarbonyl)-*L*-glutamate (**199**) as a colourless solid (174 mg, 84%).

R$_f$: 0.44 (Et_2O);
m.p.: 116 - 117 °C (Petroleum ether/Et_2O);
$[\alpha]_D^{26}$: +10.5 (***c*** 0.7 in $CHCl_3$);
UV λ_{max}/nm (ϵ/M^{-1}cm^{-1}): 280 (12350) [MeOH];
^{1}H NMR (400 MHz, $CDCl_3$) **δ**H: 8.07 (1H, br s, O**H**), 7.78 (2H, d, J = 8.4 Hz, C_{Ph}**H**), 6.90 (2H, d, J = 8.4 Hz, C_{Ph}**H**), 5.30 (1H, d, J = 8.2 Hz, N**H**CHCH$_2$), 5.27 (2H, s, C(O)C**H**$_2$O), 4.26 (1H, ddd, J = 8.2, 7.0, 7.0 Hz, NHC**H**CH$_2$), 2.68 - 2.48 (2H, m, NHCHCH$_2$C**H**$_2$), 2.23 (1H, ddt, J = 14.0, 7.0, 7.0 Hz, NHCHC**H**$_A$H$_B$CH$_2$), 2.02 (1H, ddt, J = 14.0, 7.0, 7.0 Hz, NHCHCH$_A$**H**$_B$CH$_2$), 1.47 (9H, s, OC(C**H**$_3$)$_3$), 1.44 (9H, s, OC(C**H**$_3$)$_3$);
^{13}C NMR (100 MHz, $CDCl_3$) **δ**C: 207.8 (**C**O), 191.1 (**C**O), 190.5 (**C**O), 172.5 (**C**$_{Ph}$OH), 162.0 (**C**$_{Ph}$), 155.7 (**C**O), 130.3 (**C**$_{Ph}$H), 115.8 (**C**$_{Ph}$H), 82.5 (O**C**(CH$_3$)$_3$),

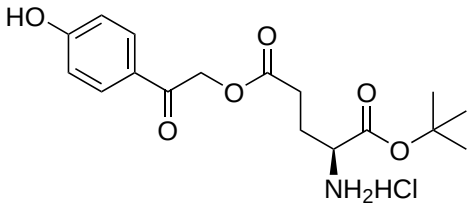
80.2 (O**C**$(CH_3)_3$), 65.8 (C(O)**C**H_2O), 53.3 (NH**C**HCH_2), 30.9 (NHCHCH_2**C**H_2), 30.0 (NHCH**C**H_2CH_2), 28.3 (OC(**C**$H_3)_3$), 27.9 (OC(**C**$H_3)_3$);

LRMS *m/z* (ESI$^+$): 438 (100% $[M + H]^+$);

HRMS *m/z* (ESI$^+$): Found 460.1938 $[M + Na]^+$ ($C_{22}H_{31}NNaO_8{}^+$ requires 460.1942 $[M + Na]^+$);

IR (ν_{max} cm^{-1}): 3417 (w), 3233 (w, br, O-H), 2976 (w), 1731 (m, C=O), 1697 (w), 1670 (w), 1603 (w), 1574 (m, Ar C-C), 1511 (m, Ar C-C), 1448 (w), 1366 (m), 1292 (w), 1248 (m), 1227 (m, C-N), 1146 (s, C-O), 1091 (w), 1046 (w), 969 (w), 842 (w), 807 (w), 778 (w), 742 (w).

1-(*tert*-Butyl) 5-(2-(4-hydroxyphenyl)-2-oxoethyl) *L*-glutamate hydrochloride



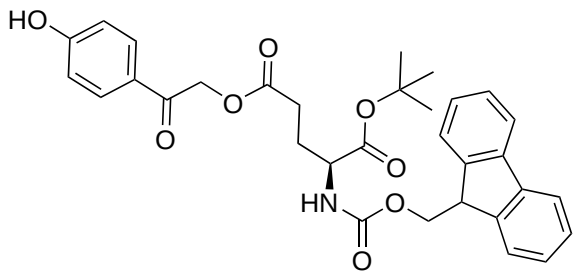
200

1-(*tert*-Butyl) 5-(2-(4-hydroxyphenyl)-2-oxoethyl) (*tert*-butoxycarbonyl)-*L*-glutamate (**199**) (666 mg, 1.52 mmol, 1.00 eq) was dissolved in a 2.0 M HCl in Et_2O (38.1 mL, 76.0 mmol, 50.0 eq) solution. The reaction mixture was stirred at RT under an Ar atmosphere for 24 h, after which time the reaction was adjudged to be complete by TLC analysis. The white precipitate was isolated by filtration, washed with Et_2O, and dried under suction to afford 1-(*tert*-butyl) 5-(2-(4-hydroxyphenyl)-2-oxoethyl)-*L*-glutamate (**200**) as a colourless solid (498 mg, 88%).

R_f: 0.22 (CH_2Cl_2:MeOH = 9:1);
m.p.: 133 - 134 °C (Hexane/MeOH);
$[\alpha]_D^{26}$: +24.7 (***c*** 0.3 in $CHCl_3$);
UV λ_{max}/nm (ϵ/M^{-1}cm^{-1}): 280 (1480) [MeOH];
^{1}H NMR (400 MHz, CD_3OD) **δ**H: 7.88 (2H, d, J = 8.9 Hz, C_{Ph}**H**), 6.88 (2H, d, J = 8.9 Hz, C_{Ph}**H**), 5.47 (1H, d, J = 16.5 Hz, C(O)C**H**$_A$H$_B$O), 5.42 (1H, d, J = 16.5 Hz, C(O)CH$_A$**H**$_B$O), 4.10 (1H, dd, J = 6.6, 6.6 Hz, NH_2C**H**CH_2), 2.82 - 2.67 (2H, m, NH_2CHCH_2C**H**$_2$), 2.36 - 2.15 (2H, m, NH_2CHC**H**$_A$H$_B$$CH_2$, NH_2CHCH_A**H**$_B$$CH_2$), 1.55 (9H, s, OC(C**H**$_3$)$_3$);
^{13}C NMR (100 MHz, CD_3OD) **δ**C: 206.8 (**C**O), 193.0 (**C**O), 173.1 (**C**O), 169.5 (**C**C$_{Ph}$OH), 164.8 (**C**$_{Ph}$), 131.7 (**C**$_{Ph}$H), 116.7 (**C**$_{Ph}$H), 85.7 (O**C**(CH$_3$)$_3$), 67.6 (C(O)**C**H$_2$O), 53.7 (NH_2**C**HCH$_2$), 30.6 (NH_2CHCH_2**C**H$_2$), 28.3 (OC(C**H**$_3$)$_3$), 27.1 (NH_2CH**C**H$_2CH_2$);
LRMS *m/z* (ESI$^+$): 338 (100% [M + H]$^+$), 360 (74% [M + Na]$^+$);
HRMS *m/z* (ESI$^+$): Found 338.1598 [M + H]$^+$ ($C_{17}H_{24}NO_6^+$ requires 338.1598 [M + H]$^+$);
IR (ν_{max} cm^{-1}): 3180 (w, br, O-H), 2977 (w), 2927 (w), 2362 (w), 2166 (w), 2026 (w), 1955 (w), 1744 (m, C=O), 1665 (m, C=O), 1605 (m, N-H), 1577 (s, Ar C-C), 1508 (w, Ar C-C), 1375 (m), 1316 (w), 1290 (w), 1235 (m), 1177 (s, C-N), 1158 (s,

C-O), 1076 (w), 1039 (w), 974 (w), 935 (w), 841 (m), 748 (w), 682 (w), 656 (w), 616 (w).

1-(*tert*-Butyl) 5-2-(4-hydroxyphenyl)-2-oxoethyl) (((9*H*-fluoren-9-yl)methoxy)carbonyl)-*L*-glutamate



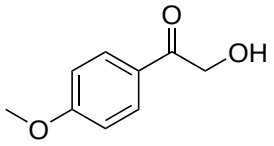
198

1-(*tert*-Butyl) 5-(2-(4-hydroxyphenyl)-2-oxoethyl) *L*-glutamate hydrochloride (**200**) (500 mg, 1.34 mmol, 1.00 eq) was dissolved in H_2O (25.0 mL). $NaHCO_3$ (250 mg, 2.97 mmol, 2.22 eq) was added and the reaction mixture was stirred at RT for 0.5 h. A solution of *N*-(9-fluorenylmethoxycarbonyloxy)succinimide (749 mg, 2.22 mmol, 1.66 eq) in 1,4-dioxane (25.0 mL) was added and the reaction mixture was stirred at RT for 18 h, after which time the reaction was adjudged to be complete by TLC analysis. The reaction mixture was acidified to pH = 2.0 with aq. 1 M HCl and extracted with Et_2O (3 × 200 mL). The combined organic extracts were washed with brine (200 mL), dried over $MgSO_4$, and filtered. The solvent was removed under reduced pressure and the resulting crude residue was purified by silica gel flash column chromatography, eluting with $CHCl_3$ to $CHCl_3$:Acetone = 9:1, to afford 1-(*tert*-butyl) 5-(2-(4-hydroxyphenyl)-2-oxoethyl) (((9*H*-fluoren-9-yl)methoxy)carbonyl)-*L*-glutamate (**198**) as a colourless foam (217 mg, 32%).

$\mathbf{R_f}$: 0.17 ($CHCl_3$:Acetone = 9:1);
m.p.: 65 - 67 °C (Petroleum ether/Acetone);
$\boldsymbol{[\alpha]_D^{26}}$: +11.2 (***c*** 1.2 in $CHCl_3$);
UV $\boldsymbol{\lambda_{max}}$/nm ($\boldsymbol{\epsilon}$/$\mathbf{M^{-1}cm^{-1}}$): 265 (33010) [MeOH];
^{1}H NMR (400 MHz, $CDCl_3$) $\boldsymbol{\delta}$H: 7.79 - 7.72 (4H, m, $C_{Ar}\mathbf{H}$, $C_{FmocAr}\mathbf{H}$), 7.61 (2H, d, J = 7.4 Hz, $C_{FmocAr}\mathbf{H}$), 7.39 (2H, t, J = 7.4 Hz, $C_{FmocAr}\mathbf{H}$), 7.30 (2H, t, J = 7.4 Hz, $C_{FmocAr}\mathbf{H}$), 6.86 (2H, d, J = 8.7 Hz, $C_{Ar}\mathbf{H}$), 5.75 (1H, d, J = 8.2 Hz, N**H**$CHCH_2CH_2$), 5.29 (1H, d, J = 16.2 Hz, C(O)C$\mathbf{H}_A$$H_B$O), 5.24 (1H, d, J = 16.2 Hz, C(O)$CH_A\mathbf{H}_B$O), 4.40 (2H, d, J = 7.1 Hz, $C_{Fmoc}\mathbf{H}_2$), 4.38 - 4.34 (1H, m, NHC**H**CH_2CH_2), 4.22 (1H, t, J = 7.1 Hz, $C_{Fmoc}\mathbf{H}$), 2.69 - 2.53 (2H, m, $NHCHCH_2C\mathbf{H}_2$), 2.37 - 2.25 (1H, m, NHCHC$\mathbf{H}_A$$H_B$$CH_2$), 2.13 - 2.02 (1H, m, $NHCHCH_A\mathbf{H}_BCH_2$), 1.49 (9H, s, OC($C\mathbf{H}_3$)$_3$);

^{13}C NMR (100 MHz, $CDCl_3$) δC: 190.7 (**C**O), 172.5 (**C**O), 171.1 (**C**O), 162.0 (**C**O), 156.4 ($\mathbf{C}_{Ar}OH$), 143.8 ($\mathbf{C}_{FmocAr}$), 141.3 ($\mathbf{C}_{FmocAr}$), 130.4 ($\mathbf{C}_{Ar}H$), 127.8 ($\mathbf{C}_{FmocAr}H$), 127.1 ($\mathbf{C}_{FmocAr}H$), 126.4 ($\mathbf{C}_{FmocAr}H$), 125.2 ($\mathbf{C}_{Ar}C(O)CH_2O$), 120.0 ($\mathbf{C}_{FmocAr}H$), 115.8 ($\mathbf{C}_{Ar}H$), 82.8 (O**C**$(CH_3)_3$), 67.3 ($\mathbf{C}_{Fmoc}H_2$), 65.9 (C(O)**C**H_2O), 53.9 (NH**C**HCH_2CH_2), 47.1 ($\mathbf{C}_{Fmoc}H$), 30.1 (NHCHCH_2**C**H_2), 28.0 (OC(**C**$H_3)_3$), 27.8 (NHCH**C**H_2CH_2);
LRMS *m/z* (ESI$^+$): 506 (95% $[M + H]^+$), 582 (100% $[M + Na]^+$);
HRMS *m/z* (ESI$^+$): Found 506.2276 $[M + H]^+$ ($C_{32}H_{34}NO_8^+$ requires 506.2279 $[M + H]^+$);
IR (ν_{max} cm^{-1}): 3341 (w, br, O-H), 2978 (w), 2166 (w), 1690 (s, C=O), 1602 (m, Ar C-C), 1517 (m, Ar C-C), 1447 (m), 1369 (m), 1281 (w), 1224 (m, C-N), 1152 (s, C-O), 1050 (m), 970 (m), 840 (m), 739 (s).

2-Hydroxy-1-(4-methoxyphenyl)ethan-1-one



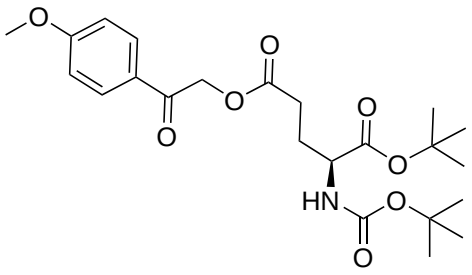
147

A solution of 2-bromo-4'-methoxyacetophenone (**146**) (5.00 g, 16.7 mmol, 1.00 eq) and sodium formate (9.10 g, 134 mmol, 8.00 eq) in EtOH (150 mL) was stirred under reflux for 4 h, after which time the reaction was adjudged to be complete by TLC analysis. The solvent was removed under reduced pressure and the obtained residue was redissolved in CH_2Cl_2 (150 mL) and washed with H_2O (150 mL). The solvent was removed under reduced pressure and the crude residue was purified by silica gel flash column chromatography, eluting with CH_2Cl_2:Et_2O = 8:2, to afford 2-hydroxy-1-(4-methoxyphenyl)ethan-1-one (**147**) as a colourless solid (2.02 g, 73%).

$\mathbf{R_f}$: 0.25 (Petroleum ether:Et_2O = 1:1);
m.p.: 99 - 101 °C (Petroleum ether/Et_2O) [Literature value: 98.5 - 100.5 °C][225];
UV λ_{max}/nm (ϵ/$M^{-1}cm^{-1}$): 275 (15980) [MeOH];
^{1}H NMR (400 MHz, $CDCl_3$) δH: 7.91 (2H, d, J = 8.9 Hz, C_{Ar}**H**), 6.98 (2H, d, J = 8.9 Hz, C_{Ar}**H**), 4.83 (2H, d, J = 4.7 Hz, C(O)C**H**$_2$OH), 3.90 (3H, s, OC**H**$_3$), 3.58 (1H, t, J = 4.7 Hz, C(O)CH$_2$O**H**);
^{13}C NMR (100 MHz, $CDCl_3$) δC: 196.7 (**C**O), 164.4 (**C**$_{Ar}$), 130.0 (**C**$_{Ar}$H), 126.3 (**C**$_{Ar}$), 114.2 (**C**$_{Ar}$H), 65.0 (C(O)**C**H$_2$OH), 55.6 (O**C**H$_3$);
LRMS *m/z* (ESI$^+$): 189 (100% [M + Na]$^+$);
IR (ν_{max} cm^{-1}): 3409 (br, w, O-H), 2923 (w), 2845 (w), 1733 (w), 1673 (s, C=O), 1594 (s, Ar C-C), 1512 (w, Ar C-C), 1415 (m), 1305 (W), 1236 (s), 1174 (m, C-O, 1103 (m, C-O), 1028 (w), 975 (m), 826 (s).

Data are concordant with literature values.[226]

1-(*tert*-Butyl) 5-(2-(4-methoxyphenyl)-2-oxoethyl) (*tert*-butoxycarbonyl)-*L*-glutamate



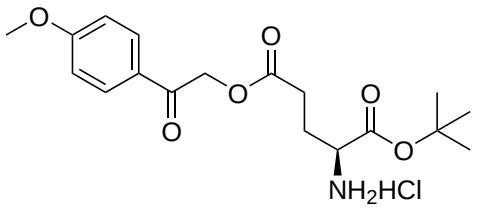
165

2-Bromo-4'methoxyacetophenone (**146**) (200 mg, 0.87 mmol, 1.00 eq) and Boc-Glu-O^{t}Bu (**138**) (264 mg, 0.87 mmol, 1.00 eq) were dissolved in anhydrous THF (10.0 mL). The solution was cooled to 0 °C and 1,8-diazabicyclo[5.4.0]undec-7-ene (146 mg, 0.14 mL, 0.96 mmol, 1.10 eq) was added dropwise. The reaction solution was stirred at RT under an Ar atmosphere for 24 h, after which time the reaction was adjudged to be complete by TLC analysis. The reaction mixture was filtered to remove the DBU salt and the solvent was removed under reduced pressure. The obtained crude residue was redissolved in CH_2Cl_2 (200 mL) and washed with H_2O (200 mL). The solvent was removed under reduced pressure and the crude oil was purified by silica gel flash column chromatography, eluting with petroleum ether 30 - 40:Et_2O = 1:1, to afford 1-(*tert*-butyl)5-(2-(4-methoxyphenyl)-2-oxoethyl) *tert*-butoxycarbonyl)-*L*-glutamate (**165**) as a pale yellow oil (292 mg, 74%).

R_f: 0.20 (Petroleum ether:Et_2O = 1:1);
$[\alpha]_D^{26}$: +7.5 (***c*** 2.6 in $CHCl_3$);
UV λ_{max}/nm (ϵ/M^{-1}cm^{-1}): 275 (17280) [MeOH];
^{1}H NMR (400 MHz, $CDCl_3$) **δ**H: 7.88 (2H, d, J = 8.9 Hz, C_{Ph}**H**), 6.94 (2H, d, J = 8.9 Hz, C_{Ph}**H**), 5.32 (1H, d, J = 16.3 Hz, C(O)C**H**$_A$H$_B$O), 5.28 (1H, d, J = 16.3 Hz, C(O)CH$_A$**H**$_B$O), 5.19 (1H, d, J = 8.2 Hz, N**H**CHCH$_2$), 4.23 (1H, ddd, J = 8.2, 7.7, 4.9 Hz, NHC**H**CH$_2$), 3.87 (3H, s, OC**H**$_3$), 2.66 - 2.49 (2H, m, NHCHCH$_2$C**H**$_2$), 2.30 - 2.16 (1H, m, NHCHC**H**$_A$H$_B$CH$_2$), 2.05 - 1.92 (1H, m, NHCHCH$_A$**H**$_B$CH$_2$), 1.46 (9H, s, OC(C**H**$_3$)$_3$), 1.43 (9H, s, OC(C**H**$_3$)$_3$);
^{13}C NMR (100 MHz, $CDCl_3$) **δ**C: 190.5 (**C**O), 172.4 (**C**O), 171.3 (**C**O), 164.1 (**C**$_{Ph}$OCH$_3$), 155.4 (**C**O), 130.1 (**C**$_{Ph}$H), 127.2 (**C**$_{Ph}$), 114.1 (**C**$_{Ph}$H), 82.2 (O**C**(CH$_3$)$_3$), 79.7 (O**C**(CH$_3$)$_3$), 65.8 (C(O)**C**H$_2$O), 55.6 (O**C**H$_3$), 53.4 (NH**C**HCH$_2$),

30.10 ($NHCHCH_2\mathbf{C}H_2$), 28.3 ($OC(\mathbf{C}H_3)_3$), 28.1 ($NHCH\mathbf{C}H_2CH_2$), 28.0 ($OC(\mathbf{C}H_3)_3$);
LRMS *m/z* (ESI$^+$): 452 (68% $[M + H]^+$), 474 (100% $[M + Na]^+$);
HRMS *m/z* (ESI$^+$): Found 452.2273 $[M + H]^+$ ($C_{33}H_{34}NO_8{}^+$ requires 452.2279 $[M + H]^+$);
IR (ν_{max} cm^{-1}): 3380 (w), 2978 (w), 2363 (s), 2335 (m), 1669 (s, C=O), 1605 (w, Ar C-C), 1515 (w, Ar C-C), 1455 (w), 1424 (w), 1371 (m), 1251 (m), 1157 (s, C-O), 1027 (m), 970 (m), 826 (w), 672 (w), 623 (w).

1-(*tert*-Butyl) 5-(2-(4-methoxyphenyl)-2-oxoethyl)-*L*-glutamate hydrochloride



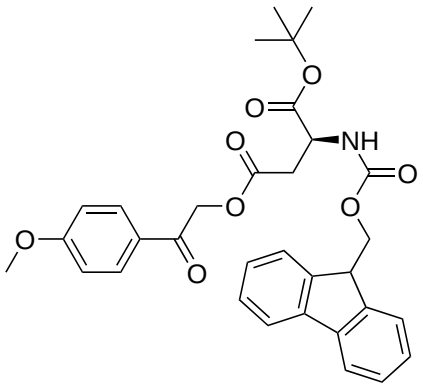
277

1-(*tert*-Butyl) 5-(2-(4-methoxyphenyl)-2-oxoethyl) *tert*-butoxycarbonyl)-*L*-glutamate (**165**) (250 mg, 0.55 mmol, 1.00 eq) was dissolved in a 2.0 M HCl solution in Et_2O (5.54 mL, 11.1 mmol, 20.0 eq). The reaction solution was stirred at RT under an Ar atmosphere for 24 h, after which time the reaction was adjudged to be complete by TLC analysis. The reaction mixture was filtered and the obtained precipitate was washed with Et_2O, and dried under suction to afford 1-(*tert*-butyl) 5-(2-(4-methoxyphenyl)-2-oxoethyl-*L*-glutamate (**277**) as a colourless solid (102 mg, 48%).

R_f: 0.01 (Petroleum ether:Et_2O = 1:1);
m.p.: 137 - 139 °C (Hexane/MeOH);
$[\alpha]_D^{26}$: +25.4 (***c*** 0.1 in $CHCl_3$);
UV λ_{max}/nm (ϵ/M^{-1}cm^{-1}): 275 (15460) [MeOH];
^{1}H NMR (400 MHz, CD_3OD) **δ**H: 7.97 (2H, d, J = 9.0 Hz, C_{Ph}**H**), 7.05 (2H, d, J = 9.0 Hz, C_{Ph}**H**), 5.50 (1H, d, J = 16.6 Hz, C(O)C**H**$_A$H$_B$O), 5.45 (1H, d, J = 16.6 Hz, C(O)CH$_A$**H**$_B$O), 4.10 (1H, dd, J = 6.7, 6.7 Hz, NHC**H**CH_2), 3.89 (3H, s, C_{Ph}OC**H**$_3$), 2.83 - 2.66 (2H, m, NHCHCH_2C**H**$_2$), 2.35 - 2.16 (2H, m, NHCHC**H**$_A$H$_B$CH_2, NHCHCH$_A$**H**$_B$CH_2), 1.55 (9H, s, OC(C**H**$_3$)$_3$);
^{13}C NMR (100 MHz, CD_3OD) **δ**C: 191.6 (**C**O), 171.6 (**C**O), 168.0 (**C**O), 164.6 (**C**$_{Ph}$OCH_3), 129.9 (**C**$_{Ph}$H), 126.8 (**C**$_{Ph}$), 113.9 (**C**$_{Ph}$H), 84.2 (O**C**(CH_3)$_3$), 66.1 (C(O)**C**H_2O), 54.8 (C_{Ph}O**C**H_3), 52.2 (NH_2**C**HCH_2), 29.0 (NH_2CHCH_2**C**H_2), 26.7 (OC(**C**H_3)$_3$), 25.6 (NH_2CH**C**H_2CH_2);
LRMS *m/z* (ESI$^+$): 352 (100% [M + H]$^+$), 374 (82% [M + Na]$^+$);
HRMS *m/z* (ESI$^+$): Found 352.1756 [M + H]$^+$ ($C_{18}H_{26}NO_{6^+}$ requires 352.1755 [M + H]$^+$);
IR (ν_{max} cm^{-1}): 2846 (w), 2605 (w), 1745 (m, C=O), 1730 (m, C=O), 1689 (m, C=O), 1599 (m, Ar C-C), 1517 (w, Ar C-C), 1491 (w), 1423 (w), 1370 (w), 1317 (w),

1243 (m, C-N), 1166 (s, C-O), 1081 (w), 1032 (w), 968 (m), 841 (m, N-H), 780 (w), 745 (w), 667 (w).

1-(*tert*-Butyl) 4-(2-(4-methoxyphenyl)-2-oxoethyl) (((9*H*-fluoren-9-yl)methoxy)carbonyl)-*L*-aspartate



209

2-Hydroxy-1-(4-methoxyphenyl)ethan-1-one (**147**) (100 mg, 0.60 mmol, 1.00 eq), Fmoc-Asp-O^{t}Bu (**221**) (247 mg, 0.60 mmol, 1.00 eq) and *N*,*N*,*N*',*N*'-tetramethyl-*O*-(1*H*-benzotriazol-1-yl)uronium hexafluorophosphate (239 mg, 0.63 mmol, 1.10 eq) were dissolved in anhydrous DMF (5.00 mL). The reaction solution was stirred at RT under an Ar atmosphere for 0.5 h. *N*,*N*-Diisopropylethylamine (155 mg, 0.21 mL, 1.20 mmol, 2.00 eq) was added dropwise and the reaction solution was stirred at RT under an Ar atmosphere for 18 h, after which time the reaction was adjudged to be complete by TLC analysis. The reaction was quenched with Et_2O (100 mL), washed with H_2O (100 mL), and brine (100 mL), dried over $MgSO_4$, and filtered. The solvent was removed under reduced pressure and the obtained crude residue was purified by silica gel flash column chromatography, eluting with petroleum ether 30 - 40:Et_2O = 1:1, to afford 1-(*tert*-butyl 4-(2-(4-methoxyphenyl)-2-oxoethyl) (((9*H*-fluoren-9-yl)methoxy)carbonyl-*L*-aspartate (**209**) as a yellow solid (272 mg, 81%).

R_f: 0.17 (Petroleum ether:Et_2O = 1:1);
m.p.: 54 - 55 °C (Petroleum ether/Et_2O);
$[\alpha]_D^{26}$: +24.8 (***c*** 3.8 in $CHCl_3$);
UV λ_{max}/nm (ϵ/M^{-1}cm^{-1}): 265 (31570) [MeOH];
^{1}H NMR (400 MHz, $CDCl_3$) δH: 7.92 (2H, d, J = 8.6 Hz, C_{Ph}**H**), 7.77 (2H, d, J = 7.5 Hz, C_{FmocAr}**H**), 7.71 (2H, t, J = 7.0 Hz, C_{FmocAr}**H**), 7.40 (2H, t, J = 7.5 Hz, C_{FmocAr}**H**), 7.35 - 7.28 (2H, m, C_{FmocAr}**H**), 6.96 (2H, d, J = 8.6 Hz, C_{Ph}**H**), 6.49 (1H, d, J = 8.7 Hz, N**H**CHCH$_2$), 5.49 (1H, d, J = 16.2 Hz, C(O)C**H**$_A$H$_B$O), 5.27 (1H, d, J = 16.2 Hz, C(O)CH$_A$**H**$_B$O), 4.66 (1H, ddd, J = 8.7, 4.6, 4.2 Hz, NHC**H**CH$_2$),

4.46 - 4.32 (2H, m, $C_{Fmoc}\mathbf{H}_2$), 4.28 (1H, dd, J = 7.3, 7.3 Hz, $C_{Fmoc}\mathbf{H}$), 3.88 (3H, s, $C_{Ph}O\mathbf{H_3}$), 3.25 (1H, dd, J = 16.5, 4.0 Hz, NHCHC$\mathbf{H}_A$$H_B$), 3.05 (1H, dd, J = 16.6, 4.6 Hz, NHCHC$H_A\mathbf{H}_B$), 1.49 (9 H, s, OC(C$\mathbf{H}_3$)$_3$);

^{13}C NMR (100 MHz, $CDCl_3$) $\boldsymbol{\delta}$C: 190.2 (**C**O), 170.1 (**C**O), 169.6 (**C**O) 164.3 ($\mathbf{C}_{Ph}OCH_3$), 156.3 (**C**O), 144.0 ($\mathbf{C}_{FmocAr}$), 141.3 ($\mathbf{C}_{FmocAr}$), 130.2 ($\mathbf{C}_{Ph}$H), 127.7 ($\mathbf{C}_{FmocAr}$H), 127.1 ($\mathbf{C}_{FmocAr}$H), 126.9 ($\mathbf{C}_{Ph}$), 125.5 ($\mathbf{C}_{FmocAr}$H), 119.9 ($\mathbf{C}_{FmocAr}$H), 114.2 ($\mathbf{C}_{Ph}$H), 82.6 (O**C**$(CH_3)_3$), 67.3 ($\mathbf{C}_{Fmoc}H_2$), 66.0 (CO**C**H_2O), 55.6 (C_{Ph}O**C**H_3), 51.0 (NH**C**HCH_2), 47.2 ($\mathbf{C}_{Fmoc}$H), 37.0 (NHCH**C**H_2), 27.9 (OC(**C**H_3)$_3$);

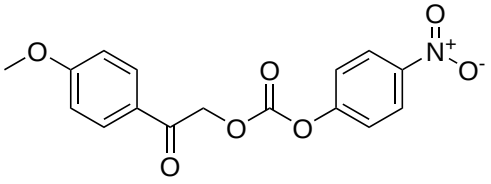
LRMS *m/z* (ESI$^+$): 560 (25% $[M + H]^+$), 582 (100% $[M + Na]^+$);

HRMS *m/z* (ESI$^+$): Found 582.2096 $[M + Na]^+$ ($C_{32}H_{33}NNaO_8{}^+$ requires 582.2098 $[M + Na]^+$);

IR ($\boldsymbol{\nu_{max}}$ cm^{-1}): 3348 (w), 2938 (w), 1732 (s, C=O), 1601 (m, Ar C-C), 1517 (m, Ar C-C), 1450 (w), 1370 (w), 1246 (m, C-N), 1161 (s, C-O), 1080 (m), 973 (w), 837 (w), 750 (w), 644 (w);

HPLC: 15.17 min (95.3%).

2-(4-Methoxyphenyl)-2-oxoethyl (4-nitrophenyl) carbonate

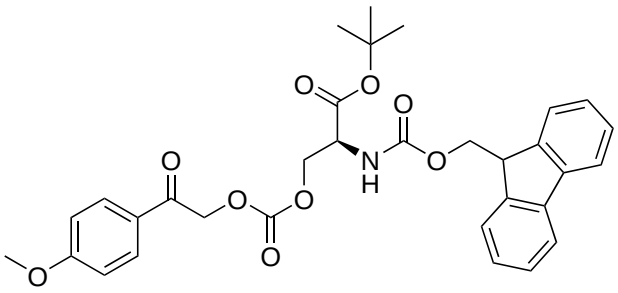


210

4-Nitrophenyl chloroformate (181 mg, 0.90 mmol, 1.50 eq) was dissolved in anhydrous CH_2Cl_2 (5.00 mL). Pyridine (52.2 mg, 0.05 mL, 0.66 mmol, 1.10 eq) was added dropwise and the solution was cooled to 0 °C. 2-Hydroxy-1-(4-methoxyphenyl)ethan-1-one (**147**) (100 mg, 0.60 mmol, 1.00 eq) was added portionwise and the resulting solution was allowed to warm to RT and stirred under an Ar atmosphere for 18 h, after which time the reaction was adjudged to be complete by TLC analysis. The reaction was quenched with CH_2Cl_2 (50.0 mL) and washed with aq. 1 M HCl (50.0 mL), and H_2O (50.0 mL). The solvent was removed under reduced pressure and 2-(4-methoxyphenyl)-2-oxoethyl (4-nitrophenyl) carbonate (**210**) was isolated as a pale yellow solid (228 mg, 77%) and used without further purification.

R_f: 0.60 (Petroleum ether:Acetone = 7:3);
m.p.: 84 - 86 °C (Petroleum ether/Et_2O);
^{1}H NMR (400 MHz, $CDCl_3$) **δ**H: 8.31 (2H, d, J = 9.2 Hz, C_{Ar}**H**), 7.92 (2H, d, J = 9.0 Hz, C_{Ph}**H**), 7.48 (2H, d, J = 9.2 Hz, C_{Ar}**H**), 7.00 (2H, d, J = 9.0 Hz, C_{Ph}**H**), 5.47 (2H, s, C(O)C**H_2**O), 3.91 (3H, s, C_{Ph}OC**H_3**);
LRMS *m/z* (ESI$^+$): Ion observed in MS of product hydrolysed by MeOH, 248 (62% $[M + H]^+$);
IR (ν_{max} cm^{-1}): 2363 (w), 1777 (m, C=O), 1694 (w, C=O), 1596 (w, Ar C-C), 1525 (m, N-O), 1491 (w, Ar C-C), 1426 (w), 1349 (m, N-O), 1220 (s, C-N), 1184 (m, C-O), 1102 (w), 1014 (w), 936 (w), 861 (m), 753 (w).

***tert*-Butyl *N*-(((9*H*-fluoren-9-yl)methoxy)carbonyl)-*O*-((2-(4-methoxyphenyl)-2-oxoethoxy)carbonyl)-*L*-serinate**



211

2-Hydroxy-1-(4-methoxyphenyl)ethan-1-one (**147**) (50.0 mg, 0.30 mmol, 1.00 eq), 4-nitrophenyl chloroformate (90.7 mg, 0.45 mmol, 1.50 eq) and 4-(dimethylamino)pyridine (11.0 mg, 0.09 mmol, 0.30 eq) were dissolved in anhydrous CH_2Cl_2 (2.50 mL). Pyridine (23.7 mg, 0.02 mL, 0.30 mmol, 1.00 eq) was added dropwise and the reaction solution was stirred at RT under an Ar atmosphere for 18 h, after which formation of the intermediate was adjudged to be complete by TLC analysis. *tert*-Butyl (((9*H*-fluoren-9-yl)methoxy)carbonyl)-*L*-serinate (**185**) (115 mg, 0.30 mmol, 1.00 eq) was added, followed immediately by the addition of $NaHCO_3$ (25.2 mg, 0.30 mmol, 1.00 eq). The reaction mixture was stirred at RT under an Ar atmosphere for 18 h, after which time the reaction was adjudged to be complete by TLC analysis. The reaction was quenched with CH_2Cl_2 (50.0 mL) and washed with H_2O (100 mL). The solvent was removed under reduced pressure and the obtained crude residue was subjected to two successive purifications by silica gel flash column chromatography, eluting with petroleum ether 30 - 40:Et_2O = 1:1 then CH_2Cl_2 to CH_2Cl_2:Et_2O = 95:5 - 9:1, to afford *tert*-butyl *N*-(((9*H*-fluoren-9-yl)methoxy)carbonyl)-*O*-((2-(4-methoxyphenyl)-2-oxoethoxy)carbonyl)-*L*-serinate (**211**) as a colourless solid (69.7 mg, 40%).

R_f: 0.23 (Petroleum ether:Et_2O = 1:1);
m.p.: 52 - 54 °C (Petroleum ether/Et_2O);
$[\alpha]_D^{26}$: +25.7 (***c*** 0.4 in $CHCl_3$);
UV λ_{max}/nm (ϵ/M^{-1}cm^{-1}): 265 (31580) [MeOH];
^{1}H NMR (400 MHz, $CDCl_3$) **δ**H: 7.87 (2H, d, J = 8.9 Hz, C_{Ph}**H**), 7.77 (2H, d, J = 7.5 Hz, C_{FmocAr}**H**), 7.65 (2H, d, J = 7.5 Hz, C_{FmocAr}**H**), 7.43 - 7.38 (2H, m, C_{FmocAr}**H**), 7.35 - 7.30 (2H, m, C_{FmocAr}**H**), 6.93 (2H, d, J = 8.9 Hz, C_{Ph}**H**), 5.86 (1H, d, J = 7.6 Hz, N**H**CHCH$_2$), 5.29 (2H, s, C(O)C**H**$_2$O), 4.68 - 4.52 (3H, m, NHC**H**CH$_2$,

NHCHC$\mathbf{H}_{\mathrm{A}}\mathrm{H}_{\mathrm{B}}$, NHCHC$\mathrm{H}_{\mathrm{A}}C\mathbf{H}_{\mathrm{B}}$), 4.41 (1H, dd, J = 14.2, 7.1 Hz, $\mathrm{C}_{\mathrm{Fmoc}}\mathbf{H}_{\mathrm{A}}\mathrm{H}_{\mathrm{B}}$), 4.38 (1H, dd, J = 14.2, 7.1 Hz, $\mathrm{C}_{\mathrm{Fmoc}}\mathrm{H}_{\mathrm{A}}\mathbf{H}_{\mathrm{B}}$), 4.25 (1H, dd, J = 7.1, 7.1 Hz, $\mathrm{C}_{\mathrm{Fmoc}}\mathbf{H}$), 3.85 (3H, s, $\mathrm{C}_{\mathrm{Ph}}\mathrm{OC}\mathbf{H}_3$), 1.52 (9H, s, $\mathrm{OC}(\mathrm{C}\mathbf{H}_3)_3$);

^{13}C NMR (100 MHz, CDCl_3) $\boldsymbol{\delta}$C: 188.8 (**C**O) 166.9 (**C**O), 163.2 ($\mathbf{C}_{\mathrm{Ph}}\mathrm{OCH}_3$), 154.9 (**C**O), 153.6 (**C**O), 142.8 ($\mathbf{C}_{\mathrm{FmocAr}}$), 140.2 ($\mathbf{C}_{\mathrm{FmocAr}}$), 129.0 ($\mathbf{C}_{\mathrm{Ph}}\mathrm{H}$), 126.7 ($\mathbf{C}_{\mathrm{FmocAr}}\mathrm{H}$), 126.1 ($\mathbf{C}_{\mathrm{FmocAr}}\mathrm{H}$), 125.7 ($\mathbf{C}_{\mathrm{Ph}}$), 124.2 ($\mathbf{C}_{\mathrm{FmocAr}}\mathrm{H}$), 118.9 ($\mathbf{C}_{\mathrm{FmocAr}}\mathrm{H}$), 113.1 ($\mathbf{C}_{\mathrm{Ph}}\mathrm{H}$), 82.3 ($\mathrm{O}\mathbf{C}(\mathrm{CH}_3)_3$), 67.6 ($\mathrm{C(O)}\mathbf{C}\mathrm{H}_2\mathrm{O}$), 67.2 ($\mathrm{NH}\mathbf{C}\mathrm{HCH}_2$), 66.3 ($\mathbf{C}_{\mathrm{Fmoc}}\mathrm{H}_2$), 54.5 ($\mathrm{C}_{\mathrm{Ph}}\mathrm{O}\mathbf{C}\mathrm{H}_3$), 52.5 ($\mathrm{NHCH}\mathbf{C}\mathrm{H}_2$), 46.0 ($\mathbf{C}_{\mathrm{Fmoc}}\mathrm{H}$), 26.9 ($\mathrm{OC}(\mathbf{C}\mathrm{H}_3)_3$);

LRMS *m/z* (ESI$^+$): 576 (32% $[\mathrm{M} + \mathrm{H}]^+$), 598 (100% $[\mathrm{M} + \mathrm{Na}]^+$);

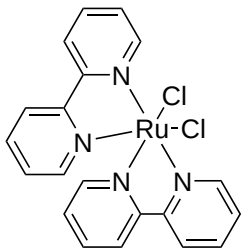
HRMS *m/z* (ESI$^+$): Found 598.2043 $[\mathrm{M} + \mathrm{Na}]^+$ ($\mathrm{C}_{32}\mathrm{H}_{33}\mathrm{NNaO}_9{}^+$ requires 598.2048 $[\mathrm{M} + \mathrm{Na}]^+$);

IR ($\boldsymbol{\nu}_{\mathbf{max}}$ cm^{-1}): 3356 (w), 2978 (w), 2165 (w), 1752 (s, C=O), 1692 (s, C=O), 1601 (m, Ar C-C), 1512 (m), 1449 (m, Ar C-C), 1427 (m), 1372 (m), 1347 (w), 1225 (s, C-O), 1154 (s, C-O), 1085 (w), 1029 (m, C-N), 955 (m), 837 (m), 784 (m), 760 (m), 738 (s), 618 (w).

7.10 Red-Shifted Caging Groups

7.10.1 Ruthenium Bipyridyl Caging Group

***cis*-$(bpy)_2RuCl_2 \cdot 2H_2O$**



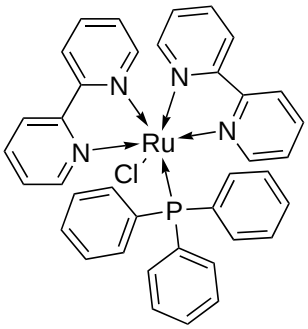
229

$RuCl_3 \cdot 3H_2O$ 325 (100 mg, 0.38 mmol, 1.00 eq), 2,2'-bipyridyl (120 mg, 0.77 mmol, 2.01 eq) and LiCl (1.27 mg, 0.03 mmol, 0.07 eq) were dissolved in DMF (5.00 mL). The resulting solution was stirred under reflux for 8 h. The reaction mixture was allowed to cool to RT and acetone (20.0 mL) was added. The resulting solution was left at 0 °C for 18 h. The suspension was filtered and the solid was washed with H_2O, and Et_2O, and dried by suction under vacuum to afford *cis*-$(bpy)_2RuCl_2 \cdot 2H_2O$ (**229**) as a black microcrystalline solid (72.6 mg, 35%).

R_f: 0.01 ($CHCl_3$:MeOH = 8:2);
m.p.: 308 °C (Acetone);
UV λ_{max}/nm (ϵ/$M^{-1}cm^{-1}$): 450 (1070) [MeOH];
^{1}H NMR (400 MHz, $(CD_3)_2SO$) δH: 9.97 (2H, d, J = 5.5 Hz, C_{bpy}**H**), 8.64 (2H, d, J = 8.1 Hz, C_{bpy}**H**), 8.48 (2H, d, J = 8.1 Hz, C_{bpy}**H**), 8.06 (2H, t, J = 7.7 Hz, C_{bpy}**H**), 7.77 (2H, t, J = 6.6 Hz, C_{bpy}**H**), 7.67 (2H, t, J = 7.7 Hz, C_{bpy}**H**), 7.51 (2H, d, J = 5.5 Hz, C_{bpy}**H**), 7.10 (2H, t, J = 6.6 Hz, C_{bpy}**H**);
^{13}C NMR (100 MHz, $(CD_3)_2SO$) δC: 160.2 (**C**$_{bpy}$), 158.2 (**C**$_{bpy}$), 153.2 (**C**$_{bpy}$H), 152.0 (**C**$_{bpy}$H), 134.5 (**C**$_{bpy}$H), 133.3 (**C**$_{bpy}$H), 125.3 (**C**$_{bpy}$H), 125.2 (**C**$_{bpy}$H), 122.8 (**C**$_{bpy}$H), 122.5 (**C**$_{bpy}$H);
LRMS *m/z* (ESI$^+$): 449 (100% $[M + Cl]^+$), 507 (20%, $[M + Na]^+$);
HRMS *m/z* (ESI$^+$): Found 507.0161 $[M + Na]^+$ ($C_{20}H_{16}Cl_2N_4NaRu^+$ requires 506.9688 $[M + Na]^+$);
IR (ν_{max} cm^{-1}): 3486 (w), 3040 (w), 1598 (w, Ar C-C), 1443 (m, Ar C-C), 1416 (m), 1307 (w), 1260 (m, C-N), 1157 (w), 1120 (w), 1014 (m), 884 (w), 800 (w), 761 (s), 724 (m), 653 (w).

Data are concordant with literature values.[227]

***cis*-(bpy)$_2$Ru(PPh$_3$)Cl·2H$_2$O**



230

cis-(bpy)$_2$RuCl$_2$·2H$_2$O (**229**) (50.0 mg, 0.10 mmol, 1.00 eq) was dissolved in MeOH (5.00 mL) and triphenylphosphine (28.9 mg, 0.11 mmol, 1.15 eq) was added. The reaction mixture was stirred ensuring complete dissolution prior to the addition of H_2O (2.00 mL). The reaction solution was stirred under reflux for 2 h, cooled and the solvent was removed under reduced pressure. The obtained crude residue was resuspended in acetone and cooled to 0 °C for 1 h. The suspension was filtered and the solid washed with portions of cold acetone and Et_2O, and dried by suction under vacuum, to afford *cis*-(bpy)$_2$Ru(PPh$_3$)Cl·2H$_2$O (**230**) as a red solid (73.7 mg, 94%).

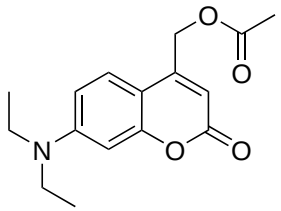
R$_f$: 0.01 ($CHCl_3$:MeOH = 8:2);
m.p.: 256 °C (Acetone);
UV λ_{max}/nm (ϵ/M^{-1}cm^{-1}): 450 (7770) [MeOH];
^{1}H NMR (400 MHz, $(CD_3)_2SO$) δH: 9.12 (1H, d, J = 5.5 Hz, C$_{bpy}$**H**), 9.07 (1H, d, J = 5.5 Hz, C$_{bpy}$**H**), 8.78 (1H, d, J = 8.0 Hz, C$_{bpy}$**H**), 8.72 (1H, d, J = 8.2 Hz, C$_{bpy}$**H**), 8.61 (1H, d, J = 8.0 Hz, C$_{bpy}$**H**), 8.49 (1H, d, J = 8.2 Hz, C$_{bpy}$**H**), 8.18 (1H, td, J = 7.9, 1.2 Hz, C$_{bpy}$**H**), 8.05 (2H, tt, J = 7.9, 1.2 Hz, C$_{bpy}$**H**), 7.77 (1H, td, J = 7.2, 1.2 Hz, C$_{bpy}$**H**), 7.54 (1H, t, J = 6.1 Hz, C$_{bpy}$**H**), 7.39 (1H, t, J = 7.2 Hz, C$_{bpy}$**H**), 7.40 (1H, t, J = 7.1 Hz, C$_{bpy}$**H**), 7.35 - 7.27 (9H, m, C$_{Ph}$**H**), 7.24 - 7.17 (6H, m, C$_{Ph}$**H**), 7.16 (1H, d, J = 5.6 Hz, C$_{bpy}$**H**), 7.12 (1H, d, J = 5.6 Hz, C$_{bpy}$**H**), 6.89 (1H, t, J = 6.1 Hz, C$_{bpy}$**H**);
^{13}C NMR (100 MHz, $(CD_3)_2SO$) δC: 165.5 (**C**$_{bpy}$), 158.4 (**C**$_{bpy}$), 157.8 (**C**$_{bpy}$H), 156.6 (**C**$_{bpy}$), 156.3 (**C**$_{bpy}$), 153.2 (**C**$_{bpy}$H), 151.4 (**C**$_{bpy}$H), 148.4 (**C**$_{bpy}$H), 138.1 (**C**$_{bpy}$H), 137.5 (**C**$_{bpy}$H), 136.8 (**C**$_{bpy}$H), 135.7 (**C**$_{bpy}$H), 133.0 (d, J = 9.5 Hz, **C**$_{Ph}$H), 131.7 (d, J = 38.9 Hz, **C**$_{Ph}$), 129.5 (**C**$_{Ph}$H), 128.1 (d, J = 8.7 Hz, **C**$_{Ph}$H), 126.8

($\mathbf{C}_{\text{bpy}}$H), 126.7 ($\mathbf{C}_{\text{bpy}}$H), 126.6 ($\mathbf{C}_{\text{bpy}}$H), 126.3 ($\mathbf{C}_{\text{bpy}}$H), 124.2 ($\mathbf{C}_{\text{bpy}}$H), 123.7 ($\mathbf{C}_{\text{bpy}}$H), 123.3 ($\mathbf{C}_{\text{bpy}}$H), 123.2 ($\mathbf{C}_{\text{bpy}}$H);
^{31}P NMR (162 MHz, $(CD_3)_2SO$) $\boldsymbol{\delta}$P: 42.94 (1P, s, $\mathbf{P}(Ph)_3$)
LRMS *m/z* (ESI$^+$): 711 (100% $[M]^+$);
HRMS *m/z* (ESI$^+$): Found 711.1017 $[M]^+$ ($C_{38}H_{31}ClN_4PRu^+$ requires 711.1013 $[M]^+$);
IR ($\boldsymbol{\nu}_{\mathbf{max}}$ cm^{-1}): 3371 (w), 3063 (w), 3016 (w), 2980 (w), 2363 (w), 1712 (w), 1627 (w), 1599 (w, Ar C-C), 1471 (m, Ar C-C), 1435 (m), 1358 (w), 1311 (w), 1268 (w), 1221 (w), 1160 (w), 1120 (w), 1088 (m), 998 (w), 759 (s), 698 (s), 625 (w).

Data are concordant with literature values.[228]

7.10.2 DEATC Caged Amino Acids

(7-(Diethylamino)-2-oxo-2*H*-chromen-4-yl)methyl acetate



233

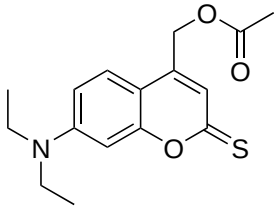
7-(Diethylamino)-4-(hydroxymethyl)-2*H*-chromen-2-one (**153**) (300 mg, 1.21 mmol, 1.00 eq), 1,3-dicyclohexylcarbodiimide (299 mg, 1.45 mmol, 1.20 eq) and 4-(dimethylamino)pyridine (177 mg, 1.45 mmol, 1.20 eq) were dissolved in anhydrous CH_2Cl_2 (30.0 mL). To this solution was added glacial acetic acid (87.1 mg, 0.08 mL, 1.45 mmol, 1.20 eq) dropwise, at 0 °C. The reaction solution was stirred at 0 °C for 10 min, then slowly allowed to warm to RT and stirred under an Ar atmosphere for 16 h, after which the reaction was adjudged to be complete by TLC analysis. The cloudy yellow suspension was filtered and the filtrate was diluted with CH_2Cl_2 (50.0 mL), washed with aq. 1 M HCl (100 mL), and sat. aq. $NaHCO_3$ (100 mL). The solvent was removed under reduced pressure and the obtained crude residue was purified by silica gel flash chromatography, eluting with petroleum ether:Et_2O = 1:1, to afford (7-(diethylamino)-2-oxo-2*H*-chromen-4-yl)methyl acetate (**233**) as a yellow solid (304 mg, 87%).

R_f: 0.52 ($CHCl_3$:Acetone = 9:1);
m.p.: 107 - 109 °C (Hexane/Acetone) [Literature value: 111 - 113 °C (propan-2-ol)][229];
UV λ_{max}/nm (ϵ/$M^{-1}cm^{-1}$): 385 (24470) [MeOH];
^{1}H NMR (400 MHz, $CDCl_3$) **δ**H: 7.28 (1H, d, J = 9.0 Hz, $C_{DEACMAr}$**H**), 6.58 (1H, dd, J = 9.0, 2.5 Hz, $C_{DEACMAr}$**H**), 6.51 (1H, d, J = 2.5 Hz, $C_{DEACMAr}$**H**), 6.13 (1H, t, J = 1.2 Hz, $C_{DEACMAlkene}$**H**), 5.22 (2H, d, J = 1.2 Hz, C**H_2**O), 3.41 (4H, q, J = 7.2 Hz, N(C**H_2**CH_3)$_2$), 2.19 (3H, s, C**H_3**), 1.20 (6H, t, J = 7.2 Hz, N(CH_2C**H_3**)$_2$);
^{13}C NMR (100 MHz, $CDCl_3$) **δ**C: 170.2 (**C**O), 161.9 (**C**O), 156.2 ($\mathbf{C}_{DEACMAr}$), 150.6 ($\mathbf{C}_{DEACMAr}$), 149.4 ($\mathbf{C}_{DEACMAr}$), 124.3 ($\mathbf{C}_{DEACMAr}$H), 108.6 ($\mathbf{C}_{DEACMAr}$H), 106.3 ($\mathbf{C}_{DEACMAlkene}$H), 105.9 ($\mathbf{C}_{DEACMAlkene}$), 97.7 ($\mathbf{C}_{DEACMAr}$H), 61.3 (**C**H_2O), 44.7 (N(**C**$H_2$$CH_3$)$_2$), 20.7 (**C**$H_3$), 12.4 (N($CH_2$**C**$H_3$)$_2$);

LRMS *m/z* (ESI$^+$): 290 (100% $[M + H]^+$);
HRMS *m/z* (ESI$^+$): Found 312.1206 $[M + Na]^+$ ($C_{16}H_{19}NNaO_4^+$ requires 312.1206 $[M + Na]^+$);
IR (ν_{max} cm^{-1}): 2973 (w), 1749 (m), 1707 (s, C=O), 1598 (s, Ar C-C), 1525 (m), 1441 (m, Ar C-C), 1413 (m), 1343 (m), 1266 (m, C-N), 1242 (s, C-O), 1193 (w), 1169 (w), 1137 (w), 1072 (m, C-O), 1040 (w), 1008 (w), 929 (w), 897 (w), 847 (w), 833 (m), 816 (m), 656 (w).

Data are concordant with literature values.[61]

(7-(Diethylamino)-2-thioxo-2*H*-chromen-4-yl)methyl acetate



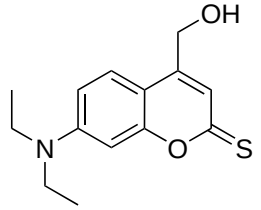
234

(7-(Diethylamino)-2-oxo-2*H*-chromen-4-yl)methyl acetate (**233**) (250 mg, 0.86 mmol, 1.00 eq) and Lawesson's reagent (227 mg, 0.56 mmol, 0.65 eq) were dissolved in anhydrous toluene (10.0 mL) at RT. The reaction mixture was heated under reflux (120 °C) and stirred under an Ar atmosphere for 18 h, after which time the reaction was adjudged to be complete by TLC analysis. The reaction solution was cooled to RT and the solvent was removed under reduced pressure. The crude residue was purified by silica gel flash column chromatography, eluting with $CHCl_3$, to afford (7-(diethylamino)-2-thioxo-2*H*-chromen-4-yl)methyl acetate (**234**) as a dark red orange solid (178 mg, 68%).

R_f: 0.79 ($CHCl_3$:Acetone = 9:1);
m.p.: 56 - 58 °C (Hexane/Acetone);
^{1}H NMR (400 MHz, $CDCl_3$) δH: 7.34 (1H, d, J = 8.5 Hz, $C_{DEATCAr}$**H**), 7.06 (1H, t, J = 1.0 Hz, $C_{DEATCAlkene}$**H**), 6.68 (1H, d, J = 2.5 Hz, $C_{DEATCAr}$**H**), 6.66 (1H, dd, J = 8.5, 2.5 Hz, $C_{DEATCAr}$**H**), 5.19 (2H, d, J = 1.0 Hz, C**H**$_2$O), 3.43 (4H, q, J = 7.1 Hz, N(C**H**$_2$CH$_3$)$_2$), 2.19 (3H, s, C**H**$_3$), 1.22 (6H, t, J = 7.1 Hz, N(CH$_2$C**H**$_3$)$_2$);
^{13}C NMR (100 MHz, $CDCl_3$) δC: 197.1 (**C**S), 170.3 (**C**O), 159.0 ($\mathbf{C}_{DEATCAr}$), 151.0 ($\mathbf{C}_{DEATCAr}$), 141.9 ($\mathbf{C}_{DEATCAr}$), 124.4 ($\mathbf{C}_{DEATCAr}$H), 120.4 ($\mathbf{C}_{DEATCAlkene}$H), 110.3 ($\mathbf{C}_{DEATCAr}$H), 108.1 ($\mathbf{C}_{DEATCAlkene}$), 97.4 ($\mathbf{C}_{DEATCAr}$H), 60.9 (C**H**$_2$O), 44.9 (N(**C**H$_2$CH$_3$)$_2$), 20.8 (**C**H$_3$), 12.4 (N(CH$_2$**C**H$_3$)$_2$);
LRMS *m/z* (ESI$^+$): 197 (100%), 306 (81% $[M + H]^+$);
HRMS *m/z* (ESI$^+$): Found 306.1159 $[M + H]^+$ ($C_{16}H_{20}NO_3S^+$ requires 306.1158 $[M + H]^+$);
IR (ν_{max} cm^{-1}): 3383 (w), 2974 (w), 2923 (w), 2871 (w), 1700 (m, C=O), 1601 (s, Ar C-C), 1518 (m), 1422 (m, Ar C-C), 1346 (m, C=S), 1289 (w), 1228 (w), 1188 (w), 1140 (w), 1079 (s, C-O), 969 (w), 899 (w), 820 (m), 797 (m), 748 (w), 712 (w), 663 (w), 635 (w).

Data are concordant with literature values.[61]

7-(Diethylamino)-4-(hydroxymethyl)-2*H*-chromene-2-thione



235

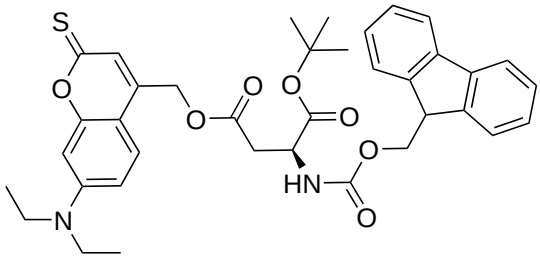
1.25 M Ethanolic HCl (1.00 mL, 1.23 mmol, 2.50 eq), generated by the dropwise addition of acetyl chloride (98.1 mg, 0.09 mL, 1.25 mmol, 2.50 mmol) to EtOH (1.00 mL) at 0 °C, was added to a solution of (7-(diethylamino)-2-thioxo-2*H*-chromen-4-yl)methyl (**234**) (150 mg, 0.49 mmol, 1.00 eq) in EtOH (100 mL). The reaction solution was heated under reflux (100 °C) and stirred under an Ar atmosphere for 18 h, after which time the reaction was adjudged to be complete by TLC analysis. The reaction solution was allowed to cool to RT and the solvent was removed under reduced pressure. The obtained crude residue was immediately purified by silica gel flash column chromatography, eluting with $CHCl_3$, to afford 7-(diethylamino)-4-(hydroxymethyl)-2*H*-chromene-2-thione (**235**) as a dark orange solid (649 mg, 50%).

R_f: 0.46 ($CHCl_3$:Acetone = 9:1);
m.p.: 117 - 119 °C (Hexane/Acetone);
UV λ_{max}/nm (ϵ/M^{-1}cm^{-1}): 460 (20970) [MeOH];
^{1}H NMR (400 MHz, ($(CD_3)_2CO$) δH: 7.52 (1H, d, J = 9.0 Hz, $C_{DEATCAr}$**H**), 7.12 (1H, t, J = 1.2 Hz, $C_{DEATCAlkene}$**H**), 6.80 (1H, dd, J = 9.0, 2.6 Hz, $C_{DEATCAr}$**H**), 6.65 (1H, d, J = 2.6 Hz, $C_{DEATCAr}$**H**), 4.81 (2H, dd, J = 5.7, 1.2 Hz, C**H**$_2$OH), 4.65 (1H, t, J = 5.7 Hz, O**H**), 3.54 (4H, q, J = 7.1 Hz, N(C**H**$_2$CH$_3$)$_2$), 1.22 (6H, t, J = 7.1 Hz, N(CH$_2$C**H**$_3$)$_2$);
^{13}C NMR (100 MHz, ($(CD_3)_2CO$) δC: 198.4 (**C**S), 159.7 ($C_{DEATCAr}$), 151.9 ($C_{DEATCAr}$), 149.3 ($C_{DEATCAr}$), 125.9 ($C_{DEATCAr}$H), 120.2 ($C_{DEATCAlkene}$H), 111.1 ($C_{DEATCAr}$H), 109.1 ($C_{DEATCAlkene}$), 97.5 ($C_{DEATCAr}$H), 60.3 (**C**H$_2$OH), 45.4 (N(**C**H$_2$CH$_3$)$_2$), 12.8 (N(CH$_2$**C**H$_3$)$_2$);
LRMS *m/z* (ESI$^+$): 264 (100% $[M + H]^+$);
HRMS *m/z* (ESI$^+$): Found 264.1054 $[M + H]^+$ ($C_{14}H_{18}NO_2S^+$ requires 264.1053 $[M + H]^+$);
IR (ν_{max} cm^{-1}): 3645 (w), 2956 (m), 2924 (s), 2855 (m), 2362 (w), 1717 (w), 1616 (m, C=O), 1578 (m, Ar C-C), 1518 (w), 1435 (m, Ar C-C), 1361 (w, C=S), 1294 (w),

1255 (m, C-N), 1190 (w), 1153 (w), 1082 (m, C-O), 1021 (m, C-O), 862 (w), 800 (m), 666 (w), 625 (w).

Data are concordant with literature values.[61]

1-(*tert*-Butyl) 4-((7-(diethylamino)-2-thioxo-2*H*-chromen-4-yl)methyl (((9*H*-fluoren-9-yl)methoxy)carbonyl-*L*-aspartate



232

Fmoc-Asp-O^{t}Bu (**221**) (156 mg, 0.38 mmol, 1.00 eq) and *N*,*N*,*N*',*N*'-tetramethyl-*O*-(1*H*-benzotriazol-1-yl)uronium hexafluorophosphate (159 mg, 0.42 mmol, 1.10 eq) were dissolved in anhydrous DMF (5.00 mL). *N*,*N*-Diisopropylethylamine (98.2 mg, 0.13 mL, 0.76 mmol, 2.00 eq) was added and the reaction solution was stirred at RT under an Ar atmosphere for 1 h. 7-(Diethylamino)-4-(hydroxymethyl)-2*H*-chromene-2-thione (**235**) (50.0 mg, 0.19 mmol, 1.00 eq) was added and the reaction solution was stirred under an Ar atmosphere at RT for 18 h, after which time the reaction was adjudged to be complete by TLC analysis. The reaction was quenched with EtOAc (100 mL), washed with aq. 1 M HCl (100 mL), sat. aq. $NaHCO_3$ (100 mL), H_2O (100 mL), and brine (100 mL). The solvent was removed under reduced pressure and the obtained crude residue was purified by silica gel flash column chromatography, eluting with $CHCl_3$, to afford 1-(*tert*-butyl) 4-((7-(diethylamino)-2-thioxo-2*H*-chromen-4-yl)methyl (((9*H*-fluoren-9-yl)methoxy)carbonyl-*L*-aspartate (**232**) as a brown foam (121 mg, 97%).

$\mathbf{R_f}$: 0.71 ($CHCl_3$:Acetone = 9:1);
m.p.: 79 - 81 °C (Petroleum ether/Acetone);
$[\boldsymbol{\alpha}]_{\boldsymbol{D}}^{\mathbf{26}}$: +11.3 (***c*** 0.9 in $CHCl_3$);
UV $\boldsymbol{\lambda_{max}}$/nm ($\boldsymbol{\epsilon}$/$\mathbf{M^{-1}cm^{-1}}$): 465 (9090) [MeOH];
^{1}H NMR (400 MHz, $(CD_3)_2SO$) $\boldsymbol{\delta}$H: 7.77 (2H, d, J = 7.7 Hz, $C_{FmocAr}\mathbf{H}$), 7.62 (2H, d, J = 7.4 Hz, $C_{FmocAr}\mathbf{H}$), 7.47 (1H, d, J = 9.2 Hz, $C_{DEATCAr}\mathbf{H}$), 7.36 (2H, t, J = 7.7 Hz, $C_{FmocAr}\mathbf{H}$), 7.27 (2H, t, J = 7.4 Hz, $C_{FmocAr}\mathbf{H}$), 6.95 (1H, t, J = 1.0 Hz, $C_{DEATCAlkene}\mathbf{H}$), 6.74 (1H, dd, J = 9.2, 2.5 Hz, $C_{DEATCAr}\mathbf{H}$), 6.57 (1H, d, J = 2.5 Hz, $C_{DEATCAr}\mathbf{H}$), 5.24 (2H, br s, $C\mathbf{H}_2O$), 4.52 (1H, dd, J = 7.6, 5.4 Hz, $NHC\mathbf{H}CH_2$), 4.34 - 4.28 (2H, m, $C_{Fmoc}\mathbf{H}_2$), 4.17 (1H, t, J = 7.3 Hz, $C_{Fmoc}\mathbf{H}$), 3.42 (4H, q, J = 7.1 Hz, $N(C\mathbf{H}_2CH_3)_2$), 3.01 (1H, dd, J = 16.5, 5.4 Hz, $NHCHC\mathbf{H}_AH_B$), 2.90 (1H, dd, J

= 16.5, 7.6 Hz, NHCHCH$_A$**H**$_B$), 1.43 (9H, s, OC(C**H**$_3$)$_3$), 1.16 (6H, t, J = 7.1 Hz, N(CH$_2$C**H**$_3$)$_2$);

^{13}C NMR (100 MHz, (CD$_3$)$_2$SO) δC: 195.8 (**C**S), 169.8 (**C**O), 169.6 (**C**O), 158.6 (**C**$_{\text{DEATCAr}}$), 155.9 (**C**O), 150.9 (**C**$_{\text{DEATCAr}}$), 143.7 (**C**$_{\text{FmocAr}}$), 140.7 (**C**$_{\text{FmocAr}}$), 127.7 (**C**$_{\text{FmocAr}}$H), 127.1 (**C**$_{\text{FmocAr}}$H), 125.9 (**C**$_{\text{DEATCAr}}$H), 125.2 (**C**$_{\text{FmocAr}}$H), 120.1 (**C**$_{\text{FmocAr}}$H), 119.6 (**C**$_{\text{DEATCAlkene}}$H), 110.7 (**C**$_{\text{DEATCAr}}$H), 107.6 (**C**$_{\text{DEATCAlkene}}$), 96.2 (**C**$_{\text{DEATCAr}}$H), 81.2 (O**C**(CH$_3$)$_3$), 65.7 (**C**$_{\text{Fmoc}}$H$_2$), 61.4 (**C**H$_2$O), 51.0 (NH**C**HCH$_2$), 46.6 (**C**$_{\text{Fmoc}}$H), 44.2 (N(**C**H$_2$CH$_3$)$_2$), 35.8 (NHCH**C**H$_2$), 27.5 (OC(**C**H$_3$)$_3$), 12.3 (N(CH$_2$**C**H$_3$)$_2$);

LRMS *m/z* (ESI$^+$): 322 (100%), 657 (45% [M + H]$^+$);

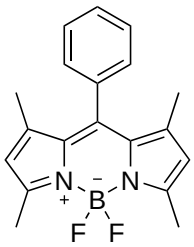
HRMS *m/z* (ESI$^+$): Found 655.2578 [M - H]$^-$($C_{37}H^{39}N_2O_7S^-$ requires 655.2473 [M - H]$^-$);

IR (ν_{max} cm^{-1}): 3352 (w), 2976 (w), 2932 (w), 1726 (s, C=O), 1628 (s, C=O), 1580 (s, Ar C-C), 1518 (s), 1438 (m, Ar C-C), 1398 (w), 1354 (m, C=S), 1294 (m), 1256 (m), 1225 (m), 1181 (m), 1150 (s, C-O), 1104 (w), 1074 (m), 847 (w), 757 (m), 620 (w);

HPLC: 16.50 min (97.2%).

7.10.3 BODIPY Caged Amino Acids

5,5-Difluoro-1,3,7,9-tetramethyl-10-phenyl-5*H*-4λ4,5λ4-dipyrrolo[1,2-c:2',1'-f][1,3,2]diazaborinine



238

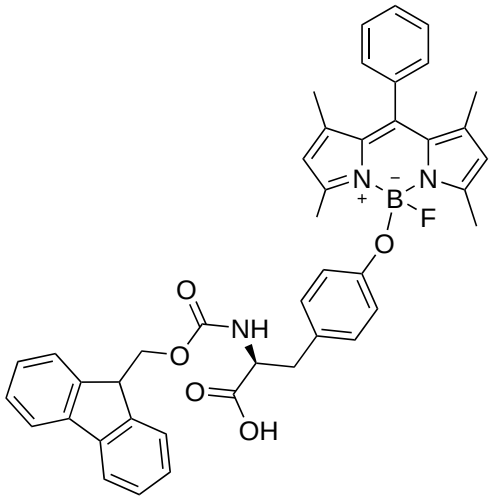
A solution of 2,4-dimethylpyrrole (**236**) (1.85 g, 2.00 mL, 19.4 mmol, 2.00 eq) and benzoyl chloride (1.42 g, 1.16 mL, 10.0 mmol, 1.03 eq) in anhydrous CH_2Cl_2 (100 mL) was stirred at RT under an Ar atmosphere for 18 h, after which time formation of the intermediate was adjudged to be complete by TLC analysis. The resulting solution was cooled to 0 °C and NEt_3 (7.28 g, 10.01 mL, 71.9 mmol, 7.40 eq), and $BF_3{\cdot}OEt_2$ (11.6 g, 10.07 mL, 81.6 mmol, 8.40 eq) were added dropwise. The reaction solution was allowed to warm to RT and stirred under an Ar atmosphere for 6 h, after which time the reaction was adjudged to be complete by TLC analysis. The reaction mixture was poured in H_2O (200 mL) and extracted with CH_2Cl_2 (2 × 200 mL). The solvent was removed under reduced pressure and the obtained crude residue was purified by silica gel flash column chromatography, eluting with petroleum ether 30 - 40:Et_2O = 9:1, to afford 5,5-difluoro-1,3,7,9-tetramethyl-10-phenyl-5*H*-4**λ**4,5**λ**4-dipyrrolo[1,2-c:2',1'-f][1,3,2]diazaborinine (**238**) as a green orange solid (793 mg, 25%).

R_f: 0.36 (Petroleum ether:Et_2O = 8:2);
m.p.: 170 - 171 °C (CH_2Cl_2/Petroleum ether) [Literature value: 168 - 169 °C][230];
UV λ_{max}/nm (ϵ/$M^{-1}cm^{-1}$): 500 (70140) [MeOH];
^{1}H NMR (400 MHz, $CDCl_3$) **δ**H: 7.53 - 7.47 (3H, m, C_{Ph}**H**, C_{Ph}**H**), 7.31 - 7.27 (2H, m, C_{Ph}**H**), 5.99 (2H, s, $C_{BODIPYAr}$**H**), 2.57 (6H, s, C**H**$_3$), 1.39 (6H, s, C**H**$_3$);
^{13}C NMR (100 MHz, $CDCl_3$) **δ**C: 155.4 (**C**$_{BODIPY}$), 143.1 (**C**$_{BODIPY}$) 141.7 (**C**$_{BODIPY}$), 134.9 (**C**$_{BODIPY}$), 131.4 (**C**$_{Ph}$), 129.1 (**C**$_{Ph}$H), 128.9 (**C**$_{Ph}$H), 127.9 (**C**$_{Ph}$H), 121.2 (**C**$_{BODIPY}$H), 14.5 (**C**H$_3$), 14.3 (**C**H$_3$);
^{19}F NMR(377 MHz, $CDCl_3$) **δ**F: -146.3 (2F, q, J = 33.5 Hz, B**F**$_2$);
LRMS *m/z* (ESI$^+$): 325 (64% $[M + H]^+$), 658 (100% $[2M]^+$);

HRMS *m/z* (ESI$^+$): Found 325.1679 $[M + H]^+$ ($C_{19}H_{20}N_2BF_2^+$ requires 325.1682 $[M + H]^+$);
IR (ν_{max} cm^{-1}): 1539 (m, Ar C-C), 1504 (m), 1467 (w), 1406 (w), 1366 (w), 1303 (m, C-N), 1257 (w), 1189 (m), 1151 (m), 1112 (w), 1063 (m), 972 (s), 921 (w), 887 (w), 811 (m), 718 (s), 627 (w).

Data are concordant with literature values.[230]

***tert*-Butyl (*S*)-2-((((9*H*-fluoren-9-yl)methoxy)carbonyl)amino)-3-(4-((5-fluoro-1,3,7,9-tetramethyl-10-phenyl-5*H*-4λ4,5λ4-dipyrrolo[1,2-c:2',1'-f][1,3,2]diazaborinin-5-yl)oxy)phenyl)propanoate**



244

5,5-Difluoro-1,3,7,9-tetramethyl-10-phenyl-5*H*-4λ4,5λ4-dipyrrolo[1,2-c:2',1'-f][1,3,2]diazaborinine (**238**) (50.0 g, 0.15 mmol, 1.00 eq) and $AlCl_3$ (10.7 mg, 0.08 mmol, 0.50 eq) were dissolved in anhydrous CH_2Cl_2 (5.00 mL) and stirred under reflux for 10 min. Heating was stopped, Fmoc-Tyr-OH (64.5 mg, 0.16 mmol, 1.05 eq) was dissolved in anhydrous CH_2Cl_2 (2.00 mL), and added dropwise to the aforementioned solution. The reaction mixture was left to stir under reflux for 0.5 h, after which heating was stopped and the reaction mixture was allowed to cool to RT. The solvent was removed under reduced pressure and the obtained crude residue was purified by silica gel flash column chromatography, eluting with $CHCl_3$, to afford *tert*-butyl (*S*)-2-((((9*H*-fluoren-9-yl)methoxy)carbonyl)amino)-3-(4-((5-fluoro-1,3,7,9-tetramethyl-10-phenyl-5*H*-4λ4,5λ4-dipyrrolo[1,2-c:2',1'-f][1,3,2]di-azaborinin-5-yl)oxy)-phenyl)propanoate (**244**) as a bright orange solid (7.8 mg, 8%).

R_f: 0.58 ($CHCl_3$:Acetone = 9:1);
m.p.: 159 - 161 °C (CH_2Cl_2/Petroleum ether);
$[\alpha]_D^{26}$: +2.1 (***c*** 0.3 in $CHCl_3$);
UV λ_{max}/nm (ϵ/$M^{-1}cm^{-1}$): 500 (12730) [MeOH];
^{1}H NMR (400 MHz, $CDCl_3$) **δ**H: 7.75 (2H, d, J = 7.6 Hz, C_{FmocAr}**H**), 7.57 - 7.50 (2H, m, C_{FmocAr}**H**), 7.50 - 7.45 (3H, m, C_{Ph}**H**), 7.42 - 7.36 (3H, m, C_{FmocAr}**H**, C_{Ph}**H**), 7.32 - 7.27 (3H, m, C_{FmocAr}**H**, C_{Ph}**H**), 6.86 (2H, d, J = 8.6 Hz, C_{TyrAr}**H**), 6.60 (2H, d,

J = 8.6 Hz, $C_{TyrAr}\mathbf{H}$), 5.98 (1H, s, $C_{Pyrrole}\mathbf{H}$), 5.96 (1H, s, $C_{Pyrrole}\mathbf{H}$), 5.30 (1H, d, J = 8.1 Hz, N**H**$CHCH_2$), 4.58 (1H, ddd, J = 8.1, 6.0, 6.0 Hz, NHC**H**CH_2), 4.35 (1H, dd, J = 10.5, 7.1 Hz, $C_{Fmoc}\mathbf{H}_AH_B$), 4.22 (1H, dd, J = 10.5, 7.1 Hz, $C_{Fmoc}H_A\mathbf{H}_B$), 4.16 (1H, dd, J = 7.1, 7.1 Hz, $C_{Fmoc}\mathbf{H}$), 3.20 (1H, dd, J = 14.0, 6.0 Hz, NHCHC$\mathbf{H}_AH_B$), 2.95 (1H, dd, J = 14.0, 6.0 Hz, NHCHC$H_A\mathbf{H}_B$), 2.48 (3H, s, C$\mathbf{H}_3$), 2.43 (3H, s, C$\mathbf{H}_3$), 1.41 (3H, s, C$\mathbf{H}_3$), 1.37 (3H, s, C$\mathbf{H}_3$);

^{13}C NMR (100 MHz, CD_3OD) $\boldsymbol{\delta}$C: 175.6 (**C**OOH), 158.6 (**C**O), 158.5 (**C**O), 157.7 ($\mathbf{C}_{Ar}$O), 157.4 ($\mathbf{C}_{Ar}$O), 156.9 ($\mathbf{C}_{BODIPY}$), 145.4 ($\mathbf{C}_{FmocAr}$), 145.4 ($\mathbf{C}_{FmocAr}$), 144.3 ($\mathbf{C}_{FmocAr}$), 143.8 ($\mathbf{C}_{BODIPY}$), 142.7 ($\mathbf{C}_{BODIPY}$), 136.6 ($\mathbf{C}_{BODIPY}$), 133.6 ($\mathbf{C}_{Ph}$), 131.5 ($\mathbf{C}_{Ar}$H), 130.6 ($\mathbf{C}_{Ph}$H), 130.4 ($\mathbf{C}_{Ph}$H), 129.5 ($\mathbf{C}_{Ar}$), 129.4 ($\mathbf{C}_{Ph}$H), 128.9 ($\mathbf{C}_{FmocAr}$H), 128.3 ($\mathbf{C}_{FmocAr}$H), 126.5 ($\mathbf{C}_{FmocAr}$H), 126.4 ($\mathbf{C}_{FmocAr}$H), 122.6 ($\mathbf{C}_{BODIPY}$H), 121.0 ($\mathbf{C}_{FmocAr}$H), 116.3 ($\mathbf{C}_{Ar}$H), 68.1 ($\mathbf{C}_{Fmoc}H_2$), 57.3 (NH**C**HCH_2), 48.5 ($\mathbf{C}_{Fmoc}$H), 38.0 (NHCH**C**H_2), 14.8 ($C_{BODIPY}\mathbf{C}H_3$), 14.8 ($C_{BODIPY}\mathbf{C}H_3$), 14.7 ($C_{BODIPY}\mathbf{C}H_3$);

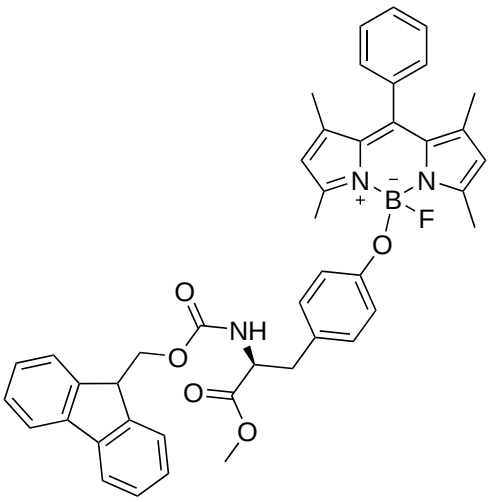
^{19}F NMR(470 MHz, $CDCl_3$) $\boldsymbol{\delta}$F: -153.0 (1F, q, J = 25.2 Hz, B**F**);

LRMS *m/z* (ESI$^+$): 730 (100% $[M + Na]^+$);

HRMS *m/z* (ESI$^+$): Found 730.2859 $[M + Na]^+$ ($C_{43}H_{39}BFN_3NaO_5^+$ requires 730.2870 $[M + Na]^+$);

IR ($\boldsymbol{\nu}_{\mathbf{max}}$ cm^{-1}): 2962 (w), 2925 (w), 2815 (w), 2356 (w), 2024 (w), 1731 (w, C=O), 1547 (s, Ar C-C), 1510 (s, Ar C-C), 1468 (w), 1445 (w), 1409 (w), 1366 (w), 1303 (m, C-N), 1260 (w), 1203 (m, C-O), 1260 (w), 1186 (m, C-O), 1155 (m, C-O), 1120 (m, C-N), 1025 (w), 981 (m), 943 (w), 803 (w), 774 (w), 722 (m), 654 (w).

Methyl (*S*)-2-((((9*H*-fluoren-9-yl)methoxy)carbonyl)amino)-3-(4-((5-fluoro-1,3,7,9-tetramethyl-10-phenyl-5*H*-4λ4,5λ4-dipyrrolo[1,2-c:2',1'-f][1,3,2]diazaborinin-5-yl)oxy)phenyl)propanoate



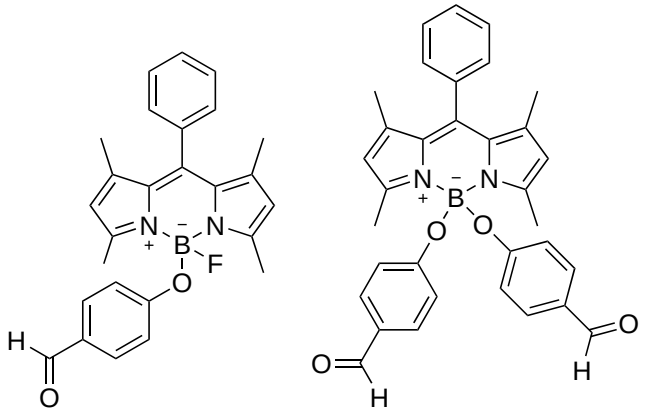
245

5,5-Difluoro-1,3,7,9-tetramethyl-10-phenyl-5*H*-4$\boldsymbol{\lambda}$4,5$\boldsymbol{\lambda}$4-dipyrrolo[1,2-c:2',1'-f][1,3,2]diazaborinine (**238**) (200 mg, 0.62 mmol, 1.00 eq) and $AlCl_3$ (66.7 mg, 0.50 mmol, 0.80 eq) were dissolved in anhydrous CH_2Cl_2 (16.0 mL). The resulting mixture was heated under reflux and stirred under an Ar atmosphere for 15 min. Heating was stopped and a solution of methyl (((9*H*-fluoren-9-yl)methoxy)carbonyl)-*L*-tyrosinate (**247**) (259 mg, 0.62 mmol, 1.00 eq) in anhydrous CH_2Cl_2 (12.0 mL) was added dropwise to the aforementioned solution. The reaction mixture was heated under reflux and stirred under an Ar atmosphere for 0.5 h. Heating was stopped and the reaction mixture was allowed to cool to RT. The solvent was removed under reduced pressure and the obtained crude residue was purified by silica gel flash column chromatography, eluting with CH_2Cl_2 to CH_2Cl_2:Et_2O = 98:2 - 95:5 - 90:10, to afford methyl (*S*)-2-((((9*H*-fluoren-9-yl)methoxy)carbonyl)amino)-3-(4-((5-fluoro-1,3,7,9-tetramethyl-10-phenyl-5*H*-4$\boldsymbol{\lambda}$4,5$\boldsymbol{\lambda}$4-dipyrrolo[1,2-c:2',1'-f][1,3,2]diazaborinin-5-yl)oxy)-phenyl)propanoate (**245**) as a bright orange foam (132 mg, 28%).

$\mathbf{R_f}$: 0.46 (CH_2Cl_2:Et_2O = 9:1);
m.p.: 88 - 89 °C (CH_2Cl_2/Petroleum ether);
$[\boldsymbol{\alpha}]_{\boldsymbol{D}}^{\mathbf{26}}$: -12.8 (***c*** 1.3 in $CHCl_3$);
UV $\boldsymbol{\lambda_{max}}$/nm ($\boldsymbol{\epsilon}$/$\mathbf{M^{-1}cm^{-1}}$): 500 (80780) [MeOH];

^{1}H NMR (400 MHz, CD_3OD) δH: 7.77 (2H, d, J = 7.2 Hz, $C_{FmocAr}\mathbf{H}$), 7.57 - 7.53 (2H, m, $C_{FmocAr}\mathbf{H}$), 7.52 - 7.46 (3H, m, $C_{Ph}\mathbf{H}$, $C_{Ph}\mathbf{H}$), 7.36 (2H, t, J = 7.2 Hz, $C_{FmocAr}\mathbf{H}$), 7.29 - 7.22 (3H, m, $C_{FmocAr}\mathbf{H}$, $C_{Ph}\mathbf{H}$), 7.12 (1H, d, J = 6.8 Hz, $C_{Ph}\mathbf{H}$), 6.93 (2H, d, J = 8.5 Hz, $C_{Ar}\mathbf{H}$), 6.38 (2H, d, J = 8.5 Hz, $C_{Ar}\mathbf{H}$), 5.87 (1H, s, $C_{BODIPY}\mathbf{H}$), 5.81 (1H, s, $C_{BODIPY}\mathbf{H}$), 4.36 (1H, dd, J = 9.5, 5.0 Hz, NHC$\mathbf{H}$$CH_2$), 4.28 (1H, dd, J = 10.0, 6.5 Hz, $C_{Fmoc}\mathbf{H}_A H_B$), 4.09 - 3.99 (2H, m, $C_{Fmoc}H_A\mathbf{H}_B$, $C_{Fmoc}\mathbf{H}$), 3.64 (3H, s, COOC$\mathbf{H}_3$), 3.00 (1H, dd, J = 14.0, 5.0 Hz, NHCHC$\mathbf{H}_A H_B$), 2.78 (1H, dd, J = 14.0, 9.5 Hz, NHCHC$H_A\mathbf{H}_B$), 2.42 (3H, s, $C_{BODIPY}C\mathbf{H}_3$), 2.36 (3H, s, $C_{BODIPY}C\mathbf{H}_3$), 1.28 (3H, s, $C_{BODIPY}C\mathbf{H}_3$), 1.26 (3H, s, $C_{BODIPY}C\mathbf{H}_3$);
^{13}C NMR (100 MHz, CD_3OD) δC: 174.2 ($\mathbf{C}OOCH_3$), 158.3 ($\mathbf{C}O$), 157.1 ($\mathbf{C}_{Ar}O$), 157.0 ($\mathbf{C}_{Ar}O$), 156.4 ($\mathbf{C}_{BODIPY}$), 156.4 ($\mathbf{C}_{BODIPY}$), 145.5 ($\mathbf{C}_{FmocAr}$), 145.2 ($\mathbf{C}_{FmocAr}$), 144.7 ($\mathbf{C}_{FmocAr}$), 143.7 ($\mathbf{C}_{BODIPY}$), 142.7 ($\mathbf{C}_{BODIPY}$), 142.6 ($\mathbf{C}_{BODIPY}$), 136.6 ($\mathbf{C}_{BODIPY}$), 133.1 ($\mathbf{C}_{Ph}$), 133.0 ($\mathbf{C}_{Ph}$), 131.2 ($\mathbf{C}_{Ar}H$), 130.6 ($\mathbf{C}_{Ph}H$), 130.5 ($\mathbf{C}_{Ph}H$), 130.4 ($\mathbf{C}_{Ph}H$), 130.0 ($\mathbf{C}_{Ar}$), 129.3 ($\mathbf{C}_{Ph}H$), 129.0 ($\mathbf{C}_{FmocAr}H$), 128.9 ($\mathbf{C}_{FmocAr}H$), 128.3 ($\mathbf{C}_{FmocAr}H$), 126.6 ($\mathbf{C}_{FmocAr}H$), 126.4 ($\mathbf{C}_{FmocAr}H$), 122.6 ($\mathbf{C}_{BODIPY}H$), 121.1 ($\mathbf{C}_{FmocAr}H$), 119.5 ($\mathbf{C}_{Ar}H$), 68.1 ($\mathbf{C}_{Fmoc}H_2$), 57.2 (NH$\mathbf{C}$$HCH_2$), 52.8 (COO$\mathbf{C}H_3$), 48.5 ($\mathbf{C}_{Fmoc}H$), 38.0 (NHCH$\mathbf{C}H_2$), 15.1 ($C_{BODIPY}\mathbf{C}H_3$), 14.8 + 14.7 ($C_{BODIPY}\mathbf{C}H_3$);
^{19}F NMR(470 MHz, CD3OH) δF: -150.1 (1F, q, J = 25.2 Hz, B$\mathbf{F}$);
LRMS *m/z* (ESI$^+$): 708 (82% $[M - F]^+$), 812 (100%);
HRMS *m/z* (ESI$^+$): Found 722.3180 $[M + H]^+$ ($C_{44}H_{42}BFN_3O_5^+$ requires 722.3196 $[M + H]^+$);
IR (ν_{max} cm^{-1}): 3336 (w), 3062 (w), 2951 (w), 1701 (s, C=O), 1611 (w), 1544 (m, Ar C-C), 1509 (s, Ar C-C), 1470 (w), 1443 (m), 1405 (w), 1349 (w), 1293 (w), 1247 (m, C-N), 1214 (s, C-O), 1182 (s, C-O), 1157 (m, C-O), 1106 (w), 1052 (m), 980 (m), 872 (w), 829 (w), 738 (s), 643 (w), 619 (w).

4-((5-Fluoro-1,3,7,9-tetramethyl-10-phenyl-5*H*-4λ4,5λ4-dipyrrolo[1,2-c:2',1'-f][1,3,2]diazaborinin-5-yl)oxy)benzaldehyde and 4,4'-((1,3,7,9-tetramethyl-10-phenyl-5*H*-4λ4,5λ4-dipyrrolo[1,2-c:2',1'-f][1,3,2]diazaborinine-5,5-diyl)-bis-(oxy))dibenzaldehyde



239 **240**

5,5-Difluoro-1,3,7,9-tetramethyl-10-phenyl-5*H*-4**λ**4,5**λ**4-dipyrrolo[1,2-c:2',1'-f][1,3,2]diazaborinine (**238**) (250 mg, 0.77 mmol, 1.00 eq) and $AlCl_3$ (50.7 mg, 0.38 mmol, 0.50 eq) were dissolved in anhydrous CH_2Cl_2 (20.0 mL) and stirred under reflux for 10 min. Heating was stopped, 4-hydroxybenzaldehyde (100 mg, 0.81 mmol, 1.05 eq) was added and the reaction mixture was stirred under reflux for 0.5 h (a larger excess of 4-hydroxybenzaldehyde and longer reactions times favoured the formation of the disubstituted adduct). Heating was stopped and the reaction mixture was allowed to cool to RT. The solvent was removed under reduced pressure and the obtained crude residue was purified by silica gel flash column chromatography, eluting with petroleum ether:Et_2O = 8:2, to afford 4-((5-fluoro-1,3,7,9-tetramethyl-10-phenyl-5*H*-4**λ**4,5**λ**4-dipyrrolo[1,2-c:2',1'-f][1,3,2]diazaborinin-5-yl)oxy)benzaldehyde (**239**) as a bright orange solid (112 mg, 35%), and 4,4'-((1,3,7,9-tetramethyl-10-phenyl-5*H*-4**λ**4,5**λ**4-dipyrrolo[1,2-c:2',1'-f][1,3,2]diazaborinine-5,5-diyl)bis(oxy))dibenzaldehyde (**240**) as a bright orange solid (78.2 mg, 19%).

i) Data for 4-((5-fluoro-1,3,7,9-tetramethyl-10-phenyl-5*H*-4**λ**4,5**λ**4-dipyrrolo[1,2-c:2',1'-f][1,3,2]diazaborinin-5-yl)oxy)benzaldehyde (**239**):
R_f: 0.26 (Petroleum ether:Et_2O = 7:3);
m.p.: 161 - 163 °C (Petroleum ether/Et_2O);
UV λ_{max}/nm (ϵ/$M^{-1}cm^{-1}$): 500 (44810) [MeOH];

^{1}H NMR (400 MHz, $CDCl_3$) δH: 9.79 (1H, s, CO**H**), 7.70 - 7.65 (2H, m, C_{Ar}**H**) 7.59 - 7.49 (3H, m, C_{Ph}**H**, C_{Ph}**H**), 7.37 - 7.32 (1H, m, C_{Ph}**H**), 7.32 - 7.28 (1H, m, C_{Ph}**H**), 6.73 - 6.67 (2H, m, C_{Ar}**H**), 5.96 (2H, s, $C_{BODIPYAr}$**H**), 2.50 (6H, s, C**H**$_3$), 1.41 (6H, s, C**H**$_3$);
^{13}C NMR (100 MHz, $CDCl_3$) δC: 191.0 (**C**O), 162.4 (**C**$_{Ar}$), 156.0 (**C**$_{BODIPYAr}$C$_{Ph}$), 143.7 (N**C**$_{BODIPYAr}$CH$_3$), 141.9 (N**C**$_{BODIPYAr}$), 134.7 (NC**C**$_{BODIPYAr}$CH$_3$), 132.0 (**C**$_{Ar}$H), 131.6 (**C**$_{Ph}$), 129.3 (**C**$_{Ph}$H), 129.2 (**C**$_{Ph}$H), 128.9 (**C**$_{Ar}$), 127.9 (**C**$_{Ph}$H), 121.8 (NC**C**$_{BODIPYAr}$H), 118.2 (**C**$_{Ar}$H), 14.8 (**C**H$_3$), 14.5 (**C**H$_3$);
^{19}F NMR(377 MHz, $CDCl_3$) δF: -148.2 (1F, q, J = 25.8 Hz, B**F**);
LRMS m/z (ESI^-): 425 (62% [M - H]$^-$);
HRMS *m/z* (ESI^+): Found 425.18571 [M - H]$^-$($C_{26}H_{23}BFN_2O_2^-$ requires 425.18421 [M - H]$^-$);
IR (ν_{max} cm^{-1}): 1691 (m, C=O), 1599 (m, Ar C-C), 1570 (w), 1542 (m, Ar C-C), 1504 (w), 1467 (w), 1439 (w), 1404 (w), 1368 (w), 1298 (m, C-N), 1249 (w), 1189 (s, C-O), 1155 (s), 1063 (w), 1024 (m), 971 (s), 834 (m), 810 (m), 760 (w), 723 (s), 651 (w), 624 (w).

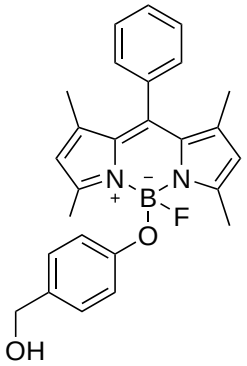
Data are concordant with literature values.[71]

ii) Data for 4,4'-((1,3,7,9-tetramethyl-10-phenyl-5*H*-4λ4,5λ4-dipyrrolo[1,2-c:2',1'-f][1,3,2]diazaborinine-5,5-diyl)bis(oxy))dibenzaldehyde (**240**)

R$_f$: 0.06 (Petroleum ether:Et_2O = 8:2);
m.p.: 238 - 240 °C (Petroleum ether/Et_2O);
UV λ_{max}/nm (ϵ/M^{-1}cm^{-1}): 500 (29800) [MeOH];
^{1}H NMR (400 MHz, $CDCl_3$) δH: 9.81 (2H, s, CO**H**), 7.72 - 7.67 (4H, m, C_{Ar}**H**), 7.62 - 7.53 (3H, m, C_{Ph}**H**), 7.32 (2H, dd, J = 7.7, 1.6 Hz, C_{Ph}**H**), 6.81 - 6.76 (4H, m, C_{Ar}**H**), 5.93 (2H, s, C_{BODIPY}**H**), 2.48 (6H, s, C**H**$_3$), 1.43 (6H, s, C**H**$_3$);
^{13}C NMR (100 MHz, $CDCl_3$) δC: 191.1 (**C**OH), 162.3 (O**C**$_{Ar}$), 156.5 (**C**$_{BODIPY}$), 144.3 (**C**$_{BODIPY}$), 144.2 (**C**$_{BODIPY}$), 134.3 (**C**$_{BODIPY}$), 131.9 (**C**$_{Ar}$H), 129.5 (**C**$_{Ph}$H), 129.4 (**C**$_{Ph}$), 129.2 (**C**$_{Ph}$H), 129.1 (**C**$_{Ar}$), 127.8 (**C**$_{Ph}$H), 122.4 (**C**$_{BODIPY}$H), 118.6 (**C**$_{Ar}$H), 15.0 (**C**H$_3$), 14.6 (**C**H$_3$);
LRMS *m/z* (ESI^+): 529 (10% [M + H]$^+$), 583 (100% [M + MeOH + Na]$^+$);
HRMS *m/z* (ESI^+): Found 551.2116 [M + Na]$^+$ ($C_{33}H_{29}BN_2NaO_4^+$ requires 551.2113 [M + Na]$^+$);
IR (ν_{max} cm^{-1}): 2962 (w), 2924 (w), 2818 (w), 2729 (w), 1691 (m, C=O), 1595 (m, Ar C-C), 1542 (m), 1501 (s), 1467 (m, Ar C-C), 1402 (w), 1365 (w), 1297 (m), 1267

(s, C-N), 1212 (w), 1182 (m), 1153 (s, C-O), 1109 (w), 1075 (w), 1042 (m), 1003 (s), 973 (s), 873 (w), 831 (m), 771 (m), 714 (m), 634 (w).

(4-((5-Fluoro-1,3,7,9-tetramethyl-10-phenyl-5*H*-4λ4,5λ4-dipyrrolo[1,2-c:2',1'-f][1,3,2]diazaborinin-5-yl)oxy)phenyl)methanol



241

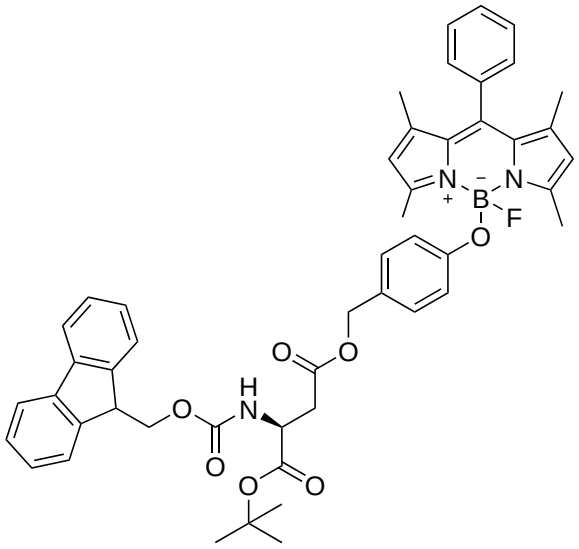
4-((5-Fluoro-1,3,7,9-tetramethyl-10-phenyl-5*H*-4$\boldsymbol{\lambda}$4,5$\boldsymbol{\lambda}$4-dipyrrolo[1,2-c:2',1'-f][1,3,2]diazaborinin-5-yl)oxy)benzaldehyde (**239**) (250 mg, 0.59 mmol, 1.00 eq) was dissolved in MeOH (25.0 mL) and $NaBH_4$ (22.3 mg, 0.59 mmol, 1.00 eq) was added. The reaction mixture was stirred at RT for 2 h. Additional $NaBH_4$ (11.2 g, 0.30 mmol, 0.50 eq) was added and the reaction mixture was stirred at RT for 0.5 h, after which time the reaction was adjudged to be complete by TLC analysis. The reaction was quenched with acetone and the solvent was removed under reduced pressure. The obtained crude residue was purified by silica gel flash column chromatography, eluting with $CHCl_3$, to afford (4-((5-fluoro-1,3,7,9-tetramethyl-10-phenyl-5*H*-4$\boldsymbol{\lambda}$4,5$\boldsymbol{\lambda}$4-dipyrrolo[1,2-c:2',1'-f][1,3,2]diazaborinin-5-yl)oxy)phenyl)methanol (**241**) as a bright orange solid (198 mg, 77%).

R_f: 0.45 ($CHCl_3$:Acetone = 9:1);
m.p.: 162 - 164 °C (Hexane/Acetone);
UV λ_{max}/nm (ϵ/$M^{-1}cm^{-1}$): 500 (54590) [MeOH];
^{1}H NMR (400 MHz, $CDCl_3$) **δ**H: 7.56 - 7.47 (3H, m, C_{Ph}**H**, C_{Ph}**H**), 7.36 - 7.31 (1H, m, C_{Ph}**H**), 7.28 - 7.24 (1H, m, C_{Ph}**H**), 7.14 - 7.09 (2H, m, C_{Ar}**H**), 6.60 - 6.55 (2H, m, C_{Ar}**H**), 5.93 (2H, s, $C_{BODIPY\,Ar}$**H**), 4.54 (2H, s, $C_{Ar}C$**H**$_2$OH), 2.52 (6H, s, C**H**$_3$), 1.39 (6H, s, C**H**$_3$);
^{13}C NMR (100 MHz, $CDCl_3$) **δ**C: 155.9 (**C**$_{Ar}$), 155.9 (**C**$_{BODIPY}$), 143.2 (**C**$_{BODIPY}$), 141.7 (**C**$_{BODIPY}$), 135.0 (**C**$_{BODIPY}$), 131.8 (**C**$_{Ph}$), 131.7 (**C**$_{Ar}$), 129.2 (**C**$_{Ph}$H), 129.0 (**C**$_{Ph}$H), 128.6 (**C**$_{Ar}$H), 128.0 (**C**$_{Ph}$H), 121.6 (**C**$_{BODIPY}$H), 118.0 (**C**$_{Ar}$H), 65.3 (**C**H$_2$OH), 14.9 (**C**H$_3$), 14.4 (**C**H$_3$);

^{19}F NMR(377 MHz, $CDCl_3$) δF: -148.4 (1F, q, J = 25.9 Hz,B**F**);
LRMS *m/z* (ESI$^+$): 305 (100%), 408 (20% [M - F]$^+$), 451 (27% [M + Na]$^+$);
HRMS *m/z* (ESI$^+$): Found 451.1964 [M + Na]$^+$ ($C_{26}H_{26}BFN_2NaO_2^+$ requires 451.1964 [M + Na]$^+$);
IR (ν_{max} cm^{-1}): 2964 (w), 2363 (m), 2164 (w), 1980 (w), 1726 (m), 1616 (w), 1551 (m, Ar C-C), 1509 (m, Ar C-C), 1468 (w), 1407 (w), 1368 (w), 1303 (m, C-N), 1252 (w), 1188 (s, C-O), 1154 (s, C-O), 1067 (m), 1028 (m), 975 (w), 826 (m), 720 (m), 625 (w).

Data are concordant with literature values.[71]

1-(*tert*-Butyl) 4-(4-((5-fluoro-1,3,7,9-tetramethyl-10-phenyl-5*H*-4λ4,5λ4-dipyrrolo[1,2-c:2',1'-f][1,3,2]diazaborinin-5-yl)oxy)benzyl)(((9*H*-fluoren-9-yl)methoxy)carbonyl-*L*-aspartate



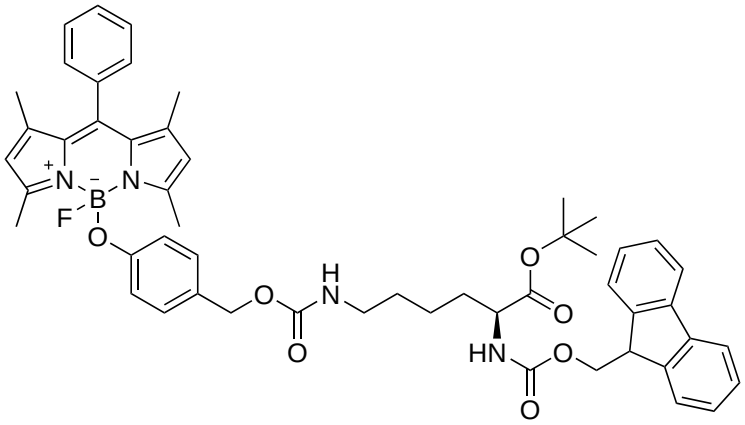
242

Fmoc-Asp-O^{t}Bu (**221**) (24.7 mg, 0.06 mmol, 1.00 eq) and (benzotriazol-1-yloxy)tripyrrolidinophosphonium hexafluorophosphate (31.2 mg, 0.06 mmol, 1.10 eq) were dissolved in anhydrous CH_2Cl_2 (2.50 mL). *N*,*N*-Diisopropylethylamine (15.5 mg, 0.02 mL, 0.12 mmol, 2.00 eq) was added dropwise and the reaction solution was stirred at RT under an Ar atmosphere for 1 h. (4-((5-Fluoro-1,3,7,9-tetramethyl-10-phenyl-5*H*-4λ4,5λ4-dipyrrolo[1,2-c:2',1'-f][1,3,2]diazaborinin-5-yl)oxy)phenyl)methanol (**241**) (25.0 mg, 0.06 mmol, 1.00 eq) was added and the reaction solution was stirred at RT under an Ar atmosphere for 18 h, after which time the reaction was adjudged to be complete by TLC analysis. The reaction was quenched with CH_2Cl_2 (5.00 mL) and the solvent was removed under reduced pressure. The crude residue was subjected to two successive purifications by silica gel flash column chromatography, eluting with $CHCl_3$:Acetone = 95:5 then petroleum ether:Et_2O = 6:4 - 1:1, to afford 1-(*tert*-butyl) 4-(4-((5-fluoro-1,3,7,9-tetramethyl-10-phenyl-5*H*-4λ4,5λ4-dipyrrolo[1,2-c:2',1'-f][1,3,2]diazaborinin-5-yl)oxy)benzyl)(((9*H*-fluoren-9-yl)methoxy)carbonyl)-*L*-aspartate (**242**) as a bright orange solid (40.2 g, 84%).

R_f: 0.62 ($CHCl_3$:Acetone = 9:1);
m.p.: 77 - 79 °C (Hexane/Acetone);
$[\alpha]_D^{26}$: +23.4 (***c*** 0.2 in $CHCl_3$);

UV λ_{max}/nm (ϵ/$M^{-1}cm^{-1}$): 500 (74120) [MeOH];
^{1}H NMR (400 MHz, $(CD_3)_2SO$) δH: 7.89 (2H, d, J = 7.6 Hz, C_{FmocAr}**H**), 7.74 (1H, d, J = 8.4 Hz, N**H**CHCH_2), 7.69 (2H, d, J = 7.4 Hz, C_{FmocAr}**H**), 7.61 - 7.52 (3H, m, C_{Ph}**H**, C_{Ph}**H**), 7.44 - 7.38 (1H, m, C_{Ph}**H**), 7.41 (2H, t, J = 7.6 Hz, C_{FmocAr}**H**), 7.31 (2H, t, J = 7.4 Hz, C_{FmocAr}**H**), 7.29 - 7.26 (1H, m, C_{Ph}**H**), 7.10 (2H, d, J = 8.6 Hz, C_{Ar}**H**), 6.42 (2H, d, J = 8.6 Hz, C_{Ar}**H**), 6.10 (2H, s, C_{BODIPY}**H**), 4.92 (2H, s, C_{Ar}C**H**$_2$O), 4.35 - 4.25 (3H, m, NHC**H**CH_2, C_{Fmoc}**H**$_2$), 4.21 (1H, t, J = 6.9 Hz, C_{Fmoc}**H**), 2.76 (1H, dd, J = 16.2, 6.0 Hz, NHCHC**H**$_A$H$_B$), 2.64 (1H, dd, J = 16.2, 7.7 Hz, NHCHCH_A**H**$_B$), 2.40 (6H, s, $C_{Pyrrole}$C**H**$_3$), 1.32 (6H, s, $C_{Pyrrole}$C**H**$_3$), 1.31 (9H, s, OC(C**H**$_3$)$_3$);
^{13}C NMR (100 MHz, $(CD_3)_2SO$) δC: 169.9 (**C**O), 169.9 (**C**O), 156.1 (**C**$_{Ar}$O), 156.0 (**C**$_{Ar}$O), 155.8 (**C**O), 155.2 (**C**$_{BODIPY}$), 143.7 (**C**$_{FmocAr}$), 142.7 (**C**$_{BODIPY}$), 141.9 (**C**$_{BODIPY}$), 140.7 (**C**$_{FmocAr}$), 134.0 (**C**$_{BODIPY}$), 131.1 (**C**$_{Ph}$), 129.9 (**C**$_{Ar}$H), 129.4 (**C**$_{Ph}$H), 129.3 (**C**$_{Ph}$H), 127.7 (**C**$_{Ph}$H), 127.6 (**C**$_{FmocAr}$H), 127.1 (**C**$_{FmocAr}$H), 126.6 (**C**$_{Ar}$), 125.2 (**C**$_{FmocAr}$H), 121.6 (**C**$_{BODIPY}$H), 120.1 (**C**$_{FmocAr}$H), 117.3 (**C**$_{Ar}$H), 81.04 (O**C**$(CH_3)_3$), 65.8 (C_{Ar}**C**H_2O), 65.7 (**C**$_{Fmoc}H_2$), 51.0 (NH**C**HCH_2), 46.6 (**C**$_{Fmoc}$H), 36.0 (NHCH**C**H_2), 27.4 (OC(**C**$H_3)_3$), 14.4 (C_{BODIPY}**C**H_3), 14.0 (C_{BODIPY}**C**H_3);
^{19}F NMR(470 MHz, $(CD_3)_2SO$) δF: -146.42 (1F, q, J = 26.8 Hz, B**F**);
LRMS *m/z* (ESI$^+$): 822 (68% $[M + H]^+$), 844 (100% $[M + Na]^+$);
HRMS *m/z* (ESI$^+$): Found 822.3746 $[M + H]^+$ ($C_{49}H_{50}BFN_3O_7^+$ requires 822.3720 $[M + H]^+$);
IR (ν_{max} cm^{-1}): 2976 (w), 2362 (w), 1730 (m, C=O), 1613 (w), 1546 (s, Ar C-C), 1511 (s, Ar C-C), 1470 (w), 1450 (w), 1408 (w), 1369 (w), 1303 (m, C-N), 1278 (w), 1254 (w), 1219 (w), 1189 (s, C-O), 1156 (s, C-O), 1044 (m), 982 (m), 842 (w), 759 (m), 743 (m), 722 (m), 637 (w).

***tert*-Butyl N^2-(((9*H*-fluoren-9-yl)methoxy)carbonyl)-N^6-(((4-((5-fluoro-1,3,7,9-tetramethyl-10-phenyl-5*H*-4λ4,5λ4-dipyrrolo[1,2-c:2',1'-f][1,3,2]diazaborinin-5-yl)oxy)benzyl)oxy)carbonyl)-*L*-lysinate**



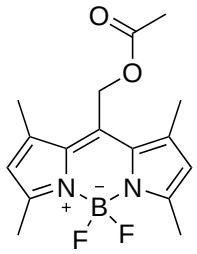
243

4-Nitrophenyl chloroformate (36.3 g, 0.18 mmol, 1.50 eq) was dissolved in anhydrous CH_2Cl_2 (5.00 mL). To this solution was added *N*-methyl morpholine (18.2 mg, 0.02 mL, 0.18 mmol, 1.50 eq) dropwise. The reaction solution was cooled to 0 °C and a solution of (4-((5-fluoro-1,3,7,9-tetramethyl-10-phenyl-5*H*-4l4,5l4-dipyrrolo[1,2-c:2',1'-f][1,3,2]diazaborinin-5-yl)oxy)phenyl)methanol (**241**) (0.050 g, 0.12 mmol, 1.0 eq) in anhydrous CH_2Cl_2 (5.00 mL) was added dropwise. The reaction solution was allowed to warm to RT and stirred under an Ar atmosphere for 3 h. *tert*-Butyl (((9*H*-fluoren-9-yl)methoxy)carbonyl)-*L*-lysinate (**187**) (51.0 mg, 0.12 mmol, 1.00 eq) was added as a solution in CH_2Cl_2 (0.60 mL), followed immediately by the addition of 4-(dimethylamino)pyridine (14.7 mg, 0.12 mmol, 1.00 eq). The reaction solution was stirred under an Ar atmosphere for 18 h, after which time the reaction was adjudged to be complete by TLC analysis. The reaction was quenched with CH_2Cl_2 (10.0 mL) and the solvent was removed under reduced pressure. The crude residue was purified by silica gel flash column chromatography, eluting with CH_2Cl_2:Acetone = 98:2 - 90:10, to afford *tert*-butyl N^2-(((9*H*-fluoren-9-yl)methoxy)carbonyl)-N^6-(((4-((5-fluoro-1,3,7,9-tetramethyl-10-phenyl-5*H*-4**λ**4,5**λ**4-dipyrrolo[1,2-c:2',1'-f][1,3,2]diazaborinin-5-yl)oxy)-benzyl)oxy)carbonyl)-*L*-lysinate (**243**) as an orange solid (15.4 mg, 14%).

R_f: 0.73 (CH_2Cl_2:Et_2O = 8:2);
m.p.: 81 - 83 °C (Hexane/Acetone);
$[\alpha]_D^{26}$: +8.7 (***c*** 0.5 in $CHCl_3$);

UV λ_{max}/nm (ϵ/M^{-1}cm^{-1}): 500 (89120) [MeOH];
^{1}H NMR (400 MHz, $CDCl_3$) δH: 7.77 (2H, d, J = 7.5 Hz, C_{FmocAr}**H**), 7.61 (2H, d, J = 7.5 Hz, C_{FmocAr}**H**), 7.54 - 7.49 (3H, m, C_{Ph}**H**, C_{Ph}**H**), 7.40 (2H, t, J = 7.5 Hz, C_{FmocAr}**H**), 7.37 - 7.33 (1H, m, C_{Ph}**H**), 7.31 (2H, t, J = 7.5 Hz, C_{FmocAr}**H**), 7.28 - 7.24 (1H, m, C_{Ph}**H**), 7.08 (2H, d, J = 8.4 Hz, C_{Ar}**H**), 6.51 (2H, d, J = 8.4 Hz, C_{Ar}**H**), 5.95 (2H, s, C_{BODIPY}**H**), 5.36 (1H, d, J = 7.8 Hz, N**H**$CHCH_2$), 4.89 (2H, s, C**H**$_2$OCO), 4.77 (1H, t, J = 7.0 Hz, N**H**CH_2CH_2), 4.37 (2H, d, J = 6.9 Hz, C_{Fmoc}**H**$_2$), 4.21 (1H, t, J = 6.9 Hz, C_{Fmoc}**H**), 4.17 (1H, ddd, J = 8.0, 7.8, 5.0 Hz, NHC**H**CH_2), 3.13 (2H, dt, J = 7.0, 6.5 Hz, NHC**H**$_2CH_2$), 2.46 (6H, s, C**H**$_3$), 1.84 - 1.74 (1H, m, NHCHC**H**$_A$H$_B$$CH_2$), 1.69 - 1.60 (1H, m, NHCHCH_A**H**$_B$$CH_2$), 1.54 - 1.47 (2H, m, $NHCH_2$C**H**$_2$), 1.44 (9H, s, OC(C**H**$_3$)$_3$), 1.39 (6H, s, C**H**$_3$), 1.37 - 1.29 (2H, m, $NHCHCH_2$C**H**$_2$);
^{13}C NMR (100 MHz, $CDCl_3$) δC: 172.1 (**C**O), 157.1 (O**C**ONH), 157.0 (O**C**ONH), 156.4 (C_{Ph}), 156.3 (OC_{Ar}), 144.5 (C_{FmocAr}), 144.1 (C_{BODIPY}), 142.7 (C_{FmocAr}), 141.8 (C_{BODIPY}), 135.4 (C_{BODIPY}), 132.2 (C_{BODIPY}), 130.3 (C_{Ar}H), 129.8 (C_{Ph}H), 129.7 (C_{Ph}H), 129.6 (C_{Ph}H), 128.6 (C_{Ph}H), 128.6 (C_{Ph}H), 128.3 ($C_{Ar}CH_2O$), 128.2 (C_{FmocAr}H), 127.6 (C_{FmocAr}H), 125.6 (C_{FmocAr}H), 122.0 (C_{BODIPY}H), 120.5 (C_{FmocAr}H), 118.3 (C_{Ar}H), 82.4 (O**C**$(CH_3)_3$), 67.2 ($C_{Fmoc}H_2$), 67.0 (**C**H_2O), 54.8 (NH**C**HCH_2), 47.8 (C_{Fmoc}H), 41.1 (NH**C**H_2CH_2), 32.8 (NHCH**C**H_2CH_2), 30.0 ($NHCH_2$**C**H_2), 28.3 (OC(**C**$H_3)_3$), 22.8 ($NHCHCH_2$**C**H_2), 15.1 (C_{BODIPY}**C**H_3), 14.8 (C_{BODIPY}**C**H_3);
^{19}F NMR (377 MHz, CD_2Cl_2) δF: -148.7 (1F, q, J = 25.5 Hz, B**F**);
LRMS m/z (ESI$^+$): 901 (100% $[M + Na]^+$);
HRMS m/z (ESI$^+$): Found 901.4126 $[M + Na]^+$ ($C_{52}H_{56}BFN_4NaO_7^+$ requires 901.4118 $[M + Na]^+$);
IR (ν_{max} cm^{-1}): 3332 (w), 2932 (w), 2363 (w), 1714 (m, C=O), 1611 (w), 1544 (s, Ar C-C), 1509 (s, Ar C-C), 1467 (w), 1447 (w), 1405 (w), 1366 (w), 1301 (w, C-N), 1249 (w), 1186 (m, C-O), 1155 (m, C-O), 1106 (w), 1043 (m), 977 (s), 834 (w), 805 (w), 720 (s), 641 (w).

(5,5-Difluoro-1,3,7,9-tetramethyl-5*H*-4λ4,5λ4-dipyrrolo[1,2-c:2',1'-f][1,3,2]diazaborinin-10-yl)methyl acetate



249

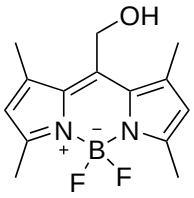
A solution of 2,4-dimethyl pyrrole (**236**) (500 mg, 0.54 mL, 5.26 mmol, 2.00 eq) and acetoxyacetyl chloride (431 mg, 0.34 mL, 3.16 mmol, 1.20 eq) in anhydrous CH_2Cl_2 (100 mL) was stirred at RT under an Ar atmosphere for 18 h. The reaction solution was cooled to 0 °C and NEt_3 (2.02 g, 2.78 mL, 20.0 mmol, 3.80 eq) and $BF_3{\cdot}OEt_2$ (3.19 g, 2.78 mL, 22.5 mmol, 4.30 eq) were added dropwise. The reaction solution was stirred at RT under an Ar atmosphere for 18 h, after which time the reaction was adjudged to be complete by TLC analysis. The reaction was quenched with CH_2Cl_2 (50.0 mL) and washed with H_2O (200 mL). The solvent was removed under reduced pressure and the obtained crude residue was purified by neutral alumina gel flash column chromatography, eluting with petroleum ether:Et_2O = 1:1, to afford (5,5-difluoro-1,3,7,9-tetramethyl-5*H*-4**λ**4,5**λ**4-dipyrrolo[1,2-c:2',1'-f][1,3,2]diazaborinin-10-yl)methyl acetate (**249**) as a orange green solid (502 mg, 60%).

R_f: 0.54 (CH_2Cl_2:Et_2O = 8:2);
m.p.: 196 - 198 °C (CH_2Cl_2);
UV λ_{max}/nm (ϵ/$M^{-1}cm^{-1}$): 515 (39680) [MeOH];
^{1}H NMR (400 MHz, $CDCl_3$) **δ**H: 6.09 (2H, s, C_{BODIPY}**H**), 5.30 (2H, s, C**H_2**O), 2.53 (6H, s, C_{BODIPY}C**H_3**), 2.36 (6H, s, C_{BODIPY}C**H_3**), 2.14 (3H, s, OCOC**H_3**);
^{13}C NMR (100 MHz, $CDCl_3$) **δ**C: 170.5 (O**C**O), 156.6 (**C_{BODIPY}**), 141.5 (**C_{BODIPY}**), 133.3 (**C_{BODIPY}**), 132.6 (**C_{BODIPY}**), 122.3 (C_{BODIPY}H), 57.8 (**C**H_2O), 20.6 (OCO**C**H_3), 15.6 (C_{BODIPY}**C**H_3), 14.7 (C_{BODIPY}**C**H_3);
^{19}F NMR(377 MHz, $CDCl_3$) **δ**F: -146.2 (2F, q, J = 32.9 Hz, B**F_2**);
LRMS *m/z* (ESI^+): 301 (100% $[M - F]^+$), 321 (49% $[M + H]^+$);
HRMS *m/z* (ESI^+): Found 343.1403 $[M + Na]^+$ ($C_{16}H_{19}BF_2N_2NaO_2^+$ requires 343.1400 $[M + Na]^+$);

IR (ν_{max} cm^{-1}): 2927 (w), 1734 (s, C=O), 1554 (m, Ar C-C), 1508 (m, Ar C-C), 1468 (w), 1431 (w), 1402 (m), 1370 (m), 1310 (m, C-N), 1217 (s, C-O), 1156 (m), 1078 (m), 1021 (m), 970 (s), 913 (w), 834 (m), 809 (m), 716 (m).

Data are concordant with literature values.[231]

(5,5-Difluoro-1,3,7,9-tetramethyl-5*H*-4λ4,5λ4-dipyrrolo[1,2-c:2',1'-f][1,3,2]diazaborinin-10-yl)methanol



250

Method A:
To a solution of (5,5-difluoro-1,3,7,9-tetramethyl-5*H*-4λ4,5λ4-dipyrrolo[1,2-c:2',1'-f][1,3,2]diazaborinin-10-yl)methyl acetate (**249**) (200 mg, 0.62 mmol, 1.00 eq) in a mixture of CH_2Cl_2:MeOH (1:2, 15.00 mL) was added 0.2 M aq. NaOH (1.22 mL, 0.24 mmol, 0.40 eq) and the reaction solution was stirred at RT for 2 h. Additional 2.0 M aq. NaOH (1.00 mL, 0.20 mmol, 0.32 eq) was added and the reaction solution was stirred at RT for 0.5 h, after which time the reaction was adjudged to be complete by TLC analysis. The solvent was removed under reduced pressure and the obtained crude residue was purified by silica gel flash column chromatography, eluting with CH_2Cl_2:petroleum ether = 8:2 to CH_2Cl_2 to CH_2Cl_2:Et_2O = 9:1, to afford (5,5-difluoro-1,3,7,9-tetramethyl-5*H*-4λ4,5λ4-dipyrrolo[1,2-c:2',1'-f][1,3,2]diazaborinin-10-yl)methanol (**250**) as an orange solid (18.4 mg, 11%).

Method B:
(5,5-Difluoro-1,3,7,9-tetramethyl-5*H*-4λ4,5λ4-dipyrrolo[1,2-c:2',1'-f][1,3,2]diazaborinin-10-yl)methyl acetate (**249**) (250 mg, 0.78 mmol, 1.00 eq) was dissolved in CH_2Cl_2 (5.00 mL). The solution was cooled to 0 °C and 0.2 M NaOMe (54.2 mg, 0.78 mmol,1.0 eq) in MeOH (5.00 mL) was added. The reaction solution was stirred at 0 °C for 2 h. Additional 0.2 M NaOMe (27.1 mg, 0.39 mmol, 0.50 eq) in MeOH (2.50 mL) was added and the reaction solution was stirred at 0 °C for a further 2 h, after which time the reaction was adjudged to be complete by TLC analysis. The reaction solution was neutralised with Amberlite ® IR120 Hydrogen form Dowex resin and filtered through a cotton plug. The solvent was removed under reduced pressure and the obtained crude residue was purified by silica gel flash column chromatography, eluting with CH_2Cl_2 to CH_2Cl_2:Et_2O = 9:1, to afford (5,5-difluoro-1,3,7,9-tetramethyl-5*H*-4λ4,5λ4-dipyrrolo[1,2-c:2',1'-f][1,3,2]diazaborinin-10-yl)methanol (**250**) as an orange solid (94.0 mg, 43%).

Method C:
(5,5-Difluoro-1,3,7,9-tetramethyl-5*H*-4$\boldsymbol{\lambda}$4,5$\boldsymbol{\lambda}$4-dipyrrolo[1,2-c:2',1'-f][1,3,2]diazaborinin-10-yl)methyl acetate (**249**) (100 mg, 0.31 mmol, 1.00 eq) was dissolved in MeOH (5.00 mL). K_2CO_3 (44.2 mg, 0.32 mmol, 1.05 eq) was added and the reaction stirred at RT for 1 h. Additional K_2CO_3 (22.1 mg, 0.16 mmol, 0.50 eq) was added and the reaction mixture was stirred at RT for 0.5 h, after which time the reaction was adjudged to be complete by TLC analysis. The solvent was removed under reduced pressure and the obtained crude residue was purified by silica gel flash column chromatography, eluting with CH_2Cl_2:petroleum ether = 8:2 to CH_2Cl_2 to CH_2Cl_2:Et_2O = 9:1, to afford (5,5-difluoro-1,3,7,9-tetramethyl-5*H*-4$\boldsymbol{\lambda}$4,5$\boldsymbol{\lambda}$4-dipyrrolo[1,2-c:2',1'-f][1,3,2]diazaborinin-10-yl)methanol (**250**) as an orange solid (30.2 mg, 39%).

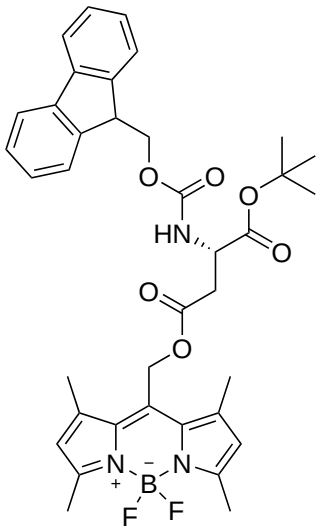
Method D:
(5,5-Difluoro-1,3,7,9-tetramethyl-5*H*-4$\boldsymbol{\lambda}$4,5$\boldsymbol{\lambda}$4-dipyrrolo[1,2-c:2',1'-f][1,3,2]diazaborinin-10-yl)methyl acetate (**249**) (300 mg, 0.94 mmol, 1.00 eq) was dissolved in MeOH (30.0 mL). The solution was cooled to 0 °C and K_2CO_3 (155 mg, 1.12 mmol, 1.20 eq) was added. The reaction mixture was stirred at 0 °C for 1 h, after which time the reaction was adjudged to be complete by TLC analysis. The reaction mixture was then neutralised with Amberlite ® IR120 Hydrogen form Dowex resin and filtered through a cotton plug. The solvent was removed under reduced pressure and the obtained crude residue was purified by silica gel flash column chromatography, eluting with CH_2Cl_2 to CH_2Cl_2:Et_2O = 95:5 - 9:1 - 8:2, to afford (5,5-difluoro-1,3,7,9-tetramethyl-5*H*-4$\boldsymbol{\lambda}$4,5$\boldsymbol{\lambda}$4-dipyrrolo[1,2-c:2',1'-f][1,3,2]diazaborinin-10-yl)methanol (**250**) as an orange solid (128 mg, 50%).

R_f: 0.46 ($CHCl_3$:Acetone = 9:1);
m.p.: 232 °C (CH_2Cl_2);
UV $\boldsymbol{\lambda_{max}}$/nm ($\boldsymbol{\epsilon}$/$\mathbf{M^{-1}cm^{-1}}$): 510 (15790) [MeOH];
^{1}H NMR (400 MHz, $(CD_3)_2SO$) $\boldsymbol{\delta}$H: 6.23 (2H, s, $C_{BODIPY}\mathbf{H}$), 5.55 (1H, t, J = 5.0 Hz, $CH_2O\mathbf{H}$), 4.70 (2H, d, J = 5.0 Hz, $C\mathbf{H}_2OH$), 2.48 (6H, s, $C_{BODIPY}C\mathbf{H}_3$), 2.41 (6H, s, $C_{BODIPY}C\mathbf{H}_3$);
^{13}C NMR (100 MHz, $(CD_3)_2SO$) $\boldsymbol{\delta}$C: 154.5 ($\mathbf{C}_{BODIPY}$), 142.1 ($\mathbf{C}_{BODIPY}$), 141.0 ($\mathbf{C}_{BODIPY}$), 131.8 ($\mathbf{C}_{BODIPY}$), 121.6 ($\mathbf{C}_{BODIPY}$H), 54.1 ($\mathbf{C}H_2OH$), 15.2 ($C_{BODIPY}\mathbf{C}H_3$), 14.2 ($C_{BODIPY}\mathbf{C}H_3$);
^{19}F NMR(377 MHz, $(CD_3)_2SO$) $\boldsymbol{\delta}$F: -143.9 (2F, q, J = 33.5 Hz, $B\mathbf{F}_2$);
LRMS m/z (ESI^-): 277 (100% $[M - H]^-$);

HRMS *m/z* (ESI$^+$): Found 277.1329 [M - H]$^-$($C_{14}H_{16}BF_2N_2O^-$ requires 277.1318 [M - H]$^-$);
IR (ν_{max} cm^{-1}): 3549 (m, O-H), 2361 (m), 2338 (w), 1554 (s, Ar C-C), 1507 (m, Ar C-C), 1474 (w), 1441 (w), 1406 (w), 1368 (w), 1305 (m, C-N), 1253 (w), 1198 (s, C-O), 1159 (s), 1126 (m), 1078 (w), 1034 (m), 967 (s), 842 (w), 812 (m), 718 (m), 666 (w), 632 (w).

Data are concordant with literature values.[231]

1-(*tert*-Butyl) 4-((5,5-difluoro-1,3,7,9-tetramethyl-5*H*-4λ4,5λ4-dipyrrolo[1,2-c:2',1'-f][1,3,2]diazaborinin-10-yl)methyl) (((9*H*-fluoren-9-yl)methoxy)carbonyl)-*L*-aspartate



251

Method A:
(5,5-Difluoro-1,3,7,9-tetramethyl-5*H*-4λ4,5λ4-dipyrrolo[1,2-c:2',1'-f][1,3,2]diazaborinin-10-yl)methanol (**250**) (40.0 mg, 0.14 mmol, 1.00 eq), Fmoc-Asp-O^{t}Bu (**221**) (60.0 mg, 0.14 mmol, 1.00 eq) and (benzotriazol-1-yloxy)tripyrrolidinophosphonium hexafluorophosphate (83.5 mg, 0.16 mmol, 1.10 eq) were dissolved in anhydrous CH_2Cl_2 (5.00 mL). *N*,*N*-Diisopropylethylamine (37.5 mg, 0.05 mL, 0.29 mmol, 2.00 eq) was added dropwise and the reaction solution was stirred at RT under an Ar atmosphere for 24 h, after which time the reaction was adjudged to be complete by TLC analysis. The reaction was quenched with CH_2Cl_2 (5.00 mL) and the solvent was removed under reduced pressure. The obtained crude residue was purified by silica gel flash column chromatography, eluting with CH_2Cl_2 to CH_2Cl_2:Et_2O = 9:1 - 8:2, to afford 1-(*tert*-butyl) 4-((5,5-difluoro-1,3,7,9-tetramethyl-5*H*-4λ4,5λ4-dipyrrolo[1,2-c:2',1'-f][1,3,2]diazaborinin-10-yl)methyl) (((9*H*-fluoren-9-yl)methoxy)carbonyl)-*L*-aspartate (**251**) as a pink solid (23.3 mg, 24%).

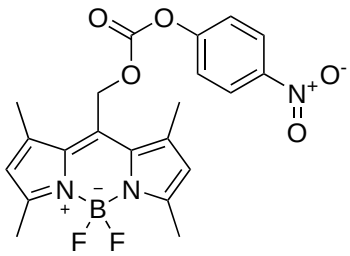
Method B:
Fmoc-Asp-O^{t}Bu (**221**) (300 mg, 0.72 mmol, 1.00 eq) was dissolved in anhydrous CH_2Cl_2 (10.0 mL). To this solution was added *N*,*N*'-dicyclohexylcarbodiimide (200 mg, 0.72 mmol, 1.00 eq) and 4-(dimethylamino)pyridine (36.7 mg, 0.30 mmol, 0.40

eq). The resulting solution was stirred at RT under an Ar atmosphere for 0.5 h. The solution was cooled to 0 °C and a solution of (5,5-difluoro-1,3,7,9-tetramethyl-5*H*-4$\boldsymbol{\lambda}$4,5$\boldsymbol{\lambda}$4-dipyrrolo[1,2-c:2',1'-f][1,3,2]diazaborinin-10-yl)methanol (**250**) (200 mg, 0.72 mmol, 1.00 eq) in CH_2Cl_2 (5.00 mL) was added dropwise. The reaction solution was allowed to warm to RT and stirred under an Ar atmosphere for 18 h, after which time the reaction was adjudged to be complete by TLC analysis. The reaction mixture was filtered to remove any insolubles prior to concentration of the solvent under reduced pressure. The crude residue was purified by silica gel flash column chromatography, eluting with CH_2Cl_2 to CH_2Cl_2:Et_2O = 9:1 - 8:2, to afford 1-(*tert*-butyl) 4-((5,5-difluoro-1,3,7,9-tetramethyl-5*H*-4$\boldsymbol{\lambda}$4,5$\boldsymbol{\lambda}$4-dipyrrolo[1,2-c:2',1'-f][1,3,2]diazaborinin-10-yl)methyl) (((9*H*-fluoren-9-yl)methoxy)carbonyl)-*L*-aspartate (**251**) as a pink solid (105 mg, 21%).

R_f: 0.56 (CH_2Cl_2:Acetone = 9:1);
m.p.: 73 - 75 °C (Petroleum ether/Et_2O);
$[\alpha]_D^{26}$: +58.4 (***c*** 0.1 in $CHCl_3$);
UV λ_{max}/nm (ϵ/$M^{-1}cm^{-1}$): 515 (62380) [MeOH];
^{1}H NMR (500 MHz, $(CD_3)_2SO$) **δ**H: 7.90 (2H, d, J = 7.5 Hz, C_{FmocAr}**H**), 7.79 (1H, d, J = 8.5 Hz, N**H**CHCH$_2$), 7.69 (2H, d, J = 6.9 Hz, C_{FmocAr}**H**), 7.42 (2H, t, J = 7.5 Hz, C_{FmocAr}**H**), 7.33 (2H, t, J = 6.9 Hz, C_{FmocAr}**H**), 6.25 (2H, s, C_{BODIPY}**H**), 5.30 (2H, s, C_{BODIPY}C**H**$_2$O), 4.34 (1H, dd, J = 9.8, 6.7 Hz, C_{Fmoc}**H**$_A$H$_B$), 4.32 (1H, ddd, J = 8.5, 8.3, 5.9 Hz, NHC**H**CH$_2$), 4.26 (1H, dd, J = 9.8, 6.7 Hz, C_{Fmoc}H$_A$**H**$_B$), 4.21 (1H, dd, J = 6.7, 6.7 Hz, C_{Fmoc}**H**), 2.91 (1H, dd, J = 16.3, 5.9 Hz, NHCHC**H**$_A$H$_B$), 2.74 (1H, dd, J = 16.3, 8.3 Hz, NHCHCH$_A$**H**$_B$), 2.42 (6H, s, C_{BODIPY}C**H**$_3$), 2.31 (6H, s, C_{BODIPY}C**H**$_3$), 1.34 (9H, s, OC(C**H**$_3$)$_3$);
^{13}C NMR (100 MHz, $(CD_3)_2SO$) **δ**C: 169.9 (**C**O), 169.8 (**C**O), 155.8 (**C**O), 155.8 (**C**$_{BODIPY}$), 143.7 (**C**$_{FmocAr}$), 142.1 (**C**$_{BODIPY}$), 140.7 (**C**$_{FmocAr}$), 133.9 (**C**$_{BODIPY}$), 131.9 (**C**$_{BODIPY}$), 127.6 (**C**$_{FmocAr}$H), 127.0 (**C**$_{FmocAr}$H), 125.2 (**C**$_{FmocAr}$H), 125.1 (**C**$_{FmocAr}$H), 122.3 (**C**$_{BODIPY}$H), 120.1 (**C**$_{FmocAr}$H), 81.2 (O**C**(CH$_3$)$_3$), 65.7 (**C**$_{Fmoc}$H$_2$), 57.7 (C_{BODIPY}**C**H$_2$O), 51.1 (NH**C**HCH$_2$), 46.6 (**C**$_{Fmoc}$H), 35.6 (NHCH**C**H$_2$), 27.4 (OC(**C**H$_3$)$_3$), 15.1 (C_{BODIPY}**C**H$_3$), 14.3 (C_{BODIPY}**C**H$_3$);
^{19}F NMR(470 MHz, $(CD_3)_2SO$) **δ**F: -143.8 (2F, q, J = 33.2 Hz, B**F**$_2$);
LRMS *m/z* (ESI^+): 694 (100% $[M + Na]^+$);
HRMS *m/z* (ESI^+): Found 694.2871 $[M + H]^+$ ($C_{37}H_{41}BF_2N_3O_6^+$ requires 694.2870 $[M + H]^+$);

IR (ν_{max} cm^{-1}): 2971 (w), 2363 (w), 1728 (s, C=O), 1559 (s, Ar C-C), 1510 (m, Ar C-C), 1448 (w), 1410 (w), 1369 (w), 1308 (m, C-N), 1225 (w), 1192 (s, C-O), 1153 (s, C-O), 1075 (m), 1029 (m), 977 (s), 840 (w), 740 (m), 719 (m); HPLC: 16.33 min (100%).

(5,5-Difluoro-1,3,7,9-tetramethyl-5*H*-4λ4,5λ4-dipyrrolo[1,2-c:2',1'-f][1,3,2]diazaborinin-10-yl)methyl (4-nitrophenyl) carbonate



255

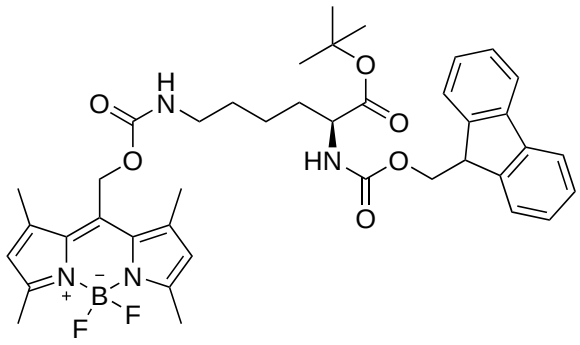
Method A:
4-Nitrophenyl chloroformate (35.0 mg, 0.17 mmol, 1.20 eq) was dissolved in anhydrous CH_2Cl_2 (5.00 mL). To this solution was added *N*-methyl morpholine (17.2 mg, 0.02 mL, 0.17 mmol, 1.20 eq) dropwise and the resulting solution was cooled to 0 °C. (5,5-Difluoro-1,3,7,9-tetramethyl-5*H*-4$\boldsymbol{\lambda}$4,5$\boldsymbol{\lambda}$4-dipyrrolo[1,2-c:2',1'-f][1,3,2]diazaborinin-10-yl)methanol (**250**) (40.0 mg, 0.14 mmol, 1.00 eq) was added dropwise as a solution in anhydrous CH_2Cl_2 (3.00 mL) and the reaction solution was allowed to warm to RT and stirred under an Ar atmosphere for 2 h, after which time the reaction was adjudged to be complete by TLC analysis. The solvent was removed under reduced pressure and the obtained crude residue was purified by silica gel flash column chromatography, eluting with petroleum ether:CH_2Cl_2 = 7:3, to afford (5,5-difluoro-1,3,7,9-tetramethyl-5*H*-4$\boldsymbol{\lambda}$4,5$\boldsymbol{\lambda}$4-dipyrrolo[1,2-c:2',1'-f][1,3,2]diazaborinin-10-yl)methyl (4-nitrophenyl) carbonate (**255**) as a red solid (28.4 mg, 45%).

Method B:
(5,5-Difluoro-1,3,7,9-tetramethyl-5*H*-4$\boldsymbol{\lambda}$4,5$\boldsymbol{\lambda}$4-dipyrrolo[1,2-c:2',1'-f][1,3,2]diazaborinin-10-yl)methanol (**250**) (100 mg, 0.36 mmol, 1.00 eq) and 4-nitrophenyl chloroformate (290 mg, 1.44 mmol, 4.00 eq) were dissolved in anhydrous THF (20.0 mL). To this solution was added *N*,*N*-diisopropylethylamine (233 mg, 0.31 mL, 1.80 mmol, 5.00 eq) and pyridine (7.12 mg, 0.01 mL, 0.09 mmol, 0.25 eq). The reaction mixture was allowed to stir under an Ar atmosphere for 1 h, after which time the reaction was adjudged to be completely by TLC analysis. The reaction mixture was diluted with Et_2O (100 mL), washed with aq. 1 M HCl (100 mL) and back extracted with Et_2O (2 × 100 mL). The combined organics were washed with sat. aq. $NaHCO_3$ (100 mL), then dried over $MgSO_4$ and filtered. The solvent was removed under reduced pressure and the obtained crude residue was purified by silica gel flash column chromatography, eluting with

petroleum ether:CH_2Cl_2 = 1:1, to afford (5,5-difluoro-1,3,7,9-tetramethyl-5*H*-4$\boldsymbol{\lambda}$4,5$\boldsymbol{\lambda}$4-dipyrrolo[1,2-c:2',1'-f][1,3,2]diazaborinin-10-yl)methyl (4-nitrophenyl) carbonate (**255**) as a red solid (107 mg, 67%).

R_f: 0.50 (CH_2Cl_2);
m.p.: 216 - 218 °C (Petroleum ether/CH_2Cl_2);
^{1}H NMR (400 MHz, CD_2Cl_2) $\boldsymbol{\delta}$H: 8.19 (2H, d, J = 9.3 Hz, C_{Ar}**H**), 7.32 (2H, d, J = 9.3 Hz, C_{Ar}**H**), 6.07 (2H, s, C_{BODIPY}**H**), 5.48 (2H, s, $C_{BODIPY}C$**H**$_2$O), 2.42 (6H, s, $C_{BODIPY}C$**H**$_3$), 2.38 (6 H, s, $C_{BODIPY}C$**H**$_3$);
^{13}C NMR (100 MHz, CD_2Cl_2) $\boldsymbol{\delta}$C: 157.8 (**C**O) 155.9 (**C**$_{Ar}$O), 152.8 (**C**$_{Ar}NO_2$), 146.2 (**C**$_{BODIPY}$), 142.4 (**C**$_{BODIPY}$), 133.1 (**C**$_{BODIPY}$), 131.8 (**C**$_{BODIPY}$), 125.9 (**C**$_{Ar}$H), 123.2 (**C**$_{BODIPY}$H), 122.3 (**C**$_{Ar}$H), 62.2 (C_{BODIPY}**C**H$_2$O), 16.1 (C_{BODIPY}**C**H$_3$), 15.1 (C_{BODIPY}**C**H$_3$);
^{19}F NMR(377 MHz, CD_2Cl_2) : -146.2 (2F, q, J = 33.0 Hz, B**F**$_2$);
LRMS *m/z* (ESI$^+$): 130 (100%), 424 (60% [M - F]$^+$), 444 (92% [M + H]$^+$);
HRMS *m/z* (ESI$^+$): Found 466.1357 [M + Na]$^+$ ($C_{21}H_{20}BF_2N_3NaO_5^+$ requires 466.1356 [M + Na]$^+$);
IR ($\boldsymbol{\nu}_{\mathbf{max}}$ cm^{-1}): 1751 (m, C=O), 1559 (w, Ar C-C), 1510 (w, Ar C-C), 1409 (w, N-O), 1369 (w), 1346 (m, N-O), 1308 (m, C-N), 1257 (m), 1206 (m, C-O), 1190 (m, C-O), 1151 (w), 1074 (m), 1052 (w), 1022 (w), 969 (s), 866 (m), 816 (m), 776 (w), 746 (w), 719 (m), 676 (w), 659 (w), 625 (w).

***tert*-Butyl N^2-(((9*H*-fluoren-9-yl)methoxy)carbonyl)-N^6-(((5,5-difluoro-1,3,7,9-tetramethyl-5*H*-4λ4, 5λ4-dipyrrolo[1,2-c:2',1'-f][1,3,2]diazaborinin-10-yl)methoxy)carbonyl)-*L*-lysinate**



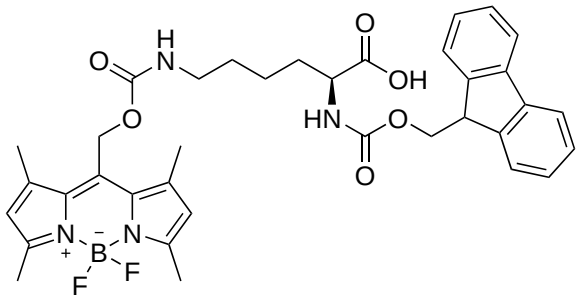
253

4-Nitrophenyl chloroformate (54.4 mg, 0.27 mmol, 1.50 eq) was dissolved in anhydrous CH_2Cl_2 (4.00 mL). To this solution was added *N*-methyl morpholine (27.3 mg, 0.03 mL, 0.27 mmol, 1.50 eq). The resulting solution was cooled to 0 °C and a solution of (5,5-difluoro-1,3,7,9-tetramethyl-5*H*-4**λ**4,5**λ**4-dipyrrolo[1,2-c:2',1'-f][1,3,2]diazaborinin-10-yl)methanol (**250**) (50.0 mg, 0.18 mmol, 1.0 eq) in anhydrous CH_2Cl_2 (1.00 mL) was added dropwise. The reaction solution was allowed to warm to RT and stirred under an Ar atmosphere for 18 h, after which time formation was the intermediate was adjudged to be complete by TLC analysis. *tert*-Butyl (((9*H*-fluoren-9-yl)methoxy)carbonyl)-*L*-lysinate (**187**) (76.0 mg, 0.18 mmol, 1.00 eq) and 4-(dimethylamino)pyridine (22.0 mg, 0.18 mmol, 1.00 eq) were added and the reaction solution was stirred at RT under an Ar atmosphere for 18 h, after which time the reaction was adjudged to be complete by TLC analysis. The reaction was quenched with CH_2Cl_2 (5.00 mL) and the solvent was removed under reduced pressure. The obtained crude residue was purified by silica gel flash column chromatography, eluting with CH_2Cl_2 to CH_2Cl_2:Acetone = 98:2 - 95:5 - 90:10 to afford *tert*-butyl N^2-(((9*H*-fluoren-9-yl)methoxy)carbonyl)-N^6-(((5,5-difluoro-1,3,7,9-tetramethyl-5*H*-4**λ**, 5**λ**4-dipyrrolo[1,2-c:2',1'-f][1,3,2]diazaborinin-10-yl)methoxy)carbonyl)-*L*-lysinate (**253**) as a pink solid (19.7 mg, 15%).

R_f: 0.66 (CH_2Cl_2:Acetone = 9:1);
m.p.: 156 - 158 °C (Hexane/Acetone);
$[\alpha]_D^{26}$: +79.1 (***c*** 0.1 in $CHCl_3$);
UV λ_{max}/nm (ϵ/M^{-1}cm^{-1}): 515 (22030) [MeOH];

^{1}H NMR (400 MHz, $CDCl_3$) δH: 7.77 (2H, d, J = 7.1 Hz, $C_{FmocAr}\mathbf{H}$), 7.60 (2H, d, J = 7.3 Hz, $C_{FmocAr}\mathbf{H}$), 7.45 - 7.35 (2H, m, $C_{FmocAr}\mathbf{H}$), 7.31 (2H, t, J = 7.3 Hz, $C_{FmocAr}\mathbf{H}$), 6.08 (2H, s, $C_{BODIPY}\mathbf{H}$), 5.49 - 5.36 (1H, m, N$\mathbf{H}$CHCH$_2$CH$_2$), 5.23 (2H, s, $C_{BODIPY}C\mathbf{H}_2O$), 5.08 - 4.94 (1H, m, N$\mathbf{H}$CH$_2$CH$_2$), 4.48 - 4.33 (2H, m, $C_{Fmoc}\mathbf{H}_2$) 4.29 - 4.10 (2H, m, $C_{Fmoc}\mathbf{H}$, NHC$\mathbf{H}$CH$_2$CH$_2$), 3.25 (1H, ddt, J = 12.0, 6.0, 6.0 Hz, NHC$\mathbf{H}_A$H$_B$CH$_2$), 3.17 (1H, ddt, J = 12.0, 6.0, 6.0 Hz, NHCH$_A\mathbf{H}_B$CH$_2$), 2.48 (6H, s, $C_{BODIPY}C\mathbf{H}_3$), 2.38 (6H, s, $C_{BODIPY}C\mathbf{H}_3$), 1.88 - 1.74 (1H, m, NHCHC$\mathbf{H}_A$H$_B$CH$_2$), 1.73 - 1.53 (3H, m, NHCHCH$_A\mathbf{H}_B$CH$_2$, NHCH$_2$C$\mathbf{H}_2$), 1.45 (9H, s, OC(C$\mathbf{H}_3$)$_3$), 1.38 - 1.29 (2H, m, NHCHCH$_2$C$\mathbf{H}_2$),
[With impurity, inseparable by silica flash column chromatography, of hydrolysed 4-nitrophenyl chloroformate at 8.17 (2H, d, J = 8.8 Hz) and 7.25 (2H, d, J = 8.8 Hz)]
;
^{13}C NMR (100 MHz, $CDCl_3$) δC: 171.5 (**C**O), 156.3 (**C**O), 155.7 (**C**O), 144.0 ($\mathbf{C}_{FmocAr}$), 143.9 ($\mathbf{C}_{BODIPY}$), 142.0 ($\mathbf{C}_{BODIPY}$), 141.3 ($\mathbf{C}_{FmocAr}$), 134.3 ($\mathbf{C}_{BODIPY}$), 132.6 ($\mathbf{C}_{BODIPY}$), 127.7 + 126.6 ($\mathbf{C}_{FmocAr}$H), 127.0 ($\mathbf{C}_{FmocAr}$H), 124.9 ($\mathbf{C}_{FmocAr}$H), 122.1 ($\mathbf{C}_{BODIPY}$H), 119.9 ($\mathbf{C}_{FmocAr}$H), 81.9 (O$\mathbf{C}$(CH$_3$)$_3$), 66.6 ($\mathbf{C}_{Fmoc}$H$_2$), 57.7 ($C_{BODIPY}\mathbf{C}$H$_2$O), 54.2 (NH$\mathbf{C}$HCH$_2$CH$_2$), 47.3 ($\mathbf{C}_{Fmoc}$H), 41.0 + 40.8 (NH$\mathbf{C}$H$_2$CH$_2$), 32.2 (NHCH$\mathbf{C}$H$_2$CH$_2$), 29.4 (NHCH$_2\mathbf{C}$H$_2$), 27.7 (OC($\mathbf{C}$H$_3$)$_3$), 22.2 (NHCHCH$_2\mathbf{C}$H$_2$), 15.4 ($C_{BODIPY}\mathbf{C}$H$_3$), 14.4 ($C_{BODIPY}\mathbf{C}$H$_3$),
[With impurity, inseparable by flash column chromatography, of hydrolysed 4-nitrophenyl chloroformate at 155.9, 143.9, 132.6, 125.0, 121.9];
^{19}F NMR(377 MHz, CD_2Cl_2) δF: -146.3 (2F, q, J = 32.2 Hz, B$\mathbf{F}_2$);
LRMS *m/z* (ESI$^+$): 751 (100% [M + Na]$^+$);
HRMS *m/z* (ESI$^+$): Found 751.3451 [M + Na]$^+$ ($C_{40}H_{47}BF_2N_4NaO_6^+$ requires 751.3449 [M + Na]$^+$);
IR (ν_{max} cm^{-1}): 3330 (w), 2972 (w), 2363 (s), 2335 (m), 2165 (w), 2044 (w), 1980 (w), 1701 (s, C=O), 1602 (m, C=O), 1557 (m, Ar C-C), 1516 (s, Ar C-C), 1445 (m), 1417 (m), 1308 (w, C-N), 1251 (w), 1195 (m, C-O), 1155 (m, C-O), 1074 (m, C-O), 981 (s), 836 (w), 738 (s), 664 (w).

N^2-(((9*H*-Fluoren-9-yl)methoxy)carbonyl)-N^6-(((5,5-difluoro-1,3,7,9-tetramethyl-5*H*-4λ4,5λ4-dipyrrolo[1,2-c:2',1'-f][1,3,2]diazaborinin-10-yl)methoxy)carbonyl)-*L*-lysine



256

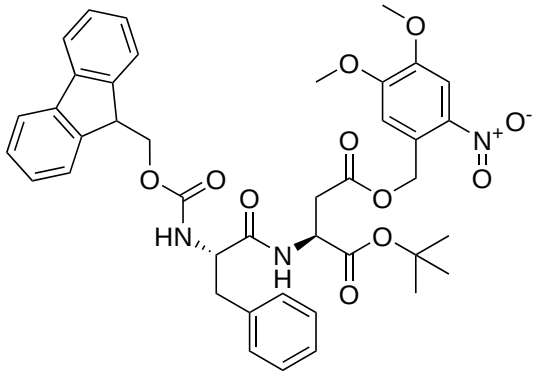
4-Nitrophenyl chloroformate (109 mg, 0.54 mmol, 1.50 eq) was dissolved in anhydrous CH_2Cl_2 (8.00 mL). To this solution was added *N*-methyl morpholine (72.8 mg, 0.08 mL, 0.72 mmol, 2.00 eq) and the resulting solution was cooled to 0 °C. A solution of (5,5-difluoro-1,3,7,9-tetramethyl-5*H*-4**λ**4,5**λ**4-dipyrrolo[1,2-c:2',1'-f][1,3,2]diazaborinin-10-yl)methanol (**250**) (100 mg, 0.36 mmol, 1.00 eq) in CH_2Cl_2 (2.00 mL) was added dropwise and the reaction solution was stirred at RT under an Ar atmosphere for 3 h, after which time formation of the intermediate was adjudged to be complete by TLC analysis. Fmoc-Lys-OH (133 mg, 0.36 mmol, 1.00 eq) was dissolved in H_2O:Acetonitrile (1:1, 10.0 mL) and $NaHCO_3$ (60.5 mg, 0.72 mmol, 2.00 eq) was added to the solution. The above prepared organic solution containing the nitrophenyl carbamate intermediate, was added dropwise to the solution containing the dissolved amino acid to form a biphasic mixture and 4-(dimethylamino)pyridine (100 mg, 0.72 mmol, 2.00 eq) was added. The resulting biphasic reaction mixture was stirred at RT for 18 h, after which time the reaction was adjudged to be complete by TLC analysis. The reaction was quenched with CH_2Cl_2 (100 mL) and washed with aq. 1 M HCl (100 mL). The aqueous layer was extracted with CH_2Cl_2 (2 × 50.0 mL) and the solvent was removed under reduced pressure. The obtained crude residue was purified by silica gel flash column chromatography, eluting with $CHCl_3$:AcOH = 100:1 to $CHCl_3$:MeOH:AcOH = 99:1:1 - 97:3:1, to afford N^2-(((9*H*-fluoren-9-yl)methoxy)carbonyl)-N^6-(((5,5-difluoro-1,3,7,9-tetramethyl-5*H*-4**λ**4,5**λ**4-dipyrrolo[1,2-c:2',1'-f][1,3,2]diazaborinin-10-yl)methoxy)carbonyl)-*L*-lysine (**256**) as a pink solid (78.4 mg, 33%).

$\mathbf{R}_f$: 0.24 ($CHCl_3$:MeOH = 9:1);

m.p.: 167 - 169 °C (Hexane/MeOH);
$[\boldsymbol{\alpha}]_{\boldsymbol{D}}^{\mathbf{26}}$: +40.4 (***c*** 0.2 in $CHCl_3$);
UV $\boldsymbol{\lambda_{max}}$/nm ($\boldsymbol{\epsilon}$/$\mathbf{M^{-1}cm^{-1}}$): 515 (43380) [MeOH];
^{1}H NMR (400 MHz, $(CD_3)_2SO$) $\boldsymbol{\delta}$H: 7.89 (2H, d, J = 7.4 Hz, $C_{FmocAr}\mathbf{H}$), 7.72 (2H, d, J = 7.3 Hz, $C_{FmocAr}\mathbf{H}$), 7.58 (1H, d, J = 8.5 Hz, N**H**$CHCH_2$), 7.41 (2H, t, J = 7.4 Hz, $C_{FmocAr}\mathbf{H}$), 7.46 - 7.37 (1H, m, N**H**CH_2CH_2), 7.32 (2H, t, J = 7.3 Hz, $C_{FmocAr}\mathbf{H}$), 6.25 (2H, s, $C_{BODIPY}\mathbf{H}$), 5.20 (2H, s, $C_{BODIPY}C\mathbf{H}_2O$), 4.28 (2H, d, J = 7.4 Hz, $C_{Fmoc}\mathbf{H}_2$), 4.21 (1H, t, J = 7.4 Hz, $C_{Fmoc}\mathbf{H}$), 3.92 - 3.84 (1H, m, NHC**H**CH_2), 2.99 (2H, dt, J = 7.0, 7.0 Hz, NHC$\mathbf{H}_2CH_2$), 2.42 (6H, s, $C_{BODIPY}C\mathbf{H}_3$), 2.37 (6H, s, $C_{BODIPY}C\mathbf{H}_3$), 1.74 - 1.64 (1H, m, NHCHC$\mathbf{H}_A$$H_B$$CH_2$), 1.63 - 1.55 (1H, m, NHCH$CH_A\mathbf{H}_BCH_2$), 1.44 - 1.36 (2H, m, $NHCH_2C\mathbf{H}_2CH_2$), 1.34 - 1.24 (2H, m, $NHCHCH_2C\mathbf{H}_2$);
^{13}C NMR (100 MHz, $CDCl_3$) $\boldsymbol{\delta}$C: 173.9 (**C**OOH), 156.1 (**C**O), 155.5 (**C**O), 143.9 ($\mathbf{C}_{FmocAr}$), 143.8 ($\mathbf{C}_{BODIPY}$), 142.0 ($\mathbf{C}_{BODIPY}$), 140.7 ($\mathbf{C}_{FmocAr}$), 135.3 ($\mathbf{C}_{BODIPY}$), 131.9 ($\mathbf{C}_{BODIPY}$), 127.6 ($\mathbf{C}_{FmocAr}$H), 127.1 ($\mathbf{C}_{FmocAr}$H), 125.3 ($\mathbf{C}_{FmocAr}$H), 122.1 ($\mathbf{C}_{BODIPY}$H), 120.1 ($\mathbf{C}_{FmocAr}$H), 65.5 ($\mathbf{C}_{Fmoc}H_2$), 57.0 ($C_{BODIPY}\mathbf{C}H_2O$), 53.8 (NH**C**HCH_2), 46.7 ($\mathbf{C}_{Fmoc}$H), 30.4 (NH**C**H_2CH_2), 28.9 (NHCH**C**H_2CH_2), 27.6 ($NHCH_2\mathbf{C}H_2$), 22.9 ($NHCHCH_2\mathbf{C}H_2$), 15.1 ($C_{BODIPY}\mathbf{C}H_3$), 14.3 ($C_{BODIPY}\mathbf{C}H_3$);
^{19}F NMR(470 MHz, $(CD_3)_2SO$) $\boldsymbol{\delta}$F: -143.9 (2F, q, J = 34.2 Hz, BF2);
LRMS *m/z* ($\mathbf{ESI^+}$): 695 (100% $[M + Na]^+$);
HRMS *m/z* ($\mathbf{ESI^+}$): Found 695.2822 $[M + Na]^+$ ($C_{36}H_{39}BF_2N_4NaO_6^+$ requires 695.2822 $[M + Na]^+$);
IR ($\boldsymbol{\nu_{max}}$ $\mathbf{cm^{-1}}$): 3317 (w, br, O-H), 2939 (w, br), 1690 (s, C=O), 1560 (s, Ar C-C), 1516 (s, Ar C-C), 1444 (m), 1411 (m), 1310 (m, C-N), 1254 (w), 1227 (w), 1194 (s, C-O), 1155 (s, C-O), 1117 (w), 1079 (s), 1030 (m), 979 (s), 822 (w), 734 (s).

7.11 Caged Peptides - Solution Phase Synthesis

1-(*tert*-Butyl) 4-(4,5-dimethoxy-2-nitrobenzyl) (((9*H*-fluoren-9-yl)methoxy)-carbonyl)-*L*-phenylalanyl-*L*-aspartate



278

1-(*tert*-Butyl) 4-(4,5-dimethoxy-2-nitrobenzyl) (((9*H*-fluoren-9-yl)methoxy)carbonyl)-*L*-aspartate (**212**) (170 mg, 0.28 mmol, 1.00 eq) was dissolved in anhydrous DMF (2.50 mL). The solution was cooled to 0 °C, piperidine (238 mg, 0.28 mL, 2.80 mmol, 10.0 eq) was added, and the reaction solution was stirred at 0 °C under an Ar atmosphere for 0.5 h, after which time the reaction was adjudged to be complete by TLC analysis. The reaction was quenched with EtOAc (10.0 mL), washed with H_2O (10.0 mL), and brine (10.0 mL). The solvent was removed by azeotropic distillation with toluene and the crude yellow residue was used without further purification:

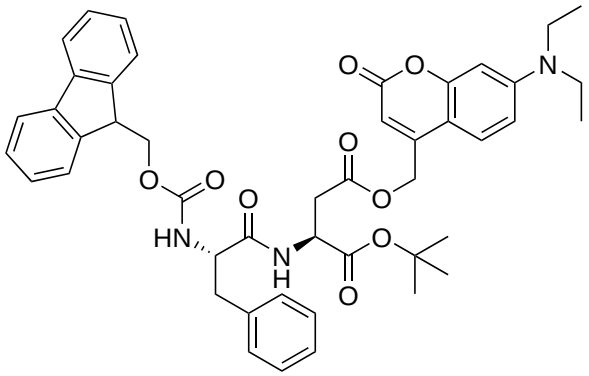
R_f: 0.17 ($CHCl_3$:Acetone = 9:1);
LRMS *m/z* (ESI$^+$): 385 (100% $[M + H]^+$).

Fmoc-Phe-OH (108 mg, 0.28 mmol, 1.00 eq) and *N*,*N*,*N*',*N*'-tetramethyl-*O*-(1*H*-benzotriazol-1-yl)uronium hexafluorophosphate (118 mg, 0.31 mmol, 1.10 eq) were dissolved in anhydrous DMF (8.00 mL). *N*,*N*-Diisopropylethylamine (72.4 mg, 0.10 mL, 0.56 mmol, 2.00 eq) was added dropwise and the resulting solution was stirred at RT under an Ar atmosphere for 1 h. The above crude yellow solid was added and the reaction solution was stirred at RT under an Ar atmosphere for 18 h, after which time the reaction was adjudged to be complete by TLC analysis. The reaction was quenched with EtOAc (50.0 mL), washed with aq. 1 M HCl (50.0 mL), sat. aq. $NaHCO_3$ (50.0 mL), H_2O (50.0 mL), and brine (50.0 mL), dried over $MgSO_4$, and filtered. The solvent was removed under reduced pressure and the crude residue was

purified by silica gel flash column chromatography, eluting with $CHCl_3$, to afford 1-(*tert*-butyl) 4-(4,5-dimethoxy-2-nitrobenzyl) (((9*H*-fluoren-9-yl)methoxy)carbonyl)-*L*-phenylalanyl-*L*-aspartate (**278**) as a colourless solid (642 mg, 30% over 2 steps).

R_f: 0.13 (Petroleum ether:Acetone = 75:25);
m.p.: 147 - 149 °C (Petroleum ether/CH_2Cl_2);
$[\alpha]_D^{26}$: +1.3 (***c*** 1.2 in $CHCl_3$);
UV λ_{max}/nm (ϵ/M^{-1}cm^{-1}): 335 (7560) [MeOH];
^{1}H NMR (400 MHz, $(CD_3)_2SO$) δH: 8.58 (1H, d, J = 8.1 Hz, N**H**C$_{Asp}$HCH$_2$), 7.86 (2H, d, J = 7.5 Hz, C$_{FmocAr}$**H**), 7.67 (1H, d, J = 8.9 Hz, N**H**C$_{Phe}$H), 7.66 (1H, s, C$_{DMNBAr}$**H**), 7.60 (2H, t, J = 7.4 Hz, C$_{FmocAr}$**H**), 7.39 (2H, t, J = 7.5 Hz, C$_{FmocAr}$**H**), 7.35 - 7.29 (1H, m, C$_{PheAr}$**H**), 7.31 (2H, t, J = 7.4 Hz, C$_{FmocAr}$**H**), 7.29 - 7.23 (3H, m, C$_{PheAr}$**H**), 7.21 - 7.16 (1H, m, C$_{PheAr}$**H**), 7.20 (1H, s, C$_{DMNBAr}$**H**), 5.42 (2H, s, C$_{DMNB}$**H**$_2$O), 4.67 - 4.59 (1H, m, NHC$_{Asp}$**H**CH$_2$), 4.32 - 4.23 (1H, m, NHC$_{Phe}$**H**CH$_2$), 4.13 - 4.05 (3H, m, C$_{Fmoc}$**H**, C$_{Fmoc}$**H**$_2$), 3.91 (3H, s, OC**H**$_3$), 3.83 (3H, s, OC**H**$_3$), 3.00 (1H, dd, J = 13.6, 3.8 Hz, NHCHC$_{Asp}$**H**$_A$H$_B$), 2.92 (1H, dd, J = 16.5, 6.6 Hz, NHCHC$_{Phe}$H$_A$**H**$_B$), 2.84 - 2.72 (2H, m, NHCHC$_{Asp}$**H**$_A$H$_B$, NHCHC$_{Phe}$H$_A$**H**$_B$), 1.35 (9H, s, O(C(C**H**$_3$)$_3$);
^{13}C NMR (100 MHz, $(CD_3)_2SO$) δC: 171.7 (**C**O), 169.8 (**C**O), 169.6 (**C**O), 155.8 (**C**O), 153.3 (**C**$_{DMNBAr}$), 147.9 (**C**$_{DMNBAr}$), 143.7 (**C**$_{FmocAr}$), 140.63 (**C**$_{FmocAr}$), 139.6 (**C**$_{DMNBAr}$), 138.14 (**C**$_{PheAr}$), 129.2 (**C**$_{FmocAr}$H), 128.1 (**C**$_{PheAr}$H), 127.6 (**C**$_{PheAr}$H), 127.0 (**C**$_{FmocAr}$H), 126.3 (**C**$_{DMNBAr}$), 126.1 (**C**$_{PheAr}$H), 125.3 (**C**$_{FmocAr}$H), 120.1 (**C**$_{FmocAr}$H), 111.2 (**C**$_{DMNBAr}$H), 108.1 (**C**$_{DMNBAr}$H), 81.2 (O**C**(CH$_3$)$_3$), 65.6 (**C**$_{Fmoc}$H$_2$), 63.0 (**C**$_{DMNB}$H$_2$O), 56.3 (O**C**H$_3$), 56.1 (O**C**H$_3$), 56.0 (**C**$_{Phe}$H), 49.1 (**C**$_{Asp}$H), 46.5 (**C**$_{Fmoc}$H), 37.4 (**C**$_{Phe}$H$_2$), 35.87 (**C**$_{Asp}$H$_2$), 27.5 (OC(**C**H$_3$)$_3$);
LRMS *m/z* (ESI$^+$): 754 (38% [M + H]$^+$), 776 (100% [M + Na]$^+$);
HRMS *m/z* (ESI$^+$): Found 754.2965 [M + H]$^+$ ($C_{41}H_{44}N_3O_{11}^+$ requires 754.2970 [M + H]$^+$);
IR (ν_{max} cm^{-1}): 3327 (w, br), 2936 (w), 2363 (w), 1727 (m, C=O), 1692 (m, C=O), 1662 (m, C=O), 1582 (w, Ar C-C), 1523 (s, N-O), 1446 (w, Ar C-C), 1366 (w), 1329 (w, N-O), 1279 (m, C-N), 1219 (w), 1158 (m, C-O), 1070 (m, C-O), 1030 (w), 989 (w), 879 (w), 797 (w), 740 (m), 702 (w), 650 (w).

1-(*tert*-Butyl) 4-((7-(diethylamino)-2-oxo-2*H*-chromen-4-yl)methyl) (((9*H*-fluoren-9-yl)methoxy)carbonyl)-*L*-phenylalanyl-*L*-aspartate



279

1-(*tert*-Butyl) 4-((7-(diethylamino)-2-oxo-2*H*-chromen-4-yl)methyl) (((9*H*-fluoren-9-yl)methoxy)carbonyl)-*L*-aspartate (**215**) (200 mg, 0.31 mmol, 1.00 eq) was dissolved in anhydrous DMF (2.77 mL) and the solution was cooled to 0 °C. Piperidine (266 mg, 0.31 mL, 3.12 mmol, 10.0 eq) was added and the reaction solution was stirred at 0 °C under an Ar atmosphere for 1 h, after which time the reaction was adjudged to be complete by TLC analysis. The reaction was quenched with EtOAc (100 mL) and washed with aq. 1 M HCl (100 mL). The aqueous layer was basified with sat. aq. $NaHCO_3$ to neutral pH and extracted with CH_2Cl_2 (3 × 100 mL). The solvent was removed under reduced pressure and the crude yellow residue was used without further purification.

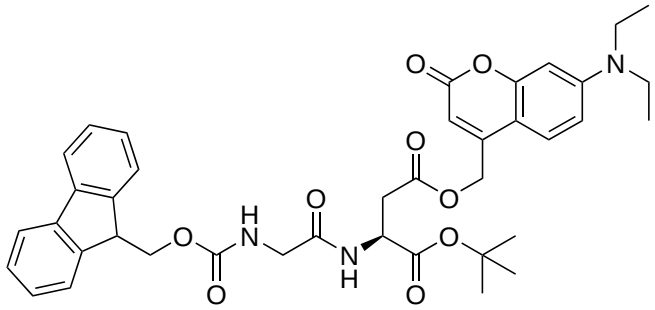
$\mathbf{R_f}$: 0.15 ($CHCl_3$:Acetone = 9:1).

Fmoc-Phe-OH (120 mg, 0.31 mmol, 1.00 eq) and *N*,*N*,*N*',*N*'-tetramethyl-*O*-(1*H*-benzotriazol-1-yl)uronium hexafluorophosphate (129 mg, 0.34 mmol, 1.10 eq) were dissolved in anhydrous DMF (10.0 mL). *N*,*N*-Diisopropylethylamine (80.1 mg, 0.11 mL, 0.62 mmol, 2.00 eq) was added dropwise and the resulting solution was stirred at RT under an Ar atmosphere for 1 h. The above crude solid was added as a solution in DMF (5.00 mL) and the reaction solution was stirred at RT under an Ar atmosphere for 18 h, after which time the reaction was adjudged to be complete by TLC analysis. The reaction was quenched with EtOAc (100 mL), washed with aq. 1 M HCl (100 mL), sat. aq. $NaHCO_3$ (100 mL), H_2O (100 mL), and brine (100 mL), dried over $MgSO_4$, and filtered. The solvent was removed under reduced pressure and the crude residue was purified by silica gel flash column chromatography, eluting with

petroleum ether:acetone = 8:2 - 7:3, to afford 1-(*tert*-butyl) 4-((7-(diethylamino)-2-oxo-2*H*-chromen-4-yl)methyl) (((9*H*-fluoren-9-yl)methoxy)carbonyl)-*L*-phenylalanyl-*L*-aspartate (**279**) as a bright yellow fluffy foam (198 mg, 82% over 2 steps).

R_f: 0.72 ($CHCl_3$:Acetone = 9:1);
m.p.: 106 - 108 °C (Hexane/Acetone);
$[\alpha]_D^{26}$: -34.9 (***c*** 0.9 in $CHCl_3$);
UV λ_{max}/nm (ϵ/$M^{-1}cm^{-1}$): 380 (25040) [MeOH];
^{1}H NMR (400 MHz, $CDCl_3$) **δ**H: 7.74 (2H, d, J = 7.6 Hz, $C_{FmocAr}\mathbf{H}$), 7.56 - 7.49 (2H, m, $C_{FmocAr}\mathbf{H}$), 7.38 (2H, t, J = 7.6 Hz, $C_{FmocAr}\mathbf{H}$), 7.32 - 7.24 (6H, m, $C_{FmocAr}\mathbf{H}$, $C_{PheAr}\mathbf{H}$, $C_{PheAr}\mathbf{H}$), 7.25 - 7.17 (1H, m, $C_{PheAr}\mathbf{H}$), 7.21 (1H, d, J = 9.0 Hz, $C_{DEACMAr}\mathbf{H}$), 7.05 (1H, d, J = 6.6 Hz, $N\mathbf{H}C_{Asp}HCH_2$), 6.55 (1H, dd, J = 9.0, 2.5 Hz, $C_{DEACMAr}\mathbf{H}$), 6.50 (1H, d, J = 2.5 Hz, $C_{DEACMAr}\mathbf{H}$), 6.03 (1H, s, $C_{DEACMAlkene}\mathbf{H}$), 5.83 (1H, d, J = 7.8 Hz, $N\mathbf{H}C_{Phe}HCH_2$), 5.23 (1H, d, J = 15.5 Hz, $C_{DEACM}\mathbf{H}_AH_B$), 5.16 (1H, d, J = 15.5 Hz, $C_{DEACM}H_A\mathbf{H}_B$), 4.75 - 4.68 (1H, m, $NHC_{Asp}\mathbf{H}CH_2$), 4.57 - 4.47 (1H, m, $NHC_{Phe}\mathbf{H}CH_2$), 4.35 (1H, dd, J = 10.4, 7.4 Hz, $C_{Fmoc}\mathbf{H}_AH_B$), 4.24 (1H, dd, J = 10.4, 7.4 Hz, $C_{Fmoc}H_A\mathbf{H}_B$), 4.16 (1H, dd, J = 7.4, 7.4 Hz, $C_{Fmoc}\mathbf{H}$), 3.40 (4H, q, J = 7.1 Hz, $N(C\mathbf{H}_2CH_3NEt_3)$, 3.25 (1H, dd, J = 13.7, 5.0 Hz, $NHCHC_{Phe}\mathbf{H}_AH_B$), 3.11 - 3.01 (3H, m, $NHCHC_{Phe}H_A\mathbf{H}_B$, $NHCHC_{Asp}\mathbf{H}_AH_B$, $NHCHC_{Asp}H_A\mathbf{H}_B$), 1.43 (9H, s, $OC(C\mathbf{H}_3)_3$), 1.20 (6H, t, J = 7.1 Hz, $N(CH_2C\mathbf{H}_3)_2$);
^{13}C NMR (100 MHz, $CDCl_3$) **δ**C: 171.0 ($\mathbf{C}O$), 170.0 ($\mathbf{C}O$), 168.7 ($\mathbf{C}O$), 162.0 ($\mathbf{C}O$), 156.2 ($\mathbf{C}O$), 150.7 ($\mathbf{C}_{DEACMAr}$), 143.8 ($\mathbf{C}_{DEACMAr}$), 143.7 ($\mathbf{C}_{FmocAr}$), 141.2 ($\mathbf{C}_{FmocAr}$), 136.4 ($\mathbf{C}_{PheAr}$), 129.3 ($\mathbf{C}_{FmocAr}H$), 128.6 ($\mathbf{C}_{FmocAr}H$), 127.6 ($\mathbf{C}_{PheAr}H$), 127.0 ($\mathbf{C}_{FmocAr}H$), 126.9 ($\mathbf{C}_{PheAr}H$), 125.2 ($\mathbf{C}_{DEACMAr}$), 125.1 ($\mathbf{C}_{PheAr}H$), 124.2 ($\mathbf{C}_{DEACMAr}H$), 119.9 ($\mathbf{C}_{FmocAr}H$), 108.7 ($\mathbf{C}_{FmocAr}H$), 105.8 ($\mathbf{C}_{FmocAlkene}$), 105.7 ($\mathbf{C}_{FmocAlkene}H$), 97.8 ($\mathbf{C}_{DEACMAr}H$), 83.1 ($O\mathbf{C}(CH_3)_3$), 67.2 ($\mathbf{C}_{Fmoc}H_2$), 61.6 ($\mathbf{C}_{DEACM}H_2$), 56.2 ($\mathbf{C}_{Phe}H$), 49.5 ($\mathbf{C}_{Asp}H$), 47.0 ($\mathbf{C}_{Fmoc}H$), 44.7 ($N(\mathbf{C}H_2CH_3)_2$), 37.9 ($\mathbf{C}_{Phe}H_2$), 36.3 ($\mathbf{C}_{Asp}H_2$), 27.8 ($OC(\mathbf{C}H_3)_3$), 12.4 ($N(CH_2\mathbf{C}H_3)_2$);
LRMS *m/z* (ESI^+): 788 (100% $[M + H]^+$);
HRMS *m/z* (ESI^+): Found 810.3359 $[M + Na]^+$ ($C_{46}H_{49}N_3NaO_9^+$ requires 810.3361 $[M + Na]^+$);
IR (ν_{max} cm^{-1}): 3310 (w, br), 2976 (w), 2163 (w), 1974 (w), 1720 (s, C=O), 1603 (s, C=O), 1527 (m, Ar C-C), 1422 (m, Ar C-C), 1355 (w), 1229 (w), 1147 (s, C-O), 1073 (m, C-O), 844 (w), 795 (w), 741 (s), 701 (w), 617 (w).

1-(*tert*-Butyl) 4-((7-(diethylamino)-2-oxo2*H*-chromen-4-yl)methyl) (((9*H*-fluoren-9-yl)methoxy)carbonyl)glycyl-*L*-aspartate



224

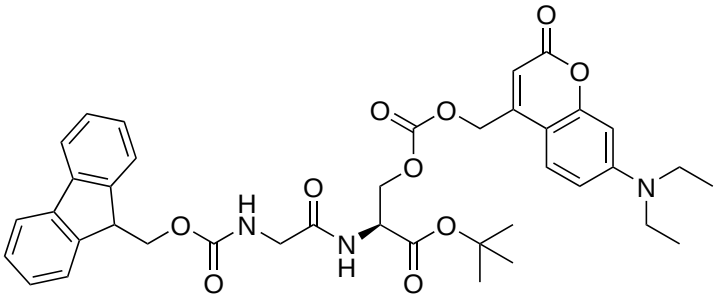
1-(*tert*-Butyl) 4-((7-(diethylamino)-2-oxo-2*H*-chromen-4-yl)methyl) (((9*H*-fluoren-9-yl)methoxy)carbonyl)-*L*-aspartate (**215**) (500 mg, 0.78 mmol, 1.00 eq) was dissolved in anhydrous DMF (7.00 mL) and the resulting solution was cooled to 0 °C. Piperidine (665 mg, 0.77 mL, 7.81 mmol, 10.0 eq) was added and the reaction solution was stirred at 0 °C under an Ar atmosphere for 0.5 h, after which time the reaction was adjudged to be complete by TLC analysis. The reaction was quenched with Et_2O (10.0 mL) and washed with brine (10.0 mL). The solvent was removed under reduced pressure and the yellow residue used without further purification.

$\mathbf{R_f}$: 0.23 ($CHCl_3$:Acetone = 8:2).

Fmoc-Gly-OH (226 mg, 0.76 mmol, 0.95 eq) and *N*,*N*,*N*',*N*'-tetramethyl-*O*-(1*H*-benzotriazol-1-yl)uronium hexafluorophosphate (326 mg, 0.86 mmol, 1.10 eq) were dissolved in anhydrous DMF (10.0 mL) and *N*,*N*-diisopropylethylamine (202 mg, 0.27 mL, 1.56 mmol, 2.00 eq) was added. The reaction solution was stirred at RT under an Ar atmosphere for 1 h. The above obtained yellow solid was added and the reaction solution was stirred at RT under an Ar atmosphere for 18 h, after which time the reaction was adjudged to be complete by TLC analysis. The reaction was quenched with Et_2O (20.0 mL), washed with aq. 1 M HCl (20.0 mL), sat. aq. $NaHCO_3$ (20.0 mL), and brine (20.0 mL), dried over $MgSO_4$, and filtered. The solvent was removed under reduced pressure and the crude residue was purified by silica gel flash column chromatography, eluting with $CHCl_3$ to $CHCl_3$:Acetone = 9:1, to afford 1-(*tert*-butyl) 4-((7-(diethylamino)-2-oxo-2*H*-chromen-4-yl)methyl) (((9*H*-fluoren-9-yl)methoxy)carbonyl)glycyl-*L*-aspartate (**224**) as a yellow foam (188 mg, 53% over 2 steps).

R_f: 0.64 ($CHCl_3$:Acetone = 9:1);
m.p.: 103 - 105 °C (Hexane/Acetone);
$[\alpha]_D^{26}$: -3.1 (***c*** 0.9 in $CHCl_3$);
UV λ_{max}/nm (ϵ/$M^{-1}cm^{-1}$): 380 (23250) [MeOH];
^{1}H NMR (400 MHz, $CDCl_3$) δH: 7.75 (2H, d, J = 7.4 Hz, $C_{FmocAr}\mathbf{H}$), 7.61 (2H, d, J = 7.3 Hz, $C_{FmocAr}\mathbf{H}$), 7.39 (2H, t, J = 7.4 Hz, $C_{FmocAr}\mathbf{H}$), 7.30 (2H, t, J = 7.3 Hz, $C_{FmocAr}\mathbf{H}$), 7.21 (1H, d, J = 9.0 Hz, $C_{DEACMAr}\mathbf{H}$), 7.05 (1H, d, J = 7.0 Hz, $N\mathbf{H}C_{Asp}HCH_2$), 6.55 (1H, dd, J = 9.0, 2.3 Hz, $C_{DEACMAr}\mathbf{H}$), 6.50 (1H, d, J = 2.3 Hz, $C_{DEACMAr}\mathbf{H}$), 6.01 (1H, s, $C_{DEACMAlkene}\mathbf{H}$), 6.00 (1H, t, J = 4.1 Hz, $N\mathbf{H}C_{Gly}H_2$), 5.22 (2H, s, $C_{DEACM}\mathbf{H}_2$), 4.77 (1H, ddd, J = 7.0, 6.0, 6.0 Hz, $NHC_{Asp}\mathbf{H}CH_2$), 4.44 - 4.33 (2H, m, $C_{Fmoc}\mathbf{H}_AH_B$, $C_{Fmoc}H_A\mathbf{H}_B$), 4.23 (1H, dd, J = 7.2, 7.2 Hz, $C_{Fmoc}\mathbf{H}$), 4.01 (1H, dd, J = 17.0, 6.0 Hz, $NHCHC_{Asp}\mathbf{H}_AH_B$), 3.94 (1H, dd, J = 17.0, 6.0 Hz, $NHCHC_{Asp}H_A\mathbf{H}_B$), 3.40 (4H, q, J = 7.1 Hz, $N(C\mathbf{H}_2CH_3)_2$), 3.10 (2H, d, J = 4.1 Hz, $NHC_{Gly}\mathbf{H}_2$), 1.45 (9H, s, $OC(C\mathbf{H}_3)_3$), 1.20 (6H, t, J = 7.1 Hz, $N(CH_2C\mathbf{H}_3)_2$);
^{13}C NMR (100 MHz, $CDCl_3$) δC: 170.2 ($\mathbf{C}O$), 169.2 ($\mathbf{C}O$), 169.0 ($\mathbf{C}O$), 162.1 ($\mathbf{C}O$), 156.8 ($\mathbf{C}O$), 156.2 ($\mathbf{C}_{DEACMAr}$), 150.8 ($\mathbf{C}_{DEACMAr}$), 149.4 ($\mathbf{C}_{DEACMAr}$), 143.8 ($\mathbf{C}_{FmocAr}$), 141.3 ($\mathbf{C}_{FmocAr}$), 127.7 ($\mathbf{C}_{FmocAr}H$), 127.1 ($\mathbf{C}_{FmocAr}H$), 125.3 ($\mathbf{C}_{FmocAr}H$), 124.3 ($\mathbf{C}_{DEACMAr}H$), 120.0 ($\mathbf{C}_{FmocAr}H$), 108.8 ($\mathbf{C}_{DEACMAr}H$), 105.8 ($\mathbf{C}_{DEACMAlkene}H$), 105.7 ($\mathbf{C}_{DEACMAlkene}$), 97.8 ($\mathbf{C}_{DEACMAr}$), 83.3 ($O\mathbf{C}(CH_3)_3$), 67.4 ($\mathbf{C}_{Fmoc}H_2$), 61.7 ($\mathbf{C}_{DEACM}H_2O$), 49.4 ($NH\mathbf{C}_{Asp}H$), 47.1 ($\mathbf{C}_{Fmoc}H$), 44.8 ($N(\mathbf{C}H_2CH_3)_2$), 44.5 ($\mathbf{C}_{Asp}H_2$), 36.3 ($\mathbf{C}_{Gly}H_2$), 27.9 ($OC(\mathbf{C}H_3)_3$), 12.4 ($N(CH_2\mathbf{C}H_3)_2$);
LRMS *m/z* (ESI^+): 698 (100% $[M + H]^+$);
HRMS *m/z* (ESI^+): Found 720.2888 $[M + Na]^+$ ($C_{39}H_{43}N_3NaO_9^+$ requires 720.2892 $[M + Na]^+$);
IR (ν_{max} cm^{-1}): 3311 (w, br), 2974 (w), 1717 (s, C=O), 1602 (s, C=O), 1526 (m, Ar C-C), 1422 (m, Ar C-C), 1340 (m, C-N), 1272 (m, C-N), 1229 (m, C-N), 1145 (s, C-O), 1072 (m, C-O), 998 (w), 900 (w), 844 (w), 796 (w), 760 (m), 740 (s), 645 (w), 621 (w).

***tert*-Butyl *N*-((((9*H*-fluoren-9-yl)methoxy)carbonyl)glycyl)-*O*-(((7-(diethylamino)-2-oxo-2*H*-chromen-4-yl)methoxy)carbonyl)-*L*-serinate**



280

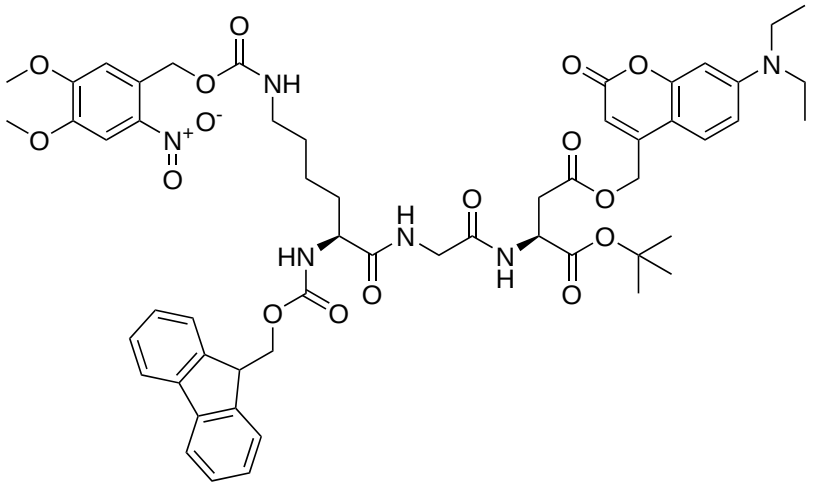
tert-Butyl *N*-(((9*H*-fluoren-9-yl)methoxy)carbonyl)-*O*-(((7-(diethylamino)-2-oxo-2*H*-chromen-4-yl)methoxy)carbonyl)-*L*-serinate (**217**) (170 mg, 0.26 mmol, 1.00 eq) was dissolved in anhydrous DMF (2.50 mL) and the resulting solution was cooled to 0 °C. Piperidine (221 mg, 0.26 mL, 2.60 mmol, 10.0 eq) was added and the reaction solution was stirred at 0 °C under an Ar atmosphere for 20 min, after which time the reaction was adjudged to be complete by TLC analysis. The reaction was quenched with CH_2Cl_2 (10.0 mL) and washed with brine (20.0 mL). The solvent was removed under reduced pressure to afford a yellow solid that was used without further purification.

$\mathbf{R_f}$: 0.15 ($CHCl_3$:Acetone = 9:1).

Fmoc-Gly-OH (91.2 mg, 0.30 mmol, 1.20 eq) and (benzotriazol-1-yloxy)tripyrrolidinophosphonium hexafluorophosphate (174 mg, 0.34 mmol, 1.30 eq) were dissolved in anhydrous DMF (5.00 mL). *N*,*N*-Diisopropylethylamine (78.8 mg, 0.11 mL, 0.61 mmol, 2.30 eq) was added dropwise and the resulting solution was stirred at RT under an Ar atmosphere for 1 h. The above prepared crude yellow solid was added and the reaction solution was stirred at RT under an Ar atmosphere for 18 h, after which time the reaction was adjudged to be complete by TLC analysis. The reaction was quenched with Et_2O (100 mL), washed with brine (100 mL), aq. 1 M HCl (100 mL), sat. aq. $NaHCO_3$ (100 mL) and brine (100 mL), dried over $MgSO_4$, and filtered. The solvent was removed under reduced pressure and the crude residue was purified by silica gel flash column chromatography, eluting with $CHCl_3$ to $CHCl_3$:Acetone = 98:2 - 95:5 - 90:10, to afford *tert*-butyl *N*-((((9*H*-fluoren-9-yl)methoxy)carbonyl)glycyl)-*O*-(((7-(diethylamino)-2-oxo-2*H*-chromen-4-yl)methoxy)carbonyl)-*L*-serinate (**280**) as a pale yellow foam (128 mg, 69% over 2 steps).

R_f: 0.42 ($CHCl_3$:Acetone = 9:1);
m.p.: 95 - 97 °C (Hexane/Acetone);
$[\alpha]_D^{26}$: +4.3 (***c*** 0.5 in $CHCl_3$);
UV λ_{max}/nm (ϵ/$M^{-1}cm^{-1}$): 380 (3700) [MeOH];
^{1}H NMR (400 MHz, $CDCl_3$) **δ**H: 7.75 (2H, d, J = 7.5 Hz, $C_{FmocAr}\mathbf{H}$), 7.62 (2H, d, J = 7.5 Hz, $C_{FmocAr}\mathbf{H}$), 7.39 (2H, t, J = 7.5 Hz, $C_{FmocAr}\mathbf{H}$), 7.31 (2H, t, J = 7.5 Hz, $C_{FmocAr}\mathbf{H}$), 7.25 (1H, d, J = 8.9 Hz, $C_{Ar}\mathbf{H}$), 6.55 (1H, dd, J = 8.9, 2.3 Hz, $C_{Ar}\mathbf{H}$), 6.50 (1H, d, J = 2.3 Hz, $C_{Ar}\mathbf{H}$), 6.11 (1H, s, $C_{Alkene}\mathbf{H}$), 5.84 (1H, d, J = 7.5 Hz, $N\mathbf{H}C_{Ser}HCH_2$), 5.57 (1H, t, J = 5.6 Hz, $N\mathbf{H}C_{Gly}H_2$), 5.29 (1H, d, J = 15.3 Hz, $C\mathbf{H}_AH_BO$), 5.18 (1H, d, J = 15.3 Hz, $CH_A\mathbf{H}_BO$), 4.63 (1H, dd, J = 11.0, 2.3 Hz, $NHC_{Ser}HC\mathbf{H}_AH_B$), 4.54 (1H, ddd, J = 7.5, 4.0, 2.3 Hz, $NHC_{Ser}\mathbf{H}CH_2$), 4.48 (1H, dd, J = 11.0, 4.0 Hz, $NHC_{Ser}HCH_A\mathbf{H}_B$), 4.41 (2H, d, J = 7.4 Hz, $C_{Fmoc}\mathbf{H}_2$), 4.24 (1H, t, J = 7.4 Hz, $C_{Fmoc}\mathbf{H}$), 4.02 (2H, d, J = 5.6 Hz, $NHC_{Gly}\mathbf{H}_2$), 3.40 (4H, q, J = 7.1 Hz, $N(C\mathbf{H}_2CH_3)_2$), 1.49 (9H, s, $OC(C\mathbf{H}_3)_3$), 1.20 (6H, t, J = 7.1 Hz, $N(CH_2C\mathbf{H}_3)_2$);
^{13}C NMR (100 MHz, $CDCl_3$) **δ**C: 169.6 ($\mathbf{C}O$), 167.7 ($\mathbf{C}O$), 162.0 ($\mathbf{C}O$), 156.4 ($\mathbf{C}O$), 156.2 ($\mathbf{C}O$), 154.9 ($\mathbf{C}_{Ar}O$), 150.6 ($\mathbf{C}_{Ar}N$), 150.1 ($\mathbf{C}_{Ar}$), 143.8 ($\mathbf{C}_{FmocAr}$), 141.2 ($\mathbf{C}_{FmocAr}$), 127.7 ($\mathbf{C}_{FmocAr}H$), 127.1 ($\mathbf{C}_{FmocAr}H$), 125.1 ($\mathbf{C}_{FmocAr}H$), 124.3 ($\mathbf{C}_{Ar}H$), 119.9 ($\mathbf{C}_{FmocAr}H$), 108.6 ($\mathbf{C}_{Ar}H$), 105.9 ($\mathbf{C}_{Alkene}H$), 105.9 ($\mathbf{C}_{Alkene}$), 97.8 ($\mathbf{C}_{Ar}H$), 83.6 ($O\mathbf{C}(CH_3)_3$), 67.3 ($\mathbf{C}_{Fmoc}H_2$), 64.8 ($NH\mathbf{C}_{Ser}HCH_2$), 62.1 ($C_{Ar}\mathbf{C}H_2O$), 54.0 ($NHC_{Ser}H\mathbf{C}H_2$), 47.1 ($\mathbf{C}_{Fmoc}H$), 44.7 ($N(\mathbf{C}H_2CH_3)_2$), 42.7 ($NH\mathbf{C}_{Gly}H_2CO$), 27.9 ($OC(\mathbf{C}H_3)_3$), 12.4 ($N(CH_2\mathbf{C}H_3)_2$);
LRMS *m/z* (ESI$^+$): 714 (100% $[M + H]^+$);
HRMS *m/z* (ESI$^+$): Found 714.3023 $[M + H]^+$ ($C_{39}H_{44}N_3O_{10}^+$ requires 714.3021 $[M + H]^+$);
IR (ν_{max} cm^{-1}): 3318 (w, br), 2975 (w), 2164 (w), 1710 (s, C=O), 1605 (s, C=O), 1526 (m, Ar C-C), 1423 (w), 1339 (w), 1274 (w, C-N), 1227 (w), 1193 (w), 1147 (m), 1083 (m, C-O), 1004 (w), 946 (w), 900 (w), 843 (w), 795 (w), 740 (m).

1-(*tert*-Butyl) 4-((7-(diethylamino)-2-oxo-2*H*-chromen-4-yl)methyl) N^2-(((9*H*-fluoren-9-yl)methoxy)carbonyl)-N^6-(((4,5-dimethoxy-2-nitrobenzyl)oxy)carbonyl)-*L*-lysylglycyl-*L*-aspartate



225

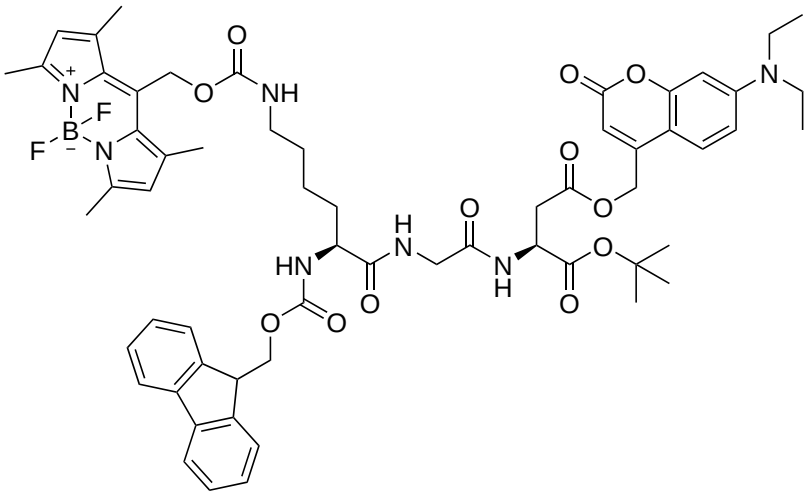
1-(*tert*-Butyl) 4-((7-(diethylamino)-2-oxo-2*H*-chromen-4-yl)methyl) (((9*H*-fluoren-9-yl)methoxy)carbonyl)glycyl-*L*-aspartate (**224**) (90.0 mg, 0.13 mmol, 1.00 eq) was dissolved in anhydrous DMF (1.15 mL) and the solution was cooled to 0 °C. Piperidine (110 mg, 0.13 mL, 1.29 mmol, 10.0 eq) was added and the reaction solution was stirred at 0 °C for 1 h under an Ar atmosphere, after which time the reaction was adjudged to be complete by TLC analysis. The crude reaction solution was loaded directly only silica gel and eluted with petroleum ether:acetone = 4:6 - 2:8, to afford a yellow residue which was used without further purification. N^2-(((9*H*-Fluoren-9-yl)methoxy)carbonyl)-N^6-(((4,5-dimethoxy-2-nitrobenzyl)oxy)carbonyl)-*L*-lysine (**214**) (73.0 mg, 0.12 mmol, 1.00 eq) and *N*,*N*,*N*',*N*'-tetramethyl-*O*-(1*H*-benzotriazol-1-yl)uronium hexafluorophosphate (50.0 g, 0.13 mmol, 1.10 eq) were dissolved in anhydrous DMF (1.00 mL). *N*,*N*-Diisopropylethylamine (31.0 mg, 0.04 mL, 0.24 mmol, 2.00 eq) was added and the resulting solution was stirred at RT under an Ar atmosphere for 1 h. To this solution was added the crude yellow solid obtained above and the reaction solution was stirred at RT under an Ar atmosphere for 24 h, after which time the reaction was adjudged to be complete by TLC analysis. The reaction was quenched with EtOAc (20.0 mL), washed with aq. 1 M HCl (20.0 mL), sat. aq. $NaHCO_3$ (20.0 mL), and brine (20.0 mL), dried over $MgSO_4$, and filtered. The solvent was removed under reduced pressure and the crude residue was purified by silica gel flash column chromatography, eluting with $CHCl_3$ to

$CHCl_3$:acetone = 9:1 - 8:2 - 6:4 - 1:1, to afford 1-(*tert*-butyl) 4-((7-(diethylamino)-2-oxo-2*H*-chromen-4-yl)methyl) N^2-(((9*H*-fluoren-9-yl)methoxy)carbonyl)-N^6-(((4,5-dimethoxy-2-nitrobenzyl)oxy)carbonyl)-*L*-lysylglycyl-*L*-aspartate (**225**) as a yellow solid (27.4 mg, 21% over 2 steps).

$\mathbf{R_f}$: 0.33 ($CHCl_3$:Acetone = 6:4);
m.p.: 81 - 83 °C (from Petroleum ether/Et_2O);
$\mathbf{[\alpha]_D^{26}}$: +1.8 (***c*** 0.4 in $CHCl_3$);
UV $\boldsymbol{\lambda_{max}}$/nm ($\boldsymbol{\epsilon}$/$\mathbf{M^{-1}cm^{-1}}$): 375 (4600) [MeOH];
^{1}H NMR (400 MHz, CD_3OD) $\boldsymbol{\delta}$H: 7.71 (1H, d, J = 7.7 Hz, $C_{FmocAr}\mathbf{H}$), 7.69 (1H, d, J = 7.7 Hz, $C_{FmocAr}\mathbf{H}$), 7.67 (1H, s $C_{DMNBAr}\mathbf{H}$), 7.61 (1H, d, J = 7.7 Hz, $C_{FmocAr}\mathbf{H}$), 7.59 (1H, d, J = 7.7 Hz, $C_{FmocAr}\mathbf{H}$), 7.33 (1H, d, J = 8.9 Hz, $C_{DEACMAr}\mathbf{H}$), 7.32 (1H, t, J = 7.7 Hz, $C_{FmocAr}\mathbf{H}$), 7.29 (1H, t, J = 7.7 Hz, $C_{FmocAr}\mathbf{H}$), 7.24 (1H, t, J = 7.7 Hz, $C_{FmocAr}\mathbf{H}$), 7.22 (1H, t, J = 7.7 Hz, $C_{FmocAr}\mathbf{H}$), 7.11 (1H, s, $C_{DMNBAr}\mathbf{H}$), 6.64 (1H, dd, J = 8.9, 2.4 Hz, $C_{DEACMAr}\mathbf{H}$), 6.45 (1H, d, J = 2.4 Hz, $C_{DEACMAr}\mathbf{H}$), 5.92 (1H, s, $C_{DEACMAlkene}\mathbf{H}$), 5.40 (2H, s, $C_{DMNBAr}C\mathbf{H_2}O$), 5.23 (1H, d, J = 15.2 Hz, $C_{DEACMAr}C\mathbf{H_A}H_BO$), 5.14 (1H, m, $C_{DEACMAr}CH_A\mathbf{H_B}O$), 4.75 (1H, dd, J = 6.2, 6.2 Hz, $NHC_{Asp}\mathbf{H}CH_2CO$), 4.34 (1H, dd, J = 10.6, 7.1 Hz, $C_{Fmoc}\mathbf{H_A}H_B$), 4.29 (1H, dd, J = 10.6, 7.1 Hz, $C_{Fmoc}H_A\mathbf{H_B}$), 4.11 (1H, dd, J = 7.1, 7.1 Hz, $C_{Fmoc}\mathbf{H}$), 4.02 (1H, dd, J = 8.2, 5.7 Hz, $NHC_{Lys}\mathbf{H}CH_2CH_2$), 3.90 (3H, s, $C_{DMNBAr}OC\mathbf{H_3}$), 3.86 (3H, s, $C_{DMNBAr}OC\mathbf{H_3}$), 3.43 (4H, q, J = 7.1 Hz, $N(C\mathbf{H_2}CH_3)_2$), 3.17 (2H, t, J = 6.5 Hz, $NHC_{Lys}\mathbf{H_2}CH_2CH_2$), 2.95 (1H, dd, J = 16.6, 6.2 Hz, $NHC_{Asp}HC\mathbf{H_A}H_B$), 2.89 (1H, dd, J = 16.6, 6.2 Hz, $NHC_{Asp}HCH_A\mathbf{H_B}$), 2.63 (2H, s, $NHC_{Gly}\mathbf{H_2}CO$), 1.86 - 1.78 (1H, m, $NHC_{Lys}HC\mathbf{H_A}H_BCH_2$) 1.77 - 1.70 (1H, m, $NHC_{Lys}HCH_A\mathbf{H_B}CH_2$) 1.69 - 1.62 (2H, m, $NHC_{Lys}H_2C\mathbf{H_2}CH_2$), 1.58 - 1.52 (2H, m, $NHC_{Lys}HCH_2C\mathbf{H_2}$), 1.41 (9H, s, $OC(C\mathbf{H_3})_3$), 1.17 (6H, t, J = 7.1 Hz, $N(CH_2C\mathbf{H_3})_2$);
^{13}C NMR (100 MHz, CD_3OD) $\boldsymbol{\delta}$C: 175.7 (**C**O), 171.6 (**C**O), 171.4 (**C**O), 170.8 (**C**O) 164.5 (**C**O), 158.9 (**C**O), 158.6 (**C**O), 157.6 ($\mathbf{C}_{DMNBAr}$), 155.4 ($\mathbf{C}_{DEACMAr}O$), 152.6 ($\mathbf{C}_{DMNBAr}OCH_3$), 152.5 ($\mathbf{C}_{DMNBAr}OCH_3$), 149.7 ($\mathbf{C}_{DEACMAr}N$), 145.3 ($\mathbf{C}_{FmocAr}$), 142.6 ($\mathbf{C}_{FmocAr}$), 141.0 ($\mathbf{C}_{DMNBAr}CH_2O$), 129.8 ($\mathbf{C}_{DEACMAr}$), 128.9 + 128.9 ($\mathbf{C}_{FmocAr}H$), 128.3 ($\mathbf{C}_{FmocAr}H$), 126.5 ($\mathbf{C}_{DEACMAr}H$), 126.4 + 126.3 ($\mathbf{C}_{FmocAr}H$), 121.0 ($\mathbf{C}_{FmocAr}H$), 111.2 ($\mathbf{C}_{DMNBAr}H$), 110.6 ($\mathbf{C}_{DEACMAr}H$), 109.4 ($\mathbf{C}_{DMNBAr}H$), 107.2 ($\mathbf{C}_{DEACMAlkene}$), 106.4 ($\mathbf{C}_{DEACMAlkene}H$), 98.4 ($\mathbf{C}_{DEACMAr}H$), 83.8 ($O\mathbf{C}(CH_3)_3$), 68.3 ($\mathbf{C}_{Fmoc}H_2$), 64.5 ($C_{DMNBAr}\mathbf{C}H_2O$), 63.0 ($C_{DEACMAr}\mathbf{C}H_2O$), 57.1 ($NH\mathbf{C}_{Lys}HCH_2CH_2$), 57.1 ($C_{DMNBAr}O\mathbf{C}H_3$), 56.9 ($C_{DMNBAr}O\mathbf{C}H_3$), 56.2 ($NH\mathbf{C}_{Gly}H_2CO$), 51.1 ($NH\mathbf{C}_{Asp}HCH_2CO$), 48.5 ($\mathbf{C}_{Fmoc}H$), 45.8 ($N(\mathbf{C}H_2CH_3)_2$), 41.5 ($NH\mathbf{C}_{Lys}H_2CH_2CH_2$), 37.0 ($NHC_{Asp}H\mathbf{C}H_2CO$),

32.2 ($NHC_{Lys}H\mathbf{C}H_2CH_2$), 30.6 ($NHC_{Lys}H_2\mathbf{C}H_2CH_2$), 28.3 ($OC(\mathbf{C}H_3)_3$), 24.9 ($NHC_{Lys}HCH_2\mathbf{C}H_2$), 12.9 ($N(CH_2\mathbf{C}H_3)_2$);
LRMS *m/z* (ESI$^+$): 1065 (100% $[M + H]^+$);
HRMS *m/z* (ESI$^+$): Found 1087.4265 $[M + Na]^+$ ($C_{55}H_{64}N_6NaO_{16}{}^+$ requires 1087.4271 $[M + Na]^+$);
IR (ν_{max} cm^{-1}): 2931 (w), 2361 (m), 2341 (m), 1715 (w, C=O), 1605 (w, C=O), 1522 (w, Ar C-C), 1455 (w, N-O), 1277 (w, C-N), 1220 (w), 1156 (w, C-O), 1069 (w, C-O), 845 (w), 773 (s), 639 (w), 614 (w); HPLC: 14.80 min (100%).

1-(*tert*-Butyl) 4-((7-(diethylamino)-2-oxo-2*H*-chromen-4-yl)methyl) N^2-(((9*H*-fluoren-9-yl)methoxy)carbonyl)-N^6-(((5,5-difluoro-1,3,7,9-tetramethyl-5*H*-4λ4,5λ4-dipyrrolo[1,2-c:2',1'-f][1,3,2]diazaborinin-10-yl)methoxy)carbonyl)-*L*-lysylglycyl-*L*-aspartate



257

1-(*tert*-Butyl) 4-((7-(diethylamino)-2-oxo-2*H*-chromen-4-yl)methyl) (((9*H*-fluoren-9-yl)methoxy)carbonyl)glycyl-*L*-aspartate (**224**) (50.0 mg, 0.07 mmol, 1.00 eq) was dissolved in anhydrous DMF (0.64 mL). The solution was cooled to 0 °C and piperidine (61.3 mg, 0.07 mL, 0.72 mmol, 10.0 eq) was added dropwise. The reaction solution was stirred at 0 °C under an Ar atmosphere for 10 minutes, after which time the reaction was adjudged to be complete by TLC analysis. The reaction was quenched with Et_2O (5.00 mL) and washed with brine (10.0 mL). The solvent was removed by exposure to a stream of N_2 gas. The crude yellow residue was used without further purification.

$\mathbf{R_f}$: 0.05 ($CHCl_3$:Acetone = 9:1).

N^2-(((9*H*-Fluoren-9-yl)methoxy)carbonyl)-N^6-(((5,5-difluoro-1,3,7,9-tetramethyl-5*H*-4λ4,5λ4-dipyrrolo[1,2-c:2',1'-f][1,3,2]diazaborinin-10-yl)methoxy)carbonyl)-*L*-lysine (**256**) (48.0 mg, 0.07 mmol, 1.00 eq) and (benzotriazol-1-yloxy)tripyrrolidinophosphonium hexafluorophosphate (41.2 mg, 0.08 mmol, 1.10 eq) were dissolved in anhydrous DMF (5.00 mL). To this solution was added *N*,*N*-diisopropylethylamine (18.1 mg, 0.02 mL, 0.14 mmol, 2.00 eq) dropwise and the reaction solution was stirred at RT under an Ar atmosphere for 1 h. The yellow residue was added dropwise as

a solution in anhydrous CH_2Cl_2 (2.00 mL) and the reaction solution was stirred at RT under an Ar atmosphere for 18 h, after which time the reaction was adjudged to be complete by TLC analysis. The reaction was quenched with Et_2O (100 mL), washed with brine (100 mL), aq. 1 M HCl (100 mL), sat. aq. $NaHCO_3$ (100 mL), and brine (100 mL), dried over $MgSO_4$, and filtered. The solvent was removed under reduced pressure and the obtained crude residue was subjected to two successive purifications by silica gel flash column chromatography, eluting with $CHCl_3$ to $CHCl_3$:MeOH = 95:5 - 90:10 - 80:20, then $CHCl_3$ to $CHCl_3$:acetone 90:10 - 80:20 - 70:30 - 60:40, to afford 1-(*tert*-butyl) 4-((7-(diethylamino)-2-oxo-2*H*-chromen-4-yl)methyl) N^2-(((9*H*-fluoren-9-yl)methoxy)carbonyl)-N^6-(((5,5-difluoro-1,3,7,9-tetramethyl-5*H*-4$\boldsymbol{\lambda}$4,5$\boldsymbol{\lambda}$4-dipyrrolo[1,2-c:2',1'-f][1,3,2]diazaborinin-10-yl)methoxy)-carbonyl)-*L*-lysylglycyl-*L*-aspartate (**257**) as a pink solid (22.4 mg, 21%).

$\mathbf{R_f}$: 0.45 ($CHCl_3$:Acetone = 6:4);
m.p.: 117 - 119 °C (Hexane/Acetone);
$[\boldsymbol{\alpha}]_{\boldsymbol{D}}^{\mathbf{26}}$: +4.1 (***c*** 0.9 in $CHCl_3$);
UV $\boldsymbol{\lambda_{max}}$/nm ($\boldsymbol{\epsilon}$/$\mathbf{M^{-1}cm^{-1}}$): 380 (810), 515 (2650) [MeOH];
^{1}H NMR (400 MHz, $CDCl_3$) $\boldsymbol{\delta}$H: 7.71 (2H, d, J = 7.6 Hz, $C_{FmocAr}\mathbf{H}$), 7.57 (2H, d, J = 6.9 Hz, $C_{FmocAr}\mathbf{H}$), 7.49 (1H, dd, J = 4.7, 4.7 Hz, $N\mathbf{H}C_{Gly}H_2CO$), 7.37 (2H, t, J = 7.6 Hz, $C_{FmocAr}\mathbf{H}$), 7.33 - 7.28 (2H, m, $C_{FmocAr}\mathbf{H}$), 7.16 (1H, d, J = 8.6 Hz, $C_{DEACMAr}\mathbf{H}$), 7.08 (1H, d, J = 5.2 Hz, $N\mathbf{H}C_{Asp}HCH_2CO$), 6.53 (1H, dd, J = 8.6, 1.7 Hz, $C_{DEACMAr}\mathbf{H}$), 6.46 (1H, d, J = 1.7 Hz, $C_{DEACMAr}\mathbf{H}$), 6.05 (2H, s, $C_{BODIPY}\mathbf{H}$), 5.87 (1H, s, $C_{DEACMAlkene}\mathbf{H}$), 5.63 (1H, d, J = 8.2 Hz, $N\mathbf{H}C_{Lys}HCH_2CH_2$), 5.25 (1H, d, J = 13.8 Hz, $C_{BODIPY}C\mathbf{H}_AH_BO$), 5.21 (1H, d, J = 13.8 Hz, $C_{BODIPY}CH_A\mathbf{H}_BO$), 5.22 - 5.17 (1H, m, $N\mathbf{H}CH_2CH_2$), 5.18 (1H, d, J = 15.2 Hz, $C_{DEACMAlkene}C\mathbf{H}_AH_BO$), 5.14 (1H, d, J = 15.2 Hz, $C_{DEACMAlkene}CH_A\mathbf{H}_BO$), 4.78 - 4.65 (1H, m, $NHC_{Asp}\mathbf{H}CH_2CO$), 4.45 - 4.31 (2H, m, $C_{Fmoc}\mathbf{H}_2$), 4.22 - 4.03 (3H, m, $C_{Fmoc}\mathbf{H}$, $NHC_{Lys}\mathbf{H}CH_2CH_2$, $NHC_{Gly}\mathbf{H}_AH_BCO$), 3.89 (1H, dd, J = 17.0, 4.7 Hz, $NHC_{Gly}H_A\mathbf{H}_B$), 3.39 (4H, q, J = 6.6 Hz, $N(C\mathbf{H}_2CH_3)_2$), 3.25 - 3.16 (2H, m, $NHC_{Lys}\mathbf{H}_2CH_2$), 3.12 - 3.02 (2H, m, $NHC_{Asp}HC\mathbf{H}_AH_BCO$, $NHC_{Asp}HCH_A\mathbf{H}_BCO$), 2.51 (6H, s, $C_{BODIPY}C\mathbf{H}_3$), 2.37 (6H, s, $C_{BODIPY}\mathbf{C}_3$), 1.89 (1H, dd, J = 10.8, 5.3 Hz, $NHC_{Lys}HC\mathbf{H}_AH_BCH_2$), 1.76 - 1.69 (1H, m, $NHC_{Lys}HCH_A\mathbf{H}_BCH_2$), 1.52 - 1.48 (2H, m, $NHCH_2C\mathbf{H}_2$), 1.43 (9H, s, $OC(C\mathbf{H}_3)_3$), 1.39 - 1.35 (2H, m, $NHCHCH_2C\mathbf{H}_2$), 1.19 (6H, t, J = 6.6 Hz, $N(CH_2C\mathbf{H}_3)_2$);
^{13}C NMR (100 MHz, $CDCl_3$) $\boldsymbol{\delta}$C: 172.5 (**C**O) 170.1 (**C**O) 169.1 (**C**O) 168.9 (**C**O), 162.7 (**C**O), 156.4 (**C**O), 156.1 (**C**O), 156.0 ($\mathbf{C}_{DEACMAr}O$), 150.9 ($\mathbf{C}_{DEACMAr}N$),) 150.2 ($\mathbf{C}_{BODIPY}$), 143.7 ($\mathbf{C}_{FmocAr}$), 141.7 ($\mathbf{C}_{FmocAr}$), 141.2 ($\mathbf{C}_{BODIPY}$), 133.9 ($\mathbf{C}_{BODIPY}$),

132.7 ($\mathbf{C}_{\mathrm{BODIPY}}$), 127.7 + 127.6 ($\mathbf{C}_{\mathrm{FmocAr}}$H), 127.1 ($\mathbf{C}_{\mathrm{FmocAr}}$H), 125.1 ($\mathbf{C}_{\mathrm{FmocAr}}$H), 124.2 ($\mathbf{C}_{\mathrm{DEACMAr}}$H), 122.2 ($\mathbf{C}_{\mathrm{BODIPY}}$H), 120.0 ($\mathbf{C}_{\mathrm{DEACMAr}}$), 119.9 + 119.9 ($\mathbf{C}_{\mathrm{FmocAr}}$H), 108.91 ($\mathbf{C}_{\mathrm{DEACMAr}}$H), 105.6 ($\mathbf{C}_{\mathrm{DEACMAlkene}}$), 104.5 ($\mathbf{C}_{\mathrm{DEACMAlkene}}$H), 97.7 ($\mathbf{C}_{\mathrm{DEACMAr}}$H), 83.1 (O$\mathbf{C}$($CH_3$)$_3$), 67.0 ($\mathbf{C}_{\mathrm{Fmoc}}H_2$), 61.4 ($C_{\mathrm{DEACMAlkene}}\mathbf{C}H_2O$), 57.9 ($C_{\mathrm{BODIPY}}\mathbf{C}H_2O$), 55.3 (NH$\mathbf{C}_{\mathrm{Lys}}HCH_2CH_2$), 49.8 (NH$\mathbf{C}_{\mathrm{Asp}}HCH_2$CO), 47.1 ($\mathbf{C}_{\mathrm{Fmoc}}$H), 44.8 (N($\mathbf{C}H_2CH_3$)$_2$), 43.0 (NH$\mathbf{C}_{\mathrm{Gly}}H_2$CO), 40.5 (NH$\mathbf{C}_{\mathrm{Lys}}H_2CH_2$), 36.2 (NHC$_{\mathrm{Asp}}H\mathbf{C}H_2$CO), 31.7 (NHC$_{\mathrm{Lys}}H\mathbf{C}H_2CH_2$), 29.4 (NHC$_{\mathrm{Lys}}H_2\mathbf{C}H_2$), 27.8 (OC($\mathbf{C}H_3$)$_3$), 22.3 (NHC$_{\mathrm{Lys}}HCH_2\mathbf{C}H_2$), 15.6 ($C_{\mathrm{BODIPY}}\mathbf{C}H_3$), 14.7 ($C_{\mathrm{BODIPY}}\mathbf{C}H_3$), 12.4 (N(CH$_2\mathbf{C}H_3$)$_2$);

^{19}F NMR(376 MHz, $CDCl_3$) $\boldsymbol{\delta}$F: -146.3 (2F, q, J = 32.2 Hz, B$\mathbf{F}_2$);

LRMS *m/z* (ESI$^+$): 1131 (100% [M + H]$^+$);

HRMS *m/z* (ESI$^+$): Found 1152.5048 [M + Na]$^+$ ($C_{60}H_{70}BF_2N_7NaO_{12}{}^+$ requires 1152.5036 [M + Na]$^+$);

IR ($\boldsymbol{\nu}_{\mathbf{max}}$ cm^{-1}): 2965 (w, br), 2862 (w), 2362 (s), 2193 (w), 1723 (m, C=O), 1602 (m, C=O), 1559 (m, Ar C-C), 1514 (m, Ar C-C), 1456 (w), 1365 (w), 1266 (m, C-N), 1191 (m, C-O), 1075 (w), 982 (w), 915 (w), 813 (w), 747 (w), 667 (m); HPLC: 15.56 min (91.4%).

7.12 Caged Peptides - Solid Phase Peptide Synthesis

Solid Phase Peptide Synthesis was conducted at and in conjunction with **Peptide Protein Reseach Ltd.**. Peptides were supplied at > 95% purity.
Non-modified amino acids were added to the peptide chain, held on the resin, through use of a peptide synthesiser, following standard peptide coupling protocols.
Modified amino acids were added to the peptide chain, held on the resin, manually following the procedures listed below.

7.12.1 Linking Amino Acid to Resin

A P10 was washed with acetone and allowed to dry on a heating block for 30 min. To the resin (300 mg) was added the amino acid (loading = 0.4 mmol/g), DIPEA (0.50 mL), DMF (1.00 mL) and CH_2Cl_2 (1.00 mL). The resin was left to shake for 1 h before plunging out the solution.
To the resin was added DIPEA (0.50 mL), DMF (1.00 mL) and MeOH (2.50 mL) to cap any unreacted resin. The resin was left to shake for 1 h before being washed with DMF (3 × 5.00 mL) and CH_2Cl_2 (3 × 5.00 mL). The resin was then used for further peptide synthesis.

7.12.2 Addition of Amino Acid to Peptide Chain

To the resin (300 mg) was added PyBOP (150 mg), DIPEA (125 µL), NMP (1.00 mL) and the amino acid (2 - 5 eq) to be coupled. The resin was left to shake for 1 h before being washed with DMF (3 × 5.00 mL) and CH_2Cl_2 (3 × 5.00 mL).
If the reaction did not go to completion, the resin could be subjected to further repeat reactions following the protocol above.

7.12.3 Cleavage of Peptide from CTR Resin

The resin (300 mg) was washed with 50% HFIP in CH_2Cl_2 (3 × 5.00 mL), shaking the resin in the solution for 10 min each time and collecting all the washings. The combined washings were concentrated under reduced pressure to afford the crude peptide.

7.12.4 Experimental Data

7.12.4.1 Tripeptides

KLD
Colourless solid;
LCMS *m/z* (ESI$^+$): 597.2 (100% $[M + H]^+$); 3.91 min (100%)

KLD-DEACM
Pale yellow solid;
UV λ_{max}/nm (ϵ/M^{-1}cm^{-1}): 380 (22840) [MeOH];
LCMS *m/z* (ESI$^+$): 826.2 (100% $[M + H]^+$); 5.07 min (100%)

BODIPY-KLD
Bright orange solid;
UV λ_{max}/nm (ϵ/M^{-1}cm^{-1}): 515 (65340) [MeOH];
LCMS *m/z* (ESI$^+$): 918.3 (100% $[M + NH_4]^+$); 5.48 min (100%)

BODIPY-KLD-DEACM
Bright pink solid;
UV λ_{max}/nm (ϵ/M^{-1}cm^{-1}): 380 (28560), 520 (60470) [MeOH];
LCMS *m/z* (ESI$^+$): 1130.3 (100% $[M + H]^+$); 6.23 min (97%)

7.12.4.2 Hexapeptides

KGSTAD
Colourless solid;
LCMS *m/z* (ESI$^+$): 798.3 (100% $[M - H]^-$); 3.05 min (%)

KGSTAD-DEACM
Pale yellow solid;
UV λ_{max}/nm (ϵ/M^{-1}cm^{-1}): 385 (8440) [H_2O];
LCMS *m/z* (ESI$^+$): 1027.4 (100% $[M - H]^-$); 3.81 min (%)

BODIPY-KGSTAD
Orange solid;
UV λ_{max}/nm (ϵ/M^{-1}cm^{-1}): 520 (680) [H_2O];

LCMS m/z (ESI^+): 1102.5 (100% $[M - H]^-$); 4.94 min (%)

BODIPY-KGSTAD-DEACM

Coral pink solid;

UV λ_{max}/nm ($\epsilon/M^{-1}cm^{-1}$): 385 (2310), 525 (3570) [H_2O];

LCMS m/z (ESI^+): 1331.6 (100% $[M + H]^+$); 5.46 min (%)

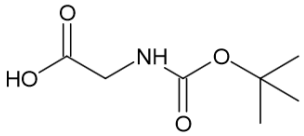
Appendix A

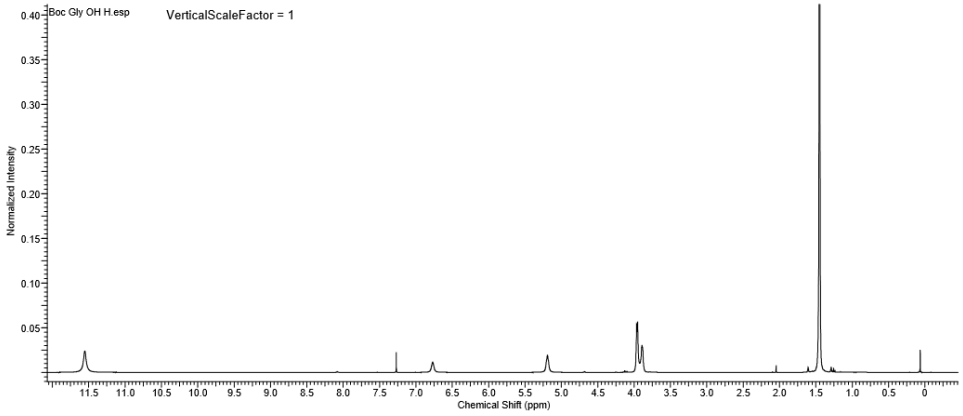
NMR Spectra

A.1 DMNB Caged GSH and ESG

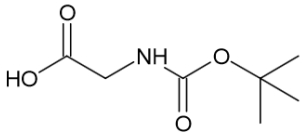
Compound 130

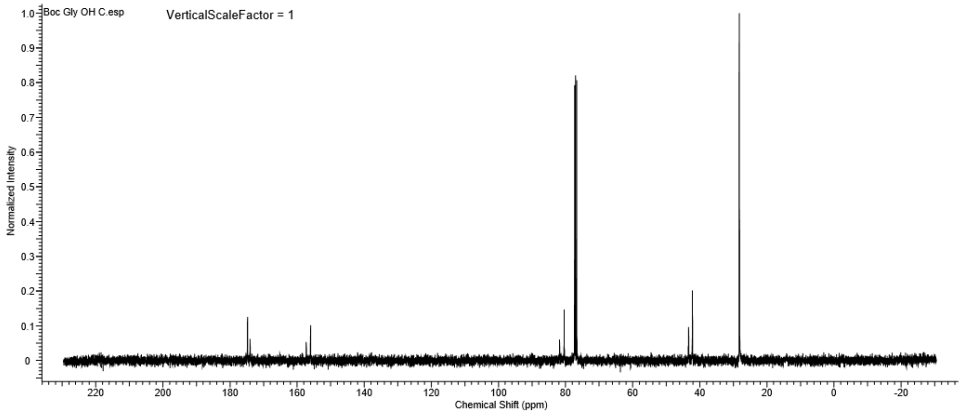
Acquisition Time (sec)	3.9584	*Comment*	Instrument DQX400 Chemist MLS Group SJC MLS01024 h1acq au CDCl3 {E:\NMR2011} sjcgrp 23				
Date	12 Sep 2011 20:12:00			*Date Stamp*	12 Sep 2011 20:12:00		
File Name	D:\Gnomeeee\NMR\Ken\Boc Gly OH\Sep12-2011-23\1\PDATA\1\1r			*Frequency (MHz)*	400.20	*Nucleus*	1H
Number of Transients	16	*Origin*	av400	*Original Points Count*	32768	*Owner*	dp-nmrgroup
Points Count	32768	*Pulse Sequence*	zg60	*Receiver Gain*	40.30	*SW(cyclical) (Hz)*	8278.15
Solvent	CHLOROFORM-d	*Spectrum Offset (Hz)*	2468.9956	*Spectrum Type*	STANDARD	*Sweep Width (Hz)*	8277.89
Temperature (degree C)	27.000						





Acquisition Time (sec)	0.6259	*Comment*	Instrument DQX400 Chemist MLS Group SJC MLS01024 c13acq au CDCl3 {E:\NMR2011} sjcgrp 23				
Date	12 Sep 2011 20:26:56			*Date Stamp*	12 Sep 2011 20:26:56		
File Name	D:\Gnomeeee\NMR\Ken\Boc Gly OH\Sep12-2011-23\3\PDATA\1\1r			*Frequency (MHz)*	100.63	*Nucleus*	13C
Number of Transients	256	*Origin*	av400	*Original Points Count*	16384	*Owner*	dp-nmrgroup
Points Count	32768	*Pulse Sequence*	zgpg30	*Receiver Gain*	32768.00	*SW(cyclical) (Hz)*	26178.01
Solvent	CHLOROFORM-d	*Spectrum Offset (Hz)*	10020.1807	*Spectrum Type*	STANDARD	*Sweep Width (Hz)*	26177.21
Temperature (degree C)	27.000						

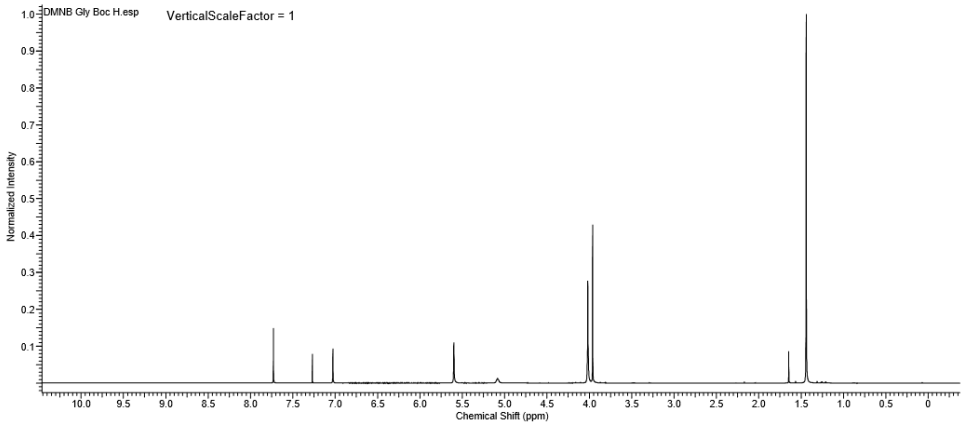




Compound 131

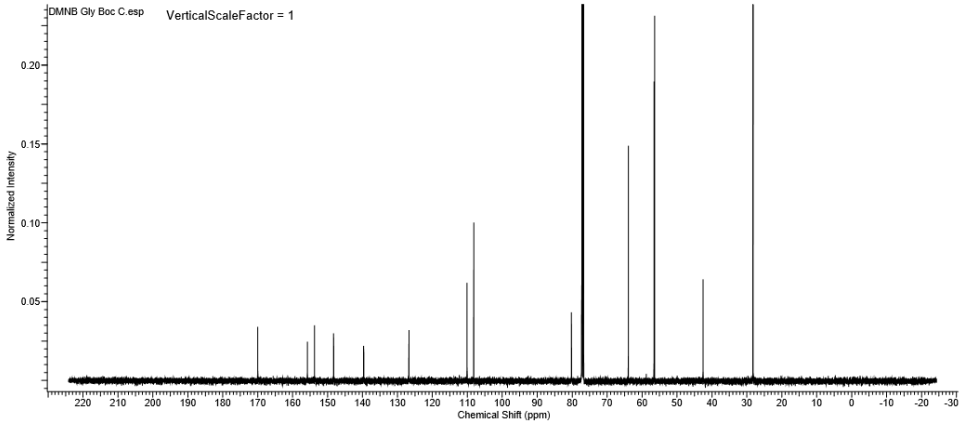
Acquisition Time (sec)	3.1719	*Comment*	Instrument AVC500 Group SJC 7534 Michelle Savage 19/1/12			*Date*	19 Jan 2012 09:12:32
Date Stamp	19 Jan 2012 09:12:32			*File Name*	D:\Gnomeeee\NMR\Kef\DMNB Gly Boc\1\fid		
Frequency (MHz)	500.30	*Nucleus*	1H	*Number of Transients*	16	*Origin*	avc500
Original Points Count	32768	*Owner*	dp-nmrgroup	*Points Count*	32768	*Pulse Sequence*	zg30
Receiver Gain	4.00	*SW(cyclical) (Hz)*	10330.58	*Solvent*	CHLOROFORM-d		
Spectrum Offset (Hz)	3066.0798	*Spectrum Type*	STANDARD	*Sweep Width (Hz)*	10330.26	*Temperature (degree C)*	24.970





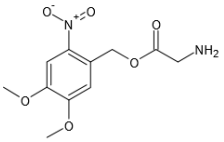
Acquisition Time (sec)	1.0486	*Comment*	Instrument AVC500 Group SJC 7534 Michelle Savage 19/1/12			*Date*	19 Jan 2012 09:46:40
Date Stamp	19 Jan 2012 09:46:40			*File Name*	D:\Gnomeeee\NMR\Kef\DMNB Gly Boc\4\fid		
Frequency (MHz)	125.80	*Nucleus*	13C	*Number of Transients*	256	*Origin*	avc500
Original Points Count	32768	*Owner*	dp-nmrgroup	*Points Count*	32768	*Pulse Sequence*	zgpg30
Receiver Gain	1820.00	*SW(cyclical) (Hz)*	31250.00	*Solvent*	CHLOROFORM-d		
Spectrum Offset (Hz)	12569.1221	*Spectrum Type*	STANDARD	*Sweep Width (Hz)*	31249.05	*Temperature (degree C)*	24.970

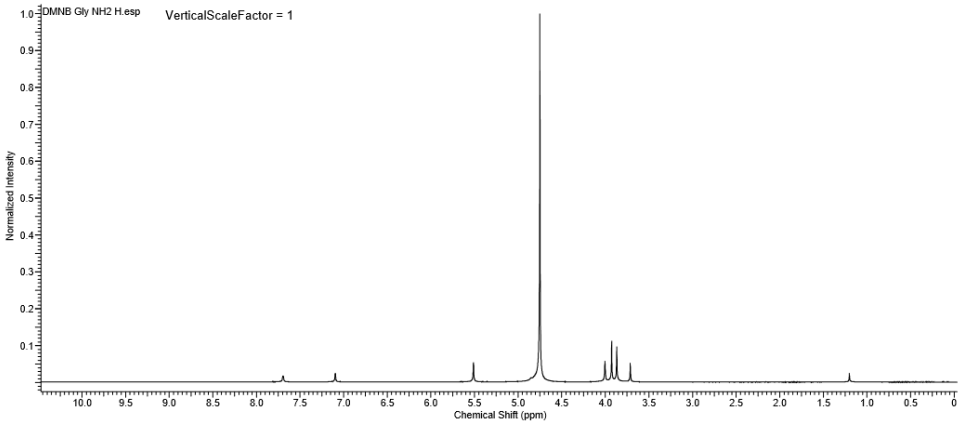




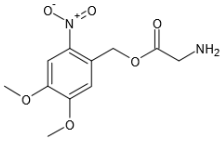
Compound 132

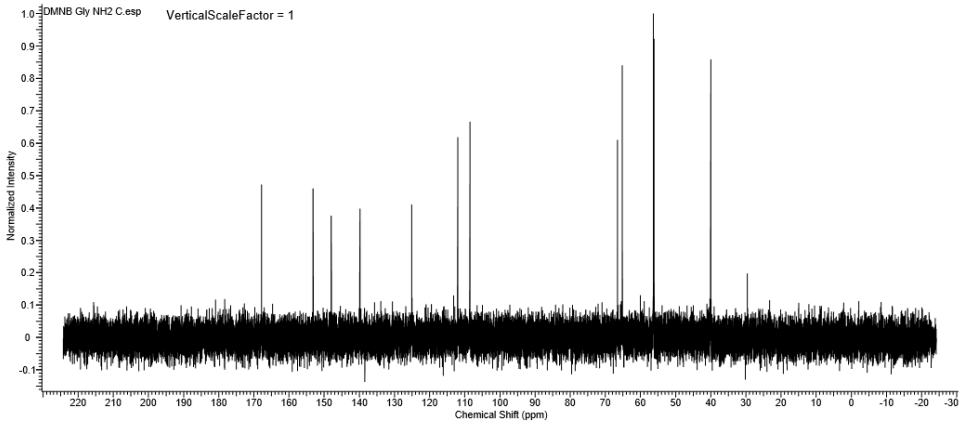
Acquisition Time (sec)	3.1719	*Comment*	Instrument AVC500 Group SJC 7535 Michelle Savage 20/1/12	*Date*	20 Jan 2012 09:50:56		
Date Stamp	20 Jan 2012 09:50:56			*File Name*	D:\Gnomeeee\NMR\Kef\DMNB Gly NH2\1\fid		
Frequency (MHz)	500.39	*Nucleus*	1H	*Number of Transients*	16	*Origin*	avc500
Original Points Count	32768	*Owner*	dp-nmrgroup	*Points Count*	32768	*Pulse Sequence*	zg30
Receiver Gain	4.00	*SW(cyclical) (Hz)*	10330.58	*Solvent*	DEUTERIUM OXIDE		
Spectrum Offset (Hz)	3112.0938	*Spectrum Type*	STANDARD	*Sweep Width (Hz)*	10330.26	*Temperature (degree C)*	24.970





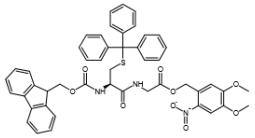
Acquisition Time (sec)	1.0486	*Comment*	Instrument AVC500 Group SJC 7535 Michelle Savage 20/1/12	*Date*	20 Jan 2012 10:27:12		
Date Stamp	20 Jan 2012 10:27:12			*File Name*	D:\Gnomeeee\NMR\Kef\DMNB Gly NH2\4\fid		
Frequency (MHz)	125.80	*Nucleus*	13C	*Number of Transients*	256	*Origin*	avc500
Original Points Count	32768	*Owner*	dp-nmrgroup	*Points Count*	32768	*Pulse Sequence*	zgpg30
Receiver Gain	1820.00	*SW(cyclical) (Hz)*	31250.00	*Solvent*	DEUTERIUM OXIDE		
Spectrum Offset (Hz)	12580.1094	*Spectrum Type*	STANDARD	*Sweep Width (Hz)*	31249.05	*Temperature (degree C)*	24.970

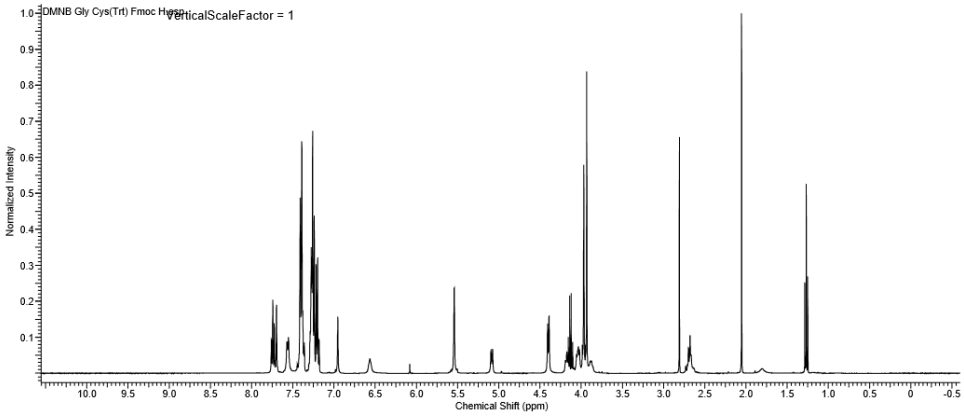




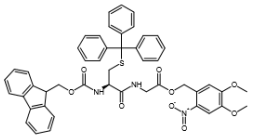
Compound 133

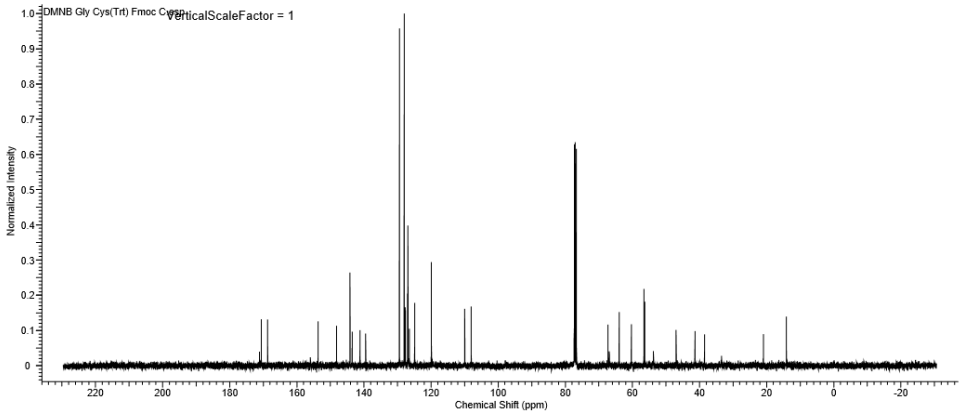
Acquisition Time (sec)	3.9584	*Comment*	Instrument DQX400 Chemist MLS Group SJC MLS01098 h1acq.au CDCl3 (E:\NMR2011) sjcgrp 17				
Date	21 Dec 2011 14:26:08			*Date Stamp*	21 Dec 2011 14:26:08		
File Name	D:\Gnomeeee\NMR\Kef\DMNB Gly Cys(Trt) Fmoc\Dec21-2011-17\1\PDATA\1\1r					*Frequency (MHz)*	400.20
Nucleus	1H	*Number of Transients*	16	*Origin*	av400	*Original Points Count*	32768
Owner	dp-nmrgroup	*Points Count*	32768	*Pulse Sequence*	zg60	*Receiver Gain*	35.90
SW(cyclical) (Hz)	8278.15	*Solvent*	CHLOROFORM-d	*Spectrum Offset (Hz)*	2468.5974	*Spectrum Type*	STANDARD
Sweep Width (Hz)	8277.89	*Temperature (degree C)*	27.000				





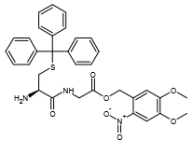
Acquisition Time (sec)	0.6259	*Comment*	Instrument DQX400 Chemist MLS Group SJC MLS01098 c13acq.au CDCl3 (E:\NMR2011) sjcgrp 17				
Date	21 Dec 2011 14:38:56			*Date Stamp*	21 Dec 2011 14:38:56		
File Name	D:\Gnomeeee\NMR\Kef\DMNB Gly Cys(Trt) Fmoc\Dec21-2011-17\3\PDATA\1\1r					*Frequency (MHz)*	100.63
Nucleus	13C	*Number of Transients*	256	*Origin*	av400	*Original Points Count*	16384
Owner	dp-nmrgroup	*Points Count*	32768	*Pulse Sequence*	zgpg30	*Receiver Gain*	32768.00
SW(cyclical) (Hz)	26178.01	*Solvent*	CHLOROFORM-d	*Spectrum Offset (Hz)*	10012.1914	*Spectrum Type*	STANDARD
Sweep Width (Hz)	26177.21	*Temperature (degree C)*	27.000				

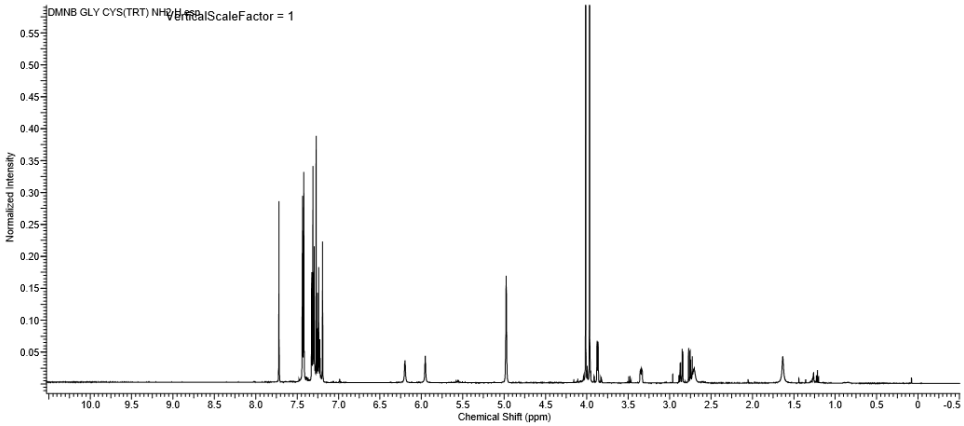




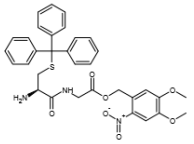
Compound 134

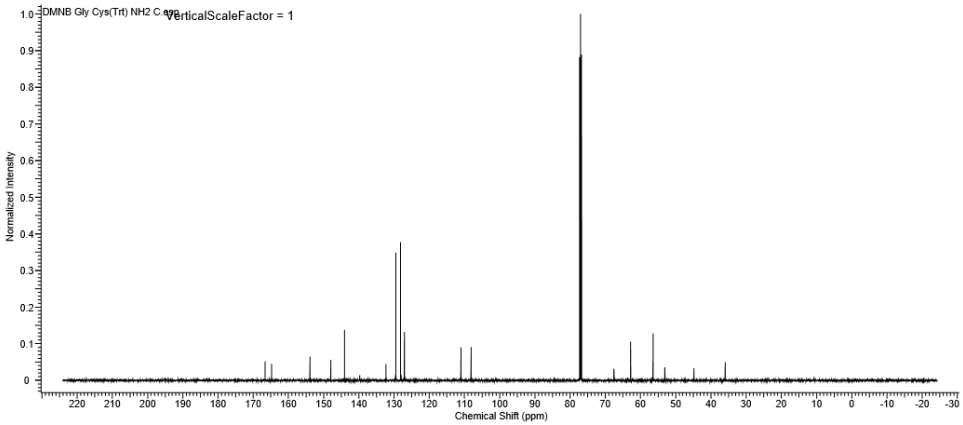
Acquisition Time (sec)	3.1719	*Comment*	Instrument AVC500 Group SJC 7659 Michelle Savage 25/1/12			*Date*	25 Jan 2012 11:48:16
Date Stamp	25 Jan 2012 11:48:16			*File Name*	D:\GNOMEEEE\NMR\KEF\DMNB GLY CYS(TRT) NH2\1\FID		
Frequency (MHz)	500.30	*Nucleus*	1H	*Number of Transients*	16	*Origin*	avc500
Original Points Count	32768	*Owner*	dp-nmrgroup	*Points Count*	32768	*Pulse Sequence*	zg30
Receiver Gain	4.00	*SW(cyclical) (Hz)*	10330.58	*Solvent*	CHLOROFORM-d		
Spectrum Offset (Hz)	3066.3953	*Spectrum Type*	STANDARD	*Sweep Width (Hz)*	10330.26	*Temperature (degree C)*	24.970





Acquisition Time (sec)	1.0486	*Comment*	Instrument AVC500 Group SJC 7659 Michelle Savage 25/1/12			*Date*	25 Jan 2012 12:16:00
Date Stamp	25 Jan 2012 12:16:00			*File Name*	D:\Gnomeeee\NMR\Kef\DMNB Gly Cys(Trt) NH2\4\fid		
Frequency (MHz)	125.80	*Nucleus*	13C	*Number of Transients*	512	*Origin*	avc500
Original Points Count	32768	*Owner*	dp-nmrgroup	*Points Count*	32768	*Pulse Sequence*	zgpg30
Receiver Gain	1820.00	*SW(cyclical) (Hz)*	31250.00	*Solvent*	CHLOROFORM-d		
Spectrum Offset (Hz)	12571.3047	*Spectrum Type*	STANDARD	*Sweep Width (Hz)*	31249.05	*Temperature (degree C)*	25.076

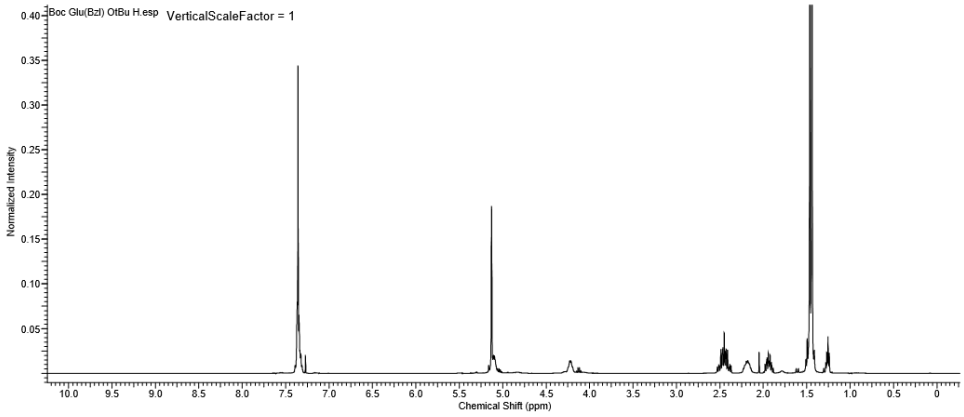




Compound 137

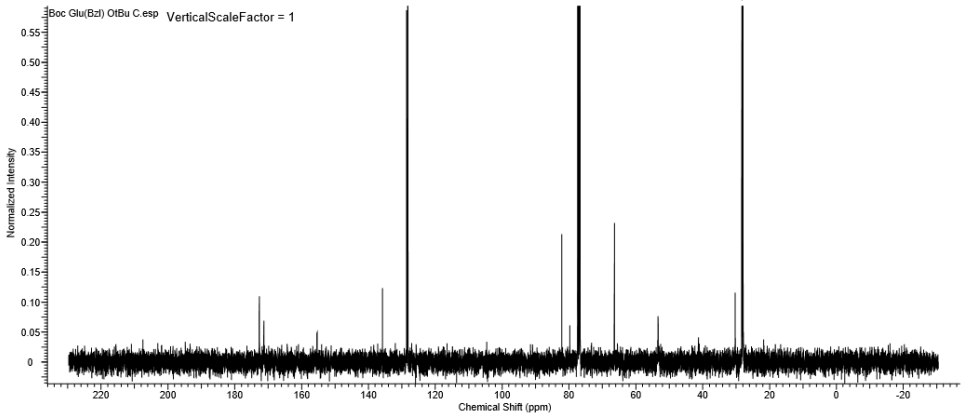
Acquisition Time (sec)	3.9584	*Comment*	Instrument DQX400 Chemist MLS Group SJC MLS01064 h1acq.au CDCl3 {E:\NMR2011} sjcgrp 52				
Date	26 Oct 2011 19:54:56			*Date Stamp*	26 Oct 2011 19:54:56		
File Name	D:\Gnomeeee\NMR\Kefi\Boc Glu(Bzl)OtBu\Oct26-2011-52\6\PDATA\1\1r					*Frequency (MHz)*	400.20
Nucleus	1H	*Number of Transients*	16	*Origin*	av400	*Original Points Count*	32768
Owner	dp-nmrgroup	*Points Count*	32768	*Pulse Sequence*	zg60	*Receiver Gain*	40.30
SW(cyclical) (Hz)	8278.15	*Solvent*	CHLOROFORM-d	*Spectrum Offset (Hz)*	2469.5007	*Spectrum Type*	STANDARD
Sweep Width (Hz)	8277.89	*Temperature (degree C)*	27.000				





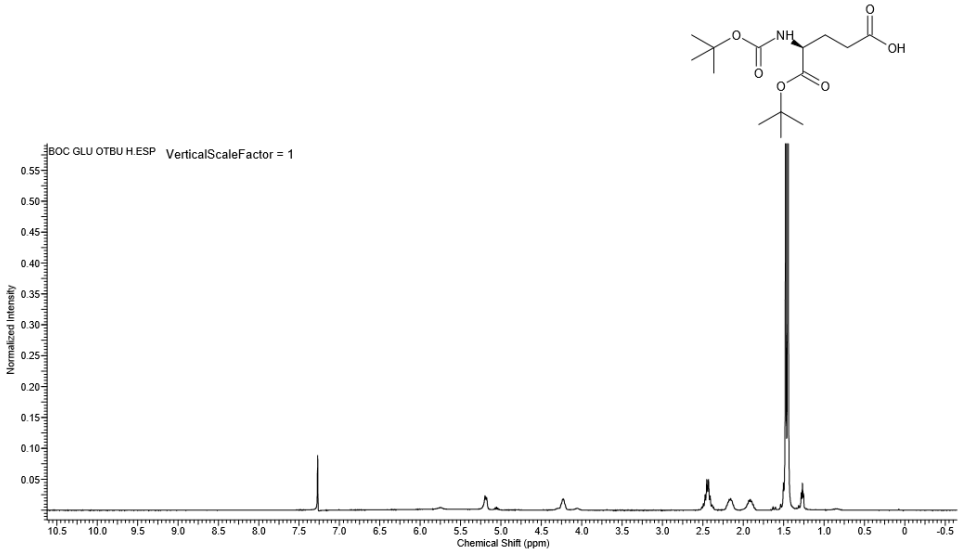
Acquisition Time (sec)	0.6259	*Comment*	Instrument DQX400 Chemist MLS Group SJC MLS01064 c13acq.au CDCl3 {E:\NMR2011} sjcgrp 52				
Date	26 Oct 2011 20:07:44			*Date Stamp*	26 Oct 2011 20:07:44		
File Name	D:\Gnomeeee\NMR\Kefi\Boc Glu(Bzl)OtBu\Oct26-2011-52\8\PDATA\1\1r					*Frequency (MHz)*	100.63
Nucleus	13C	*Number of Transients*	256	*Origin*	av400	*Original Points Count*	16384
Owner	dp-nmrgroup	*Points Count*	32768	*Pulse Sequence*	zgpg30	*Receiver Gain*	32768.00
SW(cyclical) (Hz)	26178.01	*Solvent*	CHLOROFORM-d	*Spectrum Offset (Hz)*	10021.2939	*Spectrum Type*	STANDARD
Sweep Width (Hz)	26177.21	*Temperature (degree C)*	27.000				





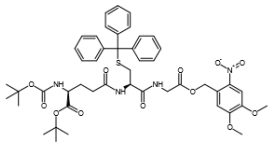
Compound 138

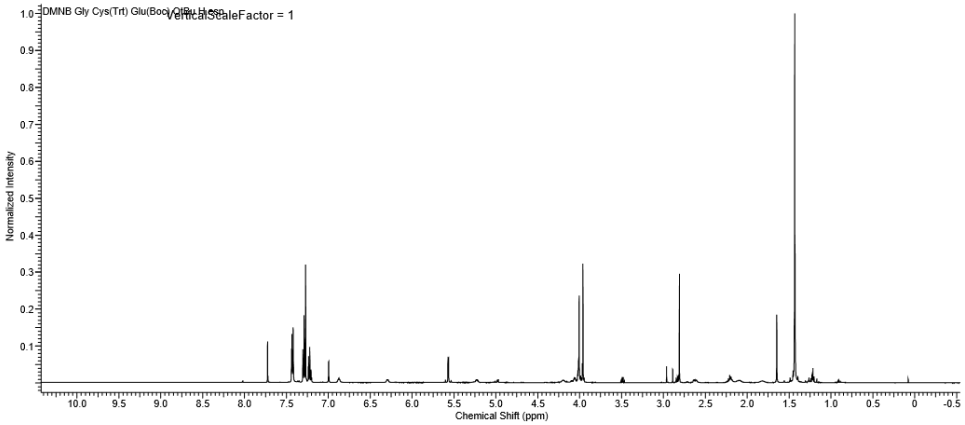
Acquisition Time (sec)	3.9584	*Comment*	Instrument DQX400 Chemist MLS Group SJC MLS01068 h1acq au CDCl3 (E:\NMR2011) sjcgrp 15				
Date	21 Dec 2011 13:26:24			*Date Stamp*	21 Dec 2011 13:26:24		
File Name	D:\Gnomeeee\NMR\Kef\Boc Glu OtBu\1\PDATA\1\1r			*Frequency (MHz)*	400.20	*Nucleus*	1H
Number of Transients	16	*Origin*	av400	*Original Points Count*	32768	*Owner*	dp-nmrgroup
Points Count	32768	*Pulse Sequence*	zg60	*Receiver Gain*	228.10	*SW(cyclical) (Hz)*	8278.15
Solvent	CHLOROFORM-d	*Spectrum Offset (Hz)*	2468.4902	*Spectrum Type*	STANDARD	*Sweep Width (Hz)*	8277.89
Temperature (degree C)	27.000						



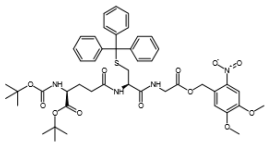
Compound 135

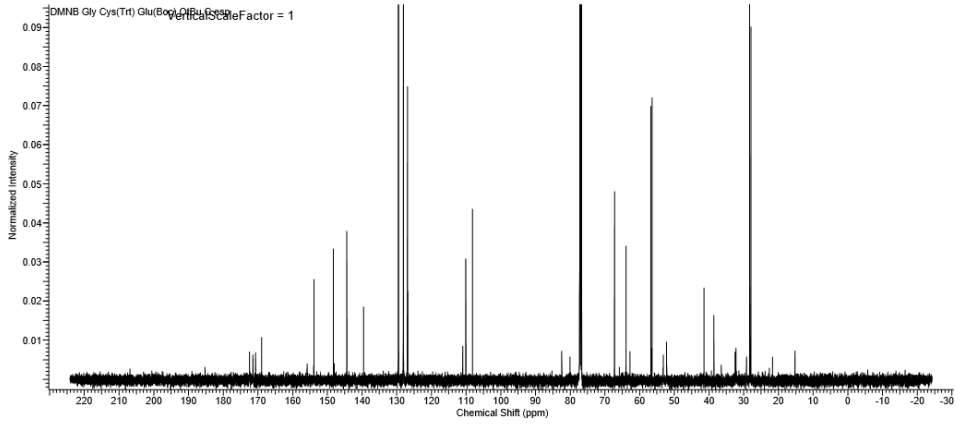
Acquisition Time (sec)	3.1719	*Comment*	Instrument AVC500 Group SJC 7660 Michelle Savage 25/1/12			*Date*	25 Jan 2012 12:43:44
Date Stamp	25 Jan 2012 12:43:44			*File Name*	D:\Gnomeeee\NMR\Kef\DMNB Gly Cys(Trt) Glu(Boc) OtBu\1\fid		
Frequency (MHz)	500.30	*Nucleus*	1H	*Number of Transients*	16	*Origin*	avc500
Original Points Count	32768	*Owner*	dp-nmrgroup	*Points Count*	32768	*Pulse Sequence*	zg30
Receiver Gain	4.00	*SW(cyclical) (Hz)*	10330.58	*Solvent*	CHLOROFORM-d		
Spectrum Offset (Hz)	3066.3953	*Spectrum Type*	STANDARD	*Sweep Width (Hz)*	10330.26	*Temperature (degree C)*	24.970





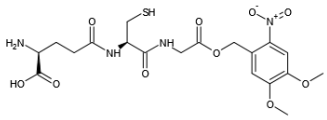
Acquisition Time (sec)	1.0486	*Comment*	Instrument AVC500 Group SJC 7660 Michelle Savage 25/1/12			*Date*	25 Jan 2012 13:32:48
Date Stamp	25 Jan 2012 13:32:48			*File Name*	D:\Gnomeeee\NMR\Kef\DMNB Gly Cys(Trt) Glu(Boc) OtBu\4\fid		
Frequency (MHz)	125.80	*Nucleus*	13C	*Number of Transients*	512	*Origin*	avc500
Original Points Count	32768	*Owner*	dp-nmrgroup	*Points Count*	32768	*Pulse Sequence*	zgpg30
Receiver Gain	812.00	*SW(cyclical) (Hz)*	31250.00	*Solvent*	CHLOROFORM-d		
Spectrum Offset (Hz)	12571.0293	*Spectrum Type*	STANDARD	*Sweep Width (Hz)*	31249.05	*Temperature (degree C)*	24.970

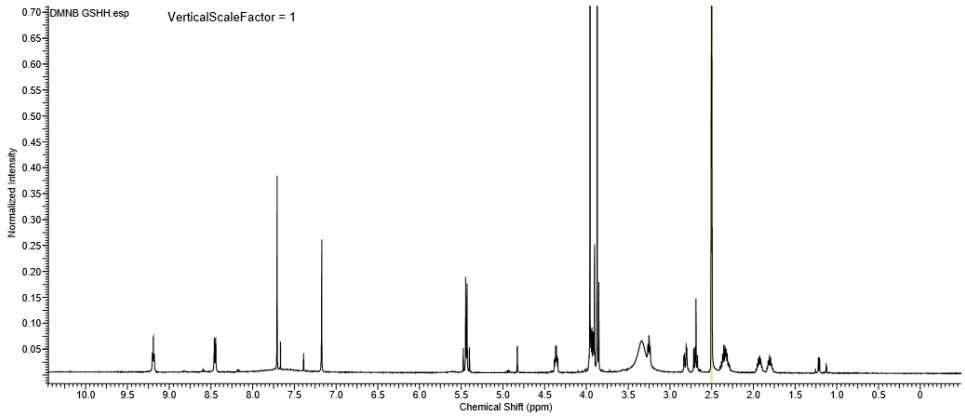




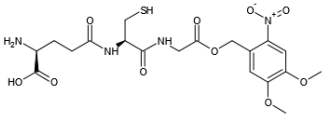
Compound 1

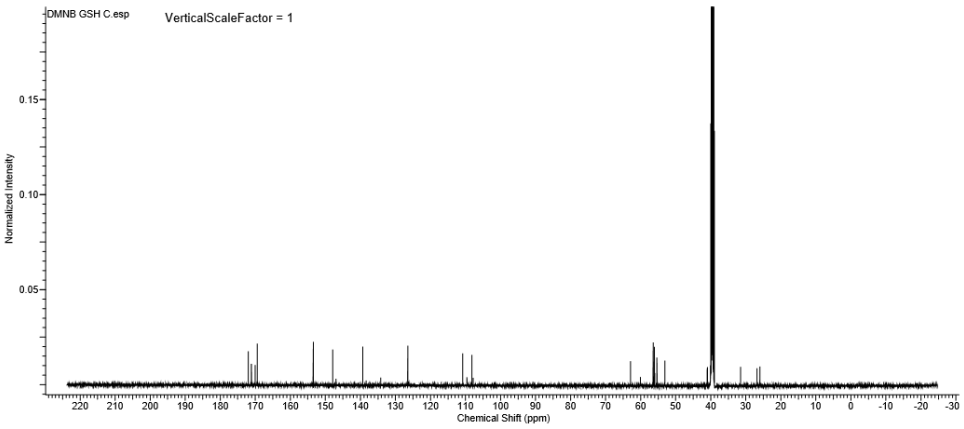
Acquisition Time (sec)	3.1719	*Comment*	Instrument AVC500 Group SJC 7384 Michelle Savage 9/1/12				
Date	09 Jan 2012 14:53:52			*Date Stamp*	09 Jan 2012 14:53:52		
File Name	D:\Gnomeeee\NMR\Kef\DMNB GSH\1\fid			*Frequency (MHz)*	500.30	*Nucleus*	1H
Number of Transients	16	*Origin*	avc500	*Original Points Count*	32768	*Owner*	dp-nmrgroup
Points Count	32768	*Pulse Sequence*	zg30	*Receiver Gain*	4.00	*SW(cyclical) (Hz)*	10330.58
Solvent	DMSO-d6	*Spectrum Offset (Hz)*	3084.1689	*Spectrum Type*	STANDARD	*Sweep Width (Hz)*	10330.26
Temperature (degree C)	24.970						





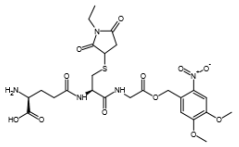
Acquisition Time (sec)	1.0486	*Comment*	Instrument AVC500 Group SJC 7384 Michelle Savage 9/1/12			*Date*	09 Jan 2012 15:21:36
Date Stamp	09 Jan 2012 15:21:36			*File Name*	D:\Gnomeeee\NMR\Kef\DMNB GSH\4\fid		
Frequency (MHz)	125.80	*Nucleus*	13C	*Number of Transients*	1536	*Origin*	avc500
Original Points Count	32768	*Owner*	dp-nmrgroup	*Points Count*	32768	*Pulse Sequence*	zgpg30
Receiver Gain	1820.00	*SW(cyclical) (Hz)*	31250.00	*Solvent*	DMSO-d6	*Spectrum Offset (Hz)*	12519.1904
Spectrum Type	STANDARD	*Sweep Width (Hz)*	31249.05	*Temperature (degree C)*	24.970		

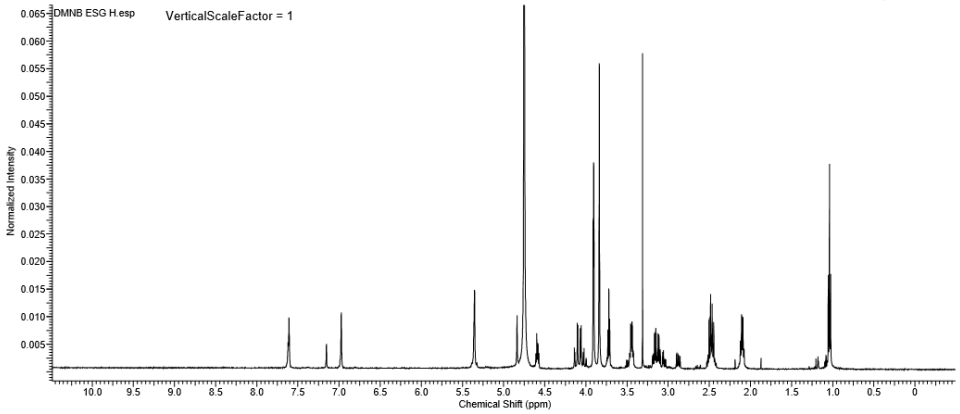




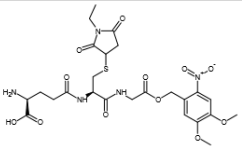
Compound 2

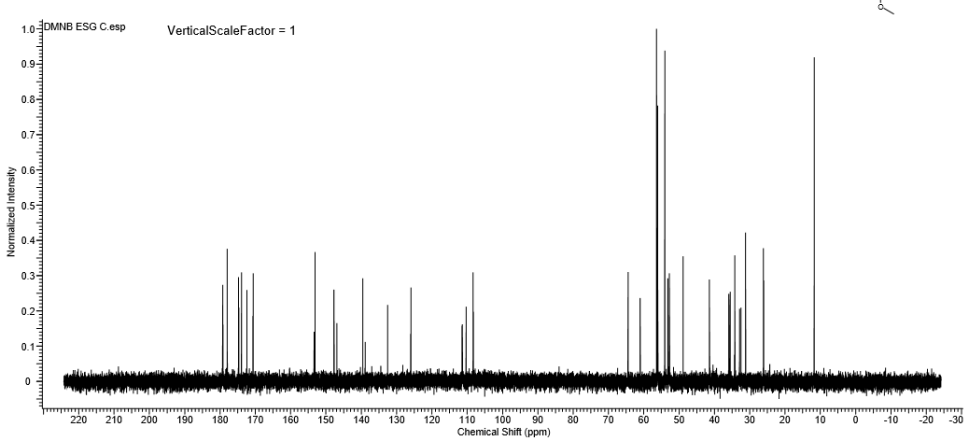
Acquisition Time (sec)	3.1719	*Comment*	Instrument AVC500 Group SJC 7452 Michelle Savage 13/1/12				
Date	13 Jan 2012 10:14:24			*Date Stamp*	13 Jan 2012 10:14:24		
File Name	D:\Gnomeeee\NMR\ms74521301\1\fid			*Frequency (MHz)*	500.30	*Nucleus*	1H
Number of Transients	16	*Origin*	avc500	*Original Points Count*	32768	*Owner*	dp-nmrgroup
Points Count	32768	*Pulse Sequence*	zg30	*Receiver Gain*	4.00	*SW(cyclical) (Hz)*	10330.58
Solvent	DEUTERIUM OXIDE			*Spectrum Offset (Hz)*	3112.7246	*Spectrum Type*	STANDARD
Sweep Width (Hz)	10330.26	*Temperature (degree C)*	24.970				





Acquisition Time (sec)	1.0486	*Comment*	Instrument AVC500 Group SJC 7452 Michelle Savage 13/1/12	*Date*	13 Jan 2012 11:33:20		
Date Stamp	13 Jan 2012 11:33:20			*File Name*	D:\Gnomeeee\NMR\Kef\DMNB ESG\4\fid		
Frequency (MHz)	125.80	*Nucleus*	13C	*Number of Transients*	1454	*Origin*	avc500
Original Points Count	32768	*Owner*	dp-nmrgroup	*Points Count*	32768	*Pulse Sequence*	zgpg30
Receiver Gain	1820.00	*SW(cyclical) (Hz)*	31250.00	*Solvent*	DEUTERIUM OXIDE		
Spectrum Offset (Hz)	12580.1094	*Spectrum Type*	STANDARD	*Sweep Width (Hz)*	31249.05	*Temperature (degree C)*	24.970

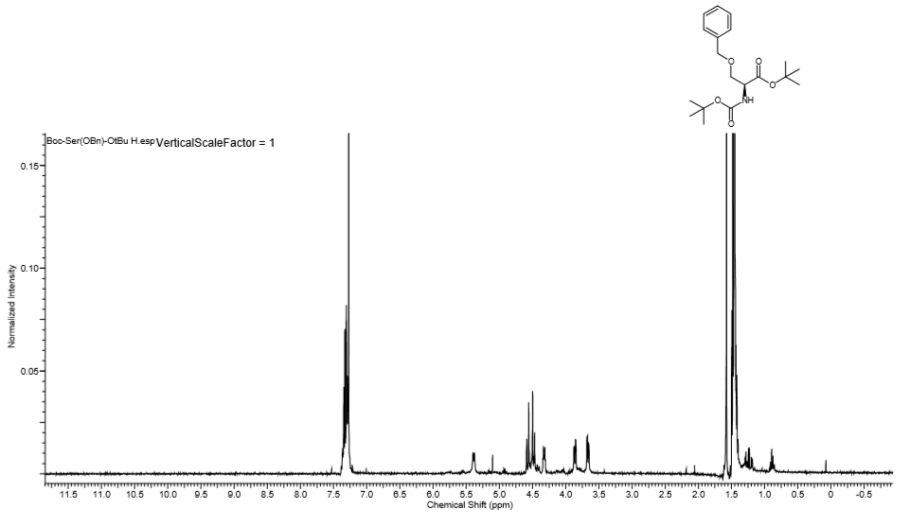




A.2 Amino Acid Residues

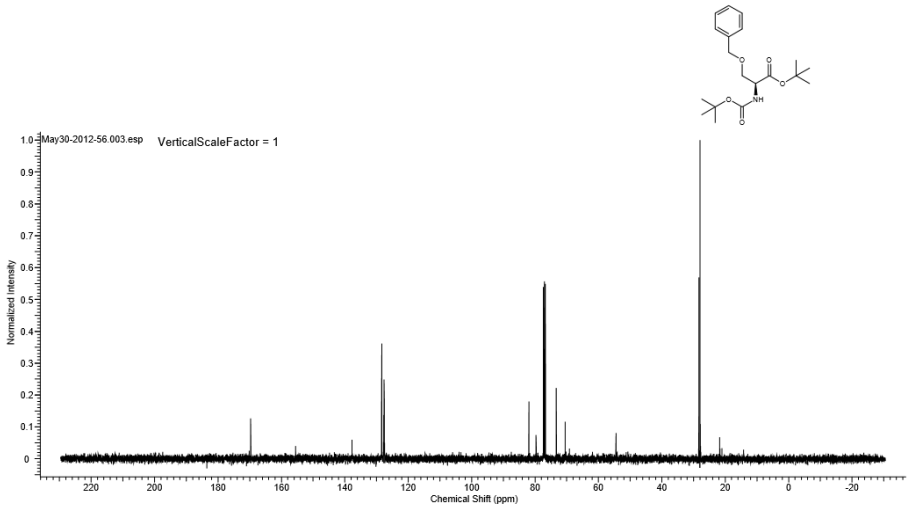
Compound 156

Acquisition Time (sec)	2.9295	*Comment*	Instrument DPX400 Chemist MLS Group SJC MLS01120 Qh1acq.au CDCl3 (C:\NMR) sjcgrp 56				
Date	22 Feb 2012 13:11:28			*Date Stamp*	22 Feb 2012 13:11:28		
File Name	F:\NMR\Amino Acid Residues\Boc Ser(OBn) OtBu\Feb22-2012-56\1\fid					*Frequency (MHz)*	400.13
Nucleus	1H	*Number of Transients*	16	*Origin*	dpx400	*Original Points Count*	16384
Owner	dp-nmrgroup	*Points Count*	16384	*Pulse Sequence*	zg30	*Receiver Gain*	228.10
SW(cydical) (Hz)	5592.84	*Solvent*	CHLOROFORM-d	*Spectrum Offset (Hz)*	1983.0062	*Spectrum Type*	STANDARD
Sweep Width (Hz)	5592.50	*Temperature (degree C)*	27.000				



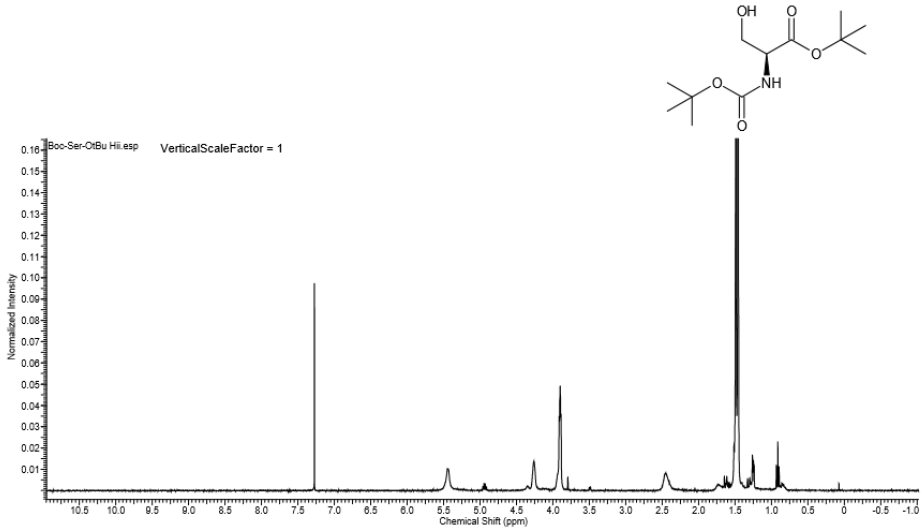
21/12/2014 3:33:45 PM

Acquisition Time (sec)	0.6259	*Comment*	Instrument DQX400 Chemist MLS Group SJC MLS01204 c13acq.au CDCl3 (E:\NMR2012) sjcgrp 56				
Date	31 May 2012 03:54:56			*Date Stamp*	31 May 2012 03:54:56		
File Name	F:\NMR\Amino Acid Residues\Boc Ser(OBn) OtBu\May30-2012-56\3\fid					*Frequency (MHz)*	100.63
Nucleus	13C	*Number of Transients*	256	*Origin*	av400	*Original Points Count*	16384
Owner	dp-nmrgroup	*Points Count*	16384	*Pulse Sequence*	zgpg30	*Receiver Gain*	32768.00
SW(cydical) (Hz)	26178.01	*Solvent*	CHLOROFORM-d	*Spectrum Offset (Hz)*	10021.2939	*Spectrum Type*	STANDARD
Sweep Width (Hz)	26176.41	*Temperature (degree C)*	27.000				



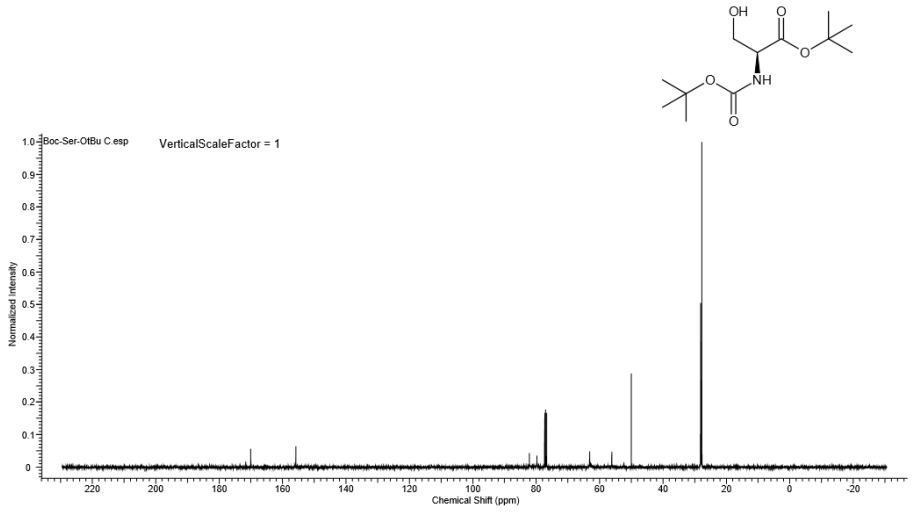
Compound 157

Acquisition Time (sec)	3.2768	*Comment*	Instrument AVG400 Group SJC Chemist MLS MLS04064 h1acq.orl CDCl3 (C:\NMR) sicgrp 40				
Date	16 Oct 2013 09:53:20			*Date Stamp*	16 Oct 2013 09:53:20		
File Name	F:\NMR\Amino Acid Residues\Boc Ser OtBu\Oct16-2013-40\1\fid			*Frequency (MHz)*	400.20	*Nucleus*	1H
Number of Transients	16	*Origin*	avq400	*Original Points Count*	32768	*Owner*	nmr-user
Points Count	32768	*Pulse Sequence*	zg30	*Receiver Gain*	255.20	*SW(cyclical) (Hz)*	10000.00
Solvent	CHLOROFORM-d	*Spectrum Offset (Hz)*	2482.2192	*Spectrum Type*	STANDARD	*Sweep Width (Hz)*	9999.70
Temperature (degree C)	21.700						



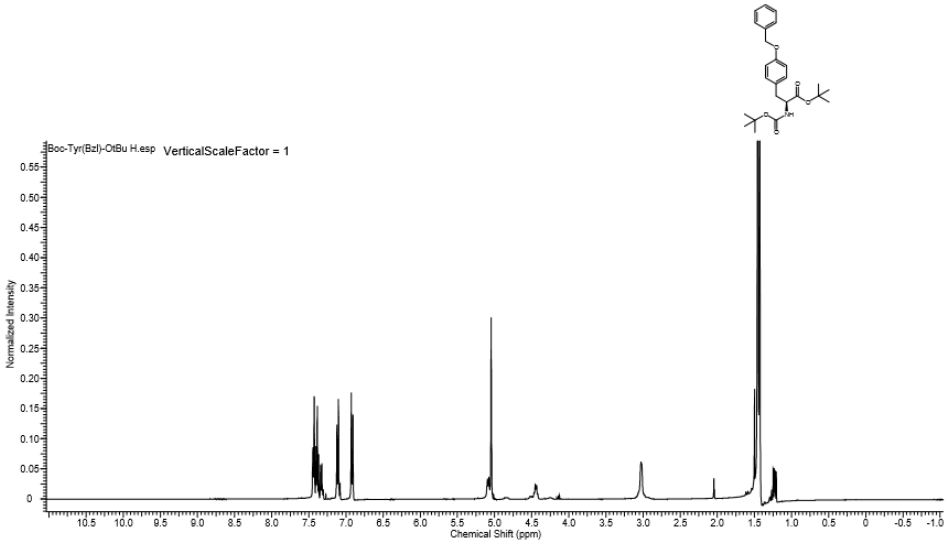
21/12/2014 4:28:47 PM

Acquisition Time (sec)	0.6259	*Comment*	Instrument DQX400 Chemist MLS Group SJC MLS01124 c13acq.au CDCl3 (E:\NMR2012) sicgrp 49				
Date	22 Feb 2012 14:51:44			*Date Stamp*	22 Feb 2012 14:51:44		
File Name	F:\NMR\Amino Acid Residues\Boc Ser OtBu\Feb22-2012-49\3\fid			*Frequency (MHz)*	100.63	*Nucleus*	13C
Number of Transients	256	*Origin*	av400	*Original Points Count*	16384	*Owner*	dp-nmrgroup
Points Count	16384	*Pulse Sequence*	zgpg30	*Receiver Gain*	32768.00	*SW(cyclical) (Hz)*	26178.01
Solvent	CHLOROFORM-d	*Spectrum Offset (Hz)*	10010.1943	*Spectrum Type*	STANDARD	*Sweep Width (Hz)*	26176.41
Temperature (degree C)	27.000						



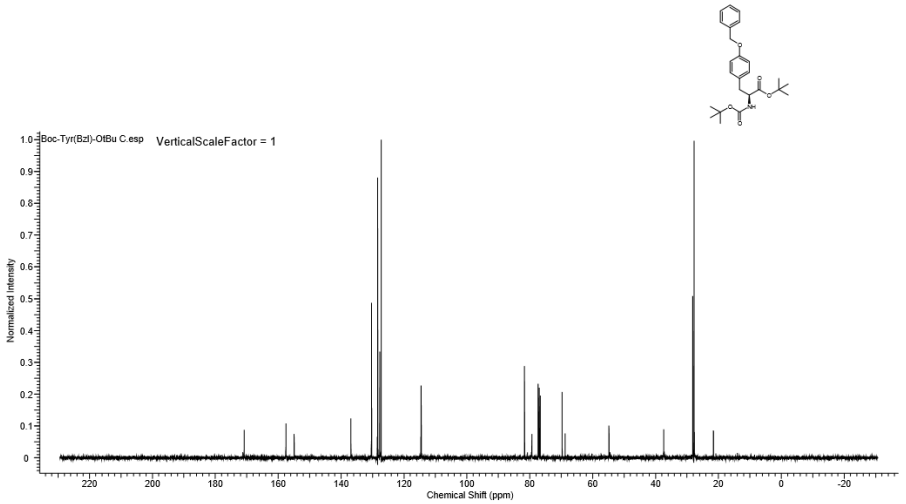
Compound 159

Acquisition Time (sec)	3.9584	*Comment*	Instrument DQX400 Chemist MLS Group SJC MLS01152 h1acq.au CDCl3 (E:\NMR2012) sjcgrp 13				
Date	14 Apr 2012 03:22:56			*Date Stamp*	14 Apr 2012 03:22:56		
File Name	F:\NMR\Amino Acid Residues\Boc Tyr(Bzl) OtBu\Apr13-2012-13\1\fid			*Frequency (MHz)*	400.20	*Nucleus*	1H
Number of Transients	16	*Origin*	av400	*Original Points Count*	32768	*Owner*	dp-nmrgroup
Points Count	32768	*Pulse Sequence*	zg30	*Receiver Gain*	12.70	*SW(cyclical) (Hz)*	8278.15
Solvent	CHLOROFORM-d	*Spectrum Offset (Hz)*	2469.5007	*Spectrum Type*	STANDARD	*Sweep Width (Hz)*	8277.89
Temperature (degree C)	27.000						



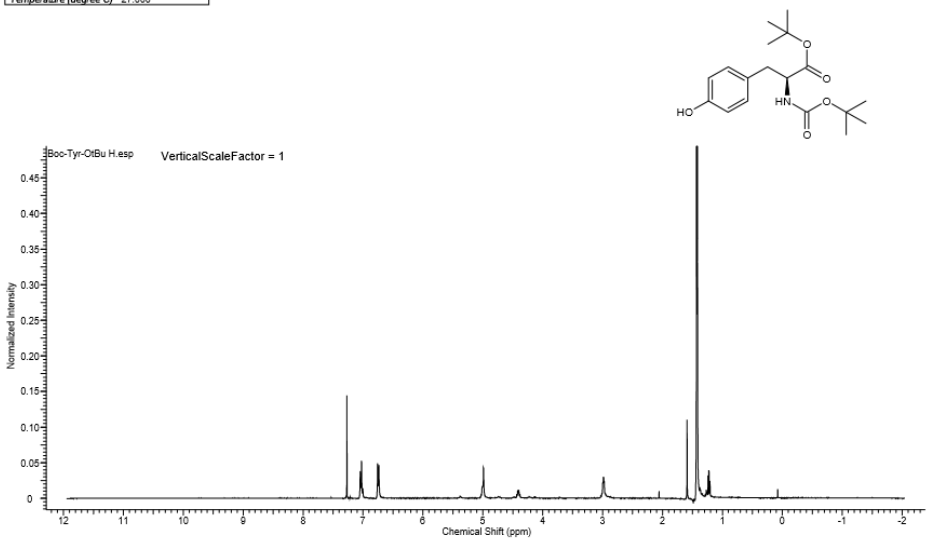
21/12/2014 5:48:46 PM

Acquisition Time (sec)	0.6259	*Comment*	Instrument DQX400 Chemist MLS Group SJC MLS01152 c13acq.au CDCl3 (E:\NMR2012) sjcgrp 13				
Date	14 Apr 2012 03:35:44			*Date Stamp*	14 Apr 2012 03:35:44		
File Name	F:\NMR\Amino Acid Residues\Boc Tyr(Bzl) OtBu\Apr13-2012-13\3\fid			*Frequency (MHz)*	100.63	*Nucleus*	13C
Number of Transients	256	*Origin*	av400	*Original Points Count*	16384	*Owner*	dp-nmrgroup
Points Count	16384	*Pulse Sequence*	zgpg30	*Receiver Gain*	32768.00	*SW(cyclical) (Hz)*	26178.01
Solvent	CHLOROFORM-d	*Spectrum Offset (Hz)*	9999.0098	*Spectrum Type*	STANDARD	*Sweep Width (Hz)*	26176.41
Temperature (degree C)	27.000						



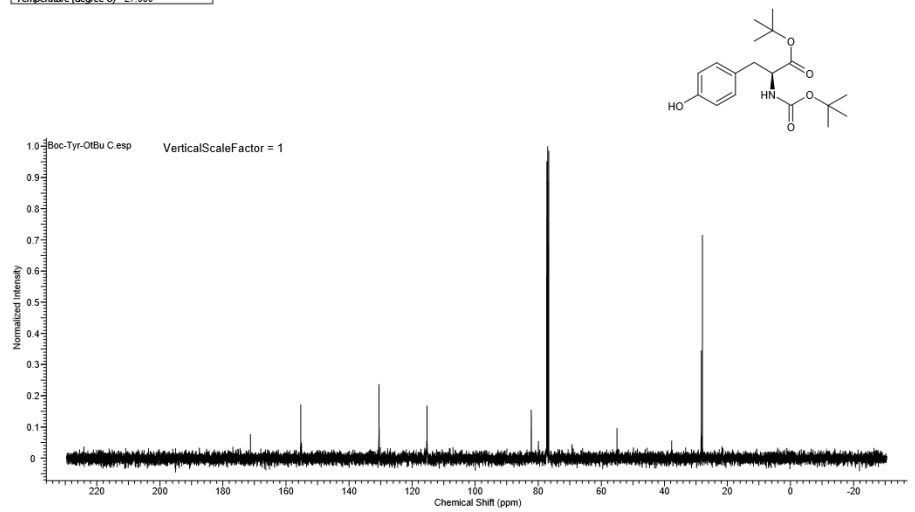
Compound 160

Acquisition Time (sec)	2.9295	*Comment*	Instrument DPX400 Chemist MLS Group SJC MLS01170 Qh1acq.au CDCl3 (C:\NMR) sjcgrp 52				
Date	23 Apr 2012 11:20:48			*Date Stamp*	23 Apr 2012 11:20:48		
File Name	F:\NMR\Amino Acid Residues\Boc Tyr OtBu\Apr23-2012-52\1\fid			*Frequency (MHz)*	400.13	*Nucleus*	1H
Number of Transients	16	*Origin*	dpx400	*Original Points Count*	16384	*Owner*	dp-nmrgroup
Points Count	16384	*Pulse Sequence*	zg30	*Receiver Gain*	228.10	*SW(cyclical) (Hz)*	5592.84
Solvent	CHLOROFORM-d	*Spectrum Offset (Hz)*	1982.6649	*Spectrum Type*	STANDARD	*Sweep Width (Hz)*	5592.50
Temperature (degree C)	27.000						



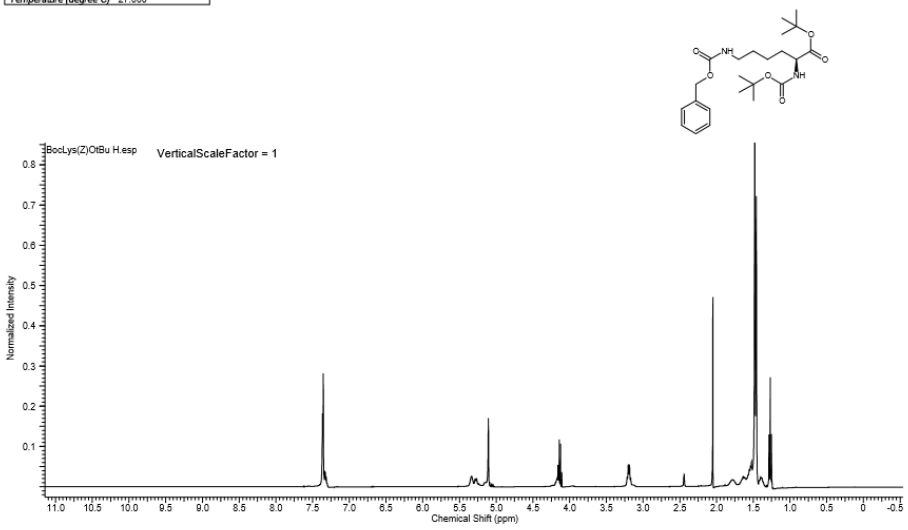
22/12/2014 12:13:48 PM

Acquisition Time (sec)	0.6259	*Comment*	Instrument DQX400 Chemist MLS Group SJC MLS01170 c13acq.au CDCl3 (E:\NMR2012) sjcgrp 6				
Date	23 Apr 2012 11:52:48			*Date Stamp*	23 Apr 2012 11:52:48		
File Name	F:\NMR\Amino Acid Residues\Boc Tyr OtBu\Apr23-2012-6\3\fid			*Frequency (MHz)*	100.63	*Nucleus*	13C
Number of Transients	256	*Origin*	av400	*Original Points Count*	16384	*Owner*	dp-nmrgroup
Points Count	16384	*Pulse Sequence*	zgpg30	*Receiver Gain*	32768.00	*SW(cyclical) (Hz)*	26178.01
Solvent	CHLOROFORM-d	*Spectrum Offset (Hz)*	10018.1836	*Spectrum Type*	STANDARD	*Sweep Width (Hz)*	26176.41
Temperature (degree C)	27.000						



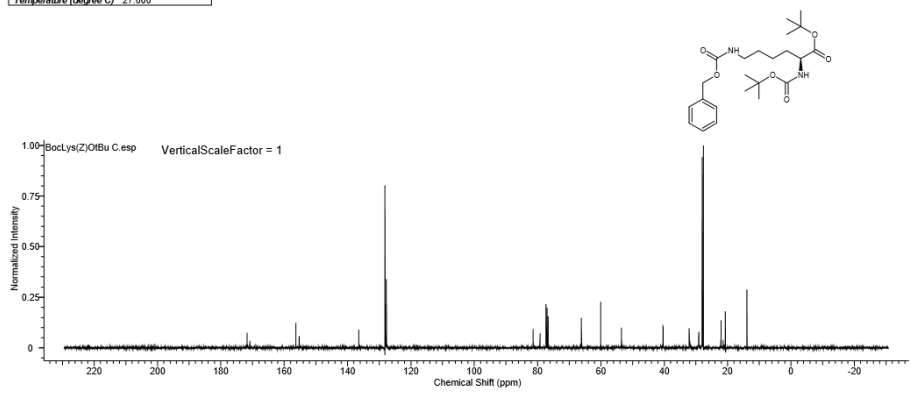
Compound 162

Acquisition Time (sec)	3.9584	*Comment*	Instrument DQX400 Chemist MLS Group SJC MLS02096 - Boc-Lys(Z)-OtBu h1acq.au CDCl3 (E:\NMR2012) sjcgrp 23				
Date	08 Aug 2012 11:16:32			*Date Stamp*	08 Aug 2012 11:16:32		
File Name	F:\NMR\Amino Acid Residues\BocLys(Z)OtBu\Aug08-2012-23\1\fid			*Frequency (MHz)*	400.20	*Nucleus*	1H
Number of Transients	16	*Origin*	av400	*Original Points Count*	32768	*Owner*	dp-nmrgroup
Points Count	32768	*Pulse Sequence*	zg30	*Receiver Gain*	12.70	*SW(cyclical) (Hz)*	8278.15
Solvent	CHLOROFORM-d	*Spectrum Offset (Hz)*	2506.5818	*Spectrum Type*	STANDARD	*Sweep Width (Hz)*	8277.89
Temperature (degree C)	27.000						



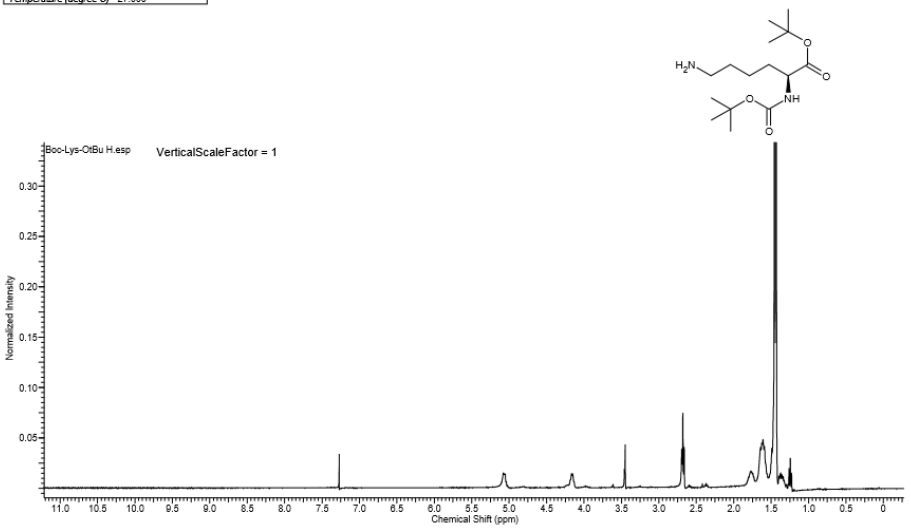
22/12/2014 1:26:04 PM

Acquisition Time (sec)	0.6259	*Comment*	Instrument DQX400 Chemist MLS Group SJC MLS02096 - Boc-Lys(Z)-OtBu c13acq.au CDCl3 (E:\NMR2012) sjcgrp 23				
Date	08 Aug 2012 11:27:12			*Date Stamp*	08 Aug 2012 11:27:12		
File Name	F:\NMR\BocLys(Z)OtBu\Aug08-2012-23\3\fid			*Frequency (MHz)*	100.63	*Nucleus*	13C
Number of Transients	256	*Origin*	av400	*Original Points Count*	16384	*Owner*	dp-nmrgroup
Points Count	16384	*Pulse Sequence*	zgpg30	*Receiver Gain*	32768.00	*SW(cyclical) (Hz)*	26178.01
Solvent	CHLOROFORM-d	*Spectrum Offset (Hz)*	9999.0107	*Spectrum Type*	STANDARD	*Sweep Width (Hz)*	26176.41
Temperature (degree C)	27.000						



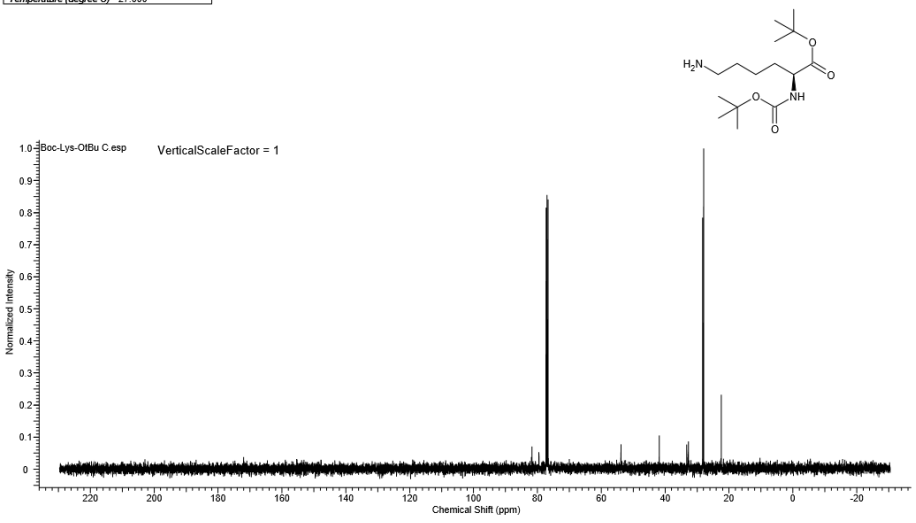
Compound 163

Acquisition Time (sec)	3.9584	Comment	Instrument DQX400 Chemist MLS Group SJC MLS02098 - Boc-Lys-OtBu h1acq.au CDCl3 (E:\NMR2012) sjcgrp 1				
Date	11 Aug 2012 23:24:00			Date Stamp	11 Aug 2012 23:24:00		
File Name	F:\NMR\Amino Acid Residues\BocLysOtBu\Aug11-2012-1\1\fid			Frequency (MHz)	400.20	Nucleus	1H
Number of Transients	16	Origin	av400	Original Points Count	32768	Owner	dp-nmrgroup
Points Count	32768	Pulse Sequence	zg30	Receiver Gain	90.50	SW(cyclical) (Hz)	8278.15
Solvent	CHLOROFORM-d	Spectrum Offset (Hz)	2468.9956	Spectrum Type	STANDARD	Sweep Width (Hz)	8277.89
Temperature (degree C)	27.000						



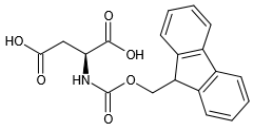
22/12/2014 1:57:02 PM

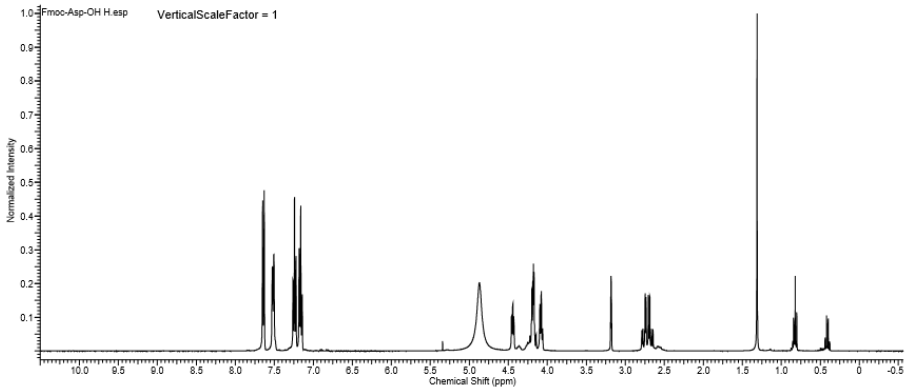
Acquisition Time (sec)	0.6259	Comment	Instrument DQX400 Chemist MLS Group SJC MLS02098 - Boc-Lys-OtBu c13acq.au CDCl3 (E:\NMR2012) sjcgrp 1				
Date	11 Aug 2012 23:34:40			Date Stamp	11 Aug 2012 23:34:40		
File Name	F:\NMR\Amino Acid Residues\BocLysOtBu\Aug11-2012-1\3\fid			Frequency (MHz)	100.63	Nucleus	13C
Number of Transients	256	Origin	av400	Original Points Count	16384	Owner	dp-nmrgroup
Points Count	16384	Pulse Sequence	zgpg30	Receiver Gain	32768.00	SW(cyclical) (Hz)	26178.01
Solvent	CHLOROFORM-d	Spectrum Offset (Hz)	10018.1836	Spectrum Type	STANDARD	Sweep Width (Hz)	26176.41
Temperature (degree C)	27.000						



Compound 271

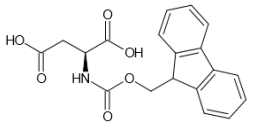
Acquisition Time (sec)	3.2768	*Comment*	Instrument AVG400 Group SJC Chemist MLS MLS06160 h1acq.crl MeOD (C:\NMR) sjcgrp 7				
Date	25 Jul 2014 13:39:28			*Date Stamp*	25 Jul 2014 13:39:28		
File Name	F:\NMR\Amino Acid Residues\Fmoc Asp OH\Jul25-2014-7\1\pdata\1\1r					*Frequency (MHz)*	400.20
Nucleus	1H	*Number of Transients*	16	*Origin*	avg400	*Original Points Count*	32768
Owner	nmr-user	*Points Count*	65536	*Pulse Sequence*	zg30	*Receiver Gain*	141.58
SW(cyclical) (Hz)	10000.00	*Solvent*	METHANOL-d4	*Spectrum Offset (Hz)*	2408.7976	*Spectrum Type*	STANDARD
Sweep Width (Hz)	9999.85	*Temperature (degree C)*	21.500				

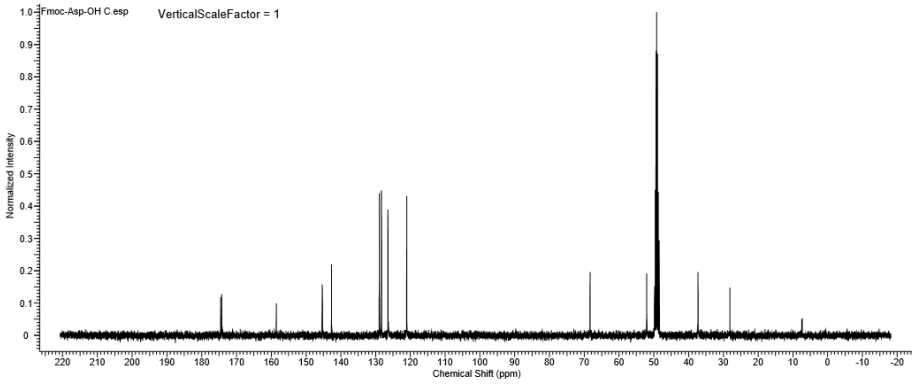




26/12/2014 10:39:21 PM

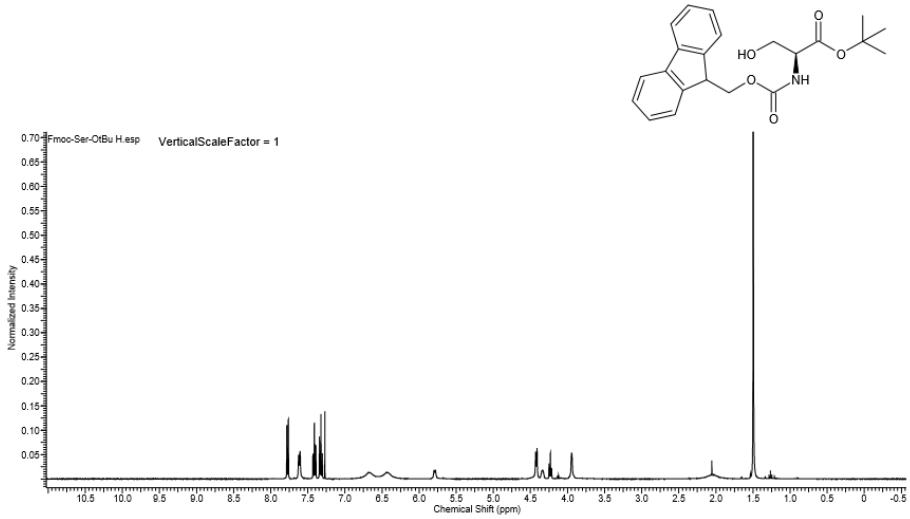
Acquisition Time (sec)	1.3631	*Comment*	Instrument AVG400 Group SJC Chemist MLS MLS06160 c13acq.crl MeOD (C:\NMR) sjcgrp 7				
Date	25 Jul 2014 22:52:00			*Date Stamp*	25 Jul 2014 22:52:00		
File Name	F:\NMR\Amino Acid Residues\Fmoc Asp OH\Jul25-2014-7\3\pdata\1\1r					*Frequency (MHz)*	100.63
Nucleus	13C	*Number of Transients*	256	*Origin*	avg400	*Original Points Count*	32768
Owner	nmr-user	*Points Count*	32768	*Pulse Sequence*	zgpg30	*Receiver Gain*	2050.00
SW(cyclical) (Hz)	24038.46	*Solvent*	METHANOL-d4	*Spectrum Offset (Hz)*	10192.2920	*Spectrum Type*	STANDARD
Sweep Width (Hz)	24037.73	*Temperature (degree C)*	21.500				





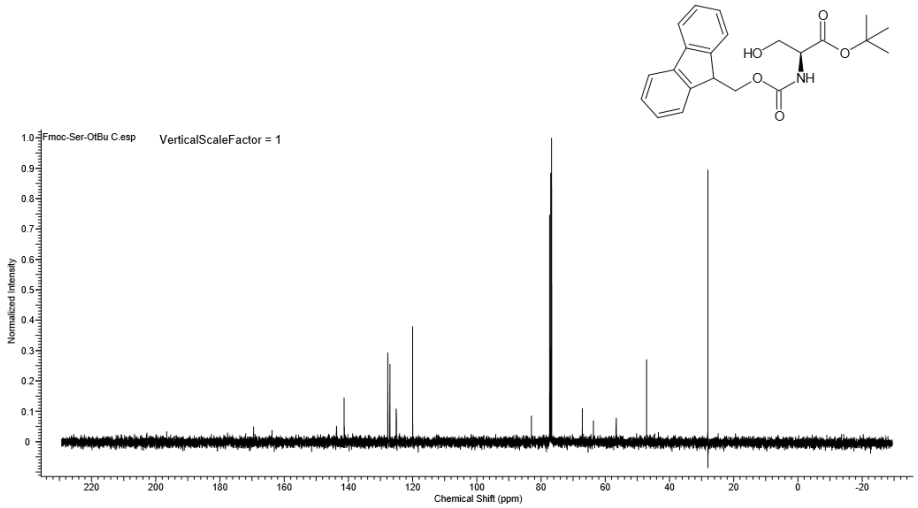
Compound 185

Acquisition Time (sec)	4.0894	*Comment*	Instrument AVN400 Chemist MLS Group SJC MLS03188: Fmoc-Ser-OtBu h1acq.crl CDCl3 (C:\NMR) sjcgrp 7				
Date	17 Jun 2013 13:09:36			*Date Stamp*	17 Jun 2013 13:09:36		
File Name	F:\NMR\Amino Acid Residues\Fmoc Ser OtBu\Jun17-2013-7\1\fid			*Frequency (MHz)*	400.25	*Nucleus*	1H
Number of Transients	16	*Origin*	avn400	*Original Points Count*	32768	*Owner*	dp-nmrgroup
Points Count	32768	*Pulse Sequence*	zg30	*Receiver Gain*	93.00	*SW(cyclical) (Hz)*	8012.82
Solvent	CHLOROFORM-d	*Spectrum Offset (Hz)*	2393.9775	*Spectrum Type*	STANDARD	*Sweep Width (Hz)*	8012.58
Temperature (degree C)	21.924						



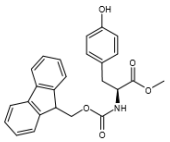
22/12/2014 7:52:22 PM

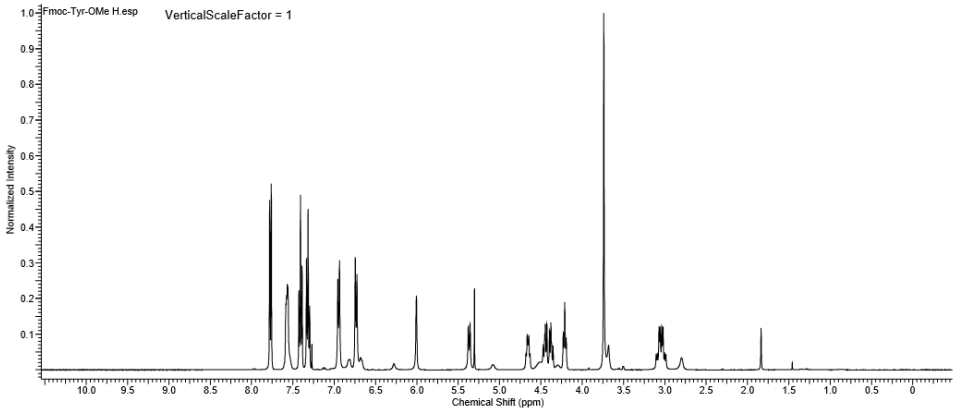
Acquisition Time (sec)	0.6291	*Comment*	Instrument AVN400 Chemist MLS Group SJC MLS03188: Fmoc-Ser-OtBu c13acq.crl CDCl3 (C:\NMR) sjcgrp 7				
Date	17 Jun 2013 13:22:24			*Date Stamp*	17 Jun 2013 13:22:24		
File Name	F:\NMR\Amino Acid Residues\Fmoc Ser OtBu\Jun17-2013-7\3\fid			*Frequency (MHz)*	100.64	*Nucleus*	13C
Number of Transients	256	*Origin*	avn400	*Original Points Count*	16384	*Owner*	dp-nmrgroup
Points Count	16384	*Pulse Sequence*	zgpg30	*Receiver Gain*	205.43	*SW(cyclical) (Hz)*	26041.67
Solvent	CHLOROFORM-d	*Spectrum Offset (Hz)*	10058.1934	*Spectrum Type*	STANDARD	*Sweep Width (Hz)*	26040.08
Temperature (degree C)	22.774						



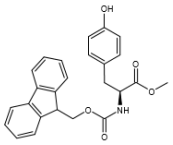
Compound 247

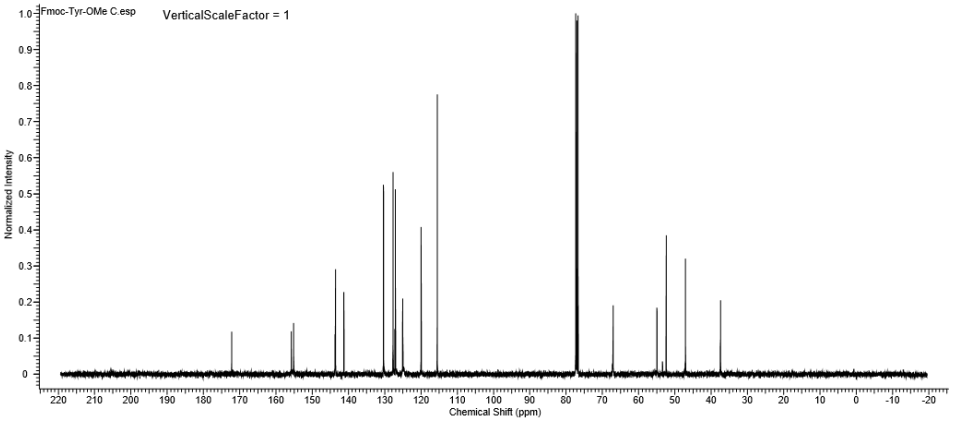
Acquisition Time (sec)	3.2768	*Comment*	Instrument AVG400 Group SJC Chemist MLS Fmoc-Tyr-OMe h1acq.crl CDCl3 {C:\NMR} sjcgrp 1				
Date	17 Apr 2015 08:38:40			*Date Stamp*	17 Apr 2015 08:38:40		
File Name	D:\Gnomeeee\NMR\Amino Acid Residues\Fmoc-Tyr-OMe\Apr17-2015-1-\1\PDATA\1\1r					*Frequency (MHz)*	400.20
Nucleus	1H	*Number of Transients*	8	*Origin*	avg400	*Original Points Count*	32768
Owner	nmr-user	*Points Count*	65536	*Pulse Sequence*	zg60	*Receiver Gain*	66.06
SW(cyclical) (Hz)	10000.00	*Solvent*	CHLOROFORM-d	*Spectrum Offset (Hz)*	2465.8047	*Spectrum Type*	STANDARD
Sweep Width (Hz)	9999.85	*Temperature (degree C)*	25.015				





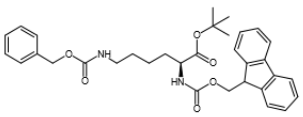
Acquisition Time (sec)	1.3631	*Comment*	Instrument AVG400 Group SJC Chemist MLS Fmoc-Tyr-OMe c13acq.crl CDCl3 {C:\NMR} sjcgrp 1				
Date	17 Apr 2015 08:57:52	*Date Stamp*	17 Apr 2015 08:57:52	*File Name*	D:\Gnomeeee\NMR\Amino Acid Residues\Fmoc-Tyr-OMe\Apr17-2015-1-\3\PDATA\1\1r		
Frequency (MHz)	100.63	*Nucleus*	13C	*Number of Transients*	256	*Origin*	avg400
Original Points Count	32768	*Owner*	nmr-user	*Points Count*	32768	*Pulse Sequence*	zgpg30
Receiver Gain	206.87	*SW(cyclical) (Hz)*	24038.46	*Solvent*	CHLOROFORM-d	*Spectrum Offset (Hz)*	10055.3301
Spectrum Type	STANDARD	*Sweep Width (Hz)*	24037.73	*Temperature (degree C)*	25.004		

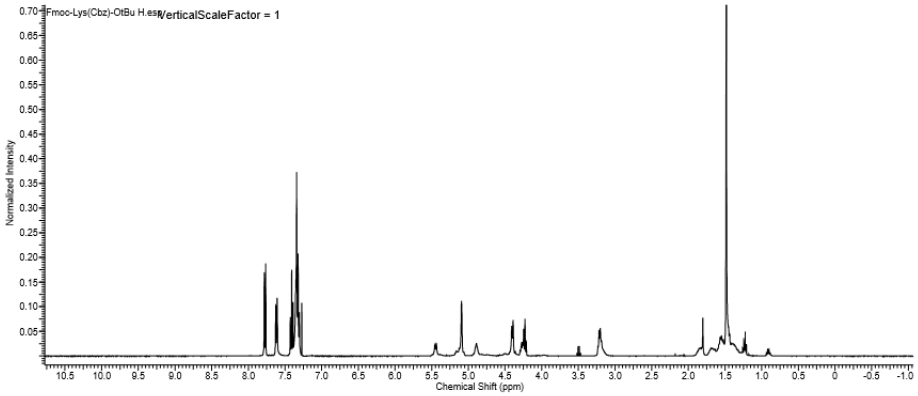




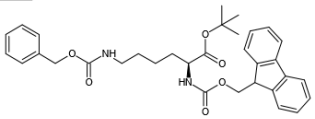
Compound 189

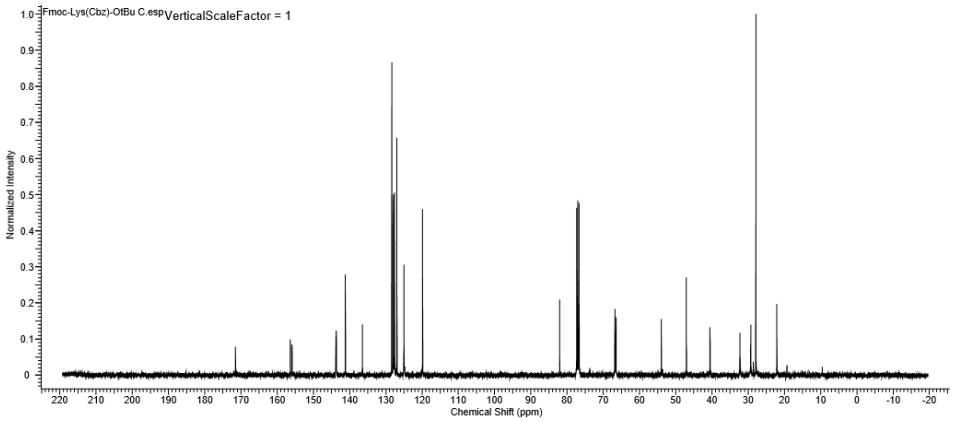
Acquisition Time (sec)	3.2768	*Comment*	Instrument AVG400 Group SJC Chemist MLS MLS04058 h1acq.crl CDCl3 {C:\NMR} sjcgrp 17				
Date	10 Oct 2013 10:23:12			*Date Stamp*	10 Oct 2013 10:23:12		
File Name	F:\NMR\Amino Acid Residues\Fmoc Lys(Z) OtBu\Oct10-2013-17\2\fid					*Frequency (MHz)*	400.20
Nucleus	1H	*Number of Transients*	16	*Origin*	avg400	*Original Points Count*	32768
Owner	nmr-user	*Points Count*	32768	*Pulse Sequence*	zg30	*Receiver Gain*	118.31
SW(cyclical) (Hz)	10000.00	*Solvent*	CHLOROFORM-d	*Spectrum Offset (Hz)*	2463.1345	*Spectrum Type*	STANDARD
Sweep Width (Hz)	9999.70	*Temperature (degree C)*	21.600				





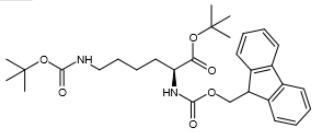
Acquisition Time (sec)	1.3631	*Comment*	Instrument AVG400 Group SJC Chemist MLS MLS04058: Fmoc-Lys(Cbz)-OtBu c13acq.crl CDCl3 {C:\NMR} sjcgrp 50				
Date	03 Feb 2015 21:26:24	*Date Stamp*	03 Feb 2015 21:26:24	*File Name*	F:\NMR\Amino Acid Residues\Fmoc Lys(Z) OtBu\Feb03-2015-50-\3\pdata\1\1r		
Frequency (MHz)	100.63	*Nucleus*	13C	*Number of Transients*	256	*Origin*	avg400
Original Points Count	32768	*Owner*	nmr-user	*Points Count*	32768	*Pulse Sequence*	zgpg30
Receiver Gain	2050.00	*SW(cyclical) (Hz)*	24038.46	*Solvent*	CHLOROFORM-d	*Spectrum Offset (Hz)*	10045.7930
Spectrum Type	STANDARD	*Sweep Width (Hz)*	24037.73	*Temperature (degree C)*	21.400		

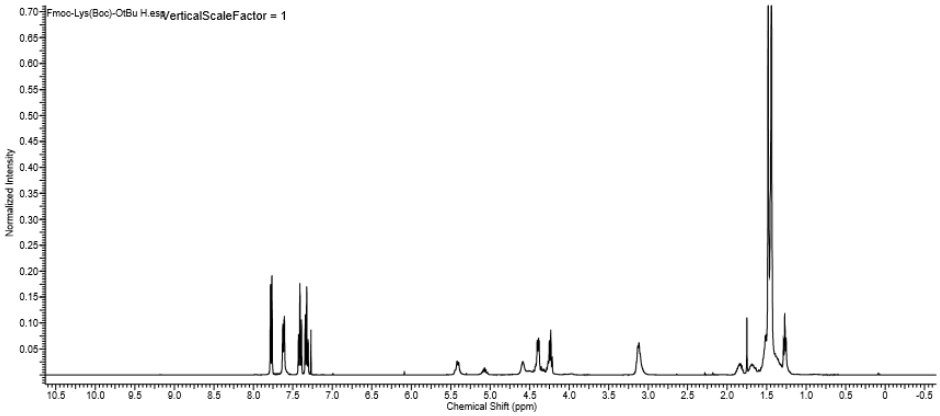




Compound 191

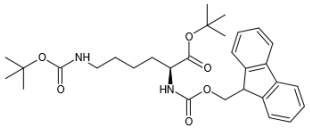
Acquisition Time (sec)	3.2768	*Comment*	Instrument AVG400 Group SJC Chemist MLS MLS05106: Fmoc-Lys(Boc)-OtBu h1acq.crl CDCl3 (C:\NMR) sjcgrp 18				
Date	24 Mar 2014 10:10:08	*Date Stamp*	24 Mar 2014 10:10:08	*File Name*	F:\NMR\Amino Acid Residues\Fmoc Lys(Boc) OtBu\Mar24-2014-18\1\PDATA\1\1r		
Frequency (MHz)	400.20	*Nucleus*	1H	*Number of Transients*	16	*Origin*	avg400
Original Points Count	32768	*Owner*	nmr-user	*Points Count*	65536	*Pulse Sequence*	zg30
Receiver Gain	128.54	*SW(cyclical) (Hz)*	10000.00	*Solvent*	CHLOROFORM-d	*Spectrum Offset (Hz)*	2462.1428
Spectrum Type	STANDARD	*Sweep Width (Hz)*	9999.85	*Temperature (degree C)*	21.600		

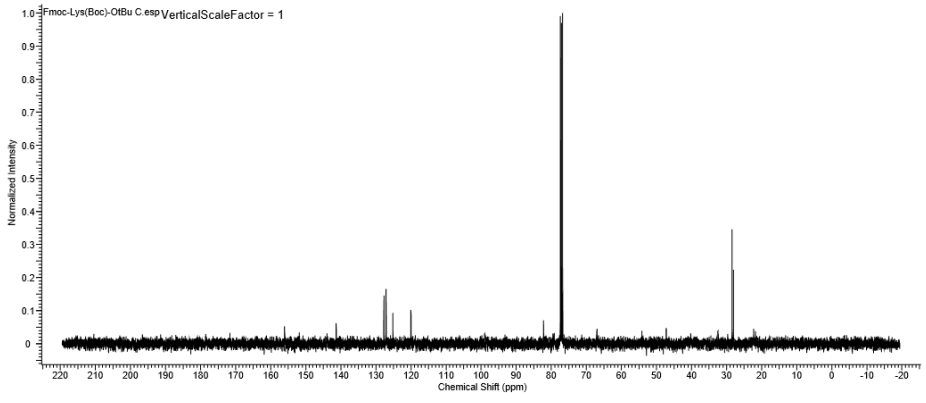




27/12/2014 5:10:33 PM

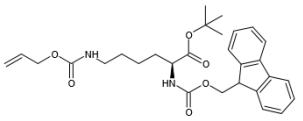
Acquisition Time (sec)	1.3631	*Comment*	Instrument AVG400 Group SJC Chemist MLS MLS05106: Fmoc-Lys(Boc)-OtBu c13acq.crl CDCl3 (C:\NMR) sjcgrp 18				
Date	24 Mar 2014 17:04:00	*Date Stamp*	24 Mar 2014 17:04:00	*File Name*	F:\NMR\Amino Acid Residues\Fmoc Lys(Boc) OtBu\Mar24-2014-18\3\PDATA\1\1r		
Frequency (MHz)	100.63	*Nucleus*	13C	*Number of Transients*	256	*Origin*	avg400
Original Points Count	32768	*Owner*	nmr-user	*Points Count*	32768	*Pulse Sequence*	zgpg30
Receiver Gain	2050.00	*SW(cyclical) (Hz)*	24038.46	*Solvent*	CHLOROFORM-d	*Spectrum Offset (Hz)*	10062.6055
Spectrum Type	STANDARD	*Sweep Width (Hz)*	24037.73	*Temperature (degree C)*	21.600		

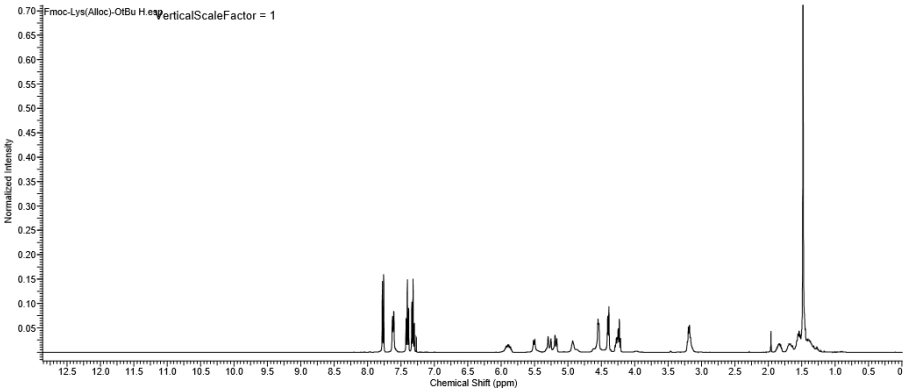




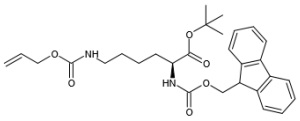
Compound 193

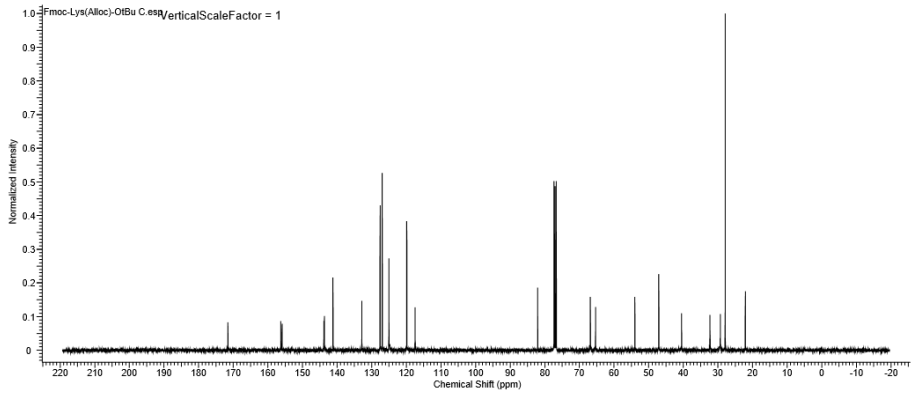
Acquisition Time (sec)	3.2768	*Comment*	Instrument AVG400 Group SJC Chemist MLS MLS05148 h1acq.crl CDCl3 (C:\NMR) sjcgrp 10				
Date	18 Apr 2014 11:54:56			*Date Stamp*	18 Apr 2014 11:54:56		
File Name	F:\NMR\Amino Acid Residues\Fmoc Lys(Alloc) OtBu\Apr18-2014-10\1\pdata\1\1r					*Frequency (MHz)*	400.20
Nucleus	1H	*Number of Transients*	16	*Origin*	avg400	*Original Points Count*	32768
Owner	nmr-user	*Points Count*	65536	*Pulse Sequence*	zg30	*Receiver Gain*	52.52
SW(cyclical) (Hz)	10000.00	*Solvent*	CHLOROFORM-d	*Spectrum Offset (Hz)*	2462.1426	*Spectrum Type*	STANDARD
Sweep Width (Hz)	9999.85	*Temperature (degree C)*	21.400				





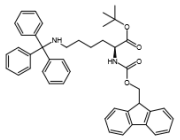
Acquisition Time (sec)	1.3631	*Comment*	Instrument AVG400 Group SJC Chemist MLS MLS05148 c13acq.crl CDCl3 (C:\NMR) sjcgrp 10				
Date	18 Apr 2014 13:45:52			*Date Stamp*	18 Apr 2014 13:45:52		
File Name	F:\NMR\Amino Acid Residues\Fmoc Lys(Alloc) OtBu\Apr18-2014-10\3\pdata\1\1r					*Frequency (MHz)*	100.63
Nucleus	13C	*Number of Transients*	256	*Origin*	avg400	*Original Points Count*	32768
Owner	nmr-user	*Points Count*	32768	*Pulse Sequence*	zgpg30	*Receiver Gain*	2050.00
SW(cyclical) (Hz)	24038.46	*Solvent*	CHLOROFORM-d	*Spectrum Offset (Hz)*	10047.9941	*Spectrum Type*	STANDARD
Sweep Width (Hz)	24037.73	*Temperature (degree C)*	21.300				

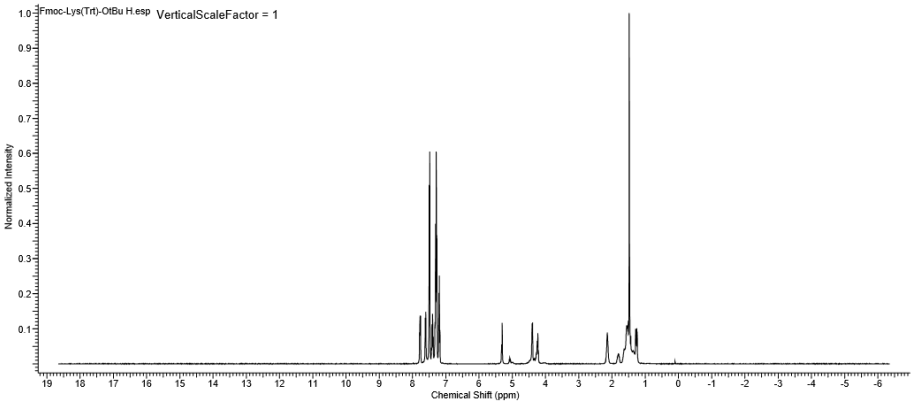




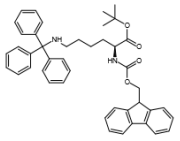
Compound 195

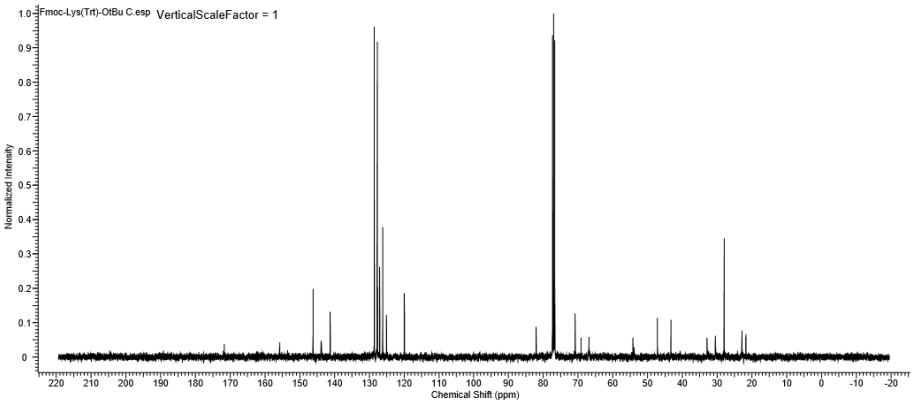
Acquisition Time (sec)	3.2768	*Comment*	Instrument AVG400 Group SJC Chemist MLS MLS06062: Fmoc-Lys(Trt)-OtBu h1acq.crl CDCl3 {C:\NMR} sjcgrp 41				
Date	24 Jun 2014 01:36:16	*Date Stamp*	24 Jun 2014 01:36:16	*File Name*	F:\NMR\Amino Acid Residues\Fmoc Lys(Trt) OtBu\Jun23-2014-41\1\pdata\1\1r		
Frequency (MHz)	400.20	*Nucleus*	1H	*Number of Transients*	16	*Origin*	avq400
Original Points Count	32768	*Owner*	nmr-user	*Points Count*	65536	*Pulse Sequence*	zg30
Receiver Gain	166.74	*SW(cyclical) (Hz)*	10000.00	*Solvent*	CHLOROFORM-d	*Spectrum Offset (Hz)*	2462.1428
Spectrum Type	STANDARD	*Sweep Width (Hz)*	9999.85	*Temperature (degree C)*	21.400		





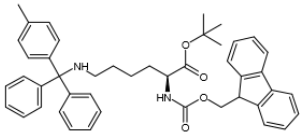
Acquisition Time (sec)	1.3631	*Comment*	Instrument AVG400 Group SJC Chemist MLS MLS06062: Fmoc-Lys(Trt)-OtBu c13acq.crl CDCl3 {C:\NMR} sjcgrp 41				
Date	24 Jun 2014 02:04:00	*Date Stamp*	24 Jun 2014 02:04:00	*File Name*	F:\NMR\Amino Acid Residues\Fmoc Lys(Trt) OtBu\Jun23-2014-41\3\PDATA\1\1r		
Frequency (MHz)	100.63	*Nucleus*	13C	*Number of Transients*	256	*Origin*	avq400
Original Points Count	32768	*Owner*	nmr-user	*Points Count*	32768	*Pulse Sequence*	zgpg30
Receiver Gain	2050.00	*SW(cyclical) (Hz)*	24038.46	*Solvent*	CHLOROFORM-d	*Spectrum Offset (Hz)*	10054.5967
Spectrum Type	STANDARD	*Sweep Width (Hz)*	24037.73	*Temperature (degree C)*	21.700		

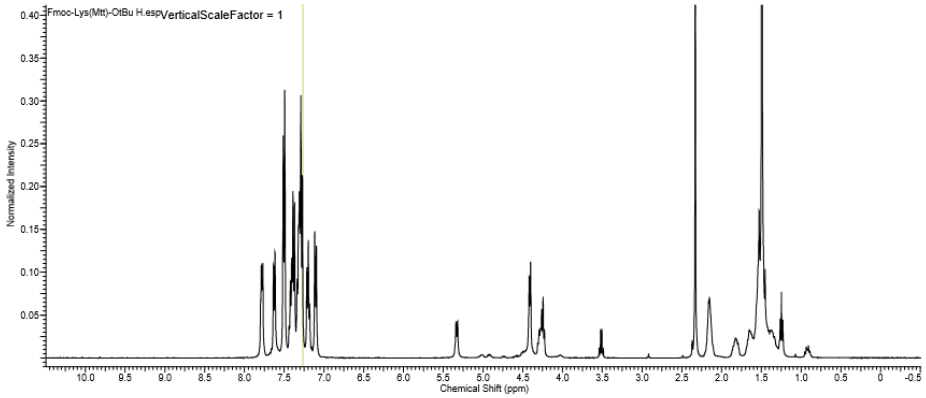




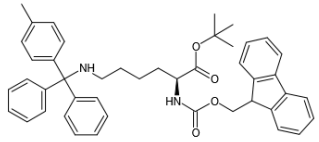
Compound 197

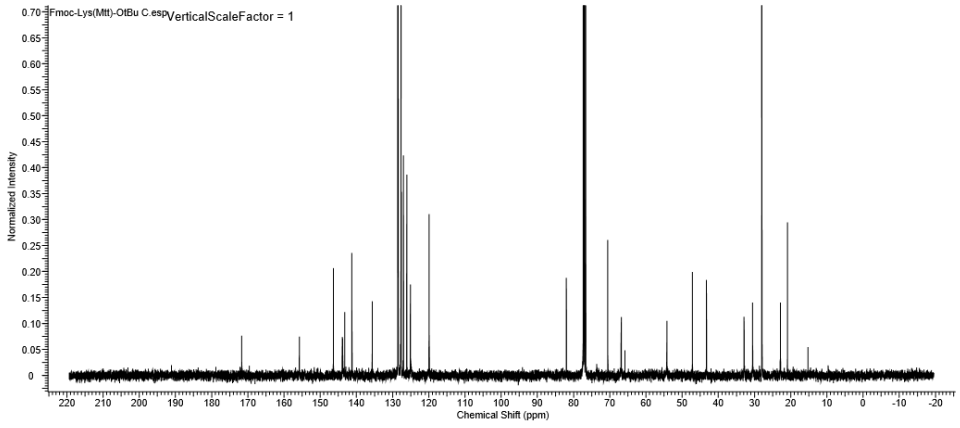
Acquisition Time (sec)	3.2768	*Comment*	Instrument AVG400 Group SJC Chemist MLS MLS09038: Fmoc-Lys(Mtt)-OtBu h1acq.crl CDCl3 {C:\NMR} sjcgrp 41				
Date	24 Feb 2015 15:53:36			*Date Stamp*	24 Feb 2015 15:53:36		
File Name	D:\Gnomeeee\NMR\Amino Acid Residues\Fmoc-Lys(Mtt)-OtBu\1\PDATA\1\1r					*Frequency (MHz)*	400.20
Nucleus	1H	*Number of Transients*	16	*Origin*	avq400	*Original Points Count*	32768
Owner	nmr-user	*Points Count*	65536	*Pulse Sequence*	zg30	*Receiver Gain*	93.53
SW(cyclical) (Hz)	10000.00	*Solvent*	CHLOROFORM-d	*Spectrum Offset (Hz)*	2462.4478	*Spectrum Type*	STANDARD
Sweep Width (Hz)	9999.85	*Temperature (degree C)*	21.100				





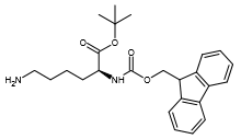
Acquisition Time (sec)	1.3631	*Comment*	Instrument AVG400 Group SJC Chemist MLS MLS09038: Fmoc-Lys(Mtt)-OtBu c13acq.crl CDCl3 {C:\NMR} sjcgrp 41				
Date	25 Feb 2015 04:48:00	*Date Stamp*	25 Feb 2015 04:48:00	*File Name*	D:\Gnomeeee\NMR\Amino Acid Residues\Fmoc-Lys(Mtt)-OtBu\3\PDATA\1\1r		
Frequency (MHz)	100.63	*Nucleus*	13C	*Number of Transients*	256	*Origin*	avq400
Original Points Count	32768	*Owner*	nmr-user	*Points Count*	32768	*Pulse Sequence*	zgpg30
Receiver Gain	2050.00	*SW(cyclical) (Hz)*	24038.46	*Solvent*	CHLOROFORM-d	*Spectrum Offset (Hz)*	10052.3955
Spectrum Type	STANDARD	*Sweep Width (Hz)*	24037.73	*Temperature (degree C)*	22.700		

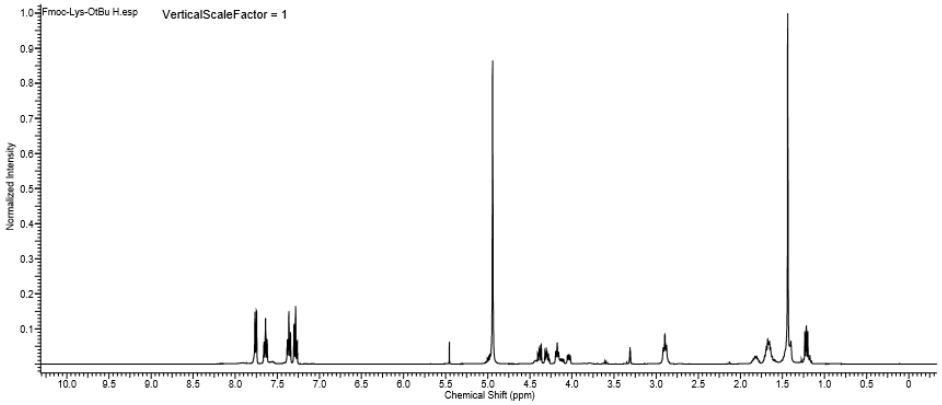




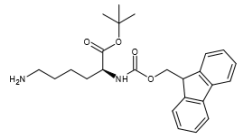
Compound 187

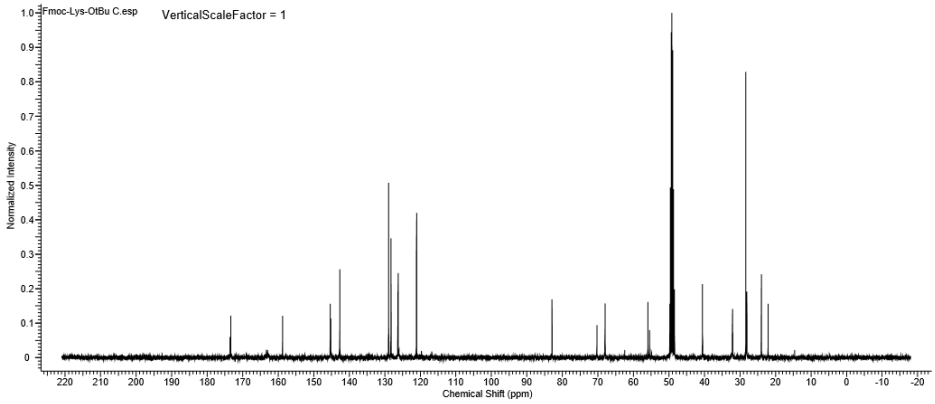
Acquisition Time (sec)	3.2768	*Comment*	Instrument AVG400 Group SJC Chemist MLS MLS06066: Fmoc-Lys-OtBu h1acq.crl MeOD {C:\NMR} sjcgrp 48				
Date	24 Jun 2014 09:14:56			*Date Stamp*	24 Jun 2014 09:14:56		
File Name	F:\NMR\Amino Acid Residues\Fmoc Lys OtBu\Jun24-2014-48\1\PDATA\1\1r					*Frequency (MHz)*	400.20
Nucleus	1H	*Number of Transients*	16	*Origin*	avg400	*Original Points Count*	32768
Owner	nmr-user	*Points Count*	65536	*Pulse Sequence*	zg30	*Receiver Gain*	52.52
SW(cyclical) (Hz)	10000.00	*Solvent*	METHANOL-d4	*Spectrum Offset (Hz)*	2460.1448	*Spectrum Type*	STANDARD
Sweep Width (Hz)	9999.85	*Temperature (degree C)*	21.000				





Acquisition Time (sec)	1.3631	*Comment*	Instrument AVG400 Group SJC Chemist MLS MLS06066: Fmoc-Lys-OtBu c13acq.crl MeOD {C:\NMR} sjcgrp 48				
Date	24 Jun 2014 09:36:16			*Date Stamp*	24 Jun 2014 09:36:16		
File Name	F:\NMR\Amino Acid Residues\Fmoc Lys OtBu\Jun24-2014-48\3\pdata\1\1r					*Frequency (MHz)*	100.63
Nucleus	13C	*Number of Transients*	256	*Origin*	avg400	*Original Points Count*	32768
Owner	nmr-user	*Points Count*	32768	*Pulse Sequence*	zgpg30	*Receiver Gain*	2050.00
SW(cyclical) (Hz)	24038.46	*Solvent*	METHANOL-d4	*Spectrum Offset (Hz)*	10209.1641	*Spectrum Type*	STANDARD
Sweep Width (Hz)	24037.73	*Temperature (degree C)*	21.200				

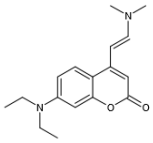


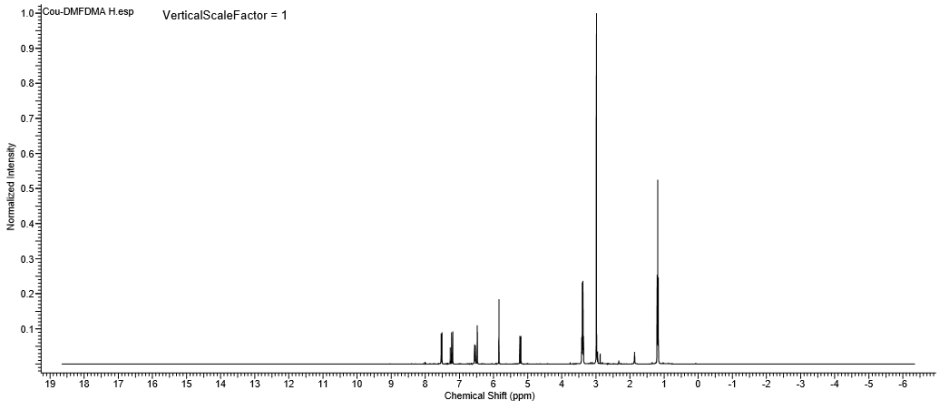


A.3 DEACM Caged Amino Acids

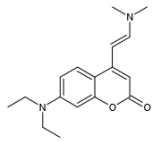
Compound 154

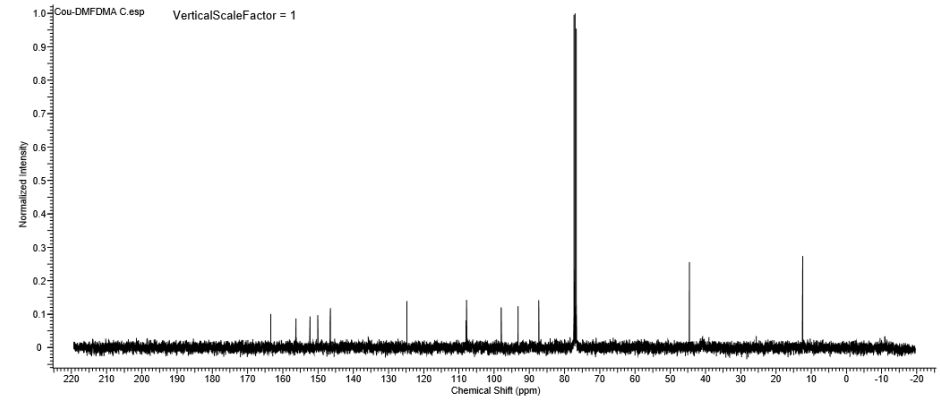
Acquisition Time (sec)	3.2768	*Comment*	Instrument AVG400 Group SJC Chemist MLS MLS05054 h1acq.crl CDCl3 {C:\NMR} sjcgrp 9				
Date	10 Mar 2014 14:51:44			*Date Stamp*	10 Mar 2014 14:51:44		
File Name	F:\NMR\Cou Stuff\MLS05054 Cou DMFDMA\2\PDATA\1\1r			*Frequency (MHz)*	400.20	*Nucleus*	1H
Number of Transients	16	*Origin*	avg400	*Original Points Count*	32768	*Owner*	nmr-user
Points Count	65536	*Pulse Sequence*	zg30	*Receiver Gain*	175.70	*SW(cyclical) (Hz)*	10000.00
Solvent	CHLOROFORM-d	*Spectrum Offset (Hz)*	2461.9902	*Spectrum Type*	STANDARD	*Sweep Width (Hz)*	9999.85
Temperature (degree C)	21.000						





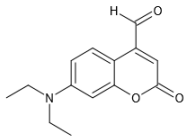
Acquisition Time (sec)	1.3631	*Comment*	Instrument AVG400 Group SJC Chemist MLS MLS05054 c13acq.crl CDCl3 {C:\NMR} sjcgrp 9				
Date	10 Mar 2014 23:55:44			*Date Stamp*	10 Mar 2014 23:55:44		
File Name	F:\NMR\Cou Stuff\MLS05054 Cou DMFDMA\4\PDATA\1\1r			*Frequency (MHz)*	100.63	*Nucleus*	13C
Number of Transients	256	*Origin*	avg400	*Original Points Count*	32768	*Owner*	nmr-user
Points Count	32768	*Pulse Sequence*	zgpg30	*Receiver Gain*	2050.00	*SW(cyclical) (Hz)*	24038.46
Solvent	CHLOROFORM-d	*Spectrum Offset (Hz)*	10053.8633	*Spectrum Type*	STANDARD	*Sweep Width (Hz)*	24037.73
Temperature (degree C)	21.500						

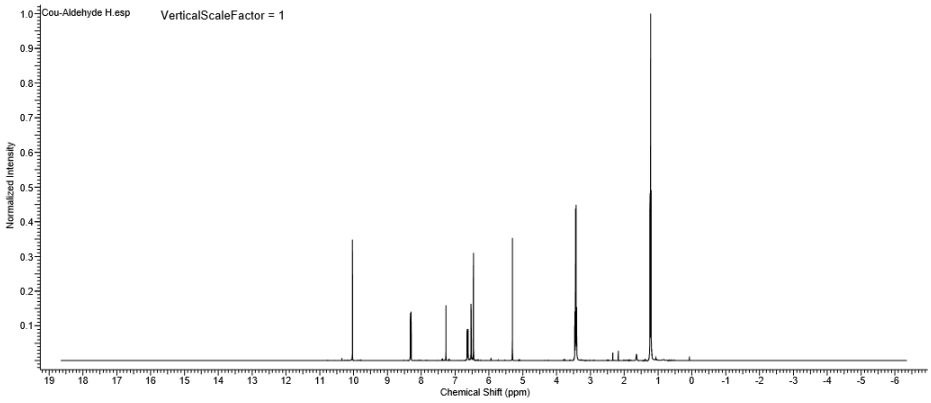




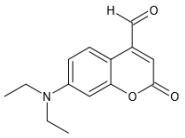
Compound 152

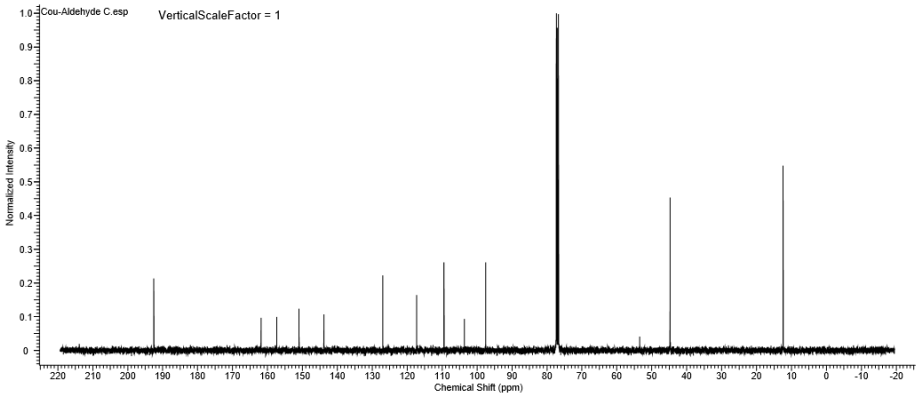
Acquisition Time (sec)	3.2768	*Comment*	Instrument AVG400 Group SJC Chemist MLS MLS06058: Cou Aldehyde h1acq.crl CDCl3 (C:\NMR) sjcgrp 25				
Date	19 Jun 2014 13:43:44			*Date Stamp*	19 Jun 2014 13:43:44		
File Name	F:\NMR\Cou Stuff\MLS06058 Cou Aldehyde\1\PDATA\1\1r			*Frequency (MHz)*	400.20	*Nucleus*	1H
Number of Transients	16	*Origin*	avg400	*Original Points Count*	32768	*Owner*	nmr-user
Points Count	65536	*Pulse Sequence*	zg30	*Receiver Gain*	255.20	*SW(cyclical) (Hz)*	10000.00
Solvent	CHLOROFORM-d	*Spectrum Offset (Hz)*	2461.8376	*Spectrum Type*	STANDARD	*Sweep Width (Hz)*	9999.85
Temperature (degree C)	21.100						





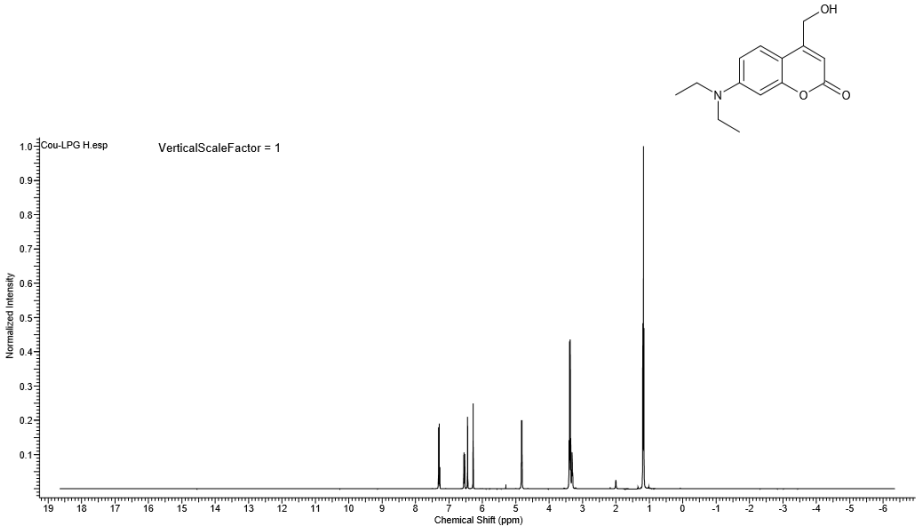
Acquisition Time (sec)	1.3631	*Comment*	Instrument AVG400 Group SJC Chemist MLS MLS06058: Cou Aldehyde c13acq.crl CDCl3 (C:\NMR) sjcgrp 25				
Date	19 Jun 2014 17:46:56			*Date Stamp*	19 Jun 2014 17:46:56		
File Name	F:\NMR\Cou Stuff\MLS06058 Cou Aldehyde\3\PDATA\1\1r			*Frequency (MHz)*	100.63	*Nucleus*	13C
Number of Transients	256	*Origin*	avg400	*Original Points Count*	32768	*Owner*	nmr-user
Points Count	32768	*Pulse Sequence*	zgpg30	*Receiver Gain*	2050.00	*SW(cyclical) (Hz)*	24038.46
Solvent	CHLOROFORM-d	*Spectrum Offset (Hz)*	10056.7969	*Spectrum Type*	STANDARD	*Sweep Width (Hz)*	24037.73
Temperature (degree C)	21.400						



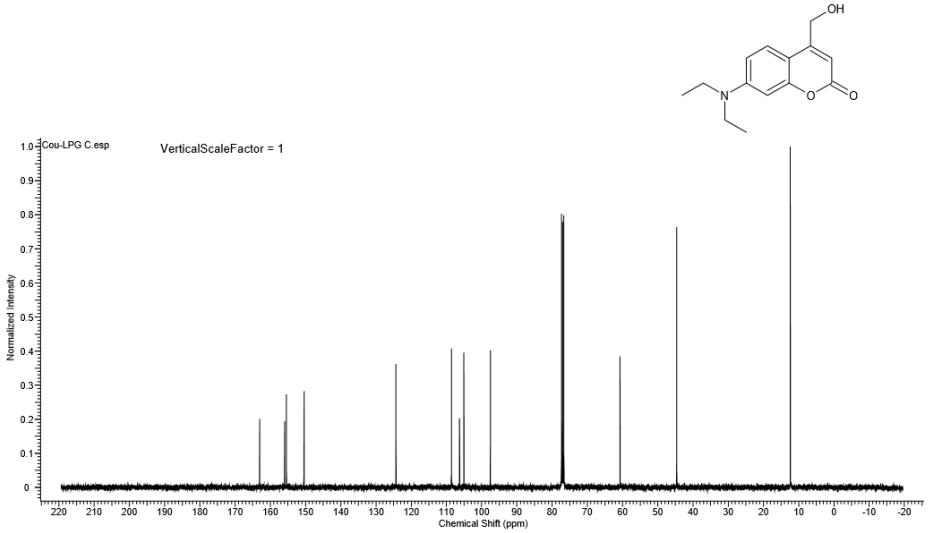


Compound 153

Acquisition Time (sec)	3.2768	*Comment*	Instrument AVG400 Group SJC Chemist MLS MLS06064: Cou LPG h1acq.crl CDCl3 {C:\NMR} sjcgrp 39		
Date	24 Jun 2014 00:17:20			*Date Stamp*	24 Jun 2014 00:17:20
File Name	F:\NMR\Cou Stuff\MLS06064 Cou LPG\2\PDATA\1\1r			*Frequency (MHz)*	400.20
Nucleus	1H	*Number of Transients*	16	*Origin*	avg400
Original Points Count	32768	*Owner*	nmr-user	*Points Count*	65536
Pulse Sequence	zg30	*Receiver Gain*	166.74	*SW(cyclical) (Hz)*	10000.00
Solvent	CHLOROFORM-d	*Spectrum Offset (Hz)*	2461.9902	*Spectrum Type*	STANDARD
Sweep Width (Hz)	9999.85	*Temperature (degree C)*	21.200		

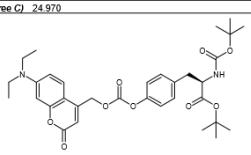


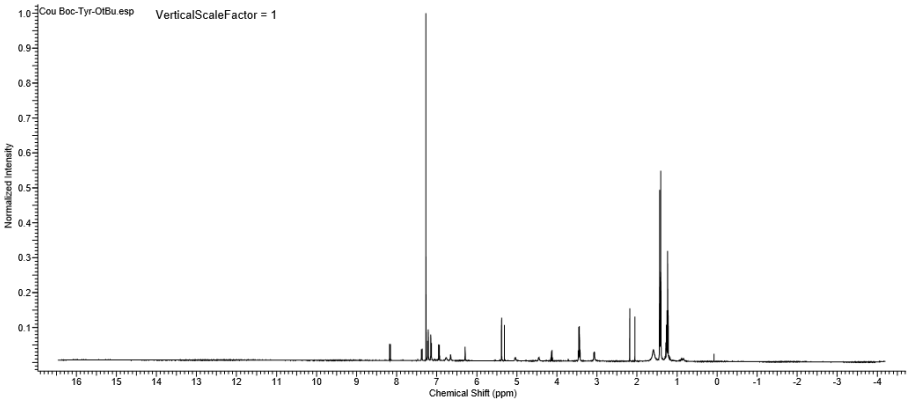
Acquisition Time (sec)	1.3631	*Comment*	Instrument AVG400 Group SJC Chemist MLS MLS06064: Cou LPG c13acq.crl CDCl3 {C:\NMR} sjcgrp 39		
Date	24 Jun 2014 00:38:40			*Date Stamp*	24 Jun 2014 00:38:40
File Name	F:\NMR\Cou Stuff\MLS06064 Cou LPG\4\pdata\1\1r			*Frequency (MHz)*	100.63
Nucleus	13C	*Number of Transients*	256	*Origin*	avg400
Original Points Count	32768	*Owner*	nmr-user	*Points Count*	32768
Pulse Sequence	zgpg30	*Receiver Gain*	2050.00	*SW(cyclical) (Hz)*	24038.46
Solvent	CHLOROFORM-d	*Spectrum Offset (Hz)*	10053.8633	*Spectrum Type*	STANDARD
Sweep Width (Hz)	24037.73	*Temperature (degree C)*	21.500		



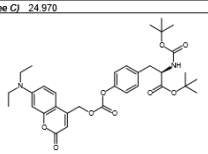
Compound 181

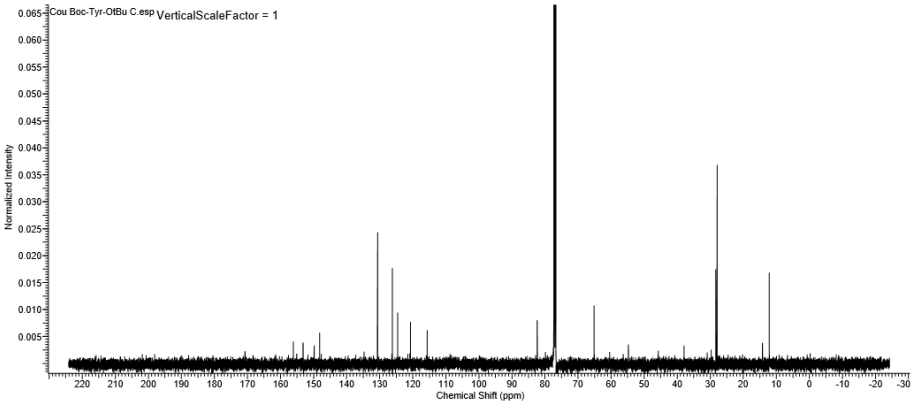
Acquisition Time (sec)	3.1719	*Comment*	Instrument AVC500 Group SJC 1203 M. Savage 22/8/12			*Date*	22 Aug 2012 12:18:24
Date Stamp	22 Aug 2012 12:18:24			*File Name*	F:\NMR\ms12032208\1\fid		
Frequency (MHz)	500.30	*Nucleus*	1H	*Number of Transients*	16	*Origin*	avc500
Original Points Count	32768	*Owner*	dp-nmrgroup	*Points Count*	32768	*Pulse Sequence*	zg30
Receiver Gain	4.00	*SW(cyclical) (Hz)*	10330.58	*Solvent*	CHLOROFORM-d		
Spectrum Offset (Hz)	3065.5417	*Spectrum Type*	STANDARD	*Sweep Width (Hz)*	10330.26	*Temperature (degree C)*	24.970





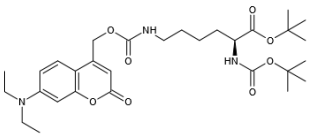
Acquisition Time (sec)	1.0486	*Comment*	Instrument AVC500 Group SJC 1203 M. Savage 22/8/12			*Date*	22 Aug 2012 12:41:52
Date Stamp	22 Aug 2012 12:41:52			*File Name*	F:\NMR\Cou Stuff\Cou Boc-Tyr-OtBu\4\fid		
Frequency (MHz)	125.80	*Nucleus*	13C	*Number of Transients*	1024	*Origin*	avc500
Original Points Count	32768	*Owner*	dp-nmrgroup	*Points Count*	32768	*Pulse Sequence*	zgpg30
Receiver Gain	1820.00	*SW(cyclical) (Hz)*	31250.00	*Solvent*	CHLOROFORM-d		
Spectrum Offset (Hz)	12571.9844	*Spectrum Type*	STANDARD	*Sweep Width (Hz)*	31249.05	*Temperature (degree C)*	24.970

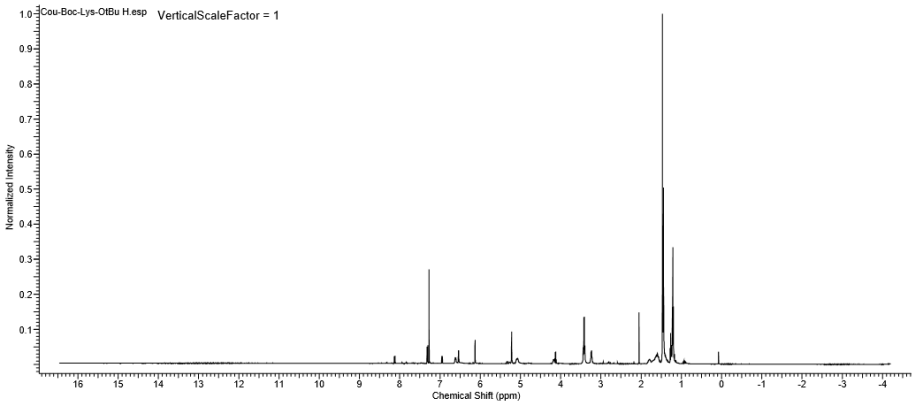




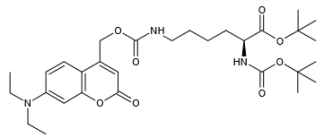
Compound 182

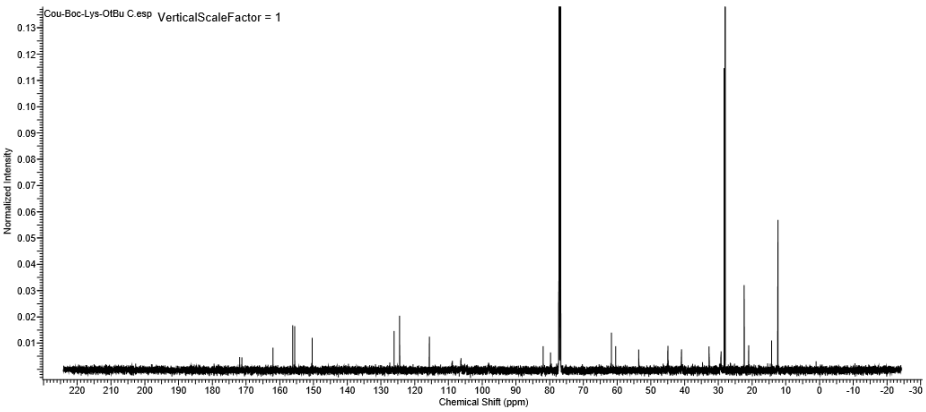
Acquisition Time (sec)	3.1719	*Comment*	Instrument AVC500 Group SJC 1200 M. Savage 20/8/12			*Date*	20 Aug 2012 14:43:28
Date Stamp	20 Aug 2012 14:43:28			*File Name*	F:\NMR\rms12002008\1\fid		
Frequency (MHz)	500.30	*Nucleus*	1H	*Number of Transients*	16	*Origin*	avc500
Original Points Count	32768	*Owner*	dp-nmrgroup	*Points Count*	32768	*Pulse Sequence*	zg30
Receiver Gain	4.00	*SW(cyclical) (Hz)*	10330.58	*Solvent*	CHLOROFORM-d		
Spectrum Offset (Hz)	3066.0798	*Spectrum Type*	STANDARD	*Sweep Width (Hz)*	10330.26	*Temperature (degree C)*	24.970





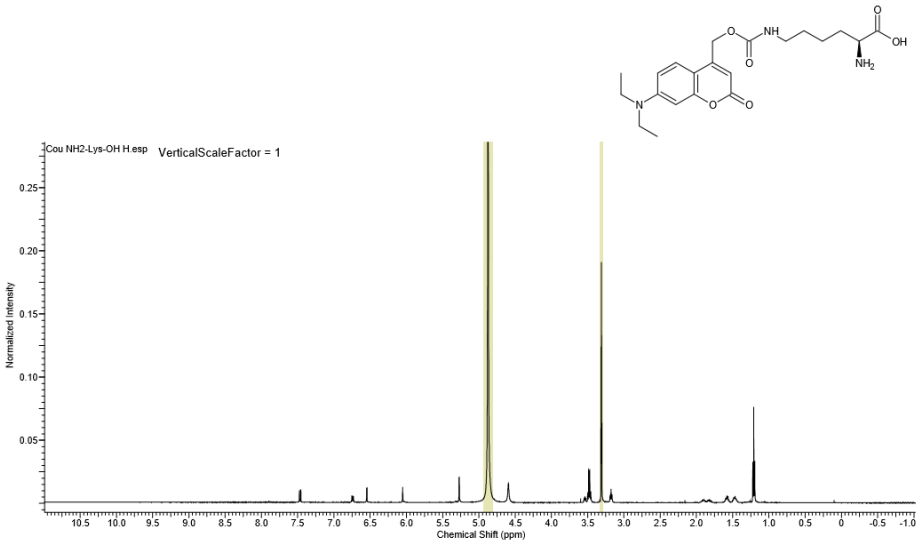
Acquisition Time (sec)	1.0486	*Comment*	Instrument AVC500 Group SJC 1200 M. Savage 20/8/12			*Date*	20 Aug 2012 15:19:44
Date Stamp	20 Aug 2012 15:19:44			*File Name*	F:\NMR\Cou Stuff\Cou Boc-Lys-OtBu\4\fid		
Frequency (MHz)	125.80	*Nucleus*	13C	*Number of Transients*	512	*Origin*	avc500
Original Points Count	32768	*Owner*	dp-nmrgroup	*Points Count*	32768	*Pulse Sequence*	zgpg30
Receiver Gain	1820.00	*SW(cyclical) (Hz)*	31250.00	*Solvent*	CHLOROFORM-d		
Spectrum Offset (Hz)	12571.0293	*Spectrum Type*	STANDARD	*Sweep Width (Hz)*	31249.05	*Temperature (degree C)*	24.970



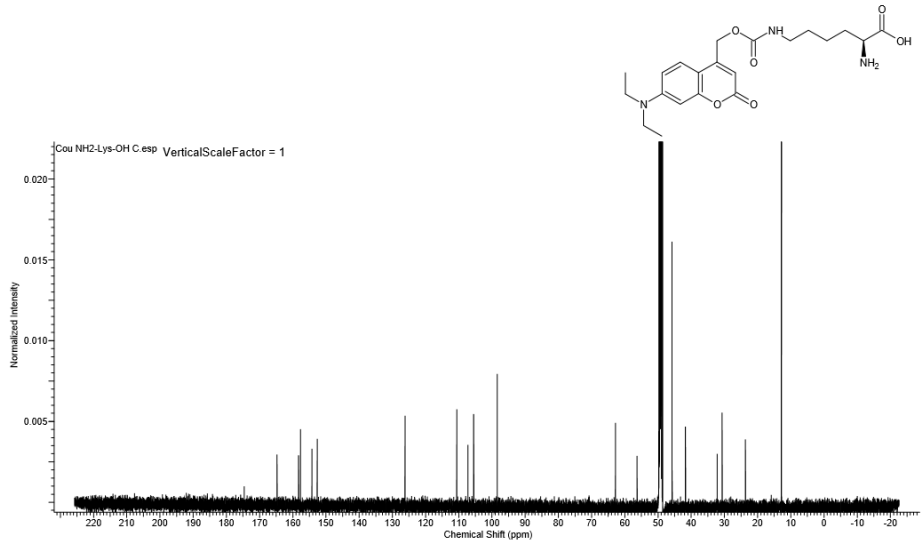


Compound 183

Acquisition Time (sec)	3.1719	*Comment*	Instrument AVC500 Group SJC 1201 M. Savage 21/8/12	*Date*	21 Aug 2012 08:32:16		
Date Stamp	21 Aug 2012 08:32:16			*File Name*	F:\NMR\ms12012108\1\fid		
Frequency (MHz)	500.30	*Nucleus*	1H	*Number of Transients*	16	*Origin*	avc500
Original Points Count	32768	*Owner*	dp-nmrgroup	*Points Count*	32768	*Pulse Sequence*	zg30
Receiver Gain	4.00	*SW(cyclical) (Hz)*	10330.58	*Solvent*	METHANOL-d4		
Spectrum Offset (Hz)	3078.6228	*Spectrum Type*	STANDARD	*Sweep Width (Hz)*	10330.26	*Temperature (degree C)*	24.970

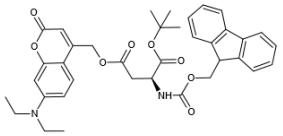


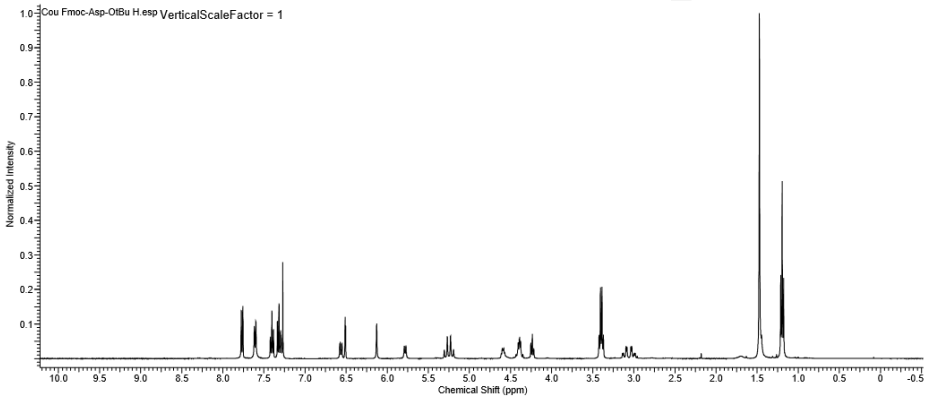
Acquisition Time (sec)	1.0486	*Comment*	Instrument AVC500 Group SJC 1201 M. Savage 21/8/12	*Date*	21 Aug 2012 09:06:24		
Date Stamp	21 Aug 2012 09:06:24			*File Name*	F:\NMR\ms12012108\4\fid		
Frequency (MHz)	125.80	*Nucleus*	13C	*Number of Transients*	1024	*Origin*	avc500
Original Points Count	32768	*Owner*	dp-nmrgroup	*Points Count*	32768	*Pulse Sequence*	zgpg30
Receiver Gain	1820.00	*SW(cyclical) (Hz)*	31250.00	*Solvent*	METHANOL-d4		
Spectrum Offset (Hz)	12773.4541	*Spectrum Type*	STANDARD	*Sweep Width (Hz)*	31249.05	*Temperature (degree C)*	24.970



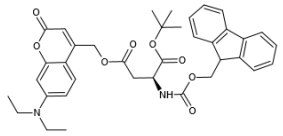
Compound 215

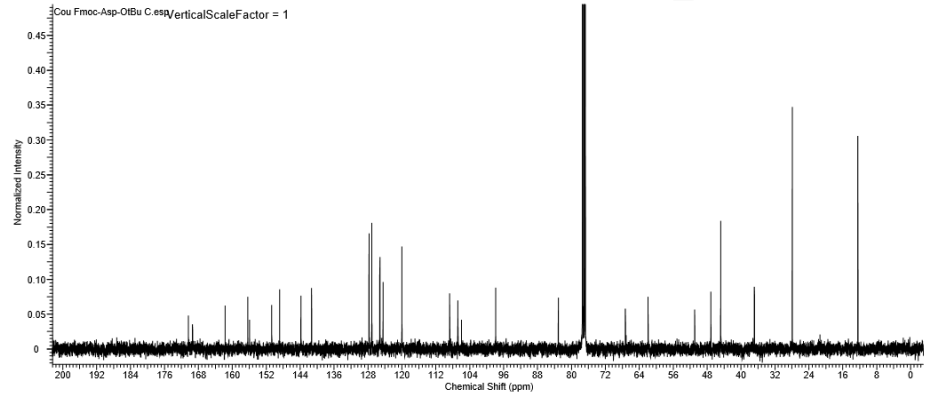
Acquisition Time (sec)	3.2768	*Comment*	Instrument AVG400 Group SJC Chemist MLS MLS05064: Cou (Fmoc) Asp (OtBu) h1acq crl CDCl3 {C:\NMR} sjcgrp 38				
Date	07 Jun 2014 20:35:28			*Date Stamp*	07 Jun 2014 20:35:28		
File Name	F:\NMR\Cou Stuff\Cou Asp\MLS05064\1\PDATA\1\1r			*Frequency (MHz)*	400.20	*Nucleus*	1H
Number of Transients	16	*Origin*	avg400	*Original Points Count*	32768	*Owner*	nmr-user
Points Count	65536	*Pulse Sequence*	zg30	*Receiver Gain*	202.31	*SW(cyclical) (Hz)*	10000.00
Solvent	CHLOROFORM-d	*Spectrum Offset (Hz)*	2461.9902	*Spectrum Type*	STANDARD	*Sweep Width (Hz)*	9999.85
Temperature (degree C)	25.000						





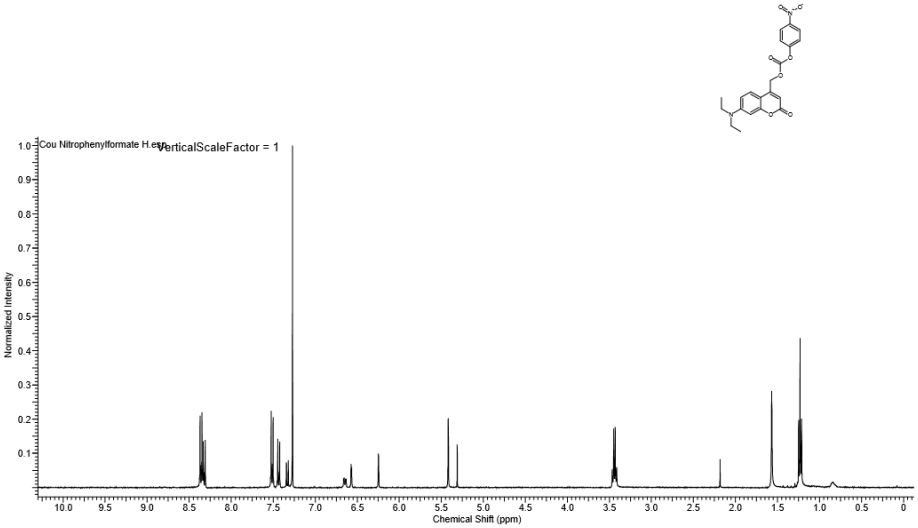
Acquisition Time (sec)	1.3631	*Comment*	Instrument AVG400 Group SJC Chemist MLS MLS05064: Cou (Fmoc) Asp (OtBu) c13acq crl CDCl3 {C:\NMR} sjcgrp 38				
Date	07 Jun 2014 21:03:12			*Date Stamp*	07 Jun 2014 21:03:12		
File Name	F:\NMR\Cou Stuff\Cou Asp\MLS05064\3\pdata\1\1r			*Frequency (MHz)*	100.63	*Nucleus*	13C
Number of Transients	256	*Origin*	avg400	*Original Points Count*	32768	*Owner*	nmr-user
Points Count	32768	*Pulse Sequence*	zgpg30	*Receiver Gain*	2050.00	*SW(cyclical) (Hz)*	24038.46
Solvent	CHLOROFORM-d	*Spectrum Offset (Hz)*	10062.6055	*Spectrum Type*	STANDARD	*Sweep Width (Hz)*	24037.73
Temperature (degree C)	27.000						



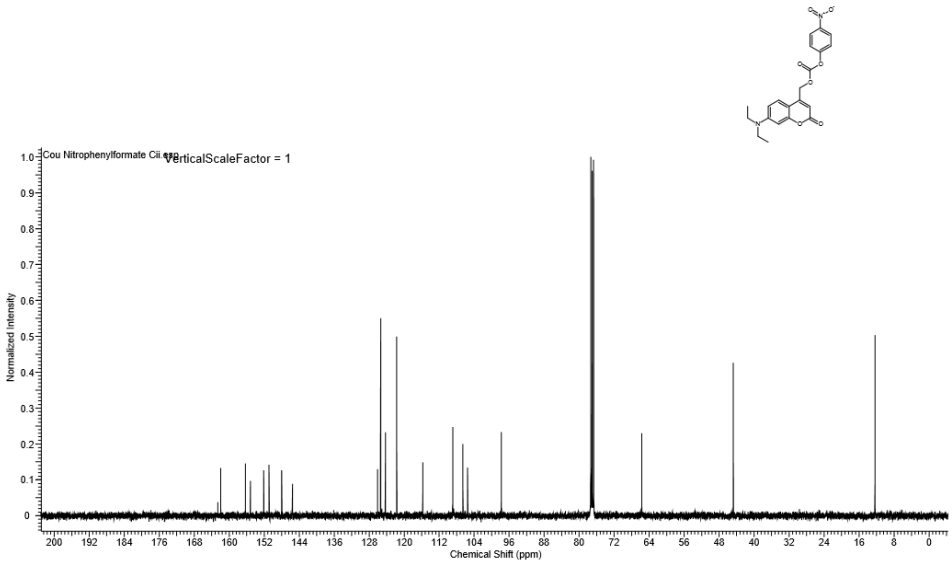


Compound 273

Acquisition Time (sec)	3.2768	*Comment*	Instrument AVG400 Group SJC Chemist MLS MLS06074: Cou i/m h1acq.crl CDCl3 (C:\NMR) sjcgrp 11				
Date	27 Jun 2014 10:40:16			*Date Stamp*	27 Jun 2014 10:40:16		
File Name	F:\NMR\MLS06074\1\pdata\1\1r			*Frequency (MHz)*	400.20	*Nucleus*	1H
Number of Transients	16	*Origin*	avg400	*Original Points Count*	32768	*Owner*	nmr-user
Points Count	65536	*Pulse Sequence*	zg30	*Receiver Gain*	788.56	*SW(cyclical) (Hz)*	10000.00
Solvent	CHLOROFORM-d			*Spectrum Offset (Hz)*	2461.8376	*Spectrum Type*	STANDARD
Sweep Width (Hz)	9999.85	*Temperature (degree C)*	20.900				

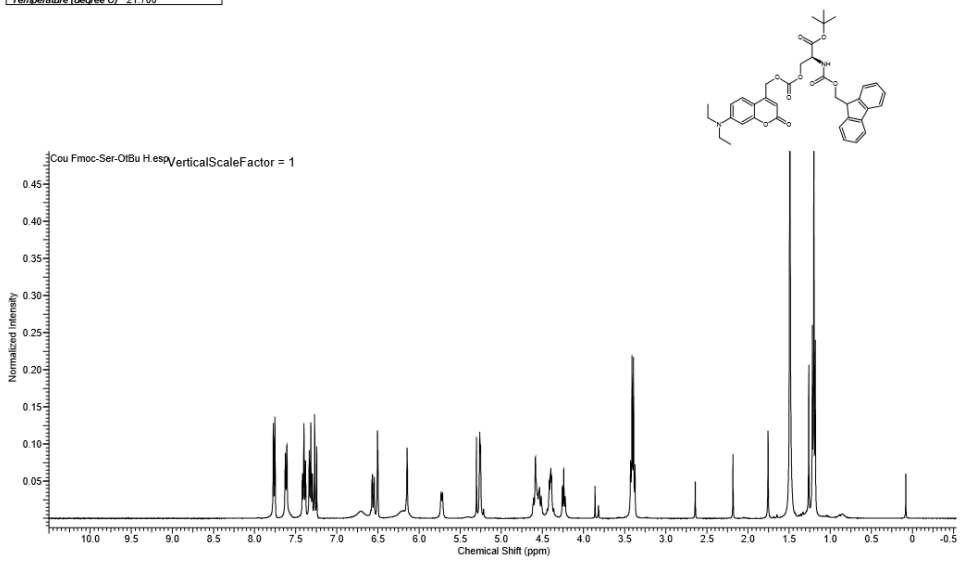


Acquisition Time (sec)	1.3631	*Comment*	Instrument AVG400 Group SJC Chemist MLS MLS08118: Cou i/m c13acq.crl CDCl3 (C:\NMR) sjcgrp 10				
Date	07 Jan 2015 22:09:04	*Date Stamp*	07 Jan 2015 22:09:04	*File Name*	F:\NMR\Cou Stuff\Cou Nitrophenylformate MLS06074\Jan07-2015-10-\3\pdata\1\1r		
Frequency (MHz)	100.63	*Nucleus*	13C	*Number of Transients*	256	*Origin*	avq400
Original Points Count	32768	*Owner*	nmr-user	*Points Count*	32768	*Pulse Sequence*	zgpg30
Receiver Gain	2050.00	*SW(cyclical) (Hz)*	24038.46	*Solvent*	CHLOROFORM-d	*Spectrum Offset (Hz)*	10055.3301
Spectrum Type	STANDARD	*Sweep Width (Hz)*	24037.73	*Temperature (degree C)*	21.800		

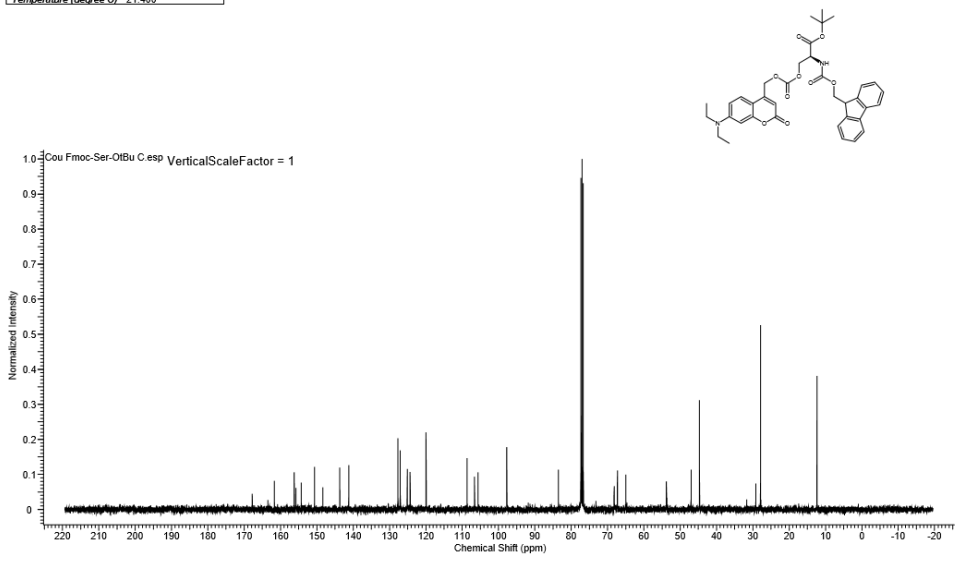


Compound 217

Acquisition Time (sec)	3.2768	*Comment*	Instrument AVG400 Group SJC Chemist MLS MLS08126: Cou Fmoc-Ser-OtBu h1acq.crl CDCl3 {C:\NMR} sjcgrp 4		
Date	12 Jan 2015 09:08:16		*Date Stamp*	12 Jan 2015 09:08:16	
File Name	F:\NMR\Cou Stuff\Cou Fmoc-Ser-OtBu\Jan12-2015-4-\1\pdata\1\1r		*Frequency (MHz)*	400.20	*Nucleus* 1H
Number of Transients	16	*Origin*	avg400	*Original Points Count*	32768	*Owner*	nmr-user
Points Count	65536	*Pulse Sequence*	zg30	*Receiver Gain*	166.74	*SW(cyclical) (Hz)*	10000.00
Solvent	CHLOROFORM-d	*Spectrum Offset (Hz)*	2462.1426	*Spectrum Type*	STANDARD	*Sweep Width (Hz)*	9999.85
Temperature (degree C)	21.700						

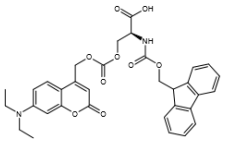


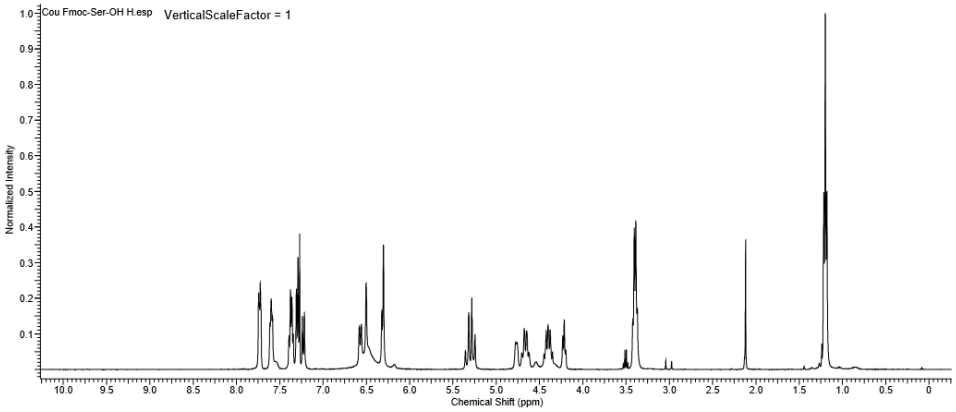
Acquisition Time (sec)	1.3631	*Comment*	Instrument AVG400 Group SJC Chemist MLS MLS08126: Cou Fmoc-Ser-OtBu c13acq.crl CDCl3 {C:\NMR} sjcgrp 4		
Date	12 Jan 2015 21:28:32		*Date Stamp*	12 Jan 2015 21:28:32	
File Name	F:\NMR\Cou Stuff\Cou Fmoc-Ser-OtBu\Jan12-2015-4-\3\pdata\1\1r		*Frequency (MHz)*	100.63	*Nucleus* 13C
Number of Transients	256	*Origin*	avg400	*Original Points Count*	32768	*Owner*	nmr-user
Points Count	32768	*Pulse Sequence*	zgpg30	*Receiver Gain*	2050.00	*SW(cyclical) (Hz)*	24038.46
Solvent	CHLOROFORM-d	*Spectrum Offset (Hz)*	10053.8633	*Spectrum Type*	STANDARD	*Sweep Width (Hz)*	24037.73
Temperature (degree C)	21.400						



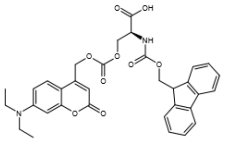
Compound 218

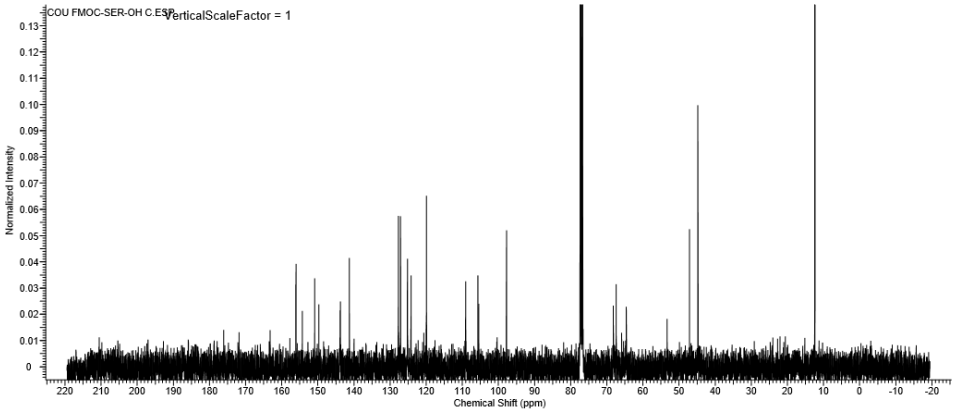
Acquisition Time (sec)	3.2768	*Comment*	Instrument AVG400 Group SJC Chemist MLS Cou Fmoc-Ser-OH h1acq.crl CDCl3 {C:\NMR} sjcgrp 54				
Date	01 Apr 2015 14:07:12			*Date Stamp*	01 Apr 2015 14:07:12		
File Name	D:\Gnomeeee\NMR\Cou Stuff\Cou Fmoc-Ser-OH\Apr01-2015-54-\1\PDATA\1\1r					*Frequency (MHz)*	400.20
Nucleus	1H	*Number of Transients*	8	*Origin*	avg400	*Original Points Count*	32768
Owner	nmr-user	*Points Count*	65536	*Pulse Sequence*	zg60	*Receiver Gain*	114.66
SW(cyclical) (Hz)	10000.00	*Solvent*	CHLOROFORM-d	*Spectrum Offset (Hz)*	2465.6523	*Spectrum Type*	STANDARD
Sweep Width (Hz)	9999.85	*Temperature (degree C)*	24.995				





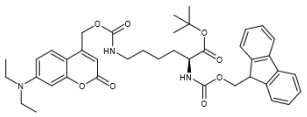
Acquisition Time (sec)	1.3631	*Comment*	Instrument AVG400 Group SJC Chemist MLS Cou Fmoc-Ser-OH c13acq.crl CDCl3 {C:\NMR} sjcgrp 54				
Date	02 Apr 2015 21:58:40			*Date Stamp*	02 Apr 2015 21:58:40		
File Name	D:\Gnomeeee\NMR\Cou Stuff\Cou Fmoc-Ser-OH\Apr01-2015-54-\3\PDATA\1\1r					*Frequency (MHz)*	100.63
Nucleus	13C	*Number of Transients*	256	*Origin*	avg400	*Original Points Count*	32768
Owner	nmr-user	*Points Count*	32768	*Pulse Sequence*	zgpg30	*Receiver Gain*	206.87
SW(cyclical) (Hz)	24038.46	*Solvent*	CHLOROFORM-d	*Spectrum Offset (Hz)*	10062.6055	*Spectrum Type*	STANDARD
Sweep Width (Hz)	24037.73	*Temperature (degree C)*	24.995				

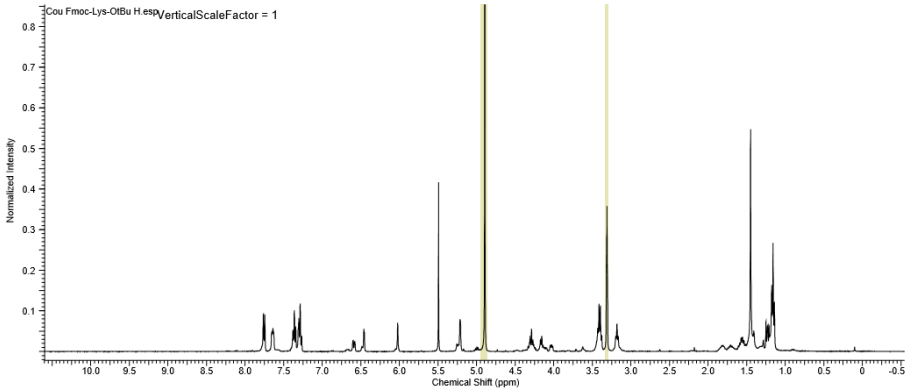




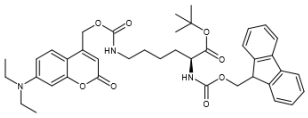
Compound 219

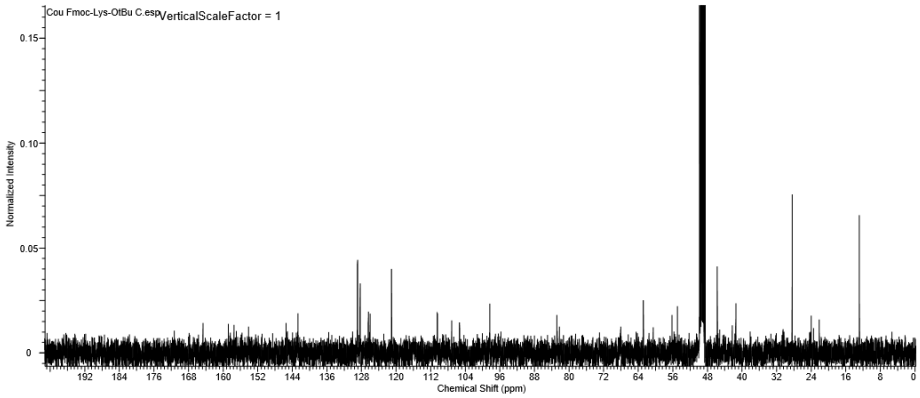
Acquisition Time (sec)	3.2768	*Comment*	Instrument AVG400 Group SJC Chemist MLS MLS06034 + MLS06042 h1acq crl MeOD {C:\NMR} sjcgrp 20				
Date	12 Jun 2014 15:11:12			*Date Stamp*	12 Jun 2014 15:11:12		
File Name	F:\NMR\Cou Stuff\Cou Fmoc-Lys-OtBu\Jun12-2014-20\1\PDATA\1\1r			*Frequency (MHz)*	400.20	*Nucleus*	1H
Number of Transients	16	*Origin*	avg400	*Original Points Count*	32768	*Owner*	nmr-user
Points Count	65536	*Pulse Sequence*	zg30	*Receiver Gain*	279.35	*SW(cyclical) (Hz)*	10000.00
Solvent	METHANOL-d4	*Spectrum Offset (Hz)*	2459.9922	*Spectrum Type*	STANDARD	*Sweep Width (Hz)*	9999.85
Temperature (degree C)	20.700						





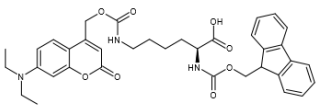
Acquisition Time (sec)	1.3631	*Comment*	Instrument AVG400 Group SJC Chemist MLS MLS06034 + MLS06042 c13acq crl MeOD {C:\NMR} sjcgrp 20				
Date	12 Jun 2014 19:35:44			*Date Stamp*	12 Jun 2014 19:35:44		
File Name	F:\NMR\Cou Stuff\Cou Fmoc-Lys-OtBu\Jun12-2014-20\3\PDATA\1\1r			*Frequency (MHz)*	100.63	*Nucleus*	13C
Number of Transients	256	*Origin*	avg400	*Original Points Count*	32768	*Owner*	nmr-user
Points Count	32768	*Pulse Sequence*	zgpg30	*Receiver Gain*	2050.00	*SW(cyclical) (Hz)*	24038.46
Solvent	METHANOL-d4	*Spectrum Offset (Hz)*	10217.2344	*Spectrum Type*	STANDARD	*Sweep Width (Hz)*	24037.73
Temperature (degree C)	21.200						

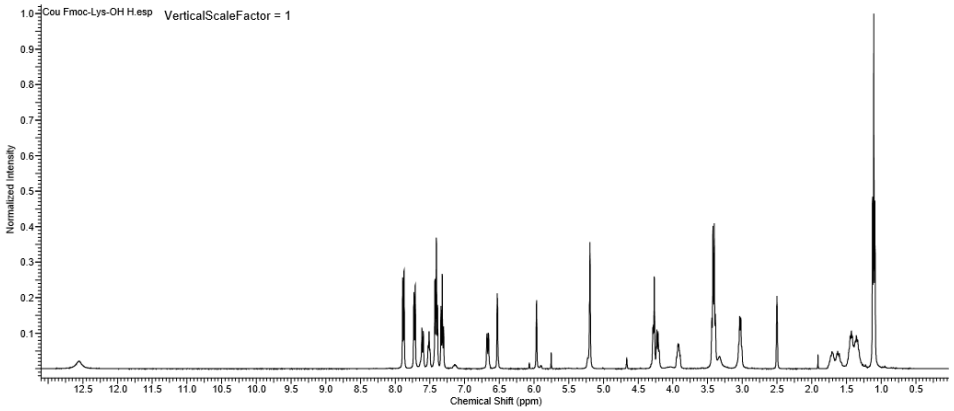




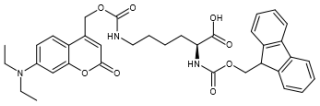
Compound 220

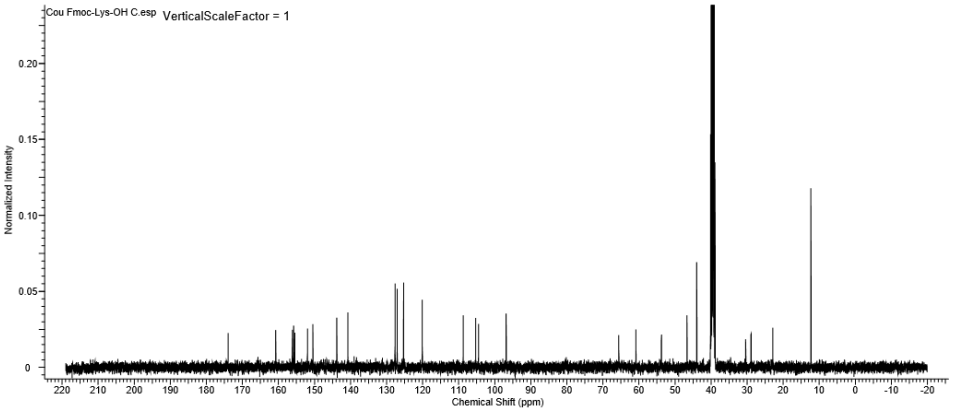
Acquisition Time (sec)	3.2768	*Comment*	Instrument AVG400 Group SJC Chemist MLS Cou Fmoc-Lys-OH h1acq.crl DMSO {C:\NMR} sjcgrp 60				
Date	01 Apr 2015 14:11:28			*Date Stamp*	01 Apr 2015 14:11:28		
File Name	D:\Gnomeeee\NMR\Cou Stuff\Cou Fmoc-Lys-OH\Apr01-2015-60-\1\PDATA\1\1r					*Frequency (MHz)*	400.20
Nucleus	1H	*Number of Transients*	8	*Origin*	avg400	*Original Points Count*	32768
Owner	nmr-user	*Points Count*	65536	*Pulse Sequence*	zg60	*Receiver Gain*	66.06
SW(cyclical) (Hz)	10000.00	*Solvent*	DMSO-d6	*Spectrum Offset (Hz)*	2468.3193	*Spectrum Type*	STANDARD
Sweep Width (Hz)	9999.85	*Temperature (degree C)*	25.005				





Acquisition Time (sec)	1.3631	*Comment*	Instrument AVG400 Group SJC Chemist MLS Cou Fmoc-Lys-OH c13acq.crl DMSO {C:\NMR} sjcgrp 60				
Date	02 Apr 2015 22:32:48			*Date Stamp*	02 Apr 2015 22:32:48		
File Name	D:\Gnomeeee\NMR\Cou Stuff\Cou Fmoc-Lys-OH\Apr01-2015-60-\3\PDATA\1\1r					*Frequency (MHz)*	100.63
Nucleus	13C	*Number of Transients*	256	*Origin*	avg400	*Original Points Count*	32768
Owner	nmr-user	*Points Count*	32768	*Pulse Sequence*	zgpg30	*Receiver Gain*	206.87
SW(cyclical) (Hz)	24038.46	*Solvent*	DMSO-d6	*Spectrum Offset (Hz)*	10013.7646	*Spectrum Type*	STANDARD
Sweep Width (Hz)	24037.73	*Temperature (degree C)*	24.994				

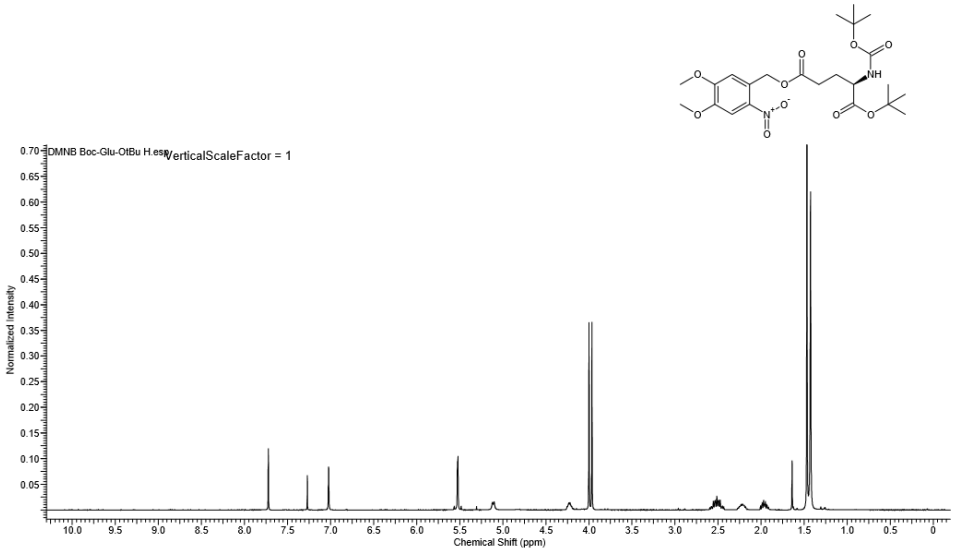




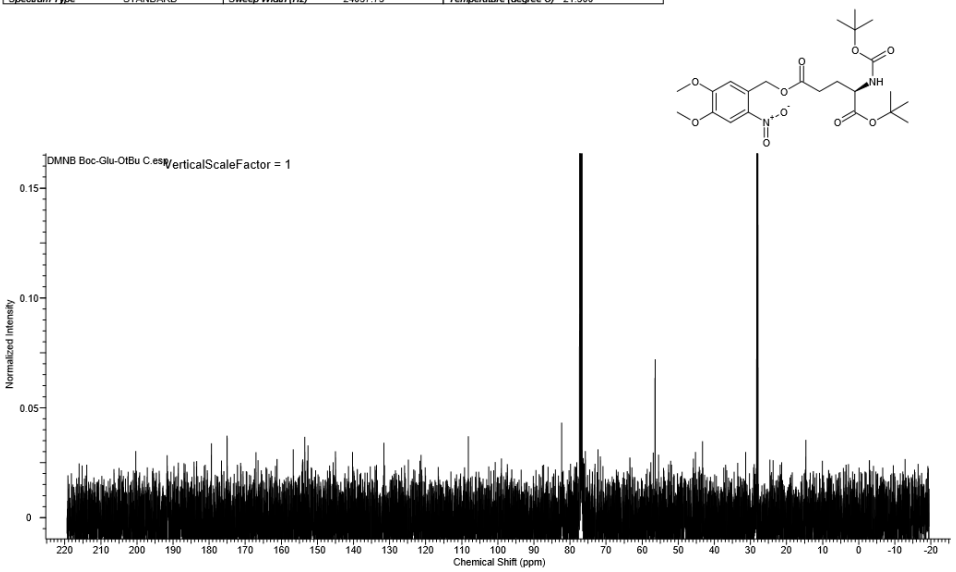
A.4 DMNB Caged Amino Acids

Compound 177

Acquisition Time (sec)	3.2768	*Comment*	Instrument AVG400 Group SJC Chemist MLS MLS05080: DMNB-(Fmoc)Glu(OtBu) h1acq.crl CDCl3 {C:\NMR} sjcgrp 30				
Date	17 Mar 2014 17:44:32			*Date Stamp*	17 Mar 2014 17:44:32		
File Name	F:\NMR\DMNB Stuff\DMNB Boc-Glu-OtBu\Mar17-2014-30\2\PDATA\1\1r					*Frequency (MHz)*	400.20
Nucleus	1H	*Number of Transients*	16	*Origin*	avg400	*Original Points Count*	32768
Owner	nmr-user	*Points Count*	65536	*Pulse Sequence*	zg30	*Receiver Gain*	221.01
SW(cyclical) (Hz)	10000.00	*Solvent*	CHLOROFORM-d	*Spectrum Offset (Hz)*	2461.8376	*Spectrum Type*	STANDARD
Sweep Width (Hz)	9999.85	*Temperature (degree C)*	20.700				

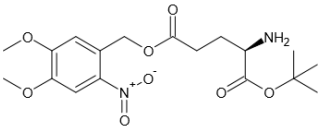


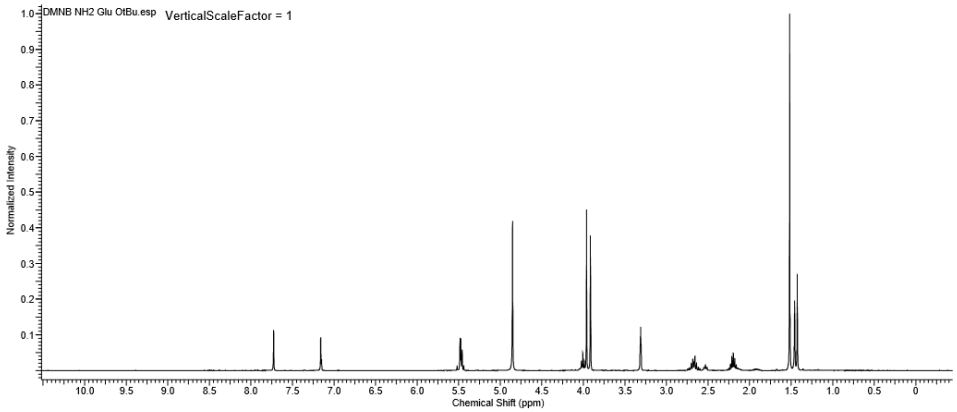
Acquisition Time (sec)	1.3631	*Comment*	Instrument AVG400 Group SJC Chemist MLS MLS05080: DMNB-(Fmoc)Glu(OtBu) c13acq.crl CDCl3 {C:\NMR} sjcgrp 30				
Date	18 Mar 2014 00:17:04	*Date Stamp*	18 Mar 2014 00:17:04	*File Name*	F:\NMR\DMNB Stuff\DMNB Boc-Glu-OtBu\Mar17-2014-30\4\pdata\1\1r		
Frequency (MHz)	100.63	*Nucleus*	13C	*Number of Transients*	256	*Origin*	avg400
Original Points Count	32768	*Owner*	nmr-user	*Points Count*	32768	*Pulse Sequence*	zgpg30
Receiver Gain	2050.00	*SW(cyclical) (Hz)*	24038.46	*Solvent*	CHLOROFORM-d	*Spectrum Offset (Hz)*	10057.5303
Spectrum Type	STANDARD	*Sweep Width (Hz)*	24037.73	*Temperature (degree C)*	21.500		



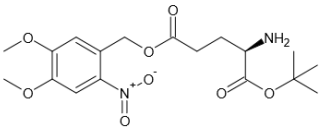
Compound 275

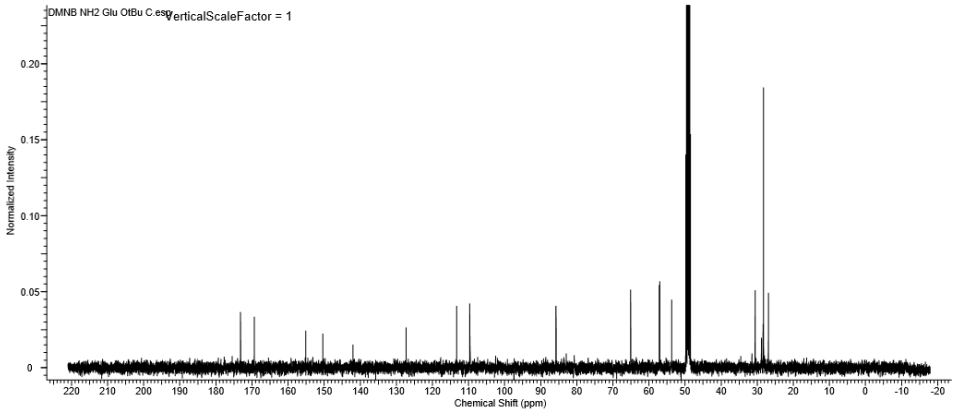
Acquisition Time (sec)	3.2768	*Comment*	Instrument AVG400 Group SJC Chemist MLS DMNB NH2 Glu OtBu h1acq.crl MeOD {C:\NMR} sjcgrp 31				
Date	01 May 2015 19:05:52			*Date Stamp*	01 May 2015 19:05:52		
File Name	D:\Gnomeeee\NMR\DMNB Stuff\DMNB NH2-Glu-OtBu\May01-2015-31-1\1\PDATA\1\1r					*Frequency (MHz)*	400.20
Nucleus	1H	*Number of Transients*	8	*Origin*	avg400	*Original Points Count*	32768
Owner	nmr-user	*Points Count*	65536	*Pulse Sequence*	zg60	*Receiver Gain*	114.66
SW(cyclical) (Hz)	10000.00	*Solvent*	METHANOL-d4	*Spectrum Offset (Hz)*	2463.9595	*Spectrum Type*	STANDARD
Sweep Width (Hz)	9999.85	*Temperature (degree C)*	24.995				





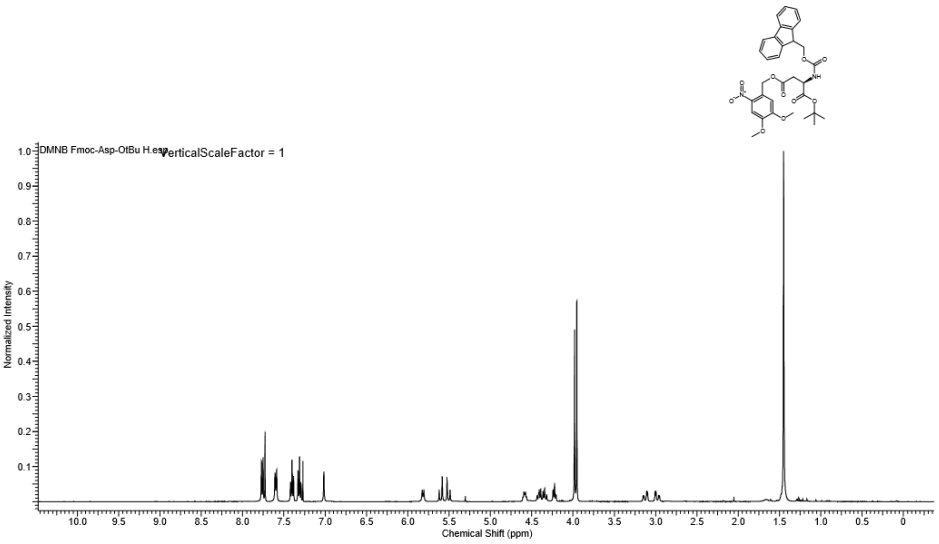
Acquisition Time (sec)	1.3631	*Comment*	Instrument AVG400 Group SJC Chemist MLS DMNB NH2 Glu OtBu c13acq.crl MeOD {C:\NMR} sjcgrp 31				
Date	02 May 2015 12:14:08			*Date Stamp*	02 May 2015 12:14:08		
File Name	D:\Gnomeeee\NMR\DMNB Stuff\DMNB NH2-Glu-OtBu\May01-2015-31-3\PDATA\1\1r					*Frequency (MHz)*	100.63
Nucleus	13C	*Number of Transients*	256	*Origin*	avg400	*Original Points Count*	32768
Owner	nmr-user	*Points Count*	32768	*Pulse Sequence*	zgpg30	*Receiver Gain*	206.87
SW(cyclical) (Hz)	24038.46	*Solvent*	METHANOL-d4	*Spectrum Offset (Hz)*	10217.9678	*Spectrum Type*	STANDARD
Sweep Width (Hz)	24037.73	*Temperature (degree C)*	25.004				



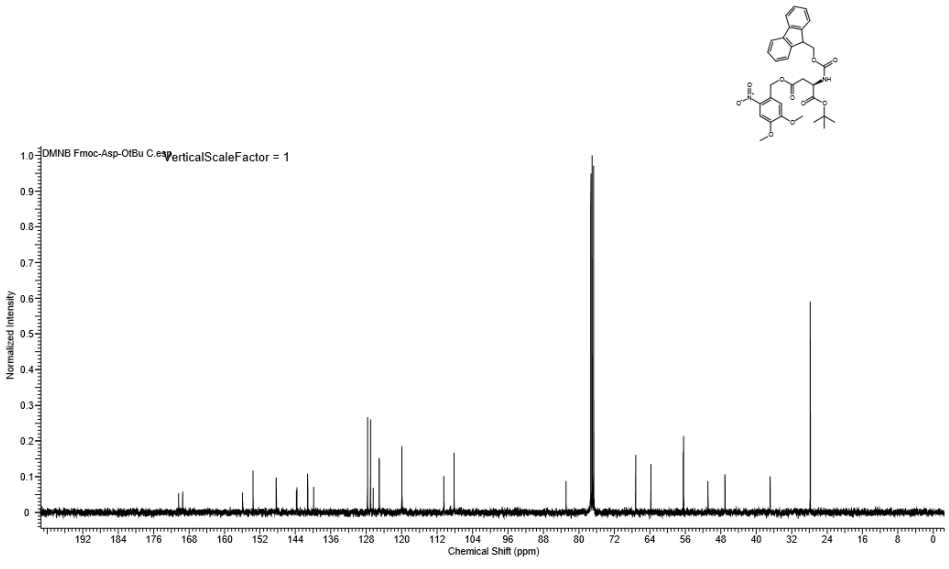


Compound 212

Acquisition Time (sec)	3.2768	*Comment*	Instrument AVG400 Group SJC Chemist MLS MLS05070: DMNB (Fmoc) Asp (OtBu) h1acq.crl CDCl3 (C:\NMR) sjcgrp 39				
Date	07 Jun 2014 20:39:44			*Date Stamp*	07 Jun 2014 20:39:44		
File Name	F:\NMR\DMNB Stuff\DMNB Fmoc-Asp-OtBu MLS05070\1\pdata\1\1r			*Frequency (MHz)*	400.20	*Nucleus*	1H
Number of Transients	16	*Origin*	avq400	*Original Points Count*	32768	*Owner*	nmr-user
Points Count	65536	*Pulse Sequence*	zg30	*Receiver Gain*	202.31	*SW(cyclical) (Hz)*	10000.00
Solvent	CHLOROFORM-d	*Spectrum Offset (Hz)*	2461.8374	*Spectrum Type*	STANDARD	*Sweep Width (Hz)*	9999.85
Temperature (degree C)	25.000						

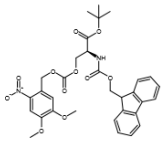


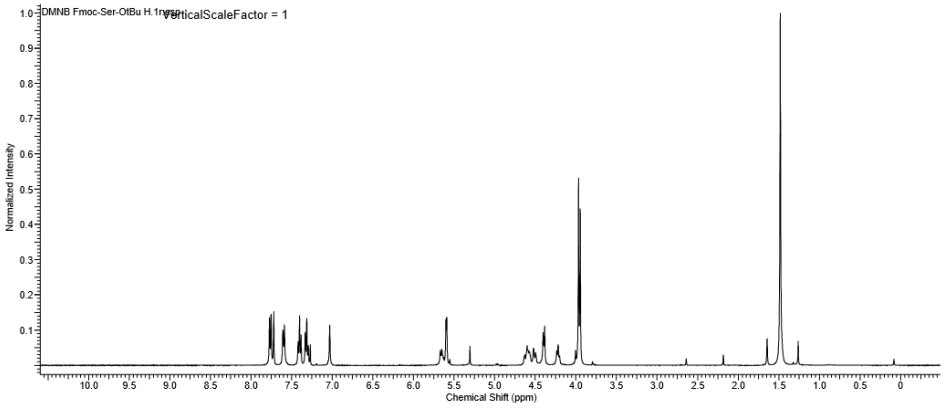
Acquisition Time (sec)	1.3631	*Comment*	Instrument AVG400 Group SJC Chemist MLS MLS05070: DMNB (Fmoc) Asp (OtBu) c13acq.crl CDCl3 (C:\NMR) sjcgrp 39				
Date	07 Jun 2014 21:41:36	*Date Stamp*	07 Jun 2014 21:41:36	*File Name*	F:\NMR\DMNB Stuff\DMNB Fmoc-Asp-OtBu MLS05070\3\pdata\1\1r		
Frequency (MHz)	100.63	*Nucleus*	13C	*Number of Transients*	256	*Origin*	avq400
Original Points Count	32768	*Owner*	nmr-user	*Points Count*	32768	*Pulse Sequence*	zgpg30
Receiver Gain	2050.00	*SW(cyclical) (Hz)*	24038.46	*Solvent*	CHLOROFORM-d	*Spectrum Offset (Hz)*	10055.3301
Spectrum Type	STANDARD	*Sweep Width (Hz)*	24037.73	*Temperature (degree C)*	27.000		



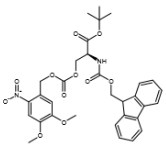
Compound 213

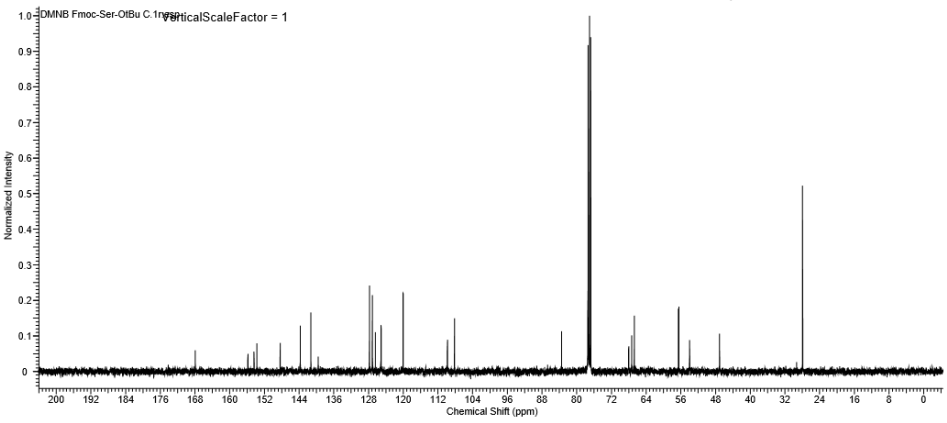
Acquisition Time (sec)	3.2768	*Comment*	Instrument AVG400 Group SJC Chemist MLS MLS08120: DMNB Fmoc-Ser-OtBu h1acq.crl CDCl3 (C:\NMR) sjcgrp 9				
Date	09 Jan 2015 08:51:12			*Date Stamp*	09 Jan 2015 08:51:12		
File Name	F:\NMR\DMNB Stuff\DMNB Fmoc-Ser-OtBu\Jan09-2015-9-\1\pdata\1\1r			*Frequency (MHz)*	400.20	*Nucleus*	1H
Number of Transients	16	*Origin*	avg400	*Original Points Count*	32768	*Owner*	nmr-user
Points Count	65536	*Pulse Sequence*	zg30	*Receiver Gain*	175.70	*SW(cyclical) (Hz)*	10000.00
Solvent	CHLOROFORM-d	*Spectrum Offset (Hz)*	2462.4480	*Spectrum Type*	STANDARD	*Sweep Width (Hz)*	9999.85
Temperature (degree C)	20.900						





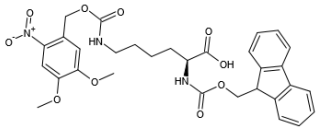
Acquisition Time (sec)	1.3631	*Comment*	Instrument AVG400 Group SJC Chemist MLS MLS08120: DMNB Fmoc-Ser-OtBu c13acq.crl CDCl3 (C:\NMR) sjcgrp 9				
Date	09 Jan 2015 23:04:32	*Date Stamp*	09 Jan 2015 23:04:32	*File Name*	F:\NMR\DMNB Stuff\DMNB Fmoc-Ser-OtBu\Jan09-2015-9-\3\pdata\1\1r		
Frequency (MHz)	100.63	*Nucleus*	13C	*Number of Transients*	256	*Origin*	avg400
Original Points Count	32768	*Owner*	nmr-user	*Points Count*	32768	*Pulse Sequence*	zgpg30
Receiver Gain	2050.00	*SW(cyclical) (Hz)*	24038.46	*Solvent*	CHLOROFORM-d	*Spectrum Offset (Hz)*	10062.6055
Spectrum Type	STANDARD	*Sweep Width (Hz)*	24037.73	*Temperature (degree C)*	21.800		

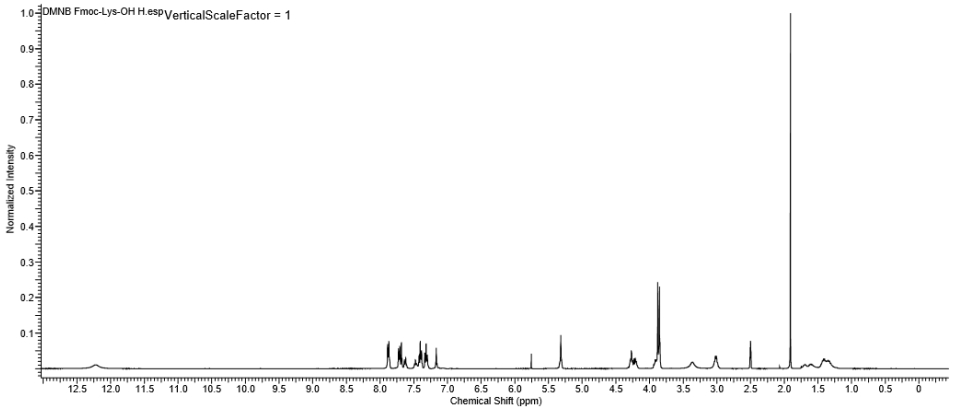




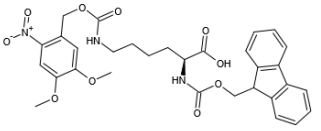
Compound 214

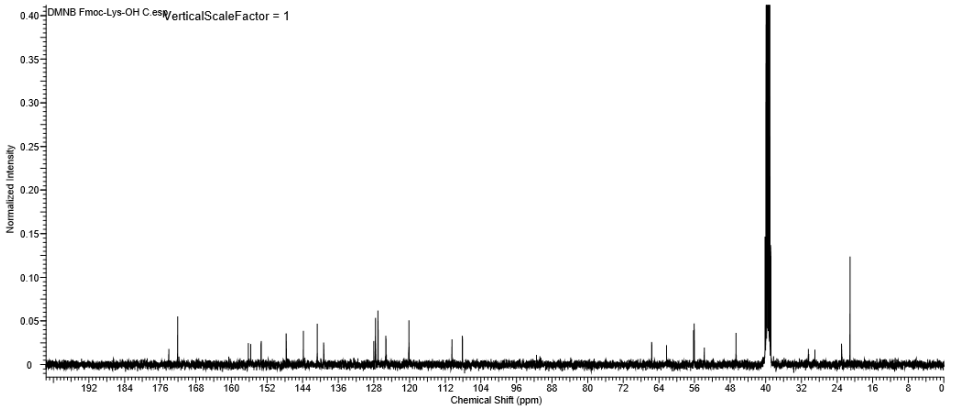
Acquisition Time (sec)	3.2768	*Comment*	Instrument AVG400 Group SJC Chemist MLS MLS07206: DMNB Fmoc-Lys-OH h1acq crl DMSO {C:\NMR} sjcgrp 39				
Date	07 Nov 2014 08:27:44			*Date Stamp*	07 Nov 2014 08:27:44		
File Name	F:\NMR\DMNB Stuff\DMNB Fmoc-Lys-OH\Nov06-2014-39\1\pdata\1\1r					*Frequency (MHz)*	400.20
Nucleus	1H	*Number of Transients*	16	*Origin*	avg400	*Original Points Count*	32768
Owner	nmr-user	*Points Count*	65536	*Pulse Sequence*	zg30	*Receiver Gain*	175.70
SW(cyclical) (Hz)	10000.00	*Solvent*	DMSO-d6	*Spectrum Offset (Hz)*	2464.6572	*Spectrum Type*	STANDARD
Sweep Width (Hz)	9999.85	*Temperature (degree C)*	21.000				





Acquisition Time (sec)	1.3631	*Comment*	Instrument AVG400 Group SJC Chemist MLS MLS07206: DMNB Fmoc-Lys-OH c13acq crl DMSO {C:\NMR} sjcgrp 39				
Date	07 Nov 2014 23:32:16			*Date Stamp*	07 Nov 2014 23:32:16		
File Name	F:\NMR\DMNB Stuff\DMNB Fmoc-Lys-OH\Nov06-2014-39\3\pdata\1\1r			*Frequency (MHz)*	100.63	*Nucleus*	13C
Number of Transients	256	*Origin*	avg400	*Original Points Count*	32768	*Owner*	nmr-user
Points Count	32768	*Pulse Sequence*	zgpg30	*Receiver Gain*	2050.00	*SW(cyclical) (Hz)*	24038.46
Solvent	DMSO-d6	*Spectrum Offset (Hz)*	10018.1660	*Spectrum Type*	STANDARD	*Sweep Width (Hz)*	24037.73
Temperature (degree C)	21.200						



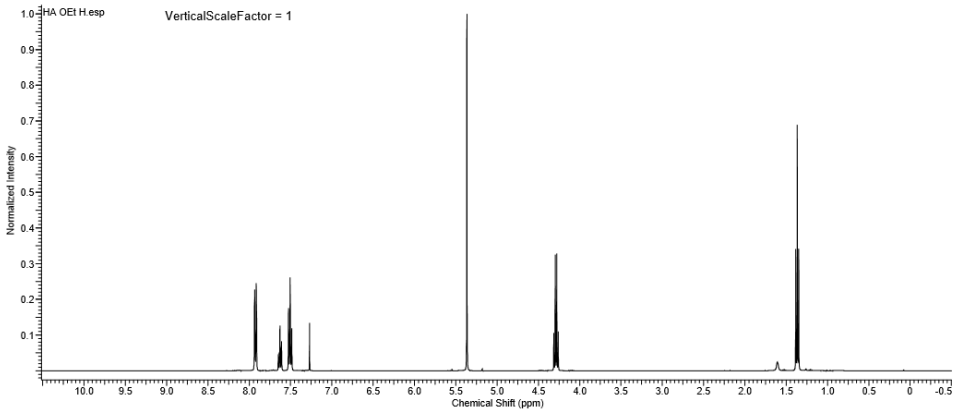


A.5 Phenacyl Caged Amino Acids

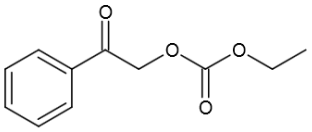
Compound 170

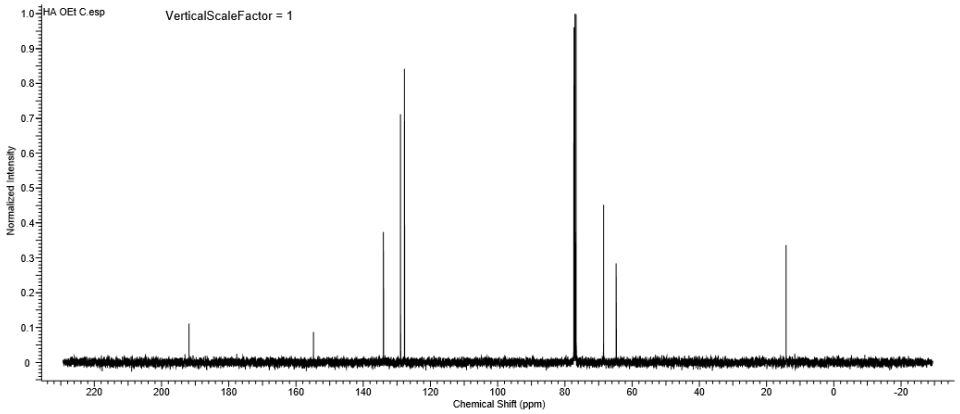
Acquisition Time (sec)	4.0894	*Comment*	Instrument AVN400 Chemist MLS Group SJC 2-HA-Et h1acq.crl CDCl3 (C:\NMR) sjcgrp 29				
Date	02 Apr 2013 10:31:44			*Date Stamp*	02 Apr 2013 10:31:44		
File Name	D:\Gnomeeee\NMR\Phenacyl Stuff\Benzaldehyde Model\Apr02-2013-29\1\PDATA\1\1r					*Frequency (MHz)*	400.25
Nucleus	1H	*Number of Transients*	16	*Origin*	avn400	*Original Points Count*	32768
Owner	dp-nmrgroup	*Points Count*	32768	*Pulse Sequence*	zg60	*Receiver Gain*	93.00
SW(cyclical) (Hz)	8012.82	*Solvent*	CHLOROFORM-d	*Spectrum Offset (Hz)*	2394.4668	*Spectrum Type*	STANDARD
Sweep Width (Hz)	8012.58	*Temperature (degree C)*	22.252				





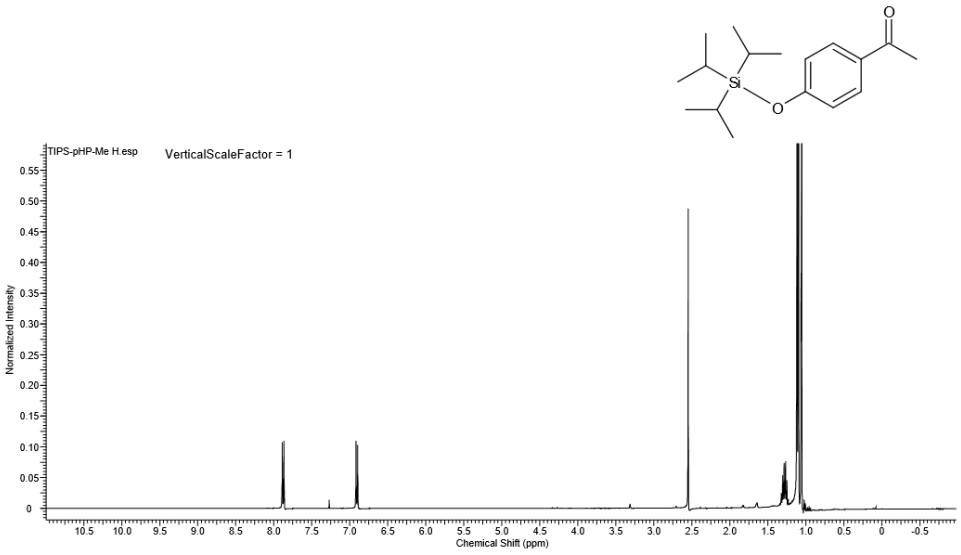
Acquisition Time (sec)	0.6291	*Comment*	Instrument AVN400 Chemist MLS Group SJC 2-HA-Et c13acq.crl CDCl3 (C:\NMR) sjcgrp 29				
Date	02 Apr 2013 10:44:32			*Date Stamp*	02 Apr 2013 10:44:32		
File Name	D:\Gnomeeee\NMR\Phenacyl Stuff\Benzaldehyde Model\Apr02-2013-29\3\PDATA\1\1r					*Frequency (MHz)*	100.64
Nucleus	13C	*Number of Transients*	256	*Origin*	avn400	*Original Points Count*	16384
Owner	dp-nmrgroup	*Points Count*	32768	*Pulse Sequence*	zgpg30	*Receiver Gain*	205.43
SW(cyclical) (Hz)	26041.67	*Solvent*	CHLOROFORM-d	*Spectrum Offset (Hz)*	10060.9756	*Spectrum Type*	STANDARD
Sweep Width (Hz)	26040.87	*Temperature (degree C)*	23.452				



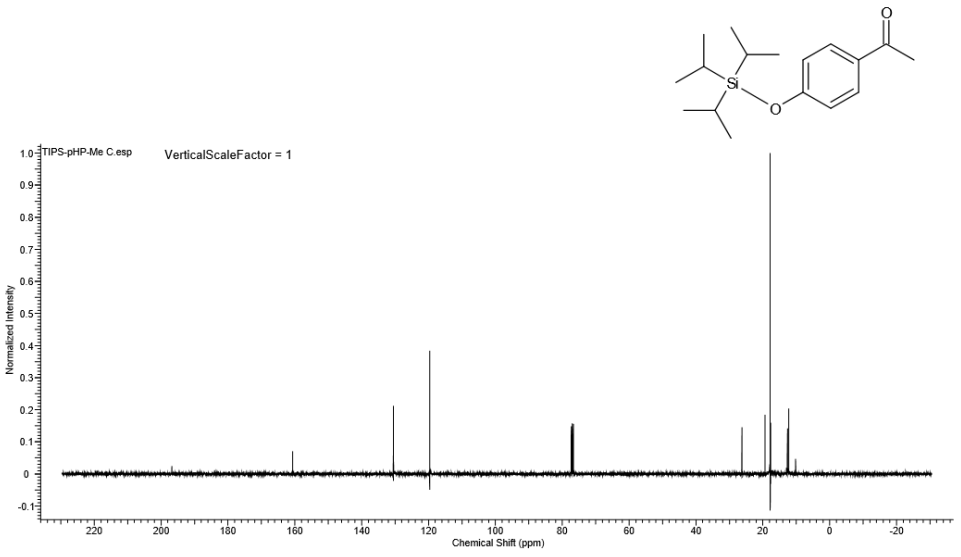


Compound 202

Acquisition Time (sec)	3.9584	*Comment*	Instrument DQX400 Chemist MLS Group SJC MLS01168 h1acq.au CDCl3 (E:\NMR2012) sjcgrp 14				
Date	14 Apr 2012 03:52:48			*Date Stamp*	14 Apr 2012 03:52:48		
File Name	F:\NMR\Phenacyl Stuff\TIPS-pHP-Me MLS04186\Apr13-2012-14\1\fid			*Frequency (MHz)*	400.20	*Nucleus*	1H
Number of Transients	16	*Origin*	av400	*Original Points Count*	32768	*Owner*	dp-nmrgroup
Points Count	32768	*Pulse Sequence*	zg60	*Receiver Gain*	25.40	*SW(cyclical) (Hz)*	8278.15
Solvent	CHLOROFORM-d	*Spectrum Offset (Hz)*	2468.9956	*Spectrum Type*	STANDARD	*Sweep Width (Hz)*	8277.89
Temperature (degree C)	27.000						

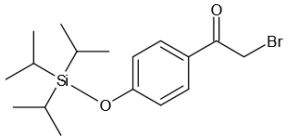


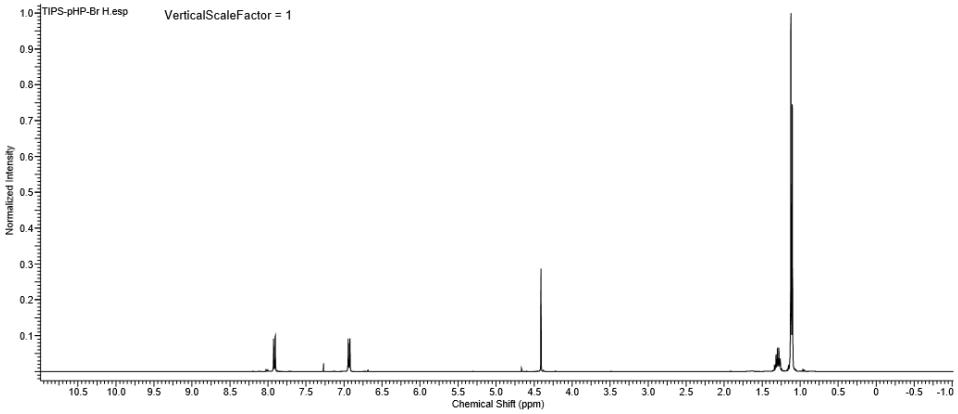
Acquisition Time (sec)	0.6259	*Comment*	Instrument DQX400 Chemist MLS Group SJC MLS01168 c13acq.au CDCl3 (E:\NMR2012) sjcgrp 14				
Date	14 Apr 2012 04:03:28			*Date Stamp*	14 Apr 2012 04:03:28		
File Name	F:\NMR\Phenacyl Stuff\TIPS-pHP-Me MLS04186\Apr13-2012-14\3\fid			*Frequency (MHz)*	100.63	*Nucleus*	13C
Number of Transients	256	*Origin*	av400	*Original Points Count*	16384	*Owner*	dp-nmrgroup
Points Count	16384	*Pulse Sequence*	zgpg30	*Receiver Gain*	32768.00	*SW(cyclical) (Hz)*	26178.01
Solvent	CHLOROFORM-d	*Spectrum Offset (Hz)*	10018.1836	*Spectrum Type*	STANDARD	*Sweep Width (Hz)*	26176.41
Temperature (degree C)	27.000						



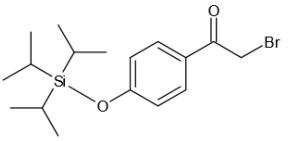
Compound 203

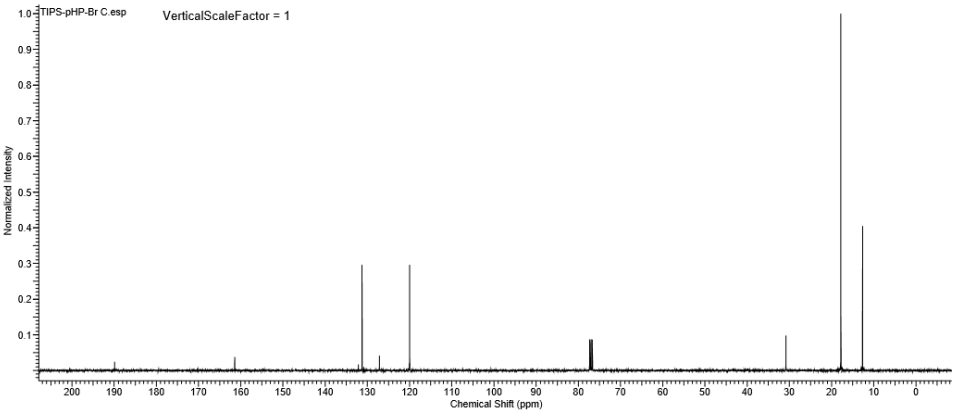
Acquisition Time (sec)	4.0894	*Comment*	Instrument AVF400 Chemist MLS Group SJC MLS04188: TIPS-pHP-Br h1acq.crl CDCl3 (C:\NMR) sjcgrp 52				
Date	21 Feb 2014 10:48:32			*Date Stamp*	21 Feb 2014 10:48:32		
File Name	F:\NMR\Phenacyl Stuff\TIPS-pHP-Br MLS04188\1\pdata\1\1r			*Frequency (MHz)*	400.25	*Nucleus*	1H
Number of Transients	16	*Origin*	avf400	*Original Points Count*	32768	*Owner*	nmr-user
Points Count	32768	*Pulse Sequence*	zg60	*Receiver Gain*	25.89	*SW(cyclical) (Hz)*	8012.82
Solvent	CHLOROFORM-d	*Spectrum Offset (Hz)*	2393.9775	*Spectrum Type*	STANDARD	*Sweep Width (Hz)*	8012.58
Temperature (degree C)	23.708						





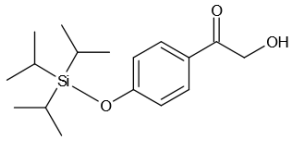
Acquisition Time (sec)	0.6291	*Comment*	Instrument AVF400 Chemist MLS Group SJC MLS04188: TIPS-pHP-Br c13acq.crl CDCl3 (C:\NMR) sjcgrp 52				
Date	21 Feb 2014 11:14:08			*Date Stamp*	21 Feb 2014 11:14:08		
File Name	F:\NMR\Phenacyl Stuff\TIPS-pHP-Br MLS04188\4\pdata\1\1r			*Frequency (MHz)*	100.64	*Nucleus*	13C
Number of Transients	256	*Origin*	avf400	*Original Points Count*	16384	*Owner*	nmr-user
Points Count	32768	*Pulse Sequence*	zgpg30	*Receiver Gain*	205.43	*SW(cyclical) (Hz)*	26041.67
Solvent	CHLOROFORM-d	*Spectrum Offset (Hz)*	10059.3848	*Spectrum Type*	STANDARD	*Sweep Width (Hz)*	26040.87
Temperature (degree C)	24.869						

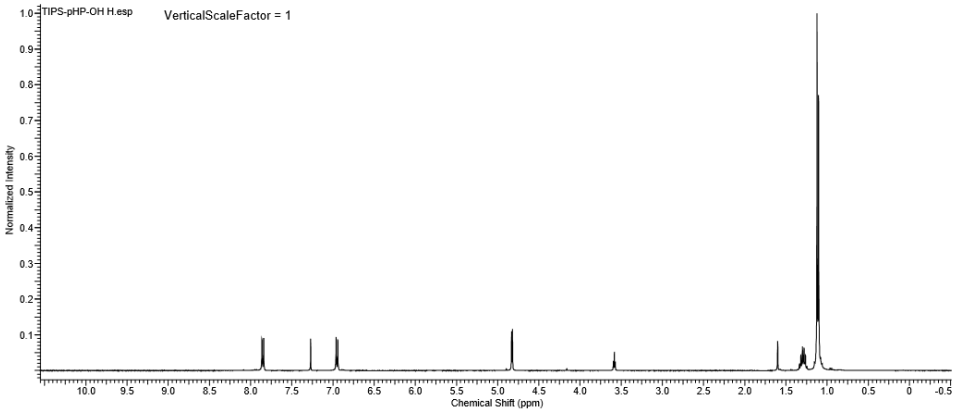




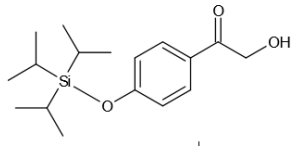
Compound 204

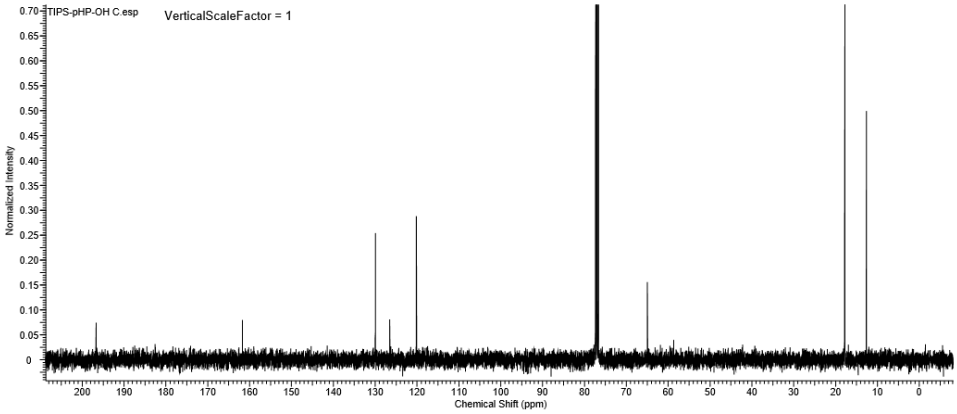
Acquisition Time (sec)	3.2768	*Comment*	Instrument AVG400 Group SJC Chemist MLS MLS04190: TIPS-pHP-OH h1acq crl CDCl3 {C:\NMR} sjcgrp 5				
Date	23 Feb 2014 16:12:48	*Date Stamp*	23 Feb 2014 16:12:48				
File Name	F:\NMR\Phenacyl Stuff\TIPS-pHP-OH MLS04190\TIPS-pHP-OH MLS04190 retake\1\PDATA\1\1r					*Frequency (MHz)*	400.20
Nucleus	1H	*Number of Transients*	16	*Origin*	avg400	*Original Points Count*	32768
Owner	nmr-user	*Points Count*	65536	*Pulse Sequence*	zg30	*Receiver Gain*	279.35
SW(cyclical) (Hz)	10000.00	*Solvent*	CHLOROFORM-d	*Spectrum Offset (Hz)*	2460.9219	*Spectrum Type*	STANDARD
Sweep Width (Hz)	9999.85	*Temperature (degree C)*	21.200				





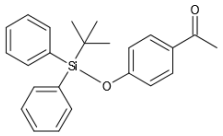
Acquisition Time (sec)	1.3631	*Comment*	Instrument AVG400 Group SJC Chemist MLS MLS04190: TIPS-pHP-OH c13acq crl CDCl3 {C:\NMR} sjcgrp 11				
Date	23 Feb 2014 19:16:16			*Date Stamp*	23 Feb 2014 19:16:16		
File Name	F:\NMR\Phenacyl Stuff\TIPS-pHP-OH MLS04190\3\pdata\1\1r			*Frequency (MHz)*	100.63	*Nucleus*	13C
Number of Transients	256	*Origin*	avg400	*Original Points Count*	32768	*Owner*	nmr-user
Points Count	32768	*Pulse Sequence*	zgpg30	*Receiver Gain*	2050.00	*SW(cyclical) (Hz)*	24038.46
Solvent	CHLOROFORM-d	*Spectrum Offset (Hz)*	10056.7969	*Spectrum Type*	STANDARD	*Sweep Width (Hz)*	24037.73
Temperature (degree C)	22.000						

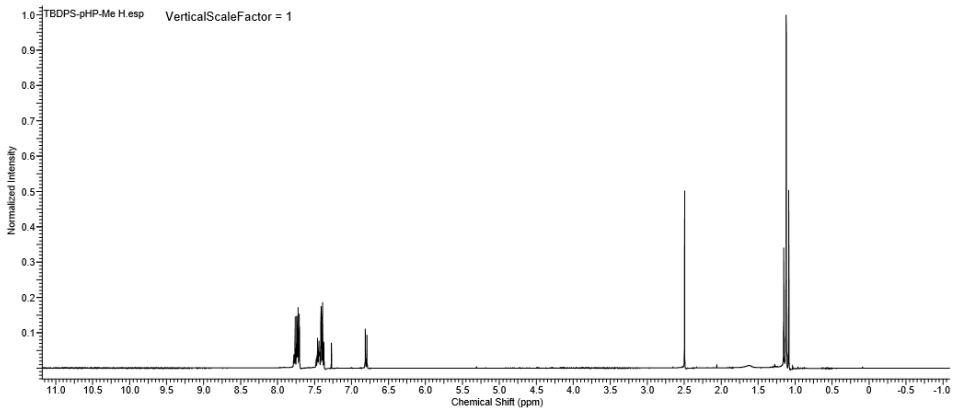




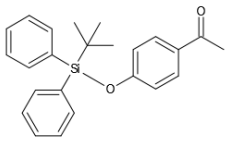
Compound 175

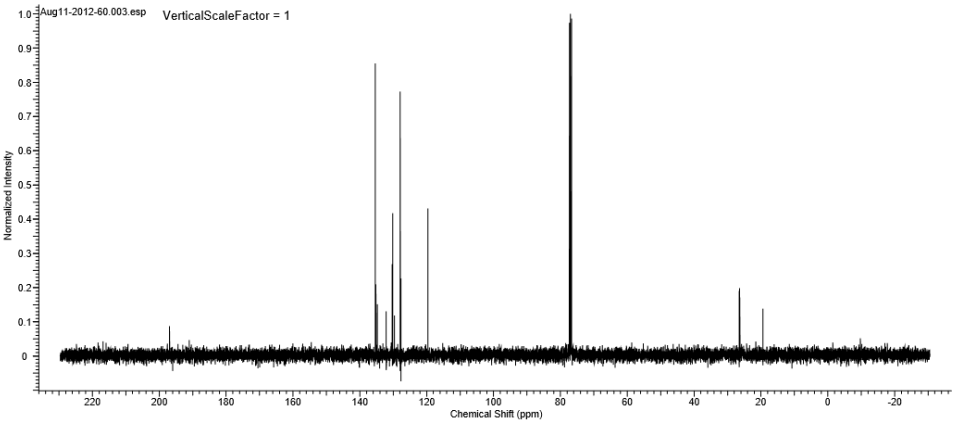
Acquisition Time (sec)	3.9584	*Comment*	Instrument DQX400 Chemist MLS Group SJC MLS02100 - TBDPS pHp h1acq.au CDCl3 (E:\NMR2012) sjcgrp 60				
Date	11 Aug 2012 22:54:08			*Date Stamp*	11 Aug 2012 22:54:08		
File Name	F:\NMR\Phenacyl Stuff\TBDPS-pHP\TBDPS-pHP-Me\Aug11-2012-60\1\fid					*Frequency (MHz)*	400.20
Nucleus	1H	*Number of Transients*	16	*Origin*	av400	*Original Points Count*	32768
Owner	dp-nmrgroup	*Points Count*	32768	*Pulse Sequence*	zg60	*Receiver Gain*	161.30
SW(cyclical) (Hz)	8278.15	*Solvent*	CHLOROFORM-d	*Spectrum Offset (Hz)*	2468.9956	*Spectrum Type*	STANDARD
Sweep Width (Hz)	8277.89	*Temperature (degree C)*	27.000				





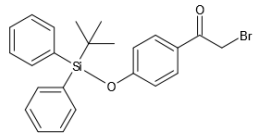
Acquisition Time (sec)	0.6259	*Comment*	Instrument DQX400 Chemist MLS Group SJC MLS02100 - TBDPS pHp c13acq.au CDCl3 (E:\NMR2012) sjcgrp 60				
Date	11 Aug 2012 23:06:56	*Date Stamp*	11 Aug 2012 23:06:56	*File Name*	F:\NMR\Phenacyl Stuff\TBDPS-pHP\TBDPS-pHP-Me\Aug11-2012-60\3\fid		
Frequency (MHz)	100.63	*Nucleus*	13C	*Number of Transients*	256	*Origin*	av400
Original Points Count	16384	*Owner*	dp-nmrgroup	*Points Count*	16384	*Pulse Sequence*	zgpg30
Receiver Gain	32768.00	*SW(cyclical) (Hz)*	26178.01	*Solvent*	CHLOROFORM-d	*Spectrum Offset (Hz)*	10018.1836
Spectrum Type	STANDARD	*Sweep Width (Hz)*	26176.41	*Temperature (degree C)*	27.000		

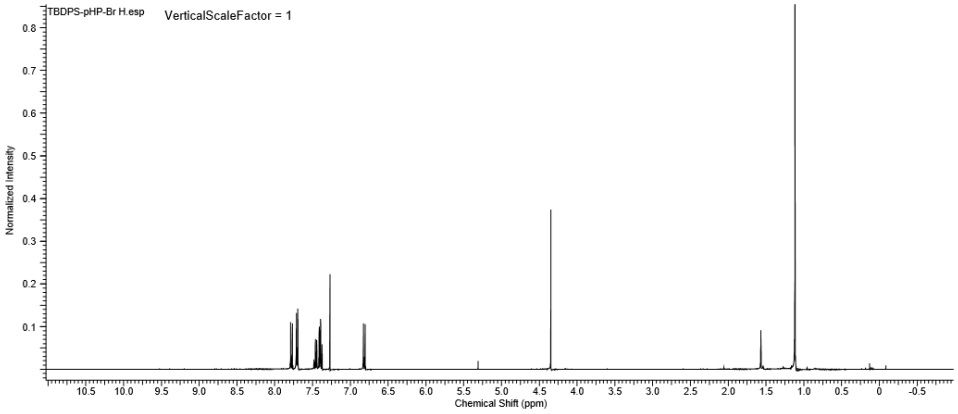




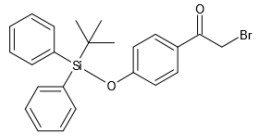
Compound 176

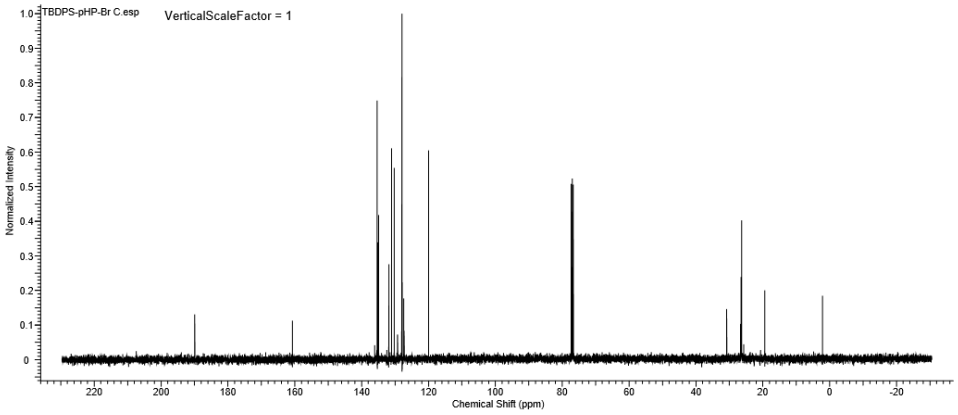
Acquisition Time (sec)	3.9584	*Comment*	Instrument DQX400 Chemist MLS Group SJC MLS02128 - Spot 1 h1acq au CDCl3 {E:\NMR2012} sjcgrp 38				
Date	17 Sep 2012 12:18:24	*Date Stamp*	17 Sep 2012 12:18:24				
File Name	G:\Gnomeeeel\NMR\Phenacyl Stuff\TBDPS-pHP\TBDPS-pHP-Br\MLS02128\Sep17-2012-38\1\fid					*Frequency (MHz)*	400.20
Nucleus	1H	*Number of Transients*	16	*Origin*	av400	*Original Points Count*	32768
Owner	dp-nmrgroup	*Points Count*	32768	*Pulse Sequence*	zg60	*Receiver Gain*	322.50
SW(cyclical) (Hz)	8278.15	*Solvent*	CHLOROFORM-d	*Spectrum Offset (Hz)*	2468.2375	*Spectrum Type*	STANDARD
Sweep Width (Hz)	8277.89	*Temperature (degree C)*	27.000				





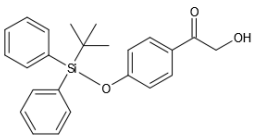
Acquisition Time (sec)	0.6259	*Comment*	Instrument DQX400 Chemist MLS Group SJC MLS02102 - TBDPS pHp Br c13acq au CDCl3 {E:\NMR2012} sjcgrp 13				
Date	09 Aug 2012 22:34:56	*Date Stamp*	09 Aug 2012 22:34:56				
File Name	G:\Gnomeeeel\NMR\Phenacyl Stuff\TBDPS-pHP\TBDPS-pHP-Br\MLS02102\Aug09-2012-13\3\fid					*Frequency (MHz)*	100.63
Nucleus	13C	*Number of Transients*	256	*Origin*	av400	*Original Points Count*	16384
Owner	dp-nmrgroup	*Points Count*	16384	*Pulse Sequence*	zgpg30	*Receiver Gain*	32768.00
SW(cyclical) (Hz)	26178.01	*Solvent*	CHLOROFORM-d	*Spectrum Offset (Hz)*	10016.5859	*Spectrum Type*	STANDARD
Sweep Width (Hz)	26176.41	*Temperature (degree C)*	27.000				

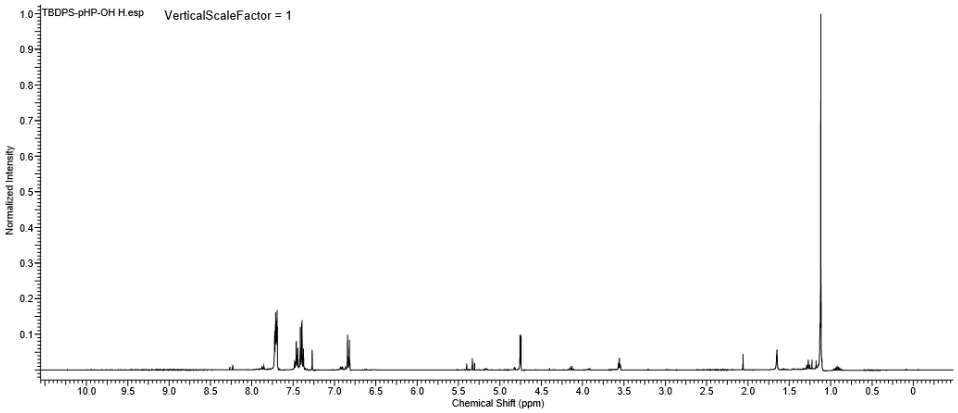




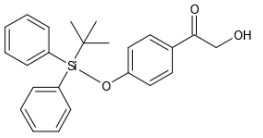
Compound 171

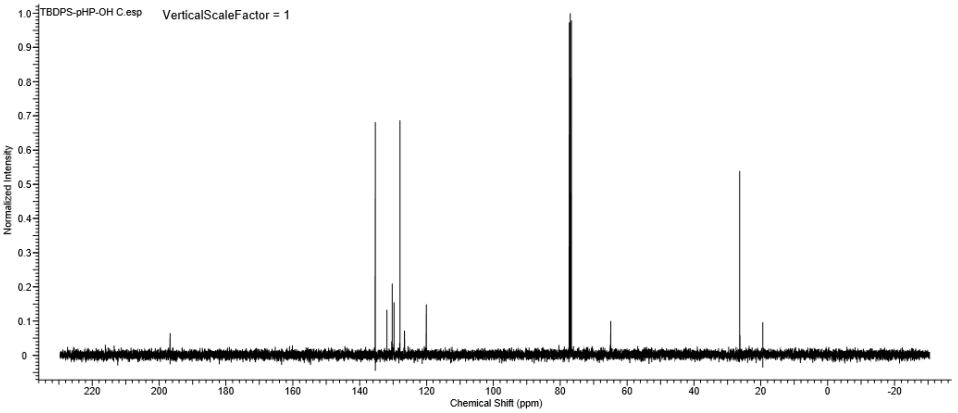
Acquisition Time (sec)	3.9584	*Comment*	Instrument DQX400 Chemist MLS Group SJC MLS02104 - TBDPS pHp OH h1acq.au CDCl3 (E:\NMR2012) sjcgrp 59				
Date	11 Aug 2012 22:26:24	*Date Stamp*	11 Aug 2012 22:26:24				
File Name	G:\Gnomeeee\NMR\Phenacyl Stuff\TBDPS-pHP\TBDPS-pHP-OH\MLS02104\Aug11-2012-59\1\fid					*Frequency (MHz)*	400.20
Nucleus	1H	*Number of Transients*	16	*Origin*	av400	*Original Points Count*	32768
Owner	dp-nmrgroup	*Points Count*	32768	*Pulse Sequence*	zg60	*Receiver Gain*	128.00
SW(cyclical) (Hz)	8278.15	*Solvent*	CHLOROFORM-d	*Spectrum Offset (Hz)*	2468.5974	*Spectrum Type*	STANDARD
Sweep Width (Hz)	8277.89	*Temperature (degree C)*	27.000				





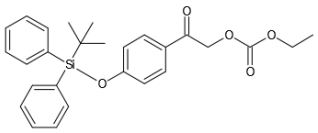
Acquisition Time (sec)	0.6259	*Comment*	Instrument DQX400 Chemist MLS Group SJC MLS02104 - TBDPS pHp OH c13acq.au CDCl3 (E:\NMR2012) sjcgrp 59				
Date	11 Aug 2012 22:37:04	*Date Stamp*	11 Aug 2012 22:37:04				
File Name	G:\Gnomeeee\NMR\Phenacyl Stuff\TBDPS-pHP\TBDPS-pHP-OH\MLS02104\Aug11-2012-59\3\fid					*Frequency (MHz)*	100.63
Nucleus	13C	*Number of Transients*	256	*Origin*	av400	*Original Points Count*	16384
Owner	dp-nmrgroup	*Points Count*	16384	*Pulse Sequence*	zgpg30	*Receiver Gain*	32768.00
SW(cyclical) (Hz)	26178.01	*Solvent*	CHLOROFORM-d	*Spectrum Offset (Hz)*	10018.1836	*Spectrum Type*	STANDARD
Sweep Width (Hz)	26176.41	*Temperature (degree C)*	27.000				

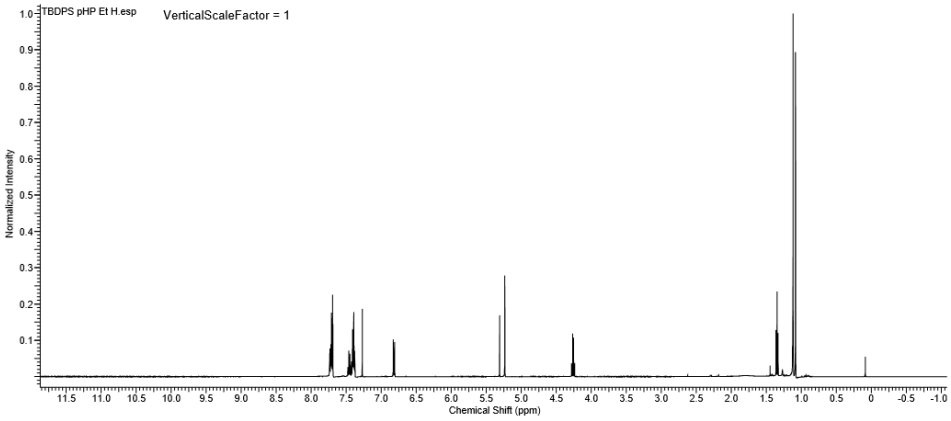




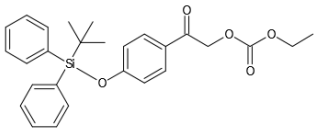
Compound 172

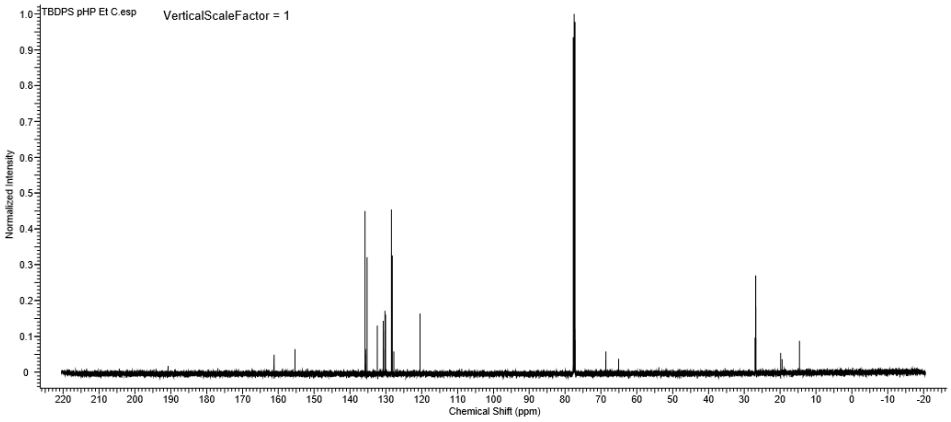
Acquisition Time (sec)	3.1719	*Comment*	TBDPS-pHP-Et h1acqbbo CDCl3 (C:\NMR) sjcogroup 21			*Date*	23 Apr 2013 16:19:28
Date Stamp	23 Apr 2013 16:19:28			*File Name*	G:\Gnomeeee\NMR\Phenacyl Stuff\TBDPS-pHP\TBDPS pHP Et\1\fid		
Frequency (MHz)	500.13	*Nucleus*	1H	*Number of Transients*	16	*Origin*	drx500
Original Points Count	32768	*Owner*	sjcogroup	*Points Count*	32768	*Pulse Sequence*	zg60
Receiver Gain	143.70	*SW(cyclical) (Hz)*	10330.58	*Solvent*	CHLOROFORM-d		
Spectrum Offset (Hz)	2476.8765	*Spectrum Type*	STANDARD	*Sweep Width (Hz)*	10330.26	*Temperature (degree C)*	24.694





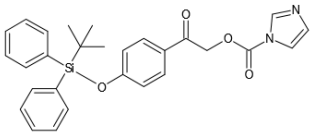
Acquisition Time (sec)	1.0813	*Comment*	TBDPS-pHP-Et c13acqbbo CDCl3 (C:\NMR) sjcogroup 21			*Date*	23 Apr 2013 17:00:00
Date Stamp	23 Apr 2013 17:00:00			*File Name*	G:\Gnomeeee\NMR\Phenacyl Stuff\TBDPS-pHP\TBDPS pHP Et\3\fid		
Frequency (MHz)	125.76	*Nucleus*	13C	*Number of Transients*	512	*Origin*	drx500
Original Points Count	32768	*Owner*	sjcogroup	*Points Count*	32768	*Pulse Sequence*	zgpg30
Receiver Gain	2896.30	*SW(cyclical) (Hz)*	30303.03	*Solvent*	CHLOROFORM-d		
Spectrum Offset (Hz)	12575.7764	*Spectrum Type*	STANDARD	*Sweep Width (Hz)*	30302.11	*Temperature (degree C)*	24.694

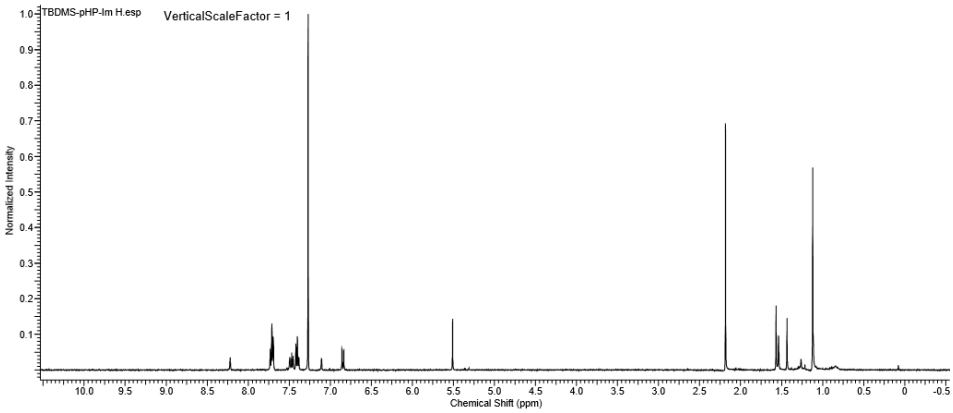




Compound 276

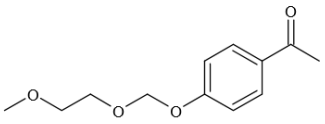
Acquisition Time (sec)	3.2768	*Comment*	Instrument AVG400 Group SJC Chemist MLS MLS04128 h1acq.crl CDCl3 (C:\NMR) sjcgrp 43				
Date	08 Jan 2014 17:08:16			*Date Stamp*	08 Jan 2014 17:08:16		
File Name	G:\Gnomeeee\NMR\Phenacyl Stuff\TBDPS-pHP\TBDPS-pHP-Im\Jan08-2014-43\2\PDATA\1\1r					*Frequency (MHz)*	400.20
Nucleus	1H	*Number of Transients*	16	*Origin*	avg400	*Original Points Count*	32768
Owner	nmr-user	*Points Count*	65536	*Pulse Sequence*	zg30	*Receiver Gain*	647.17
SW(cyclical) (Hz)	10000.00	*Solvent*	CHLOROFORM-d	*Spectrum Offset (Hz)*	2461.6851	*Spectrum Type*	STANDARD
Sweep Width (Hz)	9999.85	*Temperature (degree C)*	20.900				

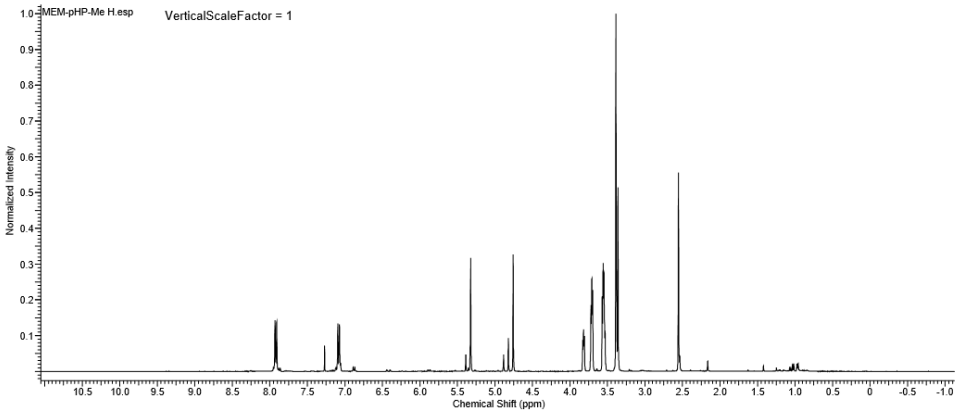




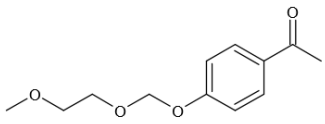
Compound 206

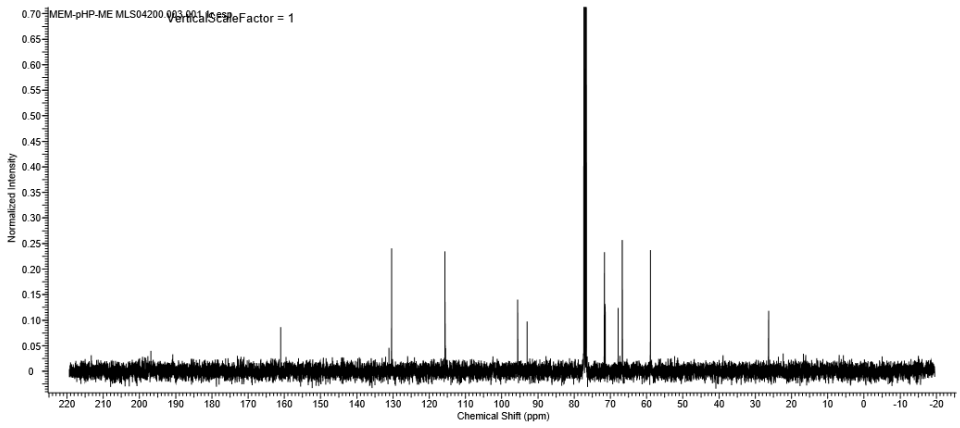
Acquisition Time (sec)	3.2768	*Comment*	Instrument AVG400 Group SJC Chemist MLS MLS04200: MEM-pHP h1acq.crl CDCl3 {C:\NMR} sjcgrp 23				
Date	27 Feb 2014 08:23:28	*Date Stamp*	27 Feb 2014 08:23:28				
File Name	G:\GNOMEEEE\NMR\PHENACYL STUFF\MEM\MEM-PHP-ME MLS04200\1\PDATA\1\1R					*Frequency (MHz)*	400.20
Nucleus	1H	*Number of Transients*	16	*Origin*	avg400	*Original Points Count*	32768
Owner	nmr-user	*Points Count*	65536	*Pulse Sequence*	zg30	*Receiver Gain*	141.58
SW(cyclical) (Hz)	10000.00	*Solvent*	CHLOROFORM-d	*Spectrum Offset (Hz)*	2461.8374	*Spectrum Type*	STANDARD
Sweep Width (Hz)	9999.85	*Temperature (degree C)*	21.300				





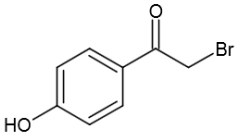
Acquisition Time (sec)	1.3631	*Comment*	Instrument AVG400 Group SJC Chemist MLS MLS04200: MEM-pHP c13acq.crl CDCl3 {C:\NMR} sjcgrp 23				
Date	27 Feb 2014 22:51:44	*Date Stamp*	27 Feb 2014 22:51:44	*File Name*	G:\Gnomeeee\NMR\Phenacyl Stuff\MEM\MEM-pHP-ME MLS04200\3\PDATA\1\1r		
Frequency (MHz)	100.63	*Nucleus*	13C	*Number of Transients*	256	*Origin*	avg400
Original Points Count	32768	*Owner*	nmr-user	*Points Count*	32768	*Pulse Sequence*	zgpg30
Receiver Gain	2050.00	*SW(cyclical) (Hz)*	24038.46	*Solvent*	CHLOROFORM-d	*Spectrum Offset (Hz)*	10054.5967
Spectrum Type	STANDARD	*Sweep Width (Hz)*	24037.73	*Temperature (degree C)*	21.800		

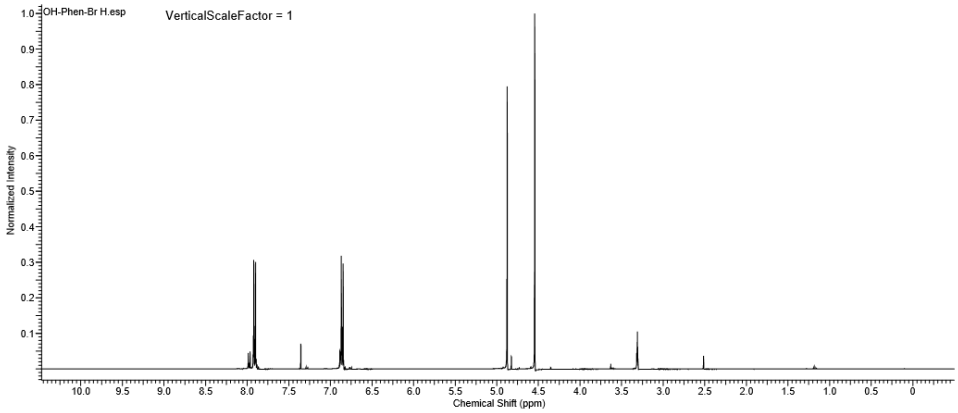




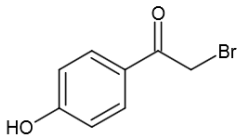
Compound 41

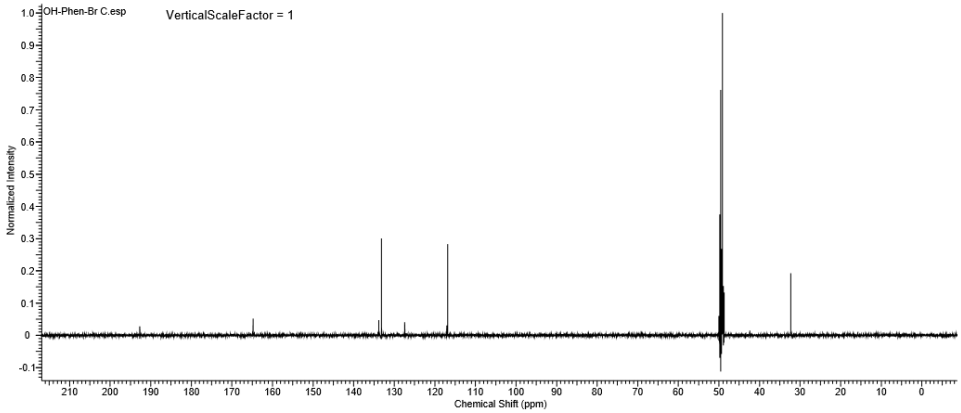
Acquisition Time (sec)	3.9584	*Comment*	Instrument DQX400 Chemist MLS Group SJC MLS01122 h1acq.au CDCl3 (E:\NMR2012) sjcgrp 48				
Date	22 Feb 2012 14:09:04			*Date Stamp*	22 Feb 2012 14:09:04		
File Name	F:\NMR\Phenacyl Stuff\OH-Phen-Br\Feb22-2012-48\1\fid			*Frequency (MHz)*	400.20	*Nucleus*	1H
Number of Transients	16	*Origin*	av400	*Original Points Count*	32768	*Owner*	dp-nmrgroup
Points Count	32768	*Pulse Sequence*	zg60	*Receiver Gain*	90.50	*SW(cyclical) (Hz)*	8278.15
Solvent	METHANOL-d4	*Spectrum Offset (Hz)*	889.7614	*Spectrum Type*	STANDARD	*Sweep Width (Hz)*	8277.89
Temperature (degree C)	27.000						





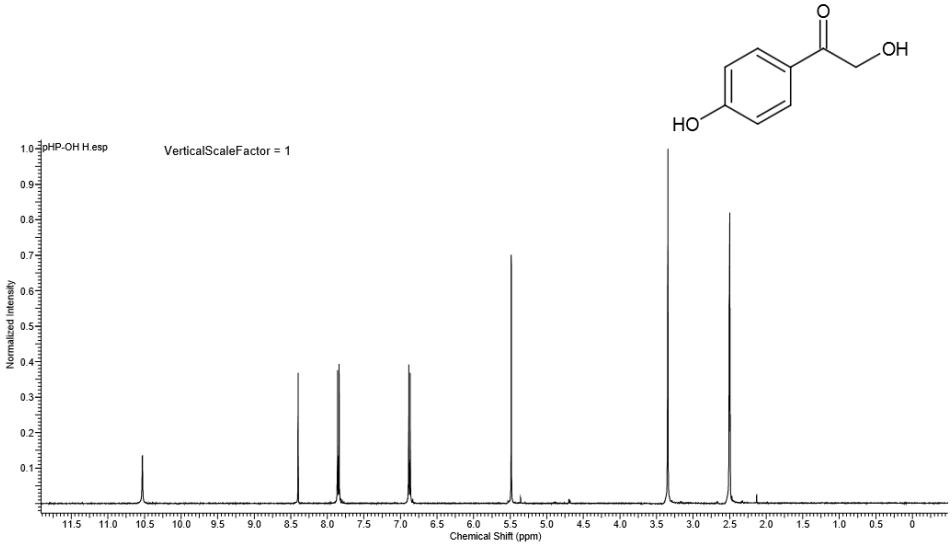
Acquisition Time (sec)	0.6259	*Comment*	Instrument DQX400 Chemist MLS Group SJC MLS01122 c13acq.au CDCl3 (E:\NMR2012) sjcgrp 48				
Date	22 Feb 2012 14:21:52			*Date Stamp*	22 Feb 2012 14:21:52		
File Name	F:\NMR\Phenacyl Stuff\OH-Phen-Br\Feb22-2012-48\3\fid			*Frequency (MHz)*	100.63	*Nucleus*	13C
Number of Transients	256	*Origin*	av400	*Original Points Count*	16384	*Owner*	dp-nmrgroup
Points Count	16384	*Pulse Sequence*	zgpg30	*Receiver Gain*	32768.00	*SW(cyclical) (Hz)*	26178.01
Solvent	METHANOL-d4	*Spectrum Offset (Hz)*	9799.2363	*Spectrum Type*	STANDARD	*Sweep Width (Hz)*	26176.41
Temperature (degree C)	27.000						





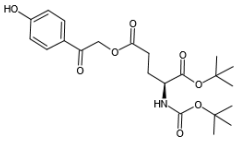
Compound 48

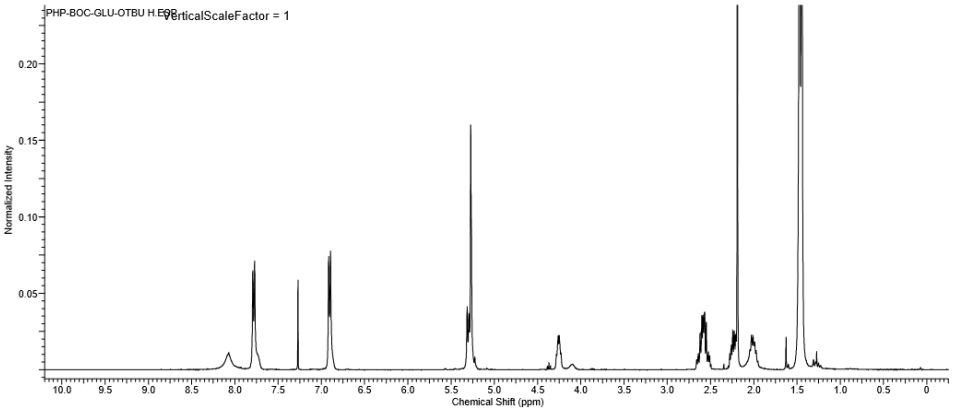
Acquisition Time (sec)	2.9295	*Comment*	Instrument DPX400 Chemist MLS Group SJC MLS01176 Qh1acq.au DMSO (C:\NMR) sjcgrp 53				
Date	23 Apr 2012 11:25:04			*Date Stamp*	23 Apr 2012 11:25:04		
File Name	G:\Gnomeeee\NMR\Phenacyl Stuff\pHP\pHP-OH\Apr23-2012-53\1\fid					*Frequency (MHz)*	400.13
Nucleus	1H	*Number of Transients*	16	*Origin*	dpx400	*Original Points Count*	16384
Owner	dp-nmrgroup	*Points Count*	16384	*Pulse Sequence*	zg60	*Receiver Gain*	645.10
SW(cyclical) (Hz)	5592.84	*Solvent*	DMSO-d6	*Spectrum Offset (Hz)*	1997.9495	*Spectrum Type*	STANDARD
Sweep Width (Hz)	5592.50	*Temperature (degree C)*	27.000				



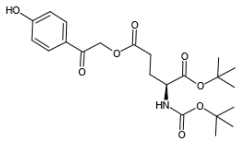
Compound 199

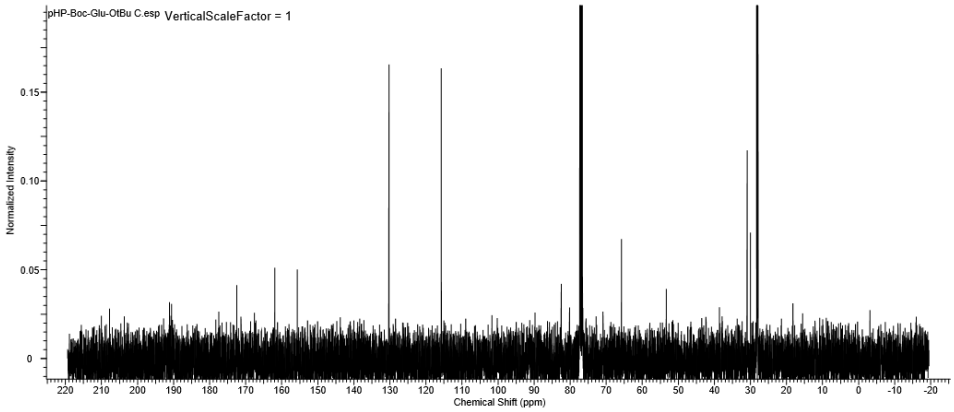
Acquisition Time (sec)	3.2768	*Comment*	Instrument AVG400 Group SJC Chemist MLS MLS04202: pHP-Boc-Glu-OtBu h1acq.crl CDCl3 {C:\NMR} sjcgrp 33				
Date	02 Mar 2014 15:21:36	*Date Stamp*	02 Mar 2014 15:21:36				
File Name	D:\Gnomeeee\NMR\Phenacyl Stuff\pHP\pHP-Boc-Glu-OtBu\Mar02-2014-33\1\PDATA\1\1r					*Frequency (MHz)*	400.20
Nucleus	1H	*Number of Transients*	16	*Origin*	avg400	*Original Points Count*	32768
Owner	nmr-user	*Points Count*	65536	*Pulse Sequence*	zg30	*Receiver Gain*	166.74
SW(cyclical) (Hz)	10000.00	*Solvent*	CHLOROFORM-d	*Spectrum Offset (Hz)*	2462.1428	*Spectrum Type*	STANDARD
Sweep Width (Hz)	9999.85	*Temperature (degree C)*	21.200				





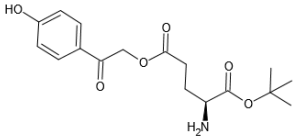
Acquisition Time (sec)	1.3631	*Comment*	Instrument AVG400 Group SJC Chemist MLS MLS04202: pHP-Boc-Glu-OtBu c13acq.crl CDCl3 {C:\NMR} sjcgrp 33				
Date	02 Mar 2014 15:42:56	*Date Stamp*	02 Mar 2014 15:42:56				
File Name	D:\Gnomeeee\NMR\Phenacyl Stuff\pHP\pHP-Boc-Glu-OtBu\Mar02-2014-33\3\PDATA\1\1r					*Frequency (MHz)*	100.63
Nucleus	13C	*Number of Transients*	256	*Origin*	avg400	*Original Points Count*	32768
Owner	nmr-user	*Points Count*	32768	*Pulse Sequence*	zgpg30	*Receiver Gain*	2050.00
SW(cyclical) (Hz)	24038.46	*Solvent*	CHLOROFORM-d	*Spectrum Offset (Hz)*	10056.0635	*Spectrum Type*	STANDARD
Sweep Width (Hz)	24037.73	*Temperature (degree C)*	21.200				

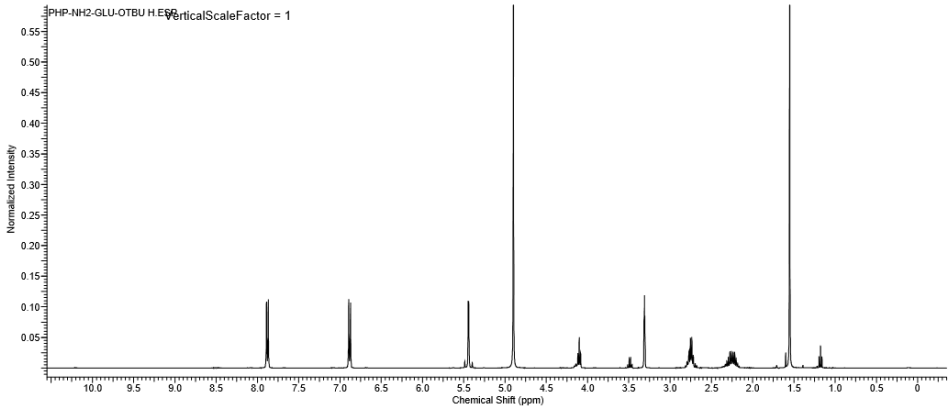




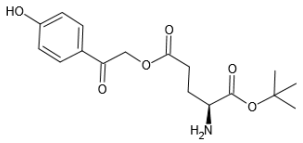
Compound 200

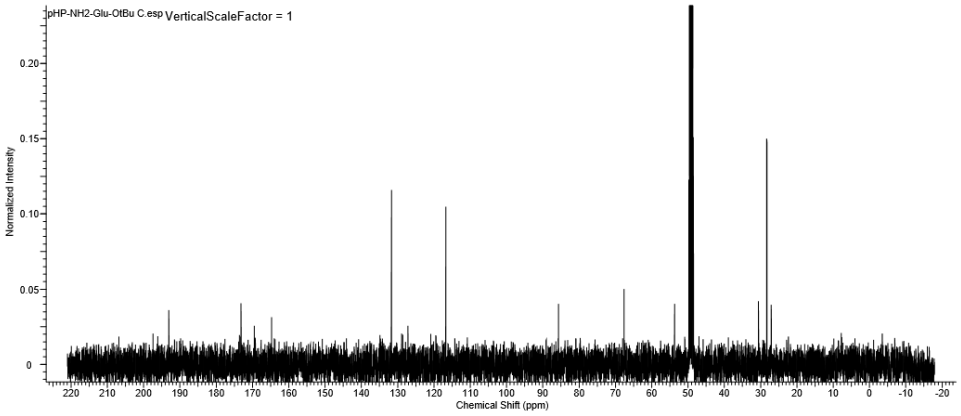
Acquisition Time (sec)	3.2768	*Comment*	Instrument AVG400 Group SJC Chemist MLS MLS05022: pHP-Glu-OtBu h1acq.crl MeOD {C:\NMR} sjcgrp 34				
Date	02 Mar 2014 16:02:08	*Date Stamp*	02 Mar 2014 16:02:08				
File Name	D:\Gnomeeee\NMR\Phenacyl Stuff\pHP\pHP NH2-Glu-OtBu\Mar02-2014-34\1\PDATA\1\1r					*Frequency (MHz)*	400.20
Nucleus	1H	*Number of Transients*	16	*Origin*	avg400	*Original Points Count*	32768
Owner	nmr-user	*Points Count*	65536	*Pulse Sequence*	zg30	*Receiver Gain*	255.20
SW(cyclical) (Hz)	10000.00	*Solvent*	METHANOL-d4	*Spectrum Offset (Hz)*	2460.2974	*Spectrum Type*	STANDARD
Sweep Width (Hz)	9999.85	*Temperature (degree C)*	21.200				





Acquisition Time (sec)	1.3631	*Comment*	Instrument AVG400 Group SJC Chemist MLS MLS05022: pHP-Glu-OtBu c13acq.crl MeOD {C:\NMR} sjcgrp 34				
Date	02 Mar 2014 16:23:28	*Date Stamp*	02 Mar 2014 16:23:28				
File Name	D:\Gnomeeee\NMR\Phenacyl Stuff\pHP\pHP NH2-Glu-OtBu\Mar02-2014-34\3\PDATA\1\1r					*Frequency (MHz)*	100.63
Nucleus	13C	*Number of Transients*	256	*Origin*	avg400	*Original Points Count*	32768
Owner	nmr-user	*Points Count*	32768	*Pulse Sequence*	zgpg30	*Receiver Gain*	2050.00
SW(cyclical) (Hz)	24038.46	*Solvent*	METHANOL-d4	*Spectrum Offset (Hz)*	10216.5000	*Spectrum Type*	STANDARD
Sweep Width (Hz)	24037.73	*Temperature (degree C)*	21.400				

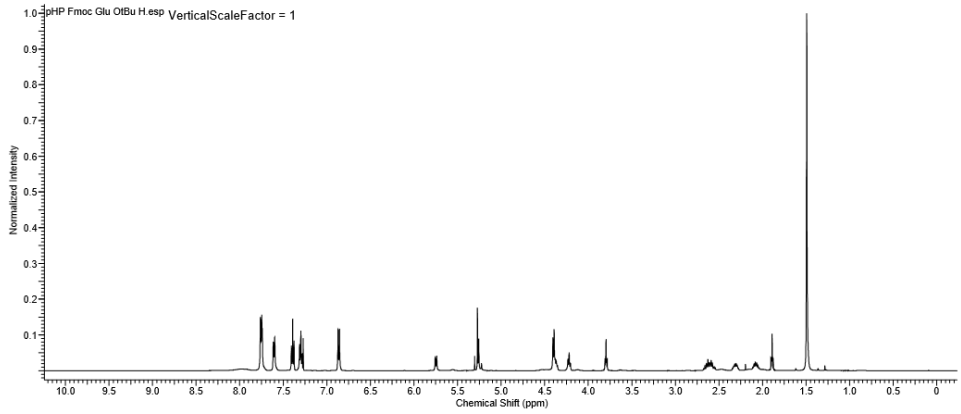




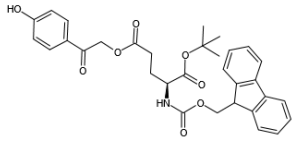
Compound 198

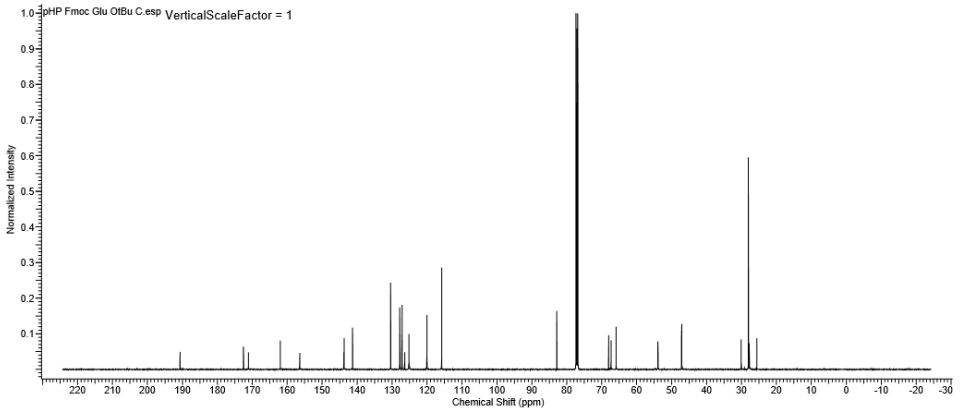
Acquisition Time (sec)	3.1719	*Comment*	Instrument AVC500 Group SJC 1122 M. Savage 30/4/15			*Date*	30 Apr 2015 08:10:56
Date Stamp	30 Apr 2015 08:10:56						
File Name	D:\Gnomeeee\NMR\Phenacyl Stuff\pHP\pHP-Fmoc-Glu-OtBu\pHP Fmoc Glu OtBu I\1\PDATA\1\1r					*Frequency (MHz)*	500.30
Nucleus	1H	*Number of Transients*	16	*Origin*	avc500	*Original Points Count*	32768
Owner	nmr-user	*Points Count*	65536	*Pulse Sequence*	zg30	*Receiver Gain*	2.80
SW(cyclical) (Hz)	10330.58	*Solvent*	CHLOROFORM-d	*Spectrum Offset (Hz)*	3081.2913	*Spectrum Type*	STANDARD
Sweep Width (Hz)	10330.42	*Temperature (degree C)*	24.970				





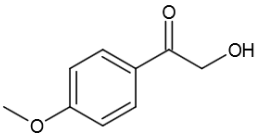
Acquisition Time (sec)	1.0486	*Comment*	Instrument AVC500 Group SJC 1122 M. Savage 30/4/15			*Date*	30 Apr 2015 08:36:32
Date Stamp	30 Apr 2015 08:36:32						
File Name	D:\Gnomeeee\NMR\Phenacyl Stuff\pHP\pHP-Fmoc-Glu-OtBu\pHP Fmoc Glu OtBu I\4\PDATA\1\1r					*Frequency (MHz)*	125.80
Nucleus	13C	*Number of Transients*	250	*Origin*	avc500	*Original Points Count*	32768
Owner	nmr-user	*Points Count*	32768	*Pulse Sequence*	zgpg30	*Receiver Gain*	912.00
SW(cyclical) (Hz)	31250.00	*Solvent*	CHLOROFORM-d	*Spectrum Offset (Hz)*	12580.1094	*Spectrum Type*	STANDARD
Sweep Width (Hz)	31249.05	*Temperature (degree C)*	24.970				

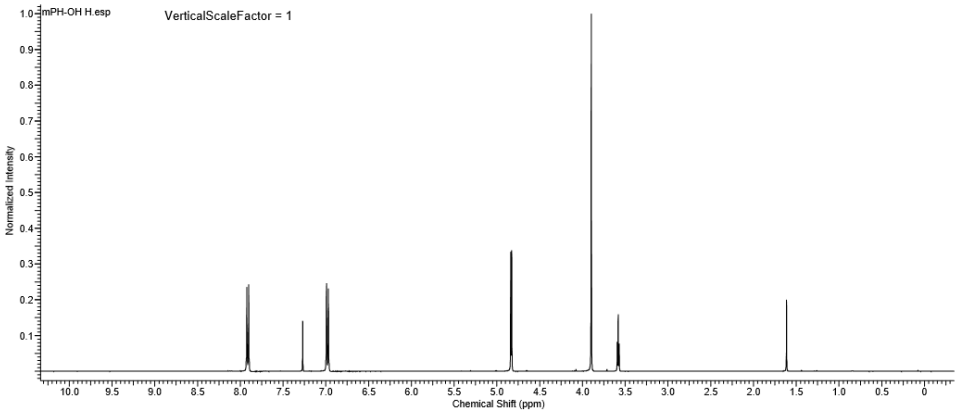




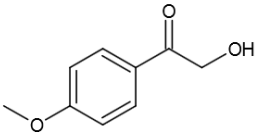
Compound 147

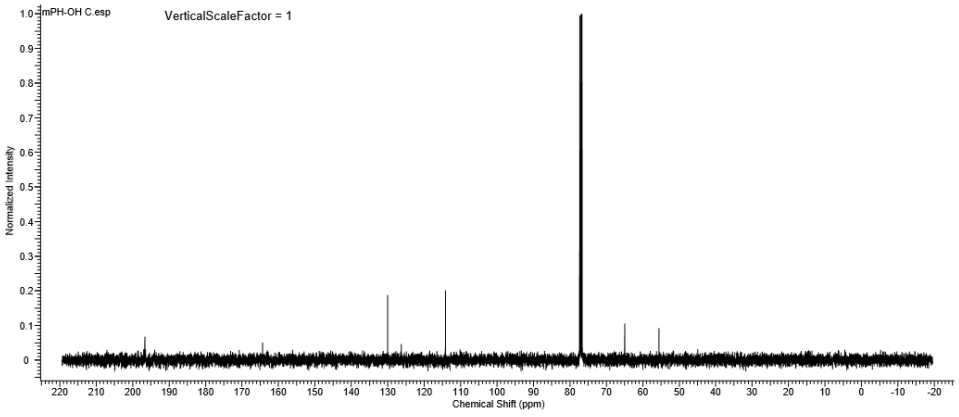
Acquisition Time (sec)	3.2768	*Comment*	Instrument AVG400 Group SJC Chemist MLS MLS05110 h1acq.crl CDCl3 {C:\NMR} sjcgrp 45				
Date	24 Mar 2014 20:22:24			*Date Stamp*	24 Mar 2014 20:22:24		
File Name	G:\Gnomeeee\NMR\Phenacyl Stuff\mPH\mPH LPG\1\PDATA\1\1r			*Frequency (MHz)*	400.20	*Nucleus*	1H
Number of Transients	16	*Origin*	avg400	*Original Points Count*	32768	*Owner*	nmr-user
Points Count	65536	*Pulse Sequence*	zg30	*Receiver Gain*	411.88	*SW(cyclical) (Hz)*	10000.00
Solvent	CHLOROFORM-d	*Spectrum Offset (Hz)*	2462.1426	*Spectrum Type*	STANDARD	*Sweep Width (Hz)*	9999.85
Temperature (degree C)	21.200						





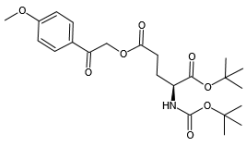
Acquisition Time (sec)	1.3631	*Comment*	Instrument AVG400 Group SJC Chemist MLS MLS05110 c13acq.crl CDCl3 {C:\NMR} sjcgrp 45				
Date	24 Mar 2014 23:06:40			*Date Stamp*	24 Mar 2014 23:06:40		
File Name	G:\Gnomeeee\NMR\Phenacyl Stuff\mPH\mPH LPG\3\PDATA\1\1r			*Frequency (MHz)*	100.63	*Nucleus*	13C
Number of Transients	256	*Origin*	avg400	*Original Points Count*	32768	*Owner*	nmr-user
Points Count	32768	*Pulse Sequence*	zgpg30	*Receiver Gain*	2050.00	*SW(cyclical) (Hz)*	24038.46
Solvent	CHLOROFORM-d	*Spectrum Offset (Hz)*	10058.2637	*Spectrum Type*	STANDARD	*Sweep Width (Hz)*	24037.73
Temperature (degree C)	21.900						

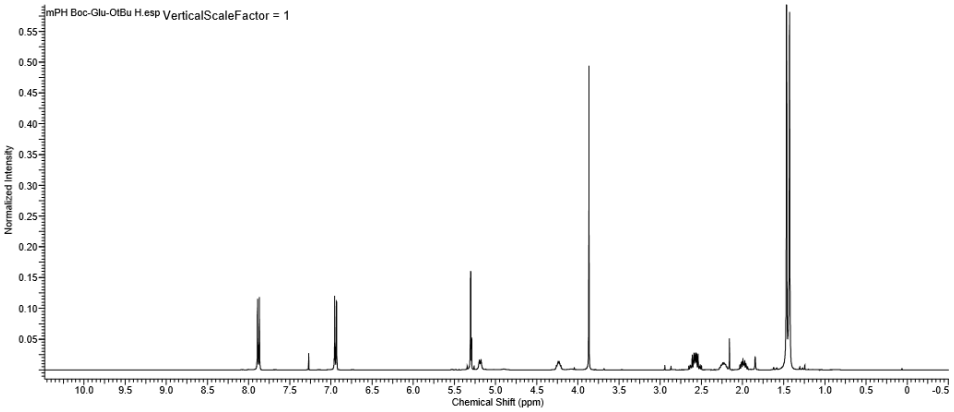




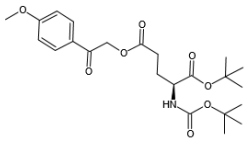
Compound 165

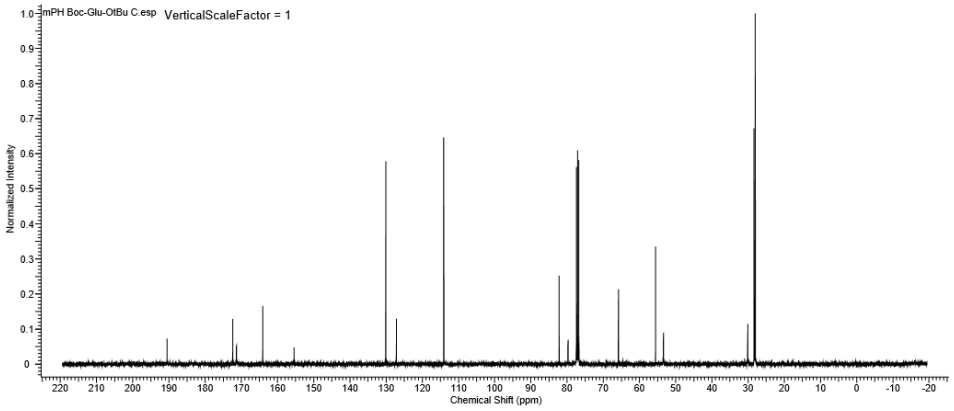
Acquisition Time (sec)	3.2768	*Comment*	Instrument AVG400 Group SJC Chemist MLS MLS05134: pMP-(Boc)Glu(OtBu) h1acq.crl CDCl3 {C:\NMR} sjcgrp 25				
Date	10 Apr 2014 09:59:44	*Date Stamp*	10 Apr 2014 09:59:44				
File Name	D:\Gnomeeee\NMR\Phenacyl Stuff\mPH\mPH Boc-Glu-OtBu\Apr10-2014-25\1\PDATA\1\1r					*Frequency (MHz)*	400.20
Nucleus	1H	*Number of Transients*	16	*Origin*	avg400	*Original Points Count*	32768
Owner	nmr-user	*Points Count*	65536	*Pulse Sequence*	zg30	*Receiver Gain*	102.60
SW(cyclical) (Hz)	10000.00	*Solvent*	CHLOROFORM-d	*Spectrum Offset (Hz)*	2463.3635	*Spectrum Type*	STANDARD
Sweep Width (Hz)	9999.85	*Temperature (degree C)*	21.100				





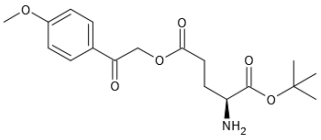
Acquisition Time (sec)	1.3631	*Comment*	Instrument AVG400 Group SJC Chemist MLS MLS05134: pMP-(Boc)Glu(OtBu) c13acq.crl CDCl3 {C:\NMR} sjcgrp 25				
Date	10 Apr 2014 22:54:08	*Date Stamp*	10 Apr 2014 22:54:08				
File Name	D:\Gnomeeee\NMR\Phenacyl Stuff\mPH\mPH Boc-Glu-OtBu\Apr10-2014-25\3\PDATA\1\1r					*Frequency (MHz)*	100.63
Nucleus	13C	*Number of Transients*	256	*Origin*	avg400	*Original Points Count*	32768
Owner	nmr-user	*Points Count*	32768	*Pulse Sequence*	zgpg30	*Receiver Gain*	2050.00
SW(cyclical) (Hz)	24038.46	*Solvent*	CHLOROFORM-d	*Spectrum Offset (Hz)*	10062.6055	*Spectrum Type*	STANDARD
Sweep Width (Hz)	24037.73	*Temperature (degree C)*	21.700				

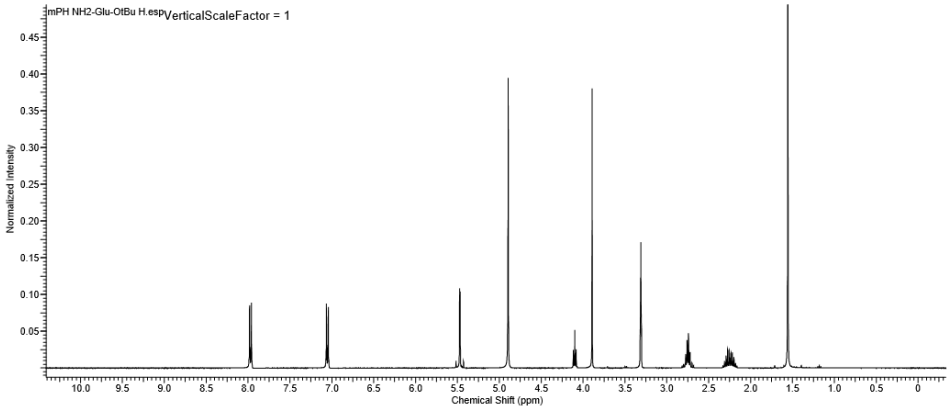




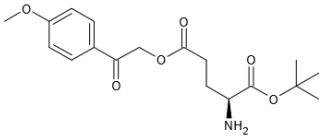
Compound 277

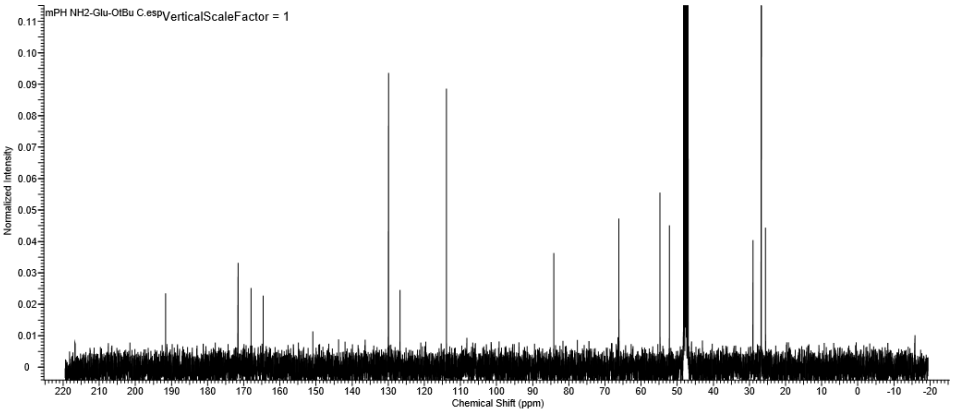
Acquisition Time (sec)	3.2768	*Comment*	Instrument AVG400 Group SJC Chemist MLS MLS05138: pMP(NH2)Glu(OtBu) h1acq.crl MeOD {C:\NMR} sjcgrp 15				
Date	13 Apr 2014 17:10:40	*Date Stamp*	13 Apr 2014 17:10:40				
File Name	D:\Gnomeeee\NMR\Phenacyl Stuff\mPH\mPH NH2-Glu-OtBu\Apr13-2014-15\1\PDATA\1\1r					*Frequency (MHz)*	400.20
Nucleus	1H	*Number of Transients*	16	*Origin*	avg400	*Original Points Count*	32768
Owner	nmr-user	*Points Count*	65536	*Pulse Sequence*	zg30	*Receiver Gain*	321.10
SW(cyclical) (Hz)	10000.00	*Solvent*	METHANOL-d4	*Spectrum Offset (Hz)*	2459.9922	*Spectrum Type*	STANDARD
Sweep Width (Hz)	9999.85	*Temperature (degree C)*	21.000				





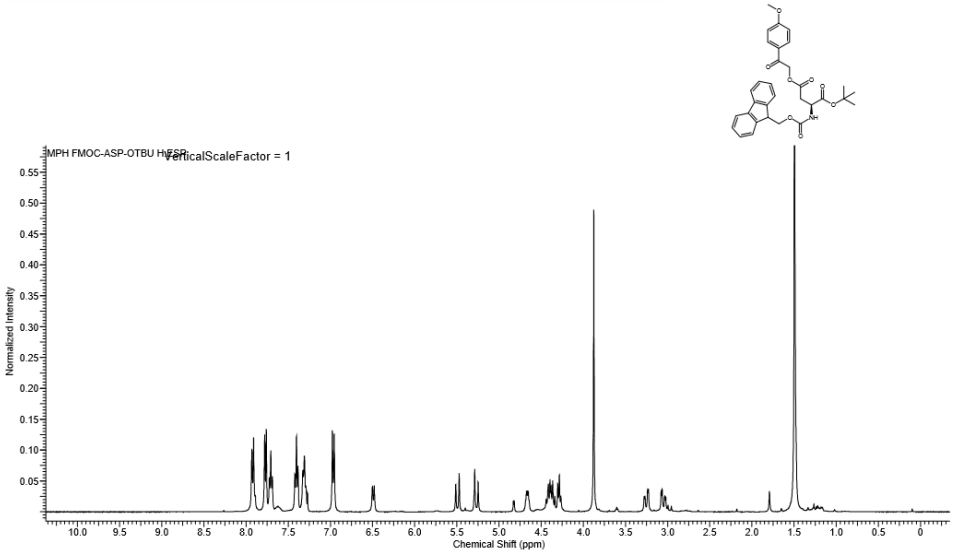
Acquisition Time (sec)	1.3631	*Comment*	Instrument AVG400 Group SJC Chemist MLS MLS05138: pMP(NH2)Glu(OtBu) c13acq.crl MeOD {C:\NMR} sjcgrp 15				
Date	13 Apr 2014 17:32:00	*Date Stamp*	13 Apr 2014 17:32:00				
File Name	D:\Gnomeeee\NMR\Phenacyl Stuff\mPH\mPH NH2-Glu-OtBu\Apr13-2014-15\3\PDATA\1\1r					*Frequency (MHz)*	100.63
Nucleus	13C	*Number of Transients*	256	*Origin*	avg400	*Original Points Count*	32768
Owner	nmr-user	*Points Count*	32768	*Pulse Sequence*	zgpg30	*Receiver Gain*	2050.00
SW(cyclical) (Hz)	24038.46	*Solvent*	METHANOL-d4	*Spectrum Offset (Hz)*	10062.6055	*Spectrum Type*	STANDARD
Sweep Width (Hz)	24037.73	*Temperature (degree C)*	21.500				



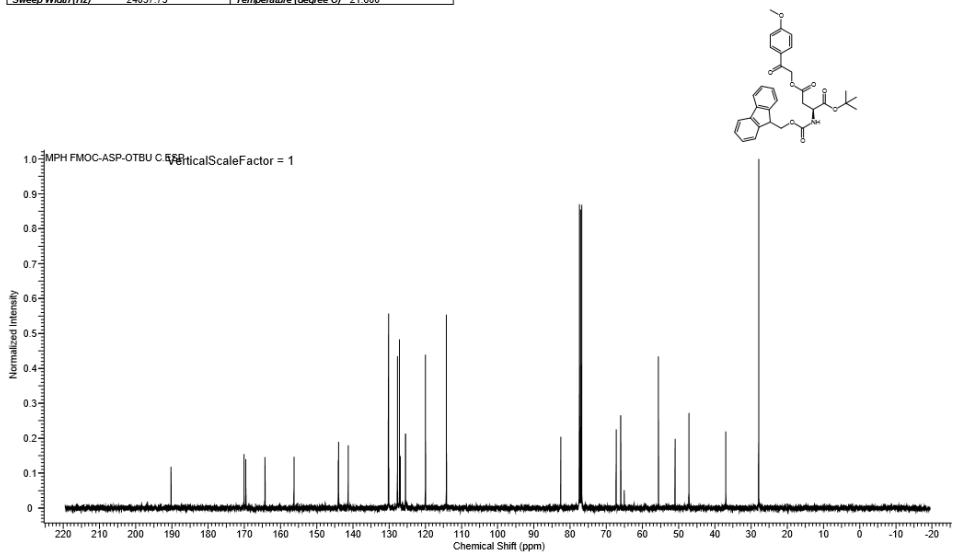


Compound 209

Acquisition Time (sec)	3.2768	*Comment*	Instrument AVG400 Group SJC Chemist MLS MLS05132: pMP-(Fmoc)Asp(OtBu) h1acq.crl CDCl3 {C:\NMR} sjcgrp 5				
Date	08 Apr 2014 10:01:52	*Date Stamp*	08 Apr 2014 10:01:52	*File Name*	D:\Gnomeeee\NMR\Phenacyl Stuff\mPH\mPH Fmoc-Asp-OtBu\MLS05132\1\PDATA\1\1r		
Frequency (MHz)	400.20	*Nucleus*	1H	*Number of Transients*	16	*Origin*	avg400
Original Points Count	32768	*Owner*	nmr-user	*Points Count*	65536	*Pulse Sequence*	zg30
Receiver Gain	102.60	*SW(cyclical) (Hz)*	10000.00	*Solvent*	CHLOROFORM-d	*Spectrum Offset (Hz)*	2462.1428
Spectrum Type	STANDARD	*Sweep Width (Hz)*	9999.85	*Temperature (degree C)*	21.000		

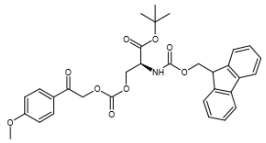


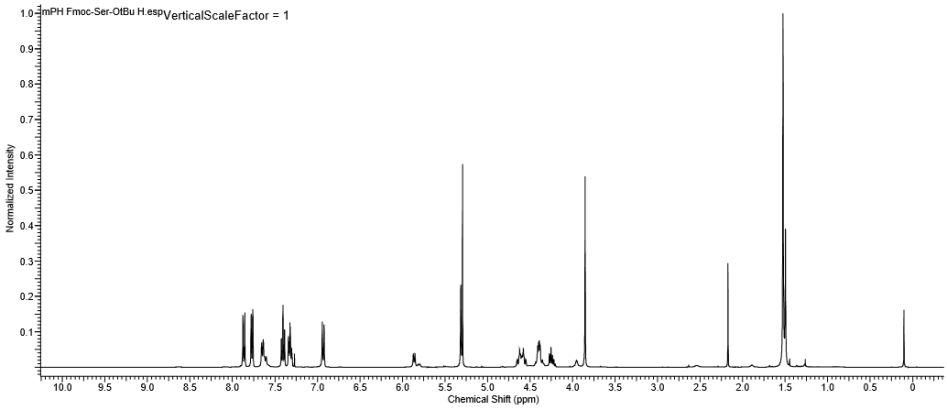
Acquisition Time (sec)	1.3631	*Comment*	Instrument AVG400 Group SJC Chemist MLS MLS05132: pMP-(Fmoc)Asp(OtBu) c13acq.crl CDCl3 {C:\NMR} sjcgrp 5				
Date	08 Apr 2014 21:43:44	*Date Stamp*	08 Apr 2014 21:43:44				
File Name	D:\Gnomeeee\NMR\Phenacyl Stuff\mPH\mPH Fmoc-Asp-OtBu\MLS05132\3\PDATA\1\1r					*Frequency (MHz)*	100.63
Nucleus	13C	*Number of Transients*	256	*Origin*	avg400	*Original Points Count*	32768
Owner	nmr-user	*Points Count*	32768	*Pulse Sequence*	zgpg30	*Receiver Gain*	2050.00
SW(cyclical) (Hz)	24038.46	*Solvent*	CHLOROFORM-d	*Spectrum Offset (Hz)*	10062.6055	*Spectrum Type*	STANDARD
Sweep Width (Hz)	24037.73	*Temperature (degree C)*	21.600				



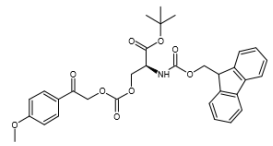
Compound 211

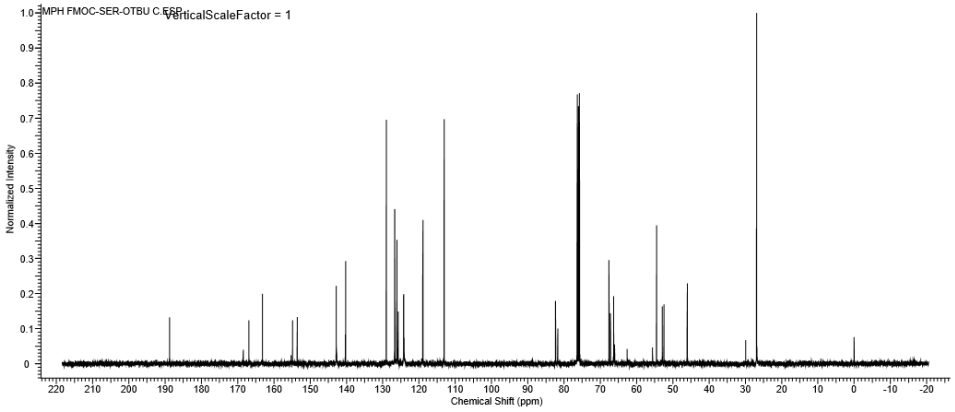
Acquisition Time (sec)	3.2768	*Comment*	Instrument AVG400 Group SJC Chemist MLS MLS05144 h1acq.crl CDCl3 (C:\NMR) sjcgrp 51				
Date	18 Apr 2014 10:06:08			*Date Stamp*	18 Apr 2014 10:06:08		
File Name	D:\Gnomeeee\NMR\Phenacyl Stuff\mPH\mPH Fmoc-Ser-OtBu\Apr18-2014-51\1\PDATA\1\1r						
Nucleus	1H	*Number of Transients*	16	*Origin*	avg400	*Original Points Count*	32768
Owner	nmr-user	*Points Count*	65536	*Pulse Sequence*	zg30	*Receiver Gain*	52.52
SW(cyclical) (Hz)	10000.00	*Solvent*	CHLOROFORM-d	*Spectrum Offset (Hz)*	2462.1428	*Spectrum Type*	STANDARD
Sweep Width (Hz)	9999.85	*Temperature (degree C)*	21.000				





Acquisition Time (sec)	1.3631	*Comment*	Instrument AVG400 Group SJC Chemist MLS MLS05144 c13acq.crl CDCl3 (C:\NMR) sjcgrp 51				
Date	18 Apr 2014 10:27:28	*Date Stamp*	18 Apr 2014 10:27:28				
File Name	D:\Gnomeeee\NMR\Phenacyl Stuff\mPH\mPH Fmoc-Ser-OtBu\Apr18-2014-51\3\PDATA\1\1r					*Frequency (MHz)*	100.63
Nucleus	13C	*Number of Transients*	256	*Origin*	avg400	*Original Points Count*	32768
Owner	nmr-user	*Points Count*	32768	*Pulse Sequence*	zgpg30	*Receiver Gain*	2050.00
SW(cyclical) (Hz)	24038.46	*Solvent*	CHLOROFORM-d	*Spectrum Offset (Hz)*	9954.0781	*Spectrum Type*	STANDARD
Sweep Width (Hz)	24037.73	*Temperature (degree C)*	21.300				



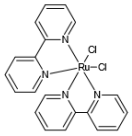


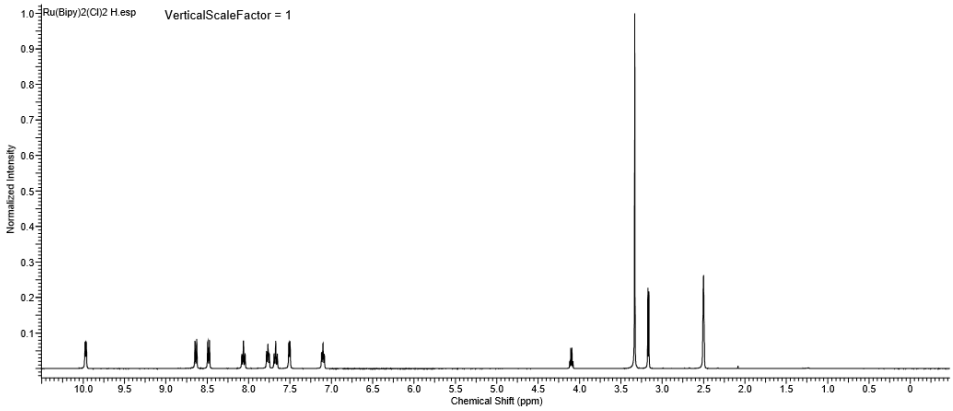
A.6 Red-Shifted Caging Groups

A.6.1 Ruthenenium Bipyridyl Caging Group

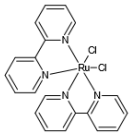
Compound 229

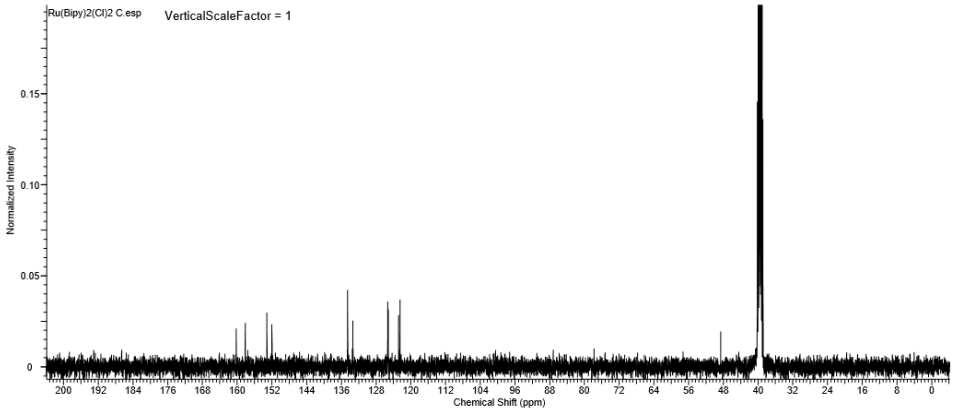
Acquisition Time (sec)	3.2768	*Comment*	Instrument AVG400 Group SJC Chemist MLS MLS06046: Ru(BiPee)2Cl2 h1acq.crl DMSO {C:\NMR} sjcgrp 29		
Date	11 Jun 2014 16:47:12			*Date Stamp*	11 Jun 2014 16:47:12
File Name	F:\NMR\Ru Stuff\Ru(Bipy)2(Cl)2\Ru(Bipy)2(Cl)2 MLS06046\1\pdata\1\1r				
Nucleus	1H	*Number of Transients*	16	*Origin*	avg400
Owner	nmr-user	*Points Count*	65536	*Pulse Sequence*	zg30
SW(cyclical) (Hz)	10000.00	*Solvent*	DMSO-d6	*Spectrum Offset (Hz)*	2466.1831
Sweep Width (Hz)	9999.85	*Temperature (degree C)*	23.800		





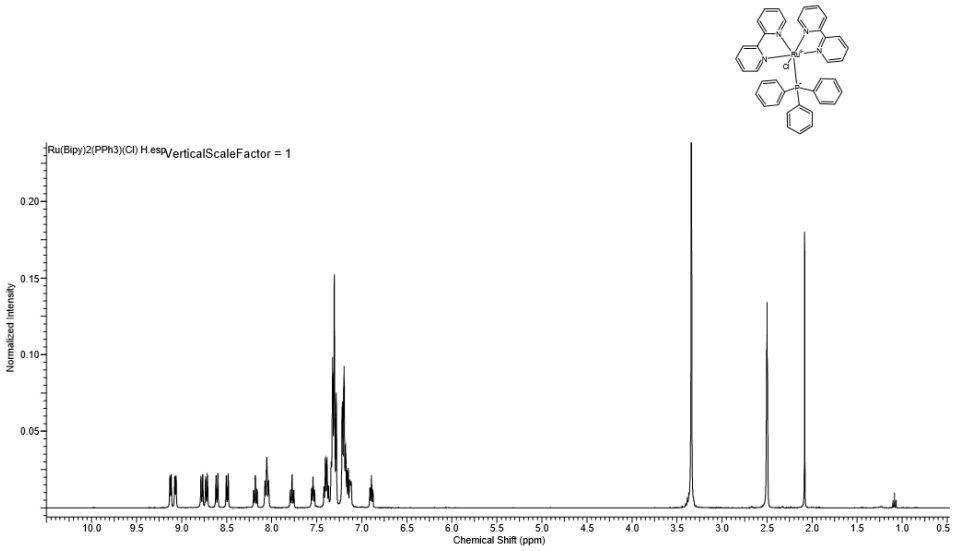
Acquisition Time (sec)	1.3631	*Comment*	Instrument AVG400 Group SJC Chemist MLS MLS06046: Ru(BiPee)2Cl2 c13acq.crl DMSO {C:\NMR} sjcgrp 29		
Date	11 Jun 2014 17:08:32			*Date Stamp*	11 Jun 2014 17:08:32
File Name	F:\NMR\Ru Stuff\Ru(Bipy)2(Cl)2\Ru(Bipy)2(Cl)2 MLS06046\3\pdata\1\1r				
Nucleus	13C	*Number of Transients*	256	*Origin*	avg400
Owner	nmr-user	*Points Count*	32768	*Pulse Sequence*	zgpg30
SW(cyclical) (Hz)	24038.46	*Solvent*	DMSO-d6	*Spectrum Offset (Hz)*	10013.7646
Sweep Width (Hz)	24037.73	*Temperature (degree C)*	24.100		



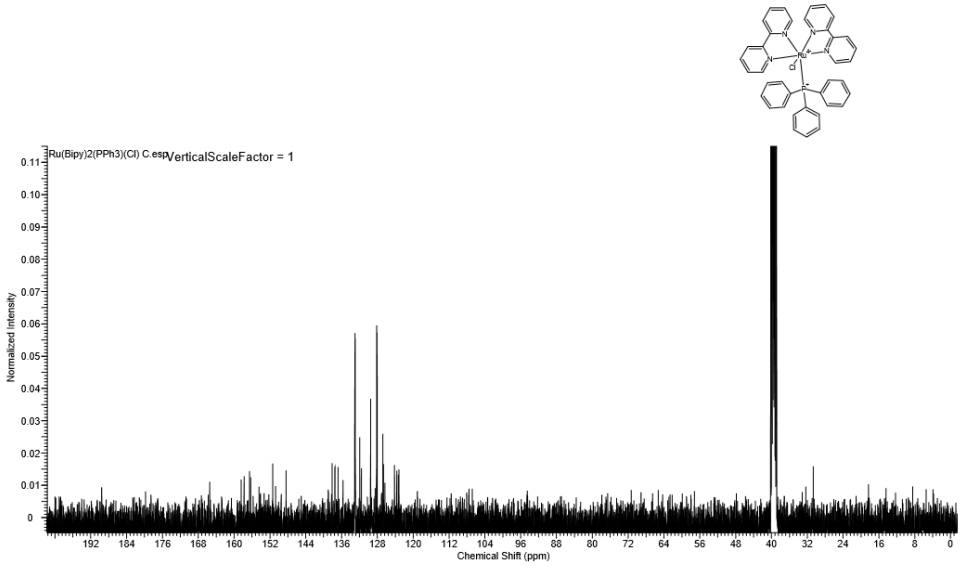


Compound 230

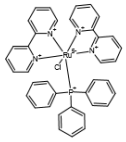
Acquisition Time (sec)	4.0894	*Comment*	Instrument AVF400 Chemist MLS Group SJC MLS06050: Ru(BiPee)2(PPH3)(Cl) h1acq.crl DMSO {C:\NMR} sjcgrp 45				
Date	13 Jun 2014 02:21:04			*Date Stamp*	13 Jun 2014 02:21:04		
File Name	F:\NMR\Ru Stuff\Ru(Bipy)2(PPh3)(Cl)\Ru(Bipy)2(PPh3)(Cl) MLS06050\1\pdata\1\1r						
Nucleus	1H	*Number of Transients*	16	*Origin*	avf400	*Frequency (MHz)*	400.25
Owner	nmr-user	*Points Count*	32768	*Pulse Sequence*	zg60	*Original Points Count*	32768
SW(cyclical) (Hz)	8012.82	*Solvent*	DMSO-d6	*Spectrum Offset (Hz)*	2395.3125	*Receiver Gain*	93.00
Sweep Width (Hz)	8012.58	*Temperature (degree C)*	23.491			*Spectrum Type*	STANDARD

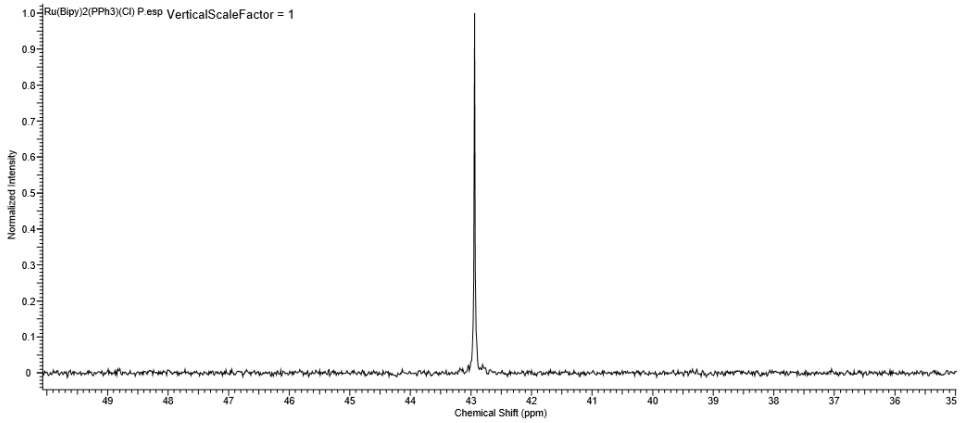


Acquisition Time (sec)	0.6291	*Comment*	Instrument AVF400 Chemist MLS Group SJC MLS06050: Ru(BiPee)2(PPH3)(Cl) c13acq.crl DMSO {C:\NMR} sjcgrp 45				
Date	13 Jun 2014 02:36:00	*Date Stamp*	13 Jun 2014 02:36:00	*File Name*	F:\NMR\Ru Stuff\Ru(Bipy)2(PPh3)(Cl)\Ru(Bipy)2(PPh3)(Cl) MLS06050\3\pdata\1\1r		
Frequency (MHz)	100.64	*Nucleus*	13C	*Number of Transients*	256	*Origin*	avf400
Original Points Count	16384	*Owner*	nmr-user	*Points Count*	32768	*Pulse Sequence*	zgpg30
Receiver Gain	205.43	*SW(cyclical) (Hz)*	26041.67	*Solvent*	DMSO-d6	*Spectrum Offset (Hz)*	10014.3535
Spectrum Type	STANDARD	*Sweep Width (Hz)*	26040.87	*Temperature (degree C)*	24.561		



Acquisition Time (sec)	0.5112	*Comment*	Instrument AVF400 Chemist MLS Group SJC MLS06050: Ru(BiPee)2(PPH3)(Cl) p31dec2.crl DMSO {C:\NMR} sjcgrp 45				
Date	13 Jun 2014 02:55:12	*Date Stamp*	13 Jun 2014 02:55:12	*File Name*	F:\NMR\Ru Stuff\Ru(Bipy)2(PPh3)(Cl)\Ru(Bipy)2(PPh3)(Cl) MLS06050\7\pdata\1\1r		
Frequency (MHz)	162.02	*Nucleus*	31P	*Number of Transients*	16	*Origin*	avf400
Original Points Count	32768	*Owner*	nmr-user	*Points Count*	32768	*Pulse Sequence*	zgpg30
Receiver Gain	205.43	*SW(cyclical) (Hz)*	64102.56	*Solvent*	DMSO-d6	*Spectrum Offset (Hz)*	0.0001
Spectrum Type	STANDARD	*Sweep Width (Hz)*	64100.61	*Temperature (degree C)*	24.255		

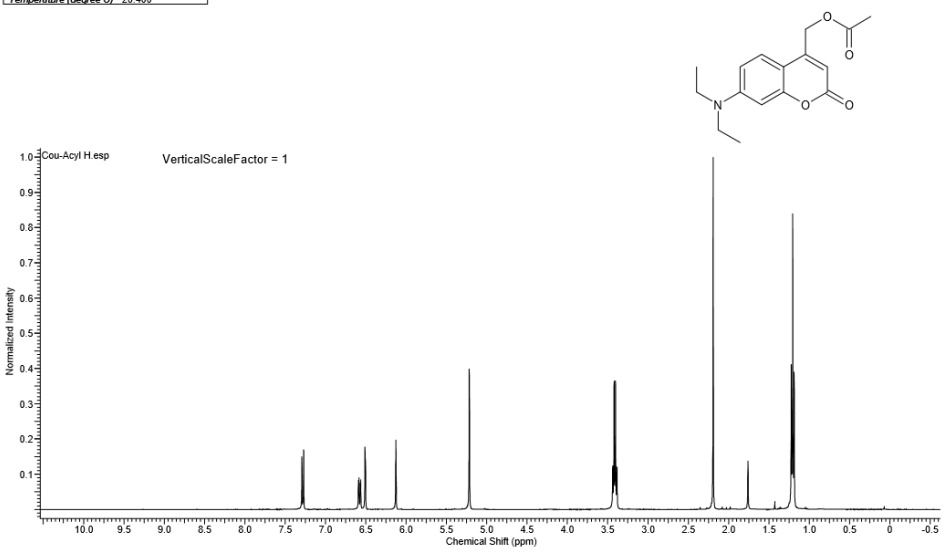




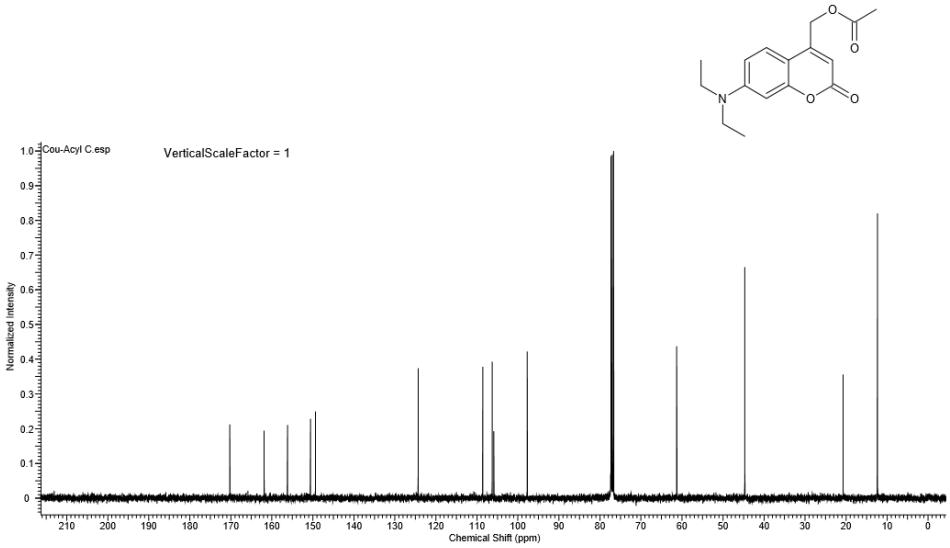
A.6.2 DEATC Caged Amino Acids

Compound 233

Acquisition Time (sec)	3.2768	*Comment*	Instrument AVG400 Group SJC Chemist MLS MLS07072: Cou Acyl h1acq.crl CDCl3 (C:\NMR) sjcgrp 5				
Date	18 Sep 2014 09:17:04			*Date Stamp*	18 Sep 2014 09:17:04		
File Name	F:\NMR\Thiocoumarin\Cou-Acyl\1\pdata\1\1r			*Frequency (MHz)*	400.20	*Nucleus*	1H
Number of Transients	16	*Origin*	avg400	*Original Points Count*	32768	*Owner*	nmr-user
Points Count	65536	*Pulse Sequence*	zg30	*Receiver Gain*	175.70	*SW(cyclical) (Hz)*	10000.00
Solvent	CHLOROFORM-d	*Spectrum Offset (Hz)*	2463.3635	*Spectrum Type*	STANDARD	*Sweep Width (Hz)*	9999.85
Temperature (degree C)	20.400						

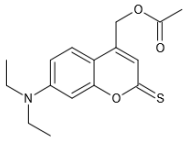


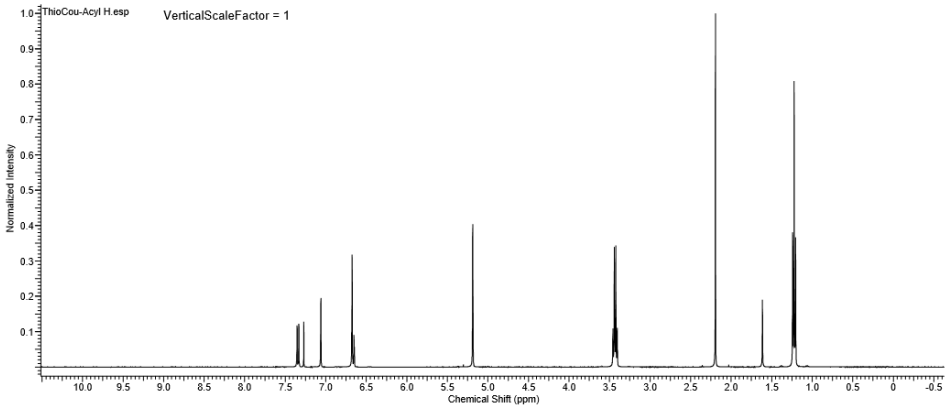
Acquisition Time (sec)	1.3631	*Comment*	Instrument AVG400 Group SJC Chemist MLS MLS07072: Cou Acyl c13acq.crl CDCl3 (C:\NMR) sjcgrp 5				
Date	18 Sep 2014 22:26:24			*Date Stamp*	18 Sep 2014 22:26:24		
File Name	F:\NMR\Thiocoumarin\Cou-Acyl\3\pdata\1\1r			*Frequency (MHz)*	100.63	*Nucleus*	13C
Number of Transients	256	*Origin*	avg400	*Original Points Count*	32768	*Owner*	nmr-user
Points Count	32768	*Pulse Sequence*	zgpg30	*Receiver Gain*	2050.00	*SW(cyclical) (Hz)*	24038.46
Solvent	CHLOROFORM-d	*Spectrum Offset (Hz)*	10053.8633	*Spectrum Type*	STANDARD	*Sweep Width (Hz)*	24037.73
Temperature (degree C)	21.500						



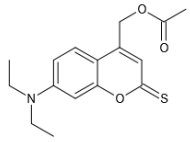
Compound 234

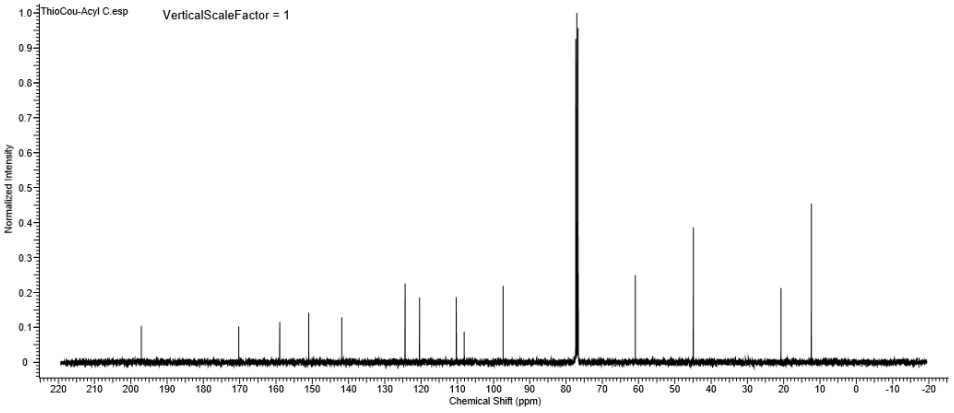
Acquisition Time (sec)	3.2768	*Comment*	Instrument AVG400 Group SJC Chemist MLS MLS07076: Thio Cou Acyl h1acq.crl CDCl3 {C:\NMR} sjcgrp 17				
Date	25 Sep 2014 09:53:20			*Date Stamp*	25 Sep 2014 09:53:20		
File Name	F:\NMR\Thiocoumarin\ThioCou-Acyl\1\pdata\1\1r			*Frequency (MHz)*	400.20	*Nucleus*	1H
Number of Transients	16	*Origin*	avg400	*Original Points Count*	32768	*Owner*	nmr-user
Points Count	65536	*Pulse Sequence*	zg30	*Receiver Gain*	255.20	*SW(cyclical) (Hz)*	10000.00
Solvent	CHLOROFORM-d	*Spectrum Offset (Hz)*	2461.8376	*Spectrum Type*	STANDARD	*Sweep Width (Hz)*	9999.85
Temperature (degree C)	21.600						





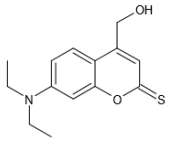
Acquisition Time (sec)	1.3631	*Comment*	Instrument AVG400 Group SJC Chemist MLS MLS07076: Thio Cou Acyl c13acq.crl CDCl3 {C:\NMR} sjcgrp 17				
Date	25 Sep 2014 11:01:36			*Date Stamp*	25 Sep 2014 11:01:36		
File Name	F:\NMR\Thiocoumarin\ThioCou-Acyl\3\pdata\1\1r			*Frequency (MHz)*	100.63	*Nucleus*	13C
Number of Transients	256	*Origin*	avg400	*Original Points Count*	32768	*Owner*	nmr-user
Points Count	32768	*Pulse Sequence*	zgpg30	*Receiver Gain*	2050.00	*SW(cyclical) (Hz)*	24038.46
Solvent	CHLOROFORM-d	*Spectrum Offset (Hz)*	10055.3301	*Spectrum Type*	STANDARD	*Sweep Width (Hz)*	24037.73
Temperature (degree C)	21.500						

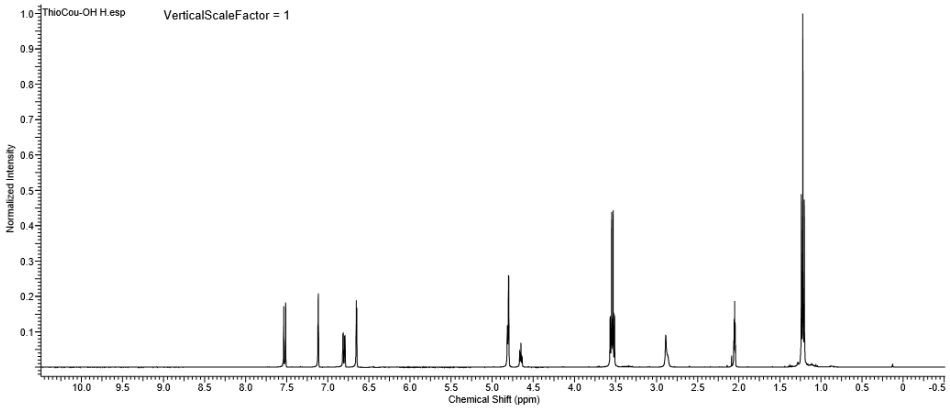




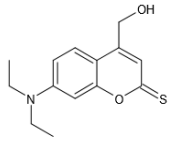
Compound 235

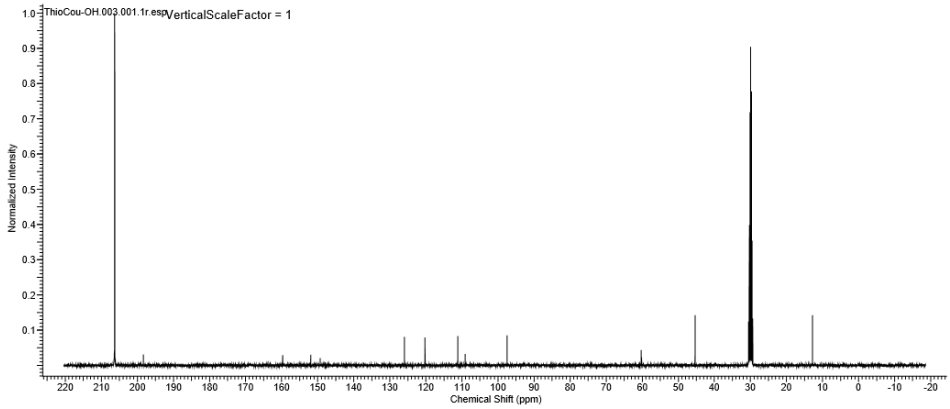
Acquisition Time (sec)	3.2768	*Comment*	Instrument AVG400 Group SJC Chemist MLS MLS07086: ThioCou LPG h1acq.crl Acetone {C:\NMR} sjcgrp 21				
Date	26 Sep 2014 09:17:04			*Date Stamp*	26 Sep 2014 09:17:04		
File Name	F:\NMR\Thiocoumarin\ThioCou-OH\1\pdata\1\1r			*Frequency (MHz)*	400.20	*Nucleus*	1H
Number of Transients	16	*Origin*	avg400	*Original Points Count*	32768	*Owner*	nmr-user
Points Count	65536	*Pulse Sequence*	zg30	*Receiver Gain*	221.01	*SW(cyclical) (Hz)*	10000.00
Solvent	Acetone	*Spectrum Offset (Hz)*	2460.8064	*Spectrum Type*	STANDARD	*Sweep Width (Hz)*	9999.85
Temperature (degree C)	21.100						





Acquisition Time (sec)	1.3631	*Comment*	Instrument AVG400 Group SJC Chemist MLS MLS07086: ThioCou LPG c13acq.crl Acetone {C:\NMR} sjcgrp 21				
Date	26 Sep 2014 15:24:00			*Date Stamp*	26 Sep 2014 15:24:00		
File Name	F:\NMR\Thiocoumarin\ThioCou-OH\3\pdata\1\1r			*Frequency (MHz)*	100.63	*Nucleus*	13C
Number of Transients	256	*Origin*	avg400	*Original Points Count*	32768	*Owner*	nmr-user
Points Count	32768	*Pulse Sequence*	zgpg30	*Receiver Gain*	2050.00	*SW(cyclical) (Hz)*	24038.46
Solvent	Acetone	*Spectrum Offset (Hz)*	10156.4482	*Spectrum Type*	STANDARD	*Sweep Width (Hz)*	24037.73
Temperature (degree C)	21.500						

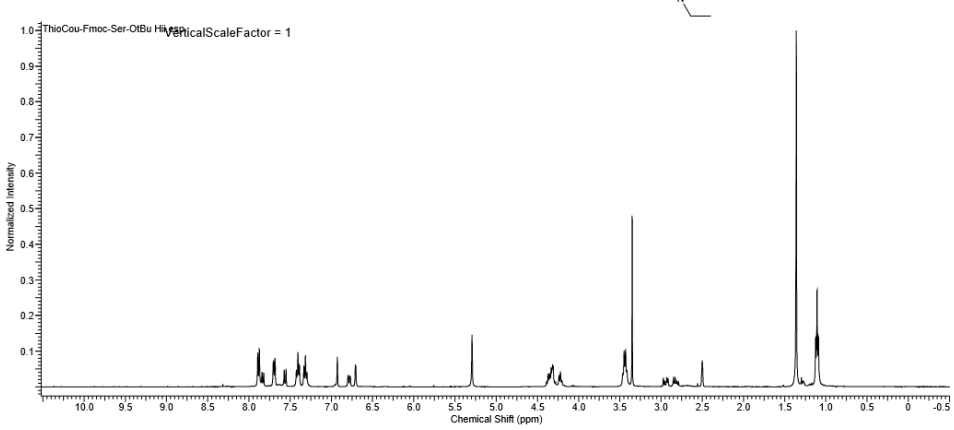




Compound 232

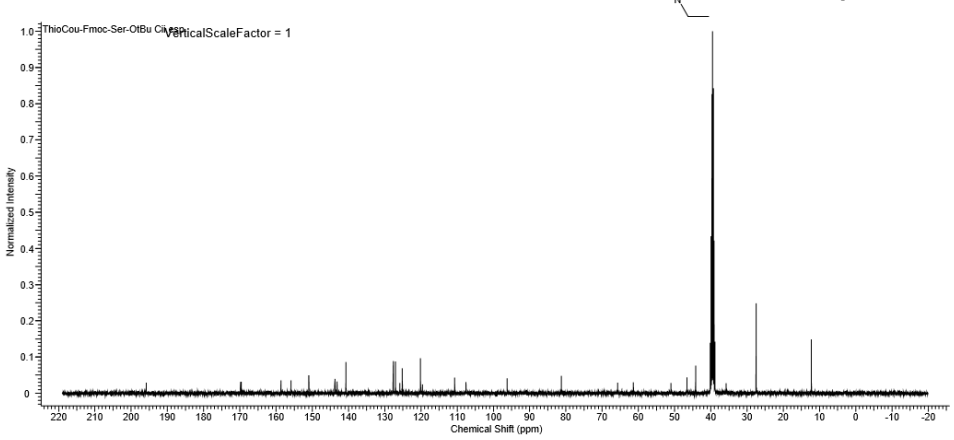
Acquisition Time (sec)	3.2768	*Comment*	Instrument AVG400 Group SJC Chemist MLS MLS07088: ThioCou Fmoc-Asp-OtBu h1acq crl DMSO {C:\NMR} sjcgrp 11				
Date	19 Jan 2015 09:31:44			*Date Stamp*	19 Jan 2015 09:31:44		
File Name	F:\NMR\Thiocoumarin\ThioCou-Fmoc-Asp-OtBu\Jan19-2015-11-\1\pdata\1\1r					*Frequency (MHz)*	400.20
Nucleus	1H	*Number of Transients*	16	*Origin*	avg400	*Original Points Count*	32768
Owner	nmr-user	*Points Count*	65536	*Pulse Sequence*	zg30	*Receiver Gain*	141.58
SW(cyclical) (Hz)	10000.00	*Solvent*	DMSO-d6	*Spectrum Offset (Hz)*	2464.6572	*Spectrum Type*	STANDARD
Sweep Width (Hz)	9999.85	*Temperature (degree C)*	21.500				





Acquisition Time (sec)	1.3631	*Comment*	Instrument AVG400 Group SJC Chemist MLS MLS07088: ThioCou Fmoc-Asp-OtBu c13acq crl DMSO {C:\NMR} sjcgrp 11				
Date	19 Jan 2015 22:13:20	*Date Stamp*	19 Jan 2015 22:13:20	*File Name*	F:\NMR\Thiocoumarin\ThioCou-Fmoc-Asp-OtBu\Jan19-2015-11-\3\pdata\1\1r		
Frequency (MHz)	100.63	*Nucleus*	13C	*Number of Transients*	256	*Origin*	avg400
Original Points Count	32768	*Owner*	nmr-user	*Points Count*	32768	*Pulse Sequence*	zgpg30
Receiver Gain	2050.00	*SW(cyclical) (Hz)*	24038.46	*Solvent*	DMSO-d6	*Spectrum Offset (Hz)*	10014.4980
Spectrum Type	STANDARD	*Sweep Width (Hz)*	24037.73	*Temperature (degree C)*	21.500		

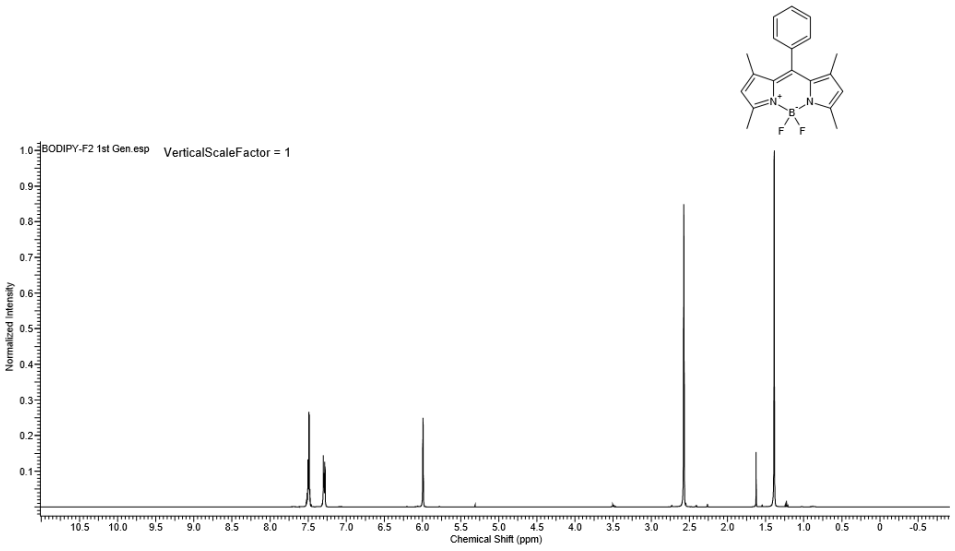




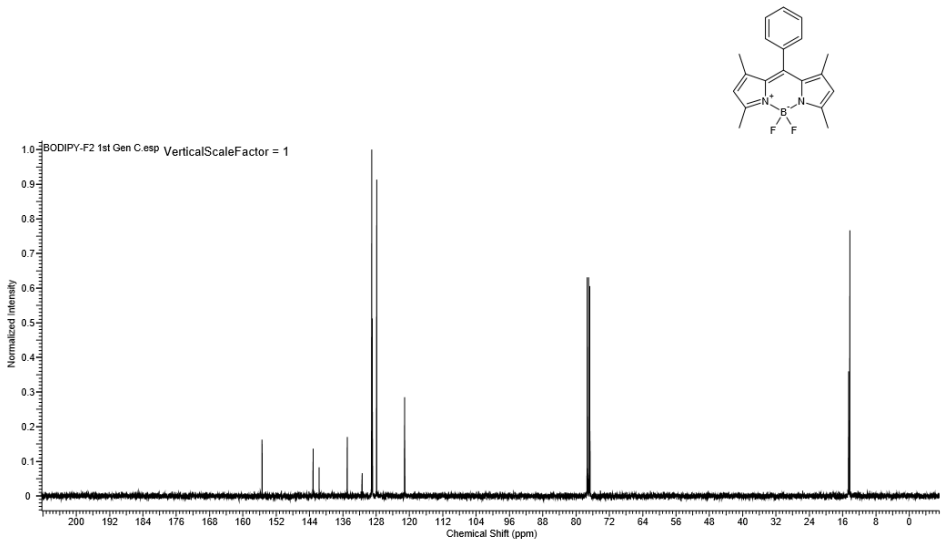
A.6.3 BODIPY Caged Amino Acids

Compound 238

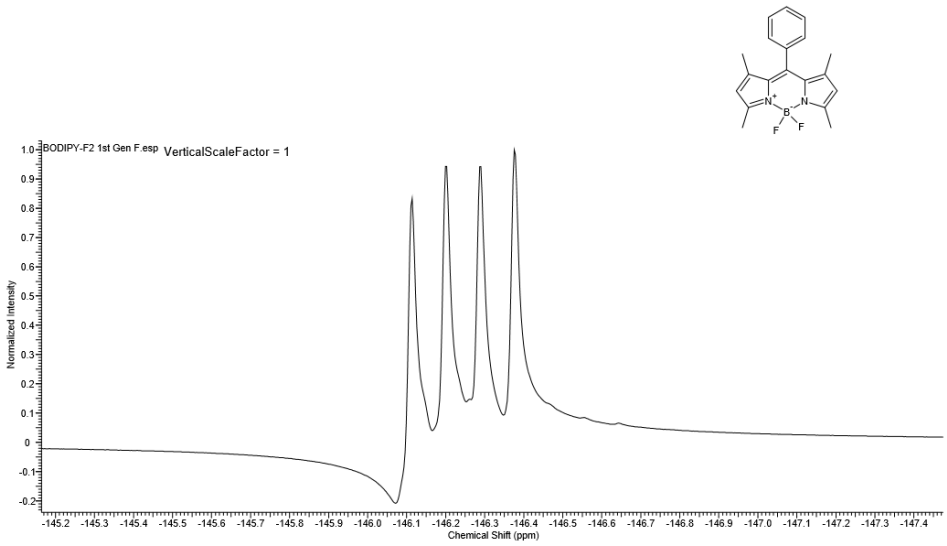
Acquisition Time (sec)	4.0894	*Comment*	Instrument AVF400 Chemist MLS Group SJC MLS07134: BODIPY LPG h1acq.crl CDCl3 {C:\NMR} sjcgrp 50		
Date	15 Oct 2014 04:52:32			*Date Stamp*	15 Oct 2014 04:52:32
File Name	F:\NMR\BODIPY Stuff\BODIPY-F2 1st Gen\1\pdata\1\1r			*Frequency (MHz)*	400.25
Nucleus	1H			*Number of Transients*	16
Origin	avf400	*Original Points Count*	32768	*Owner*	nmr-user
Points Count	32768	*Pulse Sequence*	zg60	*Receiver Gain*	45.32
SW(cyclical) (Hz)	8012.82	*Solvent*	CHLOROFORM-d	*Spectrum Offset (Hz)*	2395.9338
Spectrum Type	STANDARD	*Sweep Width (Hz)*	8012.58	*Temperature (degree C)*	22.589



Acquisition Time (sec)	0.6291	*Comment*	Instrument AVF400 Chemist MLS Group SJC MLS07134: BODIPY LPG c13acq.crl CDCl3 {C:\NMR} sjcgrp 50		
Date	15 Oct 2014 05:05:20			*Date Stamp*	15 Oct 2014 05:05:20
File Name	F:\NMR\BODIPY Stuff\BODIPY-F2 1st Gen\3\pdata\1\1r			*Frequency (MHz)*	100.64
Nucleus	13C			*Number of Transients*	256
Origin	avf400	*Original Points Count*	16384	*Owner*	nmr-user
Points Count	32768	*Pulse Sequence*	zgpg30	*Receiver Gain*	205.43
SW(cyclical) (Hz)	26041.67	*Solvent*	CHLOROFORM-d	*Spectrum Offset (Hz)*	10058.5908
Spectrum Type	STANDARD	*Sweep Width (Hz)*	26040.87	*Temperature (degree C)*	23.680

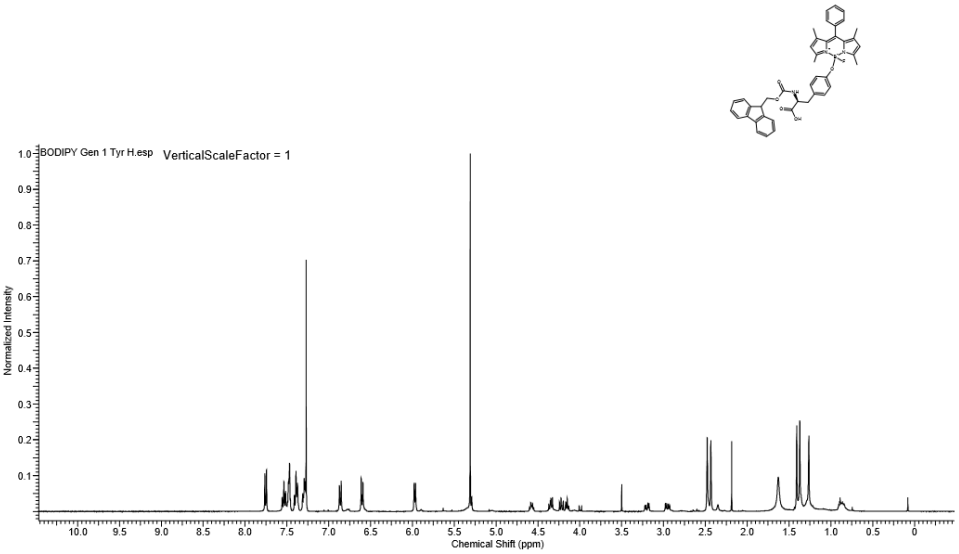


Acquisition Time (sec)	0.8738	*Comment*	Instrument AVF400 Chemist MLS Group SJC MLS07134: BODIPY LPG f19acq_256.crl CDCl3 (C:\NMR) sjcgrp 50				
Date	15 Oct 2014 05:37:20			*Date Stamp*	15 Oct 2014 05:37:20		
File Name	F:\NMR\BODIPY Stuff\BODIPY-F2 1st Gen\9\pdata\1\1r			*Frequency (MHz)*	376.61	*Nucleus*	19F
Number of Transients	256	*Origin*	avf400	*Original Points Count*	65536	*Owner*	nmr-user
Points Count	65536	*Pulse Sequence*	zgflqn	*Receiver Gain*	205.43	*SW(cyclical) (Hz)*	75000.00
Solvent	CHLOROFORM-d	*Spectrum Offset (Hz)*	-56491.6914	*Spectrum Type*	STANDARD	*Sweep Width (Hz)*	74998.86
Temperature (degree C)	22.768						

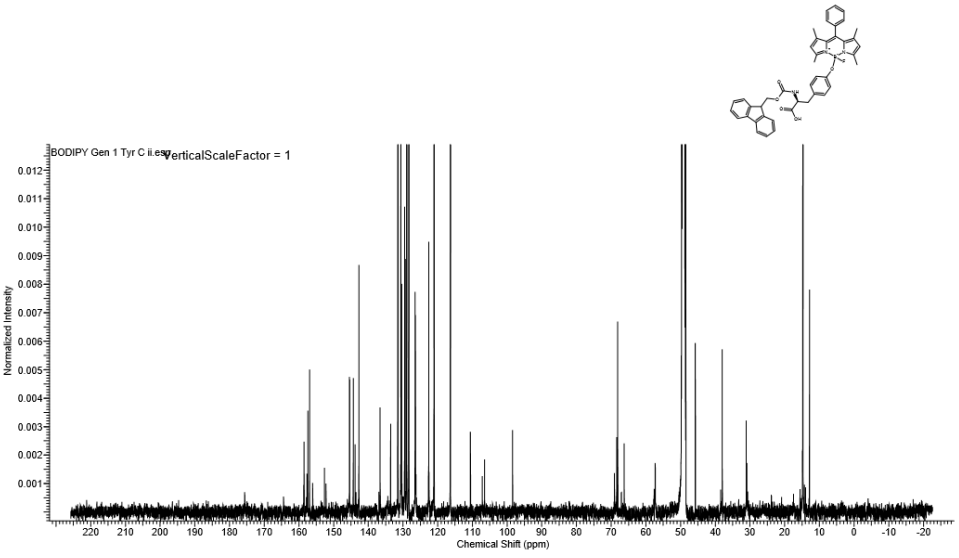


Compound 244

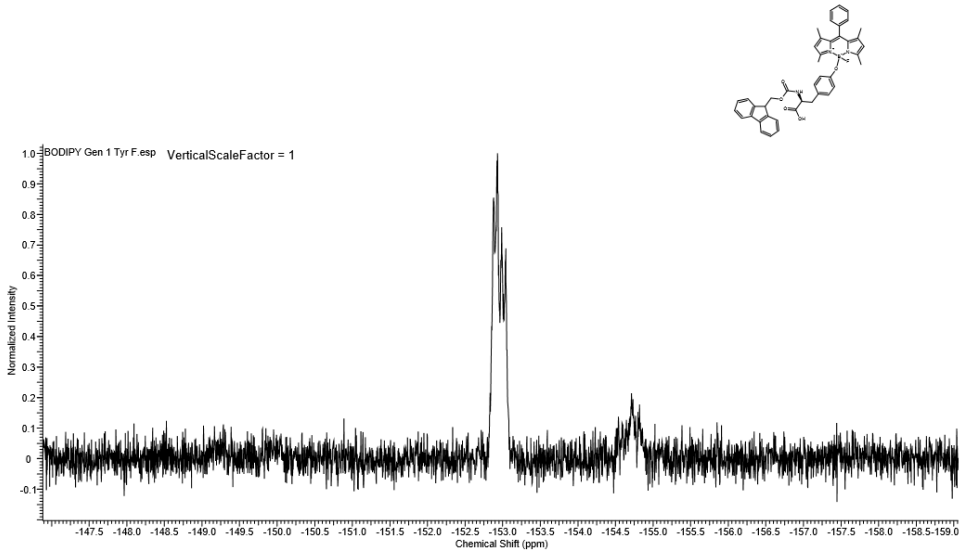
Acquisition Time (sec)	4.0894	*Comment*	Instrument AVF400 Chemist MLS Group SJC MLS07144: BODIPY Tyr h1acq.crl CDCl3 {C:\NMR} sjcgrp 9				
Date	31 Oct 2014 13:22:08			*Date Stamp*	31 Oct 2014 13:22:08		
File Name	F:\NMR\BODIPY Stuff\BODIPY Tyr\Oct30-2014-9\1\pdata\1\1r			*Frequency (MHz)*	400.25	*Nucleus*	1H
Number of Transients	16	*Origin*	avf400	*Original Points Count*	32768	*Owner*	nmr-user
Points Count	32768	*Pulse Sequence*	zg60	*Receiver Gain*	93.00	*SW(cyclical) (Hz)*	8012.82
Solvent	CHLOROFORM-d	*Spectrum Offset (Hz)*	2393.2444	*Spectrum Type*	STANDARD	*Sweep Width (Hz)*	8012.58
Temperature (degree C)	20.710						



Acquisition Time (sec)	1.0486	*Comment*	Instrument AVC500 Group SJC 1123 M. Savage 1/5/15			*Date*	01 May 2015 09:10:40
Date Stamp	01 May 2015 09:10:40						
File Name	D:\Gnomeeee\NMR\BODIPY Stuff\BODIPY 1\BODIPY Fmoc Tyr OH\ms112301051\4\PDATA\1\1r					*Frequency (MHz)*	125.80
Nucleus	13C	*Number of Transients*	1210	*Origin*	avc500	*Original Points Count*	32768
Owner	nmr-user	*Points Count*	32768	*Pulse Sequence*	zgpg30	*Receiver Gain*	912.00
SW(cyclical) (Hz)	31250.00	*Solvent*	METHANOL-d4	*Spectrum Offset (Hz)*	12775.3701	*Spectrum Type*	STANDARD
Sweep Width (Hz)	31249.05	*Temperature (degree C)*	24.970				

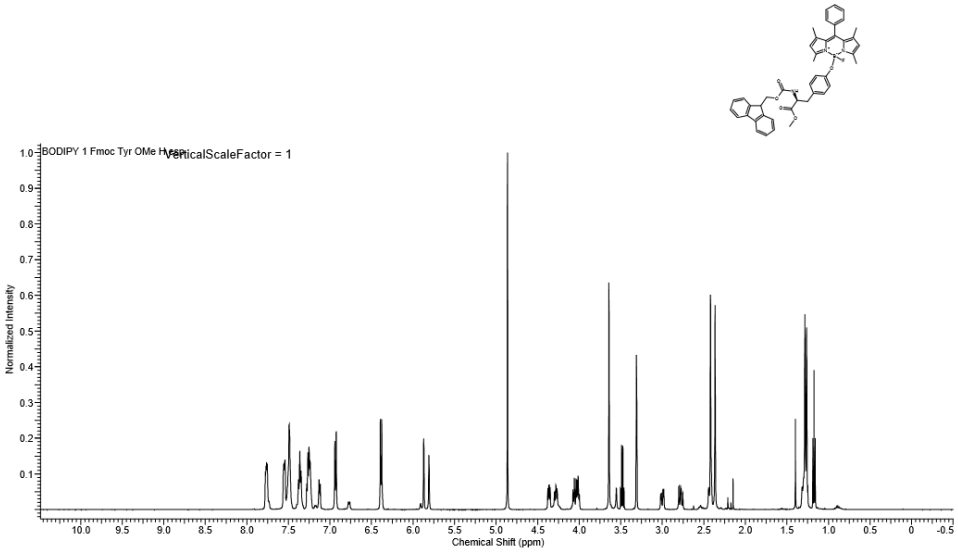


Acquisition Time (sec)	0.5767	*Comment*	Instrument AVB500 1123 M. Savage 30/4/15			*Date*	30 Apr 2015 09:25:36
Date Stamp	30 Apr 2015 09:25:36						
File Name	D:\Gnomeeee\NMR\BODIPY Stuff\BODIPY 1\BODIPY Fmoc Tyr OH\ms11230105\ms11233004.19F\1\PDATA\1\1r					*Frequency (MHz)*	470.45
Nucleus	19F	*Number of Transients*	16	*Origin*	avb500	*Original Points Count*	65536
Owner	nmr-user	*Points Count*	65536	*Pulse Sequence*	zgfhigqn.tfi	*Receiver Gain*	2050.00
SW(cyclical) (Hz)	113636.37	*Solvent*	METHANOL-d4	*Spectrum Offset (Hz)*	-47044.7344	*Spectrum Type*	STANDARD
Sweep Width (Hz)	113634.63	*Temperature (degree C)*	25.000				

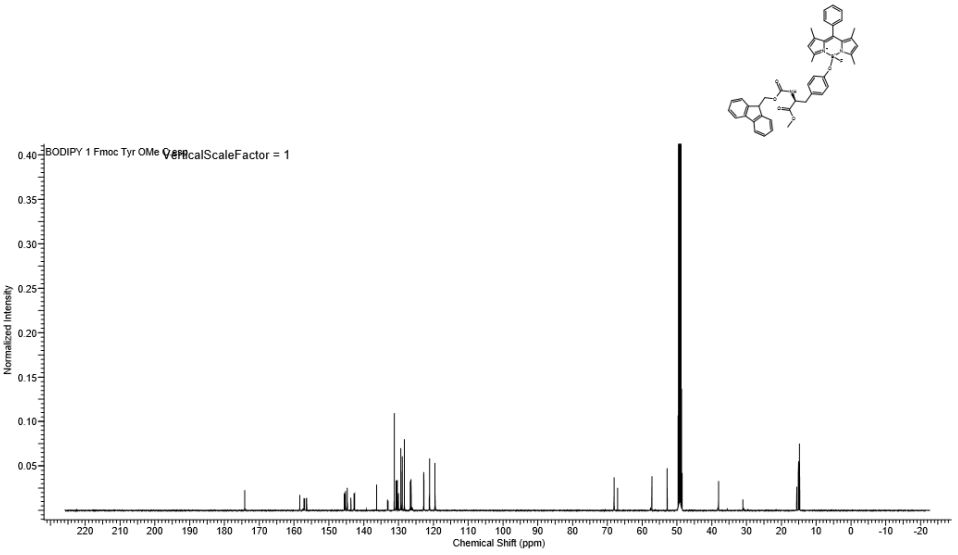


Compound 245

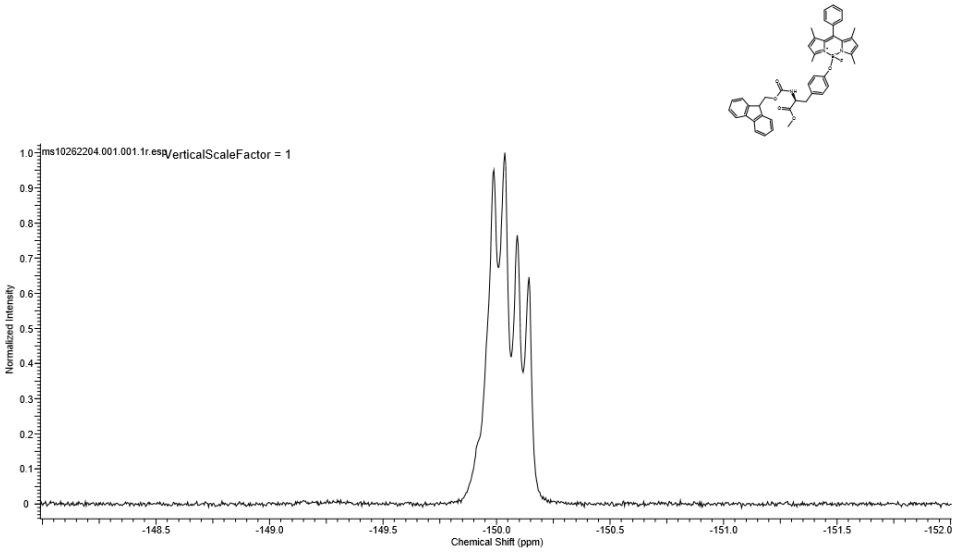
Acquisition Time (sec)	3.1719	*Comment*	Instrument AVC500 Group SJC 1026 M. Savage 22/4/15			*Date*	22 Apr 2015 08:04:32
Date Stamp	22 Apr 2015 08:04:32						
File Name	D:\Gnomeeee\NMR\BODIPY Stuff\BODIPY 1\BODIPY 1 Fmoc-Tyr-OMe\ms10262204\1\PDATA\1\1r					*Frequency (MHz)*	500.30
Nucleus	1H	*Number of Transients*	16	*Origin*	avc500	*Original Points Count*	32768
Owner	nmr-user	*Points Count*	65536	*Pulse Sequence*	zg30	*Receiver Gain*	3.20
SW(cyclical) (Hz)	10330.58	*Solvent*	METHANOL-d4	*Spectrum Offset (Hz)*	3078.7017	*Spectrum Type*	STANDARD
Sweep Width (Hz)	10330.42	*Temperature (degree C)*	24.970				



Acquisition Time (sec)	1.0486	*Comment*	Instrument AVC500 Group SJC 1026 M. Savage 22/4/15			*Date*	22 Apr 2015 09:44:48
Date Stamp	22 Apr 2015 09:44:48						
File Name	D:\Gnomeeee\NMR\BODIPY Stuff\BODIPY 1\BODIPY 1 Fmoc-Tyr-OMe\ms10262204\4\PDATA\1\1r					*Frequency (MHz)*	125.80
Nucleus	13C	*Number of Transients*	2048	*Origin*	avc500	*Original Points Count*	32768
Owner	nmr-user	*Points Count*	32768	*Pulse Sequence*	zgpg30	*Receiver Gain*	912.00
SW(cyclical) (Hz)	31250.00	*Solvent*	METHANOL-d4	*Spectrum Offset (Hz)*	12773.4629	*Spectrum Type*	STANDARD
Sweep Width (Hz)	31249.05	*Temperature (degree C)*	24.970				

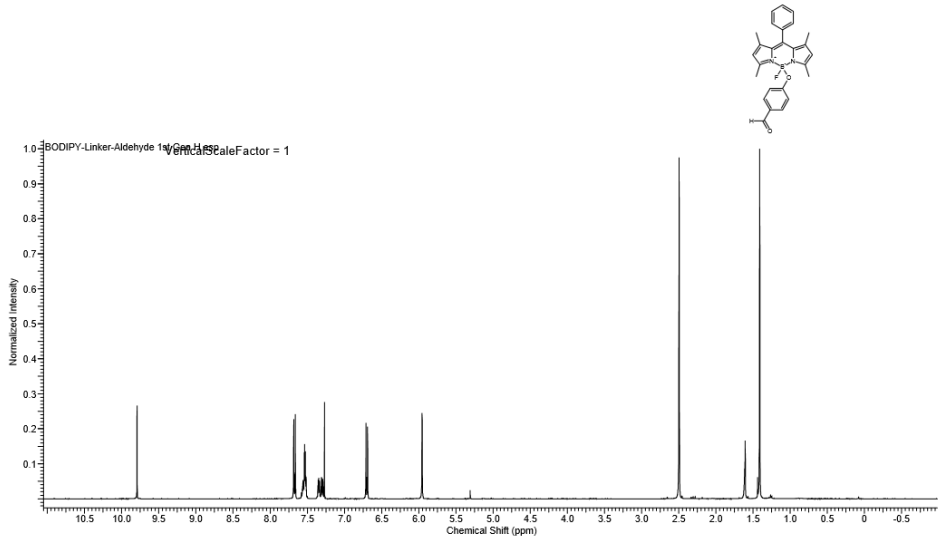


Acquisition Time (sec)	0.5767	*Comment*	Instrument AVB500 M SAVAGE 41026 22/4/15			*Date*	22 Apr 2015 11:27:12
Date Stamp	22 Apr 2015 11:27:12						
File Name	D:\Gnomeeee\NMR\BODIPY Stuff\BODIPY 1\BODIPY 1 Fmoc-Tyr-OMe\19F\ms10262204\1\1\PDATA\1\1r					*Frequency (MHz)*	470.45
Nucleus	19F	*Number of Transients*	16	*Origin*	avb500	*Original Points Count*	65536
Owner	nmr-user	*Points Count*	65536	*Pulse Sequence*	zgfhigqn.tfi	*Receiver Gain*	2050.00
SW(cyclical) (Hz)	113636.37	*Solvent*	METHANOL-d4	*Spectrum Offset (Hz)*	-47044.7344	*Spectrum Type*	STANDARD
Sweep Width (Hz)	113634.63	*Temperature (degree C)*	25.000				

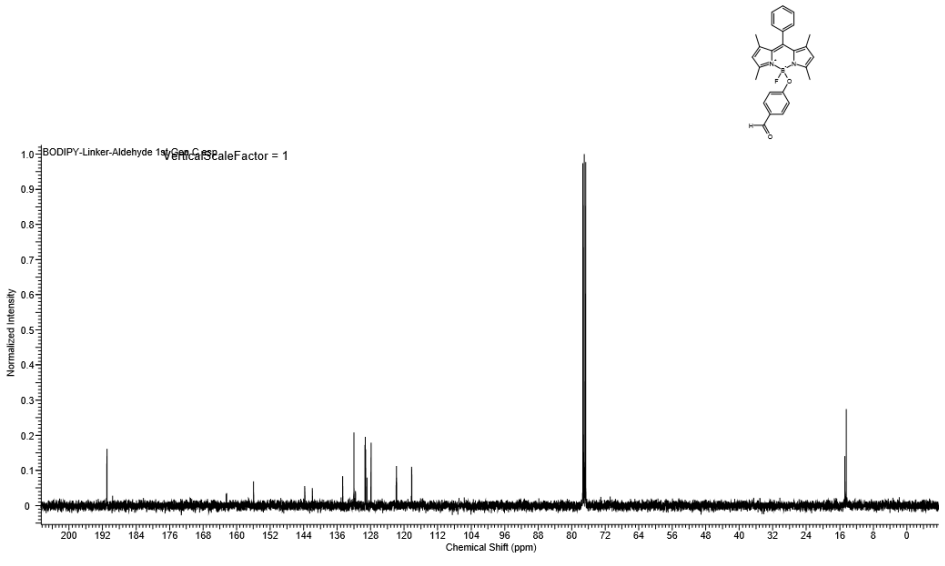


Compound 239

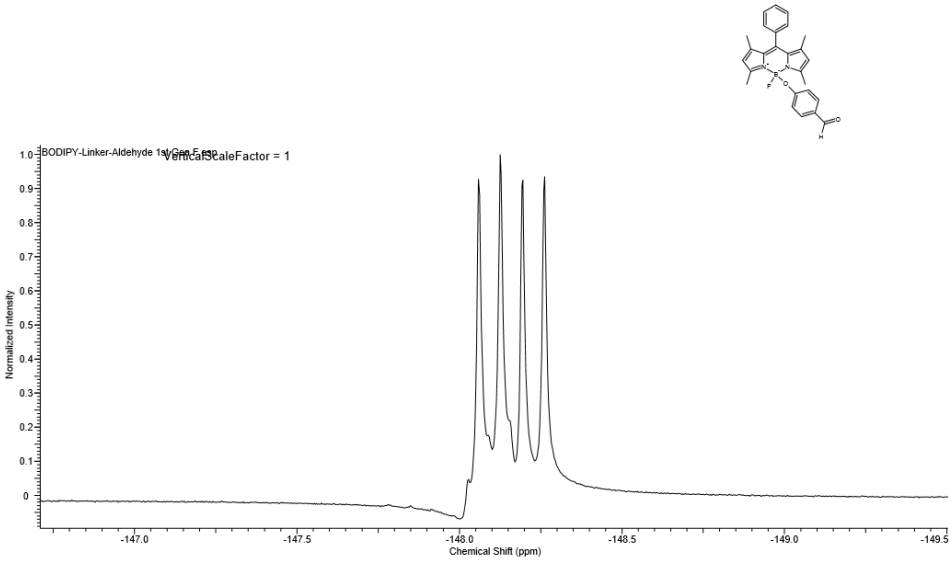
Acquisition Time (sec)	4.0894	*Comment*	Instrument AVF400 Chemist MLS Group SJC MLS07138: Spot 2 h1acq crl CDCl3 {C:\NMR} sjcgrp 18				
Date	17 Oct 2014 11:27:12			*Date Stamp*	17 Oct 2014 11:27:12		
File Name	F:\NMR\BODIPY Stuff\BODIPY-Linker-Aldehyde 1st Gen\Oct17-2014-1\$\1\pdata\1\1r					*Frequency (MHz)*	400.25
Nucleus	1H	*Number of Transients*	16	*Origin*	avf400	*Original Points Count*	32768
Owner	nmr-user	*Points Count*	32768	*Pulse Sequence*	zg60	*Receiver Gain*	93.00
SW(cyclical) (Hz)	8012.82	*Solvent*	CHLOROFORM-d	*Spectrum Offset (Hz)*	2393.4885	*Spectrum Type*	STANDARD
Sweep Width (Hz)	8012.58	*Temperature (degree C)*	22.447				



Acquisition Time (sec)	0.6291	*Comment*	Instrument AVF400 Chemist MLS Group SJC MLS07138: Spot 2 c13acq crl CDCl3 {C:\NMR} sjcgrp 18				
Date	17 Oct 2014 11:50:40	*Date Stamp*	17 Oct 2014 11:50:40	*File Name*	F:\NMR\BODIPY Stuff\BODIPY-Linker-Aldehyde 1st Gen\Oct17-2014-1\$\4\pdata\1\1r		
Frequency (MHz)	100.64	*Nucleus*	13C	*Number of Transients*	256	*Origin*	avf400
Original Points Count	16384	*Owner*	nmr-user	*Points Count*	32768	*Pulse Sequence*	zgpg30
Receiver Gain	205.43	*SW(cyclical) (Hz)*	26041.67	*Solvent*	CHLOROFORM-d	*Spectrum Offset (Hz)*	10060.9756
Spectrum Type	STANDARD	*Sweep Width (Hz)*	26040.87	*Temperature (degree C)*	23.603		

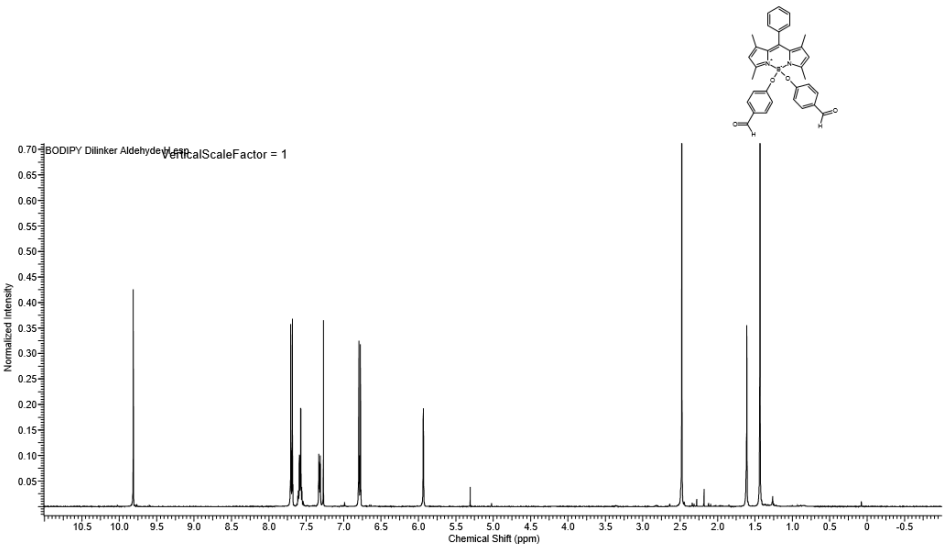


Acquisition Time (sec)	0.8738	*Comment*	Instrument AVF400 Chemist MLS Group SJC MLS07138: Spot 2 f19dec_256.crl CDCl3 {C:\NMR} sjcgrp 18				
Date	17 Oct 2014 12:16:16	*Date Stamp*	17 Oct 2014 12:16:16	*File Name*	F:\NMR\BODIPY Stuff\BODIPY-Linker-Aldehyde 1st Gen\Oct17-2014-1\6\pdata\1\1r		
Frequency (MHz)	376.61	*Nucleus*	19F	*Number of Transients*	256	*Origin*	avf400
Original Points Count	65536	*Owner*	nmr-user	*Points Count*	65536	*Pulse Sequence*	zgfhigqn
Receiver Gain	205.43	*SW(cyclical) (Hz)*	75000.00	*Solvent*	CHLOROFORM-d	*Spectrum Offset (Hz)*	-56491.6992
Spectrum Type	STANDARD	*Sweep Width (Hz)*	74998.86	*Temperature (degree C)*	23.124		

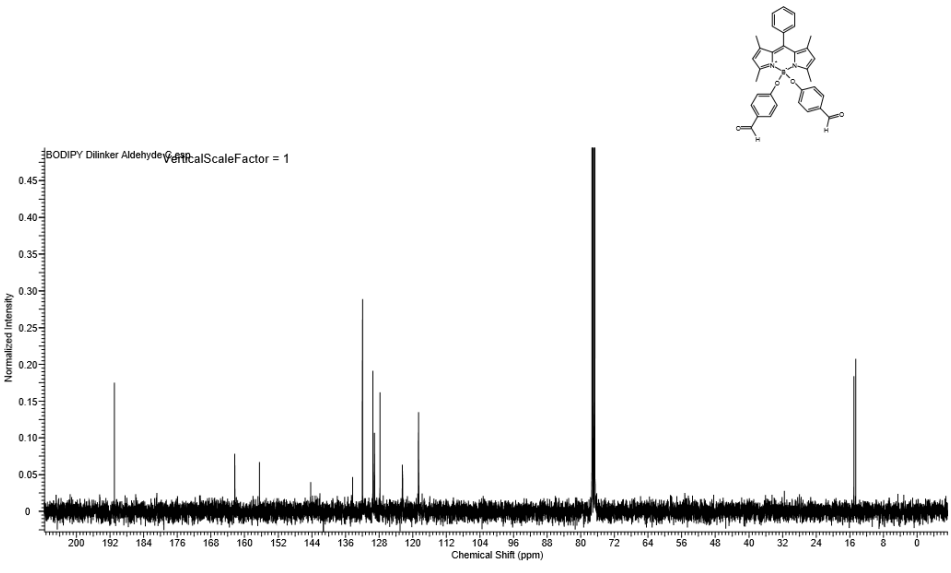


Compound 240

Acquisition Time (sec)	4.0894	*Comment*	Instrument AVF400 Chemist MLS Group SJC MLS07138: Spot 3 h1acq.crl CDCl3 {C:\NMR} sjcgrp 19				
Date	17 Oct 2014 12:20:32			*Date Stamp*	17 Oct 2014 12:20:32		
File Name	F:\NMR\BODIPY Stuff\BODIPY-DiLinker Aldehyde 1st Gen\Oct17-2014-19\1\pdata\1\1r					*Frequency (MHz)*	400.25
Nucleus	1H	*Number of Transients*	16	*Origin*	avf400	*Original Points Count*	32768
Owner	nmr-user	*Points Count*	32768	*Pulse Sequence*	zg60	*Receiver Gain*	149.73
SW(cyclical) (Hz)	8012.82	*Solvent*	CHLOROFORM-d	*Spectrum Offset (Hz)*	2393.7332	*Spectrum Type*	STANDARD
Sweep Width (Hz)	8012.58	*Temperature (degree C)*	22.650				

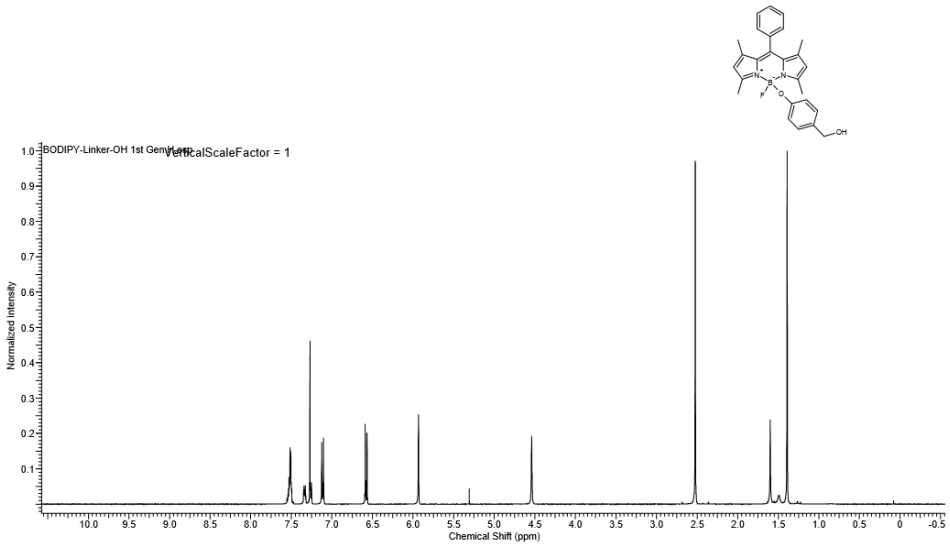


Acquisition Time (sec)	0.6291	*Comment*	Instrument AVF400 Chemist MLS Group SJC MLS07138: Spot 3 c13acq.crl CDCl3 {C:\NMR} sjcgrp 19				
Date	17 Oct 2014 12:46:08	*Date Stamp*	17 Oct 2014 12:46:08	*File Name*	F:\NMR\BODIPY Stuff\BODIPY-DiLinker Aldehyde 1st Gen\Oct17-2014-19\4\pdata\1\1r		
Frequency (MHz)	100.64	*Nucleus*	13C	*Number of Transients*	256	*Origin*	avf400
Original Points Count	16384	*Owner*	nmr-user	*Points Count*	32768	*Pulse Sequence*	zgpg30
Receiver Gain	205.43	*SW(cyclical) (Hz)*	26041.67	*Solvent*	CHLOROFORM-d	*Spectrum Offset (Hz)*	10060.9756
Spectrum Type	STANDARD	*Sweep Width (Hz)*	26040.87	*Temperature (degree C)*	23.725		

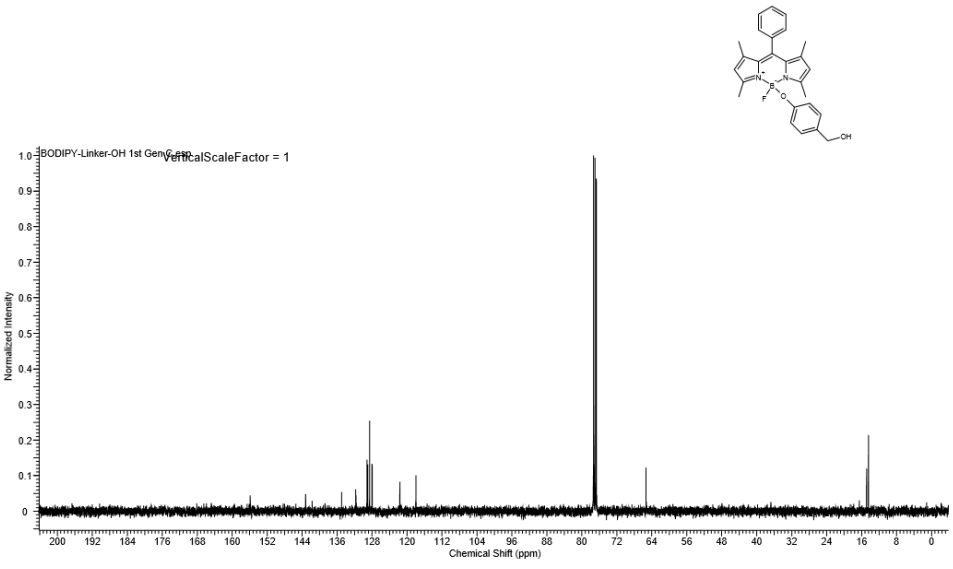


Compound 241

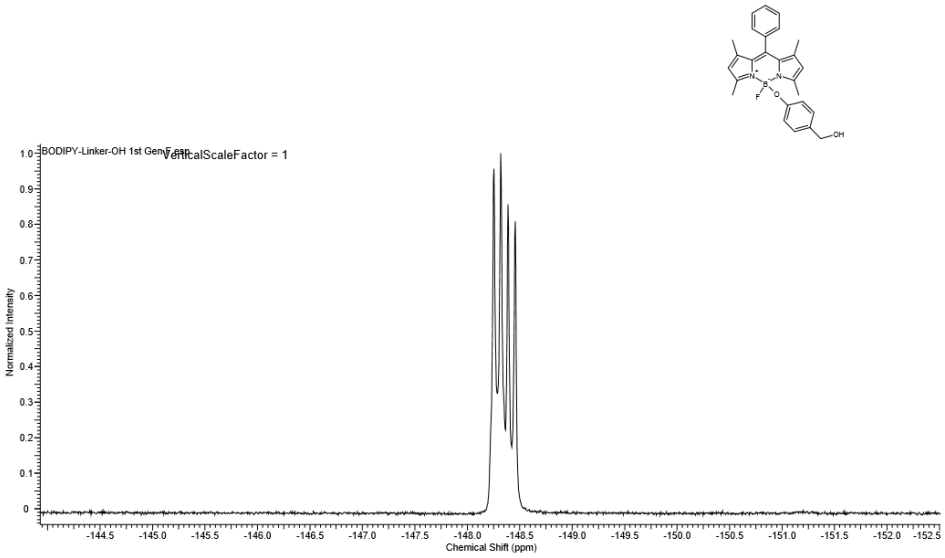
Acquisition Time (sec)	4.0894	*Comment*	Instrument AVF400 Chemist MLS Group SJC MLS07146: BoDIPy Linker OH h1acq.crl CDCl3 {C:\NMR} sjcgrp 43				
Date	21 Oct 2014 12:24:48			*Date Stamp*	21 Oct 2014 12:24:48		
File Name	F:\NMR\BODIPY Stuff\BODIPY-Linker-OH 1st Gen\Oct21-2014-43\1\pdata\1\1r						
Nucleus	1H	*Number of Transients*	16	*Origin*	avf400	*Frequency (MHz)*	400.25
Owner	nmr-user	*Points Count*	32768	*Pulse Sequence*	zg60	*Original Points Count*	32768
SW(cyclical) (Hz)	8012.82	*Solvent*	CHLOROFORM-d	*Spectrum Offset (Hz)*	2393.4885	*Receiver Gain*	93.00
Sweep Width (Hz)	8012.58	*Temperature (degree C)*	22.547			*Spectrum Type*	STANDARD



Acquisition Time (sec)	0.6291	*Comment*	Instrument AVF400 Chemist MLS Group SJC MLS07146: BoDIPy Linker OH c13acq.crl CDCl3 {C:\NMR} sjcgrp 43				
Date	21 Oct 2014 12:48:16	*Date Stamp*	21 Oct 2014 12:48:16	*File Name*	F:\NMR\BODIPY Stuff\BODIPY-Linker-OH 1st Gen\Oct21-2014-43\4\pdata\1\1r		
Frequency (MHz)	100.64	*Nucleus*	13C	*Number of Transients*	256	*Origin*	avf400
Original Points Count	16384	*Owner*	nmr-user	*Points Count*	32768	*Pulse Sequence*	zgpg30
Receiver Gain	205.43	*SW(cyclical) (Hz)*	26041.67	*Solvent*	CHLOROFORM-d	*Spectrum Offset (Hz)*	10060.9756
Spectrum Type	STANDARD	*Sweep Width (Hz)*	26040.87	*Temperature (degree C)*	23.837		

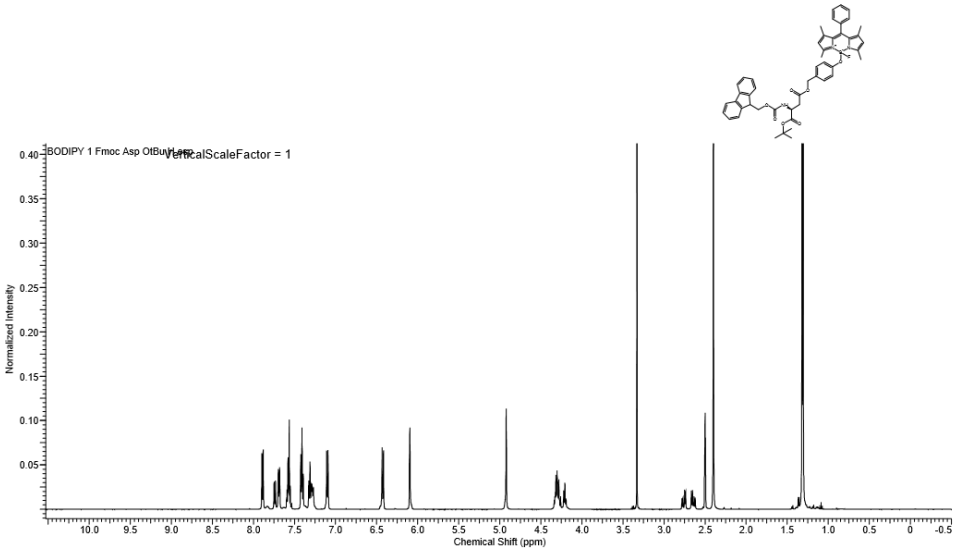


Acquisition Time (sec)	0.5767	*Comment*	Instrument AVF-400 Chemist MLS Group SJC MLS07146: BoDiPy Linker OH f19acq2_256.crl CDCl3 (C:\NMR) sjcgrp 43				
Date	21 Oct 2014 18:18:56	*Date Stamp*	21 Oct 2014 18:18:56	*File Name*	F:\NMR\BODIPY Stuff\BODIPY-Linker-OH 1st Gen\Oct21-2014-43\7\pdata\1\1r		
Frequency (MHz)	376.61	*Nucleus*	19F	*Number of Transients*	256	*Origin*	avf400
Original Points Count	65536	*Owner*	nmr-user	*Points Count*	65536	*Pulse Sequence*	zgflqn
Receiver Gain	205.43	*SW(cyclical) (Hz)*	113636.37	*Solvent*	CHLOROFORM-d	*Spectrum Offset (Hz)*	-18830.5742
Spectrum Type	STANDARD	*Sweep Width (Hz)*	113634.63	*Temperature (degree C)*	22.537		

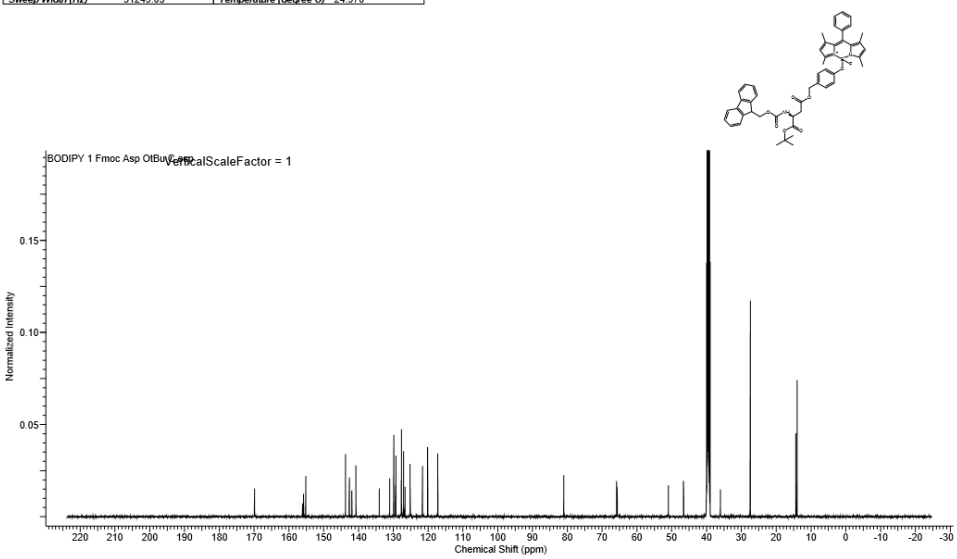


Compound 242

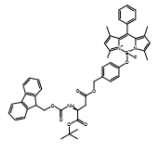
Acquisition Time (sec)	3.1719	*Comment*	Instrument AVC500 Group SJC 1124 M. Savage 1/5/15			*Date*	01 May 2015 12:14:08
Date Stamp	01 May 2015 12:14:08						
File Name	D:\Gnomeeee\NMR\BODIPY Stuff\BODIPY 1\BODIPY Linker Fmoc-Asp-OtBu\ms11240105\1\PDATA\1\1r					*Frequency (MHz)*	500.30
Nucleus	1H	*Number of Transients*	16	*Origin*	avc500	*Original Points Count*	32768
Owner	nmr-user	*Points Count*	65536	*Pulse Sequence*	zg30	*Receiver Gain*	3.56
SW(cyclical) (Hz)	10330.58	*Solvent*	DMSO-d6	*Spectrum Offset (Hz)*	3084.4055	*Spectrum Type*	STANDARD
Sweep Width (Hz)	10330.42	*Temperature (degree C)*	24.970				

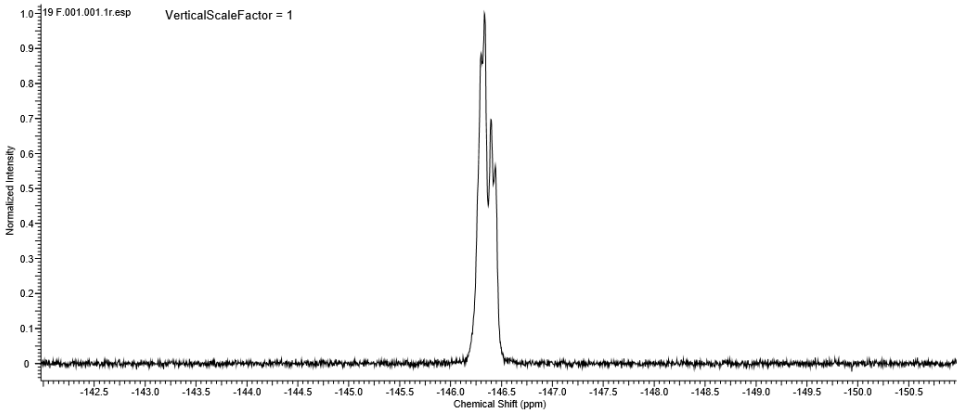


Acquisition Time (sec)	1.0486	*Comment*	Instrument AVC500 Group SJC 1124 M. Savage 1/5/15			*Date*	01 May 2015 13:11:44
Date Stamp	01 May 2015 13:11:44						
File Name	D:\Gnomeeee\NMR\BODIPY Stuff\BODIPY 1\BODIPY Linker Fmoc-Asp-OtBu\ms11240105\4\PDATA\1\1r					*Frequency (MHz)*	125.80
Nucleus	13C	*Number of Transients*	704	*Origin*	avc500	*Original Points Count*	32768
Owner	nmr-user	*Points Count*	32768	*Pulse Sequence*	zgpg30	*Receiver Gain*	912.00
SW(cyclical) (Hz)	31250.00	*Solvent*	DMSO-d6	*Spectrum Offset (Hz)*	12520.1416	*Spectrum Type*	STANDARD
Sweep Width (Hz)	31249.05	*Temperature (degree C)*	24.970				



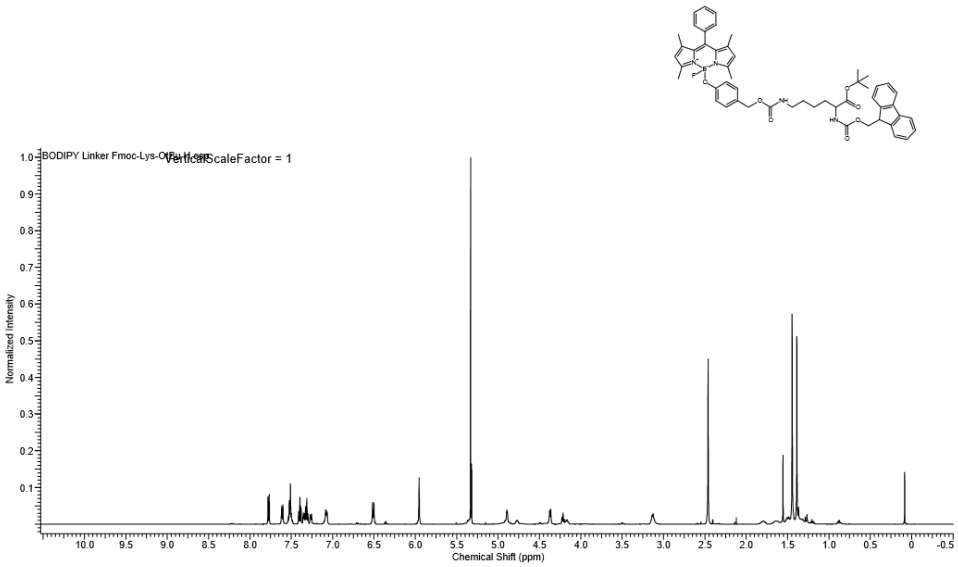
Acquisition Time (sec)	0.5767	*Comment*	Instrument AVB500 1124 M. Savage 30/4/15			*Date*	30 Apr 2015 09:40:32
Date Stamp	30 Apr 2015 09:40:32						
File Name	D:\Gnomeeee\NMR\BODIPY Stuff\BODIPY 1\BODIPY Linker Fmoc-Asp-OtBu\ms11240105\19 F\1\PDATA\1\1r					*Frequency (MHz)*	470.45
Nucleus	19F	*Number of Transients*	16	*Origin*	avb500	*Original Points Count*	65536
Owner	nmr-user	*Points Count*	65536	*Pulse Sequence*	zgfhigqn.tfi	*Receiver Gain*	2050.00
SW(cyclical) (Hz)	113636.37	*Solvent*	DMSO-d6	*Spectrum Offset (Hz)*	-47044.7344	*Spectrum Type*	STANDARD
Sweep Width (Hz)	113634.63	*Temperature (degree C)*	25.000				



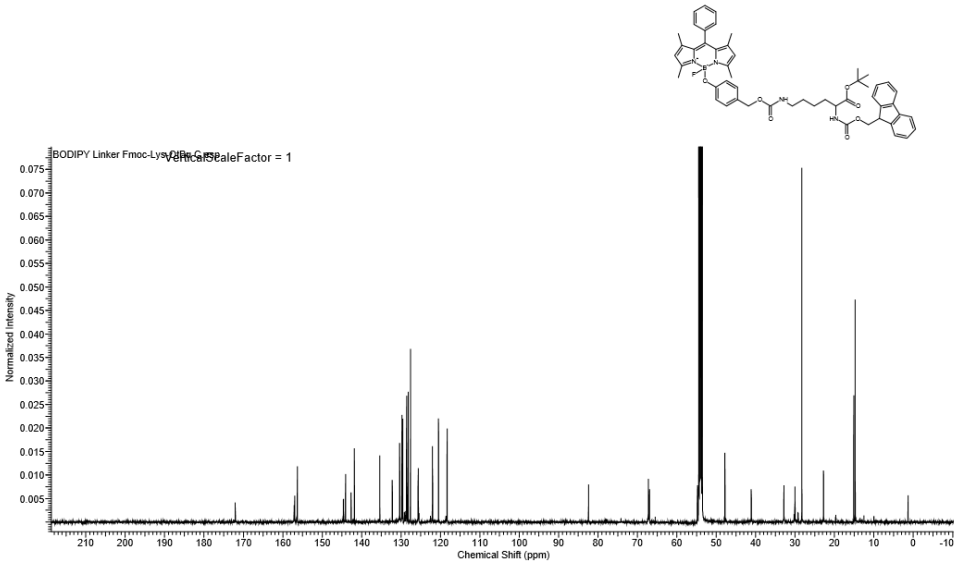


Compound 243

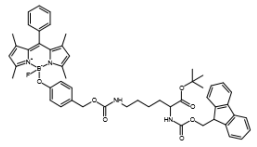
Acquisition Time (sec)	3.1719	*Comment*	Instrument AVC500 Group SJC 0621 M. Savage 10/3/15	*Date*	10 Mar 2015 11:44:00
Date Stamp	10 Mar 2015 11:44:00			*File Name*	D:\Gnomeeee\NMR\BODIPY Stuff\BODIPY Linker Fmoc-Lys-OtBu\1\PDATA\1\1r
Frequency (MHz)	500.30	*Nucleus*	1H	*Number of Transients*	16
Origin	avc500	*Original Points Count*	32768	*Owner*	nmr-user
Points Count	65536	*Pulse Sequence*	zg30	*Receiver Gain*	3.20
SW(cyclical) (Hz)	10330.58	*Solvent*	DICHLOROMETHANE-d2	*Spectrum Offset (Hz)*	3068.9966
Spectrum Type	STANDARD	*Sweep Width (Hz)*	10330.42	*Temperature (degree C)*	24.970

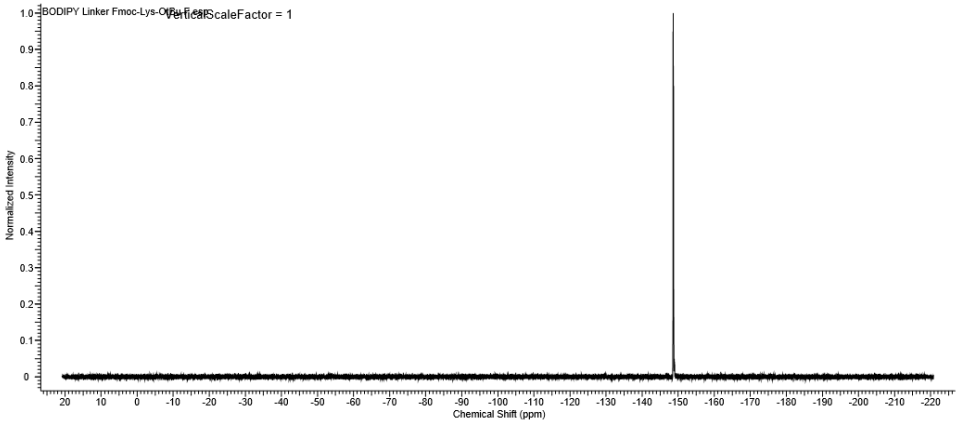


Acquisition Time (sec)	1.0486	*Comment*	Instrument AVC500 Group SJC 0621 M. Savage 10/3/15	*Date*	10 Mar 2015 12:26:40
Date Stamp	10 Mar 2015 12:26:40			*File Name*	D:\Gnomeeee\NMR\BODIPY Stuff\BODIPY Linker Fmoc-Lys-OtBu\4\PDATA\1\1r
Frequency (MHz)	125.80	*Nucleus*	13C	*Number of Transients*	2048
Origin	avc500	*Original Points Count*	32768	*Owner*	nmr-user
Points Count	32768	*Pulse Sequence*	zgpg30	*Receiver Gain*	912.00
SW(cyclical) (Hz)	31250.00	*Solvent*	DICHLOROMETHANE-d2	*Spectrum Offset (Hz)*	12651.1729
Spectrum Type	STANDARD	*Sweep Width (Hz)*	31249.05	*Temperature (degree C)*	24.970



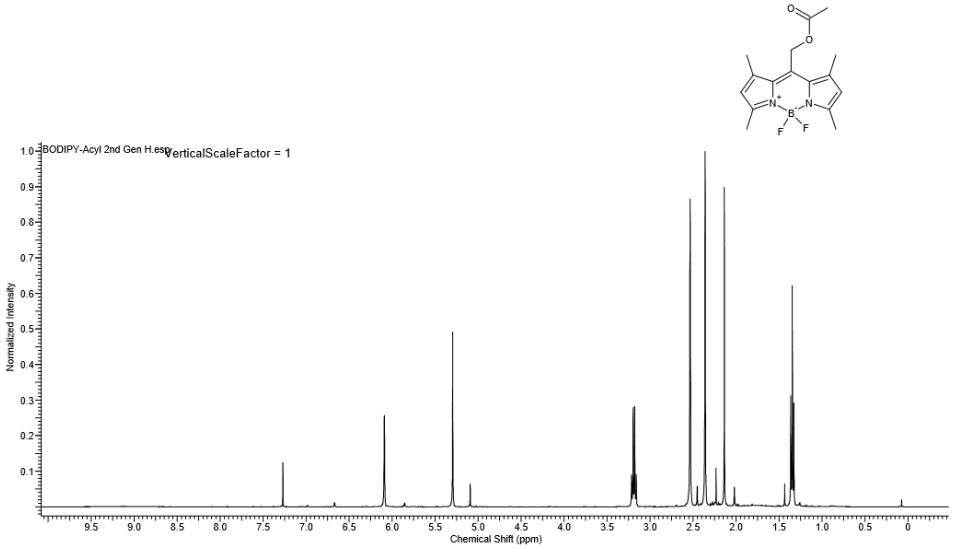
Acquisition Time (sec)	0.5767	*Comment*	Instrument AVB500 M.SAVAGE 40621 10/3/15			*Date*	10 Mar 2015 15:10:56
Date Stamp	10 Mar 2015 15:10:56			*File Name*	D:\Gnomeeee\NMR\BODIPY Stuff\BODIPY Linker Fmoc-Lys-OtBu\19F\1\PDATA\1\1r		
Frequency (MHz)	470.45	*Nucleus*	19F	*Number of Transients*	64	*Origin*	avb500
Original Points Count	65536	*Owner*	nmr-user	*Points Count*	65536	*Pulse Sequence*	zgfhigqn.tfi
Receiver Gain	2050.00	*SW(cyclical) (Hz)*	113636.37	*Solvent*	DICHLOROMETHANE-d2		
Spectrum Offset (Hz)	-47044.7344	*Spectrum Type*	STANDARD	*Sweep Width (Hz)*	113634.63	*Temperature (degree C)*	27.000



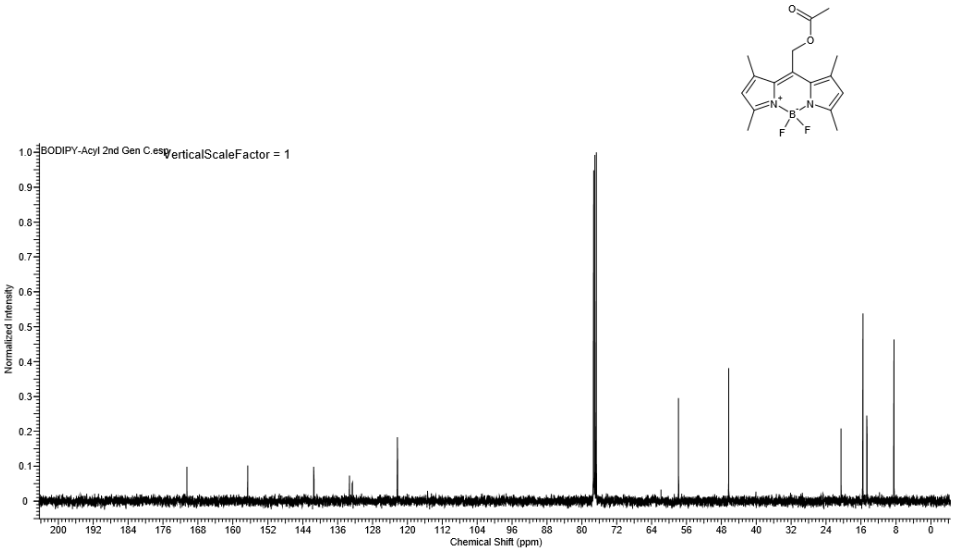


Compound 249

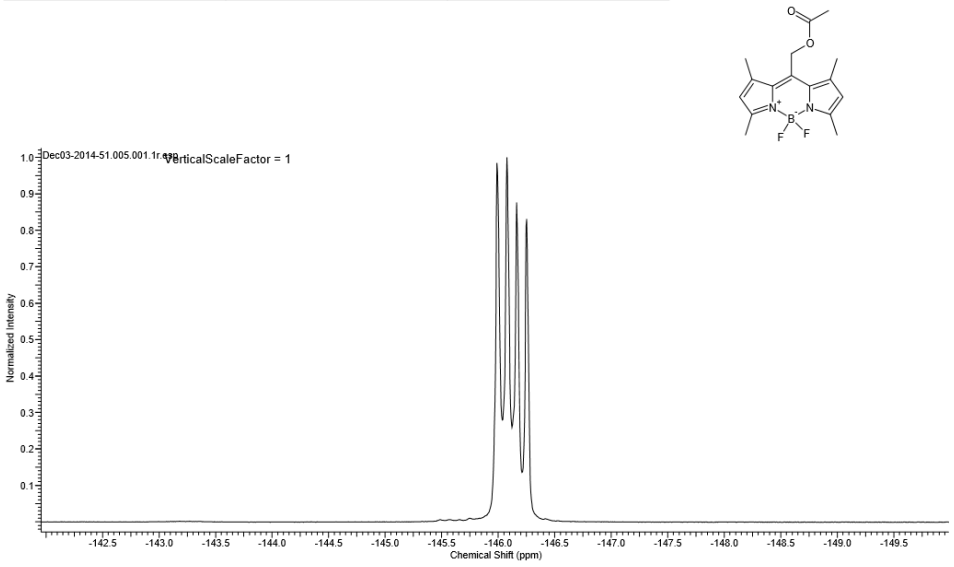
Acquisition Time (sec)	4.0894	*Comment*	Instrument AVF400 Chemist MLS Group SJC MLS08104: BODIPY 2nd Gen Acyl h1acq.crl CDCl3 {C:\NMR} sjcgrp 8				
Date	08 Dec 2014 09:12:32			*Date Stamp*	08 Dec 2014 09:12:32		
File Name	F:\NMR\BODIPY Stuff\BODIPY Acyl 2nd Gen\Dec08-2014-8\1\pdata\1\1r					*Frequency (MHz)*	400.25
Nucleus	1H	*Number of Transients*	16	*Origin*	avf400	*Original Points Count*	32768
Owner	nmr-user	*Points Count*	32768	*Pulse Sequence*	zg60	*Receiver Gain*	93.00
SW(cyclical) (Hz)	8012.82	*Solvent*	CHLOROFORM-d	*Spectrum Offset (Hz)*	2393.9775	*Spectrum Type*	STANDARD
Sweep Width (Hz)	8012.58	*Temperature (degree C)*	22.315				



Acquisition Time (sec)	0.6291	*Comment*	Instrument AVF400 Chemist MLS Group SJC MLS08104: BODIPY 2nd Gen Acyl c13acq.crl CDCl3 {C:\NMR} sjcgrp 8				
Date	08 Dec 2014 09:38:08			*Date Stamp*	08 Dec 2014 09:38:08		
File Name	F:\NMR\BODIPY Stuff\BODIPY Acyl 2nd Gen\Dec08-2014-8\4\pdata\1\1r			*Frequency (MHz)*	100.64	*Nucleus*	13C
Number of Transients	256	*Origin*	avf400	*Original Points Count*	16384	*Owner*	nmr-user
Points Count	32768	*Pulse Sequence*	zgpg30	*Receiver Gain*	205.43	*SW(cyclical) (Hz)*	26041.67
Solvent	CHLOROFORM-d	*Spectrum Offset (Hz)*	10060.1807	*Spectrum Type*	STANDARD	*Sweep Width (Hz)*	26040.87
Temperature (degree C)	23.480						

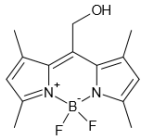


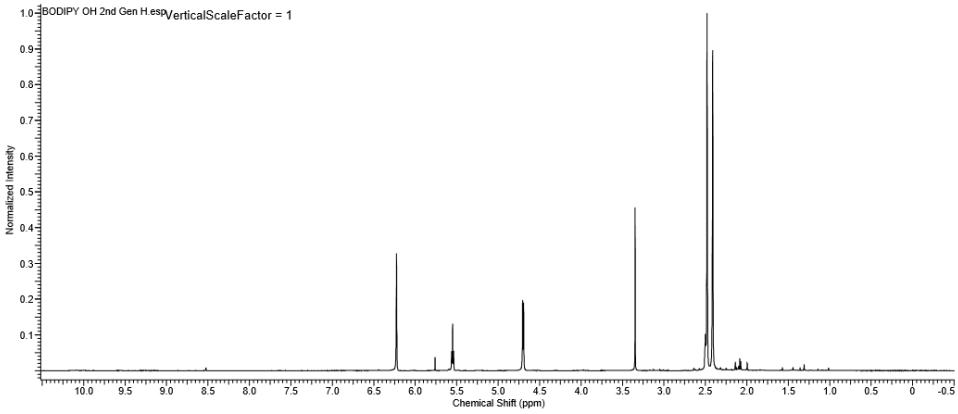
Acquisition Time (sec)	0.5767	*Comment*	Instrument AVF400 Chemist MLS Group SJC MLS08100: BODIPY Acyl 2nd Gen f19dec2_256.crl CDCl3 (C:\NMR) sjcgrp 51				
Date	03 Dec 2014 14:56:00	*Date Stamp*	03 Dec 2014 14:56:00	*File Name*	F:\NMR\BODIPY Stuff\BODIPY Acyl 2nd Gen\Dec03-2014-51\5\pdata\1\1r		
Frequency (MHz)	376.61	*Nucleus*	19F	*Number of Transients*	256	*Origin*	avf400
Original Points Count	65536	*Owner*	nmr-user	*Points Count*	65536	*Pulse Sequence*	zgfhigqn
Receiver Gain	205.43	*SW(cyclical) (Hz)*	113636.37	*Solvent*	CHLOROFORM-d	*Spectrum Offset (Hz)*	-18830.6113
Spectrum Type	STANDARD	*Sweep Width (Hz)*	113634.63	*Temperature (degree C)*	21.939		



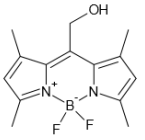
Compound 250

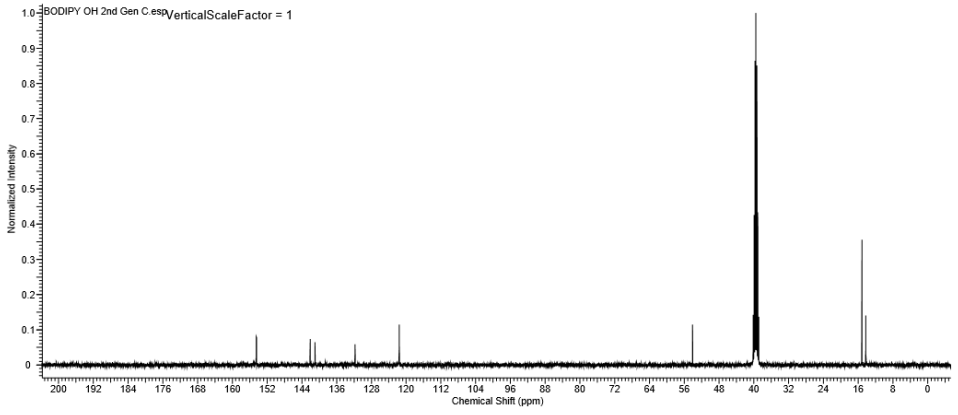
Acquisition Time (sec)	3.2768	*Comment*	Instrument AVG400 Group SJC Chemist MLS MLS08122: BODIPY 2nd Gen OH h1acq.crl DMSO (C:\NMR) sjcgrp 28				
Date	08 Jan 2015 09:31:44			*Date Stamp*	08 Jan 2015 09:31:44		
File Name	F:\NMR\BODIPY Stuff\BODIPY OH 2nd Gen\Jan08-2015-28-\1\pdata\1\1r					*Frequency (MHz)*	400.20
Nucleus	1H	*Number of Transients*	16	*Origin*	avg400	*Original Points Count*	32768
Owner	nmr-user	*Points Count*	65536	*Pulse Sequence*	zg30	*Receiver Gain*	202.31
SW(cyclical) (Hz)	10000.00	*Solvent*	DMSO-d6	*Spectrum Offset (Hz)*	2463.4365	*Spectrum Type*	STANDARD
Sweep Width (Hz)	9999.85	*Temperature (degree C)*	21.200				



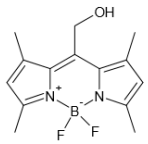


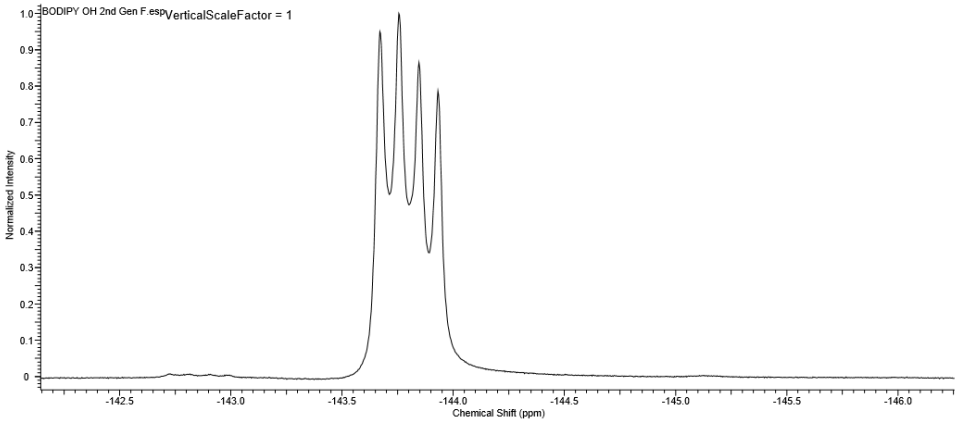
Acquisition Time (sec)	1.3631	*Comment*	Instrument AVG400 Group SJC Chemist MLS MLS08122: BODIPY 2nd Gen OH c13acq.crl DMSO (C:\NMR) sjcgrp 28				
Date	08 Jan 2015 21:34:56			*Date Stamp*	08 Jan 2015 21:34:56		
File Name	F:\NMR\BODIPY Stuff\BODIPY OH 2nd Gen\Jan08-2015-28-\3\pdata\1\1r					*Frequency (MHz)*	100.63
Nucleus	13C	*Number of Transients*	256	*Origin*	avg400	*Original Points Count*	32768
Owner	nmr-user	*Points Count*	32768	*Pulse Sequence*	zgpg30	*Receiver Gain*	2050.00
SW(cyclical) (Hz)	24038.46	*Solvent*	DMSO-d6	*Spectrum Offset (Hz)*	10015.9648	*Spectrum Type*	STANDARD
Sweep Width (Hz)	24037.73	*Temperature (degree C)*	21.800				





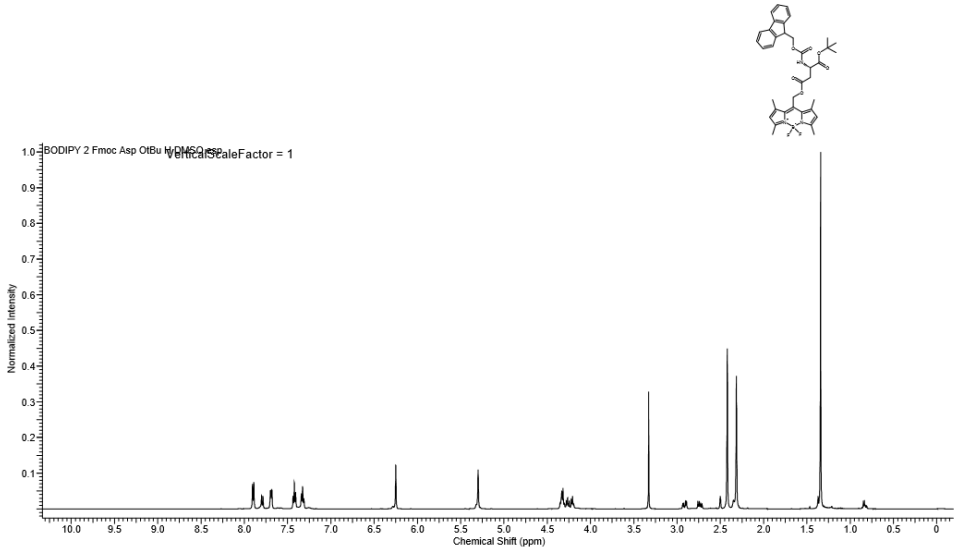
Acquisition Time (sec)	0.8738	*Comment*	Instrument AVF400 Chemist MLS Group SJC MLS08140: BODIPY-OH 2nd Gen f19acq_256.crl DMSO {C:\NMR} sicgrp 16				
Date	16 Jan 2015 19:35:28	*Date Stamp*	16 Jan 2015 19:35:28	*File Name*	F:\NMR\BODIPY Stuff\BODIPY OH 2nd Gen\Jan16-2015-16-l6\pdata\1\1r		
Frequency (MHz)	376.61	*Nucleus*	19F	*Number of Transients*	256	*Origin*	avf400
Original Points Count	65536	*Owner*	nmr-user	*Points Count*	65536	*Pulse Sequence*	zgflqn
Receiver Gain	205.43	*SW(cyclical) (Hz)*	75000.00	*Solvent*	DMSO-d6	*Spectrum Offset (Hz)*	-56491.6914
Spectrum Type	STANDARD	*Sweep Width (Hz)*	74998.86	*Temperature (degree C)*	23.661		



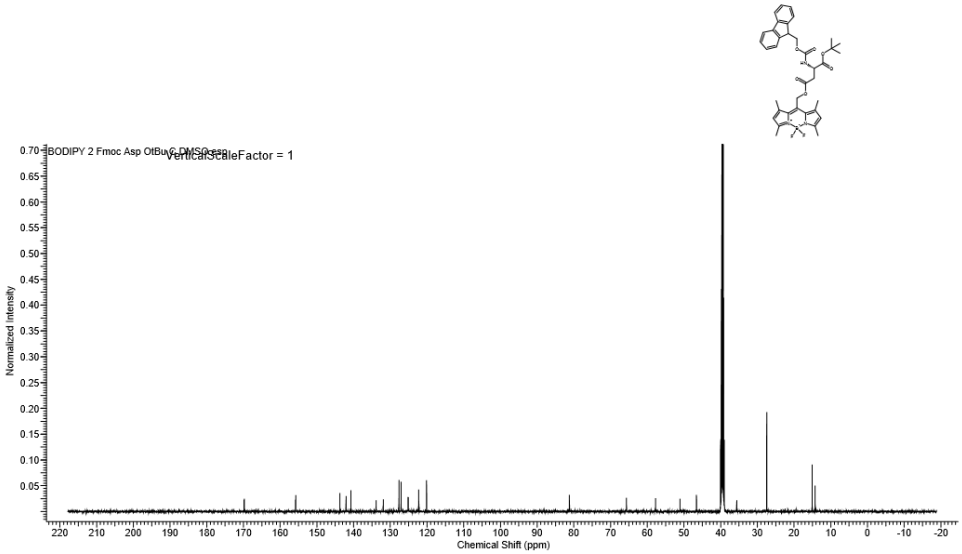


Compound 251

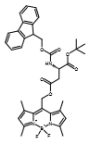
Acquisition Time (sec)	3.2768	*Comment*	Group NMR Service Instrument AVX500 AVX500 1H M SAVAGE SJC GROUP 41125 6/5/15				
Date	06 May 2015 14:56:16			*Date Stamp*	06 May 2015 14:56:16		
File Name	D:\Gnomeeee\NMR\BODIPY Stuff\BODIPY 2\BODIPY 2nd Gen Fmoc-Asp-OtBu\ms11250605\1\PDATA\1\1r					*Frequency (MHz)*	500.13
Nucleus	1H	*Number of Transients*	16	*Origin*	avx500	*Original Points Count*	32768
Owner	nmr-user	*Points Count*	65536	*Pulse Sequence*	zg60	*Receiver Gain*	30.91
SW(cyclical) (Hz)	10000.00	*Solvent*	DMSO-d6	*Spectrum Offset (Hz)*	2496.4341	*Spectrum Type*	STANDARD
Sweep Width (Hz)	9999.85	*Temperature (degree C)*	25.000				

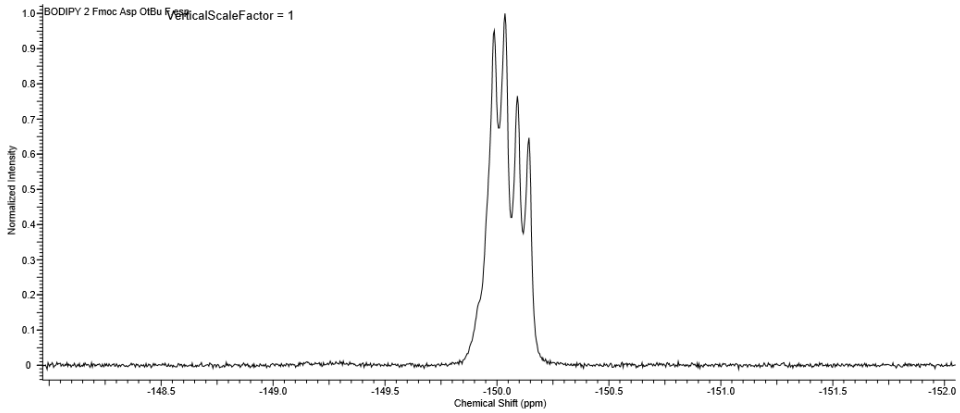


Acquisition Time (sec)	1.1010	*Comment*	Group SJC Instrument AVX500 AVX500 1H M SAVAGE 4115 DMSO-d6 6/5/15				
Date	06 May 2015 14:37:04			*Date Stamp*	06 May 2015 14:37:04		
File Name	D:\Gnomeeee\NMR\BODIPY Stuff\BODIPY 2\BODIPY 2nd Gen Fmoc-Asp-OtBu\ms11250605\4\PDATA\1\1r					*Frequency (MHz)*	125.76
Nucleus	13C	*Number of Transients*	1890	*Origin*	avx500	*Original Points Count*	32768
Owner	nmr-user	*Points Count*	32768	*Pulse Sequence*	zgpg30	*Receiver Gain*	191.37
SW(cyclical) (Hz)	29761.90	*Solvent*	DMSO-d6	*Spectrum Offset (Hz)*	12514.9785	*Spectrum Type*	STANDARD
Sweep Width (Hz)	29761.00	*Temperature (degree C)*	24.998				



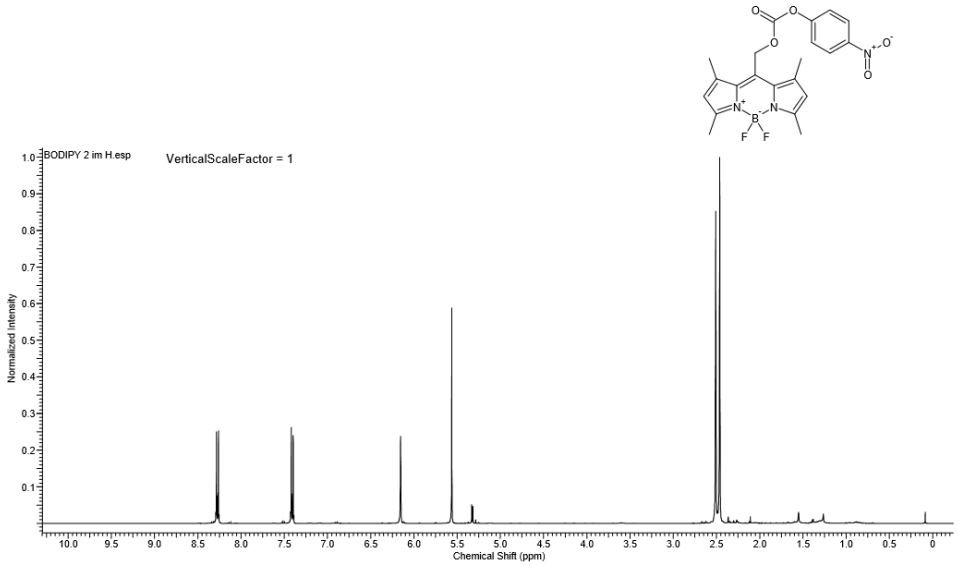
Acquisition Time (sec)	0.5767	*Comment*	Instrument AVB500 M SAVAGE 41026 22/4/15			*Date*	22 Apr 2015 11:27:12
Date Stamp	22 Apr 2015 11:27:12						
File Name	D:\Gnomeeee\NMR\BODIPY Stuff\BODIPY 2\BODIPY 2nd Gen Fmoc-Asp-OtBu\H & C\19F\1\PDATA\1\1r					*Frequency (MHz)*	470.45
Nucleus	19F	*Number of Transients*	16	*Origin*	avb500	*Original Points Count*	65536
Owner	nmr-user	*Points Count*	65536	*Pulse Sequence*	zgfhigqn.tfi	*Receiver Gain*	2050.00
SW(cyclical) (Hz)	113636.37	*Solvent*	METHANOL-d4	*Spectrum Offset (Hz)*	-47044.7344	*Spectrum Type*	STANDARD
Sweep Width (Hz)	113634.63	*Temperature (degree C)*	25.000				



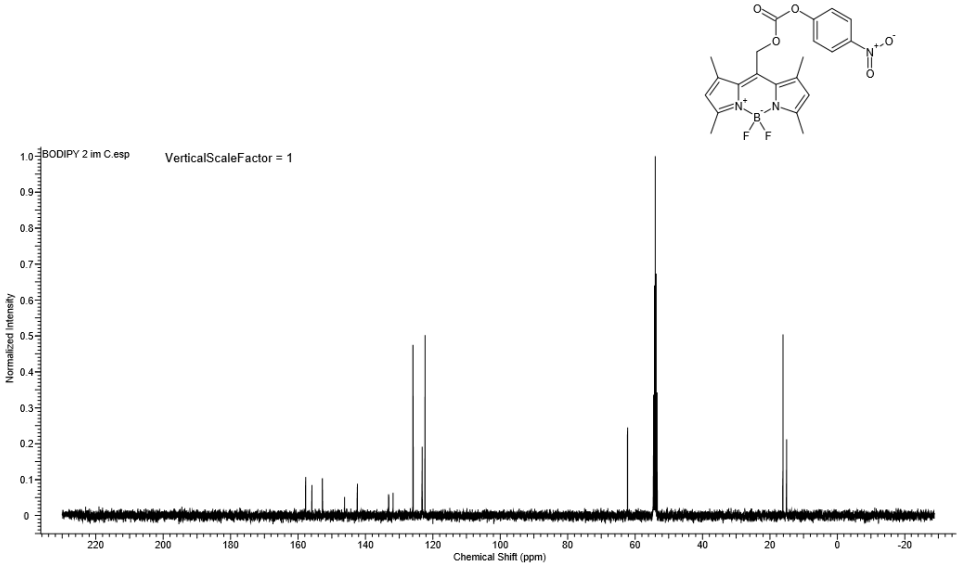


Compound 255

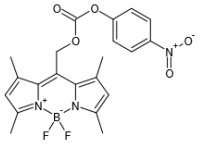
Acquisition Time (sec)	4.0894	*Comment*	Instrument AVF400 Chemist MLS Group SJC MLS08202: BODIPY Gen 2 i/m h1acq.crl CD2Cl2 {C:\NMR} sjcgrp 8				
Date	12 Feb 2015 20:03:12	*Date Stamp*	12 Feb 2015 20:03:12	*File Name*	D:\Gnomeeee\NMR\BODIPY Stuff\BODIPY 2 im\Feb12-2015-8-\1\PDATA\1\1r		
Frequency (MHz)	400.25	*Nucleus*	1H	*Number of Transients*	16	*Origin*	avf400
Original Points Count	32768	*Owner*	nmr-user	*Points Count*	32768	*Pulse Sequence*	zg60
Receiver Gain	93.00	*SW(cyclical) (Hz)*	8012.82	*Solvent*	DICHLOROMETHANE-d2		
Spectrum Offset (Hz)	2384.0103	*Spectrum Type*	STANDARD	*Sweep Width (Hz)*	8012.58	*Temperature (degree C)*	22.865

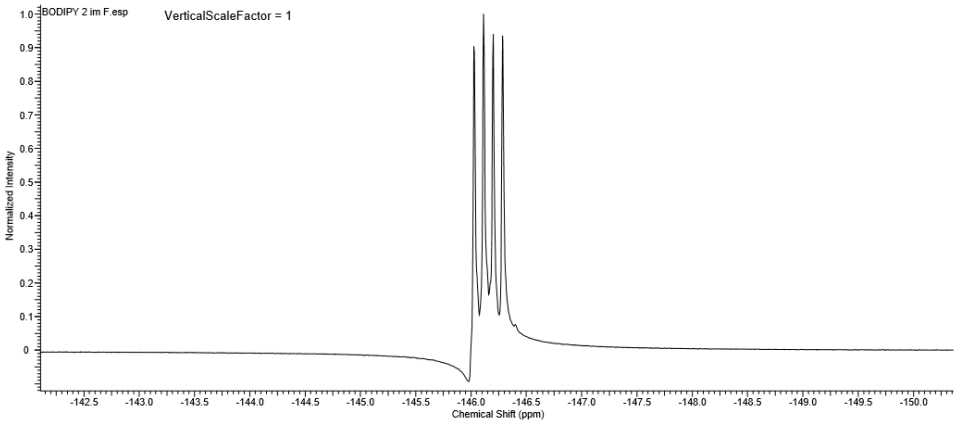


Acquisition Time (sec)	0.6291	*Comment*	Instrument AVF400 Chemist MLS Group SJC MLS08202: BODIPY Gen 2 i/m c13acq.crl CD2Cl2 {C:\NMR} sjcgrp 8				
Date	12 Feb 2015 20:11:44	*Date Stamp*	12 Feb 2015 20:11:44	*File Name*	D:\Gnomeeee\NMR\BODIPY Stuff\BODIPY 2 im\Feb12-2015-8-\2\PDATA\1\1r		
Frequency (MHz)	100.64	*Nucleus*	13C	*Number of Transients*	256	*Origin*	avf400
Original Points Count	16384	*Owner*	nmr-user	*Points Count*	32768	*Pulse Sequence*	zgpg30
Receiver Gain	205.43	*SW(cyclical) (Hz)*	26041.67	*Solvent*	DICHLOROMETHANE-d2		
Spectrum Offset (Hz)	10121.6309	*Spectrum Type*	STANDARD	*Sweep Width (Hz)*	26040.87	*Temperature (degree C)*	23.868



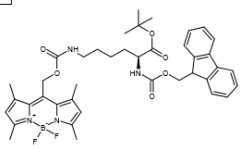
Acquisition Time (sec)	0.5767	*Comment*	Instrument AVF400 Chemist MLS Group SJC MLS08202: BODIPY Gen 2 i/m f19acq2_256.crl CD2Cl2 {C:\NMR} sjcgrp 8				
Date	12 Feb 2015 20:30:56	*Date Stamp*	12 Feb 2015 20:30:56	*File Name*	D:\Gnomeeee\NMR\BODIPY Stuff\BODIPY 2 im\Feb12-2015-8-1\5\PDATA\1\1r		
Frequency (MHz)	376.61	*Nucleus*	19F	*Number of Transients*	256	*Origin*	avf400
Original Points Count	65536	*Owner*	nmr-user	*Points Count*	65536	*Pulse Sequence*	zgflqn
Receiver Gain	205.43	*SW(cyclical) (Hz)*	113636.37	*Solvent*	DICHLOROMETHANE-d2		
Spectrum Offset (Hz)	-18830.5742	*Spectrum Type*	STANDARD	*Sweep Width (Hz)*	113634.63	*Temperature (degree C)*	22.837

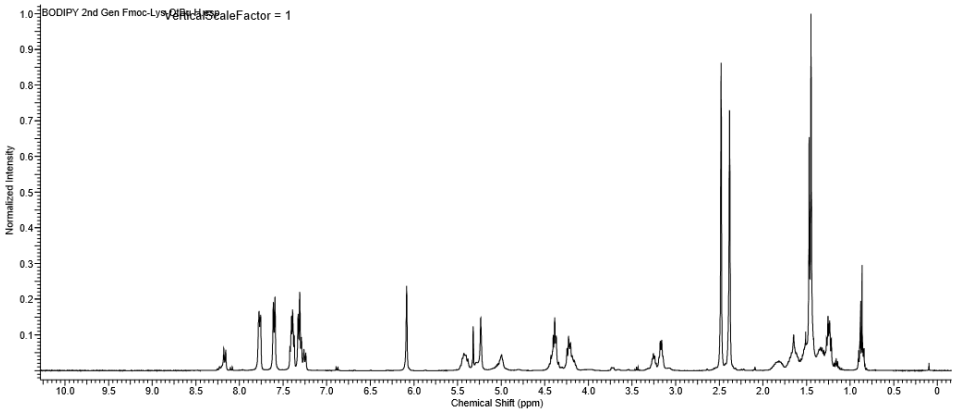




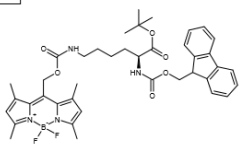
Compound 253

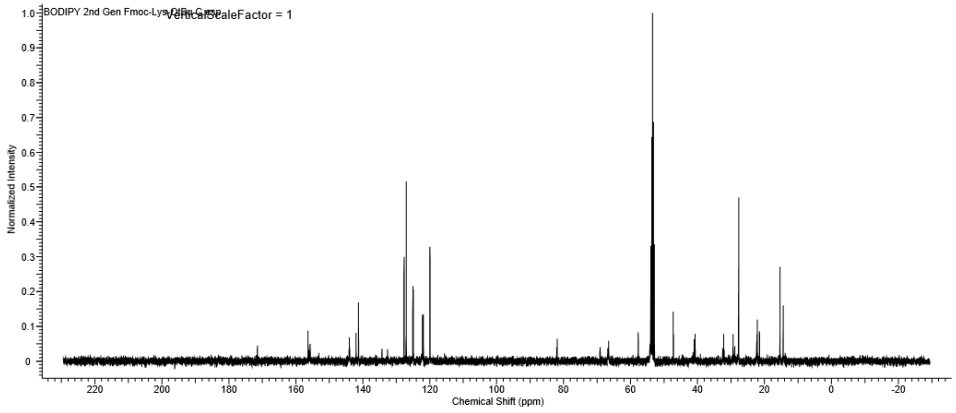
Acquisition Time (sec)	4.0894	*Comment*	Instrument AVF400 Chemist MLS Group SJC MLS08206: BODIPY Gen 2 Fmoc-Lys-OtBu h1acq.crl CD2Cl2 {C:\NMR} sjcgrp 3				
Date	15 Feb 2015 16:19:12	*Date Stamp*	15 Feb 2015 16:19:12				
File Name	D:\Gnomeeee\NMR\BODIPY Stuff\BODIPY 2\BODIPY 2nd Gen Fmoc-Lys-OtBu\1\PDATA\1\1r					*Frequency (MHz)*	400.25
Nucleus	1H	*Number of Transients*	16	*Origin*	avf400	*Original Points Count*	32768
Owner	nmr-user	*Points Count*	32768	*Pulse Sequence*	zg60	*Receiver Gain*	33.03
SW(cyclical) (Hz)	8012.82	*Solvent*	DICHLOROMETHANE-d2			*Spectrum Offset (Hz)*	2384.0103
Spectrum Type	STANDARD	*Sweep Width (Hz)*	8012.58	*Temperature (degree C)*	22.842		



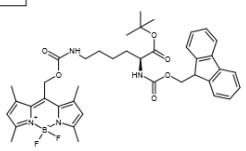


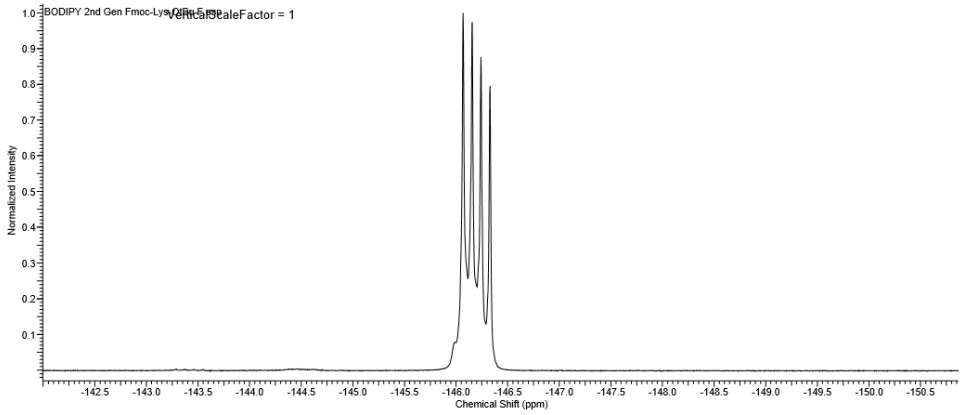
Acquisition Time (sec)	0.6291	*Comment*	Instrument AVF400 Chemist MLS Group SJC MLS08206: BODIPY Gen 2 Fmoc-Lys-OtBu c13acq.crl CD2Cl2 {C:\NMR} sjcgrp 3				
Date	15 Feb 2015 16:44:48	*Date Stamp*	15 Feb 2015 16:44:48				
File Name	D:\Gnomeeee\NMR\BODIPY Stuff\BODIPY 2\BODIPY 2nd Gen Fmoc-Lys-OtBu\4\PDATA\1\1r					*Frequency (MHz)*	100.64
Nucleus	13C	*Number of Transients*	256	*Origin*	avf400	*Original Points Count*	16384
Owner	nmr-user	*Points Count*	32768	*Pulse Sequence*	zgpg30	*Receiver Gain*	205.43
SW(cyclical) (Hz)	26041.67	*Solvent*	DICHLOROMETHANE-d2			*Spectrum Offset (Hz)*	10064.2930
Spectrum Type	STANDARD	*Sweep Width (Hz)*	26040.87	*Temperature (degree C)*	24.078		





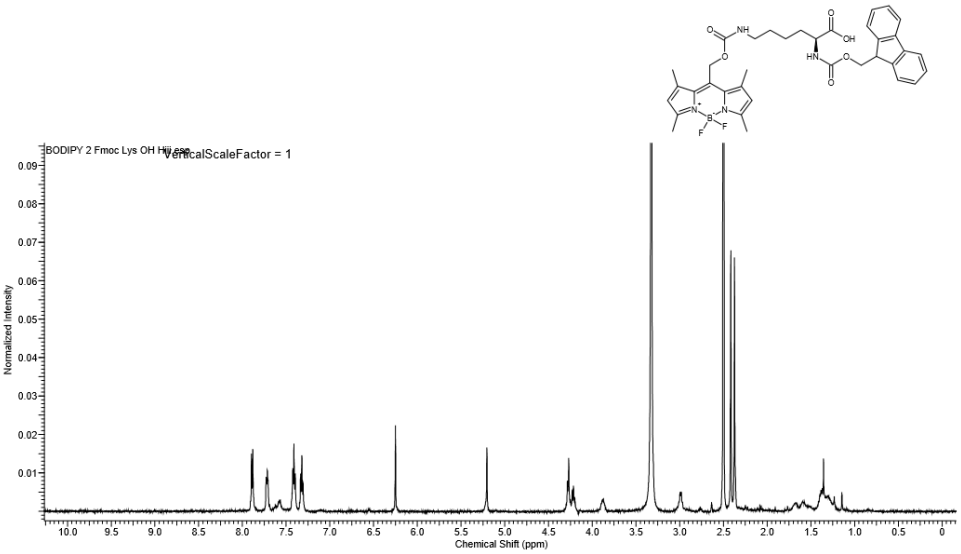
Acquisition Time (sec)	0.8738	*Comment*	Instrument AVF400 Chemist MLS Group SJC MLS08206: BODIPY Gen 2 Fmoc-Lys-OtBu f19dec_256.crl CD2Cl2 {C:\NMR} sjcgrp 3				
Date	15 Feb 2015 16:57:36	*Date Stamp*	15 Feb 2015 16:57:36				
File Name	D:\Gnomeeee\NMR\BODIPY Stuff\BODIPY 2\BODIPY 2nd Gen Fmoc-Lys-OtBu\6\PDATA\1\1r					*Frequency (MHz)*	376.61
Nucleus	19F	*Number of Transients*	256	*Origin*	avf400	*Original Points Count*	65536
Owner	nmr-user	*Points Count*	65536	*Pulse Sequence*	zgfhigqn	*Receiver Gain*	205.43
SW(cyclical) (Hz)	75000.00	*Solvent*	DICHLOROMETHANE-d2			*Spectrum Offset (Hz)*	-56491.6992
Spectrum Type	STANDARD	*Sweep Width (Hz)*	74998.86	*Temperature (degree C)*	23.489		



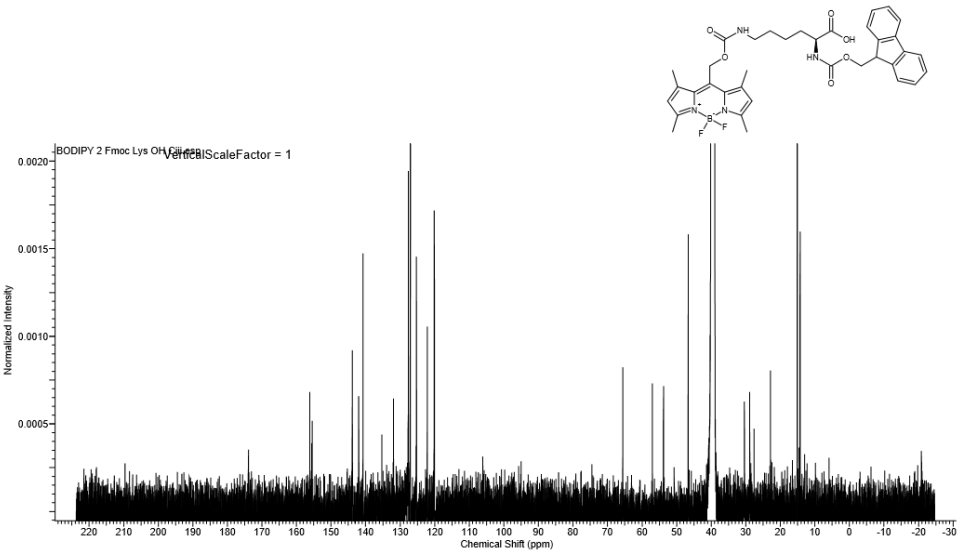


Compound 256

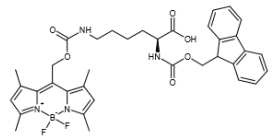
Acquisition Time (sec)	3.1719	*Comment*	Instrument AVC500 Group SJC 1126 M. Savage 11/5/15			*Date*	11 May 2015 12:31:12
Date Stamp	11 May 2015 12:31:12						
File Name	D:\Gnomeeee\NMR\BODIPY Stuff\BODIPY 2\BODIPY 2nd Gen Fmoc-Lys-OH\ms112611105\1\PDATA\1\1r					*Frequency (MHz)*	500.30
Nucleus	1H	*Number of Transients*	16	*Origin*	avc500	*Original Points Count*	32768
Owner	nmr-user	*Points Count*	65536	*Pulse Sequence*	zg30	*Receiver Gain*	2.00
SW(cyclical) (Hz)	10330.58	*Solvent*	DMSO-d6	*Spectrum Offset (Hz)*	3084.4055	*Spectrum Type*	STANDARD
Sweep Width (Hz)	10330.42	*Temperature (degree C)*	24.970				

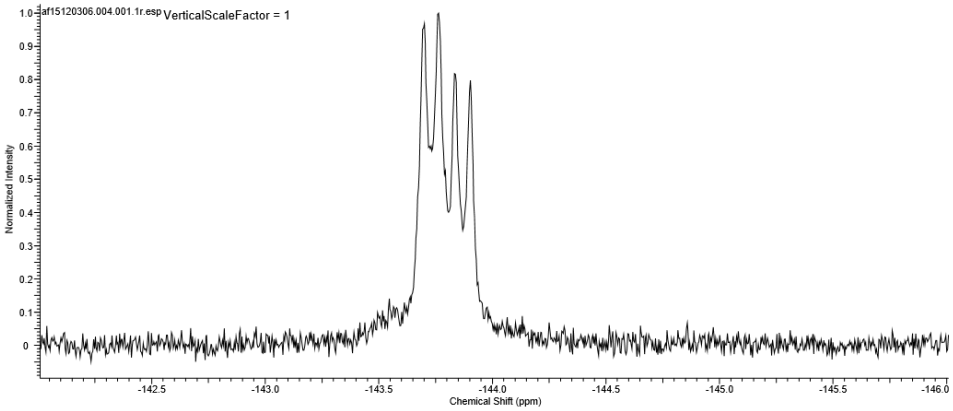


Acquisition Time (sec)	1.0486	*Comment*	Instrument AVC500 Group SJC 1126 M. Savage 11/5/15			*Date*	11 May 2015 13:18:08
Date Stamp	11 May 2015 13:18:08						
File Name	D:\Gnomeeee\NMR\BODIPY Stuff\BODIPY 2\BODIPY 2nd Gen Fmoc-Lys-OH\ms112611105\4\PDATA\1\1r					*Frequency (MHz)*	125.80
Nucleus	13C	*Number of Transients*	2048	*Origin*	avc500	*Original Points Count*	32768
Owner	nmr-user	*Points Count*	32768	*Pulse Sequence*	zgpg30	*Receiver Gain*	912.00
SW(cyclical) (Hz)	31250.00	*Solvent*	DMSO-d6	*Spectrum Offset (Hz)*	12520.1416	*Spectrum Type*	STANDARD
Sweep Width (Hz)	31249.05	*Temperature (degree C)*	24.970				



Acquisition Time (sec)	0.5767	*Comment*	Instrument AVB500 ALISTAIR FARLEY 41512 3/6/15			*Date*	03 Jun 2015 10:10:24
Date Stamp	03 Jun 2015 10:10:24						
File Name	D:\Gnomeeee\NMR\BODIPY Stuff\BODIPY 2\BODIPY 2nd Gen Fmoc-Lys-OH\af15120306\4\PDATA\1\1r					*Frequency (MHz)*	470.45
Nucleus	19F	*Number of Transients*	256	*Origin*	avb500	*Original Points Count*	65536
Owner	nmr-user	*Points Count*	65536	*Pulse Sequence*	zgfhigqn.tfi	*Receiver Gain*	2050.00
SW(cyclical) (Hz)	113636.37	*Solvent*	DMSO-d6	*Spectrum Offset (Hz)*	-47044.7344	*Spectrum Type*	STANDARD
Sweep Width (Hz)	113634.63	*Temperature (degree C)*	25.000				

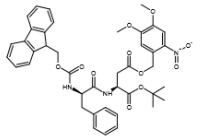


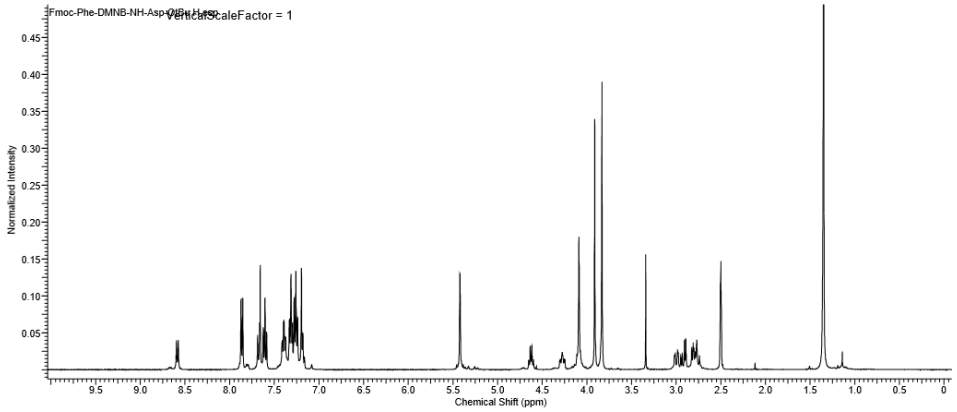


A.7 Caged Peptides

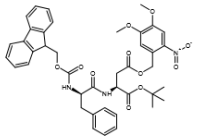
Compound 278

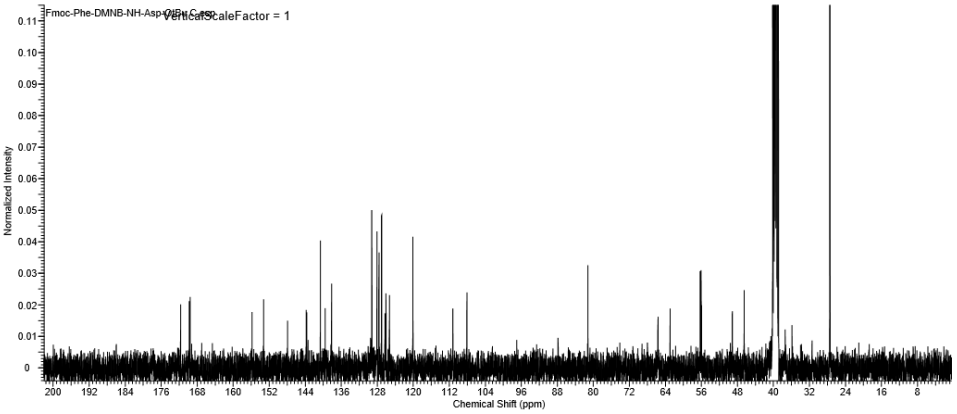
Acquisition Time (sec)	3.2768	*Comment*	Instrument AVG400 Group SJC Chemist MLS MLS07082: Fmoc-Phe-DMNB-Asp-OtBu h1acq.crl DMSO (C:\NMR) sjcgrp 22				
Date	07 Mar 2015 16:17:04	*Date Stamp*	07 Mar 2015 16:17:04				
File Name	D:\Gnomeeee\NMR\Sequential Tripeptide\Fmoc-Phe-DMNB-NH-Asp-OtBu\Mar07-2015-22-\1\PDATA\1\1r					*Frequency (MHz)*	400.20
Nucleus	1H	*Number of Transients*	16	*Origin*	avg400	*Original Points Count*	32768
Owner	nmr-user	*Points Count*	65536	*Pulse Sequence*	zg30	*Receiver Gain*	221.01
SW(cyclical) (Hz)	10000.00	*Solvent*	DMSO-d6	*Spectrum Offset (Hz)*	2463.2839	*Spectrum Type*	STANDARD
Sweep Width (Hz)	9999.85	*Temperature (degree C)*	21.200				





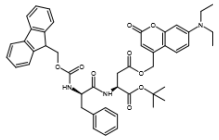
Acquisition Time (sec)	1.3631	*Comment*	Instrument AVG400 Group SJC Chemist MLS MLS07082: Fmoc-Phe-DMNB-Asp-OtBu c13acq.crl DMSO (C:\NMR) sjcgrp 22				
Date	07 Mar 2015 17:12:32	*Date Stamp*	07 Mar 2015 17:12:32				
File Name	D:\Gnomeeee\NMR\Sequential Tripeptide\Fmoc-Phe-DMNB-NH-Asp-OtBu\Mar07-2015-22-\3\PDATA\1\1r					*Frequency (MHz)*	100.63
Nucleus	13C	*Number of Transients*	256	*Origin*	avg400	*Original Points Count*	32768
Owner	nmr-user	*Points Count*	32768	*Pulse Sequence*	zgpg30	*Receiver Gain*	2050.00
SW(cyclical) (Hz)	24038.46	*Solvent*	DMSO-d6	*Spectrum Offset (Hz)*	10015.2314	*Spectrum Type*	STANDARD
Sweep Width (Hz)	24037.73	*Temperature (degree C)*	21.000				

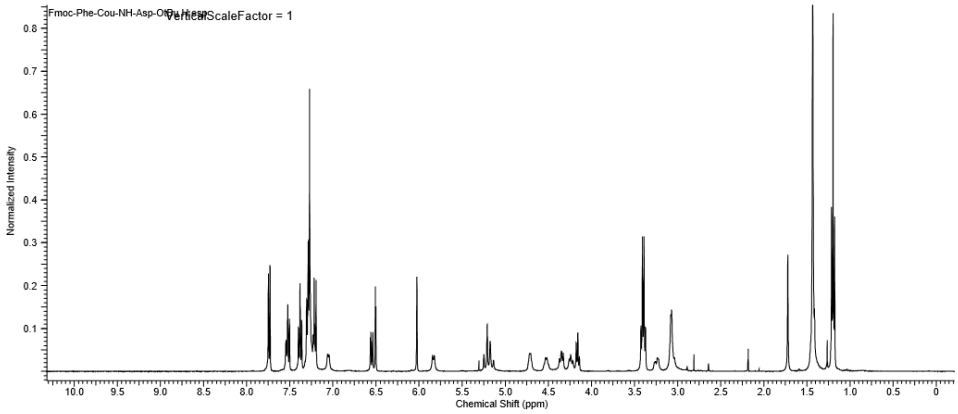




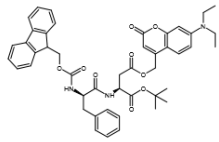
Compound 279

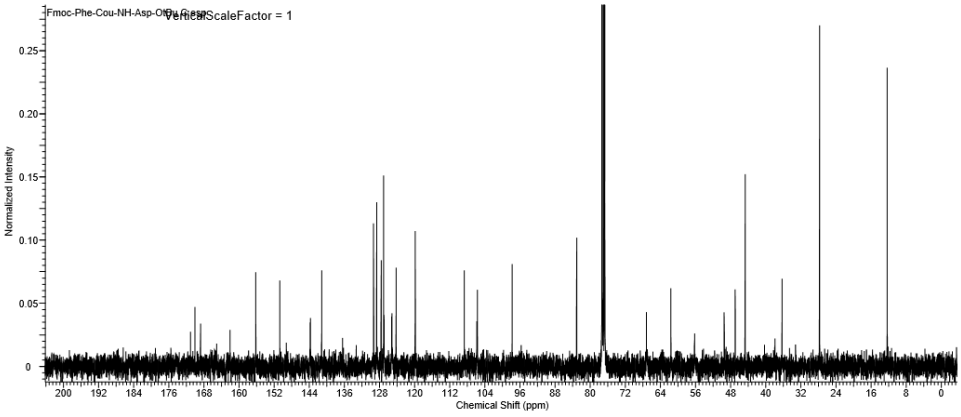
Acquisition Time (sec)	3.2768	*Comment*	Instrument AVG400 Group SJC Chemist MLS MLS07054: Dipetide (Cou Asp - Phe) h1acq.crl CDCl3 {C:\NMR} sjcgrp 1				
Date	13 Sep 2014 13:26:40	*Date Stamp*	13 Sep 2014 13:26:40				
File Name	D:\Gnomeeee\NMR\Sequential Tripeptide\Fmoc-Phe-Cou-NH-Asp-OtBu\Sep13-2014-1\1\pdata\1\1r					*Frequency (MHz)*	400.20
Nucleus	1H	*Number of Transients*	16	*Origin*	avg400	*Original Points Count*	32768
Owner	nmr-user	*Points Count*	65536	*Pulse Sequence*	zg30	*Receiver Gain*	202.31
SW(cyclical) (Hz)	10000.00	*Solvent*	CHLOROFORM-d	*Spectrum Offset (Hz)*	2461.5322	*Spectrum Type*	STANDARD
Sweep Width (Hz)	9999.85	*Temperature (degree C)*	20.600				





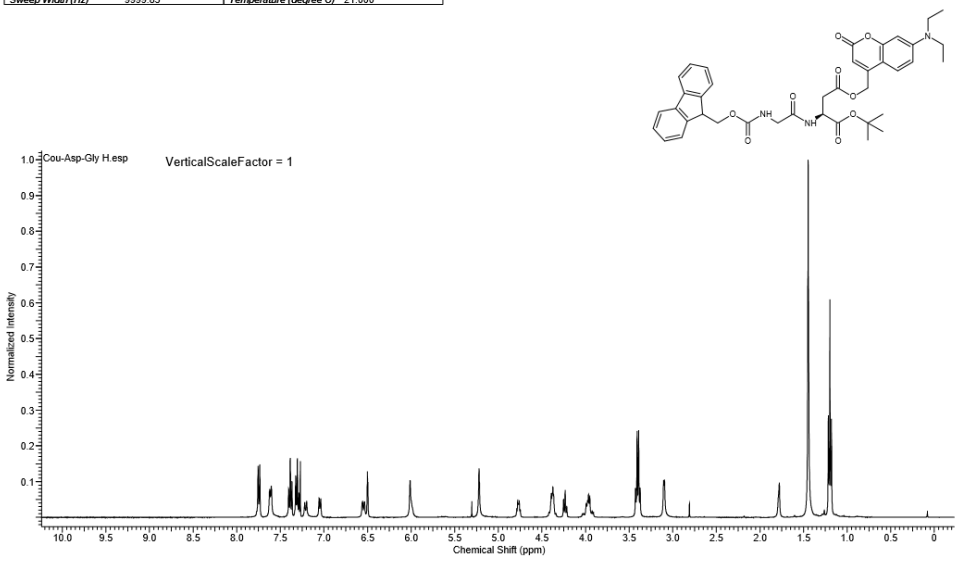
Acquisition Time (sec)	1.3631	*Comment*	Instrument AVG400 Group SJC Chemist MLS MLS07054: Dipetide (Cou Asp - Phe) c13acq.crl CDCl3 {C:\NMR} sjcgrp 1				
Date	13 Sep 2014 13:48:00	*Date Stamp*	13 Sep 2014 13:48:00				
File Name	D:\Gnomeeee\NMR\Sequential Tripeptide\Fmoc-Phe-Cou-NH-Asp-OtBu\Sep13-2014-1\3\PDATA\1\1r					*Frequency (MHz)*	100.63
Nucleus	13C	*Number of Transients*	256	*Origin*	avg400	*Original Points Count*	32768
Owner	nmr-user	*Points Count*	32768	*Pulse Sequence*	zgpg30	*Receiver Gain*	2050.00
SW(cyclical) (Hz)	24038.46	*Solvent*	CHLOROFORM-d	*Spectrum Offset (Hz)*	10055.3301	*Spectrum Type*	STANDARD
Sweep Width (Hz)	24037.73	*Temperature (degree C)*	21.400				



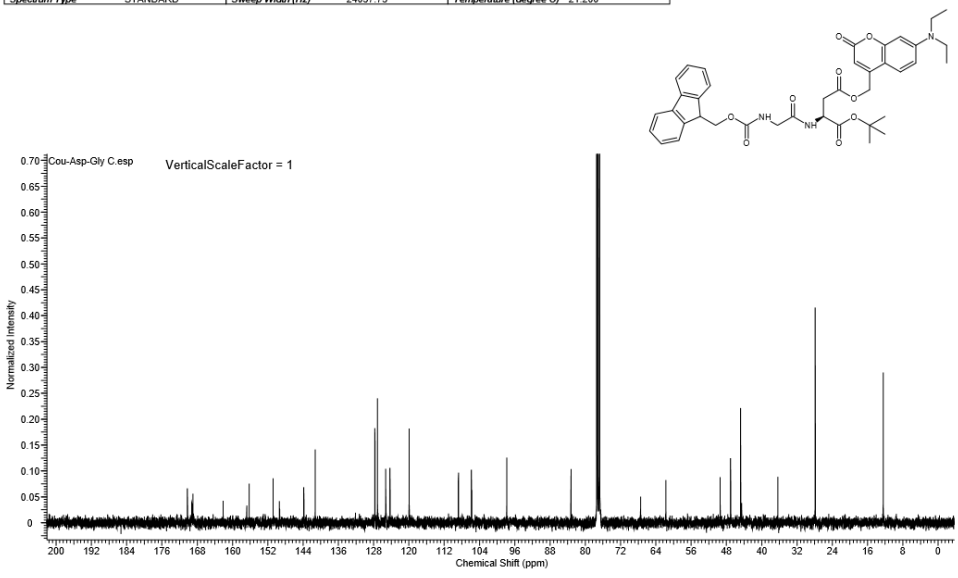


Compound 224

Acquisition Time (sec)	3.2768	*Comment*	Instrument AVG400 Group SJC Chemist MLS MLS08034: Cou Asp - Gly h1acq.crl CDCl3 {C:\NMR} sjcgrp 43				
Date	07 Nov 2014 08:42:40			*Date Stamp*	07 Nov 2014 08:42:40		
File Name	D:\Gnomeeee\NMR\Sequential Tripeptide\Cou-Asp-Gly\Nov06-2014-43\3\PDATA\1\1r					*Frequency (MHz)*	400.20
Nucleus	1H	*Number of Transients*	16	*Origin*	avg400	*Original Points Count*	32768
Owner	nmr-user	*Points Count*	65536	*Pulse Sequence*	zg30	*Receiver Gain*	202.31
SW(cyclical) (Hz)	10000.00	*Solvent*	CHLOROFORM-d	*Spectrum Offset (Hz)*	2462.1428	*Spectrum Type*	STANDARD
Sweep Width (Hz)	9999.85	*Temperature (degree C)*	21.000				

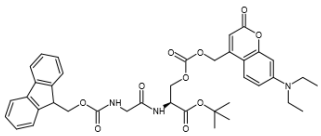


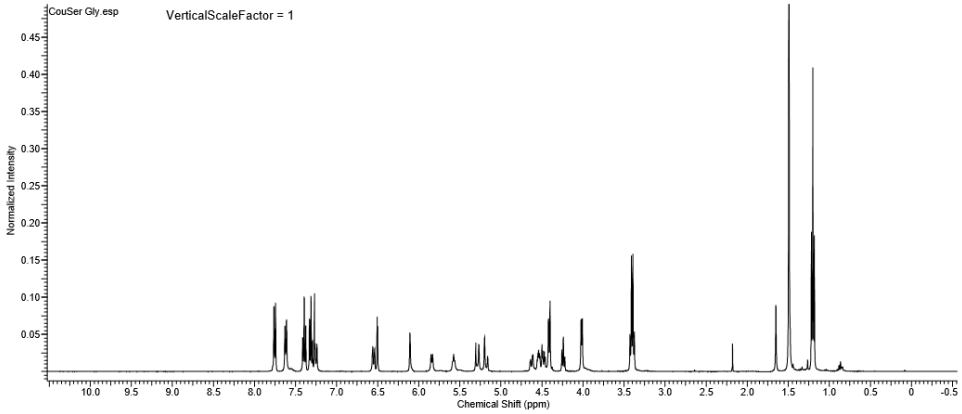
Acquisition Time (sec)	1.3631	*Comment*	Instrument AVG400 Group SJC Chemist MLS MLS08034: Cou Asp - Gly c13acq.crl CDCl3 {C:\NMR} sjcgrp 43				
Date	08 Nov 2014 00:49:04	*Date Stamp*	08 Nov 2014 00:49:04	*File Name*	D:\Gnomeeee\NMR\Sequential Tripeptide\Cou-Asp-Gly\Nov06-2014-43\3\PDATA\1\1r		
Frequency (MHz)	100.63	*Nucleus*	13C	*Number of Transients*	256	*Origin*	avg400
Original Points Count	32768	*Owner*	nmr-user	*Points Count*	32768	*Pulse Sequence*	zgpg30
Receiver Gain	2050.00	*SW(cyclical) (Hz)*	24038.46	*Solvent*	CHLOROFORM-d	*Spectrum Offset (Hz)*	10062.6055
Spectrum Type	STANDARD	*Sweep Width (Hz)*	24037.73	*Temperature (degree C)*	21.200		



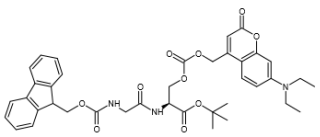
Compound 280

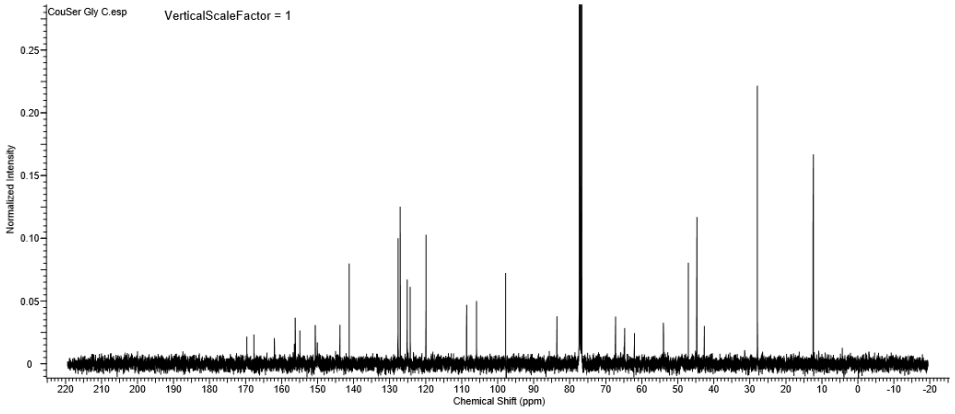
Acquisition Time (sec)	3.2768	*Comment*	Instrument AVG400 Group SJC Chemist MLS Cou Ser(OtBu) - Gly-NHFmoc h1acq crl CDCl3 {C:\NMR} sjcgrp 35				
Date	30 Mar 2015 19:05:52	*Date Stamp*	30 Mar 2015 19:05:52				
File Name	D:\Gnomeeee\NMR\Sequential Tripeptide\Cou-Ser-Gly-Fmoc\Mar30-2015-35-\1\PDATA\1\1r					*Frequency (MHz)*	400.20
Nucleus	1H	*Number of Transients*	8	*Origin*	avg400	*Original Points Count*	32768
Owner	nmr-user	*Points Count*	65536	*Pulse Sequence*	zg60	*Receiver Gain*	107.77
SW(cyclical) (Hz)	10000.00	*Solvent*	CHLOROFORM-d	*Spectrum Offset (Hz)*	2465.6523	*Spectrum Type*	STANDARD
Sweep Width (Hz)	9999.85	*Temperature (degree C)*	25.000				





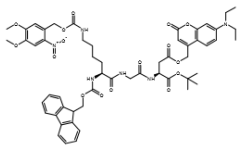
Acquisition Time (sec)	1.3631	*Comment*	Instrument AVG400 Group SJC Chemist MLS Cou Ser(OtBu) - Gly-NHFmoc c13acq crl CDCl3 {C:\NMR} sjcgrp 35				
Date	31 Mar 2015 00:15:12	*Date Stamp*	31 Mar 2015 00:15:12				
File Name	D:\Gnomeeee\NMR\Sequential Tripeptide\Cou-Ser-Gly-Fmoc\Mar30-2015-35-\3\PDATA\1\1r					*Frequency (MHz)*	100.63
Nucleus	13C	*Number of Transients*	256	*Origin*	avg400	*Original Points Count*	32768
Owner	nmr-user	*Points Count*	32768	*Pulse Sequence*	zgpg30	*Receiver Gain*	206.87
SW(cyclical) (Hz)	24038.46	*Solvent*	CHLOROFORM-d	*Spectrum Offset (Hz)*	10058.9980	*Spectrum Type*	STANDARD
Sweep Width (Hz)	24037.73	*Temperature (degree C)*	24.996				

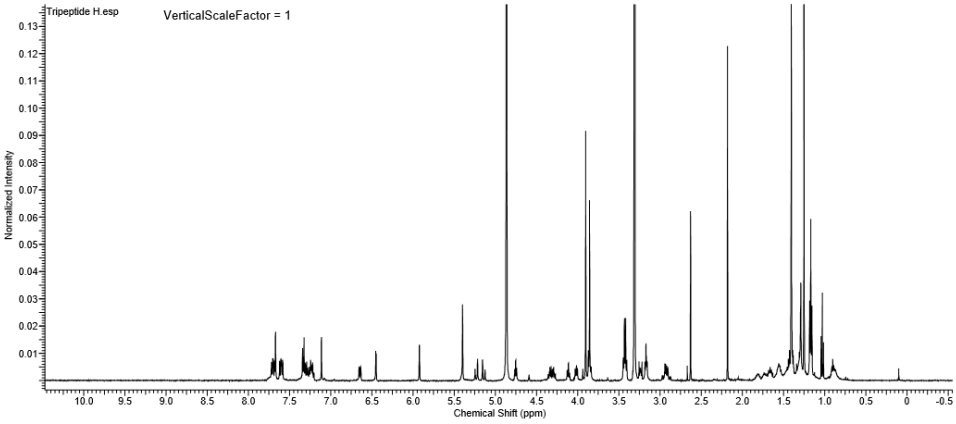




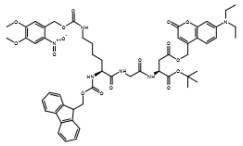
Compound 225

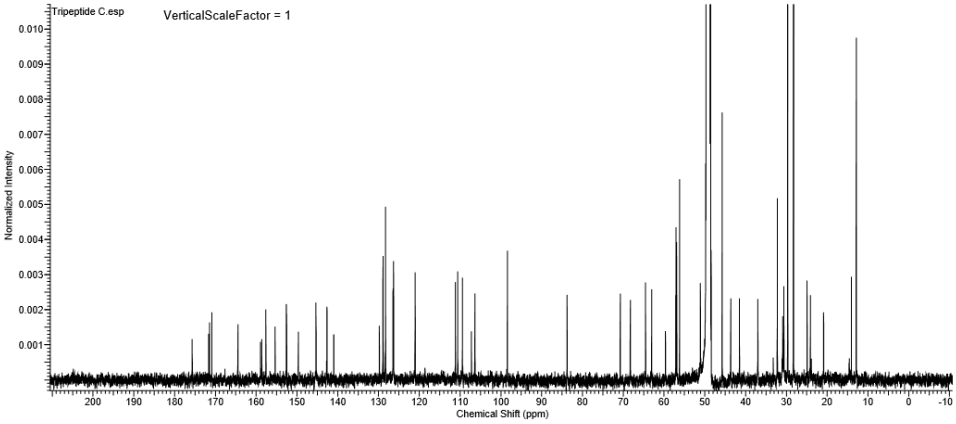
Acquisition Time (sec)	3.1719	*Comment*	Instrument AVC500 Group SJC 9676 Michelle Savage 19/11/14			*Date*	19 Nov 2014 10:57:04
Date Stamp	19 Nov 2014 10:57:04			*File Name*	D:\Gnomeeee\NMR\Sequential Tripeptide\ms96761911\1\1\PDATA\1\1r		
Frequency (MHz)	500.30	*Nucleus*	1H	*Number of Transients*	16	*Origin*	avc500
Original Points Count	32768	*Owner*	nmr-user	*Points Count*	65536	*Pulse Sequence*	zg30
Receiver Gain	3.56	*SW(cyclical) (Hz)*	10330.58	*Solvent*	METHANOL-d4	*Spectrum Offset (Hz)*	3078.8594
Spectrum Type	STANDARD	*Sweep Width (Hz)*	10330.42	*Temperature (degree C)*	24.970		





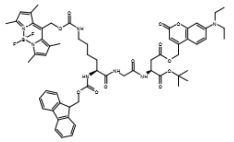
Acquisition Time (sec)	1.0486	*Comment*	Instrument AVC500 Group SJC 9676 Michelle Savage 19/11/14			*Date*	19 Nov 2014 13:28:32
Date Stamp	19 Nov 2014 13:28:32			*File Name*	D:\Gnomeeee\NMR\Sequential Tripeptide\ms96761911\4\PDATA\1\1r		
Frequency (MHz)	125.80	*Nucleus*	13C	*Number of Transients*	3072	*Origin*	avc500
Original Points Count	32768	*Owner*	nmr-user	*Points Count*	32768	*Pulse Sequence*	zgpg30
Receiver Gain	912.00	*SW(cyclical) (Hz)*	31250.00	*Solvent*	METHANOL-d4	*Spectrum Offset (Hz)*	12775.3701
Spectrum Type	STANDARD	*Sweep Width (Hz)*	31249.05	*Temperature (degree C)*	24.970		

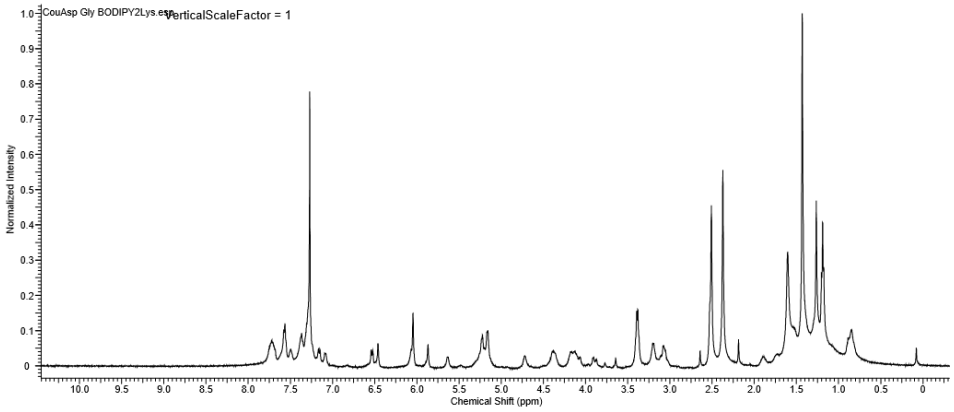




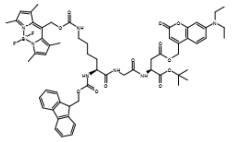
Compound 257

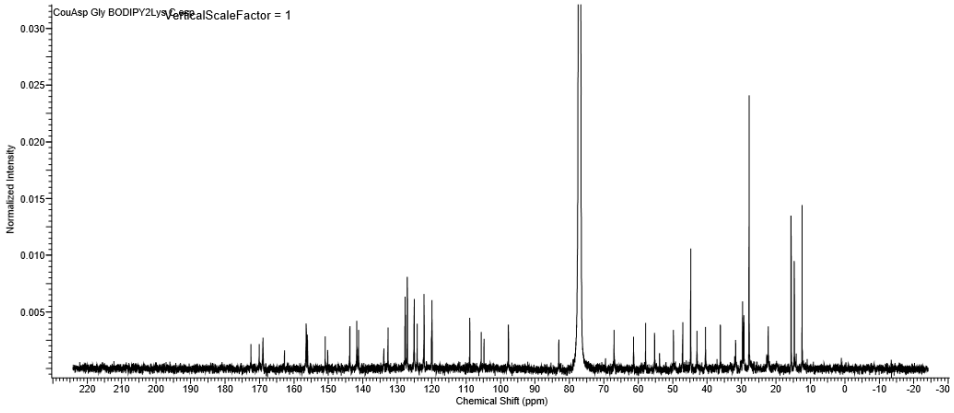
Acquisition Time (sec)	3.1719	*Comment*	Instrument AVC500 Group SJC 0875 Michelle Savage 2/4/15			*Date*	02 Apr 2015 11:35:44
Date Stamp	02 Apr 2015 11:35:44						
File Name	D:\Gnomeeee\NMR\Sequential Tripeptide\Cou Asp Gly Lys BODIPY 2\ms08750204\1\1\PDATA\1\1r					*Frequency (MHz)*	500.30
Nucleus	1H	*Number of Transients*	16	*Origin*	avc500	*Original Points Count*	32768
Owner	nmr-user	*Points Count*	65536	*Pulse Sequence*	zg30	*Receiver Gain*	3.56
SW(cyclical) (Hz)	10330.58	*Solvent*	CHLOROFORM-d	*Spectrum Offset (Hz)*	3081.1340	*Spectrum Type*	STANDARD
Sweep Width (Hz)	10330.42	*Temperature (degree C)*	24.970				



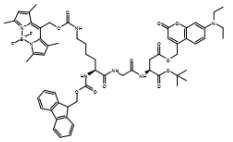


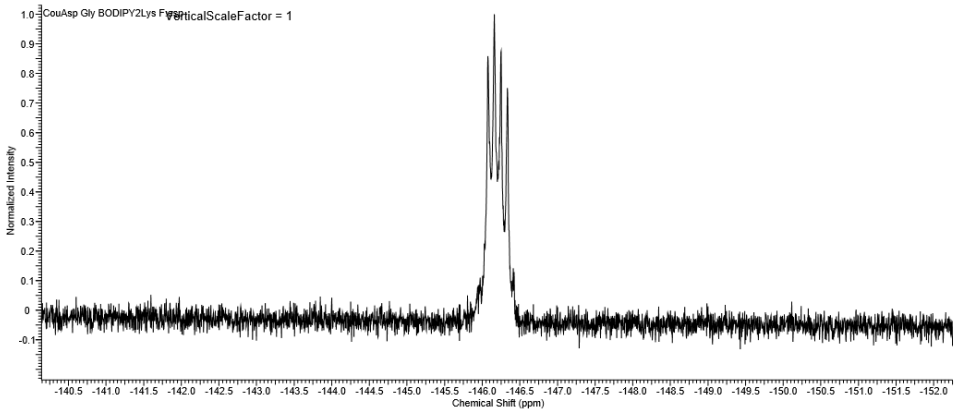
Acquisition Time (sec)	1.0486	*Comment*	Instrument AVC500 Group SJC 0875 Michelle Savage 2/4/15			*Date*	02 Apr 2015 12:01:20
Date Stamp	02 Apr 2015 12:01:20						
File Name	D:\Gnomeeee\NMR\Sequential Tripeptide\Cou Asp Gly Lys BODIPY 2\ms08750204\4\PDATA\1\1r					*Frequency (MHz)*	125.80
Nucleus	13C	*Number of Transients*	2048	*Origin*	avc500	*Original Points Count*	32768
Owner	nmr-user	*Points Count*	32768	*Pulse Sequence*	zgpg30	*Receiver Gain*	912.00
SW(cyclical) (Hz)	31250.00	*Solvent*	CHLOROFORM-d	*Spectrum Offset (Hz)*	12580.1094	*Spectrum Type*	STANDARD
Sweep Width (Hz)	31249.05	*Temperature (degree C)*	24.970				





Acquisition Time (sec)	0.7340	*Comment*	Instrument AVB400 MICHELLE SAVAGE 40875 2/4/15			*Date*	02 Apr 2015 16:00:16
Date Stamp	02 Apr 2015 16:00:16						
File Name	D:\Gnomeeee\NMR\Sequential Tripeptide\Cou Asp Gly Lys BODIPY 2\19F\ms08750204\1\PDATA\1\1r					*Frequency (MHz)*	376.50
Nucleus	19F	*Number of Transients*	16	*Origin*	avb400	*Original Points Count*	65536
Owner	nmr-user	*Points Count*	65536	*Pulse Sequence*	zgfhigqn	*Receiver Gain*	197.74
SW(cyclical) (Hz)	89285.71	*Solvent*	CHLOROFORM-d	*Spectrum Offset (Hz)*	-41414.7969	*Spectrum Type*	STANDARD
Sweep Width (Hz)	89284.35	*Temperature (degree C)*	25.087				





Appendix B

Photolysis Experiments

B.1 Determination of Calibration Curves by HPLC

B.1.1 Calibration of Fmoc-Asp-O^{t}Bu (221)

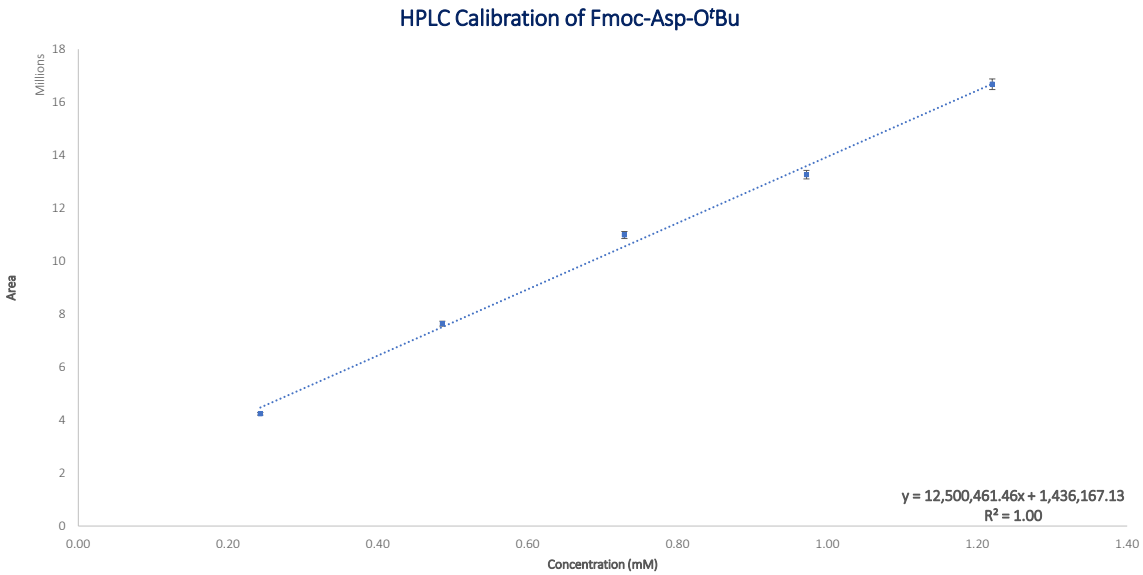


Figure B.1: Linear relationship of absorbance vs. concentration of Fmoc-Asp-O^{t}Bu (**221**).

Table B.1: HPLC calibration data for Fmoc-Asp-O^{t}Bu (**221**).

Fmoc-Asp-O^{t}Bu		
Entry	*c* (mM)	Area
1	0.24	4,238,360
2	0.49	7,641,060
3	0.73	10,986,300
4	0.97	13,264,500
5	1.22	16,677,300

Gradient $= 12.5 \times 10^6$
Intercept $= 1.44 \times 10^6$

B.1.2 Calibration of Fmoc-Ser-O^{t}Bu (185)

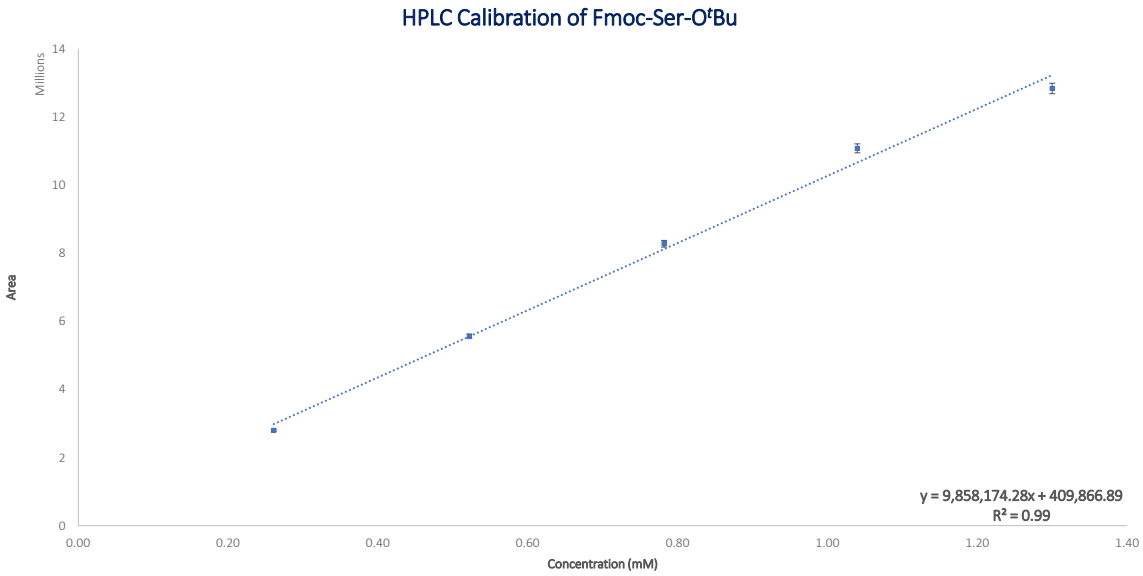


Figure B.2: Linear relationship of absorbance vs. concentration of Fmoc-Ser-O^{t}Bu (**185**).

Table B.2: HPLC calibration data for Fmoc-Ser-O^{t}Bu (**185**).

Fmoc-Ser-OᵗBu		
Entry	*c* (mM)	Area
1	0.26	2,797,660
2	0.52	5,560,266
3	0.78	8,276,337
4	1.04	11,075,610
5	1.30	12,835,632

Gradient $= 9.86 \times 10^6$
Intercept $= 0.410 \times 10^6$

B.1.3 Calibration of Fmoc-Asp(DEACM)-O^{t}Bu (215)

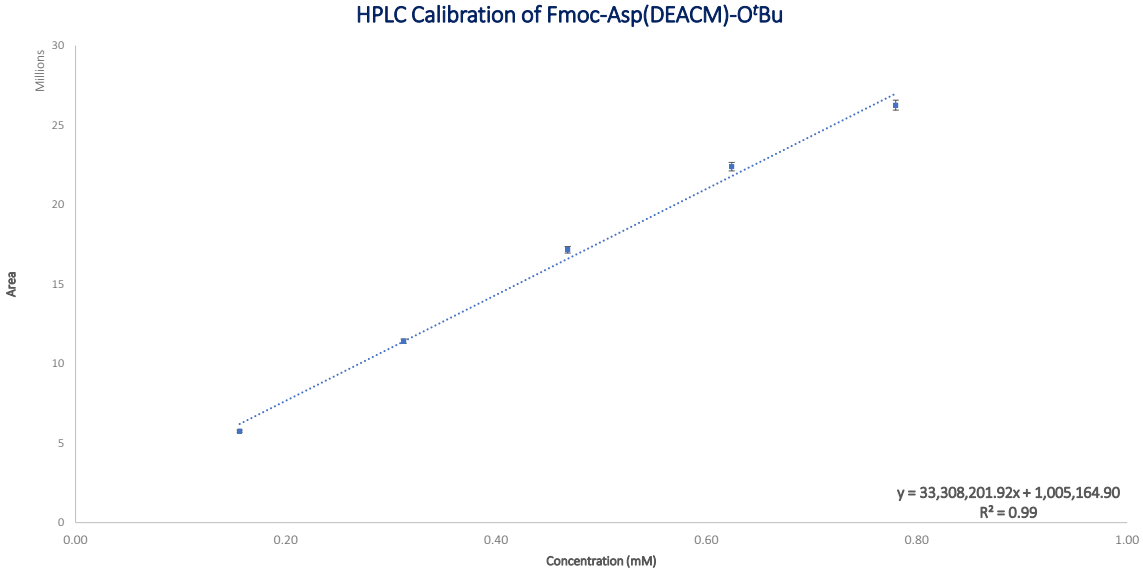


Figure B.3: Linear relationship of absorbance vs. concentration of Fmoc-Asp(DEACM)-O^{t}Bu (**215**).

Table B.3: HPLC calibration data for Fmoc-Asp(DEACM)-O^{t}Bu (**215**).

Fmoc-Asp(DEACM)-O^{t}Bu		
Entry	*c* (mM)	Area
1	0.16	5,757,186
2	0.31	11,416,287
3	0.47	17,155,558
4	0.62	22,384,518
5	0.78	26,253,468

Gradient $= 33.3 \times 10^6$
Intercept $= 1.01 \times 10^6$

B.1.4 Calibration of Fmoc-Ser(DEACM)-O^{t}Bu (217)

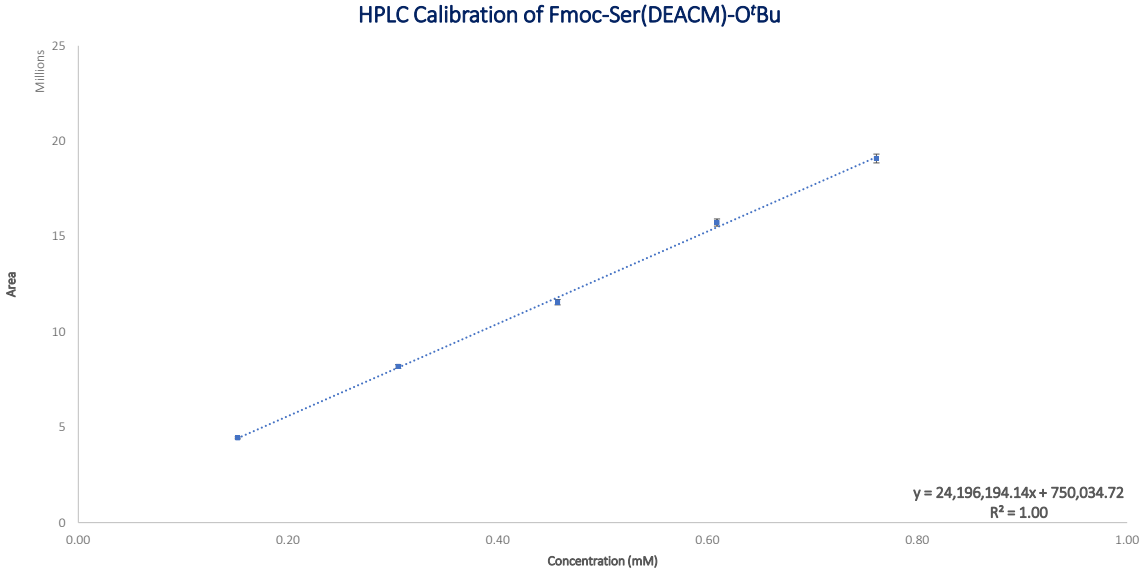


Figure B.4: Linear relationship of absorbance vs. concentration of Fmoc-Ser(DEACM)-O^{t}Bu (**217**).

Table B.4: HPLC calibration data for Fmoc-Ser(DEACM)-O^{t}Bu (**217**).

Fmoc-Ser(DEACM)-O^{t}Bu		
Entry	*c* (mM)	Area
1	0.15	4,447,240
2	0.31	8,187,790
3	0.46	11,559,741
4	0.61	15,730,015
5	0.76	19,089,495

Gradient $= 24.2 \times 10^6$
Intercept $= 0.750 \times 10^6$

B.1.5 Calibration of Fmoc-Asp(DMNB)-O^{t}Bu (212)

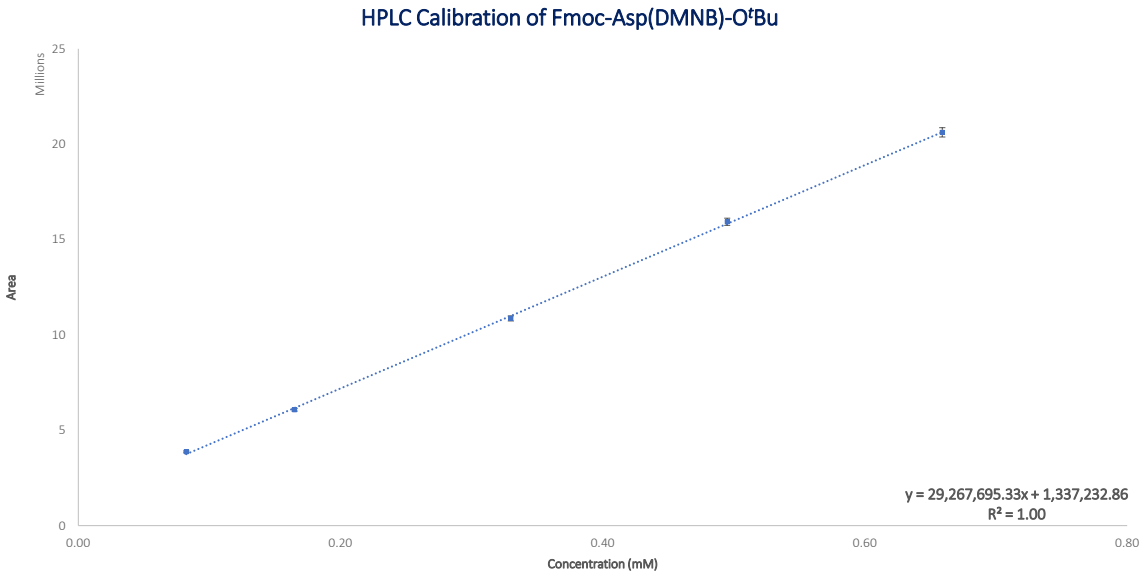


Figure B.5: Linear relationship of absorbance vs. concentration of Fmoc-Asp(DMNB)-O^{t}Bu (**212**).

Table B.5: HPLC calibration data for Fmoc-Asp(DMNB)-O^{t}Bu (**212**).

Fmoc-Asp(DMNB)-O^{t}Bu		
Entry	*c* (mM)	Area
1	0.08	3,871,046
2	0.17	6,076,044
3	0.33	10,864,395
4	0.50	15,930,595
5	0.66	20,618,172

Gradient $= 29.3 \times 10^6$
Intercept $= 1.34 \times 10^6$

B.1.6 Calibration of Fmoc-Ser(DMNB)-O^{t}Bu (213)

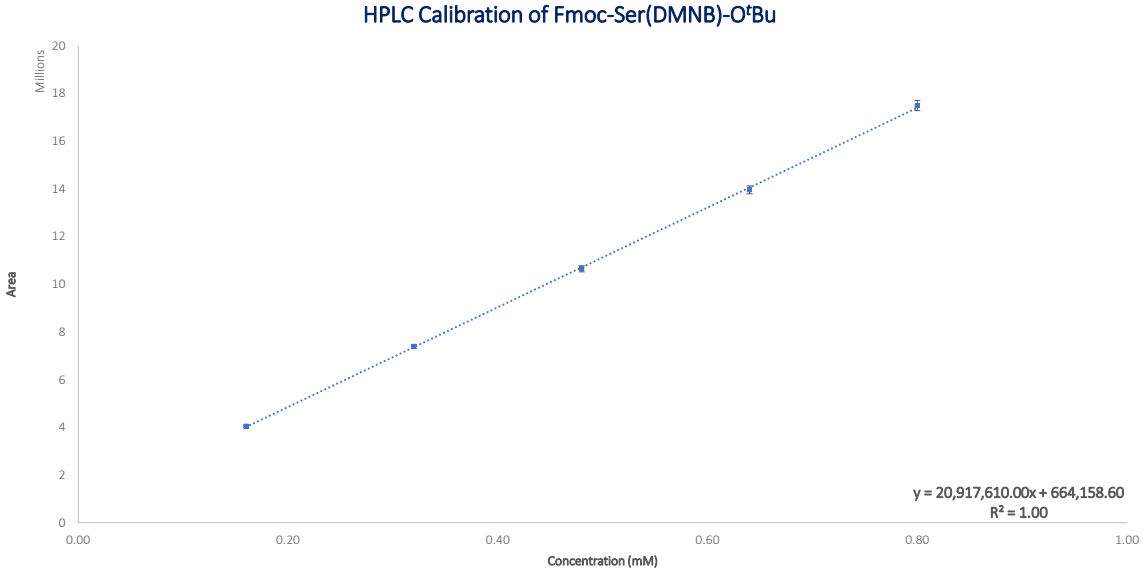


Figure B.6: Linear relationship of absorbance vs. concentration of Fmoc-Ser(DMNB)-O^{t}Bu (**213**).

Table B.6: HPLC calibration data for Fmoc-Ser(DMNB)-O^{t}Bu (**213**).

Fmoc-Ser(DMNB)-O^{t}Bu		
Entry	*c* (mM)	Area
1	0.16	4,043,281
2	0.32	7,386,082
3	0.48	10,644,905
4	0.64	13,956,758
5	0.80	17,492,031

Gradient $= 20.9 \times 10^6$
Intercept $= 0.664 \times 10^6$

B.1.7 Calibration of Fmoc-Asp(MPH)-O^{t}Bu (209)

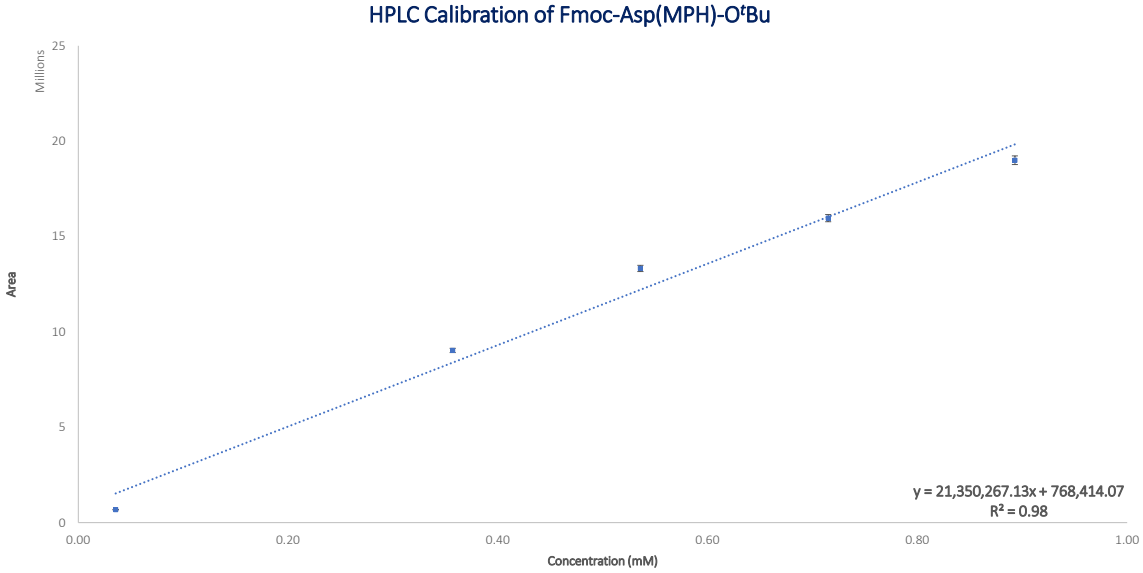


Figure B.7: Linear relationship of absorbance vs. concentration of Fmoc-Asp(MPH)-O^{t}Bu (**209**).

Table B.7: HPLC calibration data for Fmoc-Asp(MPH)-O^{t}Bu (**209**).

Fmoc-Asp(MPH)-O^{t}Bu		
Entry	*c* (mM)	Area
1	0.036	681,698
2	0.36	9,027,890
3	0.54	13,328,469
4	0.72	15,964,156
5	0.89	18,999,080

Gradient $= 21.4 \times 10^6$
Intercept $= 0.768 \times 10^6$

B.1.8 Calibration of Fmoc-Asp(DEATC)-O^{t}Bu (232)

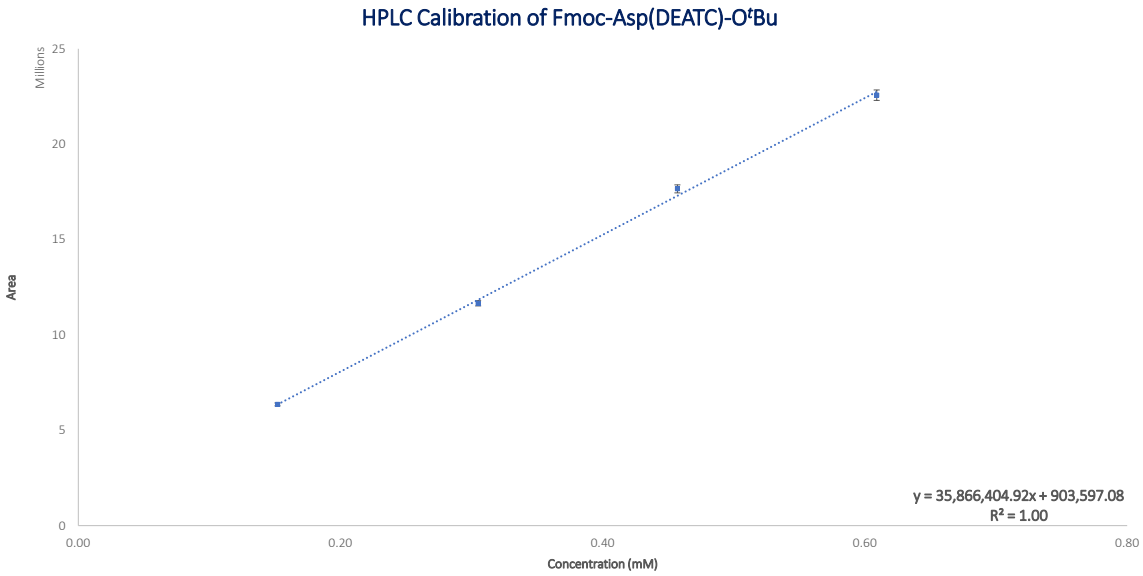


Figure B.8: Linear relationship of absorbance vs. concentration of Fmoc-Asp(DEATC)-O^{t}Bu (**232**).

Table B.8: HPLC calibration data for Fmoc-Asp(DEATC)-O^{t}Bu (**232**).

Fmoc-Asp(DEATC)-O^{t}Bu		
Entry	*c* (mM)	Area
1	0.15	6,358,658
2	0.31	11,656,565
3	0.46	17,656,991
4	0.61	22,566,709

Gradient $= 35.9 \times 10^6$
Intercept $= 0.904 \times 10^6$

B.1.9 Calibration of Fmoc-Asp(BODIPY-2)-O^{t}Bu (251)

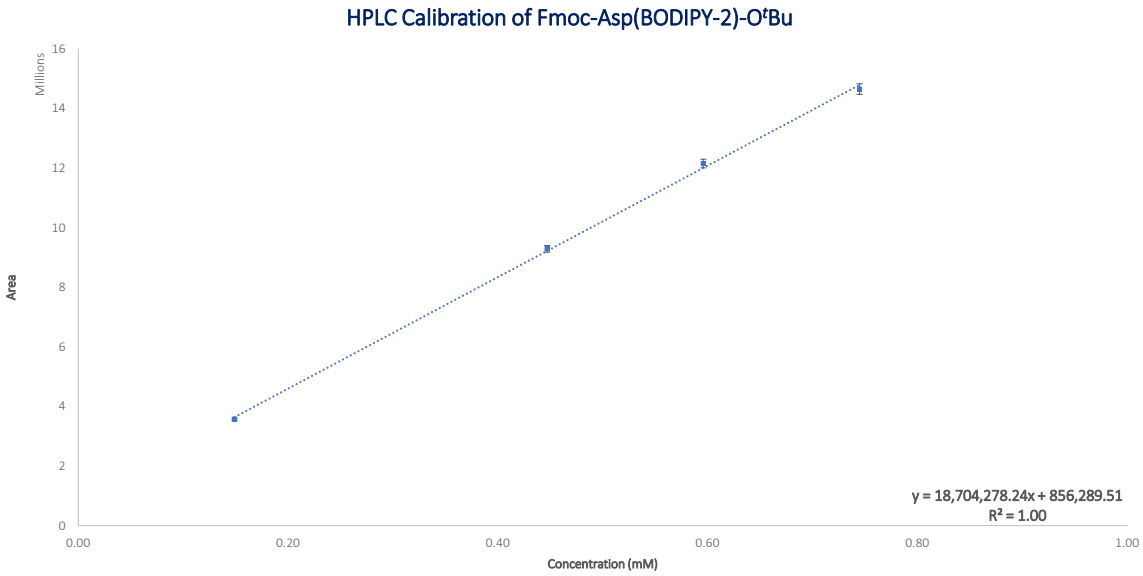


Figure B.9: Linear relationship of absorbance vs. concentration of Fmoc-Asp(BODIPY-2)-O^{t}Bu (**251**).

Table B.9: HPLC calibration data for Fmoc-Asp(BODIPY-2)-O^{t}Bu (**251**).

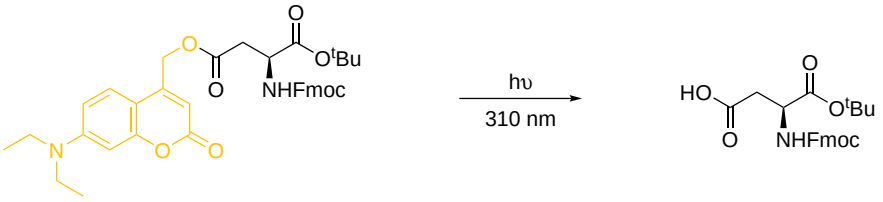
Fmoc-Asp(BODIPY-2)-O^{t}Bu		
Entry	*c* (mM)	Area
1	0.15	3,572,410
2	0.45	9,286,616
3	0.60	12,148,279
4	0.75	14,648,040

Gradient $= 18.7 \times 10^6$
Intercept $= 0.856 \times 10^6$

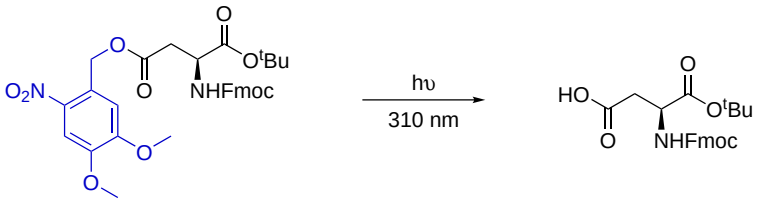
B.2 Photolysis Data as Measured by HPLC

B.2.1 Irradiation at $\lambda = 310$ nm

310 nm Irradiation of Fmoc-Asp(DEACM)-O^{t}Bu (215)


O
O
O

310 nm Irradiation of Fmoc-Asp(DMNB)-O^{t}Bu (212)



212 **221**

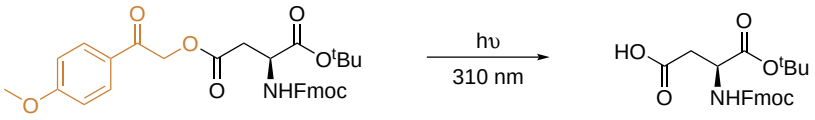
Scheme B.2: 310 nm photolysis of Fmoc-Asp(DMNB)-O^{t}Bu (**212**).

Table B.11: Determination of percentage composition of Fmoc-Asp(DMNB)-O^{t}Bu (**212**) and uncaged Fmoc-Asp-O^{t}Bu (**221**) following irradiation at 310 nm.

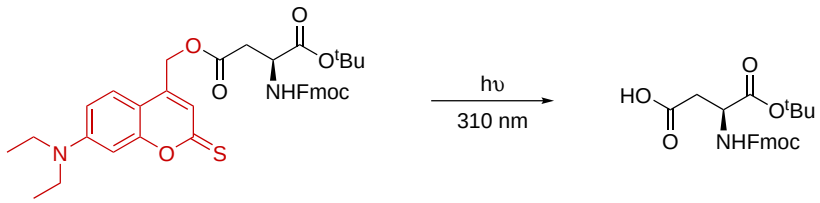
310 nm Irradiation of Fmoc-Asp(DMNB)-O^{t}Bu							
Entry	t (h)	Area [Caged]	Area [AA]	*c* [Caged] (mM)	*c* [AA] (mM)	% [Caged]	% [AA]
1	0	22,814,100	-	0.71	0.00	100	0
2	0.5	14,209,300	2,453,190	0.44	0.17	62	24
3	1	8,477,220	3,996,370	0.26	0.28	37	40
4	2	4,066,480	5,967,580	0.13	0.42	18	59
5	3	1,738,330	6,770,250	0.05	0.48	8	67
6	4	1,685,560	6,598,010	0.05	0.47	8	66

Near complete photolysis of Fmoc-Asp(DMNB)-O^{t}Bu (**212**) was observed following irradiation at 310 nm for 4 h, accompanied by a maximum 67% release of uncaged Fmoc-Asp-O^{t}Bu (**221**).

310 nm Irradiation of Fmoc-Asp(MPH)-O^{t}Bu (209)


O
O
O

310 nm Irradiation of Fmoc-Asp(DEATC)-O^{t}Bu (232)



232 **221**

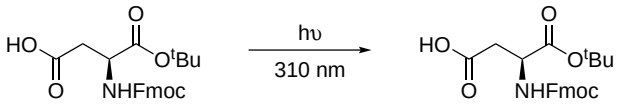
Scheme B.4: 310 nm photolysis of Fmoc-Asp(DEATC)-O^{t}Bu (**232**).

Table B.13: Determination of percentage composition of Fmoc-Asp(DEATC)-O^{t}Bu (**232**) and uncaged Fmoc-Asp-O^{t}Bu (**221**) following irradiation at 310 nm.

310 nm Irradiation of Fmoc-Asp(DEATC)-O^{t}Bu							
Entry	t (h)	Area [Caged]	Area [AA]	*c* [Caged] (mM)	*c* [AA] (mM)	% [Caged]	% [AA]
1	0	24,549,900	-	0.65	0.00	100	0
2	0.5	1,419,720	4,688,890	0.04	0.33	6	51
3	1	-	5,822,710	0.00	0.41	0	64

Complete photolysis of Fmoc-Asp(DEATC)-O^{t}Bu (**232**) was observed following irradiation at 310 nm for 1 h. This was accompanied by a maximum 64% release of uncaged Fmoc-Asp-O^{t}Bu (**221**).

310 nm Irradiation of Fmoc-Asp-O^{t}Bu (221) [Control Experiment]



221 **221**

Scheme B.5: 310 nm photolysis of Fmoc-Asp-O^{t}Bu (**221**).

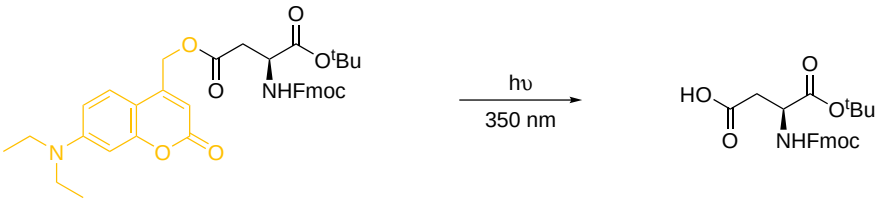
Table B.14: Determination of percentage composition of Fmoc-Asp-O^{t}Bu (**221**) following irradiation at 310 nm [Control Experiment].

310 nm Irradiation of Fmoc-Asp-O^{t}Bu							
Entry	t (h)	Area [Caged]	Area [AA]	*c* [Caged] (mM)	*c* [AA] (mM)	% [Caged]	% [AA]
1	0		17,874,600		1.26		100
2	0.5		16,356,700		1.16		92
3	1		15,428,400		1.09		86
4	2		13,282,500		0.94		74
5	4		10,768,900		0.76		60

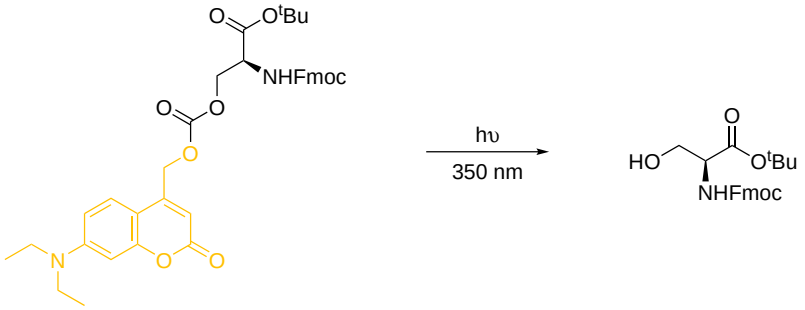
A control experiment was conducted exposing Fmoc-Asp-O^{t}Bu (**221**) to irradiation at 310 nm for 4 h. A 40% decrease in percentage composition was observed indicating possible photolytic decomposition at this wavelength.

B.2.2 Irradiation at $\lambda = 350$ nm

350 nm Irradiation of Fmoc-Asp(DEACM)-O^{t}Bu (215)


O
O
O

350 nm Irradiation of Fmoc-Ser(DEACM)-O^{t}Bu (217)



217 **185**

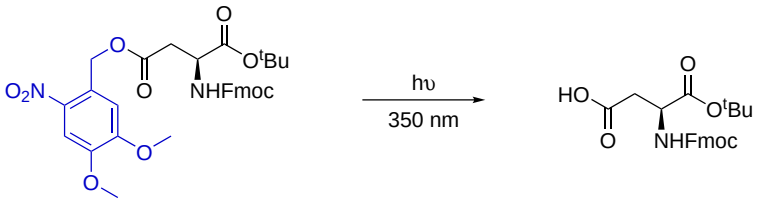
Scheme B.7: 350 nm photolysis of Fmoc-Ser(DEACM)-O^{t}Bu (**217**).

Table B.16: Determination of percentage composition of Fmoc-Ser(DEACM)-O^{t}Bu (**217**) and uncaged Fmoc-Ser-O^{t}Bu (**185**) following irradiation at 350 nm.

350 nm Irradiation of Fmoc-Ser(DEACM)-O^{t}Bu							
Entry	t (h)	Area [Caged]	Area [AA]	*c* [Caged] (mM)	*c* [AA] (mM)	% [Caged]	% [AA]
1	0	13,131,000	-	0.52	0.00	100	0
2	1	2,290,770	5,254,560	0.09	0.51	17	100
3	2	386,732	6,386,180	0.02	0.62	3	100
4	3	-	6,401,970	0.00	0.62	0	100

After 3 h, complete photolysis of Fmoc-Ser(DEACM)-O^{t}Bu (**217**) was observed when irradiating at 350 nm, accompanied by complete conversion to uncaged Fmoc-Ser-O^{t}Bu (**185**). The increase in the rate of photolysis, relative to the caged aspartic acid species (**215**), could be attributed to the increased entropic effect from the release of CO_2 following photolysis of Fmoc-Ser(DEACM)-O^{t}Bu (**217**).

350 nm Irradiation of Fmoc-Asp(DMNB)-O^{t}Bu (212)



212 **221**

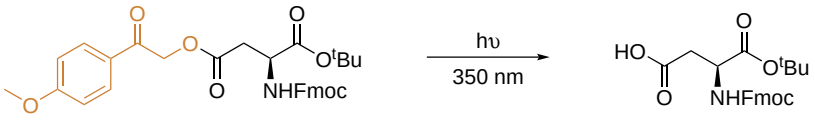
Scheme B.8: 350 nm photolysis of Fmoc-Asp(DMNB)-O^{t}Bu (**212**).

Table B.17: Determination of percentage composition of Fmoc-Asp(DMNB)-O^{t}Bu (**212**) and uncaged Fmoc-Asp-O^{t}Bu (**221**) following irradiation at 350 nm.

350 nm Irradiation of Fmoc-Asp(DMNB)-O^{t}Bu							
Entry	t (h)	Area [Caged]	Area [AA]	*c* [Caged] (mM)	*c* [AA] (mM)	% [Caged]	% [AA]
1	0	26,458,500	-	0.83	0.00	100	0
2	1	9,730,050	4,062,520	0.30	0.29	37	35
3	2	5,907,710	3,892,590	0.18	0.28	22	33
4	3	4,062,520	6,226,080	0.13	0.44	15	53
5	4	-	6,897,720	0.00	0.49	0	59
6	5	-	8,520,700	0.00	0.60	0	73
7	6	-	7,403,920	0.00	0.52	0	64

Following 4 h of irradiation at 350 nm, complete photolysis of Fmoc-Asp(DMNB)-O^{t}Bu (**212**) was observed, accompanied by a maximum release of 73% uncaged Fmoc-Asp-O^{t}Bu (**221**).

350 nm Irradiation of Fmoc-Asp(MPH)-O^{t}Bu (209)



209 **221**

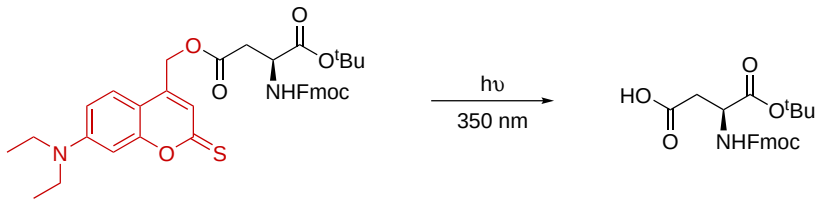
Scheme B.9: 350 nm photolysis of Fmoc-Asp(MPH)-O^{t}Bu (**209**).

Table B.18: Determination of percentage composition of Fmoc-Asp(MPH)-O^{t}Bu (**209**) and uncaged Fmoc-Asp-O^{t}Bu (**221**) following irradiation at 350 nm.

350 nm Irradiation of Fmoc-Asp(MPH)-O^{t}Bu							
Entry	t (h)	Area [Caged]	Area [AA]	*c* [Caged] (mM)	*c* [AA] (mM)	% [Caged]	% [AA]
1	0	15,362,400	-	0.68	0.00	100	0
2	1	14,097,000	-	0.63	0.00	92	0
3	2	13,879,400	-	0.62	0.00	90	0
4	4	11,653,300	-	0.52	0.00	76	0
5	6	11,437,400	-	0.51	0.00	74	0
6	8	9,933,230	-	0.44	0.00	65	0

A 35% decrease in the percentage composition of Fmoc-Asp(MPH)-O^{t}Bu (**209**) was observed following irradiation at 350 nm for 8 h. However, no conversion to uncaged Fmoc-Asp-O^{t}Bu (**221**) was observed, indicating the possibility of photolytic degradation at this wavelength.

350 nm Irradiation of Fmoc-Asp(DEATC)-O^{t}Bu (232)



232 **221**

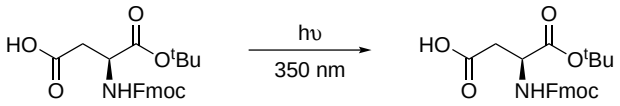
Scheme B.10: 350 nm photolysis of Fmoc-Asp(DEATC)-O^{t}Bu (**232**).

Table B.19: Determination of percentage composition of Fmoc-Asp(DEATC)-O^{t}Bu (**232**) and uncaged Fmoc-Asp-O^{t}Bu (**221**) following irradiation at 350 nm.

350 nm Irradiation of Fmoc-Asp(DEATC)-O^{t}Bu							
Entry	t (h)	Area [Caged]	Area [AA]	*c* [Caged] (mM)	*c* [AA] (mM)	% [Caged]	% [AA]
1	0	24,549,900	-	0.65	0.00	100	0
2	0.5	3,358,250	4,834,570	0.09	0.34	14	53
3	1	254,413	5,755,990	0.01	0.41	1	63
4	2	-	7,496,460	0.00	0.53	0	82
5	3	-	7,163,020	0.00	0.51	0	79

Complete photolysis of Fmoc-Asp(DEATC)-O^{t}Bu (**232**) was observed following 2 h of irradiation at 350 nm. This was accompanied by a maximum 82% release of uncaged Fmoc-Asp-O^{t}Bu (**221**).

350 nm Irradiation of Fmoc-Asp-O^{t}Bu (221) [Control Experiment]



221 **221**

Scheme B.11: 350 nm photolysis of Fmoc-Asp-O^{t}Bu (**221**).

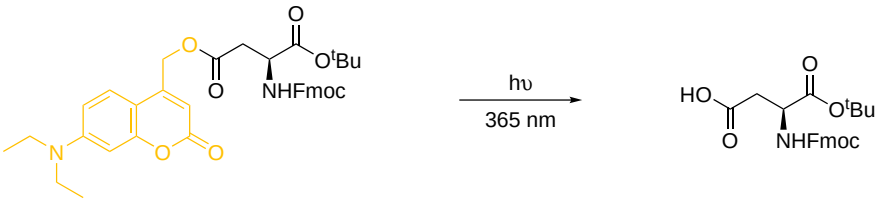
Table B.20: Determination of percentage composition of Fmoc-Asp-O^{t}Bu (**221**) following irradiation at 350 nm [Control Experiment].

350 nm Irradiation of Fmoc-Asp-O^{t}Bu							
Entry	t (h)	Area [Caged]	Area [AA]	*c* [Caged] (mM)	*c* [AA] (mM)	% [Caged]	% [AA]
1	0		17,874,600		1.26		100
2	1		15,886,600		1.12		89
3	2		16,336,500		1.16		91
4	3		15,780,000		1.12		88
5	4		16,257,500		1.15		91
6	5		16,870,000		1.19		94
7	6		17,408,200		1.23		97
8	7		17,421,100		1.23		97

A control experiment was conducted, exposing Fmoc-Asp-O^{t}Bu (**221**) to irradiation at 350 nm for 7 h. A slight decrease in percentage composition of Fmoc-Asp-O^{t}Bu (**221**) was observed, indicating the possibility of a small degree of photolytic decomposition.

B.2.3 Irradiation at $\lambda = 365$ nm

365 nm Irradiation of Fmoc-Asp(DEACM)-O^{t}Bu (215)



215 **221**

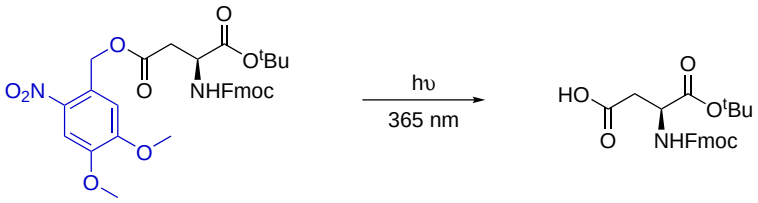
Scheme B.12: 365 nm photolysis of Fmoc-Asp(DEACM)-O^{t}Bu (**215**).

Table B.21: Determination of percentage composition of Fmoc-Asp(DEACM)-O^{t}Bu (**215**) and uncaged Fmoc-Asp-O^{t}Bu (**221**) following irradiation at 365 nm.

365 nm Irradiation of Fmoc-Asp(DEACM)-O^{t}Bu							
Entry	t (h)	Area [Caged]	Area [AA]	*c* [Caged] (mM)	*c* [AA] (mM)	% [Caged]	% [AA]
1	0	26,253,500	-	0.75	0.00	100	0
2	1	13,117,900	3,554,150	0.37	0.25	50	34
3	2	8,177,250	5,974,130	0.23	0.42	31	56
4	3	4,444,230	7,057,350	0.13	0.50	17	67
5	4	2,671,660	8,188,610	0.08	0.58	10	77
6	5	1,502,410	8,986,750	0.04	0.64	6	85
7	7	-	9,929,210	0.00	0.70	0	94

Following 7 h of irradiation at 365 nm, complete photolysis of Fmoc-Asp(DEACM)-O^{t}Bu was observed, accompanied by 94% release of uncaged Fmoc-Asp-O^{t}Bu (**221**).

365 nm Irradiation of Fmoc-Asp(DMNB)-O^{t}Bu (212)



212 **221**

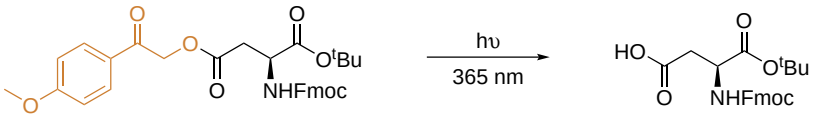
Scheme B.13: 365 nm photolysis of Fmoc-Asp(DMNB)-O^{t}Bu (**212**).

Table B.22: Determination of percentage composition of Fmoc-Asp(DMNB)-O^{t}Bu (**212**) and uncaged Fmoc-Asp-O^{t}Bu (**221**) following irradiation at 365 nm.

365 nm Irradiation of Fmoc-Asp(DMNB)-O^{t}Bu							
Entry	t (h)	Area [Caged]	Area [AA]	*c* [Caged] (mM)	*c* [AA] (mM)	% [Caged]	% [AA]
1	0	22,814,100	-	0.71	0.00	100	0
2	1	13,822,500	1,397,700	0.43	0.10	61	14
3	2	10,712,100	2,704,970	0.33	0.19	47	27
4	3	8,232,770	4,291,480	0.26	0.30	36	43
5	4	5,720,180	5,668,270	0.18	0.40	25	56
6	5	3,890,310	6,772,620	0.12	0.48	17	67
7	6	2,122,530	6,801,920	0.07	0.48	9	68
8	7	1,242,050	7,833,200	0.04	0.55	5	78
9	8	360,239	7,801,570	0.01	0.55	2	78

Near complete photolysis of Fmoc-Asp(DMNB)-O^{t}Bu (**212**) was observed following irradiation at 365 nm for 8 h. This was accompanied by 78% release of uncaged Fmoc-Asp-O^{t}Bu (**221**).

365 nm Irradiation of Fmoc-Asp(MPH)-O^{t}Bu (209)



209 **221**

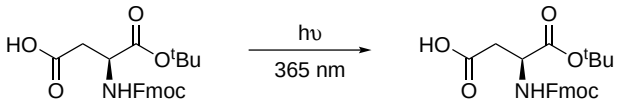
Scheme B.14: 365 nm photolysis of Fmoc-Asp(MPH)-O^{t}Bu (**209**).

Table B.23: Determination of percentage composition of Fmoc-Asp(MPH)-O^{t}Bu (**209**) and uncaged Fmoc-Asp-O^{t}Bu (**221**) following irradiation at 365 nm.

365 nm Irradiation of Fmoc-Asp(MPH)-O^{t}Bu							
Entry	t (h)	Area [Caged]	Area [AA]	*c* [Caged] (mM)	*c* [AA] (mM)	% [Caged]	% [AA]
1	0	18,999,100	-	0.85	0.00	100	0
2	1	19,605,600	-	0.87	0.00	103	0
3	2	18,532,500	-	0.83	0.00	98	0
4	3	18,648,300	-	0.83	0.00	98	0
5	4	18,082,400	-	0.81	0.00	95	0
6	5	16,783,600	-	0.75	0.00	88	0
7	7	17,929,400	-	0.80	0.00	94	0
8	8	17,198,100	-	0.77	0.00	91	0

Following 8 h of irradiation at 365 nm, the percentage composition of Fmoc-Asp(MPH)-O^{t}Bu (**209**) had decreased to 91%; no uncaged Fmoc-Asp-O^{t}Bu (**221**) was observed. These results indicated the MPH caging group to be photostable as this wavelength.

365 nm Irradiation of Fmoc-Asp-O^{t}Bu (221) [Control Experiment]



221 **221**

Scheme B.15: 365 nm photolysis of Fmoc-Asp-O^{t}Bu (**221**).

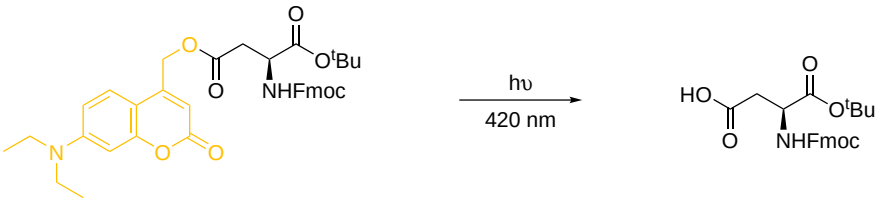
Table B.24: Determination of percentage composition of Fmoc-Asp-O^{t}Bu (**221**) following irradiation at 365 nm [Control Experiment].

365 nm Irradiation of Fmoc-Asp-O^{t}Bu							
Entry	t (h)	Area [Caged]	Area [AA]	*c* [Caged] (mM)	*c* [AA] (mM)	% [Caged]	% [AA]
1	0		19,328,000		1.37		100
2	1		19,218,000		1.36		99
3	2		19,069,500		1.35		99
4	8		19,537,300		1.38		100

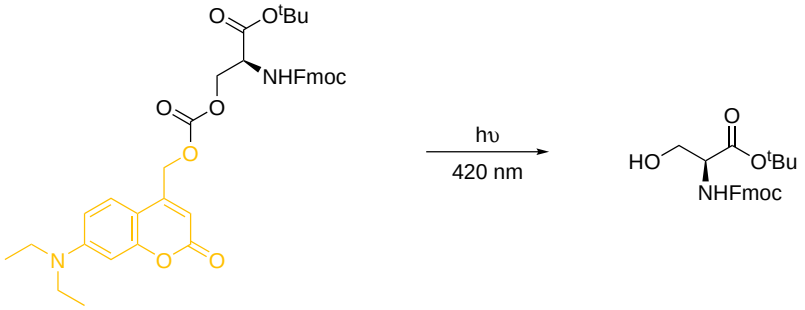
A control experiment was conducted exposing Fmoc-Asp-O^{t}Bu (**221**) to irradiation at 365 nm for 8 h. No decrease in percentage composition of Fmoc-Asp-O^{t}Bu (**221**) was observed. These results are indicative of the stability of Fmoc-Asp-O^{t}Bu (**221**) to the reaction conditions and irradiation at 365 nm.

B.2.4 Irradiation at $\lambda = 420$ nm

420 nm Irradiation of Fmoc-Asp(DEACM)-O^{t}Bu (215)


O
O
O

420 nm Irradiation of Fmoc-Ser(DEACM)-O^{t}Bu (**217**)



217 **185**

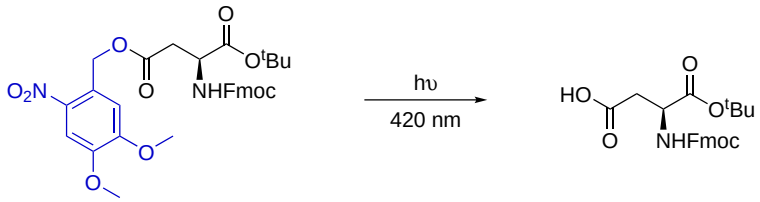
Scheme B.17: 420 nm photolysis of Fmoc-Ser(DEACM)-O^{t}Bu (**217**).

Table B.26: Determination of percentage composition of Fmoc-Ser(DEACM)-O^{t}Bu (**217**) and uncaged Fmoc-Ser-O^{t}Bu (**185**) following irradiation at 420 nm.

420 nm Irradiation of Fmoc-Ser(DEACM)-O^{t}Bu							
Entry	t (h)	Area [Caged]	Area [AA]	*c* [Caged] (mM)	*c* [AA] (mM)	% [Caged]	% [AA]
1	0	26,626,800	-	1.04	0.00	100	0
2	1	17,776,300	7,535,520	0.70	0.73	67	70
3	2	9,540,790	11,113,700	0.37	1.08	36	100
4	3	3,443,990	14,605,700	0.14	1.42	13	100
5	4	1,430,020	14,690,100	0.06	1.43	5	100
6	5	607,167	14,683,000	0.02	1.43	2	100
7	6	288,185	14,972,300	0.01	1.46	1	100

Near complete photolysis of Fmoc-Ser(DEACM)-O^{t}Bu (**217**) was observed following 6 h of irradiation at 420 nm, accompanied by complete conversion to uncaged Fmoc-Ser-O^{t}Bu (**185**).

420 nm Irradiation of Fmoc-Asp(DMNB)-O^{t}Bu (212)



212 **221**

Scheme B.18: 420 nm photolysis of Fmoc-Asp(DMNB)-O^{t}Bu (**212**).

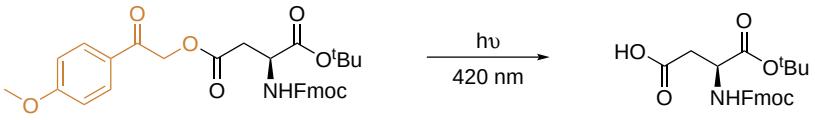
Table B.27: Determination of percentage composition of Fmoc-Asp(DMNB)-O^{t}Bu (**212**) and uncaged Fmoc-Asp-O^{t}Bu (**221**) following irradiation at 420 nm.

420 nm Irradiation of Fmoc-Asp(DMNB)-O^{t}Bu							
Entry	t (h)	Area [Caged]	Area [AA]	*c* [Caged] (mM)	*c* [AA] (mM)	% [Caged]	% [AA]
1	0	17,464,500	-	0.54	0.00	100	0
2	1	16,757,800	-	0.52	0.00	96	0
3	2	16,387,000	-	0.51	0.00	94	0
4	3	16,754,700	-	0.52	0.00	96	0
5	4	16,147,000	-	0.50	0.00	92	0
6	5	15,512,200	-	0.48	0.00	89	0
7	6	15,515,100	-	0.48	0.00	89	0
8	8	13,805,700	-	0.43	0.00	79	0

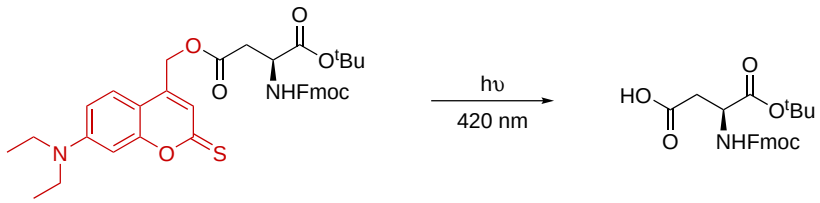
Following 8 h of irradiation at 420 nm, the percentage composition of Fmoc-Asp(DMNB)-O^{t}Bu (**212**) had dropped to 79%. No uncaged Fmoc-Asp-O^{t}Bu (**221**) was observed, indicating the decrease was likely the result of photolytic decomposition and that the DMNB caging group was stable to photolysis at 420 nm.

These results demonstrated the possibility of achieving wavelength selectivity with the DMNB and DEACM caging groups.

420 nm Irradiation of Fmoc-Asp(MPH)-O^{t}Bu (209)


O
O
O

420 nm Irradiation of Fmoc-Asp(DEATC)-O^{t}Bu (**232**)



232 **221**

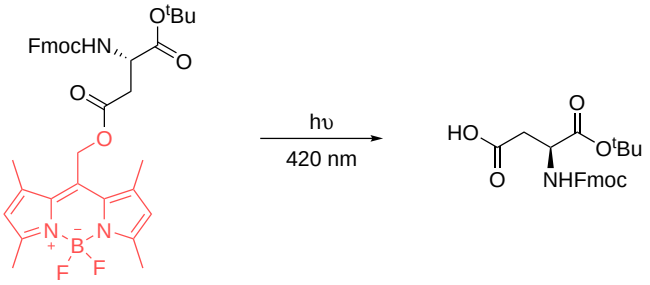
Scheme B.20: 420 nm photolysis of Fmoc-Asp(DEATC)-O^{t}Bu (**232**).

Table B.29: Determination of percentage composition of Fmoc-Asp(DEATC)-O^{t}Bu (**232**) and uncaged Fmoc-Asp-O^{t}Bu (**221**) following irradiation at 420 nm.

420 nm Irradiation of Fmoc-Asp(DEATC)-O^{t}Bu							
Entry	t (h)	Area [Caged]	Area [AA]	*c* [Caged] (mM)	*c* [AA] (mM)	% [Caged]	% [AA]
1	0	24,549,900	-	0.65	0.00	100	0
2	0.5	2,904,810	6,028,200	0.08	0.43	12	66
3	1	-	6,062,870	0.00	0.43	0	66
4	2	-	6,568,700	0.00	0.47	0	72

Complete photolysis of Fmoc-Asp(DEATC)-O^{t}Bu (**232**) was observed following irradiation at 420 nm for 1 h. This was accompanied by 72% release of uncaged Fmoc-Asp-O^{t}Bu (**221**).

420 nm Irradiation of Fmoc-Asp(BODIPY-2)-O^{t}Bu (251)



251 **221**

Scheme B.21: 420 nm photolysis of Fmoc-Asp(BODIPY-2)-O^{t}Bu (**251**).

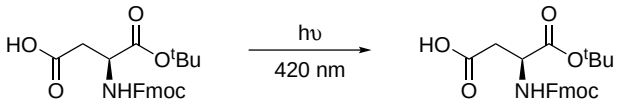
Table B.30: Determination of percentage composition of Fmoc-Asp(BODIPY-2)-O^{t}Bu (**232**) and uncaged Fmoc-Asp-O^{t}Bu (**221**) following irradiation at 420 nm.

420 nm Irradiation of Fmoc-Asp(BODIPY-2)-O^{t}Bu							
Entry	t (h)	Area [Caged]	Area [AA]	*c* [Caged] (mM)	*c* [AA] (mM)	% [Caged]	% [AA]
1	0	14,648,000	-	0.73	0.00	100	0
2	2	13,835,500	326,432	0.69	0.02	94	3
3	4	13,863,900	621,203	0.69	0.04	95	6
4	8	12,771,100	1,313,370	0.63	0.09	87	13

Following 8 h of irradiation at 420 nm, the percentage composition of Fmoc-Asp(BODIPY-2)-O^{t}Bu (**251**) had dropped to 87%, accompanied by 13% release of uncaged Fmoc-Asp-O^{t}Bu (**221**).

The slow rate of photolysis at 420 nm indicated the possibility of achieving wavelength orthogonality with the DEACM and BODIPY caging groups.

420 nm Irradiation of Fmoc-Asp-O^{t}Bu (221) [Control Experiment]



221 **221**

Scheme B.22: 420 nm photolysis of Fmoc-Asp-O^{t}Bu (**221**).

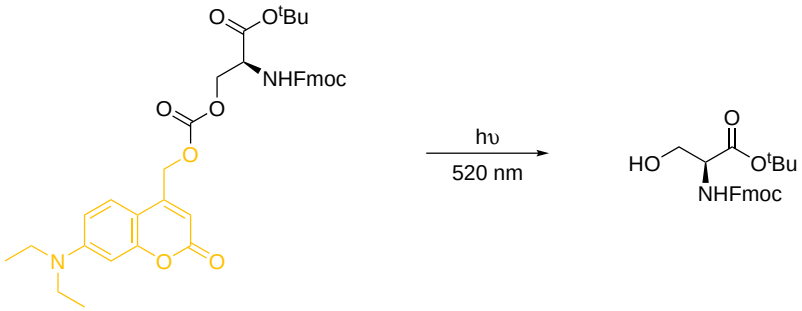
Table B.31: Determination of percentage composition of Fmoc-Asp-O^{t}Bu (**221**) following irradiation at 420 nm [Control Experiment].

420 nm Irradiation of Fmoc-Asp-O^{t}Bu							
Entry	t (h)	Area [Caged]	Area [AA]	*c* [Caged] (mM)	*c* [AA] (mM)	% [Caged]	% [AA]
1	0	-	16,873,900	-	1.19	-	100
2	1	-	15,968,800	-	1.13	-	95
3	2	-	17,085,100	-	1.21	-	100
4	3	-	16,568,100	-	1.17	-	98
5	4	-	15,876,900	-	1.12	-	94
6	5	-	16,616,900	-	1.18	-	98
7	6	-	16,550,000	-	1.17	-	98
8	7	-	16,705,600	-	1.18	-	99
9	8	-	17,063,200	-	1.21	-	100

A control experiment was conducted, exposing Fmoc-Asp-O^{t}Bu (**221**) to irradiation at 420 nm for 8 h. No change in percentage composition was observed indicating Fmoc-Asp-O^{t}Bu (**221**) to be stable to the reaction conditions and photolysis at 420 nm.

B.2.5 Irradiation at $\lambda = 520$ nm

520 nm Irradiation of Fmoc-Ser(DEACM)-O^{t}Bu (217)



217 **185**

Scheme B.23: 520 nm photolysis of Fmoc-Ser(DEACM)-O^{t}Bu (**217**).

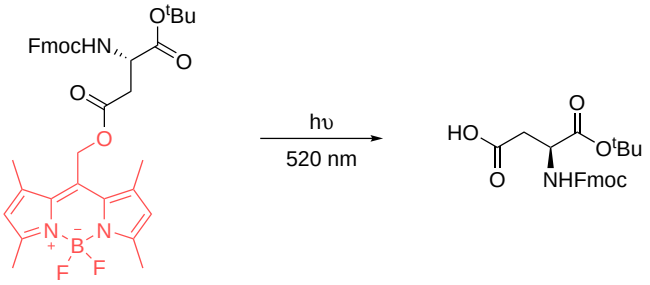
Table B.32: Determination of percentage composition of Fmoc-Ser(DEACM)-O^{t}Bu (**217**) and uncaged Fmoc-Ser-O^{t}Bu (**185**) following irradiation at 520 nm.

520 nm Fmoc-Ser(DEACM)-O^{t}Bu							
Entry	t (h)	Area [Caged]	Area [AA]	*c* [Caged] (mM)	*c* [AA] (mM)	% [Caged]	% [AA]
1	0	19,654,700	-	0.77	0.00	100	0
2	2	20,405,000	-	0.80	0.00	100	0
3	4	20,684,300	-	0.81	0.00	100	0
4	6	19,191,400	298,217	0.75	0.03	98	4
5	8	20,326,100	359,126	0.80	0.04	100	5

Following exposure to irradiation at 520 nm for 8 h, no decrease in percentage composition of Fmoc-Ser(DEACM)-O^{t}Bu (**217**) was observed. A 5% increase in uncaged Fmoc-Ser-O^{t}Bu (**185**) was also observed.

These results indicated the DEACM caging group to be photostable at this wavelength and the possibility for wavelength orthogonality to be achieved alongside the BODIPY caging group.

520 nm Irradiation of Fmoc-Asp(BODIPY-2)-O^{t}Bu (251)



251 **221**

Scheme B.24: 520 nm photolysis of Fmoc-Asp(BODIPY-2)-O^{t}Bu (**251**).

Table B.33: Determination of percentage composition of Fmoc-Asp(BODIPY-2)-O^{t}Bu (**251**) and uncaged Fmoc-Asp-O^{t}Bu (**221**) following irradiation at 520 nm.

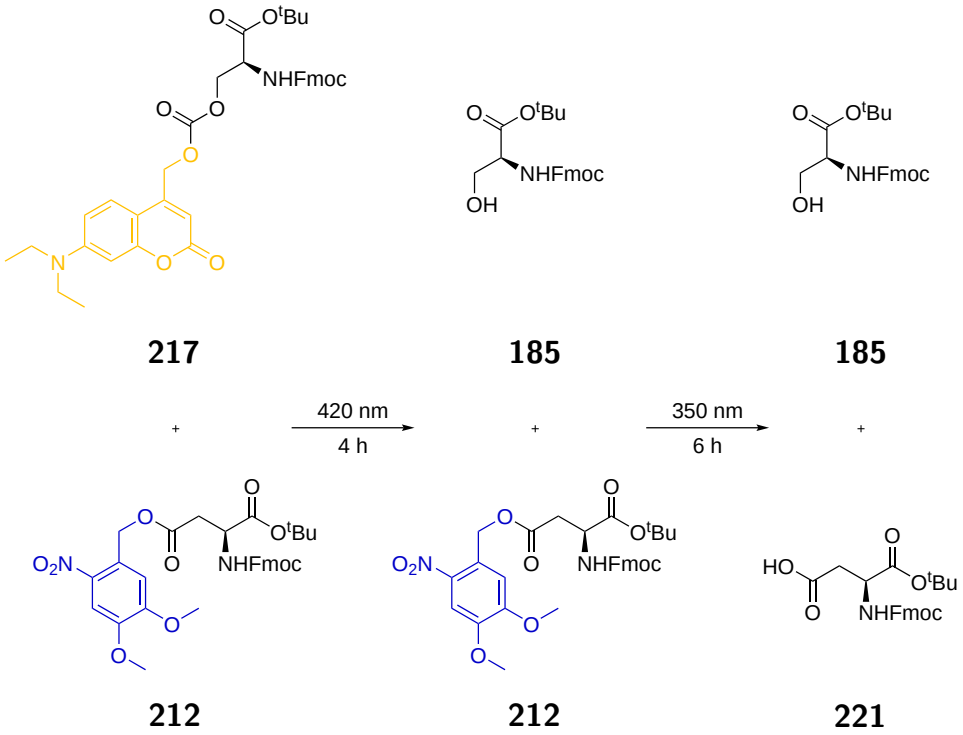
520 nm Irradiation of Fmoc-Asp(BODIPY-2)-O^{t}Bu							
Entry	t (h)	Area [Caged]	Area [AA]	*c* [Caged] (mM)	*c* [AA] (mM)	% [Caged]	% [AA]
1	0	14,648,000	-	0.73	0.00	100	0
2	2	11,720,800	1,351,840	0.58	0.10	80	13
3	4	10,838,900	2,640,190	0.54	0.19	74	26
4	8	8,791,410	4,858,120	0.44	0.34	60	47

Following 8 h of irradiation at 520 nm, a 40% decrease in Fmoc-Asp(BODIPY-2)-O^{t}Bu (**251**) was observed, accompanied by 47% release of uncaged Fmoc-Asp-O^{t}Bu (**221**).

These results indicated the possibility of achieving wavelength orthogonality through use of the BODIPY and DEACM caging groups.

B.2.6 Irradiation of a Sequential System

420 nm (4 h) then 350 nm (6 h) Irradiation of Fmoc-Ser(DEACM)-O^{t}Bu (217) and Fmoc-Asp(DMNB)-O^{t}Bu (212)



Scheme B.25: 420 nm then 350 nm photolysis of a mixture of Fmoc-Ser(DEACM)-O^{t}Bu (**217**) and Fmoc-Asp(DMNB)-O^{t}Bu (**212**).

Table B.34: Determination of percentage composition of Fmoc-Ser(DEACM)-O^{t}Bu (**217**) and uncaged Fmoc-Ser-O^{t}Bu (**185**) following irradiation of mixture at 420 nm (4 h) then 350 nm (6 h).

420 then 350 nm Irradiation of Fmoc-Asp(DMNB)-O^{t}Bu & Fmoc-Ser(DEACM)-O^{t}Bu							
Entry	t (h)	Area [Caged]	Area [AA]	*c* [Caged] (mM)	*c* [AA] (mM)	% [Caged]	% [AA]
1	0	12,792,900	0	0.50	0	100	0
2	1	4,692,930	5,287,920	0.18	0.52	37	78
3	2	747,271	5,656,250	0.03	0.55	6	100
4	3	120,716	5,628,390	0.00	0.55	1	100
5	4	0	6,025,160	0	0.59	0	100
6	5	0	5,826,800	0	0.57	0	100
7	6	0	6,323,550	0	0.62	0	100
8	7	0	6,278,550	0	0.61	0	100
9	8	0	6,767,090	0	0.66	0	100

Following 4 h of irradiation at 420 nm, complete photolysis of the Fmoc-Ser(DEACM)-O^{t}Bu (**217**) species in the mixture was observed, accompanied by complete conversion to uncaged Fmoc-Ser-O^{t}Bu (**185**). No change in percentage composition of the uncaged species was observed when the wavelength was changed to 350 nm for a further 4 h of exposure to irradiation.

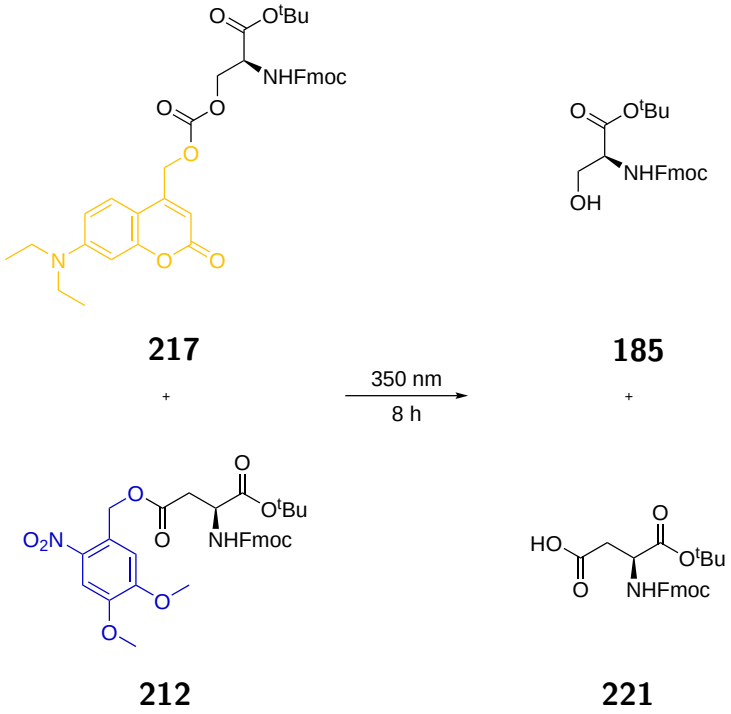
Table B.35: Determination of percentage composition of Fmoc-Asp(DMNB)-O^{t}Bu (**212**) and uncaged Fmoc-Asp-O^{t}Bu (**221**) following irradiation of mixture at 420 nm (4 h) then 350 nm (6 h).

420 then 350 nm Irradiation of Fmoc-Asp(DMNB)-O^{t}Bu & Fmoc-Ser(DEACM)-O^{t}Bu							
Entry	t (h)	Area [Caged]	Area [AA]	*c* [Caged] (mM)	*c* [AA] (mM)	% [Caged]	% [AA]
1	0	15,077,100	0	0.47	0	100	0
2	1	15,581,000	0	0.49	0	100	0
3	2	15,460,600	0	0.48	0	100	0
4	3	14,512,600	0	0.45	0	96	0
5	4	15,393,300	0	0.48	0	100	0
6	5	11,518,800	1,287,510	0.36	0.091	76	19
7	6	8,387,400	3,149,410	0.26	0.22	56	47
8	7	3,503,850	5,120,590	0.11	0.36	23	77
9	8	1,226,520	6,531,320	0.04	0.46	8	98
10	9	157,628	7,090,450	0.00	0.50	1	100
11	10	0	7,095,120	0	0.50	0	100

Following 4 h of irradiation at 420 nm, no change and hence no photolysis of the Fmoc-Asp(DMNB)-O^{t}Bu (**212**) species in the mixture was observed. A change in wavelength to 350 nm and exposure to irradiation for a further 6 h saw complete photolysis of the Fmoc-Asp(DMNB)-O^{t}Bu (**212**) species in the mixture, accompanied by complete conversion to uncaged Fmoc-Asp-O^{t}Bu (**221**).

These results indicated the possibility of wavelength selectivity between the DEACM and DMNB caging groups.

350 nm (8 h) Irradiation of Fmoc-Ser(DEACM)-O^{t}Bu (217) and Fmoc-Asp(DMNB)-O^{t}Bu (212)



Scheme B.26: 350 nm photolysis of a mixture of Fmoc-Ser(DEACM)-O^{t}Bu (**217**) and Fmoc-Asp(DMNB)-O^{t}Bu (**212**).

Table B.36: Determination of percentage composition of Fmoc-Ser(DEACM)-O^{t}Bu (**217**) and uncaged Fmoc-Ser-O^{t}Bu (**185**) following irradiation of mixture at 350 nm (8 h).

350 nm Irradiation of Fmoc-Asp(DMNB)-O^{t}Bu & Fmoc-Ser(DEACM)-O^{t}Bu							
Entry	t (h)	Area [Caged]	Area [AA]	*c* [Caged] (Mm)	*c* [AA] (mM)	% [Caged]	% [AA]
1	0	12,870,900	0	0.50	0	100	0
2	1	1,732,460	3,784,390	0.068	0.37	13	73
3	2	0	4,663,710	0	0.45	0	90
4	3	0	4,973,300	0	0.49	0	96
5	4	0	5,509,200	0	0.54	0	100
6	5	0	5,507,240	0	0.54	0	100
7	6	0	5,765,920	0	0.56	0	100
8	7	0	5,656,350	0	0.55	0	100
9	8	0	5,656,350	0	0.55	0	100

Complete photolysis of the Fmoc-Ser(DEACM)-O^{t}Bu (**217**) species in the mixture was

observed following irradiation at 350 nm for 2 h. This was accompanied by complete conversion to uncaged Fmoc-Ser-O^{t}Bu (**185**).

Table B.37: Determination of percentage composition of Fmoc-Asp(DMNB)-O^{t}Bu (**212**) and uncaged Fmoc-Asp-O^{t}Bu (**221**) following irradiation of mixture at 350 nm (8 h).

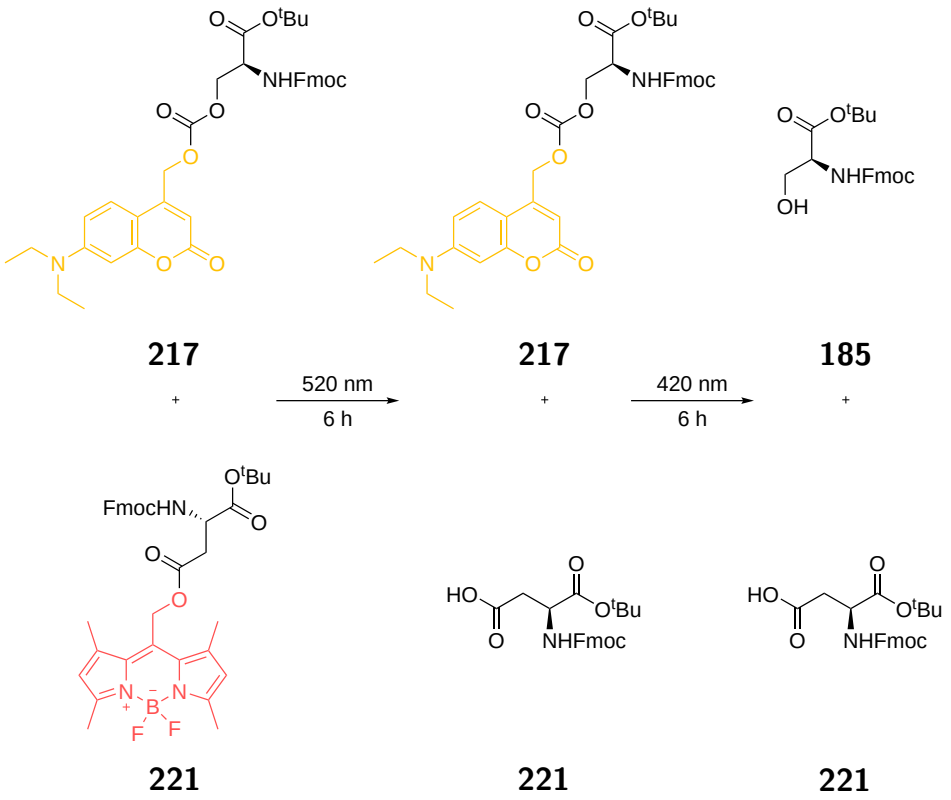
350 nm Irradiation of Fmoc-Asp(DMNB)-O^{t}Bu & Fmoc-Ser(DEACM)-O^{t}Bu							
Entry	t (h)	Area [Caged]	Area [AA]	*c* [Caged] (mM)	*c* [AA] (mM)	% [Caged]	% [AA]
1	0	16,201,400	0	0.51	0	100	0
2	1	13,021,000	1,126,260	0.41	0.08	80	16
3	2	10,029,600	2,531,220	0.31	0.18	62	35
4	3	6,741,340	4,110,870	0.21	0.29	42	58
5	4	3,767,290	6,016,100	0.12	0.43	23	84
6	5	1,308,560	6,829,640	0.04	0.48	8	96
7	6	231,840	7,267,410	0.01	0.51	1	100
8	7	0	6,706,000	0	0.47	0	94
9	8	0	5,642,920	0	0.40	0	79

Complete photolysis of the Fmoc-Asp(DMNB)-O^{t}Bu (**212**) species in the mixture was observed following 7 h irradiation at 350 nm. This was accompanied by complete conversion to uncaged Fmoc-Asp-O^{t}Bu (**221**).

These results indicated the possibility of wavelength selectivity between the DEACM and DMNB caging groups.

B.2.7 Irradiation of an Orthogonal System

520 nm (6 h) then 420 nm (6 h) Irradiation of Fmoc-Ser(DEACM)-O^{t}Bu (217) and Fmoc-Asp(BODIPY-2)-O^{t}Bu (251)



Scheme B.27: 520 nm then 420 nm photolysis of a mixture of Fmoc-Ser(DEACM)-O^{t}Bu (**217**) and Fmoc-Asp(BODIPY-2)-O^{t}Bu (**251**).

Table B.38: Determination of percentage composition of Fmoc-Ser(DEACM)-O^{t}Bu (**217**) and uncaged Fmoc-Ser-O^{t}Bu (**185**) following irradiation of mixture at 520 nm (6 h) then 420 nm (6 h).

520 then 420 nm Irradiation of Fmoc-Ser(DEACM)-O^{t}Bu & Fmoc-Asp(BODIPY)-O^{t}Bu							
Entry	t (h)	Area [Caged]	Area [AA]	*c* [Caged] (mM)	*c* [AA] (mM)	% [Caged]	% [AA]
1	0	22,361,500	0	0.88	0	100	0
2	2	22,536,300	0	0.88	0	100	0
3	4	23,187,700	0	0.91	0	100	0
4	6	22,763,700	0	0.89	0	100	0
5	8	8,846,690	8,266,410	0.35	0.81	40	92
6	10	3,193,930	11,835,300	0.13	1.15	14	100
7	12	1,107,100	14,441,700	0.04	1.41	5	100

No change in percentage composition was observed for the Fmoc-Ser(DEACM)-O^{t}Bu (**217**) species in the mixture following irradiation at 520 nm for 6 h. When the irradiation wavelength was changed to 420 nm, exposure to irradiation at this wavelength for a further 6 h led to near complete photolysis of the Fmoc-Ser(DEACM)-O^{t}Bu (**217**) species, accompanied by complete conversion to uncaged Fmoc-Ser-O^{t}Bu (**185**).

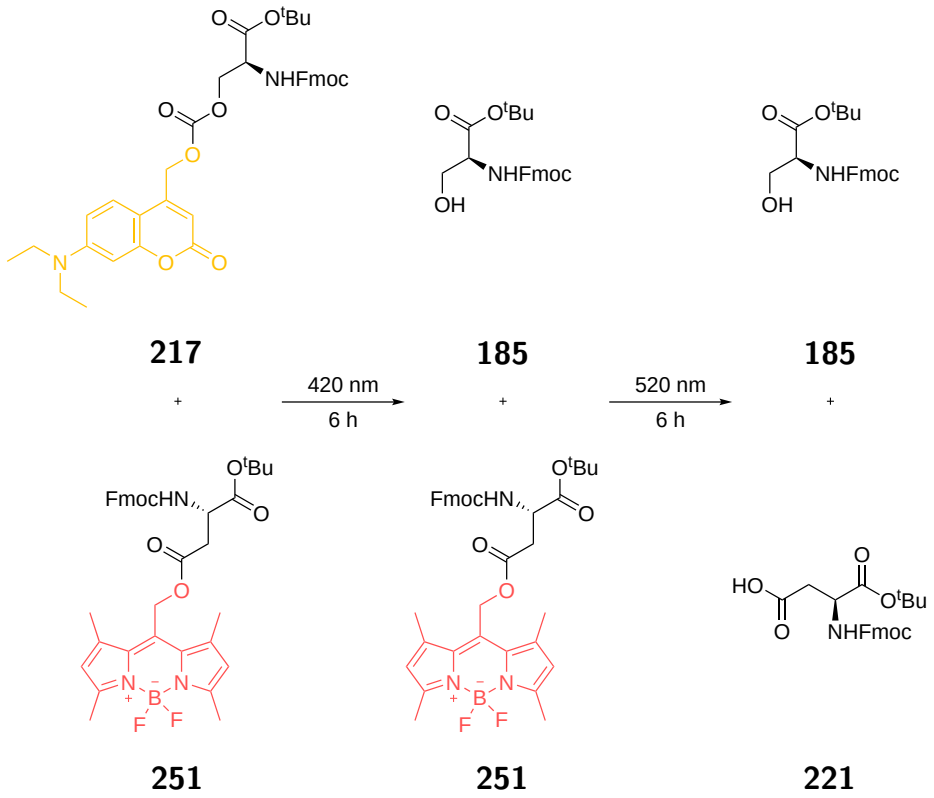
Table B.39: Determination of percentage composition of Fmoc-Asp(BODIPY-2)-O^{t}Bu (**251**) and uncaged Fmoc-Asp-O^{t}Bu (**221**) following irradiation of mixture at 520 nm (6 h) then 420 nm (6 h).

520 then 420 nm Irradiation of Fmoc-Ser(DEACM)-O^{t}Bu & Fmoc-Asp(BODIPY)-O^{t}Bu							
Entry	t (h)	Area [Caged]	Area [AA]	*c* [Caged] (mM)	*c* [AA] (mM)	% [Caged]	% [AA]
1	0	13,949,500	0	0.69	0.00	100	0
2	2	12,087,500	1,559,420	0.60	0.11	87	16
3	4	11,010,800	3,317,410	0.55	0.24	79	34
4	6	8,718,000	4,899,070	0.43	0.35	62	50
5	8	6,685,830	5,369,430	0.33	0.38	48	55
6	10	6,251,260	6,127,500	0.31	0.43	45	63
7	12	6,815,280	7,239,740	0.34	0.51	49	74

Exposure to irradiation at 520 nm for 6 h saw the percentage composition of the Fmoc-Asp(BODIPY-2)-O^{t}Bu (**251**) species in the mixture drop to 62% accompanied by 50% release of uncaged Fmoc-Asp-O^{t}Bu (**221**). When the irradiation wavelength was changed to 420 nm, initial exposure to irradiation at this wavelength saw the percentage composition of Fmoc-Asp(BODIPY-2)-O^{t}Bu (**251**) species in the mixture drop to 48% accompanied by a 5% increase in the percentage composition of uncaged Fmoc-Asp-O^{t}Bu (**221**). The percentage composition of the caged species then remained constant over the course of the remainder of the experiment which saw the percentage of composition of the uncaged species rise to 74%. This indicated that the drop of the caged species could be due to dark reaction as opposed to photolysis due to irradiation at 420 nm.

These results indicated the possibility of the DEACM and BODIPY caging groups to act as an orthogonal pair by exploiting the differences in rates of photolysis, following exposure to light at wavelengths of 420 and 520 nm, to photolyse the DEACM and BODIPY groups respectively.

420 nm (6 h) then 520 nm (6 h) Irradiation of Fmoc-Ser(DEACM)-O^{t}Bu (217) and Fmoc-Asp(BODIPY-2)-O^{t}Bu (251)



Scheme B.28: 420 nm then 520 nm photolysis of a mixture of Fmoc-Ser(DEACM)-O^{t}Bu (**217**) and Fmoc-Asp(BODIPY-2)-O^{t}Bu (**251**).

Table B.40: Determination of percentage composition of Fmoc-Ser(DEACM)-O^{t}Bu (**217**) and uncaged Fmoc-Ser-O^{t}Bu (**185**) following irradiation of mixture at 420 nm (6 h) then 520 nm (6 h).

420 then 520 nm Irradiation of Fmoc-Ser(DEACM)-O^{t}Bu & Fmoc-Asp(BODIPY)-O^{t}Bu							
Entry	t (h)	Area [Caged]	Area [AA]	*c* [Caged] (mM)	*c* [AA] (mM)	% [Caged]	% [AA]
1	0	22,459,600	0	0.88	0.00	100	0
2	2	9,317,380	7,153,820	0.37	0.70	41	79
3	4	3,735,970	10,246,600	0.15	1.00	17	100
4	6	877,397	11,611,900	0.03	1.13	4	100
5	8	899,518	11,313,800	0.04	1.10	4	100
6	10	902,985	11,839,600	0.04	1.15	4	100
7	12	839,520	11,299,900	0.03	1.10	4	100

Near complete photolysis of Fmoc-Ser(DEACM)-O^{t}Bu (**217**) was observed following irradiation at 420 nm for 6 h, accompanied by complete conversion to Fmoc-Ser-O^{t}Bu (**185**). There was no decline in the percentage composition of Fmoc-Ser-O^{t}Bu (**185**) following subsequent irradiation at 530 nm for 6 h.

Table B.41: Determination of percentage composition of Fmoc-Asp(BODIPY-2)-O^{t}Bu (**251**) and uncaged Fmoc-Asp-O^{t}Bu (**221**) following irradiation of mixture at 420 nm (6 h) then 520 nm (6 h).

420 then 520 nm Irradiation of Fmoc-Ser(DEACM)-O^{t}Bu & Fmoc-Asp(BODIPY)-O^{t}Bu							
Entry	t (h)	Area [Caged]	Area [AA]	*c* [Caged] (mM)	*c* [AA] (mM)	% [Caged]	% [AA]
1	0	14,757,400	0	0.73	0.00	100	0
2	2	13,146,800	1,206,010	0.65	0.09	89	12
3	4	12,213,900	1,810,540	0.61	0.13	83	18
4	6	11,031,100	2,308,400	0.55	0.16	75	22
5	8	9,214,960	3,606,010	0.46	0.26	62	35
6	10	8,065,530	4,984,550	0.40	0.35	55	48
7	12	6,577,740	5,736,270	0.33	0.41	45	56

Following irradiation at 420 nm for 6 h, a 25% drop in the percentage composition of Fmoc-Asp(BODIPY-2)-O^{t}Bu (**251**) was observed, accompanied by 22% release of Fmoc-Asp-O^{t}Bu (**221**). Following subsequent irradiation at 530 nm for 6 h, the percentage composition of Fmoc-Asp(BODIPY-2)-O^{t}Bu (**251**) dropped by a further 30% with the composition of released Fmoc-Asp-O^{t}Bu (**221**) rising to 56%.

These results indicated the possibility of the DEACM and BODIPY caging groups to act as an orthogonal pair by exploiting the differences in rates of photolysis following exposure to light at wavelengths of 420 and 520 nm, to photolyse the DEACM and BODIPY groups respectively.

B.3 Determination of Calibration Curves by LCMS

B.3.1 Calibration of Fmoc-Asp-O^{t}Bu (221)

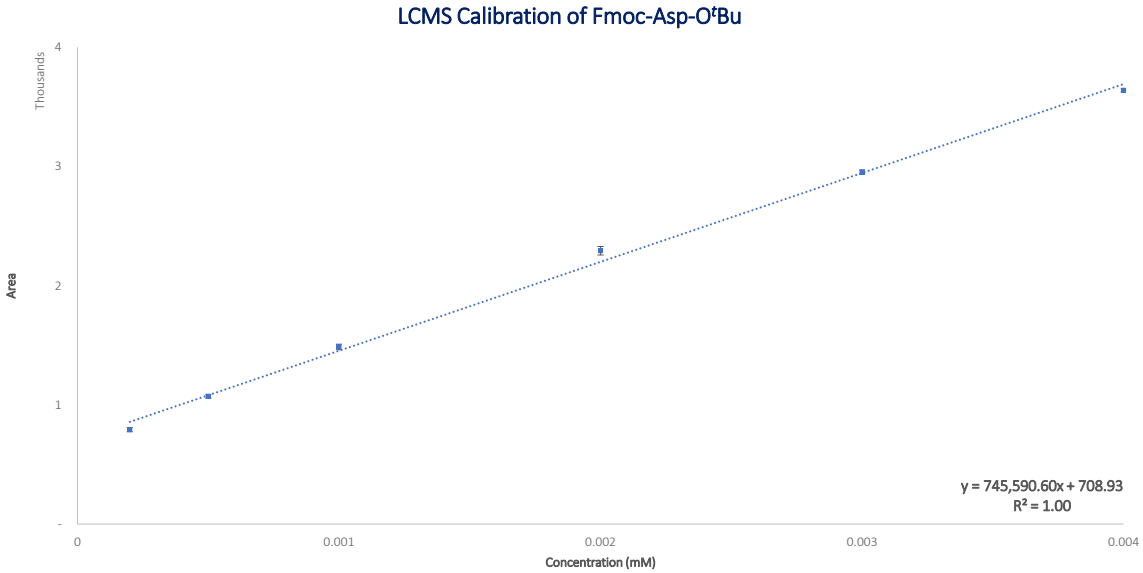


Figure B.10: Linear relationship of concentration vs. area of Fmoc-Asp-O^{t}Bu (**221**).

Table B.42: LCMS calibration data for Fmoc-Asp-O^{t}Bu (**221**).

Fmoc-Asp-O^{t}Bu		
Entry	*c* (mM)	Area
1	0.0002	792.00
2	0.0005	1072.33
3	0.001	1485.88
4	0.002	2292.08
5	0.003	2951.61
6	0.004	3637.52

Gradient $= 0.746 \times 10^6$
Intercept $= 709$

B.3.2 Calibration of Fmoc-Asp(DEACM)-O^{t}Bu (215)

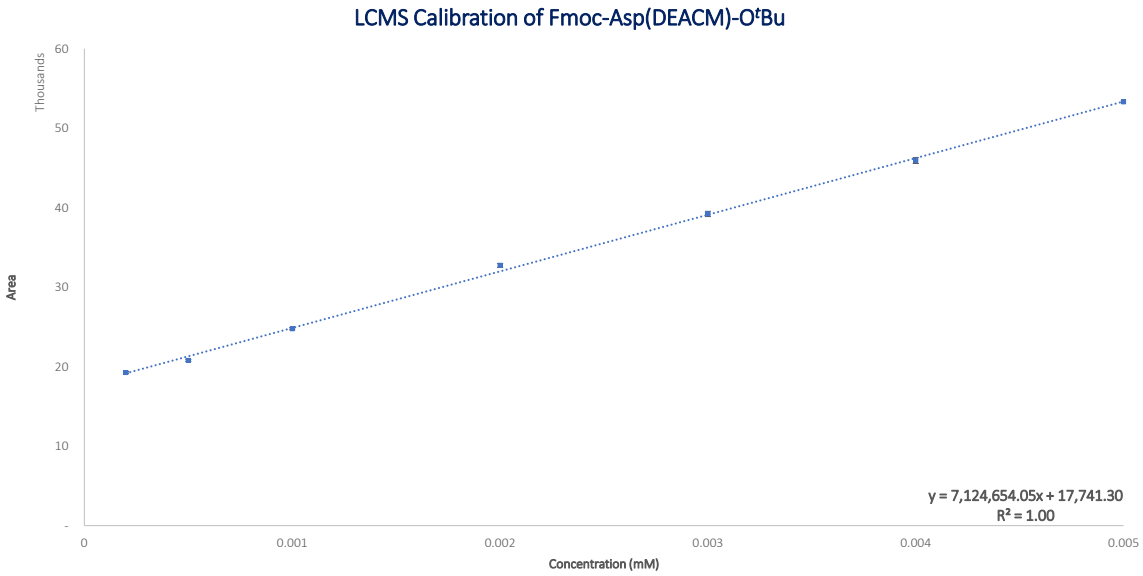


Figure B.11: Linear relationship of concentration vs. area of Fmoc-Asp(DEACM)-O^{t}Bu (**215**).

Table B.43: LCMS calibration data for Fmoc-Asp(DEACM)-O^{t}Bu (**215**).

Fmoc-Asp(DEACM)-O^{t}Bu		
Entry	*c* (mM)	Area
1	0.0002	19270.57
2	0.0005	20789.75
3	0.001	24779.59
4	0.002	32740.66
5	0.003	39221.52
6	0.004	45934.28
7	0.005	53309.78

Gradient $= 7.12 \times 10^6$
Intercept $= 17.7 \times 10^3$

B.3.3 Calibration of Fmoc-Asp(BODIPY-2)-O^{t}Bu (251)

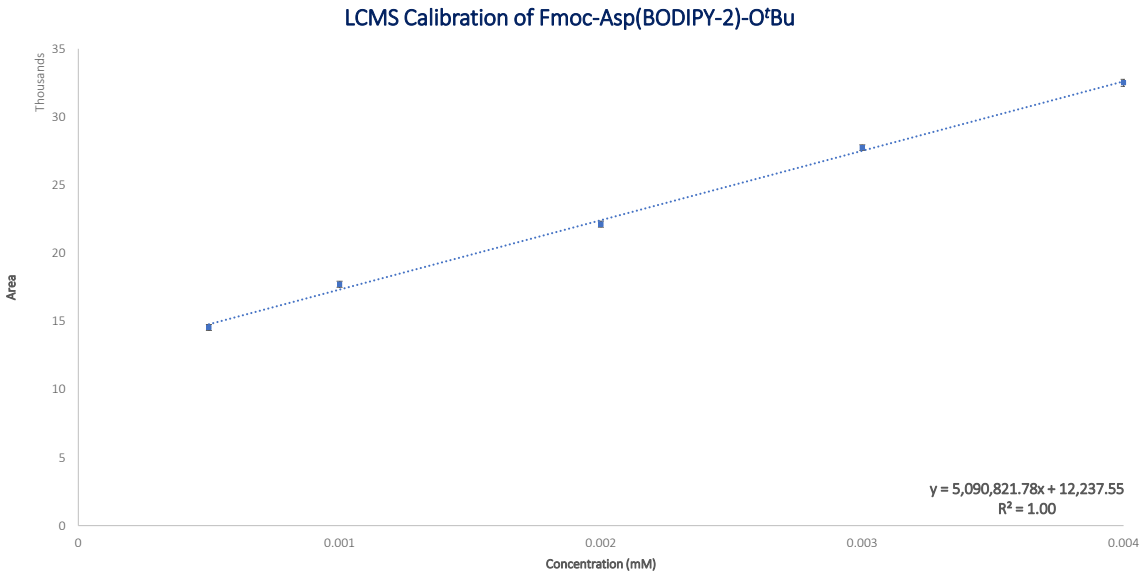


Figure B.12: Linear relationship of concentration vs. area of Fmoc-Asp(BODIPY-2)-O^{t}Bu (**251**).

Table B.44: LCMS calibration data for Fmoc-Asp(BODIPY-2)-O^{t}Bu (**251**).

Fmoc-Asp(BODIPY-2)-O^{t}Bu		
Entry	*c* (mM)	Area
1	0.0005	14546.87
2	0.001	17717.54
3	0.002	22131.36
4	0.003	27744.50
5	0.004	32501.11

Gradient $= 5.09 \times 10^6$
Intercept $= 12.2 \times 10^3$

B.3.4 Calibration of KLD (269)

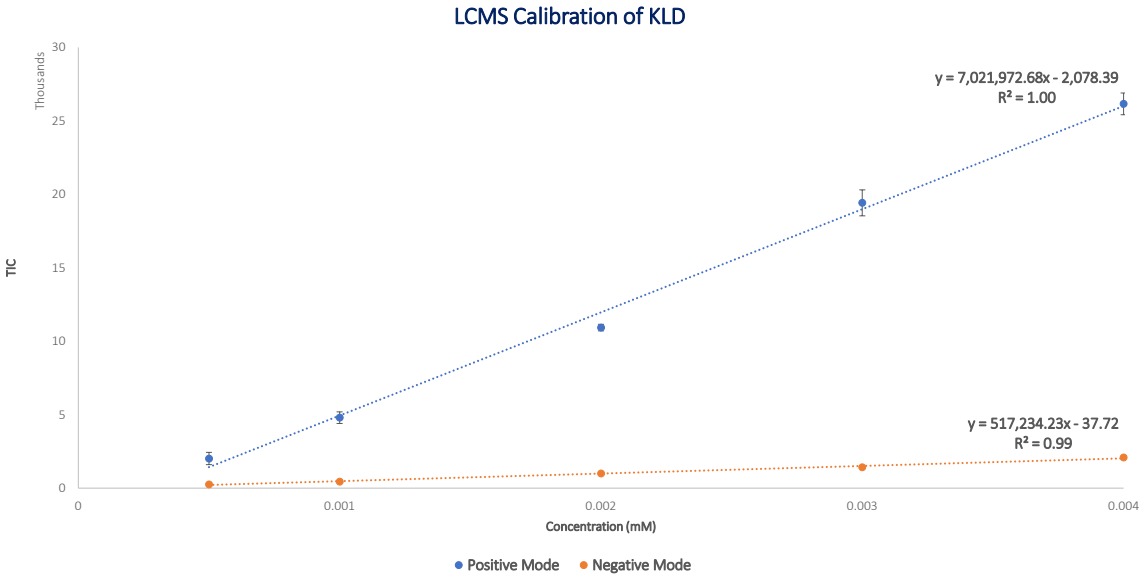


Figure B.13: Linear relationship of area vs. concentration of KLD (**269**).

Table B.45: LCMS calibration data for KLD (**269**).

KLD			
Entry	*c* (mM)	Area (+ve)	Area (-ve)
1	0.0005	2019.80	262.40
2	0.001	4803.22	450.77
3	0.002	10931.04	1009.13
4	0.003	19422.44	1430.16
5	0.004	26162.26	2089.88

Positive Mode:
Gradient = 7.02×10^6
Intercept = -2.08 $\times$ 10^3

Negative Mode:
Gradient = 0.517×10^6
Intercept = -37.7

B.3.5 Calibration of KLD-DEACM (267)

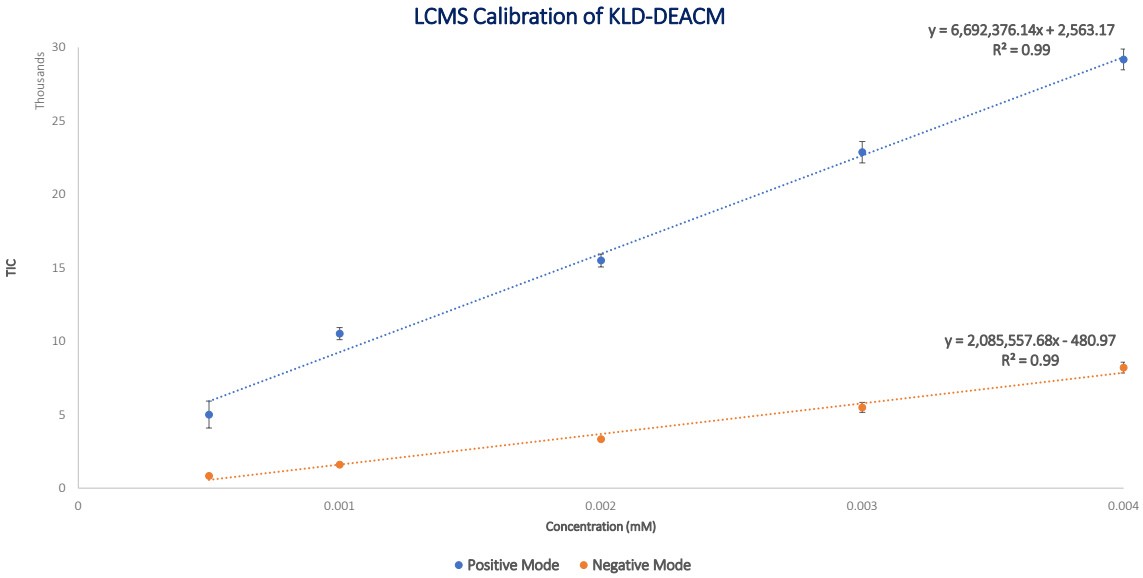


Figure B.14: Linear relationship of area vs. concentration of KLD-DEACM (**267**).

Table B.46: LCMS calibration data for KLD-DEACM (**267**).

KLD-DEACM			
Entry	*c* (mM)	Area (+ve)	Area (-ve)
1	0.0005	5012.71	835.80
2	0.001	10525.70	1610.62
3	0.002	15497.19	3338.32
4	0.003	22869.61	5502.25
5	0.004	29180.61	8206.50

Positive Mode:
Gradient = 6.69×10^6
Intercept = 2.56×10^3

Negative Mode:
Gradient = 2.09×10^6
Intercept = -481

B.3.6 Calibration of BODIPY-KLD (268)

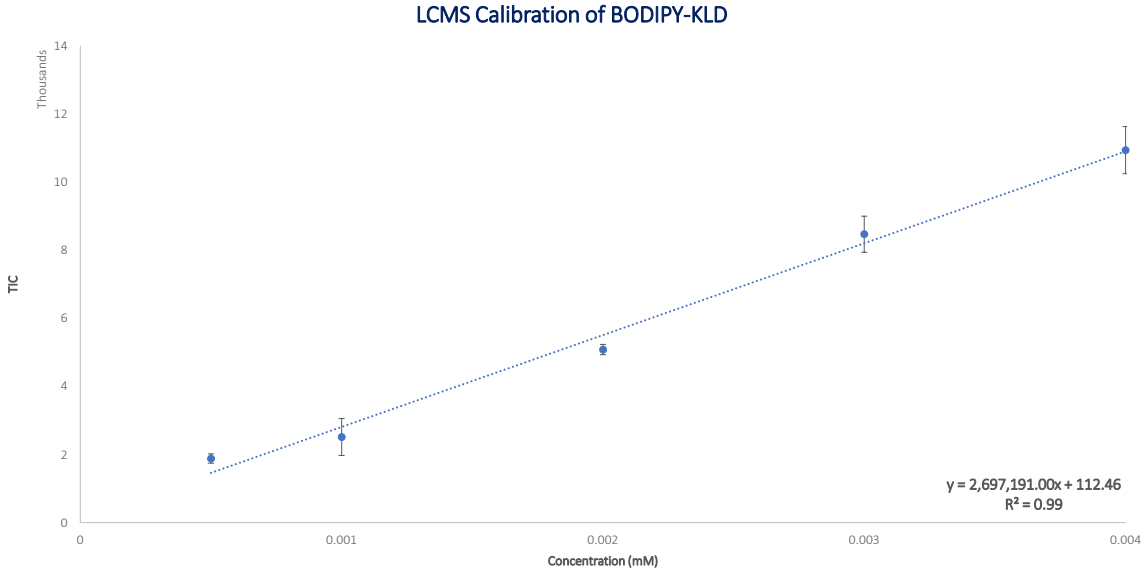


Figure B.15: Linear relationship of area vs. concentration of BODIPY-KLD (**268**).

Table B.47: LCMS calibration data for BODIPY-KLD (**268**).

BODIPY-KLD		
Entry	*c* (mM)	Area
1	0.0005	1882.41
2	0.001	2513.10
3	0.002	5082.09
4	0.003	8468.45
5	0.004	10936.75

Gradient $= 2.70 \times 10^6$
Intercept $= 112$

B.3.7 Calibration of BODIPY-KLD-DEACM (266)

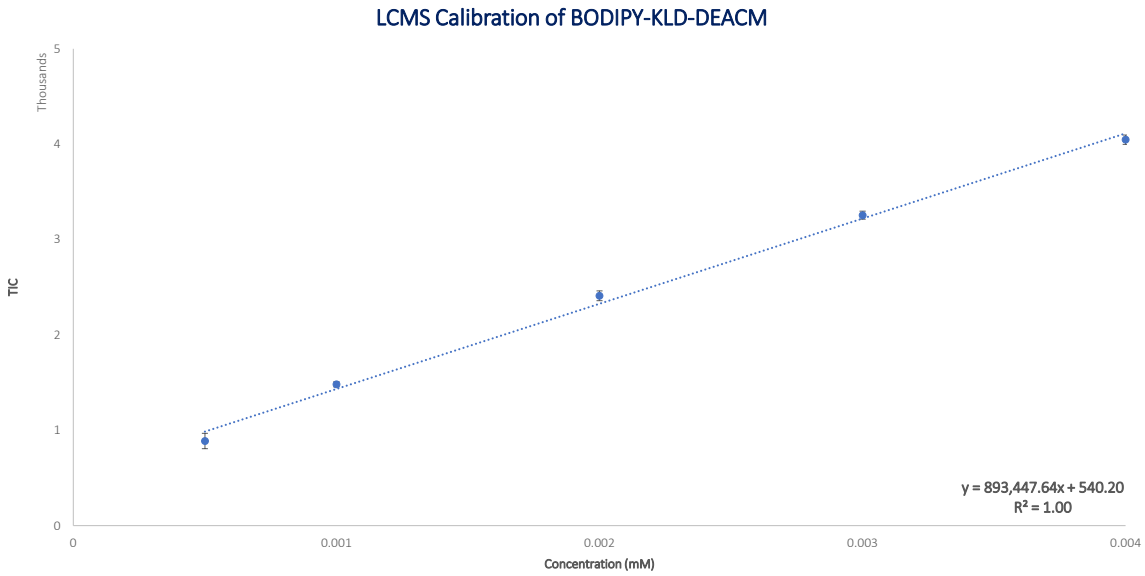


Figure B.16: Linear relationship of area vs. concentration of BODIPY-KLD-DEACM (**266**).

Table B.48: LCMS calibration data for BODIPY-KLD-DEACM (**266**).

BODIPY-KLD-DEACM		
Entry	*c* (mM)	Area
1	0.0005	888.07
2	0.001	1481.82
3	0.002	2410.68
4	0.003	3254.83
5	0.004	4046.79

Gradient $= 0.893 \times 10^6$
Intercept $= 540$

B.3.8 Calibration of KGSTAD (270)

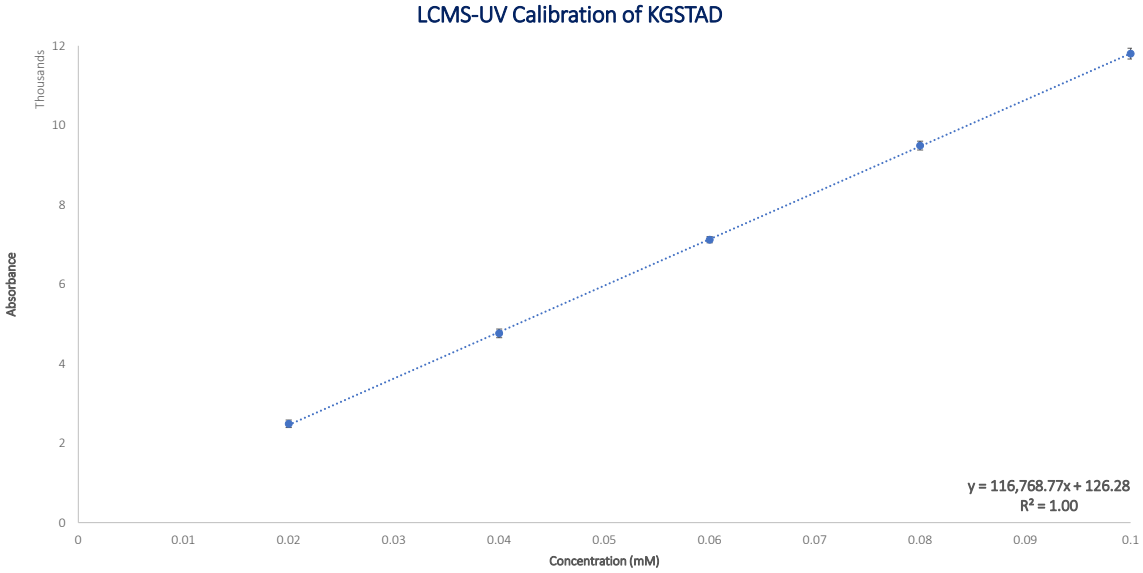


Figure B.17: Linear relationship of absorbance vs. concentration of KGSTAD (**270**).

Table B.49: LCMS calibration data for KGSTAD (**270**).

KGSTAD		
Entry	*c* (mM)	Abs (A)
1	0.02	2487.14
2	0.04	4763.54
3	0.06	7121.48
4	0.08	9488.20
5	0.10	11801.69

Gradient $= 0.117 \times 10^6$
Intercept $= 126$

B.3.9 Calibration of KGSTAD-DEACM (5)

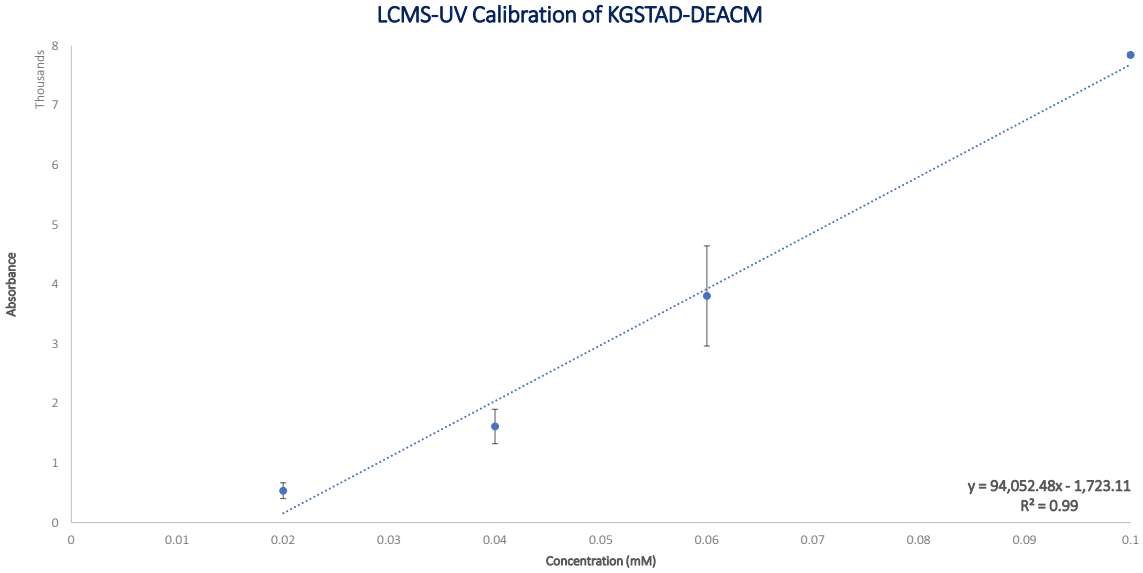


Figure B.18: Linear relationship of absorbance vs. concentration of KGSTAD-DEACM (**5**).

Table B.50: LCMS calibration data for KGSTAD-DEACM (**5**).

KGSTAD-DEACM		
Entry	*c* (mM)	Abs (A)
1	0.02	535.55
2	0.04	1613.58
3	0.06	3304.23
4	0.08	5900.73
5	0.10	7847.04

Gradient = 94.1 × 10^3
Intercept = -1.72 × 10^3

B.3.10 Calibration of BODIPY-KGSTAD (4)

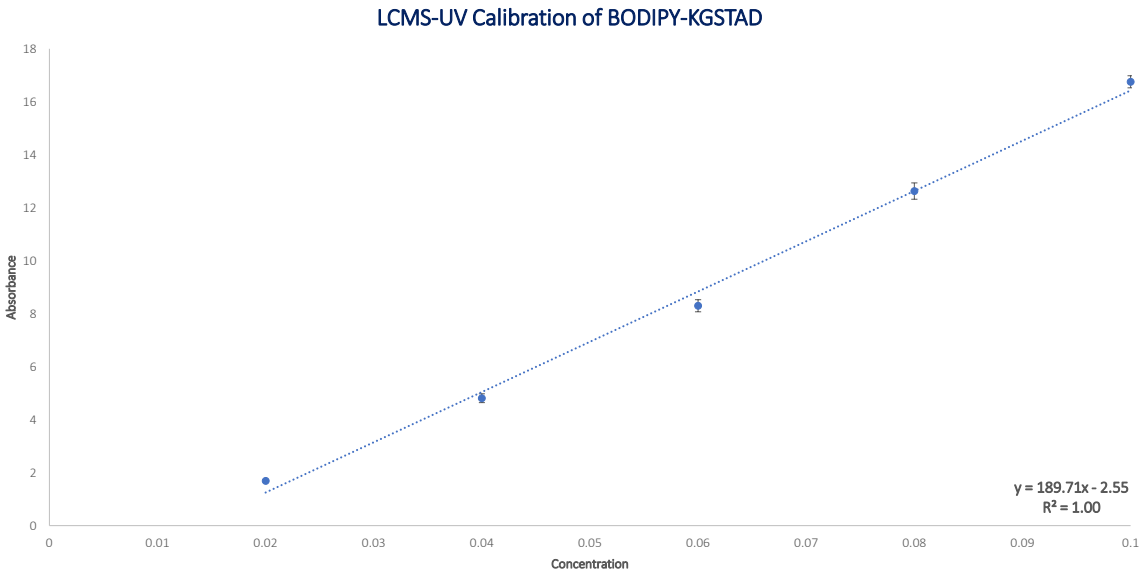


Figure B.19: Linear relationship of absorbance vs. concentration of BODIPY-KGSTAD (**4**).

Table B.51: LCMS calibration data for BODIPY-KGSTAD (**4**).

BODIPY-KGSTAD		
Entry	*c* (mM)	Abs (A)
1	0.02	1.69
2	0.04	4.81
3	0.06	8.30
4	0.08	12.63
5	0.10	16.75

Gradient = 190
Intercept = -2.55

B.3.11 Calibration of BODIPY-KGSTAD-DEACM (3)

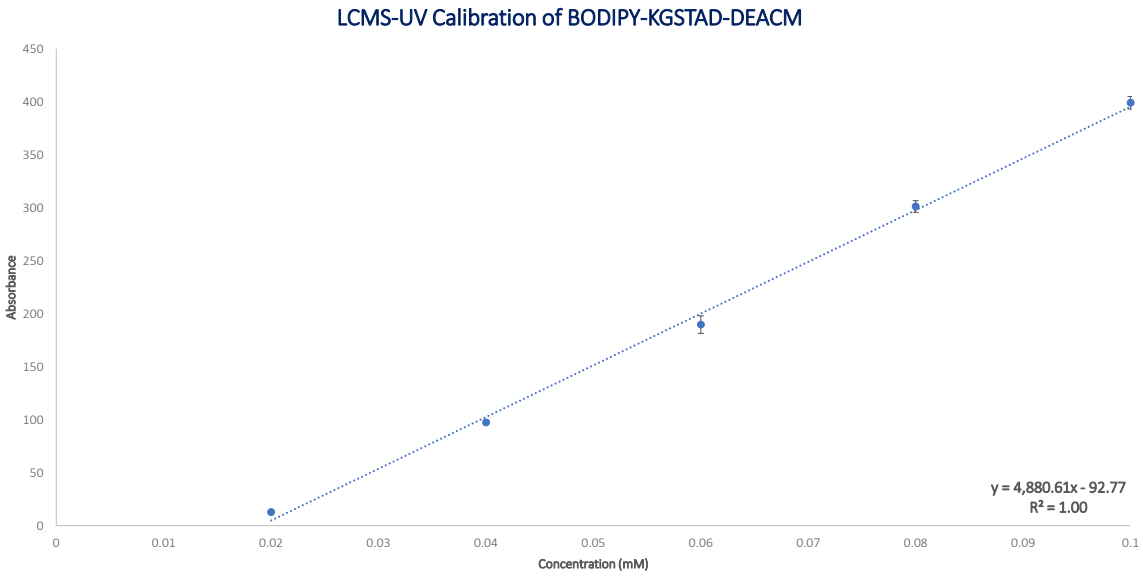


Figure B.20: Linear relationship of absorbance vs. concentration of BODIPY-KGSTAD-DEACM (**3**).

Table B.52: LCMS calibration data for BODIPY-KGSTAD-DEACM (**3**).

BODIPY-KGSTAD-DEACM		
Entry	*c* (mM)	Abs (A)
1	0.02	12.83
2	0.04	97.52
3	0.06	189.72
4	0.08	301.18
5	0.10	399.06

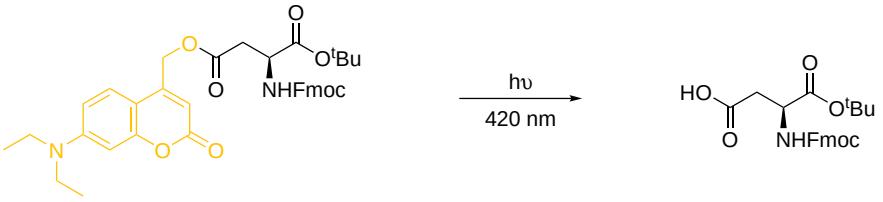
Gradient = 4.88×10^3

Intercept = -92.8

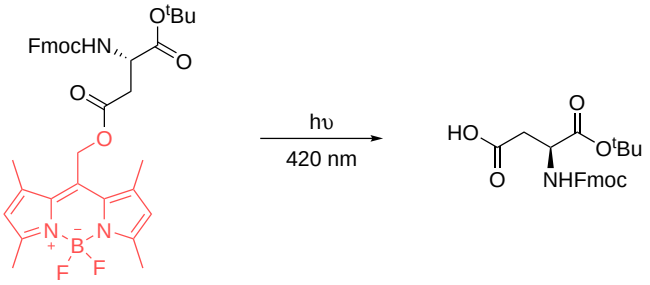
B.4 Photolysis Data as Measured by LCMS

B.4.1 Irradiation at $\lambda = 420$ nm

420 nm Irradiation of Fmoc-Asp(DEACM)-O^{t}Bu (215)


O
O
O

420 nm Irradiation of Fmoc-Asp(BODIPY-2)-O^{t}Bu (251)



251 **221**

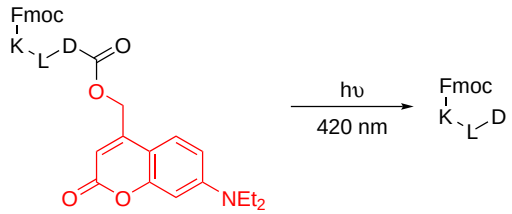
Scheme B.30: 420 nm photolysis of Fmoc-Asp(BODIPY-2)-O^{t}Bu (**251**).

Table B.54: Determination of percentage composition of Fmoc-Asp(BODIPY-2)-O^{t}Bu (**251**) and uncaged Fmoc-Asp-O^{t}Bu (**221**) following irradiation at 420 nm.

420 nm Irradiation of Fmoc-Asp(BODIPY-2)-O^{t}Bu							
Entry	t (min)	Area [Caged]	Area [AA]	*c* [Caged] (mM)	*c* [AA] (mM)	% [Caged]	% [AA]
1	0	32,488.06	-	0.00398	0.00000	100%	0%
2	0.5	32,936.59	-	0.00407	0.00000	100%	0%
3	1	32,727.23	-	0.00402	0.00000	100%	0%
4	2	33,020.90	-	0.00408	0.00000	100%	0%
5	4	32,489.59	-	0.00398	0.00000	100%	0%
6	10	32,623.37	-	0.00400	0.00000	100%	0%

The percentage composition of Fmoc-Asp(BODIPY-2)-O^{t}Bu (**251**) remained constant following exposure to irradiation at 420 nm with no released uncaged Fmoc-Asp-O^{t}Bu (**221**) observed.

420 nm Irradiation of KLD-DEACM (**267**)



267 **269**

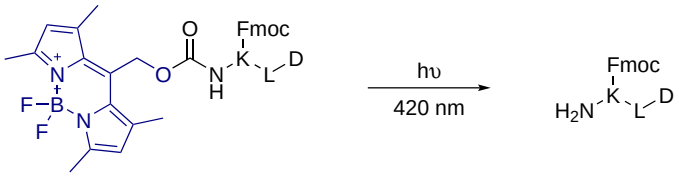
Scheme B.31: 420 nm photolysis of KLD-DEACM (**267**).

Table B.55: Determination of percentage composition of KLD-DEACM (**267**) and uncaged KLD (**269**) following irradiation at 420 nm.

420 nm Irradiation of KLD-DEACM							
Entry	t (min)	Area [Caged]	Area [AA]	*c* [Caged] (mM)	*c* [AA] (mM)	% [Caged]	% [AA]
1	0	29,548.68	-	0.00403	0.00000	100%	0%
2	0.25	20,642.14	11,288.21	0.00270	0.00190	67%	47%
3	0.5	15,828.57	15,964.95	0.00198	0.00257	49%	64%
4	0.75	10,906.46	18,967.68	0.00125	0.00300	31%	74%
5	1	8,785.01	20,741.18	0.00093	0.00325	23%	81%
6	2	2,938.92	22,802.13	0.00006	0.00354	1%	88%
7	4	1,389.31	23,622.16	0.00000	0.00366	0%	91%
8	10	681.16	24,168.31	0.00000	0.00374	0%	93%

Complete photolysis of KLD-DEACM (**267**) was observed following irradiation at 420 nm for 4 min. This was accompanied by 93% release of uncaged KLD (**269**).

420 nm Irradiation of BODIPY-KLD (268)



268 **269**

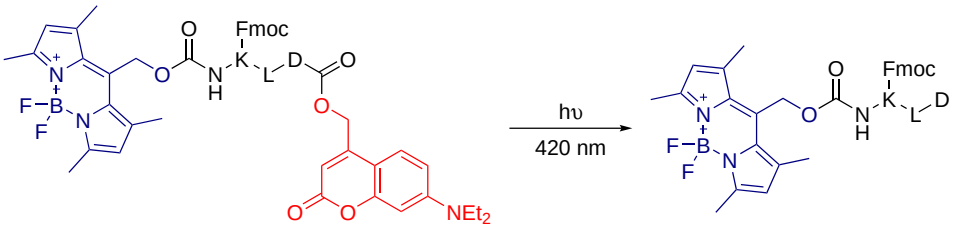
Scheme B.32: 420 nm photolysis of BODIPY-KLD (**268**).

Table B.56: Determination of percentage composition of BODIPY-KLD (**268**) and uncaged KLD (**269**) following irradiation at 420 nm.

420 nm Irradiation of BODIPY-KLD							
Entry	t (min)	Area [Caged]	Area [AA]	*c* [Caged] (mM)	*c* [AA] (mM)	% [Caged]	% [AA]
1	0	10,911.88	-	0.00400	0.00000	100%	0%
2	0.5	11,218.65	-	0.00412	0.00000	100%	0%
3	1	11,424.32	-	0.00419	0.00000	100%	0%
4	2	11,639.89	-	0.00427	0.00000	100%	0%
5	4	11,326.36	-	0.00416	0.00000	100%	0%
6	10	11,411.79	-	0.00419	0.00000	100%	0%

The percentage composition of BODIPY-KLD (**268**) remained constant following exposure to irradiation at 420 nm with no uncaged KLD (**269**) observed.

420 nm Irradiation of BODIPY-KLD-DEACM (**266**)



266 **268**

Scheme B.33: 420 nm photolysis of BODIPY-KLD-DEACM (**266**).

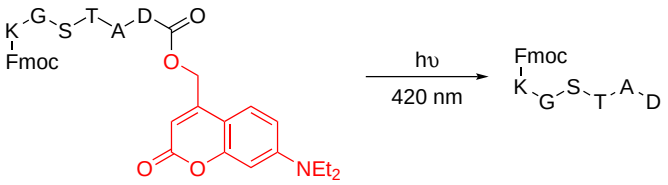
Table B.57: Determination of percentage composition of BODIPY-KLD-DEACM (**266**) and uncaged BODIPY-KLD (**268**) following irradiation at 420 nm.

420 nm Irradiation of BODIPY-KLD-DEACM							
Entry	t (min)	Area [Caged]	Area [AA]	*c* [Caged] (mM)	*c* [AA] (mM)	% [Caged]	% [AA]
1	0	4,282.68	-	0.00419	0.00000	100%	0%
2	15	3,271.64	1,479.21	0.00306	0.00051	73%	12%
3	30	2,483.16	2,524.33	0.00217	0.00089	52%	21%
4	45	2,006.46	4,652.08	0.00164	0.00168	39%	40%
5	60	1,568.61	5,955.78	0.00115	0.00217	27%	52%
6	120	879.21	7,474.40	0.00038	0.00273	9%	65%

The percentage composition of BODIPY-KLD-DEACM (**266**) dropped to 9% following 120 min of exposure to irradiation at 420 nm. This was accompanied by 65% release of uncaged BODIPY-KLD (**268**). Importantly, no products relating to uncaging of the BODIPY group at this wavelength was observed.

These results indicated the possibility of the DEACM and BODIPY caging groups to act as a pair of wavelength orthogonal caging groups.

420 nm Irradiation of KGSTAD-DEACM (**5**)



5 **270**

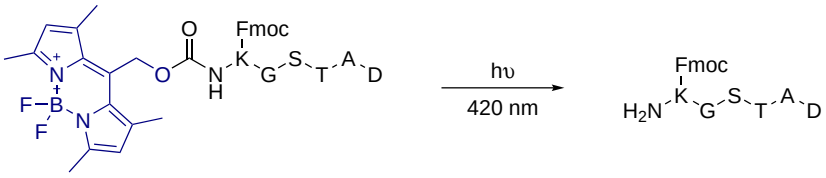
Scheme B.34: 420 nm photolysis of KGSTAD-DEACM (**5**).

Table B.58: Determination of percentage composition of KGSTAD-DEACM (**5**) and uncaged KGSTAD (**270**) following irradiation at 420 nm.

420 nm Irradiation of KGSTAD-DEACM							
Entry	t (min)	Abs [Caged]	Abs [AA]	*c* [Caged] (mM)	*c* [AA] (mM)	% [Caged]	% [AA]
1	0	8048.13	0.00	0.105	0.000	100%	0%
2	1	1946.16	6513.06	0.040	0.055	38%	52%
3	2	735.58	7483.91	0.027	0.063	26%	60%
4	5	0.00	7812.17	0.000	0.066	0%	63%
5	10	0.00	8655.36	0.000	0.073	0%	70%
6	20	0.00	8778.45	0.000	0.074	0%	71%
7	30	0.00	9195.52	0.000	0.077	0%	74%
8	45	0.00	9582.53	0.000	0.081	0%	77%
9	60	0.00	9625.76	0.000	0.081	0%	78%
10	90	0.00	10273.10	0.000	0.087	0%	83%
11	120	0.00	10669.00	0.000	0.090	0%	86%

Complete photolysis of KGSTAD-DEACM (**5**) was observed following exposure to irradiation at 420 nm for 5 min. This was accompanied by 86% release of uncaged KGSTAD (**270**) after 120 min.

420 nm Irradiation of BODIPY-KGSTAD (4)



4 **270**

Scheme B.35: 420 nm photolysis of BODIPY-KGSTAD (**4**).

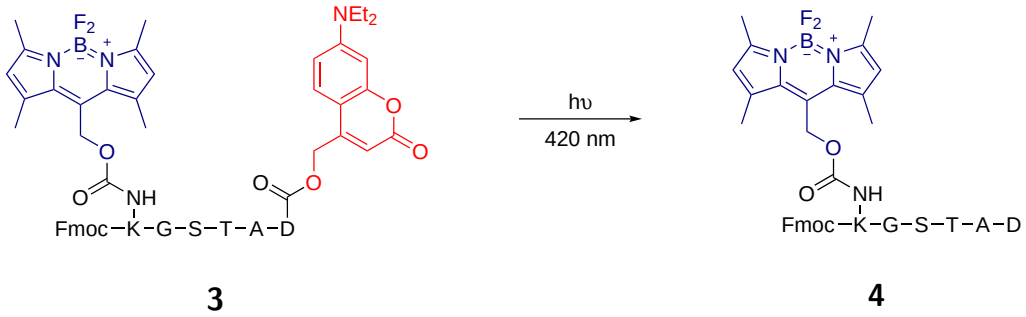
Table B.59: Determination of percentage composition of BODIPY-KGSTAD (**4**) and uncaged KGSTAD (**270**) following irradiation at 420 nm.

420 nm Irradiation of BODIPY-KGSTAD							
Entry	t (min)	Abs [Caged]	Abs [AA]	*c* [Caged] (mM)	*c* [AA] (mM)	% [Caged]	% [AA]
1	0	19.65	0.00	0.117	0.000	100%	0%
2	1	20.25	0.00	0.120	0.000	100%	0%
3	2	22.57	2.36	0.132	0.000	100%	0%
4	5	22.21	13.42	0.131	0.000	100%	0%
5	10	16.46	28.01	0.100	-0.020	86%	0%
6	20	12.06	71.95	0.077	0.003	66%	3%
7	30	6.85	94.71	0.050	0.030	42%	26%
8	45	4.78	111.74	0.039	0.041	33%	35%
9	60	3.53	119.15	0.032	0.048	27%	41%
10	120	2.06	130.73	0.024	0.056	21%	48%

Initial exposure of BODIPY-KGSTAD (**4**) to irradiation at 420 nm resulted in no change to the percentage composition of BODIPY-KGSTAD (**4**) and no formation of uncaged KGSTAD (**270**). However, prolonged exposure to irradiation at 420 nm, resulted in the percentage composition of BODIPY-KGSTAD (**4**) dropping to 21% after 120 min, accompanied by 48% release of uncaged KGSTAD (**270**).

These results indicated the possibility of exploiting the differences in kinetics between photolysis of the DEACM and BODIPY caging groups, at 420 nm and 530 nm, as a means of achieving wavelength orthogonality.

420 nm Irradiation of BODIPY-KGSTAD-DEACM (3)



3 **4**

Scheme B.36: 420 nm photolysis of BODIPY-KGSTAD-DEACM (**3**).

Table B.60: Determination of percentage composition of BODIPY-KGSTAD-DEACM (**3**) and BODIPY-KGSTAD (**4**) following irradiation at 420 nm.

420 nm Irradiation of BODIPY-KGSTAD-DEACM							
Entry	t (min)	Abs [Caged]	Abs [AA]	*c* [Caged] (mM)	*c* [AA] (mM)	% [Caged]	% [AA]
1	0	553.41	0.00	0.132	0.000	100%	0%
2	1	301.31	8.54	0.081	0.058	61%	44%
3	2	210.12	12.35	0.062	0.079	47%	59%
4	5	42.64	15.01	0.028	0.093	21%	70%
5	10	10.05	16.03	0.021	0.098	16%	74%
6	20	0.00	9.79	0.000	0.065	0%	49%
7	30	0.00	7.06	0.000	0.051	0%	38%
8	45	0.00	4.40	0.000	0.037	0%	28%
9	60	0.00	1.23	0.000	0.020	0%	15%
10	90	0.00	0.00	0.000	0.000	0%	0%
11	120	0.00	0.00	0.000	0.000	0%	0%

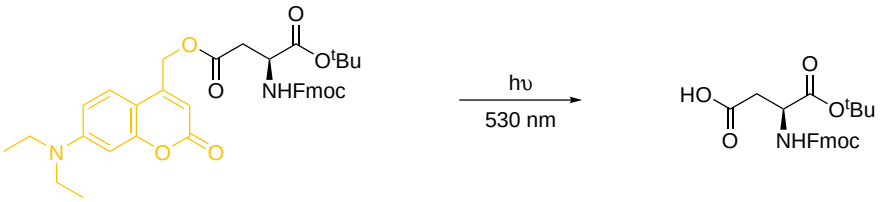
Following exposure to irradiation at 420 nm, the percentage composition of BODIPY-KGSTAD-DEACM (**3**) dropped to 16% after 10 min. This was accompanied by a maximum 74% release of uncaged BODIPY-KGSTAD (**4**) resulting from uncaging of the DEACM group. Prolonged exposure to irradiation at 420 nm then saw a decrease in the percentage composition of the released BODIPY-KGSTAD (**4**) accompanied by the release of the fully uncaged KGSTAD (**270**) species. Importantly, no KGSTAD-DEACM (**5**) resulting from uncaging of the BODIPY caging group was observed.

These results highlighted the possibility of exploiting the difference in kinetics between

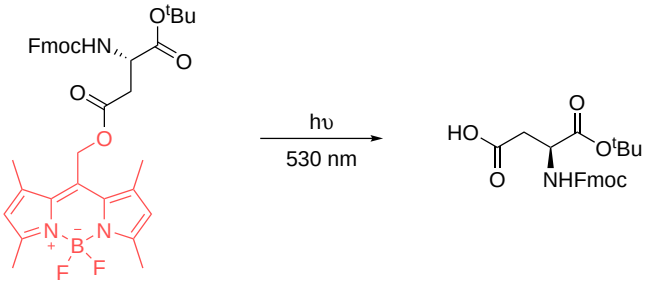
the DEACM and BODIPY groups upon exposure to irradiation at 420 nm and 530 nm as a means of achieving wavelength orthogonality.

B.4.2 Irradiation at $\lambda = 530$ nm

530 nm Irradiation of Fmoc-Asp(DEACM)-O^{t}Bu (215)


O
O
O

530 nm Irradiation of Fmoc-Asp(BODIPY-2)-O^{t}Bu (251)



251 **221**

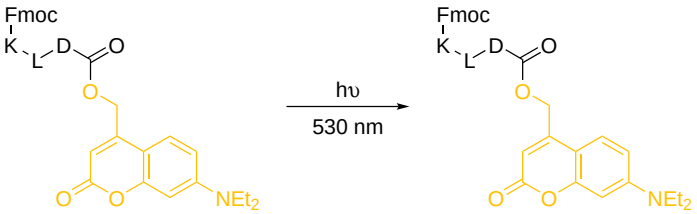
Scheme B.38: 530 nm photolysis of Fmoc-Asp(BODIPY-2)-O^{t}Bu (**251**).

Table B.62: Determination of percentage composition of Fmoc-Asp(BODIPY-2)-O^{t}Bu (**251**) and uncaged Fmoc-Asp-O^{t}Bu (**221**) following irradiation at 530 nm.

530 nm Irradiation of Fmoc-Asp(BODIPY-2)-O^{t}Bu							
Entry	t (min)	Area [Caged]	Area [AA]	*c* [Caged] (mM)	*c* [AA] (mM)	% [Caged]	% [AA]
1	0	32,300.28	-	0.00394	-	100%	0%
2	15	27,264.00	1,185.04	0.00295	0.00064	75%	16%
3	30	22,726.17	1,670.79	0.00206	0.00129	52%	33%
4	45	19,549.03	2,120.34	0.00144	0.00189	36%	48%
5	60	16,709.77	2,280.86	0.00088	0.00211	22%	53%
6	90	13,901.20	2,374.21	0.00033	0.00223	8%	57%
7	120	8,463.03	2,566.48	-0.00074	0.00249	0%	63%

Exposure to irradiation at 530 nm for 120 min saw complete photolysis of Fmoc-Asp(BODIPY-2)-O^{t}Bu (**251**), accompanied by 63% formation of uncaged Fmoc-Asp-O^{t}Bu (**221**).

530 nm Irradiation of KLD-DEACM (**267**)



267 **267**

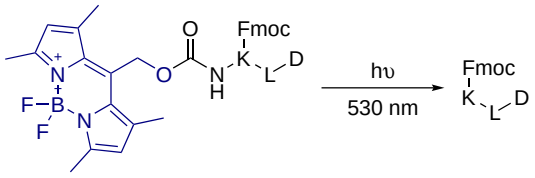
Scheme B.39: 530 nm photolysis of KLD-DEACM (**267**).

Table B.63: Determination of percentage composition of KLD-DEACM (**267**) and uncaged KLD (**269**) following irradiation at 530 nm.

530 nm Irradiation of KLD-DEACM							
Entry	t (min)	Area [Caged]	Area [AA]	*c* [Caged] (mM)	*c* [AA] (mM)	% [Caged]	% [AA]
1	0	22934.35733	-	0.01123	0.00000	100%	0%
2	15	22849.07567	-	0.01119	0.00000	100%	0%
3	30	23236.13167	-	0.01137	0.00000	100%	0%
4	60	23024.34967	-	0.01127	0.00000	100%	0%
5	120	22881.516	-	0.01120	0.00000	100%	0%

Following exposure to irradiation at 530 nm for 120 min, no change in percentage composition of KLD-DEACM (**267**) was observed. In addition, no formation of uncaged KLD (**269**) was detected.

530 nm Irradiation of BODIPY-KLD (268)



268 **269**

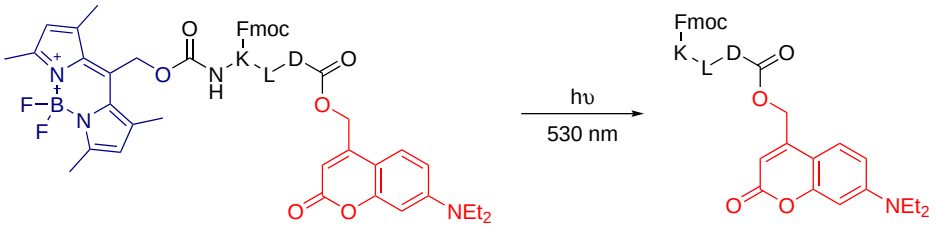
Scheme B.40: 530 nm photolysis of BODIPY-KLD (**268**).

Table B.64: Determination of percentage composition of BODIPY-KLD (**268**) and uncaged KLD (**269**) following irradiation at 530 nm.

530 nm Irradiation of BODIPY-KLD							
Entry	t (min)	Area [Caged]	Area [AA]	*c* [Caged] (mM)	*c* [AA] (mM)	% [Caged]	% [AA]
1	0	12,239.22	-	0.00450	0.00000	100%	0%
2	15	8,290.80	647.23	0.00303	0.00132	67%	29%
3	30	5,924.05	978.95	0.00215	0.00197	48%	44%
4	45	4,271.32	1,254.09	0.00154	0.00250	34%	56%
5	60	2,692.04	1,466.86	0.00096	0.00291	21%	65%
6	120	675.54	1,810.51	0.00021	0.00357	5%	79%

Exposure to irradiation at 530 nm for 120 min saw the percentage composition of BODIPY-KLD (**268**) drop to 5 %, accompanied by 79% formation of released uncaged KLD (**269**).

530 nm Irradiation of BODIPY-KLD-DEACM (266)



266 **267**

Scheme B.41: 530 nm photolysis of BODIPY-KLD-DEACM (**266**).

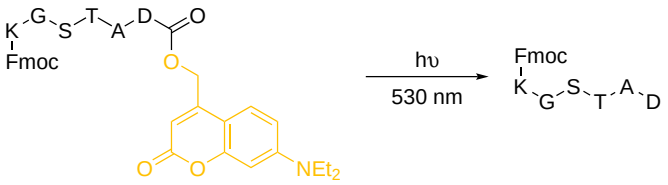
Table B.65: Determination of percentage composition of BODIPY-KLD-DEACM (**266**) and uncaged KLD-DEACM (**267**) following irradiation at 530 nm.

530 nm Irradiation of BODIPY-KLD-DEACM							
Entry	t (min)	Area [Caged]	Area [AA]	*c* [Caged] (mM)	*c* [AA] (mM)	% [Caged]	% [AA]
1	0	4351.45	0.00	0.00427	0.00000	100%	0%
2	15	3157.79	2913.63	0.00293	0.00163	69%	38%
3	30	2315.13	3566.67	0.00199	0.00194	47%	45%
4	45	1352.65	4751.51	0.00091	0.00251	21%	59%
5	60	971.98	5373.55	0.00048	0.00281	11%	66%
6	120	205.70	6441.89	0.00000	0.00332	0%	78%

Exposure of BODIPY-KLD-DEACM (**266**) to irradiation at 530 nm for 120 nm, saw complete photolysis of BODIPY-KLD-DEACM (**266**), accompanied by 78% release of KLD-DEACM (**267**), arising from photolysis of the BODIPY group. Importantly, no product arising from photolysis of the DEACM group was observed at this wavelength.

These results indicated the possibility of achieving wavelength orthogonality through use of the DEACM and BODIPY groups and irradiation at wavelengths of 420 nm and 530 nm.

530 nm Irradiation of KGSTAD-DEACM (5)



5 **270**

Scheme B.42: 530 nm photolysis of KGSTAD-DEACM (**5**).

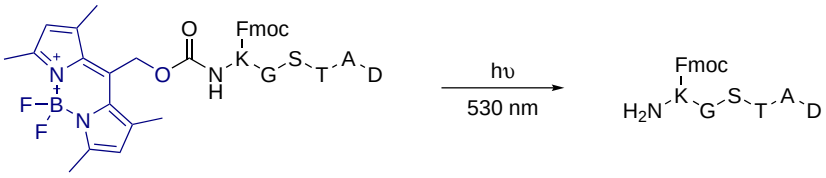
Table B.66: Determination of percentage composition of KGSTAD-DEACM (**5**) and uncaged KGSTAD (**270**) following irradiation at 530 nm.

530 nm Irradiation of KGSTAD-DEACM							
Entry	t (min)	Abs [Caged]	Abs [AA]	*c* [Caged] (mM)	*c* [AA] (mM)	% [Caged]	% [AA]
1	0	8048.13	0.00	0.105	0.000	100%	0%
2	1	8286.69	0.00	0.107	0.000	100%	0%
3	2	7907.25	0.00	0.103	0.000	99%	0%
4	10	-	391.77	-	0.002	-	2%
5	20	7648.18	318.73	0.100	0.002	96%	2%
6	30	-	764.79	-	0.006	-	5%
7	60	5539.66	1777.66	0.078	0.014	75%	14%
8	120	3481.74	2923.87	0.056	0.024	54%	23%

Initial exposure to irradiation at 530 nm saw little to no change in the percentage composition of KGSTAD-DEACM (**5**) with a 4% decrease being observed after 20 min exposure, accompanied by 2% release of uncaged KGSTAD (**270**). Prolonged exposure at this wavelength, up to 120 min, saw the percentage composition decrease to 54%, accompanied by 23% release of uncaged KGSTAD (**270**).

These results indicated the possibility of achieving wavelength orthogonality by exploiting the differences in the kinetics of photolysis of the DEACM and BODIPY caging groups following exposure to wavelengths centered at 420 nm and 530 nm.

530 nm Irradiation of BODIPY-KGSTAD (4)



4 **270**

Scheme B.43: 530 nm photolysis of BODIPY-KGSTAD (**4**).

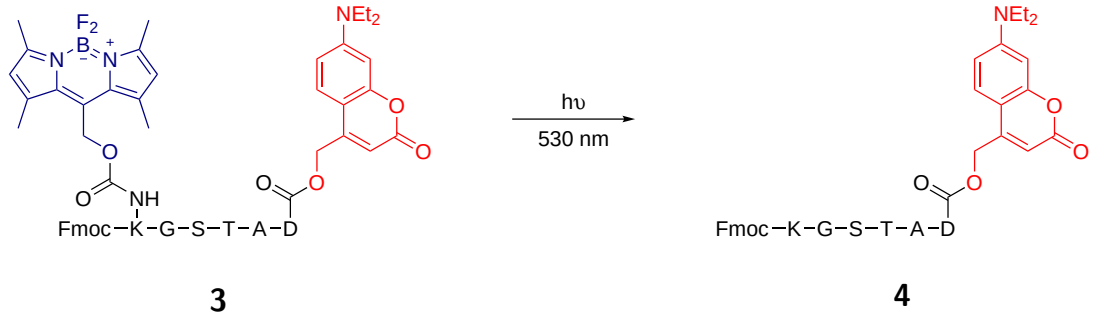
Table B.67: Determination of percentage composition of BODIPY-KGSTAD (**4**) and uncaged KGSTAD (**270**) following irradiation at 530 nm.

530 nm Irradiation of BODIPY-KGSTAD							
Entry	t (min)	Abs [Caged]	Abs [AA]	*c* [Caged] (mM)	*c* [AA] (mM)	% [Caged]	% [AA]
1	0	19.65	0.00	0.117	0.000	100%	0%
2	1	13.70	57.31	0.086	0.023	73%	20%
3	2	7.36	107.09	0.052	0.043	45%	37%
4	5	1.58	144.56	0.022	0.058	19%	49%
5	10	0.68	155.62	0.017	0.062	15%	53%
6	20	0.40	164.19	0.016	0.066	13%	56%
7	30	0.00	162.01	0.000	0.065	0%	55%
8	45	0.00	166.71	0.000	0.067	0%	57%
9	60	0.00	169.84	0.000	0.068	0%	58%
10	90	0.00	185.89	0.000	0.074	0%	64%
11	120	0.00	177.55	0.000	0.071	0%	61%

Following exposure to irradiation at 530 nm, complete photolysis of BODIPY-KGSTAD (**4**) was observed after 30 min. This was accompanied by 64% release of uncaged KGSTAD (**270**).

These results indicated the possibility of achieving wavelength orthogonality by exploiting the differences in rates of photolysis of the DEACM and BODIPY groups upon exposure to irradiation at wavelengths of 420 nm and 530 nm.

530 nm Irradiation of BODIPY-KGSTAD-DEACM (3)



3 **4**

Scheme B.44: 530 nm photolysis of BODIPY-KGSTAD-DEACM (**3**).

Table B.68: Determination of percentage composition of BODIPY-KGSTAD-DEACM (**3**) and BODIPY-KGSTAD (**4**) following irradiation at 530 nm.

530 nm Irradiation of BODIPY-KGSTAD-DEACM							
Entry	t (min)	Abs [Caged]	Abs [AA]	*c* [Caged] (mM)	*c* [AA] (mM)	% [Caged]	% [AA]
1	0	490.87	0.00	0.120	0.000	100%	0%
2	1	319.74	106.36	0.085	0.043	71%	36%
3	2	190.32	143.68	0.058	0.057	49%	48%
4	5	44.87	175.53	0.028	0.070	24%	59%
5	10	13.19	168.59	0.022	0.067	18%	56%
6	20	0.00	147.25	0.000	0.059	0%	49%
7	30	0.00	123.07	0.000	0.049	0%	41%
8	45	0.00	97.83	0.000	0.039	0%	33%
9	60	0.00	82.79	0.000	0.033	0%	28%
10	90	0.00	56.66	0.000	0.023	0%	19%
11	120	0.00	42.59	0.000	0.017	0%	14%

Initial exposure to irradiation at 530 nm saw the percentage composition of BODIPY-KGSTAD-DEACM (**3**) drop to 18% after 10 min, accompanied by 56% release of KGSTAD-DEACM (**5**). Prolonged exposure to irradiation at 530 nm resulted in a decrease in the percentage composition of the released KGSTAD-DEACM (**5**) accompanied by the formation of the fully uncaged KGSTAD (**270**) species. Importantly, no formation of BODIPY-KGSTAD (**4**), resulting from photolysis of the DEACM group was observed at this wavelength.

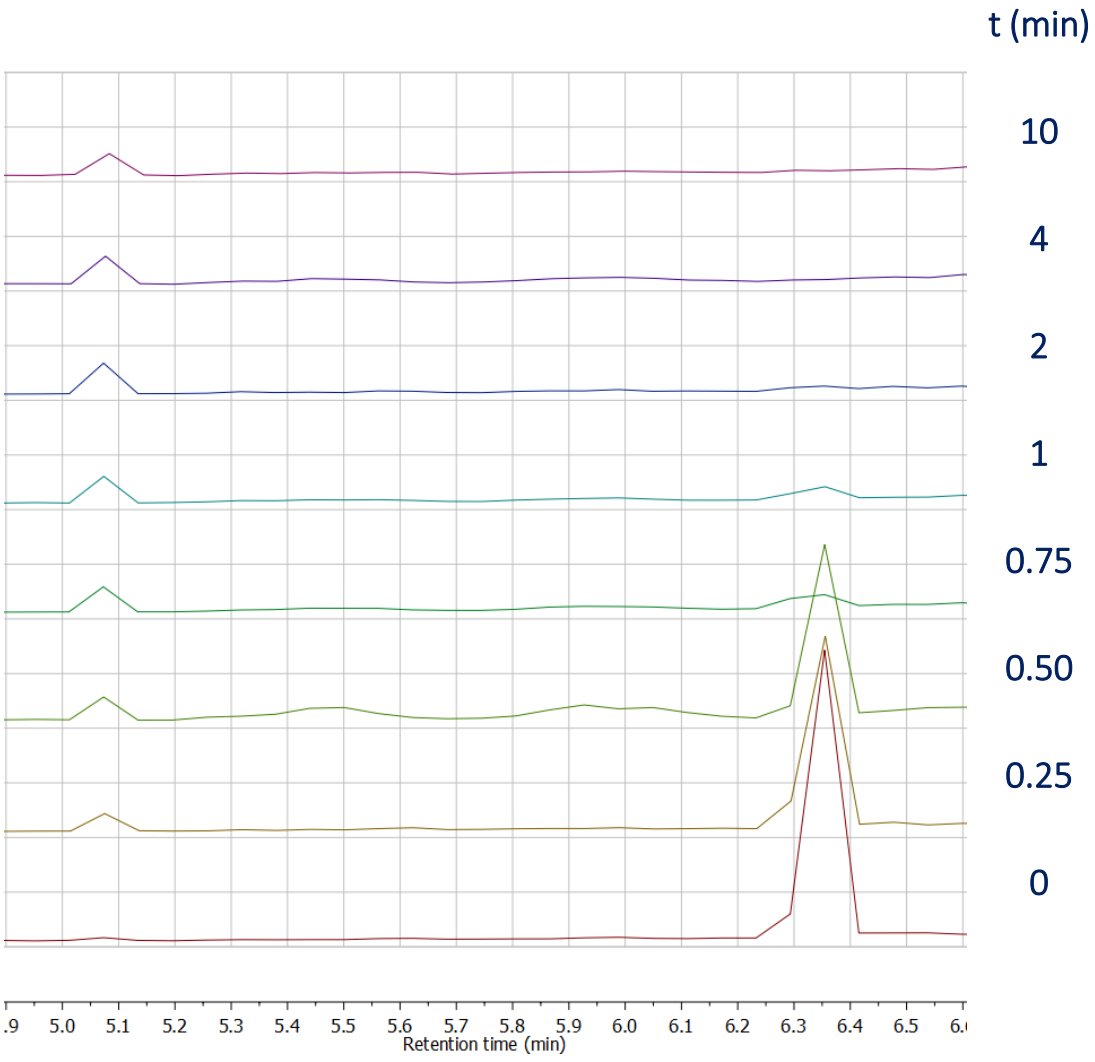
These results indicated the possibility of achieving wavelength orthogonality by exploiting the differences in kinetics of photolysis of the DEACM and BODIPY caging groups following exposure to irradiation at 420 nm and 530 nm.

Appendix C

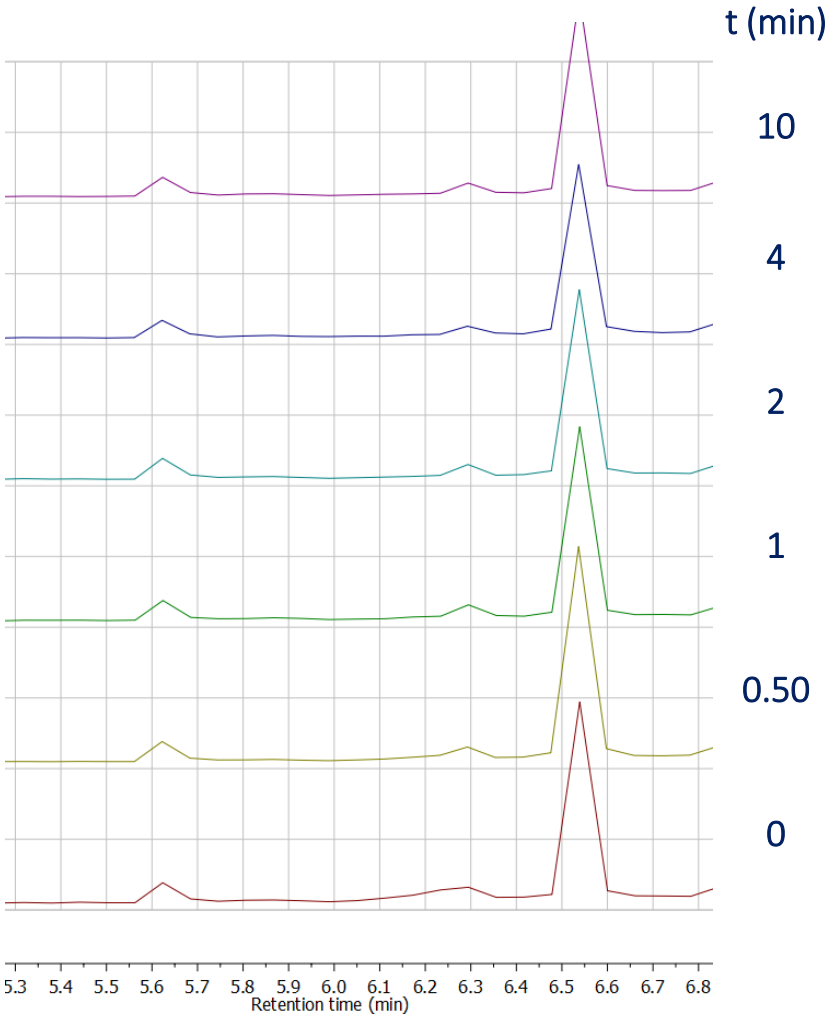
Photolysis LCMS-UV Curves

C.1 Monomers

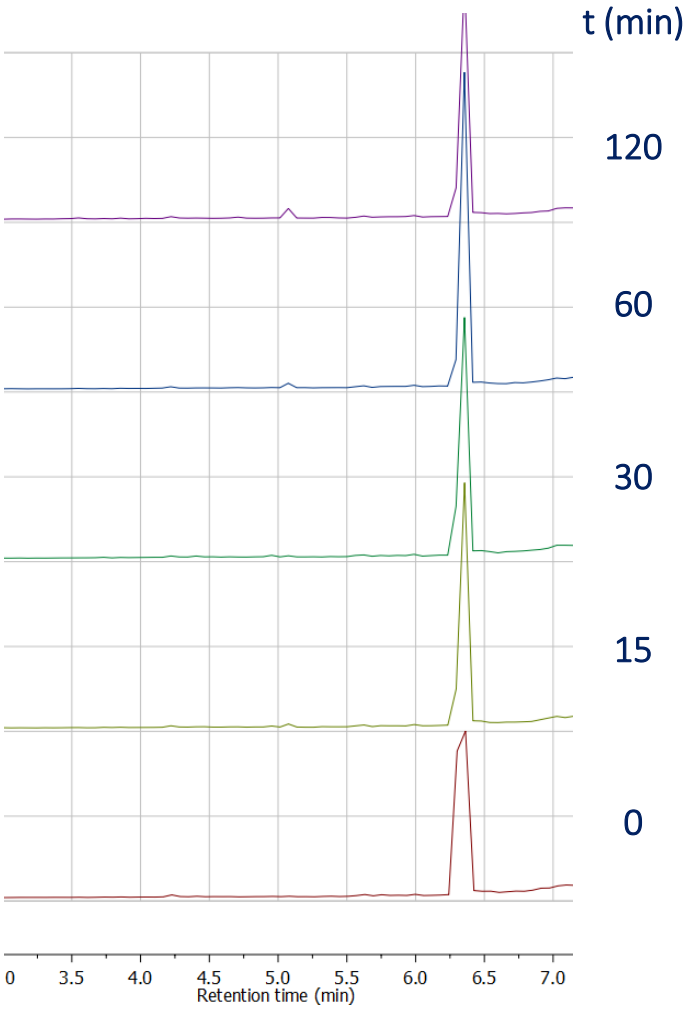
C.1.1 420 nm Irradiation of Fmoc-Asp(DEACM)-O^{t}Bu (215)



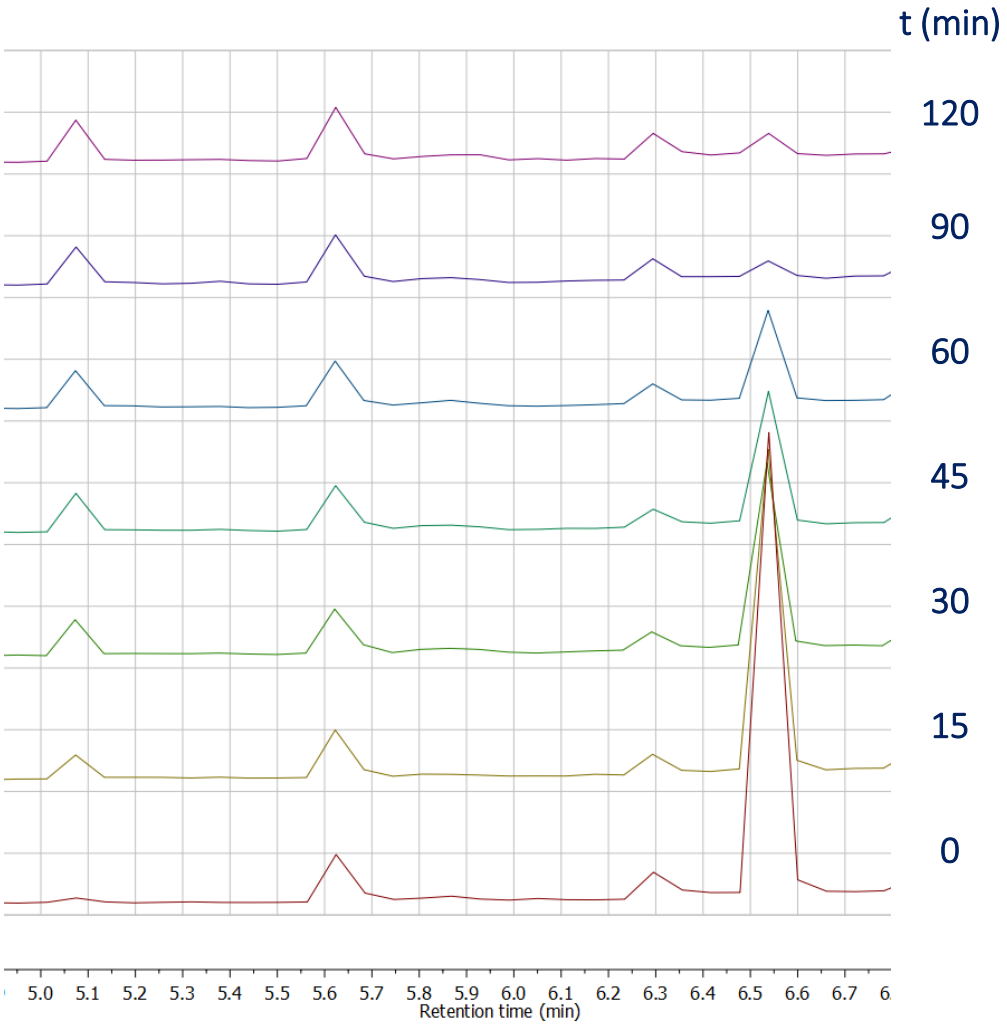
C.1.2 420 nm Irradiation of Fmoc-Asp(BODIPY)-O^{t}Bu (251)



C.1.3 530 nm Irradiation of Fmoc-Asp(DEACM)-O^{t}Bu (215)

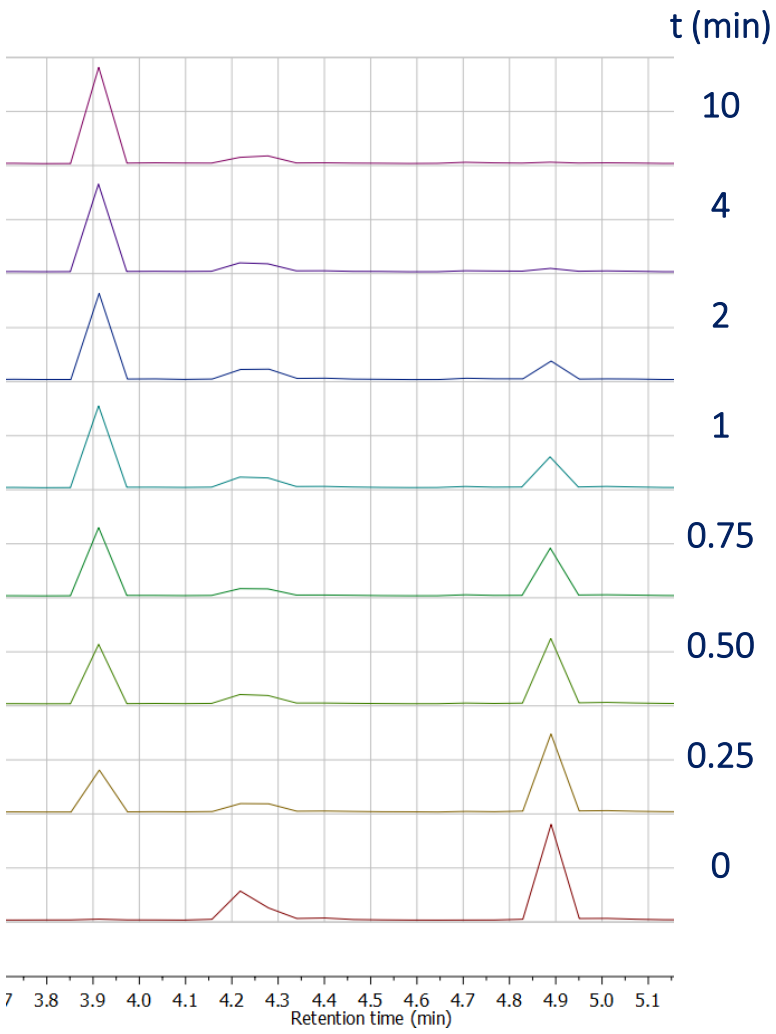


C.1.4 530 nm Irradiation of Fmoc-Asp(BODIPY)-O^{t}Bu (251)

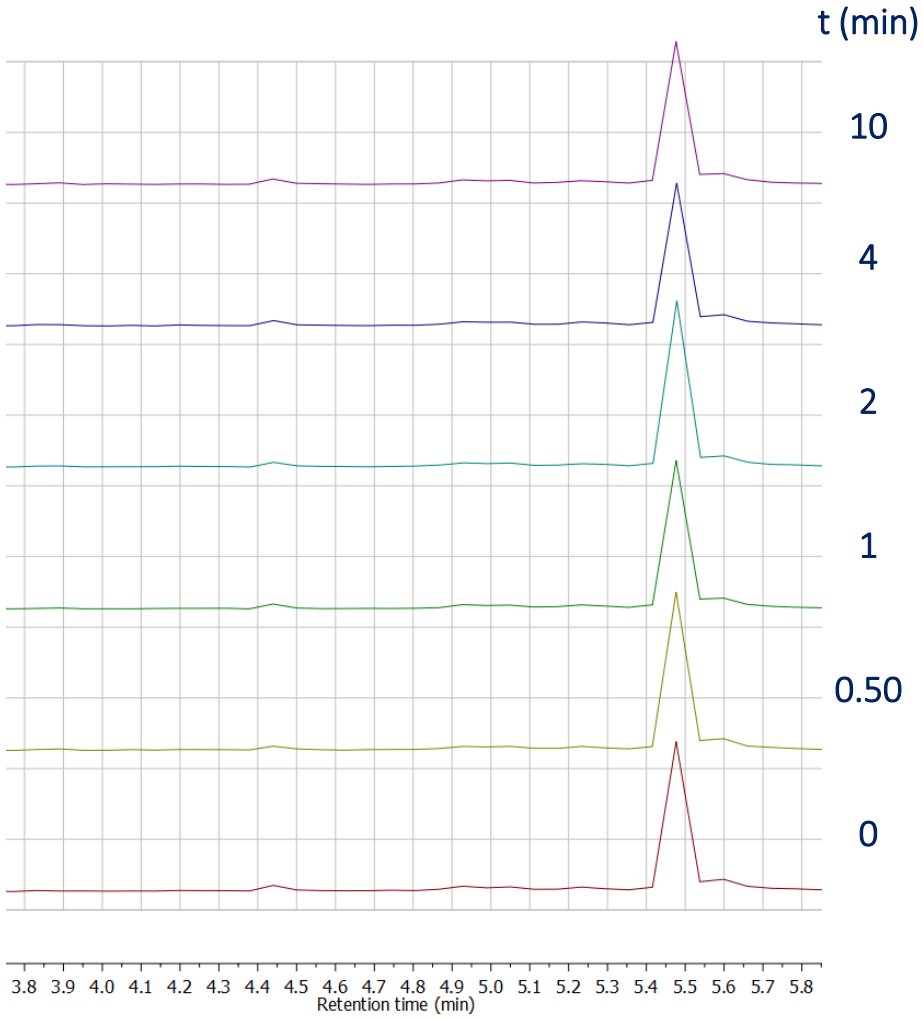


C.2 Trimers

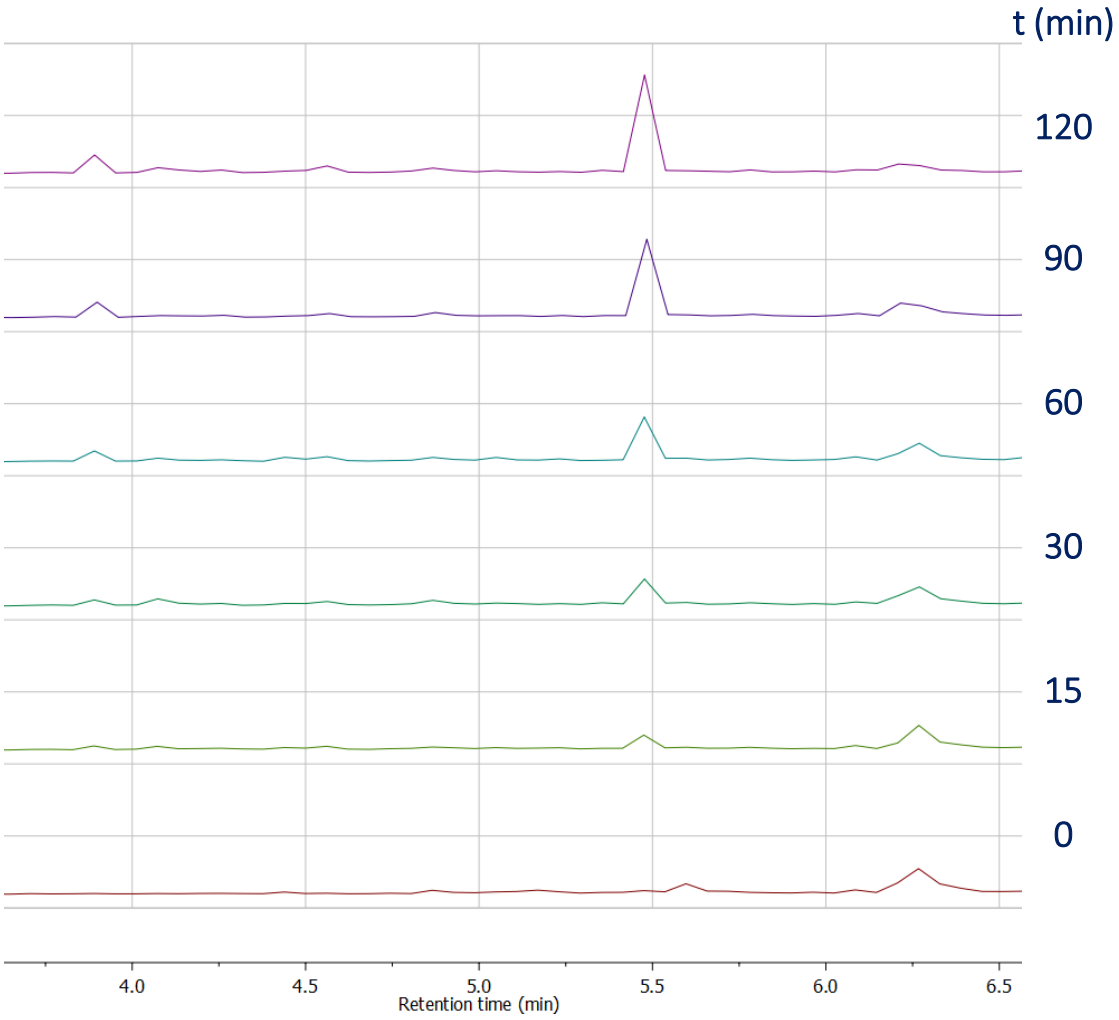
C.2.1 420 nm Irradiation of KLD-DEACM (267)



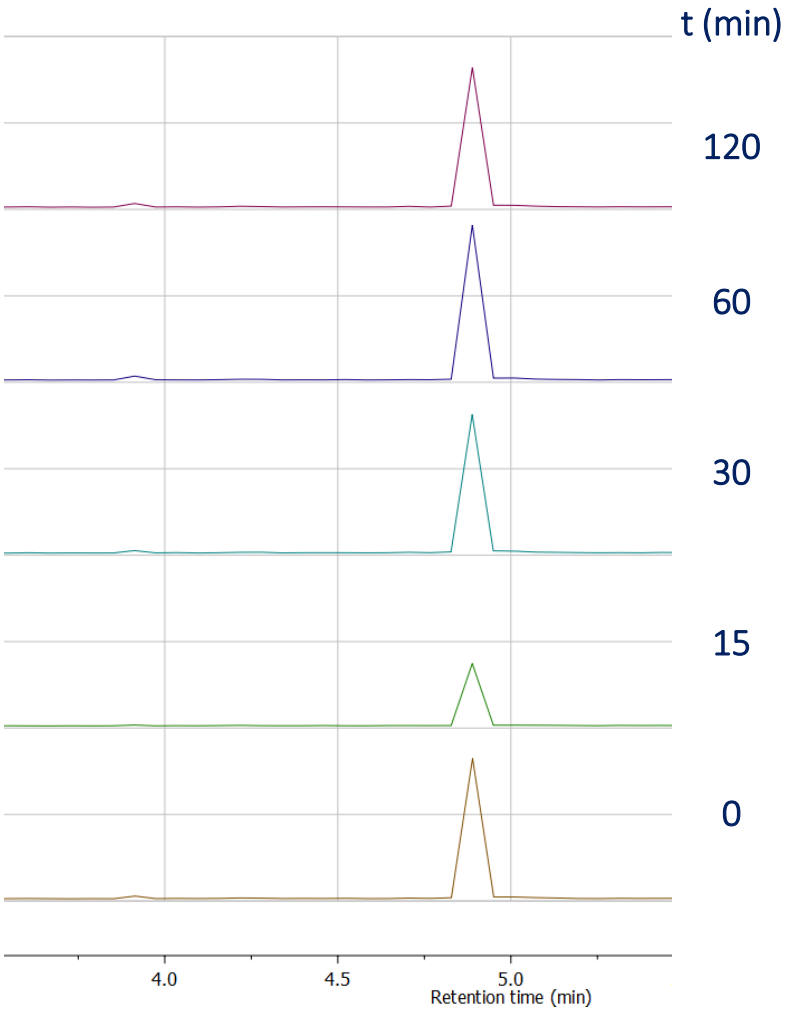
C.2.2 420 nm Irradiation of BODIPY-KLD (268)



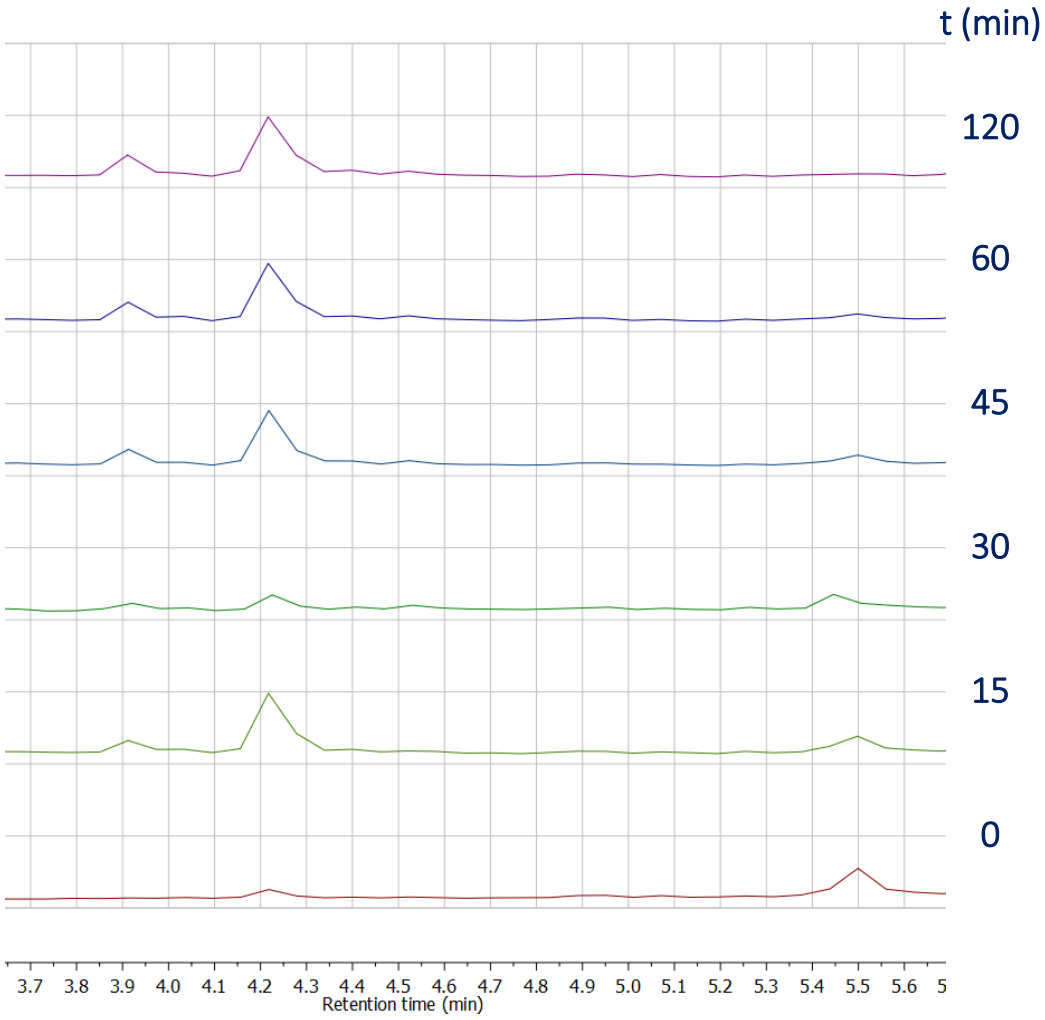
C.2.3 420 nm Irradiation of BODIPY-KLD-DEACM (266)



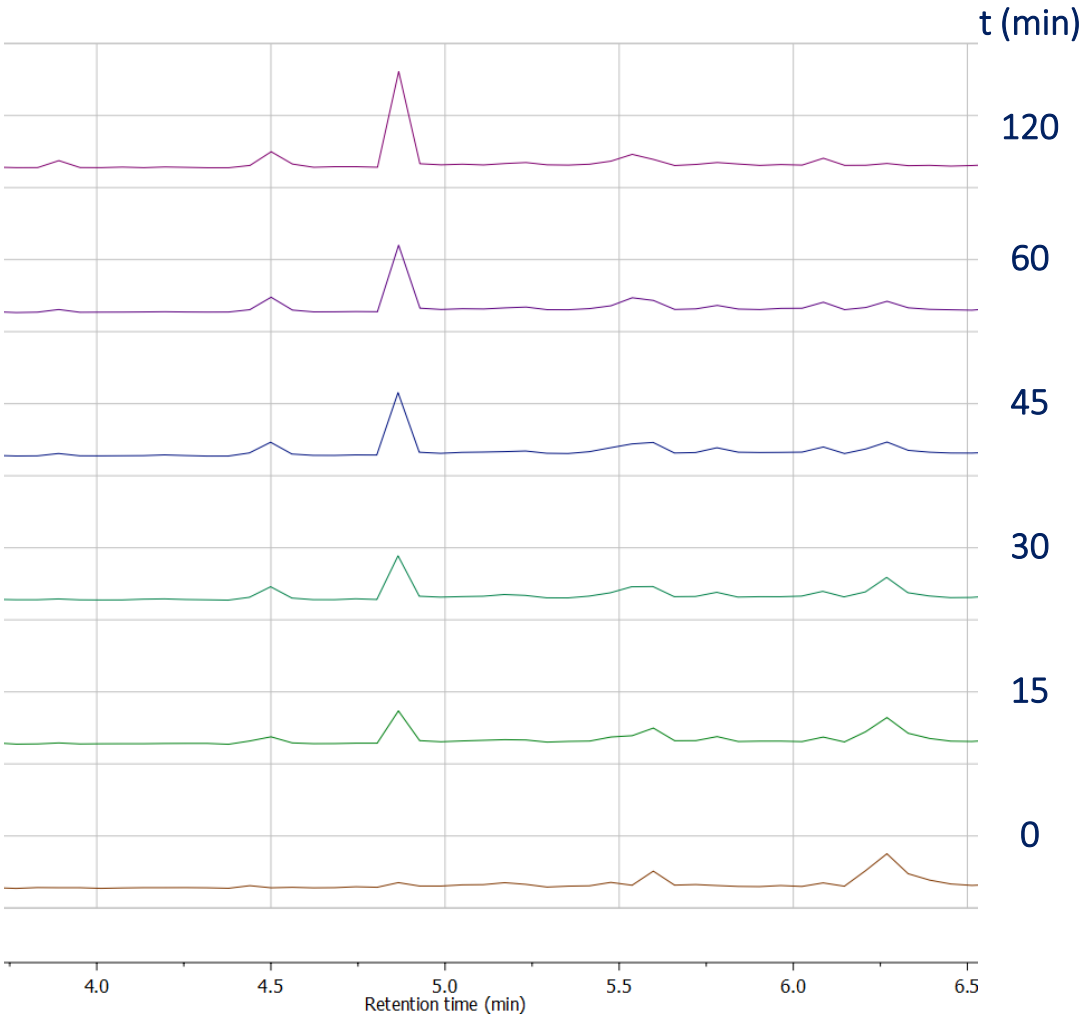
C.2.4 530 nm Irradiation of KLD-DEACM (267)



C.2.5 530 nm Irradiation of BODIPY-KLD (268)

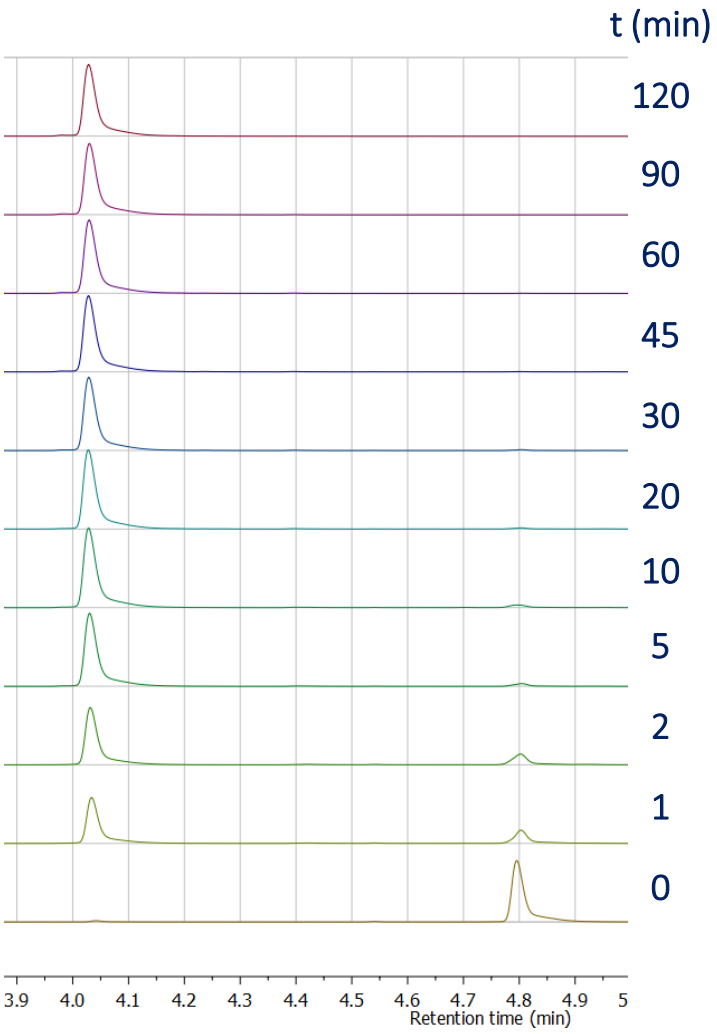


C.2.6 530 nm Irradiation of BODIPY-KLD-DEACM (266)

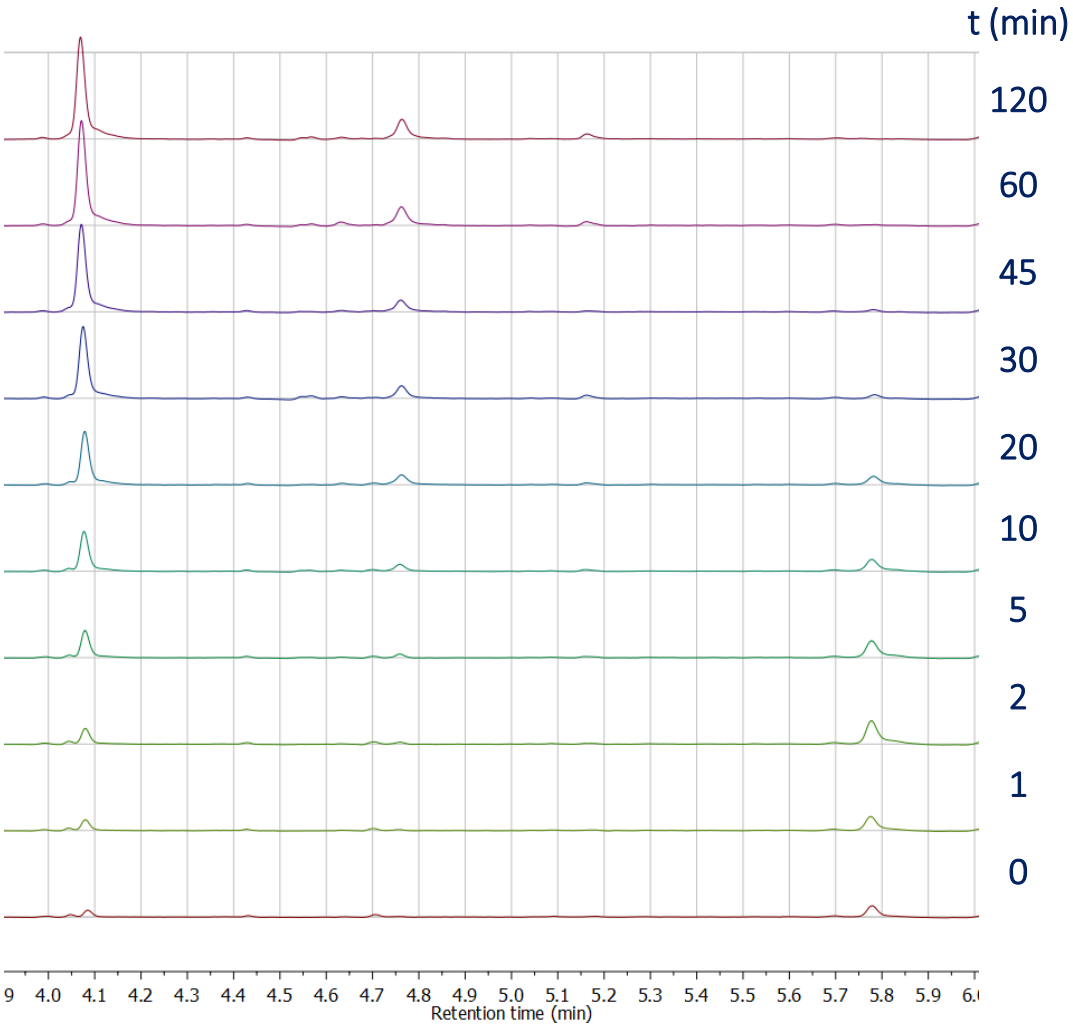


C.3 Hexamers

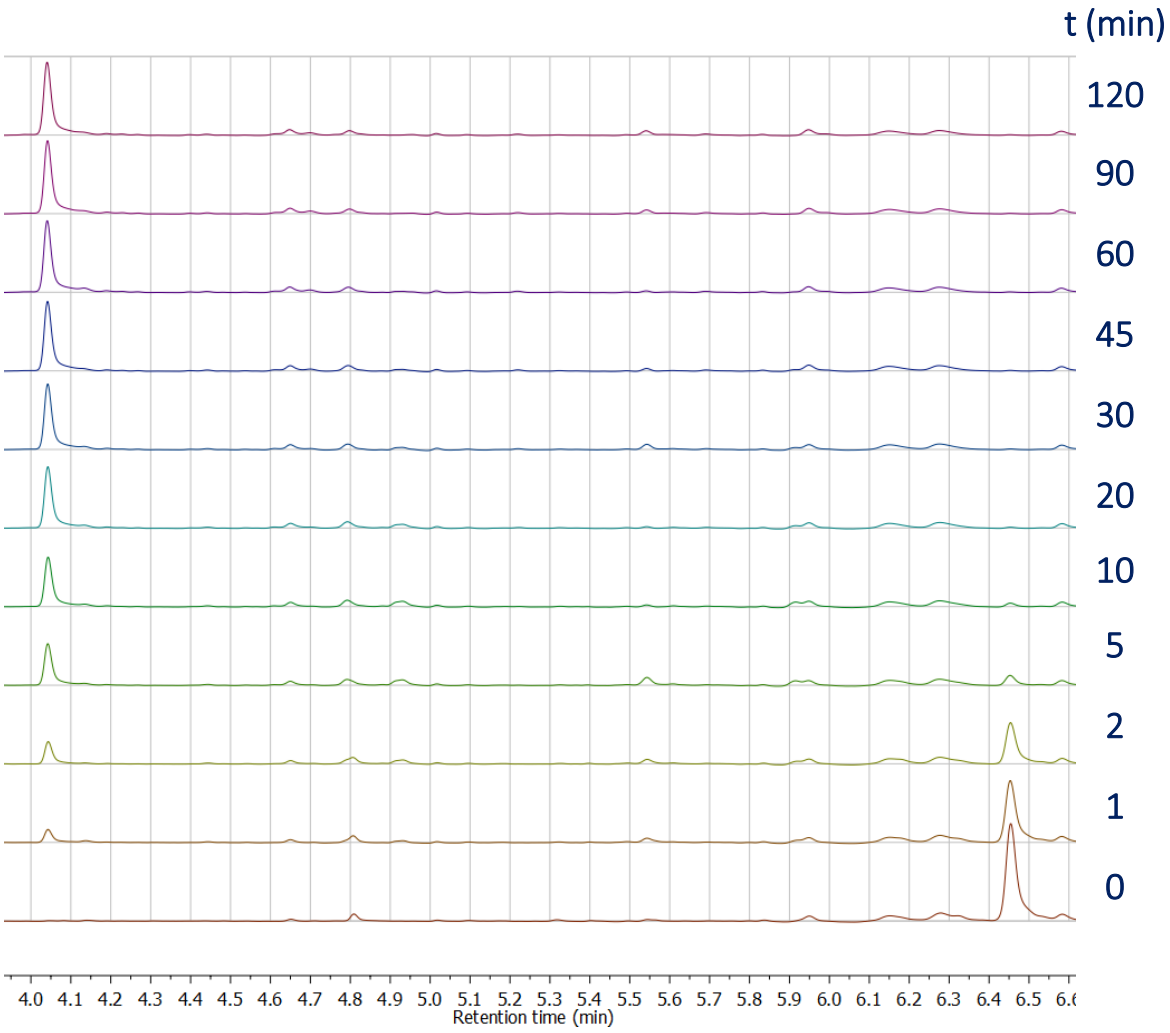
C.3.1 420 nm Irradiation of KGSTAD-DEACM (5)



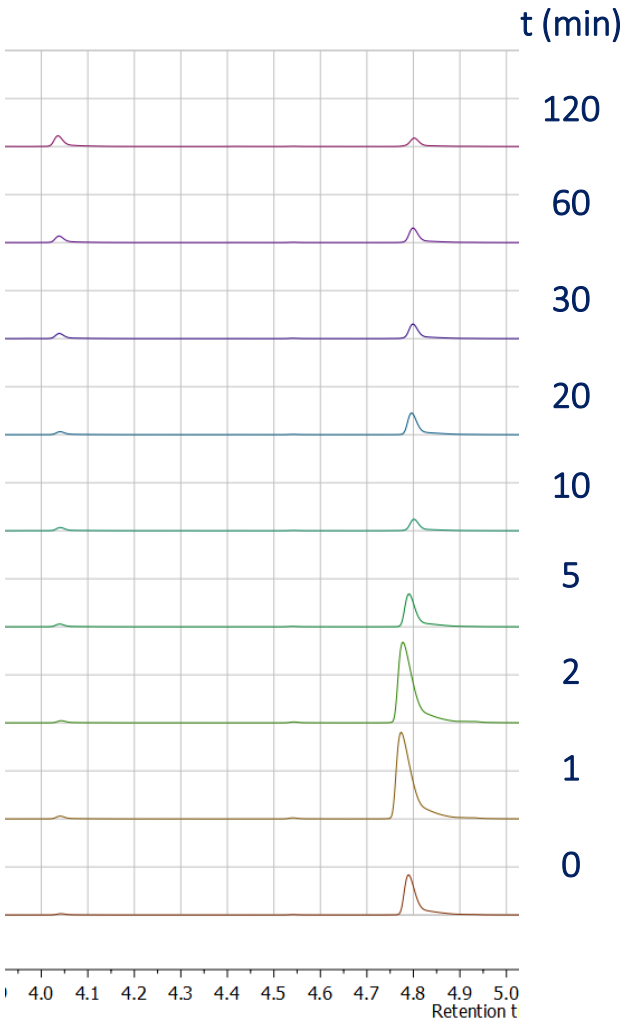
C.3.2 420 nm Irradiation of BODIPY-KGSTAD (4)



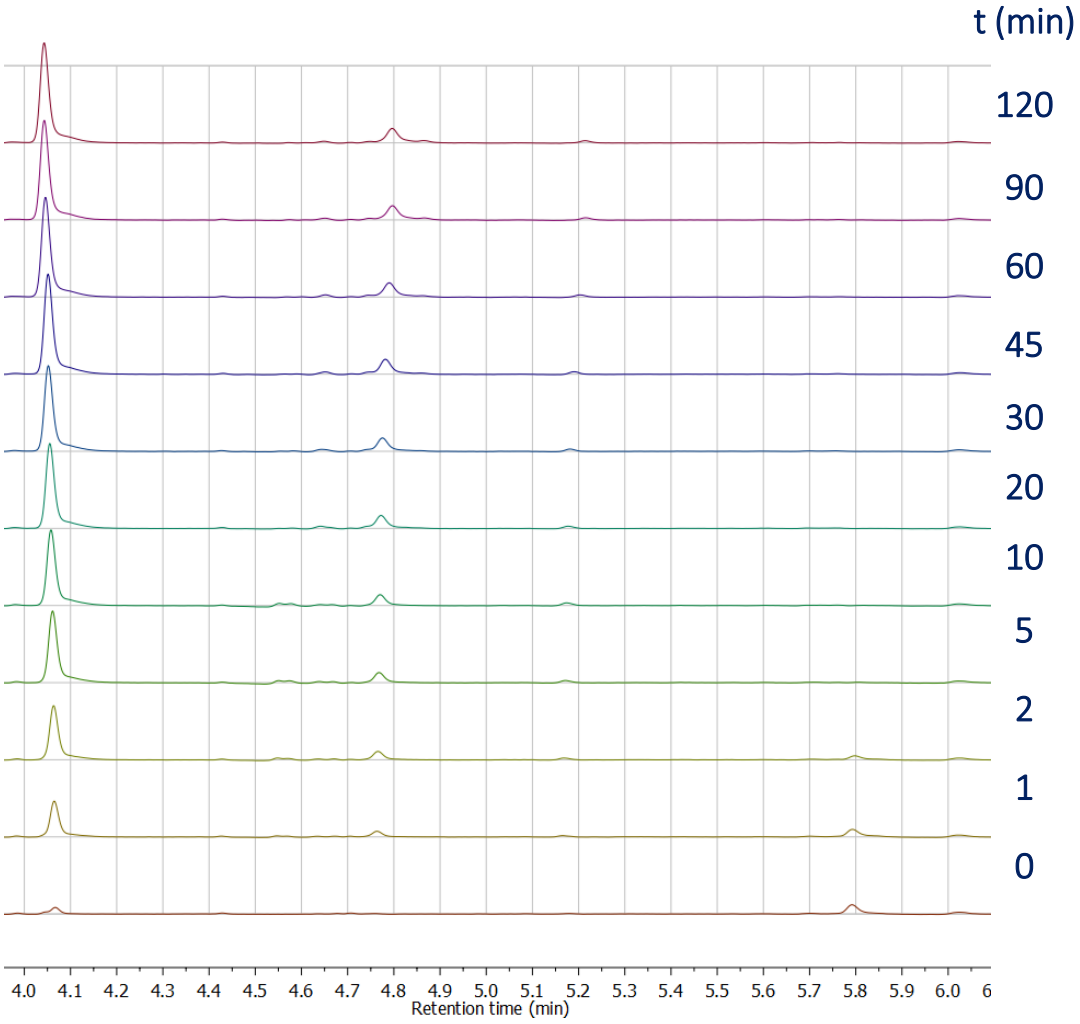
C.3.3 420 nm Irradiation of BODIPY-KGSTAD-DEACM (3)



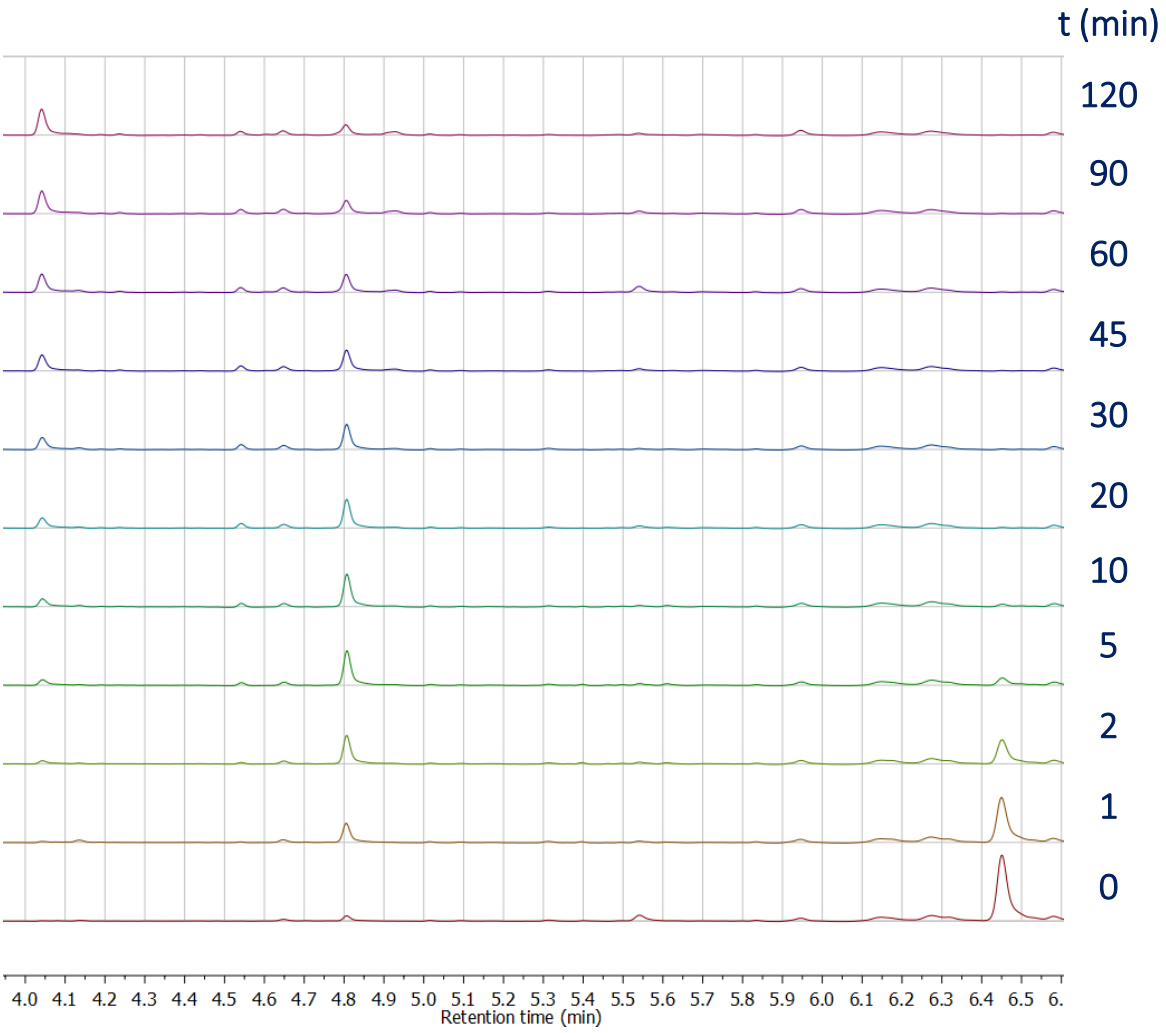
C.3.4 530 nm Irradiation of KGSTAD-DEACM (5)



C.3.5 530 nm Irradiation of BODIPY-KGSTAD (4)



C.3.6 530 nm Irradiation of BODIPY-KGSTAD-DEACM (3)

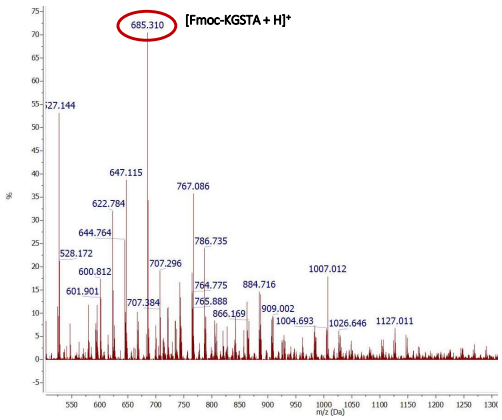


Appendix D

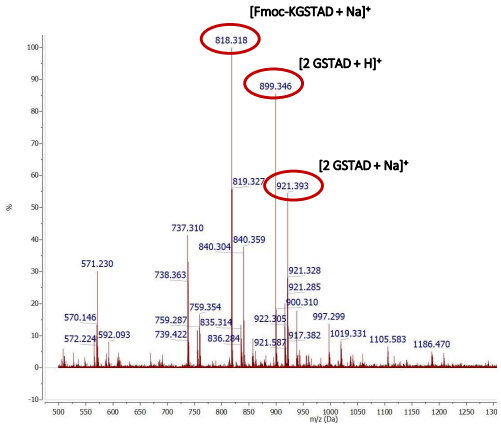
Enzyme Proteolysis Mass Spectrometry Data

D.1 Fmoc-KGSTAD (270)

Asp-*N*

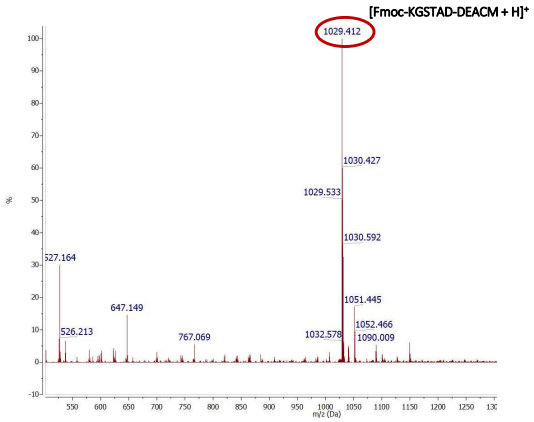


Lys-*C*

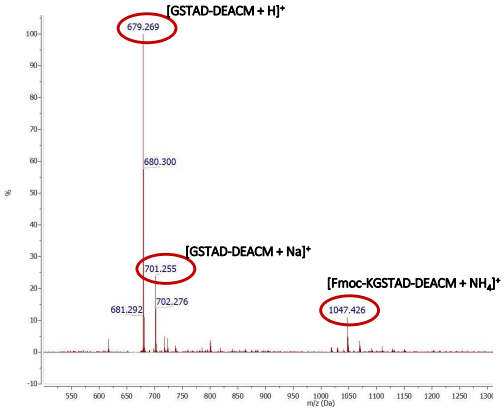


D.2 Fmoc-KGSTAD-DEACM (5)

Asp-*N*

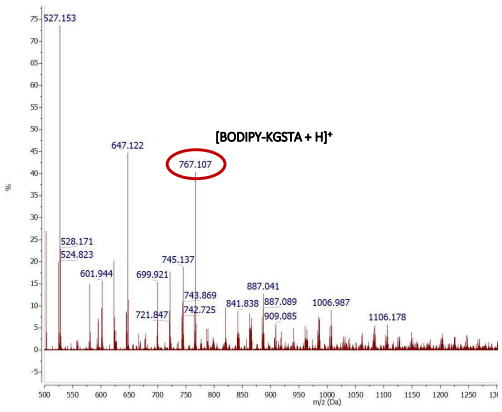


Lys-*C*

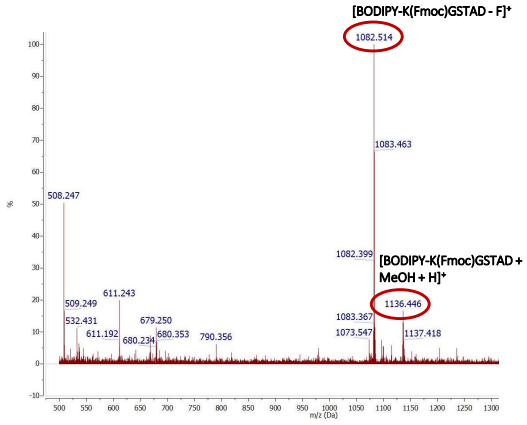


D.3 BODIPY-K(Fmoc)GSTAD (4)

Asp-*N*

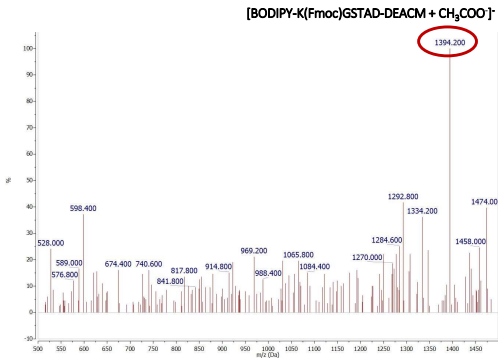


Lys-*C*

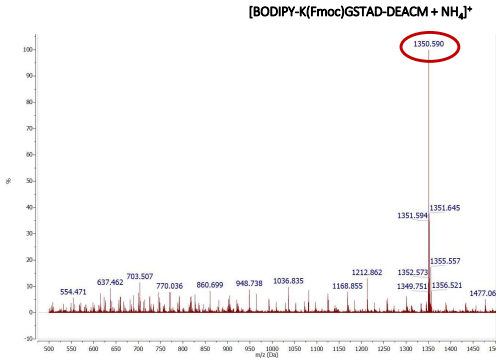


D.4 BODIPY-K(Fmoc)GSTAD-DEACM (3)

Asp-*N*

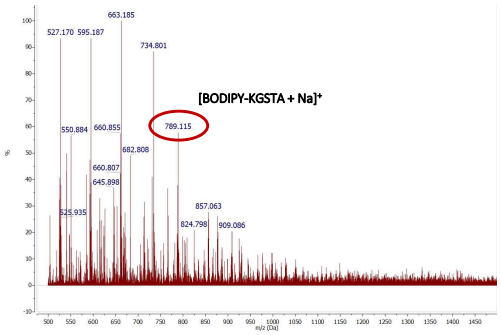


Lys-*C*

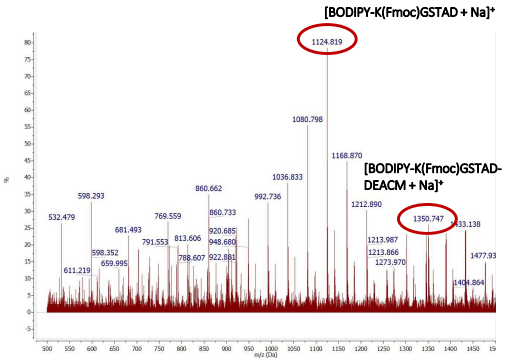


D.5 BODIPY-K(Fmoc)GSTAD-DEACM (3) following irradiation at 420 nm

Asp-*N*

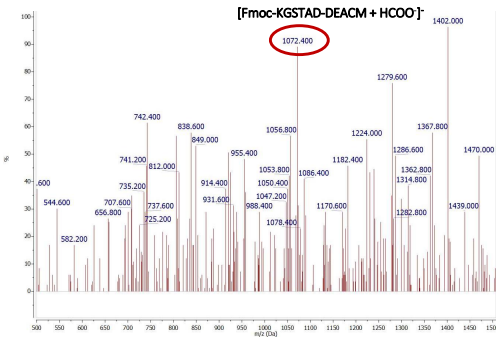


Lys-*C*

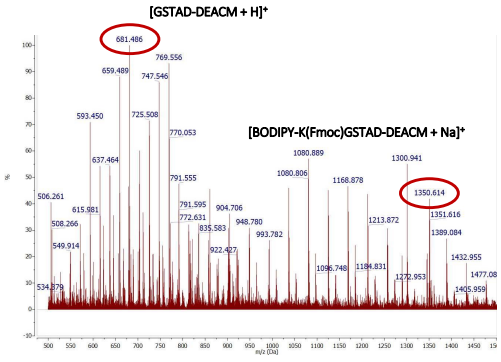


D.6 BODIPY-K(Fmoc)GSTAD-DEACM (3) following irradiation at 530 nm

Asp-*N*



Lys-*C*



References

[1] Arnaud Gautier et al. “How to control proteins with light in living systems”. In: *Nat Chem Biol* 10.7 (2014), pp. 533–541. ISSN: 1552-4450. DOI: 10.1038/nchembio.1534. URL: http://dx.doi.org/10.1038/nchembio.1534.

[2] Pharmaceutical Researchers America and Manufacturers of. “2016 Biopharmaceutical Research Industry Profile”. In: *PhRMA Profile* (2016), pp. 1–86.

[3] Web Page. 2016. URL: https://www.nobelprize.org/.

[4] Wiktor Szymański et al. “Reversible Photocontrol of Biological Systems by the Incorporation of Molecular Photoswitches”. In: *Chem. Rev.* 113.8 (2013), pp. 6114–6178. ISSN: 0009-2665. DOI: 10.1021/cr300179f. URL: http://dx.doi.org/10.1021/cr300179f.

[5] Rebecca A Craig et al. “Photosensitisers – the progression from photodynamic therapy to anti-infective surfaces”. In: *Expert Opin. Drug Deliv.* 12.1 (2015), pp. 85–101. DOI: doi:10.1517/17425247.2015.962512. URL: http://informahealthcare.com/doi/abs/10.1517/17425247.2015.962512.

[6] Chunyan Bao et al. “Building Biomedical Materials using Photochemical Bond Cleavage”. In: *Adv. Mater. (Weinheim, Ger.)* 27.10 (2015), pp. 1647–1662. ISSN: 1521-4095. DOI: 10.1002/adma.201403783. URL: http://dx.doi.org/10.1002/adma.201403783.

[7] Matthew Volgraf et al. “Reversibly Caged Glutamate: A Photochromic Agonist of Ionotropic Glutamate Receptors”. In: *J. Am. Chem. Soc.* 129.2 (2007), pp. 260–261. ISSN: 0002-7863. DOI: 10.1021/ja067269o. URL: http://dx.doi.org/10.1021/ja067269o.

[8] Petr Klán et al. “Photoremovable Protecting Groups in Chemistry and Biology: Reaction Mechanisms and Efficacy”. In: *Chem. Rev.* 113.1 (2013), pp. 119–191. ISSN: 0009-2665. DOI: 10.1021/cr300177k. URL: http://dx.doi.org/10.1021/cr300177k.

[9] Clara Brieke et al. “Light-Controlled Tools”. In: *Angew. Chem., Int. Ed.* 51.34 (2012), pp. 8446–8476. ISSN: 1521-3773. DOI: 10.1002/anie.201202134. URL: http://dx.doi.org/10.1002/anie.201202134.

[10] J. A. Barltrop and P. Schofield. “Photosensitive Protecting Groups”. In: *Tetrahedron Lett.* 3.16 (1962), pp. 697–699. ISSN: 0040-4039. DOI: http://dx.doi.org/10.1016/S0040-4039(00)70935-X. URL: http://www.sciencedirect.com/science/article/pii/S004040390070935X.

[11] D. H. R. Barton et al. “Photosensitive protection of functional groups”. In: *Tetrahedron Lett.* 3.23 (1962), pp. 1055–1057. ISSN: 0040-4039. DOI: http://dx.doi.org/10.1016/S0040-4039(00)70957-9. URL: http://www.sciencedirect.com/science/article/pii/S0040403900709579.

[12] D. H. R. Barton et al. “654. Photochemical transformations. Part XIX. Some photosensitive protecting groups”. In: *J. Chem. Soc.* 0 (1965), pp. 3571–3578. ISSN: 0368-1769. DOI: 10.1039/JR9650003571. URL: http://dx.doi.org/10.1039/JR9650003571.

[13] Joachim Engels and Ernst Juergen Schlaeger. “Synthesis, structure, and reactivity of adenosine cyclic 3’,5’-phosphate-benzyltriesters”. In: *J. Med. Chem.* 20.7 (1977), pp. 907–911. ISSN: 0022-2623. DOI: 10.1021/jm00217a008. URL: http://dx.doi.org/10.1021/jm00217a008.

[14] Jack H. Kaplan, Bliss Forbush, and Joseph F. Hoffman. “Rapid photolytic release of adenosine 5’-triphosphate from a protected analog: utilization by the sodium:potassium pump of human red blood cell ghosts”. In: *Biochemistry* 17.10 (1978), pp. 1929–1935. ISSN: 0006-2960. DOI: 10.1021/bi00603a020. URL: http://dx.doi.org/10.1021/bi00603a020.

[15] Graham C. R. Ellis-Davies. “Caged compounds: photorelease technology for control of cellular chemistry and physiology”. In: *Nature methods* 4.8 (2007), pp. 619–628. ISSN: 1548-7091 1548-7105. DOI: 10.1038/nmeth1072. URL: http://www.ncbi.nlm.nih.gov/pmc/articles/PMC4207253/.

[16] Anna Paola Pelliccioli and Jakob Wirz. “Photoremovable protecting groups: reaction mechanisms and applications”. In: *Photochem. Photobiol. Sci.* 1.7 (2002), pp. 441–458. ISSN: 1474-905X. DOI: 10.1039/B200777K. URL: http://dx.doi.org/10.1039/B200777K.

[17] C. H. Bamford and R. G. W. Norrish. “359. Primary photochemical reactions. Part VII. Photochemical decomposition of isovaleraldehyde and di-n-propyl ketone”. In: *J. Chem. Soc.* 0 (1935), pp. 1504–1511. ISSN: 0368-1769. DOI: 10.1039/JR9350001504. URL: http://dx.doi.org/10.1039/JR9350001504.

[18] Sang Tae Park, Jonathan S. Feenstra, and Ahmed H. Zewail. “Ultrafast electron diffraction: Excited state structures and chemistries of aromatic carbonyls”. In: *J. Chem. Phys.* 124.17 (2006), p. 174707. DOI: doi:http://dx.doi.org/10.1063/1.2194017. URL: http://scitation.aip.org/content/aip/journal/jcp/124/17/10.1063/1.2194017.

[19] Wei-Hai Fang and David Lee Phillips. “The Crucial Role of the S1/T2/T1 Intersection in the Relaxation Dynamics of Aromatic Carbonyl Compounds upon n* Excitation”. In: *ChemPhysChem* 3.10 (2002), pp. 889–892. ISSN: 1439-7641. DOI: 10.1002/1439-7641(20021018)3:10<889::AID-CPHC889>3.0.CO;2-U. URL: http://dx.doi.org/10.1002/1439-7641(20021018)3:10%3C889::AID-CPHC889%3E3.0.CO;2-U.

[20] John C. Sheehan and Kazuo Umezawa. “Phenacyl photosensitive blocking groups”. In: *J. Org. Chem.* 38.21 (1973), pp. 3771–3774. ISSN: 0022-3263. DOI: 10.1021/jo00961a027. URL: http://dx.doi.org/10.1021/jo00961a027.

[21] Anamitro Banerjee and Daniel E. Falvey. “Direct Photolysis of Phenacyl Protecting Groups Studied by Laser Flash Photolysis: An Excited State Hydrogen Atom Abstraction Pathway Leads to Formation of Carboxylic Acids and Acetophenone”. In: *J. Am. Chem. Soc.* 120.12 (1998), pp. 2965–2966. ISSN: 0002-7863. DOI: 10.1021/ja971431t. URL: http://dx.doi.org/10.1021/ja971431t.

[22] Petr Klán, Miroslav Zabadal, and Dominik Heger. “2,5-Dimethylphenacyl as a New Photoreleasable Protecting Group for Carboxylic Acids”. In: *Org. Lett.* 2.11 (2000), pp. 1569–1571. ISSN: 1523-7060. DOI: 10.1021/ol005789x. URL: http://dx.doi.org/10.1021/ol005789x.

[23] Radovan Ruzicka, Miroslav Zabadal, and Petr Klán. “PHOTOLYSIS OF PHENACYL ESTERS IN A TWO-PHASE SYSTEM”. In: *Synth. Commun.* 32.16 (2002), pp. 2581–2590. ISSN: 0039-7911. DOI: 10.1081/SCC-120005943. URL: http://dx.doi.org/10.1081/SCC-120005943.

[24] Petr Klan et al. “2,5-Dimethylphenacyl esters: A photoremovable protecting group for phosphates and sulfonic acids”. In: *Photochem. Photobiol. Sci.* 1.11 (2002), pp. 920–923. ISSN: 1474-905X. DOI: 10.1039/B208171G. URL: http://dx.doi.org/10.1039/B208171G.

[25] Jaromir Literak, Jakob Wirz, and Petr Klan. “2,5-Dimethylphenacyl carbonates: A photoremovable protecting group for alcohols and phenols”. In: *Photochem. Photobiol. Sci.* 4.1 (2005), pp. 43–46. ISSN: 1474-905X. DOI: 10.1039/B408851D. URL: http://dx.doi.org/10.1039/B408851D.

[26] Laxminarayana Kammari et al. “2,5-Dimethylphenacyl carbamate: a photoremovable protecting group for amines and amino acids”. In: *Photochem. Photobiol. Sci.* 6.1 (2007), pp. 50–56. ISSN: 1474-905X. DOI: 10.1039/B612233G. URL: http://dx.doi.org/10.1039/B612233G.

[27] Richard S. Givens and Chan-Ho Park. “p-Hydroxyphenacyl ATP1: A new phototrigger”. In: *Tetrahedron Lett.* 37.35 (1996), pp. 6259–6262. ISSN: 0040-4039. DOI: http://dx.doi.org/10.1016/0040-4039(96)01390-1. URL: http://www.sciencedirect.com/science/article/pii/0040403996013901.

[28] Chan-Ho Park and Richard S. Givens. “New Photoactivated Protecting Groups. 6. p-Hydroxyphenacyl: A Phototrigger for Chemical and Biochemical Probes1,2”. In: *J. Am. Chem. Soc.* 119.10 (1997), pp. 2453–2463. ISSN: 0002-7863. DOI: 10.1021/ja9635589. URL: http://dx.doi.org/10.1021/ja9635589.

[29] J. C. Anderson and C. B. Reese. “A photo-induced rearrangement involving aryl participation”. In: *Tetrahedron Lett.* 3.1 (1962), pp. 1–4. ISSN: 0040-4039. DOI: http://dx.doi.org/10.1016/S0040-4039(00)62031-2. URL: http://www.sciencedirect.com/science/article/pii/S0040403900620312.

[30] Qian Cao et al. “Ultrafast time-resolved transient infrared and resonance Raman spectroscopic study of the photo-deprotection and rearrangement reactions of p-hydroxyphenacyl caged phosphates”. In: *Faraday Discuss.* 145.0 (2010), pp. 171–183. ISSN: 1359-6640. DOI: 10.1039/B908188G. URL: http://dx.doi.org/10.1039/B908188G.

[31] Y. Chiang, A. J. Kresge, and Y. Zhu. “Flash Photolytic Generation and Study of p-Quinone Methide in Aqueous Solution. An Estimate of Rate and Equilibrium Constants for Heterolysis of the CarbonBromine Bond in p-Hydroxybenzyl Bromide”. In: *J. Am. Chem. Soc.* 124.22 (2002), pp. 6349–6356. ISSN: 0002-7863. DOI: 10.1021/ja020020w. URL: http://dx.doi.org/10.1021/ja020020w.

[32] James A. Pincock. “Photochemistry of Arylmethyl Esters in Nucleophilic Solvents: Radical Pair and Ion Pair Intermediates”. In: *Acc. Chem. Res.* 30.1 (1997), pp. 43–49. ISSN: 0001-4842. DOI: 10.1021/ar960177r. URL: http://dx.doi.org/10.1021/ar960177r.

[33] Richard S. Givens et al. “Photochemistry of .alpha.-keto phosphate esters: photorelease of a caged cAMP”. In: *J. Am. Chem. Soc.* 114.22 (1992), pp. 8708–8710. ISSN: 0002-7863. DOI: 10.1021/ja00048a059. URL: http://dx.doi.org/10.1021/ja00048a059.

[34] Richard S. Givens et al. “p-Hydroxyphenacyl photoremovable protecting groups — Robust photochemistry despite substituent diversity”. In: *Can. J. Chem.* 89.3 (2011), pp. 364–384. ISSN: 0008-4042. DOI: 10.1139/V10-143. URL: http://dx.doi.org/10.1139/V10-143.

[35] John C. Sheehan and R. Marshall Wilson. “Photolysis of Desyl Compounds. A New Photolytic Cyclization”. In: *J. Am. Chem. Soc.* 86.23 (1964), pp. 5277–5281. ISSN: 0002-7863. DOI: 10.1021/ja01077a046. URL: http://dx.doi.org/10.1021/ja01077a046.

[36] John C. Sheehan, R. Marshall Wilson, and A. W. Oxford. “Photolysis of methoxy-substituted benzoin esters. Photosensitive protecting group for carboxylic acids”. In: *J. Am. Chem. Soc.* 93.26 (1971), pp. 7222–7228. ISSN: 0002-7863. DOI: 10.1021/ja00755a017. URL: http://dx.doi.org/10.1021/ja00755a017.

[37] Christian G. Bochet. “Photolabile protecting groups and linkers”. In: *J. Chem. Soc., Perkin Trans. 1* 2 (2002), pp. 125–142. ISSN: 1472-7781. DOI: 10.1039/B009522M. URL: http://dx.doi.org/10.1039/B009522M.

[38] Chensheng Ma et al. “A Time-Resolved Spectroscopic Study of the Bichromophoric Phototrigger 3,5-Dimethoxybenzoin Diethyl Phosphate: Interaction Between the Two Chromophores Determines the Reaction Pathway”. In: *Chem. – Eur. J.* 16.17 (2010), pp. 5102–5118. ISSN: 1521-3765. DOI: 10.1002/chem.200902891. URL: http://dx.doi.org/10.1002/chem.200902891.

[39] Abraham Patchornik, B. Amit, and R. B. Woodward. “Photosensitive protecting groups”. In: *J. Am. Chem. Soc.* 92.21 (1970), pp. 6333–6335. ISSN: 0002-7863. DOI: 10.1021/ja00724a041. URL: http://dx.doi.org/10.1021/ja00724a041.

[40] Bruno Hellrung et al. “Photorelease of Alcohols from 2-Nitrobenzyl Ethers Proceeds via Hemiacetals and May Be Further Retarded by Buffers Intercepting the Primary aci-Nitro Intermediates”. In: *J. Am. Chem. Soc.* 127.25 (2005), pp. 8934–8935. ISSN: 0002-7863. DOI: 10.1021/ja052300s. URL: http://dx.doi.org/10.1021/ja052300s.

[41] Hans-Georg A. Breitinger et al. “Synthesis and Characterization of Photolabile Derivatives of Serotonin for Chemical Kinetic Investigations of the Serotonin 5-HT3 Receptor†”. In: *Biochemistry* 39.18 (2000), pp. 5500–5508. ISSN: 0006-2960. DOI: 10.1021/bi992781q. URL: http://dx.doi.org/10.1021/bi992781q.

[42] Martin Gaplovsky et al. “Photochemical reaction mechanisms of 2-nitrobenzyl compounds: 2-Nitrobenzyl alcohols form 2-nitroso hydrates by dual proton transfer”. In: *Photochem. Photobiol. Sci.* 4.1 (2005), pp. 33–42. ISSN: 1474-905X. DOI: 10.1039/B409927C. URL: http://dx.doi.org/10.1039/B409927C.

[43] Alexandre Specht and Maurice Goeldner. “1-(o-Nitrophenyl)-2,2,2-trifluoroethyl Ether Derivatives as Stable and Efficient Photoremovable Alcohol-Protecting Groups”. In: *Angew. Chem., Int. Ed.* 43.15 (2004), pp. 2008–2012. ISSN: 1521-3773. DOI: 10.1002/anie.200353247. URL: http://dx.doi.org/10.1002/anie.200353247.

[44] Isabelle Aujard et al. “o-Nitrobenzyl Photolabile Protecting Groups with Red-Shifted Absorption: Syntheses and Uncaging Cross-Sections for One- and Two-Photon Excitation”. In: *Chem. – Eur. J.* 12.26 (2006), pp. 6865–6879. ISSN: 1521-3765. DOI: 10.1002/chem.200501393. URL: http://dx.doi.org/10.1002/chem.200501393.

[45] James F. Cameron and Jean M. J. Frechet. “Photogeneration of organic bases from o-nitrobenzyl-derived carbamates”. In: *Journal of the American Chemical Society* 113.11 (1991), pp. 4303–4313. ISSN: 0002-7863. DOI: 10.1021/ja00011a038. URL: http://dx.doi.org/10.1021/ja00011a038.

[46] T. J. Mitchison et al. “[4] Caged fluorescent probes”. In: *Methods Enzymol.* Ed. by Marriott Gerard. Vol. Volume 291. Academic Press, 1998, pp. 63–78. ISBN: 0076-6879. DOI: http://dx.doi.org/10.1016/S0076-6879(98)91007-2. URL: http://www.sciencedirect.com/science/article/pii/S0076687998910072.

[47] B. Amit and A. Patchornik. “The photorearrangement of N-substituted ortho-nitroanilides and nitroveratramides. A potential photosensitive protecting group”. In: *Tetrahedron Lett.* 14.24 (1973), pp. 2205–2208. ISSN: 0040-4039. DOI: http://dx.doi.org/10.1016/S0040-4039(01)87596-1. URL: http://www.sciencedirect.com/science/article/pii/S0040403901875961.

[48] Boaz Amit, David A. Ben-Efraim, and Abraham Patchornik. “Light-sensitive amides. Photocleavage of N-acyl-1,2,3,4-tetrahydro-8-nitroquinolines to give free carboxylic acids”. In: *J. Chem. Soc., Perkin Trans. 1* 1 (1976), pp. 57–63. ISSN: 0300-922X. DOI: 10.1039/P19760000057. URL: http://dx.doi.org/10.1039/P19760000057.

[49] George Papageorgiou et al. “Synthetic and photochemical studies of substituted 1-acyl-7-nitroindolines”. In: *Photochem. Photobiol. Sci.* 4.11 (2005), pp. 887–896. ISSN: 1474-905X. DOI: 10.1039/B508756B. URL: http://dx.doi.org/10.1039/B508756B.

[50] Richard S. Givens and Bogdan Matuszewski. “Photochemistry of phosphate esters: an efficient method for the generation of electrophiles”. In: *J. Am. Chem. Soc.* 106.22 (1984), pp. 6860–6861. ISSN: 0002-7863. DOI: 10.1021/ja00334a075. URL: http://dx.doi.org/10.1021/ja00334a075.

[51] Reinhard Schmidt et al. “Kinetics Study of the Photocleavage of (Coumarin-4-yl)methyl Esters”. In: *J. Phys. Chem. A* 109.23 (2005), pp. 5000–5004. ISSN: 1089-5639. DOI: 10.1021/jp050581k. URL: http://dx.doi.org/10.1021/jp050581k.

[52] Naoko Senda et al. “Synthesis and Photochemical Properties of a New Water-Soluble Coumarin, Designed as a Chromophore for Highly Water-Soluble and Photolabile Protecting Group”. In: *Bull. Chem. Soc. Jpn.* 79.11 (2006), pp. 1753–1757. DOI: 10.1246/bcsj.79.1753.

[53] Björn Schade et al. “Deactivation Behavior and Excited-State Properties of (Coumarin-4-yl)methyl Derivatives. 1. Photocleavage of (7-Methoxycoumarin-4-yl)methyl-Caged Acids with Fluorescence Enhancement”. In: *J. Org. Chem.* 64.25 (1999), pp. 9109–9117. ISSN: 0022-3263. DOI: 10.1021/jo9910233. URL: http://dx.doi.org/10.1021/jo9910233.

[54] Francis M. Rossi and Joseph P. Y. Kao. “Nmoc-DBHQ, a New Caged Molecule for Modulating Sarcoplasmic/Endoplasmic Reticulum Ca2+ ATPase Activity with Light Flashes”. In: *J. Biol. Chem.* 272.6 (1997), pp. 3266–3271. DOI: 10.1074/jbc.272.6.3266. URL: http://www.jbc.org/content/272/6/3266.abstract.

[55] Rolf-Markus Szeimies et al. “Topical photodynamic therapy in dermatology”. In: *J. Photochem. Photobiol., B* 36.2 (1996), pp. 213–219. ISSN: 1011-1344. DOI: http://dx.doi.org/10.1016/S1011-1344(96)07375-7. URL: http://www.sciencedirect.com/science/article/pii/S1011134496073757.

[56] Agatha Schwarz et al. “Interleukin-12 suppresses ultraviolet radiation-induced apoptosis by inducing DNA repair”. In: *Nat Cell Biol* 4.1 (2002), pp. 26–31. ISSN: 1465-7392. URL: http://dx.doi.org/10.1038/ncb717.

[57] Marta Álvarez et al. “Modulating Surface Density of Proteins via Caged Surfaces and Controlled Light Exposure”. In: *Langmuir* 27.6 (2011), pp. 2789–2795. ISSN: 0743-7463. DOI: 10.1021/la104511x. URL: http://dx.doi.org/10.1021/la104511x.

[58] Dominik Wöll et al. “Triplet-Sensitized Photodeprotection of Oligonucleotides in Solution and on Microarray Chips”. In: *Helv. Chim. Acta* 87.1 (2004), pp. 28–45. ISSN: 1522-2675. DOI: 10.1002/hlca.200490015. URL: http://dx.doi.org/10.1002/hlca.200490015.

[59] Abdelaziz Houmam. “Electron Transfer Initiated Reactions: Bond Formation and Bond Dissociation”. In: *Chem. Rev.* 108.7 (2008), pp. 2180–2237. ISSN: 0009-2665. DOI: 10.1021/cr068070x. URL: http://dx.doi.org/10.1021/cr068070x.

[60] Daniel E. Falvey and Chitra Sundararajan. “Photoremovable protecting groups based on electron transfer chemistry”. In: *Photochem. Photobiol. Sci.* 3.9 (2004), pp. 831–838. ISSN: 1474-905X. DOI: 10.1039/B406866A. URL: http://dx.doi.org/10.1039/B406866A.

[61] Ludovic Fournier et al. “Coumarinylmethyl Caging Groups with Redshifted Absorption”. In: *Chem. – Eur. J.* 19.51 (2013), pp. 17494–17507. ISSN: 1521-3765. DOI: 10.1002/chem.201302630. URL: http://dx.doi.org/10.1002/chem.201302630.

[62] FP Dwyer, HA Goodwin, and EC Gyarfas. “Mono- and Bis-(2,2’-bipyridine) and -(1,10-phenanthroline) Chelates of Ruthenium and Osmium. II. Bischelates of Bivalent and Tervalent Ruthenium”. In: *Aust. J. Chem.* 16.4 (1963), pp. 544–548. DOI: http://dx.doi.org/10.1071/CH9630544. URL: http://www.publish.csiro.au/paper/CH9630544.

[63] David V. Pinnick and Bill Durham. “Photosubstitution reactions of Ru(bpy)2XYn+ complexes”. In: *Inorg. Chem.* 23.10 (1984), pp. 1440–1445. ISSN: 0020-1669. DOI: 10.1021/ic00178a028. URL: http://dx.doi.org/10.1021/ic00178a028.

[64] Leonardo Zayat et al. *Ruthenium polypyridyl phototriggers: from beginnings to perspectives*. Vol. 371. 2013. DOI: 10.1098/rsta.2012.0330. URL: http://rsta.royalsocietypublishing.org/roypta/371/1995/20120330.full.pdf.

[65] Leonardo Zayat et al. “A New Inorganic Photolabile Protecting Group for Highly Efficient Visible Light GABA Uncaging”. In: *ChemBioChem* 8.17 (2007), pp. 2035–2038. ISSN: 1439-7633. DOI: 10.1002/cbic.200700354. URL: http://dx.doi.org/10.1002/cbic.200700354.

[66] Marcelo Salierno et al. “A fast ruthenium polypyridine cage complex photoreleases glutamate with visible or IR light in one and two photon regimes”. In: *J. Inorg. Biochem.* 104.4 (2010), pp. 418–422. ISSN: 0162-0134. DOI: http://dx.doi.org/10.1016/j.jinorgbio.2009.12.004. URL: http://www.sciencedirect.com/science/article/pii/S0162013409003092.

[67] Peter Šebej et al. “Fluorescein Analogues as Photoremovable Protecting Groups Absorbing at 520 nm”. In: *J. Org. Chem.* 78.5 (2013), pp. 1833–1843. ISSN: 0022-3263. DOI: 10.1021/jo301455n. URL: http://dx.doi.org/10.1021/jo301455n.

[68] Tomáš Pastierik et al. “Near-Infrared Fluorescent 9-Phenylethynylpyronin Analogues for Bioimaging”. In: *J. Org. Chem.* 79.8 (2014), pp. 3374–3382. ISSN: 0022-3263. DOI: 10.1021/jo500140y. URL: http://dx.doi.org/10.1021/jo500140y.

[69] Alexander T. Buck, Christie L. Beck, and Arthur H. Winter. “Inverted Substrate Preferences for Photochemical Heterolysis Arise from Conical Intersection Control”. In: *J. Am. Chem. Soc.* 136.25 (2014), pp. 8933–8940. ISSN: 0002-7863. DOI: 10.1021/ja501777r. URL: http://dx.doi.org/10.1021/ja501777r.

[70] Pratik P. Goswami et al. “BODIPY-Derived Photoremovable Protecting Groups Unmasked with Green Light”. In: *J. Am. Chem. Soc.* 137.11 (2015), pp. 3783–3786. ISSN: 0002-7863. DOI: 10.1021/jacs.5b01297. URL: http://dx.doi.org/10.1021/jacs.5b01297.

[71] Nobuhiro Umeda et al. “Boron Dipyrromethene As a Fluorescent Caging Group for Single-Photon Uncaging with Long-Wavelength Visible Light”. In: *ACS Chem. Biol.* 9.10 (2014), pp. 2242–2246. ISSN: 1554-8929. DOI: 10.1021/cb500525p. URL: http://dx.doi.org/10.1021/cb500525p.

[72] John F. Kauffman et al. “Two-Photon Excitation of Substituted Enediynes”. In: *J. Phys. Chem. A* 110.1 (2006), pp. 241–251. ISSN: 1089-5639. DOI: 10.1021/jp056127y. URL: http://dx.doi.org/10.1021/jp056127y.

[73] Alexander Hopt and Erwin Neher. “Highly Nonlinear Photodamage in Two-Photon Fluorescence Microscopy”. In: *Biophys. J.* 80.4 (), pp. 2029–2036. DOI: 10.1016/S0006-3495(01)76173-5. URL: http://dx.doi.org/10.1016/S0006-3495(01)76173-5.

[74] Hsien-Ming Lee, Daniel R. Larson, and David S. Lawrence. “Illuminating the Chemistry of Life: Design, Synthesis, and Applications of “Caged” and Related Photoresponsive Compounds”. In: *ACS Chem. Biol.* 4.6 (2009), pp. 409–427. ISSN: 1554-8929. DOI: 10.1021/cb900036s. URL: http://dx.doi.org/10.1021/cb900036s.

[75] K. Fendler et al. “[17] Investigation of charge translocation by ion pumps and carriers using caged substrates”. In: *Methods Enzymol.* Ed. by Marriott Gerard. Vol. Volume 291. Academic Press, 1998, pp. 289–306. ISBN: 0076-6879. DOI: http://dx.doi.org/10.1016/S0076-6879(98)91020-5. URL: http://www.sciencedirect.com/science/article/pii/S0076687998910205.

[76] Xavier Nicol et al. “cAMP oscillations and retinal activity are permissive for ephrin signaling during the establishment of the retinotopic map”. In: *Nat Neurosci* 10.3 (2007), pp. 340–347. ISSN: 1097-6256. DOI: http://www.nature.com/neuro/journal/v10/n3/suppinfo/nn1842_S1.html. URL: http://dx.doi.org/10.1038/nn1842.

[77] Toshiaki Furuta et al. “Photochemical Properties of New Photolabile cAMP Derivatives in a Physiological Saline Solution”. In: *J. Org. Chem.* 60.13 (1995), pp. 3953–3956. ISSN: 0022-3263. DOI: 10.1021/jo00118a008. URL: http://dx.doi.org/10.1021/jo00118a008.

[78] Toshiaki Furuta et al. “Acyloxycoumarinylmethyl-Caged cAMP, the Photolabile and Membrane-Permeable Derivative of cAMP That Effectively Stimulates Pigment-Dispersion Response of Melanophores”. In: *Biochem. Biophys. Res. Commun.* 228.1 (1996), pp. 193–198. ISSN: 0006-291X. DOI: http://dx.doi.org/10.1006/bbrc.1996.1638. URL: http://www.sciencedirect.com/science/article/pii/S0006291X96916381.

[79] Nick Callamaras and Ian Parker. “[21] Caged inositol 1,4,5-trisphosphate for studying release of Ca2+ from intracellular stores”. In: *Methods Enzymol.* Ed. by Marriott Gerard. Vol. Volume 291. Academic Press, 1998, pp. 380–403. ISBN: 0076-6879. DOI: http://dx.doi.org/10.1016/S0076-6879(98)91024-2. URL: http://www.sciencedirect.com/science/article/pii/S0076687998910242.

[80] Hon Cheung Lee et al. “Caged Nicotinic Acid Adenine Dinucleotide Phosphate: SYNTHESIS AND USE”. In: *J. Biol. Chem.* 272.7 (1997), pp. 4172–4178. DOI: 10.1074/jbc.272.7.4172. URL: http://www.jbc.org/content/272/7/4172.abstract.

[81] Christof Grewer et al. “A New Photolabile Precursor of Glycine with Improved Properties: A Tool for Chemical Kinetic Investigations of the Glycine Receptor†”. In: *Biochemistry* 39.8 (2000), pp. 2063–2070. ISSN: 0006-2960. DOI: 10.1021/bi9919652. URL: http://dx.doi.org/10.1021/bi9919652.

[82] Kyle R. Gee et al. “Synthesis and Photochemistry of a Photolabile Precursor of N-Methyl-d-Aspartate (NMDA) That Is Photolyzed in the Microsecond Time Region and Is Suitable for Chemical Kinetic Investigations of the NMDA Receptor”. In: *Biochemistry* 38.10 (1999), pp. 3140–3147. ISSN: 0006-2960. DOI: 10.1021/bi9826557. URL: http://dx.doi.org/10.1021/bi9826557.

[83] Michael P. Van Ryssen et al. “Synthesis, photolysis studies and in vitro photorelease of caged TRPV1 agonists and antagonists”. In: *Org. Biomol. Chem.* 7.22 (2009), pp. 4695–4707. ISSN: 1477-0520. DOI: 10.1039/B914981C. URL: http://dx.doi.org/10.1039/B914981C.

[84] Richard S. Givens et al. “New Phototriggers 9: p-Hydroxyphenacyl as a C-Terminal Photoremovable Protecting Group for Oligopeptides”. In: *J. Am. Chem. Soc.* 122.12 (2000), pp. 2687–2697. ISSN: 0002-7863. DOI: 10.1021/ja991014b. URL: http://dx.doi.org/10.1021/ja991014b.

[85] Toshiaki Furuta et al. “Phototriggers for Nucleobases with Improved Photochemical Properties”. In: *Org. Lett.* 9.23 (2007), pp. 4717–4720. ISSN: 1523-7060. DOI: 10.1021/ol702106t. URL: http://dx.doi.org/10.1021/ol702106t.

[86] XinJing Tang and Ivan J. Dmochowski. “Synthesis of light-activated antisense oligodeoxynucleotide”. In: *Nat. Protocols* 1.6 (2007), pp. 3041–3048. ISSN: 1754-2189. URL: http://dx.doi.org/10.1038/nprot.2006.462.

[87] Hideki Ando et al. “Photo-mediated gene activation using caged RNA/DNA in zebrafish embryos”. In: *Nat Genet* 28.4 (2001), pp. 317–325. ISSN: 1061-4036. DOI: http://www.nature.com/ng/journal/v28/n4/suppinfo/ng583_S1.html. URL: http://dx.doi.org/10.1038/ng583.

[88] W. Todd Monroe et al. “Targeting Expression with Light Using Caged DNA”. In: *J. Biol. Chem.* 274.30 (1999), pp. 20895–20900. DOI: 10.1074/jbc.274.30.20895. URL: http://www.jbc.org/content/274/30/20895.abstract.

[89] Anhco Nguyen et al. “Caged phosphopeptides reveal a temporal role for 14-3-3 in G1 arrest and S-phase checkpoint function”. In: *Nat. Biotechnol.* 22.8 (2004), pp. 993–1000. ISSN: 1087-0156. DOI: http://www.nature.com/nbt/journal/v22/n8/suppinfo/nbt997_S1.html. URL: http://dx.doi.org/10.1038/nbt997.

[90] April M. Kloxin et al. “Photodegradable Hydrogels for Dynamic Tuning of Physical and Chemical Properties”. In: *Science* 324.5923 (2009), pp. 59–63. DOI: 10.1126/science.1169494. URL: http://www.sciencemag.org/content/324/5923/59.abstract.

[91] Brenda Ayers et al. “Introduction of unnatural amino acids into proteins using expressed protein ligation”. In: *Peptide Science* 51.5 (1999), pp. 343–354. ISSN: 1097-0282. DOI: 10.1002/(SICI)1097-0282(1999)51:5<343::AID-BIP4>3.0.CO;2-W. URL: http://dx.doi.org/10.1002/(SICI)1097-0282(1999)51:5%3C343::AID-BIP4%3E3.0.CO;2-W.

[92] Pamela M. England. “Unnatural Amino Acid Mutagenesis: A Precise Tool for Probing Protein Structure and Function”. In: *Biochemistry* 43.37 (2004), pp. 11623–11629. ISSN: 0006-2960. DOI: 10.1021/bi048862q. URL: http://dx.doi.org/10.1021/bi048862q.

[93] Alexander Deiters et al. “A Genetically Encoded Photocaged Tyrosine”. In: *Angewandte Chemie International Edition* 45.17 (2006), pp. 2728–2731. ISSN: 1521-3773. DOI: 10.1002/anie.200600264. URL: http://dx.doi.org/10.1002/anie.200600264.

[94] Ning Wu et al. “A Genetically Encoded Photocaged Amino Acid”. In: *Journal of the American Chemical Society* 126.44 (2004), pp. 14306–14307. ISSN: 0002-7863. DOI: 10.1021/ja040175z. URL: http://dx.doi.org/10.1021/ja040175z.

[95] Edward A. Lemke et al. “Control of protein phosphorylation with a genetically encoded photocaged amino acid”. In: *Nat Chem Biol* 3.12 (2007), pp. 769–772. ISSN: 1552-4450. DOI: http://www.nature.com/nchembio/journal/v3/n12/suppinfo/nchembio.2007.44_S1.html. URL: http://dx.doi.org/10.1038/nchembio.2007.44.

[96] Arnaud Gautier et al. “Genetically Encoded Photocontrol of Protein Localization in Mammalian Cells”. In: *Journal of the American Chemical Society* 132.12 (2010), pp. 4086–4088. ISSN: 0002-7863. DOI: 10.1021/ja910688s. URL: http://dx.doi.org/10.1021/ja910688s.

[97] Jeremy P. Olson et al. “Spectral Evolution of a Photochemical Protecting Group for Orthogonal Two-Color Uncaging with Visible Light”. In: *J. Am. Chem. Soc.* 135.42 (2013), pp. 15948–15954. ISSN: 0002-7863. DOI: 10.1021/ja408225k. URL: http://pubs.acs.org/doi/abs/10.1021/ja408225k.

[98] Christian G. Bochet. “Wavelength-selective cleavage of photolabile protecting groups”. In: *Tetrahedron Lett.* 41.33 (2000), pp. 6341–6346. ISSN: 0040-4039. DOI: http://dx.doi.org/10.1016/S0040-4039(00)01050-9. URL: http://www.sciencedirect.com/science/article/pii/S0040403900010509.

[99] George Barany and R. B. Merrifield. “A new amino protecting group removable by reduction. Chemistry of the dithiasuccinoyl (Dts) function”. In: *J. Am. Chem. Soc.* 99.22 (1977), pp. 7363–7365. ISSN: 0002-7863. DOI: 10.1021/ja00464a050. URL: http://dx.doi.org/10.1021/ja00464a050.

[100] Mickel J. Hansen et al. “Wavelength-selective cleavage of photoprotecting groups: strategies and applications in dynamic systems”. In: *Chemical Society Reviews* 44.11 (2015), pp. 3358–3377. ISSN: 0306-0012. DOI: 10.1039/C5CS00118H. URL: http://dx.doi.org/10.1039/C5CS00118H.

[101] Verónica San Miguel, Christian G. Bochet, and Aránzazu del Campo. “Wavelength-Selective Caged Surfaces: How Many Functional Levels Are Possible?” In: *J. Am. Chem. Soc.* 133.14 (2011), pp. 5380–5388. ISSN: 0002-7863. DOI: 10.1021/ja110572j. URL: http://dx.doi.org/10.1021/ja110572j.

[102] Alexandre Rodrigues-Correia, Xenia M. M. Weyel, and Alexander Heckel. “Four Levels of Wavelength-Selective Uncaging for Oligonucleotides”. In: *Org. Lett.* 15.21 (2013), pp. 5500–5503. ISSN: 1523-7060. DOI: 10.1021/ol402657j. URL: http://dx.doi.org/10.1021/ol402657j.

[103] Florian Schäfer et al. “Wavelength-Selective Uncaging of dA and dC Residues”. In: *Org. Lett.* 13.6 (2011), pp. 1450–1453. ISSN: 1523-7060. DOI: 10.1021/ol200141v. URL: http://dx.doi.org/10.1021/ol200141v.

[104] Aurélien Blanc and Christian G. Bochet. “Wavelength-Controlled Orthogonal Photolysis of Protecting Groups”. In: *J. Org. Chem.* 67.16 (2002), pp. 5567–5577. ISSN: 0022-3263. DOI: 10.1021/jo025837m. URL: http://dx.doi.org/10.1021/jo025837m.

[105] Martin Kessler et al. “Sequentially Photocleavable Protecting Groups in Solid-Phase Synthesis”. In: *Org. Lett.* 5.8 (2003), pp. 1179–1181. ISSN: 1523-7060. DOI: 10.1021/ol027454g. URL: http://dx.doi.org/10.1021/ol027454g.

[106] Megan N. Stanton-Humphreys et al. “Wavelength-orthogonal photolysis of neurotransmittersin vitro”. In: *Chem. Commun.* 48.5 (2012), pp. 657–659. ISSN: 1359-7345. DOI: 10.1039/C1CC15135E. URL: http://dx.doi.org/10.1039/C1CC15135E.

[107] Joseph M. Amatrudo et al. “Wavelength-Selective One- and Two-Photon Uncaging of GABA”. In: *ACS Chem. Neurosci.* 5.1 (2014), pp. 64–70. DOI: 10.1021/cn400185r. URL: http://dx.doi.org/10.1021/cn400185r.

[108] Alexandre Rodrigues-Correia et al. “Selective Uncaging of DNA through Reaction Rate Selectivity”. In: *Org. Lett.* 16.19 (2014), pp. 5128–5131. ISSN: 1523-7060. DOI: 10.1021/ol502478g. URL: http://dx.doi.org/10.1021/ol502478g.

[109] I R Booth. “Regulation of cytoplasmic pH in bacteria”. In: *Microbiol. Rev.* 49.4 (1985), pp. 359–378. URL: http://mmbr.asm.org/content/49/4/359.short.

[110] Tatsunosuke Nakamura et al. “KtrAB, a New Type of Bacterial K+-Uptake System from Vibrio alginolyticus”. In: *J. Bacteriol.* 180.13 (1998), pp. 3491–3494. URL: http://jb.asm.org/content/180/13/3491.abstract.

[111] Gail P. Ferguson et al. “Activation of potassium channels during metabolite detoxification in Escherichia coli”. In: *Molecular Microbiology* 9.6 (1993), pp. 1297–1303. ISSN: 1365-2958. DOI: 10.1111/j.1365-2958.1993.tb01259.x. URL: http://dx.doi.org/10.1111/j.1365-2958.1993.tb01259.x.

[112] Tarmo P Roosild et al. “KTN (RCK) domains regulate K+ channels and transporters by controlling the dimer-hinge conformation”. In: *Structure* 17.6 (2009), pp. 893–903. ISSN: 0969-2126.

[113] Lorna S. Ness and Ian R. Booth. “Different Foci for the Regulation of the Activity of the KefB and KefC Glutathione-gated K+ Efflux Systems”. In: *J. Biol. Chem.* 274.14 (1999), pp. 9524–9530. DOI: 10.1074/jbc.274.14.9524. URL: http://www.jbc.org/content/274/14/9524.abstract.

[114] Jessica Healy et al. “Understanding the Structural Requirements for Activators of the Kef Bacterial Potassium Efflux System”. In: *Biochemistry* 53.12 (2014), pp. 1982–1992. ISSN: 0006-2960. DOI: 10.1021/bi5001118. URL: http://dx.doi.org/10.1021/bi5001118.

[115] Samantha Miller et al. “Mutations in the Glutathione-gated KefC K+ Efflux System of Escherichia coli That Cause Constitutive Activation”. In: *J. Biol. Chem.* 272.40 (1997), pp. 24942–24947. DOI: 10.1074/jbc.272.40.24942. URL: http://www.jbc.org/content/272/40/24942.abstract.

[116] Tarmo P. Roosild et al. “Mechanism of ligand-gated potassium efflux in bacterial pathogens”. In: *Proc. Natl. Acad. Sci.* 107.46 (2010), pp. 19784–19789. DOI: 10.1073/pnas.1012716107. URL: http://www.pnas.org/content/107/46/19784.abstract.

[117] Volker Gatterdam et al. “Caged Glutathione – Triggering Protein Interaction by Light”. In: *Angewandte Chemie International Edition* 51.16 (2012), pp. 3960–3963. ISSN: 1521-3773. DOI: 10.1002/anie.201108073. URL: http://dx.doi.org/10.1002/anie.201108073.

[118] Fatemeh Jahani et al. “An efficient and highly chemoselective N-Boc protection of amines, amino acids, and peptides under heterogeneous conditions”. In: *Monatshefte für Chemie - Chemical Monthly* 142.10 (2011), p. 1035. ISSN: 1434-4475. DOI: 10.1007/s00706-011-0534-2. URL: https://doi.org/10.1007/s00706-011-0534-2.

[119] Karl E. Krueger and Sudhir Srivastava. "Posttranslational Protein Modifications: Current Implications for Cancer Detection, Prevention, and Therapeutics". In: *Mol. Cell. Proteomics* 5.10 (2006), pp. 1799–1810. DOI: 10.1074/mcp.R600009-MCP200. URL: http://www.mcponline.org/content/5/10/1799.short.

[120] Susan A. Marsh and John C. Chatham. "The paradoxical world of protein O-GlcNAcylation: a novel effector of cardiovascular (dys)function". In: *Cardiovasc. Res.* 89.3 (2011), pp. 487–488. ISSN: 0008-6363 1755-3245. DOI: 10.1093/cvr/cvq405. URL: http://www.ncbi.nlm.nih.gov/pmc/articles/PMC3028980/.

[121] Ru-Jing Ren et al. "Proteomics of protein post-translational modifications implicated in neurodegeneration". In: *Transl. Neurodegener.* 3 (2014), p. 23. ISSN: 2047-9158. DOI: 10.1186/2047-9158-3-23. URL: http://www.ncbi.nlm.nih.gov/pmc/articles/PMC4323146/.

[122] Tejaswita M. Karve and Amrita K. Cheema. "Small Changes Huge Impact: The Role of Protein Posttranslational Modifications in Cellular Homeostasis and Disease". In: *J. Amino Acids* 2011 (2011). DOI: 10.4061/2011/207691. URL: http://dx.doi.org/10.4061/2011/207691.

[123] GeorgeC Khoury and DavidC Zimmerman. "Development of Pretest Planning Methodologies for Load Dependent Ritz Vectors". In: *Rotating Machinery, Structural Health Monitoring, Shock and Vibration, Volume 5*. Ed. by Tom Proulx. Conference Proceedings of the Society for Experimental Mechanics Series. Springer New York, 2011. Chap. 1, pp. 1–13. ISBN: 978-1-4419-9427-1. DOI: 10.1007/978-1-4419-9428-8_1. URL: http://dx.doi.org/10.1007/978-1-4419-9428-8_1.

[124] Cheng-Tsung Lu et al. "An Intelligent System for Identifying Acetylated Lysine on Histones and Nonhistone Proteins". In: *Biomed. Res.* 2014 (2014), p. 11. DOI: 10.1155/2014/528650. URL: http://dx.doi.org/10.1155/2014/528650.

[125] Stuart J. Conway. "Bromodomains: Are Readers Right for Epigenetic Therapy?" In: *ACS Med. Chem. Lett.* 3.9 (2012), pp. 691–694. DOI: 10.1021/ml300221t. URL: http://dx.doi.org/10.1021/ml300221t.

[126] Mohammed Arif et al. "Protein lysine acetylation in cellular function and its role in cancer manifestation". In: *Biochim. Biophys. Acta* 1799.10–12 (2010), pp. 702–716. ISSN: 1874-9399. DOI: http://dx.doi.org/10.1016/j.bbagrm.2010.10.002. URL: http://www.sciencedirect.com/science/article/pii/S1874939910001239.

[127] Werner K. Maas, G. David Novelli, and Fritz Lipmann. "Acetylation of Glutamic Acid by Extracts of Escherichia Coli". In: *Proc. Natl. Acad. Sci. U. S. A.* 39.10 (1953), pp. 1004–1008. ISSN: 0027-8424 1091-6490. URL: http://www.ncbi.nlm.nih.gov/pmc/articles/PMC1063897/.

[128] Isabella Dalle-Donne et al. "Protein carbonylation, cellular dysfunction, and disease progression". In: *J. Cell. Mol. Med.* 10.2 (2006), pp. 389–406. ISSN: 1582-4934.

[129] Thomas Nyström. “Role of oxidative carbonylation in protein quality control and senescence”. In: *EMBO J.* 24.7 (2005), pp. 1311–1317. ISSN: 0261-4189.

[130] John F Rakus and Lara K Mahal. “New technologies for glycomic analysis: toward a systematic understanding of the glycome”. In: *Annu. Rev. Anal. Chem. (Palo Alto Calif)* 4 (2011), pp. 367–392. ISSN: 1936-1327.

[131] Danielle H. Dube and Carolyn R. Bertozzi. “Glycans in cancer and inflammation [mdash] potential for therapeutics and diagnostics”. In: *Nat Rev Drug Discov* 4.6 (2005), pp. 477–488. ISSN: 1474-1776. URL: http://dx.doi.org/10.1038/nrd1751.

[132] Agustín Albillos, Margaret Lario, and Melchor Álvarez-Mon. “Cirrhosis-associated immune dysfunction: Distinctive features and clinical relevance”. In: *J. Hepatol.* 61.6 (2014), pp. 1385–1396. ISSN: 0168-8278. DOI: http://dx.doi.org/10.1016/j.jhep.2014.08.010. URL: http://www.sciencedirect.com/science/article/pii/S0168827814005492.

[133] Gaya Thanabalasingham et al. “Mutations in HNF1A Result in Marked Alterations of Plasma Glycan Profile”. In: *Diabetes* 62.4 (2013), pp. 1329–1337. ISSN: 0012-1797 1939-327X. DOI: 10.2337/db12-0880. URL: http://www.ncbi.nlm.nih.gov/pmc/articles/PMC3609552/.

[134] Dirk Eggink et al. “Lack of complex N-glycans on HIV-1 envelope glycoproteins preserves protein conformation and entry function”. In: *Virology* 401.2 (2010), pp. 236–247. ISSN: 0042-6822. DOI: http://dx.doi.org/10.1016/j.virol.2010.02.019. URL: http://www.sciencedirect.com/science/article/pii/S0042682210001285.

[135] CI Levene, CD Ockleford, and CL Barber. “Scurvy; a comparison between ultrastructural and biochemical changes observed in cultured fibroblasts and the collagen they synthesise”. In: *Virchows Arch. B* 23.1 (1977), pp. 325–338. ISSN: 0340-6075.

[136] Elvira C. Riesgo, Xiaoqing Jin, and Randolph P. Thummel. “Introduction of Benzo[h]quinoline and 1,10-Phenanthroline Subunits by Friedländer Methodology”. In: *J. Org. Chem.* 61.9 (1996), pp. 3017–3022. ISSN: 0022-3263. DOI: 10.1021/jo952164h. URL: http://dx.doi.org/10.1021/jo952164h.

[137] Andrés Villalpando et al. “Triphosgene–Amine Base Promoted Chlorination of Unactivated Aliphatic Alcohols”. In: *J. Org. Chem.* 78.8 (2013), pp. 3989–3996. ISSN: 0022-3263. DOI: 10.1021/jo400341n. URL: http://dx.doi.org/10.1021/jo400341n.

[138] Vijayakumar Ramalingam et al. “A cucurbit[8]uril sponge”. In: *Org. Biomol. Chem.* 10.43 (2012), pp. 8587–8589. ISSN: 1477-0520. DOI: 10.1039/C2OB26774H. URL: http://dx.doi.org/10.1039/C2OB26774H.

[139] Paul F Fitzpatrick. “Mechanism of aromatic amino acid hydroxylation”. In: *Biochemistry* 42.48 (2003), pp. 14083–14091. ISSN: 0006-2960. URL: http://pubs.acs.org/doi/pdfplus/10.1021/bi035656u.

[140] Nenad Blau, Francjan J van Spronsen, and Harvey L Levy. “Phenylketonuria”. In: *Lancet* 376.9750 (2010), pp. 1417–1427. ISSN: 0140-6736.

[141] Håkan Hedstrand et al. “Identification of tyrosine hydroxylase as an autoantigen in autoimmune polyendocrine syndrome type I”. In: *Biochem. Biophys. Res. Commun.* 267.1 (2000), pp. 456–461. ISSN: 0006-291X.

[142] Lin Wang et al. “Three-dimensional structure of human tryptophan hydroxylase and its implications for the biosynthesis of the neurotransmitters serotonin and melatonin”. In: *Biochemistry* 41.42 (2002), pp. 12569–12574. ISSN: 0006-2960.

[143] Mellissa RW Mann and Marisa S Bartolomei. “Epigenetic reprogramming in the mammalian embryo: struggle of the clones”. In: *Genome Biol.* 3.2 (2002), REVIEWS1003.

[144] Xi Zhang, Hong Wen, and Xiaobing Shi. “Lysine methylation: beyond histones”. In: *Acta Biochim. Biophys. Sin.* 44.1 (2012), pp. 14–27. DOI: 10.1093/abbs/gmr100. URL: http://abbs.oxfordjournals.org/content/44/1/14.abstract.

[145] Xiao-Dong Yang, Acacia Lamb, and Lin-Feng Chen. “Methylation, a new epigenetic mark for protein stability”. In: *Epigenetics* 4.7 (2009), pp. 429–433. ISSN: 1559-2294.

[146] Ryuji Hamamoto et al. “SMYD3 encodes a histone methyltransferase involved in the proliferation of cancer cells”. In: *Nat Cell Biol* 6.8 (2004), pp. 731–740. ISSN: 1465-7392. DOI: http://www.nature.com/ncb/journal/v6/n8/suppinfo/ncb1151_S1.html. URL: http://dx.doi.org/10.1038/ncb1151.

[147] Kuo-Tai Hua et al. “The H3K9 methyltransferase G9a is a marker of aggressive ovarian cancer that promotes peritoneal metastasis”. In: *Mol. Cancer* 13 (2014), p. 189. ISSN: 1476-4598. DOI: 10.1186/1476-4598-13-189. URL: http://www.ncbi.nlm.nih.gov/pmc/articles/PMC4260797/.

[148] Frank P Vendetti and Charles M Rudin. “Epigenetic therapy in non-small-cell lung cancer: targeting DNA methyltransferases and histone deacetylases”. In: *Expert Opin. Biol. Ther.* 13.9 (2013), pp. 1273–1285. DOI: doi:10.1517/14712598.2013.819337. URL: http://informahealthcare.com/doi/abs/10.1517/14712598.2013.819337.

[149] Eric L. Greer and Yang Shi. “Histone methylation: a dynamic mark in health, disease and inheritance”. In: *Nat Rev Genet* 13.5 (2012), pp. 343–357. ISSN: 1471-0056. DOI: http://www.nature.com/nrg/journal/v13/n5/suppinfo/nrg3173_S1.html. URL: http://dx.doi.org/10.1038/nrg3173.

[150] Mohamed A. Abdelmegeed and Byoung-Joon Song. “Functional Roles of Protein Nitration in Acute and Chronic Liver Diseases”. In: *Oxid. Med. Cell. Longev.* 2014 (2014), p. 21. DOI: 10.1155/2014/149627. URL: http://dx.doi.org/10.1155/2014/149627.

[151] Harry Ischiropoulos. “Protein tyrosine nitration—an update”. In: *Arch. Biochem. Biophys.* 484.2 (2009), pp. 117–121. ISSN: 0003-9861.

[152] Fares Masri. “Role of nitric oxide and its metabolites as potential markers in lung cancer”. In: *Ann. Thorac. Med.* 5.3 (2010), pp. 123–127. ISSN: 1817-1737 1998-3557. DOI: 10.4103/1817-1737.65036. URL: http://www.ncbi.nlm.nih.gov/pmc/articles/PMC2930648/.

[153] Lani L. Hardy, Darin A. Wick, and John R. Webb. “Conversion of Tyrosine to the Inflammation-Associated Analog 3-Nitrotyrosine at Either TCR- or MHC-Contact Positions Can Profoundly Affect Recognition of the MHC Class I-Restricted Epitope of Lymphocytic Choriomeningitis Virus Glycoprotein 33 by CD8 T Cells”. In: *J. Immunol.* 180.9 (2008), pp. 5956–5962. DOI: 10.4049/jimmunol.180.9.5956. URL: http://www.jimmunol.org/content/180/9/5956.abstract.

[154] Péter Bencsik et al. “Serum lipids and cardiac function correlate with nitrotyrosine and MMP activity in coronary artery disease patients”. In: *EUR. J. CLIN. INVEST.* 45.7 (2015), pp. 692–701. ISSN: 1365-2362. DOI: 10.1111/eci.12458. URL: http://dx.doi.org/10.1111/eci.12458.

[155] Nicolas Abello et al. “Protein tyrosine nitration: selectivity, physicochemical and biological consequences, denitration, and proteomics methods for the identification of tyrosine-nitrated proteins”. In: *J. Proteome Res.* 8.7 (2009), pp. 3222–3238. ISSN: 1535-3893.

[156] Christine Salaun, Jennifer Greaves, and Luke H Chamberlain. “The intracellular dynamic of protein palmitoylation”. In: *J. Cell Biol.* 191.7 (2010), pp. 1229–1238. ISSN: 0021-9525.

[157] Nadège A Pfender et al. “Route of uptake of palmitoylated encephalitogenic peptides of myelin proteolipid protein by antigen-presenting cells: importance of the type of bond between lipid chain and peptide and relevance to autoimmunity”. In: *J. Immunol.* 180.3 (2008), pp. 1398–1404. ISSN: 0022-1767.

[158] Xiaochao Wei et al. “De novo lipogenesis maintains vascular homeostasis through endothelial nitric-oxide synthase (eNOS) palmitoylation”. In: *J. Biol. Chem.* 286.4 (2011), pp. 2933–2945. ISSN: 0021-9258.

[159] Tony Hunter. “Protein kinases and phosphatases: the yin and yang of protein phosphorylation and signaling”. In: *Cell* 80.2 (1995), pp. 225–236. ISSN: 0092-8674.

[160] Arnold J Levine and Anna M Puzio-Kuter. “The control of the metabolic switch in cancers by oncogenes and tumor suppressor genes”. In: *Science* 330.6009 (2010), pp. 1340–1344. ISSN: 0036-8075.

[161] Kevin L Moore. “The biology and enzymology of protein tyrosine O-sulfation”. In: *J. Biol. Chem.* 278.27 (2003), pp. 24243–24246. ISSN: 0021-9258.

[162] John W Kehoe and Carolyn R Bertozzi. “Tyrosine sulfation: a modulator of extracellular protein–protein interactions”. In: *Chem. Biol.* 7.3 (2000), R57–R61. ISSN: 1074-5521.

[163] Christoph Seibert and Thomas P Sakmar. “Toward a framework for sulfoproteomics: Synthesis and characterization of sulfotyrosine-containing peptides”. In: *Pept. Sci.* 90.3 (2008), pp. 459–477. ISSN: 1097-0282.

[164] KD Wilkinson. “Protein ubiquitination: a regulatory post-translational modification”. In: *Anti-Cancer Drugs* 2.2 (1987), pp. 211–229. ISSN: 0266-9536.

[165] Edward TH Yeh, Limin Gong, and Tetsu Kamitani. “Ubiquitin-like proteins: new wines in new bottles”. In: *Gene* 248.1 (2000), pp. 1–14. ISSN: 0378-1119.

[166] Lynn Bedford et al. “Ubiquitin-like protein conjugation and the ubiquitin–proteasome system as drug targets”. In: *Nat. Rev. Drug Discovery* 10.1 (2011), pp. 29–46. ISSN: 1474-1776.

[167] Adam P. Lothrop, Matthew P. Torres, and Stephen M. Fuchs. “Deciphering post-translational modification codes”. In: *FEBS Lett.* 587.8 (2013), pp. 1247–1257. ISSN: 0014-5793. DOI: http://dx.doi.org/10.1016/j.febslet.2013.01.047. URL: http://www.sciencedirect.com/science/article/pii/S0014579313000926.

[168] I. A. Eliseeva et al. “Y-box-binding protein 1 (YB-1) and its functions”. In: *Biochemistry (Moscow)* 76.13 (2011), pp. 1402–1433. ISSN: 1608-3040. DOI: 10.1134/s0006297911130049. URL: https://doi.org/10.1134/S0006297911130049.

[169] Waldemar B. Minich, Igor P. Maidebura, and Lev P. Ovchinnikov. “Purification and characterization of the major 50-kDa repressor protein from cytoplasmic mRNP of rabbit reticulocytes”. In: *European Journal of Biochemistry* 212.3 (1993), pp. 633–638. ISSN: 1432-1033. DOI: 10.1111/j.1432-1033.1993.tb17701.x. URL: http://dx.doi.org/10.1111/j.1432-1033.1993.tb17701.x.

[170] Ralf C. Bargou et al. “Nuclear localization and increased levels of transcription factor YB-1 in primary human breast cancers are associated with intrinsic MDR1 gene expression”. In: *Nature Medicine* 3 (1997), p. 447. DOI: 10.1038/nm0497-447. URL: http://dx.doi.org/10.1038/nm0497-447.

[171] Takefumi Ohga et al. “Role of the Human Y Box-binding Protein YB-1 in Cellular Sensitivity to the DNA-damaging Agents Cisplatin, Mitomycin C, and Ultraviolet Light”. In: *Cancer Research* 56.18 (1996), pp. 4224–4228. URL: http://cancerres.aacrjournals.org/content/canres/56/18/4224.full.pdf.

[172] Yuanyuan Gao et al. “Inhibition of Y-box binding protein-1 slows the growth of glioblastoma multiforme and sensitizes to temozolomide independent O<sup>6-methylguanine-DNA methyltransferase”. In: *Molecular Cancer Therapeutics* 8.12 (2009), pp. 3276–3284. DOI: 10.1158/1535-7163.mct-09-0478. URL: http://mct.aacrjournals.org/content/molcanther/8/12/3276.full.pdf.

[173] Anna L. Stratford et al. “Y-box binding protein-1 serine 102 is a downstream target of p90 ribosomal S6 kinase in basal-like breast cancer cells”. In: *Breast Cancer Research* 10.6 (2008), R99. ISSN: 1465-542X. DOI: 10.1186/bcr2202. URL: https://doi.org/10.1186/bcr2202.

[174] Marcus Lutz et al. “Proteasomal degradation of the multifunctional regulator YB-1 is mediated by an F-Box protein induced during programmed cell death”. In: *FEBS Letters* 580.16 (2006), pp. 3921–3930. ISSN: 1873-3468. DOI: 10.1016/j.febslet.2006.06.023. URL: http://dx.doi.org/10.1016/j.febslet.2006.06.023.

[175] C. Choudhary et al. “Lysine acetylation targets protein complexes and co-regulates major cellular functions”. In: *Science* 325.5942 (2009), pp. 834–840. DOI: 10.1126/science.1175371. URL: https://www.scopus.com/inward/record.uri?eid=2-s2.0-68949212379&doi=10.1126%2fscience.1175371&partnerID=40&md5=408ddeb4da708168310a56aa21565b39.

[176] T. Lu et al. “Regulation of NF-B by NSD1/FBXL11-dependent reversible lysine methylation of p65”. In: *Proceedings of the National Academy of Sciences of the United States of America* 107.1 (2010), pp. 46–51. DOI: 10.1073/pnas.0912493107. URL: https://www.scopus.com/inward/record.uri?eid=2-s2.0-76249100563&doi=10.1073%2fpnas.0912493107&partnerID=40&md5=f0602a080ec206dd0ed34440343c451f.

[177] M. H. Holshouser and M. Kolb. “Facile synthesis of glycol metabolites of phenethylamine drugs1”. In: *J. Pharm. Sci.* 75.6 (1986), pp. 619–621. ISSN: 1520-6017. DOI: 10.1002/jps.2600750621. URL: http://dx.doi.org/10.1002/jps.2600750621.

[178] Gao Shang et al. “Asymmetric Hydrogenation of -Primary and Secondary Amino Ketones: Efficient Asymmetric Syntheses of ()-Arbutamine and ()-Denopamine”. In: *Chem. – Eur. J.* 13.27 (2007), pp. 7780–7784. ISSN: 1521-3765. DOI: 10.1002/chem.200700594. URL: http://dx.doi.org/10.1002/chem.200700594.

[179] L. Carroll King and G. Kenneth Ostrum. “Selective Bromination with Copper(II) Bromide1”. In: *J. Org. Chem.* 29.12 (1964), pp. 3459–3461. ISSN: 0022-3263. DOI: 10.1021/jo01035a003. URL: http://dx.doi.org/10.1021/jo01035a003.

[180] Patent. 2011. URL: http://www.google.ee/patents/WO2002020150A3?cl=en.

[181] Lukas J. Gooßen and Arno Döhring. “A Convenient Protocol for the Esterification of Carboxylic Acids with Alcohols in the Presence of di-t-Butyl Dicarbonate”. In: *Synlett* 2004.02 (2004), pp. 0263–0266. ISSN: 0936-5214. DOI: 10.1055/s-2003-44986.

[182] H. J. Cristau et al. “Synthesis of New Arylhydroxymethylphosphinic Acids and Derivatives”. In: *Synthesis* 2003.14 (2003), pp. 2216–2220. ISSN: 0039-7881. DOI: 10.1055/s-2003-41045.

[183] Frank S. Gibson, Stephen C. Bergmeier, and Henry Rapoport. "Selective Removal of an N-BOC Protecting Group in the Presence of a tert-Butyl Ester and Other Acid-Sensitive Groups". In: *J. Org. Chem.* 59.11 (1994), pp. 3216–3218. ISSN: 0022-3263. DOI: 10.1021/jo00090a045. URL: http://dx.doi.org/10.1021/jo00090a045.

[184] Manoj B. Gawande and Paula S. Branco. "An efficient and expeditious Fmoc protection of amines and amino acids in aqueous media". In: *Green Chemistry* 13.12 (2011), pp. 3355–3359. ISSN: 1463-9262. DOI: 10.1039/C1GC15868F. URL: http://dx.doi.org/10.1039/C1GC15868F.

[185] Heiner Eckert and Barbara Forster. "Triphosgene, a Crystalline Phosgene Substitute". In: *Angew. Chem., Int. Ed. Engl.* 26.9 (1987), pp. 894–895. ISSN: 1521-3773. DOI: 10.1002/anie.198708941. URL: http://dx.doi.org/10.1002/anie.198708941.

[186] Victoria K. Rusiecki and Susan A. Warne. "Synthesis of N-Fmoc-N-Nvoc-Lysine and use in the preparation of selectively functionalized peptides". In: *Bioorg. Med. Chem. Lett.* 3.4 (1993), pp. 707–710. ISSN: 0960-894X. DOI: http://dx.doi.org/10.1016/S0960-894X(01)81259-2. URL: http://www.sciencedirect.com/science/article/pii/S0960894X01812592.

[187] Maciej Stawikowski and Gregg B. Fields. "Introduction to Peptide Synthesis". In: *Curr. Protoc. Protein. Sci.* CHAPTER (2002), Unit–18.1. ISSN: 1934-3655 1934-3663. DOI: 10.1002/0471140864.ps1801s26. URL: http://www.ncbi.nlm.nih.gov/pmc/articles/PMC3564544/.

[188] Saioa Diosdado et al. "Catalytic Enantioselective Synthesis of Tertiary Thiols From 5H-Thiazol-4-ones and Nitroolefins: Bifunctional Ureidopeptide-Based Brønsted Base Catalysis". In: *Angew. Chem., Int. Ed.* 52.45 (2013), pp. 11846–11851. ISSN: 1521-3773. DOI: 10.1002/anie.201305644. URL: http://dx.doi.org/10.1002/anie.201305644.

[189] Christine Viala and Christophe Coudret. "An expeditious route to cis-Ru(bpy)2C12 using carbohydrates as reducers". In: *Inorg. Chim. Acta* 359.3 (2006), pp. 984–989. ISSN: 0020-1693. DOI: http://dx.doi.org/10.1016/j.ica.2005.07.019. URL: http://www.sciencedirect.com/science/article/pii/S0020169305003956.

[190] Leonardo Zayat, Marcelo Salierno, and Roberto Etchenique. "Ruthenium(II) Bipyridyl Complexes as Photolabile Caging Groups for Amines". In: *Inorg. Chem.* 45.4 (2006), pp. 1728–1731. ISSN: 0020-1669. DOI: 10.1021/ic0512983. URL: http://dx.doi.org/10.1021/ic0512983.

[191] Verónica San Miguel et al. "Multiphoton Reactive Surfaces Using Ruthenium(II) Photocleavable Cages". In: *Langmuir* 28.2 (2012), pp. 1217–1221. ISSN: 0743-7463. DOI: 10.1021/la2033687. URL: http://dx.doi.org/10.1021/la2033687.

[192] Robert N. Garner et al. "[Ru(bpy)2(5-cyanouracil)2]2+ as a Potential Light-Activated Dual-Action Therapeutic Agent". In: *Inorg. Chem.* 50.19 (2011), pp. 9213–9215. ISSN: 0020-1669. DOI: 10.1021/ic201615u. URL: http://dx.doi.org/10.1021/ic201615u.

[193] Ludovic Fournier et al. "A Blue-Absorbing Photolabile Protecting Group for in Vivo Chromatically Orthogonal Photoactivation". In: *ACS Chem. Biol.* 8.7 (2013), pp. 1528–1536. ISSN: 1554-8929. DOI: 10.1021/cb400178m. URL: http://dx.doi.org/10.1021/cb400178m%20http://pubs.acs.org/doi/abs/10.1021/cb400178m.

[194] R. P. Steer and V. Ramamurthy. "Photophysics and intramolecular photochemistry of thiones in solution". In: *Accounts of Chemical Research* 21.10 (1988), pp. 380–386. ISSN: 0001-4842. DOI: 10.1021/ar00154a005. URL: http://dx.doi.org/10.1021/ar00154a005.

[195] Wanhua Wu et al. "Organic Triplet Sensitizer Library Derived from a Single Chromophore (BODIPY) with Long-Lived Triplet Excited State for Triplet–Triplet Annihilation Based Upconversion". In: *J. Org. Chem.* 76.17 (2011), pp. 7056–7064. ISSN: 0022-3263. DOI: 10.1021/jo200990y. URL: http://dx.doi.org/10.1021/jo200990y.

[196] Oliver Kreye, Hatice Mutlu, and Michael A. R. Meier. "Sustainable routes to polyurethane precursors". In: *Green Chemistry* 15.6 (2013), pp. 1431–1455. ISSN: 1463-9262. DOI: 10.1039/C3GC40440D. URL: http://dx.doi.org/10.1039/C3GC40440D.

[197] Lindsay D. Rogers and Christopher M. Overall. "Proteolytic Post-translational Modification of Proteins: Proteomic Tools and Methodology". In: *Molecular Cellular Proteomics : MCP* 12.12 (2013), pp. 3532–3542. ISSN: 1535-9476 1535-9484. DOI: 10.1074/mcp.M113.031310. URL: http://www.ncbi.nlm.nih.gov/pmc/articles/PMC3861706/.

[198] Xose S. Puente et al. "Human and mouse proteases: a comparative genomic approach". In: *Nat Rev Genet* 4.7 (2003), pp. 544–558. ISSN: 1471-0056. DOI: http://www.nature.com/nrg/journal/v4/n7/suppinfo/nrg1111_S1.html. URL: http://dx.doi.org/10.1038/nrg1111.

[199] Carlos Lopez-Otin and Christopher M. Overall. "Protease degradomics: A new challenge for proteomics". In: *Nat Rev Mol Cell Biol* 3.7 (2002), pp. 509–519. ISSN: 1471-0072. URL: http://dx.doi.org/10.1038/nrm858.

[200] Diego Ingrosso et al. "Specificity of endoproteinase Asp-N (Pseudomonas fragi): Cleavage at glutamyl residues in two proteins". In: *Biochemical and Biophysical Research Communications* 162.3 (1989), pp. 1528–1534. ISSN: 0006-291X. DOI: http://dx.doi.org/10.1016/0006-291X(89)90848-6. URL: http://www.sciencedirect.com/science/article/pii/0006291X89908486.

[201] Peter A. Jekel, Wicher J. Weijer, and Jaap J. Beintema. "Use of endoproteinase Lys-C from Lysobacter enzymogenes in protein sequence analysis". In: *Analytical Biochemistry* 134.2 (1983), pp. 347–354. ISSN: 0003-2697. DOI: http://dx.doi.org/10.1016/0003-2697(83)90308-1. URL: http://www.sciencedirect.com/science/article/pii/0003269783903081.

[202] Heinz Neumann et al. "Encoding multiple unnatural amino acids via evolution of a quadruplet-decoding ribosome". In: *Nature* 464.7287 (2010), pp. 441–444. ISSN: 0028-0836. DOI: http://www.nature.com/nature/journal/v464/n7287/suppinfo/nature08817_S1.html. URL: http://dx.doi.org/10.1038/nature08817.

[203] Yong Ling et al. "Synthesis and evaluation of nitric oxide-releasing derivatives of farnesylthiosalicylic acid as anti-tumor agents". In: *Bioorg. Med. Chem.* 18.10 (2010), pp. 3448–3456. ISSN: 0968-0896. DOI: http://dx.doi.org/10.1016/j.bmc.2010.03.077. URL: http://www.sciencedirect.com/science/article/pii/S0968089610002919.

[204] Lekkala Amarnath Reddy et al. "Synthesis and Process Optimization of Amtolmetin: An Antiinflammatory Agent". In: *Org. Process Res. Dev.* 14.2 (2010), pp. 362–368. ISSN: 1083-6160. DOI: 10.1021/op900284w. URL: http://dx.doi.org/10.1021/op900284w.

[205] M. N. Stanton-Humphreys. "Design, Synthesis and Application of Novel Light-Activated Molecular Probes". Thesis. 2010.

[206] Robert M. Adlington et al. "The synthesis of pyrimidin-4-yl substituted [small alpha]-amino acids. A versatile approach from alkynyl ketones". In: *J. Chem. Soc., Perkin Trans. 1* 8 (1999), pp. 855–866. ISSN: 0300-922X. DOI: 10.1039/A806741D. URL: http://dx.doi.org/10.1039/A806741D.

[207] Paolo Strazzolini, Tiziana Melloni, and Angelo G. Giumanini. "Selective nitrolytic deprotection of N-BOC-amines and N-BOC-amino acids derivatives". In: *Tetrahedron* 57.43 (2001), pp. 9033–9043. ISSN: 0040-4020. DOI: http://dx.doi.org/10.1016/S0040-4020(01)00900-0. URL: http://www.sciencedirect.com/science/article/pii/S0040402001009000.

[208] Amy C. Topley et al. "A Resin-Linker-Vector Approach to Radiopharmaceuticals Containing 18F: Application in the Synthesis of O-(2-[18F]-Fluoroethyl)-L-tyrosine". In: *Chem. – Eur. J.* 19.5 (2013), pp. 1720–1725. ISSN: 1521-3765. DOI: 10.1002/chem.201202474. URL: http://dx.doi.org/10.1002/chem.201202474.

[209] Toyonobu Usuki et al. "Biomimetic Chichibabin Pyridine Synthesis of the COPD Biomarkers and Elastin Cross-Linkers Isodesmosine and Desmosine". In: *Org. Lett.* 16.6 (2014), pp. 1672–1675. ISSN: 1523-7060. DOI: 10.1021/ol500333t. URL: http://dx.doi.org/10.1021/ol500333t.

[210] Tomasz Fekner et al. “A Pyrrolysine Analogue for Protein Click Chemistry”. In: *Angew. Chem., Int. Ed.* 48.9 (2009), pp. 1633–1635. ISSN: 1521-3773. DOI: 10.1002/anie.200805420. URL: http://dx.doi.org/10.1002/anie.200805420.

[211] Suneel P. Singh et al. “A Microwave-Assisted Synthesis of (S)-N-Protected Homoserine -Lactones from l-Aspartic Acid”. In: *J. Org. Chem.* 76.16 (2011), pp. 6825–6831. ISSN: 0022-3263. DOI: 10.1021/jo2008093. URL: http://dx.doi.org/10.1021/jo2008093.

[212] Laurent Le Corre, Christine Gravier-Pelletier, and Yves Le Merrer. “Towards New MraY Inhibitors: A Serine Template for Uracil and 5-Amino-5-deoxyribosyl Scaffolding”. In: *Eur. J. Org. Chem.* 2007.32 (2007), pp. 5386–5394. ISSN: 1099-0690. DOI: 10.1002/ejoc.200700527. URL: http://dx.doi.org/10.1002/ejoc.200700527.

[213] Hans Paulsen and Knut Adermann. “Synthese von O-Glycopeptid-Sequenzen des N-Terminus von Interleukin-2”. In: *Liebigs Ann. Chem.* 1989.8 (1989), pp. 751–769. ISSN: 1099-0690. DOI: 10.1002/jlac.198919890223. URL: http://dx.doi.org/10.1002/jlac.198919890223.

[214] Vajinder Kumar, Narender Yadav, and K. P. Ravindranathan Kartha. “In(III) triflate-catalyzed detritylation and glycosylation by solvent-free ball milling”. In: *Carbohydr. Res.* 397.0 (2014), pp. 18–26. ISSN: 0008-6215. DOI: http://dx.doi.org/10.1016/j.carres.2014.08.002. URL: http://www.sciencedirect.com/science/article/pii/S0008621514003127.

[215] Patent. Dec. 2015.

[216] Nicolas Maindron et al. “Synthesis and luminescence properties of new red-shifted absorption lanthanide(iii) chelates suitable for peptide and protein labelling”. In: *Org. Biomol. Chem.* 9.7 (2011), pp. 2357–2370. ISSN: 1477-0520. DOI: 10.1039/C0OB00832J. URL: http://dx.doi.org/10.1039/C0OB00832J.

[217] Alessandro Pratesi et al. “Design and solid phase synthesis of new DOTA conjugated (+)-biotin dimers planned to develop molecular weight-tuned avidin oligomers”. In: *Org. Biomol. Chem.* 13.13 (2015), pp. 3988–4001. ISSN: 1477-0520. DOI: 10.1039/C4OB02685C. URL: http://dx.doi.org/10.1039/C4OB02685C.

[218] Simone Weis et al. “Ethyl substituted coumarin-4-yl derivatives as photoremovable protecting groups for amino acids with improved stability for SPPS”. In: *J. Photochem. Photobiol., A* 241.0 (2012), pp. 52–57. ISSN: 1010-6030. DOI: http://dx.doi.org/10.1016/j.jphotochem.2012.05.014. URL: http://www.sciencedirect.com/science/article/pii/S1010603012002493.

[219] Zhen Wang, Peng Wang, and XinJing Tang. “Synthesis of Light-Induced Expandable Photoresponsive Polymeric Nanoparticles for Triggered Release”. In: *ChemPlusChem* 78.10 (2013), pp. 1273–1281. ISSN: 2192-6506. DOI: 10.1002/cplu.201300212. URL: http://dx.doi.org/10.1002/cplu.201300212.

[220] Caroline de Gracia Lux et al. “Intramolecular cyclization assistance for fast degradation of ornithine-based poly(ester amide)s”. In: *J. Polym. Sci., Part A: Polym. Chem.* 51.18 (2013), pp. 3783–3790. ISSN: 1099-0518. DOI: 10.1002/pola.26788. URL: http://dx.doi.org/10.1002/pola.26788.

[221] Patent. 27/11/2014 2014.

[222] Chensheng Ma et al. “Ultrafast Time-Resolved Transient Absorption and Resonance Raman Spectroscopy Study of the Photodeprotection and Rearrangement Reactions of p-Hydroxyphenacyl Caged Phosphates”. In: *J. Am. Chem. Soc.* 128.8 (2006), pp. 2558–2570. ISSN: 0002-7863. DOI: 10.1021/ja0532032. URL: http://dx.doi.org/10.1021/ja0532032.

[223] E. Thomas Everhart and J. Cymerman Craig. “A facile general route to enantiomeric 1-(4-hydroxyphenyl)alkanols, and an improved synthesis of 4-vinylphenol”. In: *J. Chem. Soc., Perkin Trans. 1* 7 (1991), pp. 1701–1707. ISSN: 0300-922X. DOI: 10.1039/P19910001701. URL: http://dx.doi.org/10.1039/P19910001701.

[224] DJ Beames and LN Mander. “Studies on intramolecular alkylation. IV. The preparation of spirodienones from phenolic diazoketones”. In: *Aust. J. Chem.* 27.6 (1974), pp. 1257–1268. DOI: http://dx.doi.org/10.1071/CH9741257. URL: http://www.publish.csiro.au/paper/CH9741257.

[225] Ildiko M. Kovach et al. “Rate-determining carbonyl hydration in the intramolecular hydrolysis of phenacyl phosphonate esters: isotopic probes and activation parameters”. In: *J. Am. Chem. Soc.* 115.23 (1993), pp. 10471–10476. ISSN: 0002-7863. DOI: 10.1021/ja00076a001. URL: http://dx.doi.org/10.1021/ja00076a001.

[226] John D. Nguyen, Bryan S. Matsuura, and Corey R. J. Stephenson. “A Photochemical Strategy for Lignin Degradation at Room Temperature”. In: *J. Am. Chem. Soc.* 136.4 (2014), pp. 1218–1221. ISSN: 0002-7863. DOI: 10.1021/ja4113462. URL: http://dx.doi.org/10.1021/ja4113462.

[227] Erik A. Karlsson et al. “Synthesis and Electron-Transfer Processes in a New Family of Ligands for Coupled RuMn2 Complexes”. In: *ChemPlusChem* 79.7 (2014), pp. 936–950. ISSN: 2192-6506. DOI: 10.1002/cplu.201402006. URL: http://dx.doi.org/10.1002/cplu.201402006.

[228] Sergey V. Litke, Aleksei Yu Ershov, and Thomas J. Meyer. “Deactivation Pathways for Metal-to-Ligand Charge-Transfer Excited States of Ruthenium Polypyridyl Complexes with Triphenylphosphine as a Ligand”. In: *J. Phys. Chem. A* 115.50 (2011), pp. 14235–14242. ISSN: 1089-5639. DOI: 10.1021/jp2062354. URL: http://dx.doi.org/10.1021/jp2062354.

[229] Keiichi Ito and Junko Maruyama. “Studies on Stable Diazoalkanes as Potential Fluorogenic Reagents. I. 7-Substituted 4-Diazomethylcoumarins”. In: *Chem. Pharm. Bull.* 31.9 (1983), pp. 3014–3023. DOI: 10.1248/cpb.31.3014.

[230] Alex L. Nguyen et al. “Synthesis and Reactivity of 4,4-Dialkoxy-BODIPYs: An Experimental and Computational Study”. In: *Inorg. Chem.* 54.7 (2015), pp. 3228–3236. ISSN: 0020-1669. DOI: 10.1021/ic502821m. URL: http://dx.doi.org/10.1021/ic502821m.

[231] Hao Zhu et al. “A “Distorted-BODIPY”-Based Fluorescent Probe for Imaging of Cellular Viscosity in Live Cells”. In: *Chem. – Eur. J.* 20.16 (2014), pp. 4691–4696. ISSN: 1521-3765. DOI: 10.1002/chem.201304296. URL: http://dx.doi.org/10.1002/chem.201304296.

[232] C. G. Hatchard and C. A. Parker. “A New Sensitive Chemical Actinometer. II. Potassium Ferrioxalate as a Standard Chemical Actinometer”. In: *Proceedings of the Royal Society of London. Series A. Mathematical and Physical Sciences* 235.1203 (1956), pp. 518–536. DOI: 10.1098/rspa.1956.0102.